



AGRICULTURAL RESEARCH INSTITUTE

PUSA

314724

PROCEEDINGS

OF THE

ROYAL SOCIETY OF LONDON

SERIES A

CONTAINING PAPERS OF A MATHEMATICAL AND
PHYSICAL CHARACTER

VOL CVII

LONDON

PRINTED FOR THE ROYAL SOCIETY AND SOLD BY
HARRISON AND SONS, LTD, ST MARTIN'S LANE,
PRINTERS IN ORDINARY TO HIS MAJESTY

APRIL, 1925.

LONDON

HARRISON AND SONS, LTD, PRINTERS IN ORDINARY TO HIS MAJESTY,
ST MARTIN'S LANE

CONTENTS.

SERIES A VOL. CVII.

Minutes of Meetings, December 1, 4, 1924, January 15, 22, 29, February 5, 12, 19, 26,
and March 5, 12, 19, 26, 1925

No A 741—January 1, 1925

	PAGE
Address of the President Sir Charles S Sherrington, at the Anniversary Meeting, December 1, 1924	1
On the Total Reflexion of Light By Sir Arthur Schuster, For Sec RS	15
The Structure of the Spectrum of Ionised Nitrogen By A Fowler, FRS, Yarrow Research Professor of the Royal Society, Imperial College, South Kensington (Plate 1)	31
Spheroidal Wave Functions By J W Nicholson, MA, DSc, FRS, Fellow of Balliol College, Oxford	43
Thermionic Effects caused by Vapours of Alkali Metals By Irving Langmuir and K H Kingdon, of the Research Laboratory, General Electric Company, Schenectady, NY Communicated by Prof Sir E Rutherford, FRS	61
1 2 3- Triaminopropane and its Complex Metallic Compounds By Frederick George Mann, Ph D, and Sir William Jackson Pope, FRS	80
The Union of Hydrogen and Oxygen in Presence of Silver and Gold By D L Chapman, MA, FRS, Fellow of Jesus College, Oxford J E Ramsbottom, DSc, Ph D, Superintendent Chemical Department, Royal Aircraft Establish- ment, Farnborough, and C G Trotman, BA, Jesus College, Oxford	92
The General Law of Electrical Conduction in Dielectrics By Spencer W Richardson, MA, DSc, FInstP Communicated by Sir William Bragg, KBE, FRS	101
Recent Developments in Tensile Testing By J V Howard, DSc, and S L Smith, DSc, ACGI Communicated by W E Dalby, FRS	113
The Effect of Superposed Alternating Current on the Polarizable Primary Cell Zinc Sulphuric Acid-Carbon Part I—Low-Frequency Current By A J Allmand, DSc, and V S Puri, MSc, Ph D Communicated by Prof S Smiles, FRS	126
The Spark-Spectra of Indium and Gallium in the Extreme Ultra-Violet Region By Mollie Weinberg, MA, MSc, Physical Laboratory, University of Toronto Communicated by Prof J C McLennan, FRS (Plate 2)	138

	PAGE
On the Atomic Fields of Helium and Neon By J E Jones, D Sc, 1851 Exhibition Senior Research Student, Trinity College, Cambridge Communicated by Prof S Chapman, F R S	157
No A 742 — February 2, 1925	
Experiments on the Distortion of Single Crystal Test-Pieces of Aluminum By H C H Carpenter, F R S, Professor of Metallurgy, Imperial College of Science and Technology, and Miss C F Elam, M A, Armourers' and Brasiers' Company Research Fellow (Plate 3)	171
On the Thirteen Semi-regular Solids of Archimedes, and on their Development by the Transformation of certain Plane Configurations By D'Arcy Wentworth Thompson, F R S	181
On the Formation of Water Waves by Wind By Harold Jeffreys, M A, D Sc, Fellow and Lecturer of St John's College, Cambridge Communicated by Prof G I Taylor, F R S (Plates 4 and 5)	189
The Thermal and Electrical Conductivities of some Pure Metals By F H Schofield, B A, B Sc Communicated by Sir Joseph Petavel, F R S	206
The Colours Due to Thin Films on Metals By Ulric R Evans Communicated by C T Heycock, F R S	228
On the Quantum Dynamics of Degenerate Systems By A M Mosharrafa, D Sc, Ph D Communicated by Prof O W Richardson, F R S	237
On the Effect of Temperature on the Anomalous Reflection of Silver By M de Sélincourt, Scholar of Brasenose College, Oxford Communicated by Prof F A Lindemann, F R S	247
The Catalytic Activity of Copper Part V—The Comparison of the Rates of Dehydrogenation of Various Alcohols By W G Palmer, Fellow of St John's College, Cambridge, and F H Constable, Strathcona Research Student, St John's College, Cambridge Communicated by Sir William Pope, F R S	255
The Catalytic Action of Copper Part VI—An Explanation of the Reproducibility of the Catalyst, and of the Periodic Change in its Activity, together with some Experiments on the Activation of the Catalyst by Alternate Oxidation and Reduction By F H Constable, Strathcona Research Student of St John's College, Cambridge Communicated by Sir William Pope, F R S	270
The Catalytic Action of Copper Part VII—A Study of the Effect of Pressure on the Rate of Dehydrogenation of Alcohols By F H Constable, Strathcona Research Student of St John's College, Cambridge Communicated by Sir William Pope, F R S	279
A Centrifugal Method of Making Small Pots of Electrically Fused Refractory Materials By Fred S Tritton Communicated by Dr W. Rosenhain, F R S	287
On the Precise Measurement of the Critical Potentials of Gases By E G Dymond, B A, St John's College, Cambridge Communicated by Prof Sir E Ruthenford, F R S	291

	PAGE
On the Determination of Resistance in Terms of Mutual Inductance By Albert Campbell, B A. Communicated by F E Smith, F R S	310
The Absorption of X-Rays By E C Stoner, B A, Lecturer in Physics at Leeds University, and L H Martin, M Sc, 1851 Exhibition Scholar (Melb), Trinity College, Cambridge Communicated by Prof Sir E Rutherford, F R S	312
Ionisation by Alpha-Particles in Monatomic and Diatomic Gases By R W Gurney, B A, Trinity Hall, Cambridge Communicated by Prof Sir E Rutherford, F R S	332
The Stopping-Power of Gases for Alpha Particles of Different Velocities By R W Gurney, B A, Trinity Hall, Cambridge Communicated by Prof Sir E Rutherford, F R S	340
The Ejection of Protons from Nitrogen Nuclei, Photographed by the Wilson Method By P M S Blackett, Moseley Research Student of the Royal Society and Fellow of King's College, Cambridge Communicated by Prof Sir E Rutherford, F R S (Plates 6 and 7)	349
The Apparent Tripling of Certain Lines in Arc Spectra By T Royds, D Sc, Director, Kodaikanal Observatory Communicated by J Evershed, F R S (Plate 8)	360

No A 743—March 2, 1925

On the Life Statistics of Fellows of the Royal Society By Sir Arthur Schuster, F R S	368
The Thermionic Work-Functions and Photo-electric Thresholds of the Alkali Metals By O W Richardson, F R S, Yarrow Research Professor of the Royal Society, and A F A Young, Ph D, King's College, London	377
On Experiments relating to the Spectrum of Nitrogen By T R Meiton, M A, D Sc, F R S, Professor of Spectroscopy in the University of Oxford, and J G Pille, B A	411
The Heat Developed during Plastic Extension of Metals By W S Farnen, M A, and G I Taylor, F R S, Yarrow Research Professor of the Royal Society	422
An Experimental Study of the Vibrations in the Blades and Shaft of an Airscrew By A Fage, A R C Sc, of the Aerodynamics Department, National Physical Laboratory Communicated by H Lamb, F R S	451
Thermal Diffusion Measurements By T L Ibbs, M C, M Sc Communicated by Prof S W J Smith, F R S	470
Overvoltage and Transfer Resistance By Edgar Newbery, D Sc, F I C, University of Cape Town Communicated by Prof Sir E Rutherford, F R S (Plates 9-11)	486
The Magnetic Properties of Iron Crystals By W L Webster, B A, 1851 Research Student of the University of Toronto Communicated by Prof Sir E Rutherford, F R S	496

	PAGE
On the Measurement of the Ratio of the Specific Heats using Small Volumes of Gas—The Ratios of the Specific Heats of Air and of Hydrogen at Atmospheric Pressure and at Temperatures between 20° C and -183° C By J H Brinkworth, A.R.C.S., M.Sc., D.I.C. Communicated by Prof H L Callendar, F.R.S.	510
The Interpretation of the Results of Bucherer's Experiments on e/m By Thos Lewis, B.Sc., (Harrod Thomas Fellow of the University College of Wales, Aberystwyth Communicated by Prof G A Schott, F.R.S.	544
The Variation with Temperature of the Intensity of Reflection of X-Rays from Quartz and its Bearings on the Crystal Structure By Reginald Edmund Gibbs Communicated by Sir William Bragg, F.R.S.	561
The Fulcher Hydrogen Bands By W E Curtis, D.Sc., A.R.C.S., Reader in Physics in the University of London, King's College Communicated by Prof O W Richardson, F.R.S.	570
On the Determination of the Directions of the Forces in Wireless Waves at the Earth's Surface By R. L. Smith-Rose, Ph.D., M.Sc., and R. H. Barfield, M.Sc. Communicated, by permission of the Radio Research Board, by Sir Henry Jackson, F.R.S.	587
No A 744—April 1, 1925	
Regularities in the Secondary Spectrum of Hydrogen By O W Richardson, Yarrow Research Professor of the Royal Society, and T Tanaka, Professor in the College of Nagata, Japan	602
The Lattice Points of a Circle By G H Hardy, F.R.S.	623
On the Calculation of certain Crystal Potential Constants and on the Cubic Crystal of Least Potential Energy By J E Jones, Ph.D., Trinity College, Cambridge, and A E Ingham, B.A., Trinity College, Cambridge Communicated by Prof S Chapman, F.R.S.	636
The Kinetics of Hæmoglobin III—The Velocity with which Oxygen combines with Reduced Hæmoglobin By H Hartridge, M.D., Sc.D., Fellow of King's College, Cambridge, and F J W Roughton, M.A., Fellow of Trinity College, Cambridge Communicated by Prof. J N Langley, F.R.S.	654
The Structure of Molecules in Relation to their Optical Anisotropy—Part I By K R Ramanathan, M.A., D.Sc., Assistant Lecturer in Physics, University College, Rangoon Communicated by Prof C V. Raman, M.A., D.Sc., F.R.S.	684
On the Alternating Current Resistance of Solenoidal Coils By S Butterworth, M.Sc. Communicated by F E Smith, F.R.S.	693
On the Field of Force near the Neutral Point produced by Two Equal Coaxial Coils, with Special Reference to the Campbell Standard of Mutual Inductance. By Raymond M Wilmette, B.A., National Physical Laboratory Communicated by Sir Joseph Petavel, F.R.S.	716

	PAGE
The Adiabatic Invariance of the Quantum Integrals By P A M Dirac, St John's College, Cambridge Communicated by Prof Sir E Rutherford, F.R.S	725
On the Theory of Elastic Stability By W R Dean, B A, Fellow of Trinity College, Cambridge Communicated by Prof G I Taylor, F.R.S	734
On the Fluorescence and Channelled Absorption of Bismuth at High Temperatures By K Rangadhama Rao, M A, Madras University Research Scholar Communicated by Lord Rayleigh, F.R.S (Plate 12)	760
A Note on the Absorption of the Green Line of Thallium Vapour By K Rangadhama Rao, M A, Madras University Research Scholar Communicated by Lord Rayleigh, F.R.S (Plate 13)	762

OBITUARY NOTICES OF FELLOWS DECEASED

S S Hough (with portrait)	i
Sir James Johnstone Dobbie (with portrait)	vi
John Edward Campbell (with portrait)	ix
Index	xiii

PROCEEDINGS OF THE ROYAL SOCIETY.

SECTION A — MATHEMATICAL AND PHYSICAL SCIENCES

Address of the President, Sir Charles S. Sherrington, at the Anniversary Meeting, December 1, 1924

The Anniversary Meeting brings the retrospect of the Society's year. It calls to mind the names of those whom the twelve months have taken from the Fellowship. The Society covers a range of scientific subjects which is wide and perhaps the more for that, observes at its Anniversary Meeting some reference even though brief to the work and endeavour which each name on the obituary list has stood for. Let me, so well as I may, follow that custom, based as it is on the community which, despite difference of individual work, binds all the Fellowship together.

HENRY HAVERSHAM GODWIN-AUSTEN died in his ninetieth year. One of the pioneers in the geography of the Himalaya, in that scene of his labours his name is signalised by the Godwin-Austen glacier, a tributary of the great Baltova glacier which he discovered. He was further a faunistic authority, especially competent in the Mollusca of India.

THOMAS GEORGE BONNEY, geologist, in his ninety-first year. A long life, active in many ways. It has been remarked of him as a field geologist, by one who much later re-studied areas he had studied, that "Bonney left little for a successor to find out." He brought into laboratory teaching the microscopic petrology originated by Sorby. When lecturer at Cambridge, no fewer than six of those who there followed his lectures have, as geologists, entered the Fellowship of this Society. Bonney in advanced life, making Cambridge again his home, found pleasure in again teaching there as a volunteer demonstrator in the Geological School.

GEORG HERMANN QUINCKE, physicist, elected Foreign Member in 1879, indefatigable throughout a long career. Known perhaps most widely by the researches on surface-tension, which early occupied him, he made observa-

tions of much significance in other fields of physics. It has been written of him by one well able to judge, and from personal knowledge, that "he was an experimenter of the highest rank", also that "for theories he had little affection."

THOMAS HENRY TIZARD, in his eighty-fifth year, formerly Assistant Hydrographer of the Navy. He was the senior survivor of the old navigating branch. He was navigating officer on the "Challenger" for the memorable "Challenger" expedition. He brought out a Table of Chords reducing time and labour in the chart-room. His survey work established the existence of the Wyville-Thomson Ridge across the Faroe channel, and traced the distribution of temperatures and exchange of Atlantic and Arctic waters occurring there. Surveying carried out by him provided a Report of permanent value regarding our national highway, the outer estuary of the Thames.

JOHNSON SYMINGTON, many years Professor of Anatomy at Queen's University, Belfast. His work though chiefly in detailed topography, drew attention to some essential facts re-establishing the view, advanced by Richard Owen and then discredited for thirty years, that the great callosal commissure of the brain prominent in the higher mammalia is yet, in the most primitive, not present.

ROBERT EDMUND FROUDE died in March. He had been superintendent at Haslar of the Admiralty Experimental tank constructed there for experiments on ship-models. He carried out for more than thirty years observations on hull-forms and resistance, and on propeller problems, work of the kind inaugurated by his father, William Froude, likewise Fellow of this Society.

WILLIAM MACEWEN died in March. Brilliant surgeon, he advanced scientific surgery. Early in contact with Lister and Lister's developing views, he quickly recognised their truth. Relying on them, he boldly trusted the reparatory power of nature in ways and to a degree until then scarcely ventured. He was of those who earliest proceeded to take surgical action based on Ferrier's experiments upon the localisation of function of the ape's brain. He tracked inflammation of the middle ear to be one of the commonest sources of abscess of the brain. He represented British surgery at the Australian Medical Meeting in Melbourne only last year.

GRENVILLE ARTHUR JAMES COLE had been Director of the Geological Survey of Ireland since 1905, and since 1890 Professor of Geology in the Royal College of Science, Dublin. Of London by family and birth, his scientific career began in London at the Royal School of Mines. In Ireland he entered ardently into the scientific life of that country, and took prominent part in the work of the

Royal Irish Academy. He was a facile and attractive writer, part of his library he bequeathed to the University of Liverpool.

SAMUEL GEORGE SHATTOCK had had charge for many years of the pathological section of the Hunterian Museum of the Royal College of Surgeons. He was indeed of the tradition of John Hunter. He had early given himself wholly to pathology. His was a great and ordered storehouse of knowledge on that subject, accessible to all who sought it, in morbid anatomy he ranked with the supreme masters. Single-minded and devoted, his way of life was of the simplest, ascetic, but without trace of harshness toward others. It was characteristic of him that he could never be induced to write a text book.

CHARLES WILLIAM ANDREWS died at the age of fifty-eight. His career began in school teaching, and then passed to the Department of Geology at the British Museum. His work, much interrupted by illness and suffering, contributed richly to palæontology. To wit, his study of the Fayum tertiary mammals, establishing *inter alia* Africa as the original home of the Proboscidea. Of his Catalogue, published from the British Museum in 1906, the year of his election to the Fellowship, it has in tribute been said that "it will remain always one of the classics of vertebrate palæontology."

JAMES JOHNSTON DOBBIE had given research to the chemical constitution of alkaloids and to ultra-violet absorption by organic compounds. His initiative and influence brought about the founding of the first Agricultural Department attached to a University or University College, namely, at Bangor, in 1894. Later, on reorganization of the Government Laboratory, he was the first to hold the appointment of Government Chemist. His tenure of it covered the difficult years of the war.

JETHRO JUSTINIAN HARRIS TEALL, geologist, and accomplished in all branches of that science, for thirteen years Director of the Geological Survey and of the Museum of Practical Geology. Despite engrossment in administrative duties, he had produced the well-known treatise which constituted a stride forward in Petrography. His collection of rock specimens, containing rock-slices described in his 'Petrography,' will have permanent home in the Sedgwick Museum at Cambridge. He had served twice on this Society's Council, and had been one of the Vice-Presidents of the Society.

In July last, still in full career of active research, died ROBERT KIDSTON, palæobotanist. The problem of the origin of the seed-plants had especially engaged him, and he had had notable success in obtaining evidence regarding it. In 1904 he showed the great seeds borne on fronds of the leaflets of

Neuropteria In conjunction with Prof Lang he furnished a reconstruction in detail of the oldest land-plants of which there is any certain knowledge. His place remains among the historians of the steps of structural change which have marked the evolution of the plant kingdom

WILLIAM ABBOTT HERDMAN, zoologist, for many years Professor of Natural History at Liverpool. A naturalist who loved the sea as sailor as well as naturalist, marine biology was pre-eminently his study. He founded the Marine Biological Station at Port Erin, its work and success were his constant care. His visits to and his investigation of the Ceylon Pearl Fisheries were the source of five volumes issued under the auspices of this Society. He, in conjunction with Lady Herdman, endowed in the University of Liverpool, Chairs of Geology and of Oceanography, and last year he gave further £20,000 toward the building of the geological laboratory. He was President of the British Association in 1921. He served as Foreign Secretary of the Society from 1916 to 1920. Genial, of buoyant temperament, a keen observer who had travelled far with interest in many themes, business-like and shrewd in business, his old colleagues and his many friends will long regret and miss him.

In August passed away **WILLIAM MADDOCK BAYLISS**, physiologist. Hardly a field of physiology but was touched by some research of his. Electrical responses of gland and of the heart muscle, vasodilator nerves and reflexes operating on the blood vessels, conduction by the spinal roots, the innervation intrinsic and extrinsic of the intestine, "secretin" and the proof of specific chemical messengers, "hormones," connecting and co-ordinating the activities of separate organs, osmotic pressure of colloids as studied in solutions of colloidal dye-stuffs, all these were items, and though of high importance, yet but items of the work accomplished by him. A lovable and ideal colleague, much of his work was done in collaboration. He was one of the key figures maintaining the physiological endeavour of our time. His steadiness and height of scientific aim made part of his inspiring influence. The Copley Medal of the Society was awarded him in 1919. Although without formal medical training he, during the war, devised a procedure for combating shock from hæmorrhage which was a direct advance in the treatment of an essentially clinical and surgical problem. His customary approach to a problem was from the point of view of general biology—a point of view typically illustrated by his book 'Principles of General Physiology,' first issued in 1917, a volume novel to physiology in such measure that it may be said hardly to have had any actual predecessor. The book was dedicated "to E. H. S., my fellow worker," namely, Professor Starling, along with whom so much of his work

was done and so many of his discoveries were made, that the two names always recall, and ever will recall, the one the other

SIDNEY HARRIS COX MARTIN, Professor of Clinical Medicine in the University of London and Senior Physician to University College Hospital. A Report from him, based on systematic and prolonged experiments, largely guided the conclusions of the Royal Commission on Tuberculosis in 1895. He was elected to the Fellowship that same year. He served on the Council of the Society from 1919 to 1921.

GEORGE THOMAS BEILBY, inventor in the applications of chemistry to industry, and a leader of industry. One of his early successes lay in improving the practice of oil distillation from the Scottish shales, helping to strengthen that industry for a difficult time ahead. Again, he met the need for cheap cyanide in connection with gold-recovery, by producing a satisfactory process and plant.

During the war his scientific and technical knowledge along with his practical wisdom performed services, still unwritten, for the Trench Warfare Committee, and for the Naval Board of Invention and Research. In 1917 he undertook, as Chairman and Director, the establishing of the Fuel Research Station. From this he retired last year, the work under his devoted direction having reached a stage where organization and general lines of enquiry had been established.

During the last thirty years, as and when his scanty leisure allowed, he had applied the microscope to metallurgical problems, and done great service by drawing attention to the changes wrought on metallic surfaces by mechanical working, indeed, he went far to answer the question "What is a polished surface?"

Quiet, unassertive, with a kindly humour, he had too a keen critical faculty in regard to shams of all kinds. Of his many and generous gifts he never dropped a hint, but to one of them the Society's Pension Fund bears witness.

WALTER HUME LONG, Viscount Long of Wraxall. His public services were many, and it may be recalled here that when President of the Board of Agriculture, relying on the opinion of his scientific advisers, he freed this country from the scourge of rabies and hydrophobia. In accomplishing this he had to face wide opposition and a petition with 80,000 signatures praying for his removal from office. But the measure he took was based with clear logic on Pasteur's proof that rabies is transmitted by inoculation only, and his courage persevered in enforcing the Order he had issued until, in due course,

as he and his advisers had foreseen it could do, it had eradicated rabies, and with a success enduring practically to the present time. He was elected to the Society under Statute XII.

JOHN EDWARD CAMPBELL, mathematician, had taught at Oxford for many years. His own particular studies had dealt with the theories of continuous groups and of contact transformations. He had completed shortly before his death the MS. of a work upon differential geometry. He was from 1918 to 1920 President of the London Mathematical Society.

WILLIAM BOTTING HEMSLEY, botanist, had entered service at Kew in 1860, and was Keeper of the Herbarium from 1899 to 1908. In spite of indifferent health through much of his earlier life, he contributed consistently work of value to systematic Botany. The "Challenger" Report, the *Flora Australiensis*, the *Flora of High Asia*, the *Flora of Tropical Africa*, all bear witness to his industry and knowledge.

ARCHIBALD GEIKIE, in his eighty-ninth year, geologist, eminent alike as observer, writer and administrator. Joining the Survey in 1855, and retiring from it as Director-General in the first year of this century, his own pen has portrayed the life he led and the work he did in the Survey throughout that lengthy service. Widely travelled and an excellent linguist, he was Foreign Secretary of the Society from 1889 to 1893, then Secretary from 1903 to 1908, in which latter year he became President. During his Presidency fell the 250th Anniversary of the Society, and his organising power and social gifts enhanced the success of the commemorative celebration. A facile and happy speaker, he was also a productive author, and not only in geology but in biography and in literary history. One of his latest services to the society was the biographical notice he wrote of Sir Alfred Kempe, sometime his fellow Officer in the Society. Elected Fellow in 1865, the seniority of the Fellowship had come to him two years ago. He had received many honours and distinctions, and his name was familiar to scientific circles the world over.

MAURICE FITZMAURICE, engineer, distinguished for a number of great engineering works. He was Chief Engineer to the Egyptian Government for the making of the Assuan Dam, and recently Chairman of the Nile Projects Committee of the British Foreign Office. He carried out the duplication and extension of the whole main drainage system of London. The Rotherhithe Tunnel, the new Vauxhall Bridge, the subway under Kingsway, the river Embankment by the County Hall are all features of his work for London. His opinion and experience were authoritative. He was Chairman of the Advisory Committee on Naval Works, during the war he advised, from visits

of inspection, on the drainage of the British Front in Flanders. He was President of the Institution of Civil Engineers in 1916-17.

Nor can this list conclude without reminding us that, in April last, death cut short the career of one whose name five weeks earlier had been published on the selected list for election to the Fellowship, NELSON ANNANDALE, Zoologist. Much of his work had been preparatory to a projected comprehensive study of the fauna of the rivers and lakes of India. His administrative ability had gained for him the Directorship of the Zoological Survey of India, a post he was the first to hold. Sadly enough, he was not spared to conduct further the work which he had there instituted and developed.

Proceeding to other matters, this year, the Society, at the request of the Government, organised through a Committee appointed for the purpose by the Society's Council, an Exhibition of Pure Science in the Government Building at the British Empire Exhibition. This Exhibition of Pure Science was planned to show, amid the surrounding display of commercial and industrial developments, the direction and the contribution towards them made by scientific enquiry and modern methods of pure research. It is estimated that more than three million persons visited the Pure Science Exhibition. The little volume issued as Handbook for it secured a large sale. All goes to prove that the Exhibit achieved its aim of bringing before a wide public the meaning and importance of scientific research, and of stimulating general interest in pure Science. Sir Richard Glazebrook and his colleagues of the Committee and with them Mr. Martin its Secretary, are to be congratulated on the skill and judgment which won well-deserved success for a novel and an arduous undertaking.

July last brought the centenary celebration of Lord Kelvin's birth. In that commemoration the Royal Society co-operated along with other institutions and societies united to do honour to an ever memorable name. At the instance of Dr. Russell, President both of the Physical Society and of the Institution of Electrical Engineers, a Committee was formed by the Council, on it, with Sir Richard Glazebrook as Chairman, were represented Universities and Societies with which Lord Kelvin had been connected. In response to the invitations from the Committee no fewer than forty-nine Institutions, British and foreign, sent delegates to the celebration. It was attended by men eminent in and representative of physical science in many lands. Sir Joseph Thomson delivered the Memorial Oration, the Lord Balfour presided at the Banquet. The celebration, rich in its associations, was for no participant more so than for this Society, where in such several ways Lord Kelvin's name endures.

The year has seen the allocation of a third Research Professorship provided from the munificent gift received from our Fellow, Sir Alfred Yarrow. To this Professorship has been appointed one of those rare sublunary beings who are gifted with both mathematical and experimental ability in almost equal degree, Prof. O. W. Richardson. His original contributions to science have been remarkable for their variety, their amount, and their value. Perhaps his most important work of all has been that connected with the emission of electrons from hot bodies, a subject he has made particularly his own and to which he has given the name of "thermionics". On the purely scientific side the subject provides a method of testing the extent to which the velocities of free electrons conform with Maxwell's Law of Distribution. It has also proved to be of great industrial importance, the modern use of thermionic valves in "wireless" depending to a large extent on the early advances made by Prof. Richardson. Another valuable part of his work has centred round the phenomenon of photo-electric action. He investigated this both from the theoretical and from the experimental standpoints. The important experimental results which he and his pupils obtained at Princeton in 1911-13 gave almost the first accurate knowledge of the broad quantitative facts of photo-electricity, and in its main outlines the subject still stands much where he left it. In 1912-14 he put forward a set of ideas which led to important results in connection with the photo-electric activity of black-body radiation, the recent important work of Kramers and Milne in this field is based upon concepts which are fundamentally identical with those put forward by Richardson more than ten years ago.

Prof. Richardson has greatly advanced our knowledge of radiation intermediate between the shortest ultra-violet radiation and the longest X-ray radiation. There is left now no unexplored range between these two types of radiation, the closing of that gap has been in no small measure due to work either accomplished by or inspired by our new Research Professor. Mention should also be made of Prof. Richardson's work on the gyromagnetic effect, which he predicted long before it was found experimentally.

During the war he did valuable work in connection with thermionic valves and instruments for the detection of hostile submarines. He is the author of two widely read text-books on 'The Emission of Electricity from Hot Bodies' and on 'The Electron Theory of Matter.' Like our two other Yarrow Professors, he will continue to work in a laboratory from which he has published a large part of his best work. We confidently hope that the freedom from routine duties which is secured to him by his appointment to a Yarrow Professorship will result in a still greater output of important research on his part. At the

same time it is the intention of the Royal Society that their Research Professors should be free not only to carry out their own research but also to inspire the researches of others. Arrangements have been made whereby Prof Richardson will continue to supervise a certain amount of graduate research work, and his success in guiding and stimulating the researches of others in the past lead us to hope that this may be by no means the least valuable part of his work in the future.

The rotation of the Foreign Secretaryship of the Society is four-yearly, and Sir Arthur Schuster therefore completes to-day his full term in that office. To his valued services, rendered devotedly, and despite the anxiety and indeed suffering caused him at one time by a dangerous accident, the Society owes much; we render him our heartiest thanks. It is a great pleasure to me to have the privilege of offering them to him.

If I may pass finally for a moment to biological progress which the year has witnessed, I would advert to the work which Professor Magnus and his collaborators have recently brought to approximate completion, their admirable research in nerve-physiology engaging the Utrecht laboratory during the past fifteen years. Its field has lain in nervous mechanisms which, though the highest part of the brain can have touch with them, can yet of themselves work wholly reflexly and separably from mind.

A number of simpler acts, studied for the most part in lower animal forms, have, of course, long been known to stand in that relation to the higher brain. But the Utrecht researches prove a like relation, and in the superior mammals, for acts surprisingly complex, such as the assumption and maintenance of the erect posture, of walking, running, and so forth in all their ordinary completeness. Not only have Magnus and his colleagues observed this, but they have analysed the reflex processes by which these acts are thus accomplished. They have traced the seat and nature of the stimuli at work, the principles of the co-ordination of the nervous arcs and muscles involved, and indeed all the mutual interaction which grade and secure the nicety of adjustment exhibited in such perfection.

Plant-growth orientates itself in regard to the line of gravity, geotropism; and so in the rabbit, cat, and monkey, standing, walking, running with their element in common, the erect attitude, are shown by Magnus and de Kleyn to be, shortly said, refined geotropic reflexes. Any position other than the erect one excites in the reflex animal restoration of its erectness. The head, for instance, is righted by an act having its unconscious source in the pull and pressure of two microscopic stones in a special pair of tiny gravity

organs bedded in the skull With righting of the head goes rotation of the eyeballs in the opposite sense, keeping the vertical meridian of each retina in correspondence with the actual vertical Appropriate reflexes bring the whole animal from any other position into the symmetrical right-side-up one. The well-known manœuvre which enables the cat, when inverted and falling from a short height, to right itself in the air during its fall, alighting squarely on its feet, is shown by Magnus and his colleagues to be executed perfectly by reflex action, after removal of the entire higher brain Detailed analysis proves this whole reaction to be a chain of reflexes again essentially geotropic

Following these researches we see, therefore, that it is less true to say that the higher animal under direction of its mind keeps itself right side up, than to say that the animal body by automatic mechanism is kept right side up From the animal's point of view, as a sentient being, for it to be right side up to the world is, of course, for the world to be right side up to it In other words, the body's automatism ensures that the mind looking, so to speak, out from the body, finds the world right-side-up By the Utrecht researches that relation is shown to be maintained by processes seemingly as non-mental as is digestive secretion of the bile Hence, this right-side-upness being settled without mind, and indeed prior to mind, and naive mind being, whatever else it is, utilitarian, the situation has not invited consideration from naive mind Mind has not needed, so to say, to think about a relation already established and given it from the outset Professor Magnus's researches enable us, therefore, to trace how, in the make-up of mind, right-side-upness of the world comes as an innate unargued datum, an immediate intuition, largely elusive of mental analysis, because there is wanting direct sense-experience of its origin and of its elemental processes, although confusion in mental space results when its elements conflict William James, with characteristic picturesqueness, wrote that our "pre-historic ancestors discovered the common-sense concepts," among them as he says "one-space" With that latter we may set "world right-side-upness", but as for dating its "discovery" to our prehistoric ancestors, it, as an immediate intuition, must date back not to the merely prehistoric but to the entirely prehuman.

We must now proceed to the presentation of the Medals. The Copley Medal is awarded to Sir Edward Sharpey-Schafer

Sir Edward Sharpey-Schafer's work, extending from 1874 to the present time, has illuminated many parts of physiology, and the field of microscopical anatomy

no less His earlier experimental researches dealt with the functions of the different parts of the brain, and with the anatomy of the paths of conduction in the central nervous system In 1894 he discovered, in conjunction with Dr George Oliver, the remarkable effects of intravenous injection of extract of the adrenal gland, tracing their source to the small medullary portion of the gland, and furnishing in regard to the mode of production of the effects an outline analysis which has since then undergone extension rather than revision This research proved the starting point for a great volume of work, still fraught with consequences of extreme importance to physiology and medicine This work on the adrenal was followed by somewhat similar work on another ductless gland, the pituitary, which opened a modern chapter of physiological knowledge of that organ, again with important consequences to medicine In 1909 he gave the Croonian Lecture, on "Functions of the Pituitary Body"

Reverting to his researches in microscopical anatomy, they have been wide and numerous, ranging from demonstration of the nerve-net in the swimming-bell of *Medusæ* to the development of the cells of the blood, and the intimate structure of muscle-fibres

All this large volume of original work, produced unremittingly through many years, and containing outstanding discoveries in regard to what, following his own term, is now known as Endocrinology, has constituted a great and singularly fertile advance in natural knowledge

The Rumford Medal is awarded to Mr. Charles Vernon Boys

Mr Vernon Boys has advanced physical science by producing apparatus for accurate physical measurements and by making measurements of a high order of accuracy He is known for his exceptional constructive ability, and for his insight into the adherent difficulties of a problem and the details requiring special attention if accurate determinations are to be obtained He invented the first method for producing quartz fibres and investigated their elastic properties, he showed that they were practically free from fatigue, and demonstrated how admirably suited they were for the measurement of very small forces He measured the extremely minute forces due to the mutual attraction of small masses, and he made a torsion balance of beautiful design for measuring the Constant of Gravitation The value he arrived at for that constant greatly surpassed in accuracy all previous results He invented a radio-micrometer consisting of a single thermo-junction combined with a single loop of silver wire suspended by a fine quartz fibre, and with this he made

measurements of the radiation received from the moon and the stars. He took the first photographs of a bullet in flight and studied the wave disturbances produced by them. He has made a series of researches on soap bubbles and films. Recently he has developed a gas calorimeter which is the standard instrument prescribed by the gas referees for ascertaining the calorific value of the gas supplies of towns, work of special appeal in regard to a medal commemorative of Count Rumford.

A Royal Medal is awarded to Sir Dugald Clerk.

In 1882, when the internal-combustion engine was as yet hardly more than a scientific toy, Sir Dugald Clerk furnished an important contribution to the theory of the gas engine. Four years later he described his experiments on the explosion of gaseous mixtures, providing data fundamental for the scientific development of internal-combustion engines. Valuable papers dealing with the specific heat of gases and with the experimental determination of the variation of the specific heat at high temperature appeared from him in 1896 and 1906. As Chairman of the British Association Committee for investigation of gaseous explosions, he drew together workers concerned with the thermodynamics of internal-combustion engines, and, up to and into the period of the war, experiments carried out by members of his Committee contributed results of high importance. Sir Dugald Clerk himself investigated the effect of turbulence in a gas-engine cylinder, and was successful in explaining the difference between the rate of combustion of the charge fired in a gas-engine cylinder in ordinary conditions of working and the rate of combustion of the charge fired in a bomb. That to-day the internal-combustion engine is taking the place of steam power in smaller ships and in workshops as a prime mover of moderate power, and that to-day that engine renders possible the motor-car, the aeroplane and the submarine, is due largely to the scientific work of Sir Dugald Clerk. Investigations and advances still in progress at the present time may be regarded as in many respects the continuation of his experiments and his discoveries.

A Royal Medal is awarded to Dr Henry Hallett Dale.

The high value and importance of Dr Dale's researches is illustrated by that series of them whose starting point was an inquiry into the action of Ergot. Working with successive collaborators, he showed that histamine, an amine derived from Ergot by decarboxylation of amino-acids, produces a condition resembling wound shock and toxæmic collapse. By analytic experiments he succeeded in establishing that histamine, while causing spasm of arterial and

visceral muscle, conversely paralyses the active contraction of the capillary blood vessels, and this analysis was reached at a time when the property of contractility of those vessels had not been generally recognized. He showed that their paralysis is the dominant feature in the shock and is responsible for a virtual break-down of the whole blood circulation. The contractility of the capillary wall was thus revealed as a prime factor in the local regulation of blood supply, and as essential to the very mechanics of the circulation. He has shown further that in histamine "shock" we have a paradigm for the shock effect of a large class of protein poisons, and also for the grave condition known in medicine as secondary surgical shock, toxæmic collapse, and anaphylactic shock. The work has thus furnished a fresh key both for study of the normal circulation and also for the problem of a baffling pathological condition. In regard to anaphylaxis and immunity he has further been able to give final proof that the anaphylactic response is due to a fixation of antigen, not, as had been supposed, in the blood or other tissue fluids, but within the cells themselves.

He has done much other work as well, and, as Director of the Department of Biochemistry and Pharmacology under the Medical Research Council, has contributed public service of great value in regard to applied problems, including the biological testing of salvarsan and the development of methods for the production and standardization of insulin.

The Davy Medal is awarded to Professor Arthur George Perkin.

Professor Perkin is distinguished for his researches on the natural organic colouring matters—a branch of organic chemistry which he has made his own, and enriched by numerous papers, published for the most part in the *Journal of the Chemical Society*, during the past thirty years.

During the course of his researches on Luteolin, Morin, Apigenin, Quercitrin and other Flavone compounds, he discovered and investigated certain derivatives which such dyestuffs form with acids—substances which he was able to employ as means for determining the molecular weights of these colouring matters. He has also carried out important investigations into the structures of the glucosides, tannins, catechin and similar compounds closely related to the natural colouring matters.

His classical researches on natural indigo have left few questions unanswered as regards the chemical constitution and behaviour of this important product, and he was the first to show that one of the constituents—indirubin—played no part during the process of vat dyeing with this agent. He was also the

first to prepare in large quantity crystalline Indican—the essential glucoside of natural indigo—and to study its properties.

More recently he has investigated other natural products, notably the colouring matter of cotton flowers, and has dealt with the formation and structure of the important vat-dyes derived from Benzanthrone.

The Darwin Medal is awarded to Professor Thomas Hunt Morgan

Prof Morgan, of Columbia University, New York, is an illustrious Zoologist. Since 1888 he has, with untiring industry and enthusiasm, given research to the theory of organic evolution. Among the earlier of his researches were those on the structure and development of invertebrates and of the frog, and his investigations on regeneration. His studies on polarity, on fertilization, and later on gynandromorphism and sex determination, mark distinct advances in knowledge. The discovery of two kinds of spermatozoa in phylloxera and observations on chromosomes in these and other insects helped to elucidate the nature of the determination of sex in parthenogenesis. Of late years Prof Morgan has devoted himself to the study of heredity in various animals, and especially in the fly, *Drosophila*. The results obtained by him and his collaborators have thrown light on the relation of the factors of heredity to the chromosomes, on sex-linked and sex-limited characters, and other difficult problems in heredity. Indeed, these researches mark an advance in the science of heredity with which the name of T. H. Morgan will always remain associated.

On the Total Reflexion of Light.

By SIR ARTHUR SCHUSTER, For Sec R S

(Received October 21, 1924)

1 The theory of so-called total reflexion deserves greater attention than it has hitherto received, and this applies more particularly to the oscillating disturbance which penetrates into the optically lighter medium at or beyond the critical angle. In the generally accepted equations, this disturbance appears as a progressive wave propagated parallel to the interface, and it is not clear how this wave is connected with the incident light from which it must ultimately derive its energy. This uncertainty arises from the primary assumption of the theory, that the incident wave as well as the refracting surface have infinite extension. If we remove this restriction we are compelled to use approximate methods, but the investigation leads to results which are sufficiently definite to indicate the limits within which the present theory applies. We shall, further, be led to the conclusion, that at any rate with finite surfaces, total reflexion, in the strict sense of the word, cannot be obtained.

2 In what follows the surface separating the two media is represented by $x = 0$, and the incident plane wave by

$$\zeta = \cos (nt - my) \quad (1)$$

Under these circumstances the hitherto recognized equation for the light vector in the second medium, when total reflexion has set in, has the form

$$\zeta = A_2^{-a_1} (\cos nt - my) \quad (2)$$

At the critical angle where total reflexion begins, $a_1 = 0$, and if the electric force is at right angles to the plane of incidence, $A = 2$. Hence, while all the energy of the light is supposed to be reflected, a wave of indefinite width traverses the medium, in which there should be no light with an amplitude twice as great as that of the incident light. It will be noticed that the disturbance extends in the x direction to infinity without diminution of intensity.

The electric vector in the first medium, taking account of the reflected wave, is

$$\zeta = 2 \cos ax \cos (nt - my)$$

This represents what the late Lord Rayleigh called a corrugated wave. In both media the waves are propagated in parallel directions and with the same velocity. By Poynting's theorem the energy transmitted through unit surface

is equal to the product of the electric and magnetic forces divided by 4π , when these are—as in the present case—at right angles to each other. The x component of the magnetic force is equal to the time integral of $-\frac{d\zeta}{dy}$, when the electric force is confined to the z direction.

An easy calculation shows that, omitting the divisor 4π , the average transmission of energy in the y direction at a distance x is $(2m \cos^2 \alpha x)/n$ in the first medium, and $2m/n$ in the second, the value of m and n being the same in both cases

Let us be clear what this means. A beam of light falls on a refracting surface

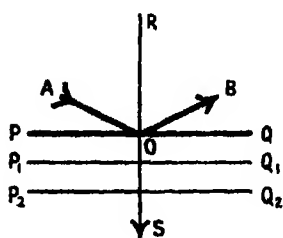


FIG 1

at the critical angle and is totally reflected (fig 1). The condition of the problem, correctly applied in its solution, secures that no energy should traverse the refracting surface PQ, and yet we find as a result of the mathematical analysis an unlimited flow of energy parallel to PQ in the second medium, twice as much energy per unit surface passing through OR as through OS. The apparent paradox implied in the conclusion will be cleared up in due course

(see Art 4). It is introduced here as an example of the difficulties into which we are led by the assumption of infinitely extended surfaces.

3 My own interpretation of the light which appears in the less dense medium beyond the critical angle is, that it is to be regarded as the remnant of the diffraction band left behind by the last ray (in the sense of Geometrical Optics), when that ray has ceased to be capable of penetrating from one medium to the other. If I am right, it is clear that the edges of the incident beam are the essential factors of the problem, and cannot be left out of account, however wide the beam may be.

Starting with incident waves which are still refracted in the normal manner, let LM (fig 2) represent the refracting surface, which may be supposed to be limited by two screens LL_1 and MM_1 . Without troubling about the incident beam, we may say that at all points on NM at right angles to the refracted beam the phases are equal. The phase at a point K of the refracting surface is determined by the optical length of the line KK_1 drawn at right angles to NM. The optical length from MN to any selected point P is $KP + KK_1$. The angle between KK_1 and KM is small, and an error of the second order only is introduced by measuring optical lengths along a path differing from the

actual one by a small quantity of the first order. Hence we may replace KK_1 by KQ . This simplification gives us a clear picture of the effects to be expected

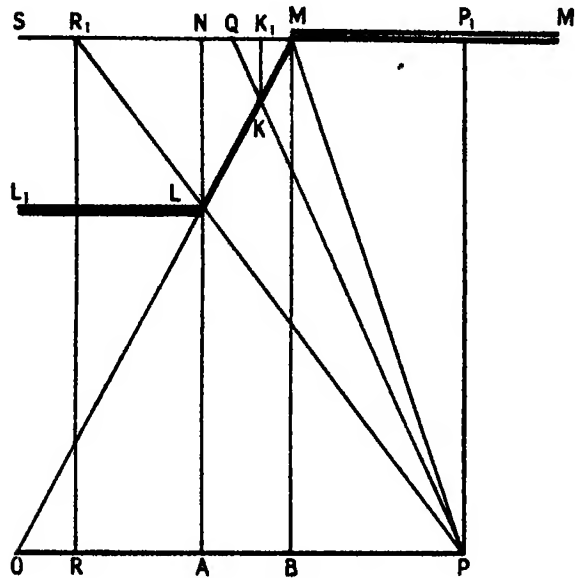


Fig 2

when the incident light approaches and ultimately passes the critical angle, and we shall further justify it by showing, that the amplitude and phase at the refracting surface can be made to agree with the known conditions by a suitable adjustment of the amplitude of the incident light

For analytical purposes the refracting surface may now be removed, and the illumination at any point P calculated, by finding the amplitude due to a plane wave-front modified by two screens LL_1 and MM_1 . If P lies between A and B we get the effects of the opening MN increased by the additional light, which may reach P from that part of the wave which is to the left of N. The light between O and A may be said to be due to diffraction from NM, modified by the obscuring effect of the screen LL_1 . We approach total reflexion if we move the point O to the right, L being stationary. M will therefore move towards N, and AB, which represents the part of the field that can be reached by the regularly-refracted light, gradually contracts. To the left of A the diffraction bands will gradually be obscured by LL_1 . The problem of refraction is, therefore, reduced to that of diffraction at an obliquely-placed rectangular aperture.

We proceed to calculate the amplitude at P by Fresnel's method

s from P_1 , along the wave-front, the effect of the strip represented by the linear element ds is, as regards amplitude, known* to be $(p\lambda)^{-\frac{1}{2}} ds$. As regards phase we have to shorten p by one-eighth part of a wave-length. If $\cos nt$ represents the light vector at the wave-front, the strip ds will contribute an amount

$$(p\lambda)^{-\frac{1}{2}} ds \cos [nt - m(p + \delta) + \epsilon]$$

to the light vector at P . In this expression ϵ stands for 45° and m for $(2\pi)/\lambda$, while $p + \delta$ is the distance from P to ds . The electric vector at P therefore becomes

$$(p\lambda)^{-\frac{1}{2}} \left\{ \cos (nt - mp + \epsilon) \int_{s_0}^{s_1} \cos m\delta \, ds + \sin (nt - mp + \epsilon) \int_{s_0}^{s_1} \sin m\delta \, ds \right\} \quad (3)$$

The next step is to express δ and the limits of integration in terms of s , changing the variable to that usually associated with Fresnel's integrals.

If Q (fig. 2) be any point on the wave-front at which s is required, and we write r for the radius vector PQ , we have

$$(r - p)(r + p) = s^2,$$

and hence, if s be small compared with p

$$\delta = (r - p) = s^2/2p$$

Denoting by x_1, x_2, x_0 , the distances from O to A, B, P , respectively, we find for the lower limit of the integrals $s_1 = x_0 - x_2$, and for the upper limit $s_2 = P_1R_1 = (x_0 - x_1)p/q$. To change to Fresnel's variable we must write

$$s = (\pi pm^{-1})^{\frac{1}{2}} v$$

so that $m\delta$ becomes $\frac{1}{2}\pi v^2$, and the limits of integration become

$$v_1 = (x_0 - x_2) \sqrt{\frac{m}{\pi p}} = (x_0 - x_2) \sqrt{\frac{2}{p\lambda}} \quad (4)$$

$$v_2 = (x_0 - x_1) q^{-1} \sqrt{\frac{2p}{\lambda}} \quad (5)$$

4 We shall confine the investigation to the case of incipient total reflexion. The diagram of fig. 2 then simplifies to that of fig. 3, the refracting surface being coincident with the refracted ray, when it is at the point of extinction.†

* Schuster, 'Phil Mag,' vol 31, p 77 (1891)

† The diffraction effect of light near the critical angle has been treated already experimentally and theoretically, in another method, by B. N. Chakravarty, 'Roy. Soc. Proc.' A, vol 99, p 503 (1921).

In order to establish complete correspondence of the problem of the shadow of a screen with that of the light transmitted at incipient total reflexion, regard must be had to the amplitude which we assign to the incident light. This may be determined by the condition that the amplitude at the edge of the shadow in one case must agree with that at the refracting surface in the other. With unit amplitude of the incident light in both cases, that at the edge of the shadow would be one half, and that at the refracting surface 2. If we assign, therefore, an amplitude 4 to the incident light in the problem of the shadow, our results will be applicable to the problem of total reflexion. We see by (4) and (5)

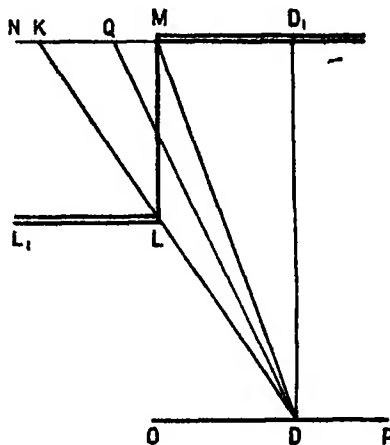


FIG 3

that v_1 diminishes and v_2 increases with p . For a given value of q the lower limit approaches zero, and the upper limit becomes infinitely large when p is infinitely great. With these limits (3), replacing p by y , becomes

$$\zeta = \sqrt{\frac{1}{2}} \left\{ \cos (nt - my + \epsilon) \int_0^{\infty} \cos \frac{1}{2} \pi v^2 dv + \sin (nt - my + \epsilon) \int_0^{\infty} \sin \frac{1}{2} \pi v^2 dv \right\}. \quad (6)$$

Both integrals are now equal to $\frac{1}{2}$, and remembering that $\cos \epsilon$ and $\sin \epsilon$ are both equal to $\sqrt{\frac{1}{2}}$, the light vector after applying, as explained above, the factor 4 reduces to

$$\zeta = 2 \cos (nt - my) \quad (6A)$$

This is the same equation as that obtained by the current theory, but we are now able to give the reason why it fails to be a correct solution of our problem. In the case of incipient total reflexion as illustrated in fig 3, x_1 and x_2 are both zero and x_0 is equal to x . The zero value of the lower limit of integration implies that x is infinitely small compared with $\sqrt{p\lambda}$. Although it is true that for any given value of x we may make p sufficiently large to reduce the lower limit below any assigned value, what we really want to know is the change of intensity along x for a given value of p . That is how the question would present itself in any actual

case If that be so, the lower limit becomes appreciable already for small distances of x , and for all values of p that have any experimental importance Even with a refracting surface 1 metre long $\sqrt{p\lambda}$ is less than a millimetre, and the equations derived from the theory which assumes p to be infinitely large are only applicable when x is small compared with that value If we further consider that the effective width of the transmitted beam increases as the square root of the length of the refracting surface, while that of the incident light increases as the length, we shall understand how the apparent paradox of paragraph 2 has arisen

We return to equation (3) As we shall only deal with intensities, the phase angle ϵ is immaterial and may be omitted The electric vector now becomes :

$$\sqrt{2}\zeta = \cos(n\epsilon - my) \int_{v_1}^{\infty} \cos \frac{\pi}{2} v^2 dv + \sin(n\epsilon - my) \int_{v_1}^{\infty} \sin \frac{\pi}{2} v^2 dv$$

where

$$v = x \sqrt{2/\lambda y} = x \sqrt{m/\pi y}$$

With the usual notation

$$C = \int_0^v \cos \frac{\pi}{2} v^2 dv, \quad S = \int_0^v \sin \frac{\pi}{2} v^2 dv,$$

the equation becomes

$$\sqrt{2}\zeta = (\frac{1}{2} - C) \cos(n\epsilon - my) + (\frac{1}{2} - S) \sin(n\epsilon - my) \quad (7)$$

Apart from the numerical factor, this is Fresnel's well-known expression, but it was necessary to go over otherwise well-known ground in order to secure numerical accuracy The square of the amplitude is

$$\frac{1}{2} [(\frac{1}{2} - C)^2 + (\frac{1}{2} - S)^2]$$

At the edge of the geometrical shadow, where C and S are zero, the intensity is one quarter that of the incident light, and not one half as given by Fresnel and others The variables x and y only enter into the result in the combination y^2/x , so that $y^2 = Ax$ is the equation to the curves for which the intensity has the same value

5 We are now in a position to determine the flow of energy in a field in which the electric vector is that represented by (7) It is convenient to apply Poynting's theorem The magnetic components α and β are determined by the well-known relations, which in the case that the electric force is parallel to the axis of ζ reduce to .

$$-\frac{d\alpha}{dt} = \frac{d\zeta}{dy}, \quad \frac{d\beta}{dt} = \frac{d\zeta}{dx},$$

t being the time.

What is required, however, is not the absolute value of the transmitted energy but its relation to that of the incident light, a measure of which is conveniently given by the square of the amplitude. In a simply-periodic wave Poynting's theorem gives, with a magnetic force H , the flow of energy as equal to $H\zeta/4\pi$, and H is equal to $c^{-1}\zeta$, where c is the velocity of light. Hence the average energy transmitted is $(8\pi c)^{-1}\zeta_0^2$, if ζ_0 is the amplitude of the original light which is here taken as being unity. In order to obtain the intensities in terms of that of the original light we shall omit the divisor 4π and divide the result by $2c$. We write (7) in the form.

$$\zeta = X \cos \omega + Y \sin \omega$$

and find

$$n\beta = \int \frac{d\zeta}{dx} dt = \frac{dX}{dx} \sin \omega - \frac{dY}{dx} \cos \omega.$$

Omitting periodic terms and replacing $\sin^2 \omega$ and $\cos^2 \omega$ by their average values we obtain for the transmitted energy, because $c = m^{-1}n$,

$$2c[\beta\zeta] = m^{-1} \left(Y \frac{dX}{dx} - X \frac{dY}{dx} \right) \quad (7A)$$

The square brackets on the left-hand side indicate the average value of $\beta\zeta$.

To save repetition of numerical factors, we omit $\sqrt{2}$ in (7), providing that the final results for the transmitted energy are to be divided by 2 or multiplied by 8, according as we deal with the problem of the shadow of a plane or with that of total reflexion. The transmitted energy in the x direction is obtained by substituting the values of X and Y in (7a):

$$I_x = m^{-1} P \frac{dv}{dx}, \quad (8)$$

if

$$P = \left(\frac{1}{2} - S\right) \cos \frac{\pi}{2} v^2 - \left(\frac{1}{2} - C\right) \sin \frac{\pi}{2} v^2. \quad (9)$$

The flux in the y direction is calculated in the same manner, but additional terms are introduced because ω depends on y . We find

$$\begin{aligned} I_y &= -m^{-1} P \frac{dv}{dy} + (X^2 + Y^2) \\ &= m^{-1} P \frac{dv}{dy} + \left(\frac{1}{2} - C\right)^2 + \left(\frac{1}{2} - S\right)^2 \end{aligned} \quad (10)$$

The flux of energy may be divided into two parts, one of which is entirely in the direction of the axis of y and the other forms angles with the axes of x

and y , the tangents of which are respectively proportional to dv/dx and $-dv/dy$

If we write $f = (\sqrt{m/\pi y})$, so that $v = fx$, we obtain f and $fx/2y$ for the flux of energy in the x and y directions respectively. This leads to the relation $dy/dx = 2y/x$, which integrates to

$$2y^2 - x^2 = K^2$$

The hyperbolas, so defined, are therefore the lines along which the energy travels in this part of the flow. But the different components into which the flux may be divided have no independent existence and must be combined.

6 The main object of this communication is to elucidate the manner in which light traverses a refracting surface at the critical angle, when it is supposed to be totally reflected. For this purpose we must examine the flow of energy in the direction along which x is measured. This, according to (9), is $(m)^{-1} P \frac{dv}{dx}$. At the surface of separation x , v , C and S are all zero, and the expression defining P then gives its value as $\frac{1}{2}$. The flow of energy through the surface becomes

$$(2m)^{-1} \frac{dv}{dx} = (2m)^{-1} \sqrt{\frac{m}{\pi y}} = \frac{1}{2} \sqrt{\frac{\lambda}{2\pi^2 y}} \quad (11)$$

This is a small fraction when y is greater than a few wave-lengths, and becomes insignificant for values of y of the order of magnitude of a millimetre. The energy enters the field, therefore, mainly through a region closely adjoining that edge of the refracting surface which is first intersected by the incident wave-front. It is to be remarked, however, that though (11) diminishes with y , its integral with regard to y increases with that variable, and must be taken into account in all questions concerning the total flux. For the total flux between $y = 0$ and $y = p$, we find from (11) the value $\frac{1}{\pi} \sqrt{\frac{\lambda p}{2}}$. Any conclusions on this head are, however, subject to certain reservations, to which attention is drawn in Art. 7.

If we investigate the flow of energy at distances large compared with the wave-length, it is found that I_0 and the first term of I_1 are small, and the flow is confined to the y direction. This seems surprising in view of the circumstance that on increasing the distance of the plane at which the light is received, the refracted light spreads out laterally. We should expect the lines of the flow to be along the parabolas of constant v , which determine the intensities. But the angles which the tangents to these parabolas form with the axis of

x are determined by dy/dx , which is equal to $2y/x$, so that the tangents are sensibly coincident with the axis of y because the light is appreciable only in the region where x is small

7 When the incident wave falls on the refracting surface beyond the critical angle, the method we have pursued fails, because there is now no wave-front, such as MS (fig. 2), at which the phases are equal and from which the optical lengths can be measured. We are, however, now in a position to extend the previous result so as to include the more general case

Disregarding diffraction, the equations, which I believe were first obtained by Stokes, for the disturbance beyond the critical angle, may be written in the form

$$\zeta = Re^{-a_1 x} \{ \cos \phi \cos (n - my) - \sin \phi \sin (n - my) \} \quad (12)$$

where R , ϕ and a_1 depend on the angle of incidence, a_1 being zero at incipient total reflexion. The solution of our problem, taking account of diffraction, must satisfy the continuity of the vector at the plane $x = 0$, and be subject to the condition that $d\zeta/dx$ for $x = 0$ is sensibly zero except close to the diffracting edge. There must also be identity with the previous results at the critical angle

With regard to the strict validity of the results obtained, two reservations have to be made. In the first place the present theory of diffraction assumes that the wave motion at the diffracting edge is not altered by the introduction of the opaque object which gives rise to the diffraction. In other words, the surface conditions at the edge of the shadow-throwing object are disregarded. But, as the late Lord Rayleigh remarks,* "except perhaps in the case of very fine gratings it is probable that the error thus caused is insignificant, for the incorrect estimation of the secondary waves will be limited to distances of a few wave-lengths only from the boundary of opaque and transparent parts."

Lord Rayleigh† himself tried to remove the objection in the case of slits, formed by narrow openings in infinitely thin and perfectly conducting sheets. While it is to be admitted that the significant part of the present investigation depends, apparently, on what is happening near the edge of the refracting body, it can be urged in answer that the error introduced could only slightly affect the main conclusion, because the total amount of light dissipated into space can be calculated from the effects observed at a distance. The light that enters the second medium may do so in a slightly different manner from that

* 'Scientific Papers,' vol. 3, p. 79.

† 'Scientific Papers,' vol. 4, p. 283, vol. 6, p. 160.

which the formulæ indicate, but its integral amount should be right within narrow limits

The second reservation concerns the division into Fresnel zones, consisting of narrow rectangular laminae. The law connecting the amplitude at a given point with the distance of that point from the lamina is not determined by strictly dynamical principles, but by the condition that the effect for the entire wave-front should be correct at small, as well as at large, distances. The answer to any objection raised on this ground would be, that the present theory claims no greater accuracy than that obtained in the corresponding problem of the diffraction at the edge of a shadow, which is universally accepted as substantially correct.

8 It is of interest to calculate the total energy dissipated into space when regular refraction ceases. At incipient total reflexion this mainly depends on the integral

$$\int_0^{\infty} (\frac{1}{2} - C)^2 + (\frac{1}{2} - S)^2 dx = \sqrt{\frac{p\lambda}{2}} \int_0^{\infty} (\frac{1}{2} - C)^2 + (\frac{1}{2} - S)^2 dv \quad (13)$$

We shall replace C and S by the variable P , defined by (9) and first introduced by Cauchy, together with another associated function —

$$Q = (\frac{1}{2} - C) \cos \frac{\pi}{2} v^2 + (\frac{1}{2} - S) \sin \frac{\pi}{2} v^2. \quad (14)$$

P and Q are connected by the relations —

$$\frac{dP}{dv} = -4\pi Q, \quad \frac{dQ}{dv} = \pi v P - 1,$$

from which it follows that

$$P^2 + Q^2 = -2 \int Q dv \quad (15)$$

The constant of integration is determined by the circumstance that

$$P^2 + Q^2 = (\frac{1}{2} - C)^2 + (\frac{1}{2} - S)^2$$

is zero when v is infinitely large. We may consequently fix the lower and higher limits as being infinity and v respectively. The total energy then becomes, for the region between $v = v_1$ and $v = \infty$,

$$\frac{1}{2} \sqrt{\frac{2}{p\lambda}} J = \int_{v_1}^{\infty} (P^2 + Q^2) dv = -2 \int_{v_1}^{\infty} \int_{\infty}^v Q dv dv$$

The numerical factor has here been introduced in accordance with the explanation given in Art. 4. Q can be expressed in terms of series proceeding by powers of v^{-1} and rapidly converging, if v exceeds values greater than 2.

Excluding powers of v^{-1} greater than 10, we have

$$Q = \frac{1}{\pi^2 v^8} - \frac{15}{\pi^2 v^9},$$

and the integration leads to

$$\int_{\infty}^v (P^2 + Q^2) dv = \frac{1}{\pi^2 v} \left(1 - \frac{1}{\pi^2 v^8} \right)$$

Q can also be expressed in a series proceeding by powers of v , but this converges very slowly when v approaches unity and is useless for our present purpose.

In default of any other available method, I have had recourse to arithmetical quadrature between $v = 0$ and $v = 2$, using for the purpose Fresnel's calculated Table for $P^2 + Q^2$. As a check, I have used both methods for the interval $v = 2$ to $v = 3$, and find that the direct quadrature and the formula lead respectively to the almost identical numbers 0.00167 and 0.00166. Dividing the whole interval between zero and infinity into two parts, I obtain for the integral between zero and two the value 0.2690, and between two and infinity 0.0503, giving for the total integral 0.3193. Hence, we have for the transmitted energy —

$$J = 2.554 \sqrt{\frac{p\lambda}{2}} \quad (16)$$

Here p stands for the distance between the refracting edge and the plane at which the energy is measured. That this distance enters into the result is due to the circumstance that although the greater part of the energy enters the field close to the edge M (fig. 3), there is a residual portion the integral of which along ML is not negligible. We are able to check our result by means of (11), the integral of which with respect to y determines the total transmitted energy. When the numerical factor is applied, this becomes

$$J_1 = \frac{8}{\pi} \sqrt{\frac{p\lambda}{2}} = 2.546 \sqrt{\frac{p\lambda}{2}}.$$

Considering the reservations that have been made, the agreement between J_1 , the energy entering the field, and J , which is the energy leaving it, is better than might have been anticipated.

The difference would disappear entirely, if it could be proved that

$$\int_0^{\infty} \left\{ \left(\frac{1}{2} - C \right)^2 + \left(\frac{1}{2} - S \right)^2 \right\} dv = \pi^{-1}.$$

We have taken no account of the first term of (10), and this requires justification. Its integral along the plane $y = p$ gives

$$\begin{aligned} J_1 &= -m^{-1} \int_0^x P \frac{dv}{dy} dx = 2 (mp)^{-1} \int_0^r P v dx \\ &= 2 (mp)^{-1} \sqrt{\frac{p\lambda}{2}} \int_0^r P v dv \end{aligned}$$

The factor varies as p^{-1} , so that however high the value of the integral may be, we can always choose a value of p sufficiently large to make it negligible.

We may now form an estimate of the light transmitted at the critical angle. If t denotes the length, measured in the plane of incidence, of the refracting surface, the width of the beams incident at the critical angle is $t\sqrt{1-\mu^{-2}}$, and this, in the units here employed, may be taken as the measure of energy falling on the surface. Taking p to be equal to t the transmitted light is $2.55\sqrt{t\lambda/2}$. The fractional loss of energy is, therefore,

$$2.55\mu\sqrt{\lambda/(\mu^2-1)2t}$$

With $\lambda = 5 \times 10^{-5}$ and $\mu = 1.5$ this becomes $0.00765\sqrt{5/t}$.

If the length of the refracting surface is 5 centimetres, the light entering the second medium amounts therefore to three-quarters per cent. of the incident light, while a length of one centimetre would increase the loss to 1.7 per cent. The energy entering the second medium must, of course, be taken away from the reflected beam, and we must draw the conclusion that the reflexion ceases to be total.

It is to be expected that the effect on the reflected beam would show itself mainly through the diffraction effects at the upper edge of the refracting surface. This may be illustrated if we alter the optical arrangement by placing the

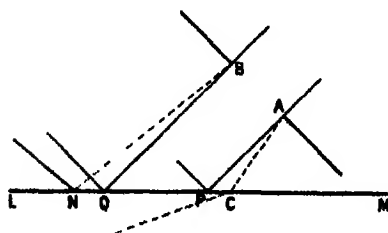


Fig. 4

aperture, which limits the beam of light, some distance away from the refracting surface. Let the incident wave pass through an aperture AB (fig. 4) and fall on the refracting surface LM at the critical angle. The optical disturbance will spread laterally by diffraction. Light passing in the direction AC , and falling on the surface at an

angle of incidence smaller than the critical angle, is able to penetrate by regular refraction. At the other edge, on the contrary, a ray such as BN

would be reflected more effectively than B Q, the angle of incidence exceeding that of total reflexion. The light that penetrates to the right of P Q diminishes the reflexion, which must then become smaller than that of the incident light.

9 The light reflected at a surface when the angle of incidence exceeds the critical angle has been studied by Fresnel and others, with special regard to its change of phase. Fresnel's treatment is based on an inspired guess, and Lord Kelvin, in his 'Baltimore Lectures' (p. 400), draws forcible attention to an error in his results, which was copied by nearly everybody who followed in Fresnel's footsteps. In consequence, wrong conclusions were arrived at as to which of the two principal components is retarded with respect to the other. This is a matter of some importance, because the relative retardation determines the direction of rotation in the elliptically polarized reflected light, and, therefore, can be tested experimentally.

The source of the confusion, as Lord Kelvin points out, is to be found in the uncertain choice of the direction in which the luminous displacement is taken to be positive. Fresnel's expression for the amplitude of the reflected light in the two principal directions is

$$\frac{\sin(\theta_1 - \theta)}{\sin(\theta_1 + \theta)}, \quad \frac{\tan(\theta_1 - \theta)}{\tan(\theta_1 + \theta)},$$

and may be taken either with the plus or minus sign, provided we adopt the same alternative in both cases. This follows from the consideration that with a diminishing angle of incidence the two expressions must converge to the same value. If different signs are chosen, an error of two right angles in the phase of one of the components occurs, and it is regrettable that this mistake also vitiates the only publication which treats the problem from the point of view of the electro-magnetic theory of light.*

There is no difficulty when the light vector is at right angles to the plane of incidence, and the reader may be referred to the late Lord Rayleigh's article in the 'Encyclopædia Britannica'†. When the light vector is in the plane of incidence, the directions of the displacements, which are to be taken as positive in the incident, reflected, and refracted wave, are fixed relatively to each other by the condition that as the angle between the incident wave-front and the surface of separation diminishes the three directions must coincide.

For the electric vector in the first medium, we may write

$$e^i(-am + by + cz) + re^r(am + by + cz)$$

* Drude, 'Lehrbuch der Optik,' p. 277.

† 'Scientific Papers,' vol. 3, p. 184.

The vector in the second medium is

$$se^{i(a'u+by+ct)},$$

r and s are the amplitudes of the reflected and refracted beams, which it is our object to determine. The refraction takes place at the plane $x = 0$, and an alteration of phase will be indicated if r and s turn out to be complex. The equations hold at all angles, but, for an incidence greater than the critical angle, a' is imaginary and we shall then substitute $-ia_1$. Confining ourselves to the case of total reflexion, and writing α for a_1/a , we have

$$a = (2\pi \cos \theta)/\lambda, \quad a_1 = ia' = (2\pi \cos \theta_1)/\lambda_1, \\ \alpha = a_1/a = (\mu \cos \theta_1)/\cos \theta = (\tan^2 \theta - \mu^{-2} \sec^2 \theta)^{\frac{1}{2}}.$$

With proper attention to the choice of these positive directions*

$$(1 - r) \sin \theta_1 = s \sin \theta, \quad (1 + r) \cos \theta = s \cos \theta_1$$

Eliminating r we find

$$s = \frac{2\mu}{1 - \mu^2 \alpha^2}. \quad (17)$$

The first of the surface conditions then leads to

$$r = 1 - \mu^{-2}s = \frac{1 + \mu^2 \alpha^2}{1 - \mu^2 \alpha^2},$$

and this reduces to the normal form

$$r = - \frac{(1 - \mu^4 \alpha^2) + 2\mu^2 \alpha}{1 + \mu^4 \alpha^2}.$$

If we denote the phase angle by 2δ , so that $r = \cos 2\delta + i \sin 2\delta$, we find

$$\cos 2\delta = \frac{\mu^4 \alpha^2 - 1}{\mu^4 \alpha^2 + 1}; \quad \sin 2\delta = - \frac{2\mu^2 \alpha}{1 + \mu^4 \alpha^2}, \quad \tan \delta = \frac{1 - \cos 2\delta}{\sin 2\delta} = - \frac{1}{\mu^2 \alpha}.$$

Some care has to be taken in determining the quadrant in which 2δ lies, having regard to the fact that the tangent of an angle draws no distinction between that angle and another differing from it by two right angles. At incipient total reflexion, where α is zero, and hence $\cos 2\delta = -1$, the formula gives a change of phase of 180° . This agrees with the tangent formula applied to the critical angle, because the latter is always greater than the polarising angle at which a reversal of phase takes place. With increasing angle of incidence α increases and $\cos 2\delta$ becomes positive when $\mu^4 \alpha^2 = 1$. Ultimately, at grazing incidence, all difference in phase disappears. In view of $\sin \delta$ being always negative, we may interpret the result more conveniently as a

* Schuster and Nicholson, 'Optics,' p. 240.

retardation, which gradually diminishes from π at the critical angle to zero at grazing incidence.

When the electric vector is at right angles to the plane of incidence Lord Rayleigh, in the publication already quoted, finds for the reflected vector in our notation

$$r_1 = (1 + \alpha)/(1 - \alpha),$$

so that if $2\delta_1$ be now the phase vector,

$$\cos 2\delta_1 = \frac{1 - \alpha^2}{1 + \alpha^2}, \quad \sin 2\delta_1 = \frac{2\alpha}{(1 + \alpha^2)},$$

whence

$$\tan \delta_1 = \alpha$$

As a positive δ denotes an acceleration, the retardation of the vector, when the vibration is in the plane of incidence relative to that which holds when it is at right angles to that plane, is expressed by $2(\delta_1 - \delta)$, and may be determined from

$$\tan(\delta_1 - \delta) = \frac{(\tan \delta_1 - \tan \delta)}{1 + \tan \delta_1 \tan \delta} = \frac{1 + \mu^2 \alpha^2}{(\mu^2 - 1)\alpha}$$

Substituting the value of α this becomes

$$\tan(\delta_1 - \delta) = \cot \theta \sqrt{\{1 - \mu^{-2} \operatorname{cosec}^2 \theta\}}$$

Rayleigh, who adopted Fresnel's expression for δ , and Drude, who fell into the error pointed out by Lord Kelvin, give the reciprocal of this expression with reversed sign. This means that an error of 180° having been committed in the phase angle 2δ , the error in δ is a right angle, interchanging the tangent and cotangent with reversed sign, and confusing the issue as to which component is retarded relatively to the other.

It remains to determine the quantities R , ϕ and a_1 in equation (12). The exponential factor a_1 , as appears from the present investigation, is given by

$$a_1 = (2\pi \cos \theta_1)/\lambda_1 = \frac{2\pi}{\lambda_1} \sqrt{(\mu^2 \sin^2 \theta - 1)},$$

the wave-length λ_1 being measured in the lighter medium.

When the light vector is in the plane of incidence $R \cos \phi$ and $R \sin \phi$ are determined by the real and imaginary parts of s in (17), which gives

$$R = \frac{2\mu}{\sqrt{1 + \mu^4 \alpha^2}}, \quad \tan \phi = \mu^2 \alpha$$

The corresponding equations, for the case where the vibration is at right

angles to the plane of incidence, are obtained from Lord Rayleigh's article,

$$R_1 = \frac{2}{\sqrt{1 + \alpha^2}}, \quad \tan \phi_1 = \alpha$$

10 The results of the investigation may now be summed up as follows —

(a) The light which enters the optically rarer medium at or beyond the critical angle is an effect of diffraction originating near the boundary of the refracting surface

(b) The analytical conditions of the problem at incipient total reflexion are the same as those applying to the light which penetrates into the geometrical shadow of an opaque screen

(c) The diffracted light derives its energy from the incident beam, and must diminish the intensity of the reflected light

(d) It follows that there can be no total reflexion in the strict sense of the word

(e) The total energy dissipated into space by diffraction increases proportionally to the square root of the length of the refracting surface, measured in the plane of incidence

(f) The ratio of the energy dissipated by diffraction to the total energy of the incident light is inversely proportional to the square root of the length of the refracting surface, and therefore tends towards zero as the size of the refracting surface increases

(g) At the critical angle the light dissipated by diffraction amounts to about 1 per cent of the incident light, when the length of the refracting surface is 3 cms. The numerical value is subject to correction depending on the approximate nature of the investigation

I have not been able to find in the literature of the subject more than one passage in which the difficulties discussed in this communication are recognised. That passage is contained in Drude's '*Lehrbuch der Optik*,' where it is suggested that the light enters the second medium at the edge of one side and returns into the first medium at the other. The results of this paper support the first, and disprove the second, suggestion.

The Structure of the Spectrum of Ionised Nitrogen

By A FOWLER, F R S, Yarrow Research Professor of the Royal Society,
Imperial College, South Kensington

(Received November 10, 1924)

[PLATE 1]

Introductory

In accordance with recent developments in the analysis of spectra, it is to be expected that while the neutral atom of nitrogen (N I) will yield a spectrum derived from systems of terms of even multiplicity, the spectrum of ionised nitrogen (N II or N^+) will be constituted from terms of odd multiplicity. The spectrum of doubly-ionised nitrogen (N III or N^{++}) is similarly expected to be formed from terms of even multiplicity.

The probable existence of the three types of line spectra representing N I, N II and N III has already been pointed out,* but few details regarding the regularities in the respective spectra have hitherto been available. A spectrum which probably represents N I has been described by Stark and Hardtke,† but accurate measurements of the lines do not appear to have been made, Bowen and Millikan,‡ however, have attributed to N I two well-known pairs of lines in the Schumann region at $\lambda\lambda$ 1745.3, 1742.7, 1494.8 and 1492.8 implying even multiplicity of the terms involved.

While the present paper has been in preparation, Ruark and his colleagues§ have recognised one of the main groups of N II lines as a multiplet of the type known as $mp - np'$, or pp' , and have indicated two pairs of lines having the separation $\Delta\nu = 51.69$. Several lines in the extreme red have further been attributed to N II by Kiess,|| and have been classified as resulting from combinations of a triple p term with an s term, another triple p term, and with a five-fold d term, all of which belong to quintet systems. None of these quintet terms have yet been found to be involved in the structure of the spectrum from λ 6650 to λ 2200 which is discussed in the present paper, all the terms

* Fowler's 'Report on Series,' p. 165 (1922)

† 'Ann. d. Phys.,' vol. 56, p. 363 (1918)

‡ 'Physical Review,' vol. 24, p. 214 (1924)

§ 'Sci. Pap. Bur. Stand., Washington,' No. 490 (1924)

|| 'Science,' vol. 60, p. 249 (Sept., 1924)

so far discovered from groups of lines in this region belong to systems of singlets and triplets

The third spectrum is still under investigation, but there is no doubt that it includes a doublet system similar to those of elements of the third group.

The present communication gives particulars of the regularities which have been recognised in the second line spectrum of nitrogen. It is not yet possible to give the absolute values of the terms, but the relative values can be stated with considerable accuracy

Observational Data

The second line spectrum of nitrogen is well known from its occurrence, in company with lines of oxygen, in the spectrum of air which appears in the ordinary spark spectra of metals. For the present purpose, however, extensive observations have also been made of the spectrum of nitrogen in vacuum tubes, with the gas at various pressures and under varying conditions of electrical discharge. In this way it has been possible to separate the different classes of lines and to obtain most of the lines with sufficient sharpness to permit accurate determinations of wave-lengths. A few lines which are of importance for the analysis of the spectrum do not appear to have been previously recorded. The spectrum has been investigated over the range λ 6650 to λ 2200, but no regularities have yet been traced on the more refrangible side of λ 3000.

All the lines between λ 6650 and λ 3000 which have been classified are collected in Table I. The wave-lengths are on the international scale, and most of them have been obtained with adequate dispersion and resolving power. Numbers in brackets following the wave-lengths indicate intensities, and the wave-numbers have been corrected to vacuum in the usual way. Term combinations are shown in the final column.

Triplets and Multiplets

The analysis of a spectrum of the kind under consideration is greatly facilitated by the assignment of a value to one of the terms, even if it be entirely arbitrary. A rough approximation to the largest term of N II, however, may be obtained from astrophysical data. In a discussion of the spectra of stars from the point of view of the stages at which typical lines attain their maximum intensity, in conjunction with ionisation potentials already determined from the series of carbon, silicon and other elements, Miss C. H. Payne* has estimated the ionisation potential of N II as 24 volts. A similar value has

* 'Harvard Coll. Obs. Circular,' No. 256 (1924).

Table I—Classified Lines of N II.

λ , I A (mty)	ν	Combinations	λ , I A (mty)	ν	Combinations
5961 25 (0)	18770 36	$p_1 - d'_3$	*4643 106 (8)	21531 30	$p_1 - p'_3$
5952 57 (3)	18794 81	$p_1 - d'_3$	4630 551 (10)	21589 67	$p_1 - p'_1$
5941 90 (8)	18824 99	$p_1 - d'_1$	4621 405 (7)	21632 41	$p_2 - p'_3$
5940 42 (2)	18829 18	$p_3 - d'_3$	4613 884 (6)	21667 66	$p_2 - p'_3$
5931 96 (7)	18853 18	$p'_3 - d'_3$	4607 167 (7)	21699 26	$p_2 - p'_3$
5928 02 (4)	18864 37	$p'_3 - d'_3$	4601 490 (8)	21726 03	$p_2 - p'_1$
5767 47 (2)	17333 83	$P - d_2$	4236 99 (8n)	23595 04	$\Delta\nu = \Delta p^2_{23}$
5747 32 (3)	17394 60	$P - d_2$	4227 738 (3n)	23646 08	
5730 04 (0)	17445 23	$p_1 - d_3$	4043 54 (2n)	24723 84	$\Delta\nu = \Delta p^2_{21}$
5710 64 (5)	17506 33	$p_1 - d_3$	4035 060 (3n)	24775 62	
5686 20 (6)	17581 57	$p_2 - d_3$	3994 995 (10)	25024 27	$P - N$
5679 49 (10)	17602 31	$p_1 - d_1$	3955 851 (5)	25271 88	$p_2 - N$
5675 96 (6)	17613 30	$p_2 - d_3$			
5666 54 (8)	17642 57	$p_2 - d_1$	3856 07 (3)	25925 81	$p'_1 - p^2_3$
5495 89 (4)	18190 38	$\Delta\nu = \Delta p^2_{23}$	3855 08 (3)	25932 48	$p'_3 - p^2_3$
5480 29 (1)	18242 15		3847 38 (2)	25984 37	$p'_3 - p^2_3$
5073 55 (1)	19704 59	$P - s$	3842 20 (2)	26019 40	$p'_3 - p^2_1$
5045 02 (5)	19816 03	$p_1 - s$	3838 39 (4)	26045 23	$p'_1 - p^2_1$
5010 54 (4)	19952 39	$p_2 - s$	3829 80 (3)	26103 65	$p'_3 - p^2_1$
5002 06 (2)	19983 81	$p_3 - s$	3615 88 (1)	27647 94	$s - p^2_3$
4810 27 (2)	20783 07	$d_1 - d'_3$	3609 09 (2)	27699 93	$s - p^2_3$
4803 30 (6)	20813 22	$d_1 - d'_1$	3593 60 (3)	27819 34	$s - p^2_1$
4793 66 (2)	20855 06	$d_3 - d'_3$	3437 162 (6)	29085 46	$P - N^2$
4788 13 (5)	20879 18	$d_3 - d'_3$	3408 136 (3)	29333 17	$p_2 - N^2$
4781 21 (2)	20909 44	$d_2 - d'_1$	3331 32 (3)	30009 52	$d_2 - p^2_3$
4779 72 (4)	20915 91	$d_3 - d'_3$	3330 30 (2)	30018 70	$d_3 - p^2_3$
4774 24 (2)	20939 91	$d_3 - d'_2$	3328 79 (4)	30032 34	$d_1 - p^2_1$
4674 98 (2)	21384 50	$P - p'_3$	3324 58 (2)	30070.37	$d_3 - p^2_2$
4667 28 (2)	21419 78	$P - p'_3$	3318 14 (2)	30128 72	$d_3 - p^2_1$
4654 57 (2)	21478 27	$P - p'_1$	†30189 69		$d_3 - p^2_1$
			3006 86 (7)	33247 67	$P - D(?)$

* The wave-lengths from λ 4643 to λ 4035, with the exception of λ 4043 54, were determined by J S Clark ('Astrophys Jour,' vol 40, p 333 (1914))

† Calculated wave number

been deduced by R H Fowler and E A Milne * The present investigation indicates that the highest term is a p term, and adopting the usual relation,† the corresponding value of the term $1p$ is 194,000 The related term, $2p$, which is applicable to the region here considered would accordingly have a value of the order of 70,000, it being assumed that the series constant is $4R$ ($R = 109678.3$) The non-appearance of certain groups which might be expected to fall within the range of spectrum observed suggests that this

* 'Mon Not R.A.S.', vol 84, p 506 (1924)

† Fowler's 'Report,' p 69.

value for $2p$ may be too low, but it will at least serve the same purpose as a value chosen at random. It is to be understood that while the values assigned to the respective terms may be considerably in error, the differences of term values are correct within the limits of error of the observations.

For the schematic representation of the structure of the triplets and multiplets, it will suffice to quote the wave-numbers of the lines, the corresponding wave-lengths may be found by reference to Table I. Numbers in brackets following the wave-numbers indicate intensities, and differences of terms are printed in italics.

The assignment of inner quantum numbers (j) is in accordance with the work of Sommerfeld and Landé,* and has led to the identification of the types of terms involved in the various groups of lines. The selection rule in relation to these inner quantum numbers, it may be mentioned is that $\Delta j = \pm 1$ or 0, with the exception that the transition 0 to 0 does not ordinarily occur. It may eventually be found convenient to adopt the inner quantum numbers as suffixes in place of those in common use for the designation of members of multiple terms, but, for the present, it has been thought desirable to continue the use of the older nomenclature and to give the values of j separately.

For the sake of brevity, combinations such as $mp - np'$ are contracted to pp' , since sequences of terms have not yet clearly entered into the discussion.

One of the most striking groups of lines of N II is that about $\lambda 4630$ (No. 3, Plate 1), and it will be convenient to consider this first, because it has been very accurately measured by Clark and fixes the triplet character of some of the terms. The structure of the group may be shown as follows —

p'_3 (0)		p'_2 (1)		p'_1 (2)	j
		21531 30(8)	58 37	21589·67(10)	p_1 (2)
		<i>136 36</i>		<i>136 36</i>	
21632 41(7)	35 25	21667 66(6)	58 37	21726·03(8)	p_2 (1)
		<i>31 60</i>			
		21699 26(7)			p_3 (0)
$p_1 = 70000 \ 00^\dagger$, $p_2 = 70136 \ 36$, $p_3 = 70167 \ 96$					
$p'_1 = 48410 \ 33$, $p'_2 = 48468 \ 70$, $p'_3 = 48503 \ 95$					

This group is clearly of the pp' type, consisting of six lines, and the inner quantum numbers adapted to the group indicate that each set of terms belongs

* 'Zeit f. Phys.,' vol 15, p. 191 (1923)

† Assumed value

to a triplet system. If the p and p' terms belonged to quartet systems, all the values of j would be increased by unity and a seventh line, $p_3p'_3$ would be expected. The p terms involved in the above combinations are doubtless equivalent to the $2p$ terms of ordinary series, since the series constant must be $4R$, the $1p$ term must be much greater. The interval rule of Landé gives a ratio of 2:1 for the separations of triplet p terms, and it will be observed that this is far from being followed in N II, the rule probably also ceases to be applicable to other elements in the first row of the periodic table.

Attention may next be directed to a complex diffuse triplet which includes the strong lines in the yellow-green about $\lambda 5680$ (Nos 1 and 2, Plate 1). This may be represented as follows:

d_3 (1)		d_2 (2)		d_1 (3)		j
17445 23(0)	61 10	17506 33(6)	96 00	17602 33(10)	p_1	(2)
136 34		136 24				
17581 57(5)	61 00	17642 57(8)			p_2	(1)
11 73						
17613 30(6)	.				p_3	(0)

$d_1 = 52397.67, d_2 = 52493.73, d_3 = 52554.71$

The triplet character of the d terms is thus fully established by the values which have to be assigned to j in order to conform with the inner quantum selection rule. The appearance of this diffuse triplet differs very considerably from that of the more familiar triplets which occur in the spectra of elements of the second group, as will be seen from fig. 1.

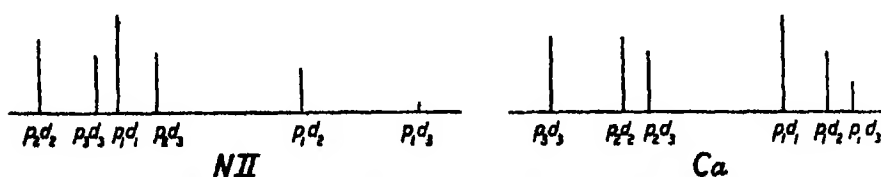


FIG. 1 —The diffuse triplet of N II near $\lambda 5680$, compared with a diffuse triplet of calcium

The apparent distortion obviously arises from the fact that in the N II group the differences between the d terms are much larger in comparison with those of the p terms than in the diffuse triplets of calcium and other elements of the second group.

The separations Δp_{12} and Δp_{23} occur also in connection with three lines

forming part of the well-known cluster of lines about $\lambda 5007$. The wave-numbers are —

p_1 (2)		p_2 (1)		p_3 (0)	j
19816 03(5)	136 36	19952 39(4)	31 42	19983 81(2)	s (1)
$s = 50184 \ 30$					

The associated term must clearly have $j = 1$, and may accordingly be a singlet P term, or an s term of a triplet system. The restrictions as to azimuthal quantum numbers, however, would ordinarily exclude P, and the term is therefore probably of the s type.

A multiplet of the triplet dd' type may be next conveniently considered. This is of 'skew-symmetrical' structure, consisting of three strong and four weaker lines and is shown as No. 3, Plate 1. The structure may be shown as below —

d'_3 (1)		d'_2 (2)		d'_1 (3)	j
		20783 07(2)	30 15	20813 22(6)	d_1 (3)
		96 11		96 22	
20855 06(2)	24 12	20879 18(5)	30 26	20909 44(2)	d_2 (2)
60 86		60 73			
20915 91(4)	24 00	20939 91(2)			d_3 (1)
$d'_1 = 31584 \ 37, d'_2 = 31614 \ 66, d'_3 = 31638 \ 75$					

The new d' terms thus introduced reappear in a $p'd'$ combination which forms a very characteristic group of lines in the orange, the brightest line being $\lambda 5941 \ 90$ (Nos. 1 and 2, Plate 1). The wave-numbers may be arranged as follows —

d'_3 (1)		d'_2 (2)		d'_1 (3)	j
16770 36(0)	24 45	16794 81(3)	30 18	16824 99(8)	p'_1 (2)
58 82		58 37			
16829 18(2)	24 00	16853 18(7)			p'_2 (1)
35 19					
16864 37(4)					p'_3 (0)

Like the pd group previously described, this group differs considerably in appearance from the more familiar diffuse triplets in the spectra of elements of the second group.

A further set of triplet terms of p type, designated p^2 for reasons given later, appears in a multiplet having its brightest member at λ 3838 (No 4, Plate 1) The new terms combine with the previously determined p' terms as shown below --

p^2_3 (0)		p^2_2 (1)		p^2_1 (2)	J
		25925 81(1)	119 42	26045 23(3)	p'_1 (2)
		58 56		58 42	
25932 48(2)	51 89	25981 37(1)	119 28	26103 65(3)	p'_2 (1)
		35 03			
		26019 40(1)			p'_3 (0)

$p^2_1 = 22365 \cdot 05$, $p^2_2 = 22484 \cdot 17$, $p^2_3 = 22536 \cdot 22$

The lines of this group are remarkable for the fact that all of them were broadened and displaced towards the red by about $0 \cdot 7\text{\AA}$ in a tube containing nitrogen at relatively high pressure. The wave-numbers quoted are from measurements on tubes at low pressures, where the lines were sharply defined.

The same phenomenon of a large displacement towards the red was observed in connection with an isolated triplet in the ultra-violet (Nos 4 and 5, Plate 1), in which the characteristic separations of the p^2 terms also appear, the wave-numbers are as follows

p^2_3 (0)		p^2_2 (1)		p^2_1 (2)	J
27647 94(1)	51 99	27699 93(2)	119 41	27819 34(3)	s (1)

The singlet term entering into this combination is the s term already deduced from sp .

The p^2 terms also enter into combination with the d terms to produce another diffuse triplet in the ultra-violet, beginning at λ 3331 (No 5, Plate 1). Thus,

d_3 (1)		d_2 (2)		d_1 (3)	J
[30189 69]	60 97	30128 72(2)	96 38	30032 34(4)	p^2_1 (2)
119 32		119 20			
30070·37(2)	60 85	30009·52(3)			p^2_2 (1)
51 66					
30018 71(2)					p^2_3 (0)

The line for which the calculated position is ν 30189 would be expected to be faint, and it is not shown on any of the photographs obtained. The members of this group, like the others in which the p^2 terms appear, show large displace-

ments towards the red when the pressure in the vacuum tubes is relatively high. The above wave-numbers have been deduced from wave-lengths measured in low-pressure tubes.

Singlets

A singlet term is indicated by the following pair of lines (Nos. 1 and 2, Plate 1) --

$$\begin{array}{rcccl}
 d_3 & & d_2 & & \\
 (1) & & (2) & & j \\
 17333 \cdot 83(2) & 60 \cdot 7 & 17394 \cdot 60(3) & P & (1) \\
 P = 69888 \cdot 51.
 \end{array}$$

A singlet P term is obviously the most appropriate for this combination, Pd_1 being then ruled out by consideration of inner quantum numbers. The P term, it will be observed, is only a trifle smaller than the p_1 term.

The P term appears also in combination with the p' terms, producing an inverted triplet which is clearly shown on the photographs (No. 3, Plate 1) although the lines are of no great intensity. Thus --

$$\begin{array}{rcccl}
 p'_3 & & p'_2 & & p'_1 \\
 (0) & & (1) & & (2) & j \\
 21384 \cdot 50(2) & 30 \cdot 25 & 21419 \cdot 78(2) & 55 \cdot 49 & 21478 \cdot 27(2) & P & (1)
 \end{array}$$

A faint line at $\lambda 5073 \cdot 5$ appears to represent the combination Ps , thus, $P-s = 19704 \cdot 21$ as compared with the observed wave-number $19704 \cdot 59(1)$.

The groups of lines so far described include a majority of the chief lines, and several of the fainter ones, in the region $\lambda 6650$ – $\lambda 3300$. There are, however, a number of lines which do not occur in groups and doubtless belong to a singlet system. Four of the more important lines, beginning with $\lambda 3995$, certainly involve two of the terms which have already been deduced. The associated terms are singlets of S type ($j = 0$). Thus --

$$\begin{array}{rcl}
 25024 \cdot 27(10) = P - S_1 & & \\
 25271 \cdot 88(5) = p_2 - S_1 & \left. \begin{array}{l} \\ \\ \end{array} \right\} & S = 44864 \cdot 36. \\
 29085 \cdot 46(6) = P - S^2 & & \\
 29333 \cdot 17(3) = p_2 - S^2 & \left. \begin{array}{l} \\ \\ \end{array} \right\} & S^2 = 40803 \cdot 12
 \end{array}$$

These combinations are in complete accordance with the azimuthal and inner quantum conditions. It does not seem possible, however, to regard S and S^2 as consecutive terms of a simple Rydberg sequence because there is no line corresponding with the next following term. The spectrum in this

region is, in fact, very simple, the only other prominent singlets in the region $\lambda 4000$ – $\lambda 3000$ being $\lambda 3919.003(6)$ and $\lambda 3006.86(7)$. The latter ($v=33247.67$) is possibly the PD line and we may write—

$$D^? = 69888.51 - 33247.67 - 36640.84$$

Other Regularities

Two pairs of lines with apparently equal separations have been noted by Ruark, and a similar pair has been found in the course of the present investigation. The wave-numbers and separations are as follows —

18190.37(3n)	51.75	18248.57(1n)
23595.04(4n)	51.64	23646.68(2n)
24723.84(2n)	51.78	24775.62(4n)

The separation suggests identity with Δp^2_{23} , but the connection is not clear.

The p' and d' terms

The significance of such terms as p' and d' is not yet completely understood, but evidence has been adduced in favour of the view that they involve the simultaneous transitions of two electrons with the emission of a single quantum of energy. Russell and Saunders* and Wentzel† have found that pp' multiplets of calcium form a series of approximately Rydberg type, and converge to a limit which is higher than that of the normal series of triplets, so that some of the terms become negative. This is regarded as an indication of the emission of a greater amount of energy in the pp' transitions than could be supplied by the series electron alone, and it may be supposed that the deficiency is made good by a transition of the second valence electron.

The terms p' , d' , &c., which are thus possibly associated with the simultaneous transitions of two electrons may be distinguished from corresponding terms of ordinary type by a further selection rule to which attention has been directed by Laporte in his discussion of the arc spectrum of iron‡. In the case of iron it would appear that in the combination of ordinary and “double-transition” terms, the usual selection rule for azimuthal quantum numbers ($\Delta k = \pm 1$)§ is to be replaced by the rule $\Delta k = 0$, while $\Delta k = \pm 1$ is

* ‘Science,’ vol. 59, p. 50 (1924).

† ‘Phys. Zeit.,’ vol. 25, p. 182 (1924).

‡ ‘Zeit. f. Phys.,’ vol. 23, p. 166 (1924), vol. 26, p. 17 (1924).

§ $k = 1$ for s , 2 for p , 3 for d , and so on.

forbidden. This rule is probably also applicable to the spectrum of N II as illustrated in fig 2, which is drawn on the plan adopted by Laporte

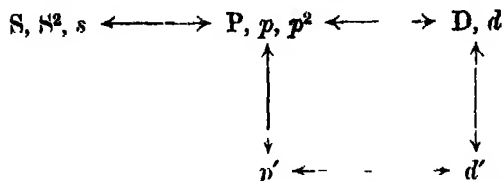


FIG 2 - -Illustrating combinations of ordinary and 'double transition' terms in N II

The combinations to be expected in accordance with the new rule, having due regard for the inner quantum number restrictions, are those indicated by arrows, it being further understood that terms which are placed in the same group do not combine with each other. All the combinations which have so far been recognised in N II are in accordance with the diagram but some of the possible combinations would yield lines outside the range of the present observations, so that their presence or absence cannot be checked. The combination pd' would fall in an observed region and definitely does not occur in N II.

The second p term behaves in combination like the first, and it has accordingly been temporarily designated p^2 in preference to p'' . The second S term has similarly been called S^2 . If p and p^2 were the consecutive terms $2p$ and $3p$ of an ordinary Rydberg sequence, $2p$ would have a value about 97,000, and the corresponding value of $1p$ would be of the order of 300,000, which is far above that suggested by astrophysical data. It seems probable that the terms do not conform closely with a Rydberg formula.

Combinations and Relative Term-values

The combinations which have been identified, and the relative values of the various terms, are collected in Table II. The combinations are stated in the order in which they have been described, and the terms are arranged in order of magnitude, p_1 being assumed as 70,000. Under k and j are the azimuthal and inner quantum numbers respectively.

It results from the foregoing investigation that the largest term is a p term, and from this it may be concluded that in the atom of N II the series electron normally occupies a 2_2 orbit. As expressed in the "spectroscopic displacement law," other investigations have shown that the spectrum of an ionised element is of the same character as that of the neutral atom of the element which immediately precedes it in the periodic table, and it follows that there is a close similarity in the arrangement of the electrons in the two atoms. The

Table II.—List of Combinations and Term-values

Combinations.	Relative Terms	
$p - p'$	h	j
$p - d$	2	$\left\{ \begin{array}{l} (0) \\ (1) \\ (2) \end{array} \right.$
$p - s$		$\left\{ \begin{array}{l} p_3 = 70167 \ 96 \\ p_2 = 70136 \ 36 \\ p_1 = 70000 \ 00 \end{array} \right.$
$d - d'$	2	(1) $P = 69888 \ 51$
$p' - d'$		$\left\{ \begin{array}{l} (1) \\ (2) \\ (3) \end{array} \right.$
$p' - p^2$	3	$\left\{ \begin{array}{l} d_3 = 52554 \ 74 \\ d_2 = 52493 \ 73 \\ d_1 = 52397 \ 67 \end{array} \right.$
$s - p^2$		
$d - p^2$	1	(1) $s = 50184 \ 30$
$P - d_{23}$		$\left\{ \begin{array}{l} (0) \\ (1) \\ (2) \end{array} \right.$
$P - p'$	2	$\left\{ \begin{array}{l} p'_3 = 48503 \ 95 \\ p'_2 = 48468 \ 70 \\ p'_1 = 48410 \ 33 \end{array} \right.$
$P - s$		
$P - S$	1	(0) $S = 44864 \ 36$
$p_2 - S$	1	(0) $S^2 = 40803 \ 12$
$P - S^2$	3	(2) $D^2 = 36640 \ 84$
$p_2 - S^2$		$\left\{ \begin{array}{l} (1) \\ (2) \\ (3) \end{array} \right.$
$P - D^2$	3	$\left\{ \begin{array}{l} d'_3 = 31638 \ 75 \\ d'_2 = 31614 \ 66 \\ d'_1 = 31584 \ 37 \end{array} \right.$
	2	$\left\{ \begin{array}{l} (0) \\ (1) \\ (2) \end{array} \right.$
		$\left\{ \begin{array}{l} p^2_3 = 22536 \ 22 \\ p^2_2 = 22484 \ 47 \\ p^2_1 = 22365 \ 05 \end{array} \right.$

conclusion with regard to ionised nitrogen is therefore of additional interest as giving an indication of the structure of the neutral atom of carbon, the spectrum of which has not yet been resolved into series. The first group of elements in

Bohr's table of atomic structures* may accordingly now be extended to carbon with considerable confidence. Thus, in the neutral atom of carbon it is probable that there are two electrons in 1_1 orbits, two in 2_1 and two in 2_2 orbits.

Summary

New observations of the second line spectrum of nitrogen (N II, or N^+) have been made in the region λ 6850– λ 2200, and 52 lines have been classified in relation to the terms which combine to produce them. In this region, all the terms which have been identified belong to singlet or triplet systems. These have been found to combine with each other in agreement with the selection rules applicable to other spectra in which p' and d' terms appear. The absolute values of the terms cannot yet be stated, but a value of 70,000 has been provisionally assigned to $2p$ in accordance with the value suggested for $1p$ by astrophysical data.

The largest term identified is a p term, and it may be inferred that the series electron in singly-ionised nitrogen normally occupies a 2_2 orbit, so that the atom of N II has two electrons in 1_1 orbits, two in 2_1 and two in 2_2 orbits. From the spectroscopic displacement law it may be further inferred that this is also the probable arrangement of orbits in the neutral atom of carbon, the spectrum of which has not yet been resolved into series.

Three groups of lines which involve one of the p terms are remarkable as showing large displacements ($> 0.5\text{\AA}$) to the red in vacuum tubes at relatively high pressures.

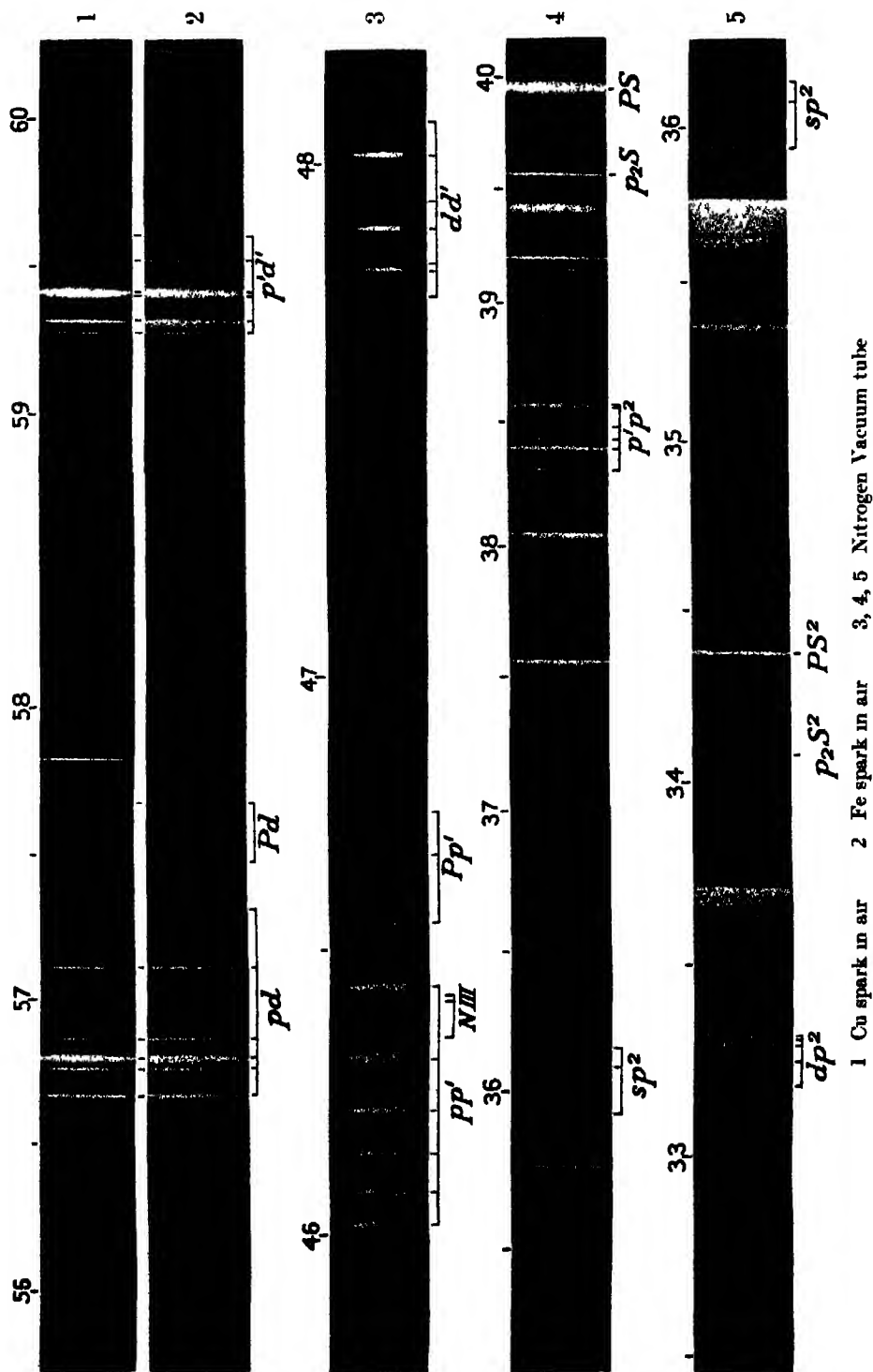
The author has pleasure in acknowledging his indebtedness to Mr. J. Brooksbank and Mr. L. J. Freeman for some of the photographs which have been utilised in the foregoing investigation.

DESCRIPTION OF PLATE 1.

- 1 Spark spectrum of copper in air
 - 2 Spark spectrum of iron in air
- } 10 feet concave grating.
- These show the groups $p'd'$, Pd , and pd
- 3 Nitrogen vacuum tube, large Lattrow prismatic spectrograph. Shows the combination groups dd' , Pp' , pp' . The short lines near the edges of the spectrum are arc lines of iron.
 4. Nitrogen vacuum tube, large quartz spectrograph. Shows the lines PS , p_2S , and the groups pp' and sp^2 . Lines of N III at $\lambda\lambda$ 4641.90, 4640.64, 4634.16 appear faintly.
 5. Nitrogen vacuum tube, large quartz spectrograph. Shows the lines PS^2 , p_2S^2 , and the groups sp^2 and dp^2 .

The bands of nitrogen which appear in 4 and 5 are mainly due to the use of an end-on tube, the bands originating in the wider part of the tube. The bright place on the red side of the strong line λ 3995 is the head of a band, λ 3998. There is also a faint band head at λ 3582 which might be mistaken for a line in the reproduction.

* 'Ann. d. Phys.,' vol. 71, p. 260 (1923)



Spheroidal Wave-Functions

By J. W. NICHOLSON, M.A., D.Sc., F.R.S., Fellow of Balliol College, Oxford

(Received August 5, 1924)

§ 1 *Introductory.*

The solution of problems relating to vibrations, in connection with spheroids—or, in two dimensions, elliptic cylinders—has hitherto only been attempted in one manner. If the vibrations have a time factor for their fundamental vector, of the form $e^{i\omega t}$, the equation of wave motion becomes, if ϕ is the fundamental vector,

$$(\nabla^2 + k^2) \phi = 0$$

where the wave-length is $2\pi/k$, and if C is the velocity of propagation of the wave in the external region, $k = p/c$. When oblate spheroidal co-ordinates are used, defined in terms of Cartesians by

$$x = a\sqrt{(1 + \mu^2)(1 + \zeta^2)} \cos \omega, \quad y = a\sqrt{(1 - \mu^2)(1 + \zeta^2)} \sin \omega, \quad z = a\mu\zeta,$$

this can be transformed, after the usual manner to

$$\frac{\partial}{\partial \mu} (1 - \mu^2) \frac{\partial \phi}{\partial \mu} + \frac{\partial}{\partial \zeta} (1 + \zeta^2) \frac{\partial \phi}{\partial \zeta} + k^2 a^2 (\mu^2 + \zeta^2) \phi = 0, \quad (1)$$

when there is symmetry round the axis of z .

This is a form which has been discussed by many writers, and notably by W. D. Niven.* The literature of the subject, in fact, goes back to Lamé and Mathieu, the latter of whom confined his attention to the similar equation arising in two-dimensional problems relating to an elliptic cylinder.

Such discussions as have been given appear to have proceeded invariably along the lines of a determination of solutions in the form

$$\phi = f_1(\zeta) f_2(\mu) f_3(\omega),$$

involving new types of normal functions $f_{1,n}(\zeta)$, $f_{2,n}(\mu)$, whose general term in an expansion in powers of ζ or μ cannot be expressed. These functions cannot, moreover, be expressed as definite integrals after the manner of Laplace's integral for the harmonic $P_n(\mu)$, and they are thus suited only to the solution of physical problems by approximate methods—in fact, their own values are only found by the method of continued approximation. No exact solution of a problem appears possible by their aid.

* 'Phil. Trans.,' A, p. 231 (1892).

We start with the hypothesis that a set of "normal" co-ordinates does not necessarily exist for a problem of wave motion with prescribed reflecting boundaries, and that, even if the set exists, it is not, of necessity, the main avenue to a solution. In other words, the solution of a problem of wave motion about a given boundary is not necessarily capable of expression in the form of a sum of solutions of the general equation of wave motion, each of which is the product of functions of one variable co-ordinate only. This will become clear in the ensuing discussion in which, in the first instance, we build up a solution of the general equation—whose general form can ultimately be found—which reduces to a prescribed form for infinite wave length, or, in fact, when the problem becomes one of electrostatics or hydrodynamics instead of a problem of waves propagated with a finite velocity.

It is convenient, in the present communication, to restrict our attention to one special case, as an illustration of a general method of procedure in passing from a solution of Laplace's equation satisfying certain boundary conditions to a solution of the equation of wave motion which satisfies the same conditions. When this is solved, we find a means of approach to a class of solutions of problems of oblate spheroids and discs, which has not hitherto been noticed. While it is not our present object to solve particular physical problems, which are reserved for a later communication, some of these are referred to in illustration of the capacity of the analysis to deal with them. Our fundamental object at present is the mathematical development of this type of analysis.

For this object we shall generalise the solution of Laplace's equation which represents the motion of an oblate spheroid through a liquid, along its axis of figure. There is a certain analogy between our method and that of Parseval,* who, by continued approximation, derived the solution of Laplace's equation in three dimensions from that in two dimensions. The analogy is derived from the fact that the equation of wave motion is essentially that of Laplace with one more dimension.

A General Solution of the Equation of Wave Motion

When a problem is symmetrical round the axis of z , the angle ω is not relevant, and a function ϕ defining a vibration satisfies

$$\frac{\partial}{\partial \zeta} (1 + \zeta^2) \frac{\partial \phi}{\partial \zeta} + \frac{\partial}{\partial \mu} (1 - \mu^2) \frac{\partial \phi}{\partial \mu} + k^2 a^2 (\mu^2 + \zeta^2) \phi = 0$$

Here $\zeta = \text{const}$ defines an oblate spheroid, $\zeta = 0$ being the circular disc

* 'Mémoires de Divers Savants,' vol I, p 379 (1805)

$z = 0$, $\rho = 0$ to a , in cylindrical co-ordinates, $\mu = 0$ defines the whole plane $z = 0$ with the disc cut out, and, more generally, $\mu = \text{const}$ defines a hyperboloid

When an oblate spheroid moves along the axis of z —its axis of figure—it creates a velocity potential, in surrounding infinite liquid, of the form

$$\phi = A\mu (1 - \zeta \cot^{-1} \zeta) = AP_1(\mu) \phi_1(\zeta) \quad (2)$$

in the notation of spheroidal harmonics,* where, if U is its velocity, so that the surface condition on $\zeta = 0$ is

$$\left(\frac{\partial \phi}{\partial z}\right) = \frac{1}{\alpha\mu} \left(\frac{\partial \phi}{\partial \zeta}\right)_{\zeta=0} = U$$

we have

$$A = -\frac{2U}{\pi a}$$

We shall proceed to determine a solution of the equation of wave motion with the properties

$$(1) \quad (\partial \phi / \partial z)_{z=0} = \text{constant},$$

$$(2) \quad \phi = 0 \text{ at infinity}$$

$$(3) \quad \phi \rightarrow B\mu (1 - \zeta \cot^{-1} \zeta) \text{ when } \lambda a \rightarrow 0$$

These are conditions appropriate to the special problem of plane sound-waves incident normally, with a velocity potential

$$\phi_1 = e^{i k (z - ct)}$$

on a circular disc at $z = 0$. The surface condition would then be, if ϕ is the disturbance scattered by the disc

$$(\partial \phi / \partial z)_{z=0} = -i k e^{-i k ct},$$

and when k is small the solution should tend to

$$\phi = \frac{2i k}{\pi} e^{-i k ct} \mu (1 - \zeta \cot^{-1} \zeta) \quad (3)$$

near the disc, as pointed out by Lord Rayleigh, the solution then being effectively that of ordinary hydrodynamics for a disc moving with velocity $-i k e^{-i k ct}$.

From several points of views this constitutes the most convenient solution for purposes of generalisation and suggestion of a type-solution

Let us therefore write, as a solution of the equation of wave motion,

$$\phi = A\mu (1 - \zeta \cot^{-1} \zeta) + (ka)^2 F_1 + (ka)^4 F_2 + \quad (4)$$

* Nicholson, 'Phil Trans,' A, vol 224, pp 48-93

where the F 's are functions of μ and of ζ , of no order in ka . We determine them, in the first instance, by successive approximation. The series from this found for ϕ , when its general term is recognised, is of considerable value in the applications, and it is not readily derived from the definite integral form ultimately obtained.

The function ϕ is restricted to vanish with μ , while its derivate with respect to ζ (or z) vanishes with ζ (or z). Now since

$$(\partial/\partial z)_{z=0} = (a\mu)^{-1} (\partial/\partial \zeta)_{\zeta=0},$$

let

$$F_0 = A\mu (1 - \zeta \cot^{-1} \zeta) \quad (5)$$

Then writing, in the equation of wave motion

$$\phi = F_0 + \omega^2 F_1 \quad (\omega = ka),$$

and retaining only the first power of ω^2 , we find

$$\begin{aligned} \frac{\partial}{\partial \mu} (1 - \mu^2) \frac{\partial}{\partial \mu} F_1 + \frac{\partial}{\partial \zeta} (1 + \zeta^2) \frac{\partial F_1}{\partial \zeta} = -(\zeta^2 + \mu^2) F_0 \\ - A\zeta\mu (1 - \zeta \cot^{-1} \zeta) - A\mu^3 (1 - \zeta \cot^{-1} \zeta), \end{aligned}$$

suggesting

$$F_1 = P\mu + Q\mu^3$$

where (P, Q) depend only on ζ . To determine P and Q , we have

$$\begin{aligned} \frac{\partial}{\partial \zeta} (1 + \zeta^2) \frac{\partial Q}{\partial \zeta} - 12Q = -A (1 - \zeta \cot^{-1} \zeta) \\ \frac{\partial}{\partial \zeta} (1 + \zeta^2) \frac{\partial P}{\partial \zeta} - 2P = -6Q - A\zeta^2 (1 - \zeta \cot^{-1} \zeta) \end{aligned}$$

We find that solution in powers of μ is preferable, as regards simplicity of analysis, to solution in a series of Legendre functions of μ .

The general solution for Q is easily shown to be

$$Q = \alpha q_3(\zeta) + \beta p_3(\zeta) + \frac{A}{18} (1 - 3\zeta^2 + 3\zeta^3 \cot^{-1} \zeta)$$

finite for all finite values of ζ . As ζ tends to infinity

$$1 - 3\zeta^2 + 3\zeta^3 \cot^{-1} \zeta = 1 - 3\zeta^2 + 3\zeta^3 \left(\frac{1}{\zeta} - \frac{1}{3}\zeta^3 + \dots \right),$$

and tends to $3/5 \zeta^2$, thus vanishing. Moreover, when $\zeta = 0$, the derivate of this function vanishes. We thus satisfy our prescribed conditions by ignoring the complementary function $\alpha q_3 + \beta p_3$, and writing

$$Q = \frac{A}{18} (1 - 3\zeta^2 + 3\zeta^3 \cot^{-1} \zeta).$$

The equation for P then becomes

$$\frac{\partial}{\partial \zeta} (1 + \zeta^2) \frac{\partial P}{\partial \zeta} - 2P = -A\zeta^2 (1 - \zeta \cot^{-1} \zeta) - \frac{A}{3} (1 - 3\zeta^2 + 3\zeta^3 \cot^{-1} \zeta) \\ = \frac{1}{3}A$$

with a remarkable simplification. The necessary solution, making P finite when $\zeta = \alpha$, and $\partial P / \partial \zeta$ zero when $\zeta = 0$, is merely

$$P = \frac{1}{6}A,$$

so that finally

$$F_1 = \frac{1}{6}A\mu + \frac{1}{18}A\mu^3 (1 - 3\zeta^2 + 3\zeta^2 \cot^{-1} \zeta) \quad (6)$$

We notice that the satisfaction of the condition at infinity (F_1 finite) has been automatic, owing to a choice of the correct form for ka null, and, in fact, involves no restriction beyond those previously made.

The third approximation to ϕ ensues by adding a term $\omega^4 F_2$, where we find at once - now retaining all powers of ω to ω^4 ,

$$\frac{\partial}{\partial \mu} (1 - \mu^2) \frac{\partial F_2}{\partial \mu} + \frac{\partial}{\partial \zeta} (1 + \zeta^2) \frac{\partial F_2}{\partial \zeta} = -(\zeta^2 + 2) F_1 \\ = -\frac{1}{6}A\mu\zeta^2 - \frac{1}{18}A\mu^3 (\zeta^2 - 3\zeta^4 + 3 + 3\zeta^3 \cot^{-1} \zeta) \\ - \frac{1}{18}A\mu^5 (1 - 3\zeta^2 + 3\zeta^3 \cot^{-1} \zeta)$$

So that we may write

$$F_2 = P_1\mu + P_3\mu^3 + P_5\mu^5$$

where, if D stands for the operation

$$D \equiv \frac{\partial}{\partial \zeta} (1 + \zeta^2) \frac{\partial}{\partial \zeta},$$

we have

$$(D - 2) P_1 = -\frac{1}{6}A\zeta^2 \\ (D - 12) P_3 = -20P_1 - \frac{1}{18}A (3 + \zeta^2 - 3\zeta^4 + 3\zeta^3 \cot^{-1} \zeta) \\ (D - 30) P_5 = -\frac{1}{18}A (1 - 3\zeta^2 + 3\zeta^3 \cot^{-1} \zeta)$$

A particular integral of the last equation is found to be

$$P_5 = \frac{A}{5!} \left(\frac{1}{3} - \frac{1}{3}\zeta^2 + \zeta^4 - \zeta^5 \cot^{-1} \zeta \right)$$

Again, this satisfies the conditions, and a complementary function is not necessary. The equation for P_3 then becomes, on reduction

$$(D - 12) P_3 = -\frac{1}{18}A (3 + \zeta^2 - 3\zeta^4 + 3\zeta^3 \cot^{-1} \zeta) \\ - \frac{A}{3!} \left(\frac{1}{3} - \frac{1}{3}\zeta^2 + \zeta^4 - \zeta^5 \cot^{-1} \zeta \right),$$

which is finally

$$(D - 12) P_3 = -\frac{1}{6}A,$$

with the satisfactory solution $P_3 = A/60$

The simplification found in F_1 thus extends to F_2 , and, as we shall see, is general. It is the first indication of a simple final result.

P_1 is then given by

$$(D-2)P_1 = -A\left(\frac{1}{10} + \frac{\zeta^2}{6}\right),$$

and its derivate vanishes with ζ if

$$P_1 = \frac{A}{5!} (1 - 5\zeta^2)$$

This is not zero at infinity, but it is not necessary for each *individual* P to vanish there, but only the final sum, as will ultimately appear.

The collected third approximation to ϕ is thus

$$\begin{aligned} \phi = & A\mu (1 - \zeta \cot^{-1} \zeta) + \frac{1}{3} A\mu \omega^2 + \frac{1}{18} A\mu^3 \omega^2 (1 - 3\zeta^2 + 3\zeta^2 \cot^{-1} \zeta) \\ & + \frac{A\mu}{5!} \omega^4 (1 - 5\zeta^2) + \frac{1}{81} A\mu^3 \omega^4 + \frac{1}{648} A\mu^5 \omega^4 (1 - \frac{1}{3}\zeta^2 + 5\zeta^4 - 5\zeta^6 \cot^{-1} \zeta) \end{aligned} \quad (7)$$

This general procedure may be continued, and it is necessary to carry it several stages further before generalisation of the results becomes possible. We shall suppress much of the detailed analyses and quote the final results. It is clearly not possible, by any simple series method applied to the differential equation directly, to find the general coefficient of any power of μ .

The final value found for F_3 is

$$\begin{aligned} F_3 = & A\mu \left(\frac{1}{7!} - \frac{\zeta^2}{360} + \frac{\zeta^4}{432} \right) + A\mu^3 \left(\frac{1}{1008} - \frac{\zeta^2}{240} \right) + \frac{A\mu^5}{8!} \\ & + A\mu^7 \left\{ \frac{1}{14 \cdot 42 \cdot 60} - \frac{\zeta^2}{42 \cdot 600} + \frac{\zeta^4}{42 \cdot 360} - \frac{\zeta^6}{42 \cdot 120} + \frac{\zeta^7 \cot^{-1} \zeta}{42 \cdot 120} \right\} \end{aligned} \quad (8)$$

and the contribution to ϕ , of the sixth order in ω , is $\omega^6 F_3$.

It is now possible to elucidate some of the structure of ϕ .

Discussion of the Fourth Approximation The Function ϕ_1 .

Let ϕ_1 be the portion of ϕ which actually vanishes term by term at infinity, namely, to the sixth order,

$$\begin{aligned} \phi_1 = & A\mu (1 - \zeta \cot^{-1} \zeta) + \frac{A}{3!} \mu^3 \omega^2 \left(\frac{1}{3} - \zeta^2 + \zeta^2 \cot^{-1} \zeta \right) \\ & + \frac{A}{5!} \mu^5 \omega^4 \left(\frac{1}{5} - \frac{1}{3}\zeta^2 + \zeta^4 - \zeta^6 \cot^{-1} \zeta \right) \\ & + \frac{A}{7!} \mu^7 \omega^6 \left(\frac{1}{7} - \frac{\zeta^2}{5} + \frac{\zeta^4}{3} - \zeta^6 + \zeta^7 \cot^{-1} \zeta \right) \end{aligned} \quad (9)$$

The law of formation of these terms is already evident, the general term of ϕ_1 being clearly

$$\frac{A\mu^{2n+1}\omega^{2n}}{2n+1!} \left(\frac{1}{2n+1} - \frac{\zeta^2}{2n-1} + \frac{\zeta^4}{2n-3} + (-)^n \zeta^{2n} + (-)^{n-1} \zeta^{2n+1} \cot^{-1} \zeta \right)$$

The result is easily proved by induction, for if this expression is called $\omega^{2n} \mu^{2n+1} \psi(n)$, it is the highest power of μ in F_n , and since

$$DF_{n+1} + \frac{\partial}{\partial \mu} (1 - \mu^2) \frac{\partial F_{n+1}}{\partial \mu} = -(\zeta^2 + \mu^2) F_n$$

the coefficients of highest powers of μ satisfy, at once,

$$D\psi_{n+1} - (2n+3)(2n+4)\psi_{n+1} = -\psi_n$$

if the expression is general. This is readily verified by direct substitution for ψ_{n+1} , ψ_n .

The importance of ϕ_1 lies in the fact that it constitutes the part of ϕ not conveniently expressible in a series of ascending powers of ζ , but very conveniently expressible in descending powers when ζ is large.

We now express ϕ_1 , whose general term is established, as a definite integral. The portion (ϕ_{11}) containing $\cot^{-1} \zeta$ as a factor, is

$$\begin{aligned} \phi_{11} &= -A \cot^{-1} \zeta \left\{ \mu \zeta - \frac{\omega^2 \mu^3 \zeta^3}{3!} + \dots \right\} \\ &= -\frac{A}{\omega} \cot^{-1} \zeta \sin(\omega \mu \zeta) \end{aligned} \quad (10)$$

The remainder, (ϕ_{12}) , is given by

$$\phi_{12} = \frac{A\mu}{1!} + \frac{A\omega^2 \mu^3}{3!} \left(\frac{1}{3} - \zeta^2 \right) + \frac{A\omega^4 \mu^5}{5!} \left(\frac{1}{5} - \frac{1}{3} \zeta^2 + \zeta^4 \right) + \dots \quad (11)$$

or rearranged as a set of absolutely convergent series

$$\begin{aligned} \phi_{12} &= A\mu \left\{ 1 + \frac{\omega^2 \mu^2}{3 \cdot 3!} + \frac{\omega^4 \mu^4}{5 \cdot 5!} + \dots \right\} \\ &\quad - A\mu \zeta^2 \left\{ \frac{\omega^2 \mu^2}{1 \cdot 3!} + \frac{\omega^4 \mu^4}{3 \cdot 5!} + \dots \right\} \\ &\quad + A\mu \zeta^4 \left\{ \frac{\omega^4 \mu^4}{1 \cdot 5!} + \frac{\omega^6 \mu^6}{3 \cdot 7!} + \dots \right\} - A\mu \zeta^6 \left\{ \frac{\omega^6 \mu^6}{1 \cdot 7!} + \frac{\omega^8 \mu^8}{3 \cdot 9!} + \dots \right\}. \end{aligned}$$

Thus

$$\phi_{12} = \int_0^1 \chi dx$$

where

$$\begin{aligned} \chi &= \frac{A\mu}{1!} + \frac{A\omega^2\mu^3}{3!}(x^2 - \zeta^2) + \frac{A\omega^4\mu^5}{5!}(x^4 - x^2\zeta^2 + \zeta^4) \\ &\quad + \frac{A\omega^6\mu^7}{7!}(x^6 - x^4\zeta^2 + x^2\zeta^4 - \zeta^6) + \dots \\ &= \frac{1}{1+x^2/\zeta^2} \left\{ \frac{A\mu}{1!} \left(1 + \frac{x^2}{\zeta^2}\right) - \frac{A\mu^3}{3!} \left(1 - \frac{x^2}{\zeta^2}\right) \omega^2\zeta^2 + \frac{A\mu^5}{5!} \left(1 + \frac{x^2}{\zeta^2}\right) \omega^4\zeta^4 \right\} \\ &= \frac{A\zeta^2}{\zeta^2 + x^2} \frac{\sin \omega\mu\zeta}{\omega\zeta} + \frac{Ax^2}{\zeta^2 + x^2} \frac{\sinh \omega\mu x}{\omega x} \end{aligned} \quad (12)$$

on summation ϕ_{12} is the integral with respect to x from zero to unity, and

$$\begin{aligned} \phi_1 = \phi_{11} + \phi_{12} &= -\frac{A \cot' \zeta}{\omega} \sin(\omega\mu\zeta) \\ &\quad + A\zeta^2 \frac{\sin \omega\mu\zeta}{\omega\zeta} \int_0^1 \frac{dx}{x^2 + \zeta^2} + \frac{A}{\omega} \int_0^1 \frac{x \sinh \omega\mu x}{x^2 + \zeta^2} dx \end{aligned}$$

which reduces merely to

$$\phi_1 = \frac{A}{\omega} \int_0^1 \frac{x \sinh \omega\mu x}{x^2 + \zeta^2} dx \quad (13)$$

The Function $F_r^s(\zeta)$.

With, as before,

$$\phi = F_0 + \omega^2 F_1 + \omega^4 F_2 + \dots$$

F_n is clearly an odd polynomial in μ of degree $2n + 1$. If we write

$$F_n = \sum_{r=0}^n F_{2r+1}^n \mu^{2r+1} \quad (14)$$

the new function F_{2r+1}^n is a function only of ζ . The functions F_1^1, F_3^2 , are the coefficients of the penultimate powers of μ in the functions F_n . The first two of the sequence are constants, and we have suggested that this fact is general.

The functions $F_1^2, F_3^3, \dots, F_{2n-3}^n$ pertain to the next lower power of μ , and may be expected, from the above fourth approximation, to be of the form $\alpha + \beta\zeta^2$, where α and β depend only on r and n . The next set similarly should be of type $\alpha + \beta\zeta^2 + \gamma\zeta^4$, and so on.

Let us consider the general relation among these functions directly from

$$(D + D_1) F_{n+1} = -(\zeta^2 + \mu^2) F_n$$

where

$$D_1 \equiv \frac{\partial}{\partial \zeta} \left(1 + \zeta^2\right) \frac{\partial}{\partial \zeta}$$

and F_n is defined by (14).

By direct substitution, we have for all values of μ ,

$$\sum_0^{n+1} \mu^{2r+1} D_1 F_{2r+1}^{n+1} - \sum_0^{n+1} (2r+1)(2r+2) \mu^{2r+1} F_{2r+1}^{n+1} \\ + \sum_0^{n+1} 2r(2r+1) \mu^{2r-1} F_{2r+1}^{n+1} = -(\mu^2 + \zeta^2) \sum_0^n \mu^{2r+1} F_{2r+1}^n,$$

and the necessary and sufficient relation becomes.—

$$[D_1 - (2r+1)(2r+2)] F_{2r+1}^{n+1} = -(2r+2)(2r+3) F_{2r+3}^{n+1} - \zeta^2 F_{2r+1}^n - F_{2r-1}^n.$$

Taking, first, $r = n+1$, we have

$$[D_1 - (2n+3)(2n+4)] F_{2n+3}^{n+1} = -F_{2n+1}^n$$

The solution of this gives the functions contained in ϕ_1 , namely, for any value of n ,

$$F_{2n+1}^n = \frac{A}{2n+1!} \left(\frac{1}{2n+1} - \frac{\zeta^2}{2n-1} + \frac{\zeta^4}{2n-3} \right. \\ \left. + (-)^n \zeta^{2n} + (-)^{n+1} \zeta^{2n+1} \cot^{-1} \zeta \right).$$

Next, taking $r = n$,

$$[D_1 - (2n+1)(2n+2)] F_{2n+1}^{n+1} = -F_{2n-1}^n - \zeta^2 F_{2n+1}^n - (2n+2)(2n+3) F_{2n+3}^{n+1} \\ = -F_{2n-1}^n - \frac{A}{(2n+1)! (2n+3)}$$

by the preceding equation.

Thus, if F_{2n-1}^n is constant, so also is F_{2n+1}^{n+1} and all functions of this type, so far as our conditions are concerned. In fact, we can take

$$F_{2n+1}^{n+1} = \frac{F_{2n-1}^n}{(2n+1)(2n+2)} + \frac{A}{(2n+1)! (2n+1)(2n+2)(2n+3)}$$

But if $n = 1$, or $n = 2$, F_{2n-1}^n takes the values $A/3!$ and $A/3 \cdot 4 \cdot 5$, so that we can readily generalize and find for every value of n , with easy reduction

$$F_{2n-1}^n = nA/(2n+1)!$$

The contribution to ϕ made by this set of functions is (ϕ_2) , where

$$\phi_2 = A \left\{ \frac{\mu \omega^2}{3!} + \frac{2\mu^3 \omega^4}{5!} + \frac{3\mu^5 \omega^6}{7!} + \dots \right\}. \quad (15)$$

The next set of function-coefficients are quadratic in ζ , as appears in the analysis automatically. They are of the form

$$P_{2n-2}^n = A_n + \zeta^2 B_n.$$

Applying the general recurrence formula with $r = n - 1$, and quoting the values already found for previous coefficients, we find this quadratic form satisfactory for all values of ζ if

$$(2n-3)(2n+2)B_{n+1} = B_n + \frac{nA}{(2n+1)!}$$

$$2B_{n+1} - 2n(2n-1)A_{n+1} = -A_n - \frac{(2n+1)(n+1)^{2n}}{2n+3!}A$$

We know the first two values from our fourth approximation, and the solution is rapid for further values. The final result, which we leave to the reader for proof, is

$$F_{2n-3}^n = \frac{1}{3}A \frac{n(n-1)(2n-1)}{(2n+1)!} - \frac{1}{4}A\zeta^2 \frac{n-1}{(2n-1)!}$$

and the contribution (ϕ_3) of such functions to ϕ is

$$\phi_3 = \frac{1}{3}A\mu\omega^4 \left\{ \frac{2}{5!} + \omega^2\mu^2 \frac{3}{7!} + \omega^4\mu^4 \frac{4 \cdot 3 \cdot 7}{9!} + \dots \right\}$$

$$- \frac{1}{4}A\zeta^2\mu\omega^4 \left\{ \frac{1}{3!} + \omega^2\mu^2 \frac{2}{5!} + \omega^4\mu^4 \frac{3}{7!} + \dots \right\} \quad (16)$$

It does not seem necessary to show that the next set of functions, of form F_{2n-5}^n , are quartic in ζ , for the same type of demonstration is effective. They can be derived from those just calculated by writing $r = n - 2$ in the general recurrence formula.

Thus $F_{2n-3}^n, F_{2n-1}^{n+1}$ are already known, and we have

$$F_{2n-5}^n = A_n + B_n\zeta^2 + C_n\zeta^4,$$

with a corresponding form for F_{2n-3}^{n+1} , and

$$[D_1 - (2n-3)(2n-2)]F_{2n-3}^{n+1} = -(2n-2)(2n-1)F_{2n-1}^{n+1} - \zeta^2 F_{2n-3}^n.$$

We thus obtain, by equating powers of ζ ,

$$-C_n + \frac{1}{4}A \frac{n-1}{2n-1!} = -(2n-3)(2n-2)C_{n+1} + 20C_{n+1}$$

$$- B_n - \frac{n(n-1)(2n-1)}{(2n+1)!} \frac{A}{6} + \frac{A}{4} \frac{n(2n-2)(2n-1)}{(2n+1)!}$$

$$= -(2n-3)(2n-2)B_{n+1} + 12C_{n+1} + 6B_{n+1}$$

$$- A_n - \frac{1}{3}A \frac{n(n+1)(2n+1)(2n-1)(2n-2)}{(2n+3)!}$$

$$= 2B_{n+1} - (2n-3)(2n-2)A_{n+1}.$$

The analysis at this point is evidently becoming cumbrous. C_n is found first, then B_n , and finally A_n . It is not perhaps necessary to exhibit the detailed calculation of C_n from the first formula and the known value

$$C_3 = A/(18 \cdot 24)$$

The final result is

$$C_n = \frac{1}{72} A \frac{n-2}{2n-3!},$$

and from the known value $B_3 = -A/360$, we can subsequently, by the second equation, generalize to

$$B_n = -\frac{1}{72} A (n-2)(n-1)(2n-3)/(2n-1!)$$

If we substitute these values, A_n is found from the third equation to satisfy

$$\begin{aligned} (2n-2)(2n-3)A_{n+1} - A_n \\ = \frac{1}{6} A (n-1)n(n+1)(2n-1)(2n-3)/(2n+3!) \end{aligned}$$

with $A_3 = A/7!$ from the fourth approximation to ϕ

The general solution is found to be

$$A_n = \frac{1}{72} A n(n-1)(n-2)(2n-1)(2n-3)/(2n+1!),$$

leading to

$$\begin{aligned} F_{2n-5}^* = \frac{1}{72} A \frac{n(n-1)(n-2)(2n-1)(2n-3)}{2n+1!} \\ - \frac{A\zeta^2}{18} \frac{(n-1)(n-2)(2n-3)}{2n-1!} + \frac{1}{72} A \zeta^4 \frac{n-2}{2n-3!} \end{aligned} \quad (17)$$

But it is clear that this procedure ultimately becomes too laborious, and that further generalization involves some intuition. At the same time there is every reason to think that a final exact expression is possible

General Structure of F_p^ when $2q-p$ is an Odd Positive Integer.*

We may write the three values so far found for the functions F_p^* as follows —

$$F_{2n-1}^* = \frac{A}{(2n-1)!} \frac{1}{2 \cdot 1!} \left(\frac{1}{2n+1} \right) \quad (18)$$

$$F_{2n-3}^* = \frac{A}{(2n-3)!} \frac{1}{4 \cdot 3!} \left(\frac{1}{2n+1} - \frac{3\zeta^2}{2n-1} \right) \quad (19)$$

$$F_{2n-5}^* = \frac{A}{(2n-5)!} \frac{1}{6 \cdot 5!} \left(\frac{1}{2n+1} - \frac{10\zeta^2}{2n-1} + \frac{5\zeta^4}{2n-3} \right), \quad (20)$$

and an inspection indicates that the next should be

$$F_{2n-7}^* = \frac{A}{(2n-7)!} \frac{1}{8 \cdot 7!} \left(\frac{1}{2n+1} - \frac{\alpha\zeta^2}{2n-1} + \frac{\beta\zeta^4}{2n-3} - \frac{\gamma\zeta^6}{2n-5} \right) \quad (21)$$

where (α, β, γ) are independent of n . We already know this function to be sextic in ζ , and it is probable that $\gamma = 7$. These suppositions are verified entirely on substitution in the general recurrence formula. It is hardly necessary to give the analysis. The values of (α, β, γ) are found to be

$$\alpha = 21, \quad \beta = 35, \quad \gamma = 7$$

In the same way, we can go on to show that

$$F_{2n-9}^{\alpha} = \frac{A}{(2n-9)!} \frac{1}{10 \cdot 9!} \left(\frac{1}{2n+1} - \frac{36\zeta^2}{2n-1} + \frac{126\zeta^4}{2n-3} - \frac{84\zeta^6}{2n-5} + \frac{9\zeta^8}{2n-7} \right),$$

and, at this point, the final generalization can be made in the form

$$F_{2n-1-2r}^{\alpha} = \frac{A}{(2n-1-2r)!} \frac{1}{2r+2} \cdot \frac{1}{2r+1!} \left(\frac{1}{2n+1} \frac{\alpha_r \zeta^2}{2n-1} \frac{\beta_r \zeta^4}{2n-3} - \dots \right)$$

the series terminating at the term in ζ^{2r} , and α_r, β_r , depending only on r .

We have the following initial scheme —

$r = 0$	$r = 1$	$r = 2$	$r = 2$	$r = 4$
$\alpha_r = 0$	$\alpha_r = 1 \cdot 3$	$\alpha_r = 2 \cdot 5$	$\alpha_r = 3 \cdot 7$	$\alpha_r = 4 \cdot 9$

and evidently, in general,

$$\alpha_r = r(2r+1)$$

The scheme for β_r is —

$r = 1,$	$r = 2,$	$r = 3,$	$r = 4,$
$\beta_r = 0,$	$\beta_r = 1 \cdot 5,$	$\beta_r = 5 \cdot 7,$	$\beta_r = 14 \cdot 9.$

These members are not decisive, though they strongly suggest the sequence

$$1^2 \cdot 5, \quad (1^2 + 2^2) 7, \quad (1^2 + 2^2 + 3^2) 9, \dots,$$

more especially as such sums of squares are already familiar in the investigation. A process of induction readily verifies this suggestion, and

$$\beta_r = (2r+1)(1^2 + 2^2 + \dots + (r-1)^2) = \frac{1}{3!} r(r-1)(4r^2-1).$$

At this point we can in fact divine the whole result completely, and verify it afterwards. With

$$\alpha_r = r(2r+1), \quad \beta_r = \frac{1}{6} (r-1)r(2r-1)(2r+1)$$

we may suggest

$$\gamma_r = \frac{1}{N} (r-2)(r-1)r(2r-3)(2r-1)(2r+1)$$

where N is numerical. Our previous work has given us the values

$$\gamma_3 = 7, \quad \gamma_4 = 8^4,$$

and these are both consistent with the suggestion, if $N = 90$. Then we may divine

$$\delta_r = \frac{1}{M} (r-3)(r-2)(r-1)r(2r-5)(2r-3)(2r-1)(2r+1),$$

and knowing δ is 9 when $r = 5$, we find $M = \frac{2}{7!}$

If these coefficients are put in the equivalent forms

$$\alpha_r = \frac{1}{2!} \frac{(2r+1)!}{(2r-1)!}, \quad \beta_r = \frac{1}{4!} \frac{(2r+1)!}{(2r-3)!}, \quad \gamma_r = \frac{1}{6!} \frac{(2r+1)!}{(2r-5)!},$$

their law of formation is simple and apparent, and if $r \neq 0$, the general value of a coefficient F is

$$F_{2n-1-2r}^* = \frac{A}{(2n-1-2r)!} \frac{1}{(2r+2)} \left\{ \frac{1}{(2n+1)(2r+1)!} - \frac{\zeta^2}{(2n-1)2!(2r-1)!} + \frac{\zeta^4}{(2n-3)4!(2r-3)!} - \dots \right\}. \quad (22)$$

It is understood that the series terminates just before a negative factorial appears. In order to complete the investigation, it is necessary to show that F satisfies the general difference equation. We have proved this by induction, but the proof is somewhat long and we do not exhibit it. We now have a solution of the equation of wave motion whose general term is expressed

Final Solution of the Equation of Wave Motion

To summarise the results, we now have a solution in oblate spheroidal co-ordinates of the form

$$\phi = \sum_0^\infty \omega^{2n} F_n \quad (23)$$

where

$$F_n = \sum_0^n \mu^{2r+1} F_{2r+1}^* \quad (24)$$

and when $r \neq n$, F is given by (22), but when $r = n$,

$$\sum_0^n F_{2n+1}^* \mu^{2n+1} = \frac{A}{\omega} \int_0^1 \frac{x \sinh \omega \mu x}{x^2 + \zeta^2} dx.$$

This solution, when $\omega \rightarrow 0$, reduces to $AP_1(\mu) q_1(\zeta)$, while its derivate to ζ is constant at $x = 0$, and identical with that of $AP_1(\mu) q_1(\zeta)$.

This is a solution on very different lines from any previously given. We now wish to sum it into a convenient form. Evidently we may write

$$F_{2n-1-2r}^* = \frac{A/2}{(2n-1-2r)!(2r+2)!} \int_{\phi}^{\infty} \frac{dx}{x^{2n+2}} \{(1 + \omega\zeta)^{2r+1} + (1 - \omega\zeta)^{2r+1}\}$$

which is equivalent to

$$F_{2m+1}^* = \frac{A/2}{(2m+1)!(2n-2m)!} \int_1^{\infty} \frac{dx}{x^{2n+2}} \{(1 + \omega\zeta)^{2n-2m-1} + (1 - \omega\zeta)^{2n-2m-1}\}.$$

Then

$$F_n = F_1^* \mu + F_3^* \mu^3 + \dots + F_{2n-1}^* \mu^{2n-1},$$

and if $\phi = \phi_1 + \phi_2$, where ϕ_1 is the function already summed,

$$\begin{aligned} \phi_2 &= \omega^2 F_1 + \omega^4 F_2 + \dots \\ &= \omega^2 \mu \{F_1^1 + \omega^2 F_1^2 + \omega^4 F_1^3 + \dots\} \\ &\quad + \omega^4 \mu^3 \{F_3^1 + \omega^2 F_3^2 + \dots\} + \omega^6 \mu^5 \{F_5^1 + \omega^2 F_5^2 + \dots\} + \dots \end{aligned}$$

where all brackets run to infinity of terms

If this is equivalent to

$$\phi_2 = \sum_{m=0}^{\infty} \lambda_m \mu^{2m+1} \quad (25)$$

we have

$$\lambda_m = \frac{1}{2} A \frac{\omega^{2m}}{(2m+1)!} \int_1^{\infty} \frac{dx}{x^{2m+2}} \left\{ \frac{1}{1 + \omega\zeta} \sum_{s=1}^{\infty} \omega^{2s} \frac{(x^{-1} + \omega\zeta)^{2s}}{2s!} + \frac{1}{1 - \omega\zeta} \sum_{s=1}^{\infty} \omega^{2s} \frac{(x^{-1} - \omega\zeta)^{2s}}{2s!} \right\},$$

the summations being absolutely convergent. Thus

$$\lambda_m = \frac{1}{2} A \frac{\omega^{2m}}{(2m+1)!} \int_1^{\infty} \frac{dx}{x^{2m+2}} \left\{ \frac{\cosh \omega (x^{-1} + \omega\zeta) - 1}{1 + \omega\zeta} + \frac{\cosh \omega (x^{-1} - \omega\zeta) - 1}{1 - \omega\zeta} \right\},$$

or, if $t = x^{-1}$,

$$\lambda_m = \frac{1}{2} A \frac{\omega^{2m}}{(2m+1)!} \int_0^1 t^{2m+1} dt \left\{ \frac{\cosh \omega (t + \omega\zeta) - 1}{t + \omega\zeta} + \frac{\cosh \omega (t - \omega\zeta) - 1}{t - \omega\zeta} \right\},$$

and thence on summation,

$$\phi_2 = \frac{A}{2\omega} \int_0^1 dt \left\{ \frac{\cosh \omega (t + \omega\zeta) - 1}{t + \omega\zeta} + \frac{\cosh \omega (t - \omega\zeta) - 1}{t - \omega\zeta} \right\}. \quad (26)$$

Clearly ϕ_2 vanishes when ζ is infinite, so that our final superposed condition is satisfied by the whole sum of terms. When this is combined with ϕ_1 , the whole result condenses into the elegant form

$$\phi = \phi_1 + \phi_2 = \frac{A}{2\omega} \int_0^1 dt \sinh \omega \mu t \left\{ \frac{\cosh \omega (t + i\zeta)}{t + i\zeta} + \frac{\cosh \omega (t - i\zeta)}{t - i\zeta} \right\}. \quad (27)$$

This is not a special case of any recognised form of solution. It expresses a certain set of converging and diverging waves, whose form is simple when expressed in terms of these co-ordinates. At a great distance it tends to the value

$$\frac{A}{2\omega\zeta} \sin \omega \zeta \left\{ \frac{\sinh \omega (1 + \mu)}{\omega (1 + \mu)} - \frac{\sinh \omega (1 - \mu)}{\omega (1 - \mu)} \right\}. \quad (28)$$

A New Class of Spheroidal Wave-forms.

By a class of wave-forms we mean a group of solutions of the equation of wave motion. The present class has not hitherto been noticed, although it is fundamental to the exact solution of problems involving the passage of waves past a circular (or oblate spheroidal) obstacle, or through a circular aperture in an infinite plane screen. The general nature of this class is suggested by the form of the function ϕ developed in this paper. This can be put in either of the forms, readily shown to be equivalent,

$$\begin{aligned} \phi &= \frac{A}{2\omega} \int_0^1 dt \sinh \omega \mu t \left\{ \frac{\cosh \omega (t + i\zeta)}{t - i\zeta} + \frac{\cosh \omega (t - i\zeta)}{t - i\zeta} \right\} \\ &= \frac{A}{\omega} \int_0^1 dt \sinh \omega \mu t \left\{ \int_0^1 d\lambda (\cos \omega \lambda \zeta \sinh \omega \lambda t) + \int_0^\infty \cos \omega \lambda \zeta e^{-\omega \lambda t} d\lambda \right\} \end{aligned}$$

The second form raises an interesting query. Under what circumstances can the equation of wave motion be satisfied by a function

$$\phi = \iint f(\lambda, t) \frac{\cos}{\sin} \left\{ \omega \lambda \zeta \frac{\cosh}{\sinh} \right\} \omega \mu t d\lambda dt \quad (29)$$

where the limits of integration are constant? We shall consider the function

$$\phi = \iint f(\lambda, t) e^{i\omega \lambda \zeta + \omega \mu t} d\lambda dt$$

where f is independent of ζ or μ . We find

$$\begin{aligned} \frac{\partial}{\partial \mu} (1 - \mu^2) \frac{\partial \phi}{\partial \mu} + \omega^2 \mu^2 \phi \\ = \iint f \cdot \{ \omega^2 t^2 (1 - \mu^2) - 2\mu \omega t + \omega^2 \mu^2 \} e^{i\omega \lambda \zeta + \omega \mu t} d\lambda dt, \end{aligned}$$

or as

$$(\omega \mu)^n e^{\omega \mu t} = (\partial / \partial t)^n e^{\omega \mu t}$$

the right-hand side becomes

$$\iint d\lambda dt f(\lambda, t) \left\{ \omega^2 t^2 - 2t \frac{\partial}{\partial t} + (1 - t^2) \frac{\partial^2}{\partial t^2} \right\} e^{\omega \mu t + i \omega \lambda \zeta}$$

This can be integrated by parts with respect to t , once and twice respectively in the second and third terms of the bracket. It is assumed that the function f and the limits are such as not to invalidate these operations.

Thus after reduction, the limits being (t_1, t_2) (λ_1, λ_2) for t and λ ,

$$\begin{aligned} \frac{\partial}{\partial \mu} (1 - \mu^2) \frac{\partial \phi}{\partial \mu} + \omega^2 \mu^2 \phi = & \iint \left\{ \omega^2 t^2 f + \frac{\partial}{\partial t} (1 - t^2) \frac{\partial f}{\partial t} \right\} e^{\omega \mu t + i \omega \lambda \zeta} d\lambda dt \\ & + \int_{\lambda_1}^{\lambda_2} d\lambda e^{i \omega \lambda \zeta} \left[(1 - t^2) \left(\omega \mu f - \frac{\partial f}{\partial t} \right) e^{\omega \mu t} \right]_{t_1}^{t_2}. \end{aligned}$$

After the same manner,

$$\begin{aligned} \frac{\partial}{\partial \zeta} (1 + \zeta^2) \frac{\partial \phi}{\partial \zeta} + \omega^2 \zeta^2 \phi \\ = \iint f d\lambda dt \left\{ -\omega^2 \lambda^2 + 2\lambda \frac{\partial}{\partial \lambda} + (\lambda^2 - 1) \frac{\partial^2}{\partial \lambda^2} \right\} e^{i \omega \lambda \zeta} + \omega \mu t, \end{aligned}$$

or, on integration by parts, becomes

$$\begin{aligned} \iint d\lambda dt \left\{ -\omega^2 \lambda^2 f - \frac{\partial}{\partial \lambda} (1 - \lambda^2) \frac{\partial f}{\partial \lambda} \right\} e^{i \omega \lambda \zeta + \omega \mu t} \\ + \int_{t_1}^{t_2} dt e^{\omega \mu t} \left[(\lambda^2 - 1) \left(i \omega \zeta f - \frac{\partial f}{\partial \lambda} \right) e^{i \omega \lambda \zeta} \right]_{\lambda_1}^{\lambda_2}. \end{aligned}$$

The equation of wave motion is thus satisfied provided that

$$\begin{aligned} \iint K d\lambda dt e^{i \omega \lambda \zeta + \omega \mu t} + \int_{\lambda_1}^{\lambda_2} d\lambda e^{i \omega \lambda \zeta} \left[(1 - t^2) \left(\omega \mu f - \frac{\partial f}{\partial t} \right) e^{\omega \mu t} \right]_{t_1}^{t_2} \\ + \int_{t_1}^{t_2} dt e^{\omega \mu t} \left[(\lambda^2 - 1) \left(i \omega \zeta f - \frac{\partial f}{\partial \lambda} \right) e^{i \omega \lambda \zeta} \right]_{\lambda_1}^{\lambda_2} = 0, \end{aligned}$$

where

$$K \equiv \frac{\partial}{\partial t} (1 - t^2) \frac{\partial f}{\partial t} - \frac{\partial}{\partial \lambda} (1 - \lambda^2) \frac{\partial f}{\partial \lambda} + \omega^2 (t^2 - \lambda^2) f = 0. \quad (30)$$

After the usual manner, we choose f to make K vanish. Then, if $\lambda = w$ is a new variable,

$$\frac{\partial}{\partial t} (1 - t^2) \frac{\partial f}{\partial t} + \frac{\partial}{\partial w} (1 + w^2) \frac{\partial f}{\partial w} + \omega^2 (t^2 + w^2) f = 0, \quad (31)$$

which is the equation of wave motion with spheroidal co-ordinates (t, w) , or $(t, -i\lambda)$. Thus if $F(\mu, \zeta)$ is any wave solution in spheroidal co-ordinates, we can take

$$f = F(t, -i\lambda)$$

in order to obtain an integral solution.

The limits $(\lambda_1, \lambda_2), (t_1, t_2)$ must be chosen to make the single integrals in (30) vanish. There is one obvious choice which is satisfactory in a majority of cases. This is $(\lambda_1, \lambda_2) = \pm 1, (t_1, t_2) = \pm 1$, provided that f and its derivatives satisfy obvious conditions of finiteness within these limits.

The sign of μ or ζ , or both, can be changed without affecting the preceding arguments, and, in fact, the following statement is true almost universally.—

If $F(\mu, \zeta)$ is a solution, in spheroidal co-ordinates, of the equation, where $ka = \omega$,

$$(\nabla^2 + k^2) \phi = 0$$

Then the double integral

$$\phi = \int_{-1}^1 \int_{-1}^1 F(t, -i\lambda) d\lambda dt e^{\pm i\omega\lambda\zeta \pm \omega\mu t} \quad (32)$$

is another solution, where the signs in the ambiguities can be combined in any manner. This gives a great variety of important solutions which may be studied, which lead to various solutions of problems of wave motion. Some of the more fundamental may be indicated at this point. The simplest solutions of the equation of wave motion are

$$F(\mu, \zeta) = e^{\pm i\omega\zeta} = e^{\pm i\omega\mu\zeta},$$

giving

$$F(t, -i\lambda) = e^{\pm \omega\lambda t},$$

and therefore, as further solutions, we have

$$\phi = \int_{-1}^1 \int_{-1}^1 e^{\pm \omega\lambda t \pm i\omega\lambda\zeta \pm \omega\mu t} d\lambda dt$$

where any ambiguous signs can be taken together. Integrating with respect to λ , solutions are

$$\phi = \frac{1}{\omega} \int_{-1}^1 e^{\pm \omega\mu t} dt \left\{ \frac{\sinh \omega(t \pm i\zeta)}{t \pm i\zeta} \right\},$$

which include as examples

$$\begin{aligned} \phi_1 &= \int_{-1}^1 dt \sinh \omega\mu t \left\{ \frac{\sinh \omega(t + i\zeta)}{t + i\zeta} - \frac{\sinh \omega(t - i\zeta)}{t - i\zeta} \right\} \\ \phi_2 &= \int_{-1}^1 dt \cosh \omega\mu t \left\{ \frac{\sinh \omega(t + i\zeta)}{t + i\zeta} + \frac{\sinh \omega(t - i\zeta)}{t - i\zeta} \right\} \end{aligned} \quad (33)$$

Limits other than ± 1 may be available. For example, with the present illustrative form of F , positive or negative infinity is at once seen to be a possible limit for λ or for t . If we take it for λ , we deduce that a solution is given by

$$\phi = \int_{-1}^1 dt \int_1^\infty d\lambda e^{-\omega\lambda t \pm i\omega\lambda\zeta \pm \omega\mu t}$$

which includes, as an important case

$$\phi_2 = e^{-i\omega\zeta} \int_0^1 \sinh \omega t \mu \left\{ \frac{e^{-\omega t}}{t + i\zeta} + \frac{e^{+\omega t}}{t - i\zeta} \right\} dt, \quad (34)$$

tending, at an infinite distance, to

$$\phi_2 = \frac{2e^{-i\omega\zeta}}{i\zeta} \int_0^1 \sinh \omega t \mu \frac{\sinh \omega t}{t} dt, \quad (35)$$

and therefore ultimately proportional, in polars, to $e^{-i\omega r}/r$, and representing a wave diverging from the primary spheroid which is the basis of the co-ordinate system. A change of the sign of i in this form of ϕ_2 gives a wave

$$\phi_2 = e^{+\omega\zeta} \int_0^1 \sinh \omega t \mu \left\{ \frac{e^{\omega t}}{t + i\zeta} + \frac{e^{-\omega t}}{t - i\zeta} \right\} dt, \quad (36)$$

converging on the spheroid.

Other solutions readily derived by this type of procedure are

$$\begin{aligned} \phi_2 &= \int_0^1 \sinh \omega \mu t \left\{ \frac{\cosh \omega (t + i\zeta)}{t + i\zeta} - \frac{\cosh \omega (t - i\zeta)}{t - i\zeta} \right\} dt, \\ \phi_2 &= \cosh \omega \mu t \left\{ \frac{\cosh \omega (t + i\zeta)}{t + i\zeta} - \frac{\cosh \omega (t - i\zeta)}{t - i\zeta} \right\} dt, \end{aligned} \quad (37)$$

of which the first is the solution derived in the earlier part of the paper, and reducing to $P_1(\mu) q_1(\zeta)$ when $\omega = 0$, and making $\partial\phi_2/\partial z$ constant over $z = 0$, $\rho < a$.

These functions ϕ_1 ϕ_2 can lead to the solution of the problem of diffraction of plane sound waves—and thence of electromagnetic waves—by an obstacle in the form of a circular disc, and also the problem of passage of plane waves through a circular aperture in an infinite plane screen. Similar analysis has been found suitable in two dimensions for the suggestion of alternative modes of solution to that of Mathieu and Lamé, in which the general form can be expressed simply.

Thermionic Effects caused by Vapours of Alkali Metals.

By IRVING LANGMUIR and K. H. KINGDON, of the Research Laboratory,
General Electric Company, Schenectady, N. Y.

(Communicated by Prof. Sir E. Rutherford, F.R.S. —Received November 18, 1924.)

Early in 1923 it was shown* that a tungsten filament heated to 1200° K or more in saturated caesium vapour converts all caesium atoms which strike it into caesium ions. Thus when the filament is surrounded by a negatively charged cylinder a positive ion current flows from the filament, which is independent of the filament temperature (above 1200° K) and independent of the applied potential, if this is sufficient to overcome the space charge effect of the positive ions. At lower voltages the currents follow the $3/2$ power law, and the currents are smaller than the corresponding electron currents obtainable from the same filament in the ratio of the square roots of the masses of the electrons and caesium ions.

The reason that the caesium atoms lose their valence electrons so readily upon contact with the filament, is merely that the electron affinity of tungsten (Richardson work function) is 4.53 volts, while the electron affinity of a caesium atom (ionising potential) is only 3.88 volts. Experiments showed in fact that if the work function for the filament is lowered to 2.69, by allowing a monatomic layer of thorium atoms to accumulate on the surface (by diffusion from the interior of a thoriated tungsten filament), the positive ion emission becomes negligible.

The positive ions must be attracted to a tungsten surface because of the electron image force. Thus it is that below about 1200° K the caesium ions evaporate so slowly from a tungsten surface that this becomes partly covered by adsorbed caesium ions. The presence of these ions, however, lowers the electron affinity of the surface, so that when about 20 per cent of the surface is covered, the work function falls below the ionising potential of the caesium. With more caesium on the surface the caesium atoms which strike the filament no longer escape in the form of ions but remain in the atomic state. Thus the positive ion currents disappear below about 1100° K. But the lowering of the electron affinity raises the electron emission, and when the surface becomes more completely covered by caesium as the temperature is lowered, the electron

* Langmuir and Kingdon, *Science*, vol. 57, p. 58 (1923), and *Phys. Rev.*, vol. 21, p. 390 (1923).

emission rises to a maximum (of about 10^{-5} amps. per cm^2 at 700°) and then decreases rapidly at still lower temperatures, in accordance with Richardson's equation

By heating a tungsten filament in a low pressure of oxygen its surface may be covered by a monatomic film of oxygen ions, which does not evaporate appreciably below 1600° K and which raises the electron affinity of the surface to 9.2 volts. On this surface, atoms such as those of copper, which have ionising potentials below about 9 volts, can be converted into positive ions, although others (such as mercury) with ionising potentials of 10 volts or more, do not form positive ions.*

Cæsium ions are held more firmly by the adsorbed oxygen film than by a surface of tungsten, so that with a cæsium vapour pressure (at 30° C) of only 0.0029 bar, the surface remains practically completely covered by cæsium ions, up to a filament temperature of 1000° K, and thus the electron emission reaches the high value of 0.35 ampere per cm^2 .

Since these results were published, detailed experimental studies of these phenomena have been made and the theory has been further developed. Full presentation of the data and the derivation of the theoretical results will be reserved for a paper to be submitted to the *Physical Review*, while in the present paper the aim will be to outline the view-point which has been arrived at and to state conclusions.

Thermal Ionisation of Cæsium Vapour.

The degree of thermal ionisation of cæsium vapour may be calculated from the ionising potential by the modified form of Saha's equation given by Fowler and Milne (*Monthly Notices, Roy. Astron. Soc.*, vol. 83, p. 403 (1923)). The ionisation of cæsium vapour at a pressure of 0.001 bar and 1200° K should be 0.00095, or only one-tenth per cent. A similar calculation for the degree of thermal excitation (corresponding to the first resonance potential of 1.48 volt) is only 6×10^{-7} .

Saha (*Phil. Mag.*, vol. 46, p. 534 (1923)) has attempted to calculate the electric conductivity of cæsium vapour from the degree of thermal ionisation, but has obtained results only partly in accord with experiments.

Let us consider an enclosure at 1200° K, having walls of tungsten and containing cæsium vapour corresponding to a pressure (ions + atoms) of 0.001 bar. Our experiments have shown that practically all cæsium atoms which strike tungsten surfaces at this temperature are converted into ions and

* Kingdon, *Phys. Rev.*, vol. 23, pp. 774, 778 (1924).

leave the surface in this condition. The normal free path of the caesium atoms, being of the order of 10^4 cm at this pressure, is so great that, with an enclosure of reasonable size, practically every atom or ion in any element of volume will have collided with the walls many times since its last collision with another particle in the free space. It is thus clear that nearly all the caesium atoms in a small enclosure at 1200° K must be converted to ions

At first sight this conclusion seems to be entirely inconsistent with the degree of ionisation of 10^{-3} calculated from the Saha equation. But we must remember that in calculating the degree of ionisation it was assumed that the concentrations of electrons and ions in the ionised gas are equal*. Since the walls of the enclosure give off electrons, there is no necessary relation between the concentrations of the ions and the electrons. What Saha's equation really gives is the equilibrium constant,

$$K_n = \frac{n_e n_p}{n_a}, \quad (1)$$

where n_e , n_p , and n_a are respectively the number of electrons, of positive ions and of atoms per unit volume. The value of K_n , when n_e , n_p , and n_a denote the numbers of particles per cm^3 , is given by

$$\log_{10} K_n = 15.385 + \frac{3}{2} \log_{10} T - \frac{19530}{T} \quad (2)$$

At 1200° K the value of K_n is 5340. The electron emission from any metal is given by

$$I = AT^2 e^{-b/T} \quad (3)$$

where, for pure tungsten, $A = 60.2$ amperes per $\text{cm}^2 \text{ deg}^{-2}$ and $b = 52,600$ degrees. The electron density n_e is obtainable from the electron emission I by the relation

$$n_e = \left(\frac{2\pi m}{e^3 kT} \right)^{1/2} I = 4.034 \times 10^{18} \frac{I}{\sqrt{T}}, \quad (4)$$

I being expressed in amperes per cm^2 and n_e in electrons per cm^3 .

Thus we find that n_e , the number of electrons per cm^3 in equilibrium with tungsten at 1200° K, is 9.25. Inserting this value of n_e in equation (1) together with the above value of K_n , 5340, we obtain $n_p/n_a = 577$. Thus if 578 caesium atoms or ions strike a tungsten surface at 1200° K, an average of only one will leave the surface as a neutral atom, while 577 leave as ions. This conclusion is in accord with the experiments.

* This tacit assumption in Saha's recent paper is largely responsible for the discrepancy between his conclusions and the experimental data.

Suppose, on the other hand, the walls of the enclosure are completely covered by a single layer of thorium atoms. The electron emission for the surface is then given by equation (3), with the constants $A = 7.0$ and $b = 31,200$, so that by equation (4) we find $n_e = 6.0 \times 10^7$. Then by equation (1) we obtain $n_p/n_a = 8.9 \times 10^{-5}$. This means that only one atom of 11,000 striking a fully thoriated tungsten surface would leave it as an ion. This is in accord with the observation that the positive ion emission from a thoriated filament in caesium vapour is negligible compared with that from pure tungsten.

Table I—Thermal Ionisation of Cæsium Vapour in Contact with Pure Surfaces of Tungsten and Thoriated Tungsten.

T	K_{∞}	Tungsten		Thoriated Tungsten	
		n_e	n_p/n_a	n_e	n_p/n_a
500	2.35×10^{-20}	5.56×10^{-37}	4230000	2.52×10^{-9}	9.33×10^{-13}
1000	2.26	1.10×10^{-4}	2060	2.52×10^8	8.96×10^{-9}
1200	5.34×10^3	9.25	577	6.00×10^7	8.90×10^{-9}
1500	1.34×10^7	8.29×10^1	162	1.52×10^{10}	8.80×10^{-9}
2000	3.72×10^{10}	8.22×10^8	45.3	4.25×10^{13}	8.75×10^{-9}
2500	4.67×10^{13}	2.21×10^{11}	21.1	1.34×10^{14}	3.49×10^{-9}

Table I gives data for the thermal ionisation of caesium vapour in enclosures of tungsten and fully activated thoriated tungsten. These figures are based on the assumption that the electron emission is that which is characteristic of the material of the walls and is not altered by the presence of the caesium vapour. This assumption is only valid if the temperatures are so high, or the vapour pressure of caesium so low, that no appreciable adsorption of caesium occurs. From the table it appears that caesium vapour in contact with tungsten walls at 500° K should be practically completely converted to ions. That this does not occur can be due only to the presence of adsorbed caesium, which increases the electron emission of the walls.

The degree of ionisation n_p/n_a decreases with rising temperature with tungsten, whereas it increases with thoriated tungsten. The positive ion emission from a pure tungsten surface in presence of caesium vapour is practically always limited by the rate at which the caesium atoms arrive at the surface, so that it is not practicable to use measurements of the positive ion currents from pure tungsten surfaces to determine experimentally the value of K_{∞} , and thus to check the theory.

With pressures of caesium corresponding to room temperature (0.001 bar), the number of positive ions generated becomes small compared to the number of atoms that strike the filament, if the filament temperature is below about 1150° K, but the electron emission at this temperature is too small to measure. At the still lower temperature at which large electron emissions are obtained from the filament due to the adsorbed caesium, the positive ion currents are too small to measure. However, by raising the pressure of the caesium vapour to 0.1 bar or more, it becomes possible to measure the positive ion and the electron emissions at the same filament temperature, and thus obtain data for determining experimentally the degree of thermal ionisation of caesium.

A pure tungsten filament was heated to 1177° K in a bulb containing saturated caesium vapour at 70° C. By applying first positive and then negative potentials to the surrounding collecting electrode, the electron and the positive ion emissions were measured. The currents increased a little with increasing voltage, because of the Schottky effect, so that they were corrected by extrapolating to zero volts by plotting the logarithms of the currents against the square roots of the voltages.*

The electron emission at 1177° K was 2.22×10^{-6} and the positive ion emission 2.06×10^{-6} ampere per cm². The electron emission from a pure tungsten surface at this temperature in absence of caesium is 3.25×10^{-12} . On raising the filament temperature to 1300° K or more, the positive ion current increased to 2.43×10^{-3} , and was then independent of the filament temperature and applied voltage, if this voltage were high enough to overcome the positive ion space charge. This ion current is thus a measure of the rate at which caesium atoms strike the filament and corresponds to 1.52×10^{16} atoms per sec per cm², or a pressure of 0.122 bar of caesium vapour.

At the lower temperature (1177° K) the atoms still strike the filament at the same rate, although the positive ion current is only 1/1180 as great as at the higher filament temperatures. The conditions at the surface of the filament must be essentially the same as though it were surrounded by an enclosure at 1177° K, containing such a concentration of caesium vapour that 1.52×10^{16} atoms strike each square cm per second. This concentration would be

$$n_e = 1.40 \times 10^{13} \text{ atoms per cm}^3$$

which corresponds to a pressure of 0.226 bar.

If the filament were in an enclosure at 1177° K under equilibrium conditions

* S. Dushman, *Gen. Electr. Rev.*, vol. 26, p. 157 (1923).

with this concentration of caesium, the filament would emit and absorb electron and ion currents equal to those measured in the bulb at 70° C. From these observed currents we may thus calculate by equation (4) the equilibrium concentration of electrons and ions. We obtain in this way

$$n_e = 2.60 \times 10^6 \text{ electrons per cm}^3,$$

$$n_p = 1.19 \times 10^9 \text{ ions per cm}^3.$$

Substituting these values of n_a , n_e and n_p , in equation (1) we obtain, for the experimentally determined value of K_n at 1177° K,

$$K_n(\text{exp}) = 2210 \text{ per cm}^3,$$

while calculation from equation (2) at 1177° K gives

$$K_n(\text{calc}) = 2500 \text{ per cm}^3$$

This difference in the two K_n 's corresponds to a very small change in temperature. To obtain $K_n = 2210$ from equation (2), we need only to substitute $T = 1174$ instead of $T = 1177$. The agreement between the observed and calculated values is thus as close as the accuracy of the temperature measurements.

A similar set of data was taken with the filament at 1254° K and the bulb at 80° C, giving a caesium vapour pressure of 0.266 bar. The electron and ion currents were 3.74×10^{-6} and 2.03×10^{-5} ampere per cm.² respectively. The value of K_n found from these measurements was 16,600, while equation (2) gives 28,700. The error is larger, but the experimental value corresponds to that given by equation (2) at $T = 1236^\circ$, which agrees reasonably well with the observed temperature of 1254°. These experimental determinations of the thermal ionisation of caesium vapour thus give results in full accord with Saha's equation, and verify the Sackur-Tetrode value of the chemical constant as applied to ionisation.

In these experiments the ion currents used in determining n_p corresponded to a negligible fraction of the atoms striking the surface (n_a). When n_p calculated from the ion current is not negligible compared to the n_a corresponding to the caesium pressure, there will be an appreciable departure from the equilibrium conditions. An analysis of the kinetics of the positive ion emission has led to the following equation for calculating K_n under these conditions,

$$K_n = \frac{n_e n_p}{n_a - n_p}. \quad (5)$$

Thus the effective concentration of caesium is not n_a , but is $n_a - n_p$.

If the collecting electrode is made positive, the positive ion current and n_p fall to zero, so that the effective concentration corresponds to n_a . Thus the amount of adsorbed caesium will be greater when the collector is made positive. For this reason, n_p in equation (5) cannot be determined from measurements of electron emission unless it is known that the amount of adsorbed caesium is too small to influence the emission. This condition, however, seems to be fulfilled with partly activated* thoriated filaments at high temperatures, for the electron emission at temperatures above 1300° is not altered when the caesium vapour pressure is raised from 0 to 0.008 bar.

A series of measurements were made of the positive ion currents and the electron currents from thoriated filaments in various states of activity. The ion currents for fully activated thoriated filaments were about 1 per cent of those from a deactivated filament for which the current was limited by the supply of caesium atoms.

The currents from the less active filaments decreased as the filament temperature was raised, while those from the more highly activated filaments increased with temperature, quite in accord with the calculated temperature variations of n_p/n_a given in Table I. But the values of K_n calculated from these data by equation (5) came out from 4 to 50 times too great. It is probable that the discrepancy is due to lack of homogeneity of the adsorbed thorium film. A few minute regions having less than the normal amount of thorium would have little effect on the electron emission, but would increase the positive ion emission and thus give too large values for K_n . Further experiments will be made to investigate these effects in more detail.

Space Charge Effects—Since in general the electron density n , and the ion density n_p are not equal, there will be space charges around a heated body in caesium vapour. For example, in a large enclosure having tungsten walls at, say, 1500° K, there is a positive space charge, which makes the potential of the space in the enclosure higher than that of the walls. This field repels ions and attracts electrons, and thus makes the concentration of the particles of the two signs in the centre of the enclosure more nearly equal. At a considerable distance from the walls the space charge and the potential gradient thus disappear, but the potential in this region may differ by several volts from that near the walls. By simultaneous solution of the Boltzmann and

* A thoriated filament is said to be *activated* when thorium is brought to its surface by diffusion from the interior, thus increasing its electron emission. A full discussion of the methods of activating these filaments and the theory of these effects was given by Langmuir, *Phys. Rev.*, vol. 22, p. 357 (1923).

Poisson equations, the potential distribution near a plane electrode can be worked out *

The Adsorbed Film of Cesium — Both electrons and ions, when they approach within less than about 10^{-8} cm of a metallic surface, are acted upon by strong forces (electric image forces) drawing them towards the surface, because of the charges of opposite sign which the particles induce in the surface. Each singly charged particle is thus attracted to the surface by a force equal to $e^2/(2x)^2$, so that within the range of this force the particles are distributed *as though* they were subjected to a potential equal to $\pm e/(4x)$ in addition to the potential resulting from space charge

Since the former potential is a fictitious one, called into play only by the presence of the particular particle upon which it acts, much confusion will be avoided if the term *potential* is not applied to it. It is, in fact, what the electro-chemist calls “electromotive force.” However, since it is measured in volts it is better not to call it a “force,” it is therefore suggested that the term *motive* be used. The *motive* is thus defined as a scalar quantity whose gradient, in any direction and at any point, represents the force-component per unit charge which *acts on an electron or ion*. The motive thus includes the potential

The concentrations n_e and n_p just beyond the range of the image force are given by equation (1), so that the product $n_e n_p$ remains constant. But within the region of the image force both n_e and n_p increase as the surface is approached, the increase of concentration being calculated from the Boltzmann equation

$$n_1/n_2 = e^{Ee/kT} \quad (6)$$

where n_1 and n_2 are the concentrations in two regions between which the motive difference is E .† Thus close to the surface the product $n_e n_p$ increases rapidly. This does not violate thermodynamic principles, because the ionising potential, which was used in calculating K_n according to equation (2), becomes a function of the distance of an atom from a surface when the atom is in the region of the image forces

We believe that the formation of an adsorbed film of cesium on a tungsten

* Since deriving the equations for this case and applying them to cesium vapour, we have found that the subject of space charge under equilibrium conditions in presence of positive ions and electrons in a metallic vapour has been treated mathematically in a recent paper by Laue, *Sitzber Preuss Akad. d Wiss* (December 6, 1923), p. 334.

† The signs of these quantities are omitted, for they are different for positive and negative charges and may be readily supplied when needed.

surface is largely the result of the high concentration n_i of ions within the region of the image force. The motive corresponding to the image force is equivalent (according to Poisson's equation) to a fictitious space charge, n_f (electrons per unit volume), given by

$$n_f = \frac{1}{8\pi x^3} = \frac{0.040}{x^3} \quad (7)$$

where x is the distance from the surface. The actual space-charge densities in the image region are enormous compared to those outside this region, but nevertheless they are usually negligible compared to n_f except when x is less than about 2×10^{-8} cm.

Thus there are no appreciable *potential differences*, such as would be necessary to alter the contact potential of a metal, except within atomic distances of the surface. Since changes in contact potential always accompany changes in electron emission, we conclude that a modification of the electron emission of a surface by caesium vapour is not due to an electron and ion atmosphere, as was suggested in our paper in *Science*, but can only be due to caesium ions or atoms in a monatomic layer on the surface.*

The concentration of ions in the image region is dependent on that outside this region, and, in fact, will be proportional to it, if the concentration is not too high. Thus, considering the data of Table I, we may understand why caesium vapour does not appreciably raise the electron emission of a fully thoriated surface at any temperature, whereas that of tungsten at 700° K may be increased 10^{16} -fold. Each adsorbed ion on the surface draws electrons into its neighbourhood and this partly offsets its positive charge. Probably considerations apply to the distribution of electrons around the adsorbed ion somewhat similar to those that Debye and Hückel† have applied to solutions of strong electrolytes.

If the adsorbed atoms are relatively far apart they probably repel one another, because of their excess of positive charge. But as they become more closely packed, the electron concentration in the spaces between the ions, varying as it does exponentially with the potential (equation 6), must increase very rapidly, and thus, as we shall see, the ions tend to be drawn together and exhibit properties like those of the molecules of liquids.

We are thus led to the conception of an *equation of state* for the adsorbed

* We shall show that in the adsorbed film no distinction can be drawn between atoms and ions.

† Debye and Hückel, *Phys. Zeit.*, vol. 24, p. 334 (1923).

caesium atoms. It has been possible, by measurements of the electron emission of tungsten filaments in presence of caesium vapour, to gain much quantitative information as to this equation of state, and also to determine the energy changes involved in the adsorption of caesium on tungsten or on a film of oxygen ions. This work is still in progress, and it is hoped that it can be extended to give the complete equation of state for even concentrated (close-packed) adsorbed films. It would seem that a study of the growth of these films, from the dilute (2-dimensional gas) state to the concentrated (liquid or solid), should throw much light on the state of the electrons within metals.

Qualitatively we have very direct evidence of the existence of two "phases" in the adsorbed films by measurements already briefly described in the paper in *Science*. The positive ion emission from a tungsten filament in caesium vapour increases discontinuously as the temperature is raised. At a certain temperature a large positive ion emission begins at one point of the filament and then spreads at a uniform rate along the filament until the whole filament gives the higher emission. If while this process is occurring the temperature is lowered, the rate of spreading of the active region is decreased, or the boundary may even be made to move back again. There are thus two distinct surface phases (a concentrated and a dilute phase) with a definite boundary between them.

Electron Emission from Dilute Caesium Films adsorbed on Tungsten

Consider a tungsten surface at such high temperature in caesium vapour that only a small fraction of its surface is covered by adsorbed caesium. The concentration n_s of ions just outside the region of the image force will be high compared to n_a , the concentration of atoms. The ions strike the surface at a rate proportional to n_s . Since the adsorbed film is dilute, the ions on the surface evaporate independently of one another, and thus the rate of evaporation of ions is proportional to n_s , the number of adsorbed ions per cm.²; so we may place

$$n_s = cn_a. \quad (8)$$

Here c is a constant at a given temperature, which is proportional to the probability of evaporation per unit time for any adsorbed ion.

It has been shown by one of us,* both theoretically and experimentally, that for dilute adsorbed films the logarithm of the electron emission is a linear function of n_s , so that

$$\frac{d \log n_e}{dn_s} = B, \quad (9)$$

* I. Langmuir, *Phys. Rev.*, vol 22, p 364 (1923).

where B is a constant at a given temperature. Combining equations (8) and (9) with (1) and integrating, we find

$$n_s \log \frac{n_s}{n_{s0}} = \frac{BK_s}{c} n_s, \quad (10)$$

where n_{s0} is the value of n_s , which corresponds to $n_0 = 0$, i.e., a surface of tungsten without adsorbed caesium. We thus see that, as the caesium pressure varies, $I \log (I/I_0)$ should increase in proportion to the pressure of caesium vapour, and that from the constant of proportionality, since we know K_s , we can determine B/c .

Experiments made for the purpose of testing this conclusion have given data in good agreement with this theory. Filament temperatures from 1450° to 1800° K were used and the caesium vapour pressures ranged from 0 to 4.07 bars (bulb at 120° C). Filament temperatures of at least 1450° were needed to give sufficient electron emission, and the high caesium vapour pressures were required to give a sufficient increase in emission to test the theory. At 1470° the electron emission with 4.07 bars of caesium vapour was 1300 times, while at 1790° it was only 3.6 times, that of a pure tungsten surface.

The conclusions drawn from these experiments are—

(1) The quantity $I \log (I/I_0)$ is proportional to the pressure of caesium vapour within the probable experimental error, except that at the highest pressures with the lowest filament temperatures the value is too high, probably because the surface film is no longer dilute. The agreement with the theory is in fact excellent for all cases where θ does not exceed about 0.13. For $\theta = 0.21$ the function $I \log (I/I_0)$ is about 1.8 times the calculated value (at 1470° K).

(2) The pure number BK_s/c has practically no temperature coefficient, and has the value 8.8×10^{-4} .

(3) Since B is approximately inversely proportional to the filament temperature, the temperature coefficient of c is only slightly less than that of K_s . By the Clapeyron equation we can thus find the heat of evaporation of positive ions from the dilute adsorbed film and obtain a value corresponding to 3.97 volts.

(4) It has been found that the values of B defined by equation (9) range from about 2.5×10^{-13} at 1500° K to 2.1×10^{-13} cm.² at 1800° K. Thus the values of c are given by

$$\log_{10} c = 9.02 + 0.5 \log_{10} T - \frac{19530}{T}. \quad (11)$$

This equation gives data for the rate of evaporation of adsorbed caesium ions on tungsten.

The Gibbs equation for the adsorption isotherm may readily be put in the form

$$\frac{d\Gamma}{d \log n_p} = n_p kT, \quad (12)$$

where Γ represents the spreading force (in dynes per cm) of the adsorbed film, which corresponds in the 2-dimensional film to a pressure in a 3-dimensional gas. An equation of state for the film is thus an equation which expresses Γ as a function of n_s and T . To obtain such an equation* we merely need to obtain a relation between n_p and n_s in order to eliminate n_p from equation (12)

But in equation (8) we have such an equation between n_p and n_s for dilute films. Combining this with equation (12), integrating, and fixing the integration constant by the condition that $\Gamma = 0$ when $n_s = 0$, we obtain as our equation of state for dilute films

$$\Gamma = n_s kT, \quad (13)$$

which corresponds exactly in 2-dimensional gases with the law $p = nkT$ for ideal 3-dimensional gases. Since, at constant temperature, the assumption $c = \text{constant}$ in equation (8) was verified by the experiments, we may take the foregoing analysis as proof that the dilute caesium films follow the laws of ideal gas films. This means that the spreading force of such films is due primarily to thermal agitation and not to repulsive forces between neighbouring adsorbed ions.

When the amount of adsorbed caesium became so great ($\theta = 0.21$) that the film was no longer dilute, we have seen that the electron emission increased faster with the caesium pressure than it should according to the theory for dilute films. This means that Γ increased less rapidly than in proportion to n_s , and thus the adsorbed ions exerted *attractive forces* on one another. We shall find further support for this conclusion in our study of concentrated adsorbed films.

The energy changes involved in the formation of dilute adsorbed films throw considerable light on the mechanism by which adsorbed atoms are held on the surface. Since the energy required to remove an adsorbed atom in the form of a positive ion is approximately the same as the ionizing potential of the atom, it is probable that the relation between the positive kernel of an adsorbed atom (the Cs^+ ion) and the electrons of the tungsten surface is substantially the same as that between the kernel and the valence electron of a free atom. Thus a

* This method of obtaining an equation of state for adsorbed films has been applied to films on liquids by Langmuir, *Journ. Amer. Chem. Soc.*, vol. 39, p. 1888 (1917).

caesium atom on a tungsten surface shares its valence electron with the tungsten very much as pairs of electrons are shared between atoms joined by the covalence bond. From this view-point there can be no real distinction between atoms and ions adsorbed on a metallic surface.

If we think of an adsorbed caesium ion on a surface as having united with, or as sharing one of the "free electrons" of, the tungsten, it may seem at first as though these atoms should be capable of evaporating as such with relatively little energy change. A closer analysis, however, shows that this is not the case.

Let U_i represent the energy associated with the ionization of a caesium atom in free space (i.e., the ionizing potential). Let U_a be the energy required for the removal of an adsorbed caesium atom (or ion) in the form of an atom. Let U_p be the energy used to remove an atom from the surface in the form of a positive ion, and finally let U_e be the work needed to remove an electron from the metallic surface. We can get an atom from the surface into the free space either by removing it as such or by removing an electron and an ion separately and then allowing these to combine in the free space. Thus we find the relation

$$U_a = U_p + U_e - U_i \quad (14)$$

For a tungsten surface having very little caesium on it $U_e = 4.54$, $U_p = 3.97$ and $U_i = 3.88$ volts, and the equation then gives us $U_a = 4.63$ as the energy involved in the evaporation of an atom as such. If $U_p = U_i$ we see that $U_a = U_e$. Thus the energy adsorption of free atoms is determined principally by the electron affinity of the metal, and results from the fact that the metal is able to take the electron that is brought to it by the atom as one of its own electrons, even though this electron is shared by the atom. Of course, the electrons which are shared by a given atom may be, and probably are, continually changing, but the conception of shared electrons is not altered thereby.

Concentrated Adsorbed Films of Caesium on Tungsten — At sufficiently low temperatures a tungsten filament in presence of caesium vapour becomes completely covered with a layer of adsorbed caesium atoms ($\theta = 1$). As the temperature is raised the emission increases, apparently in accord with the Richardson equation (equation 3), the logarithm of the electron current being practically a linear function of the reciprocal of the temperature. At a certain temperature (for each pressure of caesium) the current reaches a maximum and then decreases as the temperature is raised, since the adsorbed caesium evaporates at these higher temperatures and θ becomes much smaller than unity.

The families of curves in fig 1 give a summary of about 220 determinations of the electron emission of filaments in presence of caesium vapour. The curves have been drawn accurately from the experimental data and may be used for quantitative calculations if desired. The ordinates are the common logarithms of I_e , the electron current densities in amperes per cm.², and the abscissas are the reciprocals of the absolute temperatures of the filament, multiplied by 1000 for convenience. The temperature of the bulb which fixed the vapour pressure of the caesium is given in degrees Centigrade on each curve. The two upper curves, which appear distinctly different from the rest, were obtained with filaments which were completely covered by a film of oxygen ions before admitting the caesium vapour. The other nine curves were obtained with pure tungsten filaments which had been flashed at high temperature to remove all impurities from the surface before the readings were taken. The caesium film condensed on them, of course, when the filament temperature was lowered to that at which the currents were read.

Considering now the curves obtained with the caesium adsorbed on the pure tungsten surface, we see that each curve consists of 3 parts:—

I A low-temperature region where the emission apparently follows Richardson's equation, giving a straight line descending to the right in fig 1.

II An intermediate region where the plot in fig 1 is curved, the current reaching a maximum as the temperature is raised and then falling. This region may be regarded as a transition curve between the straight portions I and III.

III A high-temperature region, where the plot in fig 1 becomes straight again, but the current decreases with rising temperature. An equation of the Richardson type may be used to represent these lines, but the quantity b would then have a negative value.

Fig. 1 shows that both in Regions I and II the straight lines at the various pressures are approximately parallel to one another. The envelope of the family of curves is a straight line, shown as the dashed line AB. All the curves of the family are, in fact, very nearly alike,* and differ principally in being displaced in a direction parallel to AB. These displacements are found to be proportional to the logarithms of the pressures of caesium.

These conclusions may be summarized by saying that these electron emission data are given by the equation

$$\log I_e + M \log p = f(1/T + N \log p), \quad (15)$$

* This is only approximate. It will be noticed that the curves for the higher pressures have the sharper curvature in Region II.

where M and N are constants and f denotes a function characteristic of the shape of the curves in fig 1. From the data we find that the actual values of M and N are

$$M = -0.83, \quad N = 4.4 \times 10^{-5} \text{ deg}^{-1}$$

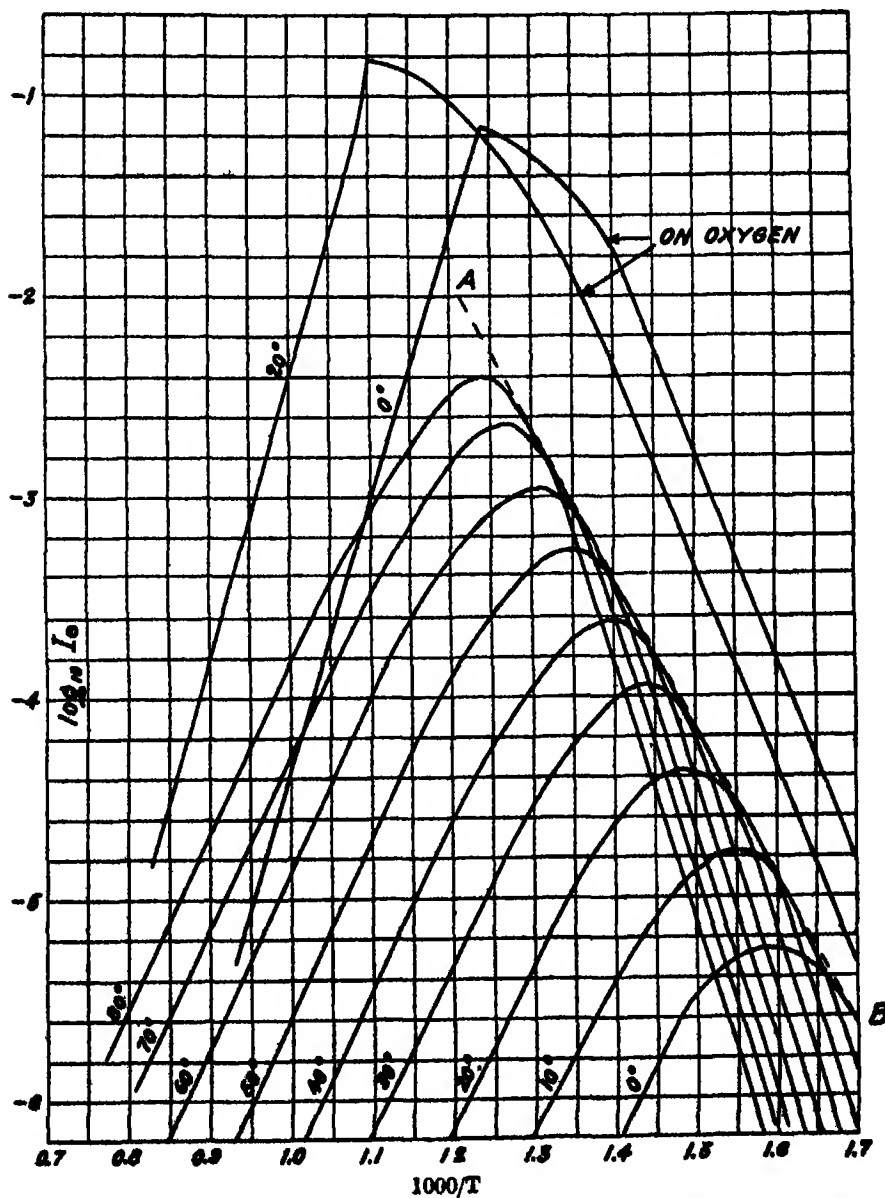


FIG. 1.—Electron emission from Tungsten filaments in Cesium vapour at various pressures

The pressures of caesium vapour used in these calculations were found by measurements of the positive ion currents obtained with filament temperatures of about 1500° K, where all the atoms that strike the filament are converted to ions. The vapour pressures obtained in this way are accurately given by the equation (p in bars)

$$\log_{10} p = 10.65 - \frac{3992}{T}. \quad (16)$$

From these considerations it may readily be seen that in Regions I and III the electron emission of a tungsten filament of temperature T in caesium vapour at a pressure p is expressible approximately by the equation

$$I_e = \alpha p^\gamma e^{-\beta/T}, \quad (17)$$

where α , β and γ are constants.

The data illustrated in fig. 1 give the following values of the constants, when I_e is in amperes per cm² and p in bars —

	α	β	γ
Caesium on Tungsten			
Region I	6.65×10^{14}	+31300	-0.70
Region III	8.6×10^{-12}	-19100	+1.66
Caesium on Adsorbed Oxygen			
Region I	1.04×10^{10}	+23400	-0.62
Region III	2.95×10^{-11}	-32200	+1.96

According to the Clapeyron equation, the heat of evaporation may be calculated from the temperature coefficient of the vapour pressure, θ remaining constant. We may generalize this and associate an energy change U_{yz} with any particular phenomenon, which varies with the temperature in such a way that the logarithm of any measured quantity y is a linear function of the reciprocal of the temperature, while another quantity x (for example, the pressure) is held constant as the temperature is changed. Thus we define U_{yz} by

$$U_{yz} = \frac{k}{e} \left(\frac{\partial \log y}{\partial (1/T)} \right)_x. \quad (18)$$

The electron charge e is used in the denominator in order to express U in the convenient form of a potential. To obtain U in volts the value of e/k may be taken to be 11600° per volt.

We can also generalize the definition of γ by the relation

$$\gamma = \left(\frac{\partial \log I_e}{\partial \log p} \right)_T, \quad (19)$$

which is consistent with equation (17)

In this way, by combination with equation (1), we may obtain the equation

$$U_{ps} = U_K - \frac{1}{\gamma} U_{ea} + \frac{1-\gamma}{\gamma} U_{es} \quad (20)$$

Here U_{ps} refers to the temperature coefficient of the *positive* ion concentration n_p near a filament, while θ is kept constant. It is therefore the heat of evaporation of ions. The quantity U_{ea} measures the temperature coefficient of the electron emission, while the pressure (concentration of atoms) remains constant. It corresponds to the value of β in equation (17). The quantity U_K measures the temperature coefficient of K_a , and is thus equivalent to the ionizing potential, while U_{es} corresponds to the temperature coefficient of the electron emission at constant θ , and thus measures the heat of evaporation of electrons.

The data of fig. 1 enable us to determine U_{ea} , we already know U_K , and thus by equation (20) we obtain a relation between U_{ps} and U_{es} , but in general we cannot determine these quantities separately from this equation. However, when $\gamma = 1$ the term involving U_{es} drops out, so that for this case we obtain the actual value of U_{ps} —

$$U_{ps} = U_K - U_{ea} \quad (21)$$

Similarly, for the case of $\gamma = 0$, the equation reduces to

$$U_{ea} = U_{es}. \quad (22)$$

It should be noted that these conclusions have been reached without assuming any knowledge of the relation between I_a and θ . If this relation were known* with sufficient accuracy for very concentrated films ($\theta > 0.9$), we should be able to determine U_{ps} and U_{es} separately for any value of θ .

Since γ is negative in Region I, and positive and greater than unity in Region III, it must pass through the values 1 and 0 while in Region II. The points for which $\gamma = 0$ are those where the curves of fig. 1 are tangent to the envelope AB, while the points corresponding to $\gamma = 1$ lie a very short distance to the left of the points where I_a is a maximum. We thus find that for $\gamma = 0$, $U_{es} = -1.24$ volts, which is thus the calculated heat of evaporation of the electrons. This value of γ corresponds roughly to about $\theta = 0.90$.

With $\gamma = 1.0$, which occurs at about $\theta = 0.87$, the value of U_{ps} is -4.3 volts. Thus the heat of evaporation of ions from these concentrated films is a little greater than the value -4.0 volts, which we found for the dilute film by an

* The linear relation between $\log I_a$ and θ , proposed by Langmuir, is a fairly good approximation up to $\theta = 0.9$ or even higher, but is not sufficiently accurate for the present purpose. A fuller discussion will appear in the *Physical Review* article.

entirely different method. The data are consistent with the assumption that U_{ee} varies gradually and steadily from -4.0 to -4.3 as θ increases from 0 to 0.9. If we make this assumption, we may calculate U_{ee} by equation (20) for all values of θ for which we know U_{ee} . Thus we find that U_{ee} , the heat of evaporation of the electrons in Region I, is about 1.5 volts and in Region III ($\theta = 0.7$) is about 1.8 volts. These data for U_{ee} are only rough, but are in general accord with our knowledge that the heat of evaporation of the electrons is greatly decreased by adsorbed caesium and must vary roughly linearly with θ . A thorough check of this part of the theory may require direct determinations of the heat of evaporation by its cooling effect. Contact potential measurements have been made with caesiated filaments and agree in general with these conclusions, but their accuracy is not yet as high as is desired.

For the caesium film on adsorbed oxygen, the heat of evaporation of ions U_{ie} comes out as 5.13 volts for $\theta = 0.95$. This is distinctly higher than that of ions adsorbed directly on tungsten and accounts for the much lower rate of evaporation of ions from the oxygen film.

An analysis of all these data from the thermodynamic standpoint by Gibbs' equation leads to the following conclusions -

With very dilute caesium films ($\theta < 0.15$) the spreading force Γ increases in proportion to θ , and in this range γ increases slowly from 0 up to nearly unity. At $\theta = 0.5$ to 0.8, γ is approximately 1.65, so somewhere between about $\theta = 0.2$ and $\theta = 0.5$, γ must be equal to unity. At this point Γ must reach a *maximum* value and then decrease as γ increases above unity. This means that strong attractive forces should render the film inherently unstable, and it should have a tendency to separate into two phases, just as has been observed in connection with the measurements of positive ion currents. However, in taking the data illustrated in fig. 1 (although in Region III Γ must decrease with rising θ), we have not observed any effects which would indicate separate surface phases.

At still higher values of θ in Region II, in the neighbourhood of $\theta = 0.87$, γ decreases again and passes through the value unity. Beyond this point Γ must again increase with rising θ , indicating that repulsive forces are beginning to come into play as the film approaches saturation.

Finally, when θ is about 0.90, γ becomes zero and then becomes negative. In this region the electron emission actually decreases as more caesium atoms become packed into the adsorbed film.

Summary

1. From thermodynamic considerations involving the Saha equation, there must be a relation between the *positive* ion emission from a heated filament in the vapour of an alkali metal and the electron emission from this surface

2 At high-filament temperatures and low pressures of the vapour, the electron emission is the same as in the absence of the vapour, so that the positive ion emission from different filaments in various vapours can be calculated Experiments with caesium and other metallic vapours, and with tungsten filaments and oxygen-coated and thorium-coated filaments, give results in accord with this theory Measurements of the positive ion and electron emissions from tungsten filaments in caesium vapour give values for the thermal ionization of caesium vapour at about 1200° K in excellent agreement with the Saha equation

3. At high-filament temperatures the positive ion emission becomes limited by the rate at which the vapour comes into contact with the filament, all atoms striking the filament being converted into ions This permits quantitative measurements of the vapour pressure to be made The vapour pressures of caesium (in bars) are given by

$$\log_{10} p = 10.65 - \frac{3992}{T}.$$

4 At lower filament temperature the electric image force causes a fraction θ of the filament surface to be covered by a layer of adsorbed ions which share electrons with the underlying metal The resulting double-layer causes an increase in electron emission and a corresponding decrease in positive ion emission Electron emissions of over 0.3 ampere per cm² at 1000° K may be obtained in caesium vapour at 30° C

5 The theory of dilute adsorbed films ($\theta < 0.2$) is developed and the equation of state for the adsorbed film is found to correspond to the ideal gas laws For more concentrated films, attractive forces draw the ions together and under certain conditions cause separate 2-dimensional phases to appear.

6 The heat of evaporation of the adsorbed caesium atoms on tungsten in the form of ions corresponds to 4.0 volts for dilute and 4.3 volts for concentrated films From adsorbed oxygen on tungsten the heat of evaporation of caesium ions is 5.1 volts

1 : 2 . 3—*Triaminopropane and its Complex Metallic Compounds.*

By FREDERICK GEORGE MANN, Ph D , and SIR WILLIAM JACKSON POPE, F.R S

(Received September 18, 1924)

The co-ordination theory of Werner (' Ann ,' vol 322, p 261 (1902)) has led to a great advance in our knowledge of complex metallic compounds , as applied to such compounds as hexamminocobaltic chloride $[\text{Co}(\text{NH}_3)_6]\text{Cl}_3$, it involves the assumption that the six component ammonia groups are situated at the apices of a regular octahedron of which the cobalt atom occupies the centre, and that the complex so constituted—the co-ordinated group—acts as a tribasic ion which combines as a whole with three equivalents of an acidic radicle For the purpose of discussing the possibilities of geometrical arrangement of the component parts of a co-ordinated group, it will be convenient to number the octahedron apices in the following manner. The outline of the plan of a regular octahedron on one of its triangular faces is bounded by a regular hexagon, each apex of which represents an angular point of the octahedron , let these latter points be numbered consecutively from one to six On the basis of this nomenclature the isomeric praseo- and violeo-compounds of the composition, $[\text{Co}(\text{NH}_3)_4\text{Cl}_2]\text{Cl}$, become, respectively, the 1 2 . 4 : 5-tetrammino-3 6-dichlorocobaltic chloride and the 1 2 3 5-tetrammino-4 6-dichlorocobaltic chloride

Werner's theory indicates the possibility of stereoisomerism, accompanied by optical activity, when certain of the six ammonia groups in hexamminocobaltic chloride are replaced by differently constituted radicles , in this respect a close correspondence has been observed between theoretical anticipation and experimental results A similar concordance between prevision and realisation has been found among compounds in which pairs of ammonia groups in the hexamminocobaltic chloride are replaced each by one molecule of ethylenediamine , theory indicates that the *ter*ethylenediaminecobaltic chloride, $[\text{Co}(\text{NH}_2\text{CH}_2\text{CH}_2\text{NH}_2)_3]\text{Cl}_3$, should be resolvable into enantiomorphously related components which contain the 1 . 2, 3 4, 5 6- and the 2 3, 4 5, 6 1-*ter*ethylenediaminecobaltic co-ordinated groups respectively, and salts of these two optically active radicles have been prepared

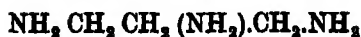
It may be stated that a very close agreement exists between the anticipations of the Werner theory and the observed facts in so far as concerns complex metallic compounds of the co-ordination number six in which univalent or

bivalent radicles or both are associated with the metallic atom within the co-ordinated group, the correspondence extends so far as to provide examples of internal compensation of the mesotartaric acid type among such salts. Since this close correspondence exists among compounds of the types named above, indicating that the theory is much more than a mere hypothesis, it seems highly desirable to extend the development of the whole subject to the study of compounds of the first type mentioned, in which triads of univalent groups are replaced each by one tervalent radicle such as 1 2 3-triaminopropane. A little consideration will show that kinds of isomerism might thus arise which would be entirely different in character from those hitherto realised and which have provided the theory with so solid an experimental foundation. Thus the compound $[\text{Co}(\text{NH}_2\text{CH}_2\text{CH}_2(\text{NH}_2)\text{CH}_2\text{NH}_2)_3]\text{Cl}_3$ might exist in the following isomeric forms: the 5 1 3, 2 4 6-*bistriaminopropanecobaltic* chloride, which should not be resolvable into optically active components, the 5 1 3, 6 2 4- and the 5 1 3, 4 6 2-isomerides, which should be obtained as an externally compensated product and should be resolvable, the 5 1 2, 3 4 6-isomeride, which would not be resolvable and should differ from the foregoing in that the points of attachment of the triamine molecule to the cobalt atom lie at three points of a square cross-section of a regular octahedron, whilst in the former types the triamine molecule is bent to an angle of 60° as between its two halves.

The subject here introduced is obviously, a large one. It may be extended usefully in the manner which Werner adopted with such brilliant results in types of cases which he studied, and may be further developed by the use of diaminomono-carboxylic acids or other compounds of mixed function, and of tricarboxylic fatty acids, and extended to the study of complex metallic compounds containing tetramines and like polyvalent components.

The first practical difficulty encountered in connection with the study of complex metallic compounds containing triacidic amines arises from the fact that the aliphatic triamines have been but little examined and are not easy to prepare. In the present paper we therefore confine ourselves to the description of an efficient method for preparing the most simple of the aliphatic triamines, the 1 2 3-triaminopropane, $\text{NH}_2\text{CH}_2\text{CH}_2(\text{NH}_2)\text{CH}_2\text{NH}_2$, and of a few compounds which prove the existence of the new class of complex metallic compounds represented by substances of the type of *bistriaminopropanecobaltic* chloride, $[\text{Co}(\text{NH}_2\text{CH}_2\text{CH}_2(\text{NH}_2)\text{CH}_2\text{NH}_2)_2]\text{Cl}_3$.

1 2 3-Triaminopropane.



1 2 3-Triaminopropane was first prepared by Brackebusch ('Ber.', vol 6, p 1290 (1873)), who converted 1 2 3-tribromopropane by the action of silver nitrite into trinitropropane, which on reduction gave the required base, the yield was low owing to contamination of the trinitropropane with trinitroglycerol, and no physical constants or analyses of the base are given. Gabriel and Michels ('Ber.', vol 25, p 3056 (1892)) prepared 1 2 3-triphtalimidopropane, which, however, on hydrolysis gave no triaminopropane. The latter was finally synthesised by Curtius and Hesse ('Jour. pr. Chem.' [11], vol 62, p 232 (1900)), who converted triethyl tricarballoylate into the corresponding trihydrazide, which when treated with nitrous acid gave tricarballoylic triazide. The latter on treatment with alcohol furnished glycerol triethylurethane, which on hydrolysis with hydrochloric acid gave the 1:2 3-triaminopropane trihydrochloride.

This synthesis, however, is unsuitable for the preparation of the base in large quantities, for, apart from the explosive nature of the intermediate compounds, the reduction of aconitic to tricarballoylic acid is a long and tedious process. Attempts were therefore made to condense 1.2 3-tribromopropane with three equivalents of *p*-toluenesulphonylsodamide, and to obtain the base by the hydrolysis of the tri-*p*-toluene sulphonamidopropane thus obtained, all such attempts proved unsuccessful, however, as under most favourable conditions only a mixture of the mono- and di-*p*-toluenesulphonamido-compounds was obtained. Since Curtius and Hesse (*loc cit*) state that tribenzoyltriaminopropane readily gives the base on acid hydrolysis, attempts were next made to prepare the former compound by the condensation of 2 3-dibromopropylbenzamide (Kay, 'Ber.', vol 26, p 2848 (1893)) with two equivalents of the sodium derivative of benzamide. These attempts also proved fruitless, owing probably to the ready conversion of the dibromopropylbenzamide into brominated oxazoline derivatives. The use of potassium phthalimide, *p*-toluenesulphonylsodamide, and sodamide in place of the sodium derivative of benzamide also failed to give the desired result.

A different synthesis was then attempted. Citric acid was converted into acetonedicarboxylic acid by Jerdan's modification ('J. Chem. Soc.', vol. 75, p 809 (1899)) of von Pechmann's method ('Ann.', vol. 261, p. 155 (1891)). The crude dicarboxylic acid on treatment with sodium nitrite solution (von Pechmann and Wehsarg, 'Ber.', vol 19, p 2465 (1886)) gave diisonitroso-

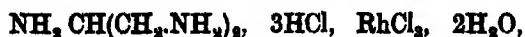
acetone, which was in turn converted to trioximinoacetone ('Ber.', vol 21, p 299 (1888)) All attempts to reduce trioximinoacetone to triaminopropane failed, in spite of the use of many reducing agents under very varied conditions, in each case the formation of ammonia indicated disruption of the trioximinoacetone complex The diisonitrosoacetone was therefore reduced with stannous chloride (Kalscher, 'Ber.', vol 28, p 1520 (1895)), and diaminoacetone isolated as its dihydrochloride The latter was then converted into diacetyldiaminoacetone by treatment with acetic anhydride (Franshimont and Friedmann, 'Rec trav chim.', vol 26, p 226 (1907)). Diacetyldiaminoacetone readily furnished the corresponding oxime, which when reduced with aluminium amalgam and hydrolysed gave the pure 1.2.3-triaminopropane trihydrochloride

Since the crude acetonedicarboxylic acid contains sulphuric acid, and the diisonitrosoacetone is contaminated with sodium cyanide, the yields of these compounds cannot be stated precisely The diaminoacetone, obtained by reduction with stannous chloride, separates as the stannochloride, and the yield of this compound from citric acid is uniformly 37 per cent of the theoretical The stannochloride on treatment with hydrogen sulphide yields diaminoacetone dihydrochloride, of which a 90 per cent yield can be readily isolated from the solution, whilst the yields of diacetyldiaminoacetone, of the oxime, and of the triaminopropane trihydrochloride are all nearly quantitative

Diaminoacetone dihydrochloride readily gives the crystalline diaminoacetoxime dihydrochloride the latter is so soluble in water that the amount isolated is small, and its reduction was not further investigated

Diacetyldiaminoacetone reacts with one molecular proportion of phenylhydrazine at ordinary temperatures to give the corresponding hydrazone, at higher temperatures or with larger quantities of phenylhydrazine the crystalline osazone, $\text{CH}_3\text{CO NH CH}_2\text{C}(\text{CH N NH C}_6\text{H}_5)_2\text{N NH C}_6\text{H}_5$, is formed

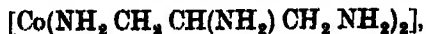
Curtius and Hesse showed that triaminopropane trihydrochloride combines with auric and platonic chlorides to yield respectively the compounds, $\text{NH}_2\text{CH}(\text{CH}_2\text{NH}_2)_2, 3\text{HCl}, \text{AuCl}_3$, and $\text{NH}_2\text{CH}(\text{CH}_2\text{NH}_2)_2, 3\text{HCl}, \text{PtCl}_4$, it is now shown that with rhodium chloride the compound



is formed In these three compounds the triaminopropane acts as a di-mono- and tri-acidic base respectively.

In accordance with the argument given above, it is found that the 1.2.3-triaminopropane yields complex metallic salts with the trivalent metals of

group eight of the periodic table ; salts are now described of the cobalt complex,



and of the corresponding rhodium complex The study of these and similar compounds will be continued with the view to ascertaining the type of configuration which they represent

Experimental

The Preparation of Diaminoacetone Dihydrochloride—Powdered crystalline citric acid (500 grms) was converted into acetone dicarboxylic acid by Jerdan's method, the product became almost dry when spread on porous plates over sulphuric acid for 48 hours, and the yield of crude material from 1,000 grms of citric acid was usually about 850 grms This acid was converted into disonitrosoacetone by the method of von Pechmann and Wehsarg, the product was contaminated with sodium cyanide, and since removal of the latter by washing with water also dissolved some disonitrosoacetone, the crude product was washed rapidly once with water and then dried, it being found that the presence of the cyanide did not affect the purity of the diaminoacetone obtained later The dry disonitrosoacetone was then reduced with stannous chloride and hydrochloric acid by Kalischer's method, and the diaminoacetone isolated as the stannochloride The latter was almost pure, and in a series of preparations it was found that the yield from 1 000 grms of citric acid was uniformly 610–630 grms, i.e., 37 per cent of the theoretical. This stannochloride, having the composition $\text{C}_3\text{H}_8\text{N}_2\text{O}$, H_2SnCl_4 , separates as colourless needles, which Kalischer states melt with decomposition at 203° . When the filtrate from these crystals is allowed to stand for several days at room temperature, it becomes orange-red in colour and deposits heavy orange-coloured crystals These, when filtered, washed with hydrochloric acid and dried, decomposed violently at 220° , and analysis showed them to be a second form of the stannochloride isolated by Kalischer (Found. $\text{H} = 2.76$, $\text{N} = 7.68$, $\text{Sn} = 33.5$ $\text{C}_3\text{H}_{10}\text{N}_2\text{Cl}_4\text{Sn}$ requires $\text{H} = 2.87$, $\text{N} = 7.98$, $\text{Sn} = 33.9$ per cent Consistent values for carbon could not be obtained) Many examples of similar polymorphism among the alkyl-substituted ammonium stannichlorides have been recorded by Ries ('Zeit für Kryst,' vol 39, p 72 (1904), vol 49, p 520 (1911)).

The diaminoacetone stannochloride (40 grms) was then dissolved in hot water (500 c.c.) containing concentrated hydrochloric acid (30 c.c.), the tin precipitated with hydrogen sulphide, and the filtered solution evaporated in

vacuo. The first crop of diaminoacetone dihydrochloride, $C_3H_5N_2O \cdot 2HCl$, H_2O , weighed 18 grms, the yield being 88 per cent of theory, a second crop was obtained by further evaporation of the filtrate *in vacuo*, or by the precipitation with an alcohol-ether mixture

Diacetyldiaminoacetone —Franchimont and Friedmann obtained this compound by heating diaminoacetone dihydrochloride with sodium acetate and acetic acid at 100° for an hour and then evaporating the filtered liquid to small bulk before allowing the diacetyldiaminoacetone to crystallise. It was found, however, that the long heating caused the diacetyl compound to be contaminated with the corresponding tetracetyl derivative. The following method avoids over-acetylation and gives the diacetyl compound in high yield. Diaminoacetone dihydrochloride (40 grms) and anhydrous sodium acetate (36.8 grms.) are well mixed and heated with acetic anhydride (160 c.c.) at 100° for 30 minutes. The mixture is quickly filtered, and the residue washed with acetic anhydride (60 c.c.) previously heated to 100° . The filtrate on cooling deposits the pure diacetyldiaminoacetone, which when filtered and washed with ether is obtained in pure white flakes (21 grms). A second crop is obtained by adding ether (600 c.c.) and petroleum (b.p. $60-80^\circ$, 200 c.c.) in turn to the filtrate. This precipitated material weighs 16 grms, the total yield of diacetyldiaminoacetone being 96 per cent of theory, it is advisable, however, to convert the crude precipitated material into the oxime before crystallising from alcohol.

Diacetyldiaminoacetoxime $(CH_3CO \cdot NH \cdot CH_2)_2C \cdot NOH$. — Hydroxylamine hydrochloride (3.7 grms) is dissolved in 15 per cent aqueous sodium hydroxide solution (150 c.c.) and diacetyldiaminoacetone (9.0 grms) added with stirring. The mixture becomes warm and soon gives a clear solution, which is kept at 50° for one hour, during which the oxime readily crystallises on scratching. The dry filtered oxime weighs 9.8 grms, and is found to contain 0.3 gm of sodium chloride, hence the yield is 97 per cent of theory. The crude product may be recrystallised from absolute alcohol, from which the *diacetyldiaminoacetoxime* separates in fine white crystals melting at $175-178^\circ$. (Found: C = 45.0, H = 6.88. $C_7H_{13}O_3N_3$ requires C = 44.9, H = 7.00 per cent.) The oxime is moderately soluble in cold water and alcohol, slightly soluble in acetone and ether, and almost insoluble in hot or cold benzene, chloroform or carbon tetrachloride.

1:2:3-Triaminopropane trihydrochloride $C_3H_5(NH_2)_3 \cdot 3HCl$, H_2O . — Diacetyldiaminoacetoxime may be reduced with sodium amalgam in the presence of acetic acid, but after hydrolysis of the acetyl groups the triaminopropane hydrochloride remains mixed with sodium chloride and has to be

isolated as the tribenzoyl-derivative. Reduction with aluminium amalgam is, therefore, far more rapid. Aluminium (20 grms), in the form of groats or very small pellets, is washed with alcohol and then treated with warm dilute sodium hydroxide solution until vigorous effervescence occurs. It is then well washed with water and treated for 2 minutes with 0.5 per cent aqueous solution of mercuric chloride. It is again washed with water and the treatment with alkali and mercuric chloride repeated. The amalgam is then washed with water and alcohol, and a hot solution of diacetyldiaminoacetoxime (10 grms) in 95 per cent. alcohol (150 c.c.) at once poured on to it. The mixture is placed in a water-bath at 45° for three hours, during which time hydrogen is evolved and aluminium hydroxide deposited; hot 95 per cent. alcohol (150 c.c.) is added in small quantities from time to time to prevent the mixture becoming too thick. Four such preparations are carried out together, the product filtered under reduced pressure, and the residual alumina thoroughly washed with hot alcohol. Filtration under these conditions is rapid, but if the reduction is carried out in the presence of acetic acid the subsequent filtration is very slow. The alcoholic filtrate is diluted with its own volume of water, acidified with hydrochloric acid and boiled down to small bulk, during which process the acetyl groups are removed by hydrolysis. The concentrated pale yellow solution is filtered, and when cool yields a large crop of triaminopropane trihydrochloride on scratching or seeding. The latter is drained at the pump, washed with alcohol and ether and obtained as fine white crystals (39.6 grms). (Found: Cl = 49.12, Calc. for $C_3H_{16}ON_3Cl_3$, Cl = 49.19 per cent). Further evaporation gives a second crop (1.7 gm) of the hydrochloride, whilst if the final filtrate is poured into alcohol a small deposit of the anhydrous hydrochloride (1.5 gm) is obtained. Thus, the total yield represents 42.9 grms of the hydrated hydrochloride, namely, 93 per cent of the theoretical yield.

Triaminopropane trihydrobromide — $C_3H_8(NH_2)_3 \cdot 3HBr, H_2O$, is prepared similarly by hydrolysing the reduced oxime with hydrobromic acid, and is obtained as fine white needles less soluble in water than the hydrochloride (Found: Br = 68.64. $C_3H_{16}ON_3Br_3$ requires Br = 68.52 per cent). The anhydrous hydrobromide is a white powder melting at 307–310° (decomp.). (Found: Br = 72.16. $C_3H_{14}N_3Br_3$ requires Br = 72.24 per cent).

1, 2, 3-Triaminopropane is not volatile in steam, and a solution of the free base is best prepared by treating a solution of the hydrochloride with an excess of silver oxide. The clear filtrate, however, retains silver in solution, and gives a white precipitate on acidification or dilution. Triaminopropane does not form a stable hydrate, and the free base is therefore easily prepared

by fractional distillation of the aqueous solution under reduced pressure. Thus triaminopropane trihydrochloride (100 grms.) is dissolved in warm water (200 c c) and the solution treated with a slight excess of freshly prepared silver oxide. The mixture is filtered, and the clear filtrate distilled under reduced pressure from an oil-bath, water distils over first, and is followed by the colourless base boiling at $105-110^{\circ}/15$ mm., a considerable viscous residue remaining in the flask. The above fraction on redistillation gives the pure 1 2 3-triaminopropane.

Triaminopropane rhodochloride $C_3H_5(NH_2)_3, H_3RhCl_6, 2H_2O$ —Crystalline sodium rhodochloride (6 grms.) is dissolved in hot water (30 c c) containing a few drops of hydrochloric acid, to this is added with stirring a solution of triaminopropane trihydrochloride (2 grms.) in boiling water (30 c c). The mixture is allowed to cool and rapidly deposits a heavy crystalline precipitate, the latter is filtered, and washed with water, alcohol and ether. *Triaminopropane rhodochloride* is thus obtained in lustrous garnet-red crystals, which are not apparently affected by heating to 310° . The chlorine was estimated volumetrically with N/10 silver nitrate solution, after fusing the compound with a mixture of sodium carbonate and peroxide (Found C = 8.04, H = 3.25, N = 9.45, Cl = 48.03. $C_3H_{18}O_2N_3Cl_6Rh$ requires C = 8.11, H = 3.86, N = 9.47, Cl = 47.94 per cent). If the triaminopropane hydrochloride solution is added to a cold concentrated solution of sodium rhodochloride, the above compound is again precipitated as an amorphous salmon-pink powder, which when washed with water and dried is pure. (Found C = 7.92, H = 3.19).

Triacetyltriaminopropane $C_3H_5(NHCOCH_3)_3$ —A mixture of anhydrous triaminopropane hydrochloride (10 grms.) and dry sodium acetate (12.4 grms.) is heated on a boiling water-bath with acetic anhydride (60 c c) for thirty minutes, and the product filtered hot, the triacetyl derivative may be isolated from the filtrate either by evaporation and crystallisation, or by precipitation with a large volume of ether. The *triacetyltriaminopropane* so obtained is recrystallised from absolute alcohol, from which it separates slowly as a fine white microcrystalline powder melting at $200-202^{\circ}$ (corr.) (Found C = 50.0, H = 8.04. $C_9H_{17}N_3O_6$ requires C = 50.2, H = 7.97 per cent). The compound is freely soluble in cold water and alcohol, sparingly soluble in hot chloroform, and almost insoluble in hot ether, acetone or benzene.

Tribenzoyltriaminopropane.—This compound is readily prepared by shaking an alkaline solution of the base with an excess of benzoyl chloride, and when recrystallised from alcohol separates slowly as a fine white amorphous powder.

which Curtius and Hesse (*loc. cit.*) state melts at 206–207°. It was found, however, that a second recrystallisation gave the tribenzoyl-compound melting at 217–218° (corr.) and further purification did not affect this melting point (Found: C = 71.48; H = 5.85, N = 10.48. Calc. for $C_{24}H_{23}O_3N_3$, C = 71.79; H = 5.78, N = 10.47 per cent.)

Diaminoacetoxime dihydrochloride. $(HCl, NH_2CH_2)_2C=NOH$ —Hydroxylamine hydrochloride (2.3 grms) is dissolved in 15 per cent aqueous sodium hydroxide solution (8.9 c.c.) and powdered diaminoacetone dihydrochloride (6 grms) added. Water (1 c.c.) is added to give a complete solution, which is maintained at 60° for one hour. On cooling and standing overnight, *diaminoacetoxime dihydrochloride* separates in long colourless needles melting at 207° (corr.) with decomposition (Found: N = 23.7, Cl = 40.5. $C_3H_{11}ON_3Cl_2$ requires N = 23.9, Cl = 40.3 per cent). The oxime thus obtained weighed 2.0 grms, the low yield (33 per cent of theory) being due to the marked solubility of the oxime in water.

The following crystal measurements were made by Mr R. Jeffery, B.A., working under the direction of Mr A. Hutchinson, F.R.S. —

“ Diaminoacetoxime Dihydrochloride

“ System —Oblique

“ Axial Ratios —a b c = 0.9094 1 0.8821 $\beta = 58^\circ 49\frac{1}{4}'$

“ Habit —The crystals were of prismatic habit, terminated by faces of the form l {001} (Fig. 1.) Only two crystals doubly terminated were observed

“ Forms Present —a {100}, m {110}, l {011}, with b {010} very small, on one crystal, and t {102}, also very small, on another.

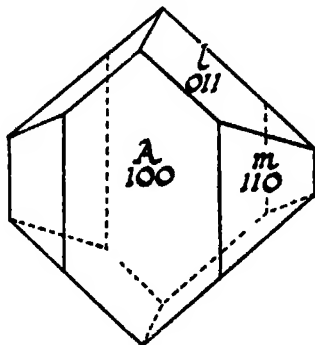


FIG. 1.

Angles Observed		No of Measurements	Limits	Mean	Calculation.
<i>a</i>	<i>m</i> = 100 . 110	9	39° 30'–36° 23'	37° 53'	—
<i>a</i>	<i>l</i> = 100 011	4	64° 35'–66° 31'	65° 35½'	—
<i>b</i>	<i>l</i> = 010 011	2	52° 50'–53° 12'	53° 1'	52° 57½'
<i>l</i>	<i>l</i> = 011 011	5	73° 55'–74° 18'	74° 5'	—
<i>l</i>	<i>m</i> = 011 110	2	46° 19'–46° 30'	46° 24½'	45° 53½'
<i>a</i>	<i>z</i> = 100 I02	1	—	88° 18'	87° 49'
<i>m</i>	<i>z</i> = 110 I02	1	—	88° 55'	88° 16½'
<i>l</i>	<i>z</i> = 011 I02	1	—	46° 14'	45° 43½'

“*Cleavage*—None observed

“*Specific gravity*—Average of three determinations 1.525 (highest value 1.528) Determined by floating the crystal in bromoform diluted with benzene

“*Optical characters*—The refractive indices were determined approximately, using the Herbert Smith refractometer, $\gamma = 1.58$, $\beta = 1.56$, $\alpha = 1.55$, and the crystal is probably positive. The optic axial plane and acute bisectrix were not determined. All the faces in the prism zone gave practically straight extinction between crossed nicols.”

Diacetyldiaminoacetonephenylhydrazone $(\text{CH}_3\text{CO NH CH}_2)_2\text{C N NH C}_6\text{H}_5$ —Diacetyldiaminoacetone readily gives an osazone with phenylhydrazine, and a deficiency of phenylhydrazine must be used in preparing the normal hydrazone. Diacetyldiaminoacetone (4 grms) is dissolved in water (6 c.c.) at 100°, and phenylhydrazine (2.3 c.c. instead of 2.5 c.c.) added. The clear solution obtained at 100° is quickly cooled to 50°, and maintained at this temperature for 30 minutes, when a heavy oil separates. The latter crystallises on cooling, and the crude dry hydrazone so obtained weighs 6 grms, the yield being 98 per cent of theory. When recrystallised from ethyl acetate, the *diacetyldiaminoacetonephenylhydrazone* is obtained in colourless crystals melting at 115–118° to a cloudy white liquid. (Found C = 59.4, H = 6.90. $\text{C}_{13}\text{H}_{18}\text{O}_2\text{N}_2$ requires C = 59.5, H = 6.90 per cent.)

Acetyldiaminomethylglyoxalosazone



Powdered diacetyldiaminoacetone (4 grms) and phenylhydrazine (5 c.c.) are added in turn to acetic acid (4 c.c.), diluted with water (4 c.c.), and the mixture kept at 50° for 3 hours, a heavy reddish-yellow oil slowly separates and finally solidifies. After standing overnight the solid product is filtered and recrystallised from alcohol, when the osazone separates in fine

lemon-yellow needles melting at 186° . (Found C = 66.2; H = 6.16, N = 22.5 $C_{17}H_{19}ON_5$ requires C = 66.0, H = 6.19, N = 22.6 per cent)

If diacetyldiaminoacetone is treated with three equivalents of phenylhydrazine under the above conditions, no further action occurs, and the above osazone remains contaminated with the excess of free hydrazine, from which it can be separated by crystallisation from alcohol. The products of hydrolysis of this osazone are under investigation.

Metallic co-ordinated derivatives of triaminopropane—In the formulæ given below, the contraction "ptn" is used to represent one molecule of triaminopropane, namely, the group $NH_2CH(CH_2NH_2)_2$.

Bispropanetriamine cobaltic trichloride $[Co\ ptn_2]Cl_3$ —A boiling aqueous solution of silver nitrate (80 grms) is treated with hot solution of potassium hydroxide (27 grms) and the precipitated silver oxide filtered and washed, and the filtrate well shaken with a solution of triaminopropane trihydrochloride (30 grms) in warm water (180 c c). The mixture is filtered, and the filtrate heated with finely powdered monochloropentamminocobaltic dichloride (7.5 grms) on the water bath. Ammonia is driven off, and when the volume of the mixture is about 40 c c, the solution is acidified with hydrochloric acid to ensure the precipitation of the silver originally dissolved in the solution of the base. The solution after filtering and cooling deposits orange-coloured crystals, which are separated, recrystallised from a little hot water, filtered and washed with alcohol. Bispropanetriamine cobaltic chloride is thus obtained in orange-coloured needles, which darken in colour at 300° and melt with decomposition at $312-314^{\circ}$ (Found C = 20.9, H = 6.43, N = 24.6, Cl = 31.0 $C_6H_{12}N_6Cl_3Co$ requires C = 20.9, H = 6.45, N = 24.5, Cl = 31.0 per cent). The salt is freely soluble in water, but almost insoluble in alcohol.

Bispropanetriamine cobaltic triiodide $[Co\ ptn_2]I_3$ —A strong aqueous solution of potassium iodide is added to a strong solution of bispropanetriamine cobaltic trichloride, and the yellowish-brown precipitate is filtered, washed with water and recrystallised from a little hot water. Bispropanetriamine cobaltic triiodide separates in orange-brown needles which undergo no apparent change when heated to 320° (Found C = 11.6; H = 3.55, I = 61.2 $C_6H_{12}N_6I_3Co$ requires C = 11.6, H = 3.59, I = 61.6 per cent). The salt is insoluble in alcohol, and considerably less soluble in water than the trichloride.

Bispropanetriamine cobaltic platinumchloride $[Co\ ptn_2]_2, 3Pt\ Cl_6, 6H_2O$.—An excess of a solution of chloroplatinic acid is added to a solution of bispropane-

triamine cobaltic trichloride, and the brown precipitate is filtered, washed with water and recrystallised from hot water, from which the platinumchloride separates in orange-brown needles. The latter lose water of crystallisation when heated at 130° , and the anhydrous bispropanetriamine cobalt platinumchloride darkens in colour at 255° and melts with decomposition at 270° (Found for the hydrated platinumchloride, $C = 8.03$, $H = 3.19$ $C_{12}H_{36}O_6N_{12}Cl_{18}Co_2Pt_3$ requires $C = 7.96$; $H = 3.12$. For the anhydrous platinumchloride, $C = 8.58$, $H = 2.73$ $C_{12}H_{34}N_{12}Cl_{18}Co_2Pt_3$ requires $C = 8.47$, $H = 2.61$ per cent.)

Bispropanetriamine rhodium triiodide $[Rh(ptn)_2]I_3$ —Triaminopropane hydrochloride (9 grms.) is dissolved in water (40 c.c.) and the solution treated as before with the oxide obtained from silver nitrate (24 grms.). The solution is filtered, added to powdered recrystallised monochloropentamminorhodium dichloride (5 grms.) and the mixture boiled under reflux for four hours. The solution is then acidified with hydrochloric acid, filtered, and when cold treated with an excess of potassium iodide solution. The white precipitate is filtered and recrystallised from a little boiling water, from which the bispropanetriamine rhodium triiodide separates in small dense cream-coloured crystals, which remain unchanged when heated to 300° (Found $C = 10.7$, $H = 3.38$, $I = 57.21$ $C_6H_{22}N_6I_3Rh$ requires $C = 10.9$, $H = 3.35$, $I = 57.53$ per cent.) If the monochloropentamminorhodium dichloride used in this preparation is impure and dark in colour, the resulting iodide is yellow or reddish-brown in colour; recrystallisation from boiling water containing animal charcoal, however, gives the pure cream-coloured triiodide. The latter is only slightly soluble in cold water, easily soluble in hot water, and insoluble in alcohol.

Bispropanetriamine rhodium platinumchloride $[Rh(ptn)_2]_2 \cdot 3PtCl_6 \cdot 4H_2O$ —A solution of bispropanetriamine rhodium triiodide in hot water is shaken with an excess of silver oxide, filtered, acidified with hydrochloric acid and allowed to cool. It is then added to a solution of an excess of chloroplatinic acid, and the platinumchloride rapidly separates. The latter is filtered, washed with hot water and alcohol, and dried over calcium chloride. Bispropanetriamine rhodium platinumchloride is thus obtained in small orange-coloured crystals, which are only slightly soluble in boiling water (Found $C = 7.75$, $H = 2.66$. $C_{12}H_{32}O_4N_{12}Cl_{18}Pt_3Rh_2$ requires $C = 7.75$, $H = 2.82$ per cent.) The anhydrous salt darkens at 295° and melts at 328° (decomp.)

Bispropanetriamine rhodium rhodochloride $[Rh(ptn)_2][RhCl_6 \cdot 4H_2O]$ —A solution of bispropanetriamine rhodochloride is prepared as in the previous

experiments and added to a solution of sodium rhodium chloride (6 grms.) in hot water (30 c c) The precipitate is filtered, washed with hot water and alcohol, and dried over calcium chloride. Bispropanetriamine rhodium rhodochloride is thus obtained as a pinkish-grey amorphous powder, which is almost insoluble in boiling water, and which undergoes no apparent change on heating to 310° (Found. N = 12.45, Cl = 32.10 $C_3H_{20}O_4N_3Cl_3Rh_2$ requires N = 12.51, Cl = 31.81 per cent.)

*The Union of Hydrogen and Oxygen in Presence of Silver
and Gold*

By D. L. CHAPMAN, M.A., F.R.S., Fellow of Jesus College, Oxford, J. E. RAMSBOTTOM, D.Sc., Ph.D., Superintendent Chemical Department, Royal Aircraft Establishment, Farnborough, and C. G. TROTMAN, B.A., Jesus College, Oxford

(Received October 4, 1924)

The action of the metals, silver and gold, in promoting the combination of hydrogen and oxygen was first investigated systematically by Bone and Wheeler ([A] 206, 1)* In the course of the research they made the very important discovery that the degree of activity of the metals depended on whether these had been heated previously to use in hydrogen or oxygen. Either metal was found to be a much more efficient catalyst after it had been heated in hydrogen.

They favoured the view that the phenomenon in question, which will for brevity be called the Bone and Wheeler effect, could be best explained by a theory very similar to that advanced by Fusinieri,† namely, that the stages in the catalytic process (in the case of silver and gold) are a condensation of hydrogen on the heated surface and a subsequent removal of this hydrogen (which was assumed to be present in an abnormally active condition) by its uniting with the oxygen present.

However, the Bone and Wheeler effect is not completely explained by such an hypothesis, unless the additional assumption is made that hydrogen is

* 'Phil. Trans.,' A, vol. 206, p. 1 (1906)

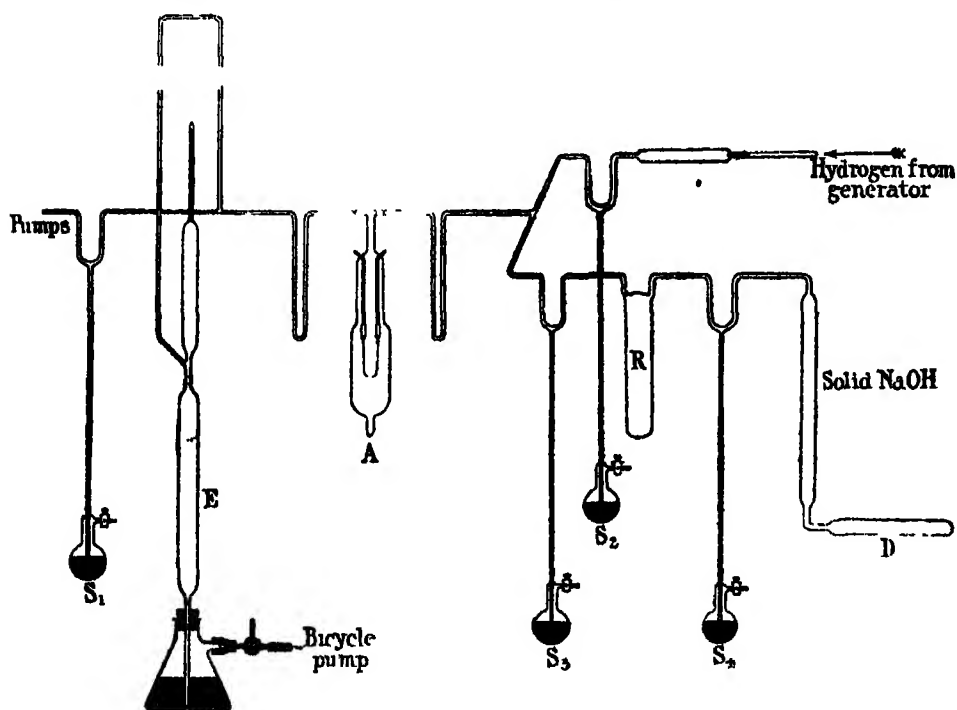
† 'Giorn. di Fisica,' vol. 8, p. 259 (1825)

adsorbed more rapidly on the surface of a metal which contains dissolved hydrogen than on the pure metal, or on one which contains dissolved oxygen for the activity of a metal, which contains only a small amount of dissolved hydrogen, is not diminished by its being employed as a catalyst to bring about the union of an indefinite amount of hydrogen with oxygen

The authors have conducted experiments which point to a different explanation of the Bone and Wheeler effect, namely, that in the case of silver and gold, dissolved oxygen acts as an inhibitor, while the presence of absorbed hydrogen does not appreciably increase or diminish the activity of the metal

Experimental.

The catalyst was in the form of a filament of the pure metal (supplied by Messrs Johnson and Matthey), 0.276 mm in diameter and approximately 10 cms in length. It was suspended in a single loop in the reaction vessel, marked A in the diagram, by fusion to thick platinum leads which were carried by two tubes inserted through the top of the vessel. The volume of the vessel was approximately 350 c cs. The filament was heated electrically, the current being regulated by a variable resistance and measured on a Cambridge and



Paul microammeter which was connected in the circuit by suitable shunts. It will be seen later that the experiments were performed in such a manner that the ammeter readings furnished all the information required.

On each side of the reaction vessel were situated U-tubes which were kept immersed in liquid air, to prevent the admission of condensable impurities, such as mercury vapour, to the vessel and to remove water formed in the reaction.

Pressure measurements were made on a McLeod gauge, and all readings were adjusted to the lowest mark (Mark 1) on the capillary tube. The pressures to be measured were generally of the order of 700 mm on the balance tube of the gauge, which corresponded to an actual pressure of 0.64 mm.

The apparatus could be exhausted by means of a mercury vapour pump of the diffusion type, working in conjunction with an automatic Sprengel pump, these being connected to the apparatus through the mercury seal S_1 . A tube, not shown in the figure, containing phosphorus pentoxide, was inserted between the pumps.

Preparation of Gases

Hydrogen, generated from pure sulphuric acid and zinc and washed by a solution of sodium hydroxide to remove acid spray, was admitted to the apparatus by diffusion through a palladium "osmosis tube" of the type supplied by Messrs Johnson and Matthey for use with X-ray bulbs. The palladium tube was protected by slipping over it a short length of quartz tubing through which the hydrogen from the generator passed, and the gas was let into the apparatus by gently warming the quartz tube. The hydrogen diffusion apparatus was connected to the apparatus through the seal S_2 .

Oxygen was prepared as required by heating carefully recrystallized potassium permanganate in the tube D, the gas being passed over pure pulverised sodium hydroxide before entering the apparatus. The oxygen required for an experiment was stored in the reservoir R, which could be isolated from the rest of the apparatus, by the seals S_3 and S_4 . The ratio of the volume enclosed between the seals S_3 and S_4 to that enclosed by the seals S_1 , S_2 and S_3 was determined.

Method of Experiment

Before commencing experiments, the apparatus was thoroughly exhausted, and the whole was heated by a large blowpipe flame to remove gases from the walls of the glass. This treatment was repeated three times.

With liquid air in position round the U-tubes, oxygen was admitted to the

exhausted apparatus by warming the potassium permanganate, until the pressure was as near as possible to the desired value of 600 mm measured from Mark 1 on the balance tube of the McLeod gauge, *i.e.*, an actual pressure of 0.552 mm. The seal S_4 was then closed, and a further seal, not shown in the figure, situated between the pumps, was also closed, so that no gas which had been in contact with the Sprengel pump should diffuse or flow back into the apparatus during subsequent operations. The pressure of the gas was adjusted in the following manner. If slightly above the value of 600 mm, the mercury was raised in the McLeod gauge balance tube to a position which was found by practice, and the seal S_1 was then closed. This, in effect, forced a little gas into the mercury vapour pump, so that when the mercury was allowed to fall to its normal level the pressure in the apparatus was diminished by the required amount.

Conversely, if the pressure was slightly lower than 600 mm, the reverse operations were performed, mercury being withdrawn from the tube E, below the McLeod gauge, while the seal S_1 was open, gas being thereby transferred from the mercury vapour pump to the apparatus. When the pressure of the oxygen had been thus adjusted, the seal S_2 was shut, so that oxygen at a known pressure was enclosed in the reservoir R. The apparatus to the left of the seal S_2 was then exhausted, and hydrogen was subsequently admitted thereto in the manner described. The pressure of the hydrogen was adjusted in the manner described above to 0.644 mm with the seals S_1 , S_2 , S_3 closed.

Since the volume of the apparatus between the seals S_1 , S_2 and S_3 was 1.85 times greater than that of the reservoir R, the mixture obtained by opening S_3 and allowing the gases to diffuse would contain hydrogen and oxygen in the ratio of 2.16 : 1. The mixtures used in all the experiments were at the same pressure and had the same composition. The mixing of the gases was hastened by drawing the mercury up and down the wide tube E, below the McLeod gauge.

As stated above, the filament was heated by an electric current, which was very gradually increased until the rate of combination of the hydrogen and oxygen corresponded to a rate of fall of pressure of 2 mm on the McLeod scale in 5 minutes.

Experiments with Silver

In a number of preliminary experiments the filament was heated previously to use either in hydrogen at 0.644 mm pressure, or in oxygen at 0.552 mm. pressure, the filament being maintained at a dull red heat for 30 minutes. It was found that the metal showed the Bone and Wheeler effect to a marked

degree. After previously heating the filament in oxygen, combination of the gases commenced when the filament was at a dull red heat, at ammeter reading 78; while after several periods of heating in hydrogen the wire became more and more active, until it eventually caused the gases to combine at ammeter reading 53

A further series of experiments with a new wire confirmed these observations. In the column W of the following table are recorded the readings of the ammeter at which combination of the gases started at the specified rate

No of experiment	Initial heating of—	W
18	30 minutes in oxygen . . .	79
19	30 minutes in oxygen .	79
20	30 mins in O ₂ , 30 mins in H ₂	62 (slight com- bination)
21	30 mins in O ₂ , 30 mins in H ₂	60
22	30 mins in O ₂ , 30 mins in H ₂	} 53
	30 mins in O ₂ , 30 mins in H ₂	
23	Do do.	53

The effect of heating the metal in a high vacuum was next investigated, and it was observed that after such treatment the filament was always in an active condition, irrespective of whether it had been previously heated in hydrogen or oxygen

No of experiment	Initial heating of—	W
24	30 mins in H ₂ , 83 mins <i>in vacuo</i> .	53
25	30 mins in O ₂ , 40 mins. <i>in vacuo</i>	53
26	80 mins. <i>in vacuo</i> .	53
27	30 mins in oxygen . . .	70
29	40 mins in O ₂ , 1 hr. 50 mins <i>in vacuo</i>	55
30	30 mins in oxygen . . .	70
31	30 mins in O ₂ , 90 mins <i>in vacuo</i>	55

In Experiment 31 evidence was sought for the emission of oxygen when the metal was heated in a vacuum, and it was found that a definite increase of pressure (which, however, was not large enough to measure accurately) occurred. A smaller apparatus was constructed later in order to make it possible to determine the pressure of this desorbed gas.

The results of Experiments 18-31 pointed to a new explanation of the Bone and Wheeler effect. They show that absorbed oxygen renders the metal inactive as a catalyst, but that it again becomes active when the oxygen is removed, the degree of activity being independent of whether this removal is effected by heating the metal in hydrogen or in a vacuum. Accordingly, absorbed hydrogen does not increase appreciably the activity of the metal, whereas absorbed oxygen has a pronounced inhibitive effect.

The prolonged heatings to which this filament had been subjected resulted in some loss of metal by evaporation, and an almost opaque film of silver was formed on the walls of the reaction vessel opposite to the filament.

A further series of experiments with a new filament confirmed the above results and showed that the metal can always be rendered inactive or active, according as to whether it is heated in oxygen or in a vacuum.

No of experiment	Initial heating of —	W
32	50 mins in oxygen	72
35	15 mins in O_2 , 80 mins in <i>vacuo</i>	66
36	30 mins in O_2 , 2 hrs 25 mins in <i>vacuo</i>	55
37	30 mins in O_2 , 90 mins in <i>vacuo</i>	53
38	Do do	50
39	Do do	50
40	Do do	49
41	30 mins in O_2 , 120 mins in <i>vacuo</i>	50
42	30 mins in oxygen	72

The following experiments were performed with the filament which had been used in Experiments 18-31 —

No of experiment	Initial heating of—	W
44	30 mins in oxygen	80
45	30 mins in O_2 , 1 hr 45 mins in <i>vacuo</i>	60
46	30 mins in O_2 , 90 mins in <i>vacuo</i>	53
47	(a) 30 mins in O_2 , 1 hr 20 mins in <i>vacuo</i>	55
	(b) 60 mins in <i>vacuo</i>	53
48	(a) 40 mins in oxygen	72
	(b) 30 mins in hydrogen	53
49	30 mins in hydrogen	49
51	30 mins in oxygen	68

Experiments were then conducted in order to determine whether a filament which had been rendered inactive by heating it in oxygen could be made more active by subsequently heating it in oxygen at a much lower pressure. For this purpose the volume of the apparatus between the seals S_1 , S_2 , and S_3 was reduced to approximately 456 c.c. and the filament employed was 11 cms. in length.

It will be seen from the following table of results that the dependence of the activity of the wire on the pressure of the oxygen in which it is heated is such that as the pressure increases from a vacuum to 0.001 mm. the activity falls very little, but that as the pressure is increased from 0.001 mm. to 0.003 mm. the activity falls to a value not much lower than that of a wire which has been heated in oxygen at a pressure more than 200 times greater—namely, 0.627 mm. It would appear, therefore, that above 0.003 mm. the activity of the wire is almost independent of the pressure of the oxygen in which it is heated, but that as the pressure falls from the former value the activity rises rapidly to the value corresponding to a vacuum. There is, in fact, a minimum degree of activity which is nearly reached when the pressure of the oxygen in which the wire is heated is above 0.005 mm.

These new facts appear to us to give a clear indication of the mechanism of the influence of absorbed oxygen. They show that the effect of the oxygen is due to the formation of an inactive film (probably of silver oxide) on the surface of the metal, the metal being completely covered with the film when the pressure of oxygen in which it is heated exceeds 0.005 mm. This, it would appear, is the only theory which can account for the fact that the activity of the wire corresponding to pressures of oxygen above this value is constant.

In Experiment 53, the pressure of oxygen evolved when the filament was heated in a vacuum was measured and was found to be 0.00077 mm. The volume of oxygen at N.T.P. corresponding to this pressure is about twice as great as that calculated from Sieverts' figures ('Zeit. Phys. Chem.' vol. 60, p. 129 (1907)) for the absorption of oxygen by silver, it being assumed in the calculation that the amount of oxygen absorbed is proportional to the square root of the pressure.

It was observed in Experiments 54–58 that the mixed gases combined slowly at the temperature of the laboratory, the maximum rate of combination observed corresponded to a rate of fall in pressure of 0.005 mm. per hour when the apparatus contained the standard mixture at a pressure of 0.575 mm. This fall in pressure persisted in each experiment at a uniform rate, until the

No of experiment	Initial heating of—	W.
52	(a) 30 mins in oxygen at 0.627 mm	
	30 mins in hydrogen at 0.627 mm	
	30 mins in oxygen at 0.627 mm	65
	(b) 30 mins in hydrogen at 0.627 mm	45
53	30 mins in oxygen at 0.627 mm	
	90 mins in <i>vacuo</i>	45
54	30 mins in oxygen at 0.627 mm	
	90 mins in oxygen at 0.0029 mm	60
55	30 mins in oxygen at 0.627 mm	
	90 mins in oxygen at 0.0017 mm	60
56	30 mins in oxygen at 0.627 mm	
	90 mins in oxygen at 0.0014 mm	56
57	30 mins in oxygen at 0.627 mm	
	90 mins in oxygen at 0.0013 mm	47
58	30 mins in oxygen at 0.627 mm	
	90 mins in oxygen at 0.0011 mm	48

temperature of the filament was raised to a point at which the gases were caused to combine by the filament. At this point for a small rise in temperature a large increase in the rate of combination was observed. As an increase of temperature of the wire below this point resulted in no alteration of the rate of combination it was concluded that the combination at the laboratory temperature was due to the film of silver deposited on the walls of the reaction vessel.

Experiments with Gold

The investigation was carried out in the same manner as that of the investigation with silver. A filament of commercially pure gold, which contained traces of copper and silver, was used for preliminary experiments. The metal blackened uniformly when it was heated in oxygen, and this was accompanied by a large fall in pressure of the gas. When the filament was heated in hydrogen or in a vacuum this coating of oxide was removed.

It was found that the clean metal caused the gases to combine at an ammeter reading of ten divisions lower than that observed when combination started in the presence of the oxidized metal. The inactive metal retained completely its blackened appearance after it had been heated to just below a dull red heat for 35 minutes in the mixture of hydrogen and oxygen.

Experiments with a filament of chemically pure gold showed that this metal behaves in the same way as silver. The difference between the active and the inactive states is, however, not so pronounced as in the case of the latter metal, being represented by only 5-6 ammeter divisions instead of 19-20 divisions.

The results of the experiments conducted with pure gold are shown in the following table

No of experiment.	Initial heating of—	W
63	30 mins. in oxygen	81
64	30 mins in O_2 , 90 mins <i>in vacuo</i>	76
65	30 mins in O_2 , 90 mins <i>in vacuo</i>	75
66	(a) 30 mins in O_2 , 30 mins in H_2 , 30 mins. in O_2	80
	(b) 30 mins in hydrogen	73
67	30 mins in O_2 , 60 mins <i>in vacuo</i>	75
68	60 mins in O_2 , 120 mins <i>in vacuo</i>	75
69	30 mins in oxygen	81
70	30 mins in hydrogen	76
71	30 mins in H_2 , 120 mins <i>in vacuo</i>	75

Conclusions

When silver is heated to dull redness in oxygen at a pressure exceeding 0.005 mm of mercury, it becomes almost completely covered with a film of oxide, which considerably impairs the efficiency of the metal as a catalyst for the reaction between hydrogen and oxygen.

The film of oxide can be removed by heating the metal to redness in a vacuum or in oxygen at a much lower pressure. The catalytic activity of the metal is then the same as that of silver which has been heated in hydrogen.

These hypotheses furnish a consistent explanation of the discovery of Bone and Wheeler that silver, after it has been heated in hydrogen, becomes a much more efficient catalyst for the reaction between hydrogen and oxygen than silver which has not been thus treated—for new silver wire which has not been heated in a reducing atmosphere would be covered with the oxide film.

The behaviour of gold is similar to that of silver, after it has been submitted to the same treatment, although in the case of the former metal the effects observed are not so pronounced.

It was found that hydrogen and oxygen will combine at the temperature of the laboratory in the presence of the silver film condensed on the inner surface of the reaction vessel

The General Law of Electrical Conduction in Dielectrics.

By SPENCER W RICHARDSON, M A , D Sc , F Inst P

(Communicated by Sir William Bragg, K B E , F R S --Received April 29, 1924)

(From the Davy Faraday Research Laboratory of the Royal Institution)

An account of a series of experiments on the behaviour of a specimen of quartz cut perpendicular to the optical axis, performed by me, has been given in two papers entitled "Some Experiments on the Properties of Dielectrics," and "The Flow of Electricity through Dielectrics," published in the 'Proceedings of the Royal Society,' A, vol 92 (1915)

In these papers I showed that if one surface of the specimen (in the form of a thin disc of area S and thickness d , silvered on both sides) be connected to the earth, and the other surface be maintained at a potential V for a time T , then the total charge accumulated in the dielectric can be represented by.—

$$(K + K') CV,$$

where

K = the specific inductive instantaneous capacity of the specimen,

K' = the maximum value of the specific inductive residual capacity of the specimen,

and

$$C = S/4\pi d$$

If the surface at potential V be now connected to the earth, then at any subsequent time t (greater than τ) the charge remaining in the dielectric can be represented by —

$$K'_t CV,$$

where

K'_t = the specific inductive residual capacity of the specimen,

$$= nK' e^{n-\alpha(t-\tau)},$$

and

n = a constant for the given specimen.

α = a function of T (the time of charging)

x = a function of both T and t

When the discharge has taken place for some time, this expression reduces to —

$$K'_t = nK' e^{-\alpha(t-\tau)} = nK' e^{-\alpha t},$$

since τ (the time taken for the potential of the surface originally at potential V to fall to zero) is small compared with t

For some years previous to the publication of the papers referred to, I

sought for information concerning the electromotive force of polarisation in the dielectric from a study of α and x . For if α and x could have been found at the instant of discharge it would have been possible to write —

$$\text{The rate at which the charge is escaping from the dielectric} = -\frac{dQ}{dt} = -\frac{P}{R},$$

where

P = the electromotive force of polarisation, and R = a constant

This information could then have been combined with that concerning the charging and polarisation currents, and the general law of electrical conduction in dielectrics could have been completely determined.

I found that I was able to calculate α from the experimental results, but I did not succeed in obtaining an expression for x which was in agreement with all the known facts. An expression of the form—

$$A_1 e^{-\alpha_1 t} + A_2 e^{-\alpha_2 t}$$

(where $A_1, A_2, \alpha_1, \alpha_2$ are suitable constants) will, for a given time of charging, lead to values of Q which approximate closely to the observed values, but the expression does not represent *exactly* what is taking place, and cannot therefore, be used for obtaining the value of $-dQ/dt$ at the instant of discharge

I then sought for experimental evidence of the existence of the electromotive force of polarisation, and, in January, 1913, I discovered that if (during charging) the applied potential V was suddenly reduced to V' (say), then, provided that V' was greater than a certain value P the current flowed through the specimen in the same direction as the original charging current, but that if V' was less than P , a current flowed (for some time) in the opposite direction. I took P to be an approximate measure of the electromotive force of polarisation in the given conditions. I calculated the rate at which the charge accumulated in the specimen and I showed that if

γ = the charging current and dQ/dT = the rate at which the charge is accumulating in the dielectric, then —

$$\gamma = \frac{dQ}{dT} + \frac{V - P}{R}.$$

That is to say —

$$\left\{ \begin{array}{c} \text{The Charging} \\ \text{Current} \end{array} \right\} = \left\{ \begin{array}{c} \text{The Polarisation} \\ \text{Current} \end{array} \right\} + \left\{ \begin{array}{c} \text{The Conduction} \\ \text{Current} \end{array} \right\}.$$

This I believe to be the general law of electrical conduction. As time goes on dQ/dT diminishes, and P tends towards a fixed value P_∞ . It would thus

appear that after the charging current has been flowing for some considerable time the equation reduces to,—

$$\gamma = \frac{V - P_{\infty}}{R},$$

and since P_{∞} is proportional to V , this may be written —

$$\gamma = \frac{V(1 - k)}{R} = \frac{V}{R_0},$$

where k and R_0 are constants

That is to say —

At sufficiently high temperatures—after the current has been flowing for some time—the behaviour of the specimen approximates to that of a metallic conductor carrying a steady current

At low temperatures dQ/dT is small,* and at the temperature of liquid air—after the instantaneous charge has been completed—both the charging and polarization currents are negligible and the equation reduces to —

$$\frac{V - P}{R} = 0$$

That is to say —

At very low temperatures the behaviour of the specimen approximates to that of an air condenser.

For the discharge the equation reduces to —

$$-\frac{dQ}{dt} = -\frac{P}{R}$$

EXPERIMENTAL RESULTS

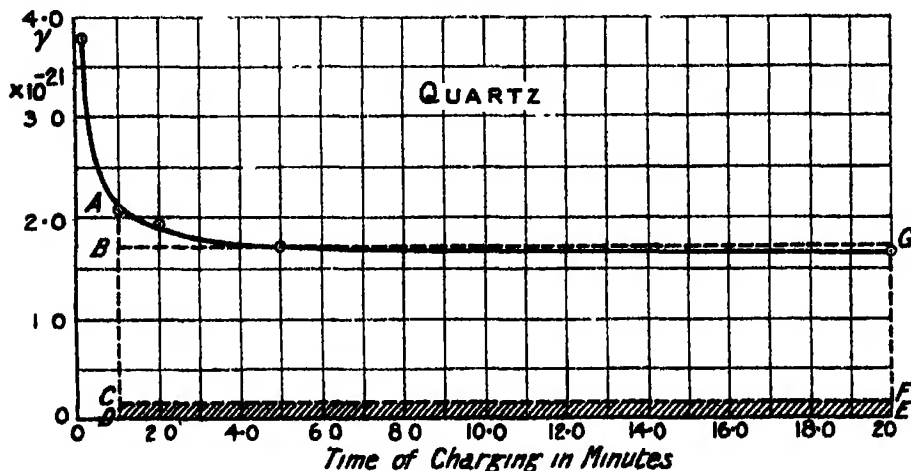
Quartz along the Optical Axis

In the paper entitled “The Flow of Electricity through Dielectrics” (‘Roy Soc Proc,’ A, vol 92, p 103 (1915)) the following table of results for a specimen of quartz (cut perpendicular to the optical axis) is given —

V = 1					
Time of Charging	γ	$\frac{dQ}{dT}$	P	Apparent Resistance	R
20 minutes	1.64×10^{-11}	0.09×10^{-13}	0.82	6.10×10^{10}	1.16×10^{10}
5 „	1.68×10^{-11}	0.20×10^{-13}	0.81	5.95×10^{10}	1.28×10^{10}
2 „	1.92×10^{-11}	0.28×10^{-13}	0.80	5.20×10^{10}	1.22×10^{10}
1 „	2.08×10^{-11}	0.39×10^{-13}	0.80	4.81×10^{10}	1.18×10^{10}
10 seconds	3.80×10^{-11}	0.88×10^{-13}	0.65	2.63×10^{10}	1.20×10^{10}
Mean					1.21×10^{10}

* Curie and Compaan, ‘Comptes Rendus’ (1902).

It will be seen that if instead of R we write $1 - P/\gamma$ (cf. Joffé, 'Annalen der Physik,' vol. 72, 1923) we obtain nearly constant results, which at first sight might lead to the conclusion that Ohm's law was obeyed. In this case, however, the values of dQ/dT are small compared with the corresponding values of γ , and the quantity of electricity that flows through the specimen in an interval of time—from $T = 1$ minute to $T = 20$ minutes (say)—is about ten times as great as the total charge accumulated in the specimen in the same interval of time. This is illustrated in the following diagram —



In the diagram are shown areas

$$\text{ADEG representing } \int_{T=1}^{T=20} \gamma dT = 1958 \times 10^{-21},$$

$$\text{CDEF representing } \int_{T=1}^{T=20} \frac{dQ}{dT} dT = 168 \times 10^{-21},$$

and

$$\text{BCFG representing } \int_{T=1}^{T=20} \frac{V-P}{R} dT = 1790 \times 10^{-21}.$$

It is clear that these results are consistent with the equation

$$\gamma = \frac{dQ}{dT} + \frac{V-P}{R}$$

Quartz across the Optical Axis.

Since the publication of the papers mentioned above I have performed a great many experiments on a specimen of quartz cut parallel to the optical

axis The specimen (in the form of a carefully cut and polished disc) was silvered on both sides—insulating gaps being produced by scraping round the edges with a sharp steel tool.

The edges of the specimen were very carefully cleaned and the specimen was kept permanently (during any series of experiments) in an air-tight chamber containing phosphorus pentoxide (see fig 1).

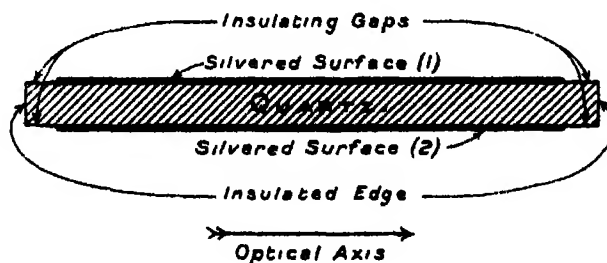


FIG 1

In these circumstances the general behaviour of the specimen was found to be in agreement with the above conclusions— but the various quantities measured (with the exception of K and P) were much less than in the case of the specimen cut perpendicular to the optical axis

The data given below relate to experiments performed at 26.4°C

$$K = 4.3.$$

In the equation $K'_t = nK'e^{-at}$

$$n = 0.50$$

The value of n for the specimen cut perpendicular to the optical axis was 0.36 (see 'Roy Soc Proc,' A, vol 92, p 49 (1915))

A series of measurements of $(K'_t - K'_\infty)$, under varying conditions as to voltage, etc, have been made, and from these the following data have been compiled. In the first column of Table I are shown times measured from the instant at which both surfaces of the specimen were brought into contact with the earth, and in the succeeding columns the corresponding values of K'_t for different times of charging are given, the last value in each column being computed and not derived from an experiment

From these data the curves plotted as figs 4-6 were obtained. Above the curves the logarithms, to the base 10, of the various values of K'_t are indicated, the logarithmic scales being shown on the right of the figures

The relation between the values of K'_t and the different times of charging is shown as fig 7.

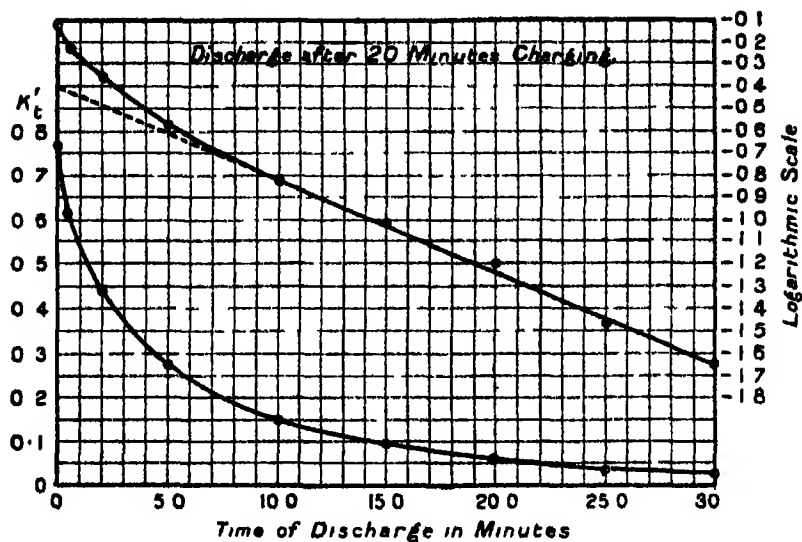


FIG. 4

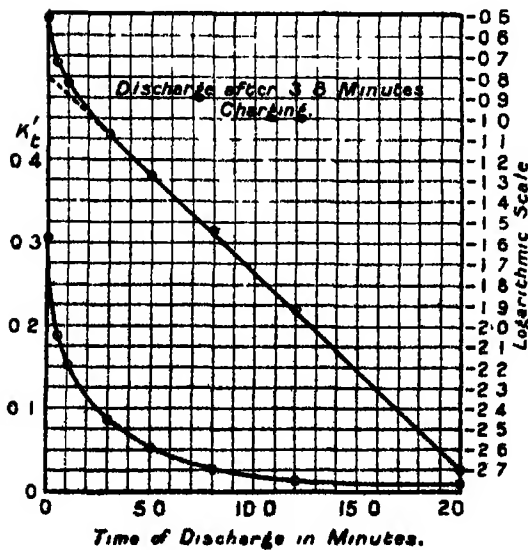


FIG. 5.

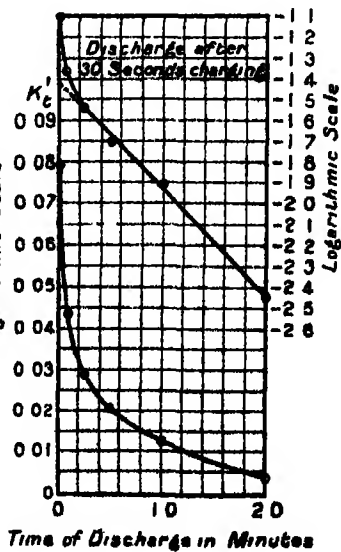


FIG. 6.

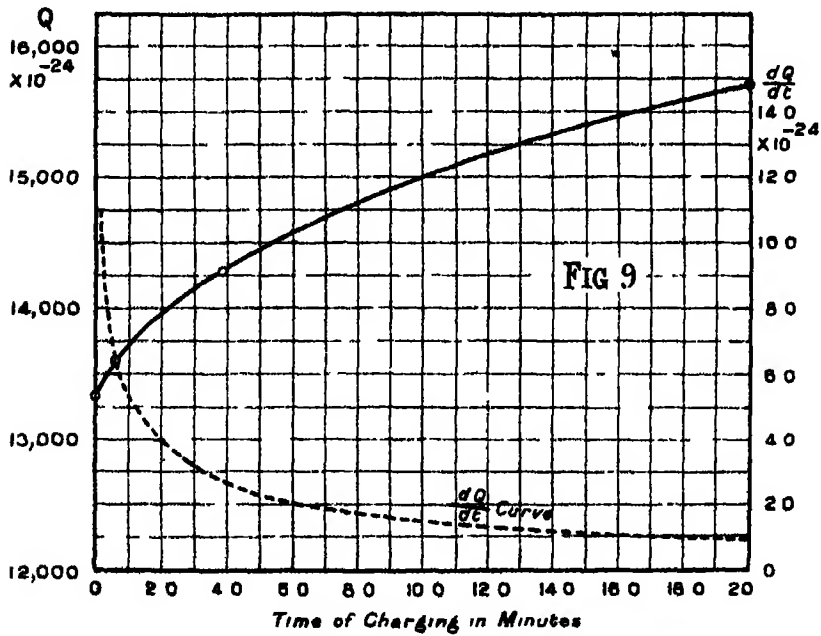
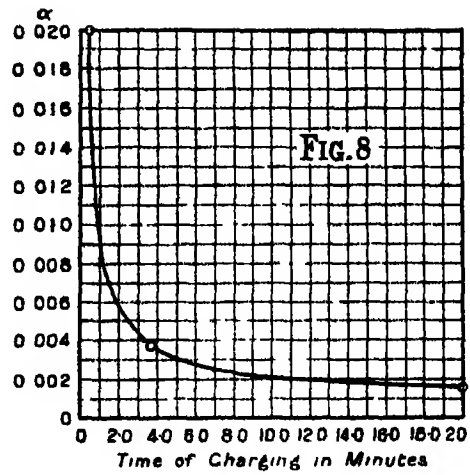
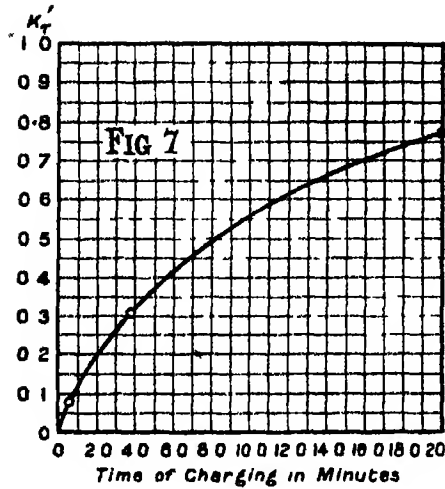


Table I

Time of discharging	Time of charging.		
	20 mins	3 8 mins	30 secs
7 secs	0 770	0 307	0 080
5 "	—	—	0 044
15 "	—	—	0 029
30 "	0 615	0 188	0 020
1 mins	—	0 151	0 012
2 "	0 440	—	0 0035
3 "	—	0 085	—
5 "	0 274	0 053	—
8 "	—	0 028	—
10 "	0 151	—	—
12 "	—	0 012	—
15 "	0 095	—	—
20 "	0 063	0 002	—
25 "	0 035	—	—
30 "	0 023	—	—

The values of α for several times of charging are given in the following Table —

Table II

Time of charging	20 mins	3 8 mins	30 secs
α	0 0016	0 0037	0 020

A curve connecting these values of α with the times of charging is shown as fig 8

Four of the values for γ , dQ/dT , and P for different times of charging are given in the following Table —

Table III

V = 1

Time of charging	γ	$\frac{dQ}{dT}$	P	Apparent Resistance	R.
10 secs	17.6×10^{-21}	11.0×10^{-21}	0 18	0.57×10^{22}	1.24×10^{22}
30 "	10.2×10^{-21}	6.5×10^{-21}	0 54	0.98×10^{22}	1.24×10^{22}
3 8 mins	4.7×10^{-21}	2.7×10^{-21}	0 75	2.11×10^{22}	1.25×10^{22}
20 "	2.5×10^{-21}	0.81×10^{-21}	0 79	4.00×10^{22}	1.24×10^{22}
Mean					1.24×10^{22}

These results are plotted as figs. 9-12. The area of the silvered surface being 4.53 sq cms, and the thickness of the specimen 0.13 cms., the specific resistance, ρ , is obtained from the relation

$$\rho = R \frac{4.53}{0.13} = 4.3 \times 10^{14}$$

This value is about 200 times greater than the corresponding value (2.0×10^{12}) found for the specimen of quartz cut perpendicular to the optical axis (*loc cut*) (See also Curie 'Annales de Chimie et de Physique, 1889')

Supplementary Note on some further Experiments relating to the Flow of Electricity through Quartz in the direction of, and perpendicular to, its Optical Axis

Curie (*loc cit*) observed that if one surface of a specimen of quartz cut parallel to the optical axis is connected to a battery (the other surface being insulated) electricity escapes from the specimen and accumulates on the insulated surface—as in other cases (see fig. 2)

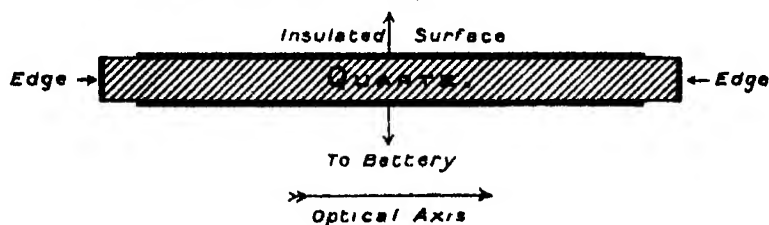


FIG 2

If, however, the edge of the specimen is uninsulated and connected to the earth, the potential of the insulated surface gradually falls as time goes on (see fig. 3)

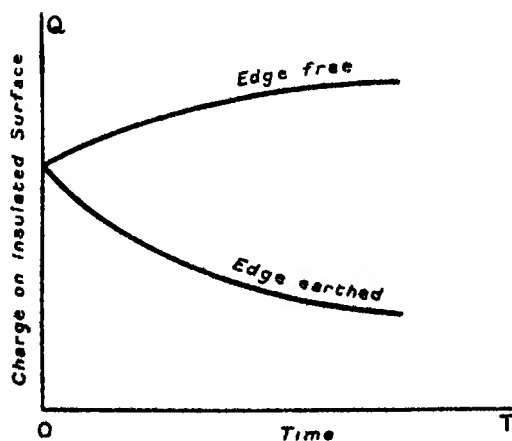
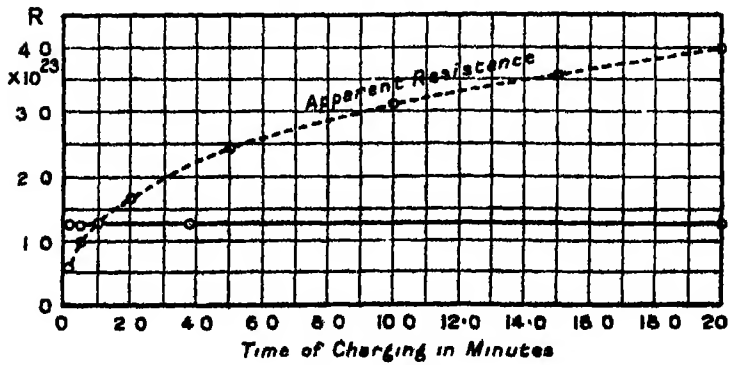
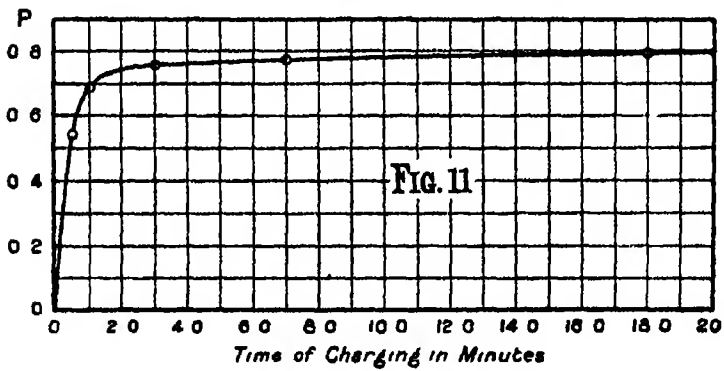
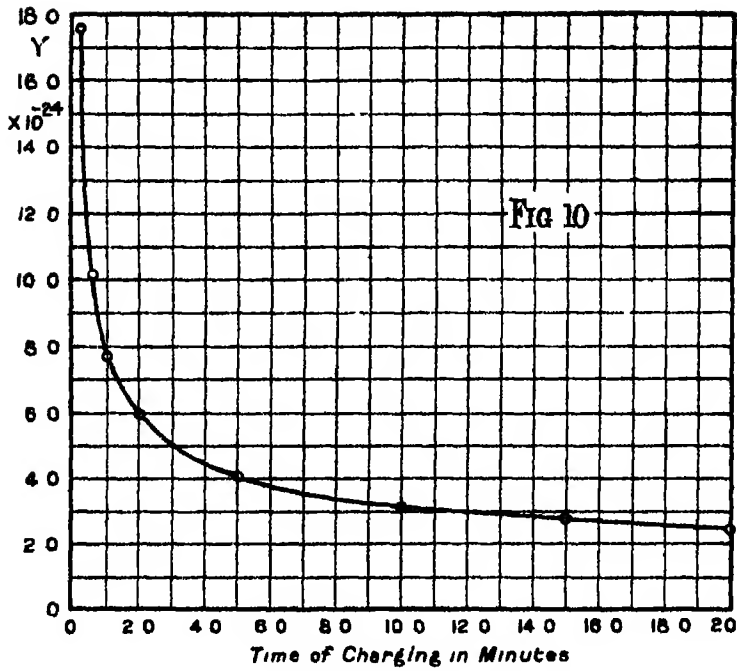
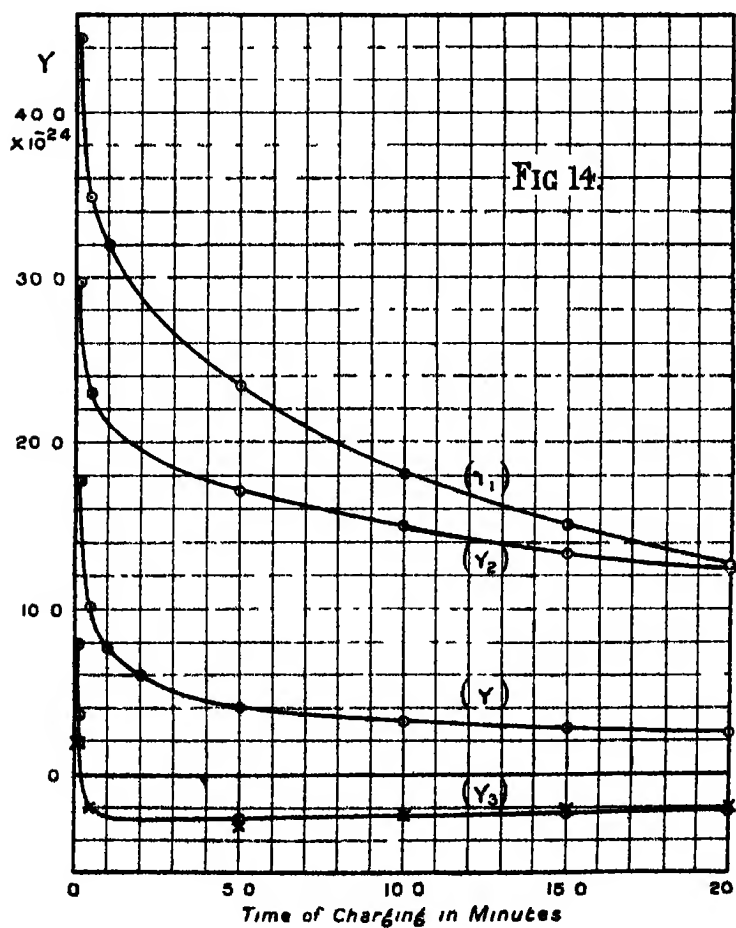
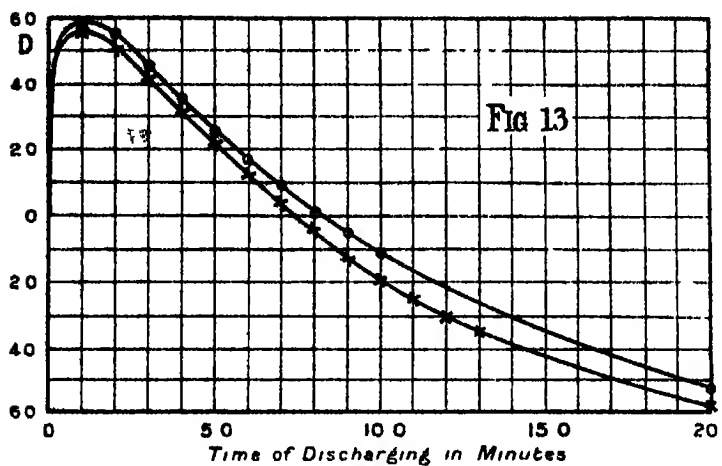


FIG 3.





I have observed that if, after charging such a specimen for some time, both surfaces are rapidly connected to the earth and then one is immediately insulated—a charge accumulates on the insulated surface for about one minute (say) and then diminishes, becomes zero and, finally, changes sign

This is illustrated in fig 13 The specimen had been charged for 10 minutes—first in one direction, and then in the other direction The ordinates represent the values of the electrometer readings in the two cases and the abscissae the corresponding times of discharge I have also observed that if one surface of the specimen (the edge being uninsulated and connected to the earth) be connected to a battery—the current, γ_3 , that flows through the insulated surface rapidly diminishes to zero and then changes sign

In order to throw some light on this phenomenon, I have performed a series of experiments (see Table IV) on —

(a) The normal current, γ , flowing through the insulated surface when the edge is free

(b) The normal current, γ_1 , flowing through the edge when one surface is free It will be seen that γ_1 is $> \gamma$

(c) The current, γ_2 , flowing through the edge when one surface is connected to the earth It will be seen that (up to 20 mins) γ_2 is $< \gamma_1$

(d) The current, γ_3 , flowing through one surface when the edge is connected to the earth These results (indicated thus \circ) are shown as fig 14

The values in the last column of Table IV (indicated thus \times in fig 14) were obtained from the *approximate* relation —

$$\gamma_3 = \gamma_2 \frac{\gamma - 0.34\gamma_1}{\gamma_1 - 0.34\gamma}$$

Table IV.

Time of charging	γ	γ_1	γ_2	γ_3	$\gamma_3 \frac{\gamma - 0.34\gamma_1}{\gamma_1 - 0.34\gamma}$
3 secs	—	—	—	7.9×10^{-21}	—
6 "	—	—	—	3.4×10^{-21}	—
10 "	17.6×10^{-21}	44.6×10^{-21}	29.7×10^{-21}	2.0×10^{-21}	1.9×10^{-21}
30 "	10.2×10^{-21}	34.9×10^{-21}	23.1×10^{-21}	—	-1.1×10^{-21}
5 mins	4.1×10^{-21}	23.4×10^{-21}	17.0×10^{-21}	-2.7×10^{-21}	-3.1×10^{-21}
10 "	3.2×10^{-21}	18.1×10^{-21}	15.0×10^{-21}	-2.5×10^{-21}	-2.7×10^{-21}
15 "	2.8×10^{-21}	15.0×10^{-21}	13.2×10^{-21}	-2.5×10^{-21}	-2.1×10^{-21}
20 "	2.5×10^{-21}	12.7×10^{-21}	12.5×10^{-21}	-2.3×10^{-21}	-1.9×10^{-21}

Recent Developments in Tensile Testing

By J V HOWARD, D Sc ; and S L SMITH, D Sc , A C G I

(Communicated by W E Dalby, F R S —Received May 30 1921)

INTRODUCTORY

The study of the behaviour of metals on removal and re-application of load has been facilitated by the Dalby Autographic Load-Extension Recorders. Prof Dalby has described these instruments and the specially designed hydraulic press in which the tensile tests are carried out,* and has shown that metal possesses elastic properties right up to fracture. Up to a certain limiting stress the extension is proportional to the applied load, when this stress is exceeded the metal loses its proportional elasticity but retains the property of non-proportional elasticity †. When the material has passed into the condition of non-proportional elasticity, the removal and re-application of the load causes a loop to be traced in the recorded load-extension diagram.

Looping is a general property of metals, and the loops obtained from different metals have distinguishing characteristics ‡. Prof Dalby has also shown that the loop area increases with permanent set, tending towards a maximum value, and that loop area plotted against permanent set gives a smooth curve §. This will be referred to as the "normal curve" for a metal.

The researches described in this paper were undertaken with a view to investigating the factors influencing the formation of these loops, and to studying the effects of variations in composition on the looping properties with special reference to tests on steel. Considerations of space render it impossible to record in detail the large amount of experimental work which has extended over the past three years. Although the paper is therefore of the nature of a summary, it may be stated that every experimental fact adduced has been checked by independent tests on different steels or by subsidiary researches.

No attempt has been made to formulate a theory to cover the experimentally established facts, but it is believed that it has been possible to extend the knowledge of properties of steel which usual methods of testing fail to reveal.

* W E Dalby, 'Strength and Structure of Steel and Other Metals,' Edward Arnold and Co, pp 31-38.

† W E Dalby, "Researches on the Elastic Properties of Metals," 'Phil Trans,' A, vol 221, p. 122.

‡ *Ibid.*, pp 125-131.

§ 'Phil Trans,' A, vol 221, p. 132.

THE PROPERTIES OF A LOOP.

1. *Recoverable Slip*—Fig 1 shows three typical loops. They were obtained in a test on a steel containing 0.63 per cent carbon. The lines O_1E_1 , O_2E_2 , and O_3E_3 have been drawn in on the diagram at a slope corresponding to the primitive modulus of elasticity determined from the elastic line at the beginning of the record *. The loop boundaries are curved, and this causes the loops, as a whole, to slope away from the "E" lines

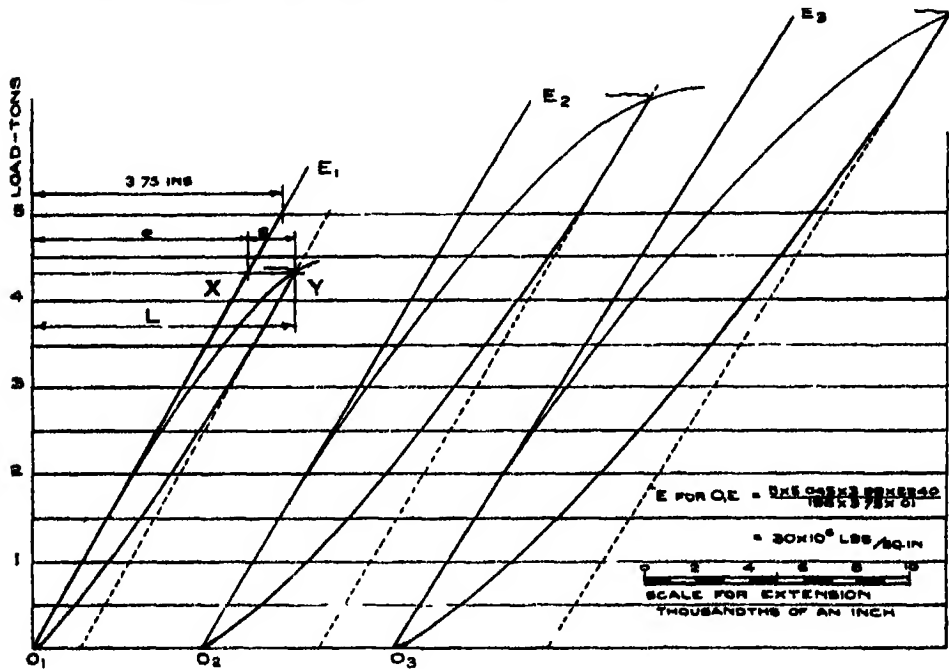


FIG 1

Referring to the first loop, on the application of the load, the spot of light which traces the record on the photographic plate moves from O_1 along the curved path O_1Y . This motion can be regarded as compounded of —

- (i) A movement from O_1 to X in the direction of the primitive elastic line, producing an extension marked "e" in the figure, and
- (ii) A plastic step or slip, XY , parallel to the extension axis, producing a further increment of extension "s" in the figure

The total stretch of the test-piece at the top of the loop is thus made up of a proportionally elastic portion and a non-proportionally elastic portion.

* W E Dalby, "Load Extension Diagrams taken with the Optical Load-Extension Indicator," Roy Soc. Proc., A, vol 88, p 285

The remarkable fact is that, on unloading the test-piece, the spot of light traces out a similar curve, so that, not only the proportionally elastic but also the non-proportionally elastic component of the extension disappears.

For want of a more suitable name, it is proposed to call this non-proportional component of the curved loop boundary the "recoverable slip." The question which immediately arises is: What is a convenient measure of recoverable slip?

2 *Loop Area as a Measure of Recoverable Slip*—From the analysis of the curved loop boundary into two steps, namely, a primitive elastic straight-line step and a plastic step parallel to the axis of extension, it is clear that the greater this second step the further will be the departure of the loop boundary from the primitive elastic "E" line. Numerous experiments have indicated that the greater this departure—or recoverable slip—the greater is the curvature of the loop boundary and, consequently, the area enclosed when the load is removed and re-applied.

This is illustrated by the two loops, obtained from tests on different steels, shown in fig 2. The steel possessing the physical property characterized by greater recoverable slip yields a loop of larger area.

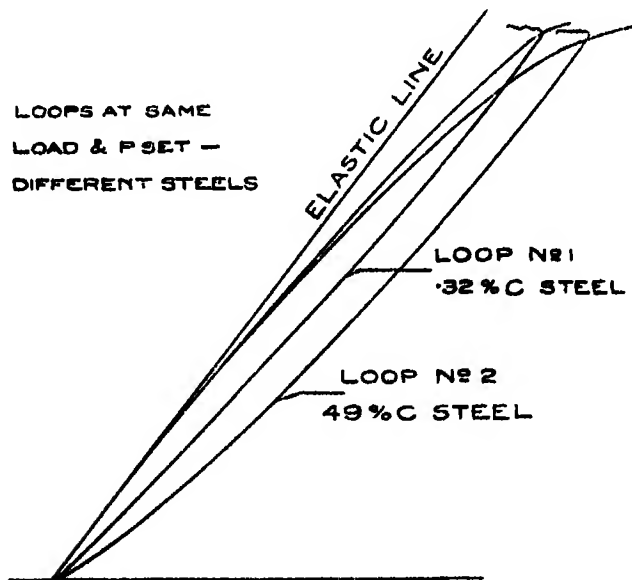


FIG. 2.

Although the steels were different, it so happened that at the load at which the loops were executed, the load-extension diagrams for the breaking tests

crossed, so that the permanent set at this load, and therefore the slope of the "E" line, was the same for both steels and the two loops are strictly comparable.

3 Recoverable Slip depends only on Stress—The actual area of a loop will depend, of course, on the load and extension scales of the diagram as well as on the diameter of the test-piece, which fixes the height of a loop for any particular stress. We have found, however, that for a given material, when the load and extension have been reduced to the corresponding values of stress and strain, the length of the second plastic step depends only on the stress and is independent of the cross-section of the test specimen.

This is demonstrated in fig 3, in which loops are shown from tests on three specimens cut from the same bar of steel. The slope of the "E" lines differs for the three loops on account of differences in cross-sectional area.

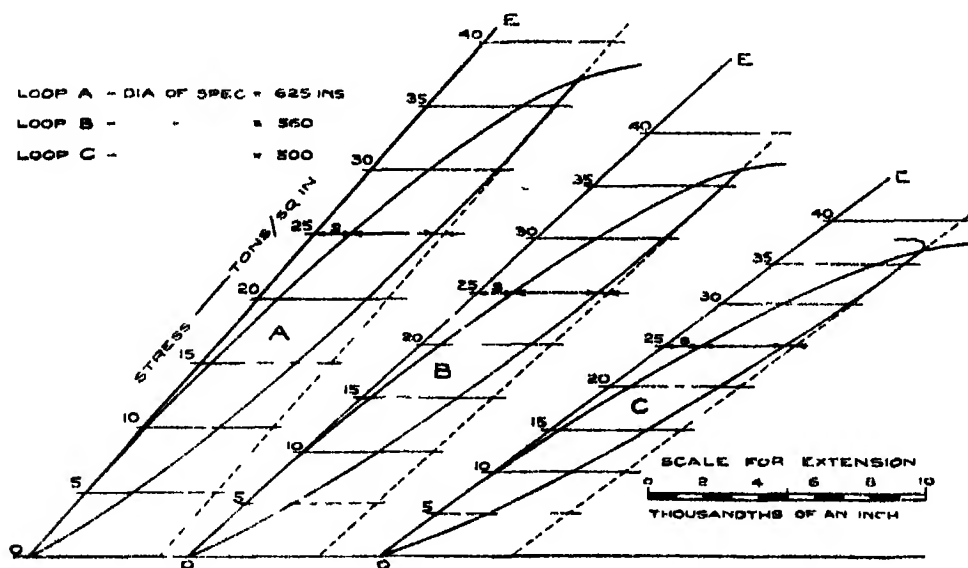


FIG 3

Notwithstanding the differences in stress scale, it will be seen that there is practical equality between the recoverable slips recorded at any particular stress. For example, the recoverable slips corresponding to a stress of 25 tons per square inch are marked "s" on the diagrams, and these have a value of 0.0013 inch in each case.

It is to be noted that the loops referred to in the foregoing remarks are what may be conveniently called the "primary loops," that is, the loops obtained

during a normal continuous looping test. Our researches have shown that, although the loop area may be reduced in various ways either by a period of rest or by a particular method of approaching the load at which the loop is recorded, the primary loop has the maximum area associated with that load.

4 *Mean Loop Width as a Measure of Recoverable Slip*—The inference from the two preceding paragraphs is that the recoverable slip produced by a given stress (and, therefore, the curvature of the loop boundaries) is an inherent physical property of the metal. It follows from this that the mean width of a loop will depend only on the stress at the top of the loop, whatever the diameter of the test piece.

This was verified in the following way. Complete looping tests up to a load approaching the maximum load for the specimen were carried out on the three test-pieces referred to in paragraph 3. The stress at the top of every loop was

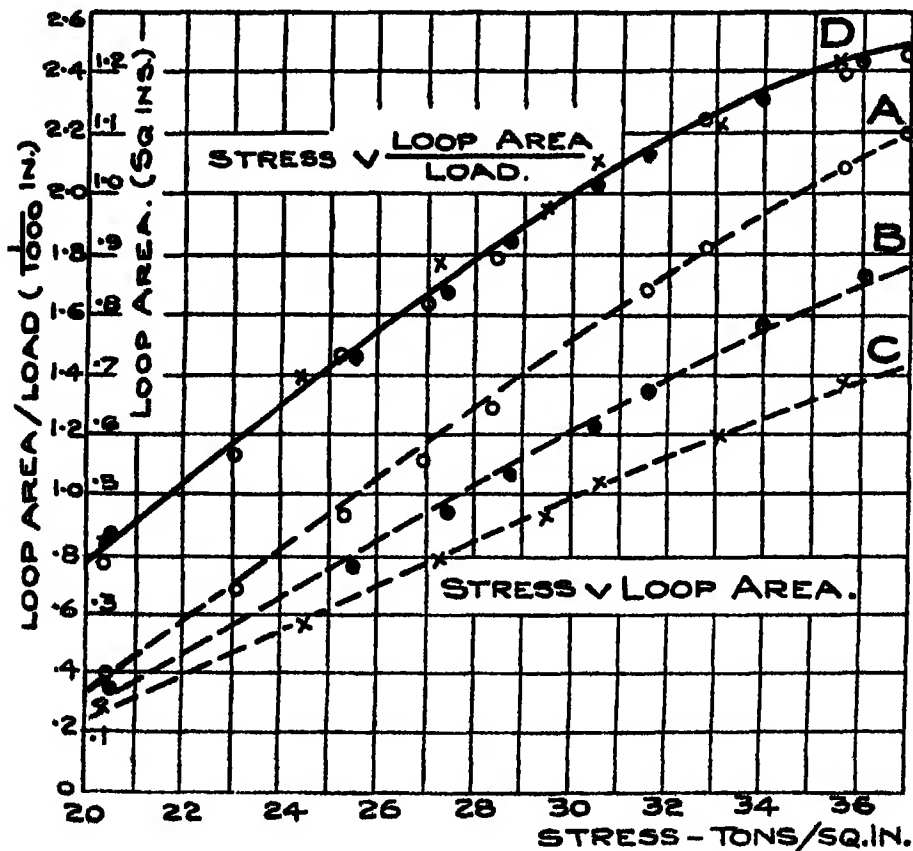


FIG. 4

calculated from the recorded load and the cross-sectional area, on the assumption that the volume of the specimen remains unchanged during the test. The curves of loop area plotted against the corresponding stress are marked A, B and C in fig 4

The mean width of the loops parallel to the extension axis was obtained by dividing each loop area by the load at the top of the loop. These values are plotted against stress in curve D in fig 4, which is the same for all three specimens. Curve D is thus a characteristic curve for the material under test. Mean loop width therefore depends only on stress and is independent of the diameter of the test-piece. It is thus a convenient measure of the property of the metal which gives rise to recoverable slip.

LOOPING AT CONSTANT LOAD

5 *Permanent Set is the Ultimate Cause of Fracture*—Two identical specimens were each looped up to a predetermined load, different for each test-piece. When this load was reached, looping was continued at constant load at the rate of 22 applications per minute. The permanent set increased continuously during the constant-load part of the test and loops were recorded at intervals of about 0.05 inches of permanent set. This was continued until the test-pieces broke.

The work done to fracture, including the energy absorbed in looping, was 15.4 and 22.4 inch-tons for the test-pieces looped at constant loads of 7 tons and 6.1 tons respectively. Apart from this looping energy, represented by the areas of the loops, the work done to fracture was 6.5 and 6.3 inch-tons.

A straight-through breaking test was also made on an identical test specimen. The work done to fracture, measured from the area under the load-extension diagram, was 6.7 inch-tons.

The total elongation was the same whether the test-piece was broken by a continuous pull or by constant-load looping at the higher or lower load. The deduction is that the ultimate cause of rupture is permanent set or plastic deformation, and not the total amount of work expended in producing this deformation.

6 *Permanent Set is caused by the Act of Looping*—When a test-piece is subjected to a steady load, it continues to stretch slowly for a considerable time and finally stops. If a loop is then executed, the stretching re-commences, continues at a decreasing rate and again stops.

Fig. 5 is a record of such a test.

The test-piece was looped normally up to a load of 6.8 tons, corresponding

to a stress of 22.1 tons per square inch. It was then left under load and readings of time and extension taken. When stretching had practically

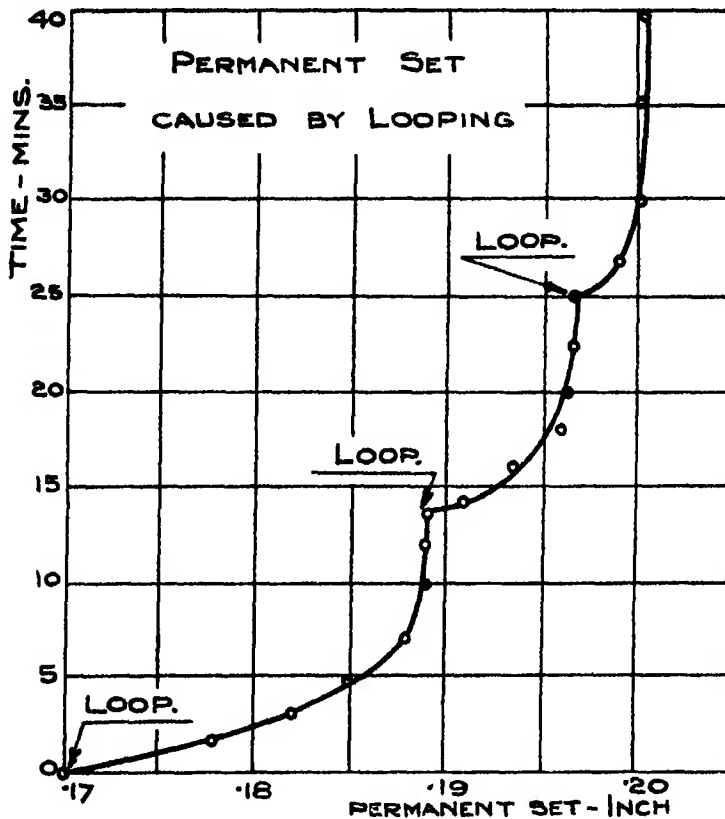


FIG 5

ceased, as shown by the curve becoming parallel to the time axis, a loop was executed and recorded and the same steady load again left on the specimen. This was repeated several times.

Fig 5 shows how the mere execution of a single loop gave an impulse to the material sufficient to start it stretching again.

The same specimen was then looped at a constant load of 6.8 tons 300 times and the load again left on the specimen. No increase in extension was observed even after several hours, but on proceeding with the looping the extension again increased. The loop areas recorded throughout the experiment were the same. This shows that when a loop is traced an internal disturbance is set up in the metal, which is a cause of the production of permanent set and therefore, ultimately, of rupture.

A PROPOSED QUALITY FACTOR

7 Recoverable slip is measured by mean loop width. For the large number of steels tested, it was found that the characteristic curves of mean loop width plotted against stress were substantially parallel. Thus, by selecting a convenient arbitrary value of mean loop width, the corresponding value of stress can be read off the characteristic curve. This stress provides a means of comparing different steels as regards that property of the metal which is revealed by this method of testing.

A mean loop width of 0.0015 inch was found to be a convenient value for test-pieces of 5-inch gauge length, and the quality factor of a steel is therefore defined as the stress in tons per square inch necessary to produce this standard loop width. A steel having a low quality factor will be characterized by large loops, and conversely

THE EFFECT ON THE QUALITY FACTOR OF VARIATIONS IN THE COMPOSITION AND HEAT-TREATMENT OF STEEL

8 The comparison of different steels by means of the quality factor defined in the last paragraph yields remarkable results. Fig. 6 records the factors derived from tests on two series of carbon steels. The carbon contents ranged

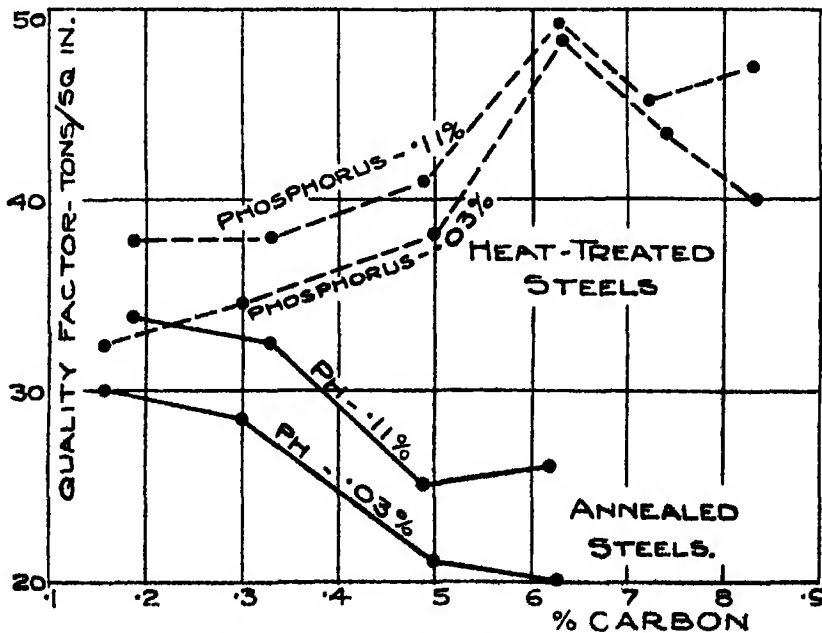


FIG. 6.—Variation of Quality Factor with Carbon Content.

from 0.16 per cent to 0.83 per cent, and the two series differed only in the amount of phosphorus present. This was 0.03 per cent in one series and 0.11 per cent in the other.

Each series was subjected to two heat-treatments before testing, one a simple anneal and the other a complete treatment consisting of quenching followed by re-heating. There are thus four groups of tests.

The influence of carbon content on quality factor appears to depend on the heat treatment which the steel has undergone. For low-carbon steels there is little difference in the factor whether this has been a simple anneal or a complete double treatment. But with heat-treated steels the factor rises with the carbon and reaches a maximum at about 0.6 per cent carbon, while, for annealed steels, it falls with rise in carbon content. The annealed series are incomplete, as the higher-carbon members were so brittle that they were liable to break suddenly with very little permanent set. To avoid risk of damage to the delicate extensometer mechanism, tests on these steels were postponed, but there are indications that the quality factor has a minimum value at 0.6 per cent carbon exactly where the maximum value of the factor occurs in the case of heat-treated steels.

As regards alloy steels, no change in quality factor could be detected with variations in nickel up to about 3 per cent. Nickel-chrome steels, containing between 0.8 and 1.2 per cent chromium, after correct heat-treatment, had a factor 1.6 times that of a straight carbon steel of the same carbon content.

9 Limit of Proportional Elasticity as affected by Variations in Composition — Looping tests on the series of steels referred to in paragraph 8 showed that variations in carbon content have practically no effect in annealed steels containing 0.11 per cent phosphorus. The elastic limit over the whole range of carbon content was 21 tons per square inch.

Reduction in phosphorus content to 0.03 per cent was accompanied by a lowering of the elastic limit. This was more pronounced at the low-carbon end of the range, so that the limit rose from 12 tons/sq. in. for steel containing 0.1 per cent carbon to 18 tons/sq. in. for that containing 0.9 per cent.

The elastic limit of the sorbitic heat-treated steels rose more or less uniformly with the carbon content, varying from 18 to 30 tons/sq. in. over a carbon range from 0.1 per cent. to 0.9 per cent.

Variations in nickel up to 3 per cent were found to have no influence on the elastic limit of steel containing 0.15 per cent carbon. When present to the amount of 4.7 per cent, nickel appears to produce a profound change in the character of the metal. This is indicated by a fundamental departure

from the typical steel load-extension diagram. The irregular yield link* is suppressed and there is a smooth transition from the elastic line to the curve of plastic extension. This change in the metal was accompanied by an elastic limit having the exceptionally low value of 9.1 tons/sq in (annealed) and 12.1 tons/sq in (heat-treated).

Annealing is an unsuitable treatment for nickel-chrome steels and was found to produce a condition somewhat similar to that conferred by high nickel. In this condition a steel containing 1.2 per cent chromium, 3.3 per cent nickel and 0.32 per cent carbon had an elastic limit of 11.2 tons/sq in. This was raised to 39 tons/sq in by correct heat-treatment.

OVERSTRAIN FOLLOWED BY REST

10 Prof Dalby has shown that some metals recover their property of proportional elasticity with time†. The following experiments were undertaken to extend the investigation to steels of different composition and heat-treatment.

The test-pieces not fractured in constant-load looping tests similar to those described in section 5 were rested for 15 days. They were then pulled under loads which were gradually increased up to the previous looping load. A record was made of each pull.

Fig 7 is the result obtained with two of the specimens. The other records were similar. In each case straight lines of proportional elasticity were

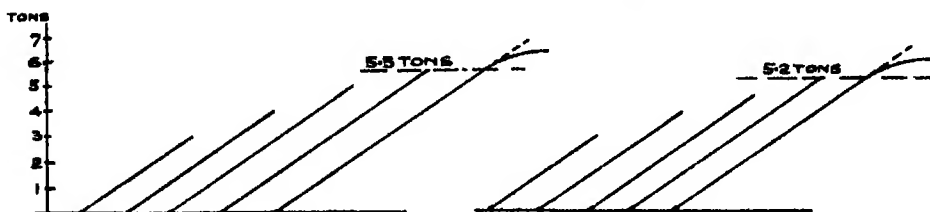


FIG 7

obtained up to the previous looping load. When this load was exceeded, small loops were traced, and a further slight increase in load caused the material to yield definitely.

The slope of the lines afforded a value for "E" the same as that for the steels in the unstrained condition. In these cases, rest under no load restored

* W. E. Dalby, "An Optical Load Extension Indicator," 'Roy Soc Proc,' A, vol. 86, p. 424.

† "Researches on the Elastic Properties of Metals," 'Phil. Trans.,' A, vol. 221, p. 120.

the elastic properties of the material and gave it a limit of proportionality equal to the previous looping load and a yield-point just above it. The steel contained 0.63 per cent carbon and had been annealed.

A number of other steels were tested in the same way after periods of rest up to three months. The conclusions drawn were —

(i) Annealed (pearlitic) hypo-eutectoid steels, including pearlitic nickel steels, completely recover their property of proportional elasticity with rest. The limit of proportional elasticity after rest is the maximum load previously applied.

(ii) Sorbitic (heat-treated) carbon steels of all compositions have no such power of recovery. On re-loading after rest, the load-extension line was curved and a loop was traced on the removal of the load.

(iii) Carbon steel of eutectoid composition does not recover whatever its previous heat-treatment.

11 *Rest under Load* — A test-piece was looped 700 times at a constant load of 6.1 tons. The total permanent set recorded was 0.261 inch. It was then left in the testing machine under this load for 18 days. During this time the permanent set remained unaltered.

On the eighteenth day the load was removed and the test-piece immediately pulled at loads ranging from 4 up to 6.1 tons. The record is shown in fig. 8. A loop was traced at each pull, and the loops at 6.1 tons were identical with the last one recorded after the original 700 loops.

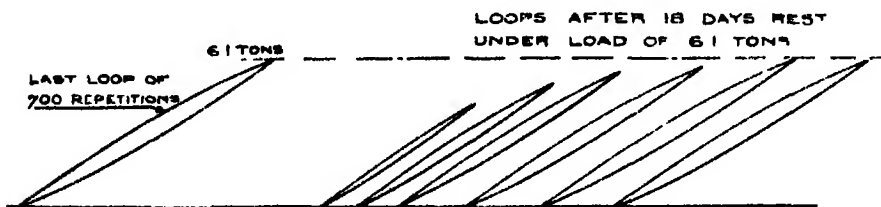


FIG. 8.

It appears that no recovery of proportional elasticity takes place while the metal remains in a condition of stress.

12 *The Normal Curve of Loop Area against Permanent Set indicates the Heat-Treatment which the Steel has undergone* — The normal curve for a typical steel consists of three parts corresponding to the three distinct stages in the complete tension test. These stages are — (i) The yield period in which a large extension takes place while the load fluctuates about a constant value. (ii) The period of plastic elongation subsequent to the yield period. (iii) The period of incipient

rupture as the maximum load for the test-piece is approached, when the loop area tends towards a maximum. In order to allow of exact comparison, the normal curves of all the steels tested were plotted logarithmically. Fig 8 relates to annealed, pearlitic carbon steels.

For the second stage in the tests, the logarithmic curve is sensibly a straight line, so that a simple approximate relation exists of the form —

$$\text{Loop Area} \propto \text{Constant (Permanent Set)}^n$$

The lines for all the steels in fig 9 are mutually parallel. The index “ n ” has the value 0.65 whatever the carbon and phosphorus content. Tests on annealed nickel and nickel-chrome steel gave the same index value so long as

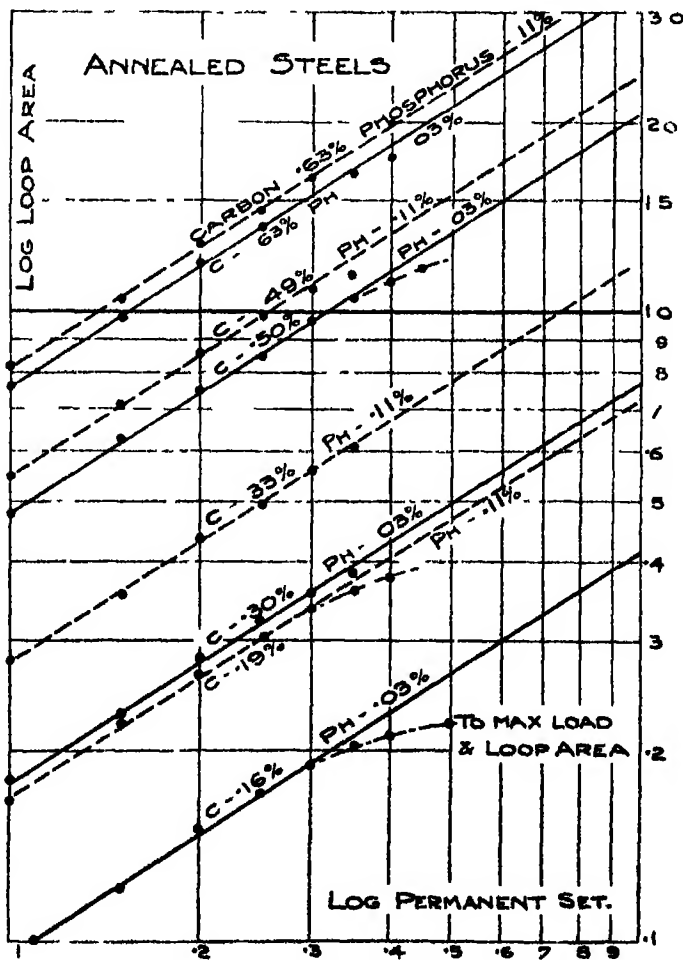


FIG 9

there was not sufficient alloy to destroy the typical steel characteristics of the metal

Similar straight lines were obtained from tests on heat-treated sorbitic steels. In general, the index corresponding to this heat-treatment was 0.40. The index is therefore a criterion as to the heat-treatment to which the steel has been subjected.

High-phosphorus, low-carbon steels (Ph 0.11 per cent, C up to 0.2 per cent) were exceptions. The value of the index for these steels after heat-treatment was 0.52. This is nearer to that for annealed steels and suggests that phosphorus in low-carbon steels impedes the action of heat-treatment.

In the high-alloy steels in which the yield link was suppressed, the index "n" had a value so low as to suggest that these steels (if they can properly be called steels) must be placed in an entirely different category.

CONCLUSION

The experimental work briefly recorded above deals only with the removal and re-application of tensile stress, without introducing the further question of reversal of stress. Even so, the research is by no means exhaustive and numerous points still await investigation.

The authors have to express their indebtedness to Prof. Dalby for his interest and valuable advice in connection with the work, and for his kind permission to use his Autographic Load-Extension Recorders which have rendered the research possible.

The Effect of Superposed Alternating Current on the Polarizable Primary Cell Zinc-Sulphuric Acid-Carbon Part I—Low-Frequency Current

By A. J. ALLMAND, D.Sc., and V. S. PURI, M.Sc., Ph.D.

(Communicated by Prof. S. Smiles, F.R.S.—Received July 22, 1924)

Under the title "Chemical Action that is Stimulated by Alternating Currents," some interesting experiments were published a few years back by Brown*. Briefly, he found that if an alternating current of suitable strength and of either 100 or 12,000 periods per second were passed through a primary cell of the type

Zinc/Dilute Sulphuric Acid/Carbon,

itself fitted up so as to discharge through a circuit of low resistance, the polarisation of the cell was destroyed and its current output materially increased. No further details are given on the experiments with 100-cycle current. Using the high frequency, however, the conclusion was come to that the increased current output was essentially the result of a changed state of affairs at the zinc, not at the carbon, electrode. Thus, when the current densities at the two electrodes were varied by altering their relative areas immersed in the electrolyte, it was found that a high alternating current density at the zinc electrode had a far greater effect in increasing the direct current output of the cell than when the high current density was employed at the carbon electrode†. In other words, a given alternating current produced a greater effect if the cell had a small zinc and a large carbon electrode than if it had a large zinc and a small carbon electrode. More conclusive was the observation that, using a small zinc and a large carbon electrode, the same effect was observed when the carbon electrode was already fully depolarised by immersion in strong nitric acid.

Brown concluded that, whilst the surface of the carbon electrode only affects the results in so far as it determines the resistance of the cell, the alternating current in some manner increases the velocity of the sulphations in the neighbourhood of and towards the zinc anode, the latter being more rapidly dissolved, particularly with a small electrode and a consequently high current density.

Several reasons led us to take up and extend Brown's experiments. Assuming for the moment that the seat of the effect is the zinc electrode, his explanation

* 'Roy. Soc. Proc.,' A, vol. 90, p. 26 (1914).

† The percentage increases in direct current were much the same in the two cases.

of the mechanism of the effect is far from convincing. Further, in practically all cases where the superposition of alternating current has been found to influence an electrode process, the latter is characterised by a marked degree of *irreversibility*. Typical examples of this kind in which the combination metal/metallion plays a part, are furnished by the anodic solution of platinum,* gold,† iron,‡ lead,§ nickel,|| and the electrodeposition of nickel ||. The anodic solution of zinc, on the contrary, is known to occur very nearly reversibly, and there is consequently an *a priori* reason for not expecting an effect with superposed alternating current. The case would appear to be quite different at the carbon electrode, at which hydrogen is evolved. Rothmund and Lessing,¶ in the course of work on the Schlömilch electrolytic detector, showed that both voltage and current output of the Smee cell were raised by the passage of electric waves, the cause being, apparently, depolarisation of hydrogen discharge, whilst Ghosh** and Goodwin and Knobel,†† using frequencies per second of 500 and of 100 downwards, respectively, also observed a marked depolarisation of cathodic hydrogen evolution.

We consequently decided to investigate the subject anew, paying particular attention to the effect of frequency, and using as our criterion of the effect the values of the electrode potentials under different conditions. The present paper gives an account of the work with low-frequency currents.

Effect of Alternating Current on the Current Delivery of the Primary Cell

The general arrangement of the apparatus is shown in fig. 1. A is a sixteen-pole alternator (made for us by the General Electric Company). It is fitted with a three-step pulley, and by the use of a specially-designed countershaft (like the motor, provided with suitably stepped pulleys) can be run at widely differing speeds, with a corresponding variation in the frequency of the currents generated between 5 and 240 cycles per second. Another machine (made by the Crocker-Wheeler Company) enabled us to work with 350-500 cycles. B allows of the adjustment of the applied alternating-current voltage, D is a Duddell thermogalvanometer, calibrated to read accurately any current between 0.001 and

* Ruer, 'Zeit für physikal. Chem.', vol. 44, p. 81 (1903).

† Wohlwill, 'Zeit für Elektrochem.', vol. 16, p. 25 (1910).

‡ Grube and Gmelin, 'Zeit. für Elektrochem.', vol. 26, p. 153 (1920).

§ Grube, 'Zeit für Elektrochem.', vol. 28, p. 275 (1922).

|| Kohlshütter and Schödl, 'Helvetica Chimica Acta,' vol. 5, p. 503 (1922).

¶ 'Ann. der Physik,' (4), vol. 15, p. 193 (1904).

** 'Jour. American Chem. Soc.', vol. 37, p. 733 (1915).

†† 'Trans. American Electrochem. Soc.', vol. 37, p. 617 (1920).

5 amperes, C is the cell, V a direct current voltmeter, M a direct current milliammeter, R_1 and R_2 resistances, and K_1 and K_2 keys

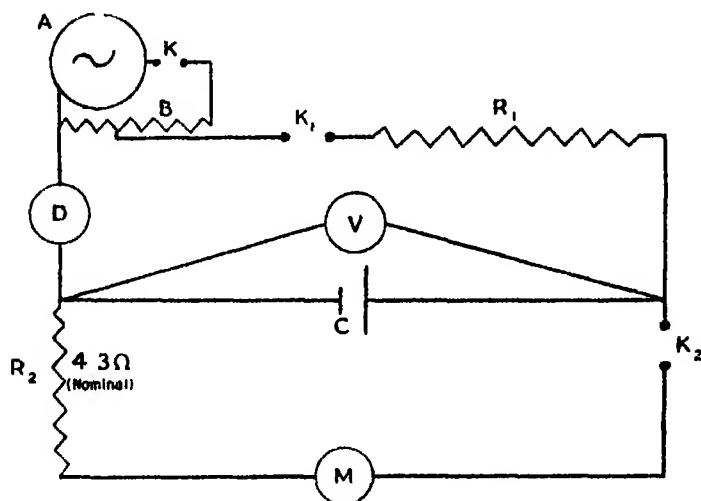


FIG 1

The zinc electrode was of rectangular cross-section (1×1 cm). Although cast from the purest zinc available it was necessary to amalgamate it, as it was otherwise attacked chemically by the electrolyte (sulphuric acid of 1.29 specific gravity). The carbon cathode was a lighting carbon, 1.1 cm in diameter. Both electrodes were filed down so as to give pointed ends, and were arranged so that any length could be immersed in the electrolyte at will.

The procedure adopted was simple. Required lengths of the two electrodes were dipped into the solution, the resistance R_1 adjusted to a pre-determined figure, and K_1 and K_2 closed. The current initially registered by M rapidly fell, and became constant in about half an hour. It was then read, as also were the cell voltage (on V), and the direct current leak into the alternating current circuit (on D). The alternator was then started. After a few minutes, when conditions had apparently become constant, M , V and D were again read. The alternating current was then switched off, when the direct current in a few minutes assumed its normal value. The whole operation was then repeated, using a different alternating current value, or varying the lengths of immersed electrodes.

It may be mentioned that, with superposed alternating current, there is a marked tendency for the bubbles of gas leaving the cathode to shoot outwards at right angles to the surface of the electrode. This was also noticed by Brown.

The results of these experiments, using a frequency of 60 cycles, are contained in Table I, and plotted in fig. 2. The figures in columns 2 and 3 are both cor-

Table I

Lengths of electrodes immersed	Alternating current in amperes	Current furnished by cell in amperes	Cell voltage in volts
Zinc 5 cm	0 0	0 033	0 125
Carbon "	0 1	0 036	0 13
	0 3	0 041	0 135
(a)	0 5	0 043	0 135
	0 7	0 045	0 16
	0 9	0 046	0 16
	1 1	0 047	0 17
Zinc tip	0 0	0 020	0 08
Carbon 5 cm	0 1	0 026	0 10
	0 3	0 028	0 11
(b)	0 5	0 031	0 11
	0 7	0 036	0 135
	0 9	0 040	0 14
	1 1	0 041	0 145
Zinc 0 6 cm	0 0	0 025	0 10
Carbon 5 cm	0 1	0 032	0 11
	0 3	0 039	0 14
(c)	0 5	0 040	0 14
	0 7	0 041	0 15
	0 9	0 042	0 15
	1 1	0 042	0 15
Zinc 5 cm	0 0	0 010	0 05
Carbon tip	0 1	0 019	0 12
	0 3	0 030	0 12
(d)	0 5	0 036	0 135
	0 7	0 042	0 14
	0 9	0 051	0 17
	1 1	0 060	0 21
Zinc 5 cm	0 0	0 021	0 07
Carbon 0 6 cm	0 1	0 025	0 10
	0 3	0 026	0 10
(e)	0 5	0 027	0 11
	0 7	0 028	0 115
	0 9	0 028	0 115
	1 1	0 029	0 115

rected for the small leak of direct current into the alternating current circuit, as determined prior to switching on the alternating current. The leak of alternating current into the direct current circuit was shown to be very small, and is neglected.

Similar experiments were done using a frequency of 400. The effects noticed were of the same order, but distinctly less than with a frequency of 60.

A comparison between fig. 2 and fig. 6 of Brown's paper is instructive. The

current deliveries of the different cells when no alternating current is flowing stand in the same order in the two cases, as would be expected. Whilst,

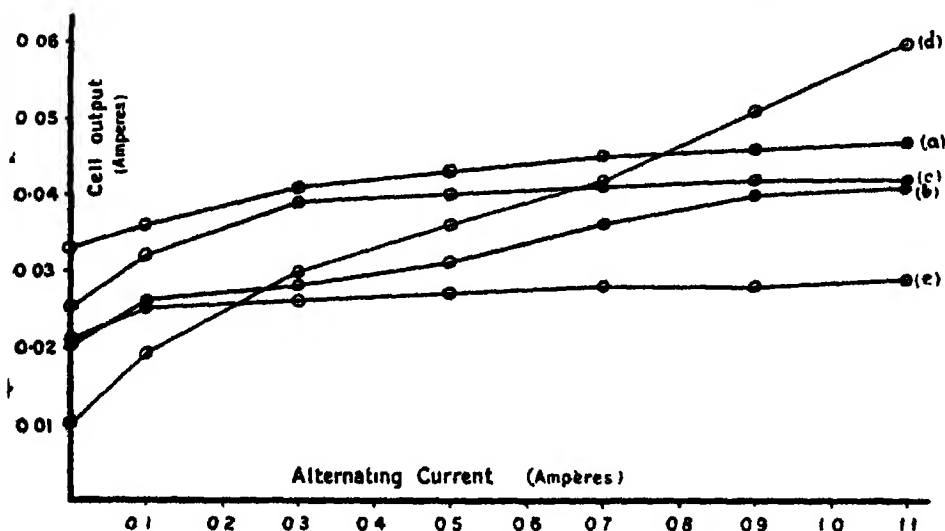


Fig 2

however, he, employing a high frequency, gets distinctly more marked effects than we do when using a small zinc and a large carbon electrode, it is quite otherwise when the carbon electrode is small compared with the zinc electrode. Our curve *d* rises more rapidly than any of the others in fig 2, whereas his curve 7 is the flattest of his series. There was, of course, the possibility that our use of amalgamated zinc might have been responsible for the difference observed, but there seemed no particular reason why this should be so. The results rather tended to confirm our anticipation that a superposed alternating current would have most effect on the carbon electrode, a view which is supported by the electrode potential measurements now to be described.

Effect of Alternating Current on the Electrode Potentials of the Primary Cell

In order to investigate separately the effects produced at the single electrodes, without disturbing directly the general working of the cell, the arrangement shown in fig 1 was modified by the introduction of an auxiliary electrode, which served to lead alternating current to the particular cell electrode under study. This, however, led to an experimental complication which is best illustrated by fig 3, in which the auxiliary electrode in every case is shown between the two cell electrodes. Imagine K and K_1 open, K_2 closed, and R_2 so adjusted as to give a reading of 0.010 ampere on M . Then, merely closing K_1

(no alternating current passing) led to a change in the reading of M, and, moreover, to the following figures —

- (a) 0·013 ampere,
- (b) 0·007
- (c) 0·002
- (d) Practically unchanged

The increased current in (a) is due to the lower current density, and therefore reduced polarisation at the carbon cathodes, the decreased currents measured

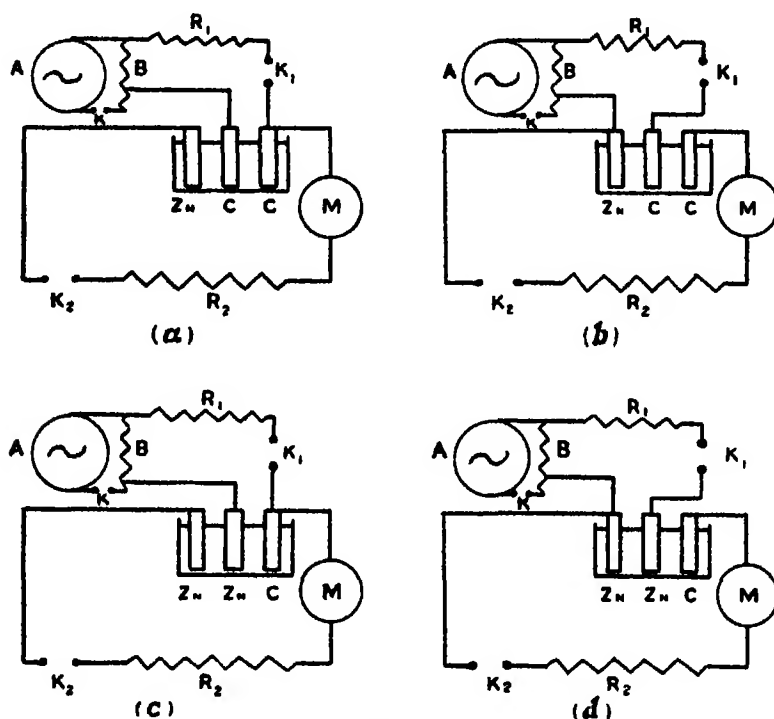


Fig 3

in (b) and (c) are clearly due to current passing through the alternating current circuit; whilst the fact that practically no increase in current takes place in (d), although the area of the anode surface is doubled, must be attributed to the extra resistance of the alternating current circuit. The procedure finally adopted was to work according to (d) when investigating the zinc electrode, and according to (a) when investigating the carbon electrode, the auxiliary electrode thus being of the same material as the direct current electrode under study. When using the circuit (a) another milliamperemeter was inserted in

the alternating current (auxiliary electrode) circuit, and the *difference* between the readings of this instrument and that of *M* taken as a measure of the direct current passing through the cell cathode

The potentials were measured by means of a Luggin capillary pressed closely against the surface of the electrode by means of rubber bands, and making connection with a normal mercurous sulphate electrode. For the rest, a metre bridge was employed, and a sensitive moving coil galvanometer. A choking coil in the potentiometer circuit prevented stray alternating currents from affecting the reading of the galvanometer, and allowed of measurements being made with a frequency as low as 20 cycles. Every instrument was insulated on wax slabs supported on glass plates or by paraffined glass insulators, and care was taken to avoid current leaks through connecting wires. These precautions were found to be very essential.

Using direct current only, two to three hours were found to be necessary for the potential of the carbon electrode to become constant within the limits

Table II.—Carbon Electrode Fed with Alternating Current

Frequency	Alternating current in amperes	Direct current in amperes	Cell voltage in volts	e_H at carbon electrode in volts	Change in P D of carbon electrode in volts
20	0 0	0 010	0 305	-0 493	—
	0 5	0 013	0 37	0 414	+0 069
	1 0	0 019	0 475	0 316	0 167
	1 5	0 024	0 58	0 216	0 267
	2 0	0 030	0 64	0 137	0 346
60	0 0	0 010	0 295	-0 515	—
	0 5	0 0115	0 325	0 481	+0 034
	1 0	0 016	0 42	0 373	0 142
	1 5	0 0225	0 55	0 266	0 249
	2 0	0 028	0 60	0 214	0 301
100	0 0	0 010	0 305	-0 488	—
	0 5	0 0105	0 33	0 466	+0 022
	1 0	0 016	0 41	0 376	0 112
	1 5	0 023	0 54	0 251	0 237
	2 0	0 027	0 595	0 195	0 293
240	0 0	0 010	0 30	-0 501	—
	0 5	0 011	0 31	0 485	+0 018
	1 0	0 015	0 40	0 388	0 113
	1 5	0 021	0 505	0 291	0 210
	2 0	0 025	0 61	0 208	0 293
400	0 0	0 010	0 295	-0 506	—
	0 5	0 0105	0 30	0 502	+0 004
	1 0	0 0135	0 385	0 416	0 090
	1 5	0 0165	0 415	0 373	0 133
	2 0	0 020	0 49	0 297	0 209

of accuracy of our measurements (0.003 volt). The amalgamated zinc electrodes settled down far more rapidly. When alternating current was switched in about 30 minutes were necessary each time for the attainment of constancy with the carbon, and five minutes with the zinc electrodes. Their respective rates of recovery on cutting off the alternating current were similar.

In the first series of experiments the direct current was first adjusted to a figure of 0.010 ampere, the alternating current switched in by regular steps, and readings taken of cell current delivery and voltage, and of electrode potential. The effects noted below an impressed alternating current of 0.5 ampere were small, and are omitted from the following Tables. It may be mentioned as showing that the apparatus was functioning well that the potential of the zinc electrode did not change perceptibly when alternating current was passing through the carbon anode, and that, with the zinc electrode under study, the change in the potential of the carbon electrode was very small, and of the order which would be expected to result from the slightly increased direct currents.

Table III — Zinc Electrode Fed with Alternating Current

Frequency	Alternating current in amperes	Direct current in amperes	Cell voltage in volts	e_H at zinc electrode in volts	Change in P.D. of zinc electrode in volts
20	0.0	0.010	0.30	-0.803	—
	0.5	0.010	0.30	0.811	-0.008
	1.0	0.0105	0.31	0.815	0.012
	1.5	0.0105	0.31	0.819	0.016
	2.0	0.011	0.31	0.822	0.019
60	0.0	0.010	0.28	-0.799	—
	0.5	0.010	0.28	0.803	-0.004
	1.0	0.0105	0.29	0.809	0.010
	1.5	0.0105	0.295	0.820	0.021
	2.0	0.011	0.295	0.822	0.023
100	0.0	0.010	0.295	-0.806	—
	0.5	0.010	0.30	0.806	-0.000
	1.0	0.010	0.30	0.816	0.010
	1.5	0.010	0.305	0.818	0.012
	2.0	0.010	0.29	0.824	0.018
240	0.0	0.010	0.30	-0.833	—
	0.5	0.010	0.31	0.835	-0.002
	1.0	0.010	0.315	0.839	0.006
	1.5	0.010	0.325	0.855	0.022
	2.0	0.010	0.33	0.859	0.026
400	0.0	0.010	0.30	-0.806	—
	0.5	0.010	0.305	0.820	-0.014
	1.0	0.010	0.32	0.826	0.020
	1.5	0.010	0.325	0.829	0.023
	2.0	0.010	0.335	0.832	0.026

Some interesting points emerge from a consideration of these Tables. There seems no doubt that, with the frequencies used in this work, the chief effect of the alternating current is confined to the carbon electrodes. The increases in current delivery and in cell voltage, and the change in the potential of the electrode under study, are all far more marked in Table II than in Table III. The figures in the relevant columns in Table II are on the whole very consistent with one another, a large change in cell voltage being paralleled by similar changes in current delivery, and in the polarisation of the carbon electrode. The results in Table III are apparently subject to error, as there is no such concordance—at all events between the current delivery and the other magnitudes. The effect of frequency is very marked in the case of the carbon electrode, and is illustrated graphically in fig 4, in which diminution in cathode

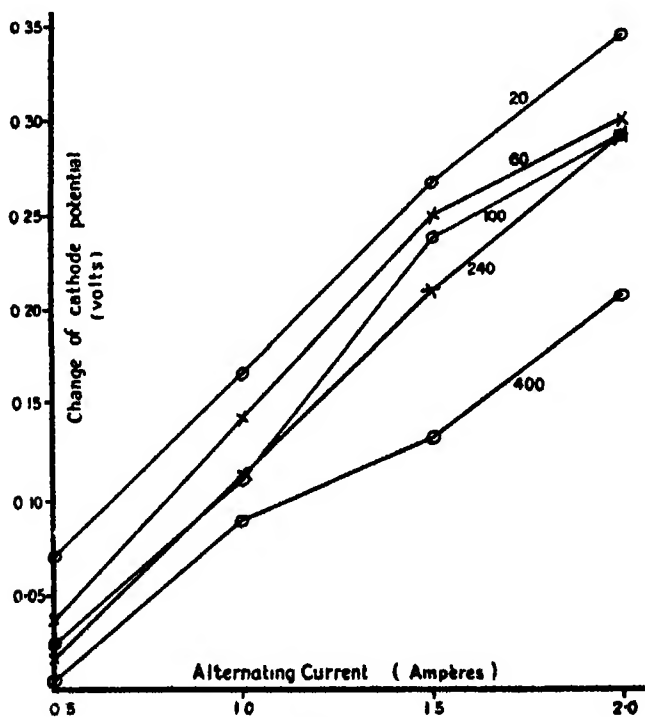


Fig. 4.

polarisation is plotted against alternating current intensity. Low frequencies produce bigger effects, the difference being more pronounced with small alternating current strengths. With the zinc electrode the change in the potential is also in the direction of a depolarisation, which would indicate, as the electrode behaves reversibly in absence of alternating current, that the

effect of the latter is to cause a dissolving zinc anode to act like a more electro-positive metal.

In the second series of experiments the same procedure was adopted, except that, by regulation of the resistance R_2 (and R_1 when working with the carbon electrode), the cell delivery was kept constant at 0.010 ampere throughout. The following table contains, for the two extreme frequencies, the results obtained when studying the carbon electrode.

Table IV

Frequency	Alternating current in amperes	Cell voltage in volts	e_R at carbon electrode in volts	Change in P.D. of carbon electrode in volts
20	0.0	0.305	-0.483	—
	0.5	0.39	0.353	+0.130
	1.0	0.54	0.253	0.230
	1.5	0.685	0.114	0.309
	2.0	0.75	0.038	0.445
400	0.0	0.295	-0.506	—
	0.5	0.305	0.500	+0.006
	1.0	0.40	0.391	0.115
	1.5	0.445	0.346	0.160
	2.0	0.575	0.226	0.280

The effects are greater with the direct current kept constant, as would be expected. The influence of frequency shows up just as in the first series. With an alternating current passing through the zinc anode, the results were much as before.

The effects observed with the zinc electrode, although in a sense forecast by the experiments of Brown, were nevertheless unexpected, for reasons already detailed, and a few more experiments were done to confirm them. Two amalgamated zinc electrodes were put in an acid zinc sulphate solution ($N ZnSO_4 + N H_2SO_4$), and a direct current, kept constant throughout at 0.01 ampere, passed through from outside. A third amalgamated zinc electrode was placed in the solution, and used as an auxiliary whereby alternating current could be led separately either to the zinc anode or to the zinc cathode. The same frequencies and alternating current strengths were used as in the above series of experiments, and electrolysis voltage and electrode potential read as before. The readings will not be given in detail, as their reproducibility does not appear to justify this. The main results can, however, be summarised as follows.—

(a) With an alternating current passing through the zinc anode, the electrolysing voltage was reduced, and the anode potential became more negative. These effects occurred to a greater extent the higher the frequency, and the greater the intensity of the alternating current, though certain readings did not fall into line with the others.

(b) With an alternating current passing through the zinc cathode, the electrolysing voltage was increased, and the cathode potential became more negative. An increase in the strength of the alternating current increased the effect, whilst an increase in frequency had no well-defined influence.

Discussion

The phenomena observed at the carbon cathode during simultaneous passage of direct and low frequency alternating current are qualitatively those which would be anticipated. There is marked depolarisation of H^+ ion discharge, its extent increasing with the strength of the alternating current. It is interesting to notice that, in most experiments, in order to get a really considerable effect, a very high ratio of alternating current/direct current was necessary. Thus the application of an alternating current *one hundred times* the direct current usually lowered the potential more than twice as much as did a current *fifty times* as great. This is particularly noticeable with the higher frequencies. No systematic experiments were carried out with very low A.C./D.C. ratios, so we are unable to express an opinion as to whether a minimum value of this ratio is necessary before H^+ ion depolarisation is facilitated, as is stated by Goodwin and Knobel* to be the case. The influence of frequency in our experiments is marked, the lowering in potential becoming considerably less as the periodicity of the alternating current is increased. This agrees qualitatively with the results of Goodwin and Knobel, working between the limits of three and one hundred cycles, and using electrodes of platinum and of lead.

The explanation and theory of these depolarisation effects are by no means clear, and we propose to say little on the subject. The views of Ghosh† and of Bancroft,‡ who attribute respectively the decreased polarisation to a surface change in the electrode material and to the removal of the adsorbed film of gas by electrical stress, do not appear applicable in the present case. There is no change of any kind visible on the surface of the hard carbon electrode, and the

* *Loc. cit.*, Cooper, 'Trans. Faraday Soc.', vol. 18, p. 102 (1922), came to a different conclusion, and Grube and Dulk ('Zeit für Elektrochem.', vol. 24, p. 237 (1918)) found the evolution of oxygen depolarised even by very small alternating currents.

† *Loc. cit.*

‡ 'Trans. American Electrochem. Soc.', vol. 29, p. 309 (1916).

effect of frequency seems to us to argue against Bancroft's idea. Oscillographic experiments, or work on the lines suggested by Jones,* are best adapted for solving the problem.

In the meantime we prefer to use an almost formal working hypothesis, viz., that the oxygen discharged during the anodic pulse of the alternating current, by combining with or displacing the "active" hydrogen at the cathode, lowers the electrolytic solution pressure of the latter. This is similar in its implications to the hypothesis used by Grube and Dulk to explain the corresponding decrease brought about by alternating current in the polarisation necessary for anodic oxygen evolution—viz., a partial reduction of the platinum oxide mixture, assumed by them to be formed on the anode in these cases.

The effects noticed at the zinc electrode require further work over a big range of frequency. This will shortly be undertaken in this laboratory. There is at present the possibility that the presence of the mercury is complicating matters. Expressed formally, the results observed correspond (whether the electrode is anode or cathode to the direct current) to an increase in the electrolytic solution pressure of the metal, or to a decrease in Zn^{++} ion concentration in the electrolyte at the electrode surface, or to both. Direct current polarisation would explain qualitatively the phenomenon at the cathode, but not at the anode.

It might be mentioned in conclusion that Ghosh† was unable to detect any change in the potential of a zinc electrode in N ZnSO_4 solution when an alternating current (no direct current) was passed through it.

The work described in this paper was mostly carried out during the session 1921-22.

* 'Trans. American Electrochem. Soc.', vol 41, p 151 (1922)

† 'Jour. American Chem. Soc.', vol 36, p 2333 (1914)

*The Spark-Spectra of Indium and Gallium in the
Extreme Ultra-Violet Region*

By MOLLIE WEINBERG, M A , M Sc , Physical Laboratory, University
of Toronto

(Communicated by Prof J C McLennan, F R S —Received July 24, 1924)

(Plate 2)

Introduction

The spark-spectrum of indium in the ultra-violet has been especially studied by Saunders,* that of gallium by Saunders and Klein † By the use of a one-metre concave grating, mounted in a brass tube which could be exhausted, Saunders was able to extend the indium spark-spectrum as far below into the ultra-violet as $\lambda = 1699 \text{ A U}$ The line of shortest wave-length as yet noted in the gallium spark-spectrum—namely, $\lambda = 2176 \text{ A U}$ —was measured by Klein with a large quartz spectrograph whose mounting was of the Lattrow type. With the object in view of making a complete and comprehensive examination of the spark-spectral lines of the above elements, that should extend right through the extreme ultra-violet and the quartz regions, the following investigations were undertaken

A —Experiments in the Quartz Region

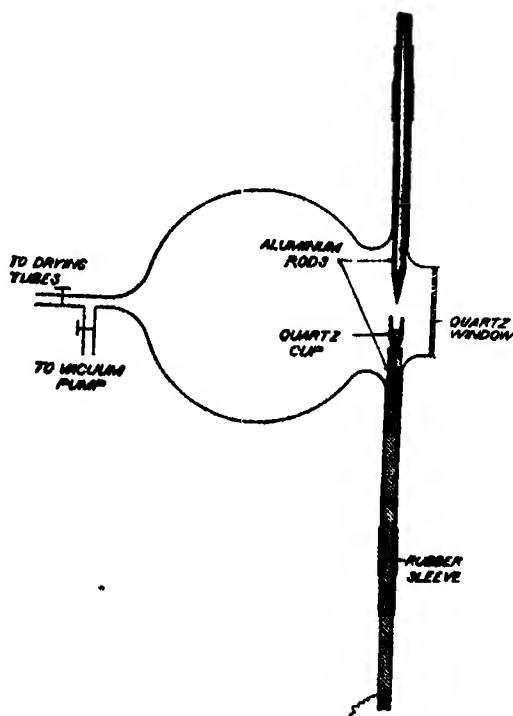
1 *Description of Apparatus*—For studying the spectra in the quartz region a spark chamber, diagrammatically shown in the figure, was employed The spark chamber proper was a pyrex bulb about 7 inches in diameter The terminals were of gallium and aluminium in the one experiment, and indium and aluminium in the other. Gallium has a very low melting point (30.2° C). It was therefore placed in a tiny quartz cup, which, supported by a long aluminium rod, formed the lower terminal for the discharge A piece of tungsten wire led from the aluminium support through the stem of the cup to the gallium. The upper electrode was of aluminium filed down to a point. Pieces of pressure tubing, 2 inches in length, lined with soft wax, fitted over the terminal supports and the tube elongations from the spark chamber. These formed gas-tight moveable joints, and served for the purpose of adjusting the spark

* Saunders, 'Astrophys. Journ.,' vol. 43, p 240 (1916)

† Klein, 'Astrophys. Journ.,' vol. 56, p 373 (1922).

gap. The gap ranged from 2 to 3 mm in width. The quartz window, through which the light passed into the spectrograph, was fastened to the spark chamber with sealing wax. One stop-cock led to the exhaust pumps, the other to the system of drying tubes. The spark was produced by a primary current of 110 volts ranging from 4 to 6 amperes. A Hilger Quartz-Prism Spectrograph, Type A, was used. All photographs were taken on Schumann plates.

While sparking was taking place, the portion of the bulb immediately around the terminals and the quartz window was kept cool by streams of cold com-



pressed air. This served to prevent the metal from running out of the cup, and the quartz window from melting away from the spark chamber.

The gallium used in these experiments was obtained by Prof. McLennan from the Adam Hilger Co. It was guaranteed to be approximately 99.5 per cent. pure. The main impurities were zinc and indium. Copper and sodium were present in spectrographic traces.

Gallium is very easily oxidizable in air, and as it has been shown* that in an atmosphere of hydrogen the gallium spectrum comes out to the best advantage,

* *Ibid.*, vol. 56, p. 373 (1922).

the spark chamber was therefore evacuated, and filled with dry hydrogen to atmospheric pressure. It was then cut off, first from the supply tank, and finally from the drying tubes

For comparison purposes the spark-spectrum was used of cadmium-zinc-lead alloy serving as one terminal, and of aluminium as the other. The spark in this case was also taken in an atmosphere of hydrogen. The following lines* were used as standards —

Element	λ —Rowland	Air Int	Element	λ —Rowland	Air Int
Al	1854.09	3	Zn	2138.66	5
Al	1930.41	2	Cd	2144.44	12
Al	1935.29	7	Cd	2194.71	10
Al	1989.90	8	Zn	2265.08	3
Zn	2025.51	8	Cd	2288.12	8
Zn	2100.06	8	Cd	2312.88	10

Exposures of the gallium spark ranged from 70 to 120 seconds, of the comparison spark from 6 to 12 seconds. The experiment with the indium was carried out in an exactly similar manner to that with the gallium, a new quartz cup being made to contain the indium.

2. *Determination of Wave-lengths* —The spectrograms obtained were measured by a Toepler Comparator. The wave-lengths were calculated from the simplified Hartmann Dispersion formula,

$$\lambda = \lambda_0 + \frac{c}{n_0 - n}$$

where n and n_0 are displacements, and λ_0 , n_0 and c are constants over a small region. The extent of the region over which the above constants were applied ranged from 120 to 200 A.U.

Three separate plates of gallium and two of indium were measured. Each plate was measured three times, and the average taken. The wave-lengths of each plate determined independently in this manner were averaged, and the resulting wave-lengths were taken to constitute the spectra of the elements.

3. *Results* —(a) Gallium —Plate 2, fig. 1A, is a photograph of the gallium spark-spectrum in the quartz region, printed directly from a Schumann plate. The wave-lengths of the lines with their relative intensities are given in Table I. The measurements of Saunders and Klein are tabulated in adjoining columns for the sake of comparison. In all, 80 lines were measured. These extended over the region from $\lambda = 1855$ to $\lambda = 2364$ A.U. Of the 80 lines, 39 occurred on more than one plate, and 41 on one plate only.

* Eder and Valenta, 'Atlas Typischer Spektren,' p. 128-135.

Table I.—Gallium Spark—Quartz Spectrograph

Int	Saunders λ —Int A	Int	Present λ —Int A	Present λ —Int. Vac	ν
		0	1855 4*	1856 0	53880
		0	1855 9	1856 6	53863
		0	1858 4	1857 1	53848
		0	1962 5*	1963 1	50939
		0	1964 1*	1964 7	50897
		0	2030 0*	2030 7	49244
		0	2042 4*	2043 1	48945
		0	2053 9*	2054 6	48672
		0	2059 7*	2060 3	48536
		0	2082 0*	2082 7	48015
		0	2084 1*	2084 8	47968
		0	2086 6*	2087 2	47911
		3	2090 5	2091 2	47819
		0	2103 5*	2104 2	47524
		0	2141 4*	2142 1	46683
		0	2142 3*	2143 0	46664
		0	2167 2*	2167 9	46129
		0	2169 4*	2170 1	46082
		0	2170 1*	2170 7	46068
		0	2175 9*	2176 5	45945
3	2176 76	0	2177 2*	2177 9	45915
		1	2181 5*	2182 2	45825
		0	2184 3*	2185 2	45672
		0	2186 5*	2187 2	45721
2	2195 63	2†	2195 7 [° 'u]	2196 4	45530
2	2205 91	—	—	—	—
		0	2206 8*	2207 5	45300
		0	2207 9*	2208 6	45279
		1	2216 5	2217 2	45102
		0	2222 5	2223 2	44979
		0	2224 2	2224 9	44945
		0	2225 4*	2226 1	44921
		1	2227 4	2228 1	44881
3	2236 17	—	—	—	—
		0	2251 1*	2251 8	44410
		0	2251 7*	2252 4	44397
		0	2253 3*	2254 0	44366
2	2255 29	1†	2255 2	2255 9	44329
1	2259 24	0	2259 7	2260 4	44241
		0	2266 8*	2267 0	44112
2	2266 84	0	2267 1	2267 8	44097
		1	2275 6	2276 3	43931
		0	2278 2*	2278 9	43881
		0	2279 7*	2280 5	43851
2	2285 19	—	—	—	—
		1	2290 6*	2291 3	43642
		0	2292 0*	2292 7	43616
2	2294 19	2	2293 6	2294 3	43588
2	2297 89	—	—	—	—
		0	2299 5*	2300 2	43475
		1	2316 9	2317 6	43148
		2	2318 7	2319 4	43115
		0	2326 7	2327 4	42966
		0	2327 8*	2328 2	42951
		0	2330 7	2331 4	42892
		1	2331 5	2332 2	42878

* Lines occurring on one plate only

† Denotes blurred lines

Table I—Galium Spark—Quartz Spectrograph—*continued*.

Int	Saunders λ —Int A	Int	Present λ —Int A	Present λ —Int Vac	ν
3	2338 24	1	2337 2	2337 9	42774
		4	2338 0	2338 7	42758
		1	2341 5	2342 2	42695
		2	2342 4	2343 1	42678
		4	2343 2	2343 9	42664
		0	2344 6	2345 3	42638
		0	2345 6	2346 3	42621
		1	2347 8	2348 5	42579
		0	2352 5*	2353 2	42494
		0	2353 3*	2354 0	42480
		0	2354 1*	2354 8	42466
		0	2355 9*	2356 6	42434
		0	2358 1*	2358 8	42395
		2	2358 8	2359 5	42381
		2	2359 8	2360 5	42363
1	2359 48 [1]	2	2360 9	2361 6	42344
		0	2362 9*	2363 6	42308
		1	2363 9	2364 6	42290

Table II.—Indium Spark—Quartz Spectrograph

Int	Saunders λ in I A Vac	Int	Present work λ in I A Vac	ν
6 5	1966 69 1977 44	0	1856 4*	53868
		9	1966 7	50846
		8	1977 3	50574
		8	2026 1	49366
		0	2032 9*	49191
		0	2033 7*	49173
		0	2048 8*	48809
		0	2052 4*	48723
		0	2058 1*	48589
		8	2062 7	48480
		0	2064 0*	48449
		0	2071 6*	48272
		0	2072 6*	48249
		0	2073 6*	48226
		0	2077 6*	48133
7	2079 28	10	2079 2	48065
		0	2081 5*	48042
		0	2082 2	48026
		0	2084 8*	47966
		0	2090 6	47833
		0	2091 5	47812
		0	2092 9*	47781
		0 [?]	2093 9*	47758
		0	2095 3	47726
		0	2096 6*	47697
		0	2098 6*	47651
		0	2106 0*	47483
		0	2106 8*	47466
		0	2108 3*	47432
		0	2109 2*	47411
		0	2115 3*	47275
		0 [?]	2122 1*	47123

* Lines occurring on one plate only

Table II—Indium Spark—Quartz Spectrograph—*continued*

Int	Saunders λ in I A Vac	Int	Present work λ in I A Vac	ν
1	2154 81	0	2128 5*	46981
		0	2129 9	46951
		0	2131 3	46920
		0	2141 6	46694
		0	2142 3*	46679
		0	2143 3	46657
		0	2147 1*	46574
		0	2147 8*	46550
		1	2154 7	46410
		1	2157 7	46346
		1	2159 1	46316
		0	2160 4*	46288
		0	2163 4	46223
		0	2164 6*	46199
		0	2166 9	46149
		0 [?]	2171 4*	46053
		0	2172 3	46034
		0	2173 4	46011
		0	2178 2	45910
		0	2182 4	45842
		0	2183 2	45804
		0	2186 3*	45740
		0	2187 3	45719
		0	2189 1	45681
		0	2196 1*	45535
		0	2197 1*	45515

Table II—Indium Spark—Quartz Spectrograph—*continued*

Int	Present work λ in I A Vac	ν	Int	Present work λ in I A Vac	ν
0	2198 2*	45492	0 [?]	2259 7*	44254
0	2200 9*	45436	0 [?]	2260 9*	44230
0 [?]	2201 4*	45426	3	2262 0	44209
0	2206 9	45312	0 [?]	2277 8*	43902
0 [?]	2207 8*	45294	0	2279 1*	43877
0	2208 8	45274	0	2284 0*	43783
0	2209 7*	45255	0	2285 2*	43760
0 [?]	2212 0*	45208	0	2286 5	43733
0	2213 0*	45188	0	2296 4*	43547
0	2214 1	45166	0	2299 1	43496
0	2215 6*	45135	0 [?]	2300 3*	43472
1	2217 0	45107	0 [?]	2301 4*	43452
0†	2220 8	45029	0	2304 9*	43386
0	2223 6*	44972	0	2310 2*	43287
0	2226 2*	44919	0	2311 4	43264
0	2227 2*	44899	0	2323 5*	43039
1	2228 2	44879	0	2325 1	43009
0 [?]	2231 8*	44807	0	2326 6	42981
0 [?]	2232 9*	44785	0	2327 9*	42958
0 [?]	2244 4*	44556	0	2332 3*	42877
0	2245 9	44526	0	2334 5*	42836
0 [?]	2248 9*	44466	0	2335 5*	42818
0	2252 0*	44405	0	2336 4*	42801
0	2253 9*	44366	0	2338 2*	42769
0	2258 3	44281			

(b) *Indium*—Fig 1B is a photograph of the indium spark-spectrum in the quartz region. Table II gives the wave-lengths of the lines, with their relative intensities. Saunders' measurements are given in an adjoining column. There were found to be more and stronger lines in the indium than in the gallium spectrum in this region. There are in all 107 indium lines, extending over the region from $\lambda = 1855$ to $\lambda = 2337$ Å U. Of these, 39 occurred on the two plates and 68 on one plate only, 19 of the latter are questionable.

The wave-length measurements in this region are given in international-vacuum units. The present measurements of the indium lines agree very closely with Saunders' results.

B—Experiments in the Extreme Ultra-violet Region

1 *Description of Apparatus*—The spark-spectra of gallium and indium in the extreme ultra-violet were studied with a vacuum grating spectrograph. This spectrograph has been described in complete detail by Lang in a paper that is at present in course of publication. The arrangement of the terminals in these gallium experiments is the same as that in the quartz region. The gallium, melted into a tiny quartz cup, constituted the lower terminal, aluminum the upper. The terminals were so adjusted that the point of the upper came exactly above the centre of the quartz cup, at a distance 1 mm or a little less above the surface of the gallium.

The spark was produced by a 20-inch induction coil operated from the 110-volt D C mains. An intermittent spark was used in order that any gases emitted by the terminal during the process of discharge might have time to be pumped off. The interrupter was adjusted to allow actual sparking to take place for 1 second during every 20. The entire exposure was equivalent to from 4 to 4½ minutes of continual sparking. Schumann plates were used throughout.

In the experiments with indium in this region both terminals were of indium. The time of exposure in these experiments was approximately the same as that in the gallium experiments.

2 *Determination of Wave-lengths*—The Toepler Comparator was again used to measure the spectrograms obtained. Each plate was measured three times, and the average for each taken. Three plates were independently measured for each of the elements studied.

A special graph had to be prepared for the purpose of translating comparator readings into Angstrom Units. The graph is based on measurements of the strong lines in the carbon and aluminum spark-spectra. These were photographed by the vacuum-grating spectrograph used in the present work. The

wave-lengths of the carbon lines used as standards are taken from Simeon's* paper, the aluminium lines from Eder and Valenta's tables † The former were already in, and the latter had first to be reduced to, international vacuum units Any wave-lengths read off from this graph are therefore in international vacuum units.

The measurements of three plates, for each of the elements studied, were separately translated into wave-lengths, and then averaged An accuracy of 0.2 to 0.3 A.U. may be claimed for this work.

3. *Results*—(a) *Gallium*—The spectrograms obtained with the vacuum-grating spectrograph prove that the spark-spectra of both indium and gallium in the extreme ultra-violet are very rich in lines. As many as from 1,000 to 1,500 appeared on one plate These were, of course, not all due to the elements studied. The impurities present were nitrogen, oxygen, hydrogen, carbon, carbon monoxide, aluminium, and copper On elimination of the impurities 828 lines remained which may be attributed to gallium These extended over the region from $\lambda = 157$ A U to 2059 A U Of these, 526 occurred on more than one plate and 302 on one plate only Of the latter, 25 are questionable

A photograph of the gallium spark in the vacuum-grating spectrograph may be seen in fig 2A The wave-lengths of the lines with their relative intensities are given in Table III The line of shortest wave-length occurring on more than one plate was $\lambda = 157$ A U It is a very faint line A few lines of shorter wave-length still were measured These were found on one plate only, and were extremely faint

(b) *Indium*—A photograph of the indium spark is given in fig 2B When all the impurities were eliminated, it was found that there were present in all 464 indium lines. There were 344 that were present on more than one plate, and 120 on one plate only, about 27 of the latter are questionable. The wave-lengths with their relative intensities are given in Table IV The line of shortest wave-length occurring on more than one plate is $\lambda = 389$ A U. The line $\lambda = 161$ A U. was extremely faint, and was found on one plate only. The wave-lengths of indium measured by Saunders are also tabulated in Table IV From a comparison of the two columns it may be seen that all of Saunders' lines are present on the plates here obtained The measurements are in good agreement, when one considers that the differences between the two lie within the limits of accuracy claimed for this work. The line $\lambda = 1774.68$, attributed by Saunders to indium, is perhaps the carbon line 1774.9 measured by Lyman

* Simeon, 'Proceedings of Royal Society,' A, vol. 102, p. 484 (1923)

† Eder and Valenta, 'Atlas Typischer Spektren,' p 135-139.

Table III.—Gallium Spark in Vacuum-Grating Spectrograph.

Int	λ	ν	Int	λ	ν	Int	λ	ν
0 [?]	124 0*	808452	0	322 9	309893	0	502 2*	199124
0	128 9*	788022	0	325 3*	307409	0	503 3	198688
0	128 2*	780031	0	326 7	306091	0	504 6*	198177
0 [?]	131 6*	759877	0	327 4*	305437	0	506 1	197581
0	142 8*	700280	0 [?]	330 0*	303030	0 [?]	509 0*	196464
0 [?]	143 6*	696378	0	334 0*	299401	3	509 8	196155
0	145 1*	689179	0 [?]	335 1*	298418	3	511 3	195579
0	150 2*	665779	0	337 1	296648	0	512 6	195084
0	151 2	661376	0	337 8	296038	0	516 1*	193761
0	151 8*	658762	0	338 7	295247	0	522 5*	191388
0	153 7	650618	0	340 6*	293599	0	524 7 [? In]	190585
0	157 2*	636132	0	343 9*	290782	0	528 4	189251
0	157 9	633312	0	351 4	284576	0	529 0*	189036
0	160 4*	623441	0	356 5*	280505	0	535 3	186811
0	163 5	611621	0	360 0*	277777	0	536 1	186532
0	165 0*	606060	0	362 0*	276243	0	544 9*	183519
0 [?]	175 6*	569476	0	362 7	275710	0	547 5 [? In]	182649
0 [?]	177 2*	564336	0	378 5	264200	0	560 0*	178571
0	181 0*	552486	0 [?]	385 3*	259538	0	561 5*	178095
0	181 7*	550358	0	389 0*	257069	0	565 7	176772
0	190 3*	525488	0	390 5	256082	0	570 1	175408
0 [?]	197 9*	505306	0	395 1*	253100	0	571 4	175009
0	203 3*	491884	0	396 4*	252270	0	572 0	174825
0	208 6*	479386	0	397 4*	251635	0	573 1*	174489
0	212 7*	470146	0	407 5*	245399	0	575 1	173883
0	214 0	467289	0	410 5*	243605	0	580 1	172384
0	216 2	462535	3	422 0	236907	0	581 2*	172058
0	217 6*	459559	0	423 3	236239	0	582 5	171674
0	220 7	453104	0	424 9	235349	0	589 0*	169779
0	223 9	446628	4	425 1	235239	0	594 4*	168237
0	225 1	444247	0	431 0*	232019	0	598 9*	166973
0	226 7	441112	0	432 0 [? In]	231481	0	601 0	166399
0	230 1*	434594	0	435 5*	229621	0	603 5*	165700
0	232 0*	431034	0	439 5*	227531	0	604 9	165316
0	232 6*	429923	0	440 5*	227015	0 [?]	606 0*	165016
0	244 0*	409836	0	442 5	225989	0	607 4	164636
0	245 0	406163	0	443 5*	225479	0	612 0*	163399
0	253 5*	394477	0	454 3	220119	0	613 9	162993
0	257 3	388651	0	455 5*	219539	1	614 6	162707
0	261 5*	382409	0	456 5*	219058	0	615 6*	162443
0	264 5*	378072	0	457 2*	218723	0	618 6	161656
0	271 4*	368459	0	460 8*	217014	2	622 0	160772
0	276 0*	362319	0	462 3*	216309	1	625 9	159769
0	277 0*	361011	0	463 2 [? In]	215889	0	627 7	159313
0	278 0*	359712	0	464 9*	215100	0	628 5	159109
0 [?]	290 9*	343761	0	469 6*	212948	0	631 2	158428
0	292 4*	341998	0	470 3*	212630	0	634 6	157579
0	293 4*	340832	0	474 6*	210704	0	637 2	156937
0	307 0*	325733	0	478 3*	209074	0	639 0*	156495
0	308 0*	324675	0	478 7*	208899	0	640 0*	156250
0	309 4*	323206	0	48003*	208333	2	645 0	155039
0	311 3	321234	0	487 1*	205297	0 [?]	646 1*	154775
0	313 8	318674	0	488 2	204834	0	647 8*	154369
0	315 5*	316957	0	491 0	203666	0	650 5*	153722
0	319 6*	312696	0	494 5*	202224	0	653 1	153116
0	320 4*	312109	0	496 4*	201451	0 [?]	653.7*	152976

* Lines occurring on one paper

† Blurred lines

‡ Probably doubles.

Table III.—Gallium Spark in Vacuum-Grating Spectrograph—*continued*.

Int.	λ	ν	Int.	λ	ν	Int.	λ	ν
0	654 5	152789	0	777 5*	128618	9	874 4	114384
0	655 8	152486	4	778 3	121848	7	875 4	114233
0	657 5*	152091	1	780 8	128074	0	877 3	113986
0 [?]	659 0*	151745	1	781 5	127059	0	877 9*	113908
0	662 6	150921	0	782 5	127796	0	879 4*	113714
0	665 3	150308	0	783 4	127649	0	891 1*	112221
0	667 8*	149746	2†	784 5	127469	0	893 2*	111957
0	668 2	149656	5	789 4	126678	1	897 3	111445
0 [?]	672 0*	148809	2	790 1*	126566	0	900 1*	111099
0	675 8	147973	3	792 2	126231	2	901 0	110968
1†	677 8*	147537	3	793 6	126009	1†	906 1	110363
0	679 9*	147080	4†	795 0	125644	7	908 0	110132
0	689 5	145033	4	798 3	125266	8	909 3	109975
0	692 0*	144508	6†	800 4	124938	3	912 0	109649
0	693 0	144300	1†	802 6	124595	3	913 5	109469
0	695 8	143719	0	803 6*	124440	0	914 3	109373
0	697 6	143349	1	804 8	124254	0	925 9*	109003
1†	698 5	143164	0	807 9	123777	5	926 7	107909
0	699 1*	143041	2	810 5	123381	8	929 9	107538
0	704 0*	142045	0	811 5	123228	2	930 7	107446
0	705 0*	141844	0	812 6	123062	0	931 4	107365
0	707 0*	141443	2	815 0	122601	2	932 9	107193
0	707 9*	141263	2	816 0	122549	5	933 7	107101
0	708 5*	141143	2	817 1	122384	1	935 7*	106872
0	709 4*	140964	0	817 9*	122264	9	938 5	106553
0	715 0*	139860	0	819 1	122085	0	940 0*	106383
0	715 9*	139684	0	820 5*	121877	4	940 7	106304
0	716 9	139489	0	821 4*	121743	1†	943 0	106045
0	722 0	138504	0	822 5*	121581	9†	947 3	105563
0	722 5*	138408	2	823 2	121477	5	949 3	105341
0	725 5	137836	2	824 1	121345	3	954 0	104822
0	726 0*	137741	0	826 9*	120934	0	956 9	104504
0	727 1*	137532	7	828 6	120685	0	958 8	104297
0	728 6	137249	7	829 8	120611	2	967 0	103413
0 [?]	731 2*	136761	0	831 5*	120265	0	968 0	103306
0	732 6*	136500	0	832 6*	120106	9	973 0	102775
0	734 7*	136110	0	836 6*	119531	3†	979 4	102103
0	736 4*	135796	0	837 3	119431	0	982 8	101760
0	738 9*	135337	7	839 9	119062	3	983 9	101636
0	739 9	135154	5	841 0	118906	7	986 8	101338
0	740 9*	134971	0	842 5*	118694	5	987 5	101266
1	744 3	134355	0	843 1*	118610	9	989 5	101081
0	745 4	134156	2	844 0	118483	4	992 9	100715
0	746 0*	134048	2	845 3	118301	0	994 8	100523
0	748 3	133637	2†	846 3	118161	0	996 5*	100351
2	750 0	133333	0	847 0*	118064	0	1000 5	99950
1	753 0	132802	0	847 7*	117966	0	1003 0 [† In]	99700
0	756 5*	132188	3	849 3	117744	1	1005 8*	99423
0	758 1	131909	0	850 4	117592	3	1008 6	99147
0	759 2*	131718	2	852 0	117371	0	1013 0	98716
0 [?]	761 6*	131303	2	854 9	116973	4	1015 4	98483
0	762 2*	131199	2	855 9	116836	6	1019 5	98087
2	765 0	130719	4	857 7	116591	0	1020 6	97981
2	766 3	130498	8	860 4	116225	5	1022 0	97847
2†	768 1	130191	0	862 3 [† In]	115969	4	1028 5	97229
1	769 0	130039	0	863 5*	115508	2	1030 1	97078
4	770 6	129769	0	865 8*	115500	3	1032 0	96899
0	773 7*	129249	0	869 5*	115009	4	1033 1	96796
0	775 7	128916	0	870 5*	114877	4	1038 6	96283
0	776 9*	128717	0 [?]	872 0*	114679	0	1041 0	96061

Table III — Gallium Spark in Vacuum-Grating Spectrograph—*continued*.

Int	λ	ν	Int	λ	ν	Int	λ	ν
3	1042 4	95932	0	1180 2*	84731	6	1345 9	74290
0	1043 8 [? In]	95903	0	1181 3	84652	0 [?]	1347 6	74206
8	1050 1	95229	0	1183 4	84502	0	1348 0 [? In]	74184
0	1052 6*	95003	6	1184 9	84395	0	1348 8*	74140
1	1055 0*	94787	3	1185 7	84339	0	1355 0*	73801
7	1057 9	94527	3†	1186 7 [? In]	84268	0	1360 6*	73497
2	1060 2	94322	0	1187 4 [? In]	84218	0	1368 4*	73078
1	1063 5	94029	0	1188 3	84154	0	1369 8	73003
0	1064 5	93940	7	1190 7	83984	0	1382 1	72354
2	1067 4 [? In]	93686	8	1192 9	83829	8	1383 7	72270
3	1068 3 [? In]	93607	8	1195 0	83682	0	1387 0*	72098
6	1069 3	93519	3	1199 2 [? In]	83389	0	1388 2*	72036
5	1071 0	93370	7	1201 4	83236	0	1399 0	71994
5	1073 5	93153	1†	1205 6	82946	7	1393 5	71762
4	1074 8	93040	1†	1208 3 [? In]	82761	0	1399 7	71444
1	1075 5	92980	4	1213 0	82440	0	1403 4	71256
0†	1076 4 [? In]	92902	0	1214 0 [? In]	82372	1	1411 0	70872
5	1078 5	92721	0	1226 7	81519	1	1412 6	70792
6	1079 4	92644	9	1228 0	81433	11	1414 4	70701
5	1080 6	92541	0	1233 0*	81103	0	1421 1*	70368
2	1081 6	92456	7	1238 4	80749	0	1421 7*	70338
1	1082 9	92345	0	1240 5*	80612	0	1422 5*	70299
4	1087 0	91990	1†	1244 0	80380	0	1423 1 [? In]	70269
3	1087 7	91937	7	1245 4	80295	0	1424 0	70225
0	1088 6	91861	0	1248 7	80083	0	1424 9 [? In]	70180
7	1090 1	91735	0	1249 4 [? In]	80039	0	1425 6	70146
9†	1091 4	91626	1†	1251 6*	79898	0	1428 1*	70023
0	1095 5 [? In]	91283	0	1252 4*	79847	7†	1437 1	69585
0	1096 3	91216	5	1256 5	79586	0	1440 4*	69425
0	1097 5	91117	10	1258 8	79440	0	1442 4*	69329
0	1098 4 [? In]	91041	8	1264 5	79083	1	1443 3	69286
10	1102 6	90695	9	1267 0	78927	0	1448 0*	69061
6†	1105 8	90432	0	1276 6*	78333	0	1453 4 [? In]	68804
7†	1113 0	89847	9	1279 2	78174	0†	1459 5	68516
8	1115 1	89678	0	1282 0*	78003	0	1461 5	68354
10	1118 0	89445	0	1284 0	77882	4	1465 7	68227
5	1118 8	89381	9	1285 2	77809	0	1470 5*	68004
8	1120 5	89246	0	1292 1	77393	7	1483 9	67390
0	1121 4	89174	10	1295 9	77167	0	1485 3 [? In]	67327
8	1126 0	88810	0	1298 0	77042	1†	1490 5	67092
15†	1128 0	88652	9	1299 5	76953	2	1493 3	66966
6	1131 0 [? In]	88417	11	1303 5	76716	1	1496 8	66809
6	1131 7	88302	0	1305 5*	76598	3	1499 0	66711
5	1132 9	88269	0	1307 2	76499	2	1500 5	66644
8	1133 5	88223	9	1309 7	76353	2	1501 1	66618
6	1135 8	88044	0	1313 1	76155	0	1503 0	66533
8	1136 9	87959	6	1314 8	76057	1	1507 6	66331
6	1138 0	87873	0	1318 6*	75938	1	1509 0	66269
0	1138 9	87804	0	1320 9*	75705	3	1512 5	66116
0	1140 0	87719	6	1322 8	75597	7††	1514 8	66018
0	1140 5	87680	1	1325 8	75427	0	1518 4	65859
0	1141 7*	87589	0	1326 1	75409	5	1523 8	65625
1	1143 0	87499	1†	1328 5 [? In]	75273	4	1529 0	65402
3	1148 0	87108	1†	1331 7 [? In]	75092	0	1531 5	65296
0	1154 2*	86640	0	1332 8*	75030	1†	1532 5	65253
10	1156 0	86505	1	1333 2	75007	12	1534 5	65168
1	1161 4*	86088	8	1338 0	74739	0	1538 4	65003
9	1163 4	85955	1†	1340 0	74627	1	1543 5	64788
0	1167 0*	85689	2	1341 6	74537	1	1552 4	64408
13	1170 3	85448	1	1344 3	74388	3††	1554 2	64342

Table III—Gallium Spark in Vacuum-Grating Spectrograph—continued

Int	λ	ν	Int	λ	ν	Int	λ	ν
0	1559 0*	64144	0	1709 3	58503	0	1812 0	55187
0	1564 4	63922	0	1710 0*	58479	9	1813 8	55133
4†	1566 5	63836	0	1710 6	58459	0	1814 3*	55118
0	1568 0	63775	3†	1711 6	58425	6†	1815 0	55096
3†	1570 3	63682	0	1713 6	58356	0	1815 6*	55078
1†	1572 7	63505	0	1714 3[? In]	58333	2†	1816 7	55045
3	1574 5	63512	0	1715 5*	58292	1	1817 8	55012
4	1575 4	63476	0	1717 7	58218	0	1820 0*	54945
1†	1575 8	63400	7†	1719 4	58150	0[?]	1820 9*	54918
0	1580 4*	63275	0	1721 3*	58096	3†	1822 6	54866
0	1583 0*	63171	0	1722 6	58052	0	1823 6	54836
0	1583 9[? In]	63135	10	1725 0	57971	0	1826 5	54750
1	1584 6	63107	0	1726 7*	57914	0	1829 3	54665
7	1586 2	63044	0	1728 0*	57870	0	1834 1	54523
0	1588 5*	62953	0	1729 0*	57837	0	1835 2	54490
0	1589 5	62913	0	1732 5[? In]	57720	0	1836 5	54451
2†	1590 6	62869	0	1733 5*	57687	0	1839 0*	54377
0†	1598 0*	62578	0[?]	1734 8*	57644	1†	1840 5*	54333
0	1600 0*	62500	0	1735 5*	57620	4†	1843 0	54259
3†	1601 0	62461	0	1736 5*	57587	8†	1845 0	54201
10	1605 8	62274	0	1737 4	57558	0	1848 0	54112
10	1612 0	62035	0	1738 6	57518	0	1848 7	54092
1†	1619 4	61751	0	1739 5	57488	3†	1852 3	53987
1†	1620 5	61709	0	1742 0	57401	0	1855 5*	53894
6	1625 3	61527	0	1746 1	57270	2†	1860 7	53743
0	1631 1*	61309	0	1748 5*	57192	0	1863 6*	53659
0	1633 0*	61237	4	1750 0	57143	1†	1865 8	53596
0	1637 6	61065	0	1753 1	57042	1	1866 5	53576
0	1641 1*	60935	0	1753 8	57019	1	1867 5	53548
0	1659 0[? In]	60278	0	1754 8*	56990	0	1868 4*	53522
0	1660 0*	60241	0	1755 8	56951	1†	1869 0	53506
0	1661 6	60183	1	1756 5	56931	3†	1871 6[? In]	53430
0	1663 3	60122	0	1757 5*	56899	0	1872 5*	53404
0	1664 6	60075	0	1758 4	56870	1	1873 4*	53379
1	1665 5	60042	6	1760 0	56818	0	1874 9*	53336
3	1668 9	59952	1	1761 3	56776	0	1876 2*	53299
11	1670 8	59852	9	1763 9	56693	3†	1877 0	53277
2†	1673 2	59766	6†	1765 6	56638	0	1880 0*	53192
0	1675 0	59702	0	1766 5	56609	1†	1881 8*	53141
2†	1679 7	59535	6	1767 5	56577	1†	1883 4*	53096
1†	1680 7	59499	0	1770 3*	56481	2†	1885 8	53028
0	1683 5	59400	0	1775 5[? In]	56322	1†	1886 9	52997
1†	1684 4*	59369	0	1776 7*	56278	1†	1887 8	52972
0	1685 7	59323	1†	1778 5	56227	0	1890 5	52896
0	1686 7*	59288	0	1779 6	56192	0	1891 9	52857
0	1687 6	59255	0	1782 0*	56116	0	1894 1*	52795
0	1689 1	59203	0	1783 5[? In]	56069	2†	1894 5	52785
0	1690 0*	59172	0	1786 0*	55991	2†	1895 5	52756
0	1691 9	59105	0	1791 0*	55835	3†	1896 6	52726
0	1694 1	59029	0	1796 3	55670	0	1897 5	52701
1†	1695 7	58973	0	1797 8*	55623	1†	1898 9	52662
0	1696 6[? In]	58942	6	1799 1	55583	0	1900 5[? In]	52617
0	1697 5	58910	0	1800 3*	55546	0	1901 0[? In]	52604
0	1698 2[? In]	58886	5†	1803 2	55457	0	1902 0	52576
0	1699 5*	58841	0	1804 2*	55426	0	1902 7	52557
0	1701 1*	58786	0	1805 6	55383	5†	1903 9	52524
0	1701 9*	58758	0	1807 1*	55337	5†	1905 0	52494
0	1704 6*	58665	4†	1808 0	55310	5†	1906 0	52466
0	1706 5*	58599	4†	1809 0	55279	0	1906 8[? In]	52444
0	1708 4*	58534	4†	1809 8	55255	2†	1908 3	52403

Table III.—Gallium Spark in Vacuum-Grating Spectrograph—*continued*.

Int	λ	ν	Int	λ	ν	Int	λ	ν
0	1909 8	52362	4†	1963 9	50919	0	2011 8*	49707
0	1910 5 [? In]	52342	2†	1964 9	50893	0	2014 3	49605
0	1916 7*	52173	2†	1966 0	50865	0	2017 8	49559
0	1917 5	52151	0	1967 6	50823	0	2018 9*	49532
0	1920 0	52083	0	1969 0	50736	3†	2020 2	49500
0	1922 1	52026	0	1969 4	50777	2†	2121 1	49478
0	1922 7*	52010	0	1970 8	50741	2†	2022 3	49449
0	1923 6	51985	1†	1971 8	50715	0	2023 3*	49424
0	1924 7	51966	0	1972 5*	50697	1†	2027 1	49331
0	1926 2*	51915	3†	1973 7	50666	0	2028 5*	49298
0	1928 0 [? In]	51867	0	1974 5*	50646	1†	2029 1*	49283
0	1928 7	51848	1†	1975 3*	50625	1†	2030 1	49259
0	1929 3*	51832	3†	1976 0	50607	0	2032 4*	49203
5†	1932 5	51748	5†	1980 0	50505	0	2033 6*	49174
0	1934 4	51696	5†	1980 5	50492	0	2036 4*	49106
7†	1935 7	51661	4†	1981 7	50462	0	2038 0*	49068
0	1937 7	51607	0	1983 6	50413	3†	2039 7	49027
0	1939 0	51573	0	1984 7	50385	3†	2040 9	48998
0	1940 5 [? In]	51533	0	1985 9	50355	2†	2041 6	48981
0	1941 0 [? In]	51520	1	1986 8	50332	0	2042 5*	48959
0	1943 2*	51462	1	1988 0	50302	0	2046 4	48910
0	1945 0*	51414	0	1994 5	50138	0	2047 8	48833
3†	1946 3	51379	0	1995 5*	50113	0	2051 8	48738
3†	1946 5	51374	0	1996 5*	50088	0	2053 2	48705
3†	1947 5	51348	0	1998 1*	50048	0	2054 3	48679
3†	1948 2	51333	0	2000 5*	49988	0	2055 7	48645
0	1949 4*	51298	0 [?]	2001 5*	49963	0	2056 8*	48619
8	1954 4	51166	0	2002 6*	49935	0	2057 5	48603
8	1955 4	51140	0	2003 2*	49920	0	2058 8	48572
8	1956 5	51112	0	2003 9	49903	0	2059 8	48549
0	1957 8	51108	0	2004 9	49878	0	2060 6	48530
0	1958 9	51049	0	2005 7	49858	2†	2062 6	48483
0	1960 4	51010	0	2006 6*	49836	1†	2063 8	48454
0	1961 2	50989	0	2007 9*	49803	1†	2065 0	48426
0	1962 4	50958	3†	2008 4	48791	0	2069 1	48330
			0	2009 3	49760	1†	2073 0	48239
			0	2010 6*	49736	2†	2074 5	48205

Table IV —Indium Spark in Vacuum-Grating Spectrograph.

Int	λ	ν	Int	λ	ν
0	161 8*	618046	0	475 5*	210904
0	181 3* [† Ga]	551571	0	476 7	209775
0	182 8*	547045	0	479 5	208550
0 [†]	240 5*	405679	0	482 5	207253
0 [†]	249 9*	400160	0 [†]	483 5*	206825
0	251 0*	398406	0	486 1*	205718
0 [†]	263 2*	379939	0	486 8 [† Ga]	205423
0	264 3 [† Ga]	378357	0	489 0*	204498
0	265 6*	376508	0	490 1	204039
0	313 5 [† Ga]	318979	0	492 6*	203004
0	314 7*	317702	0	497 5	201005
0	316 4*	316055	0	498 6	200561
0 [†]	332 0*	301204	0	501 4	199441
0	362 3 [† Ga]	276014	0	504 1	198373
0	377 1*	265181	0	510 2*	196001
0 [†]	380 8*	262605	0	513 1	194893
0	383 5*	260756	0	514 2	194476
0	386 5*	258732	0	519 8	192361
0	388 1*	257665	0 [†]	521 7*	191681
0	388 8 [† Ga]	257201	0	522 5 [† Ga]	191387
0	389 3	256871	0	523 1	191168
0	390 9 [† Ga]	255819	0	524 5 [† Ga]	190657
0	392 6	254712	0	527 7 [† Ga]	189501
0	394 0*	253807	0	531 0	188323
0	394 3*	253613	0	532 4	187828
0	397 2 [† Ga]	251762	0	539 3	186425
0	401 0*	249376	0	541 2	184774
0	402 3	248570	0	541 6 [† Ga]	184638
0 [†]	403 7*	247708	0	544 3*	183722
0	414 9*	241021	0	545 5*	183318
0 [†]	415 5*	240673	0 [†]	546 2*	183083
0	418 8	238777	0	547 7 [† Ga]	182581
0	425 0 [† Ga]	235294	0	552 2	181093
0	428 0*	233644	0	555 0*	180180
0	428 4	233426	0	557 3	179436
0	429 0	233100	0	557 6	179340
0	432 3 [† Ga]	231320	0	561 1	178221
0	436 6	229042	0	564 0	177304
0	437 1*	228780	0	566 2	176616
0 [†]	437 8*	228414	0	567 0	176366
0	441 3	226603	0	569 3	175654
0	444 7	224870	0	571 0 [† Ga]	175131
0	445 6	224416	0	576 0	173611
0	447 1	223663	0	577 5*	173160
0 [†]	449 5*	222469	0 [†]	578 3*	172920
0	455 1 [† Ga]	219731	0	579 5	172562
0	456 5 [† Ga]	219058	0	582 0	171821
0	458 3	218197	1	583 5	171379
0	461 8	216543	0 [†]	584 0*	171232
0	463 6 [† Ga]	215703	0	585 0	170940
0	465 8	214684	0	586 1*	170619
0	468 0	213675	0	587 6	170163
0	470 8 [† Ga]	212404	0	589 0 [† Ga]	169779
0	473 1	211371	0	589 6	169606
0	473 8	211059	0	591 0	169204

* Lines occurring on one plate only.

† Blurred lines

‡ Probably doubles.

Table IV.—Indium Spark in Vacuum-Grating Spectrograph—*continued*.

Int	λ	ν	Int.	λ	ν
0	592 2	168861	0	856 0*	116822
0	595 9	167813	0	860 4*	115740
0	596 1*	167757	0	861 3	116092
0	596 9*	167532	0	861 9 [? Ga]	116022
0	601 7 [? Ga]	166195	0	863 6	115794
0	603 4 [? Ga]	165727	0	865 9*	115498
0	612 9*	163158	0	871 5	114744
0 [?]	618 0*	161812	1	872 8	114573
0 [?]	619 2*	161498	0	873 9*	114429
0	621 3*	160952	0	874 6*	114337
0 [?]	627 0*	159489	0	875 7	114194
0	633 0*	157977	0	876 5 [? Ga]	114090
0	635 1*	157455	0	879 0	113765
0	639 0 [? Ga]	156494	0	880 6	113558
0	642 8	155569	0	880 9	113520
0	646 0 [? Ga]	154320	4	882 0	113378
0	649 9*	153869	0	888 0*	112612
0	650 5 [? Ga]	153727	3	890 8	112258
0†	652 5	153256	0	894 6	111782
0	659 4 [? Ga]	151653	0	898 2	111333
0	664 1*	150579	0	901 4	110938
0	667 2*	149880	0	902 4	110815
0	669 0*	149476	0	908 1*	110120
0	670 3*	149186	0	910 8	109793
0	674 0	148367	3	915 6	109218
0	675 0	148148	0	919 0	108813
0	677 5	147601	1	920 5	108636
0	679 9 [? Ga]	147080	0	922 0	108459
0	681 4	146756	1	925 2	108084
0	682 7	146477	3	926 7	107909
2	684 8	146028	0	930 6*	107457
0	688 3*	145285	2	933 5	107123
0	689 0	145137	1	934 9	106963
0	693 7	144154	0	938 0	106609
1	694 3	144029	0	939 2*	106473
0	695 1*	143864	2	940 1	106371
0	696 5*	143575	0	941 0*	106269
0	706 0*	141643	0	947 0	105596
0	707 0 [? Ga]	141442	0	948 3	105451
0	713 1	140232	0	951 2	105129
0	713 5	140154	4	954 7	104744
0	714 8 [? Ga]	139899	2†	958 9	104286
0	716 5*	139567	0	961 5	104004
0	717 3 [? Ga]	139411	0	967 5*	103359
0	720 5	138792	0 [?]	968 3*	103273
0	738 6 [? Ga]	135391	3	973 5	102722
0	740 5*	135043	0	974 8	102585
0	741 5	134862	0 [?]	986 5*	101368
0	746 3 [? Ga]	133994	0	993 0	100705
1	752 4	132908	1	994 4	100563
0	755 1 [? Ga]	132432	0 [?]	1000 8*	99920
0	755 9	132292	0	1003 1 [? Ga]	99690
0	769 7*	129920	0 [?]	1003 7*	99630
0	782 0	127875	0	1005 6	99443
0	783 2 [? Ga]	127681	0	1014 1*	98609
0	785 0	127388	0	1016 4*	98386
0 [?]	839 0*	119188	0	1018 0*	98231
0	847 6	117979	0	1019 7	98066
0	853 4	117178	0	1022 2	97828
0	854 5*	117027	4	1024 6	97599

Table IV—Indium Spark in Vacuum-Grating Spectrograph—*continued*.

Int.	λ	ν	Int.	λ	ν
4	1028 5	97228	0	1173 5	85215
0	1030 1*	97077	2	1177 0	84962
5	1031 5	96946	0	1179 5	84781
0	1032 0	96899	2	1186 6 [? Ga]	84275
0	1033 3	96777	0	1187 5 [? Ga]	84210
2	1039 7	96181	5	1192 6	83850
0	1043 9 [? Ga]	95794	2	1198 2	83599
0	1046 5	95556	1	1198 0	83472
5	1048 8	95347	2	1199 0 [? Ga]	83403
5	1052 2	95039	0	1203 2*	83112
6	1054 3	94849	2	1203 7	83077
0	1055 3	94759	0	1207 3	82829
4	1060 8	94268	1†	1208 6 [? Ga]	82740
3	1062 8	94091	3	1212 6	82488
2	1067 3 [? Ga]	93894	0	1214 0 [? Ga]	82372
2	1068 1 [? Ga]	93624	0	1216 5	82203
2	1071 6	93318	0	1218 6	82061
0	1072 6*	93231	0	1220 3	81947
0	1076 6 [? Ga]	92884	6	1222 5	81799
3	1077 5	92807	0	1223 2	81753
2	1078 9	92687	0	1224 5	81666
6	1082 0	92421	0	1227 0	81499
4	1086 1	92072	6	1233 0	81103
2†	1089 4	91793	0	1233 6*	81064
0	1089 6*	91777	0	1237 0	80840
1	1090 9	91667	6	1241 0	80580
0	1095 9 [? Ga]	91249	3	1246 5	80224
4†	1096 8	91174	0	1249 4 [? Ga]	80038
0	1098 5 [? Ga]	91033	0	1250 4	79974
2	1099 6	90942	5	1254 5	79713
0	1100 6	90858	2	1263 1	79170
1	1101 8	90760	2	1266 4	78964
0	1103 1	90653	3	1269 5	78771
0	1104 0	90579	3	1276 3	78351
2	1106 9	90342	0	1287 6	77664
1†	1108 3	90228	3†	1292 7	77357
0	1111 0	90009	1	1294 1	77274
0	1111 5	89968	0	1294 6	77244
0	1112 2	89912	9	1296 0	77160
4	1116 0	89606	0	1303 0	76746
2	1116 6	89558	6	1310 0	76336
3	1122 3	89103	0	1312 1	76214
3	1123 9	88976	4	1315 1	76040
2	1124 7	88913	6	1316 9	75936
0	1127 2	88715	2	1317 6	75895
3	1130 0	88496	7	1320 1	75751
6	1131 3 [? Ga]	88394	0	1321 5	75672
0	1140 8*	87657	0	1324 9	75477
0	1145 0	87336	0	1328 5 [? Ga]	75273
5	1146 5	87222	4	1330 6	75154
2	1150 5	86919	1	1332 0 [? Ga]	75075
4	1151 5	86843	0	1337 1	74789
0	1155 0	86584	4	1339 5	74655
1	1156 5	86468	0 [?]	1340 6*	74593
4	1157 6	86386	5	1344 5	74377
2	1159 5	86244	0	1348 0 [? Ga]	74194
0	1160 3	86185	6	1351 0	74019
2	1165 5	85900	0	1354 3	73839
2	1170 8	85412	5	1373 4	72812
3†	1172 1	85317	2	1376 6	72643

Table IV.—Indium Spark in Vacuum-Grating Spectrograph—*continued*.

Int	λ	ν	Int	λ	ν
2	1378 5	72543	7†	1513 0	66094
9	1381.7	72375	0	1519 6	65806
0	1385 0	72202	9	1521 6	65720
0	1399 6	71963	0	1524 5	65595
2	1398 5	71505	0	1528 4	65428
8	1406 0	71123	7	1530 4	65342
0	1408 0	71023	9	1533 5	65210
0 [?]	1409 9	70927	4	1578 5	63351
0	1415 9	70822	0	1583 4*	63155
0	1416 9	70577	0	1585 0 [? Ga]	63091
1	1418 0	70522	8†	1586 6	63028
0	1422 0	70324	5	1616 0	61881
0	1423 1 [? Ga]	70269	0	1617 2*	61835
0	1424 9 [? Ga]	70180	0	1618 4	61769
0	1433 6	69755	0	1620 5*	61709
11	1435 0	69086	11	1625 6	61516
5	1439 8	69454	0	1632 4	61259
0	1444 5	69228	4†	1642 3	60890
0	1449 7*	68979	0	1652 9	60499
0	1453 8 [? Ga]	68785	3	1655 6	60401
0	1455 6*	68700	0	1658 6 [? Ga]	60292
2†	1466 0	68213	0	1660 5*	60223
0	1468 1	68115	6†	1669 5	59898
4	1469 5	68050	0	1676 2	59659
7	1472 6	67906	1	1682 0	59453
0	1485 0 [? Ga]	67340	0	1692 5	59055
8	1488 3	67191	0	1695 1*	58994
0	1496 0	66845	0	1696 5 [? Ga]	58945
5	1502 0	66578	0	1698 0 [? Ga]	58893
4	1510 0	66225			

Table IV.—Indium Spark in Vacuum-Grating Spectrograph—*continued*.

Int.	Saunders	Int.	λ	ν
2	1699 86	5	1700 1	58820
		5†	1702 7	58730
		5	1707 4	58568
		0	1714 4 [? Ga]	58329
		0	1715 0	58309
1	1716 28	5	1716 8	58248
		2	1722 0	58072
		3	1726 1	57934
		0	1727 1	57900
		0	1732 1 [? Ga]	57733
		0	1733 8 [? Ga]	57677
		6	1741 6	57419
		12	1749 2	57189
5	1748 65	0	1763 0*	56721
		0	1767 4*	56580
		8†	1771 0	56485
5	1770 57	1†	1771 5*	56449
		1	1773 1	56398
		3	1775 0	56338
2	1774 68	0	1775 8 [? Ga]	56313
		0	1783 1 [? Ga]	56082
		1	1789 2	55891
		2	1793 5	55756
		0	1798 7*	55595
		3†	1808 5	55294
1	1820 38	—	—	—
		1	1832 4	54573
		2	1842 3	54279
		4	1850 5	54039
		1	1851 2	54019
		0	1853 5	53952
		0	1854 0*	53937
		3†	1856 6	53862
		0	1858 3*	53813
		0	1859 0*	53792
		0	1872 3 [? Ga]	53410
		3†	1874 1	53358
		0	1893 0	52826
		0	1900 5 [? Ga]	52617
		0	1901 4 [? Ga]	52593
		0	1907 2 [? Ga]	52433
		0	1911 0 [? Ga]	52330
		0	1927 9 [? Ga]	51869
		4	1936 5	51639
		0	1938 2*	51594
		0	1940 0 [? Ga]	51546
		0	1941 0 [? Ga]	51519
		2	1942 4	51483
		0	1947 7	51343
		0	1955 9*	51127
6	1966 69	7	1967 0	50839
		2†	1968 0	50818
		6	1977 8	50561
5	1977-44	1†	1978 8	50536
		0	2010 1	49749
		5	2079 6	48086
4	2079 28	0	2080 8*	48059
		0	2082 0*	48031

It is of interest to note that several lines of shortest optical wave-length ever measured appear on the plates taken with our vacuum-grating spectrograph. A few of the very shortest lines previously measured, which were also found in the present work, are given in the following table —

Element	Present		Millikan *
	Int	Work	
Al	0	144 3	144 3 A U
Cu	0	157 9	157 7 ..
Al	0	162 7	162 4 ..
Cu	0	189 3	189 2 ..
Al	0	219 0	219 1 .
Al	0	221 6	221 5

* Millikan and Bowen, 'Phys Rev,' vol. 23, p. 1 (1924)

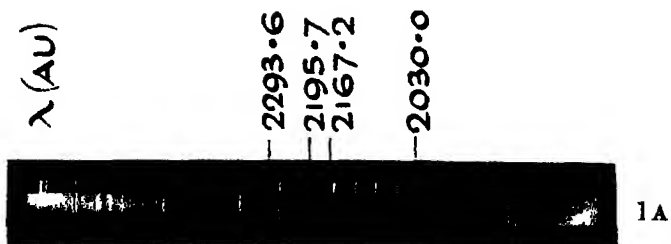
It is also quite remarkable, when one considers the extreme faintness of the lines in this region, that the agreement between Millikan's measurements and those here obtained is so close

Summary

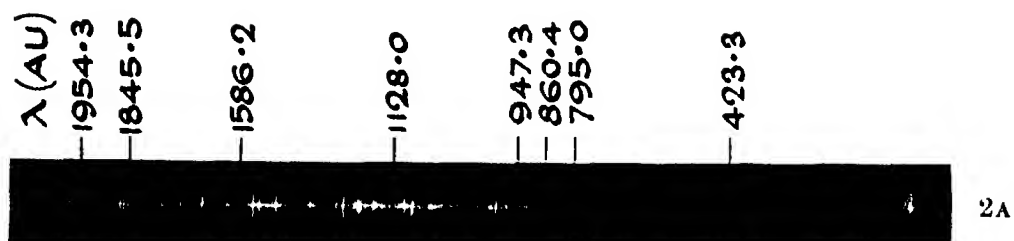
The spark-spectra of gallium and indium were examined, both in the quartz and the vacuum-grating regions. Owing to the fact that gallium and indium oxidize very easily in air, their spectra in the quartz region were taken in hydrogen. There are altogether 107 indium lines in the quartz region, some of which are extremely faint. They extend over a range of 1855 to 2337 A.U. There are fewer gallium lines in this region. These range over 1855–2364 A.U.

The vacuum-grating spectrograph revealed a great mass of lines in the extreme ultra-violet for both elements. There were from 1,000 to 1,500 lines on one plate. On elimination of the impurities, however, it was found that there were 828 gallium lines ranging over the region 157–2059 A.U., and 464 indium lines ranging over 161–2082 A.U. In gallium there were a few very faint lines extending as far down into the ultra-violet as $\lambda = 126.8$ A.U. These occurred on one plate only, and are questionable.

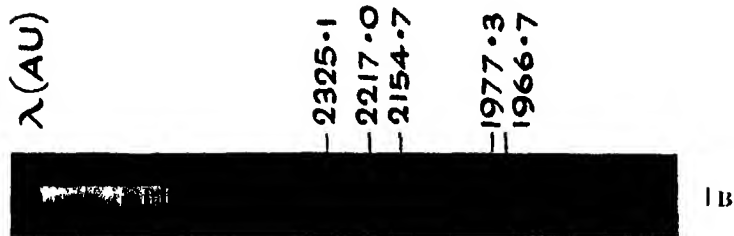
I wish to acknowledge my indebtedness to the valuable advice of Prof. J. C. McLennan, F.R.S., Director of the Department of Physics of the University of Toronto, under whose direction the investigations here described were carried out, and also to Dr. W. W. Shaver, who photographed the plates with the vacuum-grating spectrograph. I also desire to express my thanks to the Honorary Advisory Council for Scientific and Industrial Research, Ottawa, under whose auspices this investigation was conducted.



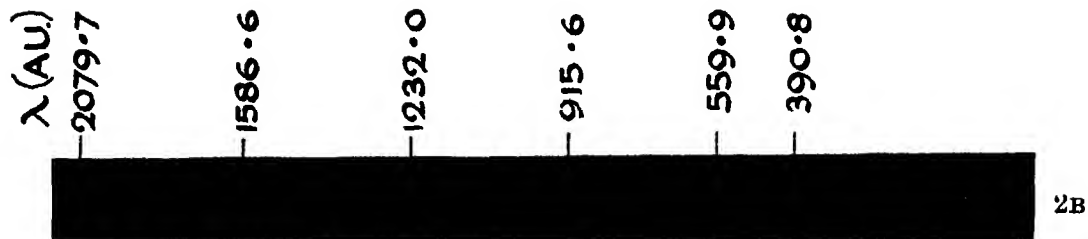
GALLIUM Quartz Spectrogram



GALLIUM Vacuum Grating Spectrogram



INDIUM - Quartz Spectrogram



INDIUM Vacuum Grating Spectrogram.

On the Atomic Fields of Helium and Neon.

By J E JONES, D Sc, 1851 Exhibition Senior Research Student, Trinity
College, Cambridge

(Communicated by Prof S Chapman, F R S —Received September 9, 1924)

§ 1 *Introduction*

The methods of determining molecular fields, described in previous papers,* are here applied with certain modifications to the cases of helium and neon. There is considerable observational material available in the case of helium, both as regards its isotherms and as regards its viscosity over a large range of temperature, but it has not as yet been used with any success to yield satisfactory information about its outer field. Keesom,† who obtained a number of theoretical formulæ for the *second virial coefficient* of the equation of state, was unable to find any which would satisfactorily explain the temperature variation of this coefficient in the case of helium, as determined experimentally by Kamerlingh Onnes ‡ in fact, the experimental coefficient showed at the higher temperatures a distinct maximum, and this property none of his theoretical formulæ possessed. The maximum property has, moreover, been confirmed by the later experimental work of Holborn and Otto §. The formula, given in a recent paper,|| is, however, more successful in this direction, and the method of using it, there described, leads to the conclusion that the field of helium can well be represented by the superposition of repulsive and attractive fields, each according to an inverse power law. Furthermore, the values of the force constants are here determined.

It has long been recognised that the temperature variation of the viscosity of helium cannot adequately be represented by the theoretical Sutherland formula, with the obvious inference that helium cannot be regarded (even roughly) as a rigid sphere with a superimposed attractive field. This is perhaps not surprising in view of the comparatively simple electronic structure of helium. Kamerlingh Onnes || has shown that the variation can best be represented by the simple law, in which the viscosity varies as a power of the temperature

* 'Roy Soc. Proc.' A, vol. 106, pp. 441 and 463 (1924).

† Keesom, 'Comm. Phys. Lab. Leiden,' Supplements Nos. 24, 25, and 26 (1912), or 'Proc. Sect. of Sciences, Amsterdam,' vol. 15 (1), p. 256 (1912).

‡ Kamerlingh Onnes, 'Comm. Phys. Lab. Leiden,' No. 102a (1908).

§ Holborn and Otto, 'Zeits. f. Phys.,' vol. 23, p. 77 (1924).

|| Kamerlingh Onnes, 'Comm. Phys. Lab. Leiden,' No. 134a, p. 18 (1913).

This formula, although first given as an empirical result, corresponds theoretically to a molecular model, in which the molecules are regarded as point centres of force repelling according to an inverse power law. The information available concerning the viscosity of helium is here used, for the first time, to determine the actual value of the repulsive force constant. It is further shown that the result is consistent with that found by the other (entirely independent) method, above described. The field thus determined is one of repulsion according to an inverse 14th power of the distance and a very weak attraction according to an inverse 5th power.

The information available concerning neon is more fragmentary and less satisfactory than that for helium. Experiments have been conducted by Crommelin, Martinez and Kamerlingh Onnes* jointly on its equation of state, but the presentment of the results renders it extremely difficult to deduce from them any definite theoretical information. They give, for instance, three sets of values for the second virial coefficient, which differ at certain temperatures by as much as 100 per cent, and it is difficult to know *a priori* which set should be used in theoretical investigations such as this. Further information on the isotherms of neon has recently been given by Holborn and Otto,† not, however, deduced from direct observations, but from the results found for a mixture of helium and neon and for helium alone, and so it is difficult to estimate how far the results can be used for theoretical purposes. In any case, the values of the second virial coefficient deduced therefrom are inconsistent with each of the sets of values just mentioned. For the present, therefore, progress in this direction does not seem to be possible.

Measurements of viscosity are also meagre in the case of neon, results for only two temperatures‡ being available, but fortunately there exist several measurements of its thermal conductivity, made by Weber,§ which can be used to give some information of its atomic field. For, from a theoretical formula due to Chapman,|| the values of the viscosity can be deduced from those of thermal conductivity, and these, being consistent with and supplementary to the direct measurements, provide sufficient data for the purpose of this investigation. As in the case of argon, already discussed elsewhere,¶ several

* Crommelin, Martinez and Kamerlingh Onnes, 'Comm Phys. Lab. Leiden,' No 154A. (1919)

† Holborn and Otto, *loc. cit.*

‡ Rankine, 'Roy Soc. Proc.,' A, vol 84, p 191 (1911).

§ Weber, 'Comm Phys. Lab. Leiden,' Supplement No 42a to Nos. 145-156 (1916).

|| Chapman, 'Roy Soc. Phil. Trans.,' vol 216, A, p 279 (1915).

¶ 'Roy Soc. Proc.,' *loc. cit.*

models can be found to explain the experimental facts, but, for each of these, the method determines the numerical values of the repulsive force constant (or the diameter in the case of the rigid sphere)

The unique determination of the model is made by using the measurements of the inter-atomic distances in the crystals of NaF and MgO, made by X-ray analysis. It is shown that the observations of thermal conductivity, of viscosity, and of crystal constants, can all be explained by one model, according to which neon is to be regarded as repelling according to an inverse 21st power of the distance. The attractive part of the field, although not actually determined, is shown to be weak.

§ 2 The Equation of State of Helium *

The isotherms of helium have been investigated by Kamerlingh Onnes† between -217°C and 100°C , and by Holborn and Otto‡ between 0°C and 400°C . The former has shown that the observed values for pv can be represented by the equation

$$pv = A + \frac{B}{v} + \frac{C}{v^2}, \quad (2.01)$$

and has determined by the method of least squares values of the coefficients A and B to fit the observations, the value of C being estimated from a theoretical formula §. The fact that the values for C are obtained in this way detracts to some extent from the reliability of the values for B. However, they are taken from the paper as given, and are reproduced in Table I.

Table I.—The Virial Coefficients of Helium from Kamerlingh Onnes

T	A	B 10^3	log B _r
$^{\circ}\text{C}$			
100.35	1.30667	0.673	1.69235
20.00	1.07273	0.534	1.69705
0	0.99970	0.512	1.70940
-103.57	0.62036	0.337	1.73499
-182.75	0.33066	0.176	1.72613
-216.56	0.20693	0.096	1.66645

* I am grateful to Mr E. V. Whitfield, B.A., Trinity College, Cambridge, for his assistance in the numerical work of this section, and in the preparation of the curves shown in figs. 1, 2, and 3.

† Kamerlingh Onnes, 'Comm. Phys. Lab. Leiden,' No. 102A (1906).

‡ Holborn and Otto, 'Zeits. f. Phys.,' vol. 10, p. 367 (1922), 'Zeits. f. Phys.,' vol. 23, p. 77 (1924), cf. also Holborn and Schultze, 'Ann. d. Phys.,' iv, vol. 47, p. 1089 (1915).

§ Kamerlingh Onnes, *loc. cit.*, eqn. (2).

Holborn and Otto also express pv in the form (2.01) above, but use as well an expansion in powers of p . Their units of pressure and volume are different, unfortunately, from those used by Kamerlingh Onnes and others, for they adopt 1 m. of Hg as the unit of pressure and define the unit of volume to be such that $pv = 1$, when $p = 1$ at 0°C . For this reason we write the equation of Holborn and Otto in the form

$$PV = a + bP + cP^2, \quad (2.02)$$

and

$$PV = a \left(1 + \frac{b'}{V} + \frac{c'}{V^2} \right) \quad (2.03)$$

Theoretically, by an inversion of the series (2.02), we should have $b = b'$, but Holborn and Otto determine their values graphically by independent methods and obtain the results given in Table II

It can be shown* that, if the relation between the two sets of units be such that a pressure p and a volume v in one set of units are the same as a pressure P and a volume V in another, with $P = lp$, $V = mv$, then

$$B = \frac{lb}{a_0 + b_0 l + c_0 l^2}, \quad (2.04)$$

where a_0 , b_0 , and c_0 are the values of the coefficients of (2.02) at 0°C . Similarly, it may be shown that in terms of a , b' , and c' ,

$$B = \frac{lb'}{a_0 + b_0' l + \frac{c_0' - b_0'^2}{a_0} l^2}. \quad (2.05)$$

Table II—The Virial Coefficients of Helium from Holborn and Otto.

T	a	b	b'	log B _N	log B' _N
°C					
0	0.99930	0.69543	0.69565	4.72313	4.72327
50	1.18223	0.68887	0.68797	4.71900	4.71846
100	1.36518	0.68804	0.67453	4.70569	4.70989
200	1.73091	0.64933	0.64894	4.69337	4.69309
300	2.09665	0.61600	0.61797	4.67043	4.67186
400	2.46244	0.59451	0.60117	4.65504	4.65989

Since one atmosphere = 76 cms. of mercury†, we have in our case $l = 0.76$, and from formulæ (2.04) and (2.05), the values of log B_N (denoted in the table

* 'Roy Soc. Proc.' A, vol. 106, p. 473 (1924)

† Note added later.—One international atmosphere at Leiden = 75.9488 cm. of mercury ('Comm. Phys. Lab. Leiden,' No. 184A, p. 4 (1919)), but this slight deviation does not affect the work of this section.

by B_N and B'_N respectively) are calculated. In the present application the mean of $\log B_N$ and $\log B'_N$ was used.

There is a slight discrepancy between these values and those of Kamerlingh Onnes between 0° and 100° , as is seen in the figure, but the lower values of Kamerlingh Onnes form a continuous curve with those obtained by Holborn and Otto.

In a former paper* it has been shown that when molecules repel according to the law $\lambda_n r^{-n}$ and attract according to the law $\lambda_m r^{-m}$ the theoretical value for the second virial coefficient is given by

$$B_N = \frac{B}{A} = \frac{2}{3} \pi v \left(\frac{\lambda_n}{n-1} - \frac{m-1}{\lambda_m} \right)^{3/(n-m)} F(y)$$

where

$$F(y) = y^{3/(n-m)} \left\{ \Gamma\left(\frac{n-4}{n-1}\right) - \sum_{\tau=1}^{\infty} f(\tau) y^\tau \right\}$$

and

$$f(\tau) = \frac{3 \Gamma\left(\frac{\tau m - 1 + n - 1}{n - 1}\right)}{\tau! (\tau m - 1 - 3)} - \frac{3 \Gamma\left(\frac{\tau m - 1 - 3}{n - 1}\right)}{\tau! (n - 1)},$$

and y is a function of the temperature given by

$$y = \frac{\lambda_m}{(m-1) kT} \left(\frac{n-1}{\lambda_n} \frac{kT}{\lambda_n} \right)^{(m-1)/(n-1)},$$

v is the molecular concentration at normal temperature and pressure.

By comparing the graphs of $\log F(y)$, plotted against $\log y$, with that of $\log B/A$ against $\log T$, the values of the force constants λ_n and λ_m are determined. The pronounced maximum of B at the higher temperatures provides a stringent test for the theoretical curves. That appropriate to the attracting rigid sphere model is, for instance, definitely unsuitable (see fig. 2), as it does not possess a maximum but increases asymptotically to a finite upper limit. The only curves which could be said to fit were those of $n=9$ and $m=5$, $n=11$ and $m=5$, $n=11$ and $m=6$, $n=14\frac{1}{2}$ and $m=5$. Of these the first could not be regarded as quite satisfactory, the second was better, the third and last best of all, the latter, in fact, was as nearly perfect as could be hoped for (see fig. 1).

The values of X and Y , the co-ordinates of the parallel transformation necessary to secure agreement between theoretical and experimental curves,

* *Loc. cit.*, p. 467

with the values of the force constants deduced therefrom, are given in Table III. The diameters are calculated from the formula*

$$\sigma = \left(\frac{2\lambda_n}{(3n-1)k} \right)^{1/n-1} \quad (2.06)$$

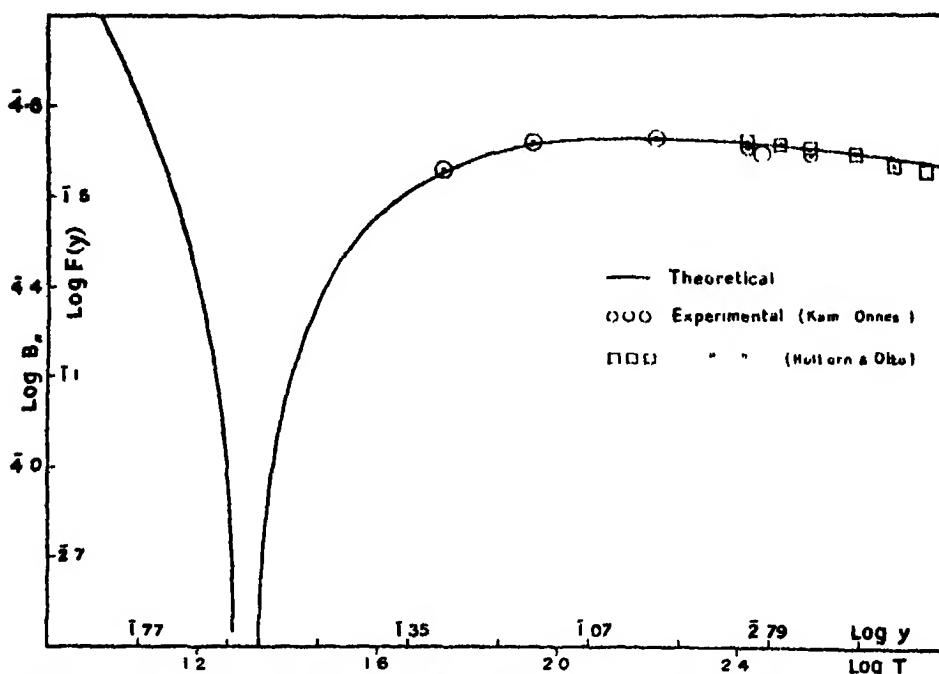


FIG. 1†—Values of Second Virial Coefficient of Neon, deduced from experiment, and Theoretical Curve (corresponding to $n = 14\frac{1}{2}$, and $m = 5$)

Table III—The Force Constants and "Diameters" of Helium from the Equation of State

n	m	X	Y	λ_n	λ_m	$\sigma \cdot 10^8 \text{ cm}$	$\phi 10^{10} \text{ (ergs)}$
9	5	0.392	3.340	$1.14 \cdot 10^{-74}$	$4.354 \cdot 10^{-45}$	4.020	2.086
11	5	0.4616	3.220	$6.25 \cdot 10^{-80}$	$2.911 \cdot 10^{-45}$	3.534	2.622
$14\frac{1}{2}$	5	0.5190	3.102	$2.15 \cdot 10^{-115}$	$1.902 \cdot 10^{-45}$	3.105	3.158
11	6	0.590	3.120	$7.47 \cdot 10^{-90}$	$1.970 \cdot 10^{-45}$	3.597	5.200

As a matter of interest, the work required to separate two atoms from the

* Cf. 'Roy. Soc. Proc.,' A, vol. 106, p. 452, eqn (4.30)

† In each figure, the left-hand portion of the curve corresponds to negative values of $F(y)$; $\log |F(y)|$ is plotted

position of relative equilibrium to an infinite distance is also included, being calculated from the formula

$$\phi = \frac{n-m}{(n-1)(m-1)} \frac{\lambda_m^{\frac{n-1}{n-m}}}{\lambda_n^{\frac{m-1}{n-m}}}$$

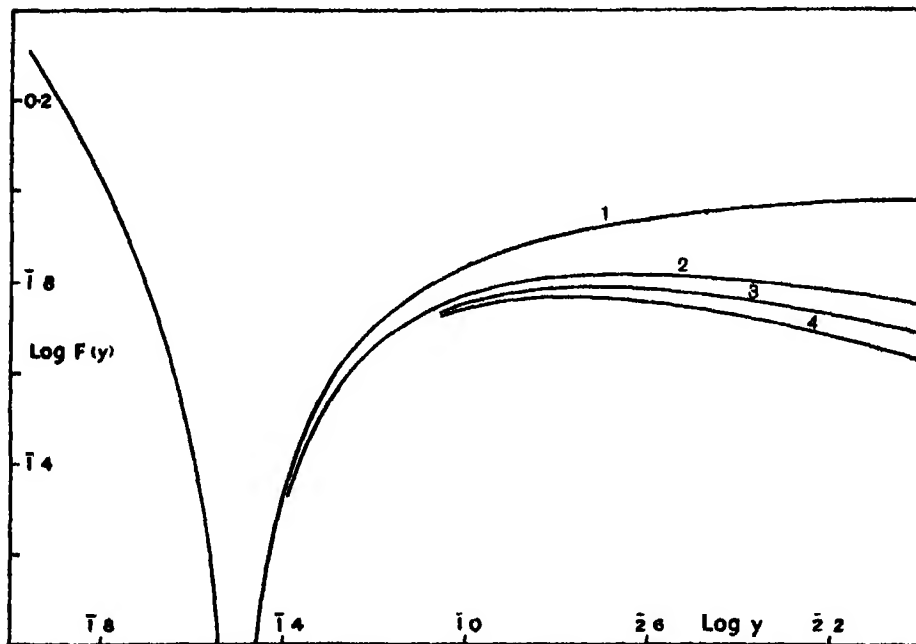


FIG. 2—Theoretical Curves for the Second Virial Coefficient for various Molecular Models

(1) $n = \infty$, $m = 5$, (2) $n = 14\frac{1}{2}$, $m = 5$,

(3) $n = 11$, $m = 5$, (4) $n = 9$, $m = 5$

(Scale shown is that appropriate to $n = \infty$, $m = 5$)

In the case of $n = 14\frac{1}{2}$, $m = 5$, the outer limits of a number of independent readings (corresponding to independent fitting of the curves) were $X = 0.5260$, $Y = 3.102$, and $X = 0.5120$, $Y = 3.102$. The corresponding values of λ_n , λ_m and σ were

$$\lambda_n = 2.196 \cdot 10^{-115} \text{ and } 2.097 \cdot 10^{-115},$$

$$\lambda_m = 1.947 \cdot 10^{-45} \text{ and } 1.857 \cdot 10^{-45},$$

$$\sigma = 3.110 \cdot 10^{-8} \text{ and } 3.099 \cdot 10^{-8}$$

In order to illustrate the difference in the theoretical curves for various values of n and m , four curves are given in fig. 2 for the same m and different values of n , and in fig. 3 for the same n and different values of m . The curves have been superimposed (with their axes parallel) so that the left-hand portion

of the curves, corresponding to negative values of $F(y)$, are as nearly as possible in coincidence. The latter are clustered about the line shown in

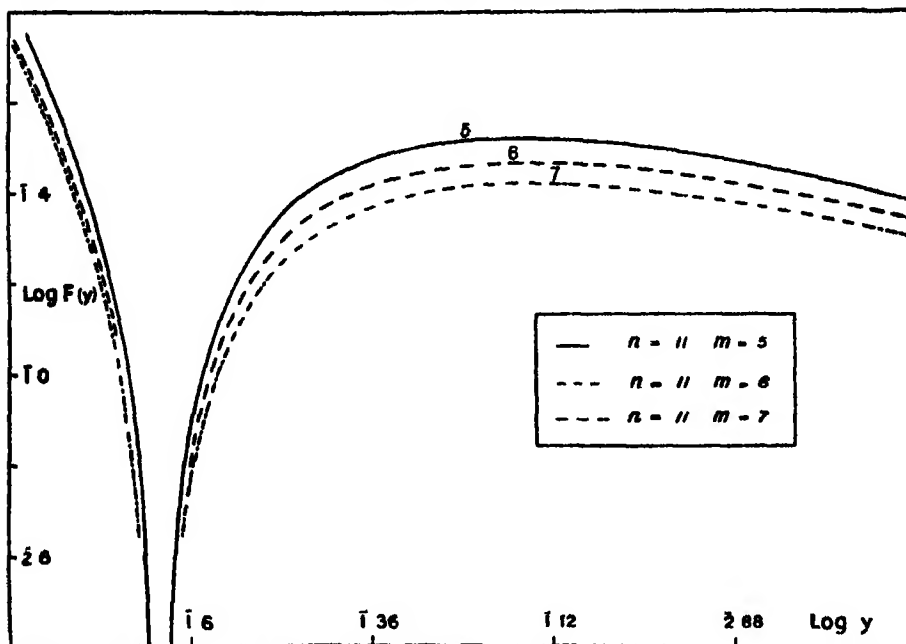


FIG. 3 — Theoretical Curves for the Second Virial Coefficient (Scale shown is that appropriate to $n = 11$, $m = 5$)

the figure, and are too near together to be reproduced in a diagram. The method is equivalent, practically, to making the "Boyle points" coincide (that is, the point for which $F(y) = 0$).

§ 3 *The Viscosity of Helium.*

Kamerlingh Onnes and Weber* have investigated the viscosity of helium from -258.1°C to 183.7°C and find that its variation with temperature is represented to a remarkable degree by the formula

$$\mu = \mu_0 \left(\frac{T}{T_0} \right)^s \quad (3.01)$$

with $\mu_0 = 1.887 \cdot 10^{-4}$ at 0°C and $s = 0.647$. This formula corresponds theoretically to a molecular model in which the molecules are point centres of force repelling (without any attraction) according to the law λr^{-n} , with $n = 14.6$.

* Kamerlingh Onnes and Weber, 'Comm. Phys. Lab. Leiden,' No. 134a, p. 18 (1913), Jeans, 'Dynamical Theory of Gases,' 3rd ed., p. 286 (1921).

The theoretical formula for the coefficient of viscosity for such a law of force is*

$$\mu = \epsilon_c \frac{5 (kmT)^{\frac{1}{2}} \pi^{\frac{1}{2}}}{8 I_2(n) \Gamma\left(4 - \frac{2}{n-1}\right)} \left(\frac{2kT}{\lambda}\right)^{3/n-1}, \quad (3.02)$$

where m is the mass of the atom or molecule, k the usual gas constant ($1.372 \cdot 10^{-16}$), † ϵ_c a number, depending only on n , which lies between the narrow limits 1.000 and 1.016‡, $I_2(n)$ is also a function only of n , its value having been computed for some values of n by Chapman§ and for others by the writer||

For our particular case $n = 14.6$, and so $\epsilon_c = 1.007$, $I_2(n) = 0.9751$. Inserting the values $\mu = 1.887 \cdot 10^{-4}$, $T = 273.1$, and $m = 6.604 \cdot 10^{-24}$ for helium, we find

$$\lambda_m^{\frac{1}{n-1}} = 2.662 \cdot 10^{-9}$$

To compare this value of the force constant with those obtained in the preceding paragraph, we calculate the "diameter" σ from the formula (2.06) and find

$$\sigma = 3.128 \cdot 10^{-8}$$

This is in remarkably close agreement with that obtained for $n = 14\frac{1}{2}$ from the equation of state. Assuming as a final result the integral value $n = 14$, we find by interpolation from the results given in Table III,

$$\sigma = 3.124 \cdot 10^{-8}$$

leading to

$$\lambda_{14}^{\frac{1}{n-1}} = 2.323 \cdot 10^{-9},$$

and

$$\lambda_{14} = 5.74 \cdot 10^{-11}$$

The corresponding value of λ_m is $1.930 \cdot 10^{-45}$.

* Cf. Enskog, 'Kinetische Theorie der Vorgänge in mässig verdünnten Gasen, Inaug. Dissertation,' Uppsala, p. 94 (1917), explicit formulæ are also given by Chapman, 'Phil. Trans. Roy. Soc.,' A, vol. 211, p. 433 (1912), 'Phil. Trans.,' A, vol. 216, p. 338, eqn. (251) (1915), and again 'Memoirs Manchester Lit. and Phil. Soc.,' vol. 66, No. 1 (1922), Appendix, Jeans, 'Dynamical Theory of Gases,' 3rd ed., p. 287 (1921). The last two formulæ should,

however, be multiplied by a factor $\left(\frac{2}{n-1}\right)^{\frac{2}{n-1}}$. A more general formula is given in 'Roy.

Soc. Proc.,' A, vol. 106, p. 441, eqn. (4.23), (1924).

† Jeans, 'Dynamical Theory of Gases,' p. 119 (1921).

‡ Chapman, *loc. cit.*, Table V (1915).

§ Chapman, 'Memoirs Manchester Lit. and Phil. Soc.,' *loc. cit.*

|| 'Roy. Soc. Proc.,' *loc. cit.*, p. 456.

From the viscosity results it would appear as though the field of helium were solely repulsive. But this is not surprising in view of the very weak attractive field possessed by helium, as evidenced by its low critical temperature and (more quantitatively) by the low values of λ_m given in Table III. The attractive force constants there given are, for example, only about 1/100 of those found for argon in a former paper. Such a weak attractive field can have little influence on the orbits of two helium atoms in collision and so little effect on the magnitude of the viscosity.

§ 4 *The Thermal Conductivity and Viscosity of Neon*

Although the viscosity of neon has been measured at only two temperatures,* viz., 13.8° C and 100° C, further values can be evaluated from the work of Weber† on its thermal conductivity at various temperatures, for it has been shown by Chapman‡ and Enskog§ that there is a theoretical relation between viscosity and thermal conductivity of the type

$$\mathfrak{S} = f\mu C_v, \quad (4.01)$$

where \mathfrak{S} is the coefficient of thermal conductivity, C_v the specific heat at constant volume, and f a numerical factor depending on the molecular model. In the case of molecules repelling according to the law r^{-n} , the value of f varies between 2.500 and 2.522 as n varies from 5 to ∞ . This theoretical formula has received quite definite support from experimental evidence,|| especially in the case of the monatomic elements. We therefore propose to assume its validity and to calculate values of μ from those of \mathfrak{S} , by taking f to be 2.500 and C_v to be given by its thermodynamical value

$$C_v = \frac{3}{2} J \frac{k}{m}, \quad (4.02)$$

when the substitutions $k = 1.372 \cdot 10^{-16}$,¶ J = 4.184 $\cdot 10^7$,** and $m = 20.2$, 1.650 $\cdot 10^{-24}$ grams†† are made, we find for neon $C_v = 0.1476$ ‡‡. The values of μ thus calculated, together with the two values obtained by measurement, are given in Table IV.

* Rankine, 'Roy Soc Proc,' A, vol 84, p 191 (1911)

† Weber, 'Comm Phys Lab Leiden,' Suppl No 42B (1918)

‡ Chapman, 'Phil Trans,' A, vol 211, 1912, and vol 216 (1915)

§ Enskog, *loc cit*

|| Enskog, *loc cit*, p 104, Jeans, 'Dynamical Theory of Gases,' 3rd ed, p. 300 (1921)

¶ Jeans, 'Dynamical Theory of Gases,' p 119 (1921)

** Jeans, *loc cit*, p 11

†† Jeans, *loc cit*, p 9

‡‡ Cf Bannawitz, 'Ann. d Phys,' vol 48, p 592 (1915).

Table IV —The Coefficients of Heat Conduction and Viscosity of Neon

T_{abs}	$\eta \cdot 10^4$	$\mu \cdot 10^4$
378.90	1.344	3.042
373.09	—	3.652*
286.89	—	3.080*
273.09	1.087	2.946
198.72	0.879	2.382
91.06	0.490	1.352

* Rankine, *loc. cit.*

Except for the value of μ calculated from η at the highest temperature, the results are quite consistent, and when plotted against T lie on a smooth curve, thus lending encouraging support to the method. It should be observed that Weber asserts that the value of η at 0°C is certainly accurate to 0.2 per cent and agrees with the measurement made by Bannawitz*. However, in making theoretical use of these results, preference must naturally be given to the observed values, and so, in the following work, we take $T_0 = 286.89$ as the temperature of reference with $\mu_0 = 3.080 \cdot 10^{-4}$.

The theoretical formula for viscosity used is that given in a former paper† corresponding to a repulsive field of type $\lambda_n r^{-n}$ with a weak attractive field, viz.,

$$\mu = \mu_0 \left(\frac{T}{T_0} \right)^{\frac{1}{2}} \frac{T_0^x + S}{T^x + S}, \quad (4.03)$$

where $x = (n-3)/(n-1)$ and S is an attractive constant, independent of temperature. To secure the best fit between theory and experiment, various values of n are chosen, and the values of S , required to give agreement between theory and experiment, are calculated from the values of μ given in Table IV. The results of this preliminary calculation from the formula

$$S = \frac{T_r^x - T_0^x \left(\frac{\mu_0}{\mu_r} \right) \left(\frac{T_r}{T_0} \right)^{\frac{1}{2}}}{\left(\frac{\mu_0}{\mu_r} \right) \left(\frac{T_r}{T_0} \right)^{\frac{1}{2}} - 1} \quad (4.04)$$

are given in Table V.

The values appropriate to 273.09 are omitted as being unreliable in view of the small range of temperature between it and T_0 . We have already seen from Table IV that one of the values of μ for 378.90°C . or for 373.09°C is wrong.

* Bannawitz, *loc. cit.*

† 'Roy. Soc. Proc.' A, vol 106, p 441

Table V—Values of the Attractive Constant (S) of Neon

T	$n = 9$	$n = 11$	$n = 15$	$n = 21$	$n = \infty$
378.90	-12.675	-11.198	-6.451	5.2549	37.631
373.09	-9.150	-6.211	0.937	10.407	56.960
198.72	-3.790	-0.012	7.758	17.173	59.429
91.66	-1.605	1.575	7.676	14.752	44.800
Value taken	4.848	-1.585	5.457	14.111	53.730

The above table shows that the measured value at 373.09 gives values more consistent with the others, and may therefore be regarded as more reliable. Average values of S calculated from this and the other two values are given at the foot of each column.

With these values of S , the repulsive force constants are then calculated from the formula*

$$\lambda_n^{\frac{2}{n-1}} = \frac{C}{I_2(n) \Gamma\left(4 - \frac{2}{n}\right) (2k)^{\frac{n-3}{n-1}} (T_0^{\frac{n-3}{n-1}} + S)}, \quad (4.05)$$

where

$$C = \frac{5\pi^{\frac{1}{2}} m^{\frac{1}{2}} (kT_0)^{\frac{1}{2}}}{4\mu_0}. \quad (4.06)$$

The values of $I_2(n)$ are obtained from a former paper†. The results, with the corresponding values of the "diameter" σ , are given in Table VI.

Table VI.—The Repulsive Force Constants of Neon

n	9	11	15	21	∞
Repulsive Force Constant	$6.663 \cdot 10^{-14}$	$4.446 \cdot 10^{-14}$	$1.764 \cdot 10^{-119}$	$3.892 \cdot 10^{-145}$	0
$\sigma \cdot 10^8$ cms	5.022	4.300	3.599	3.153	2.350

While the method does not determine the attractive field, it may be supposed that its effect is represented by the values of S given above (however interpreted), and is therefore separated from the effect of the repulsive field. The attractive field may be taken to be weak in view of the small values of S , as compared with those of argon and carbon dioxide found elsewhere.‡

* 'Roy. Soc. Proc.,' *loc. cit.*, eqn (7.01)

† 'Roy. Soc. Proc.,' *loc. cit.*, § 5.

‡ 'Roy. Soc. Proc.,' *loc. cit.*, pp 458 and 460

§ 5 Application to Crystals

Reasons have been given elsewhere* for supposing that the positive and negative ions of the elements next to the pure gases in the periodic table have the same outer field as the pure gases, plus, of course, that due to their electrostatic charges. With this assumption, theoretical calculations have been made of the inter-atomic distances in the crystals KCl and CaS from a knowledge of the field of argon, and have been shown to accord well with fact. *Vice versa*, the crystal measurements of KCl and CaS may be regarded as fixing the atomic model for argon from a series of models determined by other methods. In the same way, we can here apply the results of X-ray measurements of the crystals NaF and MgO to determine the atomic field of neon. When the repulsive field between atoms is $\lambda_n r^{-n}$, the potential of any one atom is given, as shown in the former paper by

$$\phi = \frac{(1.742) e^2 z^2}{z} - \frac{\lambda_n A_{n-1}}{(n-1) z^{n-1}},$$

z referring to the valency of the ions concerned, A_{n-1} being a function of n determined by a recent investigation,† e the unit electrostatic charge, and z the closest distance of approach between atoms. The condition that ϕ shall be a minimum leads to

$$z^{n-2} = \frac{\lambda_n A_{n-1}}{(1.742) e^2 z^2}$$

The value $z = 1$ corresponds to NaF, that of $z = 2$ to MgO. Using the values of λ_n in Table VI, we arrive at the results given in Table VII.

Table VII—Theoretical Calculations of Inter-atomic Distances in the Crystals of NaF and MgO (in Ångströms) ‡

n	9	11	15	21	∞	Measured ∞ *
NaF	1.973	2.077	2.193	2.272	2.350	2.34
MgO	1.619	1.781	1.974	2.112	2.350	2.110

* Bragg, 'X-rays and Crystal Structure,' p. 165 (1924).

The model indicated is clearly that of $n = 21$.

Finally, for this model, with $S = 14.11$, the values of the coefficient of

* 'Roy Soc. Proc.' (above).

† A. E. Ingham and J. E. Jones, 'Roy Soc. Proc.' to be published shortly. A few values of A_{n-1} have been given in 'Roy Soc. Proc.' (December, 1924).

‡ The calculated numbers would probably be diminished by (at most) 0.5 per cent if the attractive field of neon were taken into account, cf. the calculations for argon (*loc. cit.*)

viscosity have been calculated from the formula (4.03), leading to the results given in Table VIII. For comparison, the values are also calculated for the Sutherland model ($n = \infty$) with $S = 53.73$, and are included in the same table.

Table VIII —The Viscosity of Neon

T	$\mu_{\text{obs}} \cdot 10^4$	$n = 21$ ($S = 14.11$)		Sutherland ($S = 53.73$)	
		$\mu_{\text{calc}} \cdot 10^4$	Per cent diff	$\mu_{\text{calc}} \cdot 10^4$	Per cent diff
378.00*	3.042	3.705	+1.75	3.681	+1.0
373.00	3.652	3.067	+0.4	3.645	-0.02
273.00	2.946	2.979	+1.0	2.981	+1.2
198.72	2.382	2.390	+0.0	2.396	+0.6
91.06	1.352	1.359	+0.05	1.303	-3.7

* As observed above, the value of μ at this temperature is doubtful

The calculated values for $n = 21$ could obviously be brought into closer accord with experiment by reducing μ_0 by about 0.5 per cent, say, to $\mu_0 = 3.065 \cdot 10^{-4}$. The calculated values would then not differ from the observed (except in the case of the highest temperature) by more than 0.5 per cent.

The conclusion then is that neon repels according to an inverse 21st power law with $\lambda_n = 3.892 \cdot 10^{-10}$.

§6 Summary

The atomic field of helium has been determined by using conjointly the experimental results on its viscosity and on its equation of state. The conclusion is that its field can be represented by a repulsive force $\lambda_n r^{-n}$ with $n = 14$, and $\lambda_n = 5.74 \cdot 10^{-118}$ together with an attractive force $\lambda_m r^{-m}$, with $m = 5$, and $\lambda_m = 1.930 \cdot 10^{-10}$. That of neon has been determined from measurements of its thermal conductivity and its viscosity, and from measurements of the inter-atomic distances in the crystals NaF and MgO. The repulsive force $\lambda_n r^{-n}$ is shown to be given by $n = 21$ and $\lambda_n = 3.892 \cdot 10^{-165}$, the attractive force is not determined, but is shown to be weak.

*Experiments on the Distortion of Single-Crystal Test-Pieces of
Aluminium*

By H C H CARPENTER, F R S, Professor of Metallurgy, Imperial College of
Science and Technology, and Miss C F ELAM, M A, Armourers' and
Brasiers' Company Research Fellow

(Received October 30 1924)

[PLATE 3]

When aluminium test pieces are broken in tension and subsequently heated to a sufficiently high temperature, they re-crystallise and break up into a number of smaller crystals whose size depends on the amount of distortion. For example near the fracture the crystals are smallest, and they increase in size towards the shoulders of the test-piece. In order to investigate this matter further a number of single crystal test-pieces were extended to varying amounts and heated. The following Table shows the results obtained -

Table I

No	Extension per cent on 2 inches	Heat Treatment	Result
351	1	Heated for 16 hours at 550 C	No change
352	2		No change
353	3		No change
356	4		No change
359	5		No change except that crystal in shoulder re-crystallised
363	6		No change
377	7		No change
380	8		Re-crystallised
386	9		Re-crystallised
415	10		Re-crystallised

Nos 351-377 were subsequently heated at 600° C for two hours, after which no change was observed. The orientations of the crystals probably differed, so that the results are not strictly comparable, but it is evident that the crystals can be deformed as much as 7 per cent without being destroyed on heating. Those that did re-crystallise show exceptionally straight crystal boundaries, and are frequently twinned.

A round test-piece (No 78) was similarly treated. The orientation was first

determined by means of X-rays, and the bar extended 5 per cent. The position of the crystal axes was again determined, and it was noticed that the reflections on the photographic plate were not so well defined, and were spread over a large reflecting angle. This will be referred to again later. The crystal was then heated at 400°C , 500°C , and 600°C , and examined after various periods at these temperatures. There did not appear to be any change after this treat-

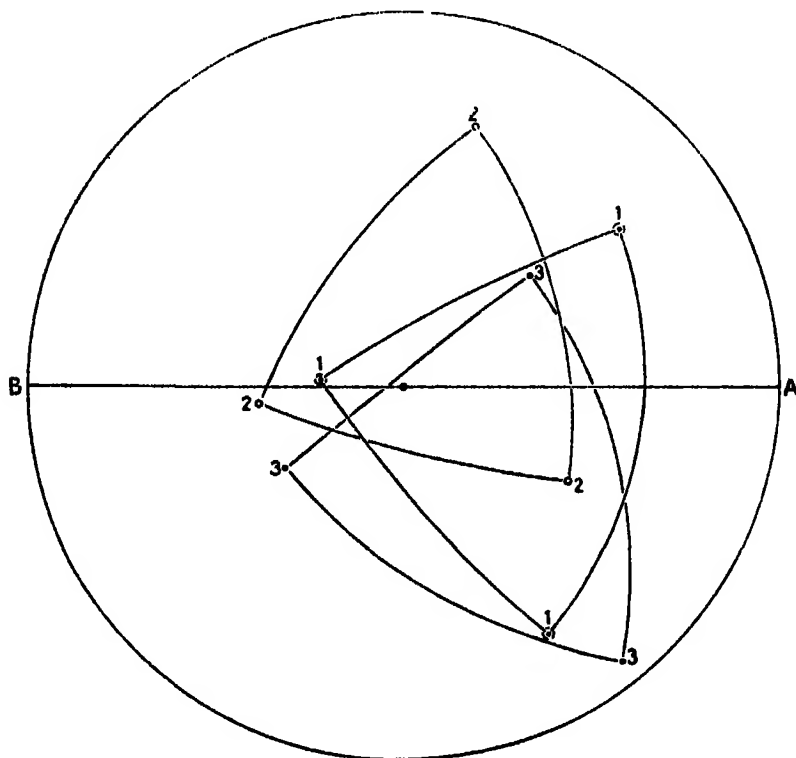


FIG 1

ment. The nature of the X-ray reflections was unaltered, and there was no change in the position of the reflecting planes.

After a second extension of 5 per cent the positions of the reflecting planes were re-determined, and the bar heated at 350°C and 450°C . No change was observed. After heating at 550°C , however, the reflections that had been found previously had disappeared, but new ones were obtained in other positions. A comparison of the reflecting planes from different parts of the bar, including opposite sides of the same reference plane, showed that it was still a single crystal, but that it possessed a totally different orientation from that of the

original Etching in caustic soda revealed an homogeneous structure in accordance with this deduction The X-ray reflections now obtained were sharp and well defined, as in the original crystal

A further extension of 5 per cent produced results similar to the first extension, and heating up to 600° C (beginning as before at 350° C) produced no change On heating after the fourth extension, however, the orientation was found

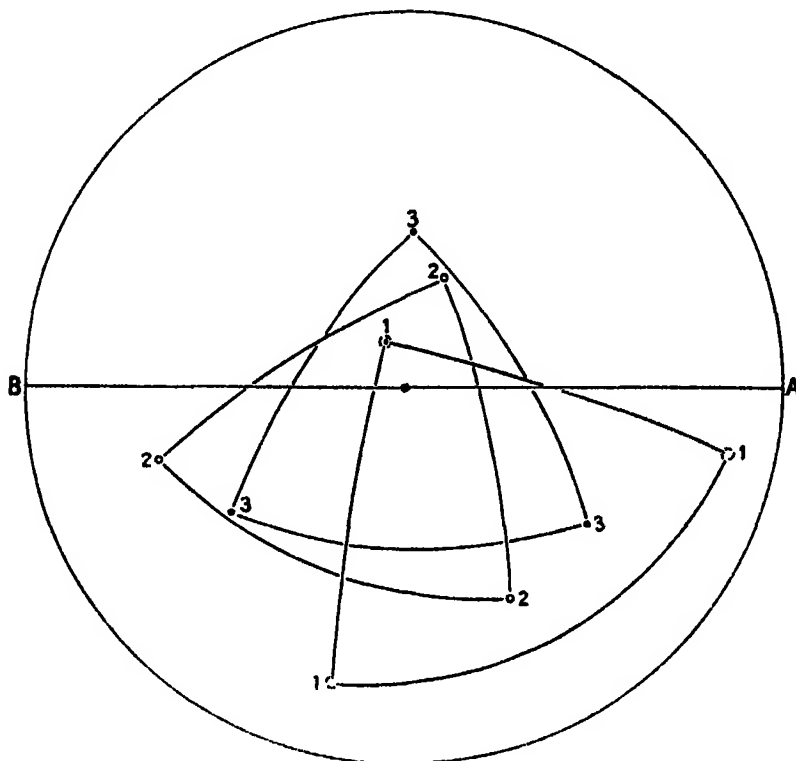


FIG 2

to have changed once more, the bar still remaining a single crystal On heating after the sixth extension a partial re-crystallisation took place

Another test-piece (No 86) was subjected to this treatment with exactly similar results The orientation was changed twice

Full details of the treatment of these bars and the positions of the crystal axes at each stage will be found in Tables II and III The figures refer always to the same reference plane

Figs 1 and 2 show the positions of the axis of the test-piece relative to the crystal axes at different stages

The positions of the cubic axes of the crystal have been plotted on the spherical diagram, in which the centre represents the axis of the test-piece and the line AB, a vertical plane to which all the X-ray measurements were referred. The great circles passing through each set of axes have been drawn, and the triangles so obtained numbered 1, 2 and 3, representing the first, second and third orientations of the test-pieces. The change in position of the spherical triangles relative to the axis of the test-piece and the reference plane shows the amount of re-orientation which has taken place after each re-crystallisation.

There does not seem to be any relation between the first, second and third orientations of the bars. It is probable that the new crystal grows from a new centre as in another bar, which had received somewhat similar treatment to the above, etching revealed the presence of new crystals while the rest of the bar gave the same X-ray reflections as it did before treatment. No intermediate stages, however, were observed in either No. 78 or No. 86.

It has already been mentioned that, after straining the X-ray reflections from the crystal planes are not so sharp or well defined, and the setting angle over which reflection occurs increases. This matter has also been referred to by Müller,* Joffé,† Ozolchralski‡ and others. It can be explained by supposing that the crystal is slightly distorted, probably by a uniform bending of the crystal planes. It has not been found that any one particular plane shows a greater distortion than the others. Fig. 3 (- Plate 3) shows photographs of X-ray reflections from an octahedral plane (111) in test-piece No. 78. No. 1 is that from the crystal before treatment, No. 2 after an extension of 5 per cent, No. 3 after an extension of 10 per cent. No. 4 refers to the same extension as No. 3, but after heating at 450° C. for thirty-six hours, while No. 5 shows the appearance of a new plane (200) due to re-crystallisation. This last is very sharp and clear, and quite unlike the diffuse spots in the previous photographs. The angle over which reflection occurs is doubled by an extension of 10 per cent, and this is reduced to the normal when the material has re-crystallised.

The most interesting feature brought out by these photographs is that heating does not destroy this effect of mechanical deformation unless the metal re-crystallises, and this will only occur if the degree of strain is sufficiently great and the temperature is sufficiently high. In this connection it is interesting to

* A. Müller, 'Roy. Soc. Proc. A', vol. 105 (1924).

† A. Joffé, M. W. Kirpitschewa, M. A. Fewitzky, 'Zeitschrift für Physik', vol. 22, No. 5.

‡ Ozolchralski, 'Zeitschrift für Metallkunde', 1923, March-May.

Table II—No 78

Extension	Heat Treatment	Reflecting Planes	
0	—	$\theta_{111} = 80^\circ 55'$ $\psi = 350^\circ 10'$	$\theta_{111} = 61^\circ 33'$ $\psi = 63^\circ 23'$
1st Extension 5 per cent	—	—	$\theta_{111} = 61^\circ 0'$ $\psi = 63^\circ 0'$
"	Heated 17 hours at 400° C	$\theta_{111} = 81^\circ 26'$ $\psi = 349^\circ 40'$	$\theta_{111} = 60^\circ 30'$ $\psi = 62^\circ 55'$
"	Heated 500° C	$\theta_{111} = 81^\circ 20'$ $\psi = 349^\circ 35'$	$\theta_{111} = 60^\circ 20'$ $\psi = 62^\circ 50'$
"	Heated 600° C	$\theta_{111} = 81^\circ 30'$ $\psi = 349^\circ 40'$	$\theta_{111} = 61^\circ 0'$ $\psi = 62^\circ 0'$
2nd Extension 5 per cent	—	$\theta_{111} = 82^\circ 25'$ $\psi = 350^\circ 40'$	$\theta_{111} = 60^\circ 25'$ $\psi = 62^\circ 20'$
"	Heated 72 hours at 350° C	$\theta_{111} = 81^\circ 30'$ $\psi = 349^\circ 40'$	$\theta_{111} = 60^\circ 10'$ $\psi = 60^\circ 30'$
"	Heated 36 hours at 450° C	$\theta_{111} = 82^\circ 25'$ $\psi = 350^\circ 40'$	$\theta_{111} = 60^\circ 25'$ $\psi = 62^\circ 20'$
"	Heated 18 hours at 550° C	$\theta_{111} = 95^\circ 30'$ $\psi = 20^\circ 46'$	$\theta_{200} = 42^\circ 30'$ $\psi = 5^\circ 25'$
3rd Extension 5 per cent	—	$\theta_{111} = 96^\circ 0'$ $\psi = 21^\circ 16'$	—
	Heated to 600° C	$\theta_{111} = 96^\circ 0'$ $\psi = 21^\circ 16'$	$\theta_{200} = 41^\circ 20'$ $\psi = 11^\circ 30'$
4th Extension 5 per cent	—	$\theta_{111} = 95^\circ 10'$ $\psi = 27^\circ 45'$	$\theta_{200} = 40^\circ 15'$ $\psi = 18^\circ 10'$
	Heated to 600° C	$\theta_{111} = 96^\circ 0'$ $\psi = 3^\circ 0'$	$\theta_{200} = 42^\circ 95'$ $\psi = 33^\circ 20'$
5th Extension 5 per cent	—	$\theta_{111} = 90^\circ 47'$ $\psi = 1^\circ 0'$	$\theta_{200} = 39^\circ 30'$ $\psi = 30^\circ 30'$
	Heated to 600° C	$\theta_{111} = 90^\circ 47'$ $\psi = 0^\circ 8'$	$\theta_{200} = 40^\circ 20'$ $\psi = 28^\circ 10'$
6th Extension 5 per cent	—	$\theta_{111} = 90^\circ 45'$ $\psi = 0^\circ 0'$	$\theta_{200} = 38^\circ 15'$ $\psi = 21^\circ 20'$
	Heated to 600° C	Partly re-crystallized	

θ = angle between vertical axis of test piece and the normal to the reflecting plane
 ψ = angle between reference plane and plane containing normal to reflecting plane ψ is measured anti clockwise

Table III—No 86

Extension	Heat Treatment	Reflecting Planes	
0	—	$\theta_{111} = 138^\circ 50'$ $\psi = 309^\circ 10'$	$\theta_{200} = 94^\circ 05'$ $\psi = 347^\circ 42'$
1st Extension 5 per cent	—	$\theta_{111} = 140^\circ 40'$ $\psi = 308^\circ 50'$	$\theta_{200} = 96^\circ 20'$ $\psi = 347^\circ 35'$
"	Heated to 600° C	$\theta_{111} = 140^\circ 11'$ $\psi = 307^\circ 05'$	$\theta_{200} = 96^\circ 10'$ $\psi = 347^\circ 36'$
2nd Extension 5 per cent	—	$\theta_{111} = 139^\circ 15'$ $\psi = 300^\circ 40'$	$\theta_{200} = 97^\circ 50'$ $\psi = 348^\circ 30'$
"	Heated to 600° C	$\theta_{111} = 124^\circ 20'$ $\psi = 3^\circ 33'$	$\theta_{111} = 90^\circ 0'$ $\psi = 86^\circ 52'$
3rd Extension 5 per cent	—	$\theta_{111} = 123^\circ 05'$ $\psi = 3^\circ 0'$	—
"	Heated to 600° C	$\theta_{111} = 123^\circ 05'$ $\psi = 2^\circ 0'$	$\theta_{111} = 88^\circ 13'$ $\psi = 67^\circ 52'$
4th Extension 5 per cent	—	$\theta_{111} = 120^\circ 55'$ $\psi = 0^\circ 35'$	$\theta_{111} = 89^\circ 45'$ $\psi = 66^\circ 22'$
"	Heated to 600° C	$\theta_{111} = 63^\circ 40'$ $\psi = 37^\circ 20'$	$\theta_{111} = 82^\circ 45'$ $\psi = 100^\circ 10'$

compare the loads required to extend the bars 5 per cent at each stage of the experiment. These are given in Table IV. In each case the load has been calculated on the cross-sectional area measured after each extension. It will be seen that the load drops after each re-crystallisation, and that with one exception it was always higher for the second extension of 5 per cent—i.e., the 2nd, 4th and 6th—than for the first—i.e., the 1st, 3rd and 5th, although the metal had been heated at 600° C between each extension. The change of orientation due to the extension is too small to account for it, although it is probably the cause of the difference observed when a new crystal is extended for the first time. It appears, therefore, that the increase in load required to extend the metal by an equal amount is chiefly due to the effect of the previous extension, and that the increase in resistance to slip is intimately connected with the change in the X-ray reflections.

It is difficult to obtain any quantitative results in this connection, as it is undesirable to compare the effects of equal amounts of deformation on crystals of different orientations. It will be noticed, however, in Table IV, that in No. 78 the second extension was 670 lbs greater than the first and the sixth extension was 615 lbs greater than the fifth. These differences are not great

Table IV

Extension			Load in lbs per sq inch
No 78 —1st	Extension 3 per cent		4,990 }
2nd	" "		5,690 }
3rd	" "		5,280 }
4th	" "		5,130 }
5th	" "		4,325 }
6th	" "		4,940 }
Re-crystallisation occurred after the 2nd, 4th and 6th extensions			
No 86 —1st	Extension 5 per cent		4,690 }
2nd	" "		5,080 }
3rd	" "		4,600 }
4th	" "		5,025 }

Re-crystallisation occurred after the 2nd and 4th extensions

The figures for the third and fourth extensions do not agree with any other similar figures in that the fourth is less than the third. It is probable that some error in measurement is the cause of this discrepancy. In No 86 the agreement is even closer, the loads for the second and fourth extensions being 390 lbs and 425 lbs greater than for the first and third.

The effect of orientation is most marked at the beginning of a tensile test, since as the deformation proceeds the crystal axes rotate and take up a fixed position with regard to the axis of the test-piece*. It is therefore possible to compare the effects of plastic deformation on a crystal during the latter stage of the extension, with the complication of changing orientation very much reduced in effect. As the final orientation assumed by aluminum crystals is the same whatever the original position of the axes, the results from a number of crystals are also comparable.

Fig 4 shows the curves obtained for four crystals by plotting the extension against the load calculated on the cross sectional area of the test-piece at each stage after it had been stretched. The actual figures are given in Tables V and VI. The curves differ considerably at the beginning of the extension, and the increase in load is relatively greater than the amount of deformation. As the extension proceeds the curves become nearly straight, and the values for all the crystals differ only slightly for the same degree of extension. This is

* G I Taylor and C F Elam, *loc cit*

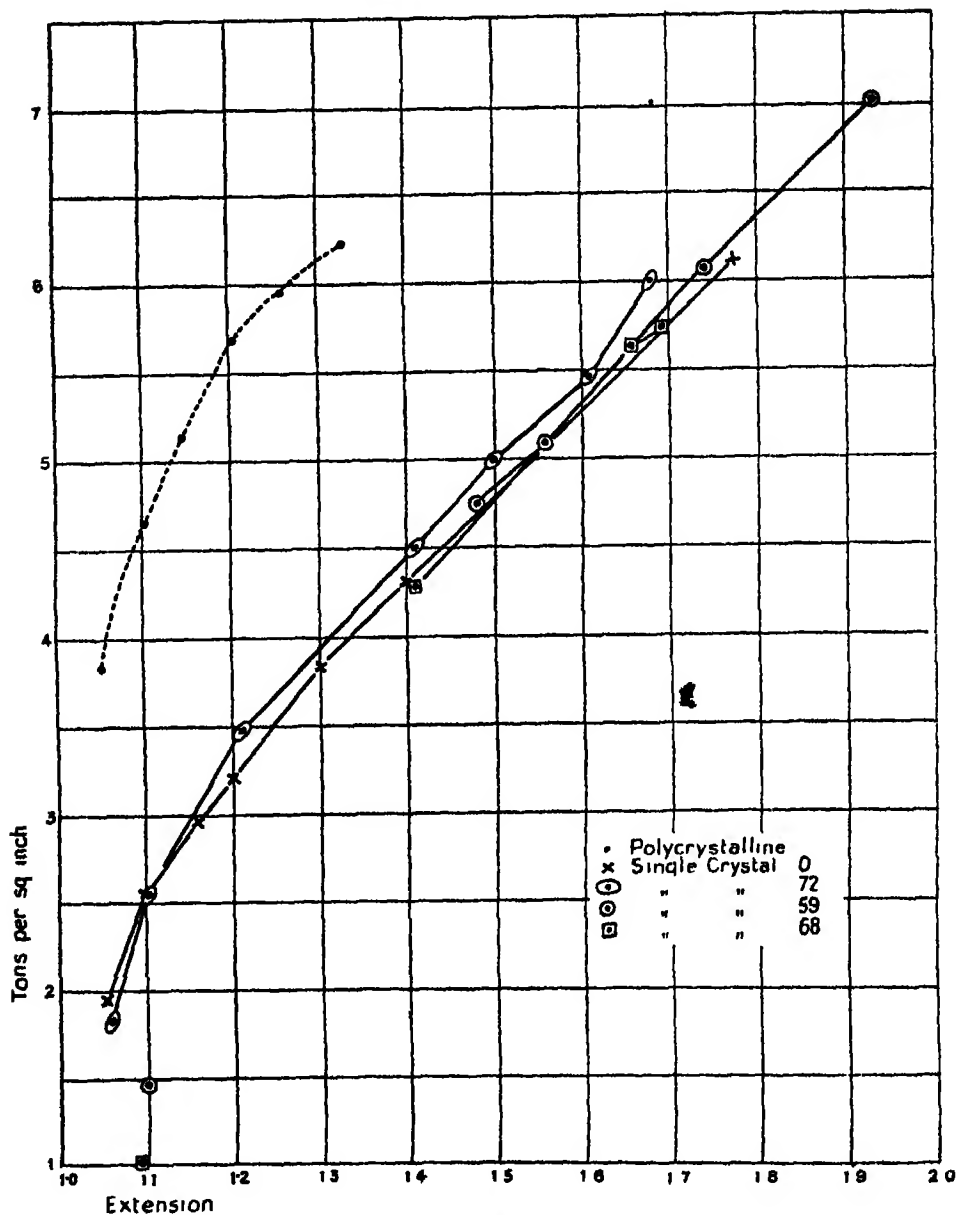


FIG 4.

evident from the diagram During the latter part of the test, therefore, the increase in hardness is directly proportional to the amount of plastic deformation The curve for a polycrystalline bar is also given It is interesting to note that the breaking load is approximately the same as for some of the single

crystals, although it is harder at all earlier stages. No. 59, a single crystal, has, however, the highest breaking load, and also the highest percentage elongation. These results show quite definitely that, in the case of aluminum crystals, the increase in hardness is intimately connected with the degree of plastic deformation, and that the original orientation of a crystal plays only a minor part. This conclusion has also been arrived at by Polanyi,* Schmid† and others.

It has already been stated that differences in orientation may account for some of the differences noticed at the beginning of the extension. There must be another factor, however, which affects the change of hardness during the earlier stages. The largest percentage increase in hardness occurs during the first 5 per cent elongation, and the value diminishes as the extension proceeds until it becomes constant as the above curves have shown. The same effect is noticeable in the initial steep rise in the stress-strain diagrams for polycrystalline metal. It appears to be connected in some way with the first break-down of the crystal, of which the actual mechanism is unknown.

Table V Polycrystalline Test-pieces

No.	Ratio of Extended to Initial Length	Cross sectional area Square inches	Load Tons per square inch
99	1.052	0.235	3.83
	1.101	0.225	4.67
	1.193	0.207	5.54
	1.225	0.199	5.87
	1.338	0.184	6.44
100	1.050	0.235	3.83
	1.102	0.225	4.71
	1.148	0.216	5.14
	1.210	0.205	5.71
	1.258	0.197	5.97
	1.301	0.1901	6.26

* Polanyi, 'Zeitschrift für Physik,' vol. 17, No. 1 (1923)

† E. Schmid, 'Zeitschrift für Physik,' vol. 22, No. 5 (1924)

Table VI.—Single-Crystal Test-pieces.

No.	Ratio of Extended to Initial Length	Cross-Sectional area, Square inches.	Load, Tons per square inch
0	1 053	0 168	1 93
	1 110	0 160	2 55
	1 161	0 152	3 95
	1 200	0 140	3 21
	1 304	0 128	3 63
	1 404	0 116	4 32
	1 785	0 080	6 13
72	1 058	0 238	1 81
	1 109	0 226	2 55
	1 210	0 205	3 47
	1 410	0 182	4 5
	1 506	0 169	5 02
	1 610	0 158	5 47
	1 687	0 146	6 01
59	1 101	0 156	1 46
	1 484	0 107	4 76
	1 560	0 102	5 08
	1 745	0 090	6 08
	1 936	0 082	7 06
8	1 093	0 108	1 10
	1 411	0 084	4 29
	1 659	0 067	5 65
	1 695	0 065	5 76

Summary

1. Single crystal test-pieces of aluminium can be extended up to 7 per cent. without re-crystallising on heating to 600° C

2 They will re-crystallise to form either another single crystal of a different orientation, or several crystals according to the degree of strain

3 The orientation of the new crystal has no apparent relation to that of the crystal from which it has formed When a large crystal grows from a number of small ones it also has neither a particular orientation nor a relation to the direction of mechanical strain.

4 The distortion of the crystal as shown by the X-ray reflections is not removed by heating unless the metal re-crystallises

5 Heating does not remove the whole of the hardness acquired through mechanical strain unless the metal re-crystallises

6. Hardening by mechanical deformation can take place independently of change of orientation

7 The proportional increase in hardening is greatest during the early stages of extension, but in the case of single crystals a stage is reached when the increase in hardness is approximately proportional to the amount of plastic deformation.

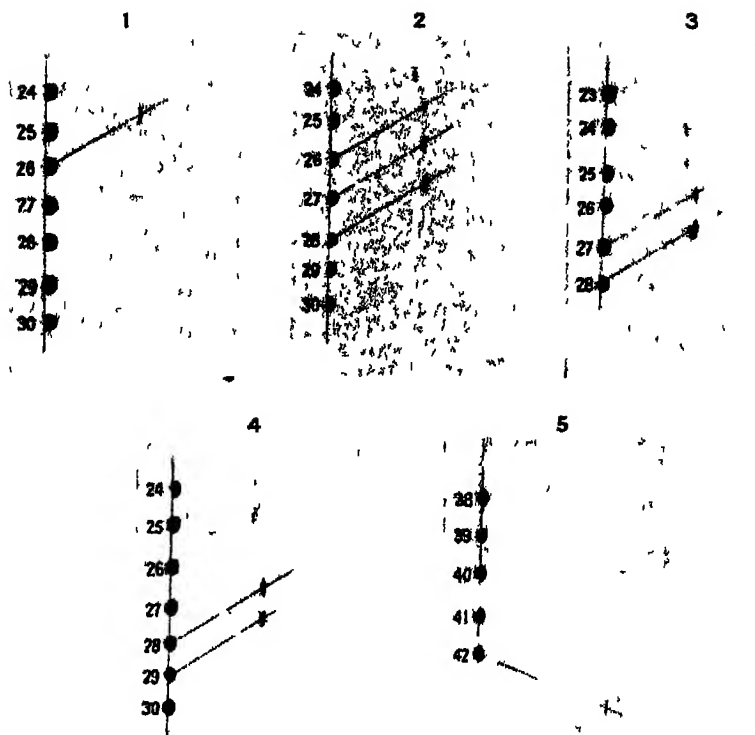


FIG 3

On the Thirteen Semi-regular Solids of Archimedes, and on their Development by the Transformation of certain Plane Configurations.

By D'ARCY WENTWORTH THOMPSON, F.R.S.

(Received November 27, 1923 — Revised November, 1924)

We learn from Pappus* that Archimedes discovered thirteen isogonal polyhedra bounded by two or by three kinds of regular polygons. Kepler† reinvestigated them, and showed that, just as the five regular solids known to the ancients are all that exist, so also the Archimedean bodies are thirteen and no more‡, that Archimedes should not only have described them but described them all, is a remarkable fact in the history of geometry.

Catalan§ investigated them again, and in doing so showed the existence of a second, or conjugate, family of thirteen isohedral but not isogonal solids of which two only (the rhombic dodecahedron and triakontahedron) had been known to Kepler. Max Brückner ('Vielecke und Vielfache,' 1900) has brought together all, or well nigh all, that is known regarding these two families.

The Archimedean bodies may be derived by truncation from the five regular solids, though in two cases (the so-called "snub cube" and "snub dodecahedron") no simple method exists for performing this operation, that the method of truncation was in Kepler's mind is plain from the names which he gives to the several bodies and it is also the method set forth in a scholium to the Vatican MS of Pappus. Catalan approached the matter in another way, namely, through spherical trigonometry,|| and found the same two polyhedra again presenting considerable difficulty. That there remains a third way of regarding, or of constructing, the Archimedean bodies is the theme of the present note.

* Pappus, 'Collectanea,' ed. Hultsch, vol. 5, pp. 352-58 (cf. Heath, 'History of Greek Mathematics,' vol. 2, pp. 98-101 (1921)).

† Kepler, 'Harmonices Mundi, Lib. II,' "De Figurarum Harmonicarum Congruentia" ('Opera,' ed. 1864, vol. 5, pp. 114-127).

‡ The number 13 was to the Greek mind a notably irregular one, and was indeed often used to denote a vague or indefinite number. To a Greek it would probably seem natural and appropriate that the regular solids should be five in number, and the semi-regular solids 13.

§ Catalan, 'Journ. de l'Ecole Polytechnique,' vol. 24, pp. 1-71 (1865).

|| "La recherche des polyèdres semi-réguliers du premier genre se réduit à la décomposition, en polygones réguliers, d'une surface sphérique" (op. cit., p. 33).

The following is a list of the Archimedean bodies, according to Kepler's order and nomenclature. We may define, or symbolise, each by a formula which shall either give the number and kind of faces in the entire polyhedron, or of those meeting in a single corner or summit—for instance, No. I, the snub cube, may be denoted by (F) $32_3 6_4$, or (C) $4_3 1_4$.

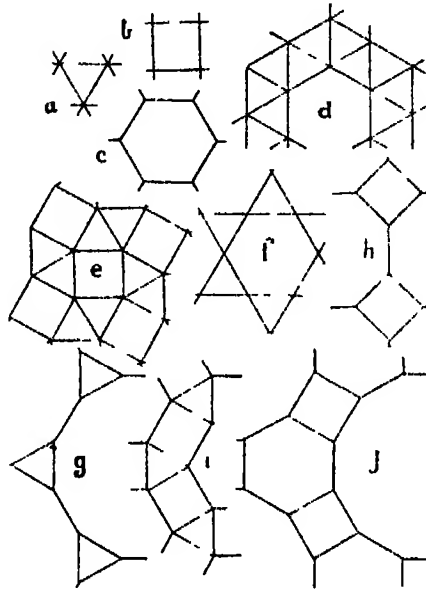
Kepler's Name and Order	Faces of Polyhedron	Faces at each Corner	F	C	E
I Cubum simum	$32_3, 6_4$	$1_3, 1_4$	38	24	60
II Cuboctahedron*	$8_1, 6_4$	$2_4, 2_4$	14	12	24
III Rhombicuboctahedron	$8_3, 18_4$	$1_4, 3_4$	26	24	48
IV Dodecahedron simum	$80_4, 12_5$	$4_3, 1_1$	92	60	150
V Icosidodecahedron	$20_3, 12_5$	$2_2, 2_5$	32	30	60
VI Tetrahedron truncum	$4_2, 4_4$	$1_3, 2_4$	8	12	18
VII Cubum truncum	$8_3, 6_4$	$1_3, 2_4$	14	24	36
VIII Dodecahedron truncum	$20_3, 12_{10}$	$1_3, 2_{10}$	42	60	90
IX Octahedron truncum	$6_4, 8_3$	$1_4, 2_3$	14	24	36
X Icosahedron truncum	$12_5, 20_6$	$1_5, 2_6$	32	60	90
XI Rhombicoidodecahedron	$20_3, 30_4, 12_5$	$1_3, 2_4, 1_5$	62	60	120
XII Cuboctahedron truncum	$12_4, 8_3, 6_4$	$1_4, 1_3, 1_4$	26	48	72
XIII Icosidodecahedron truncum	$30_4, 20_3, 12_{10}$	$1_4, 1_3, 1_{10}$	62	120	180

* Note that Kepler's "cuboctahedron" is not the figure which Von Kedorow calls by that name. Von Kedorow's cuboctahedron or heptaparallelohedron, and Kelvin's orthic tetrakaidcahedron, are identical with Kepler's "truncated octahedron," No. IX.

Kepler preceded his account of these and other more or less regular solids by an account of the various possible "congruentiæ harmonicae" of the regular polygons in a plane surface. He showed that these congruent associations are eighteen in number, but that of these eighteen, ten only are symmetrical repeating patterns. The ten are as follows:—

<i>Plane symmetrical repeating Patterns</i>	<i>Nodal formula</i>
a Contiguous triangles	6_3
b squares	4_4
c hexagons	3_6
d Hexagons, each surrounded by 18 triangles	$4_3, 1_6$
e Squares, with a triangle on each side	$3_3, 2_4$
f Hexagons, with a triangle on each side	$2_3, 2_6$
g Dodecagons, with triangles on alternate sides	$1_3, 2_{12}$
h Octagons, with squares on alternate sides	$1_4, 2_8$
i Hexagons, with a square on each side, and intercalated angles	$1_3, 2_4, 1_6$
j Dodecagons, surrounded alternately by squares and hexagons	$1_4, 1_6, 1_{12}$

We shall now see that these plane repeating polygonal patterns stand in direct relation to the isogonal polyhedra, and can be transformed into them—a fact



which Kepler does not record, nor (so far as I am aware) has any later student observed or indicated it. Let us take any one of these plane patterns, except the first, and consider the angles (each the angle of a regular polygon) which meet at a node, then let us reduce one of these angles to that of a polygon of lower order, and so on. The resulting angular combinations will then be found to be just such solid angles as go to form one or another of the isogonal polyhedra. Thus, if we take (c) the continuous sheet of hexagons, where each node is formed by three adjacent hexagons, or 3_6 , call this $2_6, 1_6$, and we have, successively —

$2_6, 1_6$	a node of the plane repeating pattern c	
$2_6, 1_6$	„	isogonal polyhedron X
$2_6, 1_4$	„	„ „ IX
$2_6, 1_3$	„	„ „ VI

Or, again,

$1_4, 1_6, 1_{12}$	a node of the plane repeating pattern	
$1_4, 1_6, 1_{10}$	„	isogonal polyhedron XIII
$1_4, 1_6, 1_8$	„	„ „ XII
$1_4, 1_6, 1_6$	„	„ „ IX

Moreover, the composition of a solid angle or corner is the fundamental

character (and is equivalent to a definition) of any isogonal solid, from which all its other characteristics may in turn be derived

We may illustrate these serial relations by concrete models Take, for instance, a ring of six hexagons (which we may construct of cardboard, joining them together by hinges of tape or paper), and slit one of the hinges, then slide *one hexagon* over another across the slit The hexagonal fenestra in the middle of the ring is thus reduced to a pentagonal fenestra, surrounded by five hexagons Slide two over two hexagons, and we get a square fenestra surrounded by four hexagons, slide three over three, and the fenestra becomes a triangle Now if, instead of a single ring of hexagons, we begin with the continuous sheet, removing alternate hexagons so that everywhere a hexagonal fenestra lies within a ring of hexagons, we find that our process of folding the sheet, or sliding the hexagons, goes on continuously, the whole system bends round and closes up into a symmetrical solid network, with twelve pentagonal windows and twenty hexagons, it is Kepler's "truncated icosihedron," the tenth on his list of the Archimedean bodies If there be more rings of hexagons than are actually required to complete the figure, the superfluous ones fold over and over upon the completed figure after it has once appeared Folding two upon two, we get in like manner Kepler's truncated octahedron (IX), Kelvin's orthic tetrakaidekahedron, or Von Fedorow's "cuboctahedron", and, folding three over three, we arrive at the truncated tetrahedron (VI) In short, we have produced successively the three possible symmetrical isogonal polyhedra in which hexagons and pentagons, hexagons and squares, and hexagons and triangles are combined

What we have done is, apparently, to impart a certain definite amount of *curvature* to a portion of our plane sheet, and then to go on applying the same amount of curvature to equally and symmetrically interspaced portions of the same sheet, the total curvature is, therefore, essentially spherical, and the plane sheet is converted into a symmetrical solid inscribable in a sphere

We may perhaps look at the operation from another point of view It seems to me to present an analogy to, and to offer an extension of, Camille Jordan's principle of "group movements" But, whereas Jordan traced the correlated movements of a rigid system, such that every point travels to a place formerly occupied by a homologous point, and the whole movement therefore leaves the system unchanged, in our case every point travels by a definite pathway to a definite point, which, however, is one in an entirely different but still symmetrical configuration And, apart from the pathways travelled, we seem to perceive very curious topological relations between the two figures, for

instance, in the superposed polygons which, coming from different parts of the plane assemblage and remaining unchanged in form, travel to the same place and, completely overlapping one another, become merged in a single face. In the whole movement of the system we seem to have a very curious combination of rigid and non-rigid parts, and a somewhat simple but very curious arrangement of degrees of freedom.

We have not yet come to the end of our series, for we may slide four hexagons over four, the fenestra is then obliterated, and all the hexagons fold flat over one another. We seem to have come, in this limiting case, to a single plane hexagon. But having passed from solid to solid, we are entitled to look upon this limiting case as a solid too, it is Klein's "solid of no volume"! So looked at, its six angles are not plane angles of 120° , but solid angles of 240° , and the number of its faces, edges and corners conform, like those of any other polyhedron, to Euler's law.

The foregoing instance may suffice for a description or illustration of the whole method. We may proceed after a similar fashion, occasionally in more ways than one, with every one of the ten plane repeating patterns, with the single exception of the continuous sheet of triangles. The snub cube (I) and snub dodecahedron (IV), which, as we have seen, are not easy to produce either by truncation of a regular solid or by partition of the sphere, are developed according to our method in as simple a fashion as any of the rest.

That the sheet of triangles is an exceptional case, and one to which our method (strictly speaking) does not apply, is obvious enough, for a triangle, or triangular fenestra, is not capable of reduction to a polygon of lower order. Moreover, the network of triangles is a six-way node system, and it is an accepted theorem (of Von Fedorow's) that we can have no solid whose nodes are all six-way, that is to say, whose corners are all hexahedral, it is a theorem analogous to that one of Euler's which tells us that we can have no solid (in the ordinary sense) whose faces are all hexagonal. But there is another method of transformation, a different but analogous method, which is still open to us. Let us consider our sheet of triangles as consisting not of so many annular assemblages of faces around a central face, but as so many hexagonal assemblages of six triangles around a *node*. Let us then slit this hexagonal ring (along a side common to two triangles), and slide one triangle over another. Formerly, we altered the shape of a central facet, now we are altering the character of a node, or composition of a corner—transforming a six-way into a five-way node. The result is to develop a frustum of an icosahedron, and by continuing the process we may proceed to build up the whole

icosahedron from our continuous sheet. Again, slide two triangles over two, then three over three, and we develop successively the octahedron and the tetrahedron. These three form a descending series of solids whose faces are all regular triangles, and which differ in the fact that their solid angles contain, successively, five-way, four-way and three-way nodes. In this manner also we may develop the cube from the plane homogeneous sheet of squares. The fact is we are now treating these regular solids as equifacial or isohedral solids, when before we were treating them as equiangular or isogonal. These regular solids are easily amenable to this mode of transformation, but it is otherwise with the semi-regular isohedral bodies which form Catalan's second family, for in these latter the alteration of the nodal angles involves a *strain* on the faces, which are thereby converted into non-regular triangles, rhombs, &c. To some extent it is possible to demonstrate the transformation, in these latter cases, by models in which the facets are represented by hinged frameworks, but I am not prepared meanwhile to pursue this subject. Returning now to our first or typical method of transformation, we find that, while the sheet of triangles does not permit of development after the same fashion as the rest, so also the dodecahedron and tetrahedron are not capable of being so developed. As to the tetrahedron, we could only hope to develop it by the continued transformation of some solid composed of triangles and squares, but of these we possess two only (I and II), from which come, as their ultimate derivatives, the icosahedron and the octahedron. They are, respectively, five-way and four-way node-systems, and the three-way system which the tetrahedron would require does not exist.

The case of the dodecahedron is peculiar. If we attempt to make a continuous network of pentagons, the net overlaps more and more, and so becomes a system of multiple sheets instead of a single sheet like the net of hexagons and the rest. We may simplify this net if we keep adding our successive pentagons only to the two outer sides of the pre-existing ones, and we then have between the pentagons (or certain of them) rhomboidal fenestræ. (Were we to add the full number of pentagons, the fenestræ would still be there, but they would be represented by regions of fewer overlaps instead of by vacant interspaces.) Now, when we begin to fold up our net we do two things, we close up the fenestræ, and we also cause more and more pentagons to overlap one another. The net folds up directly into the regular dodecahedron. The network of pentagons together with the rhomboidal interspaces is a four-way node system, and the four-way is reduced to a three-way node when we obliterate the rhombs in the process of folding. This transformation, then, is

quite analogous to that by which we have just derived the other *regular* solids

In the following table are shown the several series of polyhedra resulting from the development of the several plane, congruent, repeating patterns. In one case the hexagonal prism is introduced, as an ultimate derivative from the plane configuration j , the hexagonal prism is, of course, a semi-regular isogonal solid, though it is not included in the particular group with which we deal.

The few and very simple formulæ at the bottom of the table show how, from a knowledge of the constitution of a solid angle or corner, all the other characteristics of the several polyhedra may be deduced.

Kepler classified the Archimedean bodies into those with two and those with three kinds of faces, and further graded them in order according to the polygons of which they are composed, from triangles upwards. Catalan classified them according to the number and kind of facets which enter into the composition of each corner. Our table indicates other ways in which these thirteen bodies may be classified: (1) according to the plane polygonal patterns to which they are severally related, (2) according to the sum of the plane angles in each corner (α) and (3) by their nodal numbers (N), *i.e.*, into those with five-way, four-way or three-way nodes.

		Isogonal Polyhedra										
Plane Assemblages		360°	354°	348°	342°	336°	330°	324°	300°	270°	240°	180°
$\alpha =$												
N = 6	a (6 ₁)	—	—	—	—	—	—	—	Icosah (4 ₂ , 1 ₄)	—	—	—
5	d (4 ₂ , 1 ₄)	—	—	IV (4 ₂ , 1 ₄)	—	—	I (4 ₂ , 1 ₄)	—	Icosah (4 ₂ , 1 ₄)	—	—	—
5	e (3 ₂ , 2 ₄)	—	—	—	—	—	—	—	Icosah (3 ₂ , 2 ₄)	—	—	—
4	b (2 ₄ , 2 ₄)	—	—	—	—	—	—	—	II (2 ₄ , 2 ₄)	—	—	—
4	f (2 ₃ , 2 ₆)	—	—	—	—	—	—	—	II (2 ₃ , 2 ₆)	—	Octah (2 ₃ , 2 ₆)	—
4	i (1 ₂ , 2 ₄ , 1 ₄)	—	—	—	—	V (2 ₃ , 2 ₆)	—	—	II (2 ₃ , 2 ₄)	—	—	—
3	c (2 ₃ , 1 ₆)	—	—	—	—	—	III (1 ₂ , 2 ₄ , 1 ₄)	—	II (1 ₂ , 2 ₄ , 1 ₄)	—	—	—
3	g (2 ₃ , 1 ₆)	—	—	—	—	—	IX (2 ₃ , 1 ₆)	—	VI (2 ₃ , 1 ₆)	—	—	—
3	h (1 ₂ , 2 ₁₂)	—	—	—	—	—	VII (1 ₂ , 2 ₆)	—	VI (2 ₃ , 1 ₆)	—	—	—
3	i (1 ₄ , 2 ₆)	—	—	—	—	—	IX (1 ₄ , 2 ₆)	—	VI (1 ₄ , 2 ₆)	Cube (1 ₄ , 2 ₆)	—	—
3	j (1 ₄ , 2 ₆)	—	—	—	—	—	VII (1 ₄ , 2 ₆)	—	V (1 ₄ , 2 ₆)	—	—	—
3	k (1 ₄ , 1 ₆ , 1 ₁₂)	—	XIII (1 ₄ , 1 ₆ , 1 ₁₂)	—	XII (1 ₄ , 1 ₆ , 1 ₂)	—	IX (1 ₄ , 1 ₆ , 1 ₄)	—	Hexag prism (1 ₄ , 1 ₆ , 1 ₄)	—	—	—
5	—	—	—	—	—	—	—	Dodec (5 ₂)	—	—	—	Tetrah (3 ₂)
3	—	—	—	—	—	—	—	—	—	—	—	—
$\left. \begin{array}{l} \frac{360}{360 - \alpha} \\ \frac{C}{2} \\ \frac{E}{N} \\ \frac{F}{N - 2} \end{array} \right\} =$		∞	60	30	24	15	12	10	6	4	3	2

If p, q, \dots be the faces meeting in one corner, and f, f' (or $f, f' \dots$) the facets of the entire polyhedron,

$$f = \frac{pC}{n}, \quad f' = \frac{qC}{m}$$

On the Formation of Water Waves by Wind.

By HAROLD JEFFREYS, M A , D Sc , Fellow and Lecturer of St John's College,
Cambridge

(Communicated by Prof G I Taylor, F R S —Received October 24, 1924)

[PLATES 4-5]

It is well known that in certain circumstances a type of instability may arise at the surface of separation of two fluids when there is a finite difference between the velocities on the two sides of the surface. Some disturbances of the surface, of simple harmonic type, may increase exponentially in amplitude until the customary simplifying assumption, that the terms of the second degree in the displacements from the undisturbed state can be ignored, breaks down. One would naturally expect that in the case, for instance, of a wind blowing over the surface of water, waves would be first formed when the velocity of the wind is just great enough to make one particular type of wave grow, thus the critical wind velocity and the wave-length of the waves first formed will constitute checks on any theory of wave formation. The problem for frictionless fluids has been solved by Lord Kelvin*, subject to the restriction that the disturbances considered are two-dimensional, no horizontal displacement occurring across the relative velocity of the fluids. Since, however the possible initial deformations of a horizontal surface will not as a rule satisfy this condition, an investigation of the growth or decay of deformations of other types is desirable.

1 *Hypothesis of Irrotational Motion*

Let the two fluids be incompressible (a legitimate approximation so long as the wave velocity is small compared with that of sound in either fluid) and of great vertical extent. Let the origin be in the undisturbed position of the surface of separation and the axis of z vertically upwards. Let ζ be the elevation of the surface, and suppose the two fluids to have initially velocities U and U' parallel to the axis of x , accents referring to the upper fluid. Let the densities of the fluids be respectively ρ and ρ' , and the velocity potentials

* 'Phil. Mag' (4), vol. 42, pp. 368-370 (1871), or Lamb, 'Hydrodynamics,' p. 439 (1906).

in them ϕ and ϕ' . Let the operators $\partial/\partial t$, $\partial/\partial x$, $\partial/\partial y$, $\partial/\partial z$ be denoted by σ , p , q , and \mathfrak{S} respectively. Putting r^2 for $-(p^2 + q^2)$ we see that

$$\nabla^2 \phi = 0 \quad (1)$$

is equivalent to

$$(\mathfrak{S}^2 - r^2) \phi = 0, \quad (2)$$

whence

$$\phi = Ux + e^{rz} A, \quad (3)$$

where A is a function of x and y , determined by the value of ϕ where z is zero.

Now the vertical velocity of a particle in the surface is $d\zeta/dt$, where d/dt denotes differentiation following a particle of the fluid, and this must be equal to the value of $\mathfrak{S}\phi$ for surface particles. Hence to the first order in the small disturbances

$$(\sigma + Up)\zeta = rA \quad (4)$$

Thus

$$\phi = Ux + \frac{\sigma + Up}{r} e^{rz} \zeta \quad (5)$$

Similarly

$$\phi' = U'x - \frac{\sigma + U'p}{r} e^{-rz} \zeta \quad (6)$$

If P denote the pressure and Q the resultant velocity, the pressure integral is

$$\begin{aligned} \frac{P}{\rho} &= -\frac{\partial \phi}{\partial t} - \frac{1}{2} Q^2 - gz + \text{const} \\ &= -\sigma \phi - U e^{rz} p A - gz + \text{const}, \end{aligned} \quad (7)$$

to the first order. This becomes, when $z = \zeta$,

$$\frac{P}{\rho} = -\left\{ \frac{(\sigma + Up)^2}{r} + g \right\} \zeta + \text{const} \quad (8)$$

Similarly we have, when $z = -\zeta$,

$$\frac{P'}{\rho'} = \left\{ \frac{(\sigma + U'p)^2}{r} - g \right\} \zeta + \text{const} \quad (9)$$

Also

$$P' - P = T(p^2 + q^2) \zeta, \quad (10)$$

where T is the surface-tension. Hence ζ satisfies the differential equation

$$\{\rho(\sigma + Up)^2 + \rho'(\sigma + U'p)^2 + g(\rho - \rho')r + Tr^2\} \zeta = 0 \quad (11)$$

In particular, if ζ is proportional to $\cos(\gamma t - \kappa x) \cos \kappa' y$, where γ , κ , κ' are constants, we must have

$$\rho(\gamma - U\kappa)^2 + \rho'(\gamma - U'\kappa)^2 = g(\rho - \rho')r + Tr^2, \quad (12)$$

where

$$r^2 = \kappa^2 + \kappa'^2 \quad (13)$$

This gives

$$\gamma = \kappa \frac{\rho U + \rho' U'}{\rho + \rho'} \pm \left[\frac{g(\rho - \rho')r + Tr^3}{\rho + \rho'} - \kappa^2 \frac{\rho \rho' (U' - U)^2}{(\rho + \rho')^3} \right]^{\frac{1}{2}} \quad (14)$$

If the motion is two-dimensional, so that $\kappa' = 0$ and $r = \kappa$, the solution becomes equivalent to that of Lord Kelvin

So long as γ is purely real, the given disturbance will neither increase nor decrease in amplitude. Thus the condition for a wave to develop is that γ shall be imaginary. This gives at once

$$\kappa^2 (U' - U)^2 > \frac{\rho + \rho'}{\rho \rho'} \{g(\rho - \rho')r + Tr^3\} \quad (15)$$

$$> \frac{\rho + \rho'}{\rho \rho'} \{g(\rho - \rho')\kappa + T\kappa^3\} \quad (16)$$

$$> 2 \frac{\rho + \rho'}{\rho \rho'} \{Tg(\rho - \rho')\}^{\frac{1}{2}} \kappa^2 \quad (17)$$

the first sign of equality holding when the wind is just strong enough to increase the wave considered, the second when the wave is two-dimensional, and the third when the wave-length is such as to make $\frac{g(\rho - \rho')}{\kappa} + T\kappa$ a minimum. If the corresponding value of κ is κ_0 , we have

$$\kappa_0^2 = \frac{g(\rho - \rho')}{T} \quad (18)$$

For air and water we have

$$\rho = 1 \text{ gm./cm}^3, \quad \rho' = 0.0013 \text{ gm./cm}^3, \quad T = 73 \text{ dyne/cm} \quad (19)$$

Hence from (18) κ_0 is 3.5/cm, and the critical wave-length is $2\pi/\kappa_0$ or 1.8 cm. The critical value of $U' - U$, the velocity of the wind relative to the water, is given by

$$(U' - U)^2 = 2 \frac{\rho + \rho'}{\rho \rho'} \{Tg(\rho - \rho')\}^{\frac{1}{2}}, \quad (20)$$

making

$$U' - U = 640 \text{ cm/sec} \quad (21)$$

Again, if α be the rate of travel of the waves first formed, we have

$$\alpha = \gamma/\kappa \quad (22)$$

and

$$\alpha - U = \frac{\rho'}{\rho + \rho'} (U' - U) \quad (23)$$

$$= 0.8 \text{ cm/sec} \quad (24)$$

At each point these predictions are in disagreement with observation. The velocity of a wind just strong enough to raise waves is actually only about 110 cm./sec, the wave-length of the waves first formed by such a wind is from 6 to 8 cm, and the rate of travel of the waves is about 30 cm/sec.

A further discrepancy is provided by the wave-length of the swell in mid-ocean. Vaughan Cornish* gives 1,150 feet as the wave-length of a typical swell. This makes κ equal to 1.8×10^{-4} /cm, and hence by (16)

$$U' - U = 6.5 \times 10^4 \text{ cm/sec}$$

This is far beyond any actual velocity. It follows that no wind occurring at sea would be capable of raising a typical swell if the theory of irrotational motion were applicable to the formation of water waves.

2 *The Hypotheses of Sheltering and Skin Friction*

It therefore appears that, in any theory of wave formation that is to stand the test of quantitative comparison with observation, the hypothesis of irrotational motion must be abandoned, and the effects of quasi-discontinuities and turbulence must be included. The regular form of the waves first formed suggests that discontinuities and turbulence in the water are unimportant, at least when waves first appear, so that attention will have to be given primarily to irregular motions in the air. There are two obvious mechanisms by which the existence of waves on the surface of the water may introduce rotational motions in the air, which may then react on the water in such a way as to alter the size of the waves. The first is that the air blowing over the waves may be unable to follow the deformed surface of the water. Water flowing past a sphere does not in general flow all round it, the particles that strike the front of the sphere leave it soon after they have passed the centre, and the region behind the sphere is occupied by eddying liquid with little or no systematic motion relative to the sphere. By analogy one may suggest that if waves are once formed on water, the main air current, instead of flowing steadily down into the troughs and over the crests, merely slides over each crest and impinges on the next wave at some point intermediate between the trough and the crest. The region sheltered from the main air current contains an eddy with a horizontal axis, while smaller eddies exist along the boundary between this eddy and the main current. If such a theory is correct, the pressure of the air will be greater on the slopes facing the wind than on those away from it, for the deflexion of the air upwards when it strikes the exposed slopes

* 'Waves of the Sea and Other Water Waves,' p. 97 (1910).

implies a reaction between the air and the water. By analogy with the two-dimensional problem of the thrust of a current on a plane lamina inclined to the direction of flow,* we may infer that the reaction is approximately normal to the surface and proportional to $\rho'U' \partial\zeta/\partial x$, where U' is now the velocity of the wind over the crests. Within the sheltered region the reaction will be nearly uniform. The reaction is thus not an analytic function of x , but it could be expressed as a series of harmonic functions of multiples of x . This series would evidently contain many terms, but so long as we are considering only whether the fundamental wave will increase or decrease, it will be sufficient to consider only the term of the same wave-length as the disturbance of the surface of the water. We shall, therefore, consider the reaction as equal to $s\rho'U' \partial\zeta/\partial x$, where s is a numerical constant, not necessarily small. This hypothesis will be called the hypothesis of sheltering.

The alternative hypothesis is based on the conception of skin friction. There is a great deal of evidence to indicate that the tangential reaction of a turbulent fluid on a fixed surface is of the form $s'\rho'V^2$ where s' is a numerical coefficient about equal to 0.002 and V is the tangential velocity in the neighbourhood of the surface. We shall overestimate this effect if we neglect the reaction of this friction on the air, which reduces the velocity of the air near the surface, and simply calculate V as if the motion of the air was irrotational.

Up to a point these two hypotheses can be treated together. The equations of viscous motion of the water are three, of the form

$$\frac{du}{dt} = -\frac{1}{\rho} \frac{\partial P}{\partial x} + \nu \nabla^2 u, \quad (1)$$

where ν is the effective kinematic coefficient of viscosity. With our previous conventions we can write these

$$\{\sigma + Up - \nu(p^2 + q^2 + s^2)\} (u, v, w) = -\frac{1}{\rho} (p, q, s) P \quad (2)$$

The equation of continuity is

$$pu + qv + sw = 0 \quad (3)$$

Combining (2) and (3) we have

$$(p^2 + q^2 + s^2) P = 0, \quad (4)$$

whence

$$\frac{P}{\rho} = e^{\pi i} \Pi \quad (5)$$

* Lamb, 'Hydrodynamics,' p. 94.

where Π is a function of x and y Hence

$$u = U_1 e^{\lambda z} - \frac{p \Pi e^{\lambda z}}{\sigma + U_p}, \quad (6)$$

$$v = V e^{\lambda z} - \frac{q \Pi e^{\lambda z}}{\sigma + U_p}, \quad (7)$$

$$w = W e^{\lambda z} - \frac{r \Pi e^{\lambda z}}{\sigma + U_p}, \quad (8)$$

where U_1 , V and W are unspecified functions of x and y , and

$$\sigma + U_p - v(\lambda^2 - r^2) = 0 \quad (9)$$

In consequence of (3) we must have

$$pU_1 + qV + \lambda W = 0 \quad (10)$$

The surface condition is

$$\frac{d\zeta}{dt} = w \quad (11)$$

leading to

$$(\sigma + U_p)\zeta = W - \frac{r\Pi}{\sigma + U_p} \quad (12)$$

The stress-components across the surface $z = 0$ are

$$p_{zz} = -P + 2\nu\rho \nabla w = 2\nu\rho \lambda W - \rho\Pi \left(1 + \frac{2r^2\nu}{\sigma + U_p}\right), \quad (13)$$

$$p_{zx} = \rho\nu (\nabla u + pw) = p\nu \left(\lambda U_1 + pW - \frac{2pr\Pi}{\sigma + U_p}\right), \quad (14)$$

$$p_{zy} = p\nu \left(\lambda V + qW - \frac{2qr\Pi}{\sigma + U_p}\right) \quad (15)$$

Suppose also that these stress-components are given in terms of the surface elevation by the relations

$$p_{zz} = \rho Q\zeta, \quad p_{zx} = \rho p R\zeta, \quad p_{zy} = \rho q R\zeta \quad (16)$$

where Q and R are linear operators. Then (14) and (15) give

$$\frac{\lambda U_1}{p} = \frac{\lambda V}{q} = \frac{R\zeta}{\nu} - W + \frac{2r\Pi}{\sigma + U_p} \quad (17)$$

and on substitution in (10) we find

$$W = \frac{r^2}{\lambda^2 + r^2} \left(\frac{R\zeta}{\nu} + \frac{2r\Pi}{\sigma + U_p} \right) \quad (18)$$

Eliminating W between (12) and (18) we have, using (9),

$$\Pi = rR\zeta - \frac{\nu(\lambda^2 + r^2)}{r} (\sigma + U_p) \zeta, \quad (19)$$

and thence

$$\begin{aligned} W &= (\sigma + Up) \zeta + \frac{r^2 R \zeta}{\sigma + Up} - v(\lambda^2 + r^2) \zeta \\ &= -2vr^2 \zeta + \frac{r^2 R \zeta}{\sigma + Up} \end{aligned} \quad (20)$$

Substituting in (13) we have now

$$\begin{aligned} Q\zeta &= 2v\lambda r^2 \left(\frac{R}{\sigma + Up} - 2v \right) \zeta \\ &\quad - \left(1 + \frac{2vr^2}{\sigma + Up} \right) \left(rR\zeta - \frac{\sigma + Up + 2vr^2}{r} (\sigma + Up) \zeta \right) \end{aligned} \quad (21)$$

The amplitudes of the types of waves considered do not change by large fractions of themselves within a wave-length. Hence we shall expect that vr^2 will be small compared with $\sigma + Up$, and that $r^2 R$ will be small compared with $(\sigma + Up)^2$. If then, we omit all terms of order higher than the first in v and R , we have

$$\{(\sigma + Up + 2vr^2)^2 - Qr - Rr^2\} \zeta = 0 \quad (22)$$

which is the differential equation required. For further progress it is necessary to specify the forms of Q and R .

3 Hypothesis of Sheltering

On the hypothesis of discontinuous motion of the air there is no tangential reaction, so that R is zero. The vertical pressure across a given horizontal surface will depart from its value in the undisturbed state for three reasons. First, there is a depth ζ of water above the surface instead of an equal depth of air; hence the pressure is increased by $g(\rho - \rho')\zeta$ or since in (13) tensions are reckoned positive, p_{xx} must contain a term $-g(\rho - \rho')\zeta$. Second, as in the irrotational case, the surface tension introduces a discontinuity of amount $T(p^2 + q^2)\zeta$. Third, the pressure of the air on the side of the wave facing the wind introduces a term $s\rho'U'^2 p\zeta$, where such a velocity has been supposed superposed on the whole system that the crests of the waves have no horizontal motion. The exposed side of the wave is that facing in the direction of x increasing, if U' is negative, which will be the case considered. Thus p_{xx} is positive when $p\zeta$ is positive, and this term must therefore be associated with a positive sign. Thus in all

$$\rho Q = -g(\rho - \rho') - Tr^2 + s\rho'U'^2 p \quad (1)$$

and the differential equation satisfied by ζ becomes

$$\left\{ (\sigma + Up + 2vr^2)^2 + c^2r^2 - \frac{sp'}{\rho} U'^2 pr \right\} \zeta = 0, \quad (2)$$

where
$$\rho c^2 = \frac{q}{r} (\rho - \rho') + Tr \quad (3)$$

In accordance with our conventions the wave is a stationary one, with gradually varying amplitude. Thus we can take ζ as proportional to $e^{i\gamma} \cos \kappa x \cos \kappa' y$, where γ , κ and κ' are constants. Then

$$\sigma \zeta = \gamma \zeta, \quad p^2 \zeta = -\kappa^2 \zeta, \quad f(r^2) \zeta = f(\kappa^2 + \kappa'^2) \zeta \quad (4)$$

Then (2) gives

$$\{(\gamma + 2vr^2)^2 + c^2r^2 - U^2\kappa^2\} \zeta + \left\{ 2U(\gamma + 2vr^2) - \frac{sp'}{\rho} U'^2 r \right\} p \zeta = 0 \quad (5)$$

Neither ζ nor $p\zeta$ is in general zero, nor is their ratio a constant. Hence the coefficients must both vanish, giving

$$\gamma = -2vr^2 + \frac{sp'}{2\rho} \frac{U'^2 r}{U}, \quad (6)$$

$$\kappa^2 U^2 = c^2 r^2 + \text{a second-order quantity} \quad (7)$$

We notice from (6) that the wave will necessarily die down if U is negative. Thus when U' is negative U must be positive. Remembering that these velocities were both referred to the crests of the waves, we see that this implies that the velocity of the waves is intermediate between those of the air and the water. Again, (3) and (7) give

$$U^2 = \frac{gr}{\kappa^2} \frac{\rho - \rho'}{\rho} + \frac{T}{\rho} \frac{r^3}{\kappa^2} \quad (8)$$

and if γ is positive we must also have

$$U'^2 \geq \frac{4vp}{sp'} U r. \quad (9)$$

Let us denote the coefficient $4vp/sp'$ by C . For every value of κ , r increases steadily with κ' . Hence U and $|U'|$ both increase with κ' . But the observed speed of the wind relative to the water is $U' - U$, and its absolute value is $|U'| + U$. Hence, for any given wave-length in the x -direction, the wind velocity relative to the water needed to excite the disturbance is least when the wave-length in the y -direction is infinite, that is, when the disturbance is two-dimensional. Thus the waves produced by the gentlest wind that can ruffle the water at all should be two-dimensional.

Let us assume that the value of κ corresponding to actual waves is such as to

make $T\kappa^2/g(\rho - \rho')$ small, that is, that wind-raised waves are gravity waves and not ripples. Also let the velocity of the wind relative to the water be V . Then (9) gives

$$r \leq \frac{(V - U)^2}{CU}, \quad (10)$$

the sign of equality holding when the wave can just be maintained. Again, we have

$$r \geq \kappa \quad (11)$$

the sign of equality holding when the disturbance is two-dimensional. Then, subject to the neglect of T , we have from (8)

$$\kappa U^2 \geq g \frac{\rho - \rho'}{\rho}, \quad (12)$$

and, therefore,

$$r \geq \frac{g}{U^2} \frac{\rho - \rho'}{\rho} \quad (13)$$

From (10) and (13) then

$$U(V - U)^2 \geq Cg \rho \frac{\rho - \rho'}{\rho} \quad (14)$$

For a given value of V , the value of U between 0 and V that makes the quantity on the left greatest is

$$U = \frac{1}{3}V \quad (15)$$

so that the condition for a wind to be able to raise a wave at all is

$$V^3 \geq \frac{27}{4} Cg \rho \frac{\rho - \rho'}{\rho} \quad (16)$$

whence, with $\nu = 0.018 \text{ cm}^2/\text{sec}$

$$V \geq 73s^{-1/3} \text{ cm/sec} \quad (17)$$

and from (12)

$$\kappa^3 = 5s^2 \quad (18)$$

for the critical case. Thus so long as s is less than unity as it must be the assumption made in the neglect of the surface tension is justified.

4. Hypothesis of Skin Friction

In discussing this hypothesis the motion of the air will be treated as if unmodified by friction. In this way the velocity of the air in contact with the water surface will be exaggerated, and therefore the effects of skin friction will be over-estimated. The pressure in the air is given by

$$\begin{aligned} \frac{P'}{\rho'} &= -gz - \sigma\phi' - \frac{1}{2}Q'^2 + \text{const.} \\ &= -(\sigma + U'p)\phi' - gz + \text{const.}, \end{aligned} \quad (1)$$

and the value over the boundary is $-g\zeta + \frac{(\sigma + U'p)^2}{r}\zeta + \text{constant}$ Then

$$\rho Q\zeta = \left\{ -g(\rho - \rho') + \frac{(\sigma + U'p)^2}{r}\rho' - Tr^2 \right\} \zeta. \quad (2)$$

The tangential velocity over the surface is, to the first order, $p\phi'$, and the skin friction is $s'\rho'(p\phi')^2$. The components p_{xz} and p_{xy} cannot as a rule be put in the form used in 3 (16), except when the motion is two-dimensional. Restricting the discussion to this case, we have for the first order part of p_{xz} ,

$$\begin{aligned} p_{xz} &= -2\rho's'U'\frac{\sigma + U'p}{r}p\zeta \\ &= \rho p R\zeta, \end{aligned} \quad (3)$$

and from 3 (22)

$$\left\{ (\sigma + Up + 2\nu r^2)^2 + g\frac{(\rho - \rho')}{\rho}r + \frac{T}{\rho}r^2 - (\sigma + U'p)^2\frac{\rho'}{\rho} + \frac{2\rho's'U'}{\rho}(\sigma + U'p)r \right\} \zeta = 0 \quad (4)$$

If now we suppose, as before, that ζ is proportional to $e^{\lambda t} \cos \kappa x$, and introduce c^2 as before, we have

$$(\gamma + 2\nu\kappa^2)^2 + (c^2 - U^2)\kappa^2 - (\gamma^2 - U'^2\kappa^2 - 2s'\kappa\gamma)\frac{\rho'}{\rho} = 0 \quad (5)$$

$$(\gamma + 2\nu\kappa^2)U - \gamma U'\frac{\rho'}{\rho} + \frac{\rho's'\kappa U'^2}{\rho} \quad (6)$$

First approximations to these are

$$\gamma = -2\nu\kappa^2 - \frac{\rho'}{\rho}\frac{s'\kappa U'^2}{U} \quad (7)$$

$$U^2 = c^2 \quad (8)$$

In deriving the skin friction we have tacitly supposed U' to be positive. Hence (7) shows that for a wave to grow U must be negative, and the wave-velocity must, as before, be between those of the water and the air. But s' is known to be about 0.002. Hence, for a wave to grow we must have

$$U'^2 > 14400 \kappa c$$

and thence

$$U' - U > 120 (g\kappa)^{\frac{1}{2}} + \left(\frac{g}{\kappa}\right)^{\frac{1}{2}}.$$

The right side of this inequality has its least value when κ is $1/23$ cm., making the wave-length 140 cm. The corresponding value of $U' - U$ is 480 cm./sec.

5. Comparison with Observation

Observations on the initial stages of wave formation have been described by J Scott Russell * He states that a wind with a velocity between half a mile and two miles an hour produces small capillary waves, and that regular gravity waves, with a wave-length of about 2 inches, first develop when the wind reaches about two miles an hour

These observations seem to have been non-instrumental, and I considered it desirable to check them against a modern instrument A Negretti and Zambra Air Meter was kindly lent to me by the Meteorological Office, to the Director of which I am indebted, and observations were made on the River Cam where it enters St John's College grounds, and just above Jesus Lock, and also on a large pond at Barnwell produced by the flooding of a clay pit It was found that velocities up to 3.4 ft/sec produced no change in the appearance of the surface of the water, which always showed a slight unevenness however gentle the wind seemed, but that strong regular waves were produced by winds of 3.8 and 4 ft/sec, the latter should be reduced by a few inches per second to allow for the speed of the water On the pond ripples were once observed at a velocity of 3.6 ft/sec

These velocities are very much lower than would be consistent with either the irrotational theory or the skin-friction theory They agree well, however, with the theory of sheltering Using the relations found under this theory, we find the following values for s and for the initial wave-length for various values of the critical wind velocity—

$V \begin{cases} \text{ft/sec} \\ \text{cm/sec} \end{cases}$	3.4	3.6	3.8
	104	110	116
s	0.318	0.269	0.229
κ (1/cm)	0.79	0.71	0.64
$2\pi/\kappa$ (cm)	8.0	8.8	9.8

The quantity s is a pure number, and since it expresses the amount of a wave that is exposed to the action of the wind, it will be called the exposure co-efficient There are few *a priori* conditions to guide us as to its value, and such as there are indicate that the values just found are plausible

A crucial test of the theory should be provided, however, if the critical wave-length could be found by observation and compared with the theoretical estimates just made from the critical wind velocity. Unfortunately the critical

* 'Brit. Assoc. Report,' pp. 317-8 (1844).

wave-length is rather difficult to measure. When waves are formed the wind must be systematically somewhat above the true critical value, thus s will be systematically under-estimated, and so will κ . Thus the wave-length calculated from the velocity of the wind will, as a rule, be too great. On the other hand, a wind rather above the critical velocity will raise at first waves whose lengths differ over a finite range. The longest of these move fastest, and thus the shortest tend to remain at the rear of the group. If, then, the waves at the rear of the group are taken as the standard, the wave length will be systematically under-estimated. By eye estimation I find the length of waves raised when the wind is under 4 ft/sec to be from 6 to 8 cm, which is consistent with the above considerations, attempts were made to find the length indirectly from the number of waves passing a given fixed object in a known time, but they proved unsuccessful on account of the difficulty of counting disturbances with such a short period.

The observational evidence, therefore, appears consistent with the theory that discontinuous motion in the air plays a fundamental part in the formation of water waves.

6 OTHER ASPECTS OF THE SHELTERING THEORY

The account of the sheltering theory given in 3 describes only the initial stages of waves produced by winds. Winds with velocities greater than the critical velocity there found will be capable of raising waves with any length in either the x or the y direction within certain finite ranges. In general, all such waves will be formed, but the longer ones travel more rapidly than the shorter ones, and therefore the shortest waves are at the rear of the train produced by a given puff of wind. This agrees with observation. Again, the values of U that make 3 (14) an equality are the extreme possible values of U , and it has been seen that the equality can hold only if κ' is zero. Thus both the fastest and the slowest waves, relative to the water, that can be generated by a given wind are two-dimensional. Three-dimensional waves will be formed, but will travel with intermediate velocities. This, again, appears consistent with observation. The swiftest wave in a storm is the swell, which is a two-dimensional wave. (See Plate 4, fig 1.)

The most striking feature about waves at sea, however, is their irregularity. There is never any definite wave pattern, except in so far as the swell can be traced through the shorter and slower waves. (See fig. 2.) As a rule, the distance between consecutive maxima of elevation is of the same order of magnitude in whatever direction it is measured. Such wave-systems will be

called "short-crested," as distinguished from waves whose crests have lengths many times the distance between consecutive crests, the latter type, including as particular cases the swell and the first waves raised by a wind just strong enough to raise waves at all, will be called "long-crested"

In the case of a sudden gust with a velocity considerably more than the critical velocity (say, 6 ft /sec) the equation (14) shows easily that U may have any value from about $1/26$ of the critical wind velocity up to almost the actual wind velocity. The wave-length corresponding to the former velocity is about two centimetres. This is short enough to show that surface tension is not negligible in this case. However, it is clear that such a wind will be able to raise very short waves, and they will include short-crested waves. Now it can be observed that when such a gust occurs the first effect is to produce an irregular pattern of short-crested waves, often short enough to be considered capillary waves. This is to be expected, since it is for intermediate types of wave that the rate of growth will be most rapid. After an interval of 10 to 30 seconds the long-crested waves may be seen emerging from the catpaw having meanwhile had time to grow. (See Plate 5, fig 3)

When the wind continues steadily for a long time, several other factors become relevant. The swifter waves continually gain on the slower, so that at any intermediate point of the wave train many different types of waves might be expected to be superposed, as indeed is the case. But a new feature appears: the shorter waves are wholly obliterated. The theory of sheltering offers two explanations of this fact, which probably co-operate in producing the change. In the development of the theory all terms depending on the squares and products of the deviations from steady motion have been ignored. It has, however, been found that when a wave is actually formed its amplitude will increase exponentially with the time, so that a stage must be reached when the neglect is no longer justifiable. The nature of the change is well known. The form of the waves ceases to be purely sinusoidal: the crests become sharper and the troughs flatter than in a simple sine curve. (See fig 4) This is to be expected in waves of considerable amplitude on water unaffected by air, the wind only provides a mechanism that causes this stage to be attained.

There is a limit to the height that such waves can attain, in a gravity wave it is fixed by the fact that the crests become definitely angular, the angle being 120° . Thus a wave of given length can never grow beyond a certain height, this height being probably proportional to the wave-length. Further, wind acting on a wave in this critical state will only cause water to be projected from the crests, leaving the height unaltered. This is what actually happens,

the crests do become sharp ridges, and the tops curl over, casting white foam or spray on to the sheltered side of the wave. This effect is presumably prominent in producing turbulence in the water.

When waves of different lengths are superposed, it will not in general be possible to discuss them separately as if the equations of the problems were linear. The linearity of equations 2 (16) is due to the selection from the actual stresses across the boundary between the fluids of the harmonic constituents with wave-lengths equal to those of the wave whose history we are considering. Actually the complete expression of the stresses would require the overtones of these constituents. When two non-commensurable wave-lengths are combined the discussion becomes still more difficult.

If, however, we return to the physical description of the sheltering effect, it becomes possible to make some headway. A short wave superposed on a long one will be of smaller height than the latter when both are fully developed. Hence the short one will be sheltered from the wind for the whole time except when it is near the crest of the long one and on the exposed side. Its opportunities for growth are therefore very much less than if it were alone, while the damping effect of viscosity will be at least as great. Further, when it is on the sheltered side of the crest of the long wave, the splashing of the water from the crest of the long wave will tend to fill up the trough of the short one. On both grounds, therefore, it may be expected that the short wave will die out, its motion also will then make a contribution to the turbulence of the water.

The waves produced by a long-continued wind would therefore be expected to consist mainly of large short-crested waves, combined with a fast-travelling swell of long wave length, which has not had time to develop a height great enough to overshadow the larger short-crested waves. This is in qualitative agreement with what is observed in mid-ocean.

There are, however, difficulties in the way of a quantitative comparison, though quantitative tests may be sought in several directions. In the first place, we may consider the total thrust of the wind in a horizontal direction on the water. This should be equal to the skin friction as determined by other means. Now the horizontal component in the x -direction of the pressure of the wind on the surface is $p = \frac{\partial \zeta}{\partial x}$ approximately, and hence the thrust within a wave-length is $\int_0^{2\pi/k} \rho U^2 \left(\frac{\partial \zeta}{\partial x} \right)^2 dx$. This can only be evaluated when we have some knowledge of the relation of the height of the wave to

its length ; but an estimate of this may be made from the fact that the angle at the crest of a fully developed wave must be 120° . As an approximation let us suppose that the section of the wave is an arc of a circle, so that we can write

$$\zeta = a(1 - \cos \theta), \quad (1)$$

$$x = a \sin \theta, \quad (2)$$

and the limits for θ are 0 and $\frac{1}{2}\pi$. Then the mean value of $(\partial\zeta/\partial x)^2$ is

$$\begin{aligned} 2 \int_0^{\frac{1}{2}\pi} \sin \theta \tan \theta \, d\theta &= \log 3 - 1 \\ &= 0.0986. \end{aligned} \quad (3)$$

If then s' be the coefficient of skin friction, the horizontal thrust of the wind on the water surface will be $s'\rho V^2$ per unit area and if we take s to be 0.3 we have the relation

$$s'V^2 = 0.029U'^2. \quad (4)$$

Now when waves are just on the verge of formation we have

$$U' = \frac{2}{3}V. \quad (5)$$

Hence

$$s' = 0.013. \quad (6)$$

This value is much larger than has been found for the coefficient of skin friction in fluids flowing over smooth solids, or even rough solids where the roughnesses are irregular. Experiments have usually given numbers in the neighbourhood of 0.002. Perhaps, however, it would be premature to say that the above estimate cannot be right for the conditions it refers to, namely, a wind just strong enough to raise waves at all, blowing over water for a time long enough for them to develop fully. If the ordinary estimate for a smooth surface is correct until waves start, as would be expected, it would not be surprising if a sudden increase in the friction accompanied the formation of the first waves. The point should be capable of experimental test in a wind channel ; the stress to be sought is of the order of a gram weight per square metre.

When the velocity is greater than has just been considered, the prevalent waves travel with velocities greater than $\frac{1}{3}V$, if there is no scale effect tending to alter s , as is probable, the anticipated value of s' would therefore be smaller. Observations of the wind at sea have shown no reason to believe that it follows

laws very different from those applicable on land, so that the true value of s' is probably not very different from 0.002. Substitution in (4) now gives

$$U' = 0.26V \quad (7)$$

so that the waves that produce most of the resistance (that is, the largest waves) should travel with about three-quarters of the velocity of the wind. Cornish* makes the velocity of the waves, when well developed, about 80 to 90 per cent. of that of the wind; but as the wind was logged on the Beaufort Scale an error of 7 per cent. in the wind could escape being logged, merely on account of the coarseness of the scale. The agreement is therefore as good as could be expected.

If now we return to 3 (9) we have for the condition that a wave of given type may be able to grow at all

$$U'^2 > \frac{4\nu\rho}{s\rho'} U', \quad (8)$$

and if we apply 3 (8), taking

$$r = \kappa\sqrt{2}, \quad (9)$$

as is roughly true, we have

$$\nu < \frac{s\rho' U'^2 U}{8\rho g}, \quad (10)$$

giving with the value of U' just found

$$\nu < 6.7 \times 10^{-8} V^3 \quad (11)$$

in C.G.S. units. If the sign of equality holds, the wave will be the longest that can grow.

Now the damping of waves in mid-ocean must arise mainly from turbulence rather than true viscosity, and independent determinations of turbulence in water are available. From a comparison of the velocities of wind and ocean currents I have found† values of the eddy-viscosity in mid-ocean ranging from 4 to 460 cm.²/sec. Durst,‡ by a similar method, but with much more numerous and accurately comparable data, has recently carried out an elaborate investigation, and finds that the eddy-viscosity in mid-ocean is well represented by a formula which, when corrected for an arithmetical error, is

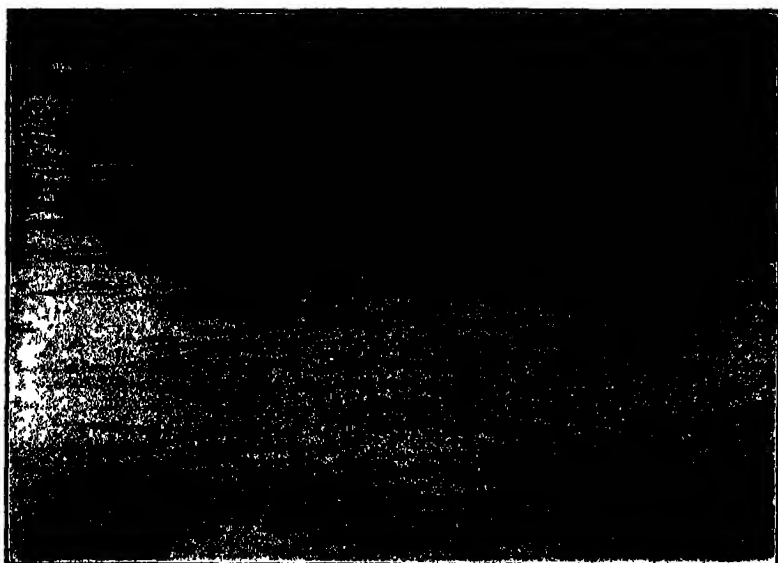
$$\nu = 8 \times 10^{-4} V^2. \quad (12)$$

His work amounts to a verification of this formula for values of V ranging from 200 to 1,200 cm./sec. For a wind of 10 m/s. this makes ν equal to 800 cm.²/sec.; whereas formula (11) makes it less than 6.7 cm.²/sec.

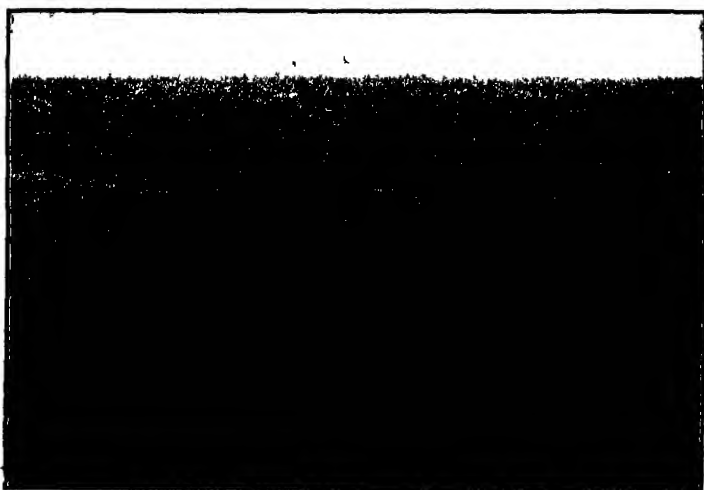
* *Zee. oit.*, pp. 111-113.

† '*Phil. Mag.*,' vol. 29, pp. 573-586 (1920).

‡ '*Q. J. R. Met. Soc.*,' vol. 50, pp. 113-119 (1924).



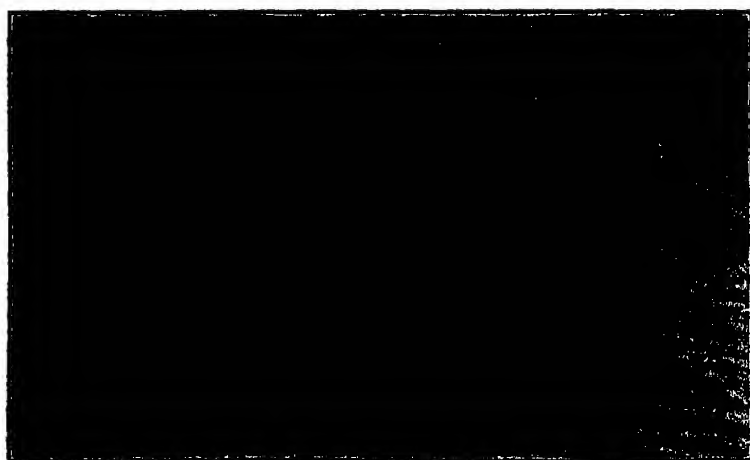
1



2.



3



4.

We have here, therefore, a definite inconsistency, which becomes more serious as the wind velocity is reduced.

A satisfactory explanation is not yet available. It might be suggested that variation of turbulence with depth would provide a possible explanation, but numerical comparison does not support this suggestion. If, for instance, ν is equal to 400 cm.²/sec, the current is reduced to e^{-1} of its surface value at a depth of 25 metres; the motion due to a wave of length 200 metres is reduced in a similar ratio at a depth of 32 metres. Thus there is no reason to expect waves and currents to be very differently affected by any variation of turbulence with depth.

Summary.

Kelvin's theory of the formation of water waves by wind, which supposed the motion in both air and water to be irrotational, has been found to lead to several quantitative predictions that disagree with observation. An alternative theory is developed in the present paper. According to this theory, the wind presses more strongly on the slopes of the waves facing it than on the sheltered slopes, and it is when the resulting tendency of the waves to grow is just able to overcome viscosity that waves are first formed. A numerical constant in the theory can be adjusted to make the wind velocity required to produce waves agree with observation, and when this is done the predicted wave-length of the waves first formed agrees with observation without further assumption. Several other facts of wave-formation are readily explained by the theory.

An attempt has been made to account for the skin friction of the wind over the seas as the resultant drag due to the horizontal thrust of the wind on the exposed sides of the waves. Agreement with the ordinarily accepted value of the skin friction can be attained if the wave velocity is about three-quarters of the wind velocity, which is in accordance with observation. The formation of waves with such a velocity, however, appears to require values of the eddy-viscosity much smaller than are indicated by observations of ocean currents, thus there is an outstanding discrepancy.

DESCRIPTION OF PLATES 4 AND 5.

PLATE 4.

FIG. 1.—Combination of two wind-formed swells in Newnham Millpond, Cambridge, June 15, 1924. Notice the remarkable straightness of the crests of the longer swell, in spite of the fact that the photograph covers in the middle distance approximately $\frac{1}{2}$ the diameter of the pond. (See p. 200.)

FIG. 2.—Short-crested waves in North Atlantic, July 31, 1924 (see p. 200). Swell is almost imperceptible.

PLATE 5

FIG. 3—Long-crested waves emerging from the front of a catspaw (Jesus Lock, Cambridge, June 29, 1924.) (See p 201.)

FIG. 4.—Effect of an increase in the wind velocity on a swell already established. The crests have become sharp and are curling over; the formation of new three-dimensional disturbances is shown by the running together of the crests. (Newnham Millpond, June 15, 1924) (See p 201)

The Thermal and Electrical Conductivities of some Pure Metals.

By F H SCHOFIELD, B A , B Sc.

(Communicated by Sir Joseph Petavel, F R S —Received October 22, 1924)

(Physics Department, the National Physical Laboratory)

I—INTRODUCTION.

The relation between the thermal and electrical conductivities of metals has for a long time engaged the attention of physicists. As far back as 1853 Wiedemann and Franz* propounded the law to the effect that the ratio of the two conductivities was the same for all metals. In 1872 Lorenz†, both on theoretical and experimental grounds, sought to establish that the above-mentioned ratio was proportional to the absolute temperature. On the development of the electron theory Drude, H A Lorentz, J J Thomson and others‡ have, on the basis of various assumptions, arrived at the same conclusion as Lorenz. Up to 1900, however, the experimental values were too uncertain to allow any definite confirmation of the theory. In that year Jaeger and Drieselhorst§ published the result of their investigation, which gave directly the ratio of the conductivities for a number of metals and alloys over the range 18° to 100° C. Lees|| has since, by an independent method, confirmed the values of Jaeger and Drieselhorst for a number of metals at 18° C. and has carried the investigation

* 'Ann. der Phys.,' vol. 89, p 497 (1853).

† 'Ann der Phys.,' vol 147, p. 429 (1872)

‡ For a critical review of the most recent theories, see Meissner, 'Jahrbuch der Radioaktivität und Elektronik,' vol. 17, p. 260 (1920).

§ 'Abh der Phys.-Tech Reichsanstalt,' vol. 3, p. 262 (1900).

|| 'Phil. Trans.,' A, vol. 208, p. 381 (1906).

down to -170°C Meissner* has experimented with some pure metals down to -250°C and Onnes and Holst† even lower

The result of these investigations has been to show that between -100°C and $+100^{\circ}\text{C}$ the value of the function $K/\lambda T$ (K and λ being the thermal and electrical conductivities and T the absolute temperature), is sensibly the same for the pure metals, with perhaps a slight tendency to fall with decreasing temperature. Below -100°C , however, the function shows an increasingly rapid fall with temperature and a considerable divergence between individual metals. Above a temperature of $+100^{\circ}\text{C}$ very few determinations of thermal conductivity have been made, and the object of the present series of experiments has been to measure, in this region, the thermal and electrical conductivities of a number of metals of the highest purity obtainable commercially

The materials used have been obtained through the kindly offices of Dr. Hutton, the Director of the British Non-Ferrous Metals Research Association, and were presented by the firms whose names appear below. In setting out the results (see Appendices I to V) it has been thought well to give, in addition to the chemical analysis of the metal, particulars as to the method of preparation and heat treatment. Dr. Rosenhain, Superintendent of the Metallurgy Department of the National Physical Laboratory, kindly undertook to advise as to the suitability of the specimens, and arranged for an examination of the aluminum specimen, of which details are included in Appendix I

II—THERMAL CONDUCTIVITY

(a) *Theory of Experiment and Reference to Previous Work*

The methods which have been adopted for measuring the thermal conductivity of metals can be classified under two main heads which, for convenience, may be termed "electrical" and "thermal" respectively. Under the former a rod of metal is heated by the passage of an electric current and measurements are made of the thermal and electrical potentials along its length. By this means the ratio of the thermal to the electrical conductivity is obtained. The determination of the latter by a separate experiment then enables the thermal conductivity to be deduced. With various modifications this method has been exploited by Jaeger and Diesselhorst,‡ Callendar,§ Meissner† and others. The method probably presents considerable experimental difficulties at high

* 'Deutsch Phys Gesell Verh,' vol 16, p 262 (1914).

† 'Proc. Acad. Amsterdam,' p 760 (1914)

‡ *Loc cit*

§ 'Encycl Britannica,' 11th ed., art "Conduction of Heat."

temperatures, and above 200° C. appears to have been tried only by Angell,* who in an ingenious way dealt with the radial, instead of the longitudinal, gradient of temperature in a bar of metal heated by an electric current.

The purely "thermal" methods of measuring conductivity are simple in theory, and generally resolve themselves into a determination of the rate of heat flow through a bar of metal, in which a longitudinal gradient of temperature is maintained

A method of this description was first used by Forbes in his well-known experiments. Forbes allowed the surface of his bar to be exposed to the atmosphere and determined the heat flow past any point on the bar by the amount given up by radiation and convection from the cooler parts. This procedure gives rise to considerable uncertainty, not only on account of the difficulty of accurate measurement of heat flow in the manner indicated, but also because it involves the necessity of estimating the temperature gradient at a particular point. With modern appliances more convenient and accurate methods of measuring the heat flow are available and, if it is possible to insulate the bar thermally so as to prevent lateral heat loss, the temperature gradient may be measured over a finite distance instead of at a point. Under the conditions indicated the rate of heat flow Q is given by the equation

$$Q = \frac{KA(\theta_1 - \theta_2)}{d}$$

where A is the cross-sectional area of the bar, θ_1 and θ_2 are the temperatures at a distance d apart, and K is the mean conductivity of the metal between the temperatures θ_1 and θ_2 , and which is assumed over this range to be a linear function of the temperature.

This is the principle of the method adopted in the present series of experiments. Before describing the details of the apparatus, it is well to refer briefly to those used by some previous workers who have adopted similar methods, particularly for experiments above atmospheric temperature. For example, Callendar and Nicholson,† when measuring the thermal conductivity of steel, used bars of considerable cross-section (about 4 inches in diameter) and lagged them with a material of low conductivity. In this way the lateral escape of heat was so reduced as to amount to only a small fraction of that conducted by the metal. The bar under test was heated at one end by steam and cooled at the

* 'Phy. Rev.', vol. 33, p. 421 (1911)

† *Loc. cit.*

other end by a flow of water. Ezer Griffiths* also used a lagged bar with electric heating at one end and water cooling at the other, and obtained the conductivity of a number of aluminium alloys up to a mean temperature of 250° C. Wilkes† eliminated lateral heat loss by an application of the guard-ring principle. He surrounded his bar with a coaxial pipe of metal, the annular space between the two being filled with a finely powdered insulating medium to prevent convection currents. At the hot end of the apparatus the bar and pipe fitted into a common end-piece of copper maintained electrically at a constant temperature. At the other end the bar and pipe were cooled independently by water circulations and the cooling was so adjusted that the same longitudinal temperature distribution was induced in the bar and pipe, thus eliminating lateral loss from the former. In the three cases mentioned above, the rate of heat flow (Q) in the test bar was determined by means of a flow calorimeter at the cold end. This method of measuring the heat flow is very accurate and convenient, but it limits the temperature to which the conductivity can be determined, since the value is given for a temperature intermediate between those of the hot and cold ends of the bar, generally the mean of these temperatures. If, however, the heat flow is determined from the energy input at the hot end, the cooler end of the bar may be kept at a higher temperature and the value of the conductivity can be obtained at a correspondingly higher mean temperature. Honda and Shimidzu‡ worked in this way in determining the conductivity of nickel and various specimens of steel to over 800° C. In their apparatus the test bar was divided into two portions centrally to allow the insertion of a small heating coil, in a very similar way to that subsequently adopted by the author (see fig 1, p 210). This specimen bar was inserted into a pipe and packed with kaolin powder, and the whole apparatus was placed inside a furnace maintained at a steady temperature. In conducting an experiment, energy was switched on in the central heating coil and was dissipated at a certain rate for about 20 minutes, at the end of which time the steady rate of heat flow was established in the bar. The temperature difference at two points at a known distance apart was then measured by differential thermocouples. Under these conditions a small amount of the energy dissipated in the central heating coil (estimated at 6 per cent) was conducted into the kaolin surrounding the bar. This amount could not be directly measured, but, on the assumption that the

* Advisory Committee for Aeronautics, Light Alloys Sub-Committee, Report No. 7 (Nov., 1917).

† 'Chem. and Met. Engineering,' vol 21, p 241 (1919)

‡ 'Sci. Reports, Tohoku Univ.,' vol 6, p 219 (1917). The author did not have access to this paper until after the conclusion of the experiments described below

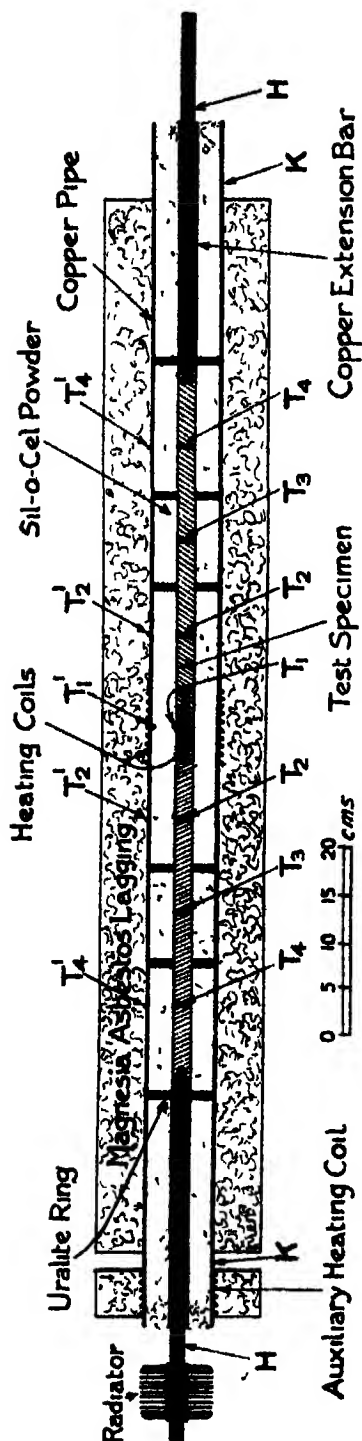


FIG 1

same fraction of heat generated was always lost by diffusion into the kaolin, relative values were obtained from room temperature up to 900°C . While this assumption may not be strictly valid over very wide ranges of temperature, for moderate ranges, at any rate, the method seems to be admirably adapted to the measurement of changes of conductivity with temperature

(b) Details of Apparatus

In the present series of experiments the attempt has been made to determine the thermal conductivity in absolute measure by adopting the guard-ring principle. For this purpose a source of heat was applied at the centre of the test bar and a sink at each end in such a way that a steady flow of heat was maintained. The guard ring consisted of a coaxial pipe of metal which surrounded the bar and which, like the bar, was heated centrally and cooled at the ends in such a way as to reproduce as closely as possible the same temperature distribution as that obtaining in the bar.

The details of the apparatus are shown in the accompanying diagrams. Fig 1 represents a section of the apparatus. The test specimen is seen to be divided into two portions (shown shaded in different directions in fig 1) which fit into each other with an overlapping joint. Each of these portions is drilled axially to a certain

depth, so that when they are brought together an enclosed space is formed, about 7.5 cms in length, for the reception of a heating unit. For purpose of clearness, the latter is not shown in fig 1, but it appears in the enlarged drawing of fig 2, and a full description of it is given below. To the ends of the test specimen are screwed copper extension pieces, and the composite bar thus formed is supported by several uralite rings inside a pipe of metal which, in order to facilitate assembly of the apparatus, is cut into halves longitudinally. The temperatures at a series of points along the bar and pipe are measured by means of thermocouples fixed at the positions marked T_1 , etc. in fig 1. These couples are of wires of platinum and 10 per cent iridium-platinum, 0.2 mm in diameter. In the case of the bar, all the couples, except the central one, were insulated with capillary tubes of pyrex glass or silica inserted into holes drilled through the bar. The precise arrangement is shown in fig 2. In order

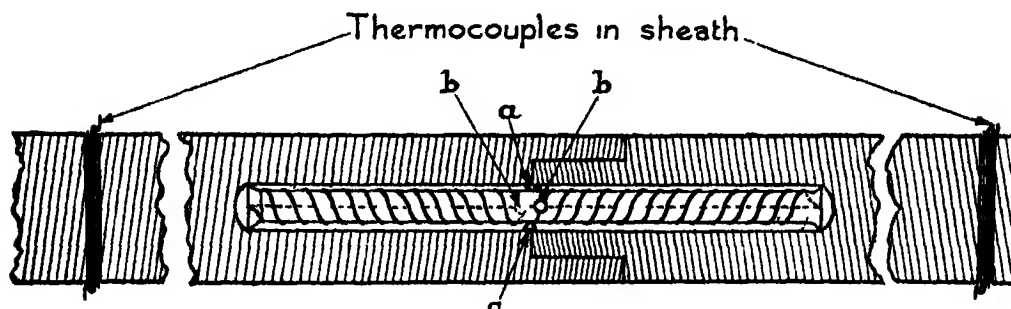


FIG 2

to fix the couple in position in the rod the capillary tubes were slightly tapered to ensure a tight fit and the wires were bent over the edges of the tubes in the manner shown. The central couple was fixed in a groove, cut in the rod, by means of a binding of platinum wire. In the case of the pipe the couples were attached directly to the metal by means of small pegs.

The central portion of the pipe was heated by means of a coil of platinum wire wound on a wrapping of mica. The length of pipe covered by the winding was equal to that of the cavity in the centre of the test bar, and in assembling the apparatus care was taken to secure that the ends of the two were in alignment. In order to reduce the heat loss from the pipe the whole apparatus was encased in magnesia-asbestos lagging.

The sinks of heat at the ends of the bar and pipe consisted of the exposed ends HH and KK, to which a number of devices for regulating the heat loss could be applied. Thus in fig 1 one end of the bar is shown fitted with a movable

sleeve to which radiating fins are attached, in order to increase the heat loss. When a still greater loss was required the ends could be wound with composition pipe, through which water was circulated. If, on the other hand, it was required to reduce the heat loss, the exposed ends could be covered with insulating material, such as asbestos string, or a still greater effect in this direction could be obtained by means of sleeves on which heating coils were wound. An auxiliary heating coil of this kind is shown in fig 1 on one end of the pipe.

As has already been indicated, the lateral interchange of heat between the bar and pipe was practically eliminated by maintaining the same temperature distribution in the two, but, in order that this device should be effective, it was necessary to secure that no interference should arise from the heating elements themselves. The respective heating coils were accordingly situated *inside* the rod and *outside* the pipe. The latter has already been described and presented no difficulty, but some experiment was necessary before a satisfactory design was evolved for a heating coil to be embedded in the rod. To secure ease of assembly it was desirable that leads should emerge close together near the centre of the heater, while to obtain the requisite efficiency it was important that there should be no obstruction between the incandescent wire of the heater and the interior surface of the bar.

The design adopted is shown in figs 2 and 3, which represent respectively

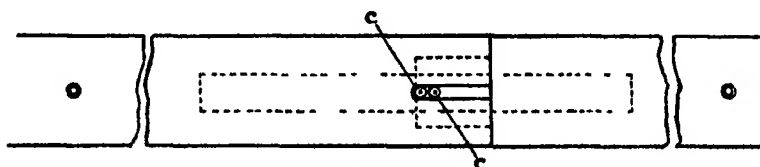


FIG 3

a section of the bar and a plan viewed from a position at right-angles to the section. The heater consists of platinum wire, 0.3 mm in diameter, wound upon a silica tube 5 mm in diameter. As is shown in fig 2, the ends of the silica tube are splayed out to prevent contact of the winding with the interior surface of the bar, and 4 knobs of silica, *aa* and *bb*, are fused to the tube near the centre. The winding is effected by belaying one end of the wire round the base of the knob *a* and winding spirally from there to the end of the silica tube. The wire then passes through a nick in the splayed end to the interior of the tube and, emerging in a similar way from the other end of the tube, is again wound spirally toward the centre and belayed round the other knob *a*. In order to prevent

overheating of the portion of the circuit inside the silica tube this section consisted of two strands of wire in parallel. The function of the knobs *b* is to prevent the short-circuiting of the complete heating coil owing to a slipping of the windings in the neighbourhood of either of the knobs *a*. Incidentally, the knobs *aa* and *bb* serve to limit any possible sagging of the silica tube at very high temperatures. It will be noticed from fig. 2 that the internal surfaces of the two portions of the bar, which are exposed to radiation from the heater, are equal.

The assembly was effected by passing the loose ends of the heating coil through the holes *cc* (see fig. 3) in the right-hand portion of the bar and drawing the heating unit in position. The left-hand portion of the bar, which was provided with a slot for clearing the holes *cc*, was then slid into position. The ends of the heating coil were insulated in the holes *cc* by means of silica tubes, and current and potential leads of platinum were attached to them where they emerged from the tubes.

In the earlier experiments asbestos wool was used for packing the space between the rod and pipe, but the material finally adopted was "Sil-o-cel," which is a finely powdered diatomaceous earth. This material has the advantage of an extremely low thermal conductivity, while its fine state of division serves to prevent convection currents and reduce the oxidation of the specimen bar.

(c) Method of Experiment

In carrying out an experiment, adjustments were made of the energy supplied to the heating coils at the centres of the rod and pipe and of the energy absorbed at the ends until the desired gradients were obtained. In all cases the gradients in the tube were made to correspond as closely as possible with those of the rod. Typical distributions of temperature for the specimens of nickel and aluminum are shown in fig. 4 (p. 214). It will be noticed that in each case the gradients in the rod and pipe are approximately straight lines.

A strict linearity of gradient would, of course, be obtained only where the metals composing the rod and pipe had conductivities not varying with temperature; where the lateral heat loss from both rod and pipe were negligible; and where the supply of heat was from sources of zero thickness in a plane at right-angles to the axis. None of these conditions was precisely fulfilled but, as will be seen from fig. 4, the nett effect in producing curvature was negligible. It should, however, be pointed out that the amount of the lateral loss through the lagging from the pipe increased with increasing temperature. The resulting sag which this would tend to produce in the temperature distribution curve

of the pipe was counteracted by using a greater thickness of lagging and by increasing the quantity of heat flowing through the metal itself. Consequently,

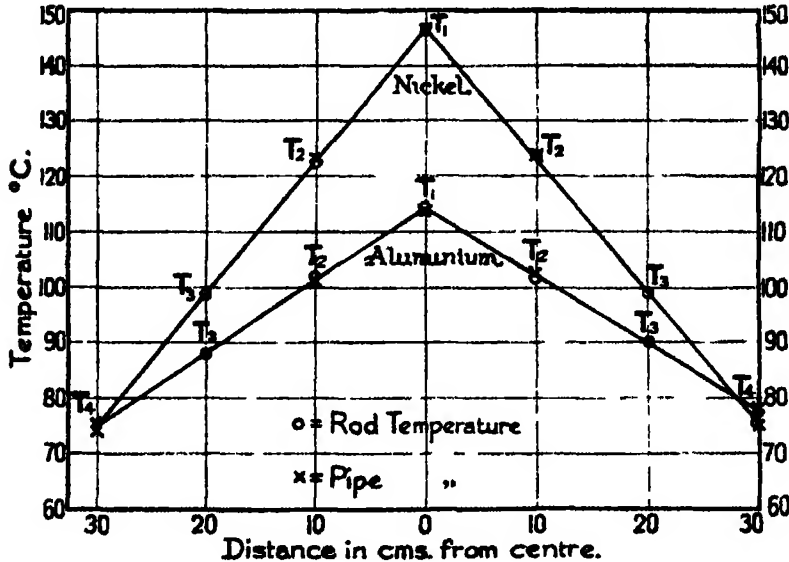


FIG 4

throughout the experiments steeper gradients were employed at the higher temperatures

As evidence that no systematic error arose from the employment of differing temperature gradients, it may be mentioned that the conductivity measurements for the same mean temperature, but with different temperature gradients, gave results agreeing within the limits of experimental error (See for example the results in Appendix I for a mean temperature of about 150° C obtained with temperature differences of 28° C, 35° C. and 50° C respectively)

(d) Magnitude of Lateral Heat Loss

Since the theory of the method presupposes the elimination of lateral heat loss from the specimen, it is important to ascertain the magnitude of any error due to failure to obtain a coincidence of temperatures over the working area of the rod and pipe. Consequently, the following series of experiments were made with the specimen of aluminum. The several temperatures of the rod and pipe were first adjusted to correspond as closely as possible, so as to obtain a value of the true conductivity of the metal. The temperatures along the pipe were then adjusted to differ by a certain amount, either above or below, from the corresponding temperatures of the rod, and when steady conditions had been

obtained the apparent conductivity was calculated. The temperature gradient between the points T_2 , T_4 (fig 1) was about 40°C . throughout, and the temperature of T_3 approximately 160°C . The results obtained are shown in fig 5,

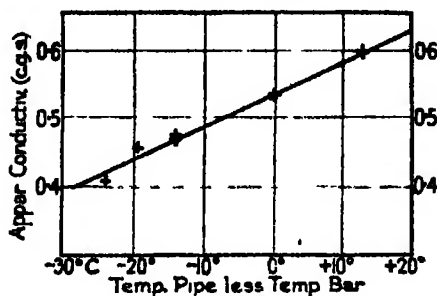


FIG. 5

and it will be observed that the error due to a mean difference of 1°C between the rod and pipe was about 1 per cent. It was estimated that the mean temperature difference between corresponding points on rod and pipe could be adjusted to between 1°C and 2°C , so that this fixes a definite limit to the accuracy of the method. This limit may be stated to be from 1 to 2 per cent. for the aluminium bar working with a temperature gradient of 40°C . Working with higher or lower temperature gradients or with metals of higher or lower conductivity the accuracy would be correspondingly greater or less.

As a check on the above conclusion, it is possible to make an approximate estimate of the lateral heat loss from the known conductivity of insulating material. No attempt can be made here to give a mathematical solution of the problem under consideration, namely, the flow of heat between coaxial cylinders with a constant difference of temperature between the corresponding points in planes at right-angles to the axis and with a longitudinal gradient in each cylinder, but as an approximation it is proposed to take the case of a constant difference in temperature, but no gradient. The formula for the lateral flow of heat per 1°C difference would then be

$$H = \frac{2 \cdot 73 K l}{\log_{10} (b/a)} \text{ cal./sec}$$

Here a and b , the diameters of the rod and pipe respectively, are 1.9 and 7.0 cms., l is taken as 30 cms., e , the complete length between T_1 and T_4 , and K , the thermal conductivity of the insulating medium at a mean temperature of 160°C , is about 0.00015 cgs units for "Sil-o-cel". Hence we get

$$H = 0.022 \text{ cal./sec.}$$

Now the flow of heat through the aluminium rod for a temperature difference of 40°C between T_2 and T_4 at a distance (d) apart of 20 cms is given by

$$H = \frac{\pi a^2 K (\theta_1 - \theta_2)}{4d} = 2.95 \text{ cal/sec}$$

So that the lateral heat loss per 1°C in the case taken is estimated as 0.7 per cent of the heat flowing in the rod, a result which is of the same order as that obtained by experiment

It may be added that the error due to lateral heat loss varies inversely as the square of the diameter of the specimen rod, provided that the ratio of the diameters of the rod and pipe is constant, so that it would be advantageous to use specimens of large diameter. The limit of the dimensions of the present apparatus was decided largely on considerations of convenience and expense

(e) *Magnitude of Longitudinal Heat Loss*

The isothermal surfaces in the lagging being adjusted so as to be approximately perpendicular to the axis, it follows that there will be a longitudinal flow of heat in the lagging, which will be contributed mainly by the pipe, but to some extent from the rod. The poorest conductor of all the metals tested, namely, nickel, having a conductivity of the order of 1,000 times that of the insulating material, it was considered safe to neglect the contribution from the rod to the longitudinal heat loss

III—ELECTRICAL CONDUCTIVITY

The measurement of the electrical conductivity of the several metals has been undertaken merely to throw light on its relation to the thermal conductivity. For this purpose an accuracy of 1 per cent. suffices, so that an elaborate investigation has not been called for. The method used consisted in a comparison of the voltage drop on a measured length of the specimen and on a standard resistance arranged in series with it, a constant current being maintained through the two.

Since this method has been adopted by a number of experimenters, a detailed description is not required here, but the following particulars should perhaps be mentioned :—

The current was led into and out of the specimen rod by copper rods 4 mm. in diameter screwed into the test rod. The voltage drop was measured by means of thin potential wires pegged into the specimen at a distance of 22 cms. apart. The specimen was fixed centrally in a tubular furnace 1.8 metres long wound with nichrome ribbon, and its temperature was measured by 3 thermocouples. The space between the specimen and the furnace tube was packed with "Sil-o-cel"

powder The current, which was supplied from a large storage battery, was of the order of 10 amps In order to eliminate any thermal E M.F.s at the potential points, measurements were made before and after reversing the main current, while the effects of thermal E M.F.s in the potentiometer circuit were eliminated by taking readings before and after a simultaneous reversal of the potential leads and the leads supplying the current to the instrument The magnitude of the difference due to these two sets of reversals seldom exceeded 2 microvolts, and it was estimated that the volt drop was obtained to better than 1 microvolt, a precision amply sufficient to meet the requirements

No special difficulty occurred in applying this method, except in the case of magnesium, where at temperatures over 300°C voltaic effects were likely to occur, which were eliminated by the use of potential leads of the same metal as the specimen

IV—DISCUSSION OF RESULTS

The detailed results of the measurements of thermal and electrical conductivity are set out in Appendices I to V The values obtained are also shown in figs 6 and 7 and, since the majority of the metals were also investigated by Lees and by Jaeger and Diesselhorst, their values over the respective ranges of -100°C to 18°C and 18°C to 100°C have been included for purposes of comparison. Some individual values given by other observers have been shown on the graphs or are referred to in the text below For the purpose of dealing with the relation of thermal to electrical conductivity, the values of Lorenz's function have been set out in Table I (p. 218)

In this table the names of the observers have been indicated by initials. Their methods of experiment have differed considerably Thus, as already stated, an "electrical" method was used by Jaeger and Diesselhorst, by Maissner and, in a considerably modified form, by Angell The other observers worked with "thermal" methods Lees, who introduced many refinements, obtained his values in absolute units, Konno was primarily interested in changes of conductivity on melting, and used a relative method, taking Lees' values at 18°C for his starting points, the method of Honda and Shimidu has already been outlined. Detailed comments on the results are appended under the heads of the several metals

Table I —Relation of Thermal and Electrical Conductivity

Metal	Purity	Ob-server	Value of Lorenz's function $K/\lambda T \times 10^6$ (K in watts/cm. ² /°C., λ in reciprocal ohms/cm.) at Temperatures of								
			-100° C.	18° C.	100° C.	200° C.	300° C.	400° C.	500° C.	600° C.	700° C.
Aluminium	99	L	1 81	2 13							
		J & D		2 19	2 27						
	99	A			2 25	2 68	3 18	3 79	4 48	5 08	
	99 7	K* S		2 30	2 25 2 23	2 29 2 36	2 26 2 44	2 23 2 53	2 14	2 03	
Copper		L	2 17	2 32							
		J & D		2 29	2 32						
		M(1)		2 25	2 33						
	99 9	M(2) S		2 26 2 31	2 34 2 31	2 36	2 34	2 37	2 34	2 35	
Magnesium	99 6	S			2 31	2 32	2 30	2 33			
Nickel	99	L	2 59	2 59							
	97	J & D		2 40	2 44						
	97	A					3 10	2 67	2 24	1 81	1 42
	97	H & S			2 37	2 53	2 71	2 68	2 71	2 75	2 75
	99 2	S			2 28	2 39	2 65	2 79	2 62	2 64	2 68
Zinc		L	2 39	2 43							
		J & D		2 31	2 33						
		K*	2 45	2 47	2 47	2 41	2 36				
	99 8	S		2 26	2 26	2 29					

* Konno's values of thermal conductivity are relative to those of Lees at 18° C., and for electrical conductivity he has taken those of Tsutsumi ('Sci. Rep.', vol 7, p 93 (1918))

Aluminium

Like Lees, and Jaeger and Diesselhorst, in their respective ranges, the author finds that the conductivity of aluminium shows a slight increase with temperature. It will be noticed from fig 6 that, at the points of overlap, the values of Jaeger and Diesselhorst are considerably lower than the other two, probably owing to impurity in their specimen. As would be expected, the electrical resistivity found by Jaeger and Diesselhorst is correspondingly higher (see fig. 7). Three other sets of values above 100° C. are available, namely, those of Ezer Griffiths, Angell and Konno. The first mentioned used material of nearly the same purity as that tested by the author, viz, 99.5 per cent., as against 99.7 per cent., and he gave values for his four specimens ranging from 0.50 to 0.52 at 100° C., and found a slight tendency to increasing conductivity with temperature up to the limit reached (250° C.). This is in very fair agreement with the results of the present experiments. On the other hand, Angell gives the value

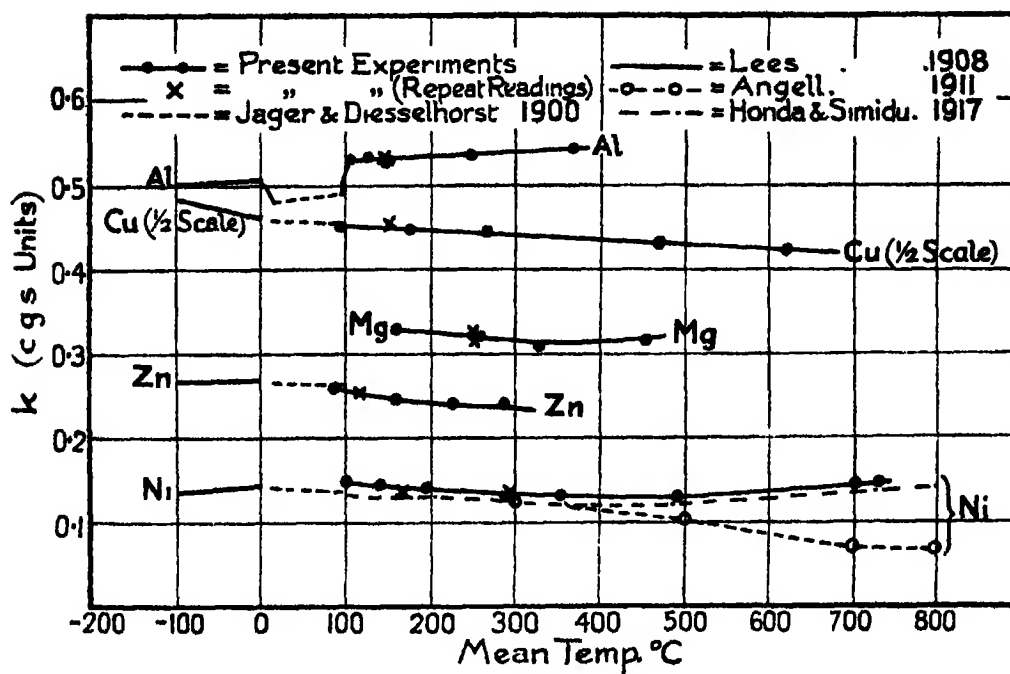


FIG. 6

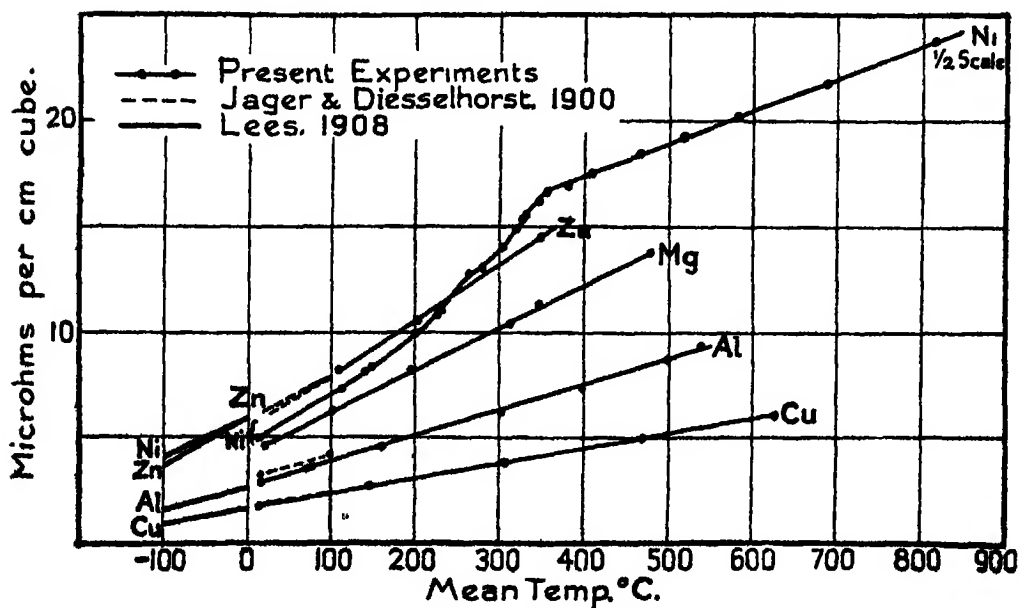


FIG. 7.

as increasing from 0.49 at 100° C to 1.0 at 600° C and Konno as decreasing from 0.50 to 0.36 over the same range

As to Lorenz's function, it will be seen that the values of the several observers are in good agreement at 100° C. Konno gives a nearly constant value throughout, and the others give values rising somewhat with temperature, those of Angell showing the greatest change.

Copper

The author's values for the thermal and electrical conductivity show a satisfactory continuity with those of Lees and of Jaeger and Diesselhorst. The copper used in all three cases seems to have been nearly 100 per cent in electrical conductivity, according to the international specification.

Further values for copper were obtained by Meissner with two specimens of the metal. One of these (No. 1) was better than, and the other (No. 2) equal to, the 100 per cent standard in conductivity. The respective values obtained are as follows —

Table II — Thermal Conductivity of Copper.

Observer	K_{100}	K_{100}
Meissner (1)	0.94	0.94
" (2)	0.92	0.92
Lees	0.91 ₅	—
Jaeger and Diesselhorst	0.91 ₅	0.90 ₅
Present paper	—	0.90 ₁

Meissner's* figure of 0.94 appears to be the highest reliable value yet obtained for copper. Schott† gives 0.98 for a natural crystal of copper, but this value is probably too high, as his figure for pure commercial copper is as large as 0.94.

With regard to Lorenz's function, it will be seen from the table that there is a good agreement at 100° C and that the author finds a nearly constant value throughout.

Magnesium.

The only previous value traced is that of Lorenz, who gives 0.37₅ for the thermal conductivity at 100° C. According to the present experiments, the value for the same temperature would be about 0.33₅.

The values for electrical conductivity are in fair agreement with those of

* 'Ann. der Phys.' (4), vol. 47, p. 1001 (1915).

† 'Verh. der Phys. Ges.', vol. 18, p. 27 (1916).

Nicolai,* the latter being on the average about 3 per cent higher. For Lorenz's function a nearly constant value is obtained, which does not differ greatly from those found for copper and zinc.

Nickel.

As will be seen from Table I, the purity of the specimens used by the several observers varied considerably. In correspondence with the purity, the values given by the present experiments at 100° C for the thermal and electrical conductivities are somewhat higher than either those of Jaeger and Diesselhorst, or Honda and Shimidu. The curve for electrical conductivity shows a pronounced change in curvature at the change point at about 350° C. The form of the curve agrees closely with those found by Nicolai, Somerville,† Pecheux,‡ and by Honda and Shimidu, while the absolute values are in close agreement with that of Pecheux, whose specimen was of 99.6 per cent purity, as compared with 99.2 for the specimen used in the present experiments. The author's values for the thermal conductivity show a decrease with temperature between 100° C and 300° C, thereafter an approximately constant value to 500° C, while the two values obtained in the neighbourhood of 700° C. show a considerable rise. The results of Honda and Shimidu give a generally similar curve, but their method permitted the taking of a large number of values with temperature differences as small as 30° C, so that they were able to trace a definite minimum of conductivity at about 400° C. With the present dimensions of the apparatus described in this paper and a metal of as low conducting power as nickel it is necessary to use gradients as high as 100° C to obtain an accuracy of 2 or 3 per cent. Consequently, the point of inflexion in the conductivity curve could not be accurately located. This fact probably accounts for the apparently high value obtained for Lorenz's function at a temperature of 400° C. It will be observed for Table I that the value tends to become constant at about 2.6 from a temperature of 300° C. upwards. A similar phenomenon was observed by Honda and Shimidu, while Angell found a steady fall in the value with rising temperature.

Zinc.

The values obtained for the thermal and electrical conductivity are slightly lower than those of Jaeger and Diesselhorst at 100° C. Like Konno, the author finds a nearly constant value for Lorenz's function.

* 'Phys. Zeits.,' vol. 9, p. 367 (1908)

† 'Phys. Rev.,' vol. 33, p. 77 (1911)

‡ 'La Lumière Électrique,' vol. 10, p. 232.

V. SUMMARY.

The thermal and electrical conductivity of a number of pure metals has been measured for mean temperatures ranging to a maximum of 700°C . The thermal conductivity of aluminium was found to increase with rising temperature, that of nickel to decrease at first and then above 500°C to show an increase. The other metals—namely, copper, magnesium, zinc—showed on the whole slight decreases of conductivity with temperature.

The values of Lorenz's function for copper, magnesium and zinc were practically constant at all temperatures, that for aluminium showed a rise with increasing temperature, that for nickel showed a rise to 300°C , above which temperature it remained nearly constant, except for an abnormal value at 400°C .

In conclusion, the author desires to make his acknowledgments, in addition to those already recorded, to the Director of the National Physical Laboratory and to Dr Kaye, the Superintendent of the Physics Department, for the ample facilities placed at his disposal. Further, he is especially indebted to Mr Challoner, observer in the Physics Department, not only for his skill in constructing the apparatus and suggesting improvements, but also for taking the majority of the observations.

APPENDIX I.

Aluminium

Particulars of Specimen (British Aluminium Co., Ltd) —The specimen was prepared as follows —Billets $6\frac{1}{2}$ inch in diameter were cast from a maximum temperature of 700°C ., annealed for $2\frac{1}{2}$ hours at 500°C , extruded at temperature of 420°C . to $\frac{3}{4}$ inch diameter, and finally annealed for $2\frac{1}{2}$ hours at 450°C .

In order to test the soundness of the material, transverse and longitudinal sections were taken from the ends of the specimen and were examined in the Metallurgy Department of the National Physical Laboratory. These were reported to be free from the more serious defects of extruded materials, viz., unsoundness, discontinuities between the core and surrounding layers, inclusion of dross and oxidised skin.

Density at 21°C . = 2.70. Purity 99.7 Al.

Thermal Conductivity.

Mean Temperature at T_1	Temperature Difference $T_2 - T_4$	Energy supplied to Bar			Conductivity c g s units	Mean Conductivity c g s units
		Amps	Volts	Cals/sec		
° C	° C					
108.7	35.7	1.360	16.60	5.38	0.528	0.528
128.6	51.7	1.135	28.95	7.84	0.532	0.532
154.0	50.0	2.585	12.20	7.53	0.528	0.528
149.4	28.1	2.030	8.70	4.22	0.526	} 0.526
149.9	28.1	2.025	8.70	4.21	0.525	
149.1	28.0	2.025	8.70	4.21	0.527	
254.0	46.9	2.395	12.50	7.15	0.536	} 0.536
253.8	46.9	2.395	12.50	7.15	0.536	
374.8	80.0	2.845	18.20	12.35	0.544	} 0.542
373.3	80.5	2.840	18.20	12.35	0.540	
371.6	80.3	2.830	18.20	12.30	0.537	
368.8	78.3	2.820	18.20	12.25	0.547	
146.4	34.8	2.180	10.20	5.24	0.527	} 0.528*
149.4	35.4	2.160	10.30	5.32	0.528	
149.7	35.5	2.160	10.40	5.36	0.530	

* Repeat reading

Electrical Resistivity.

Temperature	Resistivity	Temperature	Resistivity
° C	Ohms per cm. cube	° C	Ohms per cm. cube.
16.2	2.83×10^{-8}	302.7	6.15×10^{-8}
16.8	2.79	304.4	6.23
16.8	2.81	306.2	6.24
73.0	3.45	399.0	7.39
77.0	3.53	500.0	8.77
79.0	3.53	502.4	8.79
160.0	4.47	540.7	9.31
161.0	4.48		

APPENDIX II.

Copper.

Particulars of specimen (T Bolton & Sons, Ltd, Oakmoor)

The specimen was prepared as follows.—Billets were cast from a mixture of $\frac{1}{2}$ cathodes and $\frac{1}{2}$ electrolytic wire bars immediately after poling. They were rolled hot to 1 inch diameter, drawn cold to $\frac{7}{8}$ inch diameter, machined and polished to $\frac{3}{4}$ inch diameter, and then annealed

Density at 21° C = 8.92 Purity 99.9 Cu.

Thermal Conductivity.

Mean temperature T_s	Temperature Difference $T_s - T_i$	Energy supplied to Bar			Conductivity c.g.s. units	Mean Conductivity c.g.s. units
		Amps	Volts	Cals/sec		
°C	°C					
93.8	19.1	2.475	8.30	4.91	0.900	0.901
96.2	20.0	2.490	8.50	5.06	0.890	
95.6	19.9	2.505	8.60	5.14	0.908	
96.0	19.4	2.515	8.30	4.98	0.900	
98.4	20.9	2.590	8.75	5.41	0.907	
177.4	43.4	3.215	14.40	11.05	0.893	0.893
177.9	44.4	3.230	14.60	11.25	0.890	
172.4	44.0	3.225	14.60	11.25	0.897	
266.0	73.6	3.755	20.80	18.65	0.888	0.888
265.7	73.6	3.750	20.85	18.65	0.890	
265.7	74.0	3.750	20.85	18.65	0.885	
473.1	93.4	3.585	26.75	22.95	0.862	0.858
473.4	94.5	3.590	26.80	23.00	0.854	
472.0	93.8	3.585	26.85	23.00	0.858	
624.8	142.0	3.720	38.40	34.15	0.842	0.842
624.7	142.1	3.720	38.45	34.20	0.844	
624.7	142.3	3.790	38.45	34.20	0.839	
151.8	30.7	2.060	16.10	7.93	0.905	0.905*

* Repeat reading.

Electrical Resistivity

Temperature °C	Resistivity Ohms per cm. Cube	Temperature °C	Resistivity Ohms per cm. Cube
14.0	1.69×10^{-4}	470.0	4.88×10^{-4}
145.0	2.59	630.5	6.00
144.5	2.61	630.0	6.07
306.0	3.73		

APPENDIX III

Magnesium.

Particulars of specimen (Magnesium Co., Ltd) —The specimens were extruded to $\frac{3}{4}$ inch diameter from a billet 5 inch in diameter, annealed at 360° C for 6 hours, and allowed to cool slowly.

Density at 21° C = 1.75 Purity 99.6 Mg.

Thermal Conductivity.

Mean Temperature T_s	Temperature Difference $T_s - T_1$	Energy supplied to Bar			Conductivity c.g.s. Units	Mean Conductivity c.g.s. Units
		Amps	Volts	Cals/sec		
160.4	42.1	1.940	8.00	3.71	0.328	0.328
167.0	42.2	1.920	8.10	3.71	0.328	
158.0	40.4	1.905	7.90	3.60	0.332	
153.2	39.1	1.890	7.60	3.38	0.322	
264.0	74.7	2.290	11.85	6.48	0.324	0.318
263.0	76.5	2.300	11.85	6.51	0.317	
261.7	77.3	2.290	11.80	6.46	0.313	
258.3	75.5	2.285	11.60	6.39	0.313	
251.3	72.5	2.275	11.50	6.26	0.322	
329.5	102.4	2.495	14.20	8.47	0.308	0.300
322.0	98.6	2.460	14.00	8.23	0.311	
326.4	103.8	2.510	14.30	8.58	0.308	
456.0	104.8	1.510	24.50	8.84	0.314	0.314
456.5	104.6	1.500	24.50	8.76	0.314	
254.2	70.5	1.370	18.70	6.12	0.323	0.323*
253.0	73.0	2.230	11.40	6.08	0.311	0.314*

* Repeat readings with different heating coils.

Electrical Resistivity

Temperature °C	Resistivity Ohms per cm. Cube	Temperature °C.	Resistivity Ohms per cm. Cube
20.0	4.59×10^{-6}	199.5	8.08×10^{-6}
101.4	6.19	314.0	10.35
101.1	6.21	348.6	11.21
101.1	6.18	348.0	11.04
199.2	8.17	480.1	13.74

APPENDIX IV

Nickel

Particulars of specimen (H. Wiggins & Co., Ltd.) —The specimen was prepared as follows —Cast in 3-inch moulds, hot-rolled to $1\frac{1}{2}$ inch diameter, reheated and rolled to $\frac{7}{8}$ inch diameter, close-annealed at 800°C., cold-drawn to $\frac{11}{16}$ inch diameter, again annealed, drawn to $\frac{3}{4}$ inch diameter, and finally annealed between 750°C. and 800°C.

Density at 21°C = 8.79 Purity 99.2 Ni

Thermal Conductivity.

Mean Temperature T_s	Temperature Difference $T_s - T_0$	Energy supplied to Bar			Conductivity c.g.s. Units	Mean Conductivity c.g.s. Units.
		Amps.	Volts	Cals/sec		
99.2	47.5	1.420	5.95	2.02	0.146	0.145
100.8	48.0	1.420	5.95	2.02	0.145	
141.6	59.8	1.490	7.00	2.49	0.143	0.144
141.6	59.9	1.490	7.00	2.49	0.143	
141.8	60.0	1.490	7.00	2.49	0.145	
196.7	75.3	1.535	7.95	2.91	0.132	0.138
196.2	75.5	1.560	8.20	3.05	0.138	
196.4	75.3	1.580	8.15	3.07	0.140	
196.0	74.1	1.545	8.00	2.95	0.136	
290.2	81.6	1.510	8.45	3.05	0.128	0.128
289.7	81.5	1.510	8.45	3.04	0.128	
289.2	80.9	1.510	8.45	3.04	0.129	
288.4	80.8	1.510	8.45	3.04	0.129	
353.6	99.4	1.610	9.70	3.73	0.129	0.128
355.0	100.3	1.610	9.70	3.73	0.128	
357.3	100.3	1.610	9.75	3.75	0.128	
357.2	100.3	1.610	9.75	3.75	0.128	
491.4	105.8	1.595	10.45	3.98	0.129	0.128
491.0	106.9	1.595	10.40	3.96	0.127	
703.3	179.6	1.965	16.35	5.67	0.141	0.141
733.0	177.3	1.975	16.70	7.88	0.147	0.147
166.5	65.1	1.505	7.20	2.59	0.136*	0.136
293.7	84.1	1.575	8.70	3.27	0.133*	0.133

* Repeat reading

Electrical Resistivity

Temperature °C	Resistivity Ohms per cm. Cube	Temperature °C	Resistivity Ohms per cm. Cube
14.0	10.04×10^{-8}	320.5	29.70×10^{-8}
111.0	14.60	327.8	30.75
142.4	16.17	331.6	31.20
148.5	16.57	349.5	32.35
149.2	16.62	358.8	33.50
200.5	19.73	383.8	33.95
227.0	21.57	409.6	35.00
229.5	22.10	465.2	36.85
265.0	25.52	519.4	38.65
266.0	25.10	583.5	40.60
280.0	25.90	691.1	43.60
304.1	28.15	820.7	47.60

APPENDIX V

Zinc

Particulars of Specimen (London Zinc Mills)—The specimen was prepared as follows.—Billets were cast, were rolled at 200° C, sawn into strips and drawn cold

Density at 21° C. = 7.13 Purity 99.8 Zn

Thermal Conductivity.

Mean Temperature at T_2	Temperature Difference $T_2 - T_1$	Energy supplied to Bar			Conductivity c.g.s. Units	Mean Conductivity c.g.s. Units
		Amps	Volts.	Cals/sec		
° C	° C.					
87.5	25.0	1.520	4.90	1.78	0.256	0.258
87.7	25.0	1.520	4.85	1.77	0.256	
87.5	25.8	1.545	5.05	1.86	0.259	
87.5	25.1	1.530	4.95	1.81	0.259	
87.5	26.0	1.540	5.05	1.86	0.256	
87.8	25.0	1.540	5.00	1.84	0.264	0.246
160.5	54.4	1.910	8.10	3.70	0.244	
160.3	53.2	1.900	8.05	3.65	0.246	
160.3	53.4	1.905	8.10	3.68	0.247	
160.2	52.8	1.910	8.00	3.65	0.249	0.241
227.5	80.5	2.155	10.60	5.46	0.243	
227.1	80.0	2.160	10.30	5.32	0.239	
227.1	79.9	2.145	10.60	5.44	0.243	
224.5	79.5	2.150	10.45	5.37	0.242	
223.5	78.3	2.130	10.30	5.25	0.240	0.238
284.1	102.6	2.325	12.40	6.89	0.240	
288.5	102.7	2.320	12.40	6.88	0.239	
290.8	103.9	2.320	12.40	6.88	0.237	
291.6	104.6	2.330	12.40	6.91	0.236	0.253*
117.9	47.8	1.950	7.30	3.40	0.255	
117.7	48.6	1.955	7.30	3.40	0.251	
117.1	49.0	1.920	7.50	3.44	0.252	

* Repeat reading

Electrical Resistivity

Temperature ° C	Resistivity Ohms per cm. Cube.	Temperature ° C	Resistivity Ohms per cm. Cube.
35.0	6.08×10^{-8}	105.0	8.08×10^{-8}
107.0	8.15	200.8	10.47
106.0	8.10	200.0	10.48
105.0	8.09	350.2	14.50

The Colours Due to Thin Films on Metals.

By ULICK R. EVANS

(Communicated by C T Heycock, F R S.—Received July 29, 1924)

In recent papers* it has been shown that the corrosion of metallic objects partly covered with liquid is usually connected with electric currents set up through differences in the oxygen concentration at different parts of the metallic surface. When, for instance, a drop of sodium chloride solution is placed on a metallic surface, a current passes between the surface of the metal at the periphery of the drop and the central portion. The metal in the interior, where the concentration of oxygen is least, constitutes the anode and suffers corrosion. The peripheral zone, to which oxygen has direct access, forms the cathode, and suffers little or no corrosion in the ordinary sense of the word, the immunity, or "passivity," of this outer zone, and the local alteration of the potential, which causes the current to flow between the outer and inner portions, is best ascribed to the formation of an oxide film or oxygen film over the "aerated" part of the surface.

On iron this film is invisible, presumably because it is too thin to affect the optical properties of the surface, on copper, on the other hand, there may be seen upon the portions of the surface nearest to the edge of the drop, a series of bright rings roughly concentric with one another, green, rose and yellow in colour. It seems likely that these colours are actually due to a thin film of cuprous oxide which protects the underlying metal from further attack, and which also, by altering the potential, stimulates corrosion at the central parts to which oxygen does not diffuse readily. Since the anodic product of copper in a chloride solution is cuprous chloride, an efficient absorbent of oxygen, it follows that when once this salt has begun to accumulate at the central portion of the drop, the corrosion due to "differential aeration currents" will be stimulated.

It is naturally desirable to ascertain the order of the thickness of the oxide film which causes the ennoblement of the "aerated" portion. In cases where the refractive index is known, it would be possible to calculate the thickness from the tints produced, if we make the assumption that the colours are due

* U. R. Evans, 'J. Inst. Met.', vol. 30, p. 239 (1923), 'Proc. Camb. Phil. Soc.', vol. 22, p. 54 (1924), 'J. Soc. Chem. Ind.', vol. 43, p. 127T (1924).

to interference Tammann* has already used such a means of measuring the thickness of films in studying the action of iodine upon silver and copper at ordinary temperatures, and that of oxygen upon iron and other metals at slightly elevated temperatures. It is noteworthy that Tammann, using this optical method, found for the attack of iodine upon silver at low temperatures a parabolic relation between the thickness (y) and time (t)

$$y^2 = 2pt$$

where p is a constant The same relation was afterwards established by gravimetric methods by Pilling and Bedworth† for the high-temperature oxidation of copper, and by Vernon‡ for the low-temperature tarnishing of copper in a moist polluted atmosphere There seems little doubt that in the case of the silver iodide films produced by the attack of iodine on silver, the interference colours afford a fairly accurate measure of the thickness Many years ago Wernicke§ used the converse method to determine the refractive index of silver iodide, he obtained the thickness of the film by weighing, and then by observing the wave-length of the light extinguished by a film of known thickness, calculated the refraction index, the numbers obtained agreed fairly well with those obtained by him by the ordinary prism method Clearly when once the refractive index has been established, the colour of the film is a reliable indication of the thickness

But before this method can be applied to the case of oxide films, attention must be paid to the fact that two separate investigators have recently asserted that the tints produced by the superficial oxidation of metals are not due to interference at all Mallock|| has stated that the temper colours which appear upon steel heated in air cannot represent an interference effect, because he has attempted to reduce the thickness of the film present on "blued" steel by polishing, and has failed to obtain the yellow colour which would be characteristic of a thinner film, the blue remained blue, although its intensity decreased as the film was rubbed away Mallock attributes the colours to selective opacity depending on "damped molecular periods." It would seem, however, very unlikely that such a method as polishing could reduce the film with the uniformity required, it would surely be beyond the power of human

* G. Tammann, 'Zeitsch. Anorg. Chem.,' vol. 111, p. 78 (1920), vol. 124, p. 25 (1922); G. Tammann and W. Köster, 'Zeitsch. Anorg. Chem.,' vol. 123, p. 196 (1922)

† N. B. Pilling and R. E. Bedworth, 'J. Inst. Met.,' vol. 29, p. 529 (1923)

‡ W. H. J. Vernon, 'Trans. Faraday Soc.,' vol. 19, p. 839 (1924)

§ W. Wernicke, 'Pogg. Ann.,' vol. 142, p. 560 (1871)

|| A. Mallock, 'Roy. Soc. Proc.,' A, vol. 94, p. 566 (1918).

technique to reduce a film of, say, 200 molecules thickness, uniformly to a film of 100 molecules thickness. What probably occurred was that Mallock completely rubbed away the film at some points, whilst leaving it intact at others; this would explain the gradual diminution of intensity and the constancy of tint. Raman* also thinks that temper colours are not an interference effect, and ascribes them to a granular structure in the film.

Investigation of Mallock's Objections—Whilst Mallock failed to obtain the alteration of temper colours on steel by a process of polishing, it seemed not impossible that some other method might produce sufficiently uniform thinning to cause the desired change of tint. Chemical solvents suggested themselves, but it was necessary to choose a procedure which would give general reduction of thickness, rather than pitting or etching of the familiar kind. After some preliminary experiments, the method of reducing the thickness of the oxide coat on heated iron by cathodic treatment in dilute hydrochloric acid was adopted; apparently, the cathodic treatment reduces the magnetite which constitutes the oxide film to the state of ferrous oxide, which is at once dissolved by the acid.

A strip of iron is cleaned with emery and heated at one end in a Bunsen burner so as to produce a range of temper colours—brown, mauve, indigo, pale blue, steel colour, pink-lavender, and pale steel blue in order (passing from the cold to the hot end). When cold, the strip is connected to the negative pole of a 4-volt accumulator, and is introduced in a vertical position into a N/50 solution of hydrochloric acid, in such a way that only the lower half of the strip enters the liquid. A piece of zinc about 3 cm from the specimen serves as anode and is joined through a resistance to the positive pole of the same battery, the resistance being adjusted to give a current of about 1.7 milliamperes per square centimetre. After about $\frac{1}{4}$ minute, the specimen is taken out, washed, dried and examined. It will be found that the colours in the lower part of the strip which has been immersed in the liquid have shifted relatively to the colours in the unimmersed part of the specimen, in the manner indicated in fig. 1.

This shows that the thinning of the film produced by the treatment does actually cause the change of colour which the interference theory would predict; Mallock's objections, therefore, would not seem to possess the importance which he attaches to them. If the cathodic treatment is continued too long, although a greater lateral shift is produced, the colours grow muddy and are somewhat difficult to identify, the mauve disappears comparatively soon, although the

* C. V. Raman, 'Nature,' vol. 109, p. 105 (1922).

lighter bluish tints can be identified even after a comparatively great thinning has taken place. The diminution of brightness, and the final disappearance of colour altogether, are no doubt due to the fact that the thinning is not sufficiently uniform, pits having a depth of even a few molecules diameter would interfere considerably with the brightness of the tints.

If a similar series of colours is formed on silver foil by graduated exposure to the vapour of iodine, a similar shift of the colours may be produced by subjecting one-half of the specimen to cathodic treatment in normal sulphuric acid, for this purpose an E.M.F. of 2 volts is suitable.

Investigation of Raman's Proposal of a Granular Structure

in the Film—When lead is melted in a shallow iron dish in air a beautiful series of colours appear in order on the lead: the surface becomes brown, rose, blue, steel grey, yellow, brown, rose, blue, bright green, yellow, rose, faint green, pale rose, greenish grey, and finally the colour becomes stationary at a dirty yellowish-grey tint. A short way above the melting point the film consists of solid lead oxide, which may readily be skimmed off at any time, giving rise to a fresh sequence of the beautiful colours from the start. If, however, the lead is heated more strongly by placing one Bunsen burner below the dish and allowing another Bunsen flame to play over the lead surface, the oxide film on the surface becomes liquid, and yet the interference colours are still seen and are of the same character. If at this stage the oxidizing flame is allowed to play upon one part of the surface, the oxide may locally be blown off the lead by the current of hot gas, and at the edges of the part where the clear lead is seen a beautiful series of coloured fringes appear, which advance and retire as the flame is moved in one direction or the other. There is no doubt that the oxide film is liquid at this stage, if the flame is directed upon the edge of the vessel where solid flakes of the oxide exist, they are at once seen to melt. The production of the colours above the melting-point of lead oxide shows quite clearly that they cannot be due to a granular structure, but that they are connected with variations in the thickness of the film.

If the lead is allowed to drop below the melting-point of the oxide, it is possible to remove the film at any stage on a piece of mica or thin glass. The colours of the film may be seen when it is stripped off the lead. Examination under the microscope fails to detect any signs of a regular granulated structure

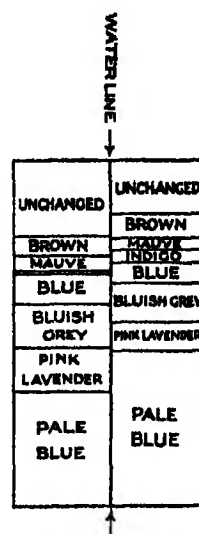


FIG 1.

which might produce diffraction-colours. The colours are less bright when viewed on glass or mica than when the film is on the lead, but nevertheless they are quite distinct. The colour when viewed by transmitted light is complementary to that seen when viewed by reflected light, which is in agreement with the interference view.

It is possible to obtain on glass a film of lead oxide of gradually increasing thickness in the following way.—A portion of the lead surface is cleared by skimming, and a very thin microscope slide-glass, held in pliers at one end, is pushed into the metal at a small angle to the horizontal, so that the other end presses on the bottom of the iron dish. The glass gradually softens and is allowed to subside slowly, as it subsides, it gradually clears away the superficial oxide at the one side, and leaves momentarily bright unoxidized lead on the other.

When the position reached is that shown in fig 2, it is evident that the lead above the glass will show the "earliest tints" characteristic of the thinnest

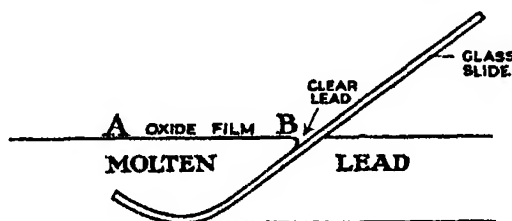


FIG 2

films at the end B, and a regular sequence will exist, until at A, where the lead has been oxidizing undisturbed for a considerable time, the later tints characteristic of thicker films are observed. At this stage, the glass may be raised, and tilted sideways to pour off the molten metal from between the oxide film and the glass. On examining the film, a regular sequence of colours (yellow, rose, blue, green etc.) is seen extending from the thin to the thick end; the order is the same by transmitted as by reflected light. Thus:

Colour by { Reflected light Transmitted light	Thin end					Thick end.
	— yellow	— red	yellow blue	red green	blue yellow	green red

At any given point the colour by transmitted light is always complementary to that seen by reflected light, as would be expected. But the

hues observed by reflected light (if the corrected angle is obtained) are often considerably brighter than those seen by transmitted light; for instance, where the colour is faint blue by transmitted light, it is a beautiful golden yellow when viewed at the proper angle by reflected light, where it is distinctly blue by reflected light, it is often only a dull yellowish-brown by transmitted light.

Scales of Colours on Different Metals—It may be of interest to tabulate the sequence of tints observed on different metals treated in different ways. They are arranged side by side, so as to show analogous tints in horizontal rows. The hues refer to metal roughened with emery (except, of course, in the case of molten lead)

Iron heated in Air	Molten lead in Air	Silver exposed to Iodine Vapour	Copper* over Dilute Solution of H_2S
Straw yellow	Yellowish brown	Yellow	Brown
Brown yellow	Brown		
Rosy mauve	Rose	Rose	Rose
Indigo		—	Mauve
Bright blue	Blue	—	Deep blue
Pale sky blue	Pale blue	Lavender	Pale blue
Steely	Steely (greenish)	Silvery (greenish)	Brilliant silver
	Yellow	Yellow	Yellow brown
	Brown		
Pale pinkish grey	Rose	Rose	Rose
Pale lavender	Blue	Lavender	Blue
Pale steel blue	Bright green	Green	Bright green
	Yellow	Yellow	Brown
	Rose	Rose (trace of lavender)	Rose
			Lavender
	Green	Dull green	Green
	Pale rose†	Dirty pink‡	Dirty rose
	Faint green†		Dirty green
	Grey	Grey	Grey

* The copper was exposed at constant or rising temperature to prevent condensation of water

† Film becomes "puckered" about this stage.

‡ On some specimens, further alternations of pink and green are just observable before the colour relapses into grey

It will be seen that in all cases the sequence of colours corresponds fairly well to that which would be expected from the interference theory, but that the surface always finally assumes a grey hue or steely blue aspect. The only remarkable feature of the phenomena was the absence or difficulty of detection of the "first-order green." The other slight departures from the theoretical sequence can mostly be explained by the fact that the metal and the film-material themselves possess specific colours. Thus we may have preferential reflection of certain wave-lengths from the surface of the metal (as from

copper), or from the film material (as from magnetite); or again we may have specific absorption of certain wave-lengths during the passage through the film (as in silver iodide). The essential similarity between the scales confirms the view that the colours are chiefly determined by interference in all cases.

It is interesting to note that colours can be produced by the formation of a thin film upon a basis which is not a metal. If a sheet of copper be exposed over a saturated solution of hydrogen sulphide in a closed vessel for a few days, a thick layer of black copper sulphide is formed, if afterwards the specimen is exposed for a few minutes to the vapours arising from concentrated hydrochloric acid, a series of tints—due to a thin film of cuprous chloride on the basis of sulphide—appears. The tarnish tints which are met with on naturally occurring specimens of sulphide minerals may be mentioned at this point.

Consideration of Tammann's Work—It is probable, therefore, that Tammann was justified in employing the principle of interference to compare the thickness of his films at different times during their formation. Unfortunately there seems to be some little doubt whether the principle has been employed correctly. Tammann and Köster,* for instance, publish the following examples of the manner in which the thickness of the silver iodide film can be estimated from the appearance of the different colours.—

Straw Yellow	.	61 $\mu\mu$	or	43 molecules Ag I
Red I	.	108 "	"	77 " " I
Red II ..		216 "	"	155 " " I
Red III		330 "	,	235 " " I
Red IV		439 "	"	313 " " I *

It will be noticed that the ratio of the thicknesses supposed to correspond to the reds of the 1st, 2nd, 3rd and 4th order is approximately 1 : 2 : 3 : 4. But the correct application of the interference principle shows that the ratio should be approximately 1 : 3 : 5 : 7. There may be some merely clerical error involved, but if the printed figures really represent part of the table which Tammann and Köster actually used throughout their research in estimating the thicknesses of the films, it is clear that the agreement between the "found" and "calculated" values in their researches was fortuitous, and that the various rather complicated equations which they claim to have established lack experimental basis.

* G. Tammann and W. Köster, 'Zeitsch. Anorg. Chem.,' vol. 123, p. 196 (1923).

Consideration of Hinshelwood's Work.—Hinshelwood,* who has carried out some interesting work on the production of brightly coloured films on copper by alternate oxidation and reduction, states that here the colours are structural, being connected with the existence of numerous spherical granules in the film of oxide. Since the oxide layer is undoubtedly porous, it would be quite conceivable that the colours might depend on the size of the granules, possibly in the same way as the colour of colloids. It is noteworthy that Schaum and Lang† have prepared a complete series of silver sols containing particles of different size, with the colour varying from orange, through red, purple, blue-violet to green as the particle-size increases, in close agreement with the accepted theory of colloidal colours. But the two facts which Hinshelwood has adduced in support of his view are quite consistent with the view that the colours are merely due to interference, caused by a thin oxide film surrounding each of the granules. These facts are.—

(1) The colours are seen to grow brighter as the chemical activity increases, that is, as the oxide presents a larger surface area. But clearly, as the layer of oxide granules becomes thicker, the rays entering the porous layer will suffer more internal reflection, and hence the colour will be brighter.

(2) The ratio of oxygen to copper in the granular film is constant for a given colour, even when different thicknesses of the granular film are examined. This is necessarily the case if the colours depend on the thickness of the oxide layer on each particle, as the interference view supposes. The ratio cannot be altered by the total number of particles, i.e., by the total thickness of the granular film.

Therefore, whilst further work on this matter might be advantageous, there is at present no reason to think that the colours of Hinshelwood's porous films are other than interference effects.

Summary.

An experimental examination has been made of the objections raised by Mallock and by Raman to the generally accepted view that the colours of thin films of oxide, sulphide and iodide on metals are interference effects. Mallock has objected to the interference theory on the grounds that he had failed to alter the colours of tempered iron by polishing the metal, it has now been shown that the colours can be changed when the thickness of the film is uniformly reduced by cathodic treatment in dilute hydrochloric acid. Raman

* C. N. Hinshelwood, 'Roy. Soc. Proc.,' A, vol. 102, p. 318 (1922).

† K. Schaum and H. Lang, 'Koll. Zeitsch.,' vol. 28, p. 243 (1921).

has proposed that the colours are due to a granular structure; but it has been shown that the colours on molten lead can be obtained as easily when the oxide film is molten as when it is solid, and thus the "granular theory" fails. The oxide films have been lifted off molten lead, and examined, supported on glass; the colours by transmitted light are complementary to those by reflected light, as is to be expected on the interference view.

Tammann and Koster were therefore justified in using the principle of interference to follow the velocity of the growth of films, but certain figures published by them suggest that the principle may have been applied incorrectly, and until this matter is cleared up their equations must be accepted with reserve.

I would like to thank Col C T Heycock, F R S, and Mr A Wood for much helpful advice and encouragement

ADDENDUM

[*Added December 17, 1924*—Since this paper was actually printed, two other papers on the same subject have appeared C W Mason ('J. Phys. Chem.', vol. 28, p 1233 (1924)), after criticising Mallock's procedure, states that he has obtained colour-transformations of oxidised steel by means of very dilute nitric acid—the blue changing to reddish-purple, and finally to straw yellow. He discusses the views of Hinshelwood and Raman, and reaches the conclusion that the colours represent an interference-effect. The present writer is in substantial agreement with Mason's views.

R. C Gale ('J Soc Chem Ind.', vol 43, p 349T (1924)) has succeeded in obtaining the alteration of blue to purple and yellow by means of polishing—the method actually tried, without success, by Mallock. Gale has also endeavoured to estimate the thickness of the film by means of the weight-increment, he states that the thickness of the film on heated iron increases, as the colour changes from yellow through purple to blue, but that (although the order of the thickness is what would be needed to produce interference) the ratio of the thicknesses corresponding to the various tints is not in accordance with the simple interference view. It must, however, be remembered that Stead ('J. Iron and Steel Inst.', vol 103, p 271 (1921)) showed that the first effect of oxygen on heated iron is to give a solid solution, and it is only when the oxygen-concentration reaches a certain value that oxide will appear as a separate phase. Any sample of iron which has been heated in air will contain oxygen below the surface (mainly on the grain-boundaries) in solid solution, and

thus the weight-increment method cannot be expected to give a very accurate measure of the thickness of the film of oxide.

The work of Chuckerbutti ('Proc Indian Assoc Cult Sci,' vol 7, p. 75 (1922)) is vitiated by the same error

Prof. T Turner has lately informed me that in the course of a research by F B Jenkins, carried out at Birmingham in 1920, it was shown possible to alter the colour of blued steel to purple and yellow by means of very dilute sulphuric acid Unfortunately Jenkins's work was never published

It would appear, therefore, that the reversed colour-changes, the existence of which Mallock regarded as essential to the interference-view, have been demonstrated independently by four different workers using four different methods]

On the Quantum Dynamics of Degenerate Systems

By A. M MOSHARRAFA, D Sc., Ph.D.

(Communicated by Prof O W Richardson, F R S —Received November 4, 1924)

§1. It is well known that if

$$F_i = n_i h, \quad i = 1, 2, \dots \quad (1)$$

be a set of quantum conditions applicable to a class of dynamical systems, then F_i must satisfy the definite condition

$$\partial F_i / \partial a = 0, \quad (2)$$

where a is a parameter, such as an external field, etc, which is allowed to undergo a slow non-systematic variation In other words, F_i must be an "adiabatic invariant" of the class of systems Burgers* has shown, on the basis of Newtonian dynamics, that

$$I_i = \int_0^1 p_i dq_i$$

fulfils this condition in the case of a conditionally periodic system of several degrees of freedom where q_i, p_i are separable Hamiltonian co-ordinates, provided the system be non-degenerate, i.e, provided no relation of the form

$$\sum_i s_i' v' = 0 \quad (3)$$

* J M Burgers, 'Ann. d. Phys.,' vol. 52, p. 195 (1917).

exist between the frequencies ν^i , where s_i^j is an integer, positive or negative. In the case of a system of charged particles, W. Wilson* has shown that on the basis of the general theory of relativity, p_i should be replaced by π_i , where

$$\pi_i = p_i + eA_i, \quad (4)$$

e being the charge on the particle involved and A the generalised magnetic vector potential. Thus the application of the quantum conditions in the form

$$J_i = \int_0 \pi_i dq_i = n_i h, \quad (5)$$

where n_i is a positive integer (including zero) and the integration is extended from $q_i = \text{minimum}$ to $q_i = \text{maximum}$ and back to $q_i = \text{minimum}$, can only be said to have been justified in the case of non-degenerate systems

§2 If now we consider a degenerate configuration, we no longer find that each of the phase-integrals J_1, J_2, \dots , is, in general, an adiabatic invariant. If, however, a "cyclic" co-ordinate q_s exist, such that the corresponding momentum co-ordinate π_s is independent of the variable parameter a , then the phase-integral

$$J_s = \int_0 \pi_s dq_s \quad (6)$$

will clearly be independent of a , i.e., will be an adiabatic invariant. For such co-ordinates we may still write

$$J_s = n_s h, \quad (7)$$

where n_s is a positive integer. An example of such a cyclic co-ordinate is the azimuthal angle ψ about the direction of the external field in the case of the hydrogen atom. Further, it has been shown† that certain linear combinations of J_1, J_2, \dots , are adiabatic invariants for degenerate systems. These are given by

$$Y_j = \sum_i r_j^i J_i, \quad (8)$$

where r_j^i is an integer, positive or negative, such that

$$\sum_i s_i^j r_j^i = 0 \quad (9)$$

and s_i^j is defined by (3) above. It is natural, therefore, to postulate that the quantum conditions for degenerate systems assume the form

$$Y_j = \tau_j h, \quad j = 1, 2, \dots \quad (10)$$

* W. Wilson, 'Roy Soc. Proc.,' A, vol 102, p. 478 (1922).

† 'Akad. van Wetensch. Amsterdam, Sitz.' v. 30, Dez 1916, note, however, that we replace the co-ordinate p_i by the corresponding π_i .

where τ_j is an integer, positive or negative, together with the general conditions (7) which apply to cyclic co-ordinates whether the system be degenerate or otherwise.

§3 The application of the postulates of the previous section to a specified problem may be illustrated by an example. Taking the case of a hydrogen atom [mass of electron m_0 , charges on electron and nucleus $(-e)$ and E respectively] in the presence of an external electric field F and referring the system to parabolic co-ordinates (ξ, η, ψ) with the origin in the nucleus and the axis of ψ in the direction of F , so that

$$q_1 = \xi, \quad q_2 = \eta, \quad q_3 = \psi, \quad (3.1)$$

we arrive at the well-known expression for the energy

$$W = \frac{-(2\pi e E)^2 m_0}{2(J_1 + J_2 + J_3)^3} - \frac{3F}{8\pi^2 m_0 E} (J_2 - J_1)(J_1 + J_2 + J_3), \quad (3.2)$$

where both the relativity refinement and higher powers of F are neglected. We calculate the frequencies from the formula

$$\nu^i = \partial W / \partial J_i, \quad (11)$$

giving.

$$\left. \begin{aligned} \nu^1 &= \frac{(2\pi e E)^2 m_0}{(J_1 + J_2 + J_3)^3} + \frac{3F}{8\pi^2 m_0 E} (2J_1 + J_3) \\ \nu^2 &= \frac{(2\pi e E)^2 m_0}{(J_1 + J_2 + J_3)^3} - \frac{3F}{8\pi^2 m_0 E} (2J_2 + J_3) \\ \nu^3 &= \frac{(2\pi e E)^2 m_0}{(J_1 + J_2 + J_3)^3} + \frac{3F}{8\pi^2 m_0 E} (J_1 - J_2) \end{aligned} \right\} \quad (3.3)$$

so that

$$\nu^1 + \nu^2 - 2\nu^3 = 0 \quad (3.4)$$

This last equation corresponds to (3) above and the system is thus seen to possess a one-fold degeneracy. In order to find a set of equations corresponding to (8) we have from (9)

$$r^1 + r^2 - 2r^3 = 0 \quad (3.5)$$

giving the two independent solutions

$$\left. \begin{aligned} r_1^1 &= r_1^2 = r_1^3 = 1 \\ r_2^1 &= -1, \quad r_2^2 = +1, \quad r_2^3 = 0 \end{aligned} \right\} \quad (3.6)$$

whence we have the two independent invariants

$$\left. \begin{aligned} Y_1 &= J_1 + J_2 + J_3 \\ Y_2 &= J_2 - J_1 \end{aligned} \right\} \quad (3.7)$$

The hypothesis (10) now leads to the quantum conditions

$$\left. \begin{aligned} J_1 + J_2 + J_3 &= \tau_1 \hbar \\ J_2 - J_1 &= \tau_2 \hbar \end{aligned} \right\} \quad (3.8)$$

and, further, as J_1, J_2, J_3 are defined in such a way as to be all positive, we see that τ_1 must remain a positive integer whilst τ_2 may be either a positive or a negative integer. The co-ordinate ψ being cyclic we, moreover, have from (7)

$$J_3 = n_3 \hbar \quad (3.9)$$

where n_3 is a positive integer subject to the condition

$$n_3 \geq \tau_1. \quad (3.10)$$

We see from (3.2) and (3.8) that the energy expression involves no other functions of J_1, J_2, J_3 than the two adiabatic invariants Y_1, Y_2 . Thus, in calculating the *frequencies* of the light emitted, we need only consider the two quantum conditions (3.8). The *polarisation* and *intensities* of the various components, on the other hand, are governed by the azimuthal condition (3.9) which refers to the direction of the external field. Thus, following Sommerfeld* we exclude the value 0 from the possible values for J_3 , since it involves a collision of the electron with the nucleus. This leads to the restriction on τ_2

$$|\tau_2| < \tau_1. \quad (3.11)$$

In order to compare the results of our theory with the already existing Epstein-Sommerfeld theory, we have, on solving (3.8) and (3.9) for J_1, J_2, J_3 .

$$\left. \begin{aligned} J_1 &= (\tau_1 - n_3 - \tau_2) \hbar / 2 \\ J_2 &= (\tau_1 - n_3 + \tau_2) \hbar / 2 \\ J_3 &= n_3 \hbar \end{aligned} \right\} \quad (3.12)$$

This is equivalent to

$$\left. \begin{aligned} J_1 &= n_1 \hbar \\ J_2 &= n_2 \hbar \\ J_3 &= n_3 \hbar \end{aligned} \right\} \quad (3.13)$$

where n_1 and n_2 (but not n_3) may simultaneously assume half-integral values. Thus if we consider the "ground orbit" of the Balmer series we have in addition to the whole-number values

$$(n_1, n_2) = (0, 1); (1, 0)$$

the fractional value

$$(n_1, n_2) = (\frac{1}{2}, \frac{1}{2})$$

* 'Atomic Structure and Spectral Lines,' English Translation, p. 238 (1923).

and for the H_s orbit ($n_1 + n_2 + n_3 = 4$) we must also permit the fractional values.

$$(n_1, n_2) \text{ or } (n_2, n_1) = (\frac{1}{2}, 2\frac{1}{2}), (1\frac{1}{2}, 1\frac{1}{2}), (\frac{1}{2}, 1\frac{1}{2}), (\frac{1}{2}, \frac{1}{2})$$

and so forth

In a previous paper* the adoption of such half-integral values has been suggested on other grounds and has been shown to account successfully for exactly those observed components of H_s which have not been explained on the Epstein-Sommerfeld theory

§4 In the foregoing section we have neglected the relativity refinement since no system of co-ordinates has hitherto been discovered in which the variables are separable on relativistic dynamics. It is, however, noteworthy that in the case of orbits which would be circular in the absence of the external field the variables actually allow themselves to be separated if we neglect products of F and $1/c^2$, where c is the velocity of light. For such orbits we have the relation

$$\left. \begin{aligned} q_1^2 + q_2^2 &= 2r \\ &= \text{constant} + \text{terms in } F \end{aligned} \right\} \quad (4.1)$$

where r is the distance of the electron from the nucleus. The relativistic Hamiltonian equation, which may be put in the form

$$\begin{aligned} p_1^2 + p_2^2 + \left(\frac{1}{q_1^3} + \frac{1}{q_2^3}\right) p_3^2 &= 2m_0 W (q_1^2 + q_2^2) - m_e F (q_1^4 - q_2^4) \\ &+ 4m_0 e E + \frac{2r}{c^2} \{W + eE/r - eF (q_1^2 - q_2^2)/2\}^2 \end{aligned} \quad (4.2)$$

is seen to allow of separation of the variables if we neglect products of F and $1/c^2$ and thus write for the last term in view of (4.1)

$$2r_0 (W_0 + eE/r_0)^2/c^2,$$

where r_0 and W_0 are calculated in the absence of the field

$$\left. \begin{aligned} r_0 &= (J_1 + J_2 + J_3)^2 / (2\pi)^2 m_0 e E \\ W_0 &= -(2\pi e E)^2 m_0 / 2 (J_1 + J_2 + J_3)^2 \end{aligned} \right\} \quad (4.3)$$

This is seen to be equivalent to replacing eE by

$$\begin{aligned} eE \{1 + r_0 (W_0 + eE/r_0)^2 / 2eEm_0 c^2\} \\ = eE \{1 + (2\pi e E)^2 / 8c^2 (J_1 + J_2 + J_3)^2\} \end{aligned} \quad (4.4)$$

* 'Roy. Soc. Proc.,' A, vol. 106, p. 641 (1924).

On using this result in the formula for the energy we have the relativistic expression for this class of orbits

$$W = -\frac{(2\pi eE)^2 m_0}{2(J_1 + J_2 + J_3)^2} - \frac{3F}{8\pi^2 m_0 E} (J_2 - J_1)(J_1 + J_2 + J_3) - \frac{(2\pi eE)^4 m_0}{8c^2 (J_1 + J_2 + J_3)^4} \quad (4.5)$$

and on applying the formula (11) above, we again have the relation (3.4) between the frequencies. Now, for this class of orbits it has been shown in a previous paper* that

$$J_2 - J_1 = 0 \quad (4.6)$$

It follows that of the fractional values which our non-relativistic analysis allows for the quantum numbers n_1, n_2 , those for which

$$n_2 - n_1 = 0 \quad (4.7)$$

are also permissible on relativistic dynamics. Hence, the adoption of such sets of values as $(n_1, n_2) = (\frac{1}{2}, \frac{1}{2})$ or $(1\frac{1}{2}, 1\frac{1}{2})$ may be claimed to have been fully justified on theoretical grounds. The success attained by adopting such values in accounting for experimental results has already been pointed out in the paper quoted above.

§5. As a further illustration of the application of the quantum conditions (10) and (7) to degenerate systems, we consider the case of the harmonic oscillator taken by Sommerfeld† as an example. First, we consider a particle (mass = m_0) acted on by forces $(-k_1x_1, -k_2x_2, -k_3x_3)$ in the directions of three mutually perpendicular axes. The energy W , on neglecting the relativity refinement, is given by

$$W = \sum_i \sqrt{k_i/m_0} J_i/2\pi, \quad (5.1)$$

where

$$J_i = \int_0^1 \sqrt{\alpha_i - m_0 k_i x_i^2} dx_i \quad (5.2)$$

and $\alpha_1, \alpha_2, \alpha_3$ are constants subject to the condition

$$\sum_i \alpha_i = 2m_0 W. \quad (5.3)$$

If k_1, k_2, k_3 are all different, the system is non-degenerate and the phase-integrals J_1, J_2, J_3 are adiabatic invariants, thus setting

$$J_i = n_i h. \quad (5.4)$$

Where n_i is a positive integer, we obtain

$$W = \sum_i \sqrt{k_i/m_0} n_i h/2\pi \quad (5.5)$$

* A. M. Mosharrafa, *loc. cit.*, p. 645.

† *Loc. cit.*, p. 559.

Next, we consider a degenerate case of the problem by putting

$$k_1 = k_2 = k \text{ (say).} \quad (5.6)$$

(5.1) and (5.2) now assume the forms

$$W = \frac{\sqrt{k/m_0}}{2\pi} (J_1 + J_2) + \frac{\sqrt{k_3/m_0}}{2\pi} J_3 \quad (5.1 A)$$

$$\left. \begin{aligned} J_1 &= \int_0^{\alpha_1} \sqrt{\alpha_1 - m_0 k x_1^2} dx_1 \\ J_2 &= \int_0^{\alpha_2} \sqrt{\alpha_2 - m_0 k x_2^2} dx_2 \\ J_3 &= \int_0^{\alpha_3} \sqrt{\alpha_3 - m_0 k_3 x_3^2} dx_3 \end{aligned} \right\} \quad (5.2 A)$$

the frequencies as given by the formula

$$\nu^i = \partial W / \partial J_i$$

conform to the relation

$$\nu^1 - \nu^2 = 0, \quad (5.7)$$

whence we have for (9)

$$r^1 - r^2 = 0 \quad (5.8)$$

and thus the adiabatic invariant corresponding to (10) is

$$Y_1 = J_1 + J_2$$

Thus we have

$$\left. \begin{aligned} J_1 + J_2 &= \tau h \\ J_3 &= n_3 h \end{aligned} \right\} \quad (5.9)$$

the last condition being clearly independent of the degenerate nature of the system. The expression for the energy is therefore

$$W = \frac{\sqrt{k/m_0}}{2\pi} \tau h + \frac{\sqrt{k_3/m_0}}{2\pi} n_3 h. \quad (5.5 A)$$

We now refer the same degenerate system to cylindrical co-ordinates (r, θ, x_3) , this gives

$$W = (2J_r + J_\theta) \sqrt{k/m_0}/2\pi + \sqrt{k_3/m_0} J_3/2\pi \quad (5.1 B)$$

where

$$\left. \begin{aligned} J_r &= \int_0^{\alpha} \sqrt{[\alpha - m_0 k r^2 - \alpha'/r^2]} dr, \\ J_\theta &= \int_0^{\alpha'} \sqrt{\alpha'} d\theta, \\ J_3 &= \int_0^{\alpha_3} \sqrt{\alpha_3 - m_0 k_3 x_3^2} dx_3. \end{aligned} \right\} \quad (5.2 B)$$

and the integration extends in each case, as throughout this paper, from the minimum value to the maximum value and back again to the minimum value of the independent variable involved. $\alpha, \alpha', \alpha_s$ are constants subject to the condition

$$\alpha + \alpha_s = 2m_0 W. \quad (5.3 B)$$

The relation between the frequencies is now

$$v^1 - 2v^2 = 0, \quad (5.7 B)$$

so that

$$r^1 - 2r^2 = 0 \quad (5.8 B)$$

and the quantum conditions are

$$\left. \begin{aligned} 2J_r + J_\theta &= \tau' h \\ J_s &= n_s h \\ J_\phi &= n_\phi h \end{aligned} \right\} \quad (5.9 B)$$

the last condition being in consequence of the hypothesis (10) for cyclic co-ordinates. The energy is given by

$$W = \frac{\sqrt{k/m_s}}{2\pi} \tau' h + \frac{\sqrt{k_s/m_0}}{2\pi} n_s h \quad (5.5 B)$$

We see that the two results (5.5 A) and (5.5 B) are in complete accord. they yield an identical set of values for the energy. In particular, we emphasise that *no discordant results concerning the orbits are yielded*. Thus one of the outstanding difficulties of the application of the quantum conditions to dynamical systems is removed.

We remark that the set of conditions (5.9 B) give for J_r half-integral multiples of h . Had we, on the other hand, integrated J_r over the complete period of the motion in the $r - \theta$ plane, namely, over twice the period of libration of r , we should have replaced $(2 J_r)$ by (J_r) in the expression for the energy (5.1 B). This, in turn, would have involved the same substitution in (5.9 B) and thus left the final expression for the energy (5.5 B) unaltered. In fact, the limits of integration for such non-cyclic co-ordinates as r in the evaluation of the phase-integrals can in no way affect the final expression for the energy on our theory. This is especially significant in consideration of the arbitrary nature that integration limits must possess for such co-ordinates in the case of degenerate systems.

§6. Consider an f -fold degenerate system with n degrees of freedom and let m of these correspond to cyclic co-ordinates. For such a system there will be

f relations of the type (3), involving the n frequencies* $\nu^1, \nu^2, \dots, \nu^n$. Consequently there will be f equations of the type (9) involving the n integers r^1, r^2, \dots, r^n . These will possess $(n-f)$ independent solutions and we shall have the $(n-f)$ quantum conditions.

$$\left. \begin{aligned} Y_1 &= r_1^1 J_1 + r_1^2 J_2 + \dots + r_1^n J_n = \tau_1 h \\ Y_2 &= r_2^1 J_1 + r_2^2 J_2 + \dots + r_2^n J_n = \tau_2 h \\ &\vdots \\ Y_{n-f} &= r_{n-f}^1 J_1 + r_{n-f}^2 J_2 + \dots + r_{n-f}^n J_n = \tau_{n-f} h \end{aligned} \right\} \quad (6.1)$$

together with the m cyclic conditions

$$J_1 = s_1 h, \quad J_2 = s_2 h, \quad J_m = s_m h \quad (6.2)$$

If now we substitute from (6.2) in (6.1) we obtain

$$\left. \begin{aligned} r_1^{m+1} J_{m+1} + r_1^{m+2} J_{m+2} + \dots + r_1^n J_n + \left\{ \sum_{i=1}^{i=m} s_i r_1^i - \tau_1 \right\} h &= 0 \\ r_2^{m+1} J_{m+1} + r_2^{m+2} J_{m+2} + \dots + r_2^n J_n + \left\{ \sum_{i=1}^{i=m} s_i r_2^i - \tau_2 \right\} h &= 0 \\ \vdots \\ r_{n-f}^{m+1} J_{m+1} + r_{n-f}^{m+2} J_{m+2} + \dots + r_{n-f}^n J_n + \left\{ \sum_{i=1}^{i=m} s_i r_{n-f}^i - \tau_{n-f} \right\} h &= 0 \end{aligned} \right\} \quad (6.3)$$

In the case where

$$m = f, \quad (6.4)$$

it will be possible to solve for the J 's, obtaining

$$J_{m+i} = \frac{s_{m+i}}{\sigma_{m+i}} h, \quad j = 1, 2, \dots, n-m. \quad (6.5)$$

where s_{m+i} involves the arbitrary integers s_i and τ_i , but σ_{m+i} is a function of the fixed integers r_j^{m+1} alone and is therefore a fixed integer

It will be observed that the example considered in §4 fulfils the condition (6.4). There the fixed integer σ_{m+i} assumed the value 2 for each of the two non-cyclic co-ordinates involved. If, on the other hand,

$$m < f,$$

then it is no longer possible to assign values to each of the non-cyclic phase-integrals separately, but only to their lineal combinations Y_1, Y_2, \dots, Y_{n-f} . It is these lineal combinations, as we have seen, which function in the expression for the energy

* If any of the frequencies are not involved at all, then the corresponding co-ordinates are clearly independent of the degenerate nature of the system and the corresponding degrees of freedom may be left out of the discussion, cf the co-ordinate x_i in §5.

§7. The analysis of the preceding sections strongly suggests that the origin of the fractional numbers defining phase-integrals is to be looked for in the mechanism of degenerate systems. Thus the denominators of the fractions involved are derived in certain cases as functions of the whole numbers governing the relations between the frequencies. It is, moreover, to be remarked that as the mechanical system becomes less and less degenerate these whole-numbers [r_j of equation (9), §1] become larger. The whole-numbers τ_1, τ_2 , etc., of the conditions (10) must therefore be assumed to increase in magnitude accordingly, if the phase-integrals are to remain finite. The quantum conditions for non-degenerate systems may therefore be looked upon as limiting forms of those for degenerate ones, where the quantum numbers τ_1, τ_2 , increase in such a way that the right-hand side of (6.5) becomes an integral multiple of h . This transition from degenerate to non-degenerate systems does not, however, correspond on the classical side to a transition from the adiabatic invariants Y_j to the phase-integrals J_j . It is more of the nature of a sudden occurrence than a gradually approached limit.

Summary

(1) A set of quantum restrictions is suggested for degenerate conditionally periodic systems, in the form

$$Y_j = \tau_j h,$$

where Y_j is a specified "adiabatic invariant."

(2) The conditions are applied to the case of the hydrogen atom in the presence of an external electric field and are shown to lead to the adoption of "half-integral orbits" in the Stark effect already suggested by the present writer on other grounds.

(3) A further example of the application of the conditions is discussed. It is shown that they lead to completely consistent results. In particular, *no discordant results concerning the orbits are yielded*.

(4) The relation of the hypothesis to the general question of fractional quantum numbers is pointed out. It is suggested that the origin of these fractions is to be sought in the mechanism of degenerate systems.

*On the Effect of Temperature on the Anomalous Reflection
of Silver*

By M. DE SÉLINCOURT, Scholar of Brasenose College, Oxford

(Communicated by Prof F A Lindemann, F R S—Received November 7, 1924.)

It has long been known that the reflection coefficient of silver, besides diminishing steadily in the ultra-violet, shows a marked anomaly in the neighbourhood of wave-length $3,200 \text{ \AA}$, sinking to a value of nearly zero, while on either side of this point it amounts to about 50 per cent. The cause of this phenomenon is unknown, though from the classical electro-magnetic point of view it would naturally be regarded as some kind of "resonance" effect, that is to say, that the "free" electrons cannot, for some reason, vibrate with frequencies corresponding to this region, for the "bound" electrons, though they could, if they were in resonance with frequency, increase the total reflection, could hardly decrease it, as actually occurs.

If this is so, and if the restoring force on the vibrating electrons varies with the distance between them and the neighbouring atoms and electrons, it may be expected that the limiting frequency on either side of this band will vary as the metal contracts or expands. A change in the temperature of the silver should then produce a corresponding shift in the position of the band of weak reflection, and measurement of the amount of this shift may afford some clue to the nature and magnitude of the forces which act upon the "free" electrons.

Lowering the temperature, which causes the metal to contract and so brings the atoms closer together, would tend to increase the force, if any ordinary law of force holds, and consequently to increase the proper frequency of the "resonance", for if the effect is due to some such cause the frequency will be proportional to the square root of the restoring force. The band will thus be shifted towards the shorter wave-lengths as the silver is cooled, while heating will obviously produce the opposite result.

The experimental method consisted in (a) photographing the continuous spectrum of a tungsten filament lamp, after causing the light to suffer reflection on its way to the spectrograph by a silver surface whose temperature could be varied, and (b) measuring the blackening of the photographic plate thus obtained photo-electrically.

The source of light used was a filament lamp fitted with a quartz window,

this was ground and sealed with sealing-wax on to the end of a side-tube, so that the wax should not be melted by the heat of the filament.

The silver was a solid plate $1\frac{1}{2}$ inches in diameter and 1 mm. in thickness, ground flat, and brought by hand to as high a polish as possible. It was suspended from a flat horizontal iron bar by means of three iron rods 12 inches in length, and was surrounded by an air-tight cylinder, the lower half of which was made of copper and the upper half of iron, these metals being chosen for their respective heat conductivities. The cylinder was supported by its lid, which had a quartz window to admit the light, inlet and outlet tubes for gas, and a passage for a thermo-element, and was bolted to the iron rods.

A parallel beam of light from the source travelled along the large iron bar and was deflected on to the silver and back into its original direction by quartz prisms placed over holes in the bar. It was finally condensed on to the slit of a large quartz spectrograph.

Owing to the far greater intensity in the visible, compared to the ultra-violet, part of the spectrum, the plate was badly fogged by scattered visible light, when the exposure was sufficient to give the desired amount of blackening in the ultra-violet. A silica tube containing bromine vapour was therefore placed in the path of the light. This absorbed all the visible light (with the exception of a small quantity in the red) but was transparent to the ultra-violet.

The wave-length of the point of minimum reflection was ascertained from a comparison spectrum of copper, placed alongside of the continuous spectrum already mentioned. It should be noticed that as the absolute coefficient of reflection was not determined, the apparent position of the band was shifted slightly as a result of the steady diminution of blackening with decreasing wave-length. The discrepancy in the absolute value of the frequency is about 4 per cent, but as the present experiment is concerned only with variations in the position and width of the band this slight general shift is unimportant.

In the first photographs, taken at room temperature, $\pm e$, at 16°C , the band was found to vary in clearness on different plates. The cause of this variation was not actually discovered, but it appeared to be connected with the polishing, as later, when greater attention was devoted to this, a reasonable constancy was attained. It was suggested that a polish containing mercury had accidentally been used, but this did not seem a likely explanation; possibly the continued friction interfered in some way with the lattice arrangement which presumably exists, as after heating the silver the band was usually restored.

to its former clearness. This, again, indicates that it is the lattice formed by the "free" electrons with which we are concerned, as the bound electrons would scarcely be affected by heating. As soon as good constancy had been secured the cylinder was immersed in a bath of liquid air, or solid carbon dioxide in alcohol, and photographs were taken with the silver plate at -183°C and -79°C .

The temperature was measured with a thermo-element, and dry hydrogen was passed through the cylinder to prevent the condensation of moisture inside as the temperature fell. A difficulty was encountered working with these temperatures, as moisture condensed and froze on the outside of the quartz window, blocking the passage of the light. At first an arrangement was made for a stream of warm dry air to keep blowing on to the outside of the window. This kept a good part of the window dry, but it was troublesome in many ways, and it was ultimately found best to keep the window moist with methylated spirit, which showed no inclination to freeze and was apparently transparent to light of all wave-lengths in the region in question. All the photographs showed that on lowering the temperature the band was shifted towards the shorter wave-lengths. Further, the band was at the same time rendered sharper and narrower.

A further set of photographs was then taken with the silver plate heated, by means of a bunsen flame, to a temperature of about 150°C . In these the band became so broad that the position of the minimum was scarcely measurable and it seemed useless to proceed to any higher temperatures. The shape of the band for each particular temperature was determined photo-electrically.

The photo-electric cell employed for this purpose was enclosed in a wooden box and the light admitted to it through a slit in the top. Over this slit the plate was held by a carrier, with slow motion in two directions at right-angles to each other. The current was measured with an electrometer and the grid of the cell was earthed through a xylene-alcohol leak. As it was principally the position of the minimum which was of interest, no calibration of the instrument was undertaken, the deflection of the electrometer being assumed to be proportional to the quantity of light entering the cell.

The measurements of wave-length were always made from the same definite line in the comparison spectrum, and the blackening of the plate was first plotted against the scale divisions of the plate carrier. These were subsequently transformed to wave-lengths by passing the copper spectrum over the slit (starting, of course, from the same line as before).

Fig. 1 shows the curves thus obtained for the four different temperatures.

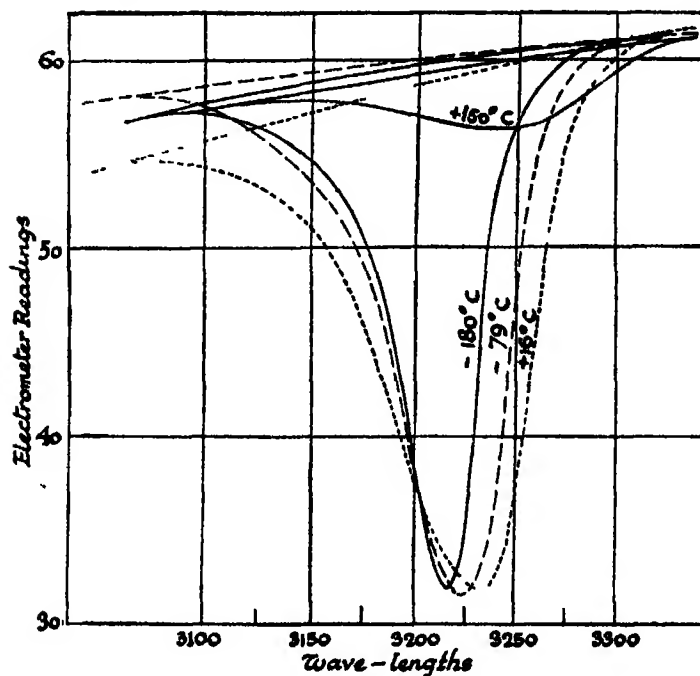


FIG 1

From these the points of minimum reflection are found to be as follows :—

Temp.	Wave length
°C	Å
- 183	3217
- 79	3227
16	3236
150	3247

If the cause of this effect is some kind of resonance the restoring force will be proportional to the square of the frequency, on the other hand, the mean distance between the points of the space lattice, *e.g.*, the centres of the atoms, is proportional to the reciprocal of the cube root of the density.

That a relation exists between these quantities is shown by the following table .—

Temp	ν^2	$\Delta\nu^2/\nu^2 = \Delta F/F$	ρ^{-1}	$\Delta\rho^{-1}/\rho^{-1} = \Delta r/r$	$\frac{\Delta r/r}{\Delta F/F}$
° C		per cent			
-183	966268	—	0.4550	—	—
-79	960289	0.6188	0.4556	0.1957	3.162
16	954255	1.1700	0.4566	0.3522	3.323
150	948505	1.8380	0.4576	0.5870	3.131

The values obtained for ν^2 are plotted against r , the mean distances between atoms, in fig. 2, and as is evident from the constancy of column 6 they lie

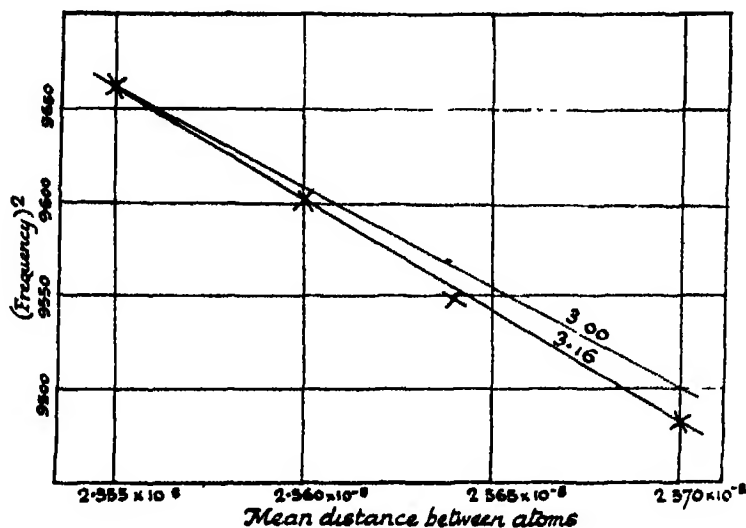


FIG. 2

approximately on a straight line, this, of course, is to be expected, as the variation in the distance is only a small fraction of the total

The ratio of the percentage change of these quantities (i.e., $\frac{dF}{F} / \frac{dr}{r}$, where F is the restoring force and r the mean distance between these atoms), is found by graphical interpolation to be 3.16

This result can be well explained by assuming that the "free" electrons form a lattice interpenetrating the atomic lattice, the electron lattice would necessarily contract with the atomic lattice, and the mean distances between the electrons would, therefore, be proportional to, and of the same order of magnitude as, the mean distances between the atoms. If the forces between electrons

are subject to the inverse-square law, then the force acting on an electron from either side may be represented by $\Sigma \frac{a_n}{r_n^2}$. If the electron is displaced by a small amount Δr the resulting force on it is

$$\Sigma \frac{a_n}{r_n^2} - \Sigma \frac{2a_n}{r_n^3} \Delta r \pm \Sigma \frac{a_n}{2r_n^4} \Delta r^2$$

Neglecting Δr^2 and higher orders, we have the restoring force proportional to $\Sigma \frac{2a_n}{r_n^3} \Delta r$, if only the neighbouring particles are effective, as is usually assumed, therefore, the restoring force will be proportional to the inverse cube of the distance between the atoms. This theoretical value is plotted in fig 2 as a contrast to the experimental value 3.16. Though the two are evidently distinct, the discrepancy is so small that it might well be due to a residual effect from the other ions.

Thus, though it gives no reason for the existence of a region where electrons cannot vibrate, the idea of an electron lattice enables us to predict a temperature shift of the observed order of magnitude, if we make the assumption that the distances between the oscillating electrons and the particles which are holding them in position vary as the distances between the atoms themselves when the whole solid expands or contracts.

This derivation, of course, implies that the restoring force is due only, or mainly, to the neighbouring free electrons, which are assumed to form a lattice interleaved with the atomic lattice. Why the positive ions are to be left out of account is not very clear, but if free electrons exist at all some such assumption seems inevitable.

If, however, the electrons form a lattice in which they are controlled solely by an inverse square law of force between themselves, we should then expect the mean amplitude of vibration to be independent of the temperature, for though the electron lattice must contract with the atomic lattice the "free" electrons cannot be regarded as attached to the atoms, while the atoms vibrate with amplitudes depending on the total heat energy, the electrons should, therefore, vibrate with constant amplitude over all temperatures, for their frequency of oscillation is too great to admit of their partaking of the heat motion of the atoms.

The breadth of the band should therefore be constant, as it depends upon the mean amplitude of vibration. For if the amplitude is zero the restoring force is constant for all electrons, whereas if the amplitude has a finite value the restoring

force on an electron, and consequently its frequency, varies according as it is nearer or further from its neighbours than in the mean position

As we have seen, experiment shows that the breadth does vary with the temperature, further, it appears to agree with the supposition that the particles controlling the electrons have an amplitude of oscillation of the same order as the atom. For if we calculate their mean amplitude from the formula $\frac{1}{2}\pi v \sqrt{\frac{kT}{m}}$ (where $v = 4.5 \times 10^{12}$, $\lambda = 1.346 \times 10^{-10}$, $m = 1.782 \times 10^{-22}$) and assume that the restoring force varies with the power 3.16 of the distance, as was found above from the shift of the band, we have for the maximum and minimum wave-lengths of resonance —

Temp	Maximum	Minimum
°C	Å.	Å
-183	3360	3110
-79	3429	3056
16	3482	3037
150	3553	3009

According to this the width of the bands at these temperatures should be in the ratio 1.1452 : 1.735 : 2.12. Since in this rough calculation the maximum and minimum wave-lengths are obtained when the neighbouring particles are at their maximum and minimum amplitudes, they may be regarded as somewhat improbable limits, and in effect the resonance band observed covers a range of wave-length only about half that predicted above, this, however, does not affect the values of the ratios of the widths.

Near the limits of possible resonance the curve scarcely differs from that corresponding to the direct beam, so that it would be extremely difficult to estimate the width of the band at this point, the depth of the curve also depends on many factors other than the resonance of silver (e.g., the exposure of the plate, development, etc.), so that the width of the curve at adjacent points would be meaningless. The width was, therefore, measured at some definite fraction of the depth of the curve.

The curve was drawn as it would probably have run had there been no resonance, but merely the diminishing reflecting power in the ultra-violet. A vertical line was then drawn up to meet it, from the minimum point, the width of the curves of weak reflection was then measured (in arbitrary units) at points $1/3$, $1/2$ and $2/3$ of the way along this line. The same was done for all except the highest-temperature curve, which was too vague to allow of

254 *Effect of Temperature on Anomalous Reflection of Silver.*

any estimate being made. The mean ratio found in these measurements for the widths of the band at -183°C , -79°C , 16°C is 1.00 : 1.43 : 1.90, and is thus not far removed from the theoretical value 1.00 : 1.452 : 1.735.

The magnitude of this effect is thus of the same order as would be expected if (a) the electrons moved in sympathy with the heat vibration of the atoms, or (b) they were controlled by the atoms themselves, though this latter view is scarcely tenable in view of the fact that the ions must carry a residual + charge, which cannot well be imagined to repel an electron. If the free electrons were controlled by the repulsion of the electrons revolving round the atoms they might well be affected by the atomic oscillations, so that a rise in temperature would produce a broadening of the band. But these start much nearer to the "free" electrons, so that a change of 1 per cent in the inter-atomic distances would mean change of at least 10 per cent in the distance over which the force acted, and the observed values of both the shift and the broadening would in this case be too small.

If, therefore, we endeavour to treat the problem from the classical point of view, we are led back to our original view of the electronic lattice, but why the electron should vibrate with amplitudes similar to those of the atom is not yet apparent. Probably here, again, a radical restatement in terms of the quantum theory will have to be undertaken.

In conclusion I must express my deep gratitude to Prof. Lindemann for the original suggestion of the experiment, and both to him and to Mr. I. O. Griffith for the continual help and advice which have enabled it to be carried out.

The Catalytic Activity of Copper. Part V.—The Comparison of the Rates of Dehydrogenation of Various Alcohols.

By W. G. PALMER, Fellow of St John's College, Cambridge, and F. H. CONSTABLE, Strathcona Research Student, St John's College, Cambridge

(Communicated by Sir William Pope, F R S —Received November 1, 1924.)

The study of the dehydrogenation velocity, and the temperature coefficient of the dehydrogenation velocity for various alcohols should give valuable information on the mechanism of the catalytic decomposition

To eliminate possible errors due to continued grain growth in the catalyst the reaction velocities for all the alcohols used were compared with that of ethyl alcohol. These measurements showed that the activity of the catalyst at a constant temperature of reduction slowly decreased, as would be expected from the results of Part IV*. This decrease does not affect the accuracy of the comparison since the grain growth is slow, and therefore the change in activity between an experiment with a selected alcohol, and another with ethyl alcohol is negligible. The ethyl alcohol behaved in a manner which was well known from the previous experiments, and moreover, since it could be obtained very pure, it afforded an excellent standard of reference.

The Purification of the Alcohols

Great care was taken to ensure the purity of the alcohols used. They were dried with lime, often twice, and then subjected to continued fractional distillation through a Dufton column till they boiled over a range of not more than 0.1°C . The apparatus was arranged to prevent the absorption of water vapour. With normal propyl, normal butyl, and one sample of iso-propyl alcohol, this process resulted in a product which was free from catalyst poisons as shown by the overlapping of the heating and cooling curves. But in the case of another sample of iso-propyl alcohol, and with iso-butyl and iso-amyl alcohols, though the boiling points were constant to 0.1°C , and the values so obtained agreed with the published values for the pure substances, rapid poisoning of the catalyst occurred. In the case of iso-amyl alcohol the velocity became negligibly small in 40 minutes. Since the poison cannot be removed by repeated fractionation, these alcohols provide an excellent opportunity for investigating the mechanism of poisoning with a constant pressure

* 'Roy. Soc. Proc.,' A, vol 106, p. 250 (1924)

of poison, the composition of the alcohol mixture being unchanged by distillation.

In the case of iso-propyl alcohol complete purification could be effected with the aid of liquid air.* The alcohol was slowly cooled in a test-tube above the liquid air. As the temperature fell the liquid became more and more viscous. The bottom of the tube was left in contact with the liquid air surface for a short time, and the liquid was stirred with a glass rod, and then the tube was scratched at the bottom. This procedure caused crystalline nuclei to form on the glass. The contents of the tube were continuously stirred and very slowly cooled, causing the separation of the pure crystalline solid at the bottom of the tube. The process was continued till three-quarters of the liquid had crystallised. The tube was then placed in a clear glass Dewar vacuum flask and allowed to warm up slowly till half the alcohol was left crystalline. The mother liquor was sucked off, by means of a pump, through a linen filter spread over the end of a capillary tube. The crystals were pressed against the linen filter to free them from as much liquid as possible. The alcohol obtained from the melted crystals did not poison the catalyst. The boiling point was unchanged.

Table 1 — Physical Constants of Alcohols used in Final Comparisons

Alcohols	Density D_0^{20}	Boiling Point at 760 mm (corr)	Boiling Point for pure substance *
<i>Primary—</i>		° C	° C
Ethyl	0.8051	78.3	78.3
Propyl	0.8174	97.4–97.5	97.4
Butyl	0.8237	117.4–117.5	116.8
Iso butyl	—	107.7–108.0	106.4 to 108.39
Iso amyl	—	131.1–131.2	131
<i>Secondary—</i>			
Iso propyl	0.8001	82.3–82.4	82.0 to 82.9
Cyclohexanol	—	160	160†
	M–P 15.6° C	Published M–P 15.0° C	

* Taken from 'Beilstein's Handbuch.'

† The cyclohexanol was frozen and filtered.

Experimental Details.

Difficulty was experienced in regulating the boiling current. The energy supplied to the heating coil is used up in radiating away energy from the glass walls of the boiler, as well as in vaporising the liquid. All alcohols have about

* Carrara and Coppadoro, 'Gazzetta,' vol 33 (1), p 343.

the same latent heat of vaporisation, but the heat lost by radiation is greater the higher the boiling point. Thus a larger boiling current must be used as the homologous series is ascended. The current cannot, however, be reduced once an experiment has started as this causes sucking-back of gas over the catalyst and subsequent poisoning, making the experiment wholly unreliable. A very low rate of boiling is likewise objectionable. From the experience gained in using the first few alcohols, the current necessary for vaporisation at the rate of about 20 c.c. an hour could easily be predicted.

Precisely the same rate of boiling was not used throughout these experiments, the variation being about 50 per cent. It has, however, been shown (Part I)* that the rate of reaction is independent of the rate of boiling above a slow limiting rate.

Preliminary Experiments

The reaction-velocity temperature curves were drawn using the constant temperature of 225° C. for the reduction of the copper oxide. Slight impurities cause marked changes in the form of the heating and cooling curves. The curve for a sample of propyl alcohol which showed a boiling range of 0–4° C. is shown in fig. 1, and is lettered EFGHIJK. It was found that AB represented the behaviour of aqueous propyl alcohol, and CD that of anhydrous alcohol. The propyl alcohol, therefore, contains a small quantity of water. The cause of this form of curve is as follows. EF represents the distillation of the constant-boiling mixture, along FG the vapour phase contained less and less water as the distillation proceeded, till at and after G anhydrous alcohol was distilling. At H poisoning commences to occur, accounting for the vertical portion HI. At about J the alcohol film has become thick enough to protect the copper, the poisoning stopped, and the curve JK has the true temperature coefficient. On further drying the heating and cooling curves for this alcohol overlapped, and agreed with the ethyl alcohol measurements.

LM shows the behaviour of iso-propyl alcohol containing poison. From this curve, and a knowledge of the rate of covering of the surface, the curve in fig. 2 was calculated. The curve NO shows a pure specimen of iso-propyl alcohol reacting through the range 220–350° C. In spite of the stability of acetone poisoning is marked above 300° C. PQ shows iso-amyl alcohol which poisoned the surface more rapidly than any of the other alcohols. Fig. 1 thus shows the principal types of curves due to the promoter action of water, and to surface poisoning.

* 'Roy. Soc. Proc.' A, vol. 98, p. 13.

The reaction-velocity-temperature curves were obtained for the alcohols in order of their ascending boiling points. One of the chief difficulties with

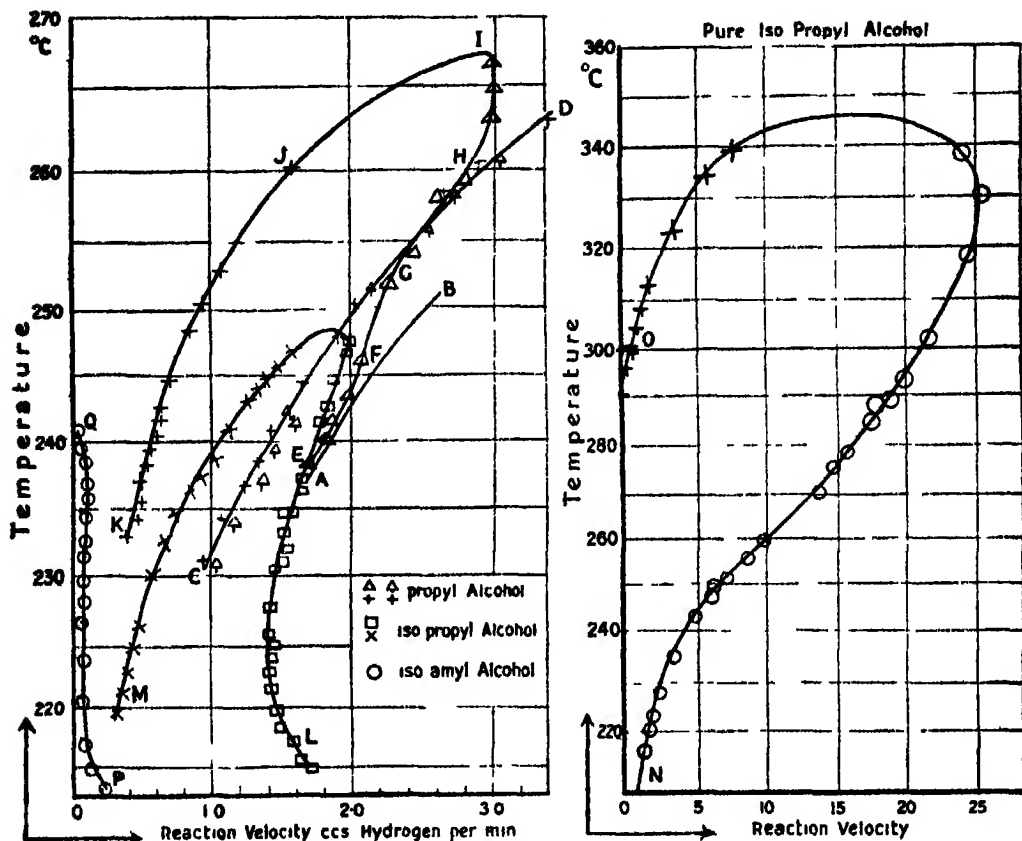


FIG 1

the higher alcohols was the removal of the reactant from the reaction tube. The Fleuss pump was worked till a pressure of about 0.1 mm was obtained. With cyclohexanol, however, the tube had to be dismantled to be cleaned.

The Results for Ethyl, Propyl and Butyl Alcohols.

The results for ethyl, normal propyl and normal butyl alcohols are shown in fig 2. Satisfactory agreement of the same sort was obtained between ethyl and propyl alcohols in the previous paper, Part IV. The number of catalyst rods used in this comparison was decreased 0.32 times for the experiments of Part V. The activity was diminished 0.42 times. Allowing for the

inequalities in the copper film on individual rods, the agreement shows that the whole of the catalyst surface was active. The results are summarised in Tables II and III.

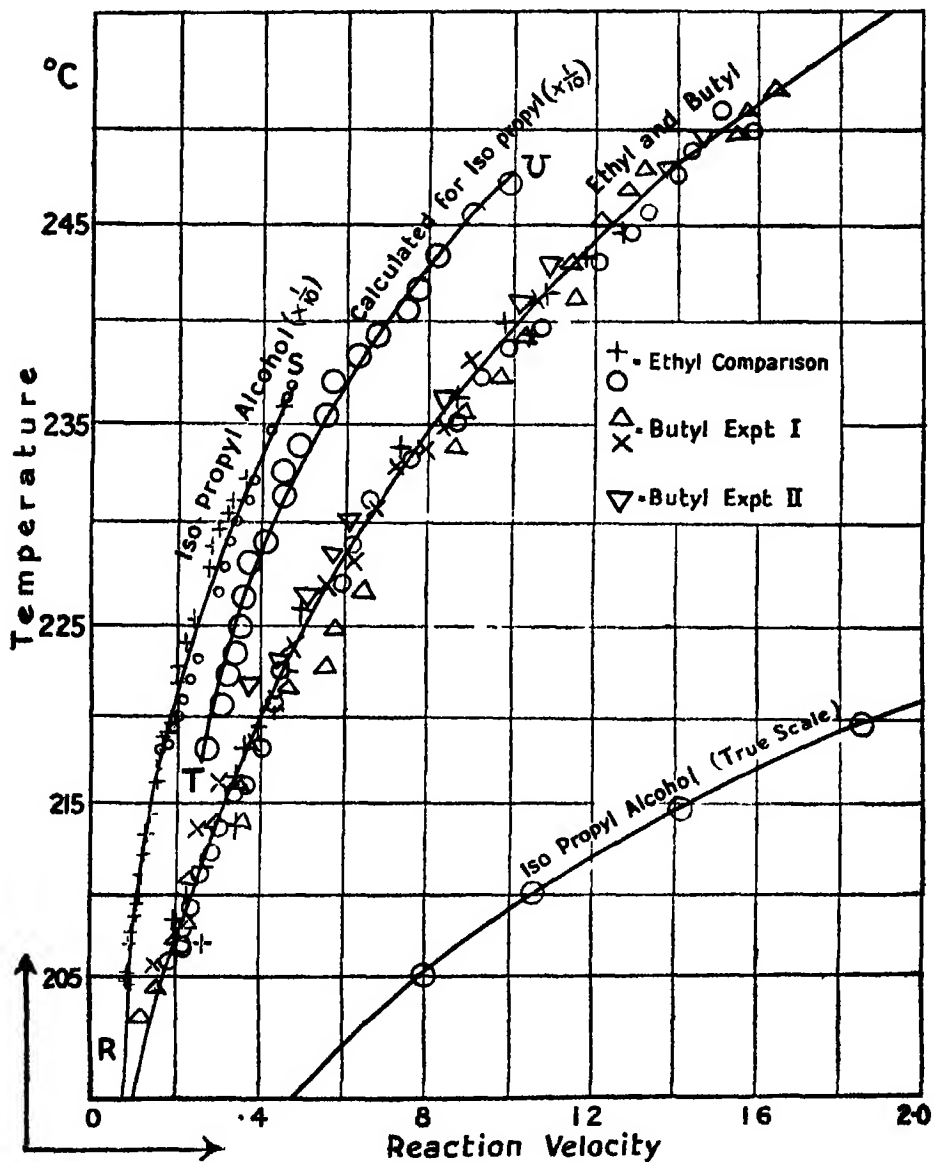


FIG 2

Table II —Reaction Velocity *

Temperature.	Ethyl Alcohol	Propyl Alcohol.
° C		
205	0 258	0 246
210	0 329	0 321
215	0 410	0 418
220	0 543	0 531
225	0 686	0 688
230	0 940	0 916
235	1 148	1 142
240	1 40	1 38
245	1 72	1 68†
250	2 04	2 19†
255	2 46	2 60†
260	2 98	3 30†
265	3 64	3 98†
270	4 26	4 90†

Temperature coefficient at 250° C { for ethyl alcohol = 1 531
 { for propyl alcohol = 1 546

* Units c cs Hydrogen per min (at 16° C and 760 mm.)

† Extrapolated from the observations at lower temperatures.

Table II —Reaction Velocity

[Observations of Part IV, *loc. cit*]

Temp	Ethyl Alcohol	Propyl Alcohol.
° C		
240	1 52	1 40
245	1 98	1 94
250	2 55	2 56
255	3 18	3 24
260	3 93	4 05
265	4 82	4 95
270	6 05	6 00
275	7 30	7 20
280	9 00	8 90

Table III.—Reaction Velocity.

Order of Experiment—	1	2	3
Temperature.	Butyl Alcohol	Ethyl Alcohol.	Butyl Alcohol.
° C			
205	0 168	0 169	0 169*
210	0 243	0 248	0 240*
215	0 320	0 331	0 306*
220	0 410	0 413	0 390
225	0 528	0 513	0 491
230	0 678	0 650	0 631
235	0 848	0 810	0 798
240	1 050	1 050	0 998
245	1 270	1 240	1 220
250	1 540	1 500	1 480
255	1 880	1 920	1 900*

Temperature coefficient at 250° C $\left\{ \begin{array}{l} \text{Butyl (1)} = 1.542 \\ \text{Ethyl (2)} = 1.533 \\ \text{Butyl (3)} = 1.543 \end{array} \right.$

* Extrapolated from exponential law

The Comparison of the Reaction Velocity when the Alcohol contains Catalyst Poisons

The curve LM in fig 1 was corrected for the rate of covering of the surface. The velocity of dehydrogenation of this sample of iso-propyl alcohol was measured at a constant temperature of 225° C. The result obtained is shown in curve III, fig 3. $\log_{10} v$ plotted against the time (t) gave the straight line V in fig 4. The straight line VI was obtained by subtracting the ordinates of V from the initial ordinate of curve V obtained by producing the straight line to meet the axis. Hence at any time (t) line VI gives the logarithm of the correcting factor by which the observed activity must be multiplied. By this means the calculated curve TU (fig 2) was obtained for iso-propyl alcohol. Comparing this curve with the result obtained from iso-propyl alcohol which had been crystallized (Table IV and fig 2, RS and TU), the method is seen to involve an error of 30 per cent. The tracking of the source of this error led to the adoption of an alternative method.

There is no doubt, however, that the velocity of dehydrogenation of iso-propyl alcohol is much greater than that of the primary alcohols.

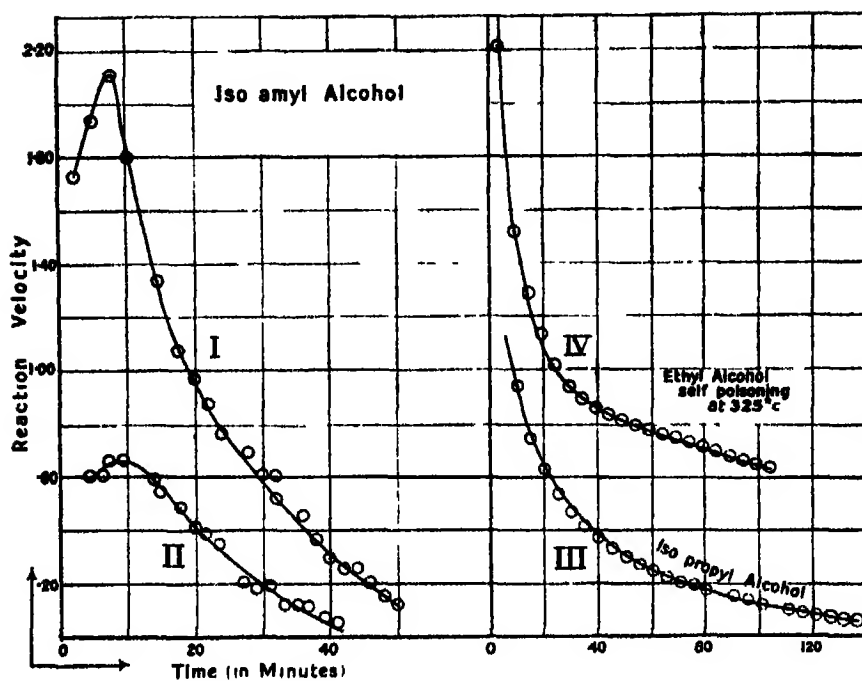


FIG 3

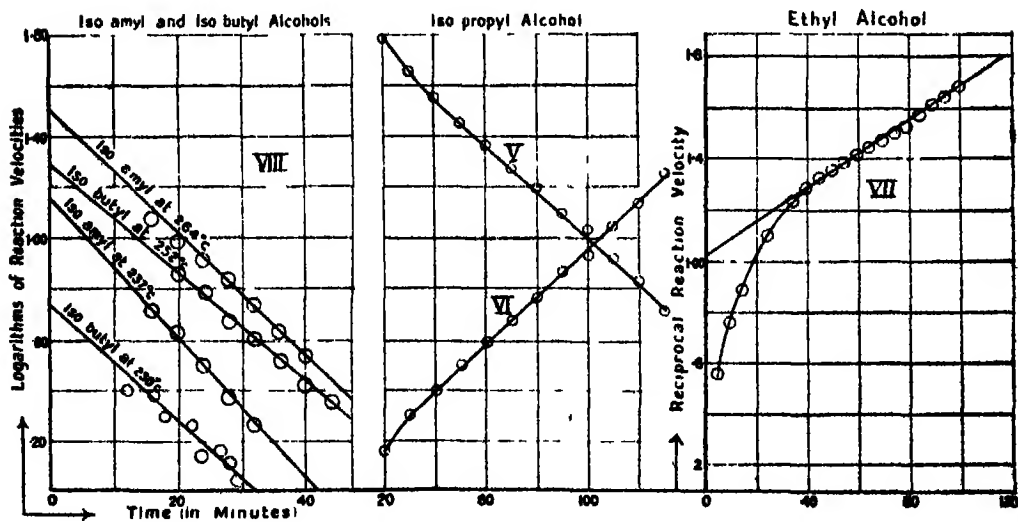


FIG 4

Table IV—Reaction Velocity

Temperature	Ethyl Alcohol	Iso-Propyl Alcohol	
		Observed	Calculated from Curve LM, fig 1.
° C			
210	0 24	1 05	—
215	0 34	1 50	2 22
220	0 43	1 96	2 84
225	0 51	2 54	3 44
230	0 70	3 32	4 32
235	0 86	4 24	5.46
240	0 99	5 31	—

Temperature coefficient at 250° C $\left\{ \begin{array}{l} \text{for ethyl alcohol} = 1.53 \\ \text{for iso propyl alcohol} = 1.633 \end{array} \right.$

Theory of the Poisoning of Catalysts.

(a) *Poisons in the Reactant*—Since the poison could not be removed by fractionation the pressure of poison in the alcohol vapour is constant during distillation

Let A = the area of the catalyst surface not covered by poison,

v = the rate of reaction at the surface

Then

$$v = \mu A, \quad (1)$$

where μ is a constant at constant temperature. But the surface A is continually being covered up by the poison from the vapour phase. Since the amount of catalyst used in these experiments is very small, the amount of poison removed from the vapour is negligible. The rate of covering of the surface is therefore proportional to the amount exposed

Hence
$$-\frac{dA}{dt} \propto A$$

But

$$v = \mu A \text{ from (1)}$$

Therefore
$$-\frac{dv}{dt} \propto v, \text{ or } -\frac{dv}{dt} = kv, \text{ where } k \text{ is a constant,}$$

i.e.,

$$\log v = -kt + c \quad (2)$$

This type of relation was found to hold for the relatively slow poisoning due to impurities in the iso-propyl alcohol, and in a modified form for iso-butyl and iso-amyl alcohols (see figs. 3 and 4)

(b) *Poisons Produced in the Reaction*—The observations of Part IV led to

the conclusion that the poisoning of the catalyst at temperatures above 280° C. was due to the bombarding of the bare surface of the catalyst by the reaction products. At constant temperature, the fraction of the exposed catalyst surface that is not covered by adsorbed alcohol, is constant.

Let this fraction be λ . Then the rate of covering the surface is proportional to λA . But the pressure of the poison is proportional to A also, and, assuming the rate of covering is proportional to the pressure of the poison, we obtain

$$\frac{dA}{dt} \propto A \times A. \quad \text{Therefore} \quad \frac{dA}{dt} \propto A^2$$

And from (1) $\frac{dv}{dt} = kv^2$, where k is constant

$$\text{Hence} \quad \frac{1}{v} = kt + c. \quad (3)$$

Owing to the assumptions made, and also to the fact that the catalyst has a finite length, this treatment is only approximate. It does show, however, that the rate of decay to be expected is much less, as the time proceeds, than would be the case with poisons present in the reactant, and the equation is in accordance with experience in the later stages of the poisoning (fig. 4, curve VII, fig. 3, curve IV). Equation (2) was tested with the impure sample of iso-propyl alcohol. The rate of poisoning was assumed independent of the temperature of the surface over a range of 20°, and the values of the reaction velocity in fig. 1 were corrected for the covering of the surface.

The corrected curve (TU, fig. 2) agrees fairly well in general character with the curve determined from pure crystallised iso-propyl alcohol, but the magnitude of the activity is 30–40 per cent in error. The method is only approximate. The sources of error were —

- (a) The assumption that the rate of poisoning is independent of the temperature
- (b) The adsorbed carbon monoxide protects the surface from poison in the early stages of the reaction
- (c) The correction for the displaced nitrogen is somewhat uncertain

The error due to (b) is serious, especially when the rate of poisoning is large. Another method was, therefore, adopted for iso-butyl and iso-amyl alcohol. This was to study the rate of poisoning at two temperatures considerably removed from one another.

Theory of the Rapid Poisoning of Surfaces

When the activity is short-lived the adsorbed carbon monoxide causes considerable depression of the activity, especially in the early stages of the reaction

Let x be the fraction of the surface covered with carbon monoxide, then the rate of removal of the carbon monoxide is proportional to the amount present. Hence

$$-\frac{dx}{dt} = ax,$$

where a is a constant at constant temperature, and the larger a the larger the rate of removal of the adsorbed gas. Therefore

$$\log x = -at + c$$

where c is an arbitrary constant, or

$$x = b e^{-at} \quad (4)$$

and b is a constant

Let A = the fraction of the surface uncovered by poison, but partially covered by carbon monoxide, then the fraction of the catalyst surface active

$$= (A - x) = (A - b e^{-at})$$

Therefore, as before,

$$-\frac{dA}{dt} = k(A - b e^{-at})$$

But from (1) $v = uA$, therefore

$$-\frac{dv}{dt} = k\left(v - \frac{b}{u} e^{-at}\right) \quad (5)$$

The time when the experiments commenced was not the instant when the alcohol first passed over the catalyst, but when the distillate first appeared in the condenser. Thus, when

$$\frac{dv}{dt} = 0, \quad \frac{b}{u} \neq v.$$

The solution to equation (5) is

$$v = L e^{-kt} + \frac{kb}{u(a-k)} e^{-at} \quad (6)$$

where L is a constant.

Since the rate of removal of carbon monoxide is much greater than the rate of covering of the surface, a is much greater than k . The equation thus takes the form

$$v = A_1 e^{-kt} + A_2 e^{-at} \quad (7)$$

where A_1 and A_2 are positive constants, and a is much greater than k

The values of v in Table V were obtained assuming $A_1 = 1.0$, $A_2 = 0.50$, $a = 0.1$, and $k = 0.01$

Table V

Time = (t)	$A_1 e^{-kt}$	$-A_2 e^{-at}$	v
1	1.000	0.452	0.548
5	0.980	0.304	0.656
10	0.905	0.184	0.821
20	0.819	0.068	0.751
30	0.741	0.019	0.722
40	0.670	0.009	0.661

The values of v show that there is a maximum in the reaction velocity, and consideration of the second term in the formula shows that this term rapidly becomes negligible. After the initial period, therefore, the poisoning progresses as if the adsorbed gas had not been present.

The predicted maximum was observed with *iso*-amyl alcohol reacting at 264°C and 237°C (fig 3), but not in the self-poisoning of ethyl alcohol at 325°C . The maximum occurred about 10 mins after the commencement of the experiment.

The foregoing considerations show that the catalyst was protected completely at first, but that no appreciable protection was afforded shortly after the maximum, the adsorbed gas being almost completely removed. Thus, the activity extrapolated from the decay curve 10 mins after the commencement will be too small, and that for the start too large, so, to obtain an approximation to the true reaction velocity, the activity was calculated for five minutes after the start.

Observations were made in this manner for *iso*-butyl and *iso*-amyl alcohol. They confirm the theoretical prediction. Fig 3, curves I and II, and fig 4, curves VIII, show also that the rate of poisoning with both *iso*-butyl and *iso*-amyl alcohol was higher the lower the temperature. This is to be expected, since the poison acts from the adsorption film, and the lower the temperature the thicker the film.

Cyclohexanol was the most difficult liquid to work with on account of its high viscosity, and also on account of its high boiling point, which caused slight local variations in temperature to have a large effect on the rate of boiling. The alcohol did not show a poisoning effect described by an exponential law, the decrease seeming irregular. The maximum value of the reaction velocity observed is given.

Table VI.—Results for Iso-Butyl Alcohol, Iso-Amyl Alcohol, and Cyclohexanol.

<i>Iso butyl Alcohol</i>		
Temperature, °C	230 0	251 9
Corrected velocity, cubic centimetres per minute	0 60	1 45
Ethyl alcohol comparison, cubic centimetres per minute	0 64	1 55
<i>Iso-amyl Alcohol</i>		
Temperature, °C.	237 2	264 0
Corrected velocity, cubic centimetres per minute	0 91	2 40
Ethyl alcohol comparison, cubic centimetres per minute	1 04	2 63
<i>Cyclohexanol.</i>		
Temperature, °C	219 1	248 7
Corrected velocity, cubic centimetres per minute	0 25	1 22
Ethyl alcohol comparison, cubic centimetres per minute	0 41	1 41

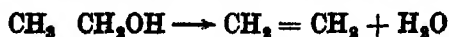
Conclusions

The rates of dehydrogenation of the primary alcohols, ethyl, propyl, butyl, iso-butyl, and iso-amyl, are all equal within the limits of experimental error, and the temperature coefficient of the velocity is the same for all. Sabatier* stated that the temperature of commencement of the reaction increased with the molecular weight of the alcohol. He neglected the poisoning effects that occur with the higher alcohols. In addition his catalyst could not be described as very reproducible. The ease of decomposition, as measured by the self-poisoning effects, increases with the molecular weight, thus confirming Sabatier's observations.

Secondary propyl alcohol reacts with a velocity about five times that of the primary alcohols, and in addition seems to have a slightly larger temperature coefficient. This is also in accord with Sabatier's observation that the temperature of commencement is much lower with the secondary alcohols.

The Mechanism of the Dehydrogenation.

Ipatiev† suggested that the production of ethylene was the



normal reaction, the aldehyde being produced by copper oxide oxidizing the alcohol, and the copper being supposed to form the intermediate oxide from the water. Sabatier* emphasised dehydrogenation as the cause of the

* 'Compt. Rend.,' vol. 136, p. 738.

† 'Ber.,' 1901, pp 596, 3579, 1902, pp. 1047 and 1057.

reaction, his chief evidence being that no trace of ethylene and water could be detected in the reaction products, and that copper does not reduce water even at 800° C

These observations also confirm his statement. Since the specific volumes of copper and copper oxide differ by about 40 per cent, the intermediate formation and reduction of the oxide at the surface of the grains would tend to shatter the structure. The activity of the catalyst was observed to remain constant for four to five hours. No shattering takes place. The hydrogen atoms are, therefore, lost directly from the alcohol molecule

Reaction occurs in an adsorption film covering the copper surface. The film becomes one molecule thick at 280° C and its thickness increases as the temperature falls. All primary alcohols contain the $\text{—CH}_2\text{OH}$ group at the end of the hydrocarbon chain. The rate of dehydrogenation has been shown to remain constant while the length of the hydrocarbon chain is doubled. It is very improbable, considering the very specific action of catalysts, that reaction could be initiated at a distance from the surface. These observations, therefore, show that the primary alcohols are adsorbed with the $\text{—CH}_2\text{OH}$ group in contact with the surface, and the hydrocarbon chains in contact perpendicular to the copper surface.

Summary.

(1) The rates of dehydrogenation of ethyl, propyl, and butyl alcohols have been compared. Direct experiment showed that the reaction velocity was the same for all. With iso-propyl alcohol the velocity was five times that of the others.

(2) One sample of iso-propyl alcohol, the iso-butyl and the iso-amyl alcohols poisoned the catalyst rapidly.

(3) An attempt to correct the observed velocity for the rate of covering the surface gave values of the right order, but 30 per cent. in error. A detailed study was therefore made of the decay curves at two constant temperatures, removed 20° to 30° C. from one another.

(4) It was deduced that for—

(a) poisons in the reactant, the law

$$\log v = -kt + c$$

should describe the poisoning; whereas for

(b) poisons produced in the reaction, the equation

$$1/v = -kt + c$$

is an approximate solution.

(5) With fast rates of poisoning correction was made for the adsorbed carbon monoxide covering the film catalyst. Investigation led to the equation —

$$v = A_1 e^{-kt} - A_2 e^{-at}$$

where A_1 and A_2 are positive constants, and a is greater than k . It was shown that a maximum was to be expected in the reaction velocity, and that an approximation to the true activity could be obtained by extrapolating the activity from the logarithmic decay curve, for a time interval after the commencement which was half that of attaining the maximum activity. The theory was confirmed by experiment.

(6) By this method it was shown that iso-butyl and iso-amyl alcohols were identical in activity (within the limits of experimental error) with ethyl alcohol.

(7) Cyclohexanol behaved irregularly, its rate of reaction being slightly less than that of ethyl alcohol.

(8) The long activity of the catalyst is further evidence in support of Sabatier's dehydrogenation mechanism.

(9) The results, taken with the probable assumption that the activated layer of molecules is uni-molecular, show that these alcohols are adsorbed with the CH_2OH group in contact with the copper surface, and the hydrocarbon chains in contact perpendicular to the surface.

The Catalytic Action of Copper. Part VI.—An Explanation of the Reproducibility of the Catalyst, and of the Periodic Change in its Activity, together with some Experiments on the Activation of the Catalyst by Alternate Oxidation and Reduction.

By F H CONSTABLE, Strathcona Research Student of St John's College, Cambridge

(Communicated by Sir William Pope, F R S —Received November 12, 1924)

The experiments of Parts I, II, III,* IV, and V,† have shown that the catalytic activity of supported copper films can be made reproducible throughout successive oxidations and reductions. Particularly was this the case during the comparison of the velocities of dehydrogenation of various alcoholic substances in Part V. The catalyst which had been reduced at 420° C showed a falling activity for several reductions at 225° C, after which the activity remained constant for almost twenty reductions. The maximum variation was about 10 per cent. In view of the random variation which is often observed in the activity of surfaces, it is interesting to attempt to discover why this film catalyst is stable under standard conditions of oxidation and reduction.

The films were activated by successive oxidation and reduction. It was thought that a study of the reaction velocity temperature curves for the dehydrogenation of ethyl alcohol during the activation might throw light on the structure of the film. The behaviour of copper films supported on copper foil has been studied by Hinshelwood,‡ and though there is still some doubt whether interference or diffraction is the cause of the colour, there seems to be little doubt that the structure is granular. He suggested that these active films have a structure "which is fine grained compared with the wave-length of light, but coarse grained compared with molecular magnitudes." The films were made active by successive oxidation and reduction. "During the activation process . . . the copper atoms are able, under the influence of surface-tension, to aggregate themselves more and more completely into small discrete units (Beilby's open formation), and the film assumes a granular structure freely permeable to gases . . . Each small unit of copper is oxidised independently,

* Palmer, 'Roy. Soc. Proc.,' A, vol 98, p. 13, vol. 99, p. 412; vol. 101, p. 178.

† Palmer and Constable, *ibid.*, vol 106, p. 250, and vol 107, p. 255.

‡ Hinshelwood, 'Roy Soc. Proc.,' A, vol 102, p. 318

and the extent to which it is converted to oxide determined the colour of the diffracted light. It is suggested that, while in oxidation each existing granule is gradually converted into oxide, reduction necessitates the growth of fresh granules, which grow about nuclei of copper, so that the film is an assemblage of growing granules of copper and diminishing granules of oxide."

There is a considerable amount of qualitative and quantitative evidence showing that reduction occurs about copper nuclei.* It does not seem obvious, however, that reduction necessitates the growth of fresh granules of copper in the case of these thin films. The reproducibility of the catalytic activity suggests that the original structure was reproduced. The structure was very open. Assuming the density of copper to be 8.95, and that of copper oxide 6.35, then there is a grain expansion of 41 per cent. on oxidation.

It is probable that the oxide grains so formed are only in contact with each other over a small area, the structure still remaining fairly open. This view is confirmed by some observations of Pease†. He has shown that a reduced copper catalyst may be heated to 350° and 400° C. without any marked change in activity, whereas a temperature of 450° C. is necessary to cause destruction of the activity. Beilby has shown that the annealing temperature of massive copper is about 230° C. This temperature is sufficient to facilitate the growth of some grains at the expense of others. The observations of Part IV show that a constant catalytic activity is maintained at temperatures ranging from 230° to 280° C., hence the effect of intergranular diffusion is very much reduced. The grains, therefore, only touch over a very small area, and sufficiently rapid growth can only occur when the high temperature of 450° C. is reached.

The volume of a grain of reduced copper is considerably less than that of the oxide from which it was formed, thus the existence of two growing nuclei separated by some distance in one grain will cause the splitting into two smaller grains, since the mass of copper now between the two nuclei is insufficient to join them. This process, by decreasing the size of the grains, increases the total surface and therefore the activity of the catalyst.

It was thus essential to attempt to obtain growth starting from the centre of the crystal grain. Since oxidation proceeds from the outside inwards, the selection of a long time for oxidation should achieve this end, the nuclei being situated very near the centre of each crystal grain. Experiment showed that four hours' oxidation at 300° C. gave the necessary conditions. By selecting

* Pease and Taylor, 'J. Amer. Chem. Soc.', vol. 43, p. 2179; Palmer, 'Roy. Soc. Proc.,' A, vol. 103, p. 454.

† 'J. Amer. Chem. Soc.', vol. 45, p. 1196 (1923).

identically the same conditions for oxidation each time, the same statistical distribution of nuclei can be ensured.* The cause of the reproducibility of this film catalyst is therefore two-fold —

- (a) The persistence of the granular structure through oxidation, which is assisted by the china-clay support,
- (b) The standardisation of the conditions of oxidation.

As the temperature of reduction was raised, a periodic variation was discovered in the activity of the catalyst. There are two factors which may change. The size of the individual grain. and hence the total surface exposed. and also the nature of the surface. There is evidence that both change. After reduction at high temperature, the value of the activity at successive constant temperature of reduction slowly falls without any corresponding change in the temperature coefficient, hence the grains were slowly growing.

In general as the temperature of reduction was raised the temperature coefficient of the reaction changed also. This cannot be accounted for by any mere change in the surface area exposed. It is necessary to conclude, therefore, that the nature of the surface has changed also. The problem thus turns on the nature of each individual grain. Whatever change that occurs is caused by the increasing temperature of reduction, and this has two effects on the factors governing the production of the grains. It increases the rate of growth of the nuclei, at the same time increasing the rate of intergranular diffusion. Both factors increase exponentially with the temperature, but the second probably does not come into consideration below 400°C , since Pease has shown that one hour's heating at this temperature has no marked effect on the catalytic activity.

The nature of the surface of the grains must change. There are three possible types of change in the grains themselves. —

- (1) Due to mixtures of the amorphous and crystalline states.
- (2) Due to the existence of allotropic forms.
- (3) Due to the existence of a definite orientation of the crystal grains at the lower temperatures breaking up as the temperature of reduction rises.

It may be that all these states occur together in the grains, but it is difficult to obtain evidence of the first two changes.

* Catalyst poisons were found not to affect the reproducibility. They cover the outside of the grains and are oxidised away very rapidly before the copper is attacked. The poisons met with were all capable of oxidation in this manner.

A preliminary experiment showed that a copper surface which had been polished with rouge had no appreciable activity on ethyl alcohol between 220° and 300° C ; hence the vitreous-flowed layer, which covered the surface, had a very small, if any, catalytic activity. There is considerable doubt, however, from the point of view of X-ray analysis, whether the amorphous state exists at all in such a layer, the reflections being as strong as those from ordinary crystalline copper *

If allotropic modifications exist, it is remarkable that they have not been observed in other connections. Cohen and Helderman† reported that copper had a transition temperature of 71.7° C, and that the transition temperature depended on the previous thermal history of the metal, and therefore more than two allotropes exist. In 1916 this was adversely criticised ‡. X-ray analysis shows no evidence of allotropic change.

On the other hand, the existence of a definite orientation in thin films of gold, silver, and copper, has been placed beyond doubt. With copper leaf the grains are orientated so that a cube face lies approximately in the plane of the leaf. As the leaf is heated this arrangement is gradually destroyed, being replaced by a random arrangement of the small crystals. Similar results were obtained with thin films of metals on glass, the transparency marking the change in orientation *

In the case of the films used as catalysts it is probable that some change in the orientation of the crystal grains took place as the temperature of reduction was increased, the grain structure being fixed at the instant of reduction and persisting at the temperatures used in the dehydrogenation. The cause of the catalytic decomposition is located in the electrostatic and electromagnetic fields at the lattice surface, and these fields change with the orientation of the grain. Some of the surface planes are more effective than others in promoting chemical decomposition. All cannot be effective, since both pure electrolytic copper and copper annealed at temperatures above 450° C are inactive. The faces on which there is the closest packing of atoms are usually cleavage planes, the fields of force between successive layers being here the weakest in the crystal. Conversely, the faces with the most open packing are those with the most intense field perpendicular to them. For chemical reaction to take place it is necessary that there should be a

* Private communications from Dr. G. Shearer.

† 'Proc. K. Akad. Wetensch. Amsterdam,' vol. 16, p. 628 (1913), vol. 17, p. 60 (1914).

‡ Burgess and Kallberg, 'J. Washington Acad. Sci.,' vol. 5, p. 657 (1916).

number of alcohol molecules each situated over some definite arrangement of copper atoms, giving a field which facilitates the release of two hydrogen atoms from the molecule. This particular arrangement of the adsorbed molecule in relation to a definite group of atoms in the surface has been called a "Reaction Centre". It has been discussed in other connections. The catalytic activity is thus influenced both by the exponential activation factor and by the density of the reaction centres on the surface. These factors are capable of independent variation. Both factors, however, will depend on the packing of the alcohol molecules on the surface as well as the actual distribution of the atoms of copper, and, therefore, the fields of force at the crystal face.

It is interesting to calculate the number of atoms of copper lying beneath one adsorbed alcohol molecule. The experiments of Part V have shown that the alcohol molecules are adsorbed with their hydroxyl groups in contact with the surface, and the hydrocarbon chains packed perpendicular to the surface. The work of Muller and Shearer,* and of N. K. Adam† has shown that the hydrocarbon chain fits into a space cell of dimensions $4.1 \times 3.7 \text{ A.U.}$ The closest packing of the alcohol molecules occurs when the cylinders of influence of the hydrocarbon chains are in contact. Copper crystallises in the cubic system, having a face-centred cubic lattice with a constant of 3.60 A.U. From these data the average number of copper atoms whose centres lie beneath an adsorbed alcohol molecule has been calculated for the three main planes of the crystal.

Face	Cube (100)	Dodecahedron (110)	Octahedron. (111)
Relative density of atoms in face	1.00	0.707	1.154
Number of atoms per alcohol molecule	2.34	1.66	2.70

A portion of the cube face has been drawn (fig. 1) showing the meaning of the fraction 2.34. No alcohol molecule has less than two atom centres beneath it. The majority have two, less have three, some have four, but none have five. The figure illustrates that for some particular face the size of the hydrocarbon chain fits the pattern on the surface. If this surface also presents the requisite

* 'J. Chem. Soc.', vol. 123, pp. 3152 and 3156 (1923).

† 'Roy. Soc. Proc.', A, vol. 101, p. 516 (1922); vol. 103, p. 676 (1923).

field, giving a low "heat of activation," it is obvious that rapid reaction will occur on this face

Probably there is more than one face on which reaction occurs. Such faces

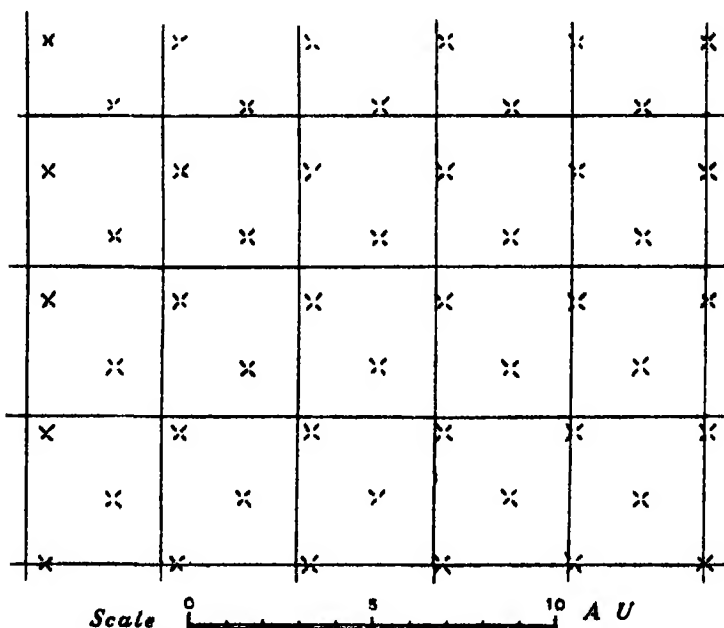


FIG. 1 —The Space Cells of the adsorbed alcohol molecules drawn over the centres of the copper atoms for the cube face

may be defined by the reaction centre density on them. It appears that there are maxima of activity corresponding to several values of the atom density on the surface.

As the temperature of reduction rises the orientation of the crystal planes exposed on the surface of the grains also changes. Each grain exposes a closed surface, and thus the lattice structure develops various faces, some of which will predominate. The edges of intersection of the faces will most probably be blunted, as the intermolecular forces are of large magnitude at the surface of such small particles. The whole exposed surface is thus made up of a large number of individual crystal faces, together with that random arrangement of atoms at the rounded intersection of the various planes, which probably results in the production of amorphous material. The small areas of contact between individual grains are most probably associated with metal that is neither in the state of orientation in the one grain nor in the other, and which is therefore probably amorphous. Since some crystal planes are more

active than others, a periodic variation will be noticed as the orientation changes from the initial to the final state

If the reaction centre density on the active faces is of the same order of magnitude, then the activity is mostly influenced by the value of the "heat of activation", hence the variation of the critical increment in the opposite sense to the reaction velocity also receives explanation

Some Experiments on the Activation of Supported Copper Films

Hinshelwood's* experiments on the activation of copper films on copper foil show that very considerable increase takes place in the rate of oxidation of these films as the number of successive oxidations is increased. A maximum activity is reached, after which a slow decrease in activity takes place. The experiments suffered from the disadvantage that it was not possible to say with certainty whether more and more massive copper was attacked. He suggested that the films should be supported on an inert substance.

As the films used in Part IV of this work were so supported, and useful information might be obtained concerning their structure, a study was made of the connection between the number of oxidations and reductions and the temperature-reaction velocity curves for the dehydrogenation of ethyl alcohol by this film catalyst.

The catalyst was prepared as described in Part IV. The films were all oxidised and reduced at a constant temperature of 320° C. to ensure that the reduction should be always complete, and in order to confirm the high value for the temperature coefficient found in the previous experiments at this temperature of reduction. For each oxidation, and between each experiment, the oxidised catalyst was kept at 320° C., the temperature being only allowed to fall to 200° C. immediately before making the reaction velocity temperature measurements. The working range was from 220° to 250° C. Heating and cooling curves were obtained, the methods of experiment being precisely those of Part IV. Overlapping occurred as before. A smooth curve was drawn through the points so obtained, and the values of the reaction velocity were read off for every 5° C. These values are shown in Table I. The family of curves were then plotted from these values. This method was adopted owing to the great difficulty in plotting the observations, due to the fact that after the first reduction the curves practically overlap, and the confusion of observations from individual curves is very great. The curves obtained are shown in fig. 2. The result of plotting $\log_{10} v$ against $1/T$ was a family of straight

* *Loc. cit.*

Table I

No of oxidations and reductions	1	2	3	4.	5	6.
Temperature °C.	Reaction velocity*					
220	0 33	0 49	0 53	0 59	0 57	0 53
225	0 44	0 64	0 67	0 74	0 72	0 67
230	0 55	0 83	0 87	0 93	0 90	0 87
235	0 69	1 04	1 12	1 18	1 13	1 11
240	0 85	1 28	1 37	1 45	1 40	1 35
245	1 06	1 58	1 74	1 82	1 77	1 71
250	1 29	1 96	2 22	2 34	2 27	2 19

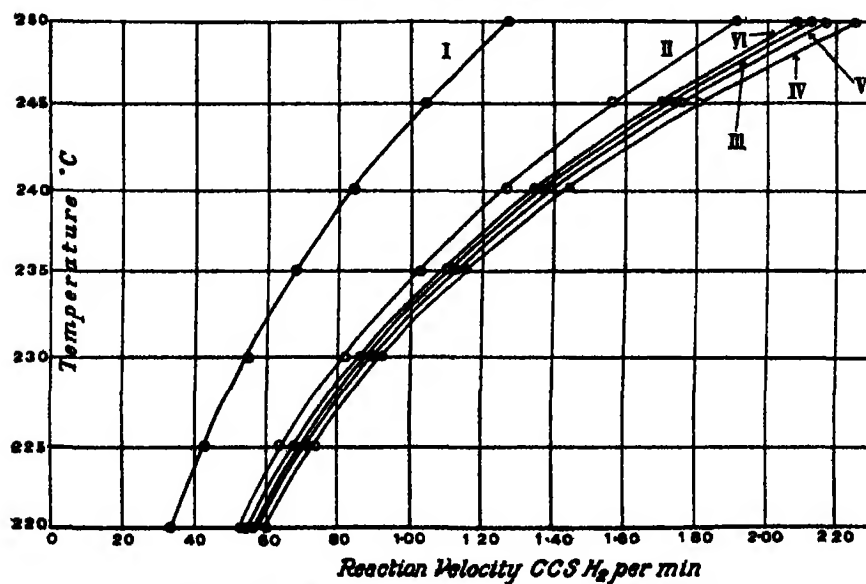
* Ccs H₂ per min at 16° C and 760 mm

FIG 2—Successive oxidations and reductions at 320° C.

lines. The values of the temperature coefficient, and also the heat of activation so deduced, are shown in Table II

Table II

No of oxidations and reductions.	Temperature coefficient (240° C)	Heat of activation in calories per gram-molecule
1	1 550	23,230
2	1 564	23,710
3	1 563	23,670
4	1 563	23,590
5	1 564	23,710
6	1 562	23,330

Discussion of Results

There is a marked increase in catalytic activity at the second reduction, after which the activity rises and then falls slightly. The curves for the third to the sixth reduction illustrate the reproducibility of this film catalyst. The temperature coefficient observed is constant, its high value is in agreement with the one already found, and its constancy shows that the nature of the surface reaction centres is practically unaltered, but the total number present is increased. Thus the nature of the surface is probably unchanged in the activation process, only the area being increased. The catalyst practically attained its full activity at the third reduction, the increase being only 75 per cent of the initial activity.

Hinshelwood found a very much larger increase for copper foil. This would be expected. The supported films have a granular structure before they are reduced, whereas the structure of the massive copper has first to be attacked and the film so formed broken down to a granular structure.

These experiments suggest that the final grain structure is attained after the third reduction, and then persists. This persistence was marked at the end of the experiments in Part V. The results are in agreement with the theory put forward in the first part of this paper.

My thanks are due to Mr W. G. Palmer for a criticism of this paper, and to Dr G. Shearer, of the Royal Institution, for evidence concerning the structure of films obtained by X-ray methods.

Summary.

(1) The reproducibility of the catalyst at constant temperature of reduction is attributed to the persistence of the granular structure throughout oxidation and reduction, assisted by the fireclay support and by standardising the conditions of oxidation. Activation experiments support this view.

(2) Chemical reaction only occurs when the alcohol molecule is adsorbed over a characteristic arrangement of copper atoms. This arrangement has been called a reaction centre.

(3) The catalyst surface exposes many crystal faces, as well as some amorphous material.

(4) There is a large variation in the number of atom centres lying beneath one adsorbed alcohol molecule on various faces of the crystal, it is thus probable that the density of reaction centres varies also.

(5) The periodic variation may be explained as due to a periodic predomination of more active planes in the surface.

(6) Two factors, at least, control the activity of the surface the value of the heat of activation and the reaction centre density. If the latter is of the same order for all the types of faces exposed, then the heat of activation plays the greater part in deciding the activity of the surface. Thus, the variation of the temperature coefficient in the opposite sense to the activity is also explained

The Catalytic Action of Copper Part VII.—A Study of the Effect of Pressure on the Rate of Dehydrogenation of Alcohols

By F. H. CONSTABLE, Strathcona Research Student of St. John's College, Cambridge

(Communicated by Sir William Pope, F.R.S.—Received November 12, 1924)

The assumption that reaction occurs in a uni-molecular film covering the surface of the copper can be tested by studying the effect of pressure on the change. If all the adsorbed molecules can react, then increasing the pressure should increase the thickness of the film, and therefore the reaction velocity. If the molecules only react in the uni-molecular film next to the catalyst surface, then varying the pressure only effects the change in so far as affects the life of a molecule in the surface layer. This effect is known to be small. Hence the reaction velocity should be practically independent of the pressure, provided the catalyst is completely covered with the adsorbed alcohol film. At low pressures the velocity would be expected to fall with pressure, since the surface is not completely covered. However, since the aldehydes are known to poison the bare copper surface, it is desirable to avoid very low pressures in the experimental work.

Experimental.

Since it was expected that the reaction velocity would be almost independent of the pressure, the composition of the distillate will be nearly constant and, therefore, will exert a constant vapour pressure at constant temperature. If, therefore, an evacuated system comprising the boiler, the reaction tube and the condenser, be shut off from the atmosphere, the increase in pressure in

the apparatus will be wholly due to the hydrogen produced in the reaction. The rate of rise of pressure thus gives the reaction velocity at the pressure measured.

The back diffusion of the reaction products must be prevented, as this will slow down the rate of reaction at the catalyst surface, and also increase the apparent volume of the apparatus. Both are serious errors, and were guarded against by inserting a trap and using the largest possible rate of boiling.

The pressure that could be used was restricted to the range 0 to 2 atmospheres by the strength of the glass boiler. The apparatus (see fig 1) was made of

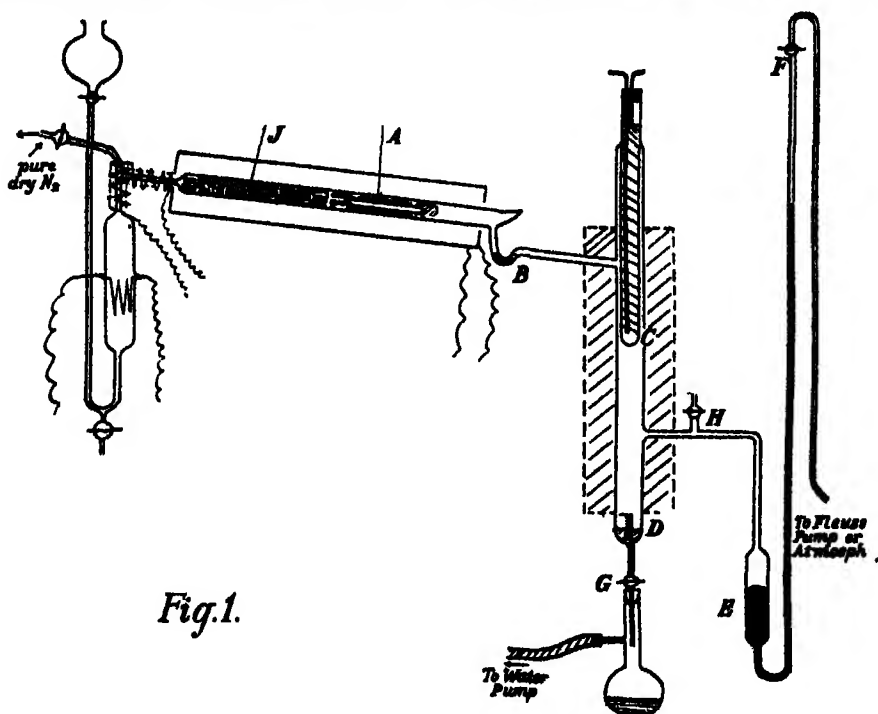


Fig.1.

glass throughout. As constancy of temperature only was desired, a new reaction tube was used that could be constructed completely of glass, the tube being packed with glass beads to heat up the alcohol vapour before it reached the catalyst. The temperature of the superheating coil was also increased. The catalyst rods A were packed symmetrically round a sealed-off glass tube in the centre of the reaction tube, and were prevented from slipping on the side furthest from the boiler by a pad of glass-wool. The bend in the tube B contained alcohol, and was used as a trap to prevent the back diffusion of hydrogen. The condenser was specially designed with a large gas space CD,

and was lagged with cotton-wool. In this space the hydrogen accumulates. The pressure gauge E was constructed with a tap F at the top. By evacuating at F with the Fleuss pump pressures from 0 to 1 atmosphere could be measured, and by opening the tap F the range was from 1 to 2 atmospheres. The gauge had the disadvantage that when the mercury ascended the tube the volume of the apparatus was slightly increased. This was corrected for by allowing alcohol to remain in the condenser at D. A scale was placed on the glass showing the required level of alcohol for each 10 cms. on the mercury manometer.* The tap G communicated with a flask evacuated by a water pump, into which the condensed alcohol was run five seconds before taking an observation of the pressure. The leak into the evacuated apparatus was less than 1 mm. in 12 hours.

The Method of Experiment

The furnace was kept at a constant temperature in the neighbourhood of 250° C. The copper oxide was reduced by carbon monoxide let in through the tap H. Alcohol was run into the boiler, and the apparatus slowly evacuated till the liquid boiled. The tap H was then shut and the alcohol electrically heated.

It was found by preliminary experiments that unless the rate of boiling is considerable the increase of pressure will ultimately stop the boiling almost completely. The reaction velocity falls off rapidly if the rate of boiling falls below some limiting value, hence it is very important to have as large a rate of boiling as is conveniently possible. Rapid boiling also assists the complete removal of hydrogen from the reaction tube. The trap also works more effectively under these conditions.

Readings of the pressure were taken every 2 minutes. At the end of each experiment the internal pressure was let off by opening the tap H, momentarily stopping the boiling current to do so, and the rate of rise of pressure was again measured for a short time. By this means it was easy to test whether poisoning had occurred (*cf.* experiments on ethyl alcohol, Table I, p. 284).

The Results of the Experiments.

The mean pressures, and the increment of pressure for some definite time interval, have been tabulated. The latter quantity is practically constant, but sometimes shows a tendency to fall with increasing pressure. The decrease in Table I is due to slight poisoning, as well as to a slight fall of the temperature of the catalyst surface consequent upon the rapid inflow of alcohol vapour.

* Scale calculated from the dimensions of the tubes.

A second experiment, quickly following the first, showed very little fall in the reaction velocity. When time was allowed for the conditions to settle down really excellent results were obtained.

Experiment 1 —A slow rate of boiling was used. It was observed that at the end of the experiment the boiling had almost stopped.

Time	Pressure in Centimetres of Mercury	Increase in Pressure in 6 minutes
10 36	76 + 2 08	—
10 38	7 72	—
10 40	13 82	—
10 42	19 61	17 52
10 44	25 30	17 58
10 46	30 58	16 76
10 48	35 64	16 03
10 50	40 78	15 48
10 52	45 34	14 76
10 54	49 72	14 08
10 56	53 85	13 07
10 58	57 62	12 28
11 00	60 92	11 20
11 2	64 20	10 25
11. 4	67 10	9 48
11. 6	69 80	8 90
11 8	72 02	7 80
11 10	74 14	7 02
11 12	76 20	6 40
11 14	77 72	5 72

The pressure in the apparatus was let down to 43 cms above atmospheric pressure, the rate of boiling was considerably increased, and the experiment was continued

Time	Pressure in Centimetres of Mercury	Increase in Pressure in 6 minutes.
11 19	76 + 53 85	—
11.21	59 20	—
11 23	65 08	—
11.25	71 00	17 15
11.27	76 55	17 35
11 29	81 40	16 32

The supply of alcohol in the boiler ran out, so the experiment had to be stopped. The result suggests that the cause of the decrease in reaction velocity is due to the slowing down of the rate of boiling, since when this is revived the velocity approaches its initial value. Poisoning certainly had not occurred.

Experiment 2—A much greater rate of boiling was used in the following experiments and measurements were made to ascertain the lowest pressure that could conveniently be obtained in the apparatus. The values of the reaction velocity obtained were practically constant over the whole pressure range

Butyl Alcohol

Pressure		Reaction velocity
Cms	Hg	
12	3	1.9
14	2	2.0
16	3	2.0
18	2	1.9
63		2.1
65		2.0
67		2.2

This preliminary experiment showed that the poisoning effect was not marked at a temperature of 250° C with a pressure as low as 12 cms. The final experiments with butyl alcohol were, therefore, commenced at this pressure and measurements were taken up to 2 atmospheres pressure. The reaction velocity was found to be practically constant, and hence the life of the molecule on the surface is little affected by the length of the hydrocarbon chain.

Typical Final Experiments

The temperature of the catalyst was about 250° C, a high rate of boiling was used and, except in Table I, time was allowed for the reaction tube to reach equilibrium before measurements were taken.

Table I —Ethyl Alcohol (showing poisoning)

Time	Reading of Pressure Gauge Zero = 4.5 cms	Reaction Velocity Increase in Pressure in 6 minutes	Pressure in Centimetres of Mercury
10 18	42.80	—	—
10 20	47.54	—	—
10 22	52.32	—	—
10 24	56.65	13.8	45.2
10 26	60.68	13.1	50.1
10 28	65.08	12.8	54.2
10 30	69.42	12.8	58.5
10 32	73.35	12.7	62.5
10 34	76.70	11.6	65.4
10 36	80.93	11.5	70.6
10 38	83.91	10.6	74.1
10 40	87.41	10.7	77.6
The tap F was opened 4.5 cms = 1 atmosphere			
10 41	18.85	—	—
10 43	23.15	—	—
10 45	27.00	—	—
10 47	30.70	11.9	96.3
10 49	33.68	10.5	99.9
10 51	37.25	10.3	102.6
10 53	40.42	9.7	105.7
10 55	43.80	10.1	108.6
10 57	46.91	9.7	113.6
10 59	50.00	9.6	116.7
The pressure was let down to atmospheric again			
11 00	21.11	—	—
11 2	24.80	—	—
11 4	28.80	—	—
11 6	32.10	11.0	98.1
11 8	35.48	10.7	101.6
11 10	38.62	10.8	105.2
11 12	42.20	10.2	108.6
11 14	45.41	9.9	111.9
11 16	48.47	9.9	115.0
11 18	51.8	9.6	118.5
11 20	54.8	9.4	121.6
11 22	57.7	9.2	124.6
11 24	61.4 —	9.6	128.1

Table II — Ethyl Alcohol

Time	Reading of Pressure Gauge Zero = 4.5 cms	Reaction Velocity Increase in Pressure in 6 minutes	Pressure in Centimetres of Mercury
10 44	36 60	—	—
10 46	40 91	—	—
10 48	45 30	—	—
10 50	49 76	13.2	37.5
10 52	54.35	13.4	42.6
10 54	58.78	13.5	47.9
10 56	63.41	13.7	52.5
10 58	67.81	13.5	56.6
11 00	72.00	13.2	60.9
11 02	76.61	13.2	65.5
11 04	80.92	13.1	69.8
Zero = 1 atmosphere			
11 12	26.0	—	—
11 14	31.55	—	—
11 16	35.00	—	—
11 18	39.12	13.0	107.6
11 20	43.58	13.2	112.6
11 22	48.50	13.5	116.7
11 24	52.85	13.7	121.5
11 26	57.22	13.6	125.4
11 28	61.45	13.9	130.0

Table III

Ethyl Alcohol		Butyl Alcohol	
Pressure	Reaction Velocity	Pressure	Reaction Velocity
35 cms	13.8	12 cms	16.6
↓	13.7	↓	15.5
↓	13.7	↓	15.8
↓	13.5	↓	15.6
↓	13.8	↓	16.1
↓	13.4	↓	16.3
↓	13.4	↓	16.7
↓	13.3	76 cms	16.6
76 cms	13.5	↓	16.6
↓	13.3	↓	16.6
↓	13.3	↓	16.1
↓	13.5	↓	15.0
↓	13.2	↓	14.3
↓	13.6	↓	14.9
↓	13.3	↓	15.7
130 cms	13.5	145 cms	15.9

Discussion of Results.

In these experiments the pressure was increased by as much as twelve times, while the reaction velocity with both ethyl and butyl alcohols remained

constant within the limits of experimental error. The evidence is therefore in favour of the assumption that reaction occurs in a uni-molecular film next to the catalyst surface. The formula for the reaction velocity to be tested takes the form

$$v = \frac{C S e^{h_1}}{\left\{ h - \frac{1}{RT} \right\} \sigma} e^{-e_1/RT}$$

where σ is the mean life of a molecule in the uni-molecular layer in which reaction occurs, and the other quantities are constant for the given surface at constant temperature. Hence these observations show that the mean life of a molecule in the activated uni-molecular layer changes very slowly with the pressure over the range investigated.

My thanks are due to Mr W G Palmer for his sympathetic interest and advice during these experiments.

Summary

(1) The apparatus used in the previous experiments was made of glass throughout, with a special condenser, and was shut off from the atmosphere.

(2) The rate of rise of pressure in the evacuated apparatus measured the reaction velocity, and the actual pressure in the apparatus was also known.

(3) The pressure range of 10 to 140 cms of mercury was studied, it was found that the reaction velocity with ethyl and butyl alcohols was independent of the pressure.

(4) The mean life of a molecule in the activated uni-molecular layer changes only slowly with the pressure over the range investigated.

A Centrifugal Method of Making Small Pots of Electrically Fused Refractory Materials.

By FREL S TRITTON

(Communicated by Dr W Rosenham, F R S—Received November 12, 1924)

(From the National Physical Laboratory.)

The present paper describes portion of a research on the alloys of iron, which is being carried out at the National Physical Laboratory, under the direction of Dr W Rosenham, for the Ferrous Alloys Research Committee. Papers dealing with other portions of the work have been published in the 'Journal of the Iron and Steel Institute'*

In the course of a research on the alloys of iron and oxygen, it became necessary to hold two immiscible layers of molten iron and iron oxide at a temperature of $1,540^{\circ}\text{C}$. It was not found possible to hold the liquid oxide at this temperature in any pot made by bonding together previously shrunk refractory material in the usual manner, such refractories as were not directly attacked became "wetted" by the oxide, which was absorbed and ran out through the pores of the pot. Experimental melts of very small quantities of oxide were made in small hollows in pieces of solid fused magnesia having a glazed surface, these showed practically no absorption of the oxide by the magnesia. Attempts were therefore made to produce a pot of pure magnesia, having an inner surface completely glazed by fusion, in the heat of an electric arc. The experiments were ultimately successful, and a method has been developed for making well-shaped pots having a glazed internal surface of fused material not only in magnesia (M P $2,800^{\circ}\text{C}$), but also in alumina (M P $2,050^{\circ}\text{C}$), zirconia (M P $2,700^{\circ}\text{C}$) and tungsten metal (M P $3,300^{\circ}\text{C}$). The time required to produce a pot (having procured the material to be fused in the form of a powder) is about 15 minutes, the time of actual fusion under the arc being about 2 minutes. Two views and a vertical section of magnesia pots made by the method to be described are shown in fig 1 (p. 288).

For making these pots it is necessary to use refractory material which has previously been fused, so as to reduce the shrinkage to a minimum. If the material has not been completely shrunk by previous fusion, large shrinkage cavities occur in the walls of the pot. The previously fused material is

* "Ferrous Alloys Research," Parts I, II and III (1924) II

crushed and ground to pass a 60-mesh sieve The tendency of the pot to crack during cooling appears to be greatly decreased by the use of pure materials

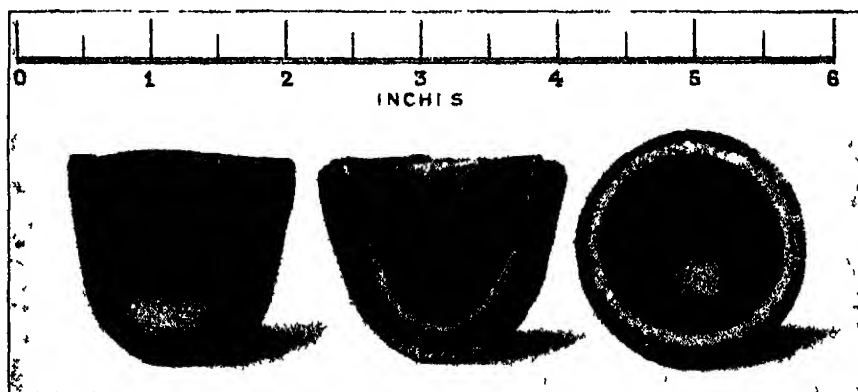


FIG 1.

The arrangement adopted for making the pots is shown in fig 2 and illustrates the apparatus ready for striking the arc This arc is used to fuse the refractory powder, while centrifugal force assists the formation of the pot

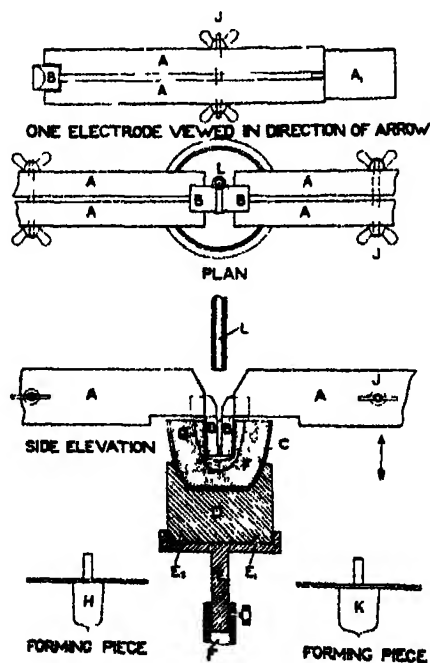


FIG 2 —Scale (approx) one-sixth

The apparatus consists of two split graphite electrodes AA, which are capable of horizontal adjustment. Each of these electrodes holds a smaller graphite rod BB of special shape, by means of pressure applied to the split electrodes AA by tightening the screws J. The ends A₁ of electrodes A are clamped into suitable cable sockets. When the apparatus is working an electric arc is struck and maintained between the two electrodes BB. These small electrodes burn away rather quickly and a fresh pair are required for the production of each pot. The powdered material to be fused is placed in the silica cup C, which is cemented into the graphite block D, as a convenient method of fitting it into the cup holder E, which can be rotated by suitable means, at various speeds. The cup and its mounting rest on holder E and are keyed to it by means of two pins E₁ and E₂.

Having placed the material to be fused in cup C (which is removed from the holder E for the purpose), a deep central depression is made in the refractory powder by pressing into it the aluminium forming piece H, this compresses the powder into a firm mass level with the top of the cup C, and at the same time moulds into it the central depression into which the electrodes BB fit quite closely. Vertical adjustment is provided by sliding the holder E into tube F. The apparatus is now ready for striking the arc. The cup C is made to rotate at a speed of about two revolutions per second, and the electric arc is struck by a horizontal movement of electrode A, causing the lower points of electrodes BB to make contact. The electric current maintaining the arc is increased, together with the speed of rotation of cup C, until the heat generated by the arc is sufficient to melt the refractory powder nearest to it. When this heat has been attained, the central depression in the refractory slowly assumes a parabolic form, as shown by the dotted line G. When sufficient material has been melted, and the size of the pot is seen to be correct, the arc is switched off and the pot allowed to cool down. The usual time taken to melt the refractory is about two minutes, and the final speed of rotation of the cup is approximately eight revolutions per second. Using 50 volts the energy required to make a pot having a capacity of approximately 15 c.c. is about 50 k.v.a., but this varies very much with the melting point of the refractory to be fused.

The arrangement just described applies to pots made of magnesia, which does not readily form carbides at high temperatures. In making pots of alumina or zirconia, special precautions must be employed to keep the molten refractory in an oxidising atmosphere, owing to the readiness with which these refractories form carbides. When fusing the latter materials a stream

of oxygen is blown between the electrodes and the refractories to be fused, through tube L, which is made of magnesia. This is found to be quite effective in stopping the production of carbides. If any carbide is formed the refractory may swell up and come in contact with the electrodes, which will be broken and impede the rotation of the cup. It is, therefore, necessary to have sufficient space between the electrode and the refractory to allow the free entry of oxygen. A former K of larger diameter than is necessary with magnesia is, therefore, employed when fusing refractories tending to form carbides.

The surface tension of the liquid refractory appears to play an important part in determining the thickness of the fused layers, alumina forms a naturally thick layer, and magnesia a very thin one. The thickness of the fused layer also depends on the amount of refractory material that is fused, and is governed in the present apparatus by the life of the electrodes BB, which are burned away in about two minutes.

The process of fusing any material in the form of a powder while subjecting it to centrifugal force, in a manner similar to that used for the centrifugal casting of liquid metals, appears to be capable of extension to the manufacture of pots of much larger sizes, and to tubes of refractory materials or metals of very high melting point.

On the Precise Measurement of the Critical Potentials of Gases

By E G DYMOND, B A , St John's College, Cambridge

(Communicated by Prof Sir E Rutherford, F R S —Received November 12, 1924)

Introduction

The aim of this research has been to attempt to increase the accuracy with which the measurement of the critical potentials of gases can be made, and so bring about a closer confirmation of the numerical relationships of the quantum theory. We must first examine the factors which have limited the accuracy of previous measurements, and then see by what means we may increase the precision of these determinations.

In all methods in common use the critical potentials are determined from singular points in the current-voltage curves of the apparatus. These points in the case of the Lenard and allied methods are upward bends or "kinks," while in the inelastic impact method of Franck and Hertz they are downward bends, that is to say, they are maxima. Were these changes ideally abrupt there would be no difficulty in fixing the critical points with great accuracy (if we ignore for the moment the question of the correction for the initial velocity of emission of the electrons and for contact potential differences), and so in conjunction with the spectroscopic evidence we could obtain independent determinations of the Planck constant h .

Unfortunately, there are two factors at least which smooth out these changes or "kinks" in the curves, first, the impossibility of obtaining an electron stream of homogeneous velocity due to the distribution, of approximately Maxwellian type, of velocities of emission from the glowing source, and second, a factor which has only recently been recognised, the fact that the probability of an electron of sufficient energy exciting or ionising an atom is not constant but rises from zero, when the electron has only just the requisite energy, to a maximum value, when it has some higher value. This probability will be denoted for brevity by $P(V)$ where V is the potential corresponding to the energy of the electron before impact. The probability that an electron shall excite or ionise in one impact will be called $p(V)$, so that

$$P(V) = np(V)$$

where n is the total number of collisions between the electron considered and the gas

The procedure which has been used, especially by Franck and Hertz, in the past in dealing with these kinks, has been to extrapolate the parts of the curve on each side of the kink, which on a large scale are nearly linear, till they meet, and to consider this intersection the required critical point. This of course is quite arbitrary and has no theoretical justification. (In the inelastic impact method the maximum of the curve has been taken with even less justification.) Leaving out of account for the moment the variation in $P(V)$ with the velocity of the electrons, we see that the point which we are most justified in taking as the critical potential is where the transition curve joins the second linear part, as here all the electrons emitted from the filament have become effective. The point where there are just sufficient electrons emitted with high velocities to register a departure from the normal curve can also be taken, if we bear in mind that its position will depend on the sensitiveness of the apparatus to record small differences of current, and also on the emission velocity distribution of the electrons.

The first step in attempting to increase the accuracy of this type of measurement would seem to be to increase the sharpness of the kinks, in other words, the sensitiveness of the apparatus, and so fix with greater precision the points mentioned. The means of doing this which obviously presents itself is to differentiate the curves.

Graphical differentiation, while rendering the bends more obvious to the eye, can plainly bring no increase in sensitivity, so recourse must be had to a type of apparatus which will directly record the differential of the current-voltage curve. This apparatus and the results from it will be discussed in the first section of this paper. A preliminary account* of this part of the work has already been published.

It was not till after these results had been obtained that the great influence of the function $P(V)$ was recognized. It is easy to see that the simple view given above of the form of the kink is not justified, for we must consider the first break-point as being the point where the quantity $P(V) \times (\text{number of fast electrons})$ becomes appreciable. As we are ignorant of the form of $P(V)$, the critical potential becomes indeterminate.

This difficulty of interpretation and efforts towards its solution, with some account of the function $P(V)$ will be considered in the second and third sections of this paper.

* Dymond, 'Proc. Camb. Phil. Soc.', vol 22, p 405 (1924)

1 *The Differentiation of the Curves*

Consider the simple Lenard apparatus. This may be made to record the differentials of its characteristic curves by the following device ---

Superimpose on the potential V_1 between the filament and grid a small alternating potential dV of frequency ω , so that the applied voltage oscillates between the values $V + dV$ and $V - dV$. The current to the plate P will accordingly oscillate between the values $I + dI$ and $I - dI$. Let now a commutator rotating with the frequency ω be placed in the circuit of P. The current, after passing through the commutator, will oscillate between $dI + I$ and $dI - I$. *i.e.*, it will consist of an alternating part I , and a unidirectional part dI . Any galvanometer whose period is large compared with ω will give a steady reading proportional to dI so that if we keep dV constant and vary V_1 the galvanometer will approximately record the differential of the $V - I$ curve, when dV is small.

It will be seen that unusually large alternating currents will be circulating in the galvanometer. It is possible to avoid this by transforming the current and then rectifying with the commutator, or by balancing out the large current by a bridge method before rectifying. The first alternative has been tried, using an intervalve transformer, from a thermionic amplifier, of lower resistance than is usual in this class of transformer. But as it was found that the simpler method first described was much more sensitive, did not damage the galvanometer (indeed the alternating portion of the current through it never exceeded 10^{-5} amp) nor caused unsteady readings with a frequency ω of 25 per second, it was adopted for permanent use.

The source of alternating potential was a potentiometer fed with current from a small battery through another commutator similar to the one used for rectification, and mounted on the same shaft with it. As one commutator was included in the circuit of a high-sensitivity galvanometer and was rotated at a high speed, the design of the contact brushes required care.

The form found most satisfactory was a thin brass strip, to the contact surface of which was soldered a sheaf of about 100 thin brass wires, diameter 0.12 mm, to ensure a large contact area. Brass gauze would doubtless have served as well, but it was not possible to obtain it in a fine enough mesh. Copper could not be used owing to the high thermo-electric effects between it and the brass segments of the commutators. These brushes required constant supervision, as the brass wires wore through rather rapidly and caused short circuits. When in good order however, the readings of the galvanometer were

free from sudden kicks, and were only subject to slow drifts of zero, which were comparatively harmless and could be allowed for. Lubricant, in the form of heavy medicinal paraffin oil, was tried to ensure steady working for longer periods. Its use seemed to have the opposite effect, so it was discarded.

Two experimental tubes were used of slightly different design. The first consisted of a tungsten filament, a cylinder of nickel closed at either end with nickel gauze to serve as grids, and a collecting plate, also of nickel. All the preliminary work was done with this tube. The range of velocities from the filament was rather wide, due to the fall of potential along it, which was about 1 volt.

In order to obtain a more homogeneous beam of electrons a second tube was constructed (fig 1). The source of electrons first tried was a sheet of thin

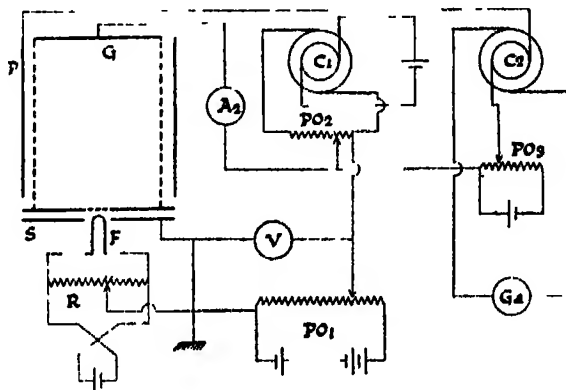


FIG 1

platinum foil, coated with oxide and heated behind by radiation from a large tungsten filament. As as much as 100 watts in this filament were found necessary to heat the platinum foil to a high enough temperature, and as a very small fraction of the electrons emitted from the very hot filament straying to the other parts of the apparatus caused very large disturbing effects, this form of source was replaced by another, which is shown in the figure. A loop of platinum foil, 2 mm wide and 0.018 mm thick, was bent into a U shape, and was coated with a mixture of Ba and Th oxides for a length of 1 mm at the end of the tip. By this means the potential drop across the portion of the strip which was actually emitting was about 0.1 volts. The "filament" F just projected through a small hole in an earthed shield S, which served to maintain a uniform field between F and the grid, and which also was used to measure the velocity distribution of emission. The centre of the filament was also earthed.

by the usual device of connecting the two ends to a high resistance R , and earthing an intermediate point.

The process of finding this point is described by Richardson and Brown * The electrons are allowed to flow across to G , with their own emission velocity without any accelerating field. If the heating current be now reversed, unless the emitting spot in the filament is at zero potential, the current to the grid will be changed.

The design of this second tube follows that used by Hertz †. The electrons make frequent collisions with the gas in the field-free space within the cylinder G , and diffuse out to the collecting plate P . As it was desired to make some subsidiary experiments on the effects of a magnetic field on the phenomena within the tube, the whole metallic part of the apparatus, with the exception of the platinum strip, was made of copper. Before assembly the metal parts were thoroughly cleaned with nitric acid. This is essential to prevent the formation of contact potentials between the various portions of the apparatus. The potential between the hot platinum filament and the copper is, of course, unavoidable. In order to facilitate the removal of the filament for repairs or alterations, it was mounted together with the shield S on a ground-glass sleeve. This was used free of all lubricant and when waxed on the outside was perfectly gas-tight. The use of this sleeve, of course, prevented the whole of the apparatus from being baked out, though all the metal parts could be subjected to treatment. But the disadvantages of having the filament inaccessible outweighed those due to the evolution of occluded gases from one end of the tube. In the process of baking out, the apparatus was inserted into the furnace to within 5 cm. of the joint, which was kept cool by a stream of water.

The general diagram of electrical connections is also shown in fig. 1. The source of potential for the main accelerating field V_1 was the potentiometer PO_1 , fed from a 40 or 80-volt battery of small secondary cells. This potentiometer in reality consisted of two, one being a fine adjustment on the other, in order to obtain steps of 0.1 volts or less. V_1 was measured on the calibrated voltmeter V . The alternating potential dV was provided by the commutator C_1 and potentiometer PO_2 . The current to the grid was measured on the microammeter A_2 , which was also connected in series with a shunted galvanometer (not shown) to record small currents. In order to take account of small variations in the emission current from the filament during a set of readings, the galvanometer (G_a) reading was always divided by the reading of the

* Richardson and Brown, 'Phil. Mag.', vol. 16, p. 380 (1908).

† Hertz, 'Proc. Roy. Acad. Amst.', vol. 25, p. 179 (1922).

microammeter, and the result was plotted. The current from the plate P passed through the commutator C_2 to the galvanometer Ga. This instrument had a sensitivity of 2×10^{-10} amp per mm at the scale distance used, and a resistance of about 1,000 ohms. Its very slow period (one minute) helped to keep the readings steady. Potentials (V_2) could be applied between P and G by means of the potentiometer PO_3 . Great care had to be exercised on the insulation of the plate circuit, as in nearly all the experiments the galvanometer Ga, the commutators, and potentiometers PO_2 and PO_3 were maintained at a potential of about 20 volts. The insulation throughout was of paraffin or freshly scraped ebonite.

The apparatus for admitting and purifying the gas presented no unusual features. Helium was chosen as the subject for these experiments, both on account of its ease of purification and because of the positive nature of the results obtained by previous workers. It was felt that a new method should be tried out on a gas on which there were abundant data already. The helium contained as impurity mostly air, with a little hydrogen. The hydrogen was removed by adding to the gas its own volume of oxygen and igniting in it a pellet of phosphorus. After admission into the apparatus by the gas manipulator the other impurities, together with any unburnt oxygen, were removed by prolonged standing over charcoal cooled in liquid air. It was found impossible to remove the H_2 line of hydrogen completely, as seen in a small spectrum tube. This requires extraordinary care in eliminating traces of water and tap grease vapours. The best test of purity was the freedom of ionisation below the ionisation potential and the constant character of the phenomena after successive repurifications.

As the metal parts of the apparatus were of copper, great care had to be taken to exclude mercury vapour from the tube. Two traps cooled in liquid air, with a tap between them, were used. The tap prevented diffusion of condensed mercury from the first trap into the apparatus overnight. A large tube filled with charcoal and cooled in liquid air was directly attached to the apparatus to remove any impurities evolved during the taking of a set of readings.

The main pumping system consisted of a condensation pump of the Langmuir type backed by a Gaede rotary mercury pump and Fleuss oil pump. This system could maintain a vacuum for purposes of baking out, etc., which was unmeasurable on the McLeod gauge, which was sensitive to 10^{-4} mm.

The baking out was conducted in a small electric furnace at 360° – 380° C. for several hours. It was not possible to glow out the metal parts in the

usual way but surface layers of gas were removed by bombardment with an intense electron stream from the filament, of 1,000 volts velocity

The inelastic impact method has been employed throughout the work. It was felt that the addition of an electrometer to a circuit containing rapidly moving contacts, such as the commutator, was undesirable when testing the possibilities of a new method. Indeed with the type of brush gear described, the irregularities introduced by it would have completely overwhelmed the effect sought, unless the electrometer were used in a very insensitive state, as they were always on the limit of measurement with the galvanometer. As the inelastic impact method is not suitable for the measurement of ionisation, because the velocity of the impinging electron after collision is indeterminate, attention has been focussed exclusively in this work on the excitation potentials. The application of the differential method to measure ionisation is identical in principle with that just described. The vindication of the differential method for excitation potentials seems sufficiently complete, so the case of ionisation has not been dealt with, especially as the more interesting problem of the interpretation of the curves supervened.

Discussion of the Results

Typical results obtained in helium are given in figs 2 and 3. Fig. 2 shows the result of the application of the normal inelastic impact method. In this

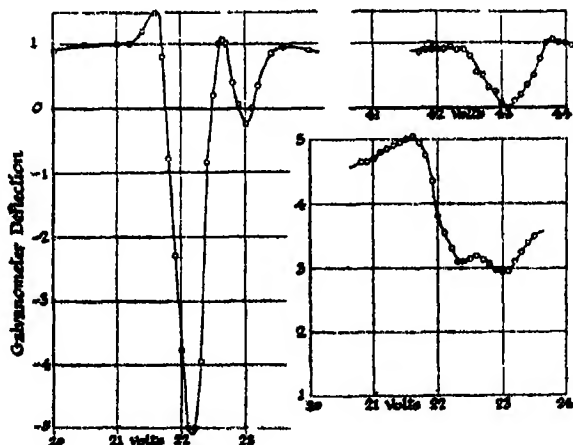


FIG 3

FIG 2

case the gas pressure was 1 mm of mercury, and the retarding potential V_r between the plate and grid was 0.5 volt. The abscissæ are uncorrected for

initial velocity and contact potential differences. The double nature of the excitation point due to the two types of excitation of helium is shown. These two points correspond to switches from the normal $1S$ (crossed orbits) state of the helium atom to the first orthohelium (coplanar orbits) $2s$ state, and to the second parahelium (crossed orbits) $2S$ state, respectively. From the optical data these should be separated by 0.8 volt. In this curve they are about 1 volt apart. Reasons for this will be discussed later.

All electrons which have made inelastic collisions with more than 0.5 volt surplus energy should theoretically not be stopped by the opposing potential, but as in practice the grid is not a perfect electrostatic shield the field V_2 must penetrate a short distance inside the "field free" space. This stray field can stop electrons of velocity greater than 0.5 volt from reaching the plate if they approach it in a slanting direction. This action will delay the recovery of the current which we should expect to be more rapid than is shown. (The imperfection of shielding of the grid must also cause the accelerating field V_1 to penetrate into the cylinder, so that electrons that have passed through the centre of the meshes of the gauze must travel some distance further before attaining their full velocity. These electrons will have a smaller chance of making effective collisions and we shall tend to obtain too high a value for the critical potential. The gauze used was of a mesh of 30 per cm and the wire was 0.3 mm diameter, so that the mesh ratio was about unity. With such a gauze this effect should be quite small, seeing that the dimensions of the cylinder were 35 mm long by 25 mm in diameter.)

The differential curve taken under very similar conditions is shown in fig. 3. The gas pressure was 1.1 mm, V_2 was 0.4 volt, the oscillating potential dV was 0.1 volt. The critical points now become very strongly marked. At first sight it looks as if this curve could fix the points with extraordinary accuracy. The maxima of the normal curves become the zero points of the differentiated curves, and these may easily be located to 0.02 volt.

We must remember firstly, however, that the maxima are not the critical points at all, they are the points where the rate of increase of the number of electrons which have collided inelastically is equal to the rate of increase of the normal current to the plate. (Although the current to the grid saturates at about 5 volts, the current to the plate continues to increase. This current is governed entirely by the diffusion outwards of the electrons from the axis of the cylinder.) We must remember also that the more important factor which renders the critical point uncertain is the correction to be applied to the readings, owing to contact potential differences and the initial velocity of

emission. These corrections are best applied by the double impact method *

If we continue to raise the potential V_1 after the first critical point is passed, those electrons which have made inelastic collisions are left with increasing amounts of energy, until a point is reached where they may be able to excite again. This point will be indicated by a second dip in the curve, and the distance between the two will give the critical potential without any complications due to contact potential differences, &c.

If the probability of single excitation is $P(V)$ that of double excitation will be $n(N - n)[p(V)]^2$, where N is the total number of collisions made, and n the number of collisions before the first inelastic impact. We see then that unless $P(V)$ is near unity the double impact point in the current curve will not be plainly marked and cannot be accurately fixed. This is shown in fig 3 where the differential of the curve at the double collision is shown on the right.

The mean distance between the break points of several sets of readings which agree to within 3/20 volt is 20.9 volts, in contradiction to the accepted value of 20.45 volts †. The spectroscopic evidence of Lyman‡, however, demands that the first excitation point should be at 19.77 volts. Franck§ gives reasons why the results of Franck and Knipping should differ from those of Lyman. Such evidence as exists goes to show that $p(V)$ for the first switch, $1S \rightarrow 2s$, which we will call the A transition, rises to a maximum a few tenths of a volt above the initial point, and then rapidly falls to a small value. (This is confirmed by the evidence brought forward in the last section of this paper.) For the second, B, $1S \rightarrow 2S$ switch however, the rise and fall are more gradual. This means that the effect due to B will far outweigh that due to A at all voltages higher than, say, 1 volt above the critical potential for A.

If in the apparatus of Franck and Knipping a potential of about 40 volts is applied, the first effective collisions begin to take place in the space between the filament and the first grid when the electron has attained about 20 volts energy, and as we have seen from the above, these collisions will result mainly in B transitions with energy loss of 20.5 volts. The electron is again accelerated and enters the space between the two grids with roughly 20 volts energy. But here the accelerating field is so small that the electron can make many collisions with substantially the same velocity. So we see that as we raise

* Franck and Hertz, 'Verh. d. D. Phys. Ges.', vol. 16, p. 45 (1914).

† Franck and Knipping, 'Zeitschr. f. Phys.', vol. 1, p. 320, 1920; Horton and Davies, 'Proc. Roy. Soc.', vol. 95, p. 408 (1919).

‡ Lyman, 'Nature', August 26 (1922), 'Astrophys. Journ.', vol. 60, p. 1 (1924).

§ Franck, 'Zeitschr. f. Phys.', vol. 11, p. 155 (1922).

the potential, at 40.3 volts collisions will occur resulting in A transitions, as here the smallness of $p(V)$ is balanced by the largeness of n , the number of collisions. Consequently the double collision point that is observed is not of AA but of BA type, and the difference between the single and double impact breaks in the curves is 20.45 and not 19.77 volts.

In the apparatus used in this work however, the distance between the filament and grid is such that very few or no collisions occur while the electron is being accelerated. It will therefore enter the second space with its full velocity of 40 volts. It has now several possibilities of losing its energy before it, but it cannot cause an A transition and pass on with nearly 20 volts energy. At 40 volts $p(V)$ must be entirely negligible. Therefore we can only hope to observe double collisions of type BB, and the distance between the break points will be 1.6 instead of 0.8 volts higher than the A excitation potential. If this view is correct we must expect to find only one break in the curve in the neighbourhood of 40 volts, and it is a fact that all efforts to find a complex structure for the double impact point, analogous to that of the single impact by the differential method, have failed.*

If the complex structure of the double impact point is not revealed by the differential method, the actual magnitude of the subsidiary critical points must be exceedingly small, for it has been found that the differential method will reveal singularities which pass quite unnoticed in the normal curves.

A good example of this is shown in figs 2 and 3 above. It will be noticed that in fig 3 the ordinate rises sharply just before the main fall. No such rise has been detected in the normal curve, and to make certain that it was not due to some new effect, the differential curve was graphically integrated. The constant of integration was adjusted to ensure that the total fall of current was the same as that in fig 2. The similarity of the two curves was very close, and affords valuable confirmation that the apparatus was working correctly.

The cause of this sharp rise is obscure, but may be connected with the effect observed by Sponer† in argon. It is known that in the rare gases very slow electrons have abnormally long free paths‡. Sponer has demonstrated this effect in a very striking way. She used an apparatus which was similar in principle to that described in this paper, with the plate and grid connected together. When the potential is raised to the excitation point of the gas in the

* I am indebted to Prof. Franck for helpful discussion of this point.

† Sponer, 'Zeit f. Phys.', vol 18, p. 249 (1923).

‡ Mayer, 'Ann. d. Phys.', vol. 64, p. 451 (1921); Ramsauer, 'Ann. d. Phys.', vol. 64, p. 513 (1921), vol. 66, p. 546 (1921), vol. 72, p. 345 (1923).

apparatus electrons with very small velocities will make their appearance, if they have abnormally long free paths they will diffuse away very rapidly. It is more probable, however, as the effect in helium is very small, that the observed rise is connected with the observation of Hertz* that slow electrons diffuse more rapidly than fast ones, independently of any variation in the free path, even in the case when there is no field

This effect of the rise of current was very marked in the first apparatus and could be seen in the normal curves. The currents used in this apparatus were considerably higher than those later employed so that the space charge and the effects due to it would be larger. It is difficult to see, however, why the effect noted should start 0.4 volt lower than the point where the arrival of the first slow electrons is indicated.

In order to explain why we find the distance between the A and B breaks to be 1 volt instead of 0.8 as previously mentioned, we must turn again to the supposed forms of the $p(V)$ curves for these two transitions. For the first one the rise is sharp, for the second it is more gradual. Now in the differential curves shown in fig. 3 the retarding potential is 0.4 volt—that is to say, we are measuring electrons which have collided elastically over a velocity range of 0.4 volt over the critical potential. We therefore see that due to the slower rise of the probability for the second type of collision it will make its appearance in this case later than it would were the excess energy of the colliding electrons only 0.1 volt or less.

If we accept the conclusion that the experimental result found is 1.6 volt higher than that of the true excitation potential, we shall obtain a value for this of 19.6 volts, compared with 19.77 volts as found spectroscopically by Lyman. As will be shown in the second section, however, we cannot say by mere inspection of the curves what point we are to take as representing the critical velocities, so that the agreement is surprisingly good.

II The Interpretation of the Critical Regions of the Curves.

We will now make a more detailed investigation into the form to be expected of the characteristic curves in the Lenard and inelastic impact methods, and from them attempt to derive the precise position of the critical potentials.

Let the potential applied to the apparatus (ignoring contact potentials) be V . Due to the velocity of emission the electrons will have velocities greater than this. If $p(u)du$ is the number of electrons emitted from the filament per second with velocities between u and $u+du$ measured in volts, this number will also

* Hertz, 'Verh. d. D. Phys. Ges.', vol. 19, p. 273 (1917)

represent the number of electrons which after acceleration by the field will have a velocity in the range $V + u$ to $V + u + du$ (This is not rigorously true, as the field being uniform increases one component only of velocity and leaves the other two unchanged. It is known that under these conditions the final distribution about the mean resultant velocity is not Maxwellian; but a solution of the problem of what this distribution is has not been obtained.)

Let $P(V)$ as before be the probability that an electron of velocity V (in volts) shall in its course through the apparatus excite an atom. Of course we have

$$P(V) = 0,$$

when $V < V_0$, where V_0 is the critical potential.

The total number of effective impacts per second will be

$$N = \int_{V_0-V}^{\infty} P(V+u) \rho(u) du \quad (1)$$

If the variation of N with V is known, together with the form of $\rho(u)$ and the excitation potential V_0 , the equation (1) may be regarded as an integral equation in P , but to determine both P and V_0 we must proceed differently.

In the experiment of Hertz* previously mentioned the number of electrons which are stopped by a small retarding field between the plate and grid is measured. In other words, the number of effective impacts by electrons whose velocities range from V_0 to $V_0 + \delta$, where δ is the retarding potential, is determined. This number is accordingly

$$y = \int_{V_0-V}^{V_0+\delta-V} P(V+u) \rho(u) du \quad (2)$$

We can by applying first a potential δ_1 and then δ_2 find the number of effective impacts by electrons in a range of velocities from δ_1 to δ_2 above the critical velocity. Put analytically we measure

$$\Delta y = \int_{V_0+\delta_1-V}^{V_0+\delta_2-V} P(V+u) \rho(u) du \quad (3)$$

If we take $\delta_2 - \delta_1$ small enough we may consider P as being linear within this range, so we have

$$\Delta y = P(V_0 + \delta) \int_{V_0+\delta_1-V}^{V_0+\delta_2-V} \rho(u) du \quad (4)$$

Now the integral represents the area in the velocity distribution curve between two ordinates $\delta_2 - \delta_1$ apart. As V_0 is unknown we do not know where on the curve they lie. If we vary V , the form of Δy will be precisely the form of the

* Hertz, 'Proc. Roy. Soc. Amst.', vol. 25, p. 179 (1922).

variation of this area as we move our two ordinates along the distribution curve. Consequently, by comparing the curve between Δy and V with that between the area and u , as determined directly from $\rho(u)$, we shall determine the position of V_0 relative to V .

The duplicity of the critical point in helium complicates the analysis of the curve by the addition of a second probability factor. That is to say, we must replace $P(V)$ by $P(V) + P^1(V)$ throughout. If we remember, however, that

$$P^1(V) = 0, \text{ for } V < V_0 + 0.8$$

$$P(V) = 0, \text{ for } V < V_0,$$

we see that if we only work a few tenths of a volt above V_0 , the second function $P^1(V)$ will not interfere.

The arrangement described in the previous section to differentiate the ordinary current-voltage curves can easily be modified to give Δy as a function of V . To do this we have to apply between the grid and plate a potential $\delta \pm h$, where $2h = \delta_2 - \delta_1$, just as previously we had to apply between the filament and grid a potential $V \pm dV$. We accordingly remove the potentiometer (PO_2 in fig. 1) and insert it in the plate circuit to provide the oscillating potential $\pm h$. The rest of the apparatus stands as before.

In order to carry out the analysis described above it is necessary to know the form of the velocity distribution curve $\rho(u)$. This was done by the method used by Richardson and Brown,* in which the number of electrons flowing from the filament under the influence of small retarding potentials is measured. The ordinate at any point on the observed curve between current and retarding potential represents the number of electrons which have velocities greater than that represented by the abscissa, that is to say,

$$n = \int_u^\infty \rho(u) du, \quad \text{or} \quad \rho(u) = \frac{dn}{du} \times \text{const}$$

Hence the area-difference to be plotted can be replaced by the difference of the ordinates of the observed curve. The function of the shield S in fig. 1 now becomes apparent. We wish to measure the energy distribution of the electrons, not, as in the case of Richardson and Brown, that of the component of velocity normal to the grid. It is not possible to do this exactly, but we can approximate by connecting the shield to the grid so that the retarding field has some measure of spherical symmetry. The approximation is, of course, not very exact, but errors in $\rho(u)$ will have only second order effects on the critical potential.

* Richardson and Brown, 'Phil Mag.', vol 16, p 360 (1908).

The general form of the curves obtained for Δy is shown in fig. 4. The data in this case are gas pressure 1 mm, retarding potential $V_2 = 0.4 \pm 0.1$ volt.

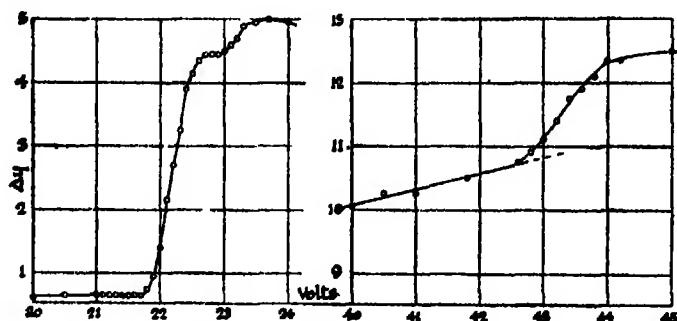


FIG. 4

For the same reasons as mentioned above, the distance between the two excitation points is not 0.8 but 1.2 volts

The retarding potential has a small effect on even fast electrons if they enter the space between the two cylinders obliquely, this is shown by the small deflection before the critical point is reached. It is however very nearly constant and can be easily allowed for.

The effect due to the double impact is small, as might be expected with this method. When the velocity of the electrons is near 40 volts the amount of ionisation is considerable, there are consequently many electrons present with indeterminate velocities, and also positive ions which are attracted to the plate by the field V_2 . The rise in the current due to the double impact is superimposed on a large effect due to ionisation and amounts only to 10 per cent of the total current.

For this reason it has not been found possible to effect an analysis of the curve due to double impacts. It will be noticed that the difference of the two "break" points is 20.9 volts (a value consistently repeated), agreeing closely with that found in the previous section by the differential method. We have no right to assume that this represents the excitation potential, as the position of the break point depends on the sensitivity of the apparatus to indicate small differences in current. If we alter the scale of the curve we shall alter the apparent position of the break point, and the scales of the single and double impact curves are widely different. An inspection, however, shows that this alteration can only be one or two-tenths of a volt, it is inadequate to account for the discrepancy of half a volt with the accepted value of the excitation potential.

Owing to the wide range of the oscillating potential used in the set of readings shown in fig 4 (0.2 volt) analysis was not carried out on this curve.

The result of a typical analysis is shown in fig 5. In this case δ was 0.3 volt.

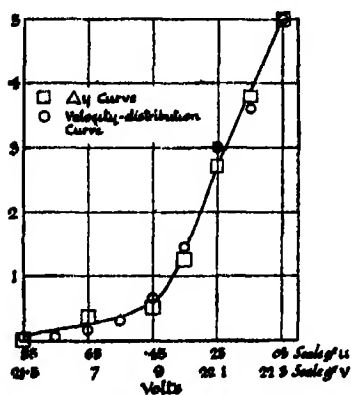


FIG 5

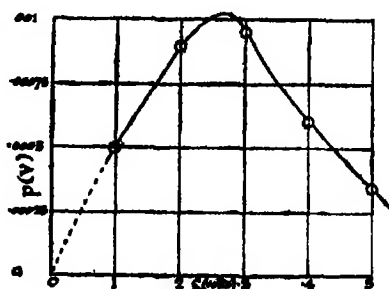


FIG 6

and $(\delta_2 - \delta_1)$ was 0.1 volt. It will be seen later that $P(V)$ is more nearly constant in this region than elsewhere.

The curve showing the rise in current (Δy) from the first break point to 0.8 volt above it is plotted, correction being made for the effect of the retarding potential on fast electrons as mentioned before. The observed velocity distribution curve is now taken, and the differences in the ordinates 0.1 volt ($= \delta_2 - \delta_1$) apart are plotted backwards against the mean potential corresponding to them. This difference curve has now to be fitted to the Δy curve, by adjusting the maximum ordinate to be equal to successive ordinates of the Δy curve. In one of these positions the two curves will be close together throughout their length. As the ordinates of the difference curves are much smaller than those of the original velocity distribution, errors in this latter will tend to be magnified. It will be seen that for this reason the points do not lie well on a smooth curve, though no such irregularities could be detected in the original observations.

We see that in fig 5 a good fit is obtained when we place the maximum ordinate of the difference curve on the point 22.3 volts. As this ordinate corresponds to a mean emission velocity of 0.05 volt we may take the critical potential to be at 22.35 volts. But as only electrons with velocities 0.25–0.35 volt greater than the critical potential are recorded, the actual position of the critical potential on the voltage scale is 22.05 volts, or about half a volt above the initial break point.

The difficulties related above in getting satisfactory curves for the double impact make this analysis of value chiefly for comparative work, in which the critical potentials of the gas under observation are measured against those of another gas as standard, these latter being checked against spectroscopic data. This calibration by a known gas has in fact been resorted to by Hertz in finding the excitation potentials of neon and argon in terms of those of helium

III *The Probability of Effective Collision*

It is of interest to investigate the form of the probability coefficient $P(V)$. Some conclusions have been arrived at from theoretical grounds concerning this function by Blackett* He considers that a condition limiting excitation of the atom by the impinging electron when it has sufficient energy is the fulfilment of the requirements of the conservation of angular momentum The atom on undergoing a quantum switch changes its total angular momentum by an amount $j\hbar/2\pi$, where j is an integer This must also be the change in angular momentum of the electron about a line through the centre of mass of the atom He shows that for velocities slightly above the excitation potential, the electron must impinge on a narrow ring around the atom to fulfil these conditions As the velocity is increased this ring expands till its area is equal to the area of the atomic disc as calculated from the kinetic theory At this point every collision should be effective, and below it the probability of excitation, $p(V)$, is represented by the ratio of the area of the ring to that of the whole atom

Plainly, when the electron has just sufficient energy to excite, the ring shrinks to a line-circle and $p(V)$ becomes zero He shows that in the case of the $1S - 2s$ switch of helium $p(V)$ should reach a maximum (of unity) 0.5 volt after the beginning of excitation

It is possible by means of the apparatus described in the previous sections to determine the form of the function $P(V)$ experimentally Consider again equation (4),

$$\Delta y = P(V_0 + \delta) \int_{V_0 + \delta_1 - V}^{V_0 + \delta_2 - V} \rho(u) du$$

If we vary δ , that is to say $(\delta_1 + \delta_2)/2$, and at the same time vary V so that the integral remains constant, Δy will be proportional to $P(V_0 + \delta)$. The integral remains constant if we keep $(V - \delta)$ constant, that is to say when V is varied by the same steps as δ

We shall not in reality obtain a true representation of $P(V)$ when the function

* Blackett, 'Proc Camb Phil Soc,' vol 22, p. 56 (1924).

is varying rapidly, but we shall approximate to its mean value in a range $(\delta_2 - \delta_1)$. In the actual experiments this range was 0.1 volt. The curve may of course be corrected for zero range by the well-known method of Rayleigh,* but the corrections so made will not be larger than the variations found from day to day.

The value of the probability for the first, 1S — 2s switch only, has been found. We are actually measuring $P(V) + P^1(V)$ as mentioned before, but by working with low values of V we may exclude $P^1(V)$. We cannot exclude $P(V)$ to measure $P^1(V)$ alone, and as this latter seems to be much smaller it has been impossible to work on it.

The averaged results of several determinations are shown in fig. 6. It is seen that $P(V)$ rises sharply and in nearly linear fashion to a maximum at 0.25 volt, with a range in different determinations from 0.2 to 0.3 volt. This is not inconsistent with Blackett's results, considering the uncertainties in his calculations. But the decrease after the maximum is unexpected and seems to have no obvious explanation. We may be reasonably assured that our interpretation of the effect we are measuring is correct, because the form of the curve remains unaltered by working with widely different portions of the velocity distribution curve, *i.e.*, with different values of V when $\delta = 0$.

Hughes and Klein† record similar curves for the probability of ionisation of helium, but on a very different scale, extending over some hundreds of volts. It is unlikely that the two phenomena have much in common.

To arrive at a numerical estimate of the maximum value of $p(V)$, we require the maximum value of $P(V)$ and the total number n of collisions with the gas which an electron suffers in traversing the apparatus. We may obtain a rough value for $P(\text{max})$ from inspection of the normal inelastic impact curve of fig. 2, in which we see that at 1 mm. pressure about 40 per cent. of the electrons make effective impacts.

The determination of the second quantity n presents greater difficulties. The exact mathematical solution of the problem has not been obtained, but we may arrive at the right order for the number of collisions from the approximate relation

$$x = l\sqrt{n} \quad \text{or} \quad n = \frac{x^2}{l^2},$$

where x is the distance traversed from the origin by an electron in n free paths each of length l . We see that n , and therefore $P(V)$, varies as the square of the pressure, a relation which has been found to be approximately true.

* Rayleigh, 'Collected Papers,' vol. 1, p. 135.

† Hughes and Klein, 'Phys. Rev.', vol. 23, p. 450 (1924).

The mean free path of a fast electron may be taken as $4\sqrt{2}$ times that of the gas in which it is moving, and is in the case of helium at 1 mm pressure about 1 mm. The dimensions of the cylindrical grid within which the collisions take place were 35 mm long by 12.5 mm radius. The mean value of x^2 , where x is the distance from where the electrons enter to a point on the circumference, is 564, which also gives the number of collisions in this case. In reality this number will be smaller, as we have assumed that an electron will have equal chances of passing through the gauze at all points. It will, in fact, tend to pass through more frequently at the end near the filament, so as we are only dealing with the roughest of approximations we may take $n = 400$. This gives

$$p(\text{max}) = \frac{P(\text{max.})}{n} = 0.001$$

This result shows that considerations of angular momentum, as treated by Blackett, while possibly controlling the form of $p(V)$ have no influence on its absolute magnitude. It should be noted, however, that he expressly states that his calculations can give only maximum values for the probability.

We are at present in the dark concerning the factor which limits $p(V)$ to so small a value. It is conceivable that the atoms of the gas were oriented by the earth's magnetic field, the stray fields of the laboratory, or that due to the current heating the filament. The experiments of Wood and Ellett* on the polarisation of the resonance radiation of mercury have shown that the presence of such small fields can exercise marked effects. Blackett has shown that a magnetic field in orienting the atoms will make the conditions of fulfilment of the angular momentum relations much more stringent, and will greatly reduce the values of $p(V)$.

In order to test the possible effect of a magnetic field on the behaviour of the probability, a solenoid capable of giving 100 gauss in the direction of the axis of the cylinder was placed round the experimental tube. The only effect observed even with the strongest field was a general increase in all the values of $P(V)$. This increase is to be expected, as the action of the field on the electrons tends to prevent them diffusing to the walls of the cylindrical grid, and so increases the number of collisions which they make before doing so. No effect on the shape of the curve was observed, and it can be said that there is no evidence of any effect of a magnetic field up to 100 gauss on the probability of effective collision.

This negative result can of course be explained by the assumption that the

* Wood and Ellett, 'Roy. Soc. Proc.,' A, vol. 103, p. 396 (1923).

atoms are already oriented by the stray fields. It has unfortunately not been possible to test this by neutralising the stray field and noting any differences in behaviour.

It must be understood that these values for the probability of excitation are only tentative, owing to the many uncertainties which arise in their determination. We have ignored entirely the small loss of energy of an electron at an elastic collision with an atom, due to the transference of momentum from one body to the other. This amounts, in the case of helium, to about $1/4000$ of the energy of the electron per collision, so that in the case considered the electron may lose 10 per cent of its energy in traversing the gas. This may increase the values of $p(V)$ by a factor of 2 or 3, which still leaves it very small, and does not bring in uncertainties of greater order than those occurring in the determination of the total number of collisions between the electron and the gas.

In order to avoid these difficulties it is necessary to work at such low gas pressures that the number of collisions is only one or two, as do Hughes and Klein. The extreme smallness of the effects to be observed at these pressures quite precludes the methods of measurement described above, and we must rest satisfied at the moment with having arrived at the order of the probability.

Summary

1 The factors limiting the accuracy of previous measurements of excitation potentials are discussed.

2 The application of automatic differentiation of the characteristic curves to increase the sharpness of the bends in them is described. The reasons for the divergence of the value found for the first excitation potential of helium, 20.9 volts, from that calculated from the optical data are discussed.

3 The problem of interpretation of the characteristic curves, taking into account the variation in the probability of effective collision and the velocity distribution of the electrons, is attacked.

4 Efforts towards finding the variation in the probability of effective collision and its numerical value are described.

In conclusion I wish to express my deep gratitude to Sir Ernest Rutherford, to whom the original suggestion of applying the differential method to finding excitation potentials is due, for his continuous interest and advice throughout the work, and also to Mr R. H. Fowler for his help in finding the total number of collisions made by the electron.

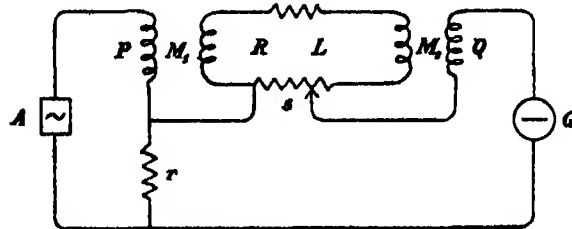
On the Determination of Resistance in Terms of Mutual Inductance.

By ALBERT CAMPBELL, B A

(Communicated by F E Smith, F R S—November 22, 1924)

Some years ago* the author made a determination of the ohm in absolute units by two alternating-current methods, both of which depended on a calculated standard of mutual inductance and a measured frequency. Each of those methods had certain disadvantages: the first required a very steady running two-phase alternator, and the limits of accuracy depended on the readings of an electrostatic voltmeter, the second method employed a condenser as intermediary and required an assumption regarding the behaviour of the condenser which was probably not quite justifiable.

The following method requires simpler apparatus than the two former, and is free from the difficulties inherent in them. The connections are shown in the figure



M_1 and M_2 are two mutual inductances, M_2 being variable. Their secondaries are connected, along with added resistance, to form a loop having total resistance R and self-inductance L , r is a non-inductive resistance, A a source of alternating current, and G a vibration galvanometer or telephone. A portion, s , of the added resistance in the loop is tapped off into the galvanometer circuit, and can be adjusted by a slide-wire contact without altering the total R . Let $\omega = 2\pi n$, where n is the frequency of the source. Then, when G shows no current,

$$\omega^2 M_1 M_2 = Rr \quad (1)$$

and

$$M_1 s = Lr. \quad (2)$$

If we fix M_1 , R , r and L , s can be adjusted once for all so as to satisfy condition (2). Then, for any given value of ω , condition (1) can be also

* 'Roy. Soc. Proc.,' A, vol. 87, p. 391 (1912)

satisfied by adjusting M_2 . If the frequency is not quite constant, and has to be averaged, M_2 can be adjusted at regular intervals. In the above simple case we have taken r as non-inductive, and the direct mutual inductance (m) between P and Q as zero. If these conditions do not quite hold, let l be the self-inductance of r . Then we have

$$\omega^2 [M_1 M_2 - L(l - m)] = Rr \quad (3)$$

and

$$M_1 s = Lr + (l - m) R \quad (4)$$

It is quite easy by experiment to set m to be zero, in which case a small correction due to l alone remains. But if m be set equal to l , the equations reduce to the original simple conditions (1) and (2). If the self-inductance of s is not quite negligible a small correction for it can be applied to M_2 .

It will be noticed that the comparison thus obtained involves two mutual inductances and two resistances. The two mutual inductances can each be accurately determined against a standard calculated from its dimensions. The resistance r is an ordinary non-inductive standard, but R includes inductive copper coils. Even when moderate frequencies are used (*e.g.*, 100 to 200 cycles per sec), the resistances of the copper portion of the loop can be made so small as to render the variation of R with temperature and frequency comparatively slight.

The method has been used to determine the ohm in absolute units. The mutual inductances M_1 and M_2 were about 14 and 10 mH respectively, and were checked against a standard kindly tested by Mr. Dye at the National Physical Laboratory, being thus derived from the calculated standard of mutual inductance set up by the author in 1907*. The resistances R and r were about 30 and 2 ohms respectively, and were checked against coils also tested at the National Physical Laboratory. L was about 3.5 mH and s about 0.5 ohm. The frequency used was about 100 cycles per sec, and was determined by a standard tuning fork which was checked by the help of a phonic wheel. The alternating current (30 to 40 milliamperes) was obtained from a single-valve generator, and the detecting instrument was a vibration galvanometer. The experiments were made in the author's small laboratory with home-made instruments.

The final results gave.—

$$\text{International ohm/true ohm} = 1.0005_4 \pm 0.0001.$$

The limits of accuracy are perhaps worse than ± 0.0001 , but the agreement

* 'Roy. Soc. Proc.,' A, vol. 79, p. 428 (1907).

of the result with the figures given by Smith and Giebe (1·00052 and 1·00051 respectively) shows that with a little more elaboration very high accuracy should be attainable. The use of the method for accurate measurement of frequency will be described elsewhere

The Absorption of X-Rays.

By E. C. STONER, B.A., Lecturer in Physics at Leeds University, and
L. H. MARTIN, M.Sc., 1851 Exhibition Scholar (Melb.), Trinity College,
Cambridge

(Communicated by Prof. Sir E. Rutherford, F.R.S.—Received Dec. 5, 1924.)

Introduction

An account is given here of the measurement, by a balance method, of the mass-absorption coefficients of a number of elements, primarily relative to aluminium, over a range of wave-lengths from 0·3 to 0·7 Å.U., and of the absolute coefficient of aluminium itself for three wave-lengths.

The main objection to the direct method of measuring absorption coefficients is the difficulty, with ordinary facilities, of obtaining an even approximately constant source of X-rays. This necessitates the use of some form of compensation or comparison method.

Siegbahn* has described such a method. Two similar monochromatic beams from the same X-ray tube are obtained with the aid of two "half spectrometers." The currents through the two ionisation chambers are opposed, and a null method is used, with an electrometer as detector. With the absorbing screen in the path of one beam, the intensity of the second is equally reduced by means of a rotating disc, the transmitting sector of which can be varied.

The present method embodies essentially the same idea, but its much greater simplicity gives it an added advantage. A single spectrometer is used, the two beams, one above the other, being reflected by a single crystal into the two ionisation chambers, which are fixed together and replace the usual single chamber of the Bragg spectrometer. After the beams are equalised in intensity

* Siegbahn and Wingårdh, 'Phys. Zeit.', vol. 21, p. 83 (1920); Wingårdh, 'Zeit. f. Phys.', vol. 8, p. 363 (1922).

the absorbing screen is placed in the path of one and the second is cut down until a balance is again obtained by moving across it a wedge of aluminium. For the determination of the absorption coefficient of aluminium the wedge was used in conjunction with a rotating sector disc.

Apparatus

General—A Coolidge medium-focus tungsten radiator-tube, the radiator covered with a water-cooling jacket, and a medium-focus water-cooled molybdenum tube were used. These were supplied with unrectified current from a Watson 100-K V oil-immersed transformer, working from the town mains.

The general arrangement of apparatus is shown in fig 1. The anticathodes

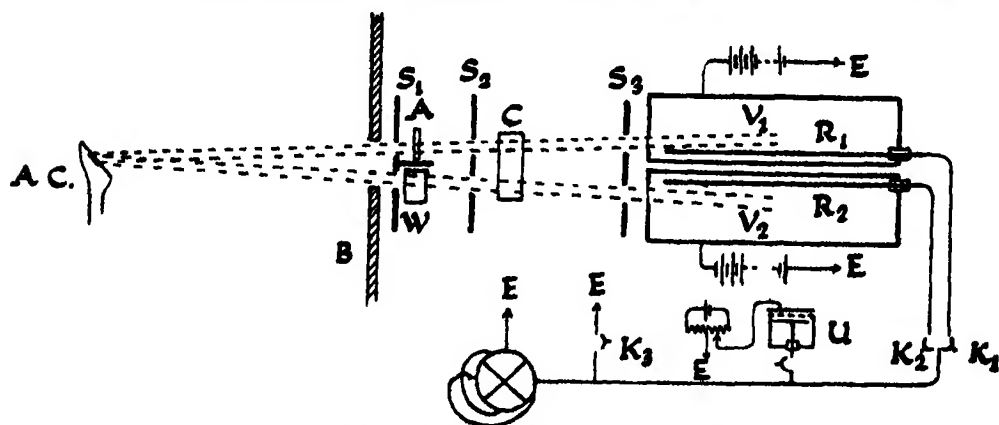


FIG 1—Diagram showing arrangement of Apparatus

were about 40 cm from the crystal, the angles of incidence of the X-rays being measured from a 24-cm circle.

The X-rays from the anticathode, A.C., pass through an aperture in the lead box, B, and are divided into two beams, slightly divergent, by the pairs of slits, S_1 , S_2 , these are reflected from the single calcite crystal, C, through the further pair of slits, S_3 , into the ionisation chambers, V_1 , V_2 . The chambers are raised to opposite potentials of 200 volts. Either or both of the insulated electrodes, R_1 , R_2 , may be connected to the electrometer by means of the keys, K_1 , K_2 . K_3 is an earthing key for the electrometer. The wires leading from the electrodes to the electrometer are surrounded by earthed tubes, while the keys, K_1 , K_2 , are within an earthed box. A quadrant electrometer of the Compton type, working at a sensitivity of $4 \rightarrow 10,000$ divisions per volt, was used. The quartz fibre was rendered satisfactorily conducting by dipping in calcium chloride solution.

For ordinary absorption measurements, A represents the position of the absorbing screen, while W is the wedge which is moved across the second beam.

The Ionisation Chambers.—The brass ionisation chambers were of semi-circular cross-section, so that the two could conveniently replace the usual single cylindrical chamber. Mica "windows" were provided and caps of lead covered the front ends of the chambers to prevent the entrance of stray radiation. The insulated electrodes placed so as to be out of the path of direct radiation passed through sulphur-quartz-ebonite plugs with guard-rings. The two chambers were separated by strips of ebonite.

The absorbing gas used was a mixture of air and ethyl bromide, the latter being placed in a small glass bulb attached directly to the chambers. A phosphorus pentoxide tube was also attached, and little trouble was experienced with leaks. These seldom exceeded a few divisions per minute and could be very exactly balanced out by applying a small voltage (a few hundredths of a volt) to an artificial leak provided by a uranium-oxide resistance, U.

The Slits.—The three slit-pieces S_1 , S_2 , S_3 were similar to the slit-pieces of an ordinary Bragg X-ray spectrometer, with the exception that they were converted in each case into a double slit by lead facings.

The front slit-piece (see fig 2) was provided with a shelf on which the absorber

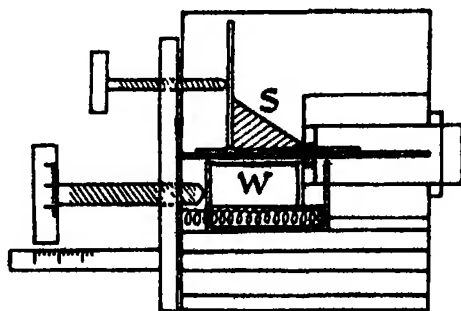


FIG 2 — Tube Slit-Piece, S_1

could be placed. Moving in a groove on this was an adjustable lead screen, S, to cut down the intensity of the upper beam, should this be necessary. This was moved by a rough screw working in a side-piece.

The Wedge Compensator.—Beneath the central shelf is a carriage for the compensating wedge, W (fig 2). This carriage slides along a lower shelf suitably grooved, and is moved by means of an accurate micrometer screw, working against a steel spring. The position of the carriage is obtained from readings on the side scale, and the graduations of the screw-head (marked in 1/100 mm.).

The wedge may be calibrated for a given slit width by taking the readings for balance against standard aluminium foils placed in the usual position of the absorbing screen (A, fig 1)

In the experiments on the absolute absorption coefficient of aluminium, the reading of the wedge was found corresponding to balance against the upper beam when its intensity was reduced to approximately half by a rotating sector disc, consisting simply of a brass lead-faced disc from which two 90° sectors were cut

Procedure

Before taking a series of readings the natural leak was accurately balanced out by means of the uranium resistance. If the two beams from the uncovered slits were not equally effective the height of the tube was adjusted to give a slightly greater ionisation in the upper chamber. The upper beam was then cut down until a balance was obtained by moving the triangular lead screen, S, across the slit, S₁

The balance was corrected before each set of two or three readings, and checked afterwards, the readings being rejected if it had changed. Variations in the balance were mainly due to the heating up of the anticathode. Time was therefore allowed for the anticathode to attain an equilibrium temperature, after which the balance ordinarily showed a most satisfactory constancy over a set of readings

With the absorbing screen in position the currents were then tuned for positions of the wedge on either side of the balance point. The main difficulties experienced were due to the smallness of the ionisation currents obtainable with the resources available. Working on the K α and β peaks with the molybdenum tube, adequate currents (12–20 divisions per second) could be obtained with slit widths only slightly greater than 0.1 mm. It was considered unsatisfactory to work with currents less than about 5 divisions per second, and this necessitated the use of wider slits when working with the white radiation from the tungsten tube, particularly at the short wave-lengths. This, however, was immaterial with the compensation method adopted, except in the neighbourhood of absorption discontinuity wave-lengths; these regions could not be “explored” with the precision which is really desirable.

The general accuracy of the actual readings is estimated to be within 1 per cent. For the shortest wave-lengths the errors are greater than this, while the readings on the Mo peaks ($\lambda = 0.631$ and 0.708) are probably correct to $\frac{1}{2}$ per cent. It should be mentioned that in working with the white radiation,

great care was taken to use voltages sufficiently low that any second-order radiation of short wave-length was quite negligible

The wedge was calibrated by means of aluminium foils placed in the position of the absorbers, so that the mass-absorption coefficients of the absorbers were obtained relative to that of the foils. A typical wedge calibration curve is shown in fig. 3. As the front slit opened asymmetrically, the same curve would

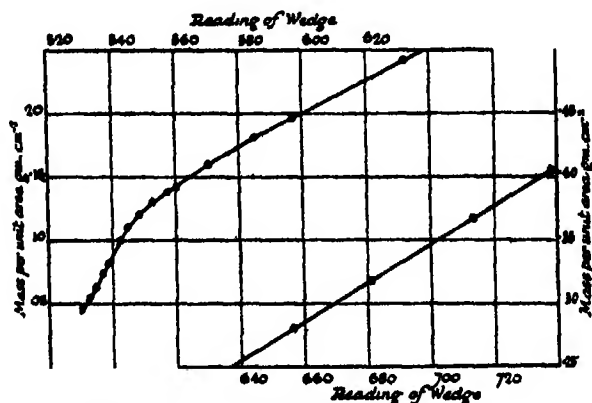


FIG 3 --Typical Wedge Calibration Curve

not serve for different slit widths, but curves for any slit width could be deduced from the standard curve for a known slit width by simple displacement, the values so obtained were in satisfactory agreement with those of actual calibrations which were carried out when the slit width was altered. The mass per unit area of aluminium corresponding to a reading of the wedge was taken from large-scale calibration curves. From the balance point readings the ratio R of the mass-absorption coefficient of an absorber to that of aluminium could thus be easily deduced, this being the inverse ratio of the balancing masses per unit area.

Although different observers give different values for the mass-absorption coefficient of aluminium for particular wave-lengths (differing by as much as 6 per cent), there is close agreement as to its mode of variation with wave-length in the range investigated ($0.3 - 0.7 \text{ \AA U}$). An accurate determination of the coefficient for the foils used for a number of wave-lengths in the range therefore enabled the ratios above obtained to be converted into mass-absorption coefficients.

Results.

Aluminium (Atomic number $Z = 13$ Atomic weight $A = 26.96$) Mass per unit area of foils used $0.1222 \text{ gm cm}^{-2}$ ($t = 0.45 \text{ mm}$), $9.152 \times 10^{-3} \text{ gm cm}^{-2}$ ($t = 0.034 \text{ mm}$). The aluminium was that supplied commercially as "pure". It was found to contain 0.31 per cent of iron*.

The rotating sector disc cut out 50.29 per cent of the radiation. The reading of the wedge corresponding to balance against this was found. Using the molybdenum tube, determinations were made on the $K\alpha$ and $K\beta$ peaks with a tube slit width of 0.13 mm. The α and α' lines were not separated in the first order, but the α' appeared as an asymmetrical hump on the intensity curve. The setting was made on the maximum. A determination was also made at $\lambda = 0.450 \text{ Å}$ with a slit width of 0.22 mm.

$\lambda = 0.708 \text{ Å U}$ —With the rotating disc cutting down the upper beam, the following were the currents for different positions of the wedge in a typical set of readings:—

Reading of Wedge	Deflection (div /mm)
555	— 10
557	+ 5
556	— 3

As the mean of a series of experiments the balance reading was found to be 556.3 ± 0.3 .

The wedge was then calibrated against aluminium foils with the following results:—

Mass per unit area of $A \text{ gm cm}^{-2}$	Wedge Reading
0.1222	550.5
1.1405	561

From the above the mass per unit area required to cut down the radiation to half value is found to be $0.1315 \text{ gm. cm}^{-2}$ and the corresponding mass-absorption coefficient 5.271.

The above example will sufficiently indicate the general method of experiment. It should be mentioned that it is a favourable one as regards order of currents. Working on the β peak the currents were roughly half as great, when white radiation was used, even with much wider slits, the currents were usually only about a quarter as great.

* We are indebted to Mr. R. Hill for this analysis.

The following table gives the results, those in the first column (Al_1) being for the material of the foils, and those of the second corrected for the iron content

μ/ρ for Al		
$\lambda \text{ \AA.U.}$	Al_1	Al
0.708	5.271	5.176
0.631	3.759	3.692
0.450	1.47	1.45

Copper (Z 29, A 63.57) Foils of commercially pure copper were used of mass per unit area $1.508 \times 10^{-2} \text{ gm cm}^{-2}$ ($t = 0.017 \text{ mm.}$) The $\lambda = 0.631$ and 0.708 readings were made with a tube slit width of 0.14 mm. the remainder with a slit width about 0.3 mm. R is the ratio of the mass-absorption coefficients to that of the aluminium foils (uncorrected for iron content) The results are graphed in fig 4

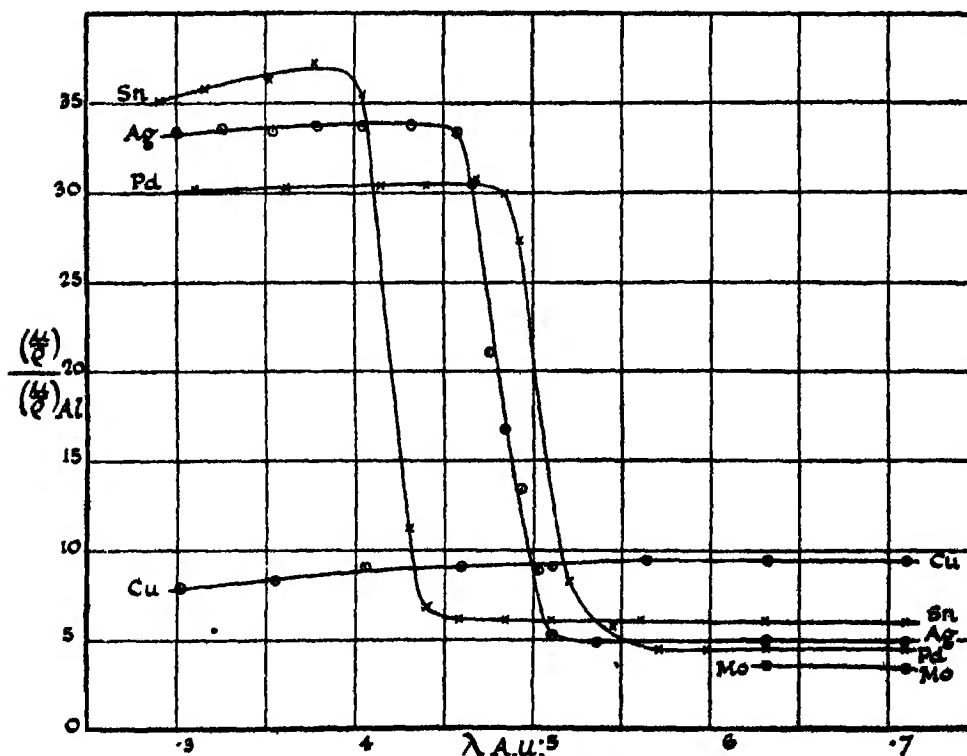


FIG 4—Ratios of Mass-Absorption Coefficients to those of Aluminium.

λ .	R.	λ .	R.
0.301	7.95	0.510	9.08
0.353	8.35	0.563	9.43
0.405	9.08	0.631	9.48
0.458	9.08	0.708	9.43

Molybdenum (Z 42, A 96) Foils 1.13×10^{-1} gm cm.⁻² ($t = 0.113$ mm.) Unfortunately, foils could not be obtained sufficiently thin to enable the absorption on the short wave-length side of the discontinuity to be investigated

λ .	R.
0.631	3.59
0.708	3.44

Palladium (Z 46, A 106.7, $\lambda_K 0.5075$).

Foils used 1.160×10^{-2} gm cm.⁻² ($t = 0.010$ mm.).

2.816×10^{-2} gm cm.⁻² ($t = 0.025$ mm.).

The palladium was supplied by Messrs Johnson Matthey as being of "the highest commercial purity, possibly 99.9 per cent. pure." The slit width used was about 0.16 mm from $\lambda = 0.48$ to 0.54, and about 0.35 mm for the other white radiation readings. The results, plotted in fig. 4, are shown in the following table —

λ .	R	λ .	R
0.310	30.2	0.520	8.30
0.362	30.3	0.545	5.82
0.415	30.4	0.571	4.50
0.440	30.4	0.598	4.50
0.467	30.8	0.631	4.55
0.484	29.9	0.708	4.50
0.493	27.3		

Silver (Z 47, A 107.88; $\lambda_K 0.484$).

Foils used 2.493×10^{-2} gm. cm.⁻² ($t = 0.024$ mm.).

9.895×10^{-2} gm. cm.⁻² ($t = 0.009$ mm.).

The silver, like the palladium, was "of the highest commercial purity, possibly

99.9 per cent. pure" The tube slit was 0.2 mm. wide from $\lambda = 0.43\mu$ to 0.53, and 0.3 mm for the other white radiation readings

λ	R.	λ	R
0.299	33.4	0.475	21.0
0.326	33.6	0.484	16.7
0.352	33.4	0.493	13.3
0.379	33.7	0.502	8.8
0.405	33.7	0.510	5.29
0.431	33.8	0.537	4.81
0.458	33.4	0.631	5.05
0.466	30.5	0.708	4.89

A further series of readings were taken with the silver foil placed immediately in front of the ionisation chamber so that a definite fraction of the secondary and fluorescent radiation excited will enter

Smaller ratios R' were found, corresponding to smaller apparent absorption $R - R'$ then gives a measure of the secondary radiation, going in a forward direction. The method was not adapted to give quantitative results, but the values of $R - R'$ serve to indicate the increase in fluorescent radiation which occurs as the incident radiation passes through the discontinuity wave-length

λ	R'	$R - R'$	λ	R	$R - R'$
0.326	31.0	2.6	0.475	18.4	3.6
0.431	30.0	3.7	0.484	13.1	3.6
0.437	29.6	4.0	0.510	4.81	0.48
0.458	30.0	3.4	0.537	4.61	0.20

Tin (Z 50, A 118.7; λ_K 0.423) Commercial "pure tin foil" (purity probably 98-99 per cent) was used, one sheet being employed on the short and six on the long wave-length side of the discontinuity. Mass per unit area 5.124×10^{-3} gm cm $^{-2}$ ($t = 0.007$ mm). Slit widths of 0.25 mm. were employed except for the shorter wave-lengths (for $\lambda = 0.3$ a slit width 0.35 was used and on the Mo peaks 0.13 mm.).

λ	R.	λ	R.
0.290	35.2	0.457	6.14
0.316	35.8	0.483	6.09
0.352	36.3	0.510	6.09
0.378	37.3	0.562	6.09
0.405	35.5	0.631	6.09
0.430	11.2	0.708	6.01
0.440	6.8		

Uranium ($Z\ 92$; $\lambda_{L_I} 0.568$; $L_{II} 0.591$; $L_{III} 0.721$). Relative measurements only were made with uranium. A filter paper was flooded with a suspension of black oxide of uranium (U_3O_8) in methylated spirits, to which a little shellac was added, and allowed to dry. By this crude method it was possible to obtain films of suitable thickness and satisfactory uniformity (as judged visually, and by the consistency of absorption readings), but the possible errors in the determination of the mass per unit area would have made an attempt at this of little value. The slit width used (except on the Mo peaks) was 0.35 mm., so that the L_I and L_{II} discontinuities were not separated. The filter paper was compensated, and as the oxygen absorption is only about 2 per cent. of that of the uranium it may be neglected. The following table gives the mass per unit area of aluminium required to balance the uranium oxide —

λ .	$(m/A)_{Al}$ gm cm ⁻²	λ .	$(m/A)_{Al}$ gm cm ⁻²
0.391	0.313	0.605	0.198
0.470	0.313	0.631	0.200
0.557	0.313	0.655	0.198
0.563	0.313	0.680	0.197
0.569	0.294	0.708	0.193
0.575	0.257	0.759	0.080
0.581	0.232	0.812	0.075

The above results are plotted in fig. 4a

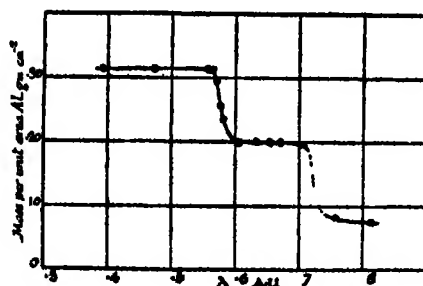


FIG. 4a.—Uranium Oxide Ratio of Mass Absorption Coefficient to that of Aluminium—Relative.

Collected Results.

The mass-absorption coefficients can be deduced from the ratios above given if the coefficient for the aluminium foils is known for the wave-lengths considered. The absorption of aluminium has been investigated over a wide

range of wave-lengths, including that involved in these experiments, by Hewlett,* Richtmyer,† and Allen‡ Though their absolute values differ (see below) there is close agreement as to the variation with wave-length. Allen's values are approximately 3 per cent higher than Richtmyer's throughout the range The values here obtained for the three wave-lengths investigated, for the aluminium uncorrected for iron content (Al'), lie between the two, being 2 per cent. higher than Richtmyer's, it is therefore possible on the basis of the measured values to give values for Al' throughout the range and hence to deduce the mass-absorption coefficients for all the elements investigated. The results for μ/ρ and μ_A (the atomic absorption coefficients) are given in the following tables, and are shown in fig 5 The ratios used in making the

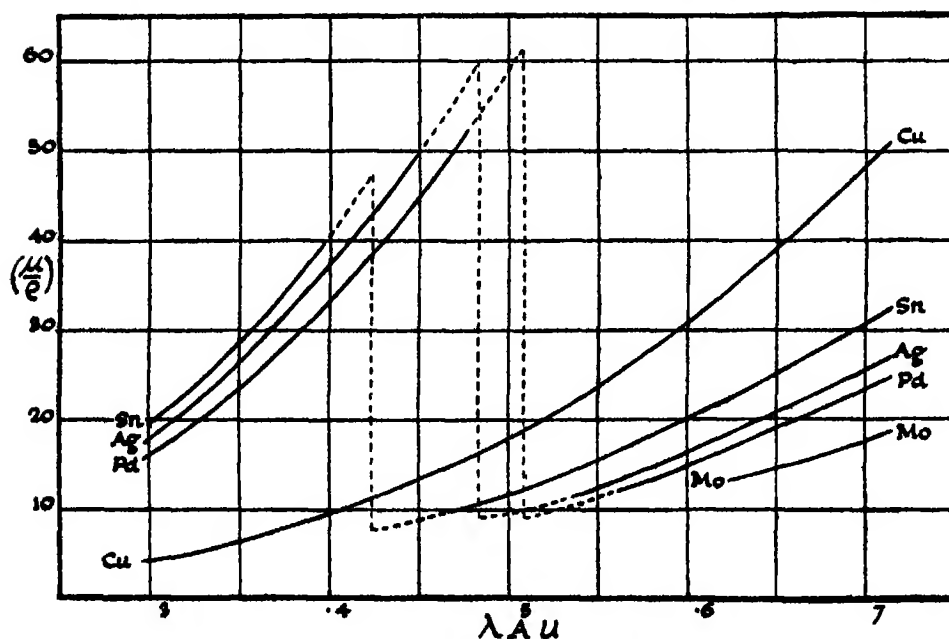


FIG 5—Mass-Absorption Coefficients.

calculations are taken from the curves of fig 4 Extrapolation is indulged in to the extent indicated by the dotted portions of the fig. 5 curves (it being assumed that the observed width of the discontinuities is almost entirely attributable to the lack of homogeneity in the radiation introduced by the wide slits). The values under Al are corrected for iron, those under Al'

* Hewlett, 'Phys. Rev.', vol 17, p. 285 (1921).

† Richtmyer, 'Phys. Rev.', vol. 18, p. 13 (1921).

‡ Allen, 'Phys. Rev.', vol 24, p. 1 (1924).

were used in the calculation of the mass-absorption coefficients from the ratios

λ \AA U	Al'	Al (13)		Cu (29)		Mo (42)	
	μ/ρ	μ/ρ	$\mu_A \times 10^{23}$	μ/ρ	$\mu_A \times 10^{23}$	μ/ρ	$\mu_A \times 10^{23}$
0.30	(0.542)	—	—	4.30	4.52	—	—
0.35	(0.780)	—	—	6.51	6.83	—	—
0.40	(1.10)	—	—	9.58	10.0	—	—
0.45	1.47	1.446	0.643	13.3	13.9	—	—
0.50	(1.92)	—	—	17.8	18.7	—	—
0.55	(2.53)	—	—	23.8	24.9	—	—
0.60	(3.27)	—	—	30.8	32.3	—	—
0.631	3.76	3.692	1.63	35.6	37.4	13.5	21.4
0.708	5.27	5.176	2.28	49.8	52.1	18.2	29.0

λ \AA U	Pd (46) λ_K 0.508		Ag (47) λ_K 0.484		Sn (50) λ_K 0.423	
	μ/ρ	$\mu_A \times 10^{23}$	μ/ρ	$\mu_A \times 10^{23}$	μ/ρ	$\mu_A \times 10^{23}$
0.30	16.2	28.6	17.9	32.3	19.3	37.9
0.35	23.5	41.3	26.3	47.0	28.7	56.5
0.40	33.5	58.9	37.2	66.6	40.3	79.1
0.45	45.0	79.4	49.7	88.7	54.05	104.6
0.50	58.7	101	65	120	71.7	138.0
0.55	75	130.3	84.4	156.1	94.4	180.2
0.60	94.8	168.2	108.4	202.2	124.0	239.2
0.631	117.2	203.3	134.1	244.0	154.4	294.0
0.708	153.8	270.0	176.0	323.3	201.7	381.1

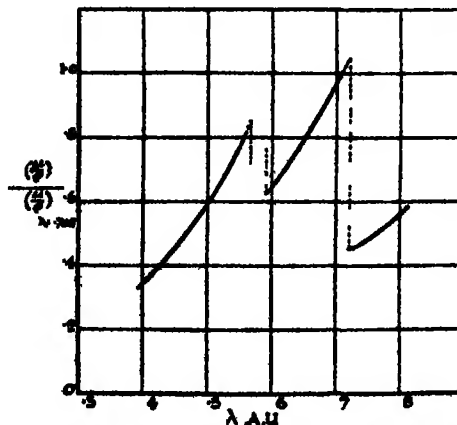


FIG. 5a.—Mass-Absorption Coefficient of Uranium Oxide relative to that at $\lambda = 0.708$.

The values for μ/ρ for U_3O_8 are next given relative to the value 1 for $\lambda = 0.708$ (The absorption due to the oxygen is of the order of 2 per cent. on the short, and 8 per cent. on the long wave-length side of the L jump.) The results are plotted in fig 5a

U_3O_8	Ur 92		λL_I 0.568		L_{II} 0.591		L_{III} 0.721		
$\lambda \text{ \AA U.}$	0.40	0.45	0.50	0.55	0.60	0.631	0.708	0.75	0.80
$\left(\frac{\mu}{\rho}\right) / \left(\frac{\mu}{\rho}\right)_{\lambda=0.708}$	0.34	0.45	0.59	0.77	0.64	0.73	1.00	0.48	0.56

Comparison with Previous Results.

The main results available for comparison are those of Richtmyer and Allen, both of whom used white radiation, and the latter molybdenum characteristic radiations in addition, of Wingårdh,* who has investigated the absorption of a large number of substances by a balance method, as previously mentioned, for $\lambda = 0.708$, and of Bragg and Pierce,† who investigated absorptions for a limited range of characteristic radiations. For aluminium there are also the results of Hewlett

As aluminium is so frequently used as a standard absorber, in the following table are collected the mass absorption coefficients as given by different observers. The first two columns give the results above quoted, uncorrected and corrected for iron

λ	S and M		R	A.	H	W
0.708	5.271	5.176	5.17	5.35	5.02	5.278
0.631	3.759	3.692	3.70	3.78	3.51	—
0.45	1.47	1.45	1.45	1.48	1.38	—

It will be observed that our corrected results agree very closely with Richtmyer's, while the uncorrected, giving the coefficient for ordinarily pure aluminium, agree with Wingårdh's, and are within 2 per cent. of Allen's values. Discrepancies between different observer's results may be due to the presence of even quite small amounts of impurities in the specimens used; and when white radiation is utilised considerable divergence may be introduced by slight errors in the assignment of wave-lengths.

* Wingårdh, 'Zeit f. Phys.,' vol. 8, p. 363 (1923).

† Bragg and Pierce, 'Phil. Mag.,' vol. 28, p. 608 (1914).

For the other elements, the results here obtained are generally somewhat lower than those recorded elsewhere. For copper, over the range concerned (0.3 to 0.7 Å.U.), the values are about 3 per cent lower than those given by Richtmyer, which, in turn, are about 3 per cent lower than Allen's. On the other hand, Wingårdh's value for $\lambda = 0.708$ is about 7 per cent lower than ours. The following gives the values for this wave-length —

Cu $\lambda = 0.708$.

S and M	R	A	W
49.8	51.3	53.7	46.3

In a more recent paper, Richtmyer* states that the mass-absorption coefficient of copper over a range from 0.12 to 0.30, which he has reinvestigated, is accurately given by $\mu/\rho = 153\lambda^3 + 0.20$, which gives for $\lambda = 0.30$, $\mu/\rho = 4.33$, in close agreement with our value 4.30. The molybdenum results are 2 per cent lower than Richtmyer's.

For palladium the only results available are those of Bragg and Pierce for some isolated wave-lengths. On the short wave-length side of the jump these are in approximate agreement, but on the long wave-length side some 20 per cent greater.

For silver the data may be summarised as follows —

Ag	λ	S and M	R	A	W
$\lambda < \lambda_K$	0.30	17.9	18.1	17.9	—
	0.45	50	55	51	—
$\lambda > \lambda_K$	0.50	9.5	11.3	10.5	—
	0.708	26	(31)	28.5	30.8

For tin, on the long wave-length side of the jump, our results are about 6 per cent lower than those given by Bragg and Pierce. On the short wave-length side Allen gives values from $\lambda = 0.11$ to $\lambda = 0.24$, extrapolation suggests that his values from $\lambda = 0.3$ to 0.4 would be some 8 per cent greater than ours. Wingårdh's value for $\lambda = 0.708$ is 35 compared with our 31.7.

It is difficult to account for the quite large discrepancies in the results of different investigators. With reference to our own results, a few points with regard to the possible sources of error may be noticed. The mass per unit area of the foils was determined with great care; they were of such thickness

* Richtmyer and Warburton, 'Phys. Rev.', vol. 22, p. 539 (1923).

that lack of uniformity—as was tested—was negligible; and foils of different thicknesses were used with consistent results. Tests were made to ensure that any second order radiation was negligible, its presence would generally have had the effect of making the observed coefficients too high (*e.g.*, on the long wave-length side of discontinuities), though its effect for the range of wave-lengths and elements investigated would be small. The effect of impurities would cause erratic variations, the Pd and Ag used were of high purity, so that the general coherence of the results for elements of different atomic number makes this unlikely as a source of any considerable errors.

All the results depend on the values taken for the material of the wedge and calibrating foils, these, however, were determined with considerable precision and show satisfactory agreement with the best previous values. An examination of the ratio curves of fig 4 will show that slight errors in the determination of the wave-lengths will not seriously affect the values arrived at except close to the jumps. Errors in the wedge calibration would make the ratios incorrect, but they would introduce comparable errors in the coefficient of aluminum itself. Unless there is some quite unrecognised source of error, it may be concluded that a balance method such as has been used is capable of yielding results far exceeding in accuracy those of direct determinations, which are inevitably subject to a large number of inherent difficulties and uncertainties.

The magnitude of the absorption discontinuity of silver, as deduced from different observers' results, is as follows —

Ag	$(\mu/\rho)_{K+L+} / (\mu/\rho)_{L+}$	
S and M.	R.	A.
6.7	6.6	7.1

Comparable results for Pd and Sn are not available, but Allen's results for a number of elements may be quoted —

Mo (42).	Ag (47).	W (74).	Pb (82).
7.4	7.1	4.7	3.9

These are in agreement with the direction of the change indicated by our results, namely:—

Pd (46).	Ag (47).	Sn (50).
6.8	6.7	6.1

though no stress should be laid on the absolute magnitudes here deduced.

Discussion of Results.

It is not intended here to enter into a discussion of the theory of X-ray absorption, but merely to bring the results, as briefly as possible, into relation with theoretical expressions which have been put forward.

The absorption of X-rays is due partly to true (photoelectric) absorption and partly to scattering, and the absorption coefficient may be written as the sum of two terms

$$\mu = \tau + \sigma. \quad (1)$$

For moderately hard X-rays and elements of low atomic number (σ/ρ) is of the order 0.20, but until more direct quantitative information as to its magnitude for a range of elements and wave-lengths is available, the division of the absorption coefficients into two terms is necessarily somewhat arbitrary and will not here be attempted. Except when μ is small, results stated for μ will apply very approximately to τ , and in any case the modification necessary can easily be made when values are assigned to σ .

For the true absorption de Broglie* deduced semi-empirically an expression which may be written

$$\tau_A = K_1 \lambda^3 \sum_n \frac{b_n}{\lambda_n^2} \quad (2)$$

where τ_A is the atomic coefficient, b_n the number of electrons in the n quantum group, and λ_n the corresponding critical wave-length. Kramers† as a result of a detailed investigation, in which an atom with only one electron is primarily considered, deduces, as an approximate expression,

$$\tau_A = K_2 \lambda^3 Z^4 \sum_n \frac{b_n}{a_n n^3} \quad (3)$$

Here Z is the atomic number, n the total quantum number of the group of electrons, and a_n the statistical weight of the electrons in the group. Assigning the usual values for the K, L, M groups, namely, $n = 1, 2, 3$ $b_n = 2, 8, 18$, $a_n = 2, 6, 12$, Kramers gives

$$\tau_A = K_2 \lambda^3 Z^4 \left(1 + \frac{1}{8} + \frac{1}{18} \right) \quad (4)$$

In both (2) and (3) the summation is to be extended only over those groups of electrons whose critical frequency is less than that of the radiation considered.

The λ^3 law.—In fig. 6 are plotted the atomic absorption coefficients divided by

* L. de Broglie, 'Jour. de Phys.', VI, vol. 3, p. 33 (1922).

† Kramers, 'Phil Mag.', vol. 44, p. 836 (1923).

λ^3 , and the curves bring out very clearly the extent to which the λ^3 law holds. For short ranges of wave-length the law holds, and the curves show that this

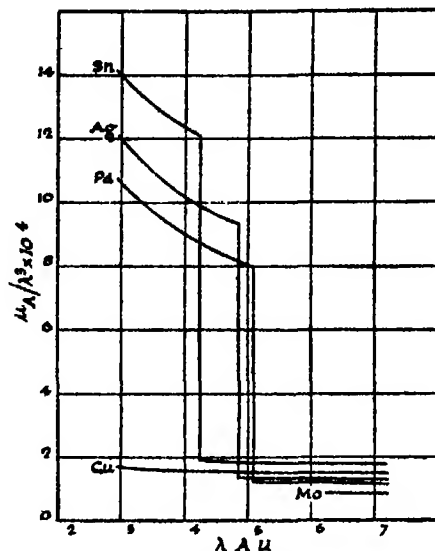


FIG 6 —Atomic Absorption Coefficients/(Wave-Length)³

is also true, with great approximation, over a large range, except when an absorption discontinuity is being approached from the short wave-length side, when the rate of increase of absorption with increase of wave-length is considerably less rapid. This has also been observed by Richtmyer. The rate of increase given by the present results for Sn, Ag, and Pd from $\lambda = 0.30$ to the jump is slightly greater than $\lambda^{3/2}$.

The general results available at present suggest that, at a given wave-length, the rate of increase of the absorption with wave-length differs slightly for different elements, being less the closer the critical absorption wave-length for the element considered, and that the λ^3 rate may be looked upon as a limit attained, when the discontinuity is sufficiently far removed, and so for X-rays of ordinary wave-length, for elements of low atomic number such as Al.

The Z^4 law.—If, as above suggested, the rate of variation of absorption with wave-length may differ somewhat for different elements, it follows that there can be no accurate relation between τ and Z which holds generally for different wave-lengths, there may, however, be simple relations for a single wave-length if this is not too close to the critical wave-lengths of any of the elements considered. The extent to which the Z^4 law holds is conveniently indicated by the values obtained by dividing the atomic absorption coefficients (or μ_A/λ^3)

by Z^4 . Owing to the various possible errors which may enter the absorption measurements themselves, and the fact that μ is used, and not τ , the results in the following table are only given to two significant figures —

$$\frac{\mu_A}{\lambda^3 Z^4} \times 10^2$$

λ	Al 13	Cu 29	Mo 42	Pd 46	Ag 47	Sn 50
0.30	—	2.3	—	2.3	2.4	2.3
0.40	—	2.2	—	2.1	2.1	2.0
0.45	2.5	2.1	—	2.0	2.0	0.31
0.50	—	2.1	—	1.9	0.38	0.29
0.631	2.3	2.1	0.27	0.27	0.27	0.28
0.708	2.2	2.1	0.26	0.26	0.27	0.28

The table shows that for a particular wave-length the Z^4 relation holds with an accuracy of about 5 per cent, before any far-reaching conclusions can be drawn, however, further investigations are undoubtedly necessary, especially in view of some remarkable observations of Allen, who finds, for example, that the K absorption of Bi (83) is actually lower than that of Pb (82). In particular it is desirable that measurements should be made with radiation of a high degree of homogeneity, a desideratum which, for short wave-lengths, presents considerable experimental difficulties.

The K Discontinuities—While De Broghe's expression (2) indicates a variation in the magnitude of the jumps, that of Kramers, (3) and (4), suggests that this should remain constant, it should be mentioned, however, that all the (necessarily) arbitrary approximations and assumptions in Kramer's treatment seem to concentrate their effect on this particular point. If (2) were correct the magnitude of the K jump should be proportional to λ_K , while this agrees approximately with our values, Allen's results over a more extended range show that it varies at least twice as rapidly as this. For the ratios of the (K + L + M) to the (L + M) absorption at the K jump, (2) gives values ranging from about 15 for Mo (42) to 9 for Pb (82), and so much greater than those observed of about 6.7 for Pd and Ag and 6.1 for Sn.

De Broghe's expression, then, is incorrect in the magnitude it attributes

to the jumps, but it indicates a change with atomic number in the right sense ; Kramer's result is incorrect in suggesting constant magnitude of the jumps, and for the elements investigated it underestimates their magnitude

If $\mu_A/\lambda^3 Z^4$ is calculated for wave-lengths considerably removed from the discontinuity on either side instead of at the discontinuity itself, it may be noted that the ratio comes out greater—of the order of 8 or 9.

The L Discontinuities.—The L absorption of uranium raises some points of interest. If (2) or (3) are even approximately correct the absorption coefficient for an element for wave-lengths longer than λ_K may be approximately written

$$(\mu/\rho) = K\lambda^3 \left[b_{L_I} + b_{L_{II}} + b_{L_{III}} + \frac{b_M}{m} + \dots \right] \quad (5)$$

where b_{L_I} , $b_{L_{II}}$ are the number of electrons in the L_I , L_{II} , . . . , M groups, m some factor

In fig 6a $(\mu/\rho)/\lambda^3$ for uranium is plotted, the vertical lines representing

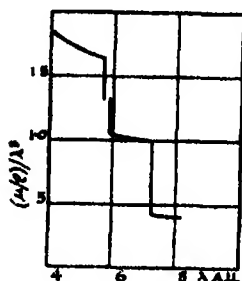


FIG 6a—Uranium Oxide
 $(\mu/\rho)/\lambda^3$ relative to value
at $\lambda = 0.708$

the position of the three critical wave-lengths. It will be seen that the increase in absorption due to the L_{III} electrons is almost exactly equal to that due to the L_I and L_{II} together. This suggests strongly that there are 4 L_{III} electrons, and 4 ($L_I + L_{II}$) electrons. This conclusion is in agreement with that of Dauvilher* based upon a somewhat similar study of the L absorption of gold. The ratio of the total ($L + M + \dots$) to the ($M + \dots$) absorption is approximately 4, in agreement with Kramer's expression

Summary.

A description is given of a balance method for the measurement of X-ray absorption. The series of slits of a Bragg spectrometer is replaced by a series of double slits (one vertically above the other) and the two beams of X-rays are reflected from a single large crystal into two separate ionisation chambers which replace the usual single chamber. The currents through the two chambers are balanced by adjusting the heights of the slits, the absorbing screen is placed in the path of one of the beams, and the absorption compen-

* Dauvilher, 'Compt. Rend.', vol 178, p 476 (1924).

sated by moving a wedge of aluminium across the path of the other beam by means of a micrometer screw. The absorption for a particular wave-length can be accurately measured in terms of the absorption of the material of the wedge.

Using a rotating sector disc, the absolute absorption coefficient of aluminium has been determined for three wave-lengths ($\lambda = 0.45, 0.631$ and 0.708 \AA U).

Primarily comparative to aluminium, the absorption of copper, palladium, silver and tin, and the relative absorption of uranium oxide have been investigated over a range of wave-lengths from 0.3 to 0.71 \AA U .

The results are compared with those of previous observers.

With reference to theories of X-ray absorption, the range of validity of the λ^3 and Z^4 laws, and the magnitude of the K and L absorption discontinuities are briefly discussed.

The above work was carried out at the Cavendish Laboratory, Cambridge. We would like to thank Prof. Sir Ernest Rutherford for his continued kindness and interest in the work, and N. Ahmad for valuable help in connection with several technical points.

One of us (E.C.S.) wishes also gratefully to acknowledge a grant from the Department of Scientific and Industrial Research.

Ionisation by Alpha-Particles in Monatomic and Diatomic Gases

By R. W. GURNEY, B.A. Trinity Hall, Cambridge

(Communicated by Prof. Sir E. Rutherford, F.R.S.—Received December 5, 1924.)

1 *Introduction*

Measurements of the total number of ions produced by alpha-particles in various gases have not hitherto given results which our ideas of ionisation-potential would lead us to expect. In 1899 Rutherford* showed that the total ionisation due to alpha-particles from uranium in H_2 , N_2 , O_2 , CO_2 , HCl , and NH_3 , was nearly the same. Measurements on these and polyatomic gases have also been made by W. H. Bragg,† Laby,‡ Kleeman§ and Hess and Hornvak||. In a gas with a high ionisation-potential we should expect the total ionisation to be smaller than in a gas with a low ionisation-potential. Taylor,¶ however, showed that in helium, which has an exceptionally high ionisation-potential, the total ionisation is greater than in hydrogen or air. It was thought that experiments on the other monatomic gases—xenon, krypton, argon, and neon—might throw light on this anomaly. This paper describes measurements on the five rare gases, which have yielded an intelligible result. Measurements have also been made on H_2 , O_2 , and N_2 .

2 *Apparatus*

The method was to send a beam of alpha-particles having a definite energy into a long ionisation chamber containing gas at sufficiently high pressure to bring the particles to rest before they reached the end of the vessel. The ions were collected by a central wire connected to a gold leaf electroscope. To obtain beams of particles of different energies the source was placed in a separate absorption chamber containing air, of which the pressure could be adjusted to any required value, and the particles passed through a mica window into the cylindrical ionisation chamber containing the gas. The

* 'Phil Mag,' vol 47, p 109

† 'Phil Mag,' vol 13, p 333 (1907).

‡ 'Roy Soc Proc,' A, vol 79, p 206 (1907)

§ 'Roy Soc Proc,' A, vol 79, p 220 (1907)

|| 'Wien Ber,' vol 129, p 661 (1920)

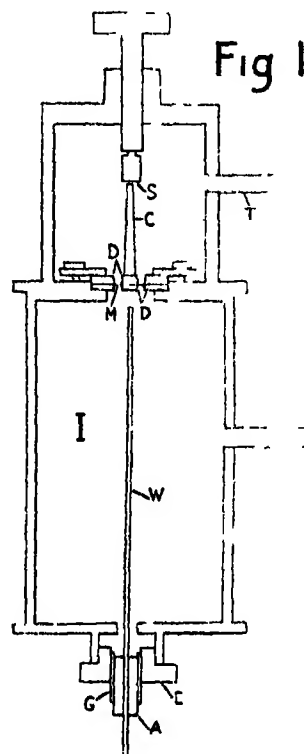
¶ 'Phil Mag,' vol 26, p 402 (1913).

ionisation chamber I (fig 1) was 8.5 cm long. The source S was of polonium deposited on copper, annular in shape with an external diameter of 4 mm. The mica window M was held between two brass discs, which were pierced with 12 small holes of 1 mm diameter, arranged on a circle of 3-mm radius. To make the window gas-tight the mica was attached to one of the discs with a little shellac, care being taken that the holes were kept clear. The large number of small holes was used instead of larger holes to reduce the bending of the mica under pressure to a negligible amount.

The alpha-particles entering through these windows combined to form a roughly cylindrical beam passing down outside the central collecting wire W. The mica had a stopping power of about 1 cm of air; it was selected from a number of pieces examined with sodium light, and showed uniform intensity over the surface by interference. To increase the homogeneity of the beam a slender brass cone C was soldered on to the upper brass disc in the centre, its point lay immediately below the centre of the annular source, and prevented particles from one side of the source from crossing over and passing through the holes on the other side of the axis.

The correct centering of the top of the cone below the source was ensured by looking at it from two directions at right angles through the side tube T before the base of the absorption chamber was fixed to the top of the ionisation chamber. The maximum difference in the distance travelled by alpha-particles from different parts of the source before reaching one of the windows was less than a fifth of a millimetre. So that the departure from homogeneity from this cause was small, except when very small residual ranges were being used, but in these cases the beam was very heterogeneous already, owing to the straggling of the particles.

The central wire passed through a plug of amber A, which was held by a brass guard-ring G fitting into the ebonite stopper E. The guard-ring was permanently earthed to prevent surface leakage of electricity to the central wire from the walls of the chamber, which were raised to a positive potential.



The central wire was earthed, and to take a measurement the earth-contact was broken

The gases were admitted from a siphon-pipette and dried by phosphorus pentoxide. The argon was purified by passing through heated tubes containing copper oxide, and a mixture of calcium oxide and magnesium powder, it was then sparked for three days with excess of oxygen, the residual oxygen being then removed by igniting phosphorus. The neon was obtained from the British Oxygen Company, originally containing 5 per cent of helium, which was removed by fractional absorption in charcoal at the temperature of liquid air, the purification being followed spectroscopically. Small fractions giving a bright helium D_2 line were removed from the gas, in which this line soon became invisible. The process was continued until the helium line could no longer be detected even in the small fractions removed, the neon now probably contained less than 1 per cent of helium. The krypton and xenon were kindly lent by Dr F. W. Aston. The helium was purified by prolonged absorption in charcoal at the temperature of liquid air. The hydrogen was taken from a commercial cylinder, nominally 99 per cent pure, measurements taken before and after application of charcoal and liquid air showed no difference, indicating that heavier impurities were present to a negligible amount. Oxygen obtained from a commercial cylinder was compared with a specimen prepared from permanganate and passed over potassium hydroxide, the difference was within the experimental error. By comparing oxygen with air the value for nitrogen could be predicted, and this was in good agreement with the observed value for nitrogen taken from a commercial cylinder.

3 *Method*

When the air in the absorption-chamber was set at definite pressures (*e.g.*, 30, 36, 42 cms of mercury), the beam of alpha-particles, emerging from the mica window, had a definite energy which was obviously independent of the gas in the ionisation chamber. Provided that the pressure of this gas was sufficient to prevent the particles from reaching the bottom of the chamber, the ionisation-current produced in any gas referred to the same rate of expenditure of energy. The method was one of simple comparison; the ionisation in each gas was compared with that in air.

The accuracy of the comparisons depended first on the reproduction of a beam of alpha-particles of definite energy, and secondly, on obtaining saturation of the ionisation current. For the former the control of the density of the air in the absorption chamber was the important factor. The meniscus of

the mercury in the manometer (which had a wide bore) was observed with a microscope and held steady by means of a fine adjustment. The brass chambers were lagged with felt to eliminate fluctuations of temperature. A thermometer with its bulb in contact with the chamber inside the lagging indicated the temperature. It was thought unnecessary to place the apparatus in a thermostat, because the change of room temperature during the short time taken to make a comparison was small, and the required correction was easily made.

With the electric field transverse to the path of the alpha-particles as described above, it is much easier to obtain saturation of the current than with it along their tracks. The risk in using a radial field, however, is that near the central wire the intensity of the field is so high that it is difficult to avoid secondary ionisation by collision. But this was obviated by the annular arrangement of the mica windows, which prevented the alpha-particles from passing near the wire, and by the direction of the field employed. When the walls of the chamber were made negative, the electrons driven into the strong field near the wire readily produced ionisation by collision in neon, even at low voltages. But with the walls of the chamber made positive no difficulty was found in obtaining saturation without ionisation by collision, using voltages from 80 volts at low pressures in argon and neon, to 480 volts at higher pressures in air and hydrogen.

The lower the pressure of the gas, the more easily is saturation of the current obtained. The pressure was therefore always lowered until the particles were travelling about three-quarters of the length of the ionisation chamber. Thus when the mean range of the particles would have been 7 mm at atmospheric pressure, the ionisation in air was measured at pressures about 8 cms of mercury. The method is based on the fact that under these conditions the ionisation is independent of the pressure. To ensure that saturation was being secured without ionisation by collision, each current was measured at different pressures and with two widely different voltages.

Since the largest current to be measured was about thirty times as great as the smallest, a condenser was connected to the gold-leaf system to reduce the sensitivity. As the measurements were all comparative, the capacity of the condenser was immaterial.

4 Results

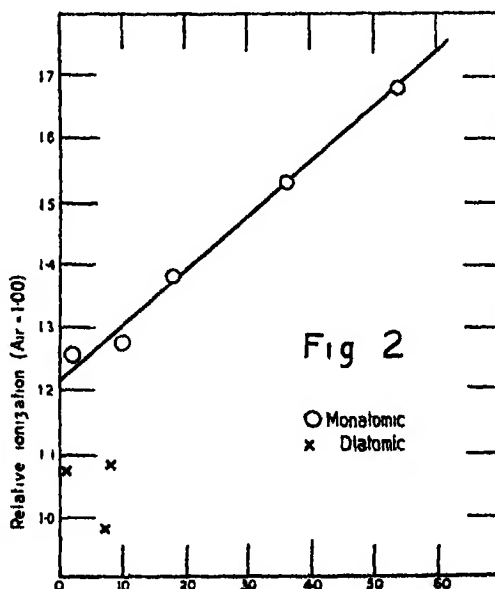
By setting the air in the absorption-chamber at different pressures values of the relative ionisation were obtained at intervals along the range up to a range of 19 mm. As an example, a set of values is shown in the following table,

taking air as unity It is for a residual range of 7 mm (which was the greatest range for which sufficient xenon and krypton were available)

Table I—Relative Ionisation by Alpha-Particles of Residual Range 7 mm

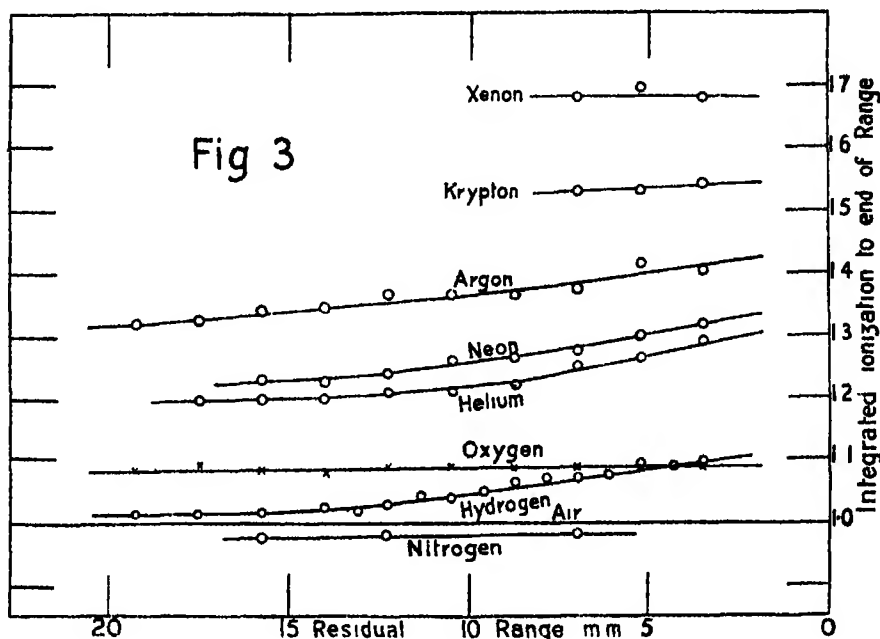
Xenon	1.68	Helium	1.26
Krypton	1.53	Oxygen	1.08
Argon	1.38	Hydrogen	1.07
Neon	1.28	Nitrogen	0.98
(Air		1.000)	

It is seen that in the diatomic gases the ionisation is less than in any of the monatomic gases. In fig 2 the values for the five monatomic gases are plotted against their atomic number, and give a linear relation.



All the measurements taken at different residual ranges are shown in fig 3. The ratios plotted at any distance from the end of the range are not for the ionisation per millimetre at that point, but for the total ionisation from the end of the range up to that point, which was the quantity actually measured. Towards the end of the range the rare gases and hydrogen show a marked increase relative to air. Since this is for the integrated values, the ionisation per mm would show a greater variation. But what is really implied is that nitrogen and oxygen show a decrease relative to the other gases. For if any of the other gases had been taken instead of air as standard, the curves for the rare gases and hydrogen would all be nearly parallel to the base-line.

This means that the variation of ionisation with range (that is, the distribution of the ionisation along the beam of alpha-particles) is similar in these gases



It is on this similarity that the method of measuring the stopping-power for slow alpha-particles, to be described in a subsequent paper, depends

5 Discussion

The least ionisation potentials of helium, neon, and argon are 24.6, 21.5, and 15.3 volts * Those of krypton and xenon have not been measured, but since the heavier members of other groups in the periodic table have progressively lower ionisation-potentials, there is little doubt that krypton and xenon have also. A relation of the kind shown in fig 2 was, therefore, to be expected.

Geiger† measured the absolute number of ions produced by an alpha-particle in the first 4 mm of range of Radium C. From the energy lost in the first 4 mm, as measured by Marsden and Taylor,‡ and by Kapitza,§ it appears that the average energy spent by a high-speed alpha-particle in producing a pair

* Hertz, 'Proc. Acad. Sci. Amsterdam,' vol 25, p 442 (1923).

† 'Roy. Soc. Proc.,' A, vol 82, p 486 (1909).

‡ 'Roy. Soc. Proc.,' A, vol 88, p 443 (1913).

§ 'Roy. Soc. Proc.,' A, vol 102, p 48 (1923).

of ions is about 33 volts. It is an interesting question whether for alpha-particles of low velocity the average energy spent per pair of ions is the same. This can be determined by comparing the energy-range curve of Marsden and Taylor, or Kapitza, with the curve obtained by integrating Henderson's* accurate ionisation-range curve. Kapitza found that over the last 3.5 cm of range the curves fitted very well. But he calculated that for an alpha-particle of 7 cm residual range the average energy spent per pair of ions is 10 per cent greater than for a particle of 3.5 cm. But the following table shows the result of integrating the area under Henderson's curve. Column 2 shows the velocity, expressed as a fraction of the initial velocity, at the range shown in column 1, which are Marsden and Taylor's observed ranges reduced to 0° C, and subtracted from 6.7 cm, the total range. Column 3 gives the energy obtained by squaring the values in column 2. The last column shows the corresponding values obtained for the areas under Henderson's curve.

Table II —Residual Energy compared with Ionisation

R	v/v_0	E/E_0	—
1.68 cm	0.60	0.36	0.358
2.47	0.70	0.49	0.491
3.54	0.80	0.64	(0.640)
4.91	0.90	0.81	0.799
6.70	1.00	1.00	0.988

The value in brackets is the one which has been made to fit. It is seen that in the first 5 cm of the range there is nowhere a divergence of more than about 1 per cent. And Kapitza found that over the last half of the range the curves fitted very well. It, therefore, appears that the average energy spent per pair of ions is about the same at the end of the range as at the beginning.

Taking Geiger's value, 33 volts for air, the observed ratios in Table I. give us the average energy spent per pair of ions in the other gases. It is interesting to compare the expenditure of energy with the lowest ionisation potential of the molecule. Of special interest are hydrogen and helium, which have only one ionisation potential. The values are compared in the following table.—

Table III

Gas	Atomic Number	Energy Spent	Ionisation Potential	Difference
		volts	volts	volts
Hydrogen	1	31	16.5*	14.5
Helium	2	26.2	24.6	1.6
Nitrogen	7	33	17	16
Oxygen	8	30.5	15.5	15
Neon	10	25.8	21.5	4.3
Argon	18	24	15.3	8.7
Krypton	36	21.5	? 1.3	? 8.5
Xenon	54	19.6	? 1.1	? 8.6

In the last column is given the difference between the values in the previous columns. In hydrogen and helium, which have only one energy level, it measures the lost energy, the energy which does not appear as ionisation, but for the other gases there is an ionisation-potential corresponding to each energy-level in the atom.

It is seen that the difference given in the last column is smallest in the case of helium. And it is remarkable that it was in this gas that Millikan† found evidence of double ionisation, for this would be expected to lead to the opposite result. A fraction of the positive ions produced by alpha-particles in helium were found to be doubly charged, and this result has been confirmed by Wilkins‡. Since it takes 1.6 times as much energy to eject both electrons from the same helium atom as it does to eject two separately, the presence of double ionisation has the effect of raising the ionisation-potential. A larger fraction of the energy of the alpha-particles appears as ionisation in helium than in hydrogen or air, and the fact that double ionisation occurs in helium and not in air accentuates the anomaly. Near the end of the range 10 per cent of the positive ions in helium were found to be doubles, this would bring the average effective ionisation-potential up to 27 volts.

We should expect about a quarter of the energy of the alpha-particles to disappear as kinetic energy of the electrons escaping from the molecules ionised. In addition to this, there will probably be further energy used up in excitation of molecules. For the average energy spent per pair of ions in helium we should have expected a value about 35 volts or even higher. But this would necessitate a value for air of 45 volts or more, instead of 33. Further discussion

* Smyth, 'Roy Soc. Proc.,' A, vol 105, p 116 (1924).

† 'Phys Rev.', vol. 18, p 460 (1921)

‡ 'Phys Rev.', vol 19, p. 210 (1922)

of this problem is postponed to a subsequent paper describing measurements of the stopping-power of these same gases

Summary

Measurements have been made of the total ionisation produced by definite beams of alpha-particles in the five monatomic gases and in the common diatomic gases. In the five rare gases the ionisation increases with increasing atomic number, which would be expected from their decreasing ionisation-potentials. But in the diatomic gases the ionisation is less than in any of the monatomic gases, indicating that energy is expended in other ways. The ratio of the value of the ionisation in air to that in the other gases is found to vary with the velocity of the alpha-particles.

In conclusion I wish to express my thanks to Sir Ernest Rutherford for his interest throughout the work, to Dr F W Aston for kindly lending the xenon and krypton, and to Mr P M S Blackett for his constant help and advice.

The Stopping-Power of Gases for Alpha-Particles of Different Velocities

By R. W GURNEY, B A, Trinity Hall, Cambridge

(Communicated by Prof Sir E Rutherford, F R S — Received December 5, 1924.)

1. Introduction

It has long been known that the stopping-power of metal foils relative to air depends on the velocity of the alpha-particles traversing the foil. It was also shown by Taylor* in 1909 that the stopping-power of hydrogen (relative to air) varied all along the range. Thus the stopping-power of a substance has little meaning, unless a small portion of the range is specified to which the value refers, and if the stopping-power of a gas is measured over the whole or a large part of the range, as has usually been done, the value obtained will be merely an average value. In this paper methods are described of selecting small portions of the range, in this way the stopping-power of gases for alpha-particles of low velocity, of high velocity and of intermediate velocity, has been separately measured. The gases examined were the five monatomic

* 'Phil Mag.', vol 18, p. 604 (1909)

gases, xenon, krypton, argon, neon and helium, and also hydrogen and oxygen

2 Apparatus and Method

The apparatus used was that already described in the paper on the ionisation of alpha-particles in these gases * The methods of purifying the gases were also given there

- (1) To measure the stopping-power at the end of the range, the gas was admitted to the ionisation chamber as in the measurements of ionisation
- (2) The alpha-particles from polonium have a range of 3.9 cm of air at N.T.P. To measure the stopping-power at the beginning of the range the gas was admitted to the chamber containing the polonium source. The first half-centimetre of the range corresponds to a decrease of velocity from about 1.6×10^9 cm/sec to 1.55×10^9 cm/sec
- (3) For still swifter alpha-particles a source of thorium C was used instead of polonium. The high-speed particles have a range of 8.6 cm and the first centimetre of the range represents a decrease of velocity from about 2.0×10^9 to 1.95×10^9 cm/sec

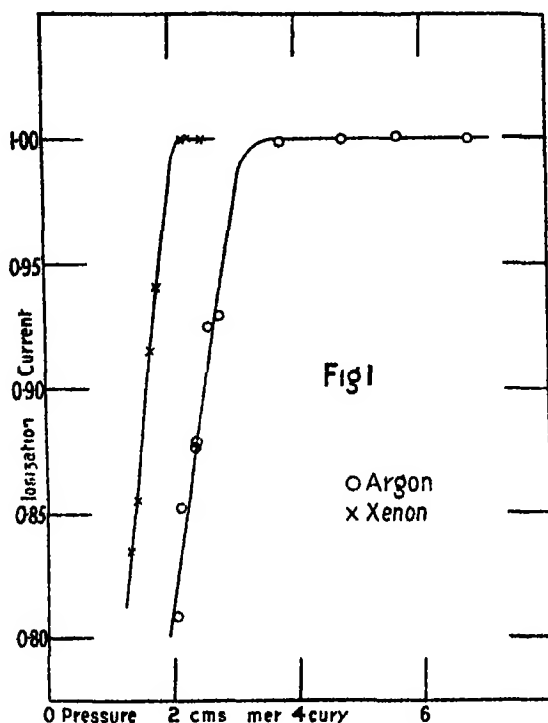
These three methods will now be described in detail

(1) The absorption being kept constant in the upper chamber, the pressure in the ionisation chamber was lowered by steps, and the decrease of the ionisation from its maximum value was determined. The pressure of any gas at which the alpha-particles begin to hit the bottom of the chamber is proportional to the range in that gas. Unfortunately, owing to the straggling, this point is not sharply defined. The ionisation, however, falls off very rapidly, as soon as the majority of the alpha-particles reach the bottom of the chamber. This is shown in fig. 1, where curves for xenon and argon are plotted, the maximum value of the ionisation-current being taken as unity in both cases (instead of their actual relative values). The form of the two curves is the same, if the abscissæ of the one are everywhere divided by a certain factor, the curves are identical. This is due to the fact mentioned in the previous paper† on ionisation, that the measurements of ionisation show that the distribution of ions along the track of the beam of alpha-particles in different gases is similar. If they were very dissimilar, the two curves in fig. 1 would be only roughly comparable. But as it is, the ratio of the abscissæ gives an accurate measure of the stopping-power

* Foregoing paper, p. 332

† P. 337 above.

The curve for argon was determined at two different room temperatures, and an expression was found from which any point on the curve for argon



could be obtained for any intermediate temperature. The other gases (including air) were referred to this as standard. As an example, one of the points plotted for xenon shows that the ionisation fell to 0.855 of its maximum value when the pressure was lowered to 1.44 cm of mercury, the temperature being 19.4°C . The corresponding pressure obtained for argon is 2.365 cm. The ratio $2.365/1.44$ gives 1.642 for the stopping-power of xenon referred to argon. The other points plotted in fig 1 yield the values 1.655, 1.688 and 1.643. The table on p 343 gives the results obtained for the mean residual range 3.5 mm.

The second column gives the number of observations made, the third gives the mean value of the stopping power referred to argon, and the fourth gives the mean error. In the fifth column are given the stopping-powers referred to air.

(2) It has been pointed out that the value of the current in the ionisation chamber is sensitive to changes of pressure in the absorption chamber, especially

Table I—Relative Stopping-Powers of Gases for Alpha-particles of Low Velocity

I	II	III	IV	V
Xenon	4	1 657	0 015	1 51
Krypton	4	1 166	0 026	1 07
Argon	-	1 000	—	0 914
Neon	9	0 500	0 013	0 457
Helium	4	0 1964	0 0026	0 179
Hydrogen	4	0 3376	0 0057	0 309
Oxygen	6	1 073	0 017	0 98
Air	9	1 094	0 013	1 000

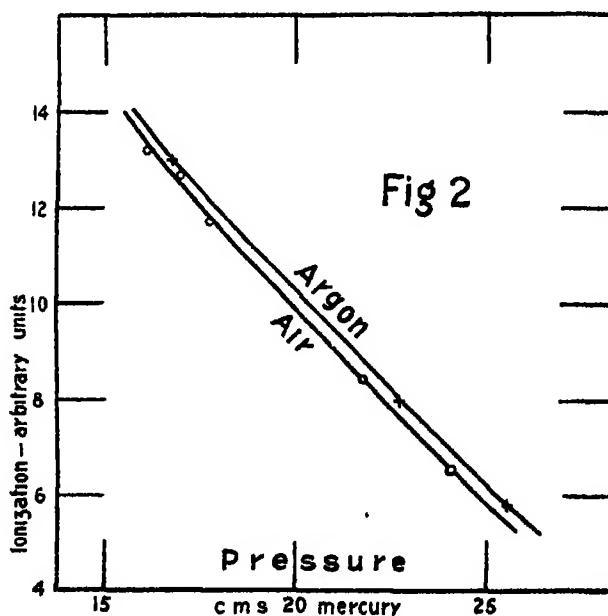
when the alpha-particles are totally absorbed. This therefore provides a method of measuring the relative stopping-powers of gases at the velocity of the alpha-particles leaving the source. The gases were admitted to the absorption chamber, and their relative stopping-powers measured directly using as indicator the value of the ionisation in the chamber below, which contained air throughout. An electrical-balance method was used. A second polonium source was placed between the plates of the condenser which had been used to reduce the sensitivity, and this acted as a radio-active leak to balance the current in the ionisation chamber. The insulated plate of the condenser being connected to the gold-leaf system, the other plate was kept at a negative potential of 120 volts.

It was decided to measure the stopping-power over the first half-centimetre of the polonium range. With the source at 2.7 cm from the mica window, this meant working with an amount of gas in the absorption chamber equivalent to air at about 15 cm of mercury. The radio-active leak was therefore chosen to balance the ionisation obtained with an absorption of about this value. The method was to find what pressure of gas in the absorption-chamber was necessary to produce the balance. In xenon, for example, it was found that at a pressure of 7.67 cm of mercury, or above, the gold-leaf rose slowly, and at 7.59 cm, or below, it fell slowly. To ensure that the conditions were stable, the balance-point in air was determined both before and after that in the gas; it was found to be at a pressure of 14.90 ± 0.15 cm of mercury. The ratio $14.90/7.63$ gives 1.95 as the stopping-power of xenon referred to air.

(3) To measure the stopping-power for still higher velocities the particles of range 8.6 cm from thorium C were used. A source of thorium B and C was collected each day on a brass disc, 4 mm in diameter, by exposure to the emanation. In addition to the long-range particles, thorium C gives out

other alpha-particles of range 5 cm. To prevent these from entering the ionisation chamber, uniform sheets of mica, of total stopping-power 5 cm., were placed above the mica window, the brass cone having been removed. When thorium C is in equilibrium with thorium B it decays with the period of the latter (half-value period, 10.6 hours). To ensure that equilibrium had been obtained, the disc was removed from the emanation two hours before measurements were to be taken. The balance method described in the last section was not used owing to the difficulty of obtaining simultaneously two sources of the right strength. Instead, a curve connecting ionisation in the ionisation chamber with pressure of air in the absorption chamber was determined. A gas was then substituted for the air in the absorption chamber and the value of the ionisation measured for three pressures of the gas.

Fig. 2 shows a comparison between argon and air (corrected for decay of the source). To ensure that there was no variation in the sensitivity of the



electroscope between the two series of measurements, and no irregularity in the decay of the source, three of the measurements for air were taken before those in the gas, and two more afterwards. As before, the ratios of corresponding pressures give the stopping-power of the gas relative to air. In these measurements the source was at a distance of 4 cm. from the mica window.

3 Results

The results for different velocities are collected in the following table —

Table II — Stopping-powers of Gases relative to Air for selected Portions of the Range

I	II	III	IV	V	VI
	8.6-7.6 cm	3.8-3.5 cm	1.4-0 cm	0.35-0 cm	*
Xenon	1.98†	1.95	—	1.51	1.804 (B)*
Krypton	1.52	1.43	—	1.07	1.330 (B)
Argon	0.98	0.93	0.92	0.914	0.930 (B)
Neon	0.623	0.597	0.555	0.437	0.580 (B)
Helium	0.173	0.175	—	0.179	0.1737 (B)
Hydrogen	0.206	0.214	0.247	0.309	0.224 (T)†
Oxygen	1.07	1.05	—	0.981	1.041 (B)

* Bates, 'Proc Roy Soc., A' vol 106, p 622 (1921)

† Taylor, 'Phil Mag,' vol 26, p 402 (1913)

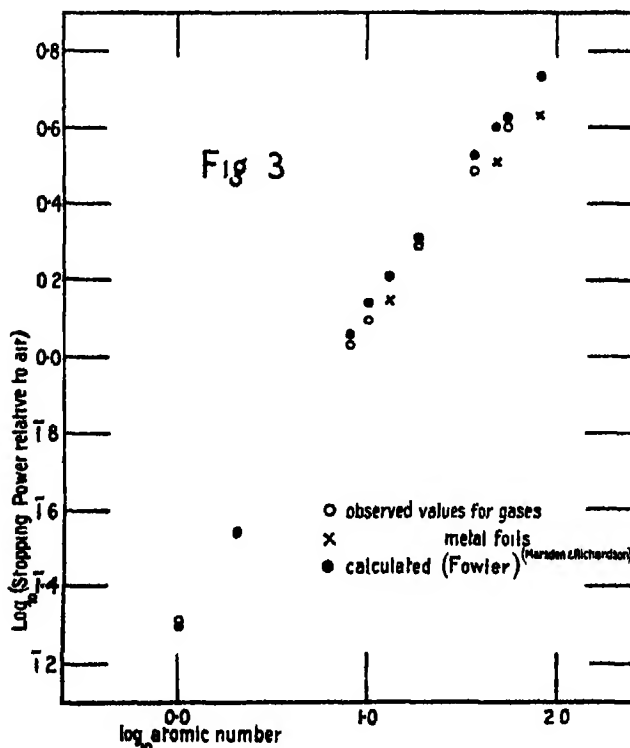
The fifth column is taken from Table I. The three measurements in column IV were made by the same method but for a residual range of 1.4 mm (there was not sufficient xenon and krypton available for measurements at this range in these gases). The values in columns II and III are for the beginning of the thorium C range and of the polonium range, respectively. In the last column are given the values of the average stopping-power over the last 4 cm of the range, obtained by Bates and by Taylor. We should expect their values to be a mean, lying intermediate between those given in column III and those in column V. This is seen to be so for each gas.

The value of most theoretical interest are those for the fastest particles, given in column II, because the theory has only been developed for the case when the velocity of the alpha-particle is great compared with the velocity of an electron in an atomic orbit. Fowler* has calculated the atomic stopping-power for high-speed alpha-particles to be expected from theory, assuming it to be due to ionisation and excitation. Since nitrogen and oxygen are diatomic, the atomic stopping-powers of the monatomic gases relative to air are double the value given in Table II.

In fig. 3 the values from column II are compared with Fowler's calculated values. Logarithms of the relative atomic stopping-power are plotted against logarithms of the atomic number. The theoretical values lie on a line slightly

* 'Proc. Camb. Phil. Soc.,' vol. 21, p. 521 (1923)

curved, and the experimental values lie on a line slightly concave in the same direction, which almost coincides



The variation of stopping-power with velocity of the alpha-particles is shown in fig 4, where the atomic stopping-powers from Table II are plotted against the range. Marsden and Richardson's measurements for foils of aluminium, silver, and gold are shown by the broken lines, and are seen to fit in well with the curves for gases. It is seen that the atomic stopping-powers all tend to converge at the end of the range.

4. Discussion.

The stopping-power of a gas is determined by the collisions of the alpha-particle itself, but only a part of the total ionisation is directly due to them. Much of the ionisation is secondary ionisation due to the delta-particles produced in the gas by the alpha-particles. Now, although the measurements of ionisation show a large difference between the behaviour of diatomic and monatomic gases, fig 3 shows that there are no such irregularities in stopping-

power. But if the stopping-power is normal, it seems that the primary ionisation must also be normal. This indicates that the anomalies found in ionisation

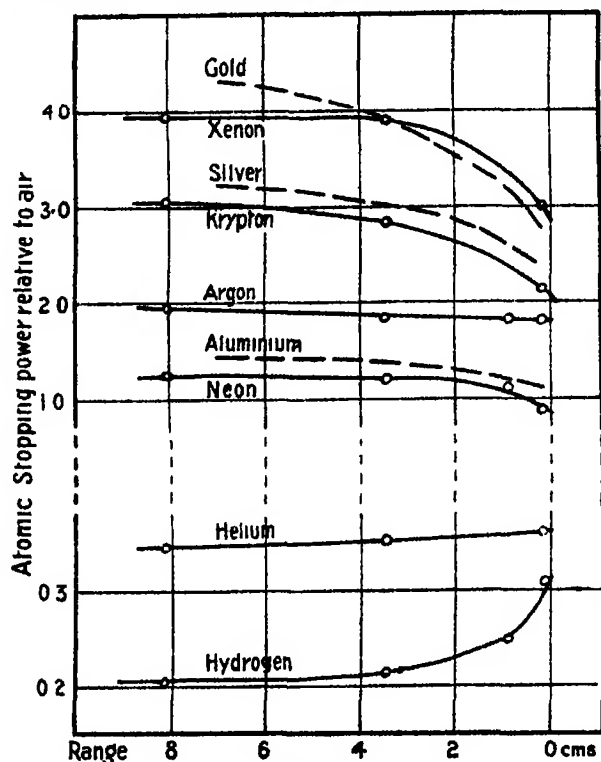


FIG. 4.

are merely anomalies in the secondary ionisation, and have no connection with the alpha-particles at all. The energy is transferred to the delta-particles, but these are apparently much less efficient ionising agents in diatomic gases than in monatomic gases. This part of the problem, then, appears to be a problem of electron-impact.

Since it is well-known that ionisation by electron-bombardment is accompanied by excitation of molecules which remain neutral it is natural to suppose that part of the energy of the delta-particles is used up in exciting radiation. There does not seem, however, to be any *a priori* reason why more energy should be spent in this way in diatomic gases than in monatomic. The obvious way to account for the greater expenditure of energy in diatomic gases would be to suppose that ionisation is accompanied by dissociation of the molecule. Smyth* determined the relative number of atomic and molecular ions produced

* 'Roy. Soc. Proc.,' A, vol 104, p 121; and vol. 105, p. 116 (1924).

by electron bombardment. In oxygen, nitrogen, and hydrogen he found that the proportion of atomic ions was small for accelerating potentials below 400 volts. The energy of most of the delta-particles must be much less than this. And, at any rate, since the energy of dissociation is only of the order of six volts, it would be insufficient to account for even half the difference between diatomic and monatomic gases, even if every molecule ionised were at the same time dissociated.

The process which would be most useful in explaining a large expenditure of energy would be dissociation, accompanied by excitation but not by ionisation, and it is this process which forms the subject of a recent paper by Hughes*. His conclusions are that in both hydrogen and nitrogen electrons of small energy readily produce dissociation, and that this dissociation is always accompanied by excitation. The evidence is somewhat indirect, but if it is confirmed it will help to explain why the ionisation in these gases is smaller than would be expected.

Fowler† showed that the absolute value of the stopping-power of air is 1.8 times as great as the value he obtained for the rate of expenditure of energy in ionisation and excitation, calculated on a basis of classical dynamics. And the present experiments show that all the gases are alike in this respect, since the values relative to air agree well with the calculated values for high-speed alpha-particles, as shown in fig. 3. As Fowler pointed out, there are two possible explanations of this excess. Either (1) the rest of the stopping-power must arise out of disturbances of the atomic system by the passing alpha-particle which do not result in a change of orbit of one of its electrons, or (2) ionisation and excitation can take place much more freely than calculations by classical dynamics can allow. The first of these explanations means that nearly half of the energy of the alpha-particles is dissipated, and if this were so it is clear that in no gas could more than about half the energy of the alpha-particles appear as ionisation. It has been shown, however, that a larger fraction than this certainly appears as ionisation in the monatomic gases, provided that Geiger's value, 33 volts for air, is nearly correct. A confirmation of this value would decide definitely in favour of the second explanation.

Summary.

By selecting small portions of the range, the relative stopping-power of gases has been measured for alpha-particles of high velocity, of low velocity,

* 'Phil. Mag.', vol. 48, p. 56 (1924).

† *Loc. cit.*

and of intermediate velocity, separately. The gases examined were xenon, krypton, argon, neon, helium, hydrogen, and oxygen. The values of the relative stopping-powers tend to converge at the end of the range. The values for high velocities are in good agreement with the relative atomic stopping powers calculated from theory by Fowler. The measurements of ionisation in these gases, previously described, are discussed in the light of this result.

In conclusion, I wish to express my thanks to Sir Ernest Rutherford for many valuable suggestions, to Dr F W Aston for kindly lending the krypton and xenon, and to Mr P M S Blackett for his advice and help

The Ejection of Protons from Nitrogen Nuclei, Photographed by the Wilson Method.

By P M S BLACKETT, Moseley Research Student of the Royal Society
and Fellow of King's College, Cambridge

(Communicated by Prof Sir E Rutherford, F R S —Received December 17, 1924.)

[PLATES 6 AND 7]

1 *Introduction*

The original experiments of Rutherford* and later those of Rutherford and Chadwick† have shown that fast alpha-particles are able by close collisions to eject protons from the nuclei of many light elements. In particular the protons from boron, nitrogen, fluorine, sodium, aluminium and phosphorus have great ranges, and are emitted in all directions relative to the velocity of the bombarding alpha-particles. The scintillation method used in these experiments can give no direct information about the motion after the collision of the residual nucleus and of the alpha-particle itself. The proton alone has sufficient range to make detection by the scintillation method possible. The Wilson Condensation Method provides the obvious and perhaps the only certain way of observing the motion of these two particles. Of the "active" elements mentioned, nitrogen can at once be selected as the most suitable for a first investigation.

* Rutherford, 'Phil Mag.', vol. 37, p. 581 (1919).

† Rutherford and Chadwick, 'Phil. Mag.', vol. 43, p. 809 (1921), vol. 44, p. 418 (1922), 'Nature,' March, 1924; 'Proc. Phys. Soc., London,' vol. 36, p. 417 (1924).

According to Rutherford and Chadwick the maximum forward and backward ranges* of the protons ejected by 7 cm alpha-particles from nitrogen are 40 and 18 cms. The total number emitted in all directions by a million 8.6 cm. alpha-particles can be estimated, from their data, to be about 20. This number decreases rapidly with the range of the alpha-particles.

In order to photograph a large number of tracks, a modified and automatic form of Wilson's apparatus was constructed, which made one expansion and took one photograph every ten or fifteen seconds. The condensation chamber itself had a floating ebonite piston similar to that described recently by Kapitza.† No mercury rings were used however and the rubber tube employed to change the volume was replaced by a corrugated metal diaphragm. A detailed description of the apparatus, which is an improved form of that previously used by the writer,‡ will be given elsewhere. The camera, designed originally by Shimizu,§ takes two photographs at right angles on standard cinematograph film ||

About 23,000 photographs have been taken of the tracks of alpha-particles in nitrogen. From 5 to 20 per cent of oxygen was added to the nitrogen to improve the sharpness of the tracks. The source used was a deposit of Thorium B + C, which gives a complex beam of 8.6 and 5.0 cm particles, the numbers being known to be in the ratio of 65 to 35. The average number of tracks on each photograph was 18, the tracks of about 270,000 alpha-particles of 8.6 cm range and 145,000 of 5.0 cm range have therefore been photographed.

2 General Results

Amongst these tracks a large number of forks were found corresponding to the elastic collisions made by alpha-particles with nitrogen (and oxygen) atoms. Reproductions of a few such tracks are given on Plate 6 (photographs 4 to 10). A description of each photograph will be found at the end of the paper.

If a particle of mass M and initial velocity V collides with another of mass m , initially at rest, and the two have velocities after collision making angles ϕ and θ with V , then the assumption that both energy and momentum are conserved leads to the relation

$$m/M = \sin \phi / \sin (2\theta + \phi). \quad (1)$$

The values of m/M calculated from the observed values of ϕ and θ are found

* Throughout the paper all ranges will refer to air at N.T.P., unless otherwise mentioned.

† Kapitza, 'Proc. Roy. Soc.' A, vol. 106, p. 602 (1924).

‡ Blackett, 'Proc. Roy. Soc.' A, vol. 102, p. 294 (1922); vol. 103, p. 62 (1923).

§ Shimizu, 'Proc. Roy. Soc.' A, vol. 99, p. 432 (1921).

|| The film was supplied and developed by Kodak, Ltd., Kingsway, London.

to agree closely with the accepted ratio of the colliding masses, thus confirming the conclusion reached in a previous paper that both energy and momentum are conserved, at least approximately, during these collisions. This result also applies to some forks due to the collision of alpha-particles with hydrogen and helium nuclei (Plate 6, Nos. 1, 2, and 3).

But amongst these normal forks due to elastic collisions, eight have been found of a strikingly different type. Six of them are reproduced on Plate 7. These eight tracks undoubtedly represent the ejection of a proton from a nitrogen nucleus. It was to be expected that a photograph of such an event would show an alpha-ray track branching into three. The ejected proton, the residual nucleus from which it has been ejected, and the alpha-particle itself, might each have been expected to produce a track. These eight forks however branch only into two. The path of the first of the three bodies, the ejected proton, is obvious in each photograph. It consists of a fine straight track, along which the ionisation is clearly less than along an alpha-ray track, and must therefore be due to a particle of small charge and great velocity. The second of the two arms of the fork is a short track similar in appearance to the track of the nitrogen nucleus in a normal fork. Of a third arm to correspond to the track of the alpha-particle itself after the collision there is no sign. On the generally accepted view, due to the work of Rutherford, the nucleus of an atom is so small, and thus the potential at its surface so large, that a positively charged particle that has once penetrated its structure (and almost certainly an alpha-particle that ejects a proton must do so) cannot escape without acquiring kinetic energy amply sufficient to produce a visible track. As no such track exists the alpha-particle cannot escape. In ejecting a proton from a nitrogen nucleus the alpha-particle is therefore itself bound to the nitrogen nucleus. The resulting new nucleus must have a mass 17, and, provided no electrons are gained or lost in the process,* an atomic number 8. The possibility of such a capture has already been suggested by Rutherford and Chadwick in a recent paper.

The argument so far has been based on the appearance of these anomalous tracks. The conclusions already drawn from their appearance are fully confirmed by measurement. The results will be summarised in this section and given in detail in the next.

In marked contrast to the normal forks, the angles between the components of each of these anomalous forks are not in general consistent with an *elastic*

* On none of the photographs is there any sign of a β -ray track, starting at the fork, longer than the usual δ -rays.

collision between an alpha-particle and a nucleus of any known or possible (i.e., integral) mass. Making the assumption that momentum alone is conserved during the collision, the velocity of the proton of assumed mass 1 is found from the measured angles of each fork to be in good agreement with those deduced by Rutherford and Chadwick from the measurement of their range. This result is independent of the mass assumed for the particle producing the short track. The momentum of the latter can also be calculated without further assumptions. The observed lengths of these tracks can be shown to be not inconsistent with the view that the particles producing them have a mass 17 and an atomic number 8.

3 *The Measurement of the Anomalous Tracks.*

There is little doubt that momentum must be conserved during these collisions, though the kinetic energy clearly is not. This assumption is supported by the observation that these anomalous forks are co-planar, as are also the normal forks. If ψ and ω are the angles between the initial track of the alpha-particle and the track of the proton and the resulting nucleus respectively, we have

$$m_p v_p \sin \psi - m_n v_n \sin \omega = 0,$$

$$m_p v_p \cos \psi + m_n v_n \cos \omega - MV = 0,$$

where m_p and m_n are the masses, and v_p and v_n the velocities, of the proton and final nucleus, and where M and V are the mass and initial velocity of the alpha-particle. We therefore find that

$$m_p v_p = MV \sin \omega / \sin (\psi + \omega), \quad (2)$$

and

$$m_n v_n = MV \sin \psi / \sin (\psi + \omega) \quad (3)$$

For each track ψ and ω are measured, while V is calculated from the distance of the fork from the source, whence from (1), assuming $m_p = 1$, we obtain v_p . Assuming with Rutherford that the range of a fast proton is proportional to the cube of its velocity and that a proton of velocity 3.08×10^9 cm. per sec. has a range of 28 cm., we find the following values for the ranges of the protons in the six photographs most suitable for measurement

Range	31,	52,	25,	18,	24,	19 cm.
ψ	41°,	63°,	65°,	79°,	84°,	150°.

Underneath each range is tabulated the angle ψ of projection of the proton. The average initial range of these six alpha-particles is 6.8 cm.

It is important to realise that since v_p is independent of m_a in (2), the ranges above are independent of the value assumed for the mass of the heavier particle. These calculated ranges are in sufficient agreement with the measurements of Rutherford and Chadwick, who found that 7.0 cm alpha-particles ejected protons from nitrogen with maximum *forward* and *backward* ranges of 40 and 18 cms. They also found that these maximum ranges were roughly proportional to the initial range of the alpha-particles. Far more data will be required before one can hope to find in the photographs any indication of this proportionality. Not only are these calculated ranges somewhat unreliable owing to their being obtained by the cubing of the measured quantities, but the two methods do not give strictly comparable results. The measurements of Rutherford and Chadwick give the *maximum* range of all the protons ejected within a cone of wide angle. The measurement of a photograph gives the *actual* range of a single proton ejected at a particular angle. The first five tracks above may be considered to represent *forward* particles, since in none of them has ψ a value greater than 85° . The last, for which ψ is 150° , is a *backward* particle.

From (3) we calculate for each fork the momentum of the particle producing the short track. Assuming its mass to be 17 we find its velocity. It can now be shown that the observed lengths of the tracks of the particles are consistent with their assumed nature and calculated velocities. From a study of the elastic collisions with nitrogen atoms the range of a nitrogen nucleus of given velocity can be determined. Below are given the observed lengths of the tracks of the particles of supposed mass 17 and atomic number 8, together with the lengths of the tracks of nitrogen atoms of the same initial velocity.

Observed length of tracks in mm.	2.36	3.10	2.78	3.14	3.64
Range of N atom of same velocity	2.00	2.50	2.70	2.90	2.80
Ratio	1.18	1.24	1.04	1.08	1.30

The ratios of the ranges in the two rows are also given. Thus, on the average the particles of assumed mass 17 have an observed range 1.16 times that of a nitrogen atom of the same initial velocity. Now the ranges of particles of the same atomic number and velocity must be proportional to their masses. Further, it has been shown by the writer (*loc cit*) that the rate of loss of energy of particles of the same velocity is roughly proportional to the square root of their atomic number*. A particle of mass 17 and atomic number 8 will therefore

* This relation, which is obtained from the ranges of hydrogen, helium, "air," and argon atoms of the same initial velocity, only holds roughly. A better approximation would be to write $1/(z^2 - 0.5)$ for $1/z^2$ in the formula, but to do this would not appreciably alter the following argument.

travel $17/14 \times (7/8)^{1/2} = 1.14$ times as far as a nitrogen atom of the same velocity. Since the mean observed ratio is 1.16 the agreement is satisfactory.

It must however be remarked that the observed length of the tracks is also consistent with the hypothesis that they have other masses than 17. For expressing the argument above as to the range R of a particle of mass m , atomic number z and velocity v , in the form

$$R \propto m z^{-1} f(v),$$

we see that it is not possible to distinguish between particles of the same momentum but of different masses, unless $f(v)$ is markedly non-linear, which, in the case of the nitrogen atom, it is not. Some results, to be described in detail elsewhere, show that R varies roughly as $v^{1.1}$ over the significant range of velocity. The range of such a particle is therefore roughly proportional to its momentum. Since it is only the momentum which is given directly by (3), it is not possible from the observed lengths of the tracks and the known momentum of the particles producing them, to determine the masses of the particles. It is however possible to determine their atomic number. Thus to explain the observed ratio of 1.16 the particles of mass 17 should have an atomic number 7.7. The actual value must of course be integral and is probably 8, as has already been shown. With more and better data it should be possible to distinguish with certainty between 8 and 7 (or 9), and so to discover whether or no any nuclear electrons, other than those in the alpha-particle itself, are gained or lost by the system during the collision.

The general result of this argument may be stated as follows. The observed lengths of the tracks are consistent with their being due to particles of atomic number roughly 8, but of any mass from, say, 12 to 20. In order to retain the conservation of mass we must of course assume that their actual mass is 17.

Knowing the masses and velocities of the two particles after the collision, their kinetic energy can be calculated. The ratio e of this energy to the initial energy of the alpha-particles is given below for six tracks.

Values of e , 0.83, 1.02, 0.72, 0.68, 0.88, 0.93. Mean 0.81.

On the average therefore there is a loss of kinetic energy of 19 per cent. This is in sufficient agreement with the value of 13 per cent. calculated by Rutherford and Chadwick, taking into account the somewhat different assumptions made by them, and the uncertainty in the measurements of the tracks, from which these values of e are calculated.

4. The Frequency of the Forks

From a study of single collisions, information can be obtained about the energy and momentum relations alone. To determine the law of force between the colliding particles a statistical analysis of the number of collisions of all types is necessary. Failing such an investigation, which, to be satisfactory, will require many more photographs than have yet been taken, the following remarks will be made tentatively.

Amongst the 270,000 alpha-particles of 8.6 cm range, whose tracks have been photographed, 14 have been deflected through angles between 45° and 90° . On the inverse-square law the number would, on the average, be about 12—in rough agreement with the observations. On the other hand the number deflected elastically through angles greater than 90° is found to be 8, while the average number on the inverse-square law would be about 1.5. This indicates that the inverse-square law between alpha-particles and nitrogen nuclei* does not hold for such intimate collisions. The discrepancy is still more marked, if the eight anomalous forks, not counted above, are considered to be due (as they certainly must be due) to very close collisions which would have resulted, had not a proton been ejected, in a deflection through a large angle. It is a fact of great interest that such collisions (photographs 7, 8, 10, Plate 6) can occur without a proton being ejected. The fact that they do, supports the view of Rutherford and Chadwick that the ejection of a proton does not necessarily occur when the initial path of the alpha-ray lies within a limiting distance of the nitrogen nucleus. There must be some other factor which determines whether an elastic collision is to be made or the alpha-particle is to be captured and a proton ejected.

The number of the anomalous forks that have been observed, 8 in 270,000 tracks of 8.6 cm and 145,000 tracks of 5.0 cm. alpha-particles, gives a somewhat higher average than that of about 20 in a million which can be deduced from the measurements of Rutherford and Chadwick. Little significance can be attached to this discrepancy in view of the probability variations to be expected with so small numbers.

5 Discussion of Results

The study of the photographs has led to the conclusion that an alpha-particle that ejects a proton from a nitrogen nucleus is itself bound to that

* Some of the large-angle deflections may be due to collisions with atoms of oxygen, one part of which was mixed with about 10 of nitrogen, but they cannot all be so due, unless one postulates an extreme departure from the inverse-square law for these nuclei.

nucleus This result is of such importance that it is useful to emphasise the evidence on which it is based.

The first step in the argument must show that the eight anomalous forks do actually represent the ejection of a proton from a nitrogen nucleus Their appearance makes this probable ; the measurements of the forks, the frequency of their occurrence and the absence of any other abnormal forks, make it certain

The second step must show that if the alpha-particle is not bound to the nitrogen nucleus after the collision, a third arm to the forks would be found This follows from the work of Rutherford,* Chadwick† and Bieler‡ on the scattering of alpha-particles These results require the force between an alpha-particle and a nucleus to be still repulsive even when their distance apart is very small. Bieler estimated the maximum potential of the electric field close to the aluminium nucleus as 4×10^6 volts from his scattering experiments Rutherford was able to detect a minimum range of protons ejected from aluminium and sulphur, corresponding to a maximum potential of about 3×10^6 volts Unless nitrogen is markedly different from these elements, this then is the order of the total kinetic energy of the alpha-particle and nucleus after separating, since it seems certain that to eject a proton an alpha-particle must penetrate within the surface of maximum potential Particles of this total kinetic energy will certainly both produce visible tracks The fact that only one track is actually found makes it therefore certain that the two particles are bound together The only possible way of avoiding this conclusion is to assume some very improbable mechanism by which the mutual potential energy of the alpha-particle and nucleus may be transformed into kinetic energy of the proton or into radiation. Provisionally this possibility may be ignored

Of the nature of the integrated nucleus little can be said without further data. It must however have a mass 17, and provided no other nuclear electrons are gained or lost in the process, an atomic number 8. It ought therefore to be an isotope of oxygen. If it is stable it should exist on the earth. If it does exist it must be in such small quantities as to escape detection in the mass spectrograph of Aston, or by its influence on the chemical atomic weight of oxygen. The fact that it certainly is not abundant is consistent with the class of elements of odd atomic weight to which it belongs, and which have been shown by Harkins to be on the whole of comparatively rare occurrence. Also

* Rutherford, 'Phil. Mag.', vol. 21, p. 669 (1911)

† Chadwick, 'Phil. Mag.', vol. 40, p. 734 (1920); vol. 42, p. 924 (1921).

‡ Bieler, 'Roy. Soc. Proc.', A, vol. 105, p. 424 (1924)

the fact shown first by Rutherford, and confirmed by this work, that the sum of the final kinetic energies of the proton and the heavy nucleus is less than the initial energy of the alpha-particle, indicates that the new integrated nucleus has a higher internal energy than the nitrogen nucleus, provided no large amount of energy is lost, for instance, by radiation. On any mechanical picture of a nucleus this greater internal energy should indicate a lower stability, in agreement, if one accepts the correlation between stability and abundance suggested by Harkins, with the certain rarity and possible non-existence on the earth of this isotope of oxygen.

It is possible that the integrated nucleus may have a short life. One can however be certain that if it breaks up again with the emission of any *positively* charged particle it must have a life greater than the time of effective supersaturation in the condensation chamber—a time of the order of $1/1000$ sec—otherwise the track of the emitted particle would be visible on the photographs.

I wish to express my thanks to Sir Ernest Rutherford, who suggested this work and assisted by his help and advice in its execution. I also wish to thank Mr C. T. R. Wilson for his interest and help in the development of the technique, and Mr. P. Kapitza for help in the design of the expansion chamber. Much of the expense of the work has been borne by grants both from the Government Grant Committee of the Royal Society and from the Research Fund of King's College, Cambridge.

DESCRIPTION OF PLATES.

The Normal Forks (Plate 6)

Each photograph shows the fork due to the elastic collision between an alpha-particle and a nucleus of hydrogen, helium or nitrogen.*

Symbols used in the description of the photographs —

- ϕ . The angle of deflection of the alpha-particle
- θ . The angle between the initial track of the alpha-particle and the track of the nucleus with which it has collided. Angles in brackets have only been measured roughly
- m/M . The ratio of the masses of the colliding particles, calculated from equation (1).

* See Note (*) under Table.

Photograph.	Type of atom struck by alpha-particle	ϕ	θ	m/M calc	m/M theory.
1	Hydrogen	8° 27'	68° 0'	0.253	0.2520
2	"	8° 39'	66° 23'	0.241	0.2520
3	Helium	38° 34'	50° 53'	0.981	1.000
4	Nitrogen*	(45°)	—	—	—
5	"	(51°)	—	—	—
6	"	(32°)	—	—	—
7	"	(121°)	—	—	—
8	"	128° 44'	20° 10'	4.1†	$\left\{ \begin{array}{l} 3.50 \\ 4.00 \end{array} \right.$
9	"	98° 51'	33° 39'	4.1†	$\left\{ \begin{array}{l} 3.50 \\ 4.00 \end{array} \right.$
10	"	(110°)	—	—	—

* A few of these collisions are probably due to collision with oxygen rather than nitrogen nuclei

† The probable error of these determinations of m/M for N and O is large, of the order of 0.6, so that these collisions may still be with N atoms

Nos. 1, 2 and 3 are all due to alpha-particles of range greater than 7 cm. The calculated values of m/M show that the collisions are approximately elastic, a result of importance in view of the very intimate nature of the collisions.

The series of photographs 4 to 10 show examples of elastic collisions of varying angles between alpha-particles and nitrogen atoms. They emphasise the marked contrast between the elastic and the inelastic collisions (Plate 7).

The track of the *nitrogen* atom itself in Nos. 6 and 10 makes a fork for which $\theta + \phi \doteq 90^\circ$. These are clearly due to the collision of one nitrogen atom with another.

The short isolated length of track in No. 8, which nearly passes through the divide of the fork, is due to "contamination," that is, to an alpha-particle emitted by some radioactive body that has strayed into the chamber itself.

The Anomalous Forks (Plate 7)

Each photograph shows the ejection by an alpha-particle of a proton from a nitrogen nucleus. The straight fine arm is the track of the proton. The short, somewhat bent arm is the track of the nucleus, of mass 17 and atomic number probably 8. The non-existence of a third arm to the forks can be seen most clearly in 1, 4 and 6. In the remaining photographs the presence of other tracks somewhat obscures the divide of the fork. Even on most of these others however a third arm, if present, would be noticeable.

Photograph No. 1.—This fork, though apparently good, is unsuitable for accurate measurement owing to—

- (a) a slight curvature of the tracks due to mass motion of the gas, caused by a slight leak ;
 (b) a small bend in the alpha-ray track immediately before the divide of the fork.

Photographs Nos 2 and 3—Note delta-ray tracks along the tracks of the protons

Photograph No 4—The visible track of the proton is short as it moves downwards out of the effective part of the chamber

Photograph No. 6—The beginning of the track of the heavy nucleus can just be detected in the left-hand image. Unfortunately its end is lost by its passing out of the effective part of the chamber.

The beaded appearance of the proton tracks, evidence of the small ionisation along them, can be seen in the photographs. Since the ionisation due to any particle is proportional to the square of its charge and the reciprocal of its velocity, the ionisation density along these proton tracks should be about one-sixth of that along the alpha-ray tracks

The measurements of the eight forks are given in the accompanying table

Row	No of Fork	1	2	3	4	5	6	7	8
	No of Photo on Plate 7	3	2	Not repro duced	Not repro duced	4	6	1	5
1	\downarrow	41° 4'	62° 46'	65° 15'	78° 52'	84° 29'	149° 42'	39° ?	—
2	ω	22° 0'	28° 51'	21° 13'	19° 24'	22° 12'	7° 54'	21 ?	—
3	$\omega + \psi$	63° 4'	91° 37'	86° 28'	98° 16'	106° 41'	157° 36'	60	79° 57'
4	R_{α} cm	6 28	7 13	7 93	7 28	6 08	6 24	7 79	8 14
5	$V \times 10^{-8}$ cm per sec	1.85	1 93	1 99	1 94	1 83	1 85	1 97	2 02
6	$v_p \times 10^{-8}$ cm per sec	3 12	3 73	2 93	2 61	2 88	2 67	3 22	—
7	R_p cm	31	52	25	18	24	19	34	—
8	$v_{\alpha} \times 10^{-8}$ cm per sec	3 20	4 04	4 20	4 52	4 46	5 76	3 37	—
9	R_{α} cm.	2 36	3 10	2 78	3 14	3 64	—	2 00	2 30
10	e	0 83	1 02	0 72	0 68	0 88	0 93	—	—

In rows 1 and 2 are given the angles of projection ψ and ω of the protons and heavy nuclei respectively. From the range of the alpha-particles before the collision (row 4) is deduced the velocity V of the alpha-particle, assuming the law of decrease of velocity with range

In row 6 are the velocities v_p of the protons, calculated from equation (2), with the corresponding ranges R_p (row 7)

The velocities v_n of the heavy nuclei, calculated from (3), are given in row 8, and their measured ranges in row 9

The ratio e of the final kinetic energy of the two bodies to the initial energy of the alpha-particle is given in row 10

The consistent variation of v_n (row 8) with R_n (row 9) confirms the assumption, that all these forks are due to the 8.6 and not to the 5 cm particles.

The Apparent Tripling of Certain Lines in Arc Spectra.

By T. ROYDS, D.Sc., Director, Kodaikanal Observatory.

(Communicated by J. Evershed, F.R.S.—Received November 12, 1924.)

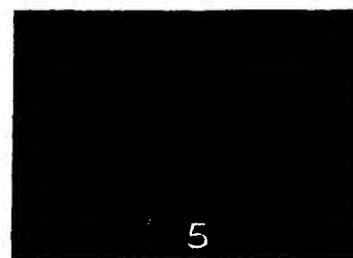
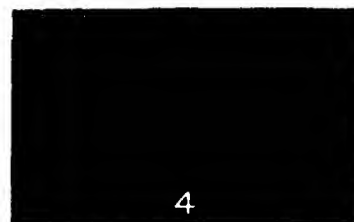
[PLATE 8]

King discovered* that the lithium line 6708, in the arc or in the furnace, changed from a doublet into a triplet by increasing the amount of Li vapour present, the separation of the triplet increasing with the amount of vapour. He suggested that the effect was due to the electrical resolution of the line by the action of interatomic fields. If this suggestion can be verified, we shall have therein a means of measuring the intensity of the interatomic fields in the arc, and from that a means of determining the interatomic fields in the sun, for in 'Kodaikanal Observatory Bulletin, No. 73,' the view was put forward that the abnormal displacements of unsymmetrical lines when the sun and arc were compared were due to interatomic electrical fields caused by ionisation, the field in the sun being roughly estimated at about 2,000 volts/cm. less than in the centre of the arc employed †

2. Consequently it seemed important to investigate more fully this observation of King, in order to find whether his suggestion of its being due to electrical

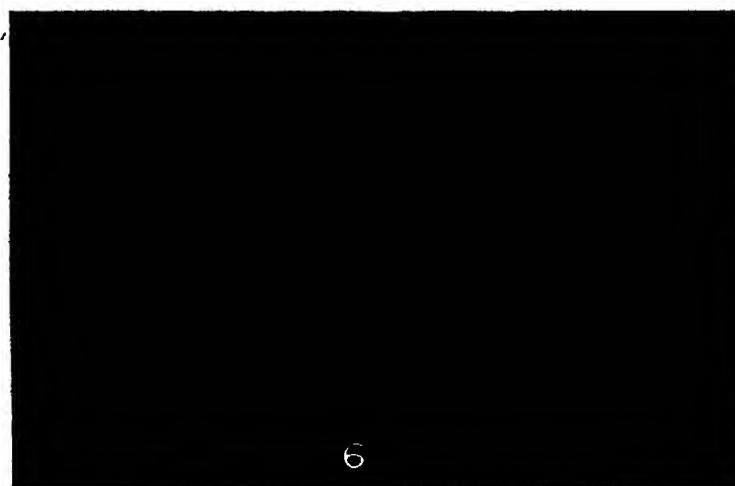
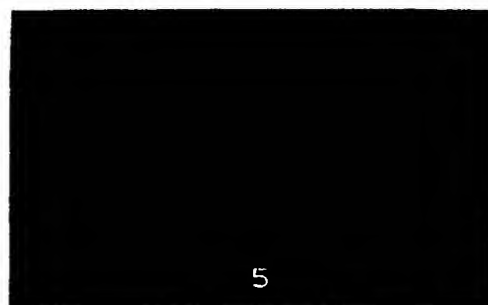
* King, 'Astrophysical Journal,' vol. 44, p. 169 (1916).

† Royds, 'Kodaikanal Observatory Bulletin, No. 73.'



Elastic Collisions between Alpha-Particles and H, He, and N Atoms.

[Facing p 860.]



Ejection of Protons from N Nuclei by fast Alpha-Particles

fields could be maintained. It was obvious that if his interpretation were correct, not merely a few exceptional lines, but the majority of spectrum lines should show a complexity on increasing the amount of material in the arc, if the resolving power of the spectroscope were sufficient to show it. As a preliminary it therefore seemed desirable to search through the whole visible region of the spectra of as many substances as were readily available in order to make a list of those lines which could be made triple or multiple by merely increasing the amount of material in the arc. From previous knowledge it seemed a foregone conclusion that the number of such lines must be small, but whether small or large, the most suitable case could then be chosen for a complete investigation of the cause, and the hypothesis revealed could be tested on the remaining examples.

3 The spectra of the following substances Li, Na, K, Rb, Cs, Cu, Ag, Mg, Ca, Si, Ba, Zn, Cd, Al, Tl, Sn, Pb, Sb, Bi, Fe were searched throughout the visible region, and the behaviour of each line, especially of the stronger and the more easily reversible lines, was watched as the amount of material under investigation in the arc was increased or decreased. The spectrograph used was the one described in 'Kodaikanal Observatory Bulletin, No 36,' observations being made with eyepieces in the 2nd, 3rd or 4th order according to the intensity of the line being examined. To avoid prejudice, no literature regarding the complexity of spectrum lines was looked up beforehand, with the exception of King's paper already referred to relating to the Li line 6708. The material was vaporised in the arc, either from metallic poles or by introducing salts into a carbon arc, the object being to secure spectrum lines as strong as possible with materials readily available, and whenever any reversal, doublet, triplet or multiplet was suspected the effect of reducing the amount of material in the arc was carefully watched.

4 Of several hundreds of lines studied the following seven are the only ones found to become complex on increasing the amount of material in the arc:—

Li 6708,* 6103, Tl 5350, Sr 4876 2, 4872, 4832, Mn pair 4235.

All these seven lines behave similarly, becoming triple when the amount of material is increased. The clearest case seemed to be that of the thallium line 5350, which was therefore chosen for exact and careful study in visual examination, and for measurement in photographs in order to determine the real nature of the change in character and position of the components as the amount of material in the arc was increased or decreased.

* Investigated by King, *loc. cit*

5 The structure of the thallium line 5350 has been studied by many observers previously* and has been found by some to be double, by others to be triple even though only temporarily, but the progressive development of this line, as described below, does not appear to have been seen before, although Nutting† gives a partial account. After introducing a little thallium salt into the arc the 5350 line passes through five distinct phases as the amount of material in the arc gradually decreases. If a continuous watch is kept on any part of the arc, the line is seen to pass through all its five phases in succession as the material is consumed, but according as the arc conditions are chosen the same phase may be exhibited along the whole length of the arc, or several phases may be simultaneously visible in different parts of the arc. The arc used was between carbon poles, 100 to 110 volts, 4 to 6 amperes, a little thallium nitrate being placed on the lower electrode. The state of several phases being simultaneously evident was very convenient for the visual examination of the behaviour of the line, and seemed best exhibited when the upper electrode of the carbon arc was made the positive pole. This arrangement was, however, not so suitable when it was desired to photograph any isolated phase, which was best achieved by making the upper electrode the negative pole, for then the phase was nearly uniform across the whole length of the arc. When all was ready to photograph any particular phase of the 5350 line, new material was introduced into the arc and allowed to burn, whilst the behaviour of the line was watched visually in a different order from that where the photograph was being taken; when the line had reached the phase desired the exposure was made, the exposing shutter being closed before a succeeding phase developed. Photographs for wavelength comparison were made by alternate exposure of the different phases of the line in juxtaposition at different heights on the plate.

6 The sequence of behaviour of the Tl 5350 line after introducing new material into the arc is as follows. For the sake of definiteness, let us suppose that a little thallium nitrate is placed on the lower, negative, carbon pole, the arc is then started and allowed to burn continuously.

Phase I—At first the line is broad with a broad reversal and appears symmetrical in width and in intensity. This is denoted as phase I, and is shown as a negative in Plate 8, fig 1. In this phase the Tl line resembles most other broad reversed lines, such as the Na D lines, Ba 5535, etc. Phase I represents beyond all doubt ordinary self-reversal, its characteristic being a broad winged emission line, the centre of which is absorbed by the cooler outer region of

* Kayser, 'Handbuch der Spectroskopie,' vol 6, p. 715.

† Nutting, 'Astrophysical Journal,' vol 23, p 64 (1906)

the arc [In this phase, the reversal does not appear absolutely black for there is a very faint, but not sharp, line in the middle of the reversal, this broad central bright line cannot be seen in fig 1 on account of its faintness, but its appearance seems common to all broadly reversed lines, the Na D lines, for example, and deserves further study] As the arc continues to burn and the material in the arc decreases, the line with its reversal becomes gradually narrower

Phase II --When the reversal has narrowed down to a certain stage, there appears a fine emission line within the reversal but nearer to the red side than to the violet At first it is faint but gradually strengthens as the amount of material in the arc *decreases* This is denoted as phase II, shown in fig 2, and represents the first triplet form which the line assumes In fig 2 the middle component is seen to be approximately twice as far from the outer component towards the violet (left in the figure) as from the outer component towards the red, but the outer components still have the wings characteristic of a broadened line At a later stage, shown in fig 3, where the middle component has grown stronger than the red outer component and at least as strong as the violet outer component, the outer components have lost most of their wings, so that the appearance begins to resemble a triplet composed of three sharp lines As the arc continues to burn the middle component gains in intensity and approaches the red outer component

Phase III --Eventually the middle component joins the red outer component, and the line has now the appearance of a doublet with the red component three or four times as wide as the violet, and somewhat more intense This is illustrated in fig 4 and designated phase III

Phase IV --Soon, however, a new central component separates from the broad red component of phase III and the line again assumes a triplet form This phase IV is shown in fig 5 The red component is the strongest and the middle component the weakest

Phase V --The middle component of phase IV gradually approaches the violet component and ultimately unites with it The line has now again assumed a doublet form denoted as phase V and shown in fig 6 The violet component is now about three times as strong as the red component of the doublet This is the final phase As the amount of material in the arc continues to decrease the two components of the doublet remain at a fixed separation until the red one becomes so faint as to be invisible

Phases II, III and IV are shown simultaneously in different parts of the arc in fig 7, and phases IV and V in fig 8 The photographs are, of course,

unretouched, but in making the print for reproduction the lower parts of figs 7 and 8 were given shorter exposure than the upper. The scale of enlargement in figs 7 and 8 is greater than in the remaining figures. It should, perhaps, be noted that, although there are two triplet forms and two doublet forms, these can never be confused as an inspection of the photographs will show, the intensities and widths of the triplet in phase II (figs. 2 and 3) are different from those in phase IV (fig 5) and the intensities and widths in phase III (fig 4) are easily distinguishable from those in phase V (fig 6).

7 The real nature of the change from one phase to another cannot be determined from a visual inspection of the line and only becomes clear by making wave-length comparisons in photographs. The final phase V was chosen as standard. In this final doublet stage the components remain fixed at a separation of 0.112 Å even when the amount of material is much diminished. Hence it cannot be a self-reversal of a single line but must be a true doublet with the red component fainter than the violet. Other phases were photographed in the manner explained in paragraph 5, in juxtaposition with phase V, under conditions for strict wave-length comparison. The clue to the whole behaviour of the Tl 5350 line is furnished by fig. 9, where phases II and V are compared. An inspection of fig 9 is almost sufficient for conviction that in phase II each line of the phase V doublet has become self-reversed, the middle component of phase II being a combination of the red component of the self-reversal of the violet line and the violet component of the self-reversal of the red line. Measurements fully confirm this, and with the additional fact that the violet line of the phase V doublet reverses more easily (i.e., with less material in the arc) than the red line, the whole behaviour of the Tl 5350 line can be readily explained as different stages in the self-reversal of the phase V doublet as follows —

Phase I —The amount of material in the outer absorbing regions of the arc is so large that the lines of the phase V doublet are broadened until they overlap, and the appearance of the line is thus indistinguishable from that of a single line self-reversed.

Phase II —The amount of material in the outer absorbing regions of the arc is now reduced until the lines of the phase V doublet no longer overlap but are gradually narrowing down. The absorptive power of the outer regions of the arc is, therefore, becoming sufficiently small in the gap between the lines for the light emitted by the core of the arc to penetrate, this is represented by the middle component appearing within the broad reversal of phase I, which will become wider and stronger as the amount of material decreases. In other

words, phase II represents the self-reversal of each line of the phase V doublet

Phase III —The material in the outer regions of the arc is now reduced until there is insufficient to reverse the red line of the phase V doublet. The red component of phase III is a blend of the unreversed red line and the red component of the reversed violet line of the phase V doublet.

Phase IV —As the material is still further reduced the self-reversal of the violet line narrows down and its red component separates from the unreversed red line of the phase V doublet. The red component of phase IV is now no longer a blend but a single line.

Phase V —Eventually the amount of material is insufficient to reverse even the violet line, and we now get two unreversed lines. Further reduction of material in the arc merely decreases the intensity of both lines without affecting their separation.

8 This explanation is adopted because the wave-length measurements reveal —

(1) That the violet line of the phase V doublet is not displaced relative to (a) the centre of the space between the violet and middle components of phase IV (fig 11), (b) the centre of the space between the two components of phase III (fig 10) and (c) the centre of the space between the violet and middle components of phase II (fig 9). The average measured displacements were (a) $+0.001$ A, (b) 0.000 A and (c) $+0.001$ A, which are inconsiderable quantities.

(2) That the red line of the phase V doublet is not displaced relative to (a) the red component of triplet of phase IV (fig 11) and (b) the centre of the space between the red and the middle components of phase II (fig 9). The average measured displacements were (a) $+0.003$ A and (b) $+0.003$ A, which are small and probably not real, as the measurement was difficult in those cases when phase III was closely approached.

(3) That the interval between the following components is constant in all photographs (a) in phase V between the two lines of the doublet, (b) in phase IV between the red component and the centre of the space between the middle and the violet components, (c) in phase II between the centre of the spaces on each side of the middle component. The average measured intervals were (a) 0.112 A, (b) 0.112 A and (c) 0.111 A.

(4) That there are no other constancies of wave-length in the varied phases of the line, e.g., the middle component of phase II has not the same wave-length as the middle component of phase IV.

It should be understood that not only have the typical phases been included

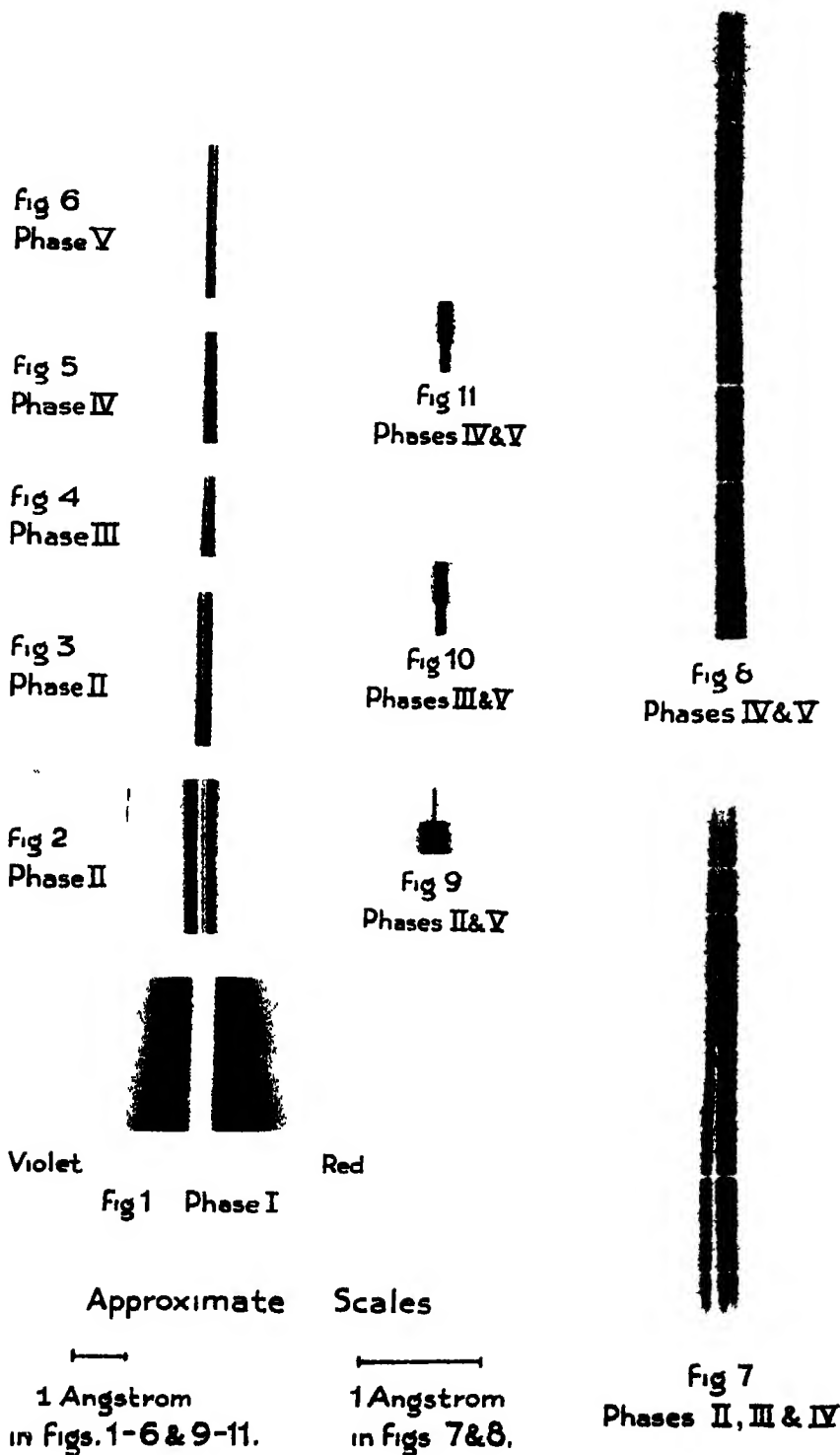
in the measurements, but also intermediate phases, where often the measurement is difficult especially when phase III is closely approached.

9. The explanation given in para. 7 that the whole behaviour of the Tl 5350 line can be explained as different stages in the self-reversal of the two lines of the doublet seems adequate and simple, and there is no need to invoke the resolution by interatomic fields suggested by King to obtain a complete explanation. There are two *a priori* reasons against the tripling in the arc being due to resolution by interatomic fields—(1) the effect in the electric arc would be an interatomic field averaged over all atoms which would be expected to result in a blending of the components into a broad line rather than a field sufficiently uniform over all atoms to yield a definite resolution into components, and (2) a field strong enough to resolve one line in the spectrum would resolve all lines sufficiently sensitive, and we should expect all lines to be complex simultaneously to a greater or less degree according to the magnitude of their Stark effect. As a matter of fact, the number of lines becoming complex when the amount of material in the arc is increased is very small. Out of hundreds of lines examined, only seven cases of complexity developing have been found, as stated in para. 4, this number might perhaps be increased by employing metals instead of salts, but it has been sufficiently proved that the effect is very exceptional.

10. The case of the Tl 5350 line having been completely investigated and a simple explanation found, it remains to test whether the same explanation suffices for the other six cases. In all these except two the final phase is a doublet, and in the two exceptional cases the tripling is so difficult to observe that the resolution of the final doublet was hardly to be expected. The details for the remaining six cases are as follows:—

La line 6708. This is very similar in appearance to the Tl line 5350, except that the lines are less sharp and that the reversals narrow down simultaneously. With a large amount of material there is a broad self-reversal corresponding to phase I of Tl 5350. Then an apparent triplet develops by the appearance of a central component nearer to the red side of the reversal than to the violet, this is the phase corresponding to phase II of the Tl 5350 line and is the self-reversal of each line of the final doublet. Since the reversals narrow down simultaneously the next phase has the appearance of a single but not sharp line, before it becomes resolved into the final doublet stage, corresponding to phase V of the Tl 5350 where the violet line has about twice the intensity of the red line.

La line 6103. This is very similar to the 6708 line, except that the unsym-



metrical character of the latter has its counterpart on the opposite side and that the lines are still less sharp. The central component in the triplet form is nearer the violet side than the red, and in the final doublet form the red line is the stronger of the two. In the third order the final doublet is only just resolved.

Sr lines 4876·2, 4872, 4832. The line 4832 triples the most readily of the three and with a small amount of material the line becomes finally double, with the violet component about one-third the intensity of the red component. The lines 4876·2 and 4872 triple less readily, and the final phase of each could not be resolved.

Mn pair 4235·4, 4235·2. With a small amount of material these two neighbouring lines are of about equal intensity, forming a "doublet," although perhaps not a physically connected doublet. When the amount of material is increased each line reverses, combining into a triplet by the merging of their adjacent components.

Summary

1. As many spectra as possible were searched through the visible region for instances of lines becoming complex when the amount of material in the arc was increased.

2. Only seven cases were found, all being of similar type in becoming apparently triple with a sufficient quantity of material.

3. The Tl line 5350 was the easiest to investigate and was found to pass through five successive phases, viz., broad simple reversal, triplet, doublet, a second triplet form, and a final doublet as the amount of material in the arc burns out.

4. It is shown that the Tl 5350 line is essentially a doublet and that all the different phases can be simply explained as different stages in the self-reversal of the two lines of the doublet.

5. The same explanation of self-reversal of an essential doublet was adopted for the six remaining instances of apparent tripling, as all except two were found to assume a doublet form as the final phase; in the two exceptions the doublet was expected to be difficult to resolve.

On the Life Statistics of Fellows of the Royal Society.

By SIR ARTHUR SCRUSTER F R S

(Received January 20, 1925)

In the year 1892, Lieut-General R Strachey communicated a paper to the Royal Society "On the probable effect of the limitation of the number of Ordinary Fellows elected into the Royal Society to fifteen in each year on the eventual total number of Fellows". The main conclusions arrived at were summarized as follows "On the whole it seems to be established that the present restriction to 15 of the number of Ordinary Fellows elected in any year will lead to an eventual maximum number not exceeding 420 and that the ultimate increase of the total strength of the Society for each additional Fellow elected in excess of 15, may be taken at 28, so that an increase of the annual number of Ordinary Fellows to 18 would lead to an ultimate total of 500 such Fellows". The results were based on a statistical examination of the average age of Fellows at election, together with such tables as were then available of the probable duration of life. The present number of Ordinary Fellows exceeds Strachey's figure by about twenty.

During recent years the question has occasionally been raised, as to whether the time has arrived for a small increase in the number of annual elections in view of the larger scientific output of the country, that has taken place since the present regulations came into force. An argument in favour of this policy might be urged if a substantial and permanent increase in the average age at election to the Fellowship had occurred in recent years, though this would not necessarily be decisive. In order to obtain the relevant facts it seemed desirable to bring the statistics up to date. The work proved to be more serious than was anticipated, because numerous and substantial errors were found to vitiate Strachey's figures, apart from the scarcity of material at his disposal. Of the 614 Ordinary Fellows elected between 1848 and 1890, there were 42 whose date of birth had not been ascertained, and their ages at election were assumed to be equal to that of the average of the known ages during successive periods of ten years. Inaccuracies, amounting in individual cases to ten years or more in the assumed age, produced errors in the annual average amounting frequently to more than a year, and once to as much as three years. One Fellow is entered as having been elected in the year 1872 at the age of 87. This is a mistake, which can only be explained by a confusion of Dr E. L Ormerod, who was elected in 1872, with G Ormerod, who died in 1873 at the

age of 88 It so happened that E L Ormerod also died in that year, but he was then only 64 years old

With one exception I have succeeded in ascertaining the year of birth of every Fellow elected since 1848 The missing date of birth is that of Captain Levett Landon Boscawen Ibbetson, a geologist of some distinction, who presented his collection of fossils to the Jermyn Street Museum He spent his last years in Germany and died at Biebrich on the Rhine on September 8, 1869 He is described in the List of Members of the Royal Society as a Knight of the Red Eagle, and as K H, which, I understand, may mean " Knight of Hanover "

Before 1847 the procedure at elections was determined by statutes which allowed a proposal to be made at any meeting the voting taking place at some subsequent meeting without restriction of numbers, but a two-third majority being required for election The Council of the Society as such, had no special powers of nomination I have collected in Table I the average number of elections under these statutes for successive periods of 25 years, together with the last short period of 23 years

Table I Average Number of Annual Elections before 1848

Period	Average Number	Period	Average Number
1675-1699	9	1775-1799	23
1700-1724	15	1800-1824	26
1725-1749	24	1825-1847	28
1750-1774	23	—	—

The maximum number elected in a single year (1834) was 50

New statutes were introduced in 1847, directing the Council to select by ballot from a list of candidates " a number not exceeding 15, to be recommended to the Society for election " In view of what followed it is necessary to quote verbatim the statute which determined the procedure at election —

" On the day of election two Scrutators shall be nominated by the President, with the approbation of the Society, to assist the Secretaries in examining the lists, and each Fellow present and voting, shall deliver to one of the Secretaries or Scrutators, one of the printed lists mentioned in Statute VIII, having erased the name of any Candidate or Candidates for whom he does not vote, and, if he shall have thought fit, having substituted or added the name of any other Candidate or Candidates contained in the printed list sent in pursuance of Statute VI of this Chapter "

The interpretation of the words "or added" in the last sentence is obscure, and in the belief that they were redundant the words were struck out in a revision of the Statutes in 1915. My suspicions were first aroused five years later when I began to revise Strachey's statistics, and found that one of his Tables gives 16 Fellows as having been elected on two occasions—1853 and 1888. This rendered it necessary to enquire further into the matter.

On referring to the Minutes of the Council, which contain the reports of the Committee who, in 1846 and 1847, drafted the new Statutes, it appears that doubts were expressed as to whether the limitation of numbers was consistent with the Charter, which vested the right of election in the "President, Council and Fellows or by any twenty-one or more of them." The matter was submitted to the Attorney and Solicitor-General, the question put being —

"Your opinion is requested whether the Council by virtue of the general power of regulating the body given them by the Charter may pass a Statute enacting that the number of Ordinary Fellows to be elected in any one year shall not exceed 15."

A reply was received in the following terms —

"The point submitted to us is not free from doubt, but after the best consideration we can give to it, we are of opinion that the Council cannot, by virtue of the general power of regulating the body given to them by the Charters, pass a Statute limiting the number of Ordinary Fellows to be elected in any one year."

Such an authoritative opinion could not be set aside, and the Committee therefore drafted the proposal for the new Statute in the form given above, the words "or added" being inserted in order to reconcile the intention of the Council with the wording of the Charter. The remedy was ingenious, but a little astute and not free from danger. Every Fellow, according to the Statute, as it was finally adopted, could add to the list of the Council's nomination as many other names as he pleased, though the chance of election was exceedingly small, unless there was some organized canvass for a particular candidate. The only body with sufficient power to combine effectively was the Council itself, and they made use of their opportunities in 1853 and 1888. The procedure adopted, so far as it can be traced, was that the Council sent round the usual list of fifteen nominations for election, but they also circulated privately a suggestion for the additional insertion of a sixteenth name, giving no doubt, their reasons for that course. No record, however, of any action they took was kept in the Council Minutes. The reason for the additional

election in 1888 is plain. A Fellow of the Society elected in 1862 defaulted, and his name was removed from the list of Fellows. Subsequently, he desired to be re-instated, and the Council was no doubt justified in thinking that his re-election should not interfere with the usual nomination of 15 candidates. They, therefore made use of the loop-hole left open by the wording of the Statute. In the last edition of the Record his name only occurs in the list of Fellows elected in 1862, but the Charter Book shows his signature twice, as he had to be admitted on two separate occasions. There is one instance of a Fellow who, after election in 1851, failed to present himself for admission within the statutory limits of time, his election was declared void, but he was nominated and elected a second time in 1868 as one of the 15.

With regard to the first occasion (1853) on which sixteen Fellows were elected, no obvious reason can be assigned for the step, except perhaps that one of the 15 Fellows elected in 1848 refused the membership of the Society, and the Council subsequently may have desired to fill the vacancy by a supernumerary election.

General Strachey states that only 14 candidates were elected on two occasions. One of these has already been mentioned, 15 being actually elected, but one refusing to take up the Fellowship. The other is given in his Tables as having occurred in 1859, but this is a mistake, the origin of which I have not been able to trace. In referring to the "Record," it will be found, indeed, that the election of only 14 is marked against the date, June 12, which was the day of election, a fifteenth is printed under the date June 5, and this gives the impression that the election took place under Statute XII. But there was no meeting of the Society on June 5, and in the Council Minutes the name of the Fellow is given as one of the 15 nominated candidates.

We may balance an election of 16 against one of 14, and, taking account of one election twice over of the same candidate and the unknown date of birth of another, we find 1,123 for the number of Fellows elected in the 75 years included in this enquiry. Of these 441 were alive on December 31, 1922 but two of these had resigned their Fellowship.

I began by calculating the average age at election for each year. These averages were collected in periods of ten years, and are given in Table II, together with that of the short concluding period of five years.

Fellows elected under Statute XII are not included in this or any of the subsequent tables.

Table II —Average Age at Election

Period.	Average Age	Period	Average Age
1848-1857	43 5	1888-1897	44 9
1858-1867	43 6	1898-1907	43 8
1868-1877	45 4	1908-1917	46 6
1878-1887	45 0	1918-1922	47 6
(40 years)	44 4	(35 years)	45 1

During the first sixty years the increase in the average age at election is not very definite. As late as 1913 it sank to 41 7, but since 1915 it never fell below 45 3.

An increase in the average age, due to few elections of men who were exceptionally young, may be counterbalanced by a simultaneous diminution of elections of men of advanced age. A better judgment of the changes that have taken place can therefore be formed by dividing the whole period into three parts of twenty-five years, and giving the figures separately for different ages at election. This is done in Table III, which shows a marked diminution during more recent years in the election of men under thirty-five, and a marked increase in the election of Fellows between forty and fifty-five. It is difficult to gauge the effect of the War, but it probably was appreciable. My impression is that the younger men were kept back in their scientific work even when they were not actually in the field, while some of maturer age were substantially assisted in obtaining the Fellowship by their war work. For this reason too much importance should not be attached to the last column.

Table III —Number of Fellows Elected at Different Ages

Age at Election	1848-1872	1873-1897	1898-1922.
24-29	16	12	1
30-34	57	49	35
35-39	71	74	66
40-44	69	64	80
45-49	54	55	73
50-54	42	46	62
55-59	31	35	30
60-64	24	15	17
65-69	7	16	8
70-74	1	3	1
75-80	1	6	2
Totals	373	375	375

The youngest man elected to the Fellowship since 1847 was John Lubbock, afterwards Lord Avebury, who entered the Society at the age of 24

It is of some interest to analyse the 29 elections of Fellows under the age of thirty with regard to subjects. These are given in Table IV

Table IV Number of Fellows Elected Under the Age of 30 Years

Physical Sciences	Number	Biological Sciences	Number
Mathematics	4	General Biology	4
Astronomy	2	Physiology and Medicine	6
Mathematical Physics	2		
Pure Physics	3		
Chemistry	5		
Engineering	1		
Meteorology	1		
Geology	1		
Total	19	Total	10

The marked preponderance of the physical sciences is emphasised by the fact that eight out of the ten elections on the biological side took place in the first ten years of the period considered. After 1858, the number of men who have obtained the Fellowship on the physical side to that on the biological side is in the ratio of three to one. I have extended the examination to Fellows elected up to the age of 35 and find that the proportion is still in the ratio of two to one for the whole period.

The number of Fellows of the Society at the beginning of 1848, when the new Statutes came into force, was 768. In consequence of the restriction in the annual elections the numbers diminished by over 100 in the first ten years and in 1891, the last year included in General Strachey's statistics, the Society contained 427 Fellows, of whom 401 were elected under the new Statutes. A supplementary Memorandum published by Strachey in the Year Book for 1900 showed that the total number of Ordinary Fellows had fallen to 418, of whom six were elected before 1818. Strachey considered that his prediction that 420 would be the ultimate maximum membership was confirmed by these figures. Table V, which gives the average number of Fellows during different periods, shows, however, that the Society continued to increase in numbers until a maximum of 451 was reached. The maximum for a single year was 455 in 1912. Since then the numbers show a steady decline.

Table V —Number of Fellows of the Society in Different Years.*

Period	Average Numbers	Period	Average Numbers
January 1 1900-1904	424	January 1 1915-1919	445
1905-1909	442	1920-1924	442
1910-1914	451	—	—

The diminution of membership during the last 10 years is partly accounted for by two deaths which may be put down to the war, and two resignations

Table VI gives the composition of the Society at the beginning of 1923 arranged in order of ages

Table VI —Composition of Society on January 1, 1923

Ages	Number of Fellows	Ages	Number of Fellows
30-34	3	65-69	52
35-39	10	70-74	42
40-44	15	75-79	24
45-49	47	80-84	17
50-54	65	85-89	8
55-59	68	90-94	1
60-64	86	95	1

Total Number of Fellows, 439 Average Age, 60.9

Table VII gives the number of Fellows alive at the beginning of 1923 arranged in the order of the years they have served in the Society. Thus we find that, at the end of 1922, fifty Fellows had been Members of the Society for more than 20 and less than 26 years. To obtain the number of men who have been Fellows for 41 years or more, we find 21 by adding the last four figures

Table VII —Years of Service in the Society on January 1, 1923

Years of Service	Number of Fellows	Years of Service	Number of Fellows
1-5	87	31-35	30
6-10	65	36-40	16
11-15	64	41-45	12
16-20	65	46-50	7
21-25	50	51-55	1
26-30	42	56-60	1

* The numbers given are exclusive of Fellows elected before 1848 or under Statute XII. The last of the former (Sir Joseph Hooker) died in 1911.

The last part of this enquiry deals with the expectancy of life of a Fellow at the age of his election. If we were only to consider those whose life has come to an end, the problem would be simple, but we should obtain too low a value of the expectancy, for the reason that the list would include Fellows who died at an exceptionally early age, while excluding those whose span of life was above the average. The difference would be negligible if the period taken into account were long compared with the duration of the average life in the Society, but this is not the case.

The following procedure was adopted. As the material is not sufficient to calculate the expectancy for each age separately, the ages at election are combined in groups of five. If y be the number of years which denotes the duration of a life after election, $n^{-1} \Sigma y$ would denote the average life for a group of five years, n being the number of Fellows in the group. This average would correspond nearly, though not exactly, to the third of the five years of the group. When the calculation has been completed for each of the groups, it is easy to apply a small correction to the average age of the group so as to make it correspond exactly to its third year.

For the Fellows who are still living we are ignorant of their ultimate life, but we find an approximate value by adding to the number (a) of years which have elapsed since election up to the end of 1922 their further expectancy (w) taken from some reliable Table of Life Statistics. I have chosen for the purpose the Table published in Whitaker's Almanack. If m denote the number of living Fellows, we take $m^{-1} \Sigma (a + w)$ as their average life after election, and correct as before to bring the average age at election in each group to that of the third year. The expectancy of life, taking account of both living and former Fellows, will then be

$$W_1 = (m + n)^{-1} \Sigma (y + a + w)$$

As shown in Table VIII the values of W_1 are substantially greater than those of w . This necessitates a revision of the calculation, substituting W_1 for w , so that the final expectancy as calculated is

$$W = (m + n)^{-1} \Sigma (y + a + W_1)$$

Table VIII represents the final results —

Table VIII - Expectancy of Life

Age	N	U	W_1	w	Expectancy
30	96	35 6	38 7	33 1	40 4
35	201	31 0	34 0	29 2	35 9
40	208	26 8	29 2	25 6	30 9
45	190	24 8	26 7	22 2	28 4
50	170	21 4	23 1	18 9	24 9
55	114	18 1	18 8	15 8	20 1
60	70	17 0	17 0	12 9	18 0
65	41	16 5	16 5	10 3	17 1

The column headed N represents the number of Fellows included in the group elected at the average age given in the first column. U represents the expectancy, taking account only of deceased Fellows, this number, as has already been explained, should be less than the true expectancy. The last column gives the expectancy calculated as indicated, and the last column but one gives the expectancy as given in the Tables of "Whitaker's Almanack". The comparison between the two last columns shows that the average life of Fellows of the Royal Society is, on the average, nearly six years longer than that given in the Tables which have been used.

It may be stated in conclusion, that Fellows who have withdrawn from the Society are included in the Life statistics but excluded from the Tables referring to the composition of the Society after the date of their resignation.

The Thermionic Work-Functions and Photo-electric Thresholds of the Alkali Metals.

By O W RICHARDSON, F R S, Yarrow Research Professor of the Royal Society, and A F A YOUNG, Ph D, King's College, London

(Received January 6, 1925)

§ 1 *Summary of Previous Knowledge*

It has generally been found that the thermionic currents from solids follow the formula $AT^b e^{-b/T}$ where A and b are two constants, over a wide range of temperature. So far as this matter is concerned, the same result holds if the index of T is replaced by 2, or, in fact, by any similar low number. For example, K K Smith* has shown in the case of tungsten that such a formula with two constants covers the thermionic currents, from 1,050° K to 2300° K, over which range of temperature the currents increase by a factor of about 10^{12} . It appears, however, that the alkali metals—at any rate, under such conditions as it is feasible to make experiments on them—do not subscribe to this requirement.

If the old values† of $\log i - 2 \log T$ (i = thermionic current, T = absolute temperature) for sodium are plotted against T^{-1} , it will be found that the curve is not a straight line, as is the case with most substances, but is definitely convex towards the origin. This can, in fact, be seen from fig 21, p 539 of the paper, which is a plot of $\log i - \frac{1}{2} \log T$, since this function behaves similarly to $\log i - 2 \log T$. This shows that the equation

$$i = CT^2 e^{-d/T} \quad (1)$$

with C and d constants is not competent to express the currents. It follows that the work function for this metal is not a single constant but its value for some electrons must differ from its value for others. The case of potassium has recently been carefully examined by one of us‡ with the result that in general the plots of $\log i - 2 \log T$ against T^{-1} are straight lines, or nearly so, at the highest and lowest temperatures of the observations. These lines have different slopes and are joined by a curved part which is convex towards the origin.

An analogous duplicity in the photo-electric phenomena has been known

* 'Phil Mag.', vol. 29, p 802 (1915)

† O W Richardson, 'Phil Trans,' A, vol. 201, p 497 (1903)

‡ A F A Young, 'Roy Soc Proc,' A, vol 104, p 611 (1923)

for some time. The curves of photo-electric yield against frequency for sodium* possess double maxima indicating the existence of at least two thresholds. The first maximum was found at 3600 Å U. and corresponds fairly closely to Pohl and Pringsheim's† maximum for the "selective" effect, and the second in the ultra-violet at 2270 Å U. If we assume that each of these maxima results from the presence of a distinct threshold in the material and that the relation‡

$$\nu_{\max} = \frac{1}{2} \nu_0 \quad (2)$$

holds, we can calculate the respective threshold frequencies ν_0 . The values found are $\nu_0 = 5.56 \times 10^{14} \text{ sec}^{-1}$ and $\nu_0 = 8.81 \times 10^{14} \text{ sec}^{-1}$ or in equivalent volts, in accordance with the $e\phi = h\nu$ relation, the values are $\phi_0 = 2.29$ volts for the "selective" threshold and $\phi_0 = 3.63$ volts for the other. The long wave threshold was directly determined by Compton and Richardson and found to be $\lambda_0 = 5770 \text{ Å U}$, which corresponds to $\phi_0 = 2.14$ volts. This, is a fair agreement with the result got from the maximum by using equation (2), but, of course, a similar check on the other maximum is not possible. It should be added that the value of λ_0 varies in some obscure way with the state of the metal surface, and a value for sodium as high as 6800 Å U has been found by Millikan§. This is the highest published value we have been able to find, and the corresponding ϕ_0 is 1.82 volts.

The old thermionic observations with sodium are open to some objections and should be repeated under better conditions, but, in view of the similar behaviour of potassium, it may be permissible to extract such information as may be obtained from them as to the probable values of the work functions. Turning to fig 21 p 539, of 'Phil Trans,' A, vol. 201, if we assume that the dotted curve for the region between $T^{-1} \times 10^4 = 14$ and $T^{-1} \times 10^4 = 15$, on the one hand, and between $T^{-1} \times 10^4 = 18.8$ and $T^{-1} \times 10^4 = 20$ on the other, has approximately reached limiting straight lines, the corresponding values of the constants representing the work function are

for $T^{-1} \times 10^4 = 14.5$, $b = 4.6 \times 10^4$, equivalent to $\phi = 3.96$ volts;

for $T^{-1} \times 10^4 = 19.4$, $b = 1.59 \times 10^4$, equivalent to $\phi = 1.37$ volts.

Whilst these quantities are much higher than the potassium values, it is interesting to note that their ratio is very close to the corresponding ratio for potassium. The upper value, 3.96 volts, does not differ from the value

* K. T. Compton and O. W. Richardson, 'Phil Mag,' vol. 26, p. 563 (1913)

† Pohl and Pringsheim, 'Verh. d. Deutsch. Physik. Ges.,' vol. 11, p. 1039 (1910)

‡ O. W. Richardson, 'Phil. Mag,' vol. 24, p. 570 (1912)

§ R. A. Millikan, 'Phys. Rev.,' vol. 7, p. 380 (1916)

$\phi_0 = 3.63$ volts deduced by the application of equation (2) to the second photo-electric maximum by more than the probable errors, but the lower value, 1.37 volts, seems definitely lower than the lowest photo-electric threshold even if Millikan's low value corresponding to 1.82 volts is taken

In the previous work by one of us with potassium it was found that the experimentally determined photo-electric threshold varied between the limits of either 1.86 to 2.02 volts or 1.72 to 1.77 volts, the higher set of values being obtained if the tail end of the spectral curves was attributed to scattered and stray light of other wave-lengths. The measured values of the two thermionic work functions for the same specimen and under the same conditions were found to lie within the ranges of 0.99 to 1.32 volts at 200° C and 0.463 and 0.694 volt at 30° C respectively. All these values are much lower than any of the estimations of the corresponding photo-electric quantity

The present experiments were undertaken to obtain further information bearing on the interesting facts outlined above. In some respects they are not as complete as we could have wished, but they are published in their present form as the collaboration of the authors has had to come to an end. The experiments were all made with potassium, and, except for modifications specifically referred to in the sequel, the apparatus was the same as that already used by one of us and described in 'Roy Soc Proc,' A, vol. 104, p. 611 (1923). As it will be necessary to make frequent reference to this paper, we shall in what follows designate it by I for brevity.

§ 2 *Theory of Patches*

It is clear from § 1, that a metal may behave as though it possessed at least two thermionic work functions and one or more of these may have a lower value than that equivalent to the lowest effective photo-electric threshold. The first explanation of these phenomena which occurred to us may be designated as the theory of patches. The idea, expressed generally, is that the surface of a substance with more than one work function is not uniform, but that there are sets of regions, each set being characterised by a particular value of the work function. We do not at this stage propose to express an opinion as to how such differences originate, though chemical contamination is an obvious possibility, and there are others which are more interesting.

In its effects the hypothesis replaces the uniform surface of the substance by a patchwork of different substances, one for each work function. To give a simple illustration of the way in which such a scheme may operate, consider a hypothetical substance which behaves as though it had two thermionic work

functions equivalent to ϕ^1 and ϕ^2 of which ϕ^1 agrees with the photo-electric threshold and ϕ^2 is much smaller than ϕ^1 . This hypothetical substance is simpler in its behaviour than either sodium or potassium according to the facts and inferences recited in § 1 but there are elements of uncertainty about some of them which prevent its absolute rejection as a possible model. At any rate the vagaries of such a substance are of the same general character as those of these alkali metals. The properties of the hypothetical substance involve an apparent contradiction, inasmuch as the photo-electric threshold is much higher than the lower thermionic threshold, whereas it is usually assumed to be a measure of the lowest possible value of this quantity. This difficulty is resolved on the theory of patches by supposing that the area of the patches afflicted with the lower value of the work function is very small compared with the area of the rest of the surface. The smallness of this area makes the photo-electric currents too small to measure until the threshold frequency for the bulk of the surface is reached, and they are, for all practical purposes, the same under all circumstances as though the small patches were not present. The thermionic effects act differently. The electron emission from unit area of the composite surface is proportional to $T^2 (C_1 e^{-d_1/T} + C_2 e^{-d_2/T})$ where C_1 and C_2 are proportional to the respective areas and d_1 and d_2 are proportional to the respective work functions. Now C_2 may be quite small compared with C_1 yet at low enough temperatures $C_2 e^{-d_2/T}$ will exceed $C_1 e^{-d_1/T}$ if d_2 is less than d_1 . We should thus expect the low work functions to dominate the thermionic emissions at low temperatures and this is what occurs. However, this particular result would be obtained on almost any view of the origin of the multiple work functions.

There is another line of evidence which tends to substantiate the real existence of specifically affected areas. If parts of the surface exist having a different work function from the rest they will have a different potential, in accordance with the relation

$$\log j_1/j_2 = e(V_2 - V_1)/kT, \quad (3)$$

where j_1, j_2 are the respective saturation current densities per unit area and V_1 and V_2 are the respective potentials. Thus, the spots of low work function will be electro-positive to the rest by the amount $V_2 - V_1$ required by (3). This will give rise to strong local fields at the surface which will tend to prevent the currents from attaining the saturation value. That the thermionic currents from potassium are difficult to saturate is shown clearly by I, figs 9, 11 and 12. That the photo-electric currents from the same metal experience no such

difficulty is shown by I, fig 16. This is to be expected on the theory of patches because the inhibitive fields of force are inoperative on the bulk of the surface from which the photo-electrons come

For a substance with a single effective threshold it is known that the thermionic current density is given with sufficient approximation by equation (1) The present point of view divides the surface of a substance whose behaviour is more complex into a patchwork (or map) in which the various patches (or countries) each behave as a simple substance For such a structure the total current density will be given by applying equation (1) to each element in proportion to its area and summing over all the areas The expression for the total current density j will therefore be

$$j = T^2 (C_1 S_1 e^{-d_1/T} + C_2 S_2 e^{-d_2/T} + \dots), \quad (4)$$

where S_1 is the proportion of unit area occupied by the patches for which the work function is measured by d_1 , S_2 is the proportion occupied by those whose work function is measured by d_2 , and so on It is possible, but not essential, that the constants C_1, C_2 , etc., which are written as characteristic for each set of patches may have a common universal value *

It has been shown by one of us† that an equation equivalent to (4) has a much more general basis than the theory of patches, so that satisfaction of this equation cannot be regarded as conclusive evidence of the existence of patches

§ 3 *Application to the Potassium Data*

We shall now show that equation (4) with two terms expresses the abnormal potassium results, such as those plotted as (a), (b), (c), and (d) of I, fig 7, to the degree of accuracy of the observations

Taking two terms only we may write (4) as

$$j = T^2 (F_1 e^{-d_1/T} + F_2 e^{-d_2/T}) = j_1 + j_2 \quad (5)$$

where

$$j_1 = F_1 T^2 e^{-d_1/T}, \quad j_2 = F_2 T^2 e^{-d_2/T} \quad (6)$$

Let $d_2 > d_1$ and write

$$j = F_1 T^2 e^{-d_1/T} \left(1 + \frac{F_2}{F_1} e^{-(d_2-d_1)/T} \right) \quad (7)$$

By taking T small enough $\frac{F_2}{F_1} e^{-(d_2-d_1)/T}$ can always be made small compared

* Cf O W Richardson, 'Roy. Soc. Proc., A, vol 105, p 387 (1924)

† O W Richardson, 'Proc Lond Phys Soc.,' vol 36, p 383 (1924)

with unity so that j always reduces to j_1 at low temperatures. The constants F_1 and d_1 can thus be extracted in the usual way from the experimental data for low temperatures. This may fail in practice if d_2 and d_1 are nearly equal, as the required value of T may be so small that the factor $e^{-d_1/T}$ will make j too small to measure. The value of the ratio F_2/F_1 might then be important. We may also write

$$j = T^2 e^{-d_2/T} (F_2 + F_1) e^{(d_2 - d_1)/T} \quad (8)$$

As $T \rightarrow \infty$, $e^{(d_2 - d_1)/T}$ approaches 1 and faster than $e^{-d_2/T}$ does ($d_2 > d_1$), so that there is a range at high temperatures in which j is nearly the same as $T^2 (F_1 + F_2) e^{-d_2/T}$, i.e., $\log j - 2 \log T$ plotted against T^{-1} has the same slope as $\log j_2 - 2 \log T$, but is displaced by an amount depending on F_2 .

We thus arrive at the following process for extracting the constants. Plot the observed values of $\log j - 2 \log T$ against T^{-1} . If two terms of equation (4) are adequate to express the data, and unless the constants have inconvenient values, the high and low temperature ends of this graph will be straight lines. The slopes of these give the values of d_2 and d_1 respectively. The absolute value at the low-temperature end gives F_1 . The other end gives $F_1 + F_2$, from which F_2 can be got by subtraction. The applicability of the process can then be checked by calculating the intermediate curved part of the graph from the values so obtained.

We have applied this process to the thermionic data for potassium from which curve (b) of 1, fig 7, was plotted. This set of data was selected as being perhaps the most complete and consistent of a number of similar sets. The values of the logarithms to the base 10 of the saturation currents (in amperes) $-T^2$ were plotted on a fairly large scale against $T^{-1} \times 10^4$. The resulting plot was found to be fitted by straight lines to within the accuracy of the observations over the ranges of $T^{-1} \times 10^4$ from 20.25 to 22.5 and from 32.0 to 34.75—that is to say, at each end over a stretch equal to about one-sixth of the full extent of the whole range of observations. The values of the constants found from these two straight lines were —

Table Ia

Degrees	Number of Electrons per sq. cm. per degree ²
$d_1 = 0.498 \times 10^4$	$F_1 = 7.96 \times 10^7$ at a mean temperature of 288° K
$d_2 = 1.296 \times 10^4$	$F_2 = 1.32 \times 10^{17}$ „ „ 490° K

The values of $2 \log_{10} T - \log_{10} j$ calculated from these data for a series of temperatures distributed along the intermediate curved part of the graph are

shown along with the observed values in Table I. These calculated values were obtained by a graphical method with the assistance of the slide rule, and will not agree with the constants above with algebraic accuracy, but these mechanical methods of calculating are accurate enough for the observational data.

Table I

$T^{-1} \times 10^4$	$2 \log_{10} T - \log_{10} j$ (calculated)	$2 \log_{10} T - \log_{10} j$ (observed)
23.47	14.332	14.285
25.00	15.126	15.104
25.91	15.548	15.537
26.88	15.946	16.009
27.03	15.999	15.953
28.41	16.439	16.405
30.12	16.874	16.854

In every case the calculated values agree with the observed within the limits of probable error, and as the values calculated from the same data fit the straight ends of the graph, it follows that the data are covered by two terms of (4) over the whole range of temperature as accurately as they have been observed.

Whilst this result is in agreement with the patch theory, it should be borne in mind that there are other possible reasons for it. These will be dealt with later (p. 405). We proceed now to consider some new experimental evidence. We shall first deal with attempts which we have made to increase the area of the hypothetical low-threshold patches.

§ 4 *The Effect of Hydrogen and Water Vapour on the Photo-electric Emission from Potassium*

The experiments of Elster and Geitel* have shown that after treatment with hydrogen, photo-electric currents may be obtained from the alkali metals with infra-red light, showing that a modification of the surface having a low value of the photo-electric work function can exist. One of us† also found a similar effect with the liquid alloy of sodium and potassium after exposure to water vapour. The manner of variation of current with wave-length was however, not accurately determined.

The present method of producing the modified surface was similar in

* Elster and Geitel, 'Phys. Zeits.', vol. 12, p. 758 (1911).

† O. W. Richardson, 'Phil. Trans.', A, vol. 222, p. 33 (1922).

principle to that of Elster and Geitel,* namely, to let hydrogen into the quartz tube containing the potassium by heating with a Bunsen flame a palladium tube, sealed through the glass situated between the quartz tube and the mercury vapour pump. When the pressure had mounted to 0.1 mm., or more, a luminous discharge was made to pass between the central electrode and the potassium surface from a 400-volt battery with a resistance of about 1200 ohms in series, the potassium being the negative electrode. To do this the electroscope connections were removed from the central electrode and the copper cylinder (I, fig. 1, W) unearthed. An induction coil was also used to produce a discharge, but this appeared to be not more effective than the 400-volt battery, probably owing to the excessive bombardment of metal parts, etc., of the tube. The discharge caused the usual change in colour of the potassium surface to a tint varying in different cases from blue-purple to dark purple, or even blackish. Photo-electric measurements were made *in a high vacuum* after pumping out the hydrogen by the mercury vapour pump. The accelerating potential difference used was from 100 to 150 volts.

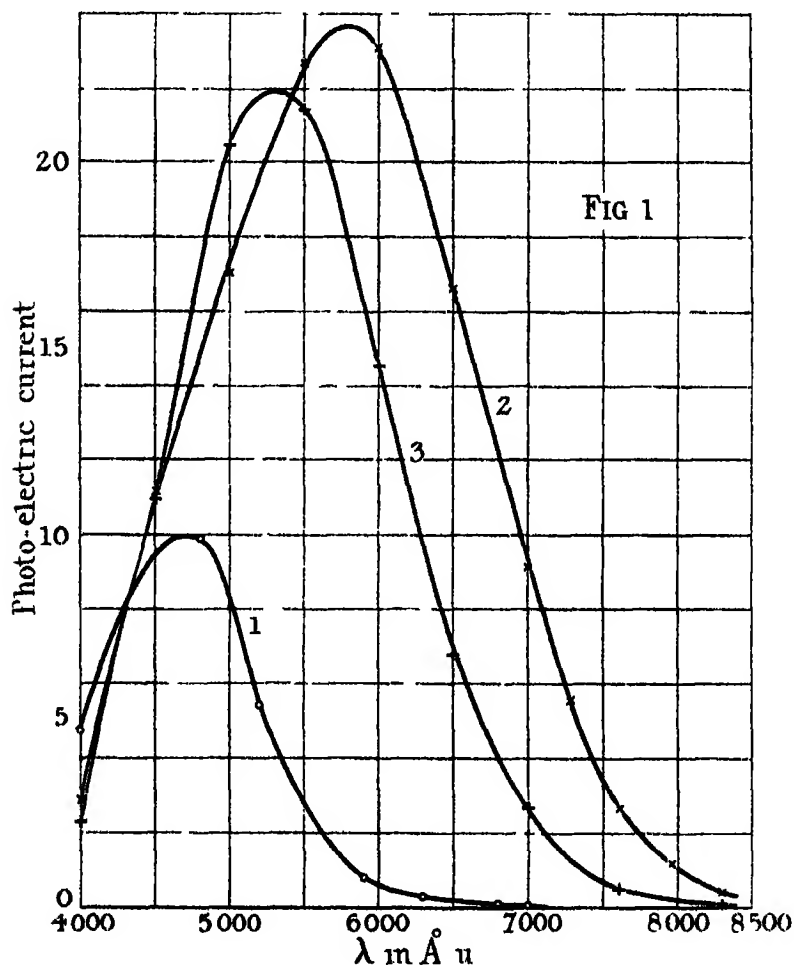
Fig. 1 shows the type of effect first obtained with the luminous discharge. The ordinates show the photo-electric current corresponding to the wave-lengths given as abscissæ. The currents are not reduced to unit intensity of the incident light, which steadily rises as we proceed towards the longer wave-lengths, being given approximately by fig. 17, I. This magnifies any effect in the region of longer wave-lengths.

It may be remarked that, as the scale on the drum of the monochromator terminated at 7000 Å U, the wave-lengths beyond this had to be extrapolated by means of an arbitrary scale drawn on the drum. This was done as follows. The beam of light from the collimator passes at minimum deviation through a quartz prism ($\epsilon = 60^\circ$) and is reflected by a quartz mirror into the telescope. Suppose the drum is set, say, at 6950 Å U. By means of the formula for the refractive index $\mu = \sin \frac{D + \epsilon}{2} / \sin \frac{\epsilon}{2}$ the deviation D through the prism may be calculated on substituting Carnelli's value $\mu = 1.54078$ for 6950 Å U. Now let the drum be turned and set at one of the arbitrary markings, then provided we know the angle θ through which the prism and table have turned, the corresponding change in deviation through the prism (20), and thus the refractive index of the light which passes through the monochromator when the drum is set to the arbitrary marking, may be

* Elster and Geitel, 'Phys. Zeits.', vol. 11, p. 257 (1910).

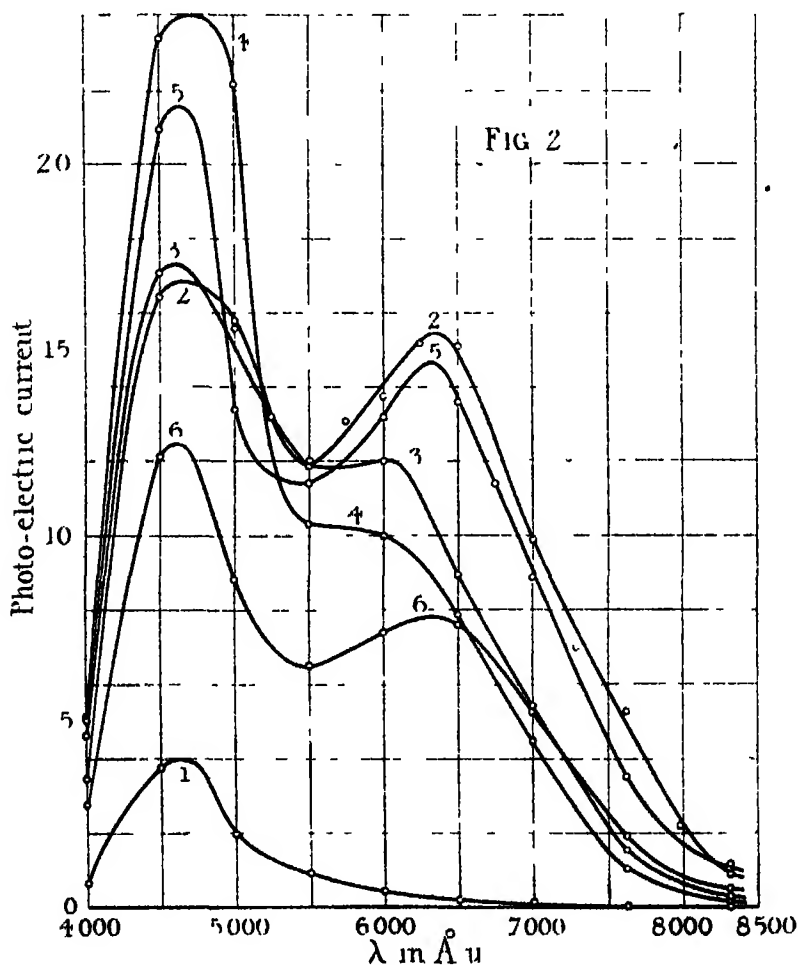
calculated. The wave-length can then be evaluated from a dispersion curve for quartz. The angle θ was measured by observing the displacement, on turning the drum, of a beam of light from a Pointolite lamp reflected from the quartz mirror on the table of the monochromator to a distant scale. The lamp and scale were situated 8.8 metres from the quartz mirror.

In fig 1, curve 1 shows the photo-electric current before sensitising, and



curve 2 that immediately after, the monochromator, etc., not being shifted during the sensitising process. Curve 3 shows the effect two days later, the tube having been left untouched meanwhile and the pressure risen to 0.01 mm. The displacements with time were always in this direction. Evidently the effect of sensitising has been to increase the magnitude of the currents by a

factor which is greatest for the region of longer wave-lengths Fig 2 shows the type of curve obtained later, which exhibits two maxima They were obtained after a side tube containing sulphuric acid, to which a drop of water had been added, had been joined on near to the quartz tube, and separable from it by a tap, in order to test the effect of water vapour Curve 1 was



obtained after the potassium had been exposed to the sulphuric acid and water for 93 hours, while 2, 3, 4 and 5 were obtained after successive glow discharges of 2, 5, 5 seconds, and 5 minutes' duration, respectively Number 6 shows the effect 15½ hours later still, the sulphuric acid tube being open for the whole 108½ hours It remains to be decided, however, as to whether the two

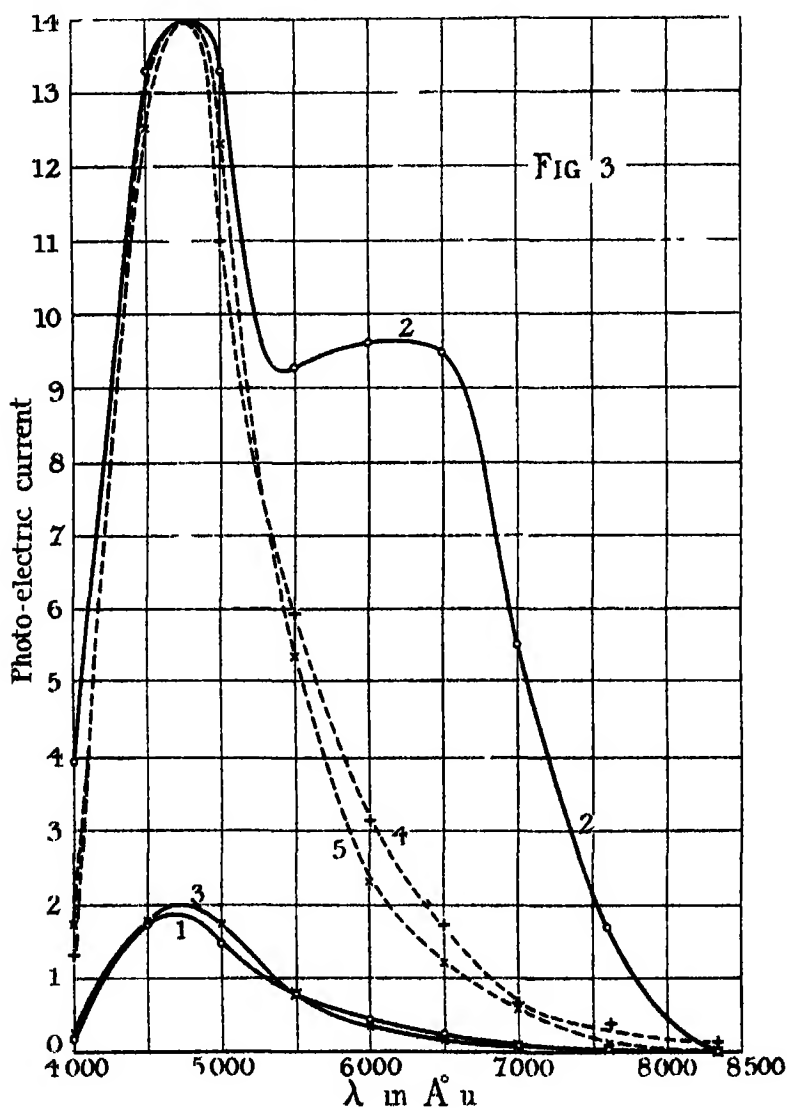
maxima were caused by water vapour. The evidence for this question will be dealt with below.

Whenever a curve exhibiting two maxima was obtained or one in which the slope decreased and then increased again in the manner of curve 4, fig. 2 the maximum nearest the ultra violet was always in the neighbourhood of 1650 \AA U , in fact for the whole series of curves it remained between 4600 and 1750 \AA U . This corresponds after allowing for the intensity distribution of the incident light to the ordinary maximum of the selective effect for potassium. In the other cases, *e.g.*, curve 2, fig. 1 where the maximum appeared to shift, the effect may possibly be due to the masking of the ordinary selective maximum by the increased effect towards the infra-red, a tendency which is exaggerated by the peculiar energy distribution of the incident light.

In all cases the currents from the sensitised potassium could be reduced approximately to their magnitude before sensitising by heating the tube containing the potassium by a Bunsen flame. Fig. 3 shows the effect of raising the temperature of the sensitised potassium to 100°C by an electric heater for about one hour in a high vacuum and then allowing it to cool. Curve 1 was that obtained before, curve 2 that after, sensitising, while curve 3 shows the effect after heating. Curves 4 and 5 are curves 1 and 3 respectively with the scales altered so that the ordinate for 1750 \AA U has the same value as for curve 2. This heat treatment also caused a fading of the colouration produced by the glow discharge.

It was found that the mere contact of the potassium with hydrogen made no difference to the photo-electric effect. Also the presence of water vapour caused no measurable increase in the photo-electric emission towards the infra-red region. Thus, for example, prior to making the observations for the curves in fig. 2, the potassium was exposed for 93 hours to sulphuric acid to which one drop of water had been added. Before exposing it in this way the potassium was heated so that a new surface was obtained by evaporation and splashing. Curve 1, fig. 4, shows the photo-electric currents in a high vacuum immediately after this had been done, while 2 shows the currents immediately after opening the sulphuric acid tube, the potassium being at the same instant shut off from the pumps. Curves 3 to 6 show the currents obtained after $1\frac{1}{2}$, $15\frac{1}{2}$, 23 and $40\frac{1}{2}$ hours respectively. Curve 7 was that obtained after 93 hours, and is identical with curve 1 in fig. 2. Immediately before curve 7 was obtained the tube was opened to the McLeod gauge, in which the pressure rose to the order of tenths of a millimetre, so that some of the variation in

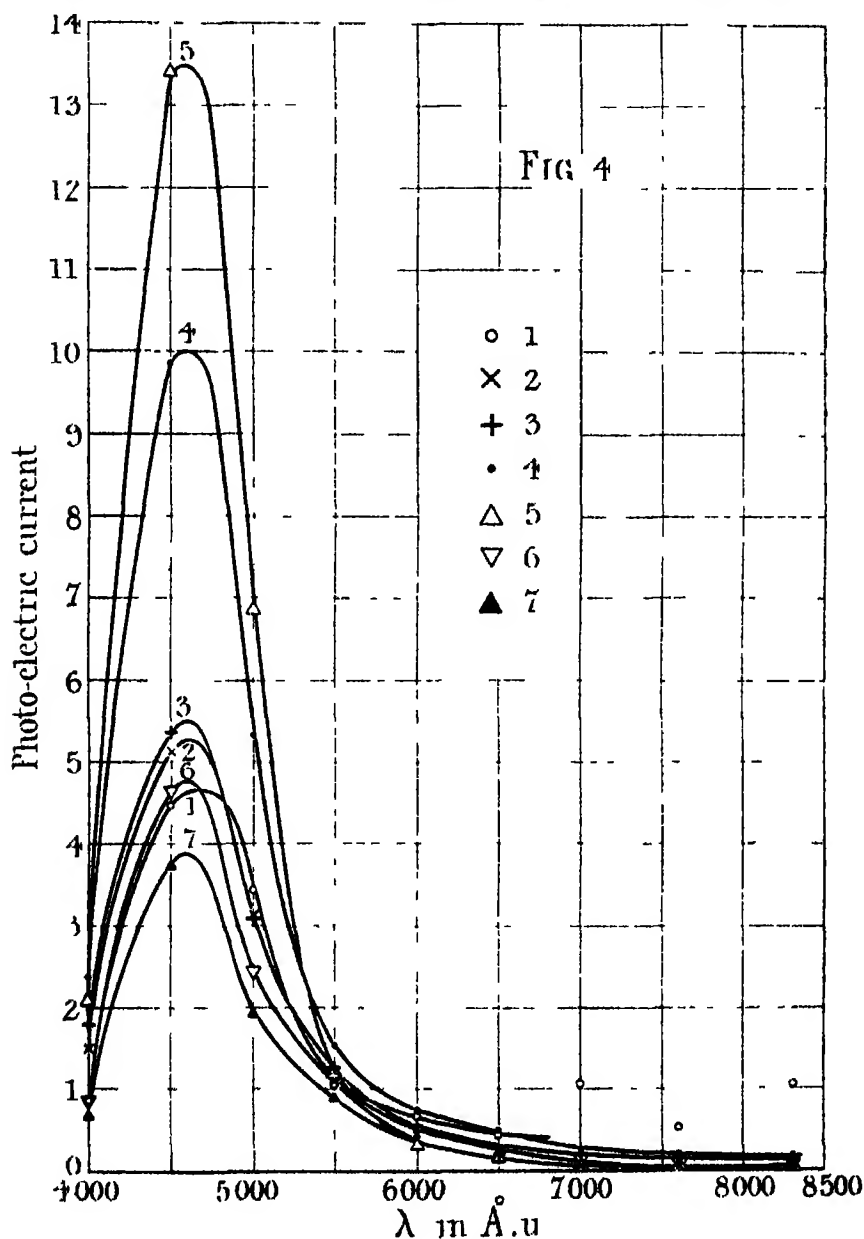
magnitude of the currents with time may be due to a varying amount of impact ionisation. At any rate, the photo-electric emission did not increase in the region of longer wave-lengths. The three stray points of curve 1 (fig 4)



may be ascribed to errors of measurement of the "dark" current, which was large for this curve.

The conditions which must obtain to give the greatest effect in the infra-red seem obscure. With the potassium first used, which had not come in contact

with water vapour, and had previously been heated in a high vacuum, which was maintained until the hydrogen was admitted, the principal effect of the



sensitising was to increase the emission in the neighbourhood of the maximum at 4700 Å U without causing much increase towards the infra-red, the effect

being roughly proportional to the time occupied by the discharge, at least for the first discharges of about a second's duration each. If no particular care was taken to avoid gaseous contamination before admitting the hydrogen, however, quite large effects were obtained on sensitising. Thus, for example, immediately before curves 1 and 2, fig 1, were obtained, the potassium had been exposed to air at atmospheric pressure from the room. Also when the potassium had been exposed for a long time to sulphuric acid containing a drop of water, the maximum effect in the extreme red was obtained at once after a discharge of only two seconds' duration, as in curve 2, fig 2. It will be noticed that the sensitivity did not continue to increase with the length of the discharge. These results point to the view that it is essential for a constituent of water to be present during the sensitising process, but on the other hand equally marked effects were obtained later with the same potassium after the sulphuric acid had been removed altogether and after the potassium and quartz tube had been thoroughly heated the Gaede pump having been taken down and cleaned in the meanwhile. Similar effects were obtained when the precaution was taken to heat the potassium and wash the apparatus out with hydrogen once or twice before letting in the hydrogen for the discharge, and also when the potassium was first heated to 315°C in an atmosphere of hydrogen.

There is a possibility in the foregoing experiments that traces of the surface modification, when once formed, were not completely removed by heating the potassium with a flame, but that the modification was only destroyed sufficiently to make the photo-electric current from it negligible. There may be a portion of the modification which is stable enough to resist heating, and which forms a nucleus from which the original state of the surface is readily built up again on re-sensitising. In Fig 3 the heating to 100°C still left an appreciable effect for wave-lengths greater than 6000 \AA U which, it will appear later, is probably not due to scattered light. Such an occurrence might give rise to the effects recounted at the end of the last paragraph.

Further experiments would be necessary to elucidate the action of water vapour.

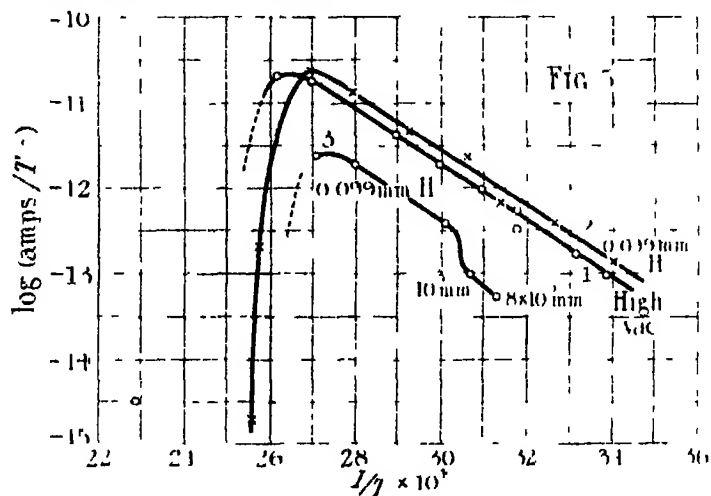
The curves with two maxima in fig. 2 are not the counter-part for potassium of the similar curves with two maxima for sodium found by Compton and Richardson*. In fig 2 the maximum for the "selective effect" for potassium is at about 4650 \AA U, and the new maximum is on the *low frequency* side of it at about 6000 \AA U. In the sodium curves the maximum for the "selective

* *Loc cit*

effect" is at 3600 Å U and the other maximum is on the *high frequency* side of it at 2270 Å U. In spite of this there may possibly be some significance in the fact that the ratio of the frequencies for the two maxima for potassium 1.36 is not very different from the value of 1.59 for the ratio of the frequencies of the two maxima on these sodium curves.

§ 5. *The Thermionic Emission from Potassium*

The effect of the presence of hydrogen at 0.099 mm. pressure is shown in fig. 5. Plotting $\log (\text{current}/T^{\frac{1}{2}})$ against $1/T$ in the usual manner curve 1 was



obtained for a high vacuum with falling temperature. Hydrogen was then admitted at room temperature, and the temperature raised giving curve 2. The sudden drop in the emission with rising temperature, to which reference was made in I (p. 619 etc.), occurred at the highest temperatures. Curve 3 was obtained on lowering the temperature, the last two points being taken while the hydrogen was being pumped out, at a pressure of 10^{-3} and 8×10^{-5} mm., respectively. The displacement of curve 2 with respect to (1) may be ascribed to impact ionisation, as also may be the bend in curve 3. The effect of the hydrogen, if any, was thus to reduce the value of A in the formula $i = AT^b e^{-b/T}$ and to leave the value of b unaltered.

The thermionic emission was also measured after sensitising the surface at room temperature. The current at a particular temperature was, however much greater with the initially rising temperature than with the subsequently falling temperature. This was probably due to the evaporation or destruction of the greater part of the surface modification during the heating.

The slopes of the two ($\log i/T^{\frac{1}{2}}, 1/T$) curves for the heating and cooling differed greatly, and in two cases gave for b a mean of 0.89×10^4 and 0.51×10^4 respectively. These values are not very reliable.

In order to obtain the values of A and b for potassium under the best possible vacuum conditions, the apparatus was set up again as follows. The copper cap R (I, fig. 1 [b]) was replaced by a glass cap with a $\frac{3}{4}$ -inch side tube fused directly to the tube L connecting to the mercury vapour pump. This tubing was made shorter and wider (1-inch bore, with two liquid air traps of $1\frac{1}{2}$ inch diameter one containing some coconut charcoal, a $\frac{3}{8}$ -inch tap, the total horizontal length between pump and quartz tube being 19 inches). The copper cylinder W was entirely removed and in its place a thin platinum wire was trailed round the inside of the quartz in a large spiral. The electrode V was made of platinum, the lower part of the connecting lead being also of platinum. The lower part of the quartz tube was well heated before melting the potassium in the side tube D.

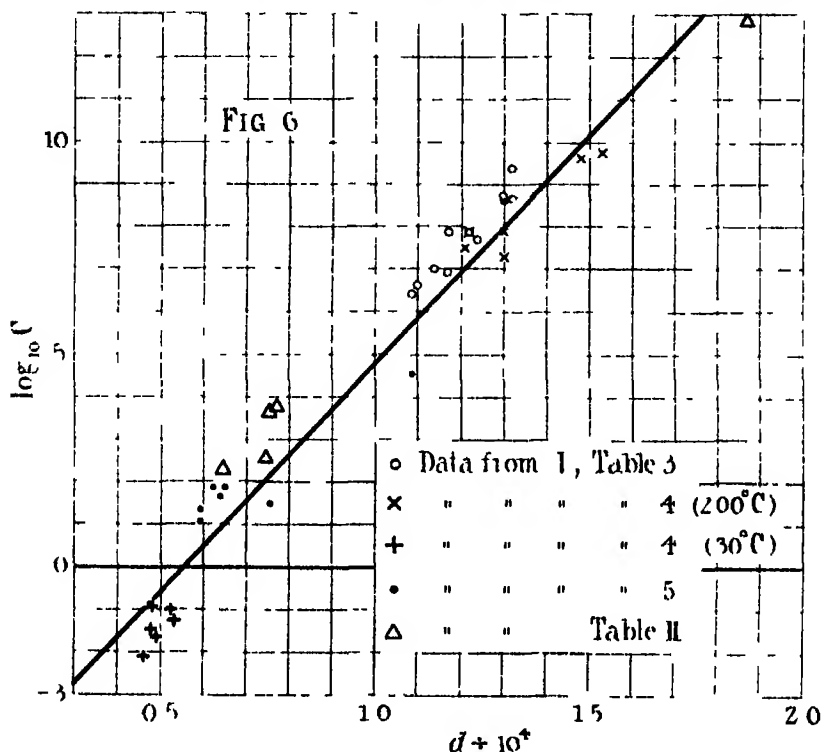
Even when these precautions were taken, and when the McLeod gauge showed an extremely small pressure, the thermionic phenomena remained the same. The sudden drop in the emission was still obtained at temperatures of from 180°C to 250°C . The ($\log i/T^{\frac{1}{2}}, 1/T$) curves for potential difference of 139 volts were approximately straight for four curves, whilst three others were curved similarly to those in I, fig. 7. All the values of A and b , except those from the steepest part of the latter curves, were of a similar low order to those already found for potassium (I, Tables III, IV, V). The new values from the four plots which were most consistent, using the formula $i = AT^{\frac{1}{2}} e^{-b/T}$ are given in Table II.

Table II

	$b \div 10^4$	A_1 (Number of Electrons per Square Centimetre)
1. { Maximum	1.900	3.5×10^{16}
{ Minimum	0.800	2.4×10^{16}
2	0.693	1.0×10^{16}
3	0.801	2.3×10^{17}
4	0.824	3.9×10^{17}

An interesting feature of the values of A_1 and b given in Table II above and in I, Tables III, IV, V, is that if $\log_{10} A_1$ is plotted against b , the points obtained are distributed near to a straight line. In fig. 6 the values of $\log_{10} C$ and d calculated by applying the formula $i = CT^{\frac{1}{2}} e^{-d/T}$ have been plotted for the

observations corresponding to the values in the above tables. This was done by subtracting $\frac{1}{2} \log_{10} T$ from the ordinates of a $(\log i/T^{\frac{1}{2}}, 1/T)$ curve and plotting



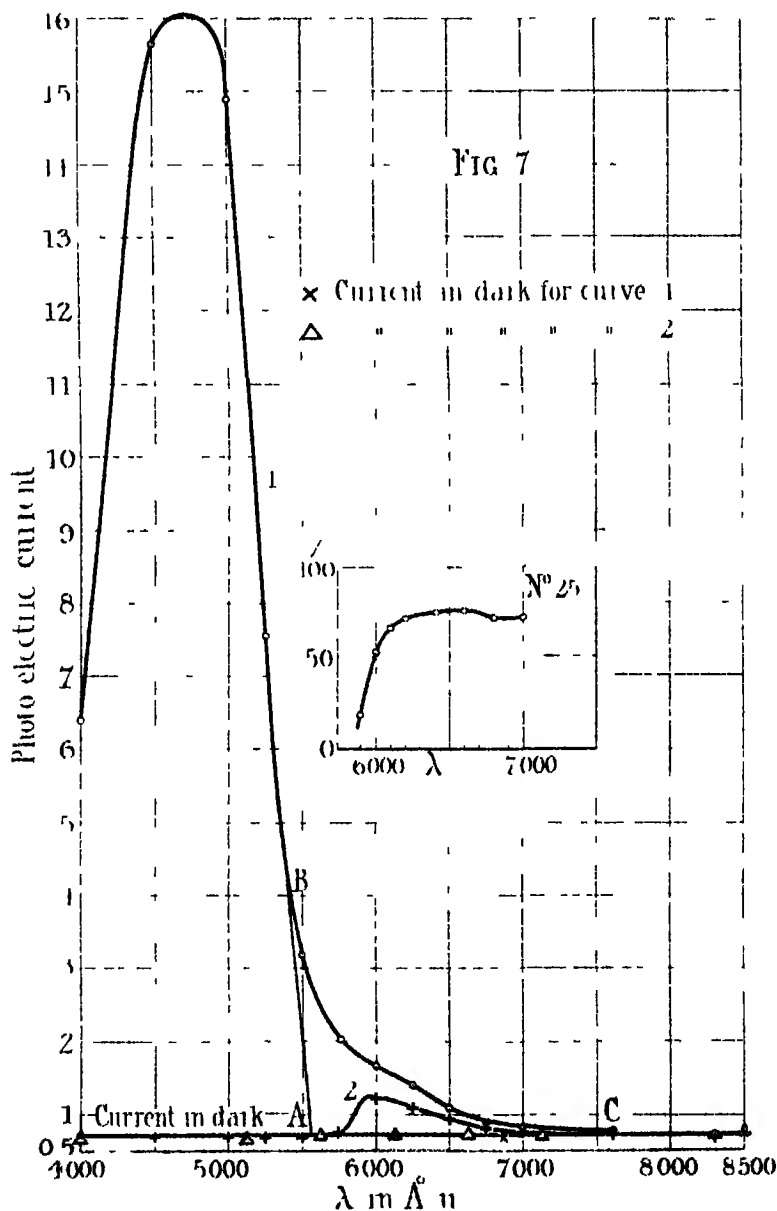
a new curve. According to this formula, A should be somewhere near to a universal constant whose value is 1.8×10^{11} E.S.U. per sq. cm. per second. It has previously been shown by one of us* that approximately a linear relation subsists between the various corresponding pairs of values of $\log A$ and b for the electron emission from tungsten and platinum and for the emission of positive ions from platinum. Fig. 6 shows that a like result holds for the thermionic electron emission from potassium.

§ 6. The Photo-electric Work Function

In paper I two values ϕ_0 and ϕ'_0 of the photo-electric work function were given, since at the time it was not known whether the asymptotic portions of the photo-electric curves at the long wave-length limit indicated a true photo-electric emission or were caused by scattered light. Referring, for example, to

* O. W. Richardson, 'Roy. Soc. Proc.' A, vol. 91, p. 524 (1915).

fig 7 curve 1 either the point A can be taken as the limiting wave-length, giving ϕ_0 , or a point such as C giving ϕ_0' . But it has since been established



that the asymptotic portion is mainly a true emission. Thus, in the case of fig 7, the interposition before the slit of the monochromator nearest the Pointo-

the source of a Wratten filter (No. 25) which cut out all the photo-electric effect for wave-lengths equal to and less than that given by A, failed to suppress the portion ABC, as is shown by curve 2. The inset is taken from the makers' "Percentage Transmission" data for the filter. Curve 1 was obtained with the apparatus set up as described in the last section and the usual thermionic currents were observed when the temperature was lowered from about 150° C. to room temperature immediately before.

It thus appears that the photo-electric work function obtained when the usual thermionic phenomena were observed is certainly less than ϕ_0 corresponding to the point A (fig. 7) and may be even less than ϕ_0' corresponding to the point C at which the photo-electric emission was immeasurable, since we cannot be certain that with a powerful enough source of illumination the currents would not be measurable for wave-lengths greater than that given by C. Incidentally the magnification of the photo-electric currents by impact ionisation in a gas might possibly be utilised to test this point. From this, and the conclusions towards the end of § 1 it appears likely that there are portions of the potassium surface which have a low work function and which are sufficiently stable to resist heating, at least to temperatures of 100–150° C.

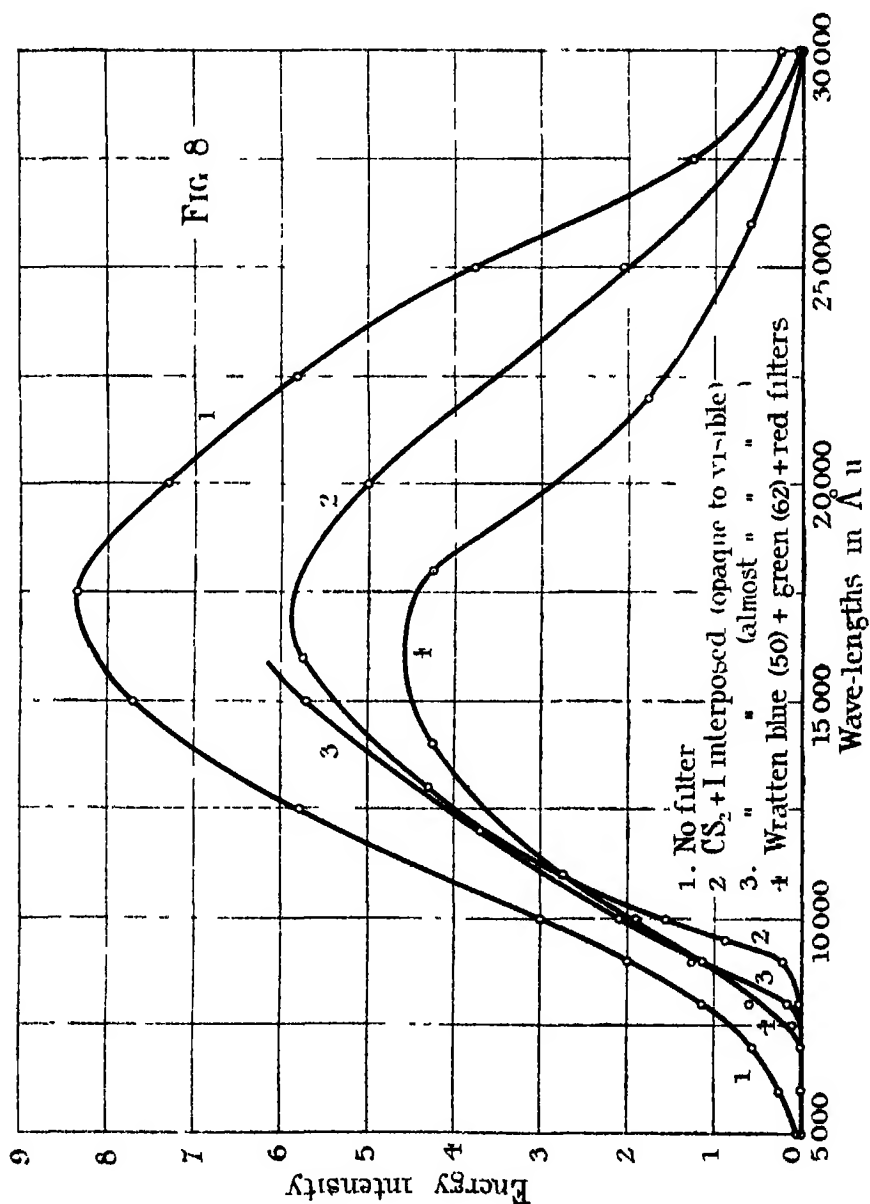
The value of the thermionic work function corresponding to the universal value of C is, from fig. 6, $\phi = 0.86 \times 10^{-4} d = 1.38$ volt. This would correspond to a photo-electric threshold of $\lambda = 12360/1.38 = 8950$ Å U. It will, however, be convenient to defer the further discussion of this question until the experiments in the next section have been considered.

§ 7. *The Infra-red Photo-electric Emission from Potassium*

Since the photo-electric measurements with the quartz monochromator could not be extended beyond 8500 Å U. some measurements were made using as monochromator a Hilger infra-red spectrometer with rock-salt prism. This instrument has a scale stretching from 5000 to 100,000 Å U. The experimental arrangements were the same as before, except that in order to obtain the maximum possible radiation-energy incident on the potassium surface, the 100 c.p. Pointolite lamp was replaced by a 500 c.p. Pointolite lamp with a concave reflector. The radiation from the plate of the lamp was focussed by a single $3\frac{1}{2}$ in. glass lens on to the slit of the spectrometer the quantity of light passing through the latter being made as large as possible. To investigate the long wave-length photo-electric emission the shorter wave length energy was absorbed by various filters.

Fig. 8 shows the spectral distribution of the energy of the dispersed radiation

leaving the second slit of the spectrometer, as indicated by means of the linear thermopile provided with the instrument and a Gambrell's galvanometer of

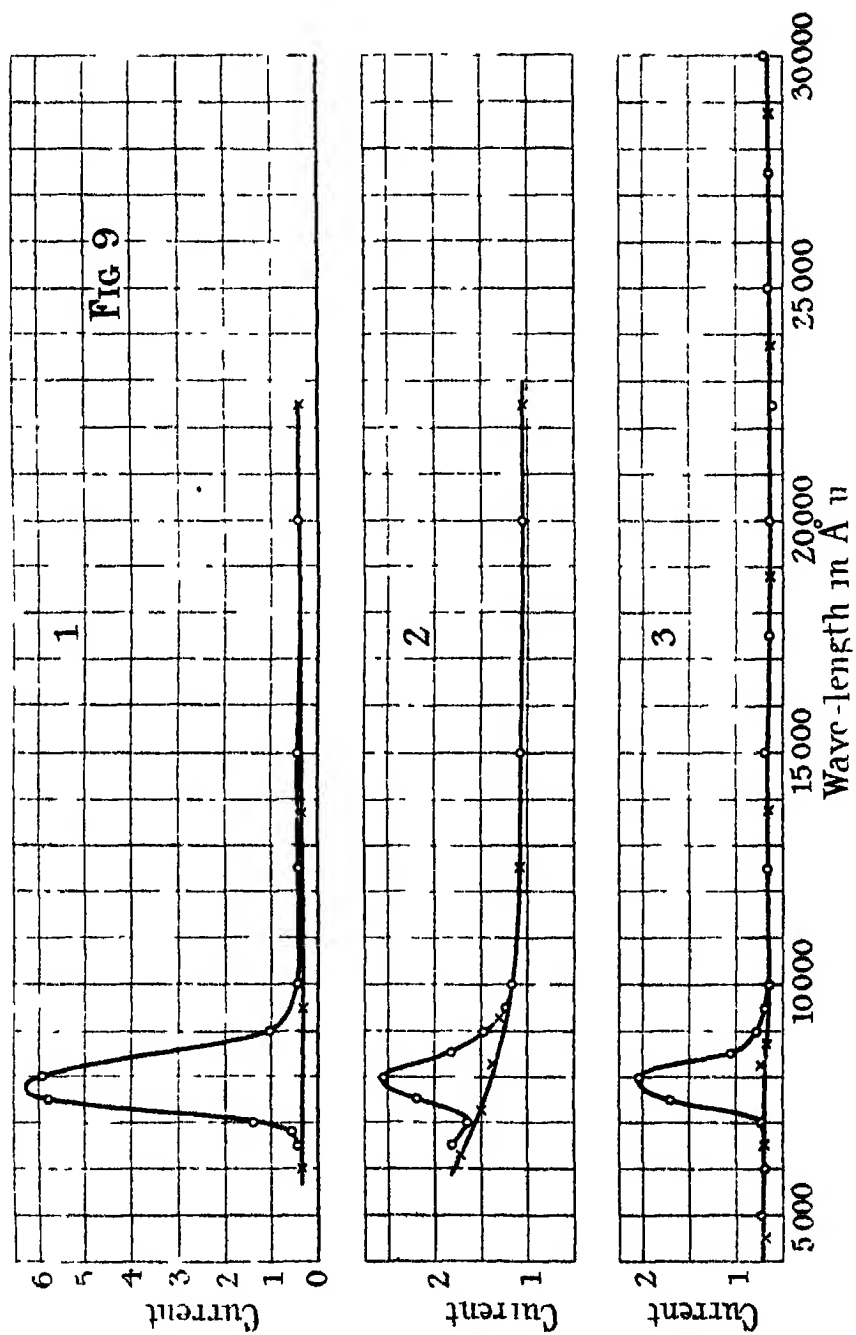


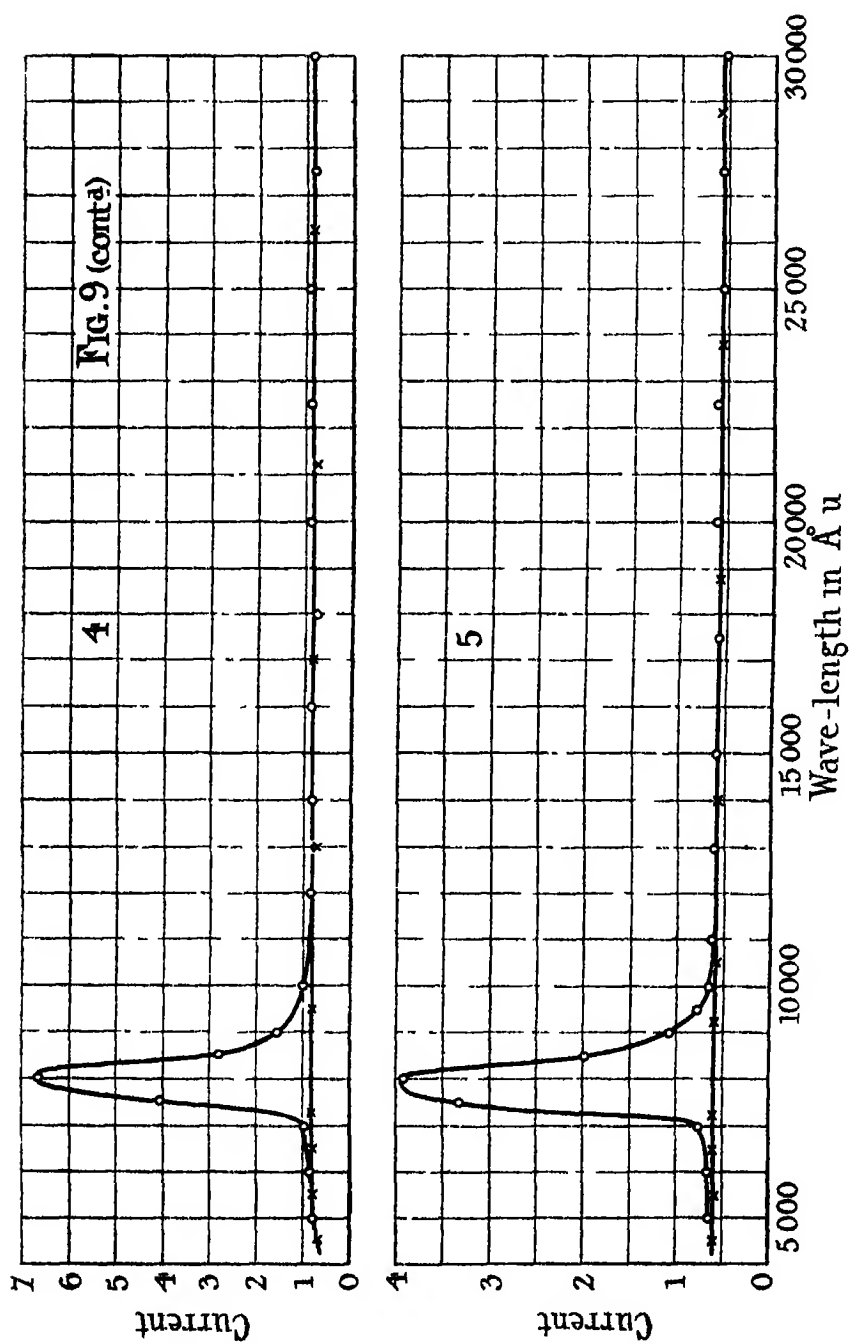
sensitivity 2.5×10^{-9} amperes per centimetre deflection per metre scale distance. Curve 1 shows the distribution without any filter interposed, curve

2 with a cell with thin microscope cover-glass ends, containing a solution of iodine in carbon disulphide of such strength that the white hot plate of the lamp was completely invisible when viewed directly through it, interposed in the non-dispersed beam before the first slit. Curve 3 shows the effect of a shorter cell of a similar solution through which the plate of the lamp could be faintly distinguished while curve 4 shows the effect of interposing simultaneously three Wratten filters (No. 50, blue, No. 62, green (both in glass) and a red gelatin filter) through which the lamp appeared a dull red. The slit widths of the spectrometer were each 0.01 inch (10 divisions), the lamp current was approximately 4.8 amperes.

Photo-electric curves obtained using the three Wratten filters together are shown in fig. 9, curves 1 to 5. The points \odot represent the total current when the surface received radiation from the spectrometer set to the wave-length shown as abscissa, while the points \times represent a residual "dark current" remaining when the radiation was cut off by a thick block of wood or brass. The accelerating potential difference was about 135 volts. In all these cases the surface had been sensitised immediately before by passing a glow discharge in dry hydrogen, for 30 seconds in the case of curve 1, and 2 minutes for curves 2, 3 and 4. The photo-electric current was found to decrease slowly with time, thus after taking measurements increasing the wave-length, on returning to the wave-length for the maximum current, that current was found to have decreased by 20—50 per cent. The effect could not have decreased much, however, in the time required to make the observations over the region of wave-lengths for which the photo-electric currents were appreciable (7000—10,000 Å U approximately). Curve 5 was taken immediately after curve 4, a further 2-minute glow discharge being passed. No water-vapour was supplied for these curves, some other observations in which water-vapour was supplied did not show larger currents or a greater effect in the infra-red, in fact, if too much water vapour was present the photo-electric currents became very small. If the photo-electric currents were measured after a previous heating of the potassium without first sensitising the latter by a glow discharge, no measurable effect could be obtained when the three Wratten filters were simultaneously interposed. The effect of interposing the perfectly opaque cell of iodine solution was to make the photo-electric currents from the sensitised surfaces completely immeasurable for all wave-lengths. The whole range of wave-lengths from 10,000 to 40,000 Å U was thoroughly investigated without finding any measurable photo-electric effect with the apparatus used.

From fig. 8, curve 4, it is apparent that the three Wratten filters together





absorb the whole of the energy of the light of wave-lengths less than 7000 \AA U ,* and the photo-electric curves of fig 9 themselves record practically no photo-electric current for wave-lengths less than this, so that it may be inferred that the whole of the photo-electric electrons from the sensitised potassium which were measured under these conditions were emitted by the incidence of light of wave-length greater than 7000 \AA U . The apparent effect for wave-lengths $5000\text{--}7000 \text{ \AA U}$ in curves 4 and 5 may be ascribed to a small quantity of scattered light, while that in curve 2 is probably due to an error. Since the emission from a surface not specially sensitised was completely suppressed by the interposition of the three filters, its emission for wave-lengths greater than 7000 \AA U must have been negligible, and this is consistent with the photo-electric curves actually obtained with such surfaces, *e g*, curve 2, fig 7, which shows no measurable emission at wave-lengths greater than 7000 \AA U . As regards the long wave-length limit of the effect with the sensitised surfaces, an inspection of the curves shows that the effect certainly extends as far as 9000 \AA U , and may extend up to 10000 \AA U . The curve near the long wave-length limit is still asymptotic and a part of the effect may be due to scattered light of shorter wave-length. At any rate, if a quantity of the same order as the possible scattering effect for $5000\text{--}7000 \text{ \AA U}$ (*e g*, curves 4 and 5) is subtracted from the effect for wave-lengths greater than 9000 \AA U , $10,000 \text{ \AA U}$ still remains as a possible limiting wave-length. The impurity of the spectrum due to finite slit-widths must have been small since curve 1 (fig 9) for which the spectrometer slits were 0.03 and 0.05 inch wide respectively is not appreciably different from curves 2-5, for which the slits were both only 0.02 inch wide.

The following are the values of the photo-electric work function ϕ_0 in volts corresponding to the given limiting wave-lengths λ in \AA U

λ	ϕ_0
9,000	1.37
9,500	1.30
10,000	1.24

The limit of the measurable photo-electric effect with the sensitised surfaces gives a work function corresponding very nearly with the value of the thermionic work function which has been found when the calculations are made using the CT² formula, and taking the value of d corresponding to the

* It is possible that the transmission might have amounted to 2 or 3 per cent at 7000 \AA U , an amount which would not be indicated by the measuring galvanometer.

universal value of C , but the significance of this may be doubtful * Much time was spent in trying to make the photo-electric effect shift further into the infra red, without success

§ 8 *Discussion of the Results*

Before drawing definite conclusions from the foregoing material it is necessary to consider the possible effects of the specific heat of potassium on its thermionic emission formula It has been shown by Lewis, Eastman and Rodebush† that the specific heat at constant volume is very appreciably higher than the Dulong and Petit value This is attributed by Lewis to the possession by the internal electrons in this metal of an appreciable heat content even at low temperatures, and Latimer‡ has shown that there is a fair correspondence between the values of σ , the specific heat of electricity (Thomson coefficient), deduced from the excess of the specific heats over the Dulong and Petit values for a number of metals and the values of σ deduced from thermo-electric data In the case of potassium in particular, the thermo-electric power deduced from the abnormal specific heat agrees exactly with the measurements of Bromewsky and Hackspill §

It is clear that the possession of this abnormal specific heat may have some effect on the temperature variation of the electron emission, but it is not clear without fuller consideration whether the effect will be of considerable magnitude such as, for example, would lead to serious error if it were assumed that the constant C in equation (1) had the universal value The effect of σ in modifying equation (1) can be elucidated by means of formulæ given in a recent paper by one of us || By taking the logarithms out of equation (32), (p 398), of that paper we have

$$p = T \frac{\gamma}{\gamma - 1} \exp \left(\frac{C_1}{k} - \frac{\omega}{kT} - \frac{e}{k} \int_0^T \frac{\sigma}{T} dT \right) \quad (9)$$

where p is the equilibrium electron pressure, γ is the ratio of the specific heats for an electron gas, C_1 is a universal constant, ω is the internal latent heat of evaporation per electron under the conditions specified on p 397 (*loc cit*), and k is Boltzmann's constant If we further assume what seems likely to be exactly true, and is certainly approximately true, that the internal latent heat

* See the discussion below

† 'Proc. Nat. Acad. of Sciences,' vol 4, p 25 (1918)

‡ 'Journal Amer Chem Soc,' vol. 44, p 2136 (1922)

§ 'C R.,' vol 153, p. 814 (1911).

|| O W. Richardson, 'Roy Soc Proc,' A, vol. 105, p 387 (1924).

ϕ of the Clausius-Clapeyron process is the same as the w of equation (9), we have (equation (22), p 394, *loc cit*)

$$\frac{dw}{dT} = \frac{k}{\gamma - 1} - e\sigma \quad (10)$$

or

$$w = \omega_0 + \frac{kT}{\gamma - 1} - \int_0^T e\sigma dT, \quad (11)$$

where ω_0 is the value of w at $T = 0^\circ \text{K}$ By combining (9) and (11)

$$p = T \frac{\gamma}{\gamma - 1} \exp \left(C_1 - \frac{1}{\gamma - 1} - \frac{\omega_0}{kT} + \frac{e}{kT} \int_0^T e\sigma dT - \frac{e}{k} \int_0^T \frac{\sigma}{T} dT \right) \quad (12)$$

This reduces to (1) with C a universal constant if the terms involving the specific heat of electricity are neglected Thus the effect of the specific heat of electricity, which, on the view we are taking, is due to the heat energy of the internal electrons, will be to multiply the thermionic currents by the factor

$$\exp \left[\frac{e}{kT} \int_0^T e\sigma dT - \frac{e}{k} \int_0^T \frac{\sigma}{T} dT \right] = \exp - \int_0^T \frac{\int_0^T e\sigma dT}{kT^2} dT \quad (13)$$

The existing thermo-electric data for potassium do not appear to be complete enough to enable us to determine the integrals in (13) with any confidence as a function of the temperature We have therefore evaluated the integrals on the left-hand side graphically, using for σ the values of the excess specific heat (C_v) given by Lewis, Eastman and Rodebush Our graphical integration is very rough, but the data are incomplete at low temperatures and otherwise the method is only approximate, so that it is probably good enough for the material In this way we estimate the value of (13) at 303°K to be $\exp 0.053 = 1.054$

It thus appears that at this temperature the electron specific heat terms only affect the currents to the extent of about five per cent Thus it seems unlikely that the specific heat terms will have any very serious effect on the constants of equation (1) even in the case of potassium As the form of (13) expressed as a function of T is unknown, it is uncertain whether the form of equation (1) will even remain unaltered, and, if it does, how such modifications as may occur will be distributed among the two constants For these reasons we shall, as a first approximation, neglect the specific heat terms

The phenomenon of electron reflection is a more serious matter If other metals can be taken as a guide this is likely to reduce the electron currents by a factor of about one-half It is likely also to affect the index of T in equation (1) If we disregard the effect on the index of T the change in C is equivalent

to an increase in the thermionic work function of 0.042 expressed in volts. If instead of assuming the standard value of C in equation (1) to be 1.8×10^{11} E.S.U. cm^{-2} , we take it to be 9×10^{10} , the corresponding value of ϕ , assuming fig. 6 to be applicable, is reduced from 1.38 to 1.354 volts, the equivalent increase in the threshold wave-length being from 8950 to 9130 Å.U. It does not seem that these considerations will move C very far from the standard value.

The essential facts as regards the photo-electric effects, so far as we have been able to ascertain them, are —

(1) With the unsensitised potassium the photo-electric currents become too small to measure at all wave-lengths in excess of about 7000 Å.U. (fig. 7)

This wave-length is almost exactly 1.5 times the wave-length (4650 Å.U.) for which the photo-electric effect as measured is a maximum. This requires a correction for the energy distribution which will probably bring the maximum to about 4400 Å.U. If the photo-electric behaviour of potassium is similar to that of other metals, we should anticipate* that the photo-electric threshold corresponding to a maximum at 4400 would be close to 6600 Å.U. This is in reasonable agreement with the determined value for which 7000 Å.U. is probably an upper limit. If they stood alone and apart from the thermionic effects the photo-electric data from the pure potassium would be quite self-consistent.

(2) With the sensitised potassium there is an additional photo-electric emission extending into the infra-red. The long wave limit at which this effect ceases to be measurable is about 10,000 Å.U. (fig. 9), and its maximum is probably in the neighbourhood of 6000 Å.U. (fig. 2)

Here again the long wave limit is not far from 1.5 times the probable maximum wave-length, so that these data are consistent with the view that the effect of sensitising is to create an abnormal form or a set of patches about half a volt electro-positive to normal potassium. The volts equivalent to thresholds of 7000 and 10,000 Å.U. are 1.77 and 1.24 respectively.

When we try to connect these results with the thermionic data we meet with considerable difficulties. In the first place, there is no clear evidence of any threshold, either photo-electric or thermionic, which agrees with the universal value of the constant C in equation (1) and the linear relation implied in fig. 6. Disregarding electron reflection, the value to agree with this should be 8950 Å.U. or 1.38 volts, or $d = 1.605 \times 10^{10}$. With one exception

* Richardson, 'Phil. Mag.' vol. 24, p. 570 (1912), Compton and Richardson, 'Phil. Mag.' vol. 26, p. 555 (1913)

all the thermionic values plotted in fig 6 are below this, most of them very much so. One of the higher temperature values taken from I, Table 4, is equal to 1.31₆ volts, and another to 1.27₆ volts. The threshold at 10,000 Å U is also fairly near (1.236 equivalent volts), but this is for potassium in an abnormal state. The value which should agree with the universal C is the photo-electric threshold at 7000 Å U, but this, expressed in volts, is far too high on fig 6. It would correspond to about 10^{15} instead of 10^{11} . It is, of course, always open to urge that our unsensitised potassium was covered with a layer of something inhibitive of photo-electric action, but this explanation seems extremely improbable. In the first place, the potassium was being continually distilled and condensed in our apparatus, with the formation of new surfaces of the metal, whilst subject to the most powerful evacuating devices known. In the second place, the determined threshold agrees with the wave-length found for the photo-electric maximum, which is quite close to the position found by Pohl and Pringsheim.

It is a fact that all the values of the work function deduced from the thermionic data for the unsensitised potassium in fig 6 which are taken from paper I, lie below the equivalent of the measured photo-electric threshold. We do not, however, infer from this that these data establish any real contradiction between the photo-electric and thermionic work functions. It follows from equation (4), and this is borne out by the experimental results, that where there are more thresholds than one the higher values only make themselves felt in the thermionic effects at the higher temperatures. It may well be that if these thermionic experiments had been pushed to higher temperatures, values of the thermionic work function would have been obtained equivalent to the measured photo-electric threshold for the unsensitised potassium. At such temperatures, however, we meet with serious practical difficulties arising from the vapour pressure of the metal, its high chemical activity, and its low ionisation and radiation potentials.

For this explanation to be reasonable it is necessary that the constants which correspond to C in equation (1), and which govern the thermionic emission should be small compared with the normal value of C, otherwise these thresholds will become effective in the photo-electric emission. This requirement is, in fact, satisfied. For example, if we turn to Table Ia, we find that F_2 is about one-thousandth part and F_1 about 10^{-12} of the normal C value. The values found for these constants are almost *invariably* of a low order, as may be seen from fig 6.

The single point in fig 6 which forms an exception to this statement, the

Δ in the top right-hand corner, may be significant. This point was determined under conditions of vacuum which were certainly not worse, and may have been better, than those in paper I. The value of d for this point is 1.87×10^4 , which is equivalent to 1.61 volts, or a threshold of 7680 Å U. This is not very far from the photo-electric threshold at 7000 Å U, which also was re-determined under the same conditions. It is possible that the value of d given by these data may even be a little higher than 1.87×10^4 , but it is difficult to determine accurately, as the $\log i - 2 \log T$, T^{-1} curve is here running into the region where the sudden reduction of the thermionic current sets in. We do not wish to overstress the value of this particular set of observations, but they do seem to afford some evidence of a tendency at high temperatures for the thermionic work function to approximate towards the photo-electric threshold. They suggest, furthermore, that the thermionic threshold which corresponds to F_2 in Table IA is removable by heating and evacuation. At the same time a thermionic threshold of a much lower order, nearer to F_1 in Table IA, persisted during these experiments, so that there is evidently another thermionic threshold which, if not permanent, is certainly more difficult to remove by such means.

The considerations so far dealt with in this section merely require that multiple thresholds exist. They afford no indication as to whether they are distributed uniformly over the surface or only exist locally in patches. The fact that the thermionic currents obey an equation of the type of (4) equally implies merely that multiple thresholds are present,* and says nothing about their superficial distribution. There is, however, definite evidence that they exist in local patches when we study the curves connecting the currents with the applied potential differences. The photo-electric curves exhibit an increase of current of the order of 5 per cent when the voltage is increased from 10 to 250. Such ready attainment of saturation is to be expected if the photo-electric emission is effective over the whole of the surface, more particularly as, on the view we are taking, some 99.9 per cent of it comes from the most electro-negative part which forms almost the whole surface.

The current E M F curves for the thermionic emission should, however, be quite different if the emitters with different thresholds are localised on the surface. Taking the figures given in Table IA as a representative sample, which is a fair way of treating the data from paper I, we see that at temperatures in the neighbourhood of 40° C practically the whole emission comes from systems which represent about 10^{-12} of what we may call the "ultimate

* O. W. Richardson, 'Proc Lond Phys Soc,' vol 36, p 383 (1924)

capacity" of the surface. If these systems are in localised areas, these areas will be electro-positive about 1.3 volts to the bulk of the surface. This would give rise to strong local fields which would tend to prevent the emitted electrons from being removed from the source by the externally applied field. At temperatures in the neighbourhood of 220°C the bulk of the emission comes from systems which represent about 10^{-3} of the ultimate capacity of the surface. If these are in localised areas, they will be electro-positive about 0.5 volt to the bulk of the surface. These will give rise to fields of force, tending to prevent the attainment of saturation, but to a much less degree than the more electro-positive areas which account for most of the thermionic activity at the lower temperatures.

Whatever may be the ultimate fate of the idea of patches, there is no doubt that these requirements are in excellent agreement with the facts. If we turn to I, figs 10 and 11, we find that the difficulty of attaining saturation at 42°C and 43°C is most striking, and that this difficulty gradually diminishes as the temperature is raised to over 200°C . If the theory of localised patches were abandoned there would remain, so far as we are aware, no alternative reasonable explanation of the remarkable difficulty of attaining saturation with the thermionic currents in the neighbourhood of 40°C .

We shall now consider the experiments with the sensitised potassium. The immediate incentive to these experiments was the hope of stimulating the formation of the low threshold modifications to such an extent that their ultimate capacity would become a considerable, instead of a very minute, fraction of the whole. In that event, we anticipated that we should obtain appreciable photo-electric currents in the infra-red, setting in at wave-lengths corresponding to the low thresholds. In this programme we did not anticipate success as regards the lowest threshold which is effective on the thermionic currents in the neighbourhood of 40°C . The photo-electric threshold corresponding to this would lie at about $30,000\text{ \AA}$, and we have been able to detect nothing in the infra-red at wave-lengths larger than $10,000\text{ \AA}$. This is, perhaps, not surprising, since at $30,000\text{ \AA}$ there was practically no energy in the arrangement we used. In any event, it may prove difficult to do much with this particular threshold. In the unsensitised potassium its ultimate capacity is about 10^{-12} . On the patch idea ultimate capacity is mainly, though not entirely, equivalent to proportion of total area. Obviously, in order to obtain any appreciable photo-electric effects we should have to multiply the amount of this modification by a factor comparable with 10^{12} . As the amount present in the unsensitised potassium

is only of the order of 10,000 atoms per square centimetre it is presumably very difficult to grow

On the other hand, our experimental results are not in conflict with the view that we have succeeded in growing the modification which is effective on the thermionic emission at about 220°C . The photo-electric threshold at about 10,000 Å U, which is brought out by sensitising, is equivalent to 1.236 volts or $d = 1.44 \times 10^4$ Å. This value falls within the range of values which we obtained from the thermionic emission from the unsensitised potassium, and which are shown thus, \times in fig. 6. It is, therefore, a possible view to take that the threshold which is effective on the thermionic emission at about 200°C in (a), (b), (c), (d) of I, fig. 7 for example, is that of the modification which is produced by subjecting the potassium to the action of a glow discharge in hydrogen. We do not feel that we have established this result beyond the possibility of doubt. It would be very difficult to do so. We also do not wish to commit ourselves as to what the particular result of the glow discharge is which is effective in altering the threshold. It may be the formation of a hydride or of an abnormal potassium atom, and, in fact there are numerous possibilities.

If the effect of the glow discharge is an extension of localised patches, which are electro-positive with respect to the normal surface, they must extend in such a way as to form a coarse and not a very fine pattern. For it appears on examination of our results that the photo-electric currents, from the sensitised surfaces, show no increase when the voltage is increased from 30 to 125. In other words, they possess the same property of easily attaining saturation as was shown by the photo-electric currents from the unsensitised potassium, but not by the thermionic currents in the neighbourhood of 200°C . If the effect of sensitising were a mere multiplication of the small patches which are supposedly effective on the thermionic emission at about 200°C , we should expect the photo-electric currents also to show lack of saturation. The lack of saturation is due to an effect which is localised at the periphery of the patches, and for this to disappear the areas must become large. The process of sensitising must consist in a growth of the individual patches and not merely in an increase of their number.

There is one fact which the foregoing explanations leave untouched, and that is the increase in the normal photo-electric emission which generally accompanies the act of sensitising. In most cases one effect of the glow discharge is to increase the maximum effect in the neighbourhood of 4400 Å U by a large factor. This increase is permanent in a high vacuum, and is thus

not due to ionisation of residual gas by impact. On the view we have been developing thus far we should not expect sensitising to increase the normal effect, as the abnormal areas have been supposed to develop at the expense of the normal areas. It appears, on the contrary, that as the low threshold effects become more responsive so also do the high threshold effects. There seems to be something to be said for the view that the low thresholds are created, or their effects augmented, by the glow discharge by a process whose effect on the surface is rather of the nature of subtraction than of addition. It may be that the thresholds are present in the unsensitised metal, but that under normal conditions most of the surface, even in the highest vacua attainable in the laboratory, is covered with a layer which either absorbs the light before it reaches the photo-electrically sensitive electrons, or tends to prevent their escape after initial liberation, and that the function of the glow discharge is to do something which is equivalent to the removal of this layer. There are obviously a considerable number of alternatives which it will require much further experimental investigation to resolve. The following is one such alternative picture of the phenomena, which appears to be consistent with the facts, and to allow of an increased normal effect from the sensitised surfaces —

(a) *Unsensitised potassium*

- (1) A maximum in the neighbourhood of 4400 \AA U , corresponding with Pohl and Fringsheim's selective maximum
- (2) An effect extending to 7000 \AA U and possibly to $10,000 \text{ \AA U}$, but too small to measure beyond 7000 \AA U

(b) *Sensitised potassium*

- (1) As for (a) (1)
- (2) A second maximum at about 6000 \AA U , giving a threshold between 9000 and $10,000 \text{ \AA U}$
- (3) Possibly an effect at $30,000 \text{ \AA U}$ —not yet detected.

(c) Assume that the effect of sensitising is merely to increase in some way (e.g., by increased absorption) the photo-electric emission from every portion of the surface, and especially for the longer wave-lengths. This is consistent with the curves actually obtained for sensitised and unsensitised surfaces. In this case all the effects with sensitised surfaces would necessarily be obtainable with unsensitised surfaces if the measuring apparatus were sensitive enough. Thus for normal potassium we should have the following thresholds —

(Selective) $\lambda = 4400 \times 1.5 = 6600$ about, equivalent to $\phi = 1.87$ volts (α),

$\lambda = 6600 \times 1.5 = 10,000$ about, equivalent to $\phi = 1.24$ volts (β) Possibly $\lambda = 30,000$ about, equivalent to $\lambda = 0.412$ volts (γ)

(d) *The thermionic data* -- Assuming that there are portions with two different work functions, the equation $i = T^2 (F_1 e^{-d_1/T} + F_2 e^{-d_2/T})$ has been found to agree well with the data from 15°C to 225°C , d_1 corresponds to the work function for an appreciable proportion of the surface and has values in the neighbourhood of 1.24 volts agreeing with threshold (β) This is also consistent with the linear relation (fig 6) and the universal value of C d_2 corresponds to a low work function and a threshold of the order of $30,000 \text{ \AA U}$ This threshold is operative only on a very minute fraction of the surface

To account for the threshold with $\phi = 1.87$ volts (selective) another term $T^2 F_0 e^{-d_0/T}$ may be added to the equation, so that $i = T^2 (F_0 e^{-d_0/T} + F_1 e^{-d_1/T} + F_2 e^{-d_2/T})$ At 225°C or 500°K , putting $d_0 = 2.17 \times 10^4 d_1 = 1.44 \times 10^4$, the term in F_2 is quite negligible compared with the other two The ratio of the first two terms to each other at this temperature is $F_0 \times e^{-10^4} F_1$ Hence unless F_1 is very small compared with F_0 the second term alone will determine the emission and the emission corresponding to the selective threshold will be negligible at 500°K

(e) The *current E M F* curves are consistent with this view --

- (1) *Thermionic Curves* Unsaturated at low temperatures when the third term is operative They are still unsaturated, but not so much so at the higher temperatures when the second term dominates the emission
- (2) *Photo-Electric Curves* -- Always saturated because the photo-electric currents will only be appreciable when they come from thresholds which are effective over a considerable proportion of the surface

Whilst the classification under (a) to (e) has seemed to merit consideration we do not feel quite satisfied with it It seems, on the whole, not unlikely that the augmentation of the "selective" photo-electric emission and the development of the low photo-electric thresholds are distinct effects There is evidence that with fresh potassium and pure hydrogen the only effect of the glow discharge is the augmentation of the "selective" emission, and that the development of the low thresholds requires the co-operation of some other element This involves a return to the interpretation on pp 29-36 with the addition of a specific effect of the hydrogen discharge in augmenting the 'selective' emission

§ 9 *Summary*

Attention is drawn to existing evidence that the thermionic work function w and the photo-electric threshold λ_0 each have more than one value for sodium and potassium. The thermionic emission i from a substance with multiple thresholds should be given as a function of the temperature by the expression $i = A_1 T^2 e^{-w_1/RT} + A_2 T^2 e^{-w_2/RT} + \dots$, with one term for each threshold. Such an expression with two terms represents typical experimental data for potassium. There are similar but less complete data for sodium. The fact that the photo-electric currents saturate readily, but the thermionic currents do not, indicates that the separate thresholds are localised in patches on the surface. The photo-electric threshold for normal potassium is close to 7000 \AA U , which agrees with the known wave-lengths of maximum activity λ_{max} and the equation $\lambda_0 = \frac{2}{3} \lambda_{\text{max}}$. Uncertain traces of a thermionic threshold agreeing with this have been found at about 200°C in one experiment but the thermionic thresholds usually effective at this and lower temperatures are of a much lower magnitude even under the best vacuum conditions. Satisfactory investigation at appreciably higher temperatures is precluded by various complications which develop. A common thermionic threshold effective at about 200°C corresponds to $\lambda_0 = \text{about } 10,000 \text{ \AA U}$. A photo-electric emission with this infra-red threshold has been got by exposing potassium to a luminous discharge in hydrogen or water vapour. It is suggested that this is due to the growth of small patches normally present. We have found no evidence of photo-electric activity further out in the infra-red, although there is a thermionic threshold which corresponds to $\lambda_0 = 30,000 \text{ \AA U}$. All the various pairs of values of A and w come near to satisfying a linear relation between w and $\log A$. The glow discharge not only brings out undeveloped thresholds, but it also augments the normal emission. A tentative classification of the effects is suggested and some unsettled alternatives are partly indicated.

In conclusion, we wish to express our thanks to the Radio Research Board for a grant to one of us (A. F. A. Y.), which has enabled this research to be brought to its present condition.

On Experiments relating to the Spectrum of Nitrogen.

By T R MERTON, M A , D Sc , F R S , Professor of Spectroscopy in the
University of Oxford, and J G PILLEY, B A

(Received January 21, 1925)

It is somewhat remarkable that the spectrum of the neutral nitrogen atom, the nitrogen arc or NI spectrum, should be the least known of the spectra associated with nitrogen. The positive and negative band spectra, associated with nitrogen molecules, have been the subject of many investigations, and of the line spectra which are developed when condensed discharges are passed through nitrogen at atmospheric pressure or through nitrogen contained in vacuum tubes, the spectrum of singly ionised nitrogen, the NII spectrum, has recently been arranged in series by Fowler ('Roy Soc Proc', vol 107, A, p 31, 1925), who has in an earlier investigation ('Monthly Notices R A S', vol 80, p 692, 1920) assigned a number of lines which have not yet been arranged in series to the doubly ionised nitrogen atom. It would appear that under ordinary conditions of excitation the lines of the arc or nitrogen I spectrum are not conspicuous and we are indebted to Hardtke ('Ann der Phys,' vol 56, p 363, 1918) for the information at present available with respect to this spectrum. Hardtke found that with discharge tubes of special construction containing nitrogen a number of lines were predominant in the spectrum of the positive rays observed in certain regions of the discharge tubes, and that the same lines were relatively enhanced in vacuum tubes of the conventional type when they were excited by condensed discharges of feeble or moderate intensities. Hardtke gave approximate measurements of a number of these lines, which he assigned to the arc spectrum.

In a series of previous investigations (Merton, 'Roy Soc Proc,' A, vol 96, p 382, 1920, Merton and Barratt, 'Phil Trans,' A, vol 222, p 369, 1922, Merton and Johnson, 'Roy Soc Proc,' A, vol 103, p 383, 1923) it has been shown that profound modifications are sometimes observed in the spectrum of a substance when a very small quantity of that substance is present in a discharge tube containing helium at a comparatively high pressure, and the tube is excited by condensed or uncondensed discharges. Thus with uncondensed discharges there is a striking change in the distribution of intensity of the lines of the secondary spectrum of hydrogen, a trace of carbon is recognised by the appearance of the "comet tail" spectrum, first observed by

Fowler ('Monthly Notices R A S,' vol 70, p 484, 1910) at very low pressures, and when both carbon and hydrogen are present a new triplet series of bands are developed

With condensed discharges of moderate intensity through helium at 30 mm. pressure containing a trace of carbon a new line spectrum was observed and it was suggested that this spectrum might be assigned to the neutral carbon atom Rayleigh ('Roy Soc Proc,' A, vol 102, p 453, 1923) has found that the spectrum of the nitrogen afterglow is modified by the presence of the inactive gases, the effect depending on the nature of the inactive gas used. The effect of argon on the secondary spectrum of hydrogen has been investigated by Barratt ('Phil Mag,' vol 6, p 627, 1923), who has observed phenomena somewhat similar to those seen in the presence of helium, but the change is not so striking, and the effect of the two gases, even qualitatively, is not exactly the same Johnson and Cameron ('Roy Soc Proc,' A, vol 106, p 195, 1924) have observed a more striking difference in the spectra of carbon in the presence of argon and helium, for whereas in the latter gas the "comet tail" spectrum and the new line spectrum appear with uncondensed and condensed discharges respectively, neither of these spectra could be observed under any conditions of excitation when argon was substituted for helium, though the new triplet series of bands could be developed in either gas In the present investigation we have examined the effect of helium on the spectrum of nitrogen, and have been successful in finding conditions under which the arc spectrum appears without any trace of the spark lines

Experimental

The preparation of the vacuum tubes has presented much greater difficulties than were encountered in the case of the tubes showing the "comet tail" spectrum and the arc spectrum of carbon For the investigation of the nitrogen lines the carbon spectrum must be eliminated, and when the pressure of the helium in the discharge tube is as great as about 30 mm of mercury, this becomes a difficult matter A procedure which would yield helium tubes showing no trace of any impurity at pressures of about 5 mm, generally results in a brilliant "comet tail" spectrum when the pressure is increased to 30 mm The tubes used were of the H pattern, with spiral aluminium electrodes and with tubes of from 8 to 12 mm internal bore in place of the usual capillary. They were provided with palladium tube regulators for admitting and removing hydrogen, and with side tubes which were blown on to a series of bulbs containing respectively phosphorus pentoxide, lumps

of caustic potash, potassium permanganate, and lastly alumina which had been moistened with a dilute solution of sodium azide and dried at a moderate temperature. In a separate side tube was sealed a short piece of platinum wire with a small head of silver fused on to the end. By passing a discharge from this silver electrode to one of the aluminium electrodes during the process of exhausting the tubes a deposit of silver was sputtered on to the walls, and this was found to be completely effective in absorbing any traces of mercury that might be present. The tubes were always washed out with dilute hydrofluoric acid followed by distilled water before the side-tubes containing the reagents were sealed on, as this had been found to be by far the most effective method of cleaning them. We are indebted to Prof J C McLennan, F R S, for a cylinder of helium which was used in this investigation. A quantity of this gas, which contained traces of neon, was transferred to an ordinary Kipp gas generator which served as a convenient reservoir. The Kipp was connected through a large U-tube containing cocoanut charcoal to the tubes to be exhausted, a mercury manometer being included between the Kipp and the charcoal tube. The apparatus was exhausted by means of a Holweck molecular pump backed by a Fleuss oil pump, and the discharge tubes and the charcoal tube were severely heated during the process of exhaustion.

A heavy discharge was passed at intervals through the tubes, which were washed out from time to time with pure oxygen admitted by gently heating one of the bulbs containing potassium permanganate. The charcoal tube was then cooled to the temperature of liquid air, and helium from the Kipp was allowed to flow very slowly through the charcoal tube into the discharge tubes, until the desired pressure of about 30 mm of mercury had been attained. At this stage the tubes, which showed a strong comet-tail spectrum, were sealed off, since the charcoal tube appeared to be quite ineffective in removing the last traces of the carbon contamination to which this spectrum is due. The elimination of the last traces of carbon could be accomplished only by admitting oxygen into the tubes by heating the permanganate and by passing a heavy discharge for a considerable time, the carbon being presumably absorbed by the potash as carbon dioxide, and at the same time nearly all the hydrogen was eliminated by absorption as water vapour by the phosphorus pentoxide. Any excess of oxygen was removed by the aluminium electrodes, and the tubes were now ready for the admission of the nitrogen by heating the alumina and the sodium azide. This had always to be carried out with the greatest possible care, for it was difficult to control the amount of nitrogen admitted. With any excess the spectrum showed nothing but the positive

and negative bands, and also the helium lines with a condensed discharge. For the excitation of the tubes a small alternating current transformer was used, and a condenser and spark gap could be included in the secondary circuit in the usual manner. It is not proposed to discuss fully in this communication the phenomena observed with uncondensed discharges, but it may be stated that under these conditions only the band spectra of nitrogen were observed, these spectra being in some respects modified by the presence of the helium, and the negative bands being greatly enhanced in intensity.

The Arc-spectrum of Nitrogen

When a condenser and a small spark gap were introduced into the secondary circuit an entirely different series of phenomena were observed. It has already been pointed out that with any excess of nitrogen only the band spectra of this gas are seen, and when the nitrogen has been absorbed by the electrodes the tubes show only the line and band spectra of helium, with traces of the neon lines. There is an intermediate stage, when the tube contains an extremely small quantity of nitrogen, in which the nitrogen and helium band spectra are both much weakened and a line spectrum appears. This line spectrum is entirely different from that observed when condensed discharges are passed between metallic poles in nitrogen at atmospheric pressure, and the strongest of its lines are not conspicuous in condensed discharges through nitrogen in vacuum tubes at reduced pressures. The lines observed include most of those recorded by Hardtke (*loc cit*), but under these conditions they are completely isolated from the spark spectrum. The tubes could only be run in this condition for a relatively short time, since the small amount of nitrogen was absorbed by the electrodes, and the admission of the requisite amount of fresh gas was difficult to control. An excess of nitrogen too small to obliterate the arc lines was nevertheless objectionable, as many of the lines of the arc spectrum were confused with lines of the band spectra, of which the negative band spectrum was particularly strong under these conditions. With very intense discharges or with narrow tubes some spark lines began to appear.

The Determination of Wave-lengths

The spectra were photographed with a grating spectrograph having a concave grating ruled with 20,000 lines to the inch, and of 4-ft. radius of curvature, the dispersion being approximately 10 Å per millimetre, and use was also made of a large Littrow spectrograph with one glass prism which

gave a dispersion of about 40 Å per millimetre at $\lambda = 7500 \text{ Å}$ and about 5 Å per millimetre at about $\lambda = 3700 \text{ Å}$. The international iron and neon lines served as standard lines, and exposures in juxtaposition were also made of the spectra of pure nitrogen and pure helium with discharge tubes of the same pattern and excited in the same manner. Lines due to the band spectra of nitrogen and the band and line spectra of helium could thus be recognised. With the wide-bore tubes which were used the intensity of the light leaves much to be desired, and very long exposures were necessary. This gave rise to great difficulties due to loss of definition and displacements with changes of temperature and the spectrograph was finally set up in a small room which was kept at a constant temperature by means of an electric heater controlled, through a relay, by an Ostwald toluene regulator. In order further to eliminate errors due to changes of temperature the comparison spectrum was put on in instalments which were spread over the period during which the nitrogen spectrum was exposed, so that a small temperature shift would show itself as a widening of the lines without sensibly displacing the positions of their maxima relative to the nitrogen lines. The plates were measured in the usual manner with a Hilger photomeasuring micrometer. The results are shown in Table I in which the wave-lengths (Å) in air and the intensities are given in the first and second columns respectively. The intensities call for some further comment. The first three lines in the table were measured with the prism instrument only. The grating gives weak spectra in this region and the plates used were not very sensitive to these wave-lengths. It is believed that the lines were really of very considerable intensity, and they have accordingly been assigned the intensities given in the table. The lines marked 0 and 00 could only be observed on plates which had been exposed for very long periods, and on which the strongest lines recorded were greatly over-exposed, and it is difficult under the circumstances to construct a uniform scale of intensities. In the third column are given the wave-numbers *in vacuo*, and in the fourth the wave-lengths recorded by Hardtke (*loc. cit.*)

The lines marked with an asterisk were measured on one plate only, a few of the lines which were very diffuse are marked *d*, and *c* denotes a line which was confused with nitrogen bands. With the condensed discharges which were used to excite the tubes the definition of the lines was not so good as that usually found when uncondensed discharges are employed, with the result that the accuracy of the wave-length determinations has not been so high as we had hoped to attain. It is believed that, with the exception of the first three lines in the table, which were recorded with the prism instrument only,

and the lines marked with an asterisk, the values given are rarely in error by more than 0.03 Å

Table I

λ (Å)	Int	Wave number (vacuo)	λ (Hardtke)	λ (Å)	Int	Wave number (vacuo)	λ (Hardtke)
7468 4	9	13386 1		5560 45	4	17979 17	5559 5
7442 4	9	13432 8		5567 63	1*	17965 97	
7423 5	7	13467 0		5563 84	3d*	17968 21	
6945 18	3	14394 51		5557 49	00	17988 74	
6926 70	2	14432 92		5545 11	0	18028 91	5544 0
6874 27	1	14543 01		5378 45	00	18587 55	
6733 33	3c	14847 40		5372 66	1d	18607 59	5372 5
6722 60	5	14871 10		5367 28	00*	18626 25	5366 5
6713 19	1*	14891 95		5356 75	3	18662 86	5357 0
6708 81	2*	14901 68		5328 67	5	18761 21	5330 0
6706 21	2*	14907 45		5310 60	00*	18825 05	
6656 53	0	15018 72		5309 48	00	18829 02	5309 0
6653 46	4	15025 05		5292 74	00	18888 57	5292 5
6646 52	2	15041 32		5281 17	1	18929 94	5282 0
6644 97	7	15044 84		5201 79	00*	19218 82	
6626 98	0*	15085 67		5197 00	00*	19236 53	
6636 94	0	15063 04					5182
6622 55	00	15095 77					5170
6499 51	1	15381 54		4935 03	9	20257 68	4935 5
6491 24	1	15401 13		4914 92	4	20340 56	4915 5
6484 88	8	15416 24		4881 67	2	20479 10	
6483 77	4	15418 87		4868 88	00*	20532 90	
6482 74	9	15421 32		4865 43	0d*	20689 77	
6481 73	3	15423 73		4830 91	0d*	20694 27	
6480 53	0	15426 58		4753 17	2	21032 73	
6471 02	0	15449 25		4750 26	2	21045 62	
6468 30	1d*	15455 75		4742 87	0	21078 40	
6462 73	0	15469 08		4735 77	1	21109 99	
6457 89	0*	15480 66					4670 0
6452 76	1	15492 98					4660 3
6448 41	1	15503 43		4494 68	5c	22242 32	
6441 70	5	15519 57		4492 45	5c*	22253 86	4492 5
6440 91	2	15521 48					4485 5
6436 75	0d	15531 50					4466 5
6420 63	2	15570 50		4358 29	7	22944 78	
6417 07	1	15579 14		4336 51	4	23053 57	4337 0
6393 74	00*	15859 23					4324 3
6285 79	0	15904 49		4317 72	4	23163 89	4317 7
6279 42	1*	15920 68		4313 11	3	23178 64	4313 3
6275 43	0	15930 75		4305 46	6	23219 83	4305 5
6272 93	2	15937 10		4284 91	2	23331 18	
6075 79	3	16454 23		4282 90	1	23345 92	
6017 74	1	16612 95		4281 35	2	23350 56	
6008 49	9	16638 52		4253 31	3	23504 51	
5999 46	5	16663 57		4230 36	4	23632 03	
5829 52	2	17149 33	5832 0	4224 90	2*	23662 56	
5752 65	2	17378 48		4223 09	5c	23672 70	4223 0
5710 77	0	17505 93					4215 0
5686 20	00	17581 58					4213 0
5625 40	00	17771 40					4193 0
5623 22	3	17778 49	5623 5				4187 0
5618 18	00	17794 44					4180 0
5616 57	4	17799 54	5617 0				4166 0
5611 36	00	17816 06		4151 44	9	24081 26	4151 0
5564 38	4	17966 47	5564 0				4145 0

Table I - (continued)

λ (I A)	Int	Wave number (vacuo)	λ (Hardtke)	λ (I A)	Int	Wave number (vacuo)	λ (Hardtke)
4117 58	4c	24161 94	4137 0	3834 20	4	26073 70	
4113 92	5	24300 88	4114 0	3830 29	9	26099 03	
4109 94	10	24324 41	4110 0	3822 00	5	26156 92	
4099 96	9	24383 62	4100 0	3818 19	1	26183 02	
4037 35	3c	24761 76		3681 14	3	27157 77	
4011 07	4	24923 99	4012 0	3650 13	5	27388 50	
3999 98	3	24993 09		3545 60	2c	28195 94	
3957 19	3	25263 32		3532 63	2c	28299 45	
3952 18	3	25295 35		3437 14	2	29085 65	
3868 95	2	25839 50					

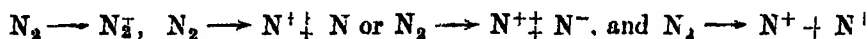
The Effect of Argon

Experiments have been made to discover whether the arc lines of nitrogen can be excited when argon is substituted for helium under the conditions of experiment which have been described above. A discharge tube similar to that used for the observations with helium was prepared, with the bulbs containing phosphorus pentoxide, potash, potassium permanganate and azide as before, and with a palladium regulator. The tube was connected to an auxiliary discharge tube provided with electrodes of aluminium, magnesium and gold. The tubes were exhausted in the usual manner and a discharge was passed between the aluminium electrode and the gold electrode, which sputtered a layer of gold on to the walls of the tube. Crude argon from a cylinder was allowed to flow into the tubes until a mercury manometer showed that a pressure of some 32 mm. of mercury had been attained, and the tube was then sealed off. The diatomic impurities in the argon were rapidly absorbed by passing a condensed discharge between the aluminium and magnesium electrodes in the auxiliary tube. During the passage of the condensed discharge the magnesium electrode appeared to be covered with bright green tufts, which showed the magnesium spectrum strongly, and the absorption of diatomic gases (with the exception of hydrogen) was very rapid. This is a convenient method of preparing pure argon. With the wide-bore tube the blue spectrum of argon was not conspicuous, even with fairly powerful condensed discharges. Small quantities of nitrogen were admitted by heating the azide, and when the tube was excited by condensed discharges of moderate intensity the nitrogen arc lines could not be seen, though the strongest of them became faintly visible when powerful discharges were used. It appears that in the presence of an

excess of argon the nitrogen arc spectrum is not developed under ordinary conditions in the same way that it appears in the presence of helium

The Excitation of Nitrogen by Cathode Rays

It has long been known that the negative band spectrum of nitrogen can readily be excited by the impact of electrons on nitrogen molecules, but the first investigation in which electrons of known velocity were employed was due to Fulcher ('*Astrophys Journ.*' vol 37, p 60, 1913), who made use of a thermionic discharge tube and found that as the speed of the electrons was increased, the positive bands first appeared and were followed at higher velocities by the negative bands. Fulcher's results were confirmed by Foote, Mohler and Meggers (Foote and Mohler, '*Origin of Spectra*,' p 191), who observed the positive bands at 7 volts and found that the negative bands were very intense at 25 volts. The ionisation of nitrogen by electron impact has formed the subject of a careful investigation by Smyth ('*Roy Soc Proc.*' A, vol. 104, p 121, 1923), who has observed critical potentials at 16.9, 24.1 and 27.7 volts, and has given cogent reasons for supposing that these potentials correspond respectively to the reactions



In the present investigation no attempt has been made to determine the potentials at which the different spectra are first observed, but an attempt has been made to observe which lines are the first to appear when the velocities of the exciting electrons are gradually increased. In the first experiments the method employed was essentially similar to that used by Foote, Meggers and Mohler (Foote and Mohler, *loc cit*, p 117). The electrons emitted by a heated strip of lime-coated platinum foil fell through a known potential in their passage from the foil to a wire grid. On the other side of the grid, and connected to it, was a flat metal plate, and the potential difference between the foil and the grid could be varied by connection to the tappings on a battery of small storage cells. Observations were made of the spectra emitted in the space between the grid and the plate.

The intensity of the light emitted under the conditions of experiment was very small in so far as the positive bands and lines were concerned, though the negative bands, which dominated the spectrum as soon as they appeared, could be photographed with comparatively short exposures. It might have been expected *a priori* that the first lines to appear would belong to the arc spectrum, but if these lines were developed at all they were of such small

intensity that they were in fact never observed under these conditions. With protracted exposures a few lines were photographed and these lines were found to belong to the spark spectrum. It was subsequently found that the same lines, with a few others, appeared with far greater brilliance in the spectrum of the glow in a hollow cathode using a wide discharge tube containing nitrogen at a pressure somewhere about a millimetre, the tube being excited by a large induction coil. The arrangement does not differ in principle from Paschen's box cathode ('Ann d Phys,' vol 50, p 901, 1916). In Table II are given the lines observed in a five-hour exposure under these conditions, the wavelengths being those given by Fowler (*loc cit*) and Porlezza ('Rend Accad Linc,' vols 5, 20, p 586 1911), whose values have been reduced to 1 A in the Table.

It will be seen that none of the arc lines are included in this list. Rayleigh ('Roy Soc Proc,' A, vol 101, p 114, 1922) has made an investigation of the nitrogen spectrum in relation to the auroral spectrum, and has also observed the line λ 3995 in the path of the cathode rays at low pressures.

Table II

λ (1 A)	
(Fowler)	(Porlezza)
	5678 94
	5675 31
	5666 03
	5004 71
	5000 92
4432 76 *	
4041 32	
3995 00	
3955 85	

Discussion

There seems to be little doubt that the spectrum recorded in Table I is to be regarded as the arc spectrum of nitrogen, and it appears that the presence of a very small proportion of this gas in helium at fairly high pressures constitutes a condition uniquely favourable to the isolation of the spectrum, which is not seen under similar conditions when argon is substituted for helium. It is probable that the analogous spectrum of carbon observed under similar conditions is due to the neutral carbon atom. It is of interest to consider how the helium acts in these cases, and in this connection it is important

to note that Johnson and Cameron (*loc cit*) were unable to observe the carbon "arc" spectrum when argon was substituted for helium, and also, as shown in the preceding section, that when nitrogen is excited by electron impacts there is apparently a direct transition from the negative band spectrum to the spark spectrum as the velocity of the electrons is increased, or at least if the NI or arc lines appear at all at an intermediate stage they are too weak to be observed under ordinary conditions. It may be inferred from this latter observation that when the nitrogen molecule is broken up, ions and not neutral atoms are the most probable product, and that the number of atoms present at any time is exceedingly small. The production of ions in the breaking up of the molecule would be consistent with the observations of Smyth (*loc cit*).

Now, with regard to the action of the helium it appears that two distinct effects may be involved. In the first place, the expectation of life of a neutral nitrogen atom will become greater as the partial pressure of that gas decreases, and in helium at a high pressure, containing a very small trace of nitrogen the conditions will be favourable both to the passage of a heavy discharge which could not be maintained at very low pressures, and also to the existence of a considerable proportion of the nitrogen in an atomic state. An effect of this kind is to be expected in the case of any of the inert gases, and the same may indeed be said with the diatomic gases as diluents, but this case need not be considered in view of the fact that at the dilutions under consideration the nitrogen lines would not be visible at all with any diluent other than the rare gases, and further complications due to the formation of compound molecules would arise. It is evident that the greater the dilution the more favourable will be the conditions for the production of line spectra, since the presence of an excess of molecules would result in a preponderating emission of band spectra, with lower radiation potentials. At relatively high pressures the mean free path would be so small that unless the proportion of molecules were very small, there would be little chance of an electron ever acquiring the energy required to excite the line spectra.

It is suggested that the helium acts also in a different manner. With condensed discharges through vacuum tubes the excitation must be regarded as very heterogeneous, and it may be supposed that forces varying over a wide range are available. It has been pointed out above that an excess of nitrogen molecules may prevent electrons from acquiring sufficient energy to excite the line spectra. The helium must act in precisely the same way, the first resonance potential of helium is at 20.4 volts (Foote and Mohler, *loc cit.*), and a

large excess of helium atoms in the discharge tube must act as "safety valves" which blow off when they are struck by 20.4-volt electrons, and which, therefore, set a superior limit to the energy which there is any significant probability that an electron will acquire. If we may assume that both in the case of nitrogen and carbon the energy required to excite the arc lines is less than 20.4 volts, and greater than this value for the excitation of the spark spectra, the above considerations show how the presence of an excess of helium may result in the complete isolation of the arc spectrum.

The resonance potential of argon is 11.5 volts (Foote and Mohler, *loc. cit.*), and it is evidently possible for spectrum lines having radiation potentials greater than this value, but less than 20.4 volts, to be suppressed by an excess of argon, though they may appear readily in the presence of helium, and it is suggested that the arc spectra of nitrogen and carbon belong to this category. On the above view it is a fortunate circumstance that helium should make it possible to isolate the arc spectra of nitrogen and carbon, but it is possible that interesting results will be obtained for other elements with other inert gases.

With uncondensed discharges the action of the helium would be similar, but it would seldom be called upon to fulfil its function as a safety-valve, electrons could undergo a large number of collisions with helium atoms without loss of energy and would acquire higher velocities than would be possible in pure nitrogen, in which collisions above a comparatively small velocity would not take place without loss of energy. With uncondensed discharges it would therefore appear that the excitation is more intense in the presence of helium for a given total pressure, and becomes greater the smaller the proportion of nitrogen or carbon in the mixture until the limit of 20.4 volts is reached. In pure gases the intensity of the excitation should increase as the pressure falls and as the potential drop between collisions increases, but at these low pressures the intrinsic brightness of the spectra is often too small for observation. The above considerations are consistent with the fact that the comet-tail spectrum can be observed either in carbon compounds at very low pressures, or else in helium at high pressures when a small trace of carbon is present, but there are complex changes in the intensity distribution which may require some further consideration.

Summary

It has been found that when helium at about 30 millimetres pressure containing a very small quantity of nitrogen is excited by feebly condensed discharges, the arc spectrum of nitrogen is developed, and under these conditions is completely isolated from the spark spectra.

The arc spectrum of nitrogen is not developed in the presence of an excess of argon under the same conditions that it appears in the presence of helium

Special precautions have to be taken to ensure the purity of the gases and the proportion of nitrogen present has to be carefully regulated

Measurements have been made of the wave-lengths of the lines of the nitrogen arc spectrum (NI)

When nitrogen is excited by electron impacts there appears to be a direct transition as the energy of the impacts is increased from the negative band spectrum to the spark spectrum, which would imply that the rupture of nitrogen molecules is generally into ions rather than neutral atoms

The action of the rare gases in modifying spectra is discussed, and the principal phenomena appear to be open to a simple explanation

We wish to express our thanks to the Department of Scientific and Industrial Research for a grant which has been made to one of us (J G P) during the course of this investigation

The Heat Developed during Plastic Extension of Metals

By W S FARREN M A and G I TAYLOR, F R S, Yarrow Research
Professor of the Royal Society

(Received November 19, 1924)

1 *Introduction*

When a soft metal, such as annealed copper or aluminum, is deformed while cold, either by stretching hammering, rolling, or other method of "cold working," it hardens, that is, the forces necessary to deform it increase as the amount of plastic deformation increases. The physical state of "cold worked" metal is undoubtedly different from that of the metal in its original soft or annealed state, and various explanations have been put forward to account for the difference. Some of these explanations involve the hypothesis that the process of hardening is associated with the formation of amorphous material at the crystal planes where slipping occurs during the deformation. The formation of amorphous material from a crystalline mass would involve a phase change, which would in general be accompanied by a change in the internal energy of the material. It has been suggested that the phase change could

be detected by measuring the heat evolved during a deformation, and comparing with the heat equivalent of the work done on the metal by the forces producing the deformation. Any difference between the two would imply a change in the internal energy of the metal.

It is curious that very few measurements of this type appear to have been made. The only reference which we have been able to find occurs in Dr Rosenham's article on "Metals," in the 'Dictionary of Physics,'* where he quotes some previously unpublished observations made by Dr Sinnat.

According to these observations, only one-tenth of the work done reappears in the form of heat, the remaining 90 per cent being presumably used up in changing the phase of the material. This result, if true, would be of very great interest, but so far no further details have been published. Dr Rosenham has informed us that he is carrying out further experiments on the subject.

On the other hand, as will be seen later, the experimental difficulties in making measurements of this kind are considerable, and if several independent workers performed such experiments along parallel lines their time would not be wasted, even if they got identical results.

2 Methods of Measurement

The simplest way to deform a metal is to take a straight bar or "test-piece" and stretch it by a longitudinal pull. The work done in any portion of the bar during an operation of this kind can be determined by measuring the pull P and the length l of the portion concerned at successive stages of the test. The work done, namely, $\int Pdl$, is represented by the area of the stress-strain curve. The stress-strain relation is usually determined in engineering laboratories by means of a testing machine in which the stress is measured by balancing the tension in the specimen against a weight on a lever, and the strain by direct measurement on the specimen.

This method was not suitable for the experiments described here, because it was necessary to do the whole of the stretching in a few seconds of time in order that the rise in temperature of the metal might be measured before any appreciable cooling had taken place. For this reason a self-recording testing machine was made which automatically produced a stress-strain curve as the specimen was being stretched. This machine is described later in some detail, because the value of our results depends entirely on the accuracy of the measurements, and it is necessary to show that the accuracy of our stress-strain curves is at least equal to that of our temperature measurements.

* Vol. 5, p. 398

To measure the heat evolved during the stretching, the use of a calorimeter naturally suggests itself, but the experimental difficulties in the way of getting accurate results in this manner appear insuperable, and even if they could be overcome the result obtained would give only the total heat evolved throughout the whole specimen, while what is wanted is the heat evolved in the middle of the bar, where the stretching is uniform.

The method adopted was to measure the rise in temperature which occurs during a rapid plastic extension of the bar. For this purpose a thermocouple was used and the temperature was recorded photographically on a moving plate.

Preliminary experiments showed that, when fixed in the testing machine and exposed to the air, the specimens first used cooled through about 4 per cent of their excess of temperature over that of the room in 1 second. It was clear, therefore, either that large cooling corrections would have to be introduced or that the temperature measurements would have to be made rapidly. The second alternative is preferable, if possible, and the first part of the work was devoted to a study of the heat losses immediately after the extension of the specimen, and to a search for the method of measuring temperature which suffered least from lag.

The cooling of the specimen was due almost entirely to conduction of heat through the ends, only a very small fraction of the heat being radiated or carried away by convection. This might have been guessed beforehand, but it was proved by observing the rate of cooling of the specimen when hung up horizontally by a silk thread, and comparing it with the rate of cooling of the specimen when fixed on the testing machine. In the former case the excess of temperature of the specimen over that of the atmosphere was reduced in the ratio 1 to e^* in 18 minutes, while in the latter the time taken was 28 seconds. It appears, therefore, that only $\frac{28}{18 \times 60}$, i.e., $\frac{1}{40}$ of the heat loss, was due to convection and radiation, and that the remaining $\frac{39}{40}$ must have been due to conduction of heat from the central uniform part of the specimen to the ends and grips of the testing machine.

The coldness of the ends takes some time to reach the middle, and it was during the interval between the time of generation of the heat and the time of arrival of the cold waves from each end of the bar that the temperature measurements were made.

* e the base of Napierian logarithms.

To find how long this interval might be expected to be it is sufficient to idealise the condition slightly. Consider a uniform bar of length l , coefficient of conductivity k , specific heat σ , density ρ , and suppose that at time $t = 0$ the temperature of the whole bar is suddenly raised by an amount T_0 , the ends being maintained subsequently at their original temperature, which may be taken as $T = 0$. The subsequent temperature at distance x from either end is represented by the series

$$T = \frac{4}{\pi} T_0 \left\{ e^{-at} \sin \frac{\pi x}{l} + \frac{1}{3} e^{-9at} \sin \frac{3\pi x}{l} + \frac{1}{5} e^{-25at} \sin \frac{5\pi x}{l} + \dots \right\} \quad (1)$$

where
$$a = \frac{\pi^2 k}{l^2 \rho \sigma}$$

When $t = 0$ $T = T_0$ for all values of x

When t is large the series reduces to the first term

$$T = \frac{4T_0}{\pi} e^{-at} \sin \frac{\pi x}{l} \quad (2)$$

When t is small this series is inconvenient for numerical calculation and the expression

$$T = T_0 \left\{ 2 - \frac{2}{\sqrt{\pi}} \int_0^{\zeta_1} e^{-\mu^2} d\mu - \frac{2}{\sqrt{\pi}} \int_0^{\zeta_2} e^{-\mu^2} d\mu \right\} \quad (3)$$

may be used where

$$\zeta_1 = \frac{x}{2} \sqrt{\frac{\rho \sigma}{\kappa t}} \quad \text{and} \quad \zeta_2 = \frac{l-x}{2} \sqrt{\frac{\rho \sigma}{\kappa t}}$$

The expression (3) is approximately the same as (1) for small values of t . The maximum errors occur first at the ends, $x = 0$ and $x = l$. When $t = 0.077 \rho \sigma l^2 / k$ the error is 1 per cent at the ends but is still quite inappreciable in the middle, where (3) gives $T = 0.594 T_0$ while (2) gives $T = 0.595 T_0$. It appears that the error in using (3) from $t = 0$ to $t = 0.077 \rho \sigma l^2 / k$ and (2) from this value to $t = \infty$ is never more than a fraction of 1 per cent.

The theoretical cooling curve for points in the middle of a bar, cooled by conduction of heat to both ends, is shown in fig. 1. It will be seen that from

$$t = 0 \quad \text{to} \quad t = 0.014 \rho \sigma l^2 / k \quad (4)$$

the temperature is practically constant. At $t = 0.014 \rho \sigma l^2 / k$ it has fallen only 1/166th of its initial value. After this the temperature begins to fall rapidly, and at $t = 0.04 \rho \sigma l^2 / k$ the curve becomes practically indistinguishable from the ordinary exponential curve (shown as a dotted line in fig. 1), which would result from Newton's law of cooling.

In the second part of the curve, when the temperature of the middle of the bar is falling exponentially, the time t_e taken to fall to $1/e$ of its value is $\rho \sigma l^2 / \pi k^2$

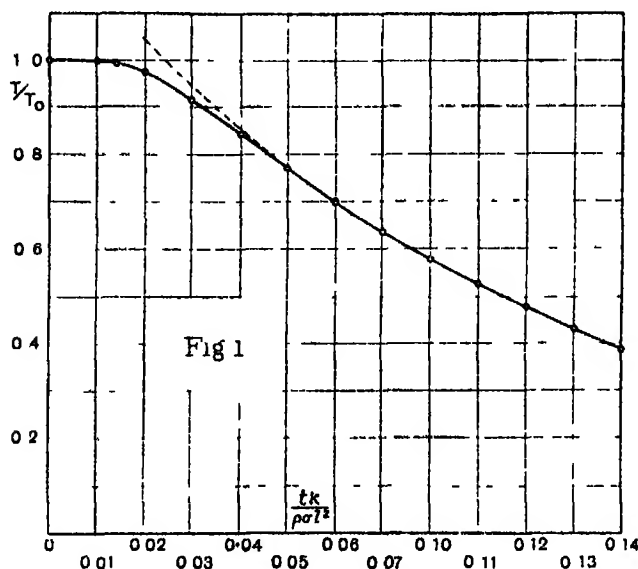


FIG 1—Theoretical cooling curve for the middle point of a bar initially at a uniform temperature and subsequently cooled by maintaining the ends at a steady temperature

or $1/a$. It appears, therefore, that if this time t_e is observed experimentally, the temperature will not fall through more than $1/166$ th of its initial value during the time $0.014 \pi^2 t_e$ after the instant when the heat is generated. If the temperature measurements can be made within this interval of time the error due to neglecting cooling corrections will not amount to 0.6 per cent.

In the first experiment with aluminium bars having a parallel portion in the middle 11 cm long before the stretching began, the time t_e was observed to be 28 seconds, so that the time available was $0.014 \times 28 = 4$ seconds, whereas using the expression (4) and inserting the known physical constants for aluminium, namely, $\rho = 2.7$, $\sigma = 0.212$, $k = 0.5$, and putting $l = 11$, the time comes out to be 1.9 seconds. The difference is due no doubt to the fact that the ends of the parallel middle portion are not in practice maintained at the temperature of the atmosphere, and it seems clear that the time during which the temperature of the middle of the bar might be expected to remain practically constant is considerably underestimated by the expression (4). This is confirmed by measurements of temperature records taken in the course of the experiments.

In some of the experiments here described it was possible to use specimens containing as much as 30 cm of parallel part in the middle, and with these there was ample time for measuring the temperature. It was not possible, however, to obtain single crystal bars of aluminium with a parallel middle portion greater than 16 cm. For this reason it was necessary to have a temperature recording system which could be relied on to give a correct reading within two or three seconds of the time of application of the strain.

For this purpose an iron-constantan thermojunction was used. This was connected directly to a galvanometer, the moving part of which reflected light from a vertical slit on to a fine horizontal slit placed close in front of a photographic plate which was made to move vertically at a constant speed by means of an electric motor fitted with a speed governor.

The galvanometer used was of the moving magnet type, but the suspended system was specially designed and made for us by Dr P. Kapitza, with a view to reducing the period to the minimum value consistent with the required sensitivity. It consisted of an astatic pair of cobalt-steel magnets, each $2\frac{1}{2}$ mm long \times 0.02 mm thick. These were fixed to a fine straight glass thread which was hung vertically by a quartz fibre. The reflecting mirror was made of thin cover slip glass, 2 mm square. A magnet was used to control the sensitivity of the system, and in the present experiments the period of oscillation was 2.3 seconds, and the damping per half-period was 0.44. The records obtained with this apparatus could be reduced to eliminate the effects of periodicity and damping in the galvanometer, in most cases, however, this was found to be unnecessary, the temperature of the middle of the bar remaining constant for a time which was long enough to allow the oscillation to die away.

3 Method of Using a Thermojunction

The usual method of using a thermojunction for measuring the temperature of solid bodies is either to insert it in a small hole in the body, or, if possible, to solder it to the surface. Neither of these methods was available in the present instance. To bore a small transverse hole in the specimen would alter the type of distortion which the metal would experience in the immediate neighbourhood of the hole. This would give rise to an error whose magnitude it would be impossible to estimate. Solder could not be used because many of the experiments were made with aluminium. It was, therefore, necessary to devise some method of attaching or pressing the thermojunction to the surface of the metal.

When a thermojunction touches a specimen on one side only, unless it can be soldered on, some other material, preferably a non-conductor, must be in contact with its other side in order to press it against the specimen. The temperature of the thermojunction will, therefore, be intermediate between that of the specimen and that of the non-conductor, and if the resistance to the passage of heat at the contact is small, presumably the temperature recorded will be close to that of the specimen, but there will be an error whose magnitude must be determined. In the experiments here described this source of error was reduced to a minimum by pressing the thermojunction against the inside of a $\frac{1}{16}$ -inch hole bored symmetrically from end to end of the specimen. The total amount of non-conducting material used for pressing the thermojunction against the inside of the hole was very small, and in any case it was certain that everything inside the hole would warm up to the temperature of the metal, whereas it was by no means certain that a thermojunction pressed on the outside of the specimen would do so.

The chief difficulty in the way of getting an accurate record of the temperature of the metal immediately after stretching was due to the lag in temperature between the thermojunction and the specimen. To test the efficiency of different ways of fitting the thermojunction a very thin-walled metal tube with a bore of $\frac{1}{16}$ -inch was made. The thermojunction was fitted into this, and a sudden change in temperature was produced by removing the tube from a jar of water and suddenly plunging it in a jar of water whose temperature was about 2° higher, and stirring vigorously. The temperature record produced in this way had to be analysed to allow for the lag in the galvanometer system. The method adopted for this purpose will next be described.

If there were no lag in the heating of the thermojunction, the record would show a damped harmonic oscillation, the characteristics of which would be determined solely by the galvanometer. In the present case the galvanometer had a period of 2.3 seconds and a damping of 0.44 per $\frac{1}{2}$ period. It is clear, therefore, that if the temperature of the thermojunction were suddenly raised from $T = 0$ to $T = T_0$, and then kept at temperature T_0 , the record would overshoot the true temperature by an amount $0.44 T_0$, so that the maximum temperature shown on the record would be $1.44 T_0$. The next minimum would be $\{1 - (0.44)^2\} T_0 = 0.81 T_0$, and so on.

If the lag in the temperature of the thermojunction were large, the recorded temperature would be close to the true temperature and there would be no maximum on the record till the true steady temperature had been attained.

For intermediate cases, where the lag in the temperature and the period of the galvanometer were of the same order of magnitude, there might be a first maximum on the record, which would necessarily be less than $1.44 T_0$, but might be greater than T_0 by an amount which would depend on the temperature lag in the thermojunction.

If T_m represents the first maximum temperature shown on the record, it is possible by measuring T_m/T_0 to measure the amount of the temperature lag in the thermojunction.

If y represents the reading of the galvanometer record when multiplied by the calibration factor, so as to reduce it to a measure of temperature, the equation which represents the galvanometer record, in the case when there is no lag in the temperature of the thermojunction, is

$$\frac{d^2y}{dt^2} + \kappa \frac{dy}{dt} + \mu y = 0, \quad (5)$$

and the solution of this is

$$y = T_0 (1 - e^{-\frac{1}{2}\kappa t} \cos nt) \quad (6)$$

where $n^2 = \mu - \frac{1}{4}\kappa^2$

$2\pi/n$ is the period of the galvanometer, while $e^{-\frac{1}{2}\kappa t}$ is the damping factor.

When there is a lag, (5) becomes

$$\frac{d^2y}{dt^2} + \kappa \frac{dy}{dt} + \mu (y - T) = 0, \quad (7)$$

where T is the temperature of the thermojunction.

If $1/\lambda$ represents the lag in the temperature of the thermojunction when the temperature outside the case containing it is suddenly changed, the equation for T may be assumed to be

$$T = T_0 (1 - e^{-\lambda t}) \quad (8)$$

This equation in fact defines the "lag."

Substituting for T in (7), solving, and inserting the condition, that when $t = 0$, $y = 0$ and $dy/dt = 0$, an equation is formed for y . Using the values for n and $\frac{1}{2}\kappa$ obtained from the experiments on the period and damping of the galvanometer, the solution of (7) which fits the conditions, is found to be

$$\frac{y}{T_0} = 1 + \frac{-8.17e^{-\lambda t} + (1.42\lambda - \lambda^2)e^{-0.71t} \cos 2.77t - (0.256\lambda^2 + 2.59\lambda)e^{-0.71t} \sin 2.77t}{\lambda^2 - 1.42\lambda + 8.17}.$$

Taking a series of different values of λ , it is found that if λ is less than 0.5 there is no maximum value for y , but that when λ is greater than 0.71, y has a maximum T_m , the values of which are given in Table I.

Table I

λ	∞	2	1	0.71
T_m/T_0	1.44	1.157	0.932	0.759

The value T_m/T_0 was measured for a number of different types of thermojunction and the results given in Table I were used to estimate the lag. It was found that the lag varied very greatly, according to the method used for pressing the thermojunction against the heated surface. In the first place the lag was always far too great unless there was actual metallic contact between the junction and the heated metal. For this reason it would be impossible to obtain accurate results if a multiple junction were used, because of the necessity in that case for having insulating material between the metal and the junction.

Various methods were tried for pressing the thermojunction directly against the inside of the hole through the specimen, but they were all failures. In every case a lag of several seconds occurred, though the lag was not so great as when there was no metallic contact.

The method which proved most successful consisted in soldering the junction to a plate of silver foil 0.1 mm thick, 7 mm long and 9 mm wide. This plate was bent round a small cylindrical piece of cork which could be forced into the hole. In this way the silver was pressed hard up against the inside of the specimen.

This method had the advantage that when the hole contracted as the specimen lengthened the only effect was to make the cork press the silver plate still harder against the metal, and even when the hole became elliptical, as it did when single crystal specimens were used, the silver foil was still pressed against the metal all over its surface.

Using this method the lag was reduced to 0.4 second (i.e., $1/\lambda = 0.4$). It will be noticed that this includes any lag which may have existed between the temperature of the copper tube and that of the water into which it was plunged, so that the lag due to the passage of heat to the thermojunction must have been less than this. In order to ensure that the temperature of the thermojunction was within 1 per cent of that of the specimen with which it was in contact it was therefore necessary to read the record at a time greater than — 0.4 log₁₀ 0.01, or 1.8 seconds, after the stretching was finished.

5 *Method of Carrying Out an Experiment*

The thermojunction was first fitted inside the middle of the specimen. The iron and constantan wires passed out through one end to the cold junction.

which was contained in an oil-filled tube dipping into a thermos flask full of water. The other end of the axial hole through the specimen was made watertight with wax, and the thermojunction was calibrated by moving the specimen from one large jar of water at the temperature of the room to another containing water about 2°C higher. The temperature of the water was found by means of Beckmann thermometers graduated in hundredths of a degree Centigrade. The water in both jars was stirred vigorously by means of small fans, run by an electric motor, but even then the specimen took some 18 seconds to attain the temperature of the surrounding water.

An actual stretching experiment lasted a few seconds only, so the speed of the falling plate on which the records were taken was reduced when the calibrations were being done (see fig 2). In order to provide a base line from which measurements of the plate could be made, an image of the same vertical slit which was used to illuminate the galvanometer mirror was cast by a fixed mirror on the horizontal slit of the recording apparatus, and the light was cut off by a shutter from both images, at regular intervals of 6 seconds, so that small simultaneous gaps appear in the temperature record and the base line.

In most of the experiments two records were taken on each plate. In fig 2 the outer and thicker line, marked A, is the calibration record.

The next step was to put the specimen in the machine and stretch it by winding the handle as rapidly as possible, till the temperature of the specimen had risen through about 2°C . The machine was then left for about 10 minutes, with the specimen still under tension, in order that it might have time to cool. It was then again stretched, till its temperature rose again by about 2°C . With the steel, copper, and aluminium specimens three such extensions were made. With the single crystals of aluminium there were five.

The load was then released suddenly and a record taken of the reversible adiabatic rise in temperature which accompanies the sudden elastic contraction. This usually amounted to about 0.3°C ., or about 3 per cent. of the total rise which would have occurred if the whole extension had been done at once.

The main object of the experiments was to determine how much of the energy put into the metal by external forces was used in increasing the internal energy of the material. For this reason it was thought that the ideal way to carry out an experiment would be to stretch the material and then immediately to release the stress, so that the material would be unstressed as a whole both before and after the experiment. This was inconvenient

and it was decided to divide up the adiabatic heating which occurred when the stress was finally released, and to distribute it among the successive stages

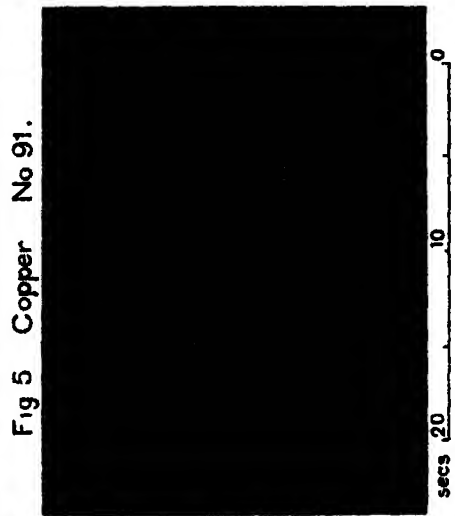
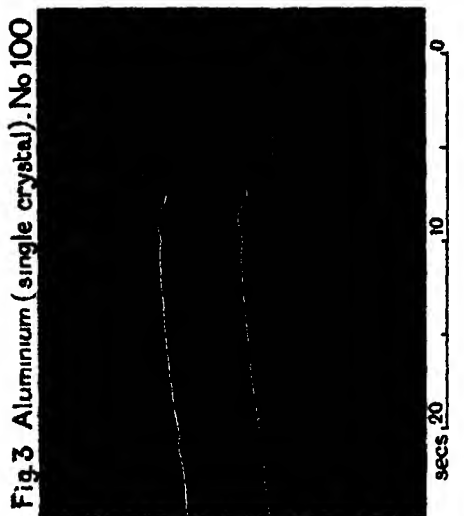
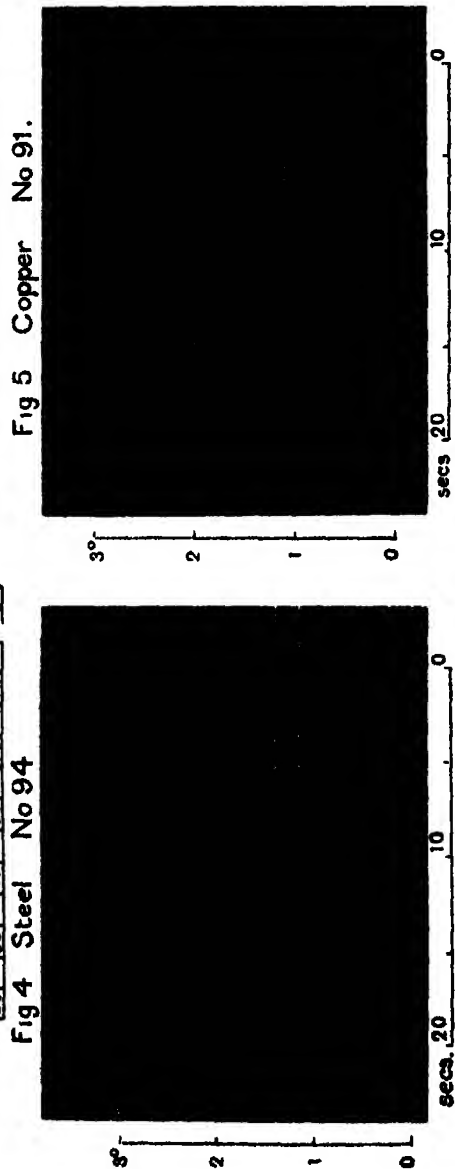
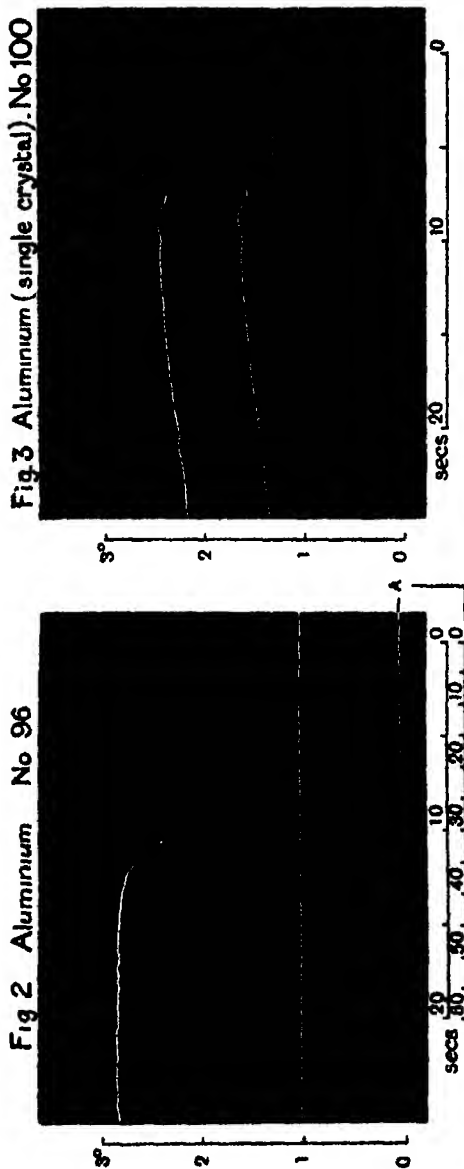


Fig 2 —Temperature record—calibration and plain aluminium Fig 3 —Temperature record—single crystal of aluminium Fig 4 —Temperature record—steel Fig 5 —Temperature record—copper

of the stretching in proportion to the change in stress which occurred in each stage. Thus if the stresses at the ends of the first three stages were p_1 , p_2 and p_3 , and if the change in temperature due to adiabatic heating on releasing

the stress p_2 was T_e , an amount $p_1 T_e / p_2$ was added to the observed rise of temperature during the first stretching, $(p_2 - p_1) T_e / p_2$ for the second stretching, and $(p_3 - p_2) T_e / p_3$ for the third. Except for the first extension in each experiment these corrections are small, but they are founded on experimental evidence that the elastic strain, and hence the adiabatic heating, is proportional to the change of stress and does not depend on the hardness of the material.

6. *Temperature Records*

Some of the temperature records are shown in figs 2-5. In each the stretching of the specimen was complete before the spot of light had travelled its maximum distance, but since the stretching was not instantaneous (it occupied about 2 seconds) the amount by which the galvanometer mirror overshot the mark was small. It is a comparatively simple matter to analyse the record so as to make allowance for the galvanometer lag and inertia, but an inspection of the records shows that the oscillation has practically died away before the specimen begins to cool, so that in most cases no correction is required. In each of the records the temperature curve has the flat top which was predicted on p. 426 (fig. 1), but it is most obvious in fig. 3 which is the record of the stretching of a single-crystal specimen of aluminium. It will be seen that the temperature did not begin to decrease till at least 5 seconds after the stretching was complete, and by that time the galvanometer oscillation had practically disappeared. In figs. 4 and 5, which are the records for annealed steel and copper, respectively, the specimens were 30 cm. long, and the rate of cooling was much slower than for the aluminium specimen, which had only 16 cm. of parallel part in the middle. The flat top in these records extends over about 8 seconds.

7. *Discussion of Results*

In order to compare the observed rise in temperature with the heat evolved the heat equivalent of the work done in each experiment has been calculated. If l_0 is the original length of the specimen between its marks, and ϵ its extension at any stage, its length is then $l_0 (1 + \epsilon)$. If P is the pull in the testing machine and a_0 the original cross-section of the specimen, the work done on unit volume of the material during a stretching between extensions ϵ_1 and ϵ_2 is $\frac{1}{l_0 a_0} \int_{\epsilon_1}^{\epsilon_2} P l_0 d\epsilon$. This integral is evaluated from the stress-strain records (see p. 448).

The cross-section of the specimen was measured in square inches and the

work done in foot-pounds Using for Joule's equivalent J the value 4.18×10^7 ergs per calorie, the factor for converting the above integral to the equivalent rise in temperature is $\frac{1.65 \times 10^{-3}}{\rho\sigma}$

The densities of the materials used were determined by weighing in water The specific heats were not measured, but their values were taken from the latest edition of Landolt and Bornstein's tables The values adopted for ρ and σ are shown in Table II below

Table II

Material	ρ	σ
Aluminum	2.70	0.212
Steel	7.80	0.106
Copper	8.93	0.092

The results of measurements on eleven specimens, namely three each of annealed copper, steel and plain aluminum, and two single crystal specimens of aluminum are given in Table III

In this table the number of the specimen is given at the top so that the figures may be compared with the reproductions of some of the temperature records (figs 2-5, p 432) and stress-strain records (fig 17, p. 448) In the first column is given the extension ϵ of the material (per cent of its unstrained length) at the end of each experiment The second gives the observed rise in temperature T_0 The third gives the correction T_a for adiabatic heating which must be added in order to give the rise in temperature which would be observed if the material were unstressed at the beginning and end of each experiment. The fourth column gives the corrected temperature $T_1 = T_0 + T_a$ The fifth column gives the temperature rise T_2 corresponding to the heat equivalent of the work done The sixth column gives the final result, namely the ratio T_1/T_2 , i.e., the proportion of the work done which is converted into heat The bottom line of each Table gives the total results for each specimen

It will be seen that in every case the observed evolution of heat falls short of the heat equivalent of the work done. The difference which represents increase in the internal energy of the material amounts to $13\frac{1}{2}$ per cent. of the work done in the case of steel, 8 to $9\frac{1}{2}$ per cent. in the case of copper, 7 to 8 per cent in the case of aluminum, and $4\frac{1}{2}$ to 5 per cent in the case of the single-crystal specimens of aluminum

Table III.

No 81.										No 84					No 95				
°	T_r	T_c	T_1	T_2	T_1/T_2	°	T_r	T_2	T_1	T_r	T_1/T_r	°	T_r	T_1	T_2	T_1	T_r	T_1/T_r	T_2/T_r
STEEL	5.92	3.41	0.28	3.69	4.20	0.88	3.99	2.14	0.25	2.39	2.79	6.11	0.66	3.71	0.06	3.71	4.29	0.865	
	9.70	2.77	0.06	2.83	3.38	0.84	8.13	3.12	0.06	3.18	3.72	10.50*	2.54	2.57	0.03	2.57	3.00	0.866	
	13.10	2.62	0.03	2.86	3.28	0.87	11.83	3.23	0.04	3.27	3.72	0.88	2.66	2.68	0.02	2.68	3.03	0.88	
Total	13.10	9.00	0.37	9.37	10.84	0.865	11.83	8.49	0.35	8.84	10.23	0.865	8.85	8.96	0.11	8.96	10.32	0.865	
No 91.										No 92					No 93. *				
°	T_r	T_c	T_1	T_2	T_1/T_2	°	T_r	T_2	T_1	T_r	T_1/T_r	°	T_r	T_1	T_2	T_1	T_r	T_1/T_r	T_2/T_r
Copper	7.66	1.91	0.22	2.13	2.31	0.92	7.78	1.79	0.22	2.01	2.25	0.895	8.76	2.41	0.23	2.41	2.72	0.885	
	12.67	2.06	0.05	2.11	2.29	0.92	13.63	2.36	0.07	2.45	2.69	0.91	15.35	2.94	0.06	2.94	3.23	0.91	
	17.45	2.32	0.04	2.36	2.57	0.92	19.90	3.08	0.04	3.13	3.44	0.91	20.20	2.53	0.03	2.53	2.76	0.915	
Total	17.45	6.29	0.31	6.60	7.17	0.92	19.90	7.26	0.33	7.59	8.38	0.905	20.20	7.88	0.32	7.88	8.71	0.905	
No 98.										No 97					No 98				
°	T_r	T_c	T_1	T_2	T_1/T_2	°	T_r	T_2	T_1	T_r	T_1/T_r	°	T_r	T_1	T_2	T_1	T_r	T_1/T_r	T_2/T_r
ALUMINUM (plain)	11.12	2.16	0.25	2.41	2.59	0.93	10.41	1.99	0.21	2.20	2.42	0.91	9.16	1.88	0.24	1.88	2.03	0.925	
	16.88	1.67	0.02	1.69	1.82	0.93	16.70	1.80	0.01	1.81	1.96	0.925	15.91	1.97	0.03	1.97	2.09	0.945	
	23.06	1.85	0.01	1.86	2.01	0.93	21.95	1.58	0.01	1.59	1.71	0.93	21.88	1.83	0.01	1.83	1.95	0.94	
Total	23.06	5.68	0.28	5.96	6.42	0.93	21.95	5.37	0.23	5.60	6.09	0.92	21.88	5.68	0.28	5.68	6.07	0.935	
No 99.										No 100					No 100				
°	T_r	T_c	T_1	T_2	T_1/T_2	°	T_r	T_2	T_1	T_r	T_1/T_r	°	T_r	T_1	T_2	T_1	T_r	T_1/T_r	T_2/T_r
ALUMINUM (single crystal)	14.58	1.58	0.13	1.71	1.80	0.95	16.19	2.12	0.16	2.24	2.37	0.96	16.19	2.24	0.16	2.24	2.37	0.96	
	24.10	1.59	0.02	1.61	1.67	0.965	25.75	1.66	0.01	1.67	1.77	0.945	25.75	1.67	0.01	1.67	1.77	0.945	
	35.25	2.07	0.02	2.09	2.20	0.95	37.70	2.24	0.01	2.25	2.38	0.945	37.70	2.25	0.01	2.25	2.38	0.945	
Total	52.72	1.96	0.01	1.97	2.09	0.94	55.72	1.82	0.00	1.82	1.93	0.945	55.72	1.82	0.00	1.82	1.93	0.945	
	52.72	8.77	0.19	8.96	9.44	0.95	55.72	9.57	0.18	9.75	10.27	0.945	55.72	9.75	0.18	9.75	10.27	0.945	

° = per cent extension at end of each experiment
 T_r = observed temperature rise
 T_c = "adiabatic" correction.
 $T_1 = T_r + T_c$
 T_2 = temperature rise equivalent to observed work in extension.

* Owing to an accident, no temperature record was obtained for the first extension, 6.11 per cent, of this specimen.

One remarkable feature of the table is the constancy of the ratio of the increase in internal energy to the work done on the specimens during different stages of the test. It is the same during the first extension when the metal is very soft and hardening rapidly as it is in the last extension when it is quite hard and only hardening slowly. It seems therefore that the increase in internal energy does not bear any very direct relationship to the hardening.

8 Description of Machine for Extending Specimen, and Recording Extensometer.

The mechanism by which the specimens were stretched was designed specially for these experiments, particularly for use with single crystals of aluminium. These have, at the breaking load of about 1 ton on an initial cross-section of $\frac{1}{2}$ square inch, an elongation of the order of 70 per cent on a length of 6 inches. Standard tensile testing machines will not deal satisfactorily with large and relatively weak specimens. The wedge grips deform the ends unduly, and require a large initial load. The force is generally applied by a weight, through a lever, and is difficult to control with such large extensions at almost constant loads. The vertical position of the specimen is inconvenient. Finally a rapid time rate of loading is almost out of the question.

In the machine described in detail below the specimen is horizontal. Its ends are screwed into steel end-pieces with spherical seatings, which fit into corresponding recesses in two moving carriages. Of these, one rests against a pair of steel springs, whose compression measures the applied load. These springs are very short and stiff, so that the energy stored is small and there is no tendency towards instability with plastic specimens. The second carriage is moved by a square thread screw, the nut being rotated by hand through a reduction gear. Loads of 2,500 lbs can be conveniently applied in about 2 seconds. The recording mechanism consists of a drum on which a celluloid film is stretched, the trace being made on it by a fine steel point. This method (due originally to Mr Collins of the Cambridge Instrument Company) has proved very satisfactory. The record is immediately available, requires no treatment, is permanent, and can be measured with great accuracy. The drum has both axial and rotational motion, the former being proportional to the compression of the springs referred to above, and the latter to the absolute movement of a point on the specimen. The scribing point has a rotational motion only, proportional to the absolute motion of another point on the specimen, situated similarly to, and some 10 cm. from, the first point.

Providing certain geometrical conditions are fulfilled the co-ordinates of the

resulting diagram are proportional to the compression of the spring and elongation of the specimen. Actually the abscissae are $1/3.59 \times$ the elongation of the specimen between the selected points, the length of the diagram in this direction varying from 6 to 15 mm. (see fig 17). The ordinates (2,000 lbs is represented by about 9 mm) are approximately twice the compression of the springs, but as the springs do not obey Hooke's Law exactly, areas are not exactly proportional to work done. The consequent distortion of the diagram from a true stress-strain figure is unimportant so far as concerns deductions from the shape of the curves, as the departure from Hooke's Law is mainly at low loads. For estimation of work done the diagrams are measured on a double stage microscope and areas of the true stress-strain curves calculated.

The calibration of the mechanism was done directly. By a system of levers described below loads were applied to the spring in the same way and through the same members as when the specimen is in place. The extension co-ordinate was calibrated by substituting for the specimen an arrangement of telescopic brass tubes incorporating a vernier reading to $1/1000$ inch.

The whole of the testing machine and recorder is self-contained and occupies a space approximately 4 feet by 1 foot 8 inches. The weight is sufficient to enable the maximum load to be applied in a few seconds without the necessity for fixing to the ground. On the other hand, the whole apparatus can be lifted by four men with ease.

9 *Tensile Testing Machine* (Fig 6)

The main frame A is rectangular, approximately 4 feet \times 1 foot 8 inches, and is made of 4-inch \times 3-inch \times $\frac{1}{2}$ -inch channel steel, bolted together with angle pieces. The longer sides A_2 are extended, carrying the recording instrument at one end and the gearing for extending the specimen at the other. To the shorter sides A_1 , A_4 , are bolted, parallel to the longitudinal axis of the machine, two bars of $1\frac{1}{4}$ -inch round steel A_3 , which act as guides for the cross head D. This cross head is moved by means of the screw B (1 inch diameter \times $\frac{1}{4}$ inch pitch). The phosphor-bronze nut through which this screw passes is mounted in bearings attached to the cross member A_1 , and is rotated by the 3 to 1 chain gearing C. The end thrust is taken by a ball bearing.

On the cross member A_4 rest two large helical springs F, held in position by short circular pieces of steel fitting freely inside them. Across their outer ends is a piece of channel steel G provided with two similar discs. To this cross bar, and to the cross head D, are attached two pieces of channel steel E_1 , E_2 , forming carriages for the ends of the specimen. E_1 is sufficiently

supported by its attachment to D To E_2 are fixed two wheels e which roll on the guide bars A_3

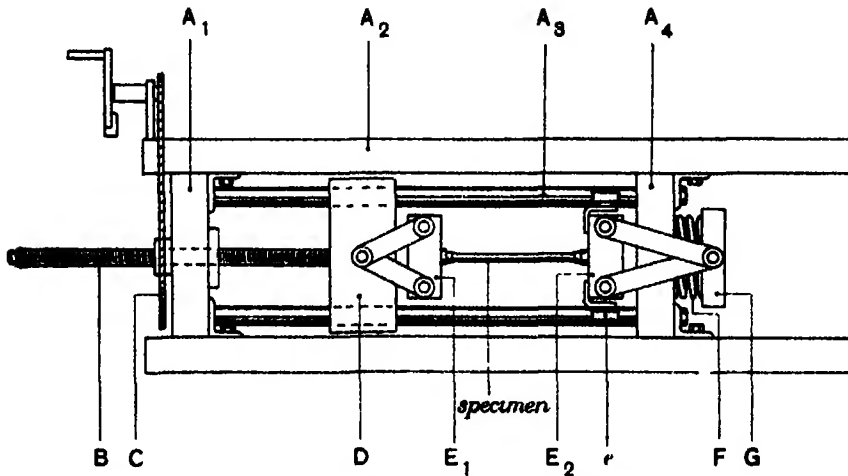


FIG 6 —Arrangement of testing machine

The ends of the specimen are screwed into end-pieces H (fig 7), which form, together with the parts E_1 , E_2 , a species of bayonet-joint. In the face of E_1 is a rectangular hole through which the end-piece H passes freely. On then

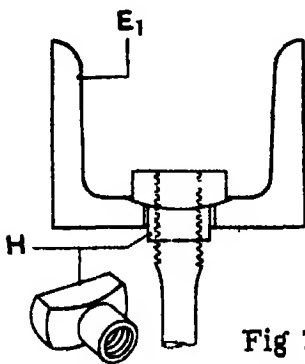


Fig 7

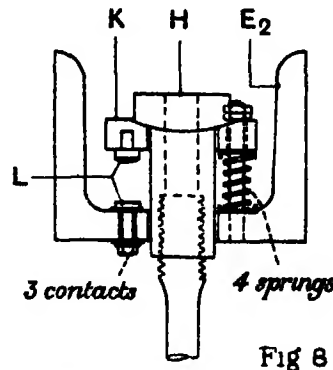


Fig 8

FIG 7 —Grip for end of specimen

FIG 8 —Grip for end of specimen with spring link

rotating the latter through approximately 90° the spherical seating on it bears on a corresponding recess in the back of E_1 . The arrangement at the other end E_2 is similar, with an additional complication described below.

The spiral springs F have each three coils of $\frac{1}{4}$ -inch diameter wire, wound on

a 2-inch mandrel, with a pitch of 0.4 inch. The pitch of the end coils decreases to zero and the ends of the spring are ground flat. This forms a suitable bearing surface and gives the spring, regarded as a strut, some stability. But it causes the law of the spring to be non-linear on account of the closing of the end coil in the early stages of compression. Since there is no actual fixture of the ends either of the specimen or of the springs, a small initial tension was necessary both in the actual experiment and in calibration. To ensure that the same amount was used always, a spring link was introduced which closed hard up at a known load, its closing being indicated electrically. In addition, in order to avoid any uncertainty which might have arisen owing to the springs seating themselves differently at different times, stops were inserted between E_2 and A_4 which prevented the springs from ever becoming slack. The initial tension (72 lbs., of the order of one-fifth of the force required to produce permanent set in the weakest specimens) was sufficient to pull E_2 away from these stops.

The spring link is shown in fig. 8. The spherical seating K, at the end nearer the springs F, is separate from the carriage E_2 , being supported on four light springs, suitably guided. Three pairs of stops L make contact when the load of 72 lbs. is applied to H, causing three lamps to light. Provided the load is applied axially, so that the lamps light nearly simultaneously, this device is very sensitive, a decrease of 2 lbs. being enough to extinguish the lamps. It was calibrated directly, the carriage E_2 being removed and suspended.

10 *Mechanism for Calibrating Springs* (See fig. 9)

The springs were calibrated in place in the machine by the application of weights through the system of levers shown diagrammatically in fig. 9. A vertical lever N, suspended by an adjustable wire, is pivoted at its lower end on a hook-piece O, which engages with the lower flange of the carriage E_1 . To this lever are attached the links M and P. The former screws into the standard end-piece H and engages, *via* the spring link (fig. 8), with the carriage E_2 , and so to the springs F. To P is attached a bell-crank lever Q, pivoted at R and carrying weights at S. All pivots (indicated by \otimes) are hardened knife-edges.

The arms of the levers are so proportioned that the force at M is approximately 10 times that at P, which is approximately double the weight S. The overall ratio is thus 20 to 1, enabling forces of 2,500 lbs. to be applied to the springs by a weight of 125 lbs. at S.

The geometry of the mechanism was restored to standard by the following

adjustments Weights being hung at S, the cross-head D was moved, carrying with it the hook O, until the lever N was parallel to a plumb line The turn-

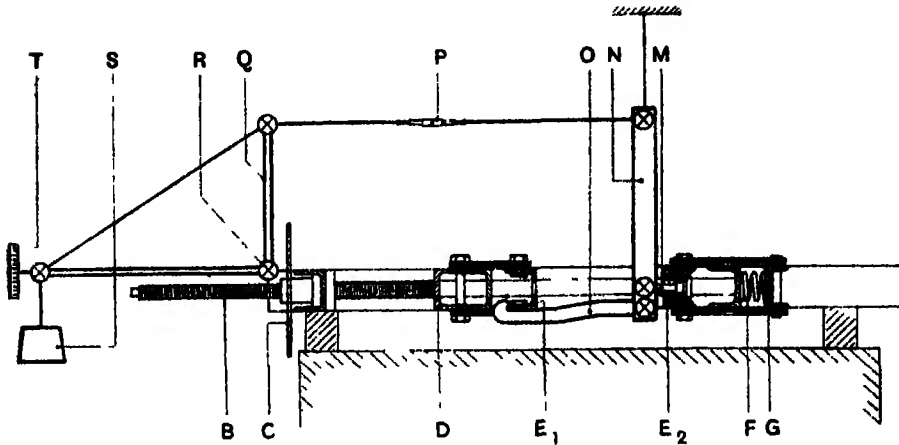


FIG. 9.—Arrangement of mechanism for calibrating springs

buckle in P was then adjusted till the bell-crank lever was in the standard position, as indicated by the index and scale T.

The accuracy of the calibration is dealt with below (§14)

11 Extensometer (See figs 10 12)

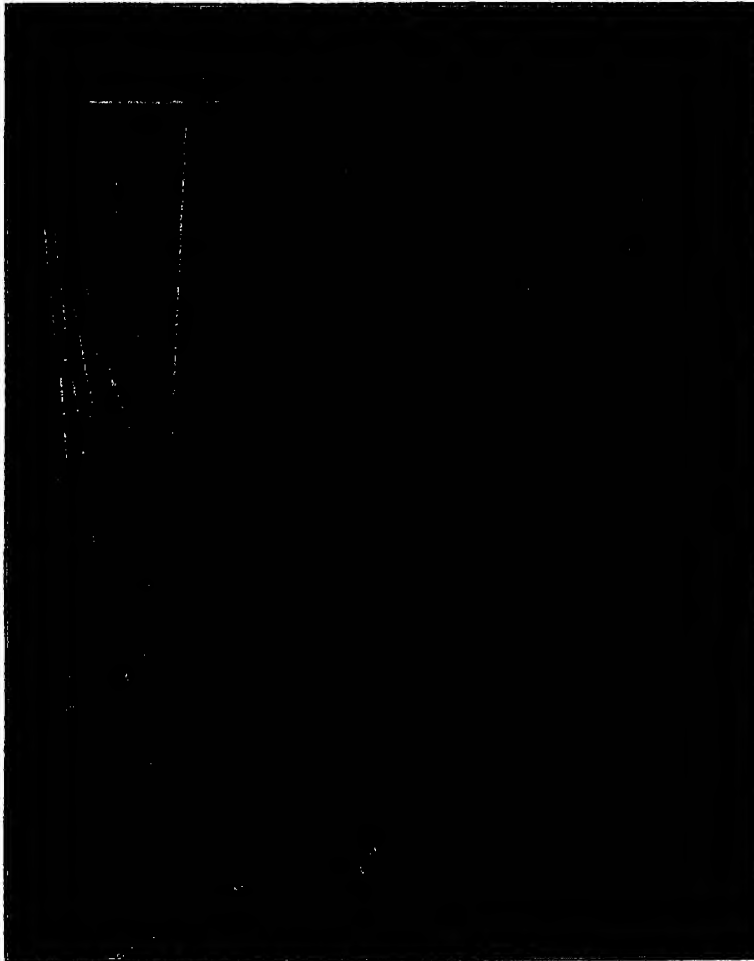
The essential problem of ordinary extensometers is the multiplying mechanism by which the minute extensions occurring within the elastic range are made visible In this instrument, with extensions of the order of 50 per cent on 10 cm., it was found desirable to use a reducing gear (actually 3.59 to 1, in all) in order to produce a convenient diagram On account of the inconvenience of very long levers, a mechanism was developed which kept the ratio of reduction constant to a high degree of accuracy with levers of reasonable length. This is shown in fig 10 Two levers, A_1 , A_2 , of special construction to avoid errors due to deflection, engage at their lower ends with the selected points on the specimen (the method of attachment is described below) Their upper ends pivot in cross-heads sliding in guides B_1 , B_2 From a point on each of these levers a connection is taken to the recorder Provided the following conditions are fulfilled, the ratio is invariable —

- (1) The points of attachment of the connections must divide the levers in the same ratio.
- (2) The guides for the upper ends of the levers must be perpendicular to the axis of the specimen and must be fixed in relation to one another

- (3) The connections to the recorder must be parallel to the axis of the specimen

The levers may be, and in fact are, of different lengths

Motion of the specimen, as a whole, in relation to the two guides B_1 , B_2 , produces no movement of the tracing-point on the drum, and hence it is not



essential, from this point of view, that the guides should be fixed, except relatively. As, however, they experience the reaction due to the force required to move the recorder, they are, in fact, fixed to the framework shown in the accompanying photograph

The levers A_1 , A_2 are tubular, stiffened by kingpost bracing tensioned

up by adjusting screws. The general arrangement can be seen in the above photograph.

One of the problems of the experiment was the attachment of the lower ends of the levers A_1 , A_2 to the selected points in the specimen. Since normal plane sections of a single crystal do not remain normal when the specimen is stretched, it is impossible to use the conventional form of attachment—namely, two screws engaging in punch-marks at opposite ends of a diameter. On the other hand, the deformation of a single crystal is so closely uniform along its whole length that the extension of any generating line of the original cylinder may be taken as the extension of the whole specimen. Two punch-marks are made about 10 cm. apart, on a generating line, the punch used being a gramophone needle. Into each of these fits a similar needle fixed into the lower end

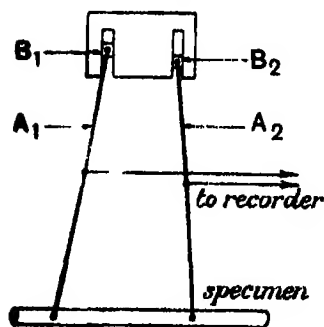


Fig 10

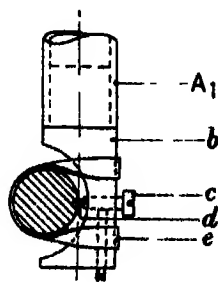


Fig 11

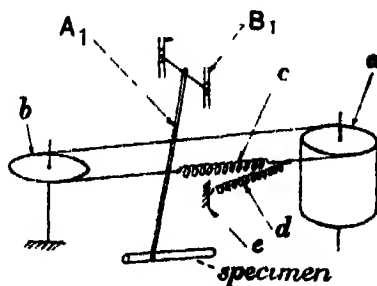


Fig 12

FIG 10.—Arrangement of extensometer mechanism.

FIG 11.—Method of attachment of extensometer to specimen.

FIG 12.—Arrangement of connections to recorder

of the lever A_1 or A_2 , the details being shown in fig. 11. In the end of the tube forming the lever is soldered a piece of brass b , shaped as shown, carrying the brass plug c , in which the needle-point d is soldered. The point is held firmly in the punch-mark by a rubber band e . It will be seen that the position of the point, practically on the axis of the tube, forming the lever A_1 , reduces the torsion on the lever to a negligible amount, and any tendency of the lever to twist as a whole is reduced by arranging the trunnions which slide in the guides B_1 , B_2 at some distance from the axis of the tube (See fig 12, B_1).

The intermediate points on the lever A_1 , A_2 are connected to the recorder by steel bands 0.1 inch wide by 0.004 inch thick. In order to avoid errors due to the slight flexural rigidity of this band, a certain minimum tension is needed. This is obtained by making each band a complete loop (see fig 12),

passing from the attachment to the lever A_1 , round the pulley a , by which the recorder is driven, back to a free pulley b at the other end of the machine, and finally returning to the lever A_1 , which therefore experiences no force due to any tension in the band. A long spiral spring c is inserted in each loop between the two pulleys mentioned above. Finally, in order to ensure that there is no lost motion in the system a light adjustable spiral spring d connects a point on each band to the framework e .

It will appear from the calibrations referred to in §14 below that these precautions had the desired result, the x co-ordinate of the records being a constant fraction of the extension between the selected points on the specimen to a high order of accuracy.

12 Recorder. (See figs 13-15)

A diagrammatic sectional view of the recorder is shown in fig 13, and its external appearance in the above photograph. It is mounted on a cross bar of channel steel attached to the extended sides of the main frame of the testing machine. On this is a bearing A , in which turns the external drum B , which carries the scribing point b_1 . On a parallel cross bar of flat steel, firmly supported by arms which are clearly visible in the photograph, is a second bearing C .

On the upper end of the drum B is formed a groove for the steel band e_2 from which it derives its motion. Three large oval panels are removed from the drum in order to enable the celluloid film to be mounted on the internal drum F . The scribing point b_1 is fixed in a triangular frame which pivots on pointed screws b_2 , attached to the drum B . It is pressed on the film by a flat spring (see photograph), which is so arranged that the point can be swung back while the film is put in place, and restored with the same pressure, when required.

The inner drum F carries the film on which the record is made. This is ordinary cinematograph film, the gelatine being first removed. The axial motion of the drum, approximately twice the compression of the springs which measure the force on the specimen, is obtained as follows. To the cross bar by which these springs are compressed (see fig 14) is attached a compensating lever a , from whose ends two steel bands pass to two equal pulleys L_1 , mounted on a spindle fixed below the recorder. In between, and integral with, these pulleys is a larger one L_2 , from whose circumference a steel band passes up to the recorder. Each band is attached to the circumference of its pulley, the compensating lever a eliminating the effect of any slight inequality in the

diameters of the smaller ones. The bands are kept taut by a spring K (fig 13) so arranged that it does not contribute to the friction of the recorder.

The band from the larger pulley L_2 is attached to the lower end of a tube H which passes up through both drums and has on its upper end a collar, against which the inner drum is pressed by a spring G, a ball thrust bearing reducing

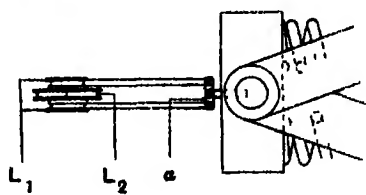
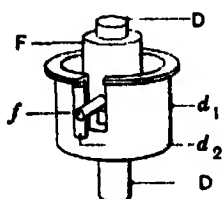
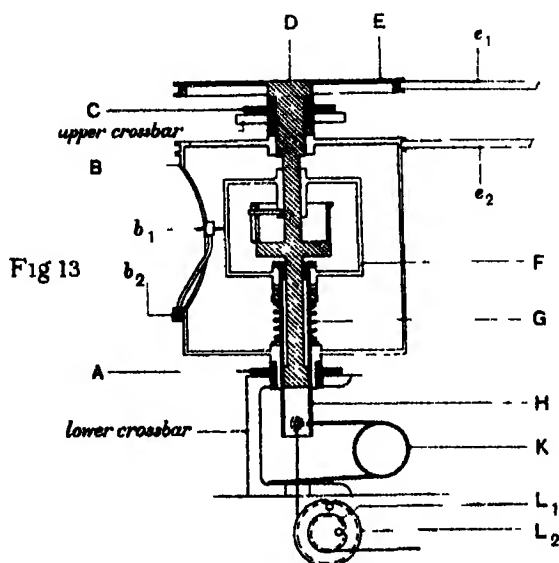


Fig 15

Fig 14

FIG 13—Arrangement of recorder

FIG 14—Connection of extensometer to springs

FIG 15—Rotational drive to drum of recorder

the friction. The spring G also serves to press the outer drum B down on to the bearing A.

The most difficult problem of the instrument was the rotational motion of the inner drum F. This is derived from the upper pulley E and steel band e_1 . The spindle D of this pulley passes down through the upper bearing C, both drums, B and F, and the tube H, the bearing surfaces being arranged

as shown in fig. 13 in order that the tension in the bands may not cause the mechanism to bind

On the part of this spindle D which is inside the drum F is mounted a cylinder d_1 (fig. 15) with a diameter approximately half that of the drum. This cylinder is open at the upper end and is slotted parallel to its axis, as shown in the sketch. To its outer surface is soldered a piece of silver steel rod d_2 , which was carefully tested for straightness. Its position is indicated in fig. 15. It was adjusted to be as nearly as possible parallel to the spindle D. Through the slot in d_1 there projects a similar piece of rod f , which is fastened to a projection of the end of the drum F. The rods f and d_2 are kept in contact by springs (not shown) to avoid backlash, and form a "key" and "keyway" connecting D and F rotationally.

This construction reduces the errors in the axial motion of the drum F to a minimum. As the result of the precautions described it is not possible to detect, on a Hilger measuring microscope, any departure from straightness in fiducial lines on the records parallel to either x or y axis (see fig. 17, below). The angle between the axes is almost exactly 90° , showing that the "key way" is practically parallel to the axis of the drum. As however the angle between the stages of the microscope could be adjusted so that the movements were parallel to the fiducial lines, the exact magnitude of this angle is not important.

13 Instrumental Errors

The errors to be anticipated in such a mechanism as has been described may be classified as follows - -

(1) *Due to strain* --The supports of all parts are very firm. The stresses in the main frame are very small and any deflection which takes place when the force is applied to the specimen is certainly elastic and, since the springs are calibrated *in situ*, is absorbed in the calibration. The steel bands driving the recorder are of ample size, and are under sufficient initial tension to ensure that their flexural rigidity is not a source of error.

(2) *Due to friction* --There is very little frictional resistance to the rotational movements of the recorder, but there is an appreciable frictional resistance to the axial motion of the inner drum. Since however the forces to be measured are of the order of 1,000 lbs. and this friction is of the order of ounces, no appreciable error arises. All the surfaces on the recorder are copiously lubricated with a fairly viscous oil, and no tendency to stick has ever been observed. It may be noted that in all experiments the motion of every part of the mechanism

is in one direction only (the fall of stress at the elastic limit with steel is the only exception and cannot give rise to any appreciable error)

(3) *Due to slack*—The precautions taken to avoid slack at every point have been described. The points which engage in the punch marks on the specimen fit very firmly, and though the latter must extend into an oval shape when the specimen is stretched, it appears from separate measurements made on the stretched specimen that the points remain in the centre of the punch marks.

(4) *Due to change of conditions between calibration and experiments*—As has been mentioned in describing the methods of calibrating, elaborate precautions were taken to ensure that, so far as the condition of the machine and recorder were concerned, the calibrations and experiments were identical.

14 Order of Accuracy of Results

The magnitude of the probable error of the final result (the area of the stress-strain figure) is influenced chiefly by the calibration of the springs. The levers used in this calibration (see §10) were found to have ratios of 1·959 and 10·21 as the mean of several calibrations by weights, giving a combined ratio of 20·00. The variations in the figures for the individual levers were of the order of 1 in 1,000 and the combined result may be relied on to 1 in 500. The "out of balance" of the bellcrank lever was determined directly to be equivalent to 21·5 lbs at the springs.

The calibration curve of the springs is shown in fig 16. It includes the

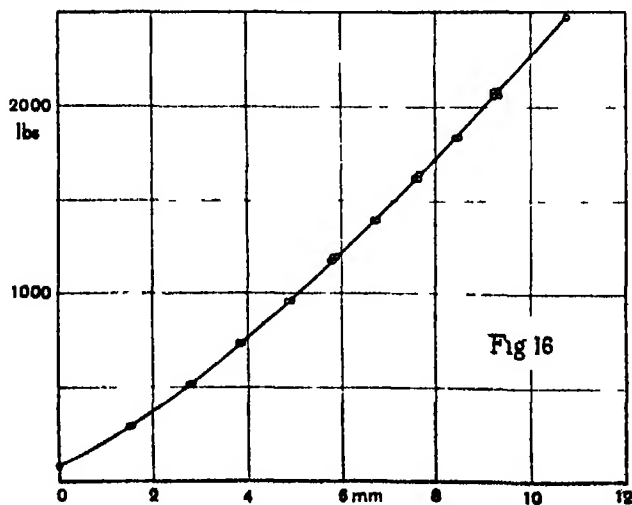


FIG 16 — Calibration curve of springs

results of calibrations taken both before and after the experiments, showing that the characteristics of the springs did not alter appreciably with time. The points nowhere depart from the curve adopted by more than 1 per cent, and it is considered that this represents the maximum error in a force measurement.

The calibration of the extension co-ordinate by the method described in §8 (p. 437) gave a ratio of 3.59 within 1 in 500, the ratio calculated from the measurements of the mechanism involved being 3.58. The former figure was used as it corresponded to a direct comparison of specimen and record, whereas the latter involved several separate measurements, one being of a type in which great accuracy could not be attained. The constancy of this ratio for extensions of both large and small amounts was within the figure given. "large" meaning of the order of 5 cm. on the specimen, and "small" of the order of 5 mm. In the experiments the actual extensions corresponding to each temperature measurement had the following average values for the materials tested —

	mm
Copper	6
Steel	1
Aluminium (plain)	7
Aluminium (single crystal)	10

The *total* extensions of each specimen averaged 18, 12, 22 and 50 mm respectively.

The actual records were measured on a Hilger comparator, on which readings could be repeated within one-hundredth of a millimetre. The final areas were computed from measurements of ordinates sufficiently closely spaced.

It is considered that the above figures enable it to be claimed that the final areas, representing the work done, are determined within 1 per cent.

15 *Stress-Strain Records*

Some examples of these are shown, enlarged 3.1 times, in fig. 17*. The upper three are from steel, copper, and plain aluminium, respectively, and the lower two from single crystal specimens of aluminium. The numbers correspond to those in the table of results (Table III) and in the temperature records, figs. 2-5.

* The definition of the lines has suffered in reproduction. As seen by transmitted light the trace of the scribing point appears as two dark lines, separated by a white line. The overall width is about 0.04 mm. In measuring the records, the cross wires of the microscope were focussed on the outer edge of one of the dark lines.

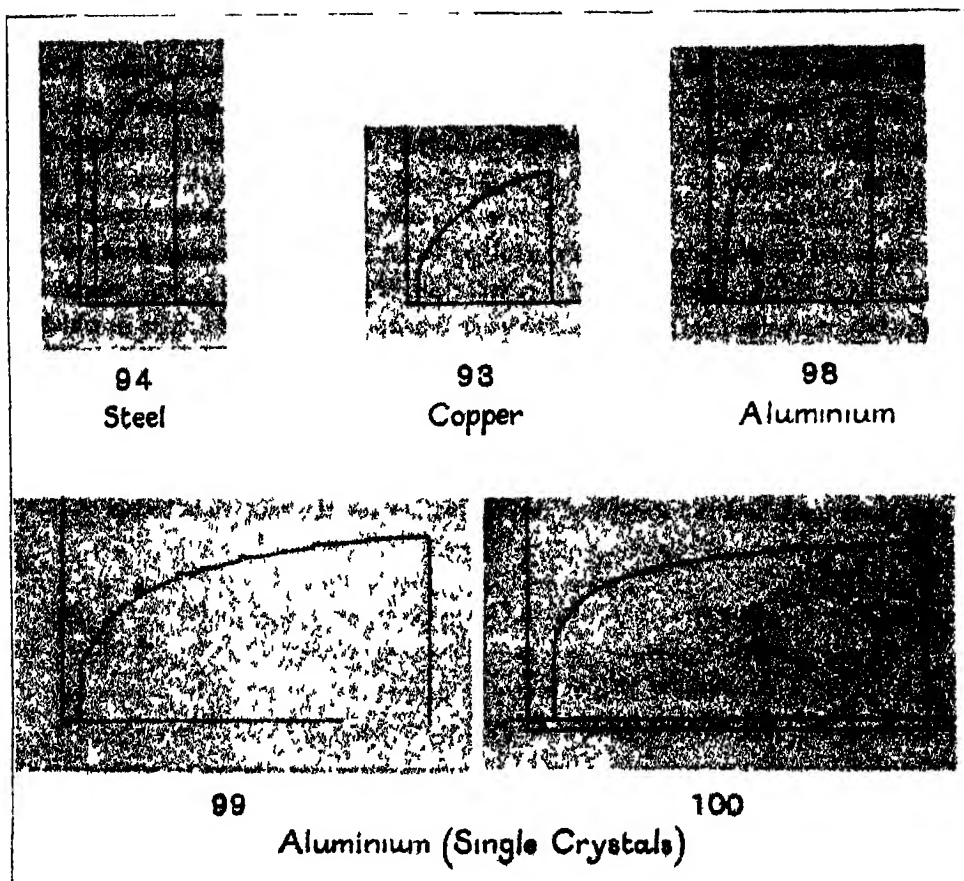


FIG 17 —Stress-strain records

The approximate scales of the diagrams as reproduced are —

Extension (x axis) 1 cm — 11·6 per cent on the original length of 10 cm.
between marks

Forces (y axis) 1 cm. = 715 lbs approximately The force scale is not
exactly linear, for reasons which have been described above.

The original dimensions of the specimens are given in the following
Table IV.

Table IV

Material	Length of parallel part	Outside diameter	Inside diameter	Cross sectional area
	cm	in	in	sq in
Steel	30	0.31	0.21	0.0422
Copper	29	0.25	0.12	0.0384
Aluminium	21	0.50	0.19	0.1688
Aluminium (single crystal)	16	0.56	0.19	0.2151

The approximate stress scales are therefore as follows —

Steel	1 cm = 17,000 lbs /square inch,
Copper	1 cm = 18,600 „ „
Aluminium	1 cm = 4,200 „ „
Aluminium (single crystal).	1 cm = 3 300 „ „

referred, in all cases, to the original cross-sectional area

The short vertical marks on the records represent the end of each experiment. With steel and aluminium they appear on the record automatically and were thought at first to be due to a defect in the instrument, but as they did not appear in experiments on copper (the marks on the record for copper were made deliberately in order to give greater precision to the measurements) they are presumably characteristic of certain materials only. Their significance is discussed below.

The interval between two extensions of any one specimen was about 10 minutes, and during this time the specimen was under tension, constant except in so far as any "creep" of the specimen allowed the springs to extend. The records show that this creep occurred with steel, and (to a much smaller extent) with plain aluminium, but not with copper or single-crystals of aluminium. It should be noted that the circumstances during this "creep" are very different from those which occur when a specimen is left under load in an ordinary testing machine. The load is then independent of any extension which may occur, whereas here extension of the specimen relieves the load rapidly. In fact, the springs extend the same amount as the specimen. The recorder magnifies extensions of the spring twice (approximately) and reduces extensions of the specimen, between the selected points, 3.59 times. Hence, if the whole length of the specimen is n times the length between the points, the line on the record representing the "creep" referred to above should slope down from left to right at an angle $\tan^{-1} 2 \times 3.59 n$. For the steel

450 *Heat Developed during Plastic Extension of Metals.*

specimen ($n = 3$) this angle is $\tan^{-1} 21.5$. Examination of the record will show that these lines do in fact slope to about this extent.

On increasing the load, for the next extension, it will be seen that with steel and aluminium (both plain and single-crystal) no extension occurs until the load has risen appreciably above that previously reached. There is then a rapid extension at almost exactly constant load, followed by a period in which both load and extension increase. The fact that the curve corresponding to the last part joins smoothly on to that representing the end of the previous extension suggested that the "kink" in the curve was instrumental, but as the phenomenon is not observed with copper (*see records*) it is presumably characteristic of certain materials only, corresponding to something analogous to sticking.

With copper the absence of the "kink" is so definite that it was sometimes found difficult to decide exactly where each separate extension ended, though the approximate point could be seen without difficulty, owing to the slightly deeper depression in the celluloid made by the scribing point resting in one position for some minutes. The marks seen in the copper records were therefore made deliberately, as mentioned above.

It will be seen that the "kinks" in the curves for single-crystals of aluminium decrease regularly as the load increases, and practically disappear when the breaking load is reached. *see in particular* No. 100, which was on the point of breaking at the end of the experiment.

The record for mild steel No. 94 shows the characteristic fall of stress at the yield-point. An actual *fall* of stress was not observed in all specimens, the variation being presumably due to slight differences in the rate of extension. The "ripples" on the record are due to slight irregularity in turning the handle of the machine. They do not appear in the records for the other materials, presumably because these have a much smaller tendency to "creep".

All the specimens were thoroughly annealed before the experiments, but there is nevertheless an appreciable "elastic range" for all except the plain aluminium. This material, however, hardens remarkably rapidly, having after 1 per cent extension an "elastic range" of about 4000 lbs/sq. in., and after 5 per cent extension a range of about 9000 lbs/sq. in., these stresses being about one-third and three-fourths respectively of its ultimate breaking stress.

When plotted on true stress-strain co-ordinates the records for all the copper and all the plain aluminium specimens tested agree very closely with

one another. The single-crystal specimens of aluminium differ considerably from one another No 99 having a lower yield point than No 100, though it is ultimately stronger.

The work was carried out in the Cavendish Laboratory through the kindness of Sir Ernest Rutherford, to whom we wish to express our thanks.

We wish also to thank Prof Carpenter and Miss Elam for presenting us with single-crystal specimens of aluminium, and Mr W W Hackett, of Messrs Accles & Pollock, Ltd, who presented us with specially annealed steel tubing from which the test-pieces were made. An analysis of this material (for which we are indebted to Mr W E Woodward, M A) showed that it contained 0.17 per cent carbon and 0.76 per cent manganese.

*An Experimental Study of the Vibrations in the Blades and
Shaft of an Airscrew*

By A. FAGE, A.R.C.Sc., of the Aerodynamics Department, National Physical
Laboratory

(Communicated by H. Lamb, F.R.S. —Received November 11, 1924.)

CONTENTS

	PAGE
§1 Introduction	451
§2 The Hot Wire Microphone	452
§3 Description of Airscrew Apparatus	453
§4 The Model Airscrews	455
§5 The Sounds of Rotation	456
§6 Measurement of Flexural Vibrations	458
§7 Calculation of Flexural Vibrations	460
§8 Discussion of Results	462
§9 Summary	468

§1 *Introduction*

This investigation* deals with the natural frequencies of flexural vibration of the blades and shaft of a rotating airscrew, and includes a comparison of

* The work described in this paper was carried out in the Aerodynamics Department of the National Physical Laboratory, and permission to communicate the results was kindly granted by the Aeronautical Research Committee.

theoretical results with those determined experimentally from an analysis of the sounds emitted. These sounds can be divided into three groups —

(a) The sounds of rotation, which, according to Lanchester,* are due to the movement in circular or spiral paths of the sources and sinks which would account for the pressure differences on the blades. Since the air pressure in the neighbourhood of the airscrew will fluctuate as the blades rotate (except at points on the axis, where in the absence of reflection from neighbouring bodies no sound is heard), the pitch of the fundamental note is equal to the product of the number of blades and the rotational speed. Harmonics of this note are also present, and these acting together have an effect on the ear which resembles that of a roar †. Experimental determinations of these frequencies have been made and are given in §5 below.

(b) Tearing sounds associated with the shedding of eddies from the blades. No attempt has been made to measure these sounds, which appear to have a high but very indefinite pitch. An analogous sound is that produced by a rotating rod, which, according to E. F. Relf,‡ emits a note of frequency equal to that of the periodic eddy formation behind the rod.

(c) Sounds arising from the vibrations of the airscrew blades and of the shaft. The frequencies of the sounds due to flexural vibration have been measured (§6), but not those due to torsion, as these were well outside the frequency range of the experiments.

The frequency measurements were made with a hot-wire microphone and a four-valve amplifier, designed and constructed by Dr W. S. Tucker, of the Signals Experimental Establishment, Woolwich Common.

§2 *The Hot-Wire Microphone*

This instrument has been developed by W. S. Tucker and E. T. Paris,§ and consists of an electrically heated platinum grid placed in the neck of a cylindrical Helmholtz resonator which is capable of being tuned by means of a sliding piston. The advantages of this type of resonator are that the resonance is sharp and that the overtones are all comparatively high and are not in harmonic relation. When in tune to the note to be measured, the oscillatory

* "Memorandum on the Emission of Sound by an Aeroplane Propeller" 'Aeronautical Research Committee, Report No. T 1058' (*Not published*)

† The variation of the intensity of this sound with rotational speed has been investigated mathematically by E. J. Lynam and H. A. Webb. "The Emission of Sound by Airscrews" 'Aeronautical Research Committee, R. & M., No. 624'

‡ 'Phil. Mag.' July, 1921

§ "A Selective Hot-Wire Microphone" 'Phil. Trans. Roy. Soc., Series A, vol. 221.

movement of air in the neck of the resonator causes a sensible change in the resistance of the wire grid. This change is compounded of a steady fall in resistance, due to the average cooling, and a periodic change due to the oscillatory air currents. Resonance may be detected, either by measurement on a Wheatstone's bridge of the steady resistance drop, or by amplifying the periodic changes of current and making use of a galvanometer or telephone. In the present experiments a four-valve amplifier, designed by Dr. Tucker, was used in conjunction with a mirror galvanometer.

The circuit values of this amplifier are given in fig. 1. Three microphones of different sizes were available for detecting resonance, the frequency ranges

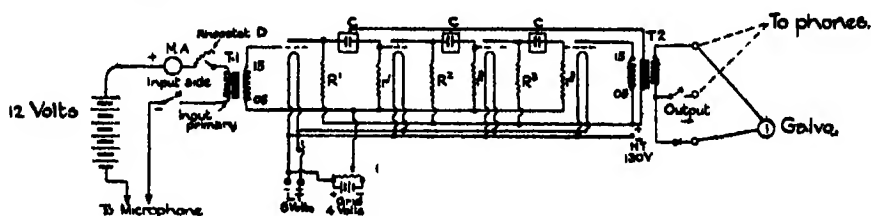


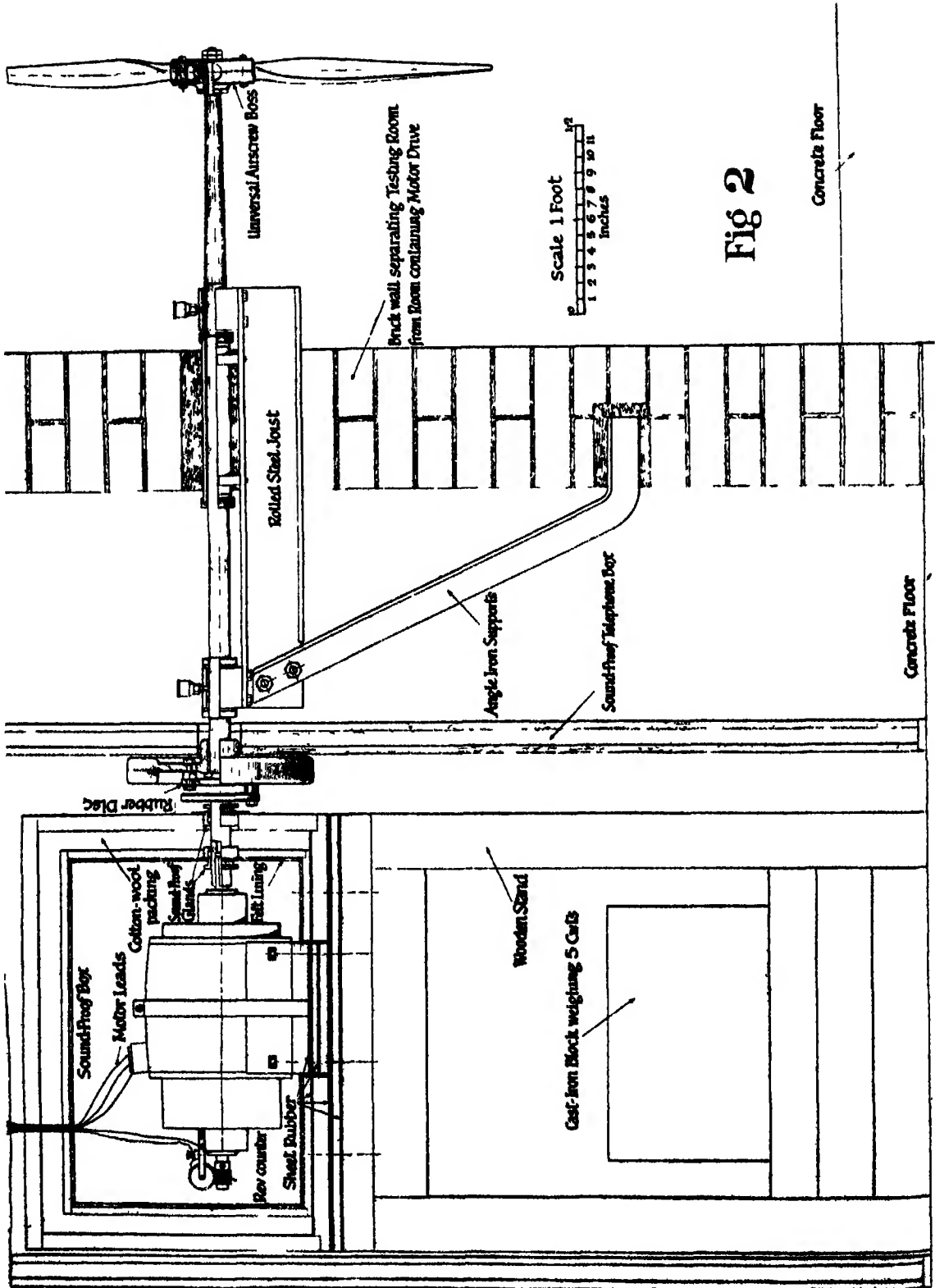
FIG. 1

being 25-50, 50-100, and 100-200 respectively. These microphones were calibrated against a standard siren at Woolwich, and check calibrations against tuning-forks, in which the vibrations were maintained electrically, were made at the National Physical Laboratory.

§3 *Description of Airscrew Apparatus.*

The chief feature of the present apparatus is the method adopted to obtain a silent electric drive for the airscrew. Preliminary experiments on electric motors showed that the sound emitted by them was built up of a large number of tones, the frequency intervals being so small that it would be almost impossible to distinguish between these notes and those from an airscrew, especially as both vary with the rotational speed. Accordingly, it was decided to enclose the motor in a sound-proof chamber, and as a further precaution to isolate this chamber outside the room in which the frequency measurements were to be made.

The general arrangement of the airscrew apparatus is shown in fig. 2. The sound-proof box had double wooden walls packed with cotton-wool, and was lined on the inside with felt. The motor and box, detached from each other, were mounted on alternate sheets of rubber and wood, on the top of a strong wooden table standing on a concrete floor. The purpose of this method of



mounting was to dissipate within the box most of the noise of the rotating parts and to damp out the motor vibrations by the rubber sheets. To increase the inertia of the stand, and so to lessen the effect of motor vibrations not dissipated in the rubber sheets, a heavy weight of about 5 cwt was carried on a lower platform. Further, the sound-proof box and stand were totally enclosed within an ordinary Post Office telephone box, on the outside of the brick wall of the experimental room.

The airscrew shaft rotated in two well-lubricated plain journal bearings carried on a rolled-steel joist, which was grouted into the brick wall and additionally stiffened with splayed angle bars. Direct transmission of sound or vibration along the airscrew shaft was prevented by the use of a rubber drive between the motor and airscrew shafts. The rotational speed was measured by a revolution counter on the motor shaft within the sound-proof box. Steadiness of running was obtained by mounting a heavy fly-wheel on the motor end of the airscrew shaft, and also by running the motor directly from a battery supply of adjustable voltage.

It was found in practice that this method of isolating the motor noises was quite satisfactory. At speeds below about 700 r p m no sound could be heard in the experimental room, above this speed and up to the highest speed of the experiments—about 1,400 r p m—only faint noises, chiefly due to the grinding of the bearings, were audible. Acknowledgment is due to Mr A. Monk, artificer in the Aerodynamics Department, for care taken in the construction and erection of the apparatus.

§4 *The Model Airscrews*

The experiments were made on four airscrews, of diameter 3 ft, which had been used in a previous investigation*. These airscrews were then designated as fourbladers Nos 1, 3 and 10, and sixblader No 11. For convenience, they are renamed 'airscrews A, B, C, and D' respectively in the present paper. Some general characteristics of the four types of blade are given in fig. 3. Except at the root, where the section was a circle of diameter 1.1 inches, the blades had similar sections at the same radii. The blade widths were in the ratios 4 : 3 : 2. The blades were of cast aluminium and were clamped into a large metal boss.

* "Experiments with a Family of Airscrews mounted in front of a Small Body" By A. Fage, C. N. H. Lock, R. G. Howard, and H. Bateman. 'R & M, No 820' Aeronautical Research Committee.'

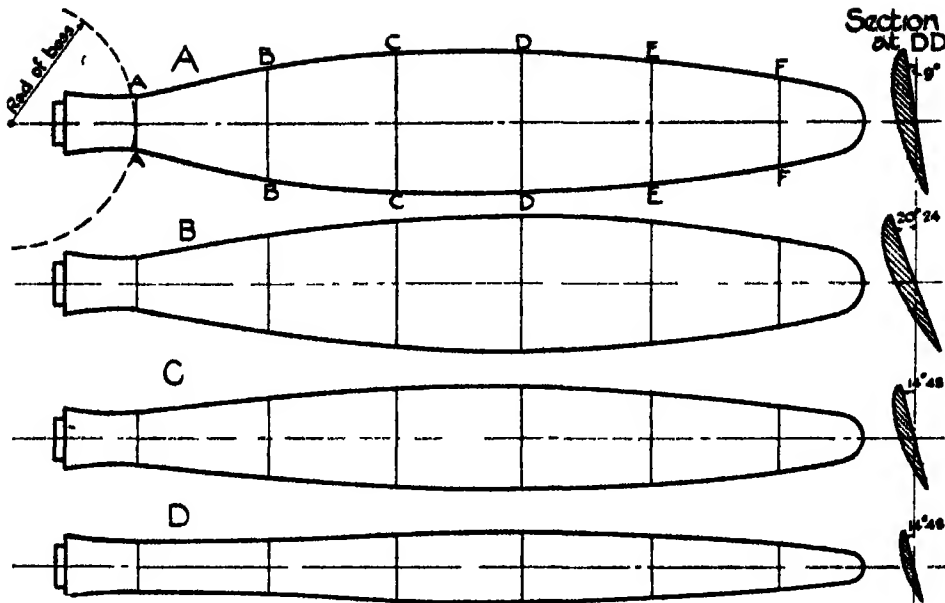


FIG 3

§5 *The Sounds of Rotation*

It would appear that most of the sound emitted from an airscrew arises, in the absence of excessive vibration, from the rotation of the source-and-sink system associated with the pressure differences on the blades. Experiments by R McKinnon Wood* have shown that this noise is composed of a large number of tones, which are harmonics of a fundamental having a frequency equal to the product of the number of blades and the rotational speed in these experiments the frequencies were estimated aurally, by comparison with a piano and pitch-pipe.

The present experiments have involved the direct measurement of these tones. The method adopted was to maintain constant the speed of rotation, and to record resonances as the tuning of the resonator was progressively changed. The alternative method of constant tuning and variable rotational speed was found to be unsatisfactory, since the changes with speed in both the intensity and character of the sound influenced the shape of the resonance curves. Variable tuning was obtained by removing the piston and placing the open end of the resonator under water, the level of which was raised at a slow and uniform rate. The frequency change per minute was about $\frac{1}{2}$ per

* "Note on Some Experiments on the Sound emitted by Airscrews" 'R. & M., No 694. Aeronautical Research Committee'

cent at a frequency of 100, and 2 per cent at a frequency of 200 With this method of variable tuning, the sensitivity of the microphone is increased by the forced convection of air over the hot-wire grid *

Resonance curves were obtained by plotting the average deflection of the mirror galvanometer taken over a period of 30 sec against the frequency of the resonator a resonance being indicated by a peak in the curve Both the valve amplification and the distance of the microphone from the airscrew were adjusted to give a convenient deflection of the galvanometer at resonance The microphone was placed in a line making an angle of about 45° with the airscrew axis

A summary of the experimental results for four-bladed airscrew B, rotating freely at a stationary point, is given in Table I

Table I

Rotational Speed n R P S	Frequency of Note p	$(p/4n)$	Remarks
15.95	127.3	2.0	1st harmonic
15.95	104.5	3.05	2nd "
12.50	48.35	0.98	Fundamental
12.50	97.50	1.95	1st harmonic
12.50	154.0	3.08	2nd "
12.50	209.5	4.18	3rd "
8.33	100.0	3.00	2nd "
8.33	129.0	3.90	3rd "
8.33	168.5	5.08	4th "
8.33	197.5	5.95	5th "
7.13	112.5	3.05	3rd "
6.97	137.0	4.93	4th "
6.97	169.0	6.08	5th "
6.97	190.5	6.85	6th "
6.97	225.0	8.10	7th "

This table shows that musical notes ranging from the fundamental (of frequency $4n$) up to the seventh harmonic, have been detected with satisfactory accuracy The higher harmonics were of faint intensity, owing to the low rotational speed which was necessary in order to keep within the frequency range of the resonators It is probable that still higher tones are present and that these would be detected with resonators of higher frequency range

Typical resonance curves are shown in fig. 4 In general, the resonances were less marked as the order of the harmonic increased An exception is shown at $n = 12.5$ r p s., where the second harmonic is more pronounced than the first, although the reverse was the case at $n = 15.95$ r p s.† It

* For explanation see the paper on "A Hot-Wire Microphone," *loc. cit.*

† Not shown in fig. 4

should be noted that the galvanometer deflections at resonance are not necessarily representative of the intensity of the note, since the response of

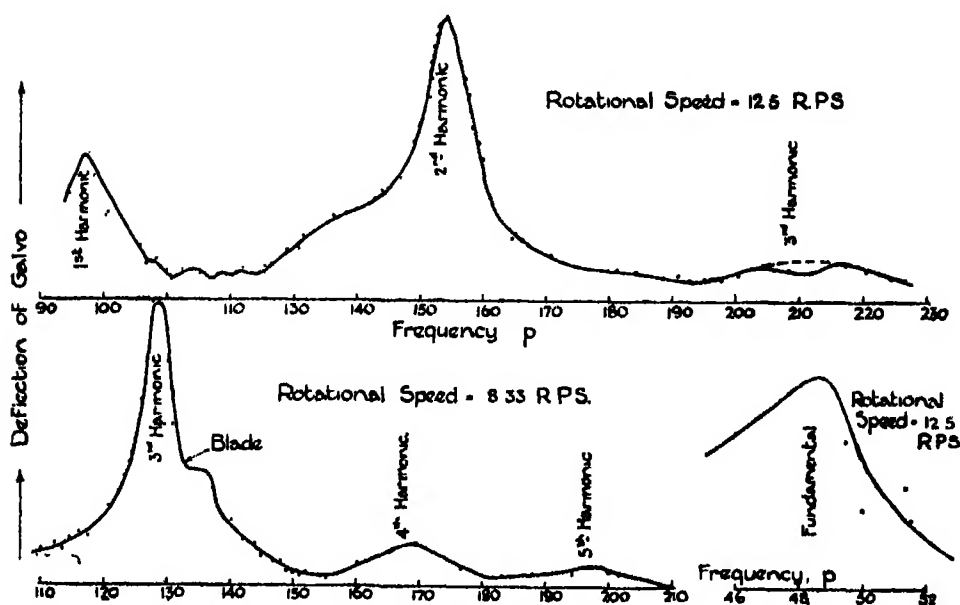


FIG 4

the resonator depends on the pitch of the note and the valve amplification may not remain constant throughout the experiments

§6 Measurement of Flexural Vibrations

In the elastic system composed of an airscrew rotating at the end of a shaft of appreciable length, there are possible two distinct types of flexural vibration, that of the blades alone and that of the airscrew shaft. Torsional vibrations are also possible, but these are not here considered, since they are well outside the frequency range of the microphones. Preliminary experiments showed that when the airscrew was rotating freely the only notes that could be measured were those of rotation and except for an occasional flutter there was no tendency for either the blades or shaft to vibrate. It was necessary, therefore to stimulate these vibrations by giving to the blades a definite number of impulses per revolution.

The method adopted was to mount behind the airscrew—i.e., in the slip-stream—a number of equally spaced radial arms, which cause the blades to vibrate when their natural period is equal either to the impulse frequency or

to one of its harmonics. Stars of 4, 7, 8, 9, 10, and 12 radial arms were used. The distance of a star behind the airscrew, and the width of the arm, were adjusted so as to make the impulse strengths just sufficient to maintain the vibrations. The arm widths were either 1 inch or 3 inches, the maximum distance of a star behind the airscrew was 4 inches. A diagrammatic sketch, showing the general arrangement of a star of 8 arms, is given in fig 5.

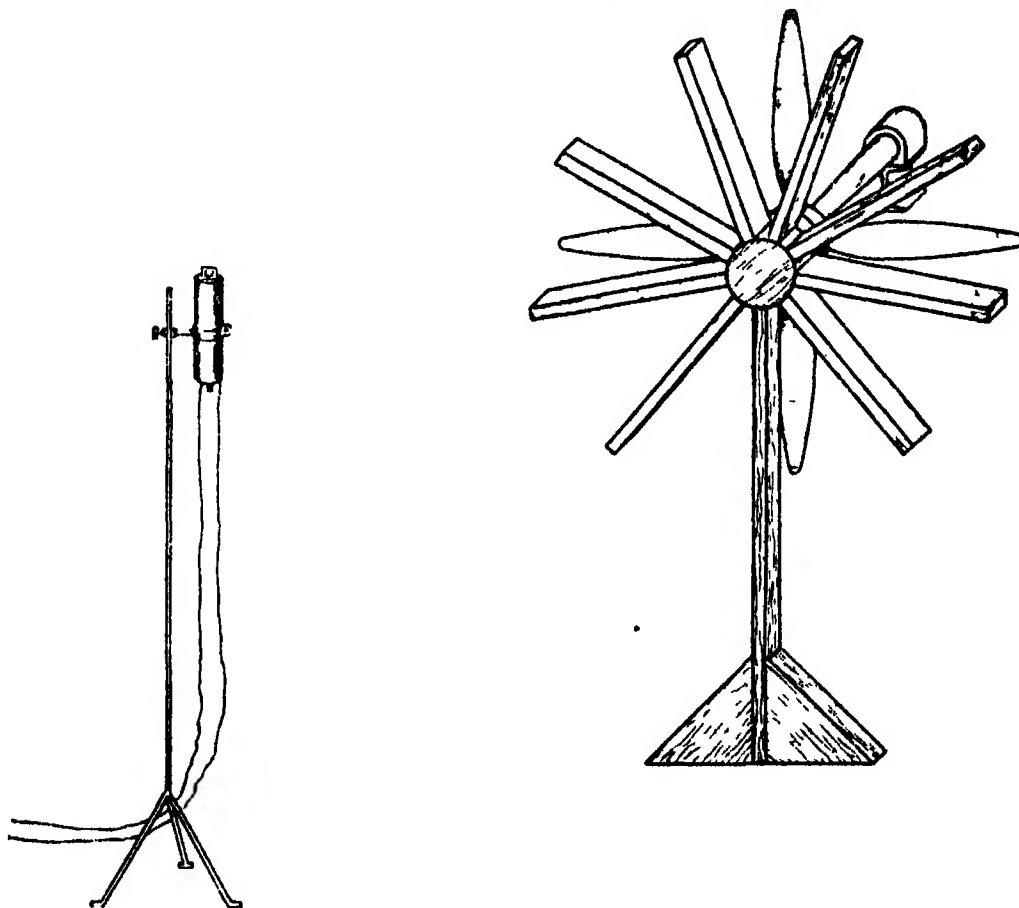


FIG. 5

It was originally contemplated that a star would excite vibrations in the blades only. It was found, however, that flexural vibrations of the shaft were also excited, presumably on account of some slight want of symmetry in the forcing system. Complete records of all the vibrations were accordingly taken, and afterwards the two types of vibration were disentangled with the aid of theory.

The method of experiment employed was to traverse a range of rotational speed in short steps, and when the rotation was steady to measure this speed and then from its known calibration to tune the resonator to a note of which the pitch was equal to the product of the number of arms and the rotational speed*. At each step the average deflection of the galvanometer taken over 3 or 4 minutes was recorded, and resonance curves were then obtained by plotting these readings against either the resonator pitch or the rotational speed.

To illustrate the general character of the results, the resonance curves for airscrew B are given in figs 6 and 6A. These curves, on which the observation points are plotted show that in nearly all cases the resonances were very pronounced, and also that with no vibration the response of the resonator is very weak, although it is always in tune with the forcing impulses.

The pitch of the notes from the non-rotating blades was determined by Mr E F Relf from a comparison with tuning-forks of standard pitch. A detailed discussion of these experimental results, and also a comparison with theoretical values, is given later (§ 8).

§7 Calculation of Flexural Vibrations

(a) *Airscrew Shaft*—The frequency of the flexural vibrations of the airscrew shaft, which is supposed to be encastré at one end and attached rigidly to the centre of inertia of the airscrew at the other, was determined by the method† described by the writer in 'Engineering,' July 20, 1917. The steel shaft used in the present experiments had an overall length of 13.2 inches, and tapered in diameter from 1.385 inches at the encastré end to 1.0 inch at the airscrew. The calculated results are given in Table II, where it will be seen that there are two periods of vibration corresponding to each rotational speed. The values of M and I_1 for each airscrew are also included in this table. M (the mass of the airscrew) is given in slugs, and I_1 (the moment of inertia of the airscrew about an axis passing through the centre of inertia at right angles to the plane of flexure) in slug-feet².

(b) *Airscrew Blades*—The frequency of the lateral vibrations of a non-rotating blade was determined by the analytical method of A. A. Griffith‡ and also by the graphical method of R. V. Southwell§. The results obtained

* In some experiments the resonator was tuned to a note of double this frequency.

† See also the method of A. Berry, published by the Aeronautical Research Committee (R. & M., No. 177). These two methods give practically the same results.

‡ 'Aeronautical Research Committee, R. & M., No. 451.'

§ 'Phil. Mag.,' March, 1921.

by these two methods were found to be in very close agreement. They are given in Table IV.

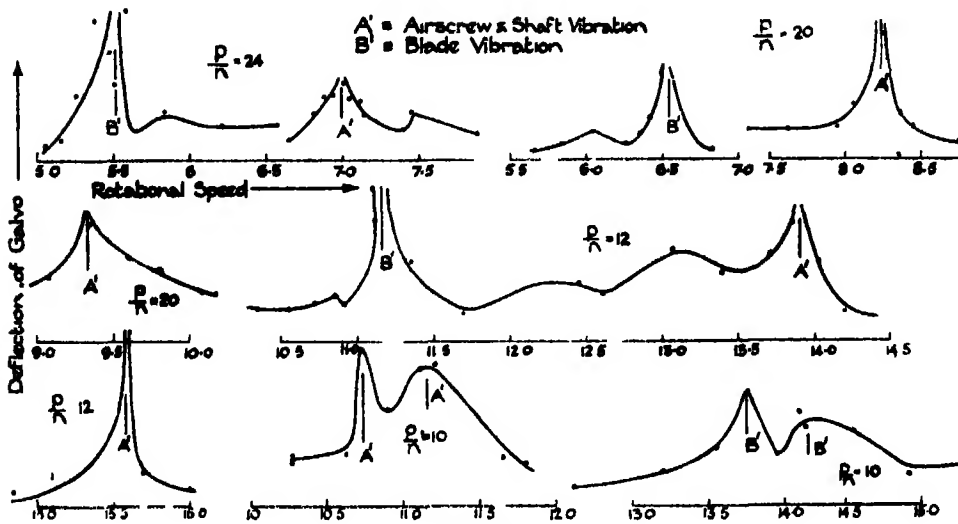


FIG 6

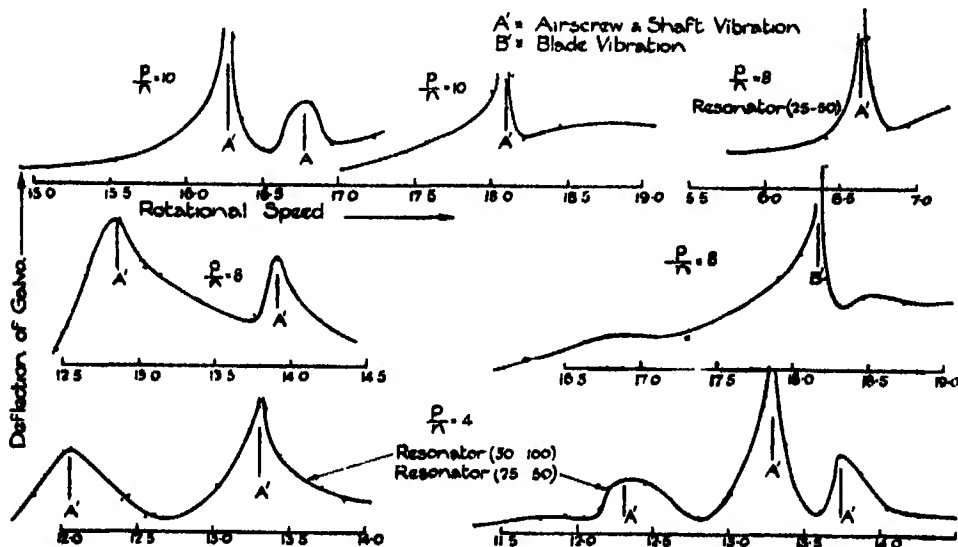


FIG 6A

The effect of rotation on the frequency of the lateral vibrations was determined by the method of R. V Southwell and Barbara S Gough,* who have

* 'Aeronautical Research Committee, R & M, No 766'

shown that the frequency p and the rotational speed ω are connected by an approximate formula of the form of $p^2 = p_0^2 + \alpha\omega^2$, where p_0 is the gravest frequency in the absence of rotation and α is a constant, the value of α cannot be determined exactly, but an upper limit to which it approaches can be estimated by an application of methods due to Lord Rayleigh

The modulus of elasticity used in the calculation of the frequency of the aluminium blades was determined by direct measurement at the Royal Aircraft Establishment, and was found to vary from 1.0×10^7 to 1.1×10^7 lbs per square inch. The density was found to vary from 0.103 to 0.105 lb per cubic inch, and a mean value 0.104 was taken in the calculations

§8 Discussion of Results

(a) *Vibrations of Airscrew Shaft* -The experimental results for three of the four airscrews are given in Table II, those for airscrews B and C are plotted in figs 7 and 8. Each frequency value given in the table was determined from resonance curves of the type shown in figs 6 and 6A. The observations for airscrew D were limited in number, as they were made only for the purpose of distinguishing the shaft vibrations from those of the blades. No measurements of the shaft vibrations were made for airscrew A, which differs from airscrew B only in its pitch-diameter ratio. The theoretical values of the shaft frequencies are also included in Table II.

The above table shows that for the airscrews C and D the measured frequencies of the fundamental modes of vibration agree with those of theory within 2 per cent. The agreement is not so satisfactory in the case of the heavier airscrew B, for which the measured values of the upper and lower fundamental modes are about 8 per cent lower than those of theory. It is probable that in this case there is some "give" at the fixed end of the shaft. It is of interest to note that overtones of the fundamental were also measured.

(b) *The Flexural Vibrations of the Blades* -The experimental results for the four airscrew blades are summarised in Table III. The results for airscrews B and C are also plotted in figs 7 and 8.

Table II.

Airscrew	Rotational Speed n R P S	Frequency of Note p	Number of Radial Arms	Remarks
Four-bladed airscrew B. M = 0 32 I₁ = 0 0454	13 30	a { 53 2 48 2* 49 3* b { 53 1 53 5 53 0	4	Lower fundamental. Average value, 53 2 Theoretical values { 57 9 at $n=0$ 57 1 at $n=15$ 55 8 at $n=25$
	12 05		4	
	12 32		4	
	13 27		4	
	13 37		4	
	6 62		4	
	12 85	102 8	4	Overtone (first harmonic) Average value, 108 2
	13 90	111 2	4	
	10 73	107 3	10	
	11 15	111 5	10	
	16 27	102 7	10	Overtone (second harmonic) Average value, 166 0
	16 77	167 7*	10	
	13 90	167 0	12	
	8 23	164 6	10	
	7 00	168 0	12	
	18 10	181 0	10	Higher fundamental Average value, 184 9 Theoretical values { 201 5 at $n=0$ 201 7 at $n=25$
	15 58	187 0	12	
	9 33	186 6	10	
Four-bladed air screw C M = 0 264 I₁ = 0 027	10 00	70 0	7	Lower fundamental Average value, 67 0 Theoretical values { 66 5 at $n=0$ 64 7 at $n=20$
	9 20	64 4†	7	
	8 33	66 6†	8	
	10 56	105 6*	10	Average value, 104 5 Overtone (perfect fifth)
	8 06	104 0*	12	
	5 78	104 0*	9	
	14 20	127 8	9	Average value, 134 8 Overtone (first harmonic)
	10 93	131 4	12	
	7 14	128 5	9	
	15 40	139 0†	9	
	11 71	140 9	12	
	7 85	141 2	9	
Six-bladed air- screw D M = 0 239 I₁ = 0 0191	6 95	62 6	9	Lower fundamental Average value, 69 2 Theoretical values { 70 9 at $n=0$ 70 0 at $n=15$
	7 48	74 8	10	
	9 30	74 4	8	
	8 10	64 8	8	

* Faint note
 a Middle resonator

† Strong note
 b Large resonator

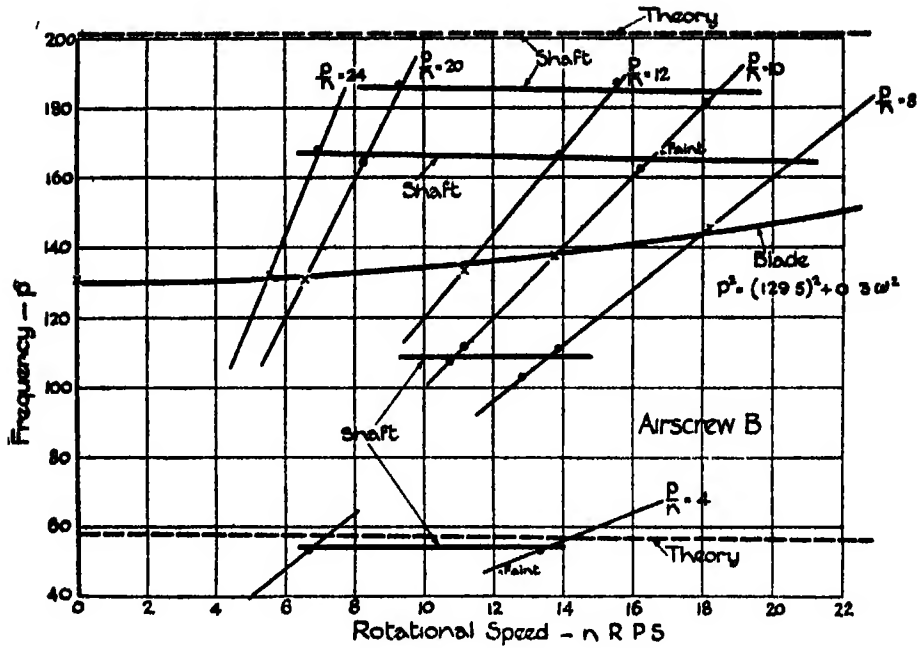


FIG 7

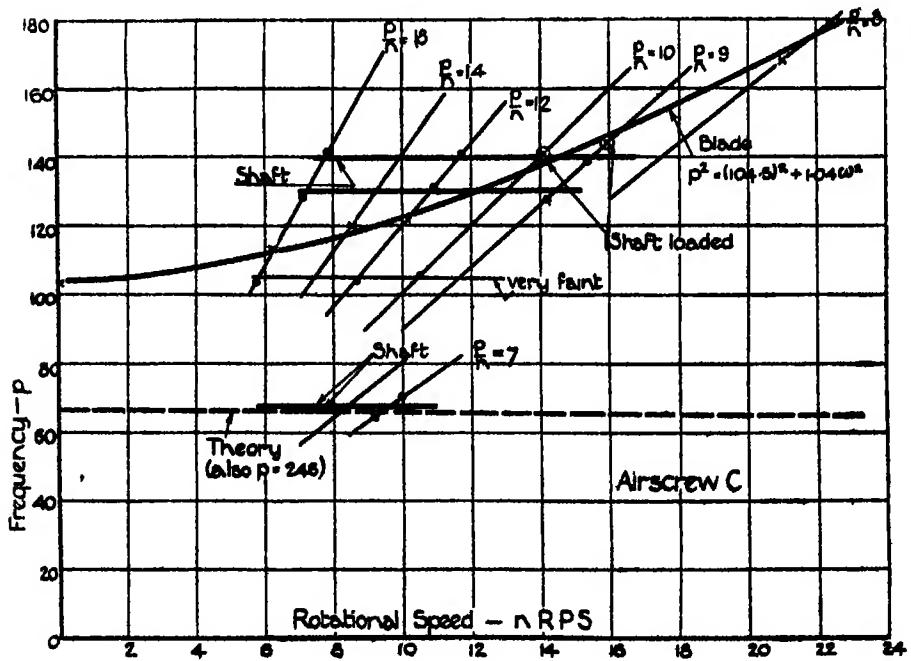


FIG. 8.

Table III

Blade Shape	Rotational Speed n R P S	Frequency of Note p	(p/n)	Number of Radial Arms	Remarks
B	0	131 0	—	—	Tuning fork measurement.
	5 51	132 0	24	12	—
	6 54	130 8	20	10	—
	11 15	133 8	12	12	—
	14 15	141 5	10	10	Faint note
	13 75	137 5	10	10	—
	18 16	145 3	8	4	—
C	0	102 0	—	—	Tuning fork measurement
	14 10	141 0	10	10	Shaft loaded to have a theoretical frequency = 52 0
	15 95	143 6	9	9	
	8 56	120 0	14	7	—
	10 15	121 8	12	12	—
	14 20	142 0	10	10	—
	16 00	144 5	9	9	Very strong note
D	0	76 5	—	—	Tuning fork measurement
	6 85	96 0	14	7	—
	8 58	103 0	12	12	—
	11 74	117 4	10	10	—
	15 96	143 7	9	9	—
	16 50	148 5	9	9	Shaft loaded to have a theoretical frequency = 59 3
A	0	128 0	—	—	Tuning fork measurement.
	6 45	129 0	20	10	—
	13 77	137 7	10	10	—
	11 00	132 0	12	12	—
	5 41	130 0	24	12	—
	18 80	150 4	8	4	—

To eliminate any uncertainty of measurement in the region where the curve of blade vibration crosses the first harmonic of the shaft fundamental (see fig 8), the shaft was loaded for airscrews C and D to have a different frequency and the experiments repeated. These additional results are also given in Table III, for the purpose of comparison the two sets of resonance curves are shown in fig 9. It should be recorded that when each of these airscrews was rotated at the speed at which the blade frequency was double that of the shaft the noise emitted was so intense, even although the forcing impulses were very weak, that it was necessary to shut down immediately. Similar trouble was not experienced with airscrews A and B, and would not be

expected, since for the range of the experiments the frequency of the blade vibrations is never a harmonic of the shaft frequency.

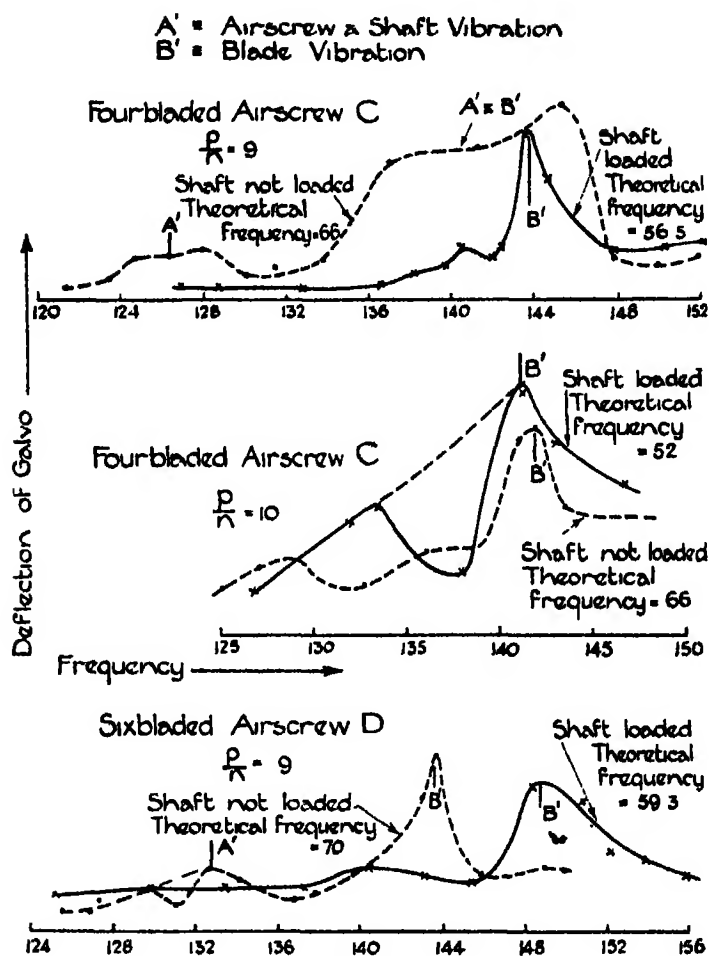


FIG. 9.

In fig 10 the experimental values of p^2 from Table III have been plotted against ω^2 . These curves show that for each of the blades C and D the frequency can be expressed with good accuracy by the approximate formula of R V Southwell and B S Gough,* viz, $p^2 = p_0^2 + \alpha\omega^2$. This linear relationship does not hold for blades A and B, although both sets of results are seen to lie on the same curve, the slope of which increases with ω^2 and has a value at $\omega^2 = 1.44 \times 10^4$ of 0.85

* *Loc. cit.*

The agreement of the experimental frequencies for blades A and B shows that a change of geometrical pitch-ratio from 0.3 to 0.7 does not appreciably influence the frequency of the flexural vibrations.

The experimental values of p_0 and α obtained from the curves of fig. 10 are given in Table IV, where comparisons are made with the theoretical values

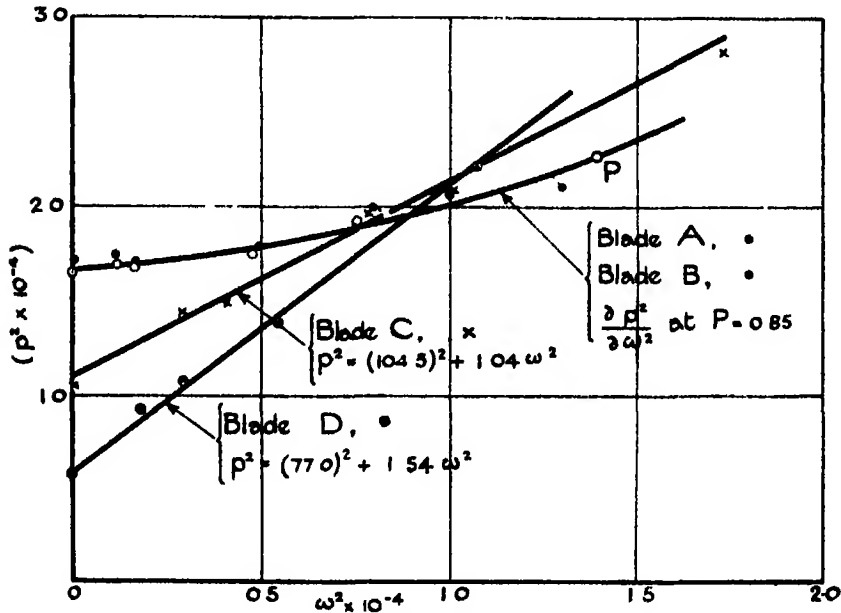


FIG. 10

Table IV

Blade Shape	$p_0 (\omega = 0)$			α		Ratio of experimental and theoretical frequencies at $n = 1,200$ r p m (Average theoretical values of p_0 taken)
	Expt	Theory		Expt	Theory * Upper Limit	
		$E = 11 \times 10^7$ lbs per sq inch	$E = 10 \times 10^7$ lbs per sq inch			
D	77 0	80 5	76 5	1 54	1 60	0 98
C	104 5	107 5	102 5	1 04	1 55	0 88
A and B	128 0	135 5	129 0	$\frac{\partial p^2}{\partial \omega^2} = 0.85$ at $\omega = 120\frac{1}{2}$	1 30	0 80

* Lower limit is unity

† Value increases with ω

For blades D and C the experimental values of p_0 lie between those of theory, whilst for blades A and B the discrepancy from the average theoretical value is only 3 per cent. Such close agreement shows that any torsion involved in the flexural vibrations* is too small to modify the frequency appreciably.

Since the blades are symmetrical in plan form, these results confirm the work of A. A. Griffith and B. Hague,† who have shown that such blades would not be expected to twist appreciably under load. The agreement between the calculated frequency and that measured on the rotating blade D is also quite satisfactory. The theory of thin rods therefore holds, and any twisting of the blade due to the centrifugal force can be neglected.

The agreement is, however, less satisfactory as the weight and width of a blade increases. If the blades were similar and the end conditions the same, both the theoretical and experimental frequencies would be independent of the scale. This is not the case, since the blades, although similar over the greater part of their length, have a common section of large diameter at the root. Blade D is therefore exceptionally strong at the root and about four times lighter.

The frequency of blades A and B would be over-estimated if the flexural vibrations were appreciably modified by torsion. In view, however, of the close agreement of theory and experiment obtained on blade D this is not to be expected, especially as these blades are stronger in torsion. A possible explanation of the low frequencies measured on blades A and B is that the assumption of an encastré end holds more closely for the thin blade D than for the heavier blades. In this connection it is of interest to note that whilst the shaft vibrations for airscrew D were in good agreement with theory, those for airscrews A and B were about 8 per cent. low.

§9 Summary.

(1) The frequencies of the flexural vibrations in the blades and shaft of a rotating airscrew have been determined from an analysis of the sounds emitted. A comparison of experimental results with those of theory is given. The experiments were made on four airscrews of different blade shape, the variables of design being width and geometrical pitch.

(2) The analysis was made with Tucker hot-wire microphones used in conjunction with a four-valve amplifier. To isolate extraneous noises the

* Neglected in the theory.

† 'Aeronautical Research Committee, R. & M., No. 455.'

electric motor driving the airscrew was enclosed in a sound-proof chamber, and a flexible rubber drive was used between the motor and airscrew shafts

(3) The sounds of rotation were analysed and found to be compounded of a large number of harmonics, having as fundamental a note of frequency equal to the product of the number of blades and the rotational speed

(4) The measured frequencies of the shaft vibrations were found to agree very closely with the calculated results, except for a discrepancy of 8 per cent obtained on the heaviest airscrew

(5) The experiments on blade vibration support the approximate formula of Southwell and Gough—viz, $p^2 = p_0^2 + \alpha\omega^2$, where p_0 is the frequency of the gravest mode of vibration in the absence of rotation, and α is a constant. Close agreement between the theoretical and experimental values of both p_0 and α was obtained on long narrow blades, the agreement was less satisfactory for the widest blade of the series

The writer wishes to acknowledge his indebtedness to Mr R V Southwell, Superintendent of the Aerodynamics Department, for the suggestion that the work should be undertaken, and for the great interest he has shown throughout the investigation, to Dr Tucker for assistance received during the initiation of the experiments, and to Dr H Lamb for valuable suggestions made during the preparation of this paper

Thermal Diffusion Measurements.

By T L IBBS, M C, M Sc.

(Communicated by Prof S W J Smith, F R S.—Received November 14, 1924)

INTRODUCTION

In a previous paper* an account was given of a series of experiments demonstrating the thermal diffusion effect† in mixtures of hydrogen and carbon-dioxide. The gas mixtures were passed through a separating device consisting of a glass tube down the middle of which ran a helix of platinum wire heated by a current. The gas was drawn off in two streams, one from near the hot helix, the other from the cooler outer parts of the tube. Analysis of the two gas streams by means of a differential katharometer showed that there was a tendency for the heavier carbon-dioxide molecules to move towards the cold side, and for the lighter hydrogen molecules to move towards the hot side, thus producing a difference in the distribution of the components of the mixture.

Although the method was useful for showing the effect of varying the temperature or of altering the proportions of the two gases, it was not suitable for measuring the amount of separation produced with the hot and cold sides under definite temperature conditions. The extremes of temperature only were known, and not the actual temperatures of the hot and cold streams of gas.

In order to make a more complete investigation of the phenomenon, further experiments were undertaken. The object of these was to measure the amount of separation produced in mixtures of different pairs of gases under definite temperature conditions. Such measurements might give information as to the influence of different types of molecules on the amount of separation produced. The continuous flow method previously used was abandoned, and preliminary experiments were made with mixtures of hydrogen and carbon-dioxide, using the principle employed in the original experiments of Chapman

* Ibbs, T L, with a note by Chapman, S, 'Roy Soc Proc,' A, vol 99, p 385 (1921)

† Enskog, D, 'Phys Zeit,' vol 12, p 538 (1911), 'Ann d Phys' (4), vol 38, pp 742, 759 (1912), Chapman, S, 'Roy Soc Proc,' A, vol 93, p 1 (1916), 'Phil. Trans,' A, vol 217, p 157 (1917), Chapman, S, and Dootson, F W, 'Phil Mag,' vol 32, p 266 (1917), Chapman, S, 'Phil. Mag,' vol 34, p 146 (1917), 'Phil. Mag,' vol 38, p. 182 (1919), Enskog, D, 'Arkiv f Nat Astron o Fysik,' Stockholm, XVI (1921), Chapman, S, and Hainsworth, W, 'Phil Mag,' vol 48, p 602 (1924)

and Dootson Two cylindrical copper vessels, each of about 200 c.c. capacity, were joined by a connecting tube of length 30 cm and diameter 0.6 cm. One vessel was heated electrically, and the other kept cool by running water. In this case, however, a katharometer block was connected by a short tube to the cold side, so that changes of composition in the gas could be measured directly. Although the thermal diffusion effect was clearly shown, this method did not appear suitable for obtaining quickly results of the required accuracy. Many hours elapsed before anything like a steady state was reached, and consistent measurements could not be obtained. With vessels of this size and shape it was difficult to ensure that uniformity in composition of the gas throughout the apparatus had been attained at the beginning of an experiment. Any want of uniformity, however small, would cause serious irregularity in the small changes observed. The long time taken to reach a settled condition would probably be partly due to the influence of water vapour arising from the inside metal surfaces, on the katharometer readings.

Owing to the large number of measurements required in the investigation of the phenomenon for a pair of gases, it was desirable to devise a form of apparatus in which the time for the effect to take place would be short.

PRINCIPLE AND METHOD OF EXPERIMENT

The system of experiment used was developed on the following lines. If a small cold cell at a steady temperature communicates by a tube with a hot vessel of large capacity and both are filled with a uniform gas mixture, the effect of thermal diffusion will be to cause a change in composition of the gas in the cold cell. There will be a tendency for the lighter and smaller molecules to leave the cold cell, and for the heavier and larger molecules to enter it. This transfer will go on, until it is finally balanced by the effect of ordinary diffusion, and a steady state is reached. As the capacity of the hot vessel is large compared with that of the cold cell, very little change of composition will occur on the hot side, and practically the whole effect will be shown in the change of composition in the cold cell. With a small cold cell the actual amount of gas transferred to bring about the change in composition is small, and we should therefore expect the time to reach the steady state to be short. In the practical arrangement of the apparatus the katharometer cell itself, with the necessary connections, is made to form the cold cell mentioned above. Changes of composition in a small quantity of gas can in this way be accurately measured.

A cylindrical glass vessel A (fig 1) drawn out at each end serves as the hot side. This is heated electrically, and surrounded by a lagging of plaster-of-

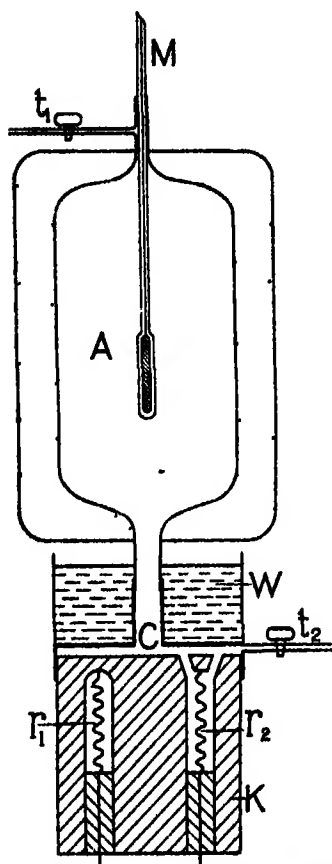


FIG. 1.—Diagram of Apparatus, showing katharometer cell forming part of cold side

Paris. Through the closed upper end of A a mercury thermometer M passes, which is used for measuring the temperature of the gas in A. A narrow-bore side-tube leading to a tap t_1 is joined to the top of A, and is used for passing gas into the apparatus. The lower end of A narrows into a tube of 0.53 cm diameter, and this leads into a brass screw cap C. This cap is screwed on to the cylindrical copper block of the katharometer K, a thin lead washer being employed to keep a small clearance space between the cap and the top of the block. This space communicates with the cell r_2 of the katharometer by three small holes. Free communication is thus established between the cell r_2 and the remainder of the apparatus. The other cell r_1 of the katharometer is sealed in dry air. A narrow-bore tube ending in a tap t_2 is joined to the screw cap as shown, and is used for passing gas out of the apparatus. A water-jacket W, through which is passed a continuous stream of water from the mains, is fixed on the top of the screw cap. This surrounds the lower part of the connecting tube, and serves to keep this part of the tube, the screw cap, and the katharometer block at a steady temperature, and particularly serves to shield the katharometer from the effects of the hot side. The temperature of the water in W gives the cold side temperature. The actual length of tube between the hot and cold sides is about 0.8 cm.

During a series of experiments on a gas mixture in which the temperature of the hot side was varied between room temperature and about 300° C, the temperature of the cold side would only alter a few degrees.

[It is important to notice that when the katharometer is used for the analysis of a gas mixture in a vessel, this instrument and the vessel to which it is con-

nected must be at the same temperature, otherwise serious errors will arise owing to the effects of thermal diffusion]

One katharometer of the standard type was used throughout the experiments. I wish to express my thanks to the inventor, Dr. G A Shakespear, for the use of this instrument, and for his willingness to give me the benefit of his wide experience with it. The instrument is very suitable for use in the gas analysis required in these experiments, and particularly for accurate work when dealing with small quantities of gas.

The instrument was used for two distinct purposes during the course of the experiments. (1) In order to analyse mixtures of two gases with an accuracy of about 0.5 per cent. (2) In order to measure as accurately as possible the small changes in composition produced by thermal diffusion.

The experiments can be divided into five groups, each group referring to mixtures in different proportions of a particular pair of gases. The different pairs were as follows —Hydrogen and carbon-dioxide (Group I), hydrogen and nitrogen (Group II), nitrogen and carbon-dioxide (Group III), hydrogen and argon (Group IV), helium and argon (Group V).

The mass ratio between the molecules of the pairs of gases chosen was very large, except in the case of mixtures of nitrogen and carbon-dioxide, and we should therefore expect the thermal separation to be considerable. There is also a large difference in the thermal conductivities of the gases making up the pairs, which will mean that mixtures will be suitable for katharometric measurement. By choosing molecules of different types there was a possibility of obtaining interesting comparisons between the results obtained.

In order to use the instrument for the analysis of gas mixtures, a calibration curve is required for each group. The curve for hydrogen and carbon dioxide used in the previous experiments was again employed, and curves for the four remaining groups were constructed. Dr Shakespear very kindly devoted some considerable time to assisting me in the preparation of these curves. For ordinary gas analysis the normal bridge arrangement of the katharometer, previously described, was employed. A number of mixtures of known composition by volume are accurately made up. The galvanometer deflection produced by each mixture when the open cell r_2 is exposed to it is noted, and thus deflection-composition curves can be constructed. The shape of the curves varies with the pair of gases used, approaching a straight line in the case of mixtures of nitrogen and carbon-dioxide. The curve for hydrogen and argon shown in fig 2 may be regarded as typical. The composition of any mixture of unknown proportions was determined by passing it through

the thermal diffusion apparatus without applying the heater, and noting the galvanometer deflection with the normal bridge arrangement mentioned

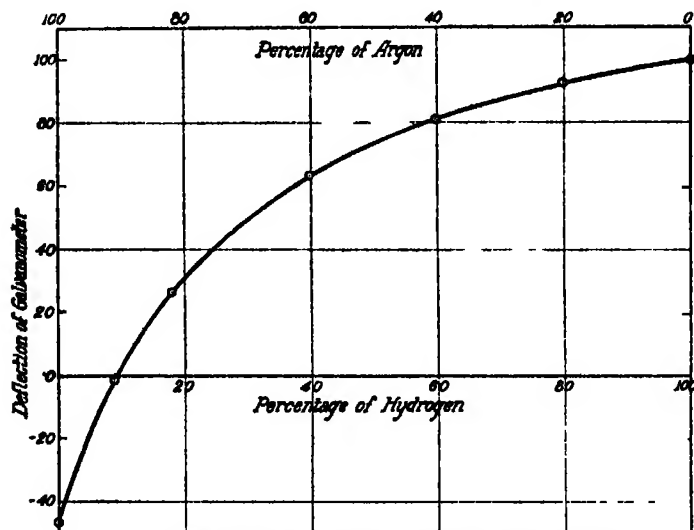


FIG. 2—Calibration curve for Hydrogen and Argon

above. By reference to the calibration curve the percentage composition could then be read off.

Although the differences in composition produced by thermal diffusion are sufficiently large to be shown with the ordinary katharometer arrangement for analysis, it is necessary to make special provision for their accurate measurement. Before dealing with this method of measurement the general procedure employed in the experiments will be described.

A stream of water is passed through the cooler, and the vessel A is heated until the conditions become steady at the required temperature. The gas mixture for examination is passed through the apparatus, entering at t_1 , passing downwards through A, then through the connecting tube into the screw cap, flowing past the holes leading to the cell r_2 , and leaving through the narrow tube and tap t_2 . The flow of the mixture opposes the tendency for thermal separation, and a steady flow can be maintained so that the separating effect is overcome, and gas of practically uniform composition fills the whole apparatus. It is found that this stream of gas attains the temperature of the containing vessel as it passes through. The form of apparatus employed, in which the gas flushes out each part in turn, assists greatly in enabling a state of uniform composition to be reached. By having the holes leading to the katharometer cell in the line of flow, the gas in the cell r_2 soon acquires uni-

formity of composition with the gas in the stream, by the ordinary process of diffusion

The flow of gas is now stopped, taps t_1 and t_2 are closed, and the thermal diffusion begins. This proceeds at first rapidly, and then more slowly as the steady state is approached. The actual progress of the effect can be followed by observing the movement on a galvanometer scale. For all mixtures, except those of nitrogen and carbon-dioxide, the change was complete in about three minutes. The change in mixtures of nitrogen and carbon-dioxide is much slower, requiring about fifteen minutes to complete. The effect was clearly shown in all the mixtures examined, and in all cases the heavier molecules tended to move towards the cold side of the apparatus.

In the "Theory of the Katharometer,"* Dr H. A. Daynes describes two ways in which the Wheatstone bridge arrangement can be used. The platinum spirals in the copper block (one sealed in air the other exposed to the gas of variable composition) form two arms of the bridge. The other arms of manganin, outside the block, may be joined by a graduated bridge wire, and the point of contact between the arms varied so that the galvanometer gives zero reading. (Cf fig 2, *loc cit*.) The other way is to keep the point of contact between the manganin arms fixed so that their resistances are equal, and read the direct deflection on the galvanometer when a change of resistance occurs in one of the platinum arms (r_2) of the bridge. This arrangement is the one used in the system of calibration, and analysis of gas mixtures, already described.

The comparatively small differences in composition produced by thermal diffusion were measured in these experiments by using a combination of the two bridge arrangements. When the steady flow of gas mixture is passing through the apparatus, thus overcoming the tendency for thermal diffusion separation, the slide wire is moved so that the galvanometer (which is more sensitive than the one used for ordinary analysis) is brought to zero. When the flow is stopped, thermal diffusion occurs, and the change of composition of the gas in the cold cell causes the galvanometer to deflect. In this way very small changes in composition can be accurately measured. From the slope of the ordinary calibration curves at any point, we can get the change in deflection which will be produced by any small change in composition. It will be noticed that the change in deflection corresponding to a definite change in composition varies with the proportions of the two gases in any mixture. Reference to fig 2 shows that this change in deflection is greatest when the

* 'Roy. Soc. Proc.' A, vol 97 (1920)

mixture contains a small proportion of the lighter gas. This means that the sensitiveness to changes of composition diminishes as the proportion of the lighter gas is increased. Deflections on the more sensitive galvanometer can be expressed in terms of changes in deflection of the ordinary calibration galvanometer, and by getting the slope of the calibration curve at a point corresponding to any mixture, the change in composition produced by thermal diffusion can be obtained.

For example, in a mixture containing 10 per cent hydrogen and 90 per cent argon, a difference of 0.005 per cent could be measured, for a mixture containing 90 per cent hydrogen and 10 per cent argon, a difference of 0.05 per cent could be measured. About the same sensitiveness is given by other mixtures, except those of nitrogen and carbon-dioxide, in which the sensitiveness is less.

The volume of the hot side A is 12.1 c.c. It was not practicable to have it greater as the quantity of helium available for the experiments was limited, and it is necessary to flush out the apparatus thoroughly before measurements are made. The volume of the cold side is 1.5 c.c. or about one-eighth that of the hot. The actual volume of the katharometer cell is about 0.5 c.c., the remainder of the cold side being made up by the cooled portion of the connecting tube and the space inside the metal cap. If the volume of the connections to the katharometer cell had been too far reduced, slowness in diffusion would have resulted.

The flow of the larger molecules to the cold side is accompanied by an equal flow of the lighter molecules from the cold to the hot side. This produces a change in composition on the hot side, which is less than the change produced on the cold side. The total effect is the sum of the change on the cold side, and the smaller change on the hot. As all the experiments are made at atmospheric pressure, the mass of any particular mixture on the hot side diminishes with rise of temperature, which is equivalent to a reduction in the effective volume of the hot side. This must be taken into account when working out the hot side change corresponding to the measured change on the cold. As the percentage separation is greater on one side than the other there will be a small change in the mean composition of the gas in the connecting tube. The influence of this on the results will be small in the range of temperatures employed.

In each group of experiments from five to ten mixtures in different proportions were made up for the pair of gases in a cylinder of 2 cubic feet capacity. This provided a good supply of each mixture with uniformity of composition. In this way one mixture can be examined with the hot side at a number of different

temperatures, enabling the relation between separation and temperature to be found. About seven such measurements were made on each mixture. In all, 43 gas mixtures were examined, giving about 300 measurements of thermal diffusion.

The change in composition is in all cases stated as a percentage change, *i.e.*, the difference in percentage composition by volume between the gas on the hot and the cold sides. The mixtures in each group are numbered in ascending order as the proportion of the lighter gas increases.

The results generally have been expressed graphically to avoid giving numerous tables of data. A typical set of results for one mixture only is given in tabulated form (Table A). This will serve as an example of the tables drawn up for all mixtures, from which the graphs are obtained. Throughout the paper T_1 represents the absolute temperature of the hot side, and T_2 the absolute temperature of the cold side.

Table A

Mixture No 5, Group II (Hydrogen-Nitrogen) Composition 32.7 per cent H_2 , 67.3 per cent N_2 Temperature of cold side $11^\circ C$

Temperature of Hot Side	Percentage Separation			$\log_{10} T_1/T_2$
	Cold Side	Hot Side	Total	
$^\circ C$	per cent	per cent	per cent	
55	0.66	0.10	0.76	0.063
106	1.47	0.24	1.71	0.125
145	1.91	0.35	2.26	0.168
183	2.08	0.42	2.50	0.206
206	2.50	0.53	3.03	0.227
237	2.83	0.63	3.46	0.254
274	2.96	0.71	3.67	0.285

Each measurement for a mixture is made separately, the apparatus being flushed out as described before another measurement is made. It is not sufficient merely to alter the temperature of the hot side as this would result in change of pressure.

For all mixtures used the total separation is found to be nearly proportional to $\log T_1/T_2$. This is in agreement with the prediction of the Enskog-Chapman theory. For a few mixtures the separation at the higher temperatures increases a little more rapidly than $\log T_1/T_2$. This small deviation may be apparent only, and due to a decrease of the effective volume of the cold side by the heating

of the gas in the connecting tube. At the higher temperatures also there is greater difficulty in keeping all the experimental conditions steady. The general agreement, however, is so close that the most effective way of demonstrating the results is by plotting graphs of separation shown against $\log_{10} T_1/T_2$. This has been done for all five groups. The cold side temperature (shown in the table of mixtures for each group) is throughout kept practically stationary. Temperature-separation curves are not now shown, as these are all of the same form as those previously obtained.*

The mixtures were made from gases, as supplied commercially, in cylinders under pressure. For purposes of thermal diffusion measurement these gases can generally be regarded as practically pure. Each gas was tested by passing it direct from the supply cylinder into the diffusion apparatus, and observing if any thermal separation could be obtained. For all the gases used except helium the effect was very small, and not sufficient to influence the nature of the results. For helium the effect obtained was equivalent to that which would be given by 3 or 4 per cent of argon mixed with the pure gas. (The probable purity of the cylinder helium is about 97 per cent, with nitrogen as the impurity.)

The results obtained for each pair of gases will be considered separately.

RESULTS

Group I (Hydrogen and Carbon-dioxide)

The results obtained for this pair of gases in the previous experiments could be regarded as comparative only, the extremes of temperature being known, and not the actual temperatures of the hot and cold sides. It was desirable, therefore, to repeat the experiments on this pair using the new form of apparatus.

The mixtures examined are shown in Table I.

Table I

Mixture No.	H ₂	CO ₂	Cold Side Temperature
	per cent	per cent	° C
1	5.8	94.2	17
2	11.8	88.2	16
3	24.3	75.7	15
4	43.3	56.7	15
5	52.6	47.4	15
6	58.8	41.2	14
7	65.0	35.0	18
8	69.5	30.5	17
9	80.5	19.5	12
10	89.5	10.5	12

* 'Roy. Soc. Proc.,' A, vol. 99, p. 392

In fig 3 is shown the relation between separation and $\log_{10} T_1/T_2$ for mixtures Nos 1, 2, 3 and 7. In order to find the effect of varying the proportions of the

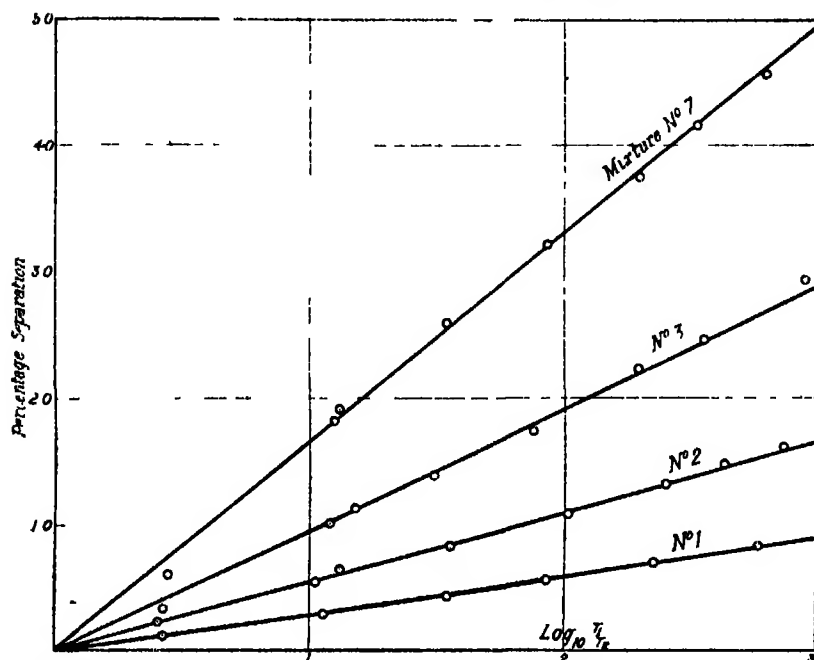


FIG 3.—Group I— H_2 and CO_2 . Relation between separation and $\log_{10} T_1/T_2$ for mixtures 1, 2, 3 and 7

two gases in the mixture the separation corresponding to $\log_{10} T_1/T_2 = 0.2$ is measured on the graph for each mixture. (This is equivalent to raising the hot side to about $185^\circ C$.) The curve in fig 4 is thus obtained showing the relation

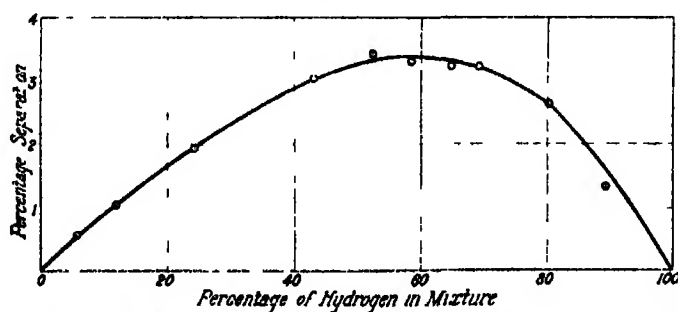


FIG 4.— H_2 — CO_2 . Relation between composition and separation ($\log_{10} T_1/T_2 = 0.2$)

between composition and separation. It is rather more symmetrical, but is of the same general form as the curves obtained in the previous series of experi-

ments (fig 7, 'Royal Soc Proc,' A, vol 99, p 393) The slight sag shown in the part of the old curve for mixtures containing small proportions of hydrogen has disappeared, and in this respect the new curve corresponds more closely with the curves obtained theoretically by Prof Chapman The system of heating now employed is preferable to the old one, with the result that greater accuracy may be expected

As was anticipated, the separations are greater than those given by corresponding temperatures with the old apparatus The observed values previously obtained are only about 0.45 of the absolute values now measured

It is interesting to notice that the separation for a 50 per cent mixture is about 0.47 of the amount calculated by Chapman and Hainsworth* for this pair of gases, on the assumption that the molecules behave like rigid elastic spheres

Group II (Hydrogen and Nitrogen)

This pair of gases was selected in order that a comparison could be made with Group I, showing the effect of substituting the lighter diatomic nitrogen molecules for carbon-dioxide molecules

The mixtures examined are shown in Table II

Table II

Mixture No	H ₂	N ₂	Cold Side Temperature
	per cent	per cent	° C
1	2.8	97.2	13
2	4.7	95.3	12
3	10.7	89.3	10
4	25.7	74.3	11
5	32.7	67.3	11
6	37.4	62.6	11
7	50.5	49.5	9
8	60.0	40.0	11
9	94.3	15.7	9

Fig 5 shows the relation between separation and $\log_{10} T_1/T_2$ for mixtures Nos 2, 3, 4, 6 and 7 Fig 6 shows the separation-composition curve for Group II, when $\log_{10} T_1/T_2 = 0.2$ Comparison with fig 4 shows that the curve is more symmetrical than the one for carbon-dioxide and hydrogen. This is of interest when we consider that the mass ratio of the molecules has been reduced from 22/1 to 14/1 for nitrogen and hydrogen. In spite of this reduction

* 'Phil Mag,' Sept., 1924, "Kinetic Theory of Viscosity, Conduction, and Diffusion."

in mass of the heavier molecule, and also a reduction in size,* it will be observed that the maximum separation has been slightly increased

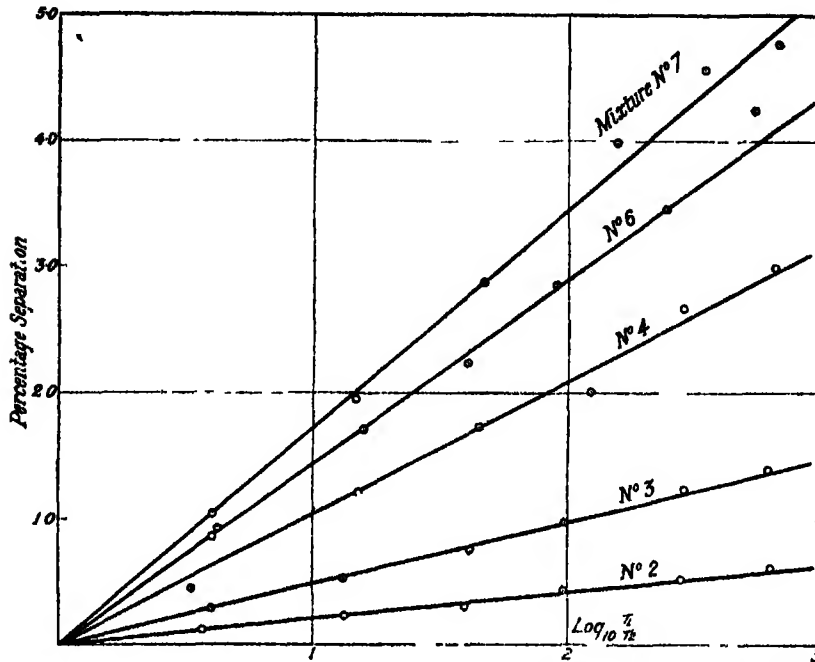


FIG. 5—Group II— H_2 and N_2 Relation between separation and $\log_{10} T_1/T_2$

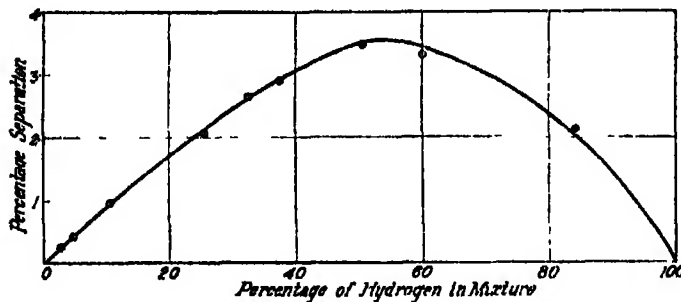


FIG. 6— H_2 and N_2 Relation between composition and separation ($\log_{10} T_1/T_2 = 0.2$)

Group III (Nitrogen and Carbon-dioxide)

Owing to the comparatively small mass ratio (3.14/1) of molecules of carbon-dioxide and nitrogen, we may expect the thermal diffusion effect to be less than that obtained in Groups I and II. The results may be valuable for purposes of

* Cf Jeans, 'Dynamical Theory,' page 327, 3rd edit.

theoretical comparison with Group I, the heavier diatomic gas nitrogen having been substituted for the light diatomic gas hydrogen

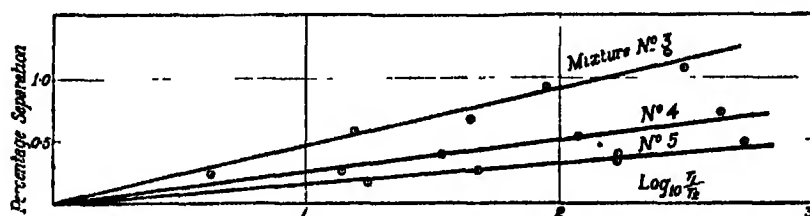
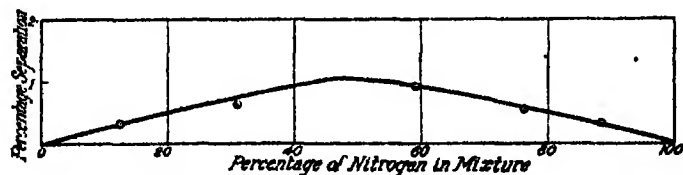
The five mixtures examined are shown in Table III

Table III

Mixture No	N ₂	CO ₂	Cold Side Temperature
	per cent	per cent	°C
1	12.6	87.4	12
2	26.0	74.0	11
3	59.4	40.6	9
4	76.5	23.5	11
5	88.0	11.4	11

Although the amount of separation and also the sensitiveness of the method are both reduced for this pair, the results obtained are sufficiently accurate to be dealt with as before

Fig 7 shows the relation between separation and $\log_{10} T_1/T_2$ for mixtures Nos 3, 4, and 5 Fig 8 shows the relation between composition and separation

FIG 7—Group III—N₂ and CO₂ Relation between separation and $\log_{10} T_1/T_2$ FIG 8—N₂ and CO₂ Relation composition to separation, as before

when $\log_{10} T_1/T_2 = 0.2$ The five points obtained lie on a decidedly symmetrical curve. It will be noticed that the separation obtained for a 20 per cent mixture of one of the gases is about the same as for a 20 per cent mixture of the other. This does not occur in any other group examined.

A point of interest which has already been mentioned is the slowness with which the effect takes place for this pair of gases

Group IV (Hydrogen and Argon)

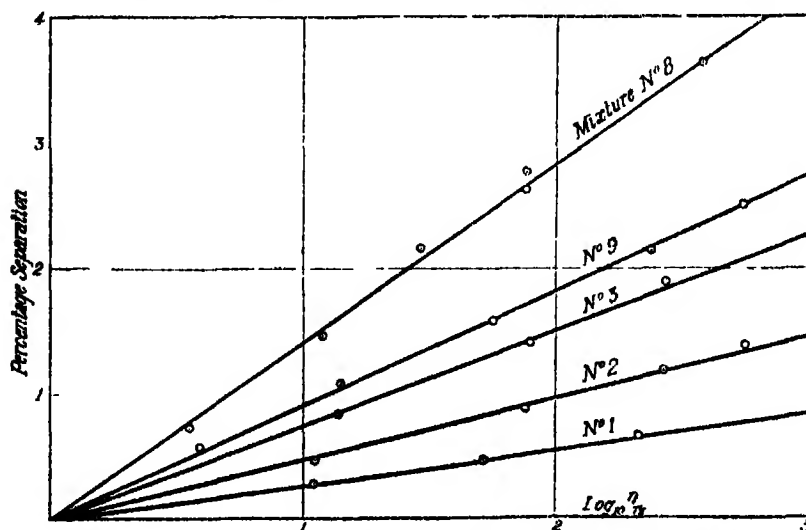
This pair of gases was selected so that a comparison could be made with the results obtained for carbon-dioxide and hydrogen, the mass ratio of the molecules in the two cases being nearly the same (reduced from 22/1 to 19.9/1)

The ten mixtures examined are shown in Table IV

Table IV

Mixture No	H ₂	A	Cold Side Temperature
	per cent	per cent	°C
1	6.0	94.0	16
2	11.0	89.0	17
3	16.1	83.9	16
4	25.7	74.3	15
5	35.5	64.5	12
6	52.8	47.2	11
7	63.7	36.3	11
8	73.5	26.5	15
9	85.0	15.0	13
10	92.2	7.8	15

Fig. 9 shows the relation between separation and $\log_{10} T_1/T_2$ for mixtures Nos. 1, 2, 3, 8, and 9. Fig. 10 shows the relation between composition and

FIG. 9.—Group IV.—H₂ and A. Relation separation and $\log_{10} T_1/T_2$.

separation when $\log_{10} T_1/T_2 = 0.2$. This curve is of the same shape, but is a little more symmetrical than the one obtained for carbon-dioxide and

hydrogen, and the maximum amount of separation is about the same. The small argon molecule is thus as effective as the bigger carbon-dioxide molecule.

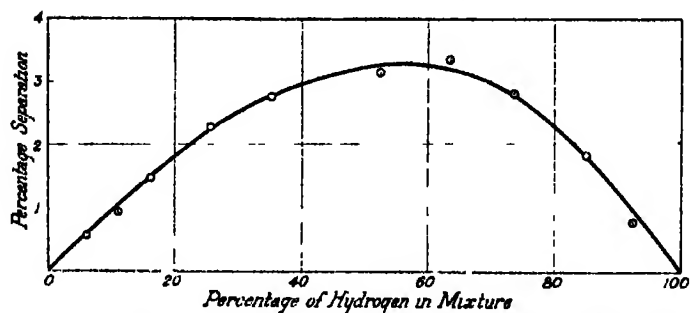


FIG. 10 — H_2 and A. Relation composition to separation, as before.

Group V (Helium and Argon)

It was important to obtain measurements on a pair of monatomic gases. Argon and helium, with a molecular mass ratio of 9.8/1, were selected as most suitable for the purpose. I am indebted to Prof. J. C. McLennan, through Dr. Shakespear, for supplying the helium used in the experiments.

The mixtures examined are shown in Table V. Mixtures containing more than 71 per cent of helium were not made, as the supply of the gas available for these experiments was limited. The nature of the effect, however, is well shown.

Table V

Mixture No.	He	A	Cold Side Temperature
	per cent	per cent	° C.
1	3.3	96.7	17
2	5.8	94.2	19
3	11.2	88.8	19
4	18.5	81.5	17
5	27.7	72.3	18
6	38.1	61.9	18
7	48.8	51.2	18
8	57.0	43.0	17
9	70.8	29.2	17

In fig. 11 is shown the relation between separation and $\log_{10} T_1/T_2$ for mixtures Nos. 1, 3, 4, 6, and 9. Fig. 12 shows the relation between composition and separation when $\log_{10} T_1/T_2 = 0.2$.

It is interesting to observe that this monatomic pair gives the greatest separation obtained in the experiments. Mixture No. 9 (70.8 per cent. helium

and 29.2 per cent argon) gives a separation of 4.5 per cent when $\log_{10} T_1/T_2 = 0.2$. The separation for a 50 per cent mixture is 0.64 of the amount

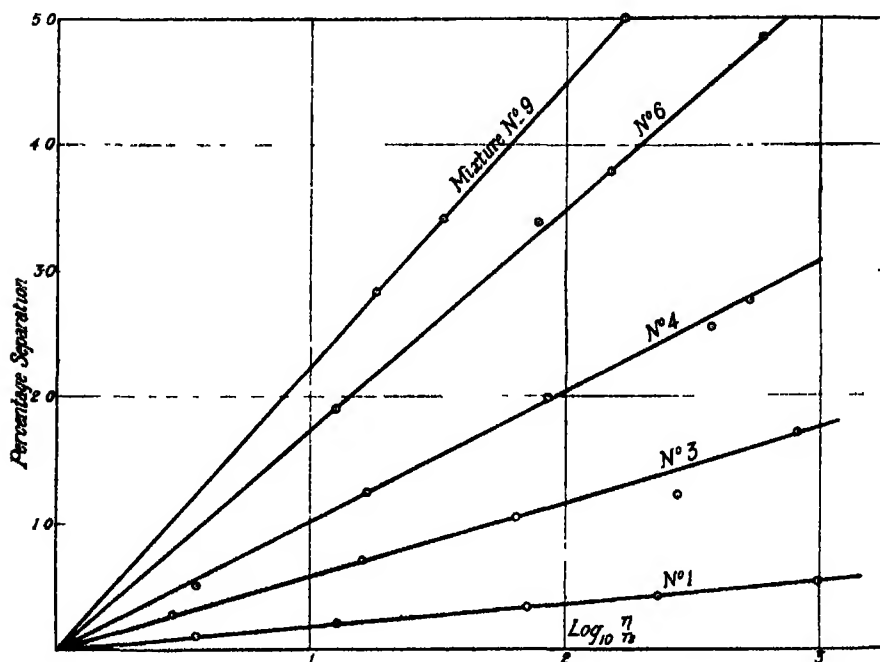


FIG. 11 —Group V —He and A Relation separation and $\log_{10} T_1/T_2$

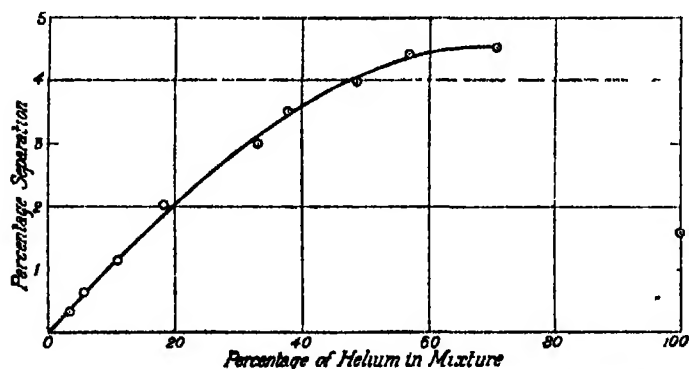


FIG. 12 —He and A Relation composition and separation, as before

calculated by Chapman and Hainsworth for these gases, on the assumption that the molecules behave as rigid elastic spheres.

In fig 12 the percentage of helium shown is that of the gas, together with the small amount of impurity. The separation shown for 100 per cent helium

is the proportional effect due to the impurity, and the completed curve for the mixtures would pass through this point. After allowance has been made for the impurity, the maximum separation is still given with a greater proportion of the lighter gas in the mixture (in the neighbourhood of 65 per cent) than for any other group.

The results as expressed in the composition-separation diagrams Nos 4, 6, 8, and 10, show the general influence of the mass ratio of the molecules on the symmetry of the curves. No 12, for helium-argon, suggests that the mass ratio may not be the only determining factor, and that the shape may be influenced to some extent by the nature of the molecules.

The results of this paper were communicated before publication to Prof S Chapman, who, with Mr W Hainsworth is preparing a discussion of their bearing on the question of the intermolecular fields.

Overvoltage and Transfer Resistance

By EDGAR NEWBERY, D Sc, F I C, University of Cape Town

(Communicated by Prof Sir E Rutherford, F R S --Received November 25, 1924)

[PLATES 9-11]

Introductory—During the last ten years there has been much controversy as to the correct method of measuring the overvoltage of an electrode in an electrolytic cell. One body of workers considers that it should be measured during the passage of current through the cell, whereas another maintains that the current should be interrupted by means of a rotating commutator or similar device before the electrode in question is connected to the potentiometer or other measuring instrument.

The question is one of considerable importance, as the results obtained by the two methods differ widely in magnitude and behaviour, and no theory of overvoltage can be generally accepted until this controversy is settled.

The vital point at issue may be shortly stated thus:—(a) Is the total opposition to the passage of current from electrode to electrolyte due to an active back electromotive force? or (b) Is a part of this opposition due to a passive resistance? In other words, is the whole of the fall of potential from electrode to electrolyte reversible, or is a part of it irreversible?

Our definition of the term "overvoltage" must rest upon a satisfactory answer to these questions, for if (b) is answered in the affirmative, it is quite as incorrect to speak of the irreversible part as a voltage as it is to speak of the voltage of a resistance coil

Possible Methods of Attack—The author has felt for some years that the above question can be satisfactorily answered only by tracing out the complete time-potential curve of an electrode when the existing current is made and broken. To do this perfectly, an oscillograph having infinite resistance, infinite frequency, and a sensitivity of not less than 1 cm per volt, would be required. The Duddell oscillograph has a very high frequency and sensitivity, but the resistance is usually less than 10 ohms. Hence, from a small electrode so much current would be taken that the true single potential would not be indicated. The string electrometer has high resistance and high sensitivity, but its frequency is of the order of 200 per second. As the total period of the make-and-break of the current is sometimes 1/100th second, such an instrument would be quite unsuitable. The cathode ray oscillograph has nearly infinite frequency and is almost electrostatic in action, but the sensitivity of the common types is about 1 cm per 100 volts. The more recent types of cathode ray tubes, in which the electrons are expelled from a heated filament and directed on to a screen with the aid of moderate voltages (200 to 500), show a much higher sensitivity, but the best of these only give 1 mm deflection for 1 volt. It is possible, however, with the aid of thermionic valves, to amplify the electromotive force given by the experimental cell, and it was finally decided to proceed along these lines.

This work was hampered for three years by lack of funds and much time wasted by the author attempting to produce home-made tubes, but a generous grant from the Royal Society overcame this difficulty.

Experimental—The apparatus used is somewhat complicated in appearance, involving no less than eight independent electric circuits. The oscillograph used was the Johnson cathode ray tube,* which requires a directing potential of 250–400 volts and has a maximum sensitivity of 1 mm per volt. The rays are emitted by a small Wehnelt cathode, and the beam, after passing through a small platinum tube which forms the anode, is prevented from spreading by the presence of a small quantity of argon, which gives rise to heavy positive ions in the body of the tube. The connections of the oscillograph itself are shown in fig. 1, but the second pair of deflecting plates was not used in this work, and was therefore short-circuited and connected to earth.

* 'J Opt Soc Amer,' vol 8, No 7 (1922).

The general arrangement of the apparatus is shown in fig 2 The main battery B_1 , 12 volts, is connected directly to two rheostats of 35 ohm and

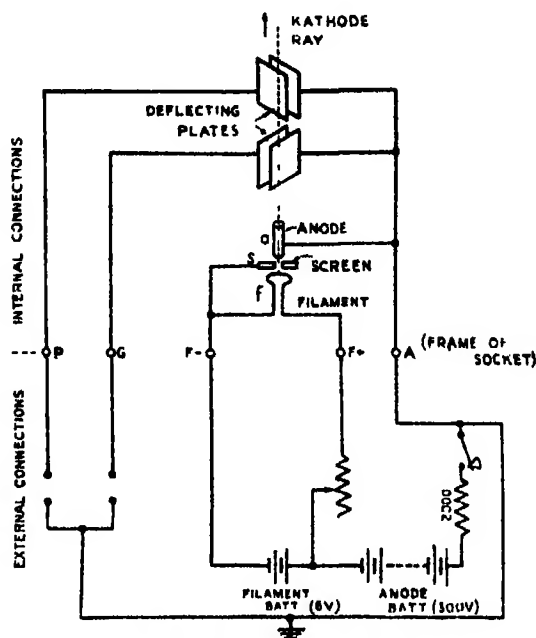


FIG 1—Cathode ray oscillograph Diagram of connections

8.5 ohm respectively, and any desired voltage from 0 to 12 may be tapped off from the sliding connections to these rheostats. The current then passes through a 3-scale milliammeter MA and a rotating contact breaker CB to the experimental cell C, which consists of a rectangular plate-glass cell 10 cm. high, 6 cm wide, and 1 cm thick (internal measurements). The cathodes used were generally in the form of plates 1 cm. wide, and consequently the jet of the standard mercurous sulphate electrode, when placed behind the cathode, was outside the field of current flow between anode and cathode. The contact breaker was divided into four equal sections and was rotated uniformly at 200 revolutions per minute. Hence the current was made and broken for equal intervals of 0.075 second.

The experimental cathode and the standard electrode were connected through the switch S_2 to the filament and grid of a thermionic valve V. By reversing S_2 , a known potential difference from the potentiometer P could be applied to the terminals of the same valve. The filament and plate of this valve were connected through a high resistance R_4 (150,000 ohms) to a battery B_4 of 30 dry

cells, 45 volts, and the terminals of R_4 connected directly to the deflecting plates of the oscillograph O. The directing potential for the cathode rays between

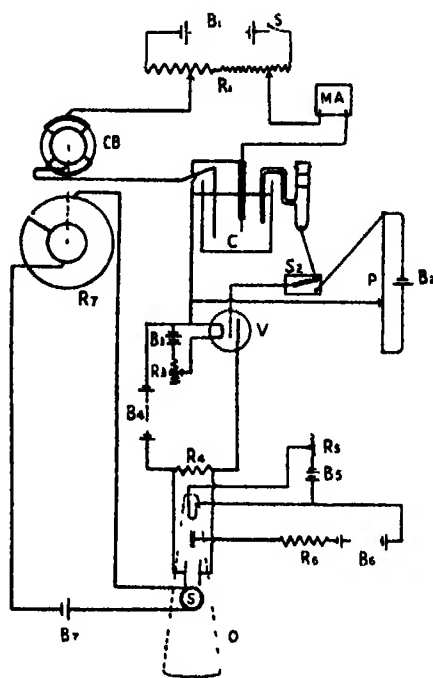


FIG 2

the Wehnelt cathode and the platinum tube was applied from the high-tension battery B_6 (275 volts) through the resistance R_6 (50,000 ohms)

With this arrangement a difference of potential of 1 volt between the experimental cathode and the standard electrode gave a deflection of about 1 cm, depending partly upon the current passed through the valve filament. As the potential of the cathode varied, the spot of light traced out a vertical line on the oscillograph screen. In order to draw out this line into a curve various arrangements were tried—rotating or vibrating mirrors, moving photographic plates etc.—but the one finally adopted is shown in the figure.

Two solenoids S were fixed above and below the oscillograph tube parallel with the deflecting plates*. These solenoids were connected to a 2-volt accumulator B_7 through the resistance R_7 . This resistance consisted of a platinum wire 0.2 mm. thick fitted on the circumference of a 3.5-inch ebonite disc rotating on the same axle as the contact breaker CB . One end of this wire was

* In the figure, for the sake of clearness, these plates are shown at right angles to their real position.

pinned to the ebonite, and the other end connected by a strip of copper to a continuous brass ring on the same axle, the distance between the ends being about 1 mm. Contact with the wire was made by means of a small platinum brush, made of a number of bits of thin platinum foil soldered to the end of a piece of watch spring. This arrangement has therefore the effect of drawing the oscillograph spot with fairly uniform velocity horizontally across the screen, together with a flyback action which is practically instantaneous. Since the rotation of the resistance is always in phase with that of the contact breaker, the pattern described on the screen will be exactly repeated as long as the periodic changes of potential of the experimental cathode remain the same.

This arrangement for recording the single potential of the cathode is not perfectly electrostatic as it should be under ideal conditions, but it is nearly so. The current passing between the cathode and the standard electrode is usually only a fraction of a micro-ampere, and even under extreme conditions—very high current density and high filament current—it does not exceed 10 micro-amperes, and the large surface of the standard electrode used may, therefore, be relied upon to maintain a constant single potential.

The photographs (Plates 9-11) were taken with an ordinary $\frac{1}{4}$ -plate stand camera, using two 2-inch diameter quartz lenses and Barnet orthochromatic plates. The cathodes used were copper, silver, zinc, cadmium, mercury, thallium, graphite, lead, chromium, nickel, and platinum, all of approximately 1 square centimetre area.

The plates were exposed for 30 seconds to the curve-tracing spot of light and then the switch S_2 was reversed and the potentiometer adjusted in three positions, giving 0.0, 0.9, and 1.8 volts respectively, and the plates exposed for 10 seconds with each position, the solenoid circuit B_2R_2 being cut out. The three spots thus marked on each plate enable an estimate of the single potential of the cathode to be made within 0.1 volt. Since the electrolyte used was NH_4SO_4 in all cases, and the potential difference between a hydrogen and a mercurous sulphate electrode in this liquid is 0.7 volt, overvoltages at any instant may be measured by the height of a point on the curve above a horizontal line representing 0.7 volt.

The current density employed in most cases was 0.1 ampere per square centimetre, with an applied E.M.F. of about 4 volts. Where other current densities were employed, the fact is definitely stated.

Discussion of Results—Inspection of the photographs reproduced will at once show that the nature of the curves obtained varies greatly with the cathode material. The factors which have been previously shown to have an

effect on overvoltage also have an influence upon the curves, but it was also observed that whereas the relative positions of the upper and lower portions of the curves were chiefly affected by the nature of the cathode and the current density, the shape of the lower portions was more affected by time and by the previous history of the electrode. This change of shape with time is very marked with certain electrodes, notably lead and mercury, and renders it difficult to obtain clear photographs in the 30 seconds required for exposure.

One point is brought out quite clearly by all the photographs, and that is the large instantaneous drop of potential when the main current is interrupted. In some cases this amounts to nearly 2 volts, and the least value observed with 0.1 ampere per square centimetre is 0.5 volt. This instantaneous change of potential must be due to an irreversible resistance effect between the cathode and the electrolyte. The question stated in the introduction as the main object of this work may therefore be definitely answered—the total opposition to the passage of a current from electrode to electrolyte is made up of two distinct parts, one reversible (true overvoltage) and the other irreversible (transfer resistance).

Attempts to measure overvoltages without the use of a commutator will, therefore, lead to errors of at least 0.5 volt, and possibly 2 volts, when the current density is 0.1 ampere per square centimetre. At this current density, therefore, the transfer resistance is from 5 to 20 ohms per square centimetre. At higher current densities the transfer resistance is lower, although the instantaneous voltage drop is greater. At very low current densities it may rise to high values, the greatest so far observed with this apparatus being 100 ohms per square centimetre at a mercury electrode with a current of 0.001 ampere per square centimetre. The condition of the electrode surface also is an important factor in determining the magnitude of the transfer resistance, rough surfaces showing lower values than polished surfaces, but the whole question needs further investigation, and work along these lines is now being carried out.

Overvoltage Measurements—It has already been stated that the overvoltage of the electrode at any instant after the current has been interrupted may be found by measuring the distance between a point on the corresponding part of the curve and a horizontal line representing 0.7 volt above the zero line, and comparing this distance with that between the points at the left of the photographs representing 0.0, 0.9 and 1.8 volts. The true overvoltage while the current is flowing will therefore be represented by the distance between

the line representing 0.7 volt and the highest point on the lower portion of the curve

In most cases the measurement of this distance presents no difficulty. Thus in the case of zinc and chromium the lower portions of the curves are horizontal straight lines and measurements may be taken from any portion. In the case of copper, silver, graphite, nickel, and platinum, the extremities of the turned-up ends of the curves are definite and clearly marked. On the other hand, with thallium, lead, and mercury these extremities are in many cases indistinct in the photographs, and if we had nothing else to rely upon, there might be some justification for contending that the curves are really continuous. This indistinctness is, however, much more marked in the photographs, which represent about 100 tracings superimposed on each other, than appears when the curves are viewed with the eye on the screen itself. To an eye rested for 10 minutes in the dark room the upper ends of the lower curves appear perfectly sharp and removed by a very definite gap from the upper curves, but at the same time the spot is moving more rapidly while these upper ends are being traced out. The indistinctness is therefore due to underexposure of the upper part of the lower curves and not to continuity of the curves.

Some idea of the effect of time may be obtained by comparing figs. "n" and "o" for lead, or "s" and "t" for mercury. In each case there appears to be a tendency for the lower sections of the curves to assume angular forms, the upper part of each section becoming less marked, but it is remarkable that although the shape of the curve changes, and also the position of the lowest portion of the curves, yet the position of the tip of the lower portion (from which the overvoltage is measured) is very little changed by time or current density. This result appears to indicate that the effects of time and current density upon overvoltage have been somewhat overestimated. On the other hand, transfer resistance, which largely determines the position of the upper sections of the curves, is greatly affected by both of these factors, the thickening of these sections in the photographs being due to the time effect. There is, however, insufficient data at present to draw very definite conclusions as to the general behaviour.

Comparison of these Results with those Obtained by Other Methods.—The author has previously* attempted to obtain reliable values for the hydrogen overvoltage of various cathodes by using the usual commutator method, and varying the speed of the commutator. By extrapolating to infinite commutator speed, values were obtained in most cases which were considered to be very

* 'J. Chem. Soc.,' vol. 121, p. 7 (1922), and vol. 125, p. 511 (1924).

near those existing while the current was flowing. The reliability of this method may be estimated from the following table

(Current density 0.1 ampere per square centimetre.)

Metal	Overvoltage by Oscillograph	Overvoltage by Variable Commutator
Copper	0.5	0.37 rising
Silver	0.3	0.30
Zinc	0.7	0.70
Cadmium	0.7	0.57 rising
Mercury	0.7	(0.83)
Graphite	0.7	0.52
Lead	0.9 to 1.0	0.50 rising
Chromium	0.4	0.41
Nickel	0.4	0.22 rising
Platinum		0.07

With copper, cadmium, lead, and nickel the commutator rotating at 1500 revolutions per minute gives low results, but also indicates the fact that these results are low. The results obtained with graphite and platinum probably owe their differences to the electrodes showing different overvoltages in the two experiments, due to variations in the nature of the surfaces and previous history of the electrodes. The values for mercury are not strictly comparable, as that given in brackets was obtained at a lower current density.

It is evident, therefore, that although the commutator method as described gives reliable results in some cases, a maximum frequency of 1500 per minute is too low, and some arrangement similar to that described by Glasstone* (which would reduce the time during which no current is flowing, and the potential measurement is taken to 0.001 second or less) would appear to be desirable for general work.

The Theory of Overvoltage—As the result of work on this subject extending over the last ten years, the author has suggested that cathodic overvoltage is due to the presence of solid solutions of metallic hydrides in the electrode surface.

Although no single phenomenon has yet been found which is definitely inconsistent with this theory, so many workers have objected to the hypothesis of hydride formation (which at present appears to be not adapted to direct

* 'J. Chem. Soc.', vol. 123, p. 2927 (1923).

proof) that the author began this work to a certain extent prejudiced against his own theory, and determined to study critically any phenomena which could possibly discredit it. In spite of this attitude of mind, the whole of the evidence obtained appears to be entirely in favour of the above theory, and this is particularly the case with the remarkable curves shown in fig "p". The two upper sections of these curves were obtained in the usual way with a lead cathode, and are almost identical with fig "n". The time of exposure was 30 seconds. Then without touching any other part of the apparatus, the switch S_1 was turned off and the exposure continued for a further 45 seconds. For about 15 seconds the spot described a nearly straight horizontal line and then rapidly fell and described the lowest set of curves, of which the summits represent the potential of a hydrogen electrode.

It will be seen from the diagram (fig. 2) that cutting off S_1 allows the experimental cathode and anode (which was about four times the area of the cathode) to discharge periodically through the resistance R_1 via the contact breaker CB, whilst the variations of single potential of the cathode are registered by the oscillograph. If we now assume the formation of a solid solution of the hydride, the explanation of these curves is simple. The middle section indicates the gradual disappearance of the hydride phase with production of current, the single potential remaining constant. The comparatively long time required for this disappearance is due to the slow diffusion of the deeply imbedded hydride, or, what is practically the same thing, the comparative stability of the solid solution.

The current given by a charged cathode under these conditions is peculiar. If a very large-surfaced standard electrode is connected with the small experimental cathode through a micro-ammeter immediately after breaking the main circuit, the current registered by the micro-ammeter is mainly determined by the rate of diffusion of the hydride and is almost unchanged by the introduction of resistances up to 10,000 ohms or more, an apparent exception to Ohm's Law.

When all the hydride has been used up, the cathode behaves as a hydrogen electrode from which current is being taken periodically at a greater rate than can be compensated by the solution of more hydrogen in the metal.

At the end of the experiment bubbles of hydrogen were still clinging to the cathode. Other electrodes give similar curves, so that this is not a property of lead alone. After all the hydrogen bubbles have disappeared, the lowest curve takes the form of a horizontal straight line, as would be expected. Further investigation of these curves is in progress.

It is extremely difficult, if not impossible, to explain these phenomena by

Newbery.

Roy. Soc Proc , A, vol 107, Pl. 9.



a Cu



d Cd



b Ag



e Tl



c Zn



f C

[Facing p. 404]

Newberry.

Roy. Soc Proc., A, vol 107, Pl 10.



g Cr



l Pb 0.01 amp



h Ni



m Pb 0.05 amp



l Pt



n Pb 0.1 amp



o Pb 0.1 amp later



r Hg 0.05 amp



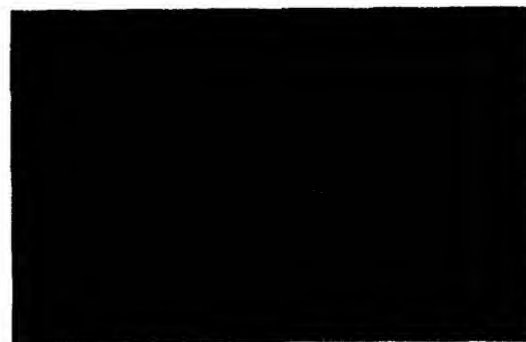
p Pb 0.1 amp



s Hg 0.1 amp



q Hg 0.01 amp



t Hg 0.1 amp later



u Hg 0.4 amp

means of any theory other than the hydride theory. The changes in the shapes of the curves with time may also be explained on the basis of the hydride theory. Lead and mercury show at least two distinct overvoltages, and therefore each forms at least two compounds. At a current density of 0.1 ampere per square centimetre the overvoltage of lead as measured by the commutator method tends to fall with time. Under similar conditions the overvoltage of mercury tends to rise. Comparison of fig. "n" with fig "o" shows that under these conditions the lower overvoltage compound of lead is produced more freely than the higher, and the electrode surface is saturated with the former compound in a comparatively short time, whereas the higher overvoltage compound is probably only formed in traces on the outer surface. Comparison of figs. "s" and "t" shows that under similar conditions the higher overvoltage compound of mercury is formed in such quantity that the potential of the lower ceases to exert any appreciable influence.

Summary.

The variations of the single potentials of a cathode during make and break of the current have been followed with the aid of a cathode ray oscillograph and a thermionic valve.

The results prove conclusively that transfer resistance is a real quantity, of anything but negligible dimensions, rising at least to 100 ohms per square centimetre under certain conditions.

Transfer resistance decreases with increasing current density, but its behaviour at very high and very low current densities has not yet been investigated.

The direct method of measuring overvoltage cannot be relied upon under any circumstances, as it includes not only the true overvoltage, but also the fall of potential across the variable transfer resistance.

The commutator method of measuring overvoltage gives reliable values, if the results obtained with varying commutator speed are extrapolated to infinite speed, but with certain cathodes it is necessary to obtain speeds at least equivalent to 1,000 per second in order to carry out satisfactory extrapolation.

All the phenomena observed are readily explainable on the hydride theory of overvoltage.

In conclusion, the author wishes to express his gratitude to the Royal Society for the grant which enabled him to purchase the oscillograph, and to Dr. B. Schonland for assistance and suggestions in connection with the thermionic valve.

The Magnetic Properties of Iron Crystals.

By W L WEBSTER, B A , 1851 Research Student of the University of Toronto

(Communicated by Prof Sir E Rutherford, F R S —Received December 5, 1924)

§ 1 *Introduction*

Comparatively little work has so far been done on the magnetic properties of ferro-magnetic crystals, and it has been confined to substances for which the saturation value of the intensity of magnetisation is small P Weiss, the chief worker in this field, did experiments on pyrrhotine, which has a saturation value of 47 absolute units It is found that, for these crystals, the direction of the magnetisation does not, in general, coincide with the direction of the applied field To account for this deviation, Weiss postulates a "molecular field" due to the mutual action of the molecules of the crystal He finds that this molecular field has components along the crystallographic axes, and that for any axis the component of the molecular field is proportional to the component of the magnetisation along that axis The proportionality factor may vary for different axes Weiss calculates values for the molecular field, which would account for the deviation of the magnetisation from the applied field, and finds values of the order of 100,000 gauss

It is obviously important to verify the extension of this theory to crystals of iron, which has a much larger saturation value for the magnetisation (about 1,600 abs units) We have been able to obtain through Miss Flam, of the Imperial College of Science, some crystals of iron large enough for the purpose of the investigation

It is to be noticed that, as iron has a cubic structure, the proportionality factor must be the same for all the axes, and therefore that the component of the molecular field along any axis cannot be simply proportional to the magnetisation along that axis For then the resultant molecular field would be in the direction of the magnetisation and could produce no deviation (See § 8.)

§ 2 *Method of Investigation*

A thin disc is cut out of the crystal, its plane being parallel to one of the (1, 0, 0) planes of the crystal The diameter of the disc is about 4 mm and the thickness about 0.4 mm It is important to make the disc thin, in order to reduce the demagnetising field as far as possible.

It is necessary to measure, for different values of the applied field, the direction

and magnitude of the intensity of magnetisation, as the direction of the applied field varies in the crystal

The measurement of the magnetisation is divided into two parts

- (a) The measurement of the component of the magnetisation *parallel* to the magnetising field
- (b) The measurement of the component *perpendicular* to the field

The methods used in both cases are essentially the same as those used by Weiss ('*Journal de Physique*,' vol 4, p 469 (1905), vol 6, p 655 (1907)) The couple exerted by a magnetic field H , on a body uniformly magnetised with an intensity I , is given by

$$C = H I \sin \phi \ v,$$

where v is the volume of the magnetised body, and ϕ is the angle between the directions of H and I

In our experiments, C is measured by balancing it against the couple of a torsion fibre H and v were known, so that $I \sin \phi$ could be determined This gives the component of the intensity of magnetisation perpendicular to the applied field The method for determining the parallel component will be considered below See § 4

§ 3 Apparatus

The apparatus used consists of an electro-magnet, torsion-head suspension system, and the case containing the suspension The electro-magnet was quite large Using pole pieces, with face area of about 30 sq cm, and a separation of 1.6 cm, fields up to 9000 gauss could easily be obtained The field was found to be quite uniform, and was measured with a ballistic galvanometer. The current was taken from a battery of accumulators, but, as these were not independent, was found to vary appreciably This made an accurate valuation of the field difficult The magnet is mounted on a strong turn-table, so that it is capable of rotation about a vertical line midway between the pole faces.

The assembly of the torsion-head and suspension is shown in fig 1 The central rod of the torsion head is threaded, and by means of two lock-nuts may be adjusted to any height This is desirable as the length of the torsion fibre or of the suspension may be varied A pointer was provided for use with a circular scale graduated in degrees But it was more accurate to measure the angle of torsion by a scale and mirror combination A small plane mirror was fixed on to the torsion head, and through it a metre scale could be viewed with a telescope. The scale-mirror distance was 240.4 cm, and the angles could be read to less than a minute The central rod carried

at its lower end a small brass spring, which protected the torsion fibres from shocks during the adjustment.

The suspension system consists of a long straight piece of brass wire. At

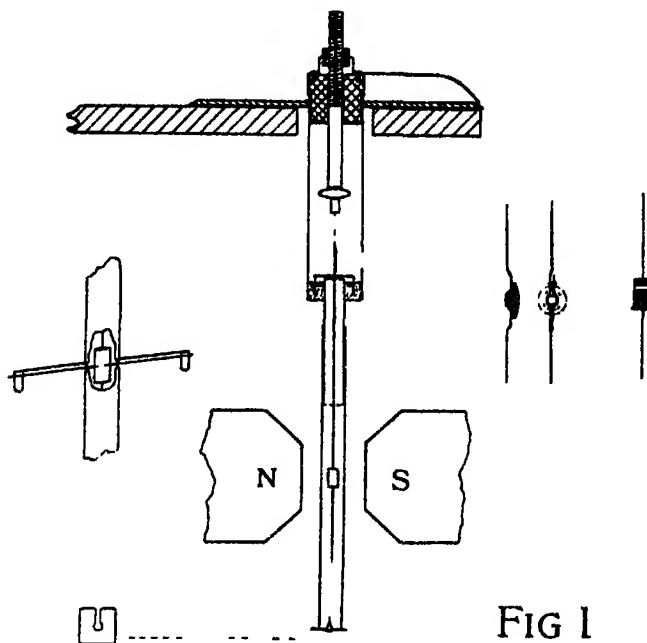


FIG 1

the upper end this carries a galvanometer mirror, and a pair of arms which dip into an annular trough, containing light oil, and carried by the case. This provides damping for the system. To overcome the attraction of the pole-pieces on the iron disc, a heavy brass weight was attached to the lower end of the suspension. For very strong fields it was better to hold the lower end by a second torsion fibre, held down by the casing tube. The crystal container, carried in the middle of the suspension, differs for the measurement of the two components. The two forms are shown in fig 1. For the parallel component the disc is carried with its plane vertical, on a rotatable spindle, at the other end of which is a brass disc carrying a scale graduated in 10-degree divisions. For the perpendicular component, the disc is carried with its plane horizontal, inside a brass cup. The disc is fastened in place with a trace of bees-wax. Care was taken to have the disc on the axis of the rod.

When measuring the component perpendicular to the field, the suspension was found to have positions of instability, the cause of which will be considered later. To take readings in this region it is necessary to reduce the free motion

of the suspension to 4 or 5 degrees. This is done by attaching a horizontal pointer to the suspension, and limiting its motion by stops fixed to the case (fig 1)

Torsion fibres of phosphor-bronze were used. Wires with a diameter of 0.008 inches, and about 1 cm in length, were generally convenient. It is convenient to hold the fibre in small brass clamps, into which the suspension may be screwed. It is then possible to interchange the two suspensions or, by attaching a bob of known inertia, to find the torsion constant of the fibre in position.

The torsion-head is fastened to a strong support fixed firmly to a stone bench, and its position is adjusted so that the axis of the torsion-head and of the suspension coincides with that of the magnet.

§ 4 Procedure

The torsion constant of the fibre having been found, the suspension is assembled and the disc put in place. The system is then adjusted till the disc-container is in the middle of the magnetic field. The torsion head is put in its zero position, and the zero position of the suspension (in the absence of a magnetic field) is noted. This is done by using the galvanometer mirror on the suspension, with a lamp and a scale, distant about 2.5 metres. It can be fixed in less than a minute.

Now, if we are measuring the parallel component, we apply the magnetic field and rotate the spindle through about 40 degrees, so that the disc is in position for the first reading. Then rotate the magnet till the suspension is in its zero position. This gives the zero position of the magnet, and we assume that the magnetic field is then parallel to the plane of the disc. The magnet is rotated through an angle of about 5 degrees, and the rotation of the torsion-head, which is required to return the suspension to its zero position, is noted. The spindle, bearing the disc, is then turned through about 10 degrees, and the process repeated. The zero position of the magnet must be found for each position of the disc, as there may be a slight wobble in the spindle. And, as the 5° rotation of the magnet must be repeated exactly, it is measured by means of a lamp, mirror and scale, which is calibrated by comparison with a circular degree scale on the magnet. The angle may then be repeated to about 1 minute. The desired series of readings may thus be obtained for any particular field strength.

Now let I' represent the projection of the magnetisation in the horizontal

plane (and this is the parallel component we wish to measure). Then we have directly,

$$I' = \frac{C}{H \cdot v \sin 5^\circ}.$$

In deriving this formula, we assume that the demagnetising coefficient for the direction perpendicular to the plane of the disc is so large that the direction of magnetisation remains in the plane of the disc. This is not the case, but we shall correct for this below.

If we are measuring the component of the magnetisation perpendicular to the field, we find, as before, the zero position of the suspension with no magnetic field. We then apply the magnetic field, and rotate the magnet through about 50 degrees to the position for the first reading. For this position of the magnet we measure the rotation of the torsion-head required to return the suspension to its zero position. We then apply our original formula (§ 2), and have,

$$I \sin \phi = \frac{C}{H \cdot v},$$

giving the required component. We now rotate the magnet, in the same direction as before, through about 5 degrees, and repeat the readings.

In the region of instability, we find it impossible to hold the suspension in its zero position by adjusting the torsion head. When we attempt to bring the suspension back to its zero position, it suddenly flies beyond it. As will be seen later, this instability is not due to instability in the crystal, but is a result of the method used. We may get rid of it by using heavier torsion fibres.

It is necessary to be able to refer the results to a known direction in the crystal disc. A fine line is scratched on the disc, and its direction relative to the suspension is noted when the disc is put in place. The direction of the magnetic field when parallel to the scratch may be determined to 4 or 5 degrees.

§ 5 *Results.*

Two crystal discs have been examined, we shall refer to them as discs A and B.

A—This disc was cut from a large crystal obtained from a blast furnace. Three (1, 0, 0) crystal faces were present, and the disc was cut from one of them. The dimensions of the disc are:—

$$\begin{aligned} \text{Diameter } (c) &= 4.74 \text{ mm.} & \text{Thickness } (a) &= 0.369 \text{ mm.} & \text{Volume } (v) \\ & & & & = 0.00650 \text{ c.c.} \end{aligned}$$

The demagnetising coefficient (D) = $\pi^2 (a/c) = 0.771$. (Maxwell, '*Elect. and Mag.*' vol 2, p. 65)

B.—The crystal from which this disc was cut was produced by Edwards, of Swansea University. The axes were determined by X-ray analysis, and the disc cut out parallel to a (1, 0, 0) plane. This was done to within 1 or 2 degrees. The dimensions of this disc are —

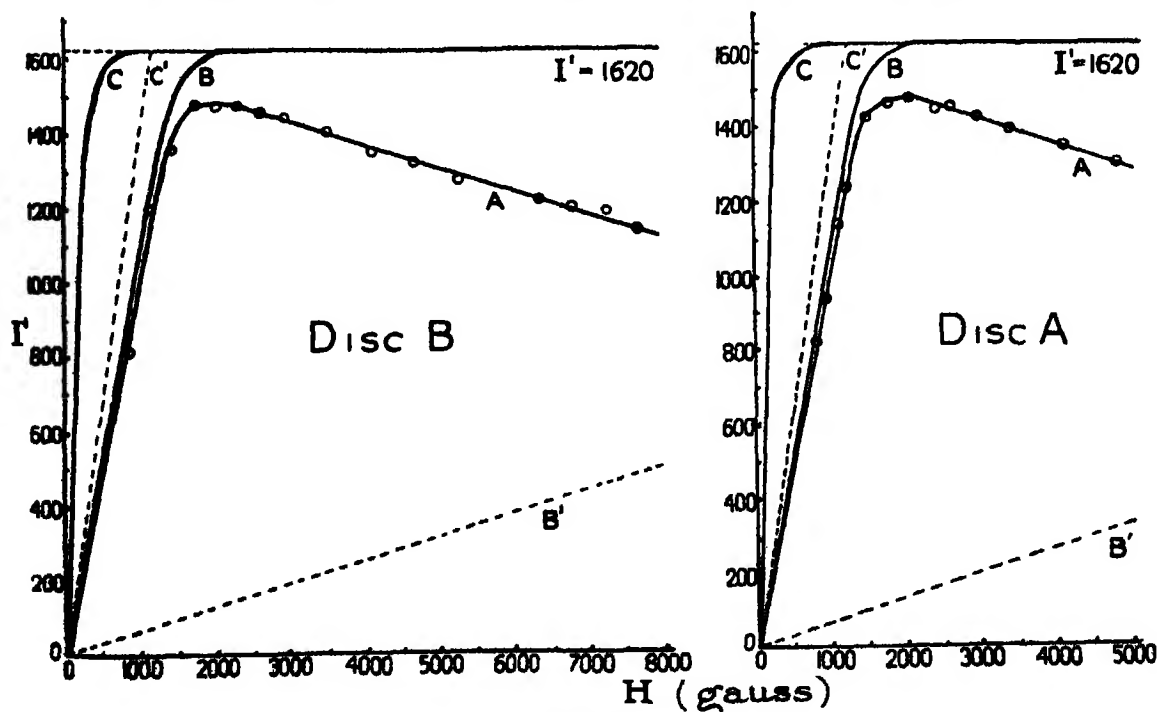
$$\text{Diameter} = 4.10 \text{ mm} \quad \text{Thickness} = 0.305 \text{ mm}$$

$$\text{Volume} = 0.00375 \text{ c.c.}$$

The demagnetising coefficient = 0.734. The results are quite similar for both discs.

§ 6. Magnetisation Parallel to the Field

We measure this component of the magnetisation for different field strengths, and plot the I - H curve. This is shown in graph 1, curve A. The curve rises sharply to a maximum, and then falls off linearly. This falling-off is due to the presence of a component of magnetisation perpendicular to the plane of the disc. To correct for this, we draw B' with the same slope as the decreasing part of A. We add the ordinate values of B' to A, and



GRAPH 1.

obtain the corrected curve B. This curve gives the true saturation value of the magnetisation. We may also correct the curve for the demagnetisation field by subtracting the abscissa values of C' from the curve B. The slope of C' is given by the demagnetising coefficient, $1/H_D = 1/D$. This gives the true I-H curve C. The saturation value of the magnetisation is found to be the same for both discs, and equals 1620 abs units. Saturation occurs at about $H = 1000$ gauss, and we have then

$$B = 21,200 \text{ abs units}$$

The demagnetising force is then equal to 1190 gauss for disc B.

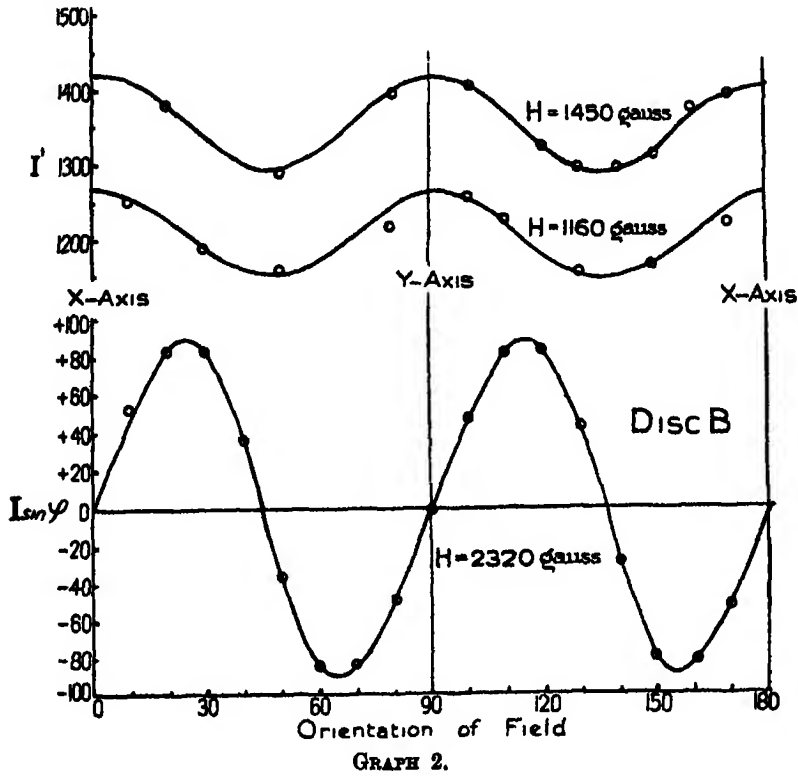
No variation in the magnetisation, for a given field strength, could be detected except in the region just below saturation (from $H = 1000$ gauss to $H = 1800$ gauss). Here, as the magnetic field changes direction with regard to the disc, the magnetisation varies regularly with a period of 90 degrees. (See graph 2.) The maximum values occur when the field is parallel to one of the crystallographic axes in the plane of the disc. The value plotted on the I-H curve is the average over a period. But as our calculations are carried out for fields giving approximately saturation, this variation does not enter into them.

§ 7 *Magnetisation Perpendicular to the Field.*

The variation of this component is shown in graph 2, for $H = 2320$ gauss; the variation of the parallel component for the same orientations is shown for $H = 1450$, and $H = 1160$ gauss. The perpendicular component also has a period of 90 degrees, but its value is zero when the magnetic field is parallel to one of the crystallographic axes. In the graph the field is parallel to one of the axes, for the orientations 0, 90, 180 degrees. The component is also zero for orientations midway between the axes. The regions of instability mentioned above occur for orientations about 10 degrees on either side of this position.

In fig. 2, let X and Y represent the crystal axes in the plane of the disc. Suppose the field H to be applied in a direction about 40 degrees from the axis of X, so that it is in the region of instability, then the direction of the magnetisation will be between H and X, and will lie two or three degrees from H. The suspension will then turn in an anti-clockwise direction. To restore the suspension to its zero position, the torsion head must be moved in a clockwise direction. But as we bring the suspension back, the magnetisation perpendicular to the field decreases, thus decreasing the magnetic couple. The

torsion couple then becomes predominant, and forces the suspension beyond its zero position



GRAPH 2.

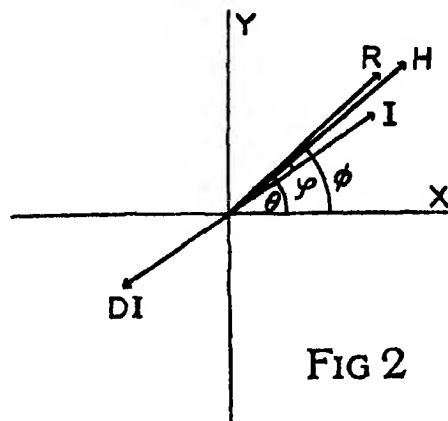
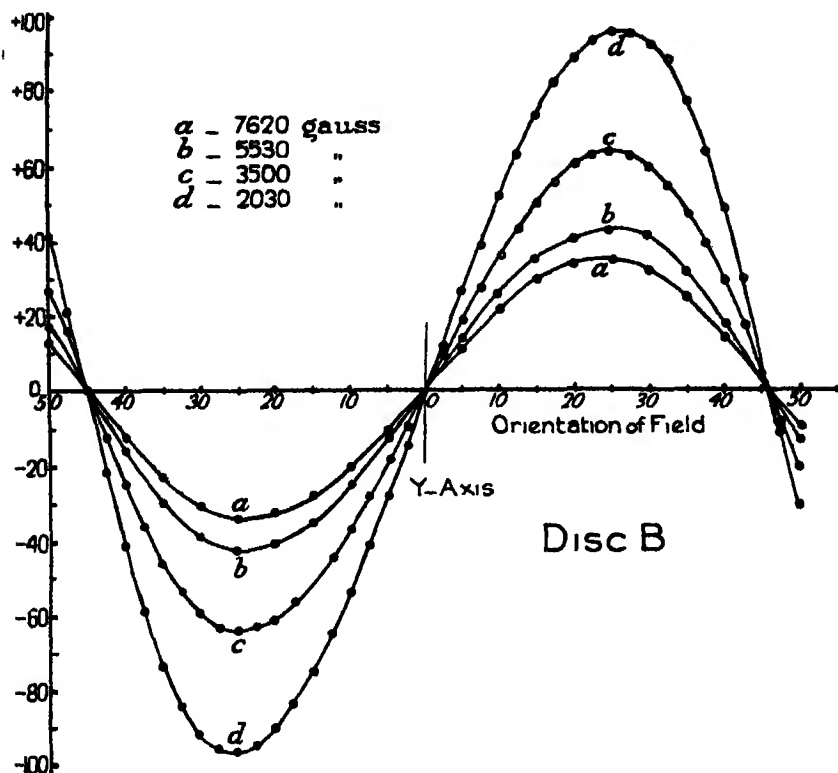


FIG 2

In graph 3 we give the curves for the perpendicular component for different field strengths. In this diagram the direction O represents one of the crystal

axes. The symmetry is seen to be quite good, showing that the crystalline structure of the disc must be fairly uniform

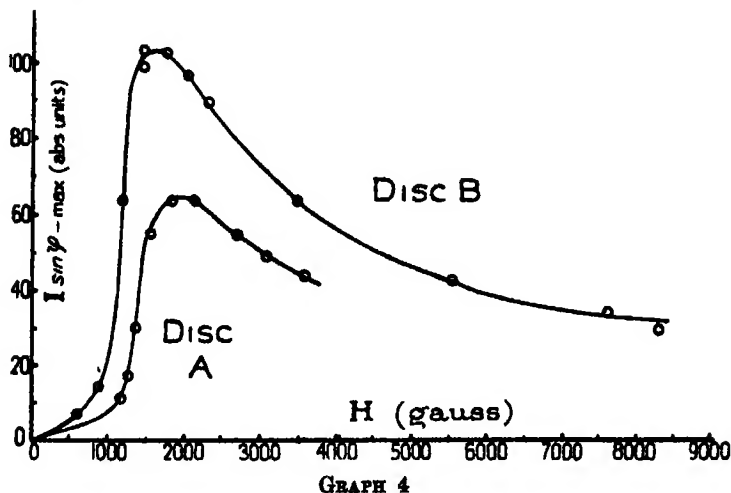


GRAPH 3

If, now, we draw a curve between the field and the maximum value of the perpendicular component, we see that at first this component is small and irregular, at about 1000 gauss it increases very rapidly, reaching a maximum at about 1800 gauss, and then gradually falling off (See graph 4)

The probable explanation of this effect is the non-uniform magnetisation with weak fields. The applied magnetic field has to overcome not only the demagnetising field, but also to a certain extent the molecular field. We have seen that the maximum demagnetising field is about 1200 gauss, and further on we find that the molecular field is about 600 gauss. This effect, in conjunction with the departure of our discs from perfect spheroidicity, is probably sufficient to prohibit a uniform magnetisation for applied magnetic fields of less than about 1800 gauss. The molecular field of the disc, while it seems to exist for applied fields of about 1000 gauss, cannot be at its full value

till much higher fields are reached. This increase to a limiting value is found to occur (See below.)



§ 8 Calculation of Molecular Field

In fig 2, let X and Y be the direction of the crystal axes in the plane of the disc. Let H be the direction of the applied magnetic field, and I that of the magnetisation. The direction of H is known, and that of I may be calculated from

$$\left(\tan \psi = \frac{\text{perpendicular component}}{\text{parallel component}} \right).$$

The direction and magnitude of the demagnetising field DI is known. We can then calculate the direction and magnitude of the resultant external field R. We have, the component of R perpendicular to the magnetisation is

$$R \sin (\phi - \theta + \psi)$$

Let M_x and M_y be the components of the molecular field along X and Y. Then these must contribute a component equal and opposite to $R \sin (\phi - \theta + \psi)$. M_x and M_y will depend on the direction of the magnetisation. Put

$$M_x = M \cdot f(\psi), \quad M_y = M \cdot f(90 - \psi),$$

where $\psi = (\theta - \phi)$, and $f(\psi)$ is some function of ψ .

Since iron has a cubic structure, one would expect the constant M to be the same for both axes. Weiss found the function $f(\psi)$ to be simply $\cos \psi$. In our case this cannot be, for the resultant molecular field would then have no component perpendicular to the direction of magnetisation.

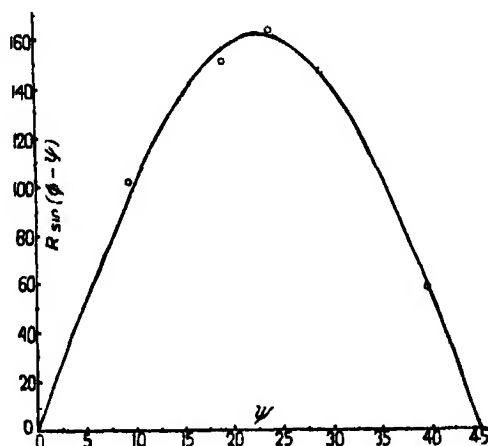
The resultant molecular field perpendicular to the magnetisation is given by

$$Mx \sin \psi - My \cos \psi = M[f(\psi) \sin \psi - f(90 - \psi) \cos \psi].$$

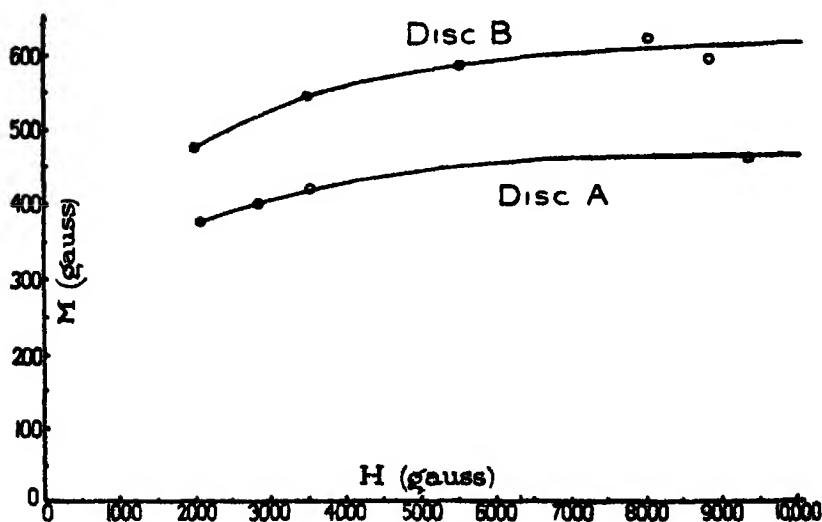
We must now determine values of M and $f(\psi)$, which will give

$$R \sin(\phi - \psi) = M[f(\psi) \sin \psi - f(90 - \psi) \cos \psi]$$

The value $f(\psi) = \cos^4 \psi$ was found to give the best agreement with experimental results. The experimental values $R \sin(\phi - \psi)$ are plotted for different values of ψ . A value of M is then taken which makes the curve, calculated from the right-hand side of the above equation, fit the experimental points—



GRAPH 5



GRAPH 6.

see graph 5, which shows the agreement obtained. For the case shown, $H = 7620$ gauss, and M is taken equal to 620 gauss

It is found that M , which we may call the molecular field, increases as H increases (see graph 6). This is to be expected if, as we assumed above, perfect alignment of the molecular magnets is not attained except for strong fields; we see that M tends to a limiting value. For the two discs measured this limit is ·

Disc B, 620 gauss Disc A, 470 gauss

§ 9 *Accuracy*

The probable error in the absolute values of the two components of the magnetisation is about 2 per cent. The largest part of this is due to uncertainty in the value of the applied magnetic field, which, as explained above, could not be fixed accurately. In the calculation of the molecular field we have other errors. As the discs could not be accurately machined, the value of the demagnetising coefficient is not known very well. This, in conjunction with the error in the saturation value of I , may involve an error of about 4 per cent in the value of the demagnetising field. There may be another serious error in the measurement of the angle θ , which could not be measured to less than three or four minutes. The estimated error in the values of M is about 10 per cent.

§ 10 *Discussion*

In discussing these results, it is necessary to point out a difference between our case and that treated by Weiss. In our iron crystals the saturation value of the magnetisation is about 35 times larger than in the pyrrhotine crystals used by Weiss. The effect of the demagnetising field must be correspondingly greater. And as our discs are not perfect spheroids, we cannot assume a uniform magnetisation except for applied fields, large enough to give nearly saturation. This same defect may account for the small initial susceptibility shown in the I - H curves. The increasing uniformity of the magnetisation, with increasing field strength, probably accounts for the increase in the value of the molecular field to be noted in graph 6. Further, as our calculations of the molecular field are only valuable if the magnetisation is uniform, we cannot find the value of the molecular field except for applied fields strong enough to give nearly saturation.

Comparing the I - H curves of the two crystals, it is found that, for disc B, saturation is reached a little sooner and more sharply than for the other. From graph 4 we see that the sudden rise in the value of the component of the magnetisation perpendicular to the field takes place for smaller applied fields,

and that this value is everywhere higher in disc B. Thus we would expect to follow from the higher value of the molecular field found for disc B.

The difference in the value of the molecular field for the two crystals is probably due to the presence of different impurities in them. The analysis, for which we are indebted to Miss Elam, is as follows —

	Disc A.	Disc B
	Per cent	Per cent
Carbon	0.048	0.105–0.130 (?)
Silicon	0.013	0.021–0.023
Sulphur	0.017	0.045–0.028 (?)
Manganese	0.024	0.380–0.440
Phosphorus	0.220	0.019–0.020

Crystal B was heated in hydrogen after this analysis was made, which probably removed all the carbon and some of the sulphur. There is a considerable difference in the impurities in the two crystals, chiefly in the phosphorus and manganese content. If we suppose that both phosphorus and manganese alter the molecular field, then it seems that phosphorus does so to a greater extent. The effect of any substance probably depends on the position it takes in the lattice of the iron crystal. Apparently the molecular field is very sensitive to impurities.

It is interesting to note that the variation of the component of the molecular field perpendicular to the direction of magnetisation, given by the expression $[\cos^4(\psi) \sin(\psi) - \sin^4(\psi) \cos(\psi)]$ is very nearly the same as the simple term $\sin(4\psi)$. The ratio of the two expressions is

$$\frac{[1 + \frac{1}{4} \sin(2\psi)]}{4 [\cos(\psi) + \sin(\psi)]}.$$

$\sin(4\psi)$ is the simplest variation demanded by the symmetry of the crystal, and is approximately the form calculated by Honda and Okubo ('Physical Review,' vol 10, p. 705 (1917)).

The properties of ordinary iron depend a great deal on the physical treatment it receives. To investigate any such effect on the molecular field, one of the discs was heated to about 600° C. and rapidly cooled. No change in the results could be detected. The molecular field must then be a stable property of the crystal.

A determination of the coercive force was made on a short rod (de-magnetising coefficient = 0.113), cut parallel to one of the axes of crystal A. A value of about 4 gauss was found, for a maximum magnetisation of 1,000 abs. units.

Comparing the values of the molecular field found above with those found by Weiss for pyrrhotine, we are at once struck by the enormous difference between them. That in pyrrhotine is many times larger than that in iron. Now in pyrrhotine (Fe_7S_8) the distance between neighbouring atoms of iron must be greater than that in pure iron, and we should expect the molecular field of pyrrhotine, if due to magnetic forces, to be less than in iron. It is probable, as has been suggested by Weiss, that the molecular field is not due to magnetic forces. The above criticism would not hold in that case.

§ 11 *Summary*

It is shown that the magnetic properties of iron crystals may be explained on the Weiss theory of molecular fields. The magnitude of the molecular field is found for two crystals, giving respectively 620 gauss and 479 gauss. The magnitude of the component of the molecular field along any axis varies as $\cos^4(\psi)$, where (ψ) is the angle between the direction of magnetisation and the axis considered.

It is shown that the molecular field is a stable property of the crystal, and that it is affected considerably by the presence of impurities. Support is found for the view that the molecular field is not due to magnetic forces.

In conclusion, I should like to express my thanks to Professor Sir Ernest Rutherford for his interest in this work, to R. L. Aston, of this laboratory, for his X-ray analysis of these crystals, and especially to Dr P. Kapitza for his very helpful guidance throughout.

[*Note, added January 20*—Since writing the above, a summary* of some work by K. Beck† on the magnetisation of crystals of iron has been found. Our results are in very good agreement with those of Beck, except that the maximum value of the component of the magnetisation perpendicular to the magnetic field, in Beck's case, is much larger than in our experiments. This seems to indicate a higher molecular field than was found for our crystals. The chemical impurities in his specimen amounted to about 2 per cent.

It is interesting to note that, in our experiments, the crystal with the greatest amount of impurities (about $\frac{1}{2}$ per cent.) also gave the largest value for the molecular field. This seems to add weight to the argument that the molecular field is not due to magnetic forces.]

* Kunz, 'Bull. Nat. Res. Council,' vol 3, Part 3, p. 180 (1922).

† K. Beck, 'Dissertation,' Zürich (1918).

On the Measurement of the Ratio of the Specific Heats using Small Volumes of Gas.—The Ratios of the Specific Heats of Air and of Hydrogen at Atmospheric Pressure and at Temperatures between 20° C. and -183° C

By J H BRINKWORTH, A R C S , M Sc , D I C

(Communicated by Prof H L Callendar, F R S —Received October 14, 1924)

Introduction.—In nearly all the previous determinations of the ratio of the specific heats of gases, from measurements of the pressures and temperatures before and after an adiabatic expansion, large expansion chambers of from 50 to 130 litres capacity have been used. Professor Callendar first suggested the use of smaller vessels, and in 1914, Mercer ('Proc Phys Soc,' vol 26, p 155) made some measurements with several gases, but at room temperatures only, using volumes of about 300 and 2000 c c respectively. He obtained values which indicated that small vessels could be used, and that, with proper corrections, a considerable degree of accuracy might be obtained. The one other experimenter who has used a small expansion chamber, capacity about 1 litre, is M C Shields ('Phys. Rev,' 1917), who measured this ratio for air and for hydrogen at room temperature, about 18° C, and its value for hydrogen at -190° C. The chief advantage gained by the use of large expansion chambers is that no correction, or at the most, a very small one, has to be made for any systematic error due to the size of the containing vessels, but it is clear that, in the determinations of the ratio of the specific heats of gases at low temperatures, the use of small vessels becomes a practical necessity in order that uniform and steady temperature conditions may be obtained.

Owing, however, to the presence of a systematic error depending upon the dimensions of the expansion chamber, the magnitude of which had not been definitely settled by experiment, the following work was undertaken with the object of investigating the method more fully, especially with regard to its applicability to the determination of this ratio at low temperatures.

The present experiments relate to air and hydrogen. Further experiments of a similar nature on other gases are in progress. Air was selected in the first instance on account of its convenience, and because the value of the ratio of the specific heats at ordinary temperatures is known with greater accuracy than for other gases. The results obtained for air in the present experiments

with small vessels, down to 35 c.c. capacity, will, therefore, afford a fair criterion of the degree of accuracy attainable under such conditions.

Hydrogen has been investigated because, in the first place, its physical properties, density, heat conductivity, &c., are so very different from those of air that it might perhaps be assumed that, if the experimental conditions requisite in the cases of air and hydrogen are known, it should not be difficult to deal with any other gas, and secondly, because a knowledge of the temperature variation of the specific heats of hydrogen is of very great importance in theoretical physics, and the experimental values at present available are few in number and are somewhat discordant.

These investigations have been made in the Physical Laboratories of the Imperial College of Science, and I wish to do homage to Prof. Callendar, the Director of those Laboratories, and to express to him my thanks for his advice and my great appreciation of the opportunity given me to develop this method of experiment.

General Outline of the Method.—The quantity actually measured in these experiments is the cooling effect in adiabatic expansion, that is to say, the ratio of the drop in temperature to the drop in pressure, when the gas in a vessel at a pressure slightly above atmospheric is allowed to expand rapidly to atmospheric pressure. The general principle of the method is the same as that of the old experiment of Clément and Désormes, except that the drop of temperature is directly measured with a sensitive thermometer, as in the experiments of Lummer and Pringsheim ('*Smithsonian Contributions to Knowledge*,' 1898) and those of Callendar and Nicolson, in an engine cylinder ('*Proc. Inst. C.E.*,' November, 1897).

Assuming an adiabatic relation between pressure and temperature of the same type as for a perfect gas, namely

$$\theta_1/p_1^m = \theta_2/p_2^m \quad A,$$

where θ_1 , θ_2 , are the initial and final temperatures on the absolute scale, and p_1 , p_2 , the corresponding pressures, we find for the index m ,

$$m = \log(\theta_1/\theta_2)/\log(p_1/p_2).$$

But, in order to facilitate comparison with the work of other observers, the results have been expressed in terms of the apparent value of the ratio of the specific heats γ , by the relation:

$$\gamma = 1/(1 - m), \quad \text{or} \quad m = (\gamma - 1)/\gamma.$$

The apparent value of γ thus obtained requires certain small corrections to

allow for deviations of the actual gases employed from the ideal state, in addition to corrections for radiation and for the volume of the vessel or the time of expansion, depending on the conditions of each experiment

The advantage of the direct measurement of the drop in temperature, as compared with the indirect method of Clément and Désormes, is that the effect of the walls of the vessel is very greatly reduced.

As compared with the method of deducing γ from the velocity of sound, the advantages of directly measuring the drop of temperature with an electric thermometer are as follows. An error of 1 per cent in the observed velocity gives an error of 2 per cent in the value of γ , whereas an error of 1 per cent. in the drop of temperature gives an error of $(\gamma - 1)$ per cent in γ or only 0.4 per cent. for air

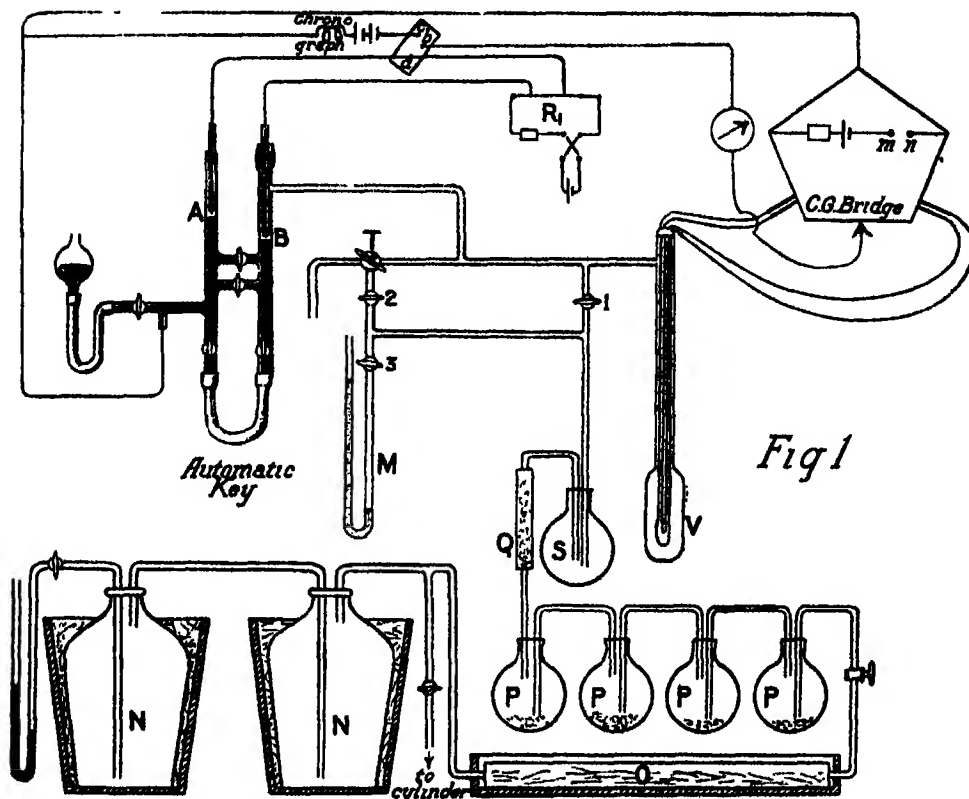
With suitable apparatus a higher order of accuracy can be attained in the measurement of the temperature drop than in the measurement of the velocity of sound, except possibly in the case of air on a large scale. With small quantities of gas at low temperatures the electric method is probably about ten times as accurate as the velocity method

Arrangement of Apparatus—The gases were obtained from Brin's Oxygen Co., in the usual gas cylinders. For the experimental measurements the gas was stored in large glass carboys N, N, together holding about 7 cubic feet, under the excess pressure of about 5 cm. of mercury. The gas circuit from these reservoirs to the expansion vessel V is shown in the diagram (fig 1), where O is a tube, 1 metre long, containing stick potash, and P, P, P, P are 2-litre flasks partly filled with phosphorus pentoxide. Q is a tube filled with glass-wool acting as a dust filter, and S another 2-litre flask which could be surrounded by a low-temperature bath, when necessary, in order to cool the gas on its way to the expansion vessel. The latter was maintained at an approximately constant temperature in a suitable medium contained in a vacuum vessel.

The difference between the initial and final pressures of the gas is read on the oil manometer M, the final pressure being that of the atmosphere, which is obtained from the barometric reading. The temperatures before and immediately after the expansion of the gas were measured electrically, by means of a compensated thermometer of platinum wire, 0.025 mm. in diameter; this was put into the electrical circuit by contacts made in the arms A and B of a mercury key

The Automatic Mercury Key.—An automatic key was employed, as it is important that the time interval between the commencement of the expansion

and the closing of the galvanometer circuit for the measurement of θ_2 should be reproducible with some consistency. If the points *a* and *b* (fig. 1) are joined and



the gas in *V* is under pressure, the galvanometer circuit can be closed in the limb *A* for the measurement of the initial temperature θ_1 . This circuit must then be open until it is again closed, at some instant after the commencement of the expansion, for the observation of the final temperature θ_2 . This second contact was made in the limb *B* by the rising of the mercury level in this limb when the vessel *V* was opened to the atmosphere. The time elapsing between the commencement of an expansion and the making of contact in *B* could be varied by adjustment of the mercury levels and the taps, shown in the figure of the key and was measured on a chronograph. The latter gave a trace of 5 cm. on the record, corresponding to a time interval of one second. R_1 is an auxiliary circuit by which a small e.m.f. can be introduced into the galvanometer circuit to compensate disturbing thermal effects.

Method of Performing an Experiment (fig. 1)—At the commencement of an

experiment taps 1, 2 and 3 were open and T connected V with the oil gauge. Contact was made in the three-way mercury switch between *a* and *b*, and the electrical circuit through the galvanometer was completed in the limb A of the automatic key. The pressure p_1 on the gas in V was first adjusted to be from 76 to 78 cm. of oil in excess of atmospheric pressure, and test observations were made to determine the steady temperature of the gas θ_1 and its constancy, the time indication of the automatic mercury key, the approximate balance point on the Callendar-Griffiths bridge corresponding to the lowest temperature reached by the gas, the absence of thermo-electromotive forces in the galvanometer circuit and the value of the heating effect caused by the current in the thermometer wire. The experimental manipulations and observations necessary for the evaluation of each individual measure of the ratio of the specific heats were then made in the following order. Two readings of the approximate balance point on the bridge wire, differing by 1 mm., and the resulting deflections obtained on reversal of the current, corresponding to temperatures slightly above and slightly below the actual steady temperature θ_1 , were recorded. The latter can be deduced by interpolation. Contact at A, in the mercury key, was then broken by raising, through a friction grip, the wire dipping into the mercury in this arm, and the contact on the bridge was adjusted to a millimetre division as near as possible to the point corresponding to the lowest temperature θ_2 attained by the gas after expansion. The readings in both limbs of the oil gauge were taken, tap 1 was closed, the large three-way tap, T, quickly turned full open to the atmosphere, and the (more or less) sudden deflection of the galvanometer needle was noted. It is convenient to call this the *KICK* deflection.

Immediately after the observation of this kick, the battery circuit through the bridge was broken at *m*, *n*, tap 2 was closed, the three-way tap T turned back to its initial position, and the pressure readings on the oil gauge were checked. The galvanometer needle was then brought to rest by means of a subsidiary damping circuit and the contact on the bridge wire was lifted and depressed. If there was no change in the position of the galvanometer needle resulting from this, it indicated the absence of thermo-electromotive forces in the circuit: if they existed, they could be neutralised by a suitable change in the balancing circuit R_1 . Tap 3 was then closed and tap 1 opened, thus refilling the bulb. During the heating up of the new supply of gas, observations were made of the atmospheric pressure and of the temperatures of the oil gauge and the barometer.

Taps 2 and 3 were then opened, the contact lowered into the arm A, and

the steady readings of the thermometer again observed. Another experiment was now made in a similar manner, except that the position of the bridge-wire contact, corresponding approximately to the temperature θ_2 , was altered by one or two millimetres in whichever direction was judged advisable from a consideration of the magnitude of the kick observed in the preceding experiment. After some five to fifteen sets of observations had been made, the time interval between the commencement of the expansion and the closing of the galvanometer circuit was again noted. To do this, the contact in the three-way switch between a and b was broken and a , c joined. The point of the wire contact in A was made just to touch the surface of the mercury in this arm of the mercury key, the chronograph was set in motion, and an expansion made, as before, by turning the three-way tap. A complete set of observations could be made in one to three hours.

Details of Apparatus Employed

The Barometer and Oil Gauge—The barometer used was of the standard Fortin type. Its indications were read to 0.01 cm and the necessary temperature corrections to 0°C were applied.

The oil gauge was that used by Swann in his measurements of the specific heats of air and of CO_2 . The scale was engraved in millimetres over a length of 81 cms on both limbs of a glass U-tube, the scale was everywhere correct to within 0.002 cm. Determinations of the density and of the temperature coefficient of expansion of the oil used gave the following relationship for the reduction of the pressure measured in centimetres of oil at $t^\circ \text{C}$, i.e. h_t , to lengths H_0 measured in centimetres of mercury at 0°C .

$$H_0 = h_t (0.06400) [1 - 0.000735 (t - 22)]$$

The indications on the gauge could easily be read to 0.01 cm, these readings being taken by the aid of low-power microscopes. The oil was somewhat viscous, but sufficient time was always allowed for stationary levels to be attained, moreover, the use of large balancing reservoirs ensured that the change in the levels of the oil between successive experiments was small. It will be noticed that during the time taken to complete any set of observations the barometric pressure remained constant to within a few tenths of a millimetre of mercury, thus showing that the atmospheric conditions were steady. It is essential that all observations should be taken only under such conditions, for on windy days the oil surfaces in the gauge were never at rest and the irregular fluctuations in pressure were sometimes as big as 2 to 3 mm. of oil. The pressure readings taken immediately before and after the expansion

were almost always identical, rarely differing by as much as 1 in 3000. When a difference existed, the mean value has been used in the calculations.

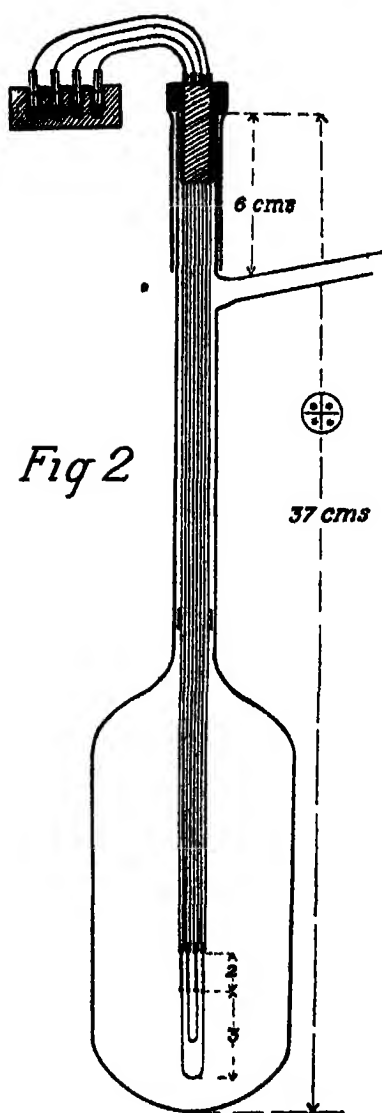


Fig 2

The Expansion Vessels (fig 2)—These were of glass, each consisting of a bulb on the end of a straight tube of 1 cm. diameter, through which the thermometer was inserted. The overall length of each vessel was the same, 37 cm, the side tube for the exit of the gas being 6 cm from the open end of the tube. Each bulb was blown with the length of the cylindrical portion of the bulb about 1.5 times its diameter.

The internal volumes of the bulbs were 697, 287.75, 34.5, 11.2 c.c. respectively, the reciprocals of the cube roots of these volumes being 0.1128, 0.1516, 0.2371, 0.3072, and 0.447.

The Galvanometer.—An astatic galvanometer of the Paschen type with a long quartz-fibre suspension, was used. It had a period of about 5 seconds and a resistance of 4 ohms. Some care was taken in making it as astatic as possible. To do this, the needle was first deflected through 90° by a small current, then a large current was flushed through the two pairs of field coils arranged in series, the magnetic field in the coils surrounding the weaker magnet being strengthened by the insertion of an iron core. Such success was obtained that it was not necessary to screen the instrument. The scale was

about 2 metres from the galvanometer.

The Platinum Thermometer Bridge.—The well-known form of bridge designed by Prof. Callendar was used, the bridge coils being cut out by means of mercury keys. Two calibrations of the coils and bridge were made, and the corrections, which were small, agreed to within 0.005 cm. of bridge wire.

The Thermometer (fig. 2).—The main leads were of No 22 copper wire, to which lengths of 0.1 mm platinum wire were hard-soldered. The main resistance consisted of a single loop of about 6 cm. of pure platinum wire 0.025 mm in diameter. The compensating leads were joined by another loop of about 2 cm. of the same wire. The value of δ in the Callendar reduction formula is 1.50 for this specimen of wire. The fine wires were joined to the ends of the thicker platinum wires by a trace of gold solder. The main leads were sheathed in glass tubes, which were fused around the thicker platinum wires, leaving about 2 cm. of the latter exposed. The sheathing tubes were firmly bound together and were fixed, at the end remote from the platinum wires, in a glass tube which just fitted into the stem-tube of the expansion vessel, the joint being made with plaster-of-Paris covered with wax. This glass tube served as a guide, and other guides, consisting of small mica frames, were placed at intervals along the stem of the thermometer.

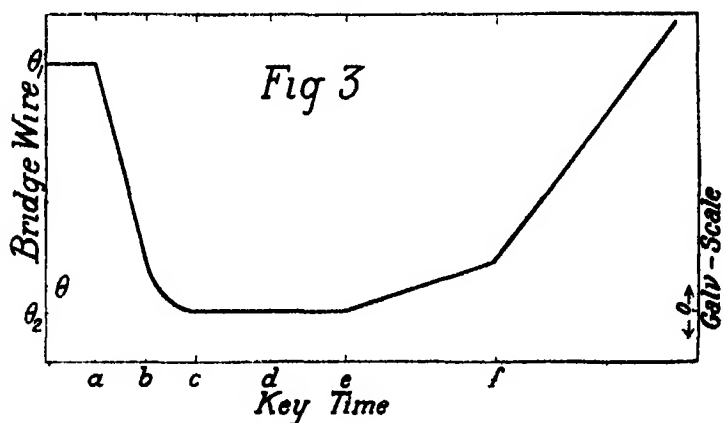
The gas-tight joint between the head of the thermometer and the bulb stem was made by a rubber tube fixed to this head, it slipped over the stem and was wound round with insulating tape and wired into position. The free ends of the four leads from the thermometer and compensator were soldered to thick copper lugs, which were connected with the flexible leads to the bridge in a 4-hole mercury cup. With this arrangement, the transference of the thermometer from one bulb to another could be accomplished easily, and it was possible, when necessary, to alter the position of the thermometer wire in a bulb and to replace the thermometer in practically the same position. It was found to be important that the thermometer should be firmly fixed in the bulb. As the result of the preliminary experiments it was decided to arrange the lower end of the loop 1 to 1.5 cm. above the bottom of the bulb in use.

Before commencing any series of experiments the loops were cleaned by heating in a spirit flame, and they were slightly stretched so that each loop lay in one plane, but the two loops were in planes at right angles to each other. The fundamental interval was then determined with the usual apparatus. After several expansions the longest loop changed its outline, due to the slight shaking, but this did not affect the fundamental interval. If the wire became bent very much out of its original plane, or if it was touched during the transference from one vessel to another, then the wires were again cleaned and straightened, and the new constants determined. In general, the fundamental interval was about 270 cm., and the resistance at 0° C about 720 cm. of bridge wire.

The current to the bridge was derived from accumulators, either 1, 2 or 4 units, in series with suitable resistances according to the conditions of the experiment

With such fine wires the effect of the bridge current in altering the resistance of the thermometer must be measured and allowed for. This heating effect in the thermometer wire was measured in the way suggested by Prof Callendar, and the variation of the effect with change of temperature was determined. It is the small difference, from 0.01 to 0.06 cm., of bridge wire, between the magnitudes of this heating effect at θ_1 and θ_2 , which affects the calculated values of γ . These differences were constantly redetermined, and very consistent values were obtained in experiments performed, on different days under similar conditions.

Estimation of the Lowest Temperature attained ---In fig 3, the probable changes in temperature of the gas are plotted against the time. Starting from an initial



temperature θ_1 , the tap T is opened at time a . There is a rapid fall of temperature at first, becoming less rapid from b to c . From c to e the temperature remains constant any cooling being balanced by heat received from outside. At e the gas has begun to rise in temperature and this rise gets more rapid as time passes. The straight portion from c to e indicates the lowest temperature θ_2 . If the moment of contact is at a time between c and e , and the bridge wire setting corresponds to θ_2 , the galvanometer needle will remain undeflected when contact is made at B. If the contact is maintained as the gas rises in temperature a gradual deflection (say, to the right) will take place. If, with the same time conditions, the bridge setting corresponds to θ , a temperature between θ_1 and θ_2 , there is an initial kick to the

left due to the want of balance. It is this initial kick which is measured. If the time of contact corresponds to b , and the bridge setting to a temperature reached after this instant, there is the possibility that, before the kick occurs to the left, there may be a small and almost instantaneous movement of the needle to the right. The latter movement was only observed when the bridge wire setting was not far removed from the point of exact balance, if it existed the time of the key was increased to correspond to a value slightly greater than c .

The expression "kick sensitiveness" is used to indicate the number of scale divisions in a kick movement corresponding to 1 mm of bridge wire. Its average value in an experiment can be deduced from a consideration of successive observations, such as are tabulated in columns b and c on pages 527 and 531. This quantity increased as the temperature at which the experiment was performed was lowered, and also, roughly, in direct proportion to a linear measurement of the bulb (fig 4). The key times usually adopted (*i.e.*, a c in

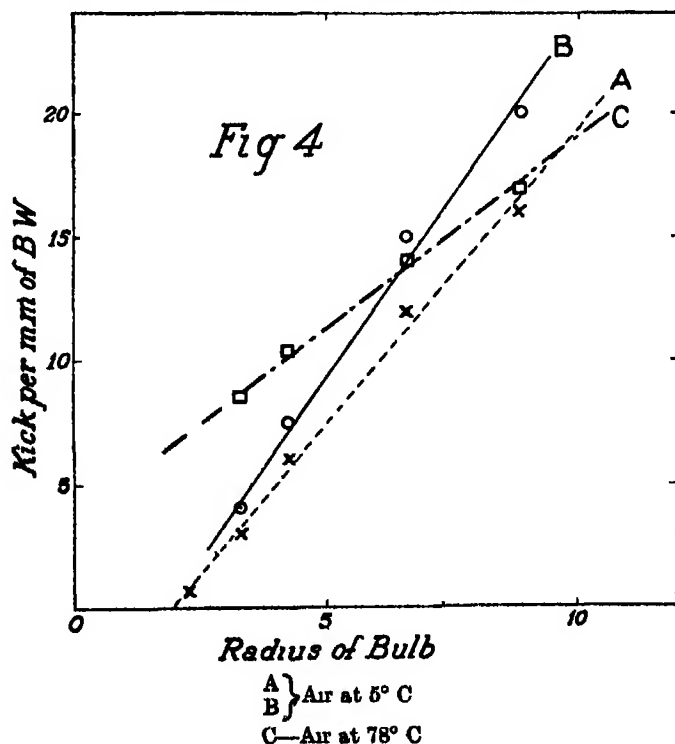


fig. 3) showed the same relationship. The latter is dependant on the extension of the pressure drop down the axis of the bulb, the former on the time

interval corresponding to oe . When experiments were made with longer times than c , but not exceeding f , the kick sensitiveness was decreased, but the calculated values of γ were only slightly reduced. This can be explained by reference to fig 3. When the key time corresponds to c there is a considerable interval of time before the needle is moved to the right, and, therefore, the galvanometer spot has time to reach its maximum kick elongation to the left. In some of the air experiments, if the time of making contact was trebled, the kick sensitiveness was reduced by about one-half. When necessary, a kick deflection could be estimated to a quarter division on a total deflection of 2 or 3 divisions, but, in general, to obtain the accuracy expected, it was only necessary to observe to the nearest scale division. A check on the value of the kick sensitiveness used is obtained from a comparison of the mean values of γ calculated from the results when the kick deflections are (a) small, (b) large. These means should agree.

Thermoelectric Effects in the Galvanometer Circuit—The current through the thermometer was kept constant in all the observations from which one mean value is deduced, the key contact at B being one to close the galvanometer circuit. The presence of thermoelectro-motive forces in this circuit is not a matter of especial consequence when it is possible, as it is in the measurement of the steady temperature, to reverse the direction of the current through the bridge. But the value of the lowest temperature is deduced from a bridge reading which represents a point of balance only existing for a short interval of time during which reversal is not possible, hence, it is of great importance that the kick deflection should be free from errors due to a zero shift occurring during the time of observation of this temperature.

Such thermo-electric effects as existed, when contact through the galvanometer circuit was made at B, were small and were reduced so as to be negligible by the insertion of a balancing e m f in this circuit. The arrangement employed (shown at R₁, in fig 1) consisted of a circuit containing an accumulator, a reversing key, a resistance box and a piece of well-lagged manganin wire. potential leads from two points on the latter being led into the galvanometer circuit. It is more especially in those cases when the movement of the needle during the kick elongation is slow that the whole effect of such a source of error will have time to show itself, but the error then introduced is minimised by the fact that, under these conditions, the magnitude of the kick deflection per mm change in the reading of the bridge is large. Such uncompensated zero changes as existed were rarely more than ± 2 divisions on the galvanometer scale, and errors thus introduced would mean out, though, no doubt,

some part of the variations between individual results is due to their presence

Initial Temperature Conditions and Reduction of Platinum Temperatures to True Temperatures.—The expansion bulb was surrounded by a suitable medium contained in a vacuum vessel. Absolute constancy of the temperature of the medium is not essential, but any change occurring must be slow, as it is not desirable that the difference between the steady temperatures, measured before and after an expansion, should differ by 0.01°C . In general, the differences observed were less than this. For all temperatures above -78°C Callendar's ('Phil. Trans.,' 1887) parabolic formula was used. Initially the observations at -78°C were reduced in the same manner, and the correction curve given by Henning ('Ann der Physik,' vol 40, p 635, 1913) for his standard thermometer was utilized in reducing the platinum temperatures observed at -118° and -183° . With these corrections the temperatures of solid CO_2 , subliming from alcohol, was -78.49° , and that of old liquid air, -183.40°C . Henning has shown that at -78° the Callendar formula gives results about 0.08° too low while at -183° the divergence is over 2° . (See also Travers and Gwyer, 'Roy Soc Proc.,' vol 74, p 528, 1904.) Henning has also shown that at -183° different platinum thermometers will vary by as much as 0.5° in their indications, but that the scales of these thermometers could be connected with that of his standard by making an additional correction calculated from a relation of the form $pt_1 - pt_2 = c \cdot pt_1 (pt_1 - 100)$

The scale finally adopted for the calculations of temperatures at and below -78° was the Henning scale with this additional correction. The temperature of a considerable quantity of liquid air used in the experiments made at the end of November was -183.40° as deduced, using Henning's standard values, and this temperature was constant to within 0.02° over a period of four hours on each of two successive days. In calculating the constant c , in the additional correction to be applied to Henning's standard values, it has been assumed that this temperature should have been -182.95°

The expansion bulb was surrounded by water, ice, and ice and salt respectively, in the experiments made at temperatures of about 17° , 0° and -21° . Lower temperatures were obtained by the use of (a) a mixture of solid CO_2 and alcohol; (b) solid ether, and (c) liquid air. These will be considered separately.

(a) Solid CO_2 was mixed with alcohol to form a pasty mass. Over the pressure range of about 2 cm. due to variations in the barometric height, the temperatures can be represented by $-78.31 + 0.16(p - 76)$.

(b) Liquid air was poured on to anhydrous ether and the solid crust which formed was rammed around the bulb. The temperatures obtained were sufficiently constant, but addition of liquid air was necessary after every two or three observations. The temperature, about -117.8° , is 0.2° lower than the value obtained by Holborn and Wien ('Wied Ann,' 1896). It has been shown by Timmermans ('Bull Soc Chem Belg,' 1911), and confirmed by Henning ('Ann d Phys.,' 1914), that solid ether is dimorphous, and that the lower transition point is at a temperature of -123.6° C.

(c) The liquid air was obtained from commercial sources and was always fairly rich in oxygen. The temperatures of the various samples were sufficiently constant for the purposes of the experiments. A check on the accuracy with which the scale adopted applies to my thermometer is obtained from the value it gives for the temperature of solid CO_2 in alcohol, a value which differs from that obtained by Holborn ('Ann der Physik,' vol 6, p 242, 1901) by only 0.03° C.

The Effect of Observational Errors—The ratio of the specific heats is usually obtained either from measurements of the velocity of sound or from a knowledge of the pressure or temperature resulting from an adiabatic expansion.

In the first method, an error in the measurement of the velocity gives rise to an error *twice* as great in the value of γ .

In the method adopted in these experiments—which, it is generally agreed, is the best of the expansion methods—we may write

$$\begin{aligned}\frac{\gamma - 1}{\gamma} &= \frac{\log \theta_1/\theta_2}{\log p_1/p_2} = \frac{\log (1 + \Delta\theta/\theta_2)}{\log (1 + \Delta p/p_2)} \\ &= \frac{p_2}{\theta_2} \frac{\Delta\theta}{\Delta p} \left[1 - \frac{1}{2} \left(\frac{\Delta\theta}{\theta_2} - \frac{\Delta p}{p_2} \right) \right]. \quad (1)\end{aligned}$$

In considering my experiments, make $p_2 = 75$ cm and $\Delta p = 5$ cm., and

at room temperature $\theta_2 = 280^{\circ}$ and $\Delta\theta = 5^{\circ}$

at liquid air temperature $\theta_2 = 88^{\circ}$ and $\Delta\theta = 2.1^{\circ}$.

Substituting in (1), we find that

$$\frac{\gamma - 1}{\gamma} = \frac{p_2}{\theta_2} \frac{\Delta\theta}{\Delta p} \text{ is correct,}$$

at both temperatures, to within $2\frac{1}{2}$ per cent., and this simple relation is sufficiently accurate if we wish only to consider to what extent errors in the quantities observed will affect the value of γ obtained. As p_2 and θ_2 can be observed to a high degree of accuracy, p_2/θ_2 may be assumed correct.

Therefore

$$\frac{d\gamma}{\gamma} = (\gamma - 1) \left(\frac{d(\Delta\theta)}{\Delta\theta} - \frac{d(\Delta p)}{\Delta p} \right) \quad (2)$$

$$- \gamma \frac{p_2}{\theta_2} \frac{\Delta\theta}{\Delta p} \left(\frac{d(\Delta\theta)}{\Delta\theta} - \frac{d(\Delta p)}{\Delta p} \right) \quad (3)$$

The most difficult observation is the determination of the value of θ_2 , but the biggest error will be that in $\theta_1 - \theta_2$, i.e., in $\Delta\theta$. Equation (2) shows that the error in γ is only about *one-half* of the observational error in $\Delta\theta$.

Equation (3) shows that the percentage error $d\gamma/\gamma$ increases with diminishing values of θ_2 . In these experiments p_2 could be measured to 1 in 7000, Δp to 1 in 4000. θ_2 , θ_1 , and $\Delta\theta$ are, on an average, correct to 0.01 cm. of bridge wire, i.e., to 0.004° C. Hence, even in the case of the experiments at liquid-air temperatures, $\Delta\theta$ should not be in error by more than 1 part in 500, or γ be wrong by more than 1 in 800. At room temperatures the error should be $2\frac{1}{2}$ -times smaller.

The indeterminable accidental errors—which, like the observational errors, disappear from a mean value—cause the differences between the mean and the individual values to be rather greater than was desired, but they are not greater than those found in the results of other observers. The general concordance obtained indicates a probable accuracy of 1 part in 1000 in all the final values of γ .

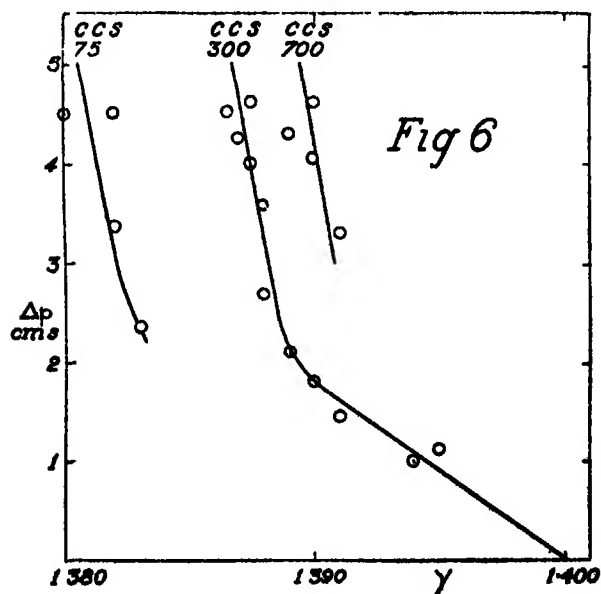
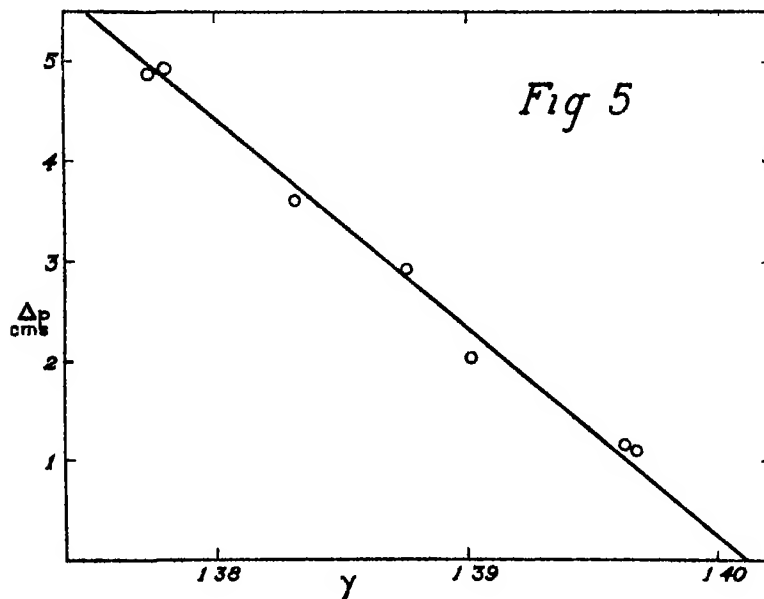
Preliminary Experiments—A large number of preliminary measurements, using air, were made throughout the year 1922, in order to determine the best experimental arrangements and how to minimize the possible errors. These experiments can conveniently be summarized into three groups—

(a) A fine wire compensated thermometer was used in a bulb of 130 c.c. capacity. The mercury key was a simple U-tube connected into the gas circuit close to the exit from the bulb.

These results are shown graphically in fig. 5, the linear relation giving an extrapolated value of γ , corresponding to zero-pressure excess, of 1.401. Though the results are not strictly comparable with those obtained by Shields, as the experimental conditions were not the same, yet they are, roughly, confirmatory of the fact that it is possible to obtain a fairly good estimate of the value of the ratio sought for, by using the method of extrapolation against the pressure excess, when a vessel of this small volume is employed.

(b) Before commencing the second group of experiments, the thermometer and expansion vessels used in these and in all the later experiments were constructed. Another mercury key, with an additional cross-arm, was used.

A fairly complete set of observations was made with the 300-c.c bulb, and the results, with some obtained with other bulbs, are shown in fig 6



It had been expected that a similar linear relation would result, although the experimental arrangements had been somewhat modified. In the experi-

ments referred to in group (a) the time of the key was about the same as the time of expansion of the gas, in this second series the key was placed near the tap T, and its time was fixed by the adjustment of the taps in the cross-arms. The movement of the mercury column in the key was not quite uniform. On opening the tap, T, the mercury surface in the arm, B, at first rose rapidly and then more slowly. When the pressure excess was small, contact was made during the time interval corresponding to the first rapid rise, and therefore the conditions were very similar to those previously existing. For the larger values of the pressure excess the key time was shorter than in the preceding experiments, but if the key time was increased the apparent values of γ became smaller. It is obvious that this method of extrapolation can only be used when the timing conditions are suitable. Both Moody and Shields allowed a definite time to elapse between the commencement of the sudden expansion and the closing of the circuit. With the slower rates of expansion used in these experiments, apparently a linear relation is only obtained when the time increases with the excess pressure. With larger vessels, when longer time intervals are allowable, the linear relation between γ and Δp will hold over a greater range.

As the values of γ obtained with excess pressures of 3 to 5 cm. of mercury, when plotted against the inverse cube roots of the volumes of the bulbs, lie near straight lines which give extrapolated values close to that generally accepted, it was thought advisable to work with excess pressures of about 4.5 to 5 cm. of mercury, the maximum value measurable on the oil gauge, and to investigate the timing conditions. As a result, the method detailed on page 518 was evolved.

(c) The final form of mercury key was adopted, and rather greater consistency between the individual values and the mean was obtained by the introduction of the thermo-electromotive-force balancing circuit. All the practical manipulations and settings were as in the final experiments and are described on page 514, but undried, unpurified air was used. The mean results with the five bulbs used are shown graphically on p. 533 in fig. 8 (dotted line), each mean being obtained from 20 to 30 separate determinations with one of the bulbs. It was not expected that very good results would be obtained with the smallest bulb, capacity 11 c.c. only, but the individual values agreed among themselves to ± 0.002 on the value of γ —viz., 1.351. This value lies, rather more than 1 per cent., below the line showing the linear relation between the results obtained with the larger vessels; the lowness of the result is probably due to the fact that the time of the key could not be made sufficiently short.

It is of interest to note that this result is only about 4 per cent lower than the value obtained when using a volume of gas over ten-thousand times greater

During the course of these experiments the variation of the kick sensitiveness with the size of the bulb and its dependence on the time of the key were ascertained. Experiments were made, in the largest bulb, with the thermometer loop at different distances above the bottom of the bulb. Consistent results were obtained, as long as the wire was not more than one-quarter way up the bulb. If higher than this the loop was bent out of the vertical plane and the results were discordant.

The *Final Experiments*, representing the results of this research, date from this time. A few reduced observations are given in order to show the steadiness of the experimental conditions and the accuracy with which results could be reproduced.

AIR FINAL EXPERIMENTS (FIG 8, p 533)

Fundamental Interval, Freezing Point and Heating Effect Observations,
in cm of Bridge Wire

Date	Temp °C	1 Cell	2 Cells	4 Cells
April 19, 1923	0 99 726	731 34 1004 67 F P 731 28	731 62 1004 86 F I 274 09	732 68 1005 66

Heating Effects (Subtractive)

Date	Temp °C	4 Cells	2 Cells
April 19	0	1 41	0 37
April 19	100	1 07	0 25
May 19	— 78	1 57	0 42
July 24	— 118	—	0 50
June 18	0	—	0 35
September 6	0	1 42	—
September 6	100	1 09	—

The value of the F.P. obtained on the latter day was 731 28.

From these observations it will be seen that the correction to be applied on account of the variation in the heating effect is only 0 02 cm in the case of the measurements at room temperatures, and it is negligible at -78° and -118° when 2 cells only were used.

Reduced Observations

Columns (a) and (d) give the values of θ_1 and θ_2 expressed in terms of cm. of bridge wire, after the application of the box coil and the heating effect corrections

Column (b) gives the bridge wire setting for the observation of θ_2 and (c) the resulting kick deflection.

May 9th. 300 c.c. Bulb $t = 28$ secs

p_2	p_1	a	b	c	d	θ_2	θ_1	γ
75 61	80 564	779 23	17 0	68	765 09	285 281	290 384	1 3877
	80 545	779 23	16 6	2	765 13	285 295	290 384	1 3881
	80 525	779 23	16 8	28	765 15	285 302	290 384	1 3895
	80 503	779 24	16 8	16	765 23	285 331	290 388	1 3892
	80 480	779 24	16 9	21	765 30	285 356	290 388	1 3890
75 59	80 456	779 24	16 9	11	765 37	285 381	290 388	1 3889
	80 418	779 24	16 95	11	765 42	285 399	290 388	1 3887
	80 397	779 25	16 95	1	765 48	285 421	290 391	1 3889
	80 378	779 25	17 0	2	765 53	285 439	290 391	1 3890
	80 356	779 26	17 1	8	765 59	285 462	290 395	1 3893
	80 338	779 26	17 05	-4	765 62	285 472	290 395	1 3902
	80 320	779 26	17 2	5	765 71	285 504	290 395	1 3885

Other values of $(\gamma - 1)$ obtained under similar conditions

April 26th -- 3901, 3895, 3896, 3901, 3875, 3895, 3895, 3899, 3890, 3890 $t = 35$ secs

May 12th -- 3893, 3888, 3883, 3888 3885, 3897, 3894, 3890, 3896, 3891 $t = 30$ secs

Summarised Results for Air

Date	Vol c c	Time, Secs	No of Obs	p_2 cm	p_1 cm	θ_2 Abs	θ_1 Abs	γ Mean
1923								
27 4	700	0 48	8	75 77	80 551	282 172	287 074	1 3916
30 4	700	0 34	7	75 98	80 814	282 326	288 294	1 3918
26 5	700	0 34	8	75 71	80 505	282 539	287 467	1 3915
26 4	300	0 35	10	74 83	79 628	282 436	287 399	1 3904
9 5	300	0 28	12	75 61	80 456	285 381	290 388	1 3889
12 5	300	0 30	10	75 08	79 909	283 007	287 998	1 3890
2 5	75	0 27	11	76 63	81 555	283 647	288 586	1 3833
2 5	75	0 23	6	76 57	81 504	283 708	288 658	1 3834
17 5	75	0 23	9	76 31	81 224	282 183	287 099	1 3827
27 6	75	0 23	8	76 46	81 338	286 077	291 021	1 3830
20 5	35	0 20	6	75 24	80 012	282 371	287 174	1 3780
20 5	35	0 20	10	75 16	79 991	282 414	287 280	1 3783
20 5	35	0 30	11	75 17	79 994	282 489	287 356	1 3782
21 5	700	0 52	8	75 82	80 686	191 400	194 788	1 3936
30 5	700	0 65	5	76 31	81 152	191 460	194 845	1 3956
30 5	700	0 65	5	76 31	81 055	191 529	194 828	1 3962
30 5	700	0 60	7	76 31	81 105	191 508	194 859	1 3953
21 5	300	0 36	9	75 77	80 533	191 420	194 738	1 3925
28 6	300	0 33	11	76 56	81 333	191 598	194 874	1 3921
28 6	300	0 33	7	76 56	81 559	191 402	194 850	1 3931
19 5	75	0 24	13	75 94	80 778	191 454	194 770	1 3857
30 5	75	0 22	16	76 29	81 170	191 521	194 861	1 3869
28 6	75	0 24	18	76 62	81 501	191 545	194 872	1 3861
19 5	35	0 20	13	75 91	80 745	191 481	194 785	1 3821
28 6	35	0 22	16	76 59	81 450	191 565	194 866	1 3823
24 7	75	0 40	15	75 92	80 798	152 502	155 200	1 3927
24 7	35	0 40	7	75 98	80 878	152 515	155 189	1 3850
24 7	35	0 40	6	75 98	80 872	152 552	155 231	1 3858

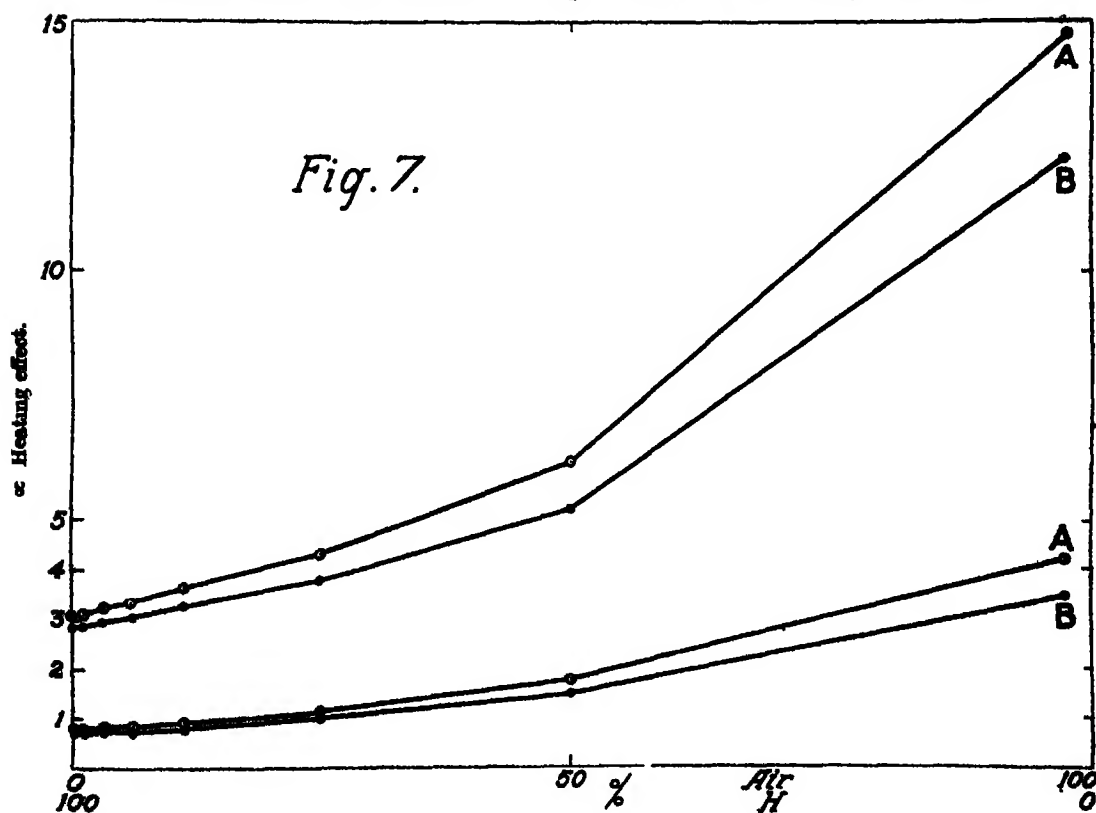
Hydrogen Experiments

Preliminary Observations.—The whole apparatus was exhausted and then filled with hydrogen, these processes being repeated until a sample of gas taken from the circuit had a purity of about 99 per cent of hydrogen. In the first experiments, using the 75 c.c. bulb, the bridge current was the same as in the previous experiments on air at room temperatures. It was at once obvious that the time of expansion was very much smaller and that the kick sensitiveness was much reduced. With times of 0 16, 0 11 and 0 07 seconds, the values of γ were about 1 35, 1 37 and 1 38 respectively. The largest bulb was then used, with the same bridge current, the value 1 395 was obtained with a key time of 0 2 seconds, the kick sensitiveness being only 2 divisions per mm., *i.e.*, about ten times smaller than in the case of the corresponding air experiments. The sensitiveness was increased by putting 100 instead of 400 ohms in circuit with the 4 accumulators. The value of γ obtained was practically the same, but the

sensitivity was now 6.5 divs per mm. of bridge wire. With such a large value for the heating effect, over 1.5°C . in the experiments at air temperatures, the variation in its values at θ_1 and θ_2 becomes of great importance; it amounts to about 0.06 cm of bridge wire and gives an additive correction to the ratio of 0.0023.

At lower temperatures, sufficient sensitiveness was obtained when using much smaller currents through the thermometer. The correction for the change in the heating effect was 0.02 cm at -78°C , 0.01 cm at -118°C , and nothing at -183°C .

Purity of the Hydrogen—The magnitude of the heating effect varied greatly with the purity of the hydrogen and its measure was a useful guide to a knowledge of this purity. As will be seen from fig 7 the heating effect changed from about 19 cm of bridge wire, when the bulb contained air, to about 4 cm, when hydrogen of the maximum purity used filled the bulb. The dependence of the heating effect on the purity was estimated in the following way. The resistance of the thermometer was measured, using 1, 2 and 4 cells through 100 ohms,



when the bulb was filled with air. The pressure in the bulb was then reduced to one half its initial value, 80 cm of mercury, and hydrogen, from the reservoir, was admitted to raise the pressure back to the original value, when similar resistance measurements were again made. This procedure was repeated.

The curves (fig 7) are obtained by plotting the differences between the resistances with 2 and 1, and with 4 and 2 cells respectively, against a rough estimate of the air content. The upper curves show that when the hydrogen is fairly pure, a difference of 1 mm on the bridge wire corresponds to about 1 per cent change in the purity of the hydrogen. The curves marked AA refer to observations made with the 300 c.c. bulb at 0° C, BB represent mean results obtained using the 700 c.c. and 75 c.c. bulbs at a temperature of about 15° C.

I am indebted to Mr D. Newitt, of the Department of Chemical Technology in the Imperial College, for some analyses of samples of hydrogen taken from the gas circuit on various occasions, chiefly when the low temperature measurements were in progress. The mean of six separate analyses gives 99.3 ± 0.5 per cent of hydrogen, the impurity being air, as there was about four to six times as much nitrogen as oxygen present in the remainder. A small correction, amounting to 1 part in 1000 on the value of ν at -183°C , has been applied to the final results.

Final Experiments—These are summarised in the following tables. The general nature of the temperature changes during the expansion of the gas was as in the air experiments (fig 3), but the time scale was reduced about five times.

HYDROGEN FINAL EXPERIMENTS (fig. 9)

Reduced Observations

P_2	P_1	a	b	c	d	μ_2	θ_1	γ
November 29th, 1923 300 c c bulb						$t = 0 \ 17 \text{ sec}$		
75 22	80 345	202 81	16 5	24	196 19	87 834	90 002	1 5872
	80 288	202 81	16 5	11	196 26	87 857	90 002	1 5872
	80 233	202 81	16 6	18	196 32	88 877	90 002	1 5882
	80 174	202 81	16 6	3	196 40	88 903	70 002	1 5873
	80 123	202 81	16 8	30	196 45	88 919	90 002	1 5894
	80 060	202 81	16 8	22	196 50	88 936	90 002	1 5917
	80 017	202 82	16 9	24	196 59	88 966	90 005	1 5924
	79 961	202 82	16 8	- 2	196 63	88 979	90 005	1 5935
	79 907	202 82	16 9	- 2	196 73	88 012	90 005	1 5885
								1 5895
						$t = 0 \ 15 \text{ sec}$		
75 26	80 254	202 83	16 6	9	196 37	87 893	90 009	1 5880
	80 198	202 83	16 8	37	196 41	87 906	90 009	1 5887
	80 140	202 84	16 7	0	196 52	87 942	90 012	1 5881
	80 082	202 85	16 8	4	196 60	87 968	90 015	1 5884
	80 028	202 85	17 0	27	196 67	87 991	90 015	1 5873
	79 970	202 85	16 9	0	196 72	88 008	90 015	1 5910
	79 916	202 85	17 0	5	196 79	88 031	90 015	1 5906
								1 5890
December 5th, 1923						$t = 0 \ 17 \text{ sec}$		
74 57	79 495	200 23	14 0	3	193 84	87 065	89 157	1 5905
	79 436	200 27	14 3	29	193 96	87 105	89 170	1 5889
	79 371	200 32	14 3	7	194 08	87 145	89 186	1 5899
	79 315	200 36	14 5	21	194 20	87 184	89 199	1 5883
	79 262	200 42	14 5	2	194 31	87 220	89 219	1 5907
								1 5897

Summarised Results for Hydrogen.

Date	Vol cc	Time, secs	No of Obs.	P_2 cm	P_1 cm	θ_2 Abs	θ_1 Abs	γ Mean
1923								
17 9	700	0 09	9	75 33	80 087	285 129	290 180	1 3982
19 9	700	0 10	10	75 73	80 575	284 682	289 754	1 3980
12 9	700	0 22	11	75 69	80 565	284 800	289 873	1 3950
27 9	700	0 15	9	76 88	81 786	284 034	289 074	1 3970
10.11	700	0 12	7	76 60	81 505	282 327	287 353	1 3981
3 10	300	0 06	8	74 76	79 620	284 789	289 903	1 3944
29 10	300	0 07	9	76 00	80 977	284 346	289 438	1 3960
31 10	300	0 06	7	76 46	81 422	284 751	289 880	1 3962
1 11	75*	0 05	10	76 45	81 389	284 507	289 520	1 3958
22 11	75*	0 04	7	75 46	80 404	280 137	285 128	1 3860
10 10	35†	—	—	—	—	—	—	1 368
1924								
31 1	300	0 09	7	76 96	81 865	268 278	273 046	1 3983
24 1	300	0 08	12	76 47	81 373	247 500	252 000	1 4084
24 1	300	0 09	9	76 45	81 210	247 593	251 968	1 4087
1923								
14 11	700	0 12	6	74 35	79 220	190 927	194 619	1 4331
14 11	700	0 12	9	74 69	79 496	191 036	194 660	1 4339
31 10	300	0 09	11	76 46	81 257	191 358	194 904	1 4312
1 11	75	0 07	12	76 63	81 422	191 417	194 897	1 4240
24 10	35	0 05	13	73 81	78 714	190 826	194 478	1 4190
22 11	35	0 05	10	75 49	80 360	191 184	194 740	1 4194
1924								
31 1	300	0 12	19	76 90	81 783	152 494	155 511	1 4676
1923								
29 11	300	0 17	9	75 22	80 123	87 919	90 002	1 5895
29 11	300	0 15	7	75 26	80 082	87 968	90 015	1 5890
5 12	300	0 17	5	74 57	79 371	87 145	89 186	1 5897
7 12	75	0 12	5	75 20	79 969	87 985	90 005	1 5838
19 12	75	0 12	14	76 57	81 500	88 061	90 114	1 5837
25 11	35‡	0 10	15	76 50	81 370	88 240	90 239	1 5764
29 12	35	0 11	8	77 08	81 968	88 155	90 157	1 5772
29 12	35	0 09	6	77 08	81 838	88 217	90 177	1 5778

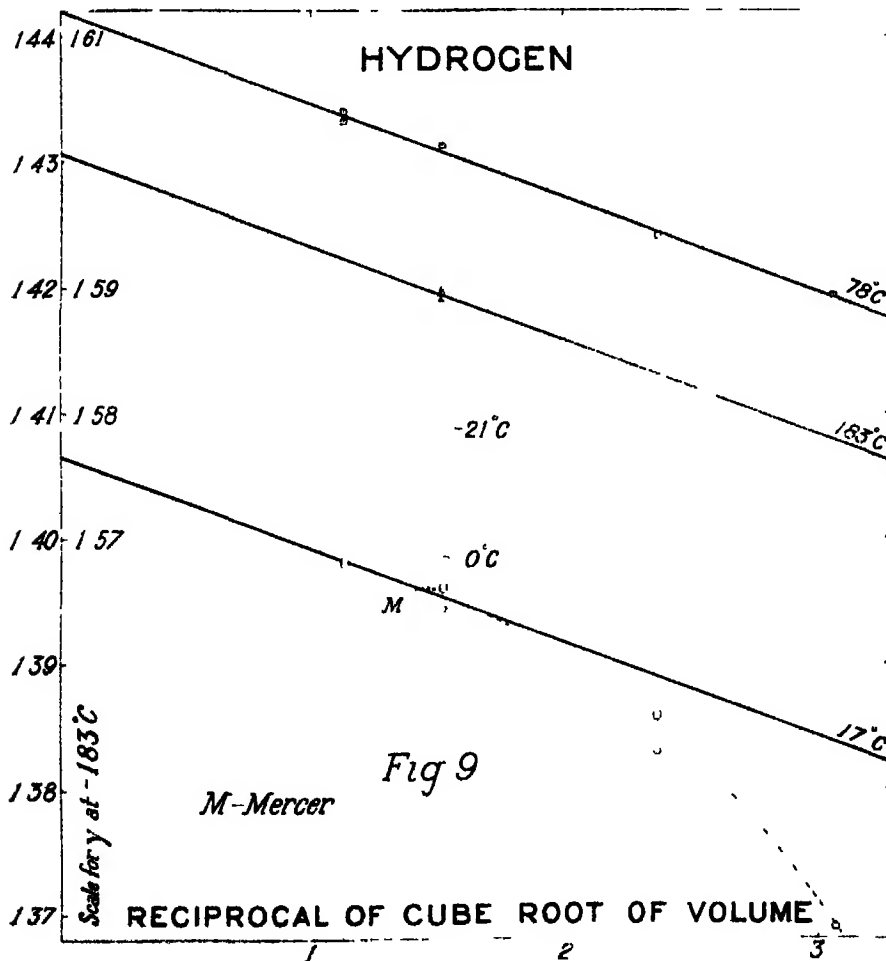
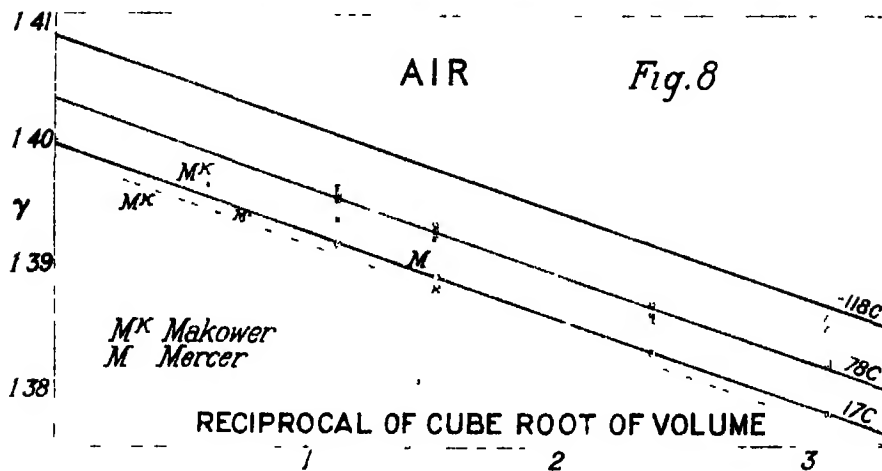
* With a key time 0 07, $\gamma = 1 383$

† Key time too small for measurement Highest value obtained

‡ With a key time 0 17, $\gamma = 1 574$ " " 0 29, $\gamma = 1 570$

Extrapolated Results—In figs. 8 and 9 the mean result obtained with each bulb is plotted against the reciprocal of a linear dimension of the bulb, i.e., the inverse cube root of the volume. It is found that the results at any temperature thus treated lie on a straight line—this law had been assumed by Mercer—and the value given by the intersection of this line with that of infinite volume is taken as the value required.

As soon as the gas in the neighbourhood of the thermometer is cooled by



the adiabatic expansion an inflow of heat occurs from the walls of the vessel. This causes a rise of temperature in the gas which will vary inversely with the volume employed θ_2 will therefore be in excess of its true value, and γ will be lower than the value corresponding to infinite volume by an amount depending on an inverse linear dimension of the vessel

There is no difficulty in deducing the relation which represents the results of the experiments on air, because a linear law is so strictly applicable to the results obtained with all four vessels. This is the case because the time of the key could be made short enough, even in the experiments with the 35 c c bulb

Hydrogen, on account of its much smaller density, expands very much more rapidly, and it was not possible to make observations with a time interval sufficiently short in the experiments with the two smaller vessels at air temperatures. The four experimental results, at about 15° C, lie on a curve which, if extrapolated on the assumption that *all the points should be equally weighted*, indicates a value for the ratio for hydrogen at this temperature slightly higher than that obtained by Shields

It was noticed how nearly the straight line through the mean results obtained with the two larger vessels passed through the value obtained by Lummer and Pringsheim, and also that this line was approximately parallel to the other straight lines representing the results with air. At a later date it was found, from the other experiments on hydrogen at lower temperatures, when, owing to the greater masses of gas in any bulb, more correct experimental conditions were obtainable with the smaller vessels, that similar nearly parallel lines were obtained

Although the gases used had such very different physical properties and the temperatures of the experiments extended over so wide a range, the slopes of all these lines, each obtained from one set of experiments, agreed to within 6 per cent. As the magnitude of the correction to be applied to the results obtained with the 300 c c bulb amounts to only 0.01 on the value of γ , the final values of γ would not be affected by as much as 1 part in 2000 by the adoption of a constant slope for all the linear relationships experimentally found. This result was wholly unexpected, it is undoubtedly due to the fact that, in attempting to observe the lowest temperature attained by the gas in the manner described previously, the time of the key is necessarily much shorter when using hydrogen than when air fills the bulb

The Radiation Correction—The thermometer wire continually receives heat from the walls of the expansion vessel. The quantity of heat received will depend on the nature of the surfaces and on the magnitudes of θ and of

Δ6. The subsequent rise in temperature of the wire, on which the radiation correction depends, will be determined not only by the quantity of heat absorbed, which is practically independent of the nature of the gas, but also by the rate of loss of heat from the wire. The latter will depend on the thermal conductivity of the surrounding gas.

The radiation corrections will, therefore, be in the inverse ratio of the thermal conductivities of the gases, as was assumed by Mercer. If the above explanation is correct, Partington's adverse criticism of this method of estimating the correction is unjustifiable. The radiation correction has been measured and applied to their results by all other observers, except by Shields. She points out that it does not apply to values of γ obtained by extrapolating against the pressure excess.

The method of determining the correction is to measure γ , first with a bright platinum wire and then with the wire coated with platinum black, all other experimental conditions being the same. Then, assuming that the absorption of a black surface is 15 times as great as that of a polished surface, the correction can be calculated. As the thermometer, after the air experiments, was used for work with hydrogen, an experiment to determine this correction has not been made, obviously, it could not safely be attempted in an atmosphere of hydrogen.

However, the smallness of the correction, and still more the concordance between the values for it which have been obtained by others, justifies the assumption of an additive quantity 0.0021 to correct for this radiation error in air at room temperatures. The values at lower temperatures have been deduced by the application of Stefan's law.

Theoretical Correction—Equation A, p 511, applies only to perfect gases which obey the law $pv = R\theta$. The adiabatic law assumed in calculating the results is $p^m/\theta = \text{constant}$. In the limit, corresponding to results deduced for a vessel of infinite volume, m is written as $\frac{\gamma' - 1}{\gamma'}$. The specific heat at constant pressure s_p , of a gas which obeys the Callendar characteristic equation, $v = b + \frac{R\theta}{p} + c$ (where b is the co-volume, and c the co-aggregation volume, which is a function of the temperature of the form $c = c_0 \left(\frac{\theta_p}{\theta}\right)^n$, n being dependent on the nature of the gas), can be calculated from the thermodynamical relation $s_p \left(\frac{d\theta}{dp}\right)_p = \theta \left(\frac{dv}{d\theta}\right)_p$. The difference of the specific heats at constant pressure and constant volume can be calculated from $s_p - s_v = \theta \left(\frac{dp}{d\theta}\right)_v \left(\frac{dv}{d\theta}\right)_p$.

$\gamma = -\frac{s_p}{s_v}$ can thus be obtained in terms of γ' , the relationship being

$$\gamma = \gamma' \left(1 + (\gamma' - 1) \frac{ncp}{R\theta} \right).$$

The numerical values adopted in calculating this correction are those given by Prof Callendar in his paper on the "Thermodynamical Correction of the Gas Thermometer" ('Phil Mag,' January, 1903)

The corrections are almost identical in magnitude with those deduced from the Berthelot characteristic equation used by Partington

Summary

Final Values for the Ratios of the Specific Heats

Gas	Temperature, °C	γ'	Radiation correction r	$\gamma' \pm \gamma'$	Thermodynamical correction factor (1 + f)	Impurity correction	Final Values of γ	Values Obtained by Other Observers
Air	17	1.3997	0.0021	1.4018	1.0010	—	1.4032	1.4025 L & P. 1.4029 Sh 1.4034 P
	-78	1.4032	0.0005	1.4037	1.0028	—	1.4077	1.4055 K.
	-118	1.4082	0.0002	1.4084	1.0050	—	1.4154	
Hydrogen	17	1.4006*	0.0004	1.4070	1.0000	—	1.4070	1.4012 Sh
	0	1.4095	0.0003	1.4098	1.0001	—	1.4099	
	-21	1.4197	0.0002	1.4199	1.0001	—	1.4200	
	-78	1.4420	0.0001	1.4421	1.0002	0.0003	1.4427	
	-118	1.4789	0.0000	1.4789	1.0004	0.0005	1.4800	
	-183	1.6007	—	1.6007	1.0020	0.0015	1.6054	1.592 Sh
	—	—	—	—	—	—	—	—

L & P, Lummer and Pringsheim, 'Ann d Phys,' 1898

K, Koch, 'Ann d Phys,' 1908

P, Partington, 'P R S,' 1921

Sh, Shields, 'Phys Rev,' 1917

* L & P, experimental value 1.4063

Criticism of Previous Measurements of γ

Summaries of the work of the many observers will be found in various papers referred to below. It will be sufficient if attention is restricted to results obtained by the method adopted in these experiments. This limits the discussion to a consideration of the methods of extrapolation used by some observers and to the results of the experiments by Lummer and Pringsheim, and by Partington.

Moody ('Phys Rev,' vol 34, p 275, 1912), and later Shields ('Phys. Rev.,' vol 10, p. 525, 1917) using thermocouples, extrapolate the observed values

of γ against the pressure excess Δp . Over the range of pressures used by the latter observer, 7 to 35 mm of mercury only, a linear relation holds with considerable accuracy. Moody, using larger pressure excesses and a vessel of 60 litres capacity, found that the linear relation did not hold good for values of Δp greater than 6 cm, the divergence of the observations from this linear law being in the same direction as that found by me (fig 6), but not so large as mine. Both these experimenters made the key contact at some definite time after the commencement of the sudden expansion, but such contact was not made automatically.

In Moody's experiments this interval was either 2 or 3 seconds. In Shields' work, with a 1-litre flask, the time was between 0.87 and 1 second in the air experiments, and from 0.62 to 0.83 second when hydrogen was used.

There can I think, be no doubt that the reason for the low values of the ratio for hydrogen obtained by Shields is because the time intervals were too long.

Both Lummer and Pringsheim and I find that the time taken for the expansion is some five times smaller in the case of hydrogen than for air, possibly Shields would have obtained a higher value if the time intervals employed had been between 0.1 and 0.2 second. Shields points out that this method of extrapolation corrects for error due to conduction along the leads of the thermo-junction as well as for the radiation effect, as these are proportional to $\Delta\theta$, which is itself zero when $\Delta p = 0$.

For the same reason any thermometric lag effect is eliminated. This method of extrapolation is objectionable chiefly because the observed values of γ obtained from experiments with small values of Δp and $\Delta\theta$, on which observational and accidental errors would produce big percentage errors, are just those of most importance in fixing the point of intersection ($\Delta p = 0$), giving the final value of γ .

Makower ('Phil. Mag.', vol 5, p 226, 1903) used air in a 50-litre globe and a compensated thermometer of 0.025 mm diameter platinum wire. From the observed measurements, he calculated the values of the adiabatic index m (see p 511) corresponding to different times of closing the circuit after the expansion, times which varied from 0.75 to 5 seconds. He assumed this variation of m to be linear and extrapolated to find the value corresponding to zero time interval. This method may, perhaps, be referred to in terms of fig. 3, as one in which observations are made at various points on the slowly upward-rising part of the temperature-time curve, i.e., between e and f . The values of m for times shorter than about 1 second are constant and give a value

of $\gamma = 1.396$, but by assuming the linear extrapolation Makower deduces $\gamma = 1.399$

It is difficult to see how such a method of extrapolation can possibly correct for any lag effect, but the close agreement of the extrapolated result with the probable value may be taken as a proof that any error due to lag effect in a wire of 0.025 mm diameter is very small, certainly not exceeding 0.001 on the value of γ . It is interesting to note that his results, for time intervals of one second and less, confirm the horizontal nature of the line c, c , in fig. 3. The experimental result 1.396 is of great value as an estimate of γ which can indubitably be associated with my own experiments.

The method of extrapolation used by Mercer and myself is not open to the two objections raised above. The observations are all made with a fairly large pressure excess, so that percentage errors in Δp and $\Delta \theta$ are minimised, moreover, as I have shown, there is a very accurate linear relation between the plotted quantities over a big range in the size of the vessel employed, and the whole variation in γ over the observed straight portion of any line is only 1 per cent.

Again, the linear extrapolation gives a value of γ corresponding not only to that obtainable with a vessel of infinite volume, but also to a long time for the key. This is clear if it be remembered that the key times had to be increased as the size of the bulb increased, in order to get near the point c (fig. 3), and during this long interval lag effects would have had time to disappear. The method would not have been satisfactory if the thermometer had not been compensated.

Before commencing the hydrogen experiments, I had expected that the much greater thermal conductivity of this gas would be indicated by an increased slope in the lines representing the results. That this is not the case shows that the correction applied depends on the size of the bulb and on the thermometer, but not, apparently, on the nature of the gas surrounding the latter. The closeness with which Makower and Mercer's values agree with mine are confirmatory to this supposition.

Lummer and Pringsheim and Partington have made measurements, using much finer wires in the thermometric system. Lummer and Pringsheim used a fine bolometer strip in a globe of 90 litres capacity. They showed that, in the case of air, the same results were obtained with an expansion time varying from 12 to 2 seconds, and that in the latter case "the galvanometer needle remained absolutely at rest for several seconds after the expansion." There must, however, be some uncertainty in their results, owing to the fact that

the bolometer strip was not compensated for conduction occurring from the thicker leads

Probably Partington's result $\gamma' = 1.4001$ ('Roy Soc Proc,' A, vol. 100, p 27, 1921), obtained for air, using a 130-litre globe and a thermometer wire of diameter 0.001 mm, may be considered as entirely free from systematic error, unless any was introduced by the "overshooting" of the gas owing to the rapidity of the expansion

He made some preliminary observations, using thermometer wires 0.05, 0.01 and 0.001 mm in diameter respectively, and found lag effects which increased with the diameters of the wires used these measurements being apparently made with no compensating leads. If this were so, the "lag" effects, i.e., the non-coincidence of the temperature of the wire with that of the gas immediately surrounding it, would be due to two causes, (a) the inertia of the wire itself, (b) conduction to the wire from the leads. Both these effects tend to maintain the wire at a temperature above that of the gas. If the two effects are operative, it does not seem justifiable to apply the full correction deduced from these preliminary observations to results obtained with compensated thermometric systems. In some later experiments on air, when a 60-litre vessel was employed, with a wire of 0.01 mm diameter forming the compensated thermometer, Partington and Howe ('Roy Soc Proc,' A, vol 105, p 225, 1924) obtained two values, 1.3928 and 1.3968, "there being some uncertainty to within 0.05" in the measurement of the final temperature in the second determination. The correction applied was deduced from the "lag" observations quoted above, and the values of γ' became 1.4004 and 1.4038 respectively

Makower's experimental value, 1.396, is only 0.004 lower than the most probable value of γ' , but Partington's first result, to which he attaches most weight, is so much lower than this, although the thermometer wire used was 2.5 times smaller in diameter, that it suggests some outstanding error in Partington's later measurements. In other experiments Partington found "overshooting" to occur when he used oxygen, but not when he used nitrogen. This seems so curious that, perhaps, it had better be considered as *sub judice*

Partington's value $\gamma' = 1.4001$ was obtained by the null method, the galvanometer being an Einthoven string galvanometer with a period of about 0.01 seconds. The resistance of the thermometer wire was about 1000 ohms, and this was not affected by variations, within reasonable limits, of the bridge current. The temperature measurements were deduced by direct comparisons with an auxiliary thermometer, which was read to 0.01° C, and corrected for

emergent stem and scale errors. Though the advantage accruing from the use of the fine wire bolometer and a dead-beat galvanometer, having a short period, are very great, there is a loss in sensitivity, as measured by the deflection of the filament corresponding to a temperature change in the thermometer wire. An estimate of this sensitiveness can be made from the experimental data given. The initial and final temperatures being fixed, $\Delta\theta = 7.72^\circ$, a pressure excess of 115.10 mm of oil caused a deflection of 0.1.

The null experiment gives $\gamma' = 1.3981$. Neglecting the deflection, the preliminary experiment gives $\gamma' = 1.3965$. The 0.1 division deflection (this is stated as being the limit to which the scale deflection could be estimated), therefore, corresponds to a temperature difference of over 0.02°C. , and the accuracy of an individual result is limited to about 0.0015 on the value of γ' .

The sensitivity may be even less than this, as the value of γ' deduced from the null experiment is 0.002 lower than the mean of all the results which vary from 1.3978 to 1.4015. Confirmation of the essential correctness of this calculation is obtained from a statement by Partington ('Roy Soc Proc,' A, vol. 105, p. 238, 1924) that "one-half a small scale division corresponds to about 0.10° temperature change," though this statement refers to his more recent, but similar, experimental arrangements.

Kundt's tube method of determining the velocity of sound in gases cannot be considered good, owing to the difficulty in measuring the length of the sound wave.

It is much better to measure the velocity of sound in small tubes by a direct method and to deduce the velocity in free gas. This has been done recently by Dixon, Campbell and Parker ('Roy Soc Proc,' A, vol. 100, p. 1, 1921) and by Dixon and Greenwood ('Roy Soc Proc,' A, vol. 105, p. 199, 1924). Their measurements were made on many different gases and vapours and extend over a wide range of high temperatures.

Great care was taken to eliminate errors inherent in the timing mechanism. The values obtained are probably more accurate than any previously recorded.

Values of the Specific Heats, fig 10

The specific heat at constant pressure, s_p , and the molecular heat at constant volume S_v , can be deduced from the final values of γ , but the error introduced on the value of each specific heat thus calculated is about three times larger than that existent on the value of γ . Nevertheless, a smooth curve drawn through my observations with Hydrogen at 90° , 155° , and 290° abs. , gives

values at 252° and 273° which agree within one part in 250 with those deduced from the experimental measurements.

The following values have been assumed in the calculations of s_p and S_v

R the gas constant	= 1 985
Molecular Weight of Air	= 28.99
Molecular Weight of Hydrogen	= 2 016

Air

$\theta^\circ \text{ A}$	$\gamma - 1$	$S_p - S_v$	S_v	s_p	Direct Measurement of s_p
290	0 4032	1 995	4 948	0 2395	0 2414 S_v , 0 237 R 0 2406 S & H
195	0 4077	2 012	4 937	0 2396	0 243 S & H, 0 237 W
155	0 4154	2 034	4 896	0 2391	0 246 S & H * (at 90° A)

Hydrogen.

$\theta^\circ \text{ A}$	$\gamma - 1$	$S_p - S_v$	S_v	s_p	Direct Measurement of s_p
290	0 4070	1 9856	4 879	3 405	3 403 S & H
273	0 4099	1 9858	4 844	3 388	3 40 R
252	0 4200	1 9863	4 729	3 331	
195	0 4427	1 9869	4 488	3 212	3 157 S & H, 3 21 *
155	0 4800	1 9884	4 142	3 041	
90	0 6054	1 9983	3 301	2 628	2 644 S & H., 2 60 *

R, Regnault, 'Mém de l'Acad,' 1862

S_v , Swann, 'Phil. Trans,' A, 1911

W, Witkowski, 'Phil Mag,' 1896

S & H, Scheel and Heuse, 'Ann d Phys,' 1912, 1913

* S & H, Scheel and Heuse, 'modified (see below)

Scheel and Heuse ('Ann der Physik,' vol 37, p 79, 1912, and vol 40, p. 473, 1913) have measured the specific heats at constant pressure for air, hydrogen and other gases. The flows, in grammes per second, were very small, so that a very long extrapolation is necessary in order to arrive at the value of s_p corresponding to infinite flow, *i.e.*, zero heat loss. If their experimental observations of $CE/Qd\theta$ are plotted against the corresponding values of $1/Q$, it will be found that considerable latitude in the values of s_p deduced is possible. The experimental results with hydrogen at -78°C , can be represented by a linear relation, fitting the points quite as well as the curve adopted, which gives the value 3.21, which is in excellent agreement with that deduced from my measurement of γ at this temperature. With regard to Scheel and Heuse's

measurements on air and hydrogen at -183°C , values rather lower than those they give can be deduced. For example, each of the three series of experiments on air at this temperature, when extrapolated linearly, will give a value of s_p in the neighbourhood of 0.246.

Regnault's value for the specific heat of air undoubtedly requires correction for the variation in the specific heat of water. In addition, if the correction suggested by Leduc ('Compt Rend,' 1898) is made, Regnault's value is raised to 0.239₆, or if the experimental values be plotted against $1/Q$, the value corresponding to infinite flow is about the same.

Eucken ('Sitz d Kon Preus Akad d Wiss,' 1912 p 141) measured the molecular heat of hydrogen as a difference between the thermal capacities of a steel vessel when empty and when filled with hydrogen. At temperatures above 190°A , the ratio, thermal capacity of the contained hydrogen/thermal capacity of vessel, was about $\frac{1}{8}$, but at lower temperatures the ratio increased. The specific heat of steel alters very rapidly at low temperatures, and as the values of this quantity are somewhat uncertain, it is clear that some considerable error may be introduced on the small difference measured. Eucken's results, the first in which the rapid change in the molecular heat of hydrogen was experimentally verified, are remarkably consistent when one remembers the extreme difficulty of the measurements.

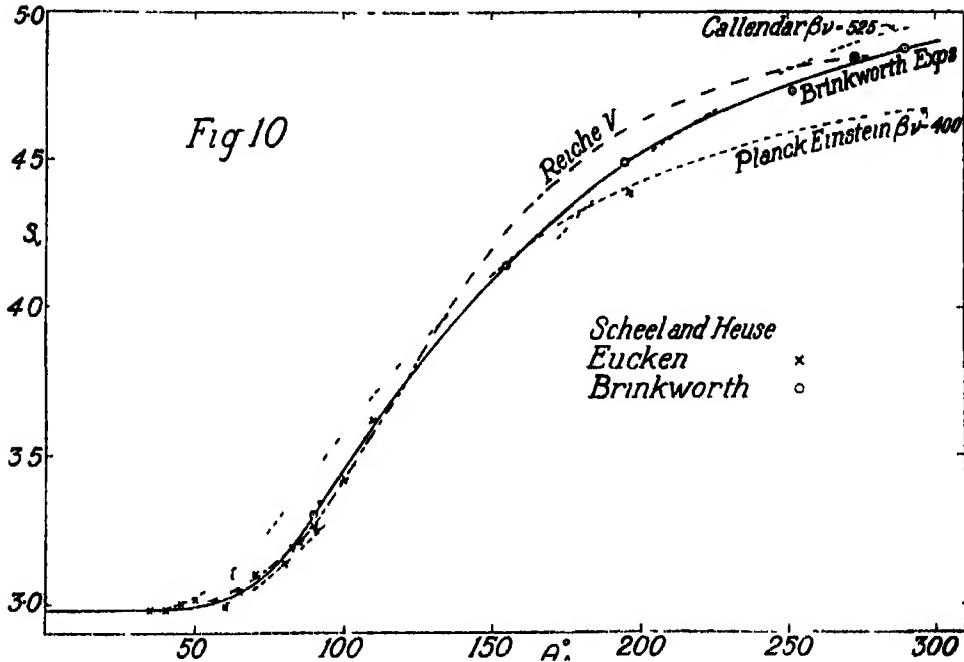
On the Variation of the Molecular Heat of Hydrogen with Temperature

The values of S_p , calculated from my experimental observations, are plotted against the corresponding absolute temperatures in fig. 10, and the continuous variation in S_p is represented by the full curve. The values obtained by Eucken (*loc cit*) and those deduced from the experiments by Scheel and Heuse (*loc cit*) are also shown. The three broken curves have been drawn from formulæ proposed by Planck-Einstein ('Ann der Physik,' vol 22, 1907), by Reiche ('Ann der Physik,' vol 58, p 657, 1919) and by Callendar ('Phil. Mag,' vol 26, p 787, 1913) respectively. Not one of these fits the experimental observations over the whole temperature range at all well, for each deviates by 2 per cent* or more from the full curve representing values which, by a very conservative estimate, are accurate to within one-half of 1 per cent.

It is not to be expected that a simple relation, involving one frequency only and however deduced, should represent the results over the whole temperature

* The divergence when measured as a percentage of the rotational specific heat is several times greater than this.

range, but Callendar's formula certainly agrees better than the simple Planck-Einstein relation whatever value of βv is adopted in the latter expression



Reiche has discussed the problem of the temperature variation of S_v , basing his calculations on a rigid model of the molecule. His curve V, which is plotted, is obtained by excluding, somewhat arbitrarily, certain quantum states. It is in fair agreement with my experimental curve below 160° and above 270° , but it also gives values which deviate by as much as 2 per cent. between these two temperatures, although so many initial assumptions have been made

*The Interpretation of the Results of Bucherer's Experiments
on e/m .*

By THOS LEWIS, B Sc, Garrod Thomas Fellow of the University College of
Wales, Aberystwyth

(Communicated by Prof G A Schott, F.R.S —Received October 24, 1924)

1. *Introduction* —In the 'Physikalische Zeitschrift,' 9 Jahrgang, No 22, pp 755-760, and again, in greater detail, in the 'Annalen der Physik,' 1909, vol 28, pp 513-536, Prof A H Bucherer gives an account of an experiment performed by him with the object of ascertaining which of the various mass formulæ attributed to the electron by theoretical physicists agrees best with experiment. The method is briefly as follows: a source of high speed electrons (a stick of radium fluoride) is fixed on the axis of a circular parallel plate condenser, one of whose plates is connected to earth, and the other to a source of high potential so as to produce a sensibly uniform electric field in the region between. Perpendicular to the electric field is applied a uniform magnetic field whose effect is to diminish, or increase, the mechanical force on the electron according as the direction of its velocity forms a left-handed or a right-handed system with those of the two fields.

Since the distance between the plates is very small compared with their radius, it follows that the velocity of projection of an electron cannot have an arbitrary value if it is to escape from the condenser. Given the direction of projection of an electron, its velocity must lie between two definite limits which depend upon the relative intensities of the two fields, and also upon the distance between the plates of the condenser.

More explicitly expressed the velocity must be such that the mechanical force on the electron, due to the magnetic field, almost balances that due to the electric field, the maximum resultant mechanical force allowable for two given fields will depend upon the distance between the plates of the condenser. We cannot diminish this distance without limit, and at the same time maintain a high difference of potential between the plates. In Bucherer's experiment the distance between the plates was 0.025 cm.

Outside the condenser, the electrons are subject to the influence of the magnetic field only, and their paths will be helices. Coaxial with the condenser is fixed a cylindrical photographic film of twice the radius, upon which the electrons are allowed to impinge, thus producing the usual photographic

effects, and enabling us to measure actual deviations which they have suffered owing to the presence of the magnetic field

Photographs of the apparatus used are reproduced in the '*Annalen der Physik*', also reproductions of two of the films are given. The double curve was obtained by reversing the field. (See fig. 3 (a), p. 559)

If we take account of the so-called compensated rays only—those for which the mechanical force inside the condenser is zero—the velocity of projection, and the deflection on the film corresponding to a given direction of projection are easily calculated. In this simple case the trace should have the same width at every point, and to a given section of the trace should correspond one, and only one, velocity. In actual practice such ideal results cannot be obtained, non-compensated rays escape, causing a widening of the trace and displacement of the curve of maximum intensity. The effect of these rays becomes more and more marked as we approach the points where the curves join the central trace attributed to γ -rays. In this paper we shall show how to construct the trace as it should be if the Lorentz formula holds for very high velocities, other circumstances being supposed ideal. The experimental material necessary for constructing the trace is very scanty—very little is known about the β -ray spectrum of radium salts in the region of high velocities. The highest velocity observed by Ellis up to date is 0.83 times the velocity of light. (See '*Royal Society Proceedings*,' January and February, 1924.) In the region explored he has identified but three strong lines, which correspond to velocities 0.64, 0.70 and 0.75 times that of light, and for whose relative intensities he has given the values 25, 30 and 40 respectively. His estimates of the relative intensities of the other lines range from 1 to 10.

These strong lines of Ellis will not account for the deviation of the experimental trace from that calculated for the compensated rays (see fig. 3a), but the assumption of sufficiently strong rays in the region observed by Danysz enables us to do so. This investigator (see '*Comptes Rendus*,' 2, 1911) has identified lines corresponding to velocities up to 0.99 times that of light, but it is very desirable that this region should be reinvestigated, and that finer estimates of the relative intensities of the lines identified should be recorded. It is hoped that this paper will serve to show the necessity of undertaking this task. We are forced to the conclusion that if the Lorentz formula is valid for all velocities, then, in order to account for the traces obtained by Bucherer, it is necessary to assume the existence of strong β -rays of very high velocities.

2. Path of the Electron—The equations of motion of an electron moving in a steady and uniform electromagnetic field, with the electric and magnetic

forces at right angles to one another, have been worked out by Prof G A Schott in his book, 'Electromagnetic Radiation,' p 301 Taking the origin on the axis of the condenser—the axis z along it, the axis of x parallel to the magnetic field, and that of y perpendicular to the first two, so as to form a right-handed system—the equations of motion are

$$x'' = 0, \quad y'' - pz' = 0, \quad z'' + py' - p^2 \sin^2 \lambda (z + k) = 0, \quad (1)$$

where the dashes denote differentiation with respect to a new variable τ

$$\text{defined by the equation } t = \int_0^\tau (1 - \beta^2)^{-\frac{1}{2}} d\tau, \quad (2)$$

$$\text{and } p = eH/cm, \quad \sin \lambda = E/H, \quad (3)$$

while k is a constant determined from the initial condition

$$c(1 - \beta_0^2)^{-\frac{1}{2}} = p \sin \lambda (z_0 + k) \quad (4)$$

(The suffix 0 will be used throughout to refer to the axis of the condenser, the suffix 1 to its edge, and the suffix 2 to the film)

Let us put

$$s = c(1 - \beta^2)^{-\frac{1}{2}} = (c^2 + w^2)^{\frac{1}{2}}, \quad \phi = \tau \cos \lambda, \quad A = y'_0 \sec \lambda - s_0 \tan \lambda, \quad (5)$$

where w denotes $\sqrt{x'^2 + y'^2 + z'^2}$, the velocity referred to τ as time variable

In Bucherer's experiment E was less than H , so that λ is real Hence the solutions of the equations (1) are

$$\left. \begin{aligned} x &= x'_0 \sec \lambda \phi \\ y &= y'_0 \sec \lambda \phi + p^{-1} \sec^2 \lambda \{A (\sin p\phi - p\phi) + z'_0 (1 - \cos p\phi)\} \\ z &= z_0 + p^{-1} \sec \lambda \{z'_0 \sin p\phi - A (1 - \cos p\phi)\} \end{aligned} \right\} \quad (6)$$

Outside the condenser there is no electric field, so $\sin \lambda = 0$, and $A = y'_1$.

$$\text{Again, let } \psi = \tau - \tau_1, \quad (7)$$

then

$$\left. \begin{aligned} x - x_1 &= x'_1 \psi = x'_0 \psi \\ y - y_1 &= y'_1 \psi + p^{-1} \{y'_1 (\sin p\psi - p\psi) + z'_1 (1 - \cos p\psi)\} \\ z - z_1 &= p^{-1} \{z'_1 \sin p\psi - y'_1 (1 - \cos p\psi)\} \end{aligned} \right\} \quad (8)$$

The values of z'_0 and A are limited by the restriction $|z - z_0| < d$ for $\phi < \phi_1$, where d is the distance between the plates of the condenser

Now, let us put

$$x'_0 = v_0 \cos \alpha, \quad y'_0 = v_0 \sin \alpha, \quad (9)$$

$$\begin{aligned} f(\phi) &= p^{-1} \sec^2 \lambda \{A (\sin p\phi - p\phi) + z'_0 (1 - \cos p\phi)\}, \\ g(\psi) &= p^{-1} \{y'_1 (\sin p\psi - p\psi) + z'_1 (1 - \cos p\psi)\}, \end{aligned} \quad (10)$$

so that

$$\left. \begin{aligned} f'(\phi) &= \sec^2 \lambda \{ A (\cos p \phi - 1) + z'_0 \sin p \phi \} \\ q'(\psi) &= y'_1 (\cos p \psi - 1) + z'_1 \sin p \psi \\ f''(\phi) &= p \sec^2 \lambda \{ -A \sin p \phi + z'_0 \cos p \phi \} \end{aligned} \right\} \quad (11)$$

Then equations (6) become

$$x = v_0 \cos \alpha \sec \lambda \phi, \quad y = v_0 \sin \alpha \sec \lambda \phi + f(\phi), \quad z = z_0 + p^{-1} \cos \lambda f'(\phi), \quad (12)$$

and equations (8) become

$$\left. \begin{aligned} x &= v_0 \cos \alpha (\sec \lambda \phi_1 + \psi), \\ y &= v_0 \sin \alpha (\sec \lambda \phi_1 + \psi) + f_1 + f'_1 \cos \lambda \psi + g(\psi) \\ z &= z_0 + p^{-1} \{ \cos \lambda (f'_1 + p^{-1} f''_1 \sin p \psi) - y'_1 (1 - \cos p \psi) \} \end{aligned} \right\} \quad (13)$$

Put

$$x = r \cos \theta, \quad y = r \sin \theta, \quad (14)$$

where r is $\sqrt{x^2 + y^2}$. Then eliminating $(\sec \lambda \phi_1 + \psi)$ between the first two of equations (13) we get

$$r \sin (\theta - \alpha) = \{ f_1 + f'_1 \cos \lambda \psi + g(\psi) \} \cos \alpha \quad (15)$$

At the edge of the condenser $\psi = 0$, and hence $g(\psi) = 0$, whilst $r = a$, the radius of the condenser. Hence (15) gives

$$a \sin (\theta_1 - \alpha) = f_1 \cos \alpha \quad (16)$$

Now from (12)

$$f_1 \cos \lambda = p \int_0^{\phi_1} (z - z_0) d\phi,$$

therefore $|f_1 \cos \lambda| < p d \phi \sim v^{-1} p da \sim 0.01$, with $d = 0.025$ cm., $a = 4$ cm., $H = 127.55$ e/m units, $\sin \lambda = 0.5154$ and $\beta = 0.6$

It follows that in writing $\theta_1 - \alpha$ for its sine in (16), the relative error is very small. It is $\frac{1}{2} (f_1 \cos \alpha / a)^2 \sim \frac{1}{2} (v^{-1} p d \cos \alpha)^2 \sim 10^{-6}$

3 Method of Approximation—The following method of successive approximation is perhaps the most convenient for solving the equation

$$\gamma \equiv a (\theta_1 - \alpha) = f_1 \cos \alpha, \quad (17)$$

where f_1 is now regarded as a function of θ_1 , for by (6), (12) and (14)

$$\phi_1 = a v_0^{-1} \sec \alpha \cos \lambda \cos \theta_1 \quad (18)$$

Let us define a sequence of values $\gamma_0, \gamma_1, \gamma_2 \dots \gamma_n$ in the following manner —

$$\begin{aligned} \gamma_0 &= f_1(0) \cos \alpha, \text{ where } f_1(0) \text{ denotes that we have written } \alpha \text{ for } \theta_1, \text{ in } f_1, \\ \gamma_1 &= f_1(\gamma_0) \cos \alpha, \quad \gamma_2 = f_1(\gamma_1) \cos \alpha, \quad \dots \gamma_n = f_1(\gamma_{n-1}) \cos \alpha, \quad n > 0 \end{aligned}$$

Then

$$|\gamma - \gamma_n| = |f_1(\gamma) - f_1(\gamma_{n-1})| \cos \alpha \\ = |(\gamma - \gamma_{n-1}) f'_1(\bar{\gamma})| \cos \alpha < |\gamma - \gamma_{n-1}| M < \gamma M^{n+1},$$

where $0 < \bar{\gamma} < \gamma$, while M is the maximum modulus of $|f'_1(\gamma)| \cos \alpha$ in the interval concerned

Hence the relative error in writing γ_n for γ is less than M^{n+1} .

By (12) $f'_1(\gamma) = p \sec \lambda (z_1 - z_0) d\phi/d\gamma = -v^{-1} p (z_1 - z_0) \sin \theta_1 \sec \alpha$, so the convergency ratio is $v^{-1} p (z_1 - z_0) \sin \theta_1 < v^{-1} p d \sim 0.0025$

Again, at the film we have $r = b$, $\theta = \theta_2$, hence by (15)

$$b \sin(\theta_2 - \alpha) = (f_1 + f'_1 \cos \lambda \psi_2 + g_2) \cos \alpha \quad (19)$$

In the neighbourhood of $\theta_2 = \lambda$, where we require the deflection on the film, we may neglect cubes of $\theta_2 - \alpha$ so that we have to solve an equation of the same type as (17), namely, the equation

$$b(\theta_2 - \alpha) = (f_1 + f'_1 \cos \lambda \psi_2 + g_2) \cos \alpha \quad (20)$$

The same method of solution is applicable to this equation as to (17)

4. *Compensated Rays*—Prof A. H. Bucherer had intended to eliminate, as far as possible, all rays other than the so-called compensated rays. In this section we shall discuss briefly the nature of the trace that would have been obtained had he entirely succeeded in his purpose

Since (inside the condenser) there is no resultant mechanical force on the electrons composing these rays, their paths are straight lines. This property of compensated rays gives rise to the two conditions

$$z'_0 = 0, \quad A = (v_0 \sin \alpha - s_0 \sin \lambda) \sec \lambda = 0 \quad (21)$$

Since in this case $w_0 = v_0$ and $s_0 = \sqrt{c^2 + v_0^2}$, the second equation gives

$$\beta = \beta_0 = v_0/s_0 = \sin \lambda \operatorname{cosec} \alpha \quad (22)$$

From this formula we see that none of these rays can escape outside the angular region defined by $\pi - \lambda > \alpha > \lambda$. The two extremes correspond to velocities equal to that of light

Again, since z'_0 and A both vanish for the compensated rays, we see from (10) that $f(\phi)$ vanishes everywhere, hence f_1, f'_1, f''_1 are all zero, and we obtain from the third of equations (13), with

$$y'_1 = v_0 \sin \alpha, \quad v_0 = c \sin \lambda (\sin^2 \alpha - \sin^2 \lambda)^{-1/2} \quad (23)$$

$$z_2 - z_0 = -p^{-1} v_0 \sin \alpha (1 - \cos p \psi_2) = -\frac{1}{2} p v_0 \sin \alpha \psi_2^2, \quad (24)$$

approximately for small values of ψ_2

From (20) and (10) we obtain

$$b(\theta_2 - \alpha) = g_2 \cos \alpha = p^{-1} v_0 \sin \alpha \cos \alpha (\sin p \psi_2 - p \psi_2) \\ = -\frac{1}{2} p^2 v_0 \sin \alpha \cos \alpha \psi_2^2 \quad (25)$$

approximately. Lastly, the first of equations (13) gives very nearly

$$v_0 \psi_2 = b - a. \quad (26)$$

Neglecting higher powers of $\alpha - \lambda$, we get from equation (23)

$$\alpha - \lambda = c^2 \tan \lambda / 2v_0^2, \quad (27)$$

which, combined with (25), gives us the equation

$$b(\theta_2 - \lambda) = \frac{1}{2} c^2 b \tan \lambda / v_0^2 - \frac{1}{2} p^2 v_0 \sin \lambda \cos \lambda \psi_2^2 \quad (28)$$

Again, eliminating v_0 and ψ_2 between (24), (26) and (28), we obtain to a first approximation

$$(z_2 - z_0)^2 = \frac{1}{2} p^2 \sin \lambda (b - a)^4 \left\{ \frac{1}{2} c^2 b \sec \lambda \right. \\ \left. - \frac{1}{2} p^2 \cos \lambda (b - a)^2 \right\}^{-1} b (\theta_2 - \lambda) \quad (29)$$

On the unrolled film the abscissa is equal to $b\theta_2$, hence the last equation shows that in the neighbourhood of $\theta_2 = \lambda$, the curve due to compensated rays behaves like a parabola of latus rectum equal to

$$\frac{1}{2} p^2 \sin \lambda (b - a)^4 \left\{ \frac{1}{2} c^2 b \sec \lambda - \frac{1}{2} p^2 \cos \lambda (b - a)^2 \right\}^{-1}$$

The parabola cuts the central line at $\theta_2 = \lambda$ perpendicularly, and is shown as curve CC' in fig 3b at the end of the paper. Bucherer's experimental curve is different, it is shown in the inset, fig 3a, and appears to touch the central line at a point for which θ_2 exceeds λ considerably. In the case of the curve measured this excess is as much as 6° . In order to account for this discrepancy we must find out where the non-compensated rays strike the film.

5 *Non-compensated Rays satisfying special conditions*—We shall find it convenient to study the class of non-compensated rays characterised by the condition $z_1 = z_0$. They have a turning point inside the condenser which will be denoted by z_m . Let us write

$$z_m - z_0 = \delta. \quad (30)$$

Then δ lies between the limits $\pm d$, d being 0.025 cm. The compensated rays belong to this class, and are given by $\delta = 0$. From (6) we see that the condition $z_1 = z_0$ gives

$$z'_0 = A \tan \frac{1}{2} p \phi_1, \quad (31)$$

where the suffix 1 refers to the edge of the condenser as usual. The turning point is determined by $z'_0 = A \tan p \phi$, so that

$$\sqrt{A^2 + z'^2_0} - A = (z_m - z_0) p \cos \lambda = \delta p \cos \lambda. \quad (32)$$

Eliminating z'_0 between (31) and (32) we obtain, using (5),

$$\delta p \cos \lambda (\sec \frac{1}{2} p \phi_1 - 1)^{-1} = A = v_0 \sin \alpha \sec \lambda - s_0 \tan \lambda \quad (33)$$

Let $\bar{\alpha}$ be the value of α belonging to a compensated ray which is projected with the same velocity as the ray considered, and therefore has the same values of v_0, s_0 . For this ray z'_0, A and $\delta = 0$, and $\sin \bar{\alpha} = (s_0/v_0) \sin \lambda$. Hence we get from (33)

$$\sin \alpha = \sin \bar{\alpha} + \delta p v_0^{-1} \cos^2 \lambda (\sec \frac{1}{2} p \phi_1 - 1)^{-1} \quad (34)$$

Again, for this class of rays we see from the last two equations (6) that $z'_1 = -z'_0 = -A \tan \frac{1}{2} p \phi_1$, $y'_1 = y'_0 = v_0 \sin \alpha$, hence we obtain from (10)

$$f_1 + g_2 = p^{-1} v_0 \sin \alpha (\sin p \psi_2 - p \psi_2) + A p^{-1} \sec^2 \lambda \{ \sin p \phi_1 - p \phi_1 + 2 \tan \frac{1}{2} p \phi_1 (\sin^2 \frac{1}{2} p \phi_1 - \cos^2 \lambda \sin^2 \frac{1}{2} p \psi_2) \} \quad (35)$$

For the high velocities which we shall consider later on ($\beta > 0.75$), it will be found that f_1 and g_2 are given to a sufficient degree of accuracy for our purpose by taking the first approximations for them (see Section 3) in the small second term, i.e., by putting $\phi_1 \sec \lambda = a/v_0$, $\psi_2 = (b-a)/v_0$. Now in Bucherer's experiment, $b = 2a$, hence, neglecting higher powers of ϕ_1 and ψ_2 , we obtain from (33) and (35)

$$f_1 + g_2 = p^{-1} v_0 \sin \alpha (\sin p \psi_2 - p \psi_2) - \frac{1}{3} p v_0^{-1} a \delta, \quad (36)$$

with $\psi_2 = (b-a)/v_0 = a/v_0 = \phi_1 \sec \lambda$

The first term on the right-hand side of (36) is the value of \bar{g}_2 , i.e., the first approximation for g_2 when $\alpha = \bar{\alpha}$. We also notice that although δ is small the last term may be the dominant one if the velocity is sufficiently high.

Again, we find by means of (8) and (31)

$$z_2 - z_0 = p^{-1} \{ -A \tan \frac{1}{2} p \phi_1 \sin p \psi_2 - v_0 \sin \alpha (1 - \cos p \psi_2) \}, \quad (37)$$

where ϕ_1 and ψ_2 are to be calculated from the formulæ

$$\phi_1 = a v_0^{-1} \sec \alpha \cos \theta_1, \quad \psi_2 = (b \cos \theta_2 - a \cos \theta_1) v_0^{-1} \sec \alpha \quad (38)$$

Curves for different values of the parameter δ are given at the end, fig. 3b.

6 Classification of Effective non-compensated Rays—Not all the rays emitted by the radium stack reach the photographic film and are effective in producing the observed trace, some strike against the condenser plates and are absorbed, and many of those which are reflected* more than once emerge from the condenser at comparatively large angles with the plates and do not take part

* When the energy exceeds 11 volts the reflection is negligible (Gehrt and Baeyer, 'Ann. der Phys.', vol. 36, p. 995 (1911)).

in the production of the trace, but merely produce a general fogging. Moreover, very little is known of the circumstances attending absorption and reflection of high-speed electrons at metal surfaces, hence we must perforce content ourselves with neglecting the effect of all pencils of rays, except those which escape from the condenser without striking the plates. In order to find the curve of maximum intensity of photographic effect on the film due to rays with a given value of β , it will be convenient to classify the rays which escape according to the positions of their turning points. Since we shall be dealing with high velocities only ($\beta > 0.75$), we may neglect the change in lateral deflection due to a change in z'_0 . (This will be justified later on.) Again, as far as the vertical motion of the electron inside the condenser is concerned, we shall treat its path as a parabola

$$z = z_0 + \mu r - \frac{1}{2} \kappa r^2 \quad (39)$$

where r is the radial distance, $\mu = z'_0/l_0$, $\kappa = Ap \cos \lambda / v_0^2$ (40)

κ is connected with the parameter δ in the following manner — By (33) $\delta = p^{-1} A \sec \lambda (\sec^2 \frac{1}{2} p \phi_1 - 1)$. Now if we take for ϕ_1 its first approximation, $a \cos \lambda / v_0$, and neglect powers higher than squares, we get as a first approximation for δ the term $\frac{1}{2} p^{-1} A a^2 \cos \lambda / v^2 = \frac{1}{2} a^2 \kappa = 2\kappa$, since $a = 4$ cm. Later, it will be seen that this approximation is justifiable, for we use κ only for the purpose of calculating the intensity of photographic effect.

The turning point and ordinate at emergence are given by

$$z_m = z_0 + \frac{1}{2} \mu^2 \kappa^{-1}, \quad z_1 = z_0 + \mu a - \frac{1}{2} \kappa a^2 \quad (41)$$

Let l denote the length of radium stick from which rays can escape when μ is given, and h the ordinate of the centre of gravity of this length relative to the mid-point of the radium stick. We shall first classify the pencils for which $\kappa < 0$, i.e., those which are concave upwards. The case $\kappa > 0$ is treated in a similar way.

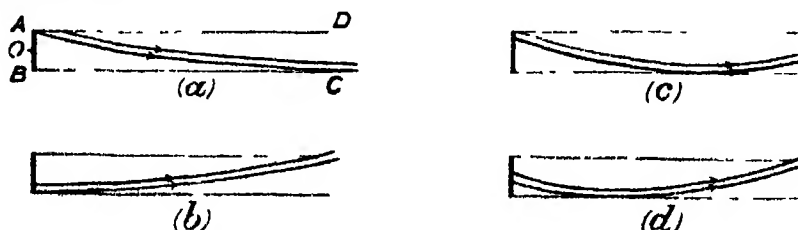


FIG. 1 — AB represents the radium stick, AD and BC the condenser plates.

(a) A length of radium stick with its upper end coinciding with A (see fig. 1a) gives rise to pencils of rays which have their turning points outside the condenser

(the rays composing a pencil are emitted with the same value of v_0 and μ_0 respectively) For these pencils $l = z_1 + \frac{1}{2}d$, $h = \frac{1}{2}(d - l)$ with $z_0 = \frac{1}{2}d$

In order that a ray may belong to this class, its initial inclination μ must lie between the limits μ' and μ'' , where μ' makes $z_1 = -\frac{1}{2}d$ when $z_0 = \frac{1}{2}d$, the ray passing through diagonally, and μ'' makes $z_1 = z_m$, the ray having its turning point at the edge of the condenser. Thus by (41)

$$l = d + a(\mu - \frac{1}{2}\kappa a), \quad h = -\frac{1}{2}a(\mu - \frac{1}{2}\kappa a), \quad \mu' = -a^{-1}(d - \frac{1}{2}\kappa a^2), \\ \mu'' = \kappa a \quad (42)$$

The groups of pencils will be found to possess a certain degree of symmetry with respect to the pencil for which $z_1 = z_0$, therefore, it will be convenient to refer them all to this as standard by making the following simple transformations

$$\mu = \xi + \frac{1}{2}\kappa a, \quad h = \eta_0 - \frac{1}{16}\kappa a^2 \quad (43)$$

Then equations (42) become

$$l = d + a\xi, \quad \eta_0 = \frac{1}{16}\kappa a^2 - \frac{1}{2}a\xi, \quad \xi' = -a^{-1}d, \quad \xi'' = \frac{1}{2}\kappa a \quad (44)$$

(b) There is another group of pencils symmetrically placed with respect to the first (see fig. 1b). The rays belonging to this class have their turning points in the region $r < 0$. For this class we obtain, after applying the transformations (43)

$$l = d - a\xi, \quad \eta_0 = \frac{1}{16}\kappa a^2 - \frac{1}{2}a\xi, \quad \xi' = -\frac{1}{2}\kappa a, \quad \xi'' = a^{-1}d \quad (45)$$

Neither of these two classes exists when κ satisfies the inequation

$$|z_1 - z_0| > d \text{ for } \mu = 0, \quad \text{i.e., if } -\frac{1}{2}\kappa a^2 > d$$

(c) Beginning with the upper end of the stick again (see fig. 1c), we find that pencils can escape which have their turning points inside the condenser in the region $\frac{1}{2}a < r < a$. For these we have, provided $-\frac{1}{2}\kappa a^2 < d$

$$l = d + \frac{1}{2}\kappa^{-1}(\xi + \frac{1}{2}\kappa a)^2, \quad \eta_0 = \frac{1}{16}\kappa a^2 - \frac{1}{2}\kappa^{-1}(\xi + \frac{1}{2}\kappa a)^2, \quad \xi' = \frac{1}{2}\kappa a, \\ \xi'' = 0, \quad (46)$$

but if $-\frac{1}{2}\kappa a^2 > d$, then (bearing in mind that $\kappa < 0$)

$$\xi' = -\sqrt{-2\kappa d} - \frac{1}{2}\kappa a. \quad (47)$$

(d) There is another class of pencils (fig. 1d) which is symmetrically placed with respect to (c), and has its turning point inside the condenser, but this time in the region $0 < r < \frac{1}{2}a$. When $-\frac{1}{2}\kappa a^2 < d$ we have

$$l = d + \frac{1}{2}\kappa^{-1}(-\xi + \frac{1}{2}\kappa a)^2, \quad \eta_0 = \frac{1}{16}\kappa a^2 - \frac{1}{2}\kappa^{-1}(-\xi + \frac{1}{2}\kappa a)^2, \\ \xi' = 0, \quad \xi'' = -\frac{1}{2}\kappa a, \quad (48)$$

$$\text{and when } -\frac{1}{2}\kappa a^2 > d, \quad \xi'' = \frac{1}{2}\kappa a + \sqrt{-2\kappa d}. \quad (49)$$

7. *Distribution of Photographic Effect on the Film*—In order to compare Bucherer's curves with the theoretical results it is necessary to be able to compute the photographic effect at any given point on the film. For this purpose we assume that the total effect can be obtained by the simple addition of the effects of the several rays which reach that point. Hence it is necessary to determine the region of the film covered by rays belonging to each pencil emitted with a given common velocity, which is able to escape from the condenser. For the photographic effect of the pencil depends upon three factors (1) the specific photographic effect of a single electron with a given velocity, (2) the number of such electrons emitted by radium, (3) the number of such electrons in the pencil and the distribution of their points of impact on the film. Very little is known concerning the effect of the first two factors, investigations such as those of Danysz and Ellis, already referred to, on the β -ray spectrum of radium and its derivatives, only give very general indications of the relative photographic effects of groups of β -rays of certain velocities under conditions only approximately similar to those of Bucherer's experiments, but they do give us some idea of the combined effect of the first two factors. The effect of the third factor is amenable to approximate calculation, as will be shown below.

Let η_a be the ordinate of the central line of any pencil at the film relative to that of the pencil of equal velocity for which $z_1 = z_0$.

From (6) and (8) we get

$$\begin{aligned} z_a &= z_0 + p^{-1} \sec \lambda \{z'_0 \sin p\phi_1 - A(1 - \cos p\phi_1)\} \\ &\quad + p^{-1} \{z'_1 \sin p\psi_2 - y'_1(1 - \cos p\psi_2)\} \\ z'_1 &= z'_0 \cos p\phi_1 - A \sin p\phi_1, \\ y'_1 &= y'_0 + \sec \lambda \{z'_0 \sin p\phi_1 - A(1 - \cos p\phi_1)\} \end{aligned}$$

Then, since η_0 is the initial ordinate of the centre of gravity of a pencil relative to the one for which $z_1 = z_0$, we obtain by (31), (40) and (43)

$$\eta_a = \eta_0 + \xi N, \quad (50)$$

where we have put

$$N = p^{-1} v_0 (\sin p\phi_1 \cos p\psi_2 \sec \lambda + \cos p\phi_1 \sin p\psi_2) \quad (51)$$

and neglected the small changes in ϕ_1 and ψ_2 due to ξ , which is very small, in no case exceeding $d/a = 1/160$.

Let us plot the two curves

$$\eta = F(\xi) \equiv \eta_a + \frac{1}{2}l, \quad \eta = G(\xi) \equiv \eta_a - \frac{1}{2}l \quad (52)$$

Then, from (44), we obtain in the region (a), $-a^{-1}d < \xi < \frac{1}{2}\kappa a$

$$F(\xi) = \frac{1}{16} \kappa a^2 + \frac{1}{2}d + \xi N, \quad G(\xi) = \frac{1}{16} \kappa a^2 - \frac{1}{2}d + \xi(N - a) \quad (53)$$

For the present purpose we may use the first approximations for ϕ_1 and ψ_2 , and neglect cubes and higher powers, i.e., we shall write $\phi_1 \sec \lambda = a/v_0$, $\psi_2 = a/v_0$, and $N = 2a$. Then, when $a = 4$ cm, $d = 0.025$ cm, $N = 8$ cm. For convenience of calculation, we shall suppose the units of the three variables ξ , η , and κ to be multiplied 80 times, so that the numerical values of the variables become one-eightieth of ξ , η , and κ respectively. Thus, the equations of the curves in the new units are found from (53) to be for the region (a)

$$\begin{aligned} &(-\frac{1}{2} < \xi < 2\kappa) \\ \eta = F(\xi) &= 1 + \kappa + 8\xi, \quad \eta = G(\xi) = -1 + \kappa + 4\xi \end{aligned} \quad (54)$$

In precisely the same way we find that the equations of the two curves in the new units for the other three regions are

$$\begin{aligned} &(b) \quad (-2\kappa < \xi < \frac{1}{2}) \\ \eta = F(\xi) &= 1 + \kappa + 4\xi, \quad \eta = G(\xi) = -1 + \kappa + 8\xi \end{aligned} \quad (55)$$

$$\begin{aligned} &(c) \quad (2\kappa < \xi < 0) \\ \eta = F(\xi) &= 1 + \kappa + 8\xi, \quad \eta = G(\xi) = -1 - \kappa + 6\xi - \frac{1}{2}\kappa^{-1}\xi^2 \end{aligned} \quad (56)$$

$$\begin{aligned} &(d) \quad (0 < \xi < -2\kappa) \\ \eta = F(\xi) &= 1 + \kappa + 4\xi, \quad \eta = G(\xi) = -1 - \kappa + 6\xi - \frac{1}{2}\kappa^{-1}\xi^2 \end{aligned} \quad (57)$$

We notice that the curve $\eta = F(\xi)$ has only one point where the tangent is discontinuous, and this occurs for $\xi = 0$. The curve $\eta = G(\xi)$ is continuous in the whole region defined, but, whereas near the ends it is straight, in the middle, where $(2\kappa < \xi < -2\kappa)$, it is a parabola which touches the straight lines at the points $\pm 2\kappa$ respectively. The general character of the curves is shown in fig. 2 below.

Fig. 2a represents the general case for which $-\frac{1}{2}\kappa a^2 < d$. $\eta = F(\xi)$ is represented by the straight lines AB and BC which intersect at the point $\xi = 0, \eta = 1 + \kappa$, AB cuts the ξ -axis at the point $\xi = -\frac{1}{8}(1 + \kappa)$. $\eta = G(\xi)$ is represented by the straight line AE, the segment ED of the parabola, and the straight line DC. The co-ordinates of the points A, E, D, and C are respectively $\xi = -\frac{1}{2}, \eta = -3 + \kappa$, $\xi = 2\kappa, \eta = -1 + 9\kappa$, $\xi = -2\kappa, \eta = -1 - 15\kappa$, and $\xi = \frac{1}{2}, \eta = 3 + \kappa$. The parabola cuts the ξ -axis at the point $\xi = 6\kappa - \sqrt{34\kappa^2 - 2\kappa}$, and the η -axis at the point $\eta = -1 - \kappa$.

As pointed out in the last section, groups (a) and (b) do not exist when $-\kappa > \frac{1}{2}$. Then, the curve $\eta = G(\xi)$ consists of the parabola only. (See fig. 2b.) Again, when $-\kappa = 1$ the points A, B, C coalesce at 0. This means that no rays escape for that value of κ . When we are dealing with the compensated rays, i.e., when $\kappa = 0$, the points E and D coalesce at F ($\xi = 0$,

$\eta = -1 + \kappa$, so that the curve $\eta = G(\xi)$ is composed of two straight lines, which together with AB and BC form a parallelogram

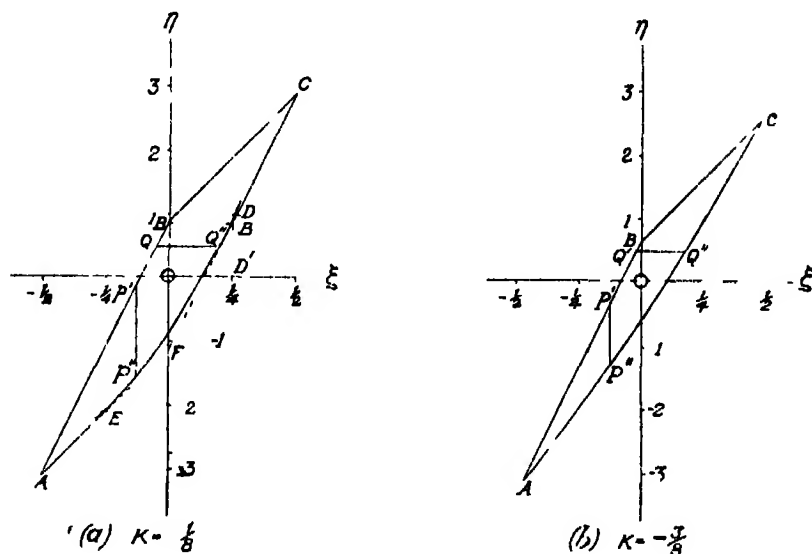


FIG. 2

Now, let us consider all the rays escaping with a given velocity v_0 and at a given inclination α to the x -axis. As shown in the last section, every ray belongs to a pencil, which in its turn belongs to one of the four classes (a), (b), (c), (d). The area of the normal cross-section of a pencil at all points along its length is the same, and is equal to $2/\rho$, where ρ is the radius of the radium stick, which we assume to have a circular cross-section. The pencil strikes the film obliquely, but the angle which the normal to the film makes with that of the cross-section of the pencil is very small in all cases, whilst the change in this angle due to the small changes in ξ with which we are concerned is very small indeed, and may be entirely neglected for the present purpose, namely, that of finding the combined photographic effect of all the pencils. Let us draw a straight line $P'P''$ parallel to the η -axis cutting the curves $\eta = F(\xi)$ and $\eta = G(\xi)$ in P' and P'' respectively (see fig. 2). This straight line represents the length and position on the film of the pencil which has the corresponding value of ξ , or ξ'_0 , relative to the lengths and positions of the other pencils with the same values of v_0 and α . The pencils are deflected laterally, and each through a slightly different angle. The expression for this lateral deflection is given by (20) and (10)

$$\begin{aligned}
 b(\theta_2 - \alpha) &= (f_1 + f', \cos \lambda \psi_2 + g_2) \cos \alpha \\
 &= p^{-1} [\sec^2 \lambda \{A (\sin p\phi_1 - p\phi_1) + z'_0 (1 - \cos p\phi_1)\} \\
 &\quad + p\psi_2 \sec \lambda \{A (\cos p\phi_1 - 1) + z'_0 \sin p\phi_1\} \\
 &\quad + y'_1 (\sin p\psi_2 - p\psi_2) + z'_1 (1 - \cos p\psi_2)] \cos \alpha
 \end{aligned}$$

Allowing only z'_0 to vary, and neglecting variations in ϕ_1 and ψ_2 , we get

$$\begin{aligned}
 b\delta(\theta_2 - \alpha) &= p^{-1} \{ \delta z'_0 (1 - \cos p\phi_1) \sec^2 \lambda + \delta y'_1 (\sin p\psi_2 - p\psi_2) \\
 &\quad + \delta z'_0 p\psi_2 \sec \lambda \sin p\phi_2 + \delta z'_1 (1 - \cos p\psi_2) \} \cos \alpha,
 \end{aligned}$$

which, by using (6), reduced to

$$\begin{aligned}
 b\delta(\theta_2 - \alpha) &= \delta z'_0 p^{-1} \{ (1 - \cos p\phi_1) \sec^2 \lambda + \sec \lambda \sin p\phi_1 (\sin p\psi_2 - p\psi_2) \\
 &\quad + p\psi_2 \sec \lambda \sin p\phi_1 + \cos p\phi_1 (1 - \cos p\psi_2) \} \cos \alpha \quad (58)
 \end{aligned}$$

In order to get a rough estimate for the value of $b\delta(\theta_2 - \alpha)$ we shall put $\phi_1 \sec \lambda = \psi_2 = a/v_0$ and neglect powers higher than squares. Then $b\delta(\theta_2 - \alpha) = 2pv_0^{-2} a^2 \cos \alpha \delta z'_0$. But we have seen that $\delta z'_0$ cannot exceed $v_0 d/a$. Hence for $\beta > 0.75$, $a = 0.025$ cm, $a = 4$ cm and $p/c = 1/16$, $b\delta(\theta_2 - \alpha) < 1/80$ cm. But the diameter of the radium stick, and hence the breadth of a pencil, is 0.05 cm, so for all practical purposes we can neglect the lateral deflection of any pencil relative to that of the standard ray given by $z_1 = z_0$, and treat all the pencils as overlapping on the film.

If we draw a straight line $Q'Q''$ parallel to the ξ -axis, cutting the curves $\eta = F(\xi)$ and $\eta = G(\xi)$ in Q' and Q'' respectively, it is easy to see that the length $Q'Q''$ gives the measure of the intensity of photographic effect for the corresponding value of η due to all the rays with which we are now concerned. As stated above, the assumption involved is if a pencil of rays falling on the film produces a photographic effect whose intensity is measured by n_1 per unit area, and another pencil produces an effect n_2 per unit area, then the combined effect of both falling upon the same area is given by $(n_1 + n_2)$ per unit area.

For $\kappa = 0$, the intensity is constant along BF, and its measure is $BB' = n = \frac{1}{4}$.

When κ is such that $DD' \gg BO$, i.e., when $-\kappa \gg \frac{1}{2}$, the point $\eta = \kappa + 1$ is one of maximum intensity.

For any given value of η , the intensity is given by $n = -\xi' + \xi''$ where ξ' and ξ'' are respectively roots of the equations

$$F(\xi) - \eta = 0, \quad G(\xi) - \eta = 0. \quad (59)$$

For the four regions defined with $\kappa < 0$ we get from (54), (55), (56) and (57)

$$(a) (-\frac{1}{2} < \xi < 2\kappa), \quad \xi' = \frac{1}{8}(\eta - 1 - \kappa), \quad \xi'' = \frac{1}{4}(\eta + 1 - \kappa) \quad (60)$$

$$(b) (-2\kappa < \xi < \frac{1}{2}), \quad \xi' = \frac{1}{4}(\eta - 1 - \kappa), \quad \xi'' = \frac{1}{8}(\eta + 1 - \kappa) \quad (61)$$

$$(c) (2\kappa < \xi < 0), \quad \xi' = \frac{1}{8}(\eta - 1 - \kappa), \quad \xi'' = 6\kappa + \sqrt{2\kappa(17\kappa - 1 - \eta)} \quad (62)$$

$$(d) (0 < \xi < -2\kappa), \quad \xi' = \frac{1}{4}(\eta - 1 - \kappa), \quad \xi'' = 6\kappa + \sqrt{2\kappa(17\kappa - 1 - \eta)} \quad (63)$$

8 Explanation of Curves and Tables—In Section 4 we have obtained an expression, (29), giving the deflection for the trace of the compensated rays in the immediate neighbourhood of the central line, or axis of abscissa of the film. This central line lies along the middle of the trace of the undeflected γ rays in fig. 3b. The curve CC' is the centre line of the trace of the compensated rays, which we saw is nearly a parabola of latus rectum

$$\frac{1}{4}p^2 \sin \lambda (b - a)^4 \left\{ \frac{1}{2}c^2b \sec \lambda - \frac{1}{6}p^2 \cos \lambda (b - a)^3 \right\}^{-1} \text{ (see Section 4)}$$

The total width of this trace is 0.075 cm (see Section 7 and fig. 2a) if we take account of all the rays for which $A = 0$, and z'_0/v_0 varies between the limits $\pm d/a$ ($\approx 1/160$). However, as explained in the last section, the intensity is constant only for the middle third of the width, whilst at each of the extreme ends it tapers to a vanishing point, as is clearly seen from fig. 2a. (Of course, the relative lateral deflection due to z'_0 is neglected.)

Again, in Section 4 we have obtained expressions, (36) and (37), giving the lateral and vertical deflections of our standard non-compensated rays (those for which $z_1 = z_0$) in terms of the parameter δ , which depends upon the velocity and direction of projection of the electrons constituting the standard ray.

We have drawn curves for given values of δ , and given values of β ($\equiv v_0/s_0 = v_0/\sqrt{c^2 + v_0^2}$), with $z_1 = z_0$. The effect of the rays for which ξ varies between the limits $\pm d/a$ is to modify the trace due to the standard non-compensated rays (for a given value of δ) in the same way as the trace of the compensated rays is modified by the rays for which $A = 0$, and $-d/a < \mu < d/a$ (see Section 7 and fig. 2). These rays serve to broaden the trace, and whereas the intensity of photographic effect along the middle strip, width $(d - \delta)$, is fairly constant for a given value of $\theta_a - \lambda$, it diminishes to zero at the edges. The total width of a trace is the difference of the ordinates of A and C, fig. 2. When $-\kappa < \frac{1}{4}$, the width is 6, or in the usual units, 0.075 cm, when $-\kappa > \frac{1}{4}$, the width of the trace is a function of κ , namely, $24(\kappa + \sqrt{-\kappa})$ in the new units.

The curves $\delta = \text{constant}$ are drawn for values $0, \pm \frac{1}{4} \pm \frac{1}{8}, \pm \frac{3}{8}$ (in the new units) as full lines in fig 3*b*. Of course, $\delta = 0$ gives the curve CC'.

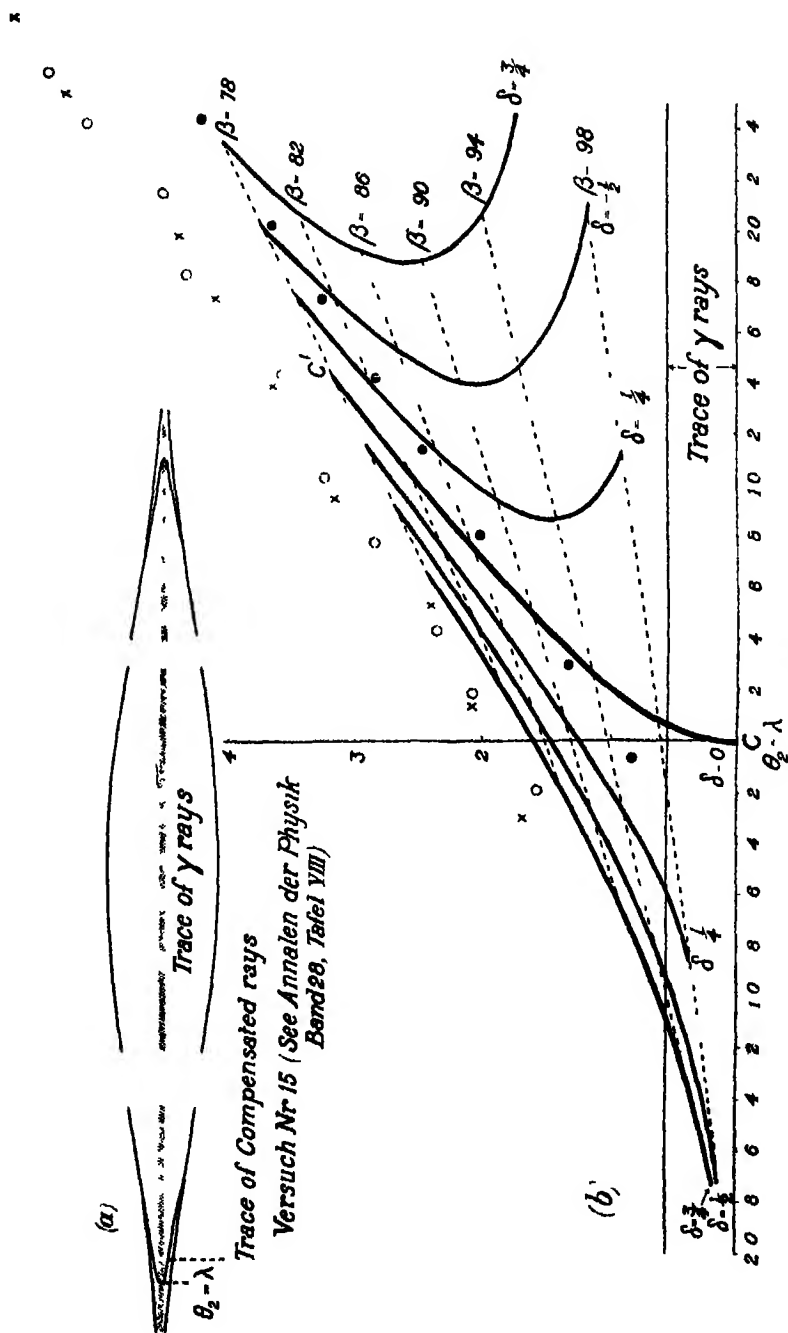
The intensity of the traces given by $\delta = \pm \frac{3}{8}$ ($\kappa = \pm \frac{3}{8}$) is about 0.75 of that for which $\delta = 0$ (see fig 2), and their width is about 0.95 of that for which $\delta = 0$. The curves drawn represent the middles of the traces for the given values of δ . The curves $\beta = \text{constant}$ are drawn for values increasing by 0.04 from 0.78 to 0.98 as broken lines in fig 3*b*.

I have measured the plate for which $E/H = \sin \lambda = 0.5154$ (see Plate 15, Table VIII, 'Annalen der Physik,' 1909, vol. 28) at both ends. Prof. A. H. Bucherer, of Bonn University, placed what was left of his original plates at my disposal, and gave me the benefit of his personal assistance and advice. My best thanks are due to him for his kindness, without which this part of my paper could not have been written.

The calculated values of the ordinate z_2 and abscissa L , measured from the point $\theta_2 = \lambda$, for compensated rays and non-compensated rays with the given values of β and δ for which the curves in fig 3*b* have been drawn, are given in Table I. The measurements made on the two ends of Bucherer's curves ($E/H = 0.5154$) are also given in the table for comparison, and the points corresponding to them are marked in fig 3*b* by crosses and circles respectively. These measurements were taken at the outside of the trace for the sake of accuracy, whilst the ordinates z_2 refer to the middle of the traces, as already explained. All the measurements are given in centimetres, but for the sake of greater clearness the ordinates in fig 3 are given on a scale five times as great as that of the abscissæ.

If we assume the actual trace to be 0.075 cm wide, we see that it coincides very nearly with the region where the theoretical curves are most dense (the full black dots represent, approximately, the inner edge of the experimental trace). The general character of the trace seems to be very much the same as that which one would expect from theoretical deductions, assuming that electrons are emitted with velocities as great as 0.94 (or 0.98) times the velocity of light. These velocities are much greater than those of the most intense rays observed by Ellis, but well within the limits of those observed by Danyasz.

At the same time the experimental material is too scanty to allow of our drawing absolutely certain conclusions as to the agreement or otherwise of the Lorentz mass formula with the experimental results for values of β exceeding 0.80, which was the extreme limit reached by Neumann in his repetition of Bucherer's original measurements, when only the maximum deflection was



560 *Interpretation of Results of Bucherer's Experiments on e/m*

used Nevertheless, the measure of agreement obtained in the present investigation is sufficient to show the desirability, from the point of view of the Theory of Relativity, of further experiments by Bucherer's method, and of a more extensive and detailed investigation of the β -ray spectrum of radium

Table I.

Observed				Compensated rays ($\delta = 0$)		$\delta = \frac{1}{2}$		$\delta = -\frac{1}{2}$	
$L \times z_2$		$L \circ z_2$		L	z	L	z	L	z
-0 298	0 168	-0 180	0 157	1 441	0 320	1 170	0 293	1 724	0 346
0 136	0 208	0 180	0 208	1 206	0 291	0 982	0 264	1 502	0 317
0 536	0 240	0 438	0 235	1 103	0 264	0 803	0 238	1 415	0 291
0 770	0 284	0 773	0 283	0 950	0 239	0 630	0 212	1 280	0 265
0 953	0 316	1 035	0 323	0 807	0 214	0 463	0 188	1 163	0 241
1 986	0 362	1 430	0 356	0 670	0 190	0 298	0 164	1 059	0 217
1 726	0 408	1 820	0 432	0 545	0 167	0 135	0 141	0 970	0 194
1 975	0 437	2 140	0 460	0 423	0 144	-0 030	0 117	0 903	0 170
2 526	0 527	2 410	0 510	0 310	0 120	-0 226	0 093	0 870	0 146
2 826	0 569	2 610	0 540	0 200	0 094	-0 442	0 068	0 914	0 121
Mean of five readings		Mean of six readings		0 098	0 064	-0 833	0 038	1 098	0 091

$\delta = \frac{1}{2}$		$\delta = -\frac{1}{2}$		$\delta = \frac{1}{2}$		$\delta = -\frac{1}{2}$		#
L	z_2	L	z_2	L	z_2	L	z_2	
0 938	0 267	2 010	0 373	0 650	0 240	2 311	0 309	0 78
0 702	0 238	1 868	0 344	0 433	0 212	2 183	0 370	0 80
0 510	0 211	1 736	0 317	0 223	0 185	2 071	0 344	0 82
0 319	0 186	1 622	0 292	0 014	0 159	1 980	0 318	0 84
0 128	0 161	1 531	0 267	-0 198	0 135	1 918	0 294	0 86
-0 063	0 137	1 462	0 243	-0 417	0 111	1 880	0 270	0 88
-0 263	0 114	1 415	0 220	-0 651	0 088	1 855	0 246	0 90
-0 494	0 091	1 408	0 197	-0 898	0 064	1 843	0 223	0 92
-0 742	0 067	1 462	0 173	-1 242	0 041	2 094	0 199	0 94
-1 089	0 041	1 641	0 147	-1 698	0 015	2 455	0 174	0 96
-1 715	0 011	2 115	0 117	-2 565	-0 015	3 635	0 144	0 98

Probable error in observed measurements less than one in the second figure after the decimal point

In conclusion, I wish to express my heartiest thanks to Prof G A. Schott, F R S, Head of the Mathematics Department in the University College of Wales, Aberystwyth, for suggesting this problem, and for his assistance and advice while the work was in progress.

The Variation with Temperature of the Intensity of Reflection of X-Rays from Quartz and its Bearing on the Crystal Structure

By REGINALD EDMUND GIBBS

(Communicated by Sir William Bragg, F R S—Received Nov 18, 1924)

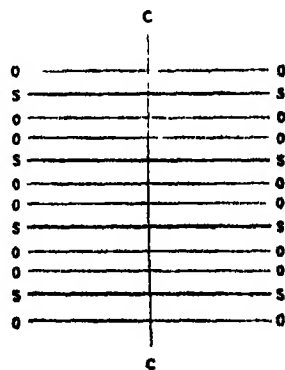
Since the appearance of Sir William Bragg's first work on the structure of quartz (these 'Proceedings,' A, vol 89, p 595 (1914)) this mineral has been the subject of many investigations. It has lent itself very well to study by the older crystallographic methods, by which, from symmetry considerations, it has been placed in the trapezohedral class of the trigonal system, i.e., it exhibits trigonal symmetry about one (c) axis and digonal symmetry about three others, lying symmetrically in a plane perpendicular to the first and intersecting in it. Two enantiomorphous forms were found to exist.

Investigation by the X-ray spectrometer method enabled Bragg to give the dimensions of the unit triangular prismatic cell as $a = 4.89 \text{ \AA U}$ and $c = 5.375 \text{ \AA U}$, whilst density considerations clearly indicated that three molecules were associated with such a unit cell. It was also shown that the three molecules were associated with the unit cell in such a way that planes of equal weight occurred at $0, c/3, 2c/3, c$, etc., along the vertical c axis.

These conclusions determined the "space group" or "molecular arrangement" of the crystal, which in the notation of Schonflies is D_3^4 . The arrangement of the atoms in the molecule, however, remains to be determined by the consideration of X-ray reflection intensities, and of any physical and chemical properties which may prove useful. There are, in fact, still four unknown parameters, viz., the "radius" of the silicon spiral and the position of the oxygen atom relative to the silicon.

The merits of the solutions suggested by Huggins ('Phys Rev.,' April, 1922, p 363), McKeehan ('Phys Rev,' May, 1923, p 503), and Sosman ('Jl Franklin Inst,' vol 194, No 6 (1922)) will be considered later.

Planes which are perpendicular to the c axis can be represented as in the diagram herewith, in which the full lines SS represent silicon-bearing planes at a



common separation of $c/3$. The oxygen planes contain the same number of atoms each as the silicon planes, and are necessarily equidistant above and below the latter, at a distance d , which may be considered as one of the four unknown parameters. This is not determined by a knowledge of the space group and must be found by fresh considerations. The relative intensities of the various orders of X-ray reflections from the basal plane of quartz—which is, of course, parallel to SS —depend entirely on d alone of the four parameters, and may be taken as giving some indication of its value. The values for the first, second, and third orders of that plane are given by Bragg as 38 40 24, and the writer's observations are in agreement with these. They are all very weak reflections, the first order being less than one-tenth of that given by the first order of, say, the 100 or the $2\bar{1}2$ planes. Now, when it is clear that the atom centres which are associated with any plane all lie in that plane, the usual ratios of intensities are about 100 20 7. There is, therefore, a very strong presumption that the oxygen planes do not coincide with the silicon planes, in other words, that d is not zero. If this is the case, the structures proposed by Huggins and McKeehan cannot be correct, for both these writers put $d = 0$.

It can be calculated that the experimental relation between intensities is very closely accounted for if d is made equal to about 0.63 \AA U. or one-third of $c/3$, and their weakness is readily accounted for by the fact that the reflections from the silicon and oxygen planes are not in the same phase. As a very small change in d materially alters the calculated values of the intensity ratios, the slight changes in the relative positions of the silicon and oxygen atoms which may be expected to occur as the temperature is raised, especially because at about 575°C quartz passes over to a second structural form, ought to show in the intensities of the basal plane reflections. It was partly for the purpose of testing this expectation, as well as in order to obtain any further information that might help to explain the transformation at 575 , that the experiments now described were undertaken. It will be seen that the expectation is fully realised, and that d must alter by a certain small amount in order to account for the large intensity changes which are found to occur.

The present arrangement of apparatus was very similar to that used originally by Bragg, and later by Backhurst. A Coolidge tube with a molybdenum target was employed, and its filament and primary coil currents adjusted so as to give as steady a source of rays as possible, whilst care was taken to run the tube for some time before starting a set of observations, in order to get

it in a steady state. Moreover, the electroscope was used in a comparatively insensitive state, and its high-tension battery maintained at a steady voltage by a potentiometer slide, all in the hope of maintaining constancy. Under the above conditions the results can be satisfactorily reproduced. The furnace was made to a design fairly similar to that used by Backhurst and temperatures up to about 800°C were employed. Several hundred readings were taken, the measurements extending over a considerable period, a fair proportion of which was required in maintaining the conditions constant and results comparable from time to time. Time did not allow of temporarily cooling the furnace to its initial temperature to get a check reading at an intermediate stage, and the whole range of temperature, both up and down, had to be dealt with progressively. Occasionally, however, readings were taken slightly out of order, owing to the furnace assuming a temperature other than the one required, but at all times the readings fitted well enough on an experimental curve.

Most points on the curves represent an average of two, three, four or even many more, up to 14, separate sets of readings, as concordant between themselves as could be hoped for. The temperature was in each case measured by a thermo-couple placed in a transparent silica tube just above the crystal. Owing to the existence of the rather large windows just near the position where the temperature had to be measured, a small vertical movement of the couple relative to the crystal made a large difference to the temperature reading. To overcome this, inside the furnace and surrounding the crystal, except for the two windows, a thick copper cylinder was placed. This helped to equalise the temperature, and, finally, a difference of about 20°C at the most was left, to allow for this the crystal was afterwards removed, and the temperature measured consecutively at the usual thermometer position, and then at the crystal position, and the necessary correction could be applied to each temperature reading. This accounts for the fact that the maximum does not always appear to occur exactly at the transition temperature.

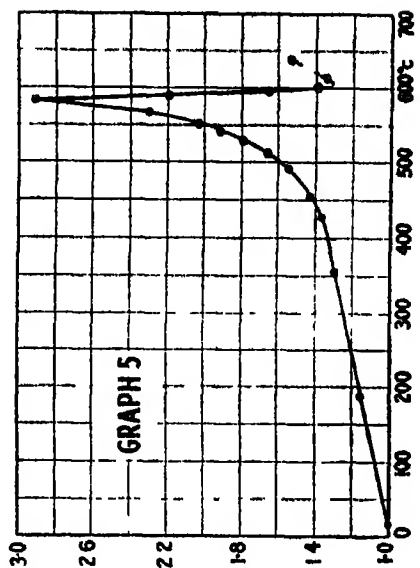
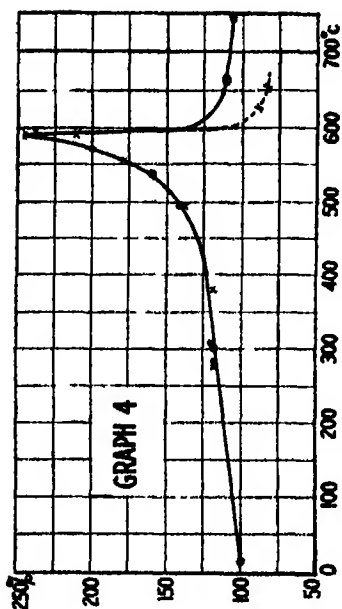
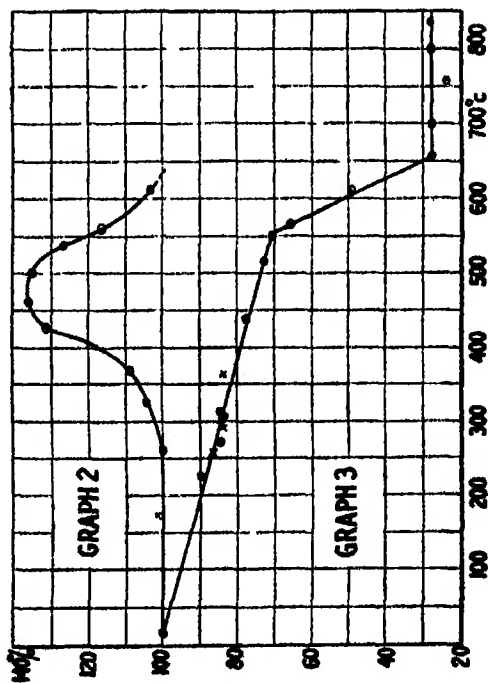
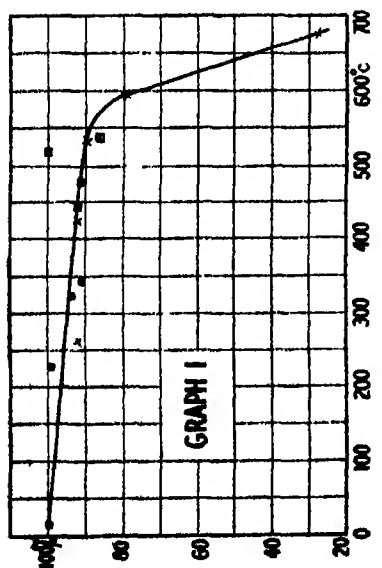
The measurements were made on the first and second orders of the planes 111, 110, 211, employing the $K\alpha$ line of molybdenum, and in any graph all observations taken during one complete experiment are indicated by the same sign. The results expressed in graphical form are as follows —

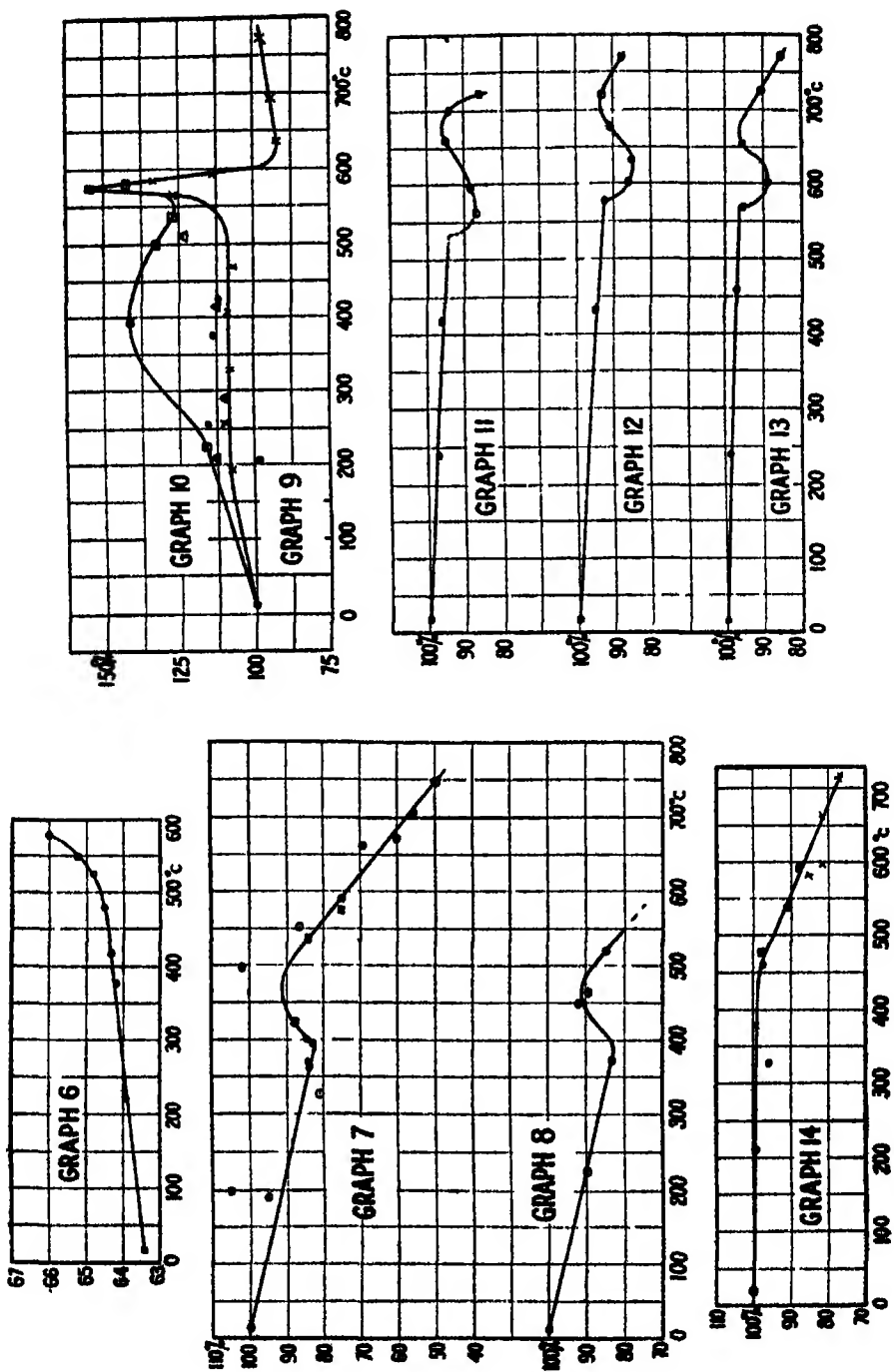
- 1 Variation with temperature of intensity of first-order reflection from the 111 plane
2. *Ditto* after rapid cooling
3. *Ditto* after subsequent slow cooling

4. Variation with temperature of intensity of a second-order reflection from the 111 plane.
- 5 Variation with temperature of the ratio of the intensities of the second order reflection to the first-order reflection from the 111 plane of quartz
- 6 Alteration of position of oxygen planes relative to silicon planes sufficient to explain the result exhibited in graph 5.
7. Variation with temperature of intensity of first-order reflection from the 110 plane
8. *Ditto*.
9. *Ditto* for second-order reflection
- 10 *Ditto* after rapid cooling
- 11 Variation with temperature of intensity of first-order reflection from the 211 plane
12. *Ditto*
- 13 *Ditto*
- 14 *Ditto* for second-order reflection.

As was expected beforehand, the most interesting and useful results are afforded by the graphs referring to the 111 plane, however it will be noticed that the $\bar{1}\bar{1}0$ gave anomalous results also, although in that case the variation was not so large. It must be remembered, however, that until more is known of the mechanism of reflection and the method of measuring its intensity, the actual shape of the curves are suggestive and not necessarily final. The ordinates were obtained by adopting the following procedure, viz., the peak position was found by the usual method on the spectrometer, then using a small crystal, all the slits were opened wide and the peak integrated uniformly over its full width, next the crystal was turned through 1° away from its peak setting and the ionisation chamber through 2° , when the same process was repeated; the latter reading subtracted from the former gave a measure of the peak intensity. The position of the peak maximum had to be continually redetermined as it altered with temperature. The intensity at room temperature was then counted as the standard and those at other temperatures expressed as a percentage of it.

It will be observed that it is possible for the oxygen atoms to move along the c axis in a manner capable of accounting for the first or rising portion of graph 6, but that the second section of this graph is not explicable by the same process, for here the difficulty is to explain the corresponding fall in the actual intensities of both the first and second order simultaneously, and, further, the variation of their relative numerical values. An idea of the power of the method





is given when it is stated that the whole of the 150 per cent increase can be explained by a movement of the oxygen layers relative to those of silicon of only 0.025 \AA U . In order to appreciate the importance of these increases it will be useful to recall the results obtained by Backhurst (these 'Proceedings,' vol 102 (1922)). It will be remembered that the usual result of raising the temperature of a crystal is that the intensity of reflection slowly decreases almost linearly, as is illustrated by such substances as graphite and ruby. For the diamond the decrease was negligible, but for other substances it was of the order of a 15 per cent decrease for a rise of temperature of about 500°C .

The variations in the α state, though large, can be reasonably explained, but those in the β state are more difficult to understand. Further, if the crystal takes up a true hexagonal structure at the transition point, then it is not clear why, after passing this point, there should be any abnormal intensity changes as in graphs 11, 12, and 13. None of the variations recorded for the other planes investigated can be correlated with the variation of any single parameter, hence their theoretical explanation must be left over until the structural changes have been more closely examined. These questions are, however, receiving further attention.

The properties of quartz have been so widely studied that it seemed advisable to recall some of the more important results and compare them as far as possible with the data obtained by means of X-rays. Crystallographers have demonstrated that at 575°C quartz undergoes a transition from the low or α to the high or β modification, in which a number of its physical properties, or rather the laws which these obey, suffer a severe change. Perhaps the most important change accompanying this transition is the increase in the symmetry of the crystal, for whereas low quartz is trigonal, high quartz displays hexagonal symmetry in its Laue photograph (Rinne, 'Die Kristalle als Vorbilder,' pp 62, 142 (1922)), and in its etch figures (Friedel, 'Bull Soc Franç Min' (1902), vol 25, p 112), belonging probably to the hexagonal trapezohedral class 24. This increase in symmetry is supported by the disappearance of any piezoelectric effect at 575°C (A. Perrier, 'Soc Suisse de Physique,' Berne, 1916, 'Arch Sci. Phys Nat' (4), t 41, p 493), and by the fact that at the transition point the elasticity surface for quartz becomes one of revolution (A. Perrier et R. de Mandrot, 'Elasticité et Symétrie du Quartz aux Températures élevées'—Univ de Lausanne, 1924).

Sudden changes have been shown to occur in the refractive index (Rinne, p. 143), and the primary interfacial angle 100.111 (F. E. Wright), whilst Le Chatelier ('Compt Rend,' vol 108, p 1046 (1889)) found a change of law

for the coefficient of expansion, in fact a reversal of sign at 575°C , and accompanying it also a sudden expansion at that temperature along both axes. Again, Randall's results ('Phys Rev,' vol 20 (1905)) on the coefficient of expansion of quartz, indicate such a rapid rise in its value towards 500°C , that the curve connecting it with the temperature might finally possess a vertical tangent. Perrier and Wolfers ('Arch Sci,' p 372 (1920)) found that not only did the law for specific heats change on passing through the transition point, but that there was also a latent heat of transformation. The existence of this latent heat can, of course, be inferred also from Perrier and Mandrot's observation of the difference existing between the adiabatic and isothermal constants near 575°C .

Before concluding, it is advisable to record some investigations on the electrical properties of quartz. Its conductivity was the subject of an investigation by Curie in 1889 ('Annales de Chimie et de Phys,' 6 S, vol 18, p 203). Amongst other things, his results indicated an extremely large increase of conductivity with temperature for a direction parallel to the c axis, while for a direction perpendicular to it the conductivity was very much smaller and decreased with rise of temperature. Despite the interest attached to an increase of two million times in the conductivity for a temperature change of about 300°C too much faith cannot be based on this value without its repetition to-day under more exacting conditions, owing to the uncertainty introduced by the surface effects of absorbed gases, moisture, etc, which must be exceedingly difficult to avoid. Recent measurements made by S W Richardson at room temperature indicate the importance of allowing for polarization, etc, and the great precautions necessary to get consistent results.

In a general way some of the properties mentioned seem to follow a gradual and continuous change up to 575°C , while at that temperature a comparatively discontinuous transition to a new state occurs, after which another steady law is followed. The present X-ray results indicate somewhat similar changes. It was uncertain, of course, whether after heating and cooling the crystal was in the same state as at the beginning, for, according to Iddings ('Rock Minerals'), the downward inversion is accompanied by intricate internal twinning and optical differences. However, the X-ray intensity measurements seemed quite similar time after time for the same crystal. Further, it has been stated by Sosman that the $\alpha \rightarrow \beta$ transition point inversion shows definite hysteresis phenomena according as the temperature is rising or falling, if such is the case, then the temperature range must be a fairly small one, for X-ray measurements taken both while the temperature is rising and falling

fit within experimental error on the same curve. Perrier and Mandrot found also that according to elasticity measurements there was complete reversibility, i.e., no effect of any type analogous to thermal hysteresis.

It is significant that on two occasions, when the crystal was cooled rather rapidly from its high temperature, that in taking a further set of readings (graphs 2 and 10) with rising temperature, a completely different curve was obtained, whilst having passed through the inversion temperature once more and cooled down again, this time slowly, a third experiment reproduced more nearly the original curves (graphs 3 and 9). Such a phenomenon must surely be analogous to the hardening and tempering of steel, in which the quick cooling causes it to remain in the state which it assumed at the higher temperature, whilst subsequent slow cooling enables it to return to its normal equilibrium state. From the accompanying graphs it would appear as though something of the nature of a spring action came into play, owing to the existence of which the atoms at first move gradually, then at an ever-increasing rate, until at the transition point a new configuration was assumed almost discontinuously. From the X-ray results it is difficult to decide whether or not the transition is discontinuous, although in general the slope on the α side of the transition point does seem more gradual than on the β side; but even so, the second gradient has a finite value. This is true also of Perrier's elasticity measurements.

Probably, whatever change is really occurring, it is one that passes through a position of thermally unstable equilibrium. If the "spring" was weak or the motion sluggish, a slow lowering of temperature would probably enable the system to reverse almost exactly its previous transition, whilst a rapid lowering might "lock" it in some stage of its configuration at high temperatures, from which it could be released only by raising the temperature slowly up to or towards its inversion-point value.

Summary.

Whilst the space group to which quartz belongs is known, the positions of the atoms in the molecule remain undetermined. It is shown that the oxygen atoms cannot lie in the same basal planes as do the silicon, but must interleave them at a distance d . Of all the four unknown parameters the variation of d alone will affect the intensity of reflection from the basal plane.

The variation of the intensity of reflection with temperature from about 0°C to 800°C has been recorded for several planes, and very marked reflection intensity changes shown to occur for all the planes at the transition point.

From the results for the 111 plane the values of d have been calculated for various temperatures

The X-ray results are compared with a number of physical properties of quartz and the type of change occurring at the transition is discussed

The above research was carried out during 1923 in the Physics Department of University College, London, at the suggestion of Sir William Bragg, for whose interest, encouragement, and constant assistance I return my warmest thanks I desire also to take this opportunity of expressing my sincere thanks to Prof. A W Porter for his continued kindness and advice In conclusion, I desire to acknowledge my indebtedness to the Scientific and Industrial Research Department, whose grant enabled this research to be pursued

The Fulcher Hydrogen Bands.

By W E CURTIS, D Sc, A R C S, Reader in Physics in the University of London, King's College

(Communicated by Prof O. W Richardson, F R S—Received Nov. 29, 1924)

1 The Fulcher Triplets

It is now some twelve years since Fulcher* discovered the two triplet and four singlet series which are now commonly associated with his name, but until quite lately our theoretical knowledge was too limited to furnish any explanation of these regularities It is now possible, however, to attempt this, and a beginning has been made by Kiuti,† and, quite recently, by H S. Allen ‡

Kiuti obtained a new series from an arc in hydrogen at nearly atmospheric pressure. This appeared to be of "Q" type, *i.e.*, a series originating at a head (instead of running to and from a head as P and R types do) and consisted of single lines The head fell about in the middle of the gap between the first (or red) and second (or green) series of Fulcher triplets, and Kiuti concluded that the latter were respectively the P and R branches associated with the new Q series Attractive though this interpretation may be, it is nevertheless very difficult to accept, for the following reasons—

* 'Astrophys Journ.', vol 37, p 60 (1913)

† 'Proc. Phys Math. Soc.', Japan, vol. 5, p 9 (1923).

‡ 'Roy. Soc. Proc.,' A, vol. 106, p. 69 (1924).

(1) The Q series is a singlet series, whilst the Fulcher series are of triplet character. Now whether a band consists of singlets, doublets or other groups, the character of each branch has always been found to be the same.

(2) The Q series is much strengthened at high pressure and the Fulcher lines at low pressure. This again is contrary to experience, no case being known in which the relative intensities of associated branches can be modified experimentally.

(3) The second differences of the Q series are of the opposite sign (-13.6) from those of the supposed P ($+10.4$) and R ($+14.4$). This means that the Q branch is degraded towards the red and the P and R towards the violet, but in all other bands these heads are turned in the same direction. Kiuti recognises this difficulty, but points out that in the case of the helium band at 26400\AA there is a similar discrepancy between the P and Q series. But further study of this spectrum has shown that these two series may not really be associated with one another, the three which indubitably are, namely P', Q and R, are all degraded in the same direction, just as in other bands.

In view of these difficulties the association of Kiuti's Q series with the Fulcher lines seems very unlikely. Further, his conclusion that the Fulcher red and green series are associated P and R branches, must be called in question. Allen has shown (*loc cit*) that the molecular moments of inertia involved are very different in the two cases, and that therefore "there does not appear to be sufficient evidence to support his (Kiuti's) supposition that these are related series, originating from the same molecular system."

2 *The Extension of the Fulcher Triplets*

The most striking contribution made by Allen is the discovery of a number of lines which may be regarded as extending the triplets into quadruplets and quintuplets.* That is to say, the triplets may be regarded as the first three members of series of which the extra lines form the succeeding members, and these series may be expressed by a parabolic formula in just the same way as corresponding members of successive triplets. The number of new lines added to each triplet varies from one to three, and they are mainly of low intensity. Since their existence is of great significance in connection with the interpretation of the triplets, it is necessary to examine their credentials very carefully, the more so as the spectrum is rich in lines and spurious series not difficult to discover. An examination of the intensities of the new lines does not at first glance

* But the association of these lines with the triplets appears to have been first recognised by Fulcher himself. See 'Phys. Rev.', vol 21, p 375 (1923).

inspire confidence in their genuineness, but this criterion is not entirely reliable, on account of the possible existence of blends, further, the Fulcher lines themselves, although unquestionably a series, have a somewhat abnormal intensity distribution, and so also have the new series recently discovered by Richardson and Tanaka *. The decision must therefore rest with the numerical relationships between the wave-numbers, and the most convenient way of studying these is by examination of the first and second differences and the regularities exhibited by them. Table I gives the wave-numbers, together with the intensities (in brackets) and horizontal and vertical first differences (in italics). To avoid confusion the second differences have been collected below.

If we confine our attention to the first band for the moment, it is seen that the vertical second differences tend to decrease upwards and to the left, and the horizontal ones decrease to the right and are more or less constant vertically. A striking feature in the latter case is the constancy of the second column from the left, except for the value 11.88, which depends on a doubtful line. This suggests that the other columns might also be constant if errors of observation could be eliminated. The values marked with an asterisk show pronounced deviations from the general tendency, but it is found that these can be removed by adjusting the wave-number of the line 16315.64. If a correction of $+0.52$ is applied to this the second differences assume the values given in brackets below the original ones, and these will be seen to fit very satisfactorily in both sets of differences. As such displacements of lines from their expected positions are not at all uncommon in band spectra, we might conclude that we are dealing here with a "perturbation," and for purposes of calculation employ the corrected value of the wave-number, 16316.16. After this conclusion had been reached an opportunity occurred of examining a plate taken by Prof. Merton and now in Prof. Richardson's possession, and it was found that the line in question showed an anomalous "helium effect" as compared with the other two members of the triplet. Its intensity, too, is somewhat greater than it should be, and, finally, it was found that Fulcher had already (*loc. cit.*, 1923) recorded that this line "is apparently double, the band line being λ 6127.20" (*i.e.*, $\nu = 16316.16$), although the reason for this conclusion is not stated.

Turning now to Fulcher's second band, the particulars of which are also included in Table I, it is seen that the data in this case are somewhat meagre, but by analogy with the first band the asterisked values are clearly irregular, and, as before, they can be brought into line by adjusting the single wave-

* 'Roy. Soc. Proc.,' A, vol. 106, p. 663 (1924)

TABLE I—Wave-numbers of Fulcher bands with First Differences

Extra lines		15919 56(0)										[16464 48]	
		44 12										43 25	
Fulcher triplets		15483 12(0) 214 34 15707 40(2) 256 22 15963 68(4) 266 71 16230 39(4) 277 34 16507 73(5)										36 59	
		31 37 33 05 15740 51(1) 257 23 15997 74(3) 265 06 16265 80(3) 278 52 16544 32(6)										22 27	
Fulcher triplets		15494 48(0) 246 02 15740 51(1) 257 23 15997 74(3) 265 06 16265 80(3) 278 52 16544 32(6)										22 27	
		25 56 26 59 15767 10(6) 258 25 16025 35(8) 269 19 16294 53(8) 279 61 16574 14(10)										22 27	
Fulcher triplets		15520 05(3) 247 05 15767 10(6) 258 25 16025 35(8) 269 19 16294 53(8) 279 61 16574 14(10)										22 27	
		19 38 15539 43(2) 247 85 15787 28(5) 259 06 16046 34(7) 269 30 16315 64(9) 280 77 16506 41(7)										15 02	
Fulcher triplets		12 98 15552 41(5) 249 32 15800 73(8) 259 58 16060 31(9) 270 35 16330 66(10) 280 77 16611 43(10)										15 02	
		15315 93(4) 236 48 15552 41(5) 249 32 15800 73(8) 259 58 16060 31(9) 270 35 16330 66(10) 280 77 16611 43(10)										15 02	
Fulcher triplets		15610 91(1) 249 02 15859 93(3) 261 66 16121 59(5) 272 07 16393 66(6) 284 93 16678 58(6)										5 97	
		2 98 15862 91(2) 263 29 16126 20(8) 273 59 16398 79(8) 284 73 16684 52(2)										7 52	
Fulcher triplets		7 18 15870 08(7) 262 16 16132 25(5) 273 27 16405 52(2) 286 52 16692 04(5)										38 54	
		35 49 15905 59(4) 263 35 16168 96(8) 274 35 16443 31(9) 287 37 16730 58(10)										38 54	
Extra lines		17541 46(0) 376 42 17917 88(0) 387 05 18304 93(1) 399 58 18704 51(1)										18641 58(1)	
		49 57 17591 33(2) 374 67 17968 00(2) 388 66 18354 66(0) 402 77 18787 43(1)										62 93	
Fulcher triplets		37 70 17629 03(3) 375 92 18004 85(4) 389 57 18394 72(5) 404 50 18799 22(5)										18704 51(1)	
		28 55 17657 58(3) 376 84 18034 42(2) 390 41 18424 83(3) 405 79 18830 62(4)										52 92	
Fulcher triplets		18 64 17678 22(5) 377 64 18053 86(7) 391 66 18445 52 6 405 97 18951 49(8)										402 77 18787 43(1)	
		37 70 17629 03(3) 375 92 18004 85(4) 389 57 18394 72(5) 404 50 18799 22(5)										41 79	

Table I (*continued*)—Second differences of wave-numbers.

First Band (excluding S_6 to S_7)								
Vertical Second Differences.					Horizontal Second Differences			
	10 06			6 66	11 88	10 49	10 68	
5 81	6 46	6 45	6 68	6 77	11 21	10 93	10 46	
6 18	6 41	6 62	7 62*	7 55	12 07	11 20	10 93	10 43
6 14	6 40	6 73	7 02	(7 10) 6 09* (7 13)	11 99	11 21	10 24* (10 76)	11 47* (10 43)
					11 84	11 26	10 77	10 42
Second Band								
Vertical Second Differences.					Horizontal Second Differences			
				10 01	10 63	12 53		
12 17	9 27	9 67	11 13		13 99	14 11		
9 15	9 28	9 95*	10 39		14 05	14 63		
9 91	10 13	(9 50) 9 42* (10 32)	10 53		13 57* (14 02)	15 38* (14 48)		
					14 02	14 31		

The extra lines, and differences involving them, are those above the dotted line in each case

number 18424·83 The correction required is about $+0.45 \text{ cm}^{-1}$, which leads to the second differences in brackets and an adopted wave-number 18425·28 This line was found by Kuri† to have an exceptionally large Stark effect (p -component $+5.3\text{\AA}$ and s -component $+4.3\text{\AA}$ in a field of 87 kv./cm), and this may have something to do with the perturbation found, which corresponds in magnitude and direction to a field of about $2\frac{1}{2}$ kv/cm

The removal of these irregularities greatly facilitates the verification of the extra lines, and, in fact, all the subsequent calculations A careful study of the sets of differences has led to the following conclusions —

First Band —15919·56 should not be included

16464·48 is doubtful

15707·46 is probably about 0.3 too low

Remainder genuine

Second band —17541·46 should not be included

18704·51 „ „

18641·58 „ „

17917·88 is doubtful.

18304·93 „

Remainder genuine

† 'Japanese Journ. Phys.,' vol. 1, p. 29 (1922).

These conclusions, derived purely from the differences, may be summarised in the statement that the Fulcher triplets have been extended into quintuplets in the case of the first band and into quadruplets in the case of the second. All the well-established lines and none of the doubtful ones are included in this scheme, and there are no gaps in it. A sounder basis for calculation has thus been established.

3 Relation between Triplets and other Series in the First Band

In addition to the triplets already discussed, Fulcher discovered in the red region four other series, which he designated S_4 to S_7 . They appear to be related to the triplets, since the horizontal first and second differences are closely similar, and Allen has found that if the triplets S_1 to S_3 are treated as half-quantum series and the series S_4 to S_7 as whole-quantum series, the values of the constants in the formulae representing the series are practically the same for all seven series. For a whole-quantum series of P type the formula is

$$P(m) = \nu_0 - C_a(2m - 1) - (C_a - C_r)m^2, \quad (1)$$

and for a half-quantum series*

$$P'(m) = \nu_0 + \frac{1}{4}(C_a - C_r) - (C_a + C_r)m + (C_a - C_r)m^2 \quad (2)$$

Here the initial moment of inertia of the molecule is $h/8\pi^2cC_a$ and the final $h/8\pi^2cC_r$, c being the velocity of light and ν_0 a frequency characteristic of the whole band, which originates in the changes in the electronic and nuclear configurations. When a Q series exists it converges approximately to ν_0 , which can therefore be determined. When this value is substituted in (1) and (2) it is at once apparent whether the series is of P or P' type. In this case there is no Q series, so that we have no certain means of distinguishing between whole and half-quantum series, and all that may legitimately be concluded from Allen's calculations is that, if one of the two sets is of P type the other is probably of P' type. There is, however, a criterion available which may help to indicate the correct numeration. Analysis of the helium band spectrum† has shown that the line P (1) does not occur, while the line P' (1) usually does. This may, perhaps, be made clearer by reference to fig. 1 below, where two such series are shown in their true relative positions and the rotational quantum changes are also indicated.

* I.e., one in which the rotation states are defined by $(m + \frac{1}{2})$ instead of m . This modification is frequently useful in correlating branches of a band.

† Curtis, 'Roy. Soc. Proc.,' A, vol. 101, p. 38 (1922); vol. 103, p. 315 (1923).

It will be seen that the first line of the P' series has a higher wave-number than the first line of the P series. Applying this to the Fulcher bands one

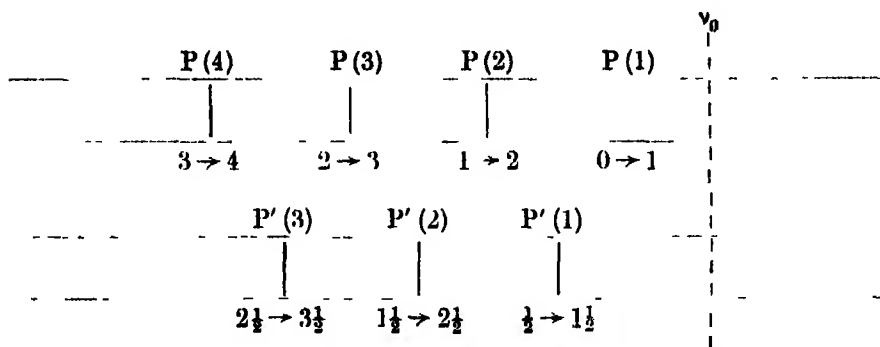


FIG. 1.—Showing relative positions of whole- and half-quantum series.

would expect that the S_4 to S_7 group, commencing at $\nu\nu$ 16678 to 16731, might be P' series, and the S_1 to S_3 group, commencing at 16574 to 16611, P series. It is true that the criterion is not decisive, since ν_0 has not the same value for all the series, but it is at least suggestive, and this alternative to Allen's representation was accordingly tried. Table II gives the results of the calculations, Allen's being reproduced for comparison. The numeration of the lines has been modified to suit the new view, ϵ , the quintet commencing at 16611 has been called $P(2)$ and the group commencing at 16730 has been taken as $P'(1)$.

If, now, the differences between successive values of C_a are examined, it will be observed that they are in every case less in the new arrangement than in the old. The same applies to C_e and to the differences between the mean C_a and C_e in the two sets. The alterations are small but so perfectly consistent that they are probably significant, and we shall, therefore, adopt the revised classification in preference to Allen's. It ought, perhaps, to be made clear that the new values of C_a and C_e are obtained merely by transformation of the old values to suit the new numeration and are thus strictly comparable with the latter. But the question is not a vital one so far as the conclusions reached in subsequent sections are concerned.

The triplet series in Fulcher's two bands resemble one another so closely, except for a difference of scale, that one would expect to find in the second band series corresponding to S_{4-7} in the first. That is to say, if the series Σ_{1-3} in the second band are of whole-quantum type, a set of related half-quantum series might possibly be found in the same region. A careful search

Table II --- Constants for the series S_1 to S_7 of the First Band.

Series	Allen		Curtis	
	Half quantum type		Whole quantum type	
	C_1	C_2	C_1	C_2
S_1	156 19	150 76	153 48	148 05
	+0 64	+0 57	+0 60	+0 54
S_2	156 83	151 33	154 08	148 59
	+0 17	+0 34	+0 36	+0 32
S_3	157 20	151 67	154 44	148 91
Mean	156 74	151 25	154 00	148 52
	Whole quantum type		Half quantum type	
	C_1	C_2	C_1	C_2
S_4	156 81	150 99	153 91	148 09
	-0 79	-0 42	0 61	-0 24
S_5	156 02	150 57	153 30	147 85
	+2 28	+1 64	+1 96	+1 32
S_6	158 30	152 21	155 26	149 17
	-0 17	0 19	-0 33	-0 05
S_7	157 83	152 02	154 93	149 12
Mean	157 24	151 45	154 35	148 50
S_4 - S_1	+0 50	+0 20	+0 35	+0 04

for lines having the appropriate intervals was accordingly made, but without result. The data available for prediction purposes are so definite that one can be pretty sure that such series do not exist, unless they should happen to be affected by considerable perturbations, which might render their detection difficult.

4 Interpretation of the Vertical Series

The discovery of the extra lines is of the first importance in connection with the interpretation of the triplets, for it implies that the new vertical series thus formed must originate from a system of related stationary states. The question is, what is the relation between them? It is not likely, for several reasons, that they are successive rotation states. For one thing, the horizontal series have already been explained in this way and furnish a reasonable value

of the moment of inertia of the molecule. But apart from this, the intensity distribution suggests a Q type, and a Q branch does not occur alone (*i.e.*, without P and R). On the other hand, if they are assumed to be R branches, the moment of inertia would have to be of the same order as that of the helium molecule, which is very unlikely. Neither can they correspond to successive electronic orbits, for they are much too close together. The only remaining alternative, so far as is known at present, is to attribute them to successive states of vibration of the nuclei within the molecule, and it is now proposed to examine this view in some detail.

Kratzer* has investigated the question theoretically and has made several very successful applications of his results, as, for example, to the well-known cyanogen bands in the blue and near ultra-violet †. He finds that for a diatomic molecule the vibrational energy can be expressed, to a first approximation, in the form

$$W_n = nh\nu_x (1 - nx),$$

where n is the vibrational quantum number, ν_x the frequency of vibration of the nuclei, and x a small constant dependent on the law of force and equal to zero if the vibrations are simple harmonic. Thus, the frequency radiated in consequence of a change in the vibration state given by $n' \rightarrow n$ will be

$$\nu_e + n'\nu'_x (1 - n'x') - n\nu_x (1 - nx),$$

$$\text{i.e.,} \quad \nu_e + (n' - n)\nu'_x + n(\nu'_x - \nu_x) - (n'^2\nu'_xx' - n^2n\nu_xx) \quad (3)$$

The quantities ν_x and x may be affected by the change of electron configuration which occurs simultaneously with the vibrational change, so initial values ν'_x and x' are assumed for them. The four terms on the right will usually be in descending order of magnitude. ν_e , the frequency characteristic of the electron transition alone, is much larger than ν_x (*e.g.*, for CN $\nu_e = 26,000$ and $\nu_x = 2,100$), and the two together determine the location of a group of bands (*e.g.*, CN 4216, 4197, 4181, 4168, 4153). The third term is mainly responsible for the position of the band in the group, and if there were no further term the constituent bands would be equally spaced in wave-number. The fourth term, however, involves the square of n and thus gives a parabolic distribution.

So far the rotational state of the molecule has been disregarded, actually, however, a rotational change is in general superposed on the other two, and the frequency due to this alone will be of the form

$$B(m-1)^2 - bm^2, \text{ i.e., } B - 2Bm + (B-b)m^2$$

* 'Zetschr f Phys,' vol 3, p 289 (1920)

† 'Phys Zetschr,' vol. 22, p 552 (1921)

in the case of a P series. The constants B and b are the same as Allen's C_a and C_v respectively, and are introduced here for the sake of preserving Kratzer's notation throughout. Before forming the expression for the total frequency radiated allowance must be made for a certain interdependence between the rotation and vibration states*. The moment of inertia, and hence the rotational energy, is dependent upon the state of vibration, since this affects the mean separation of the nuclei, and the vibrational energy is dependent upon the state of rotation (owing to centrifugal force). Kratzer† has shown that both effects can be taken into account by replacing B and b in the above formula by $B(1 - n'\alpha')$ and $b(1 - n\alpha)$, respectively, α and α' being small and constant to a first approximation.

The complete expression for the radiated frequency thus becomes, for a rotation change $(m - 1) \rightarrow m$ and a vibration change $n' \rightarrow n$,

$$P(m) = \nu_r + (n' - n)\nu'_r + n(\nu'_r - \nu_r) - (n'^2\nu'_r\alpha' - n^2\nu_r\alpha) \\ + B(1 - n'\alpha') - 2B(1 - n'\alpha')m + \{B(1 - n'\alpha') - b(1 - n\alpha)\}m^2 \quad (1)$$

It is not possible to evaluate all these quantities from data derived from only one group of bands, but it is possible to test whether such an expression is of the correct form for the representation of the series, and to determine some of the constants.

In the first place, the possible values of $n' - n$ are limited by the correspondence principle to those which are represented in the harmonic components of the vibration. If this were simple harmonic we should expect only the values ± 1 to occur. If it were nearly simple harmonic we should expect the group of bands given by $n' - n = \pm 1$ to be more intense than any other. Evidence that the vibration in this case does approximate to simple harmonic will be produced later. We therefore begin by assuming that $n' - n = \pm 1$.

The similarity between the two triplet bands obviously suggests that they might represent the two vibrational transitions ± 1 , but this unfortunately does not appear admissible. It would require that the values of $B(1 - n'\alpha')$, or Allen's C_a , should not differ greatly in the two cases, since α' can be shown to be small. The difference is actually some 40 per cent, and the same discrepancy is encountered when the coefficients of m^2 , $C_a - C_v$, are considered. The previous conclusion is thus confirmed, that the bands

* See Sommerfeld, 'Atomic Structure and Spectral Lines,' p. 422.

† 'Zetschr. f. Phys.,' vol. 3, p. 289 (1920).

originate from different molecules and must therefore be considered separately *

The abandonment of the above hypothesis leaves us with no means of determining which of the transitions $n \pm 1 \rightarrow n$ is concerned in the emission of the bands. Let us provisionally assume that it is $n + 1 \rightarrow n$, as a matter of fact the conclusions which follow would not be fundamentally altered by assuming $n - 1 \rightarrow n$ instead. Then the formula becomes

$$\begin{aligned}
 P(m) = & v_e + v'_n(1 - x') + n(v'_n - v_n - 2v'_n x') - n^2(v'_n x' - v_n x) \\
 & + B(1 - \alpha') - Bn\alpha' - 2B(1 - \frac{n}{n+1}\alpha')m \\
 & + [B\{1 - (n+1)\alpha'\} - b\{1 - n\alpha'\}]m^2
 \end{aligned} \tag{5}$$

We should get a horizontal series by giving m successive integral values (beginning at 2), n remaining constant. A vertical series should result from a similar progression of n , m remaining constant. We have already assigned values to m for all the lines, and may feel reasonably confident of their correctness. The proper values for n are in some doubt, but analogy with other bands leads us to expect that the lowest values will be associated with the strongest lines. That is to say, the lines S_3 should arise from the transition $1 \rightarrow 0$, S_2 from $2 \rightarrow 1$ and so on. With these assumptions we are in a position to compare the theoretical and observed results.

It is first necessary to represent the series by formulæ. As Allen only gives formulæ for S'_{1-3} and not for the extra lines, and as he does not state how the formulæ were obtained, fresh formulæ were calculated. These were derived in each case from the first three lines, assumed to be $P(2)$, $P(3)$ and $P(4)$. Experience has shown that this is preferable, apart from the question of labour, to calculating least-square formulæ, since after the first few lines terms in higher powers of m than the second begin to have an effect, and the quadratic formula ceases to fit. In any case the essential thing for the present purpose is to use precisely the same procedure for all the series. The results are summarised in Table III below, which gives the values of the constants in equation (1) above.

* Takahashi ('Japanese' Journ. Phys., vol. 2, p. 95 (1923)) comes to the opposite conclusion. He uses a different formula, which he has derived theoretically, but which does not appear to be so well verified by comparison with observation as Kratzer's. In any case there are discrepancies between his observed and calculated values which seem to me to render his deductions far from convincing.

Table III.—Constants for Quintuplets of First Band.

Series	C_1	C	$C_a - C$	ν_0
S_4	153 41	148 20	+5 21	17050 82
S_3	153 16	147 94	5 22	17035 03
S_2	152 84	147 62	5 22	17011 80
S_1	152 34	147 11	5 23	16980 42
$S_{(-1)}$	151 96	146 64	5 32	16942 35

Comparison of equations (1) and (5) shows that $B(1 - \overline{n+1}\alpha')$ and $b(1 - n\alpha)$ are to be identified with C_a and C_s respectively, so that with the numeration assumed the following equations result —

Δ	Δ
$B(1 - \alpha') = 153\ 41$	$b = 148\ 20$
$- 0\ 25$	$- 0\ 26$
$B(1 - 2\alpha') = 153\ 16$	$b(1 - \alpha) = 147\ 94$
$- 0\ 32$	$- 0\ 26$
$B(1 - 3\alpha') = 152\ 81$	$b(1 - 2\alpha) = 147\ 62$
$- 0\ 50$	$- 0\ 51$
$B(1 - 4\alpha') = 152\ 34$	$b(1 - 3\alpha) = 147\ 11$
$- 0\ 38$	$- 0\ 47$
$B(1 - 5\alpha') = 151\ 96$	$b(1 - 4\alpha) = 146\ 64$

The first differences are seen to be approximately constant, as required by the theory, the agreement being extraordinarily good, considering that each number is derived from three lines, each of which may easily be in error by 0.03 unit, apart from possible apparent displacements due to blending with other lines. The mean values of the constants as determined by the method of least squares are—

$$B = 153\ 86 \qquad b = 148\ 29$$

$$\alpha' = 0\ 00242 \qquad \alpha = 0\ 00266$$

The values of α are approximately equal and very small in comparison with those met with in other bands (*e g*, for CN, 0.044, 0.035, 0.136)*. For pure harmonic vibrations α would assume a small negative value, we therefore conclude, as has been assumed above, that the nuclear vibration deviates but little from the simple harmonic type.

It may also be shown that the horizontal second differences should be approximately constant vertically, this is actually the case, as has been remarked earlier in this paper. The vertical second differences should also be

* Kratzer, 'Phys Zeitschr.', vol 22, p. 554 (1921)

constant horizontally, but in both bands they show a tendency to increase to the right. This is not a vital discrepancy, however, in view of the fact that neither set of series can be accurately represented by quadratic formulae, such as have been used in the approximate theoretical expressions quoted, so that a small systematic deviation of calculated from observed values is to be anticipated.

A further comparison of equations (1) and (5) establishes the identity

$$\begin{aligned} v_0 = & v_c + v'_x(1 - x') + n(v'_x - v_x - 2v'_xx') - n^2(v'_xx' - v_xx) \\ & + B(1 - \frac{n}{n+1}\alpha') \end{aligned}$$

That is to say, the values of v_0 for the series S_3, S_2 , etc., should be expressible by a quadratic formula in n , so that their second differences should be constant. The values and differences are as follows —

Assumed n	v_0	Δ_1	Δ_2
0	17050.82		
		- 15 79	
1	17035 03		- 7.44
		- 23 23	
2	17011 80		- 8.15
		- 31 38	
3	16980 42		- 6 69
		- 38 07	
4	16942.35		

In view of the long extrapolation (about 450 cm^{-1}) involved in the determination of v_0 this is far from unsatisfactory. The second difference is here negative, whereas it is positive in the case of the cyanogen bands, but there does not appear to be any reason against this, since there is no theoretical indication of the relative magnitudes of xv and $x'v'$. It is obviously impossible to evaluate the five unknown constants v_c, v_x, v'_x, x and x' , since although five values of v_0 are available they are represented by a quadratic formula and are thus equivalent to only three.

The second band may be treated in the same way and gives similar results, which are less conclusive, however, since there are only sixteen lines available instead of thirty. The calculated values of the constants are given in Table IV.

Disregarding Σ_0 , with which there appears to be something wrong, the most probable values are found to be

$$\begin{aligned} B &= 221.05 & b &= 213.73 \\ \alpha' &= +0.00075 & \alpha &= +0.00115 \end{aligned}$$

It may be remarked that the above conclusions would only be modified in

numerical details, i.e., their general purport would be unaffected, if the vibration change had been assumed to be $(n - 1) \rightarrow n$, instead of $(n + 1) \rightarrow n$

Table IV — Constants for Quadruplets of Second Band

Series	C_1	C_2	$C_2 - C_1$	ν_0	Δ_1	Δ_2
Σ_2	220 87	213 71	7.16	19485 48	—21 51	
Σ_1	220 77	213 53	7 24	19463 97	32 39	—10 88
Σ_1	220 54	213 22	7 32	19431 58	45 10	12 71
Σ_0	219 13	212 04	7 09	19386 48		

5 Molecular Moments of Inertia derived from the Fulcher Triplets

On the basis of the foregoing assumptions it is now possible to calculate the moments of inertia with greater accuracy than hitherto. The values given below refer to the non-rotating vibrationless state

	Initial M of I	Final M of I
First Band	1.794×10^{-41}	1.862×10^{-41} gm cm ²
Second Band	1.249 „	1.292 „ „

It is worth noting that the ratios of the two initial and the two final μ of inertia are very nearly the same, being 1.437 and 1.441 respectively. If this is not purely accidental, it presumably means that the two molecules are essentially similar in structure, the difference between them being chiefly one of scale. The increase in the moment of inertia as a result of the electron transition is at first sight surprising, as one tends to picture the whole molecule contracting when the electron falls into an inner orbit. But the effect cannot be predicted in this way, depending, as it does, on the complex interactions between electrons and nuclei, and in point of fact it appears that "expansion" of the molecule is quite common, as we infer from the numerous bands which are degraded towards the violet.*

6 The Distribution of Intensity in the Bands

Up to the present we have considered solely the wave-numbers of the lines. These give information as to the energies of the stationary states. The intensities, on the other hand, depend upon the probabilities of occurrence of the states and of transitions from one to another. On account of the rather trouble-

* For this means that $C_2 - C_1$ is positive, i.e., $C_2 > C_1$, i.e., $I_2 < I_1$.

some nature of the measurements few exact data as to intensities in series have as yet been obtained, but in general these vary quite regularly. In line series they decrease steadily in the direction of the limit of the series. In band series they at first increase with the rotation quantum number, reach a maximum, and then fall off slowly. The variation of intensity with vibration quantum number does not appear to have been investigated, but inspection of the cyanogen bands suggests that the intensity decreases as the energy of vibration increases. At any rate there is no point of inflexion in the graph connecting intensity and vibration quantum number. The intensity distribution in the Fulcher bands presents some curious features, as will be apparent from Table V which gives the intensities as recorded by Merton and Barratt,[†] together with the rotation and vibration transitions as assumed above.

Table V—Intensities of Lines in Fulcher Bands

	Rotation quantum numbers						Vibration quantum numbers
	6 → 7	5 → 6	4 → 5	3 → 4	2 → 3	1 → 2	
First Band S_{-1} Z_{-1} Z_{-2} Z_{-3} Z_{-4}		0	2	4	4	5	5 → 4
		0	1	3	3	5	4 → 3
	2	3	6	8	8	10	3 → 2
	1	2	5	7	9*	7	2 → 1
	4	5	8	9	10	10	1 → 0
Second Band M_0 M_{-1} M_{-2} M_{-3}			2	2	0	3	4 → 3
			3	4	5	7	3 → 2
			3	2	3	1	2 → 1
			5	7	6	8	1 → 0

The horizontal distribution seems fairly normal, except for the one marked*, this is one of the two "perturbed" lines, and is almost certainly a blend. But the vertical distribution is peculiar, in that the rows designated 2 → 1 are both consistently weaker than their neighbours on either side. In the case of the first band this is, in fact, much more marked than the tabulated intensities would suggest—that is to say, the middle members of the Fulcher triplets are very considerably weaker than the outer ones. It is difficult to account for this on the interpretation put forward, but would seem to be no less difficult on any alternative one.

Another point relating to intensities deserves to be briefly mentioned.

[†] 'Phil. Trans.' A, vol. 222, p. 369 (1922).

Kimura and Nakamura* concluded that the S_1 series of the first band is of the enhanced type and S_8, S_6, S_5, S_7 are of the arc type. If this view were accepted the former would originate from an ionised and the latter from a neutral molecule, thus prohibiting the inclusion of S_1 and S_3 in the same series as has been done here. The numerical relationships indicate quite clearly, however, that the S_1, S_2 and S_3 series must originate from the same molecule. The explanation is probably that a more powerful electrical excitation throws more molecules into the states having greater vibrational energy, thus strengthening S_1 ($n = 3 \rightarrow n = 2$) relative to S_3 ($n = 1 \rightarrow n = 0$). The enhancement of a line by increasing the energy of excitation does not necessarily imply ionisation of the carrier. The suggested explanation thus incidentally gives some support to the numeration assumed in regard to the vibration states. Further evidence is obtainable from a study of the behaviour of the lines under the influence of the condensed discharge, as recorded by Merton and Barratt. There seems to be an unmistakable tendency for the series associated above with higher vibration quantum numbers to be relatively strengthened by the condensed discharge. This observation is a sort of generalisation of Kimura and Nakamura's result. At the same time one may note that the second band seems to be enhanced, relatively to the first, by stronger excitation.

7 General Remarks

The conclusions reached raise several questions of interest. In the first place, if the Fulcher bands are P branches we might expect to find Q and R branches associated with them. The data obtained may be extrapolated in order to predict these, but no such series have been identified in the expected positions, although an exhaustive search has yet to be made. It seems, however, that solitary branches do occasionally occur, there being several instances in the helium band spectrum. Again, whichever vibration change is assumed for these bands the reverse one must also occur, and should give rise to a set of closely similar bands. But we have no means of predicting the location of the latter, since the value of v_e is unknown. It might even be associated with a different electron transition. The frequency of the nuclear vibration in the hydrogen molecule has been calculated by Kemble and Van Vleck† from specific heat data, but refers to the normal molecule. In all probability both molecular states with which we have been dealing here are "excited."

* 'Japanese Journ Phys,' vol 1, p. 85 (1923). Similar observations have been made by Gehroke and Lau ('Preuss Akad Wiss Berlin Ber,' vol 32, p 453 (1922)).

† 'Phys Rev,' vol 21, p 653 (1923).

states, the emission resulting in the formation of the normal molecule is probably of much shorter wave-length (perhaps in the Lyman region).

Attention has been drawn to the fact that the moments of inertia derived from the two triplet bands have the same ratio, 1.44, for both final and initial states. It is remarkable that the vertical second differences are in very nearly the same ratio, namely, 1.42 (mean of 8 pairs of corresponding values). The vertical second difference has the theoretical value $-2(\nu'_n x' - \nu_n x)$, so that there is no obvious interpretation of this relation. Another curious feature of the vertical series is that they can be represented with fair accuracy, as Takahashi (*loc cit*) has shown, by formulæ of the type $A - B(n + \frac{1}{2})^2$. The significance, if any, of this is also obscure.

The interpretation of the Fulcher bands which has been offered here implies a very striking difference in structure from that of all other known bands. In the latter the contribution of the rotational term to the frequency radiated is small compared with that due to the vibrational term, so that (to use the same nomenclature as above) the spacing of the horizontal series is much smaller than that of the vertical series. The exact opposite is the case here, and the appearance of the band system is in consequence entirely changed. The difference is readily explicable if we take into consideration.—

- (1) The small moment of inertia of the molecule, resulting in a large horizontal spacing, and
- (2) the approximation of the nuclear vibration to simple harmonic character, which contracts the vertical spacing.

In conclusion, acknowledgment may be made to the invaluable tables of wave-lengths, etc., due to Merton and Barratt, since without such comprehensive and accurate data it would have been useless to undertake an investigation such as this.

8 Summary

The Fulcher lines and Allen's additions to them have been examined with a view to finding a theoretical interpretation of them. The wave-numbers of two of the strongest lines are shown to require correction by about 0.5 cm.^{-1} . The differences are then sufficiently regular to provide a criterion for the genuineness of the extra lines, which are in the main confirmed. Discarding all doubtful lines, the Fulcher triplets then become quintuplets and the second set quadruplets. The arrangement of these is shown to be consistent with the view that they originate from combinations of simultaneously occurring rotation and vibration changes. The relevant quantum numbers cannot be determined.

with certainty, but their most probable values are indicated. New and, it is believed, more accurate values of the molecular moments of inertia concerned are obtained. These, however, probably refer to an "excited" molecule.

It appears that the nuclear vibrations within the hydrogen molecule are very nearly simple harmonic, which would account, in conjunction with the small moment of inertia, for the unique structure of the system as compared with other band systems.

Although it does not seem possible that the two sets of Fulcher triplets can originate from the same molecule it is concluded that the two molecules concerned must be essentially similar in structure, as there is a remarkably close correspondence between all the constants in the two cases.

The existence of other series related to these is to be expected, and the data obtained give indications which may facilitate the search for such new series.

On the Determination of the Directions of the Forces in Wireless Waves at the Earth's Surface

By R. L. SMITH-ROSE, Ph.D., M.Sc., and R. H. BARFIELD, M.Sc.

(Communicated, by permission of the Radio Research Board, by Sir Henry Jackson, F.R.S.—Received November 26, 1924.)

1. *Introduction*

There are two outstanding problems relating to the propagation of wireless waves over the earth's surface which at present remain unsolved, viz—What is the agency which causes the waves to follow the curvature of the earth, thus rendering long-distance communication possible? And what is the cause of the large and rapid variations of the intensity and apparent direction of the waves, very commonly observed at the receiving station and confined almost entirely to the hours of darkness?

Both phenomena can be explained to some extent by the well-known Heaviside-layer theory, with the modifications proposed by Eccles, but it is generally admitted that further experimental evidence of the existence of the layer is needed. If the theory is correct and is sufficient, it follows that, a receiver experiencing either of the above phenomena, part of the energy must be arriving in a downward direction (i.e., inclined to the horizontal), and that during

the occurrence of directional variations, this downcoming wave must have an horizontally polarised component (i.e., with its electric force horizontal). It has, therefore, been generally recognised for some time that a conclusive experimental demonstration of the presence or absence of such waves, by suitable quantitative measurements in three dimensions, would aid considerably in proving or disproving the Heaviside-layer theory.

Several workers have carried out investigations on these lines. The most successful of these was T. L. Eckersley (1), who obtained results which appear to indicate definitely the presence of an abnormally polarised downcoming wave, and to show that the intensity of this wave was proportional to the magnitude of the directional error. Although it is extremely difficult to find any fault either in the experimental methods adopted or in the analysis based on the results, these conclusions are of such importance that they have naturally been submitted to some criticism, and it is highly desirable to carry out confirmatory experiments.

Other work of this nature has been carried out by Austin (2), who attempted to measure the direction of the electric field of an arriving wave by means of a large "Hertzian Rod" aerial, by Erskine-Murray and Robinson (3), who employed a combination of Hertzian rod and a frame coil mounted on three axes for determining the direction of propagation of electro-magnetic waves; by Bellini (4), who made observations on the inclination of the magnetic force to the horizontal during the occurrence of directional variations by means of a frame coil rotating about both vertical and horizontal axes; and by Sir Henry Jackson (5), who also used a frame coil with much the same object. As far as can be gathered from the published information, however, it appears that these experiments were accompanied by either instrumental or local errors which prevented the establishment of any definite facts relevant to the general problem of the propagation of waves.

The present investigation consists in following up the line of attack opened up by the above workers, in an attempt to obtain more conclusive results. The experimental methods employed are much the same in principle, but a large amount of detailed research has been carried out on the apparatus to improve its accuracy. This paper describes the first part of the investigation only, for the experiments are still in progress (September, 1924).

2 Boundary Conditions imposed at Earth's Surface.

A preliminary consideration of the problem in hand drew attention to the necessity of taking into account the boundary conditions imposed on the

forces of an electromagnetic wave at a receiver situated on the ground, i.e. effectively at the surface of separation between a non-conducting and a conducting medium. With a perfectly conducting earth, these conditions would imply that at the surface (assumed horizontal) the resultant electric force (E) must always be vertical and the resultant magnetic force (H) always horizontal, whatever might be the inclination of the wave or waves arriving at the receiver. In other words, a wave incident at any angle at the surface of separation will give rise to a reflected wave, the two interfering in such a way as to tend to eliminate the horizontal component of the electric force and the vertical component of the magnetic force.

It was, therefore, clear at the outset of the experiments, that if the earth at the receiver were of sufficiently high conductivity it would be useless to attempt to detect down-coming waves by directional measurements at the surface, since the resultant fields produced at the surface of the earth would be indistinguishable from those of a horizontally propagated wave. For this reason a knowledge of the value of this conductivity was considered to be necessary as a preliminary to the experiments.

Information on the conductivity of various soils is also to be found in tabular form in various text-books (*e.g.*, Fleming (6)). These values appear to have been obtained for the most part from the works of Brylinski (7), Lowy (8), Schmidt (9), and Uller (10).

In most of these cases the conductivity measurements were made in the laboratory on artificially treated specimens of soil, and in very few cases were they carried out at radio frequencies. In view of the heterogeneous nature of the surface and sub-soil at any ordinary site, and its varying moisture-content, it was not considered that this information was sufficiently reliable and exact for the purpose required. For example, the values given for moist earth—the nearest description to the conditions at Slough for the greater part of the year—vary from 10^7 to 10^9 electrostatic units,* limits which are somewhat wide for making satisfactory deductions as to the suitability of the site for the proposed experiments.

Considerable doubt also existed as to what effect, if any, a non-conducting subsoil such as dry sand or rock would have, when, as is usual on level ground in this country, it is covered by either water or soil of sufficient thickness for the maintenance of ordinary vegetation. In these circumstances, therefore, it was decided to determine the conductivity experimentally, employing wireless waves of ordinary commercial frequencies.

* To convert to electromagnetic units, divide by c^2 ($\approx 9 \times 10^{20}$ approx.)

3 *Determination of Conductivity of Ground at Slough.*

The method adopted was to measure the angle of inclination to the vertical, or "forward" tilt, of waves received from various transmitters situated only a few miles away, it being assumed that such waves are vertically polarised* and propagated horizontally over the earth's surface. This was effected by rotating a straight Hertzian-rod-type receiver about a horizontal axis, placed perpendicular to the direction of travel of the waves, until the signals were reduced to a minimum. The angle (β_0) then made by the rod with the horizontal is the angle of inclination of the electric field to the vertical. By a simple modification of Zenneck's formula for the ratio of the horizontal to the vertical component of the electric field of such a wave, of frequency " n ," the conductivity (σ) in electrostatic units is given by the expression

$$\sigma = \frac{n}{4 \tan^2 \beta_0} \quad (1)$$

to a close degree of approximation, when β_0 is reasonably small and σ is large compared with n , both of which conditions were found to be valid in the experiments under consideration.

The Hertzian rod used at Slough consisted of a copper wire, 30 feet long, stretched on a light wooden beam in the manner of a bowstring, the centre of this beam being carried on a horizontal axis mounted at the top of a wooden tripod 20 feet high. Leads from the centre of the rod were taken to an amplifying receiver, contained in a screened box mounted on a centre turntable, which, with the horizontal axis supporting the rod, was capable of complete rotation about a vertical axis. By this means the rod-aerial could be rotated in any required vertical plane. The success and accuracy of the instrument are largely due to the efficiency of the screening of all the apparatus and leads except the wire forming the aerial, and in the present arrangement this is so satisfactory that, when using a nine-valve amplifying receiver, the direct pick-up of signal from any transmitting station is negligible.

In making an observation the horizontal axis of rotation of the rod is set at right angles to the direction of the transmitting station, and the rod is rotated in its own vertical plane until the received signal is reduced to a minimum. The angle then made by the rod with the horizontal is the angle of inclination (β_0) of the electric field with the vertical. The minima are usually not quite sharp, owing to the fact (shown theoretically by Zenneck) that the electric force is

* The term "vertically polarised" implies that the electric force is contained in the vertical plane of propagation.

elliptically polarised in the plane of propagation of the wave. In each position the observation is repeated, after reversal of the leads between rod and receiver, and the procedure is then repeated with the horizontal axis turned through 180° . This process eliminates the error which would otherwise be caused if any residual direct pick-up of signal were still present, and also that due to any incorrect setting of the scale. The maximum error of the individual observations made is considered to be about a degree, although the mean of a number of readings is probably of a higher order of accuracy.

A series of measurements was made on wave-lengths varying from 450 metres to 6.9 km, and the values of β_0 , together with the conductivity values (σ) calculated therefrom, are given in Table I.

Table I—Values of Forward Inclination of Electric Force measured at Slough for Calculation of Conductivity of Earth

Transmitting Station	Distance (miles)	Wave length (km)	Frequency (kc per sec)	Angle β_0 (deg)	Conductivity σ (E.S.U.)
Northolt	9.0	6.90	43.5	0.7	
Ongar	36.0	3.80	79.0	0.7	
Teddington	11.5	2.60	116.0	0.6	
Teddington	11.5	0.75	400.0	2.1	0.7×10^8
Teddington	11.5	0.75*	400.0	2.0	0.8×10^8
Teddington	11.5	0.45*	670.0	2.7	0.7×10^8
Mean value of conductivity					0.7×10^8

* Indicates spark transmission, all others continuous wave

In the first three cases in the above table it is seen that the quantity measured (β_0) is of the same order of magnitude as the limits of accuracy of the apparatus, and it was therefore not considered justifiable to use these results for the calculation of conductivity.

From these observations it will be seen that the mean value of the effective conductivity of the ground at Slough for wireless-wave propagation was found to be about 0.7×10^8 electrostatic units. This mean value obtained undoubtedly represents a much closer approximation to the actual value than could be obtained from the previously existing information referred to above.

4. Boundary Conditions at Slough.

Having gained the necessary knowledge of the conductivity of the ground at the site proposed for the experiments, it was now possible to examine the boundary conditions and calculate exactly what would be the direction of

the resultant fields produced by a down-coming wave, if it existed. It will first be assumed for simplicity that a single wave only is arriving at the receiver, travelling in a downward direction with an angle of incidence, θ , to the normal. Referring to the resultant electric and magnetic forces E and H , due to the combination of the down-coming incident wave and the up-going reflected wave:—

Let β be the inclination of E to the vertical in the plane of propagation of the wave

, α be the inclination of E to the vertical in the plane at right angles to the plane of propagation

„ δ be the inclination of H to the horizontal plane

Then it can be shown from the electromagnetic equations for reflection at a conducting surface that,

(a) for a vertical polarised wave (i.e., E in plane of incidence and, therefore, $\alpha = \delta = 0$),

$$\tan \beta = \frac{1}{2} \sqrt{\frac{n}{\sigma}} \times \frac{1}{\sin \theta} \quad (2)$$

and hence from (1)

$$\tan \beta = \frac{\tan \beta_0}{\sin \theta}, \quad (3)$$

(b) for a horizontally polarised wave (i.e., E is perpendicular to plane of incidence, and, therefore, $\alpha = \frac{1}{2} \pi$, $\beta = 0$),

$$\tan \delta = \frac{1}{2} \sqrt{\frac{n}{\sigma}} \times \sin \theta \quad (4)$$

$$= \tan \beta_0 \times \sin \theta \quad (5)$$

These formulae are approximations which are substantially true if σ/n is large compared with K (the dielectric constant of the earth). Both the electric field in case (a) and the magnetic field in (b) are slightly elliptical in form, and the angles given by equations (2) and (4) give the directions of the major axes of these ellipses.

Dealing first with equation (5) it is seen that the value of the angle δ increases with the angle of incidence and is greatest for grazing incidence ($\theta = 90^\circ$) when we have, $\delta_{\max} = \beta_0$.

Now the experiments already described have shown that at Slough the angle β_0 and hence δ_{\max} varies from a small amount with long waves to about 2.5° at 450 metres, and by extrapolating to a wave-length of 100 metres, the value of β_0 and δ_{\max} becomes 4.6° . If equation (3) is now referred to

it will be seen that $\tan \beta$ is inversely proportional to $\sin \theta$. Now, for all practical conditions θ is probably never less than 45° , and the maximum value of β therefore becomes $\beta_{\max} = \sqrt{2} \beta_0$, and is therefore only 1.4 times the value of β_{\max} above. Since, as has already been shown, β_0 does not exceed 3° at Slough on commercial wave-lengths, β_{\max} would be very difficult to distinguish from β_0 with the apparatus used up to the present.

A prediction of the values of the angles in the case when two or more waves are arriving simultaneously at different angles of incidence is naturally quite impossible unless the relative amplitudes and phases of the individual waves are known. A little consideration shows, however, that the tendency will generally be for the inclination to be *less than* those obtained for single waves. The exceptions to this occur when the conditions are such that the field due to the down-coming wave and that due to the direct wave are nearly opposite in phase, in which case they will almost neutralise each other, and the resultant field will therefore probably be too small to detect. Furthermore, although in the case of a single abnormally-polarised incident wave, we have $\alpha = 90^\circ$, the resultant electric force at the surface is very small in magnitude if σ/n is large, owing to the almost complete interference between the incident and reflected waves. If, therefore, a direct normally polarised wave of any appreciable magnitude is present, the resultant electric force is inclined sideways at an angle α , which can be shown to be not greater than δ .

This brief analysis, therefore, leads to the conclusion that whatever may be the causes of the phenomena of long-distance transmission and directional errors as observed at Slough, they could not be expected to give rise to resultant fields at the receiver which differ in direction sufficiently to be distinguished with the apparatus available from those of the direct, horizontally propagated wave. For further progress it therefore seemed necessary either,

- (a) to improve the accuracy of the apparatus or use another method to enable inclinations of the desired magnitude to be detected,
- (b) to carry out the experiments on short wave-lengths of 100 metres or less, or
- (c) to find an alternative site at which the ground is of much lower conductivity than at Slough.

The latter course was chosen as the first step, since from the published information on the resistance of the earth (already referred to) it appeared to be quite possible to find a site at which the conductivity would be as low as 10^6 , on which the values of β and δ might be expected to exceed 15° , and

therefore might be conveniently measurable. It was therefore decided to measure the conductivity of a number of other kinds of soil in different parts of England, in an attempt to find a more suitable site.

5 Measurements of Conductivity of Different Soils in Southern England.

For this purpose a portable Hertzian-rod receiver was constructed, very similar in design to that installed at Slough, as described in Section 3 above, but on a smaller scale. The straight wire forming the aerial was only 15 feet long, and the height of the supporting tripod only 5 feet. Owing to the reduction in size of the aerial system, the relative magnitude of the energy directly picked up by the tuning circuits, amplifiers, subsidiary apparatus and connecting leads, was increased. By careful detailed attention to the screening of the apparatus, however, this difficulty was overcome, and the apparatus was found to be quite as accurate as the larger instrument, the instrumental error was certainly less than 1° , and the mean of several readings, as usually taken, probably being correct to about 0.5° .

With this apparatus experiments were carried out on some ten different sites, on subsoils of as varied a nature as could be found in the south of England—viz, clay, sand, chalk, granite, and serpentine rock. At several of the sites the measurements were repeated on a second occasion, in an attempt to detect possible variations, due to change in season or other causes. The results of these measurements, carried out from May to September, 1924, are summarised in Table II.

This table shows that the effective conductivity of the ground at these various sites lies between 0.14×10^8 and 4.7×10^8 , and the state of the surface of the ground does not appreciably modify this value. Omitting, in the first place, the results obtained in Cornwall, it is seen that the conductivities are of the same order as that at Slough, which gives an average representative value for the various sites selected well away from the coast. The actual value of σ at Slough, given in Table II, is somewhat higher than that obtained in the earlier measurements, given in Table I.

This discrepancy was discovered later to be due to the fact that the inclination of the electric force to the vertical varied in different parts of the field, as shown by the portable apparatus, and is evidently due to some local cause (such as the masses of trees in the vicinity) which has been previously shown to give rise to errors in apparent bearings of certain transmitting stations. This variation is not, however, large enough to affect any of the conclusions which have been drawn.

Table II.—Results of Measurements on Forward Inclination of Electric Force (Angle β_0) at various Places with Portable Rod Receiver.

Site.	Nature of Sub-soil.	State of Surface	Date of Test	Value of β_0 measured at			Distance in Miles		Remarks	Average value of σ obtained from β_0 †
				2LO, 365 m	5HW, 450 m	5HW, 750 m	From 2LO	From 5HW		
Stoke Common, Bucks Walton Heath, Surrey " " "	Clay Sand "	Very wet Moist Very dry	8.5.24 22.5.24 8.7.24	Deg 3.1 3.8 3.3	Deg 2.1 2.8 2.8	Deg 1.3 2.4 2.1	20	14	—	1.3×10^9
							17	10	After four weeks' hot, dry weather	0.6×10^9
							17	10	After four weeks' hot, dry weather	0.7×10^9
Cheam Bos, Bucks	Chalk	Wet	5.6.24	1.6	1.2	0.7	23	23	After 24 hours, continuous rain	4.7×10^9
" " "	"	Very dry	10.7.24	1.5	1.5	0.9	25	23	After four weeks' hot, dry weather	3.2×10^9
Marlborough Downs, Chisleton, Wilts	"	"	1.7.24	—	1.2	0.9	68	60	Measurements confirmed on longer waves, 2,600 m to 6,900 m — β_0 diminishing to 0.4 on latter wave	4.0×10^9
Slough, Bucks	Clay	Moist	3.7.24	2.4	1.8	1.3	18	11.5	—	1.5×10^9
" " "	"	Dry	7.7.24	2.0	1.7	1.1	18	11.5	—	2.1×10^9
Princes Risborough, Bucks	Chalk	"	15.7.24	3.5	3.6	0.9	33	29	Taken on sloping ground	1.6×10^9
" " "	"	Moist	5.8.24	1.7	1.5	1.4	33	29	On level site	2.2×10^9
"The Sands, Farnham, Surrey	" Sand	Dry	17.7.24	2.1	2.1	1.4	33	25	—	1.5×10^9
Teddington, Middlesex	"	"	24.7.24	1.7	1.4	0.7	11	1.0	—	4.2×10^9
The Lizard, Cornwall	Serpentine	"	9.9.24	5WA 351 m 1.0	6BM 385 m 1.5	FFU and GLD 600 m —	134	From 6BM 152 From GLO 23	On barren ground with outcropping rock, 1½ miles from coast	2.4×10^9
" " "	"	"	10.9.24*	5.6	5.9	1.9	134	152	On rocky cliff path, ½ mile from coast	0.51×10^9
Land's End, Cornwall	Granite	"	11.9.24*	7.1	—	5.3	143	169	On rocky cliffs, 200 yards from coast	0.17×10^9
" " "	"	"	"	5.7	7.4	6.7	143	169	As above, 100 feet nearer coast	0.14×10^9

* Note.—The ground at the sites chosen at the Lizard and Land's End on September 10 and 11 was of very broken surface and varied nature. This, together with the proximity to the cliffs, probably accounts for the relatively large discrepancies in some of the results. In each case it was noticed that a slight shift in position of the apparatus resulted in a change in the values obtained, and in several positions the electric and magnetic fields were subject to appreciable sideways inclinations.

† For comparison purposes it may be pointed out that the conductivity of sea-water is of the order 10^9 .

For comparison purposes, it is interesting to note that the previously published values of the conductivities range from 10^8 to 10^9 or less for specimens of moist and dry earth, sand, or clay. The more uniform values obtained in the present measurements are probably due to the fact that for wireless-wave propagation the effective conductivity is not solely determined by the condition at the immediate surface. In England, even in the hottest summer weather, it is doubtful if the soil ever becomes thoroughly dry to a depth of more than a few feet, and it is the moist soil below which will in this case determine the forward inclination of the wave-front. Also, as Hack (11) has previously shown, the presence of a layer of ground water at a depth of a fraction of a wave-length in a poorly conducting soil will almost entirely annul the forward tilt of the wave-front which would otherwise be set up at the surface.

Referring now to the measurements made in Cornwall, as recorded at the end of Table II, it is seen that in the first of these, at the Lizard, the conductivity obtained is similar to that at Slough. This is undoubtedly explained by the fact that the highly insulating serpentine-rock subsoil was mostly covered by a layer of one or two feet of surface soil with a moderate moisture-content, only at intervals over the surface was the rock projecting through the upper soil. As the coast is approached the depth of the soil layer decreases, and within a quarter of a mile of the edge of the cliffs the measurements show an appreciable drop in the conductivity values. For these latter measurements it was extremely difficult to find suitable sites, and the discrepancies occurring in the values of β_0 measured on the different wave-lengths are considered to be due to the uneven rock surface, the consequently varying depth of surface soil, the stratification of the rocks, and the trapping of rain-water in pools on the rock surface below the soil. In any case, the sites of these measurements would not be suitable for the proposed experiments on reception of down-coming waves, since for the study of wave-reflection problems a uniform surface of dimensions greater than a wave-length is necessary, and these particular sites were less than a wave-length from cliffs of two or three hundred feet in height. It is possible that at a more satisfactory site further inland, lower conductivity values would be obtained after a hot, dry summer, long enough to dry out the soil down to the rock surface, but the conductivity at such a place would, naturally, be subject to a large seasonal variation.

It is, therefore, to be concluded from these experiments that, although at some of the places investigated the conductivity is slightly lower than that at Slough, the difference is not sufficiently great to justify the transfer of any of the experimental work. The difference in the maximum possible inclinations

of the electric and magnetic forces as obtained from the theory already given is, in fact, almost inappreciable at all the sites investigated

(While not strictly relevant to the problem in hand, it is interesting to record here that during these measurements justification was obtained for the assumption that the inclination of the wave-front was related to the normal to the ground surface at the receiver, whereas the angles measured on the apparatus were related to the true vertical. At most places a suitable horizontal site could be obtained, but it was sometimes necessary to work on slightly sloping ground and make the necessary corrections for the direction and magnitude of the slope (usually less than 1°). On one occasion, however, a site was intentionally selected on the side of a hill sloping at about 16° , but after correcting for this, it was found that the values of β_0 agreed with those measured on a level site in the same neighbourhood.)

6 *Confirmatory Experiments at Slough*

In view of the conclusion arrived at in the last section, it is of sufficient interest to record the result of a series of measurements of the directions of the electric and magnetic forces made at Slough, mainly with the object of confirming experimentally the deductions made from the boundary conditions considered in Section 4

(a) *Method of Measurement* —The direction of the electric field was measured by means of the larger Hertzian-rod apparatus described in Section 3. That of the magnetic field was measured by means of a frame coil capable of rotation about both vertical and horizontal axes. With its plane vertical the coil is rotated about the vertical axis to the position of minimum signal, and the ordinary wireless bearing observed. The plane of the coil in this position is then parallel to the horizontal component of the magnetic field of the arriving wave. The coil is now turned through 90° about its vertical axis to the maximum signal position, and then rotated about its horizontal axis until a second position of minimum signal is obtained, when the angle made by the plane of the coil with the horizontal is observed. This reading gives the elevation of the resultant magnetic field due to the arriving wave, and the direction of the field is the line of intersection of the planes of the coil when in the two minimum positions above determined. In the complete measurements the observations are always repeated after reversing the connections of the frame coil, and the whole operation is then repeated after rotating the coil through 180° about a vertical axis. The mean readings so obtained are practically

free from any scale errors, and also from the effects of any residual direct pick-up on the leads and coupling coils of the receiver

The auxiliary apparatus used with this frame coil is the same as that employed with the Hertzian-rod receiver. In addition to the screening of the tuning circuits and amplifiers in a metal box, the operator and whole of the apparatus are contained in a wooden hut, which is well insulated from earth and entirely surrounded by a wire screen comprising open untuned loops. This type of screen has been shown previously (12) to eliminate antenna effect on the frame-coil system. The accuracy of the observations obtainable with this apparatus was considered to be about the same as that of the Hertzian rod instrument.

(b) *Discussion of Results*—Table III gives a summary of the results of a series of systematic measurements of the directions of the electric and magnetic fields as observed simultaneously at Slough, over a period of seven months, on various wave-lengths. In this table, α , β , β_0 and δ are the same quantities defined in Section 4, p 592, and γ is the angle between the observed direction of the horizontal component of the magnetic field and its normal direction, i.e., γ is the error in the observed wireless bearing.

Table III—Summary of Results of Simultaneous Directional Measurements of Electric and Magnetic Fields at Slough

Transmitting Station	Distance	Wave-length	Frequency	Extreme Readings over a Period of Seven Months.				β_0 calculated from $\sigma = 10^\circ$.
				α	β	γ	δ	
	miles	km	kc per sec	deg	deg	deg	deg	deg
Nantes	302	9 00	33 3	+0 1 -1 3	0 0 -0 5	-0 9 -1 7	-0 3 -0 7	+0 5
Leafield	48 5	8 70	34 5	+1 1 -0 7	+0 5 1 3	+12 0 -11 2	+1 0 -0 7	+0 5
Tours	165	6 80	44 2	0 0 -1 0	+1 1 0 0	+0 6 -1 4	+0 3 -1 0	+0 5
Königswusterhausen	608	5 30	56 6	0 0 -0 3	+1 5 0 0	+3 1 -9 7	+1 0 -0 3	+0 6
Nauen	576	4 70	63 8	+0 5 -1 0	+1 5 +1 0	+9 8 -5 7	+0 7 0 0	+0 6
Ongar (GLO)	36	4 40	68 2	+0 5 -0 5	+1 5 -0 7	+4 2 -6 3	+0 8 -0 9	+0 8
Ongar (GLB)	36	3 80	79 0	+1 0 -1 0	+1 5 0 0	+2 3 -2 5	+1 3 0 0	+0 8
Paris (FL)	221	2 60	116 0	0 0 -0 5	+1 0	+0 1	0 0 -0 1	+0 9
Teddington	11 5	0 75	400 0	-0 1	+2 1 +2 0	+0 6 +0 4	+0 1 -0 5	+1 7
Teddington	11 5	0 45	670 0	-0 3	+2 7 +2 6	+1 2 +0 5	+0 1 -0 1	+2 2

Many of the observations summarised above were purposely made on stations and at periods which experience had shown to be most likely to produce variations in γ (i.e., directional errors or night effect) and it will be seen that variations as large as 23° were obtained. Yet the results show that on these occasions there were no corresponding variations in the values of α , β , and δ . In fact throughout the whole series of observations and over the entire range of wavelengths the values of α and δ do not depart from zero by more than 1.3° , a value which is inappreciably greater than the limit of accuracy of the apparatus for the individual readings. It was frequently noticed during the observations on the frame coil apparatus, that the minimum obtained with the coil vertical was blurred, a common occurrence at night-time on wireless direction-finders. On all occasions, however, the minimum with coil in the horizontal position was sharp and well-defined, thus indicating that the magnetic field was of elliptical form in a horizontal plane only.

Again referring to Table III, many of the stations are sufficiently distant for the phenomena of long-distance transmission to enter, and according to the Heaviside-layer theory most of the energy would be coming downwards from the layer. Yet in no case do the values of β differ by an appreciable amount from the theoretical values of β_0 as recorded in the last column of the table, these values of β_0 having been calculated from the conductivity of the ground at Slough as found experimentally. These experiments are thus seen to support the conclusions drawn from the theoretical considerations in Section 4, and cannot, therefore, be considered as evidence for or against the existence of down-coming waves, as required by the Heaviside-layer theory.

7 Summary

This paper describes the commencement of a theoretical and experimental investigation into the determination of the directions of forces in electromagnetic waves, particularly with a view to elucidating many problems connected with the propagation of wireless waves over the earth's surface. So far as it has gone the investigation has drawn attention to the fact that the success of experiments to detect down-coming waves by directional measurements depends to a large extent upon the conductivity of the ground on which the experiments are carried out, for the boundary conditions imposed by this conductivity are such that the resultant fields at the surface tend to have the same direction in space whatever the polarisation and inclination of the component waves. In the case of a perfectly conducting earth, for example, the

electric force will always be vertical and the magnetic force horizontal at the earth's surface

It is concluded from the measurements made that the ground at Slough has an effective conductivity of about 10^8 (in absolute electrostatic units), and using this value to determine the boundary conditions it is found that on commercial wave-lengths the resultant fields of down-coming waves, incident at any likely angle (*i.e.*, greater than 45 deg to the vertical), will not be inclined sufficiently at the surface to distinguish them from horizontally propagated waves

In a search for a site for low conductivity on which experiments might be carried out with more success, an extension of the measurements was made to various parts of Southern England, which showed that all typical soils possessed conductivities of the same order as at Slough, varying between the limits of 0.6×10^8 and 4.7×10^8 . Only in the extreme cases of very rocky and broken surfaces was a conductivity as low as 0.14×10^8 experienced, and in these cases the very limited extent of suitable ground rendered the site impracticable for its required purpose. It is therefore concluded that in England, at any rate, there is no more favourable site than Slough, as regards the earth's conductivity, at which to continue the general investigation.

Finally, a summary is given of the results of the measurements at Slough of the directions of the electric and magnetic fields in arriving waves, over a period of seven months, by day and night, and over various distances, these results being in support of the above conclusions as to the impossibility of detecting inclined fields at Slough, even during the occurrence of directional errors and long-distance reception at night.

The best methods of continuing the investigation in the light of these conclusions are mentioned in Section 4. It appears that in order to obtain positive results with this directional method of attacking the propagation problem, it will be necessary to either—

- (1) Improve the accuracy of the apparatus and then repeat the experiments on the same site, or
- (2) Repeat the experiments with the existing apparatus, but on ground of lower conductivity, or
- (3) Repeat the experiments on the same site and with the same apparatus, but on a shorter wave-length

All these are possible lines of advance though all have their difficulties, and on the whole a combination of them is probably the best course to take.

It appears that in order to find a site of sufficiently low conductivity for the

purpose, it would be necessary to go to some part of the world which is much drier than England. By choosing some locality with a very limited rainfall it should be possible to find a site where the surface water is sufficiently low down not to affect the electromagnetic fields at the surface. On such a site it should be possible to obtain conclusive results with apparatus of the existing design.

This work was carried out for the Radio Research Board under the Department of Scientific and Industrial Research, and we are indebted to the Committee on Directional Wireless for their helpful criticism. The authors also wish to acknowledge the assistance rendered by Mr M G Bennet, M Sc, in the early part of the experiments.

REFERENCES

- (1) T L Eckersley, "The Effect of the Heavieside Layer on the Apparent Direction of Electromagnetic Waves" 'Radio Review,' vol II, pp 60-65, and 231-248 (1921).
 - (2) L. W Austin, "The Wave Front Angle in Radio Telegraphy," 'Journ Washington Acad Science,' vol. 40, pp 101-106 (1921)
 - (3) J Erskine-Murray and J Robinson, "An Improved Method for Determining the Direction of Propagation of Electromagnetic Waves" 'British Patent 176,' 127/1921
 - (4) E. Bellini, "Frame Aerials and Errors in Bearings," 'Electrician,' vol 89 pp 150-1 (1922)
 - (5) H B Jackson, "Directional Effects with Frame Aerials," 'Wireless World and Radio Review,' vol 9, pp 789-800 (1922)
 - (6) J A Fleming, 'Principles of Electric Wave Telegraphy,' 4th edition, p 623 (1919)
 - (7) Brylinski, 'Bull Soc Int Elect,' vol 6, pp 255-300 (1906)
 - (8) H Löwy, 'Ann der Phys,' vol 36, pp 125-133 (1911)
 - (9) H Schmidt, 'Jahr d Drahtl Tu T,' vol 4, pp 636-8 (1911)
 - (10) K. Uller, *ibid*, vol 4, pp. 638-640 (1911)
 - (11) J Zenneck, 'Wireless Telegraphy' (English Translation), pp 260-2 (1915).
 - (12) R H Barfield, "Some Experiments on the Screening of Radio Receiving Apparatus," 'Journ I.E.E,' vol 62, pp 249-262 (1924).
-

Regularities in the Secondary Spectrum of Hydrogen.

By O W RICHARDSON, Yarrow Research Professor of the Royal Society, and
T TANAKA, Professor in the College of Nigata, Japan

(Received January 24, 1925)

§ 1 This paper deals with the continuation of our endeavour to arrange the lines of this spectrum in series by starting from a study of the lines which are selectively changed in intensity in electron discharges in hydrogen at a low pressure as compared with discharges in a Geissler tube of the type which is most usual in spectroscopic observations. The previous work has been described in two papers* which we shall assume to be available in dealing with what follows.

§ 2 *A Second P, Q, R Combination*—We commence by considering the following lines which can be arranged as P, Q, and R series with the enumeration shown.

Table I—Series No 202 P (*m*)

<i>m</i>	Properties							Wave No	Int	1st Diff	2nd Diff
	(1)	(2)	(3)	(4)	(5)	(6)	(7)				δ δ Δ
2			—	U				20615 62	E2 (6)		
3					Z			20284 02	(10)	331 60	23 49 — 0 14
4								19928 93	(3)	355 09	23 77 + 0 14
5								19550 07	(9)	378 86	
										mean Δ =	23 63

Series No 110 Q (*m*)

1	++						h	21039 75I	II	III (1)	23 62	
2		+						21016 13		(1)	49 26	25 64 + 0 96
3	+							20966 87I	II	III (1)	73 37	24 11 — 0 50
4	++							20803 50I		(1)	97 73	24 36 — 0 34
5	++			+				20795 77I _m	II	III (2)		
											Δ =	24 70

* "The Striking and Breaking Potentials for Electron Discharges in Hydrogen," 'Roy Soc Proc.,' A, vol 106, p 640 (1924), and "On a P, Q, and R Combination in the Many-lined Spectrum of Hydrogen," *ibid*, p 663 (1924)

Table I—continued

<i>m</i>	Properties	Wave No	Int	1st Diff	2nd Diff
Series No 101 R (<i>m</i>)					
1	+	21440 41E3	(5)	257 82	
2	++	21698 23I II _m III	(3)	232 70	25 12 + 1 16
3	+	21930 93I† II _m III	(2)	208 98	23 72 - 0 24
4	+	22139 91I II <i>D</i>	(1)	185 95	23 03 - 0 93
5	+	22325 86	(<i>q</i>)		
				Δ -	23 96

I, II, III Denote weakened in 1st, 2nd and 3rd type discharges respectively

m Denotes much weakened.

† Denotes unresolved doublets (M and B)

E2 and E3 Denote enhanced in 2nd and 3rd type discharges respectively

D Denotes not weakened, possibly enhanced, in 3rd type

The test of the combination principle on these lines is

$$P(2) + R(1) = Q(2) + Q(1) + 0.15$$

$$P(3) + R(2) = Q(3) + Q(2) - 0.75$$

$$P(4) + R(3) = Q(4) + Q(3) - 0.51$$

$$P(5) + R(4) = Q(5) + Q(4) + 0.71$$

The agreement in the second and fourth combinations is not as good as it should be if the lines were straightforward. The ambiguity here may well be almost entirely due to the two lines P(3) and Q(5). The intensities of each of these lines is higher than it should be in comparison with the other lines of the relevant series. The apparent width of P(3) on Prof. Merton's plate is 3.58 and that of Q(5) 2.29 in wave-numbers, and it seems that these lines might conceal fainter constituents. The lines with intensity (*q*) are not given in Merton and Barratt's tables. These are faint lines which we have observed on Prof. Merton's plate and which have been measured by one of us (T. T.). Their intensities are classified in descending magnitude as (1), (0), (*p*), (*q*), (*r*) — (1) and (0), having, so far as possible, the same meaning as in Merton and Barratt's tables. It is just possible, although unlikely, that 19550.07 (*q*) = P(5)* is not a real line, as there is a strong line 19551.91 (5) very close to it, which makes the plate a little difficult to interpret just at that position. Most of the error

* On account of lack of resolution it is almost impossible to estimate the intensity of this line, which might be appreciably higher than the value stated

in the third combination may be due to R (3), which Merton and Barratt note as an unresolved doublet.

By suitable combinations of

$$P(m) = v_0 + F(m-1) - f(m), \quad m-1 \rightarrow m. \quad (1)$$

$$Q(m) = v_0 + F(m) - f(m), \quad m \rightarrow m. \quad (2)$$

$$R(m) = v_0 + F(m+1) - f(m), \quad m+1 \rightarrow m. \quad (3)$$

we deduce the successive differences in the initial and final term numbers $F(m)$ and $f(m)$ given in the following table —

Table II

$F(m+1) - F(m)$	$R(m) - Q(m)$	$Q(m+1) - P(m+1)$	Mean	2nd Diff
$F(2) - F(1)$	400 66	400 51	400 58 ₅	281 89
$F(3) - F(2)$	682 10	682 85	682 47 ₅	281 84
$F(4) - F(3)$	964 06	964 57	964 31 ₅	281 74
$F(5) - F(4)$	1246 41	1245 70	1246 05 ₅	284 04
$F(6) - F(5)$	1530 09			

$f(m+1) - f(m)$	$R(m) - Q(m+1)$	$Q(m) - P(m+1)$	Mean	2nd Diff
$f(2) - f(1)$	424 28	424 13	424 20 ₅	307 53
$f(3) - f(2)$	731 36	732 11	731 73 ₅	306 95
$f(4) - f(3)$	1037 43	1037 94	1037 68 ₅	306 10
$f(5) - f(4)$	1344 14	1343 43	1343 78 ₅	

The values of $F(m)$ are obviously characterised by very nearly constant second differences. Most, if not all, of the deviation in the fourth value in the fifth column can be accounted for if we suppose there is an error in $Q(5)$ such as would account for the error in the fourth test of the combination principle. We accordingly assume that the initial values of the F 's are represented by—

$$F(m) = B(m - P)^2 \quad (4)$$

B is half the constant second difference, and its mean (disregarding the fourth discrepant value) is 140 9116. Combining this value of B with the value 400 58₅ of $F(2) - F(1)$, which is the most accurate first difference, we find $P = +0.078575$. From these we re-calculate the following table of values of the F 's and their differences:—

Table III

m	$F(m)$ calculated	$F(m)$ computed	$F(m+1) - F(m)$ calculated	$F(m+1) - F(m)$ found
0	0 87			
1	119 64	119 64	400 58 ₆	400 58 ₆
2	520 22 ₅	520 22 ₅	682 41	682 47 ₅
3	1202 63 ₅	1202 70	964 23	964 31 ₅
4	2166 86 ₅	2167 01 ₅	1246 06 ₅	1246 06 ₅
5	3412 92	3413 07	1527 88	1530 09
6	4940 80	4943 16		

The agreement is satisfactory except in the term involving $F(6)$, as was to be expected from Table II

As regards the f 's the best procedure is not so clearly indicated. It seems likely that the second differences really diminish with increasing m , but it is not certain, owing to the small number of terms and the large errors in the tests of the combination principle, so that we shall assume, provisionally at any rate, that we can treat the second differences here also as in reality constant. Taking the mean, this gives $b = 153 \cdot 263$, whence from $f(2) - f(1) = 424 \cdot 20_6$, $\rho = +0 \cdot 11609$. These numbers give the following table of values —

Table IV

m	$f(m)$ calculated	$f(m)$ computed	$f(m+1) - f(m)$ calculated	$f(m+1) - f(m)$ found
0	2 11			
1	119 74 ₅	119 74 ₅	424 20 ₆	424 20 ₆
2	543 95	543 95	730 73	731 73 ₅
3	1274 68	1275 68 ₅	1037 26	1037 68 ₅
4	2311 94	2313 37	1343 78 ₅	1343 78 ₅
5	3655 72 ₅	3657 15 ₅		

The errors in $f(3) - f(2)$ lie beyond what is permitted by the observational data, so that the results are not adequately represented by—

$$f(m) = b(m - \rho)^2. \quad (5)$$

The disagreement could be got rid of by using

$$f(m) = b(\sqrt{m^2 - \sigma^2} - \rho)^2, \quad (6)$$

but this introduces what seem at this stage to be other difficulties, and as the same result could be obtained by almost any formula which introduced another disposable constant, we do not propose to press this point. The fact is, the

material offered by this combination is inadequate to form a satisfactory judgment on this question

As the formulæ used are not very satisfactory in the case of the final states, we shall only rely on them to determine the value of the two terms $F(1)$ and $f(1)$, the higher terms being obtained from these in combination with the successive values of $F(m+1) - F(m)$ and $f(m+1) - f(m)$ got from the line measurements. In this way we obtain the "computed" values given in the third columns of Tables III and IV. From these values by means of the equations—

$$\begin{aligned} \nu_0 &= P(m) - F(m-1) + f(m) = Q(m) - F(m) + f(m) \\ &= R(m) - F(m+1) + f(m) \end{aligned} \quad (7)$$

we can deduce 14 values of ν_0 . These have extreme values of 21039.18 and 21040.21, with a mean value of 21039.82, to which most of them are very close. On the interpretation taken, the value of ν_0 is almost coincident with $Q(1)$ ($= 21039.75$) for this combination.

From the value of B we find for the moment of inertia of the emitting molecule in the initial state $J_1 = 1.9614 \times 10^{-41}$ gm. cm², and for the moment of inertia in the final state the value of b gives $J_2 = 1.8028 \times 10^{-41}$ gm. cm². These values are similar to those which have been deduced from Fulcher's bands. Allen,* for example, with an assumed enumeration which seems not improbable, finds that all the seven series of Fulcher's first band lead to almost identical values of the constants Ca and Ce respectively, the corresponding moments of inertia being $J_1 = 1.761 \times 10^{-41}$ and $J_2 = 1.827 \times 10^{-41}$ gm. cm². It seems reasonable to suppose that the present series arise by transitions of the same molecule as in Fulcher's bands, presumably H_2 , but between different excited states.

The distribution of intensity among the different lines in the R series is in agreement with these low values of the moments of inertia and is, in fact, similar to that found in Fulcher's bands, the strongest line being at one end of the series, and the strength falling away gradually towards the other end. The same would be true of the lines of the P series, except for the line $P(3)$, which is a wide line of abnormally high intensity which probably covers up the real line belonging to the present series. This assumption has been made already in order to account for the error in the second test of the combination principle. The intensities in the Q series appear to be abnormal generally, but they are all weak lines, and their intensities are clearly very susceptible to changes in the physical conditions. $Q(5)$ appears definitely too strong. This line has considerable apparent width, and it is probably responsible for the error in

* 'Roy. Soc. Proc.,' A, vol. 106, p. 77 (1924)

the fourth test of the combination principle and in the value of $F(6)$ in Tables II and III. This line also deviates from all the other Q lines in being enhanced by helium. The intensities of the lines of 110 $Q(m)$ show a very remarkable variability on Prof Merton's two plates. On one plate we estimate their intensities as $Q(1) = (2-)$, $Q(2) = (2-)$, $Q(3) = (1)$, $Q(4) = (1)$ and $Q(5) = (2+)$, and, on the other plate, as $Q(1) = (0)$, $Q(2) = (2)$, $Q(3) = (1)$, $Q(4) = (1)$ and $Q(5) = (1-)$. On this plate their intensity distribution is evidently similar to that in the first type discharge.

The line $Q(2)$ is a low pressure line, whereas all the other four Q lines are weakened in the 1st type discharge and are high pressure lines. It is interesting to observe that there is a similar abnormality in the R series. All except $R(1)$ are enhanced by helium, and of these the two which have been tested for it show the Zeeman effect. $R(2)$, $R(3)$ and $R(4)$ are weakened in the 1st and 2nd type discharges, and $R(2)$ and $R(4)$ are high pressure lines. On the other hand, $R(1)$ is a low pressure line and definitely does not show the Zeeman effect. Thus, both $Q(2)$ and $R(1)$ appear to involve a common state to which low pressure is favourable. They both involve the same initial state $F(2)$. $P(3)$ also possesses the initial state $F(2)$, and should therefore show a similar abnormality. We have already seen reasons for believing that the real $P(3)$ is covered up by a much stronger line, so that it is not surprising that this further abnormality is not apparent.

We have looked for lines which might involve the zero quantum states $F(0)$ and $f(0)$. These are $P(1)$, $Q(0)$ and $R(0)$. Calculating $P(1)$ from $P(1) = \nu_0 + F(0) - f(1)$ we find $P(1)$ calculated = 20920.95. There is a faint line, intensity (p), at 20917.92 = $P(1)$ calc. - 3.03. $Q(0)$ calculated = $\nu_0 - F(0) + f(0) = 21041.06$. There is a faint line, intensity (p), at 21044.08 = $Q(0)$ calc. - 3.01. $R(0)$ calculated = $\nu_0 + F(1) - f(0) = 21157.35$. Merton and Barratt give a line 21158.96 (1), \cdot , $+$, \cdot , \cdot , \cdot , \cdot . This is equal to $Q(0)$ calculated + 1.61. It is curious that the first two perturbations are equal to twice the second. If these lines were assigned to $P(1)$, $Q(0)$ and $R(0)$, they would not satisfy the combination principle $P(1) + R(0) = Q(1) + Q(0)$, so that it is probable that the relation between these perturbations is a coincidence.

If we are dealing here with genuine bands which really satisfy the combination principle, the foregoing results have a quite general importance, because they show that the half quantum or other simple fractional numbers which enter into the formulæ for many band spectra have no very fundamental significance. In the present case the constants P and p do not have simple fractional values,

but are quite complicated proper fractions. It may be that these constants have a tendency to approximate round the values 0 , $\frac{1}{2}$, $\frac{1}{3}$, $\frac{2}{3}$, or 1 , as seems indicated by the behaviour of many band spectra, but the present series cannot be expressed by equations such as (5) or (6) if we are limited to such simple fractional values of the constants.

There are two lines not yet mentioned which may prove to be associated with this group, viz. 20853.80 (3) and 20526.72 (7). Their wave numbers are intermediate between those of P(1), if it existed, and P(2), and of P(2) and P(3) respectively. Together with the line 21158.96 (1), which we have already referred to as being close to the position for R(0), they practically coincide with the continuation of the R series into negative values of m . In conjunction with R(1) they can also be arranged as the following series —

Table V—No 102

m	Properties							Wave No	1st Diff	2nd Diff
	(1)	(2)	(3)	(4)	(5)	(6)	(7)			
		+			0			21440 41 (5)		$\delta \quad \delta - \Delta$
		+						21158 96 (1)	281 45	
		+						20853 80 (3)	305 16	$23 \ 71 + 0 \ 90$
					0 or			20526 72 (7)	327 08	$21 \ 92 - 0 \ 89$
					—					$\Delta \quad 22 \ 81$

If this were a genuine series with 21440.41 as the leading line, it would mean that this line which we have assigned to R(1) would have to be taken out of the foregoing combination. This would make it much less convincing. If we take 21440.41 out of both 101 and 102, we can treat the remaining lines as R' and P' series respectively, with 21440.41 (5) as the leading line of a new Q series. This series, which we may denote by Q'_1 , would have as its second line ($m=2$) 21417.40 (1), $+$, $+$, \dots , and as its third line ($m=3$) 21370.99 intensity (p). These have the successive first differences 23.01 and 46.41 and the second difference 23.40 . These give one combination

$$P'(2) + R'(1) = Q'_1(2) + Q'_1(1) - 0.62,$$

but the next combination fails. On the whole, the association we have assumed above seems much more probable than this. If we take 20853.80 (3) and 20526.72 (7) to be two lines constituting a fragment of a P' series associated with the series we have treated as P, Q and R, there is a faint line 21456.60

which in combination with $20526.72(g)$ yields $20526.72 + 21456.60 = P'(3) + R'(2) = Q(3) + Q(2) + 0.32$. An argument might be made here that the combinations are between P or R' and P' and R, as Curtis finds in the helium bands, but the matter is too uncertain to warrant further discussion without better evidence.

§ 3 *Series which may be connected with those preceding*—The following sets of lines can be arranged as Q and R series with a common ν_0 , but there does not appear to be an associated P series.

Table VI—Series No 59 Q (m)

m	Properties							Wave No		1st Diff	2nd Diff
	(1)	(2)	(3)	(4)	(5)	(6)	(7)	I	II	III	Δ
1								I	II	III	20540 59 (2)
2								x*			20503 23 (4)
3								x*			20439 11 (2)
4											20351 31 (0)
5								†			20239 07 (2)
											mean $\Delta = 24.06$

Series No 56 R (m)

1											20809 92 (0)
2											21002 27 (0)
3								x*			21167 02 (5)
4								x*			21306 74 (2)
5											21420 84 (1)
											$\Delta = 25.33$

x* Denotes weakened in 2nd and 3rd type, but not in 1st type discharge

† Denotes unresolved doublet (M and B)

I, II, III Denote weakened in 1st, 2nd and 3rd type

If we take out the lines for which $m = 1$, which may not belong to the series, the second differences for the others are very close to those in the preceding section. The relation between these and the preceding Q and R series may be shown in another way, by subtracting corresponding terms of corresponding series, when we obtain a set of numbers with almost constant differences.

This is shown by the following table, if we again except the case $m = 1$, to be particularly true of the Q series

Table VII

$m \rightarrow$	1	2	3	4	5
$\Delta Q(m) =$ $110Q(m) - 59Q(m)$	499 16	512 90	527 76	542 19	556 70
$\Delta Q(m+1) - \Delta Q(m)$	13 74	14 86	14 43	14 51	
$\Delta Q(m+2) - 2\Delta Q(m+1) + \Delta Q(m)$	+1 12	- 0 43	0 08		
$\Delta R(m) =$ $101R(m) - 56R(m)$	630 49	695 96	763 91	833 17	905 02
$\Delta R(m+1) - \Delta R(m)$	65 47	67 95	69 26	71 85	
$\Delta R(m+2) - 2\Delta R(m+1) + \Delta R(m)$	+2 48	+1 31	+1 59		

In the case of $\Delta R(m)$, the first differences are not constant but increase if we take out the exceptional case $m = 1$, in a linear way with m

If 59 and 56 are associated Q and R series, and if, as before we assume $F(m) = B(m - P)^2$ and $f(m) = b(m - \rho)^2$ we have

$$R(m) - Q(m) = F(m+1) - F(m) = B(2\overline{m - P} + 1) \quad (8)$$

$$R(m-1) - Q(m) = f(m) - f(m-1) = b(2\overline{m - \rho} - 1) \quad (9)$$

The values of these quantities are shown in the following table

Table VIII

$${}_m\Delta_m = R(m) - Q(m) = F(m+1) - F(m) = B(2\overline{m - P} + 1)$$

$m \rightarrow$	1	2	3	4	5
${}_m\Delta_m$	269 33	499 04	727 91	955 43	1181 77
${}_{m+1}\Delta_{m+1} - {}_m\Delta_m$	229 71	228 87	227 52	226 34	
Next difference	- 0 84	- 1 35	- 1 18		

$${}_{m-1}\Delta_m = R(m-1) - Q(m) = f(m) - f(m-1) = b(2\overline{m - \rho} - 1)$$

$m \rightarrow$	1	2	3	4	5
${}_{m-1}\Delta_m$		306 69	563 16	815 71	1067 67
${}_m\Delta_{m+1} - {}_{m-1}\Delta_m$		256 47	252 55	251 96	
Next difference		- 3 92	- 0 59		

If equations (8) and (9) were exact, the differences of successive Δ s should be constant. In the case of ${}_m\Delta_m$ this difference shows a small linear progression which might be given a number of interpretations. The value of ${}_2\Delta_3 - {}_1\Delta_2$ is irregular. This is due to the irregularity of R (1) which is here combined with R (2), Q (3) and Q (2). The value of ${}_2\Delta_2 - {}_1\Delta_1$ which involves the difference of the two irregular lines Q (1) and R (1) in combination with Q (2) and R (2) shows no irregularity. This suggests that Q (1) and R (1) may be abnormal lines affected by an equal displacement and is the only real justification for keeping these lines in the series.

From the values in Table VIII we deduce $\bar{B} = 114.06$, $\bar{b} = 126.13$, $P = 0.30724$ and $\rho = 0.26734$. From these we can calculate one value of $F(m)$ and $f(m)$ respectively, and from the values of the differences of these functions in Table VIII we can then proceed to calculate a table of the functions themselves. From these values we can calculate ν_0 . Using $\nu_0 = Q(2) + f(2) - F(2)$ we obtain $\nu_0 = 20555.79$ and from $\nu_0 = R(2) + f(2) - F(3)$ we obtain by two different methods of calculating $\nu_0 = 20555.75$ and $\nu_0 = 20556.19$ respectively.

The values of B and b above correspond with $B = 140.9$ and $b = 153.2$ from the combination considered in the preceding section and with $B \approx 154$ and $b \approx 148$ from the first Fulcher bands. If they are a real series their source must therefore have an appreciably higher moment of inertia than that of the source of the Fulcher bands. The maximum intensity of the lines which is at $m = 2$ for the Q series and $m = 3$ for the R series is not unreasonable for such a value of the moment of inertia.

§ 4 *Possible series having similar constants to Fulcher's bands*—We shall next deal with some possible series which have similar constants to Fulcher's bands. In the cases now under consideration we have only one branch at our disposal, so that it is not possible fully to determine the constants. The constant second differences determine the values of $Ca - Ce^*$, but the values of Ca or Ce individually and of ν_0 depend on the assigned enumeration and on whether the series are whole or fractional quantum number series. The formulæ given below are merely illustrative and intended to give some idea of the magnitudes of Ca , Ce and ν_0 . In some cases they happen to have been calculated as half quantum series, but there is no sufficient justification for assuming that they are such, the assumed enumeration, on the other hand, has been taken as on the whole the most probable one. The following three sets of five lines have fairly constant second differences, and, whilst the properties

* Cf. H. S. Allen, *loc. cit.*

and intensity sequences are not perfect, there is some evidence of coherence in each set —

Table IX—Series No. 3 P.

<i>m</i>	Properties.							Wave No	1st Diff	2nd Diff
	(1)	(2)	(3)	(4)	(5)	(6)	(7)			$\delta \quad \delta - \Delta$
1	+		+	+	Z			16774 72 (8)		
2	++							I IID 16476 14 (5)	298 58	14 86 + 0 02
3	++							Im II _m III _m 16192 42 (6)	293 72	14 74 - 0 10
4								15923 44 (0)	268 98	14 93 + 0 09
5	++		-					I 15669 39 (4)	254 05	
										$\Delta 14 \ 84$

Series No 10 P.

1								21841 16 (0)		
2		++			O			I II III 21427 59 (3)	413 57	47 15 + 0 03
3	+							I II III 20966 87 (1)	460 72	46 88 - 0 24
4								I II III 20459 27 (1)	507 60	47 33 + 0 21
5								19904 34 (0)	554 93	
										$\Delta 47 \ 12$

Series No. 11 R.

1				O				I II 19584 89 (3)		
2		+						19980 86 (4)	395 97	40 42
3	++			+				I III 20417 25 (2)	436 39	39 86
4	++							I E 20893 50 (1)	476 25	41 00
5	+							21410 75 (1)	517 25	39 16
6	++			++	O			Im II _m III _m 21967 16 (3)	556 41	

I, II, III Denote weakened, Im, II_m, III_m denote much weakened in 1st, 2nd and 3rd type discharges respectively

D. Denotes not weakened in 3rd type discharge

E. This line is the same as 110Q (4) above. The evidence as to duplicity is not clear; on one plate it is stronger, on the other weaker, than 4786 04 (2). It is rather wide, so that a line of intensity equal to or less than *p* could be concealed by it, if of ordinary sharpness and having *v* in the region 20893 23 — 20894 01.

As regards 11 R the second differences are very bad, but this may be due entirely to 20893 50, which has already been assigned to No. 110 Q (4) and

is unlikely to be No 11 P(4) as well. If 20893 50 conceals a line about 20893 90 the second differences become quite reasonable. It will be noticed that the effect of the relative weakening is to make these lines have a distribution of intensity in the 1st type discharge which makes them look more like series than in the ordinary Geissler tube discharge.

No 3 P can be represented as

$$P'(m) = 17086.27 + 1.853 - (Ca + Ce)m + 7.410m^2, \quad m = 1, 2, 3, 4, 5$$

where $Ca = 164.11$, $Ce = 156.70$, $Ca - Ce = 7.41$ and $\nu_0 = 17086.27$

Similarly

$$\text{No 10 P as } P'(m) = 22213.56 - 5.89 - 342.92m - 23.56m^2, \quad m = 1, 2, 3, 4, 5,$$

where $Ca = 159.68$, $Ce = 183.24$, $Ca - Ce = -23.56$ and $\nu_0 = 22213.56$

and No 11 R as

$$R'(m) = 19224.30 + 5.055 + 335.31m + 20.22m^2, \quad m = 1, 2, 3, 4, 5, 6,$$

where $Ca = 177.76$, $Ce = 157.54$, $Ca - Ce = 20.22$ and $\nu_0 = 19224.30$

As we have pointed out above, there are other alternatives. The values of Ca and Ce got by Allen from Fulcher's bands range between 158 and 142 for the first band, and 221 and 170 for the second.

If the four following lines are a series it has a ν_0 close to the values of ν_0 for Fulcher's second band, but the values of Ca and Ce are similar to those in Fulcher's first band.

Table X—Series No 27 P(m).

m	Properties							Wave No		1st Diff	2nd Diff
	(1)	(2)	(3)	(4)	(5)	(6)	(7)	I	II	D	$\delta \quad \delta - \Delta$
1	++			++				I	II	D	19297.46 (4)
2	++			++				I	II	D	19018.39 (5)
3	+			+							18757.48 (1)
4			++								18513.72 (0)

I Denotes weakened in 1st type discharge
 II Weakened in 2nd type discharge
 D. Not weakened in 3rd type

These lines can be represented by

$$P'(m) = \nu_0 + Cd/4 - (Ca + Ce)m + Cd m^2, \quad m = 1, 2, 3, 4,$$

where

$$\nu_0 = 19592.12, \quad Cd = Ca - Ce = 8.91, \quad Ca = 157.36 \text{ and } Ce = 148.45$$

The two second differences are far from equal, but the general appearance of the properties suggests that these lines are related

The following set of lines is very remarkable

Table XI—Series No. 20 Q (m)

m	Properties							Wave No	1st Diff	2nd Diff
	(1)	(2)	(3)	(4)	(5)	(5)	(b)			δ $\delta - \Delta$
1								23933 60 (4)	10 95	
2							I II III	23944 64 (2)	22 04	11 09 - 1 01
3							I II III	23966 68 (3)	35 20	13 16 + 1 06
4							I II III	24001 88 (1)	48 89	13 09 + 1 59
5				O			I II III	24060 77 (2)	60 78	11 99 - 1 09
6							S I III	24111 55 (0)	71 37	10 59 - 1 51
7							S I	24182 92 (0)		
										$\Delta 12 10$

I Denotes weakened in 1st type discharge
 II Weakened in 2nd type discharge
 III Weakened in 3rd type discharge

The second differences vary between the wide limits of 10.59 and 13.69, but the variation is entirely systematic, as may be seen from a plot of δ against m (fig 1). All these lines except 23933.69 ($m = 1$) are weakened in the first

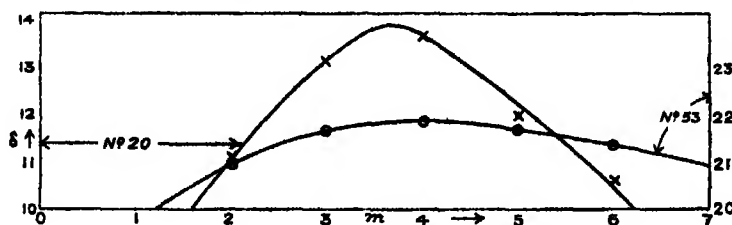


FIG 1.

type discharge, and the four stronger lines, $m = 2, 3, 4, 5$, are weakened in the second and third type discharges also. In fact, they form consecutive members of our list of lines weakened in the respective discharges. Otherwise, these lines have no particular character, the table of properties given by Merton and Barratt being practically empty. We do not consider the fact that the Stark effect happens to have been observed for two of these lines as a criterion of importance in this connection. The alternation in intensity of successive

lines similar to that in 28Q and in some of Fulcher's bands may also be noted

The following five lines can be arranged as a P series with the same ν_0 as No 20 Q (m) —

Table XII—Series No 26 P (m)

m	Properties							Wave No	1st Diff	2nd Diff
	(1)	(2)	(3)	(4)	(5)	(6)	(7)			$\delta \quad \delta - \Delta$
1		+						23648 77 (0)		
2		++						23202 88 (0)	445 89	11 06 + 0 17
3				++	0		S I	22768 05 (2)	434 83	10 70 - 0 27
4	+			++	Z		S I II m III m	22343 92 (2)	424 13	11 14 + 0 00
5				+	Z		I II m	21930 93 (2)	412 99	
										$\Delta 10 97$

I Denotes weakened in 1st type discharge

II m , III m Much weakened in 2nd and 3rd type

If (20) and (26) are connected Q and P series they give the following table

Table XIII

m	F (m)	F ($m - 1$)	Q (m) - P (m) Diff	$f (m + 1) - f (m)$	Q (m) - P ($m + 1$) Diff
1	F (1) - F (0)		284 92	$f (2) - f (1)$	730 81
2	F (2) - F (1)		741 76	$f (3) - f (2)$	1176 59
3	F (3) - F (2)		1108 03	$f (4) - f (3)$	1622 76
4	F (4) - F (3)		1657 90	$f (5) - f (4)$	2070 95
5	F (5) - F (4)		2110 84		

These would lead to, approximately, $B = 228.4$, $b = 223$, $\nu_0 = 23930$. It is far from certain that No 26 P (m) is connected with No 20 Q (m) in the way suggested. It might be an R series with ν_0 in the neighbourhood of 21600, but if it is a series at all it must have values of $C\alpha$ and $C\epsilon$ similar to some of those in Fulcher's second band, with the difference $C\alpha - C\epsilon$ similar to those in Fulcher's first band

The following lines which, like 20 Q (m), have no properties, may be connected with the two last sets

Table XIV—Series No. 60 R (*m*)

<i>m</i>	Properties							Wave No	1st Diff	2nd Diff
	(1)	(2)	(3)	(4)	(5)	(6)	(7)			
1								20314 80 (0)		5 3 - Δ
2								20641 11 (2)	326 31	
3								20955 39 (2)	314 28	12 03
4								21259 14 (1)	303 75	10 53 - 0 04
5								21552 28 (0)	293 14	10 61 + 0 04
									Mean Δ = 10 57	

I Denotes weakened in 1st type, II in 2nd type, III in 3rd type discharge

? Denotes that the inclusion of this line is doubtful

If these lines are represented by $R(m) = v_0 + Ce(2m - 1) + Cdm^2$ with the above enumeration, which is problematical even if they are a series, the values of the constants are $Ca = 165.074$, $Ce = 170.359$, $Cd = -5.285$ and $v_0 = 20151.17$

The following lines are also distinguished by the absence of special properties —

Table XV—Series No. 53 P (*m*)

<i>m</i>	Properties							Wave No	1st Diff	2nd Diff
	(1)	(2)	(3)	(4)	(5)	(6)	(7)			
1	++		--					I II III D 20888 30 (2)		5 3 Δ
2								20470 07 (1)	418 23	30 94 - 0 52
3								20072 83 (3)	397 24	21 66 + 0 15
4								19697 25 (2)	375 59	21 86 + 0 35
5								19343 53 (2)	353 72	21 67 + 0 16
6								19011 48 (0)	332 05	21 39 - 0 12
7								18700 82 (0)	310 66	Δ - 21 31

D. This is the same line as No 41Q (4) below, but we are unable to observe any appearance of duplicity in it.

The variations in the second differences are entirely systematic, as can be seen by reference to the plot-points thus:—○, in fig. 1. With the numeration shown these lines are represented by $P(m) = v_0 - Ca(2m - 1) + Cd m^2$ with the values $Ca = 225.32$, $Ce = 214.56$, $Cd = 10.75$, and $v_0 = 21102.86$. The values of Ca and Ce are similar to those in Fulcher's second band.

§ 5 Various Sequences.

The following are either Q series with nothing to suggest their further affiliations, or are P or R series with constants involving higher moments of inertia than those belonging to Fulcher's bands.

 Table XVI—Series No 81 R (*m*)

<i>m</i>	Properties							Wave No	1st Diff	2nd Diff.
	(1)	(2)	(3)	(4)	(5)	(6)	(7)			$\delta \quad \delta - \Delta$
1	++		+					16297 37 (4)		
2	++		+					I II III 16517 97 (5)	220 60	6 54 + 0 23 _s
3	+		+					III 16745 11 (3)	227 14	6 34 + 0 03 _s
4	++		+					I II III 16978 59 (6)	233 48	6 45 + 0 14 _s
5			++					LD II 17218 52 (5)	239 93	5 35
6					0			17463 80 (g)	245 28	7 79
7			++	+				<i>zD</i> II 17716 87 (3)	253 07	5 36
8				0				17975-30 (0)	258 43	
									Mean $\Delta = 6 \ 30_s$	

I, II, III Denote weakened in 1st, 2nd or 3rd type discharge respectively
z, D Denote not weakened in 1st or 3rd type respectively

The last three second differences in Table XVI are very bad, but this is entirely due to the inclusion of the faint line 17463 80, intensity (*g*) (= - 2), which we found on Prof Merton's plate, but which is not given in Merton and Barratt's tables. We have re-examined this line and find that it is rather diffuse and shows signs of being double. Its apparent breadth on the plate is 0 45 Å u, whilst those of neighbouring lines are as follows — $\sqrt{17456 \cdot 15}$ (0), 0 34 Å.u. and $\sqrt{17446 \cdot 38}$ (0), 0 36 Å u. The remeasured value of the wave-number of the line, treated as single, is $\sqrt{17463 \cdot 86}$. If it is replaced by a fictitious line with the wave-number increased by 0 81 to 17464 61, the last three second differences receive the common value 6 17, which differs by less than 0 14 from the mean value of the whole six. It seems, therefore, that the two lines $m = 7, 8$ should be retained even though the measured wave-number assigned to $m = 6$ is doubtful. We have also re-examined No. 81 R (7) $\sqrt{17716 \cdot 87}$ (3). This line is either double, with constituents which are differentially affected by helium, or it is displaced in helium in a way which simulates an unresolved doublet with these hypothetical properties.

If these lines are represented by $R(m) = v_0 + C_e(2m - 1) + C_d m^2$, the

constants are $Ca = 108.818$, $Cc = 105.666$, $Cd = 3.153$ and $v_0 = 16188.55$. Both initial and final moments of inertia are much higher than those connected with any of Fulcher's bands and approach those given by the combination 1P, 28Q, 101R dealt with in our earlier paper

The sequence shown in Table XVII is remarkable for its length, if not for the constancy of its second differences. It seems likely, however, that it is a Q series which has run by accident over into an R series

Table XVII—Series No 83 Q and R

No.	Properties							Wave No	1st Diff	2nd Diff
	(1)	(2)	(3)	(4)	(5) Z	(6)	(7)			$\delta \quad \delta - \Delta$
1	++		++		Z			Im II III 16413 35 (7)		
2	++				Z			I II III 16469 90 (7)	50 55 = $1 \times 50 \ 55$	58 29
3	++				Z			I III 16584 74 (8)	114 84 = $2 \times 57 \ 42$	53 76 + 0 12
4	++		++					I 16753 34 (8)	168 60 = $3 \times 56 \ 20$	54 06 + 0 42
5	+		++	O				III' 16976 00 (3)	222 66 = $4 \times 55 \ 67$	53 87 + 0 23
6			++	++				III' 17252 53 (4)	276 53 = $5 \times 55 \ 31$	53 23 - 0 41
7							†	17582 29 (r)	329 76 = $6 \times 54 \ 96$	53 95 + 0 31
8			++			F		17966 00 (2)	383 71 = $7 \times 54 \ 82$	53 24 - 0 40
9								18402 95 (g)	430 95 = $8 \times 54 \ 62$	$\Delta 53 \ 64$
										52 76
10								18992 66 (5)	480 71	54 12
11	++			++			II	19436 49 (3)	543 63	53 54 - 1 10
12		++	-	+				20033 86 (1)	597 37	54 97 + 0 33
13	++			O			Im II	20686 20 (8)	652 34	54 49 - 0 15
14					Z			21303 03 (2)	706 83	53 10
15				++			I	22152 96 (1)	759 93	
16							III	22963 96 (0)	811 00	164 84 + $2 \times 0 \ 31$
17								23835 63 (p)	871 67	= $2 \times 54 \ 95$
										$\Delta 54 \ 64$

I Denotes weakened in 1st type II In 2nd type III. In 3rd type discharge.

m Denotes much weakened.

† Probably a doublet

III' This part of the spectrum seems weakened generally in 2nd type discharge.

The first nine lines belong to the Q series, with values of m corresponding to the numbers, and the lines numbered 10 to 17 can be regarded as an R series, with the probable enumeration 1 to 8. It is not suggested that the Fulcher line 17966 00 (2) is really 83 Q (8). It is too strong anyway, but it may conceal a very weak line, which is the most that is wanted here. The errors in the measurements of the weak lines 17582 29 (r) and 18402 95 (q) may be greater than for the lines measured by Merton and Barratt, so that the casual errors in the second differences from $m = 5$ to $m = 9$ are about what might be expected. The line 16413 35 (7) assigned to Q (1) may not belong here. The very large δ is suspicious, but not a certain ground for rejection. All the properties seem to fit in. The properties of the lines numbered 10 to 17 seem rather miscellaneous, but the intensities seem reasonable. The line 22152 96 (1) either does not belong or is badly displaced. If the formula $R(m) = \nu_0 + C_e(2m - 1) + Cd m^2$ is applied to these lines numbered downwards from 18892 66 (5), $m = 1$, the constants are $Ca = 258.26$, $C_e = 230.94$, $Cd = 27.32$ and $\nu_0 = 18634.40$. These are not very different from some of the values which may be assigned to Fulcher's second band, but they correspond to lower values

Table XVIII—Series No 52 P (m)

m	Properties							Wave No	1st Diff	2nd Diff
	(1)	(2)	(3)	(4)	(5)	(6)	(7)			$\delta \quad \delta - \Delta$
1								19346 63 (0)		
2								II 19171 45 (2)	175 18	
3			—					II 18961 84 (5)	209 61	34 43 + 0 17
4			—					II 18718 46 (1)	243 38	33 77 - 0 49
5			+					18440 80 (0)	277 66	34 28 + 0 02
6								d 18128 55 (q)	312 25	34 59 + 0 33
7								Missing		102 26 =
8								17400 57 (0)		$3 \times 34.09 - 3 \times 0.17$
9			+					16986 06 (1)	414 51	
10			+	++				16536 82 (3)	449 24	34 73 + 0 47
11								Missing.		Mean $\Delta = 34.26$
12			+					15536.22 (3)		

II. Denotes weakened in 2nd type discharge
d Denotes a diffuse line.

of the moment of inertia of the emitter than any which have hitherto been suggested in connection with this spectrum

The following sequence (see Table XVIII) consists of lines which, except for some slight sensitiveness in the condensed discharge, are devoid of special properties

If these are represented by $P(m) = v_0 - Ca(2m - 1) + Cd m^2$ with the assigned values of m the approximate values of the constants are $Ca = 61.90$, $Ce = 79.03$, $Cd = -17.13$ and $v_0 = 19425.66$. Except for the doubtful members with high quantum numbers, the distribution of intensity among the lines is not unreasonable for such low values of Ca and Ce *

The following sequences are rather speculative, but they may possibly be useful. —

Table XIX — Series No 41 Q (m)

m	Properties							Wave No	1st Diff	2nd Diff.
	(1)	(2)	(3)	(4)	(5)	(6)	(7)			$\delta \quad \delta - \Delta$
0	++			+				I II III 20417 25 (2)		
1			=					20450 73 (1)	33 48	56 38 + 0 48
2								I II III 20540 59 (2)	89 86	55 75 - 0 15
3	++			0				Im II 20686 20 (3)	145 61	56 49 + 0 59
4	++		-					I II III D 20888 30 (2)	202 10	55 80 - 0 10
5	+							21146 20 (0)	257 90	54 81 - 1 09
6								21458 91 (p)	312 71	56 15 + 0 25
7		++		+	0			21827 77 (5)	368 86	
										$\Delta 55 90$

I, II, III Denote weakened in 1st, 2nd and 3rd type discharges respectively.

Im Denotes much weakened in 1st type discharge

D This is the same line as No 53 P (1) above, but we are unable to observe any appearance of duplicity in it

The numbers in Table XIX are fairly near to the form $Q(m) = v_0 + Cd m^2$ with v_0 about 20389 and Cd 28.0 If the last two members are dropped, the variations in the second differences hardly exceed the probable errors of measurement

* [Note added February 23, 1925 — In a paper now being written by one of us (O. W. R.) it will be shown that No 52 P (m) is the sum of two series, a P and an R, and that there are a number of other new series connected with these.]

Table XX—Series No. 38 R (m).

m	Properties							Wave No	1st Diff	2nd Diff
1	(1)	(2)	(3)	(4) O	(5)	(6)	(7)	I	20173 01 (3)	8 8 - Δ
2								I II III	20530 59 (2)	357 58
3								I	20925 97 (3)	395 38
4		+							21359 62 (2)	38 27 + 0 45
5					O				21830 67 (1)	433 65
										471 05
										Δ37 82

I, II, III Denote weakened in 1st, 2nd and 3rd type discharges respectively

If this is assumed to be $R(m) = \nu_0 + (2m - 1)Ce + m^2 Cd$, the values of the constants are $Ca = 169.34$, $Ce = 150.43$, $Cd = 18.91$ and $\nu_0 = 20003.67$. The moments of inertia are thus similar to those in Fulcher's first band.

General Discussion

It is unlikely that all the sequences we have mentioned will prove to be genuine physical series, and, in fact, the greatest difficulty of this investigation arises from the fact that there is no absolute criterion as to the genuineness of a series. It follows that, until the whole spectrum has been classified into series, it is necessary to regard each suggested series as merely provisional in character and liable to extinction at any moment as further information about alternative arrangements develops. In the following table we have set out the constants* of the known arrangements of the lines in this spectrum, and in doing so we have arranged the data in three groups. The first group contains those series which, in our judgment, seem fairly certain, the second group those which are rather probable, whilst those in the third group are to be considered merely as possibilities. In forming these judgments, we have taken into account the number of lines in a sequence, the numerical coherence of the wave-numbers, the coherence of the properties, the distribution of intensity among the lines in a sequence and its reasonableness from the point of view of the resulting moments of inertia. The first column gives the series under consideration, the second the value of ν_0 , the third the second difference $\Delta_2 F$ of the initial term number $F(m)$ and the fourth the second difference $\Delta_2 f$ of the final term number $f(m)$. Where there is not enough information to deduce these quantities,

* The actual values are, in many cases, subject to re-adjustment due to uncertainty in the numeration adopted.

622 *Regularities in the Secondary Spectrum of Hydrogen*

they are replaced by the corresponding initial and final constants $Ca = h/8\pi^2 I_a$ and $Ce = h/8\pi^2 I_e$, I_a and I_e being the initial and final moments of inertia. The values of Ca and Ce are given in the fifth and sixth columns and the difference $Cd = Ca - Ce$ in the seventh. The eighth column contains the corresponding difference $\Delta_2 F - \Delta_2 f$ for the cases in which it has been determined. The values of Ca , Ce and the corresponding ν_0 are subject to the assumed enumeration which is that which has seemed to us the most likely.

The chief thing that emerges from the numbers in Table XXI is that the values of Ca (or $\Delta_2 F$) and Ce (or $\Delta_2 f$) are spread fairly well over the whole range between the extreme values $\Delta_2 F = 44.27$ of 1P28Q201R and $Ca = 258.26$ of 83R. This relative continuity rather tends to diminish the value of the suggestion made in our previous paper that 1P28Q201R might be due to something with a more massive molecule than H_2 , such as, perhaps, H_3 . If the values

Table XXI.—Group I

Series	ν_0	$\Delta_2 F$	$\Delta_2 f$	Ca	Ce	Cd	$\Delta_2 F - \Delta_2 f$
1st Fulcher Band	17125 to 17205			157	151	+ 6	
2nd Fulcher Band	19430 to 19485			220.6	213.5	+ 7.1	
Kruti's	17206.28					- 6.8052	
1 P 28 Q 201 R	17307.43	44.27	57.59				- 13.32
20 Q	23930					+ 6	
53 P	21102.86			225.32	214.56	+10.76	
81 R	16188.55			108.82	105.67	+ 3.15	
83 Q	16413					+26.8	
52 P	19425.65			61.89	79.02	-17.13	

Group II

202 P 110 Q 101 R	21039.82	140.91	153.26				- 12.35
59 Q 56 R	20556	114.06	126.13				- 12.07
3 P	17086.27			164.11	156.70	+ 7.41	
20 Q 26 P	23930	228.4	223.0				+ 5.4
83 R	18634.40			258.26	230.94	+27.32	
41 Q	20389.2					+28.05	

Group III

11 R'	19224			177.76	157.54	+20.22	
27 P'	19592			157.36	148.45	+ 8.91	
60 R	20151			165.07	170.36	- 5.29	
38 R	20003.67			169.34	150.43	+18.91	
*10 P'	22213			159.68	183.24	-23.56	
*4 R	16058.19			124.96	144.89	-19.93	
*113 P	22992.82			64.17	73.52	- 9.35	

* These seem relatively improbable. In fact the details of 4 R and 113 P have been taken out of the paper as not worth publishing at this stage.

are spread fairly well over the whole range, it would seem more likely that these low values also arise from excited forms of H_2 . This would have the corollary that the process of excitation, whatever its nature, may give rise to relatively enormous changes in the moment of inertia of the H_2 molecule. The largest existing gaps are between 177.76 (Ca for 11R') and 213.5 (Ce for Fulcher's second band), between 230.94 and 258.26 (Ce and Ca for 83R), and between 79.02 (Ce for 52P) and 105.67 (Ce for 81R) in diminishing order. At present there is a distinct predominance of values of Ca and Ce in the neighbourhood of those belonging to Fulcher's first and second band respectively. It is, of course, possible that these features will disappear as more bands become unravelled. Up to the present we have not noticed any regularity among the values of ν_0 , but the investigation is being continued in this and in other directions.

The Lattice Points of a Circle.

By G. H. HARDY, F.R.S.

(Received December 30, 1924.)

1. *Introduction*

1.1 This note is a sequel to two with the same title printed recently in the 'Proceedings,' the first by Landau and myself* and the second by Littlewood and Walfisz†. I use the notation of the first of these notes without renewed explanations‡.

Our primary object in the first of these notes was to give two methods for the proof of the identity

$$(1.11) \quad \bar{P}(x) = \sqrt{x} \sum_{\nu=1}^{\infty} \frac{\tau(\nu)}{\sqrt{\nu}} J_1(2\pi\sqrt{\nu x})$$

The note, however, contained the kernel of a third method, which was actually used only for a subsidiary purpose§. This method leads to a proof of (1.11)

* G. H. Hardy and E. Landau, 'Roy. Soc. Proc.' (A), vol. 105, pp. 244-258 (1923). I refer to this note as I.

† J. E. Littlewood and A. Walfisz, *ibid.*, vol. 106, pp. 478-489 (1924) (with an additional note by E. Landau). I refer to this note as II.

‡ Littlewood and Walfisz use $R(x)$ for our $A(x)$.

§ See I, §3.

in some ways simpler than either of those which we gave before, and is indeed in many ways peculiarly well adapted to all these problems connected with the circle. I apply it here to the proof not only of (1.11), but of a more precise formula, embodied in Theorem 3, which gives an upper bound for the remainder of the series after x_1 terms, valid over the whole range $x \equiv \frac{1}{2}$.*

The most interesting case of this formula is†

$$(1.12) \quad P(x) = \sqrt{x} \sum_{v=1}^{x_1} \frac{r(v)}{\sqrt{v}} J_1(2\pi\sqrt{vx}) + O\left(\frac{x^{1+\epsilon}}{\sqrt{x_1}}\right),$$

where $\frac{1}{2} \equiv x_1 \equiv x$ and ϵ is any positive number. This formula may be used, as I show shortly in § 4.3, to replace Lemmas 1–3 of the investigation of Littlewood and Walfisz. The kernel of their argument, embodied in Lemmas 4 and 5, would naturally remain unchanged, but in this way we are led to a proof of their main theorem which, if not the simplest,† is on the whole the most natural and straightforward.

The method may be adapted to the more general problem of the ellipsoid in space of n dimensions, and I conclude in § 5, by a brief discussion of the case of the ordinary ellipse.

2 The Fundamental Lemma

2.1 LEMMA 1. If K_1 is the circle $u^2 + v^2 \equiv x_1$, $\psi(u, v)$ is any continuous function, and

$$(2.11) \quad f = f(u) = f(u, \delta) = \sum_{-\infty}^{\infty} e^{-(m-u)^2/\delta^2},$$

then

$$(2.12) \quad J = J_\delta = J(\delta, x_1) = \frac{1}{\pi\delta^2} \iint_{K_1} f(u) f(v) \psi(u, v) du dv \rightarrow \Sigma' \psi(\mu, \nu), \ddagger$$

where the summation extends over the lattice points of K_1 , and the dash implies that lattice points on the boundary are affected by a weight $\frac{1}{2}$, when $\delta \rightarrow 0$.

The proof differs from that of Lemma 4 of I§ only in so far as lattice points on the boundary are concerned, and it is only necessary to show that, if q is a (complete or partial) lattice square q whose lattice point (μ, ν) lies on K_1 , then

$$(2.13) \quad J_q = J_q(\delta) = \frac{1}{\pi\delta^2} \iint_q \psi \exp\left\{-\frac{(\mu-u)^2 + (\nu-v)^2}{\delta^2}\right\} du dv \rightarrow \frac{\alpha}{2\pi} \psi(\mu, \nu),$$

* The upper bounds given in I contained numbers L, M independent of x_1 , but depending on x in an unspecified manner.

† The simplest is that in Landau's note to II.

‡ I have changed the definition of J , from I, to the extent of the factor π .

§ See I, 253–254.

where α is the angle subtended at the lattice point by the part of q which lies inside K_1 *. A glance at a figure shows, in fact, that the sum of the values of α associated with a lattice point on K_1 is in all cases equal to π .

All cases which can arise for lattice points in the first quadrant are shown in fig 1, and all other cases are trivial variants of these

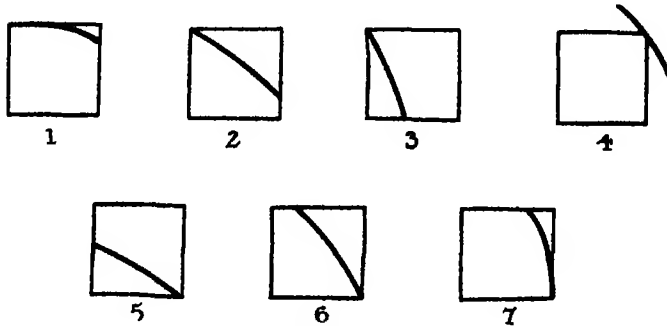


Fig 1

In each case we make the substitution

$$\mu - u = \pm U, \quad v - v = \pm V,$$

and the problem is reduced to showing that

$$(2.14) \quad I(\delta) = \frac{1}{\pi \delta^2} \iint_q \psi(U, V) e^{-(U^2+V^2)/\delta^2} dU dV \rightarrow \frac{\alpha}{2\pi} \psi(0, 0),$$

where q is a region cut off from the square of fig 2 by a circle through the origin, and α is the angle of q at the origin

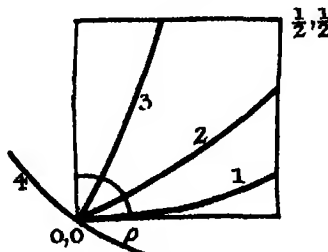


Fig 2

The proof of (2.14) is very simple, as the kernel is positive.† In the first

* That is to say, the angle between the tangent to K_1 at the lattice point and the side of q directed towards the interior of K_1 , except when q lies (apart from the lattice point) entirely inside K_1 , in which case α is $\frac{1}{2}\pi$.

† It is here that the method proves so much simpler than the ordinary "Pfeiffer" method, which uses an oscillating kernel.

place, we may ignore all of q except such of it as lies inside the small quadrant of radius ρ (fig 2), for the contribution of the remainder is

$$O\left(\frac{1}{\delta^2} e^{-\rho^2/\delta^2}\right) = o(1)$$

Next, we may replace ψ by its value at the origin, for ρ may be chosen so small that the difference is less than ϵ , and the resulting error is less than

$$\frac{\epsilon}{\pi\delta^2} \int_0^\infty \int_0^\infty e^{-(U^2+V^2)/\delta^2} dU dV = \frac{1}{2} \epsilon$$

Finally, if ρ be small enough, the circle will (in so far as it lies within the quadrant of radius ρ) be contained between radii making angles $\alpha - \epsilon$ and $\alpha + \epsilon$ with the axis of y , so that

$$\iint_q e^{-(U^2+V^2)/\delta^2} dU dV$$

lies between the two integrals

$$\frac{1}{\pi\delta^2} \int_{\frac{1}{2}\pi-\alpha+\epsilon}^{\frac{1}{2}\pi} d\theta \int_0^\rho r e^{-r^2/\delta^2} dr,$$

which tend to $(\alpha \mp \epsilon)/2\pi$ when δ tends to zero.

3. Proof of an identity for

$$P(x) = \sqrt{x} \sum_{v=1}^{x_1} \frac{r(v)}{\sqrt{v}} J_1(2\pi\sqrt{vx}),$$

and deduction of (1.11)

3.1 THEOREM 1 If x and x_1 are positive,* then

$$\begin{aligned} (3.11) \quad P(x) &= \sqrt{x} \sum_{v=1}^{x_1} \frac{r(v)}{\sqrt{v}} J_1(2\pi\sqrt{vx}) \\ &= J_0(2\pi\sqrt{xx_1}) - \sqrt{\frac{x}{x_1}} P(x_1) J_1(2\pi\sqrt{xx_1}) \\ &\quad + \sqrt{x} \sum_{v=1}^{\infty} \frac{r(v)}{\sqrt{v}} \int_{2\pi\sqrt{xx_1}}^{\infty} J_2(t) J_1\left(t\sqrt{\frac{v}{x}}\right) dt. \end{aligned}$$

The proof of this theorem, which we shall find it possible to write later in a simpler form, depends on a double application of Lemma 1.

Suppose first, in Lemma 1, that $\psi(u, v) = 1$. Then

$$A(x_1) = \pi x_1 + P(x_1) = \lim J_2 = \lim \frac{1}{\pi\delta^2} \iint_{K_1} f(u) f(v) du dv.$$

* If $x_1 < 1$, the sum on the left-hand side is empty. The identity is similar to, but simpler than, that of I, Theorem 1.

We substitute for $f(u)$ and $f(v)$ from the transformation formula,* and integrate term by term. Observing that

$$\iint_{K_1} \cos 2m\pi u \cos 2n\pi v \, du \, dv = \frac{\sqrt{x_1} J_1 \{2\pi \sqrt{(m^2+n^2)x_1}\}}{\sqrt{m^2+n^2}},$$

except when $m = 0, n = 0$, when its value is πx_1 , we obtain

$$\bar{P}(x_1) = \sqrt{x_1} \lim \sum' e^{-(m^2+n^2)\pi x_1} \frac{J_1 \{2\pi \sqrt{(m^2+n^2)x_1}\}}{\sqrt{m^2+n^2}},$$

where the summation extends over all values of m and n save the pair $(0, 0)$; or

$$(3.12) \quad P(x_1) = \sqrt{x_1} \lim \sum_1 e^{-\pi x_1 \frac{r(v)}{\sqrt{v}}} \frac{J_1(2\pi \sqrt{vx_1})}{\sqrt{v}}$$

If we could put $\delta = 0$ under the sign of summation, we should obtain (1.11) forthwith, but this, naturally, we are not yet at liberty to do.

3.2 Next, in Lemma 1, we put

$$\psi(u, v) = \frac{J_1 \{2\pi \sqrt{(u^2+v^2)x}\}}{\sqrt{u^2+v^2}},$$

it being understood that $\psi(0, 0)$ stands for $\pi\sqrt{x}$, the limit of ψ at the origin. We obtain

$$(3.21) \quad \pi\sqrt{x} + \sum_{v=1}^{\infty} \frac{r(v)}{\sqrt{v}} J_1(2\pi \sqrt{vx}) = \lim J_\delta \\ = \lim \frac{1}{\pi\delta^2} \iint_{K_1} f(u) f(v) \frac{J_1 \{2\pi \sqrt{(u^2+v^2)x}\}}{\sqrt{u^2+v^2}} \, du \, dv \dagger$$

Effecting transformations similar to those of §3.1, we obtain

$$(3.22) \quad J_\delta = \sum e^{-(m^2+n^2)\pi x_1} \iint_{K_1} \cos 2m\pi u \cos 2n\pi v \frac{J_1 \{2\pi \sqrt{(u^2+v^2)x}\}}{\sqrt{u^2+v^2}} \, du \, dv,$$

the summation here being over all values of m and n .

Now

$$(3.23) \quad \iint_{K_1} = \int_0^{\sqrt{x_1}} J_1(2\pi r \sqrt{x}) \, dr \int_0^{2\pi} \cos(2m\pi r \cos \theta) \cos(2n\pi r \sin \theta) \, d\theta \\ = 2\pi \int_0^{\sqrt{x_1}} J_1(2\pi r \sqrt{x}) J_0(2\pi r \sqrt{v}) \, dr = 2\pi \int_0^{\infty} - 2\pi \int_{\sqrt{x_1}}^{\infty},$$

* I (3.12)

† The dash in the summation has here the same meaning as in Lemma 1

where $v = m^2 + n^2$; and

$$2\pi \int_0^{\infty} J_1(2\pi r \sqrt{x}) J_0(2\pi r \sqrt{v}) dr = \frac{1}{\sqrt{x}}, \quad \frac{1}{2\sqrt{x}}, 0$$

according as $v < x$, $v = x$ or $v > x$. Hence

$$(3.24) \quad \lim J_s = \frac{A(x)}{\sqrt{x}} - 2\pi \lim \sum_{v=0}^{\infty} r(v) e^{-v^2 x} \int_{\sqrt{x_1}}^{\infty} J_1(2\pi r \sqrt{x}) J_0(2\pi r \sqrt{v}) dr,$$

provided only that one of these limits exists. Comparing (3.21) and (3.24), we see that the limits do in fact exist, and that

$$(3.25) \quad \begin{aligned} \bar{P}(x) = \bar{A}(x) - \pi x = \sqrt{x} \sum_{v=1}^{x_1} \frac{r(v)}{\sqrt{v}} J_1(2\pi \sqrt{vx}) \\ + 2\pi \sqrt{x} \lim \sum_{v=0}^{\infty} r(v) e^{-v^2 x} \int_{\sqrt{x_1}}^{\infty} J_1(2\pi r \sqrt{x}) J_0(2\pi r \sqrt{v}) dr \end{aligned}$$

Here again we are not at present, in a position to put $\delta = 0$ under the sign of summation.

3.3 We now transform the integral in (3.25) by partial integration. If $v > 0$, we have

$$\begin{aligned} 2\pi \sqrt{x} \int_{\sqrt{x_1}}^{\infty} J_1(t) J_0\left(t \sqrt{\frac{v}{x}}\right) dt \\ = -\sqrt{\frac{x}{v}} J_1(2\pi \sqrt{vx_1}) J_1(2\pi \sqrt{vx_1}) + \sqrt{\frac{x}{v}} \int_{2\pi \sqrt{vx_1}}^{\infty} J_2(t) J_1\left(t \sqrt{\frac{v}{x}}\right) dt, \end{aligned}$$

while the term $v = 0$ gives $J_0(2\pi \sqrt{xx_1})$. Hence we derive from (3.25)

$$\begin{aligned} (3.31) \quad \bar{P}(x) - \sqrt{x} \sum_{v=1}^{x_1} \frac{r(v)}{\sqrt{v}} J_1(2\pi \sqrt{vx}) = J_0(2\pi \sqrt{xx_1}) \\ - \sqrt{x} J_1(2\pi \sqrt{xx_1}) \lim \sum_{v=1}^{\infty} e^{-v^2 x} \frac{r(v)}{\sqrt{v}} J_1(2\pi \sqrt{vx_1}) \\ + \sqrt{x} \lim \sum_{v=1}^{\infty} e^{-v^2 x} \frac{r(v)}{\sqrt{v}} \int_{2\pi \sqrt{vx_1}}^{\infty} J_2(t) J_1\left(t \sqrt{\frac{v}{x}}\right) dt, \end{aligned}$$

provided only that the limits on the right exist, for which it is sufficient that either exists.

The first limit exists, by (3.12), and the second term accordingly reduces to

$$(3.32) \quad -\sqrt{\frac{x}{x_1}} J_1(2\pi \sqrt{xx_1}) \bar{P}(x_1)$$

To deal with the second limit, we require a lemma

3.4. LEMMA 2* If $\tau > A$, $N > A$, where the A 's are positive constants, then

$$(3.41) \quad \int_{\tau}^{\infty} J_2(t) J_1(Nt) dt = -\frac{\operatorname{sgn}(N-1)}{\pi N \sqrt{N}} \int_{(N-1)\tau}^{\infty} \frac{\sin u}{u} du + O\left(\frac{1}{N\tau\sqrt{N}}\right)$$

If $\tau > A$, $N > 1 + A$, then

$$(3.42) \quad \int_{\tau}^{\infty} J_2(t) J_1(Nt) dt = O\left(\frac{1}{N\tau\sqrt{N}}\right).$$

If $0 < N < 1 - A$, $N\tau > A$, then

$$(3.43) \quad \int_{\tau}^{\infty} J_2(t) J_1(Nt) dt = O\left(\frac{1}{\tau\sqrt{N}}\right).$$

We have

$$\int_{\tau}^{\infty} J_2(t) J_1(Nt) dt = -\frac{J_2(\tau) J_2(N\tau)}{N} + \frac{1}{N} \int_{\tau}^{\infty} J_2(t) J_2(Nt) dt$$

If $\tau > A$, $N > A$, the first term falls under the error term of (3.41). In the second, we may replace the J 's by their asymptotic equivalents, the error so introduced being

$$O\left\{\frac{1}{N}\left(\frac{1}{N\sqrt{N}} + \frac{1}{\sqrt{N}}\right) \int_{\tau}^{\infty} \frac{dt}{t^2}\right\} = O\left(\frac{1}{N\tau\sqrt{N}}\right).$$

There remains

$$\begin{aligned} & \frac{2}{\pi N \sqrt{N}} \int_{\tau}^{\infty} \frac{\cos(t - \frac{1}{2}\pi) \cos(Nt - \frac{1}{2}\pi)}{t} dt \\ &= -\frac{1}{\pi N \sqrt{N}} \int_{\tau}^{\infty} \frac{\sin(N-1)t}{t} dt - \frac{1}{\pi N \sqrt{N}} \int_{\tau}^{\infty} \frac{\cos(N+1)t}{t} dt \end{aligned}$$

The first term here is equal to that on the right-hand side of (3.41), while the second is of the order of the error term.

This proves (3.41). To obtain (3.42), we have only to observe that

$$\int_{(N-1)\tau}^{\infty} \frac{\sin u}{u} du = O\left(\frac{1}{\tau}\right)$$

if $N > 1 + A$.

To prove (3.43), we observe that

$$\begin{aligned} \int_{\tau}^{\infty} J_2(t) J_1(Nt) dt &= N' \int_{\tau'}^{\infty} J_2(N'u) J_1(u) du \\ &= -J_2(N'\tau') J_2(\tau') + \int_{\tau'}^{\infty} J_2(N'u) J_2(u) du, \end{aligned}$$

where $N' = 1/N$, $\tau' = N\tau$, so that $N' > 1 + A$, $\tau' > A$. The first term falls

* In view of §4, I have included in Lemma 2 rather more than is immediately necessary.

under the error term of (3.43),* and so does the error introduced when we replace the J 's in the integral by their asymptotic equivalents. There remains

$$\begin{aligned} & \frac{2}{\pi\sqrt{N}} \int_{\tau}^{\infty} \frac{\cos(N't - \frac{1}{2}\pi) \cos(t - \frac{1}{2}\pi)}{t} dt \\ &= -\frac{1}{\pi\sqrt{N'}} \int_{\tau}^{\infty} \frac{\sin(N'-1)t}{t} dt - \frac{1}{\pi\sqrt{N'}} \int_{\tau}^{\infty} \frac{\cos(N'+1)t}{t} dt \\ &= O\left(\frac{1}{\tau'\sqrt{N'}}\right) = O\left(\frac{1}{\tau\sqrt{N}}\right) \end{aligned}$$

3.5 We return to the third term on the right-hand side of (3.31). It is plain from Lemma 2 that the general term, when x and x_1 are fixed, is $O(v^{-\frac{1}{2}+\epsilon})$ for every positive ϵ , and uniformly in δ . The series is therefore absolutely and uniformly convergent, and we may make $\delta = 0$ inside the summation. When we do this we obtain (3.11), except that the finite sum now carries a dash and that $\bar{P}(x_1)$ stands for $P(x_1)$ on the right-hand side. It is plain, however, that the dash and the bar may be removed, since the discontinuities on the two sides, when x_1 is an integer, are the same. This completes the proof of (3.11).

It remains to deduce (1.1). For this, it is only necessary to show that the right-hand side of (3.11) tends to zero when $x_1 \rightarrow \infty$. This is obvious so far as the first two terms are concerned, since $P(x_1) = O(\sqrt{x_1})$.

It remains to consider the series

$$(3.51) \quad S = \sqrt{x} \sum_{v=1}^{\infty} \frac{r(v)}{\sqrt{v}} \int_{\tau}^{\infty} J_2(t) J_1(Nt) dt = \sqrt{x} \sum_{v=1}^{\infty} \frac{r(v)}{\sqrt{v}} I_v,$$

say, where $\tau = 2\pi\sqrt{xx_1}$, $N = \sqrt{v/x}$. If x is fixed, and not an integer, $|N-1| > A$ for all values of v , and, by (3.41),

$$(3.52) \quad I_v = O\left\{(xx_1)^{-1} \left(\frac{v}{x}\right)^{-1}\right\} = O(x_1^{-1} v^{-1})$$

If x is an integer, $|N-1| > A$, except when $v = x$, and then $\text{sgn}(N-1) = 0$, so that (3.52) is still valid. We have, therefore, for any fixed x ,

$$S = O\left(\frac{1}{\sqrt{x_1}} \sum_{v=1}^{\infty} \frac{r(v)}{v!}\right) = O\left(\frac{1}{\sqrt{x_1}}\right) \rightarrow 0$$

This proves (1.1).

3.6. I add here two further remarks.

* Since $\tau'\sqrt{N'} = \tau\sqrt{N}$.

(1) If we transform the integral in (3 11) by a further integration by parts, and use the identity*

$$P_1(x) = \int_0^x P(y) dy = \frac{x}{\pi} \sum_{v=1}^{\infty} \frac{r(v)}{v} J_1(2\pi\sqrt{vx}),$$

we obtain the result of I, Theorem 1 †

(2) We are now also in a position to prove

THEOREM 2 —If x and x_1 are positive, then

$$\begin{aligned} (3\ 61) \quad \bar{P}(x) - \sqrt{x} \sum_{v=1}^{x_1} \frac{r(v)}{\sqrt{v}} J_1(2\pi\sqrt{vx}) \\ = 2\pi\sqrt{x} \sum_{v=0}^{\infty} r(v) \int_{\sqrt{x_1}}^{\infty} J_1(2\pi r\sqrt{x}) J_0(2\pi r\sqrt{v}) dr. \end{aligned}$$

It is, in fact, after (3 25), sufficient to prove the convergence of the series. But this series is convergent, after §3 3, if the two series on the right-hand side of (3 31) are convergent when $\delta = 0$, and this has now been proved. The identity (3 61) is simpler than (3 11), but less useful, as the series is not absolutely convergent.

4 Proof of (1 12)

4.1. We suppose now that $x > A$, $x_1 > A$, and we proceed to determine an upper bound, in the form of a function of x and x_1 , for the right-hand side of (3 11)

THEOREM 3 —If $x > A$, $x_1 > A$, then

$$\begin{aligned} (4\ 11) \quad P(x) - \sqrt{x} \sum_{v=1}^{x_1} \frac{r(v)}{\sqrt{v}} J_1(2\pi\sqrt{vx}) \\ = O\left(\frac{x^{1+\epsilon}}{\sqrt{x_1}}\right) + O\{(xx_1)^{-1}\} + O(x^{\frac{1}{2}}x_1^{\Theta-1}), \end{aligned}$$

where Θ is any number for which $P(x_1) = O(x_1^{\Theta})$ ‡. In particular, if $A < x_1 < Ax^2$, then

$$(4\ 12) \quad \bar{P}(x) - \sqrt{x} \sum_{v=1}^{x_1} \frac{r(v)}{\sqrt{v}} J_1(2\pi\sqrt{vx}) = O\left(\frac{x^{1+\epsilon}}{\sqrt{x_1}}\right)$$

The first term on the right of (3 11) is

$$O\{(xx_1)^{-1}\},$$

and the second is

$$O(x^{\frac{1}{2}}x_1^{\Theta-1}).$$

* See I (1.22) and §3.

† I, 256.

‡ So that we may take $\Theta = \frac{1}{2}, \frac{1}{3}, \frac{1}{4}, \dots$, according as we assume what has been proved by Gauss, Sierpiński, Littlewood and Walfisz.

We write now

$$(4.13) \quad S = \sqrt{x} \sum_{v=1}^{\infty} \frac{r(v)}{\sqrt{v}} \int_{2\pi\sqrt{vx_1}}^{\infty} J_2(t) J_1\left(t\sqrt{\frac{v}{x}}\right) dt = \sqrt{x} \sum_{v=1}^{\infty} \frac{r(v)}{\sqrt{v}} I_v \\ = \sqrt{x} \sum_{v < x-\delta x} + \sqrt{x} \sum_{x-\delta x}^{x+\delta x} + \sqrt{x} \sum_{v > x+\delta x} = S_1 + S_2 + S_3,$$

say Here δ is a positive constant less than 1

In S_1 we have, in the notation of §§ 3.4-3.5,

$$0 < N = \sqrt{\frac{v}{x}} < 1 - A, \quad N\tau = 2\pi\sqrt{vx_1} > A,$$

and so, by (3.42),

$$I_v = O\left\{\frac{1}{\sqrt{xx_1}}\left(\frac{x}{v}\right)^{\frac{1}{2}}\right\} = O(x^{-\frac{1}{2}}x_1^{-\frac{1}{2}}v^{-\frac{1}{2}}), \\ (4.14) \quad S_1 = O\left(x^{\frac{1}{2}}x_1^{-\frac{1}{2}} \sum_{v < x-\delta x} \frac{r(v)}{v^{\frac{1}{2}}}\right) = O\left(\sqrt{\frac{x}{x_1}}\right)$$

In S_3 we have $\tau = 2\pi\sqrt{xx_1} > A$ and $N > 1 + A$, and so, by (3.43),

$$I_v = O\left\{\frac{1}{\sqrt{xx_1}}\left(\frac{x}{v}\right)^{\frac{1}{2}}\right\} = O(x^{\frac{1}{2}}x_1^{-\frac{1}{2}}v^{-\frac{1}{2}}), \\ (4.15) \quad S_3 = O\left(x^{\frac{1}{2}}x_1^{-\frac{1}{2}} \sum_{v > x+\delta x} \frac{r(v)}{v^{\frac{1}{2}}}\right) = O\left(\sqrt{\frac{x}{x_1}}\right)$$

Combining our results,

$$(4.16) \quad \bar{P}(x) = \sqrt{x} \sum_{v=1}^{x_1} \frac{r(v)}{\sqrt{v}} J_1(2\pi\sqrt{vx}) \\ = S_2 + O\left(\sqrt{\frac{x}{x_1}}\right) + O\{(xx_1)^{-\frac{1}{2}}\} + O(x^{\frac{1}{2}}x_1^{-\frac{1}{2}}).$$

4.2. In S_2 , $1 - A < N < 1 + A$, and

$$(4.21) \quad I_v = O\left(\left|\int_{\lambda}^{\infty} \frac{\sin u}{u} du\right|\right) + O\left(\frac{1}{\sqrt{xx_1}}\right),$$

where

$$(4.211) \quad \lambda = |N - 1| \tau = 2\pi\sqrt{x_1} |\sqrt{v} - \sqrt{x}|.$$

The second term on the right of (4.21) gives

$$O\left(\frac{1}{\sqrt{x_1}} \sum_{x-\delta x}^{x+\delta x} \frac{r(v)}{\sqrt{v}}\right) = O\left(\sqrt{\frac{x}{x_1}}\right).$$

The first term is

$$O \left\{ \text{Min} \left(1, \frac{1}{\lambda} \right) \right\} = O \left\{ \text{Min} \left(1, \frac{1}{\sqrt{x_1} |\sqrt{v} - \sqrt{x}|} \right) \right\},$$

and its contribution is $O(S)$, where

$$(4.22) \quad S = \sum_{s-\delta x}^{s+\delta x} r(v) \text{Min} \left(1, \frac{1}{\sqrt{x_1} |\sqrt{v} - \sqrt{x}|} \right)$$

We write

$$(4.23) \quad S = \sum_{x-\delta x}^{x-\lambda} + \sum_{x-\lambda}^{x+\lambda} + \sum_{x-\lambda}^{x+\delta x} = S_1 + S_2 + S_3,$$

where

$$(4.231) \quad \lambda = \eta \sqrt{\frac{x}{x_1}}$$

and η is a positive constant. Then

$$(4.24) \quad S_2 \leq \sum_{x-\lambda}^{x+\lambda} r(v) = O(x^\epsilon \lambda) = O \left(\frac{x^{1+\epsilon}}{\sqrt{x_1}} \right)$$

for every positive ϵ . Also

$$(4.25) \quad S_3 \leq \frac{1}{\sqrt{x_1}} \sum_{s+\lambda}^{s+\delta x} \frac{r(v)}{\sqrt{v} - \sqrt{x}} = O \left(\frac{x^{1+\epsilon}}{\sqrt{x_1}} \sum_{s+\lambda}^{s+\delta x} \frac{1}{v-x} \right) \\ = O \left(\frac{x^{1+\epsilon}}{\sqrt{x_1}} \sum_{\mu=1}^{\delta x} \frac{1}{\mu} \right) = O \left(\frac{x^{1+\epsilon}}{\sqrt{x_1}} \right),$$

and similarly

$$(4.26) \quad S_1 = O \left(\frac{x^{1+\epsilon}}{\sqrt{x_1}} \right)$$

From (4.23)-(4.26), we have

$$(4.27) \quad S = O \left(\frac{x^{1+\epsilon}}{\sqrt{x_1}} \right);$$

and so S_3 is of the same form. This completes the proof of (4.11).

If $x_1 < Ax^3$, and we take $\Theta = \frac{1}{3}$, the two last error terms in (4.11) are smaller than the first, and we obtain (4.12). If we only wish to use the trivial $\Theta = \frac{1}{3}$, we must suppose $x_1 < Ax$.

4.3 Since

$$J_1(2\pi\sqrt{vx}) = \frac{\cos(2\pi\sqrt{vx} - \frac{3}{4}\pi)}{(vx)^{\frac{1}{4}}} + O \left\{ \frac{1}{(vx)^{\frac{1}{2}}} \right\},$$

we have

$$(4.31) \quad \sqrt{x} \sum_{v=1}^{\frac{x}{\sqrt{x_1}}} \frac{r(v)}{\sqrt{v}} J_1(2\pi\sqrt{vx}) = \frac{x^{\frac{1}{2}}}{\pi} \sum_{v=1}^{\frac{x}{\sqrt{x_1}}} \frac{r(v)}{v^{\frac{1}{2}}} \cos(2\pi\sqrt{vx} - \frac{3}{4}\pi) + O(x^{\frac{1}{2}}).$$

If $x_1 = x^{\frac{1}{2} + \epsilon}$ the right-hand side is, after Littlewood and Walfisz,*

$$O(x^{\frac{1}{2} + \frac{1}{12} + \epsilon}) = O(x^{\frac{1}{12} + \epsilon}),$$

and the right-hand side of (4.12) is

$$O(x^{\frac{1}{2} + \epsilon - \frac{1}{12} - \frac{1}{2}\epsilon}) = O(x^{\frac{1}{12} + \frac{1}{2}\epsilon}) = O(x^{\frac{1}{12} + \epsilon})$$

Hence

$$P(x) = O(x^{\frac{1}{12} + \epsilon}),$$

their main result

5 The Ellipse

5.1 There is no difficulty in applying the same method to the ellipse

$$(5.11) \quad \phi(u, v) = \alpha u^2 + \beta uv + \gamma v^2 < x,$$

where

$$(5.12) \quad \Delta = 4D = 4\alpha\gamma - \beta^2 > 0$$

We write

$$(5.13) \quad \phi_1(u, v) = \frac{4(\gamma u^2 - \beta uv + \alpha v^2)}{\Delta}$$

for the form conjugate to $\phi(u, v)$, and

$$(5.14) \quad F(u, v) = \frac{1}{\pi\delta^2} \sum \exp \left\{ -\frac{1}{\delta^2} \phi(u-m, v-n) \right\},$$

m and n running through all integral values

If $A(x)$ and $\bar{A}(x)$ are defined for the ellipse as previously for the circle, and

$$(5.15) \quad A(x) = \frac{\pi x}{\sqrt{D}} + P(x), \quad \bar{A}(x) = \frac{\pi x}{\sqrt{D}} + \bar{P}(x),$$

we find, as in §3.1,

$$(5.16) \quad \bar{A}(x) = \frac{\pi x}{\sqrt{D}} + \bar{P}(x) = \lim J_2 = \lim \sqrt{D} \iint_{\phi < x} F(u, v) du dv.$$

5.2 The transformation formula for $F(u, v)$ is†

$$(5.21) \quad F(u, v) = \frac{1}{\sqrt{D}} \sum \sum e^{-\pi \phi_1(m, n)} \cos 2m\pi u \cos 2n\pi v.$$

* II, 482 (Lemma 4).

† See P. Epstein, "Zur Theorie allgemeiner Zetafunktionen," 'Math. Annalen,' vol. 56, pp. 615-644 (1903).

Substituting in (5.21), and using the formula

$$(5.22) \quad \iint_{\phi < x} \cos 2\pi(mu + nv) du dv = \sqrt{\frac{x}{D}} \frac{J_1(2\pi\sqrt{x\phi_1})}{\sqrt{\phi_1}}, *$$

where the arguments of ϕ_1 are m and n , we are led to

$$(5.23) \quad \bar{P}(x) = \sqrt{x} \sum_1^{\infty} \frac{r(v)}{\sqrt{v}} J_1\left(2\pi\sqrt{\frac{vx}{D}}\right).$$

Here $r(v)$ is the number of solutions of $\phi_1(m, n) = v$, or, what is the same thing, of $\phi(m, n) = v$, and the series is in the first instance defined by an Abelian limit with the convergence factor $e^{-\pi^2 v/D}$. In order to prove the convergence of the series, we have to use rather more elaborate arguments, corresponding to those of §3, but no new difficulty of principle arises. The formula corresponding to (3.61) is

$$(5.24) \quad \begin{aligned} \bar{P}(x) &= \sqrt{x} \sum_1^{\infty} \frac{r(v)}{\sqrt{v}} J_1\left(2\pi\sqrt{\frac{vx}{D}}\right) \\ &= 2\pi\sqrt{x} \sum_0^{\infty} r(v) \int_{\sqrt{x_1}}^{\infty} J_1(2\pi r\sqrt{x}) J_0(2\pi r\sqrt{v}) dr. \end{aligned}$$

* Mr. A. Oppenheim points out to me that it is rather simpler to use this integral than the corresponding integral with $\cos 2\pi r\sqrt{x} \cos 2\pi r\sqrt{v}$, used by Landau in his discussion of the O problem by Pfeiffer's method. See E. Landau, "Neue Untersuchungen über die Pfeiffer'sche Methode zur Abschätzung von Gitterpunktzahlen," 'Wiener Sitzungsberichte,' vol. 124, Abt. II A, pp. 469-505 (1915).

*On the Calculation of certain Crystal Potential Constants, and on
the Cubic Crystal of Least Potential Energy*

By J E JONES, Ph D , Trinity College, Cambridge, and

† A E INGHAM, B A , Trinity College, Cambridge

(Communicated by Prof. S. Chapman, F.R.S.—Received October 22, 1924)

§1 *Introduction*

Mathematical investigations of the physical properties of a crystal usually proceed in terms of its potential energy, and applications of the general formulæ obtained are impossible without a knowledge in explicit terms of this function. Its evaluation requires, of course, a knowledge of the interatomic forces in the crystal, but, even when this information is available, the calculation of the potential energy presents a further problem, for which there is no general solution

The present paper is designed to supply certain necessary steps in the elucidation of the latter problem in the case of the cubic crystals, when the law of force between atoms is expressed as a series of inverse powers of the distance—probably the most general form in which the force is ever likely to be expressed

The problem in its simplest form is to calculate the potential energy of any one atom of an infinite cubic crystal due to all those which surround it, when the potential between any two is inversely proportional to the s th power of the distance. The result, besides being a function of the distance of closest approach of atoms in the crystal, involves as well a function of s , which takes the form of a triple summation over the lattice points of the crystal and is a particular case of the generalised zeta-functions of Epstein *. This function, the nature of which depends on the form of the crystal, cannot easily be calculated by direct summation, except for large values of s , and special methods have to be devised. The problem considered here is the evaluation of the functions, appropriate to the three cubic structures, for integral values of $s > 3$. Each number, so evaluated, is called a *crystal potential constant*.

Two methods are already available for the discussion of the problem. One is by the use of Epstein's formulæ for the generalised zeta-function in the form

* Epstein, 'Math Annalen,' vol. 56, pp. 615-644 (1903), vol. 63, pp. 205-216 (1907). These papers will be referred to as "Epstein I" and "Epstein II" respectively.

of a series of terms involving Bessel functions * This method, or one essentially equivalent to it, has, in fact, been used by Madelung† for the particular case of *electrostatic* potentials ($s = 1$), and by the present writers‡ for another particular case ($s = 4$), but it is not one which seems well adapted to a more general treatment of the problem

The second method depends on another type of transformation of the zeta-functions, and leads to series of a different form It was used first by Ewald§ for the electrostatic case and subsequently by Emersleben for a general inverse power law Some account of the latter's work has been given in two recent papers,|| but the full details are apparently contained only in an unpublished dissertation,¶ which we have not, unfortunately, been able to consult So far as we are aware, the author has not applied his method to the actual calculation of the numbers considered in this paper

The method used here is of a different character, and is somewhat analogous, in principle, to the use of the Euler-Maclaurin sum formula for the Riemann zeta-function While it may not be so advantageous as Emersleben's formula in the calculation of the functions for individual values of s , it seems better adapted to the calculation of a series of such values, especially when a calculating machine is available

Some of these numbers have been calculated by Born** by direct summation, but most of his results differ even in the second decimal place from those obtained by the more elaborate methods of this paper

An immediate application of the evaluation of these constants is made to determine the cubic crystal form of least potential energy, when the law of force between atoms is repulsive according to one inverse power of the distance and attractive according to another It is shown that the repulsive field must fall off more rapidly than the attractive, and that the face-centred cubic has then less potential energy than the space-centred, and the space-centred less than the simple cubic The previously known result that the face-centred kind of

* Epstein I, § 8 (pp 639-644) Epstein does not state his results explicitly in this form, but his integrals may (as he observes) be expressed in terms of Bessel functions

† Madelung, 'Phys Zeit,' vol 19, pp 524-532 (1916) Madelung develops his formulae independently of Epstein, and by a method more in keeping with the physical aspects of the problem, but the formulae themselves may be derived directly from those of Epstein.

‡ J E Jones, 'Roy Soc Proc,' A, vol 106, pp 709-718 (p 713) (1924).

§ Ewald, 'Ann. d Phys,' IV, vol 64, pp 253-287 (1921).

|| Emersleben, 'Phys Zeit,' vol 24, pp 73 and 97 (1923)

¶ Emersleben, 'Dissertation,' Göttingen (1922)

** Born, 'Atomtheorie des festen Zustandes,' 2nd Auflage, p 739 (1923).

cubic crystal is the one of closest packing of attracting rigid spheres is a special case of the more general theorem given here

§2 *The Potential Constants for Cubic Crystals*

When the potential between two atoms is of the form λr^{-s} , then the potential energy of one atom in a simple cubic crystal due to all the rest is clearly given by

$$\phi = \frac{\lambda A_s}{\epsilon^s}, \quad (2.01)$$

where ϵ is the closest distance between two atoms and

$$A_s = S'_i (l_1^s + l_2^s + l_3^s)^{-s/2}, \quad (2.02)$$

the summation being a triple one over all integral values of l_1 , l_2 , and l_3 , except $l_1 = l_2 = l_3 = 0$. Obviously, A_s is a function of s only, and so is a constant for a given law of force—hence the term *crystal potential constant*.

In some cases, the lattice points of a simple cubic crystal are occupied alternately by atoms of different kinds,* and it is then necessary to calculate separately the contributions of the two sets of atoms to the potential of any selected atom. If, for instance, the potential between unlike atoms be of the type $\lambda' r^{-s'}$, and that between like atoms $\lambda'' r^{-s''}$, then the potential energy of one atom becomes

$$\frac{\lambda' A_{s'}}{\epsilon^{s'}} + \frac{\lambda'' A_{s''}}{\epsilon^{s''}}, \quad (2.03)$$

where

$$A_{s'} = S_{\substack{l_1+l_2+l_3 \\ \text{odd}}} (l_1^s + l_2^s + l_3^s)^{-s/2} \quad (2.04)$$

and

$$A_{s''} = S'_{\substack{l_1+l_2+l_3 \\ \text{even}}} (l_1^s + l_2^s + l_3^s)^{-s/2}, \quad (2.05)$$

the summations being over all values of l_1 , l_2 , and l_3 , for which $l_1 + l_2 + l_3$ is respectively odd and even.† Clearly, $A_s = A_{s'} + A_{s''}$.

The potential energy for a space-centred cubic for a similar law of force is easily seen to be

$$\phi = \frac{\lambda B_s}{\epsilon^s},$$

* Or, in other words, the crystal consists of two interpenetrating face-centred cubics, as in NaCl.

† M. Born uses the notation $S'_s(s)$, $S''_s(s)$, and $S_s(s)$ for $A_{s'}$, $A_{s''}$ and A_s respectively, *loc. cit.*, p. 739.

where

$$B_s = \left(\frac{\epsilon}{r_0}\right)^3 S'_i (l_1^2 + l_2^2 + l_3^2)^{-3/2} + \left(\frac{\epsilon}{r_0}\right)^3 S_i \{(l_1 + \frac{1}{2})^2 + (l_2 + \frac{1}{2})^2 + (l_3 + \frac{1}{2})^2\}^{-3/2} \\ = \left(\frac{\sqrt{3}}{2}\right)^3 A_s + (\sqrt{3})^3 S_i \{(2l_1 + 1)^2 + (2l_2 + 1)^2 + (2l_3 + 1)^2\}^{-3/2}, \quad (2.06)$$

r_0 being the length of the unit cube and ϵ , as before, the closest distance between atoms *

The corresponding summations for the face-centred cubic are perhaps best obtained by considering the crystal as made up of unit cells, determined by vectors \mathbf{a}_1 , \mathbf{a}_2 , and \mathbf{a}_3 , each cell containing one atom. The position of any atom in the crystal may be described by the vector \mathbf{r} , given by

$$\mathbf{r} = l_1 \mathbf{a}_1 + l_2 \mathbf{a}_2 + l_3 \mathbf{a}_3 \quad (2.07)$$

where l_1 , l_2 , and l_3 are any integers. If \mathbf{i}_1 , \mathbf{i}_2 , and \mathbf{i}_3 are unit vectors parallel to the rectangular axes of the crystal, and $2r_0$ is the length of the unit cube, we have in the case of the face-centred cubic†

$$\mathbf{a}_1 = r_0 (\mathbf{i}_2 + \mathbf{i}_3), \quad \mathbf{a}_2 = r_0 (\mathbf{i}_3 + \mathbf{i}_1), \quad \mathbf{a}_3 = r_0 (\mathbf{i}_1 + \mathbf{i}_2), \quad (2.08)$$

and so

$$\mathbf{r} = r_0 \{\mathbf{i}_1 (l_2 + l_3) + \mathbf{i}_2 (l_3 + l_1) + \mathbf{i}_3 (l_1 + l_2)\} \quad (2.09)$$

From this it follows that

$$\phi = \lambda_s C_s \epsilon^{-s}$$

where

$$C_s = \left(\frac{\epsilon}{r_0}\right)^3 S'_i \{(l_2 + l_3)^2 + (l_3 + l_1)^2 + (l_1 + l_2)^2\}^{-s/2}, \quad (2.10)$$

and ϵ has the same meaning as before, so that $\epsilon/r_0 = \sqrt{2}$. It is of interest to observe that there is an alternative form for C_s , viz

$$C_s = 3S'_i (2l_1^2 + l_2^2 + l_3^2)^{-s/2} - 2^{1-s/2} S'_i (l_1^2 + l_2^2 + l_3^2)^{-s/2} \\ = 3S'_i (2l_1^2 + l_2^2 + l_3^2)^{-s/2} - 2^{1-s/2} A_s. \quad (2.11)$$

* When the centres of the cubes are occupied by different atoms, we obviously have for the potential of any one

$$= \frac{\lambda' B'_s}{r_0^s} + \frac{\lambda'' A_s}{r_0^s}$$

where

$$B'_s = S_i \{(l_1 + \frac{1}{2})^2 + (l_2 + \frac{1}{2})^2 + (l_3 + \frac{1}{2})^2\}^{-s/2},$$

and has the following relation to A_s and B_s ,

$$B_s = \left(\frac{\epsilon}{r_0}\right)^3 A_s + \left(\frac{\epsilon}{r_0}\right)^3 B'_s \\ = \left(\frac{\sqrt{3}}{2}\right)^3 (A_s + B'_s)$$

† M. Born, *loc. cit.*, p. 566

Table I—Potential Constants for Cubic Crystals

s	A	A_1'	A_1''	B_1	C_1
4	16 5323 ₁ ²	10 1977 ₁ ¹	6 33457 ₁	22 63872 ₁	25 33830 ₁
5	10 3775 ₁ ¹	7 3780 ₁ ¹	2 99946 ₁	14 7585 ₁ ¹	16 9675 ₁ ¹
6	8 40192 ₁	6 59518 ₁	1 806740	12 2533 ₁ ¹	14 4539 ₁ ¹
7	7 4670 ₁ ¹	6 28624 ₁	1 18081 ₁	11 05424 ₁	13 3593 ₁ ¹
8	6 94580 ₁	6 14568 ₁	0 800121	10 355 ₁ ¹	12 80193 ₁
9	6 6288 ₁ ¹	6 0767 ₁ ¹	0 55209 ₁	9 8945 ₁ ¹	12 49254 ₁
10	6 4261 ₁ ¹	6 04139 ₁	0 38472 ₁	9 564 ₁ ¹	12 31124 ₁
11	6 29229 ₁	6 0226 ₁ ¹	0 26960 ₁	9 31326 ₁	12 2009 ₁ ¹
12	6 2021 ₁ ¹	6 0125 ₁ ¹	0 18956 ₁	9 11418 ₁	12 1318 ₁ ¹
13	6 140 ₁ ¹	6 0070 ₁ ¹	0 13355 ₁	8 95180 ₁	12 08772 ₁
14	6 09818 ₁	6 00397 ₁	0 094211	8 8167 ₁ ¹	12 05899 ₁
15	6 06876 ₁	6 00225 ₁	0 06651 ₁	8 70298 ₁	12 04002 ₁
16	6 04826 ₁	6 00128 ₁	0 046982	8 60625 ₁	12 02735 ₁
17	6 0339 ₁ ¹	6 00073 ₁	0 03319 ₁	8 52363 ₁	12 0198 ₁ ¹
18	6 02388 ₁	6 000419	0 023463	8 45250 ₁	12 01299 ₁
19	6 01682 ₁	6 000240	0 016585	8 39138 ₁	12 009353
20	6 011863	6 000138	0 011725	8 33860 ₁	12 006280
21	6 008369	6 0000 ₁ ¹	0 0082 ₁ ¹	8 28306 ₁	12 004496
22	6 00590 ₁	6 000046	0 005861	8 253675	12 00306 ₁
23	6 004170	6 00002 ₁	0 004144	8 219626	12 00218 ₁
24	6 002945	6 000015	0 002930	8 19015 ₁	12 001511
25	6 00208 ₁	6 000009	0 002072	8 16465 ₁	12 001075
26	6 001470	6 000005	0 001465	8 1425 ₁ ¹	12 000748
27	6 001040	6 000003	0 001036	8 123469	12 000531
28	6 000734	6 000002	0 00073 ₁	8 108921	12 00037 ₁
29	6 000519	6 000001	0 000518	8 092593	12 000263
30	6 000367	6 00000 ₁	0 00036 ₁	8 080186	12 000185

It is the evaluation of the functions A_s , B_s , and C_s for various values of s , which forms the main part of this paper. The methods by which these numbers

have been computed are described below in §4, but the results are given here so that readers, interested only in the physical aspects of the subject, may omit the necessary mathematical analysis. The limits of error are indicated in each case. Where the upper and lower bounds are not given, it is to be inferred that the number is correct to six places of decimals.

Without methods such as those here described, the calculation of these numbers would have been impracticable, even so, the computation has involved considerable labour, which could not have been undertaken without the use of a calculating machine.*

To indicate the danger of calculating these functions for small values of s by direct summation, it should be mentioned that 24 terms of the summation for A_4 , representing the contributions of the nearest 484 atoms to the potential, are less by about 15 per cent than the actual value of A_4 , while even in the case of 100 terms, corresponding to about 4,000 atoms, there is an error of 6 per cent.†

§3 *The Cubic Crystal of least Potential Energy*

The most general way in which we can as yet hope to express the field of force between two atoms is by two terms, each an inverse power of the distance, one positive to express repulsion and the other negative to express attraction. For the purpose of this paragraph, we therefore express the law of force in the form

$$f = \frac{\lambda_n}{r^n} - \frac{\lambda_m}{r^m}, \quad (3.01)$$

and proceed to find which of the cubic crystals has, for this law of force, the least potential energy. The potential energy of a crystal in its usually accepted sense, that is its capacity to do work as a result of the interatomic forces, being negative, what we require is that crystal of the greatest negative energy.

Denoting the potentials of simple, space-centred, and face-centred cubics,

* The authors take this opportunity of expressing their warmest thanks to Prof Newall, Director of the Solar Physics Observatory, Cambridge, for his kindness in placing at their disposal a Brunsviga calculating machine.

† In calculating A_s we suppose A_s expressed in the form $\sum a_n n^{-s}$ (see §4.6), and by a "term" we mean a term of *this* series.

In general, the error involved in the calculation of A_s , when atoms within a large distance R of the origin only are considered, is approximately

$$\frac{4\pi R^{3-s}}{s-3}$$

The number (N) of atoms involved is roughly $\frac{4}{3}\pi R^3$, and the number (n) of terms about R^3 .

by ϕ_a , ϕ_b , and ϕ_c , respectively, and the distance of closest approach between atoms by ϵ_a , ϵ_b , ϵ_c , we have

$$\phi_x = \frac{\lambda_n X_{n-1}}{(n-1) \epsilon_x^{n-1}} - \frac{\lambda_m X_{m-1}}{(m-1) \epsilon_x^{m-1}}, \quad \begin{matrix} (x = a, b, c) \\ (X = A, B, C) \end{matrix} \quad (3.02)$$

or, using the fact that

$$\partial\phi/\partial\epsilon = 0,$$

that is

$$\epsilon_x^{n-m} = \frac{\lambda_n X_{n-1}}{\lambda_m X_{m-1}}, \quad \begin{matrix} (x = a, b, c) \\ (X = A, B, C) \end{matrix}$$

we have

$$\phi_x = - \frac{n-m}{(n-1)(m-1)} \frac{\lambda_n^{n-1/n-m} X_{n-1}^{n-1/n-m}}{\lambda_m^{m-1/n-m} X_{m-1}^{m-1/n-m}} \quad (3.03)$$

In order that ϕ shall be negative, we must have $n > m$, which is obvious, too, on physical grounds.

Hence the ratios of ϕ_a , ϕ_b , and ϕ_c are independent of λ_n and λ_m , being given by

$$\begin{aligned} \phi_a : \phi_b : \phi_c &= \left(\frac{A_{m-1}^{1/m-1}}{A_{n-1}^{1/n-1}} \right)^{\frac{n-1}{n-m}} \left(\frac{B_{m-1}^{1/m-1}}{B_{n-1}^{1/n-1}} \right)^{\frac{n-1}{n-m}} \left(\frac{C_{m-1}^{1/m-1}}{C_{n-1}^{1/n-1}} \right)^{\frac{n-1}{n-m}} \\ &= \left[\left(\frac{A_{m-1}}{B_{m-1}} \right)^{\frac{1}{m-1}} \left(\frac{B_{n-1}}{A_{n-1}} \right)^{\frac{1}{n-1}} \right]^{\frac{n-1}{n-m}} \left[\left(\frac{C_{m-1}}{B_{m-1}} \right)^{\frac{1}{m-1}} \left(\frac{B_{n-1}}{C_{n-1}} \right)^{\frac{1}{n-1}} \right]^{\frac{n-1}{n-m}} \end{aligned} \quad (3.04)$$

or, if we write,

$$\left(\frac{A_s}{B_s} \right)^{1/s} = \psi(s), \quad \left(\frac{C_s}{B_s} \right)^{1/s} = \chi(s), \quad (3.05)$$

we have

$$\phi_a : \phi_b : \phi_c = \left[\frac{\psi(m-1)}{\psi(n-1)} \right]^{\frac{n-1}{n-m}} : 1 : \left[\frac{\chi(m-1)}{\chi(n-1)} \right]^{\frac{n-1}{n-m}}.$$

From Table II, it is clear that $\psi(s)$ and $\chi(s)$ are monotonic functions, at any rate for integral values of $s > 4$, and that when $m < n$,

$$\psi(m-1) < \psi(n-1)$$

and

$$\chi(m-1) > \chi(n-1),$$

with the result that

$$|\phi_a| < |\phi_b| < |\phi_c|.$$

Table II.

s	$\psi(s) = (A_s/B_s)^{1/s}$	$\chi(s) = (C_s/B_s)^{1/s}$	s	$\psi(s) = (A_s/B_s)^{1/s}$	$\chi(s) = (C_s/B_s)^{1/s}$
4	0.92443	1.0286	11	0.96498	1.0248
5	0.93199	1.0283	12	0.96843	1.0241
6	0.93906	1.0279	13	0.97143	1.0234
7	0.94560	1.0274	14	0.97400	1.0228
8	0.95131	1.0269	15	0.97625	1.0219
9	0.95647	1.0262	16	0.97818	1.0211
10	0.96101	1.0258	∞	1.00000	1.0000

We may express the result in the form of a theorem

Atoms, whose field can be represented by a repulsion according to one inverse power law and an attraction according to another, set in the form of a face-centred cubic crystal in preference to a space-centred, and in a space-centred in preference to a simple cubic

The previously known result that the face-centred cubic crystal is the one of closest packing of spheres is a special case of the above theorem corresponding to $n = \infty$ (with $\lim_{n \rightarrow \infty} (\lambda_n)^{1/n} = \sigma$, the diameter)

It is of interest to observe that the field of Argon has recently* been shown to be of the type $\lambda_n r^{-18} - \lambda_m r^{-5}$ and that crystalline Argon has been found to be of the face-centred cubic type

§4 The Calculation of A_s , B_s , and C_s

4.0 The generalised zeta-functions of Epstein, of which the functions A_s , B_s , and C_s are particular cases, are defined as follows † Let

$$q(u) = q(u_1, \dots, u_k) = \sum_{\lambda, \mu=1}^k d_{\lambda\mu} u_\lambda u_\mu \quad (d_{\lambda\mu} = d_{\mu\lambda})$$

be a positive definite quadratic form in the k variables u_1, \dots, u_k , with determinant

$$\begin{vmatrix} d_{11} & d_{12} \\ \cdot & \cdot \\ d_{k1} & \dots & d_{kk} \end{vmatrix} = D \quad (> 0),$$

and let g_1, \dots, g_k and h_1, \dots, h_k be two series each of k real numbers. Then the generalised zeta-function associated with the form q and with the "characteristics" (g) and (h) is defined by

$$Z \begin{vmatrix} g_1 & \dots & g_k \\ h_1 & \dots & h_k \end{vmatrix} (s) = \sum_{\ell > 0} e^{2\pi i (\ell_1 g_1 + \dots + \ell_k g_k)} \{q(\ell_1 + g_1, \dots, \ell_k + g_k)\}^{-s}, \quad (4.01)$$

* J. E. Jones, 'Roy. Soc. Proc.,' A, vol 106, p. 709 (1924).

† Epstein I.

the summation extending to all integer values of l_1, \dots, l_k , for which $q = q(l_1 + g_1, \dots, l_k + g_k) > 0$, and so to all integer values except, in case g_1, \dots, g_k are all integral, the combination $-g_1, \dots, -g_k$, which makes $q = 0$. The series on the right is absolutely convergent if $s > k$, a condition which will be assumed throughout. (4.01) will be written in the more compact form

$${}^kZ \left| \frac{g}{h} \right| (s)_q = \sum_{q>0} e^{2\pi i (M)} [q(l+g)]^{-s} \quad (4.02)$$

The following notation will also be used —

$$\{g\} = \{g_1, \dots, g_k\} = \begin{cases} 1 & \text{if all } g\text{'s are integral,} \\ 0 & \text{otherwise,} \end{cases}$$

a similar meaning being assigned to $\{h\}$. \bar{q} will denote the form reciprocal to q , namely

$$\bar{q}(u) = \sum_{\lambda, \mu=1}^k \frac{D_{\lambda\mu}}{D} u_\lambda u_\mu,$$

$D_{\lambda\mu}$ being the co-factor of $d_{\lambda\mu}$ in D . Finally $Q_\kappa(x)$ and $\mathcal{Q}_\kappa(x)$ are defined (for $x \geq 0$, $\kappa \geq 0$) by the relations

$$Q_\kappa(x) = \sum_{0 < q < x} \{x - q(l+g)\}^\kappa e^{2\pi i (M)} \quad (4.03)$$

$$\frac{Q_\kappa(x)}{\Gamma(\kappa+1)} = \frac{\{h\} \pi^{1/2} x^{\kappa+1/2}}{\Gamma(\kappa+1/2) \sqrt{D}} - \frac{\{g\} e^{-2\pi i (gh)} x^\kappa}{\Gamma(\kappa+1)} + \mathcal{Q}_\kappa(x) \quad (4.04)$$

We begin by developing, in a series of lemmas, certain transformations of the generalised zeta-functions, and then proceed to indicate their application to the calculation of A_s , B_s and C_s , for integral values of s greater than 3. These transformations depend ultimately on a formula of Landau concerning the lattice points of a k -dimensional ellipsoid. With the notation just explained this result may be expressed in the form

$$\mathcal{Q}_\kappa(x) = e^{-2\pi i (gh)} \frac{x^{\kappa+1/2}}{\pi^\kappa \sqrt{D}} \sum_{q>0} \frac{e^{-2\pi i (gq)}}{[\bar{q}(l+h)]^{\kappa+1/2}} J_{\kappa+1/2}(2\pi \sqrt{\bar{q}(l+h)} x), \quad (4.05)$$

valid certainly for integral values of $\kappa > \frac{1}{2}k$, the series on the right being then absolutely convergent.*

* E. Landau, "Über eine Aufgabe aus der Theorie der quadratischen Formen," 'Wiener Sitzungsberichte,' vol. 124 (IIa), pp. 445-468 (1915) (452, equation (6)). Landau states the result only for a particular value of κ ($= \rho = [\frac{1}{2}k] + 1$), but the argument evidently applies to any integral $\kappa > \frac{1}{2}k$, the formula (4.05) is, in fact, valid for all real $\kappa > \frac{1}{2}(k-1)$, the series on the right still being absolutely convergent. But this will not be required here.

4.1 Lemma 1. If $x > 0$ and κ is an integer ≥ 0 , then

$$\begin{aligned} {}^kZ \left| \frac{g}{h} \right| (s)_s = & \sum_{0 < g < s} e^{2\pi i(M)} [q(l+g)]^{-s} \\ & + \frac{\{h\} \pi^{1/2}}{\Gamma(\kappa + \frac{1}{2}k + 1) \sqrt{D}} \frac{s(s+2)}{2^s (s-k)} \frac{(s+2\kappa)}{x^{k(s-k)}} \\ & - e^{-2\pi i(g/h)} \frac{\{g\}}{\kappa!} \frac{(s+2)(s+4)}{2^s x^{ks}} \frac{(s+2\kappa)}{2^s x^{ks}} \\ & - \sum_{v=0}^{\kappa} \frac{s(s+2)}{2^{v+1}} \frac{(s+2v-2)}{v!} \frac{Q_v(x)}{x^{k^s+v}} + R_{\kappa}(x, s), \quad (4.11) \end{aligned}$$

where

$$R_{\kappa}(x, s) = \frac{s(s+2)}{2^{\kappa+1}} \frac{(s+2\kappa)}{x^{k^s+1}} \int_s^{\infty} Q_{\kappa}(u) u^{-s-\kappa-1} du \quad (4.12)$$

We have in fact

$$\begin{aligned} \sum_{0 < g < s} e^{2\pi i(M)} \{[q(l+g)]^{-s} - x^{-s}\} &= \sum_{0 < g < s} e^{2\pi i(M)} s \int_{q(l+g)}^x u^{-s-1} du \\ &= s \int_0^x u^{-s-1} \sum_{0 < g < u} e^{2\pi i(M)} du = s \int_0^x Q_0(u) u^{-s-1} du, * \end{aligned}$$

that is,

$$\sum_{0 < g < s} e^{2\pi i(M)} [q(l+g)]^{-s} = Q_0(x) x^{-s} + s \int_0^x Q_0(u) u^{-s-1} du \quad (4.13)$$

If $s > \frac{1}{2}k$ we may make $x \rightarrow \infty$, since $Q_0(x) = O(x^{1/2})$ as $x \rightarrow \infty$ †. If from the resulting equation we then subtract (4.13), we deduce

$$\begin{aligned} {}^kZ \left| \frac{g}{h} \right| (2s)_s - \sum_{0 < g < s} e^{2\pi i(M)} [q(l+g)]^{-s} &= -\frac{Q_0(x)}{x^s} + s \int_s^{\infty} \frac{Q_0(u)}{u^{s+1}} du \\ &= -\sum_{v=0}^{\kappa} \frac{s(s+1)}{v!} \frac{(s+v-1)}{v!} \frac{Q_v(x)}{x^{s+v}} + \frac{s(s+1)}{\kappa!} \frac{(s+\kappa)}{\kappa!} \int_s^{\infty} \frac{Q_{\kappa}(u)}{u^{s+\kappa+1}} du, \quad (4.14) \end{aligned}$$

the last formula being obtained by κ partial integrations, with the help of the relation

$$\int_0^x Q_{v-1}(u) du = \frac{Q_v(x)}{v} \quad (v > 0).$$

The desired result follows from (4.14) by substituting for $Q_{\kappa}(u)$ (in the last term) from (4.04), simplifying, and changing s into $\frac{1}{2}s$

* We may integrate down to 0, since $Q_0(u) = 0$ for a certain range $0 \leq u \leq \delta$ ($\delta > 0$).

† $|Q_0(x)|$ is not greater than the number of "lattice points" (points with integral co-ordinates) inside the k -dimensional ellipsoid $q(u_1 + g_1, \dots, u_k + g_k) = x$, and this number $\sim Ax^{1/2}$, A being a constant, namely, the volume of the ellipsoid $q(u_1, \dots, u_k) = 1$.

4.2 Lemma 2. If $\kappa > \frac{1}{2}k$, then

$$R_{\kappa}(x, s) = \frac{s(s+2)}{2^{\kappa+1}\pi^{\kappa}\sqrt{D}} \frac{(s+2\kappa)}{x^{\frac{1}{2}k+\frac{1}{2}\kappa-\frac{1}{2}k}} \frac{e^{-2\pi i(s+h)}}{x^{\frac{1}{2}k+\frac{1}{2}\kappa-\frac{1}{2}k}} \times$$

$$\sum_{\bar{q}>0} e^{-2\pi i(s+h)} \frac{j_{\kappa+\frac{1}{2}k-\frac{1}{2}}(s+\kappa-\frac{1}{2}k+\frac{1}{2}, \pi^2 \bar{q}(l+h)x)}{[\bar{q}(l+h)]^{\frac{1}{2}\kappa+\frac{1}{2}k}}, \quad (4.21)$$

where

$$j_{\mu}(\rho, X) = \int_1^{\infty} u^{-\frac{1}{2}\mu-\frac{1}{2}} J_{\mu+\frac{1}{2}}(2\sqrt{Xu}) du$$

To prove this, we have only to substitute for Q_{κ} in (4.12) from Landau's formula (4.05), integrate term by term and use the substitution $u = xu'$ in the resulting integrals. The term by term integration presents no difficulty when $\kappa > \frac{1}{2}k$, since $J_{\kappa+\frac{1}{2}}(\xi) = O(\xi^{-\frac{1}{2}})$ as $\xi \rightarrow \infty$, and

$$\sum_{\bar{q}>0} \frac{1}{[\bar{q}(l+h)]^{\frac{1}{2}\kappa+\frac{1}{2}k+\frac{1}{2}}} \int_x^{\infty} u^{-\frac{1}{2}\mu-\frac{1}{2}\kappa+\frac{1}{2}k-\frac{1}{2}} du$$

is convergent for $\kappa > \frac{1}{2}(k-1)$, $s > 0$, and so *a fortiori* for $\kappa > \frac{1}{2}k$, $s > k$.

4.3 Lemma 3. If $\rho > 0$, $\mu \geq 0$, $X > 0$, then

$$|j_{\mu}(\rho, X)| < \pi^{-1} X^{-\frac{1}{2}} G_{\mu}(X),$$

where

$$G_{\mu}(X) = \frac{1}{\Gamma(\mu+1)} \int_0^{\infty} u^{\mu} e^{-u} du \int_0^{\infty} \left(1 + \frac{uv}{4X} + \frac{u^2}{16X}\right)^{\frac{1}{2}\mu} e^{-v} dv$$

Writing for brevity $2\sqrt{X} = Y$, we have

$$j = j_{\mu}(\rho, X) = 2 \int_1^{\infty} z^{-\frac{1}{2}\mu-\frac{1}{2}} J_{\mu+\frac{1}{2}}(Yz) dz$$

$$= 2 \mathfrak{H} \int_1^{\infty} z^{-\frac{1}{2}\mu-\frac{1}{2}} H_{\mu+\frac{1}{2}}^{(1)}(Yz) dz,$$

where $H_{\mu+\frac{1}{2}}^{(1)}$ is Hankel's function*. Substituting for $H_{\mu+\frac{1}{2}}^{(1)}$ from the formula†

$$H_{\mu+\frac{1}{2}}^{(1)}(x) = \frac{1}{\Gamma(\mu+1)} \sqrt{\frac{2}{\pi x}} e^{i(x-\frac{1}{2}(\mu+1)\pi)} \int_0^{\infty} e^{-xu} \left(1 + \frac{u^2}{2x}\right)^{\frac{1}{2}\mu} du,$$

and inverting the order of the integrations in the resulting repeated integral (as is evidently legitimate if $\rho > 0$, $\mu \geq 0$), we obtain

$$j = \frac{2}{\Gamma(\mu+1)} \sqrt{\frac{2}{\pi Y}} \mathfrak{H} \left\{ e^{-i(\mu+1)\pi} \int_0^{\infty} u^{\mu} e^{-u} du \int_1^{\infty} z^{-\frac{1}{2}\mu-\frac{1}{2}} \left(1 + \frac{u^2}{2Yz}\right)^{\frac{1}{2}\mu} e^{iYz} dz \right\}$$

$$= \frac{2}{\Gamma(\mu+1)} \sqrt{\frac{2}{\pi Y}} \mathfrak{H}(I), \quad (4.31)$$

* G. N. Watson, 'Theory of Bessel Functions' (Cambridge, 1922), p. 73, §3.6.

† Watson, *loc. cit.*, p. 168, equation (3).

say. In the inner integral we may, by Cauchy's theorem, deform the path of integration into the line $(1, 1 + \infty i)$. Writing then $z = 1 + iw$, we deduce*

$$I = e^{i(Y - i\mu\pi)} \int_0^\infty w^\mu e^{-w} dw \int_0^\infty z^{-1-\rho} \left(1 + \frac{w}{2Yz}\right)^\mu e^{-Yw} dw \quad (z = 1 + iw)$$

Now we have, for $w > 0$ and $\eta = \frac{u}{2Y} > 0$,

$$|z| > 1,$$

$$\left|1 + \frac{i\eta}{z}\right|^2 = \left|\frac{1 + i(w + \eta)}{1 + iw}\right|^2 = \frac{1 + (w + \eta)^2}{1 + w^2} < 1 + 2\eta w + \eta^2,$$

and so, since $1 + \rho > 0$, $\mu \geq 0$,

$$\begin{aligned} |I| &< \int_0^\infty w^\mu e^{-w} dw \int_0^\infty \left(1 + \frac{w}{Y} + \frac{w^2}{4Y^2}\right)^\mu e^{-Yw} dw \\ &= \frac{1}{Y} \int_0^\infty w^\mu e^{-w} dw \int_0^\infty \left(1 + \frac{w}{Y} + \frac{w^2}{4Y^2}\right)^\mu e^{-w} dw \end{aligned}$$

Substituting this in (4.31) and observing that $|\Re(I)| \leq |I|$, we obtain at once the desired result

4.4 Lemma 4. *If $\kappa > \frac{1}{2}k$, then*

$$|R_\kappa(x, s)| < \frac{s(s+2)}{2^{\kappa+1}\pi^{\kappa+2}\sqrt{D}} \cdot \frac{(s+2\kappa)}{x^{s+\frac{1}{2}\kappa-\frac{1}{2}k+1}} \frac{G_{\kappa+\frac{1}{2}k-\frac{1}{2}}(\delta\pi^2 x)}{x^{s+\frac{1}{2}\kappa-\frac{1}{2}k+1}} \left|\frac{h}{0}\right| \left(\kappa + \frac{1}{2}k + \frac{1}{2}\right)_{\bar{0}},$$

where $\delta = \delta(q, h)$ is the smallest positive value, for integral l 's, of $q(l+h)$

This follows at once from Lemmas 2 and 3, if we observe that $G_\mu(X)$ is a decreasing function of X , and that

$$\begin{aligned} \mu = s + \frac{1}{2}k - \frac{1}{2} &> k - \frac{1}{2} > 0, \quad \rho = s + \kappa - \frac{1}{2}k + \frac{1}{2} > s + \frac{1}{2} > 0, \\ X = \pi^2 \bar{q}(l+h)x &\geq \delta\pi^2 x > 0 \end{aligned}$$

4.5 Lemma 5 *If $0 \leq \mu \leq 6$, $X > 0$, then*

$$G_\mu(X) < 1 + \frac{3(\mu+1)(\mu+6)}{16X} \left(1 + \frac{11}{X} + \frac{54}{X^2}\right).$$

* By $z^{-1-\rho}$, we mean, of course, the principal value. The function $\left(1 + \frac{is}{2Yz}\right)^\mu$, qua function of z , is regular for $\Re s > 0$, we take the branch which $\rightarrow 1$ as $z \rightarrow \infty$ along the real axis.

From the definition of G_μ we have, since $\frac{1}{2}\mu \leq 3$,

$$G_\mu(X) \leq \frac{1}{\Gamma(\mu+1)} \int_0^\infty u^\mu e^{-u} du \int_0^\infty \left(1 + \frac{uv}{4X} + \frac{u^2}{16X}\right)^3 e^{-v} dv \\ = k_0 + \frac{3k_1}{16X} + \frac{3k_2}{(16X)^2} + \frac{k_3}{(16X)^3},$$

where

$$k_\lambda = \frac{1}{\Gamma(\mu+1)} \int_0^\infty u^\mu e^{-u} du \int_0^\infty (4uv + u^2)^\lambda e^{-v} dv$$

We have immediately

$$k_0 = 1$$

$$k_1 = \frac{1}{\Gamma(\mu+1)} \int_0^\infty u^\mu e^{-u} (4u + u^2) du = (\mu+1)(\mu+6)$$

and for $\lambda > 1$,*

$$k_\lambda \leq \frac{2^{\lambda-1}}{\Gamma(\mu+1)} \int_0^\infty u^\mu e^{-u} du \int_0^\infty \{(4uv)^\lambda + u^{2\lambda}\} e^{-v} dv$$

The last integral may be evaluated in terms of Γ -functions, and it is easily verified that, when $0 \leq \mu \leq 6$,

$$\frac{k_2}{k_1} \leq \frac{488}{3}, \quad \frac{k_3}{k_1} \leq 9.6471,$$

from which the stated inequality immediately follows

4.6. Returning now to the functions A_n , B_n , and C_n , we have evidently by

$$(2.02) \quad A_n = {}^sZ \left| \begin{matrix} 0 \\ 0 \end{matrix} \right| (s)_{q_1} = \sum_{n=1}^\infty \frac{a_n}{n^{s+1}},$$

where

$$q_1 = u_1^2 + u_2^2 + u_3^2,$$

and a_n is the number of representations of n as a sum of three squares.† Applying Lemma 1, with $x = 25$ and $\kappa = 5$, observing that $D = 1$, $\{g\} = \{h\} = 1$, $\bar{q}_1 = q_1$, $\delta = 1$, $\kappa > \frac{1}{2}k$, and effecting some simple reductions we obtain

$$A_s = (A_s)_0 + R_s(s), \quad (4.61)$$

* We use here the inequality

$$(a + b)^\lambda \leq 2^{\lambda-1}(a^\lambda + b^\lambda) \quad (a > 0, b > 0, \lambda > 1).$$

† Attention being paid to the order and sign of the representing numbers, so that $a_1 = 6$, $a_2 = 12$, $a_3 = 3$, etc.

where

$$(A_s)_0 = \sum_{n=1}^{2s} \frac{a_n}{n^{1s}} + \frac{s(s+2)}{3 \cdot 5} \cdot \frac{(s+10)}{13} \frac{4\pi}{5^{s-3}(s-3)} \\ - \frac{(s+2)(s+4)}{5! \cdot 2^5 \cdot 5^s} \frac{(s+10)}{5^s} - \sum_{\nu=0}^5 \frac{s(s+2)}{\nu!} \frac{(s+2\nu-2)}{10^{s+2\nu}} \alpha_\nu, \quad (4.62)$$

$$\alpha_n = \sum_{\nu=1}^{21} (25-n)^\nu a_n,$$

and $R_s(s)$ (which is the $R_s(x, s)$ of Lemma 1) satisfies, by Lemma 4, the inequality

$$|R_s(s)| < \frac{s(s+2)}{2^6 \pi^7} \frac{(s+10)}{5^{s+5}} G_5 (25\pi^2) A_5 \quad (4.63)$$

The calculation of A_s consists of two parts (i) the computation of $(A_s)_0$ from the formula (4.62), and (ii) the determination of a numerical upper bound for $|R_s(s)|$

The first part involves the evaluation of the positive integers α_ν ($\nu = 0, 1, \dots, 5$), and this, even with the aid of a calculating machine in conjunction with Barlow's tables, is a rather tedious process owing to the magnitude of the numbers involved. But it should be observed that the α_ν 's are independent of s , and when once determined may be used for all values of s . The values are found to be as follows —

$\nu = 0$	1	2	3	4	5
$\alpha_\nu = 484$	5 200	74 248	1 231 168	22 274 392	426 121 840

In the actual calculation of $(A_s)_0$ it is convenient to treat separately the cases when s is even and when s is odd. It is useful also to observe that each term of $(A_s)_0$ may be derived from the corresponding term of $(A_{s-2})_0$ by means of a simple numerical factor,* so that when the separate terms of $(A_s)_0$, for example, have been computed, those of $(A_6)_0, (A_8)_0, \dots$ may be determined successively by calculations of a comparatively simple character.

We have now to estimate $|R_s(s)|$, starting from (4.63). Lemma 5 gives at once $G_5(25\pi^2) < 1.07$, so that, as $A_5 < 7$,† we have $G_5 A_5 < 7.5$. Observing further that $\pi^7 = \pi^3 \cdot \pi^4 > 30.97$, we obtain

$$|R_s(s)| < \frac{2^{s-3} s(s+2)}{97 \cdot 10^{s+5}} \frac{(s+10)}{5^{s+5}},$$

in particular

$$|R_s(4)| < 0.00000666$$

* Thus, for the term in π , the factor by which we pass from $(s-2)$ to s is $(s+10)(s-5)/(25(s-2)(s-3))$.

† The quickest verification, from the present point of view, is by means of the calculations just described. From these it appears that $(A_5)_0 < 6.95$, a crude inequality for $|R_s(s)|$ then suffices to give $A_5 < 7$.

In addition to $R_n(s)$ there will, of course, be certain errors arising in the calculation of $(A_s)_0$. In order to avoid increasing unnecessarily the error already present, these calculations have been carried to seven places of decimals and in some cases to eight. For A_4 , for example, eight places have been used in each term of \sum_1^{24} , and seven in each of the remaining terms on the right of (4.62). This enables us to obtain A_4 with a final error less in absolute value than 0.000007.

It should be observed that if we were concerned only with the larger values of s , say $s > 8$, it would be possible to calculate A_s to the degree of accuracy just indicated in the case of A_4 , by the use of smaller values of x and κ than those suggested above. But as the lower values of s have in fact to be considered, nothing would be gained by adopting a new value of x for the higher numbers, since any change in x would necessitate the calculation of a new set of numbers α_s . A reduction in κ with increasing s would not be open to the same objection, but the consequent saving of labour would be so slight as hardly to compensate for the formal complications (trivial though they are) introduced by a varying κ .

The method just described has been used for $s = 4, 5, \dots, 16$. For $s > 16$ the numbers may be calculated without serious difficulty by direct summation. For purposes of reference, the table has been extended by this method as far as $s = 30$.

4.7 For B_s we use (2.06), which we write in the form

$$B_s = \left(\frac{3}{2}\right)^{1/2} A_s + \left(\frac{3}{2}\right)^{1/2} B'_s, \quad (4.71)$$

so that

$$2^{-s} B'_s = Z \begin{vmatrix} \frac{1}{2} & \frac{1}{2} & \frac{1}{2} \\ 0 & 0 & 0 \end{vmatrix} (s)_n = \sum_1^{\infty} \frac{b_n'}{n^{1/2}},$$

where

$$q_2 = 4q_1 = 4u_1^2 + 4u_2^2 + 4u_3^2,$$

and b_n' is the number of representations of n as a sum of three *odd* squares. Clearly $b_n' = 8b_n''$, b_n'' being the number of representations of n as a sum of three *positive odd* squares. Further, $b_n' = b_n'' = 0$, unless $n \equiv 3 \pmod{8}$.*

We now apply Lemma 1, with $x = 100$, $\kappa = 5$, to $\left(\frac{3}{2}\right)^{1/2} B'_s$, writing the result in the form

$$\left(\frac{3}{2}\right)^{1/2} B'_s = \left(\frac{3}{2}\right)^{1/2} (B'_s)_0 + \left(\frac{3}{2}\right)^{1/2} R'_s(s). \quad (4.72)$$

Here (since $D = 64$ and $\bar{q}_2 = \frac{1}{2}q_1$)

$$\begin{aligned} \left(\frac{3}{2}\right)^{1/2} (B'_s)_0 &= \sum_1^{99} b_n' \left(\frac{3}{n}\right)^{1/2} + \frac{s(s+2) \cdot (s+10)}{3 \cdot 5 \cdot 13} \frac{3^{1/2} \pi}{2(s-3) 10^{s-2}} \\ &\quad - \sum_{v=0}^5 \frac{s(s+2)}{2^{v-2} v!} \frac{(s+2v-2)}{10^{s+2v}} \beta_v'', \end{aligned}$$

$$* \ b_s'' = 1, \quad b_{11}'' = 3, \quad b_{19}'' = 3, \quad b_{27}'' = 4, \dots$$

where

$$\beta_v'' = \frac{1}{8} \beta_v' = \sum_{n=1}^{100} (100-n)^v b_n''$$

The calculation of $(\frac{3}{2})^{1/2} (B_s')_0$ is similar to that of $(A_s)_0$, the values of β_v'' are found to be

$v = 0$	1	2	3	4	5
$\beta_v'' = 69$	2 613	149 541	9 973 269	725 364 741	55 795 433 973

For the first term on the right of (4.71) we substitute from (4.61) and use the values of $(A_s)_0$ already calculated

It remains to consider the error terms. We write

$$B_s = (B_s)_0 + R_b(s),$$

where

$$(B_s)_0 = (\frac{3}{2})^{1/2} (A_s)_0 + (\frac{3}{2})^{1/2} (B_s')_0$$

is to be calculated as just explained, and

$$R_b(s) = (\frac{3}{2})^{1/2} R_a(s) + (\frac{3}{2})^{1/2} R_b'(s)$$

An upper bound for $|R_a(s)|$ has been obtained in §4.6, and $|R_b'(s)|$ may be treated similarly, combining these in the obvious way we deduce an inequality for $|R_b(s)|$. For $s = 4$ this leads to

$$|R_b(4)| < 0.00000750$$

A much more precise result may, however, be obtained by combining the *explicit* expressions for R_a and R_b' given by Lemma 2, when it is found that the leading terms on the right of (4.21) cancel. We have, in fact, writing for a moment $\xi = 25$, so that $x = \xi$ in $R_a(s)$ and $x = 4\xi$ in $R_b'(s)$,

$$R_b'(s) = \frac{s(s+2)}{2^8 \pi^8 \xi^{s+1-1}} \sum_1^{\infty} \frac{(-1)^n a_n}{n^{s+1}} J_0(s+4, \pi^2 n \xi),$$

while the formula for $R_a(s)$ is to be obtained from this by omitting the factor $(-1)^n$. Hence

$$R_b(s) = (\frac{3}{2})^{1/2} \frac{s(s+2)}{2^8 \pi^8 \xi^{s+1}} \sum_1^{\infty} \frac{2a_{2m}}{(2m)^{s+1}} J_0(s+4, 2\pi^2 m \xi), \quad (4.73)$$

and an application of Lemma 3 gives

$$|R_b(s)| < \frac{3^{1/2} s(s+2)}{\pi^7 (4\xi)^{s+5/2}} G_0(2\pi^2 \xi) A_3''$$

From Lemma 5 and the calculations for A_3'' (to be described below) we deduce $G_0(50\pi^2) A_3'' < 0.84$, so that finally

$$|R_b(s)| < \frac{3^{1/2} 7s(s+2)}{24 \cdot 10^{s+5}},$$

and in particular

$$|R_0(4)| < 0.00000085.*$$

4.8 For C_s we use the form (2.10), which is evidently equivalent to

$$C_s = 2Z \begin{vmatrix} 0 \\ 0 \end{vmatrix} (s)_{q_s} = \sum_1 \frac{c_n}{n^3},$$

where

$$q_s = l_1^2 + l_2^2 + l_3^2 + l_2 l_3 + l_3 l_1 + l_1 l_2,$$

and c_n is the number of representations of n by this form. Now

$$\begin{aligned} 2q_s &= (l_2 + l_3)^2 + (l_3 + l_1)^2 + (l_1 + l_2)^2 \\ &= \lambda_1^2 + \lambda_2^2 + \lambda_3^2, \end{aligned}$$

where $\lambda_1 = l_2 + l_3$, . . . so that

$$2l_1 = -\lambda_1 + \lambda_2 + \lambda_3 = -2\lambda_1 + (\lambda_1 + \lambda_2 + \lambda_3).$$

When l_1, l_2, l_3 take all integer values, $\lambda_1, \lambda_2, \lambda_3$ clearly take all sets of integer values for which $\lambda_1 + \lambda_2 + \lambda_3$ is even, the correspondence being one to one. c_n is therefore the number of representations of $2n$ in the form $\lambda_1^2 + \lambda_2^2 + \lambda_3^2$ with the condition " $\lambda_1 + \lambda_2 + \lambda_3$ even". But this is equivalent to " $\lambda_1^2 + \lambda_2^2 + \lambda_3^2$ even" and is thus automatically satisfied, so that we have simply

$$c_n = a_{2n}, \quad (4.81)$$

a relation which greatly facilitates the calculation of the coefficients c_n .

We take, as for A_s , $x = 25$ and $\kappa = 5$, writing as before

$$C_s = (C_s)_0 + R_c(s)$$

Since $D = \frac{1}{2}$, the formula for $(C_s)_0$ may be obtained from that for $(A_s)_0$ (equation (4.62)) by changing α_n into c_n , π into $\pi\sqrt{2}$, and α_r into γ_r , where

$$\gamma_r = \sum_{n=1}^{24} (25 - n)^r c_n$$

* The arrangement of the text has been chosen as the one which gives $(B_s)_0$ directly in the form most convenient for numerical computation. But we might also start from the formula

$$B_s = 3^{1/2} 2Z \begin{vmatrix} 0 \\ 0 \end{vmatrix} (s)_{q_s},$$

where

$$q_s = 3l_1^2 + 3l_2^2 + 3l_3^2 - 2l_2 l_3 - 2l_3 l_1 - 2l_1 l_2$$

Then $\bar{q}_s = \frac{1}{3}q_s$ (see § 4.8), and for the "remainder term" we obtain a formula involving the coefficients c_n (introduced in § 4.8), and if we take $x = 4\frac{1}{2}$ ($= 100$) this formula is found, in virtue of (4.81), to be identical with (4.73). The appearance of the coefficients c_n corresponds to the geometrical fact that the reciprocal of a space-centred cubic lattice is a face-centred cubic

The values of γ_r are

$v = 0$	1	2	3	4	5
$\gamma_r = 682$	7 354	105 202	1 747 594	31 664 242	606 678 634.

For the estimation of $|R_c(s)|$ we use Lemma 4. We have

$$\begin{aligned}\tilde{q}_3 &= \frac{1}{2} (3l_1^2 + 3l_2^2 + 3l_3^2 - 2l_2l_3 - 2l_3l_1 - 2l_1l_2) \\ &= \frac{1}{2} \{(-l_1 + l_2 + l_3)^2 + (l_1 - l_2 + l_3)^2 + (l_1 + l_2 - l_3)^2\} \\ &= \frac{1}{2} (\mu_1^2 + \mu_2^2 + \mu_3^2),\end{aligned}$$

say. Since $\mu_2 + \mu_3 = 2l_1$, etc., it is clear that, as l_1, l_2, l_3 take all integral values, μ_1, μ_2, μ_3 take all sets of integral values of the same parity (i.e., all odd or all even). From this it is evident that

$${}^sZ \begin{vmatrix} 0 \\ 0 \end{vmatrix} (s)_{\tilde{q}_3} = S' \left(\frac{2}{\mu_1^2 + \mu_2^2 + \mu_3^2} \right)^{1/2} = \left(\frac{2}{3} \right)^{1/2} B_s,$$

and that $\delta = \frac{3}{2}$, so that Lemma 4 gives

$$|R_c(s)| < \frac{s(s+2)}{2^s \pi^7} \frac{(s+10) \sqrt{2}}{5^{s+5}} G_s \left(\frac{75}{2} \pi^2 \right) \left(\frac{2}{3} \right)^{1/2} B_s.$$

From Lemma 6 and the value of B_s already found, we deduce $G_s B_s < 10 \cdot 9$, whence

$$|R_c(s)| < \frac{2^{s+1} s(s+2)}{27 \cdot 10^{s+7}} \frac{(s+10)}{10^{s+7}}$$

In particular

$$|R_c(4)| < 0 \cdot 00000272$$

4.9 We have finally to consider A_s', A_s'' . Of these A_s'' is immediately deducible from C_s , in virtue of the identity (4.81), which gives

$$A_s'' = \sum_{n=1}^{\infty} \frac{a_{2n}}{(2n)^{2s}} = 2^{-1s} C_s.$$

A_s' is then obtained by subtracting this value from that of A_s already found

§5 Summary

Certain numbers, necessary in the calculation of the potential energy of the three cubic crystals, are computed by a method depending on the theory of Epstein's generalised zeta-functions.

An immediate application is made to determine the cubic crystal form of least potential energy, when the law of force between atoms is repulsive according to one inverse power of the distance and attractive according to another

*The Kinetics of Hæmoglobin. III.—The Velocity with which
Oxygen combines with Reduced Hæmoglobin*

By H HARTRIDGE, M D, Sc D, Fellow of King's College, Cambridge, and
F J W ROUGHTON, M A, Fellow of Trinity College, Cambridge *

(Communicated by Prof J N Langley, F R S —Received December 2, 1924)

(From the Physiological and Biochemical Laboratories, Cambridge)

CONTENTS

	Page
Introduction	654
I —Experimental Details	655
II —(i) The Adequacy of the Reaction Velocity Apparatus for Coping with such Rapid Reactions,	662
(ii) The Order of the Reaction	663
III —The Relation between the Velocity-constants and the Equilibrium-constant of the reaction $O_2 + Hb \rightleftharpoons O_2Hb$	668
IV —The Effect of p_{H_2} , Temperature, and other Factors	674
V —Further Consideration in regard to the Chemical Kinetics of the Reaction	678
References	683

INTRODUCTION

The velocity with which oxygen dissociates from its combination with hæmoglobin, and the factors upon which the velocity-constant of this reaction depends, have already been investigated by us in some detail in the second of the present series of papers (1) Since then we have been engaged in a similar inquiry into the velocity of the reverse reaction, *i e*, the combination of oxygen with reduced hæmoglobin The scope of the investigation, which we are now about to describe, was as follows —

(α) To determine the order of the reaction between oxygen and hæmoglobin (see p 663)

(β) To compare the value of

$$\frac{\text{the velocity-constant for the combination of } O_2 + Hb}{\text{the velocity-constant for the dissociation of } O_2Hb \rightarrow}$$

with the value of the equilibrium-constant of the reaction as determined from the dissociation curve.

(γ) To study the effect of (i) p_{H_2} , (ii) temperature, (iii) light, and (iv) salt content upon the velocity of the reaction between O_2 and hæmoglobin

* Part of this work was carried out during the tenure of the Michael Foster and George Henry Lewis Studentships.

The general methods adopted were similar to those used in studying the rate of dissociation of oxyhæmoglobin. One solution (I) consisted of water containing a considerable quantity of oxygen in solution, whereas the other solution (II) consisted of reduced hæmoglobin. These were driven by separate jets into the mixing chamber of the reaction velocity apparatus (2 and 3), and after mixing travelled steadily with known velocity down the observation tube. Spectroscopic observation of the ratio of oxyhæmoglobin to reduced hæmoglobin concentration at various points of the tube, together with a knowledge of the rate of linear flow and of the total amount of (i) oxygen and (ii) hæmoglobin in unit volume of the mixed solution, gave us all the data required for the measurement of the velocity of the reaction.

I EXPERIMENTAL DETAILS

The fact that the velocity with which oxygen combines with reduced hæmoglobin is very rapid necessitated very rapid rates of flow in our observation apparatus, and this in turn meant the use of big volumes of oxygenated water and reduced hæmoglobin solution. For the purposes of this research it was necessary to devise methods by which upwards of 50 litres of these solutions could be rapidly prepared.

(A) *The Preparation of the Solution of Oxygenated Water* For the majority of the experiments water saturated with air at barometric pressure was found to contain an appropriate quantity of dissolved O_2 . Large quantities of "aerated" water were readily prepared in the following manner —

A 20-litre earthenware bottle with bottom tubulure was filled to the brim with tap-water. About 10 litres of the latter were allowed to run out, air being drawn in on top. The connections at the top of the bottle were then closed and the bottle rolled vigorously to and fro by hand. After two minutes' rolling the gas phase and the liquid phase were found by control experiments to have reached equilibrium.

Other concentrations of dissolved oxygen were readily obtained by substituting a gas phase of appropriate composition for the 10 litres of atmospheric air with which the water was usually rolled. In a few experiments the equilibration between the gas phase and the water was performed by spraying the water several times through a glass bottle containing the gas phase.

(B) *The Preparation of the Reduced Hæmoglobin Solutions.*—The usual concentrations of hæmoglobin solution used in these experiments were either about 0.4 per cent (i.e., 1 part whole sheep blood to 40 parts water) or 0.2 per cent. Hb. Several methods (both physical and chemical) of preparing the

large quantities required were tried, and the results obtained with samples made by the different methods were found to be quite consistent with one another. The most serviceable of the different methods was —

(α) *The Rolling Method* —In this method the blood and the water were freed from O_2 independently of one another and afterwards mixed together in appropriate proportions anaerobically

(1) The removal of O_2 from the blood

About 1 litre of the blood (treated with 1 per cent boric acid and a trace of octyl alcohol) was warmed to $40^\circ C$ and then sucked into a vacuum 20-litre earthenware bottle, also standing in a warm bath at about $40^\circ C$. The bottle was then removed from the bath and rolled for a couple of minutes, the poor thermal conductivity of the walls of the bottle preventing any appreciable fall in the temperature of the blood contained therein. As a result of this rolling the blood must yield up at least 90 per cent of its chemically combined oxygen. The bottle was then restored to the warm bath, evacuated again, and once more rolled. The second rolling was sufficient to reduce the blood completely. The latter was then transferred anaerobically into a measuring cylinder (closed at the top with rubber cork and connections and previously filled with commercial N_2 and evacuated), which thereupon was placed in the cold store till ready for use.

(2) The removal of the O_2 from the water

A number of 20-litre bottles were half filled with tap-water and half with commercial N_2 . Each was rolled for 2 minutes, then evacuated, and rolled for another 2 minutes. After this treatment the residual O_2 in solution was quite negligible. Whilst still vacuum, appropriate volumes of the reduced blood were drawn into each of the bottles, and the latter, after having been filled with commercial N_2 , were stood upright, ready for use.

(β) *The Vacuum-Spray Method* —In most of our earlier experiments the water and blood was freed of O_2 by being sprayed into a vacuum glass container, the walls of which were maintained at a temperature of about $50^\circ C$. by a stream of warm water driven by a water-circulating pump. From the glass container the solution syphoned over into vacuum receivers. Tap-water was first of all passed through the apparatus, until all the receivers except the last one were full of O_2 free water, the last receiver being left only half full. After a lapse of 12 hours, during which there was time for the O_2 free water to cool

down to laboratory temperature, the strong hæmoglobin solution (1 in 4) was passed through the apparatus until the last receiver was full of fluid. The containers were then at once connected in series with a rotary pump, by means of which the warm hæmoglobin solution in the last receiver was rapidly and anaerobically mixed with the cooled water in the other receivers. Further experimental details may be obtained from the diagram of the apparatus, shown in fig 1

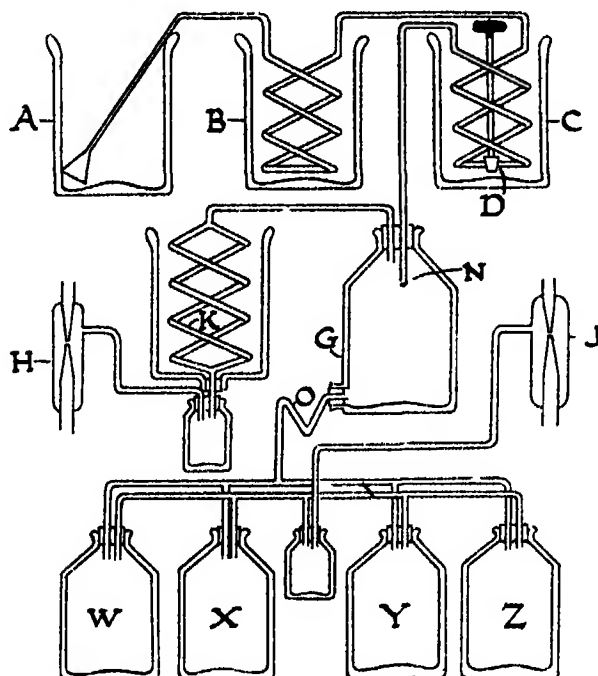


FIG 1

(γ) *The Ammonium Sulphide Method*—For experiments in the alkaline range, i.e., $p_{\text{H}} 10$ and above, the reduced hæmoglobin solution could be very readily prepared by adding 1 per cent ammonium sulphide to oxyhæmoglobin solution. After a lapse of half an hour or more (according to the temperature) the reduction was found to be complete, and control experiments, to be described later, showed that at $P_{\text{H}} > 10$, the presence of the ammonium sulphide caused no error.

(C) *The spectroscopic determination of the ratio of O_2Hb concentration to Red Hb concentration at various positions in the observation tube*—The calibration of the reversion-spectroscope for the measurement of ratio $\frac{\text{O}_2\text{Hb}}{\text{Red Hb}}$

was carried out in the manner which we have previously described (1), namely, by determining the position of the absorption bands formed by an auxiliary solution of COHb and a series of known optical mixtures of O₂Hb and Red Hb, such a series being readily obtained by having the O₂Hb and Red Hb in the two compartments of a double wedge-trough. A similar method was used by one of us in 1912 (5) for obtaining the calibration curve for the estimating of the composition of mixtures of O₂Hb and COHb. The validity of the procedure was, in the latter case, submitted to a very crucial test, namely, the comparison of the ratio $\frac{O_2Hb}{COHb}$ as obtained from the spectroscopic measurements and the calibration curve with the value of the ratio $\frac{O_2Hb}{COHb}$ as obtained with the same solutions by means of an entirely independent method, *i.e.*, the blood gas pump. Over a wide range of values of ratio $\frac{O_2Hb}{COHb}$ good agreement was obtained.

We thought it desirable to apply a similar check to the present method by comparing the values of ratio $\frac{O_2Hb}{Red\ Hb}$ obtained by its aid with the values of ratio $\frac{O_2Hb}{Red\ Hb}$ as obtained by an entirely independent method. The usual methods of blood gas analysis are not sufficiently accurate for determining independently the percentage saturation of dilute hæmoglobin solutions, and we therefore had recourse to a method similar in principle to that adopted by Haldane and Douglas for the calibration of their carmine titration method for estimating carboxy-hæmoglobin (6). The details of the procedure were as follows —

(a) A considerable quantity of reduced hæmoglobin solution (blood 1 in 60) was prepared by the physical reduction method described on page 655.

(b) Part of this solution was aerated, and a known volume of the reduced hæmoglobin was mixed anaerobically with a known volume of the aerated hæmoglobin solution by means of a mercury reservoir and a burette of capacity 130 c.c. graduated in tenths of a cubic centimetre between 100 c.c.

(c) One limb of the tap at the head of the burette was then connected to a lead entering the trough T. The latter and its connections were then filled with commercial N₂ so as to minimise the loss (or gain) of O₂ by the hæmoglobin solution when it was driven into the trough by opening the burette tap and raising the mercury reservoir.

(d) After about 50 c.c. of the hæmoglobin solution had been driven through

the trough the connections of the latter were clamped off and the percentage O_2Hb in the trough determined spectroscopically in the usual manner

(e) The O_2 -contents of the reduced hæmoglobin solution and the aerated hæmoglobin solution were estimated by the method described upon pp 660-2. With this information it is easy to calculate the total quantity of O_2 per cubic centimetre in the mixture prepared in (b)

(f) An independent value for the percentage oxy-hæmoglobin is given by the equation--

$$\text{Percentage } O_2Hb = \frac{\frac{(\text{Total quantity of } O_2 \text{ per cubic centimetre of solution}) - (\text{Quantity of } O_2 \text{ in physical solution per cubic centimetre})}{(\text{Total gas combining capacity of hæmoglobin per cubic centimetre of solution})}}$$

It only remains, therefore, to mention -

(g) The determination of total gas-combining capacity of the hæmoglobin This was carried out in the manner described on pp 660-2

(h) The quantity of O_2 in physical solution per cubic centimetre

This was usually very small in comparison with the total quantity of O_2 per cubic centimetre It was estimated indirectly in the following manner -

Samples of the hæmoglobin solution were shaken up with gas mixtures containing known small partial pressures of O_2 The percentage O_2Hb was measured SPECTROSCOPICALLY in each case, and a curve was plotted relating percentage O_2Hb as measured SPECTROSCOPICALLY and the oxygen pressure in the gas phase With the aid of this curve, and of the solubility coefficient of O_2 , it was possible to calculate the quantity of O_2 in physical solution corresponding to a given value of the percentage O_2Hb as measured SPECTROSCOPICALLY The latter had already been determined for the solution in (d) The whole procedure was then repeated for each of a series of different mixtures, it being unnecessary, however, to redetermine the total gas-combining capacity of the hæmoglobin per cubic centimetre, since this is in all cases the same. The results obtained are shown in the following table.--

Table I

Percentage O_2Hb determined --

(1) SPECTROSCOPICALLY ..	22.5	36	53	65
(2) By method of mixtures .	20.6	33	49	58.5*

* This determination was rendered somewhat inaccurate by the fact that the aerated hæmoglobin solution had to be introduced into the mixing burette in two instalments.

It will be observed that the spectroscopic values are slightly, but consistently, higher than the calculated values. Any error in determining either (i) the total gas-combining capacity of the hæmoglobin or (ii) the position of the absorption band of the 100 per cent O_2Hb solution would lead to a systematic discrepancy between the two sets of values, exactly like that shown in the above table. In view of this consideration, the agreement is as good as could be expected.

(D) *The Rate of Linear Flow*

$$= \frac{\text{Volume of fluid passing through the apparatus per second}}{\text{Cross-sectional area of the observation tube}}$$

In all the experiments in this paper rates of not less than 4 metres per second were invariably required. Consequently, it was always necessary to apply (by means of compressed nitrogen) a pressure of 50 mm Hg pressure to the two solutions in order to drive them through the apparatus fast enough. Diagrams of the apparatus used for most of the present experiments are shown in fig. 2 (A, B, C).

(E) *The total amount of (i) Oxygen, (ii) Hæmoglobin in the mixed solution* — These could be readily calculated from a knowledge of

(α) The relative delivery of the two solutions into the apparatus

This was measured by noting the actual volume of fluid lost by each bottle during the same interval. In order that the relative deliveries should remain constant during an experiment, it was found necessary to insert large filters in between each of the bottles and the mixing chamber.

(β) *The concentration of dissolved O_2 in Solution I* — The actual concentration of dissolved oxygen was estimated either—

(i) From the pressure of O_2 in the gas-phase with which the water was equilibrated and the Tables of solubility coefficients for O_2 in water (accurate to 1 per cent) or

(ii) By shaking about 200 c.c. of the water in a gas sampling tube with a 10 c.c. gas-phase consisting of O_2 free nitrogen and by analysing the gas phase afterwards for O_2 . The experimental details and the calculations involved in this method are to be described in full in a forthcoming paper.

(γ) *The concentration of hæmoglobin in Solution II.*—The gas-combining capacity of the dilute hæmoglobin solution was determined in one of three ways —

(i) By means of the Haldane-Gowers hæmoglobinometer

- (u) By aerating some of the hæmoglobin solution and mixing a known volume thereof with a known volume of water containing CO in solution,

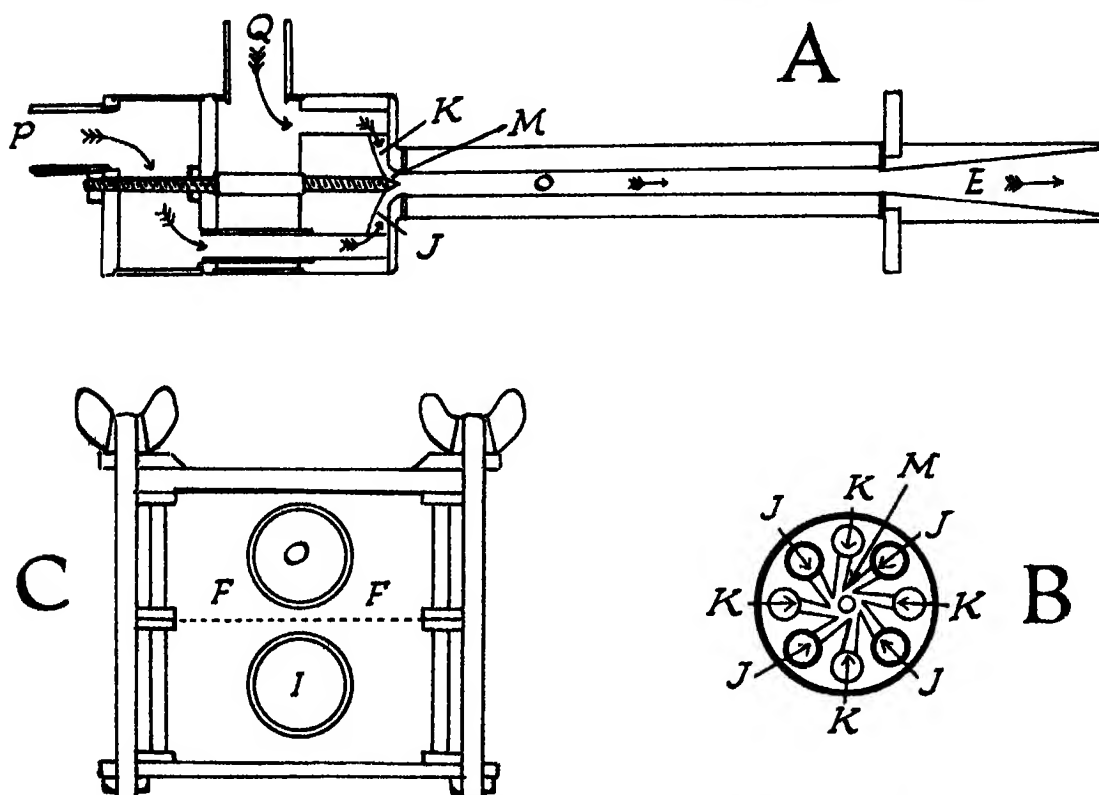


FIG 2—A Diagrammatic longitudinal section of the mixing apparatus principally used for the work recorded in this paper. The reduced hæmoglobin and the oxygenated water enter respectively through the pipes P and Q. They are then forced through the four jets J and the four jets K respectively, and enter the mixing chamber M, from which they pass immediately into the observation tube O, to flow finally out at the exit E.

B Arrangement of the jets J and K with regard to the mixing chamber.

C Arrangement of the two filter boxes through which the fluids passed on their way from the bottles to the apparatus. Fluids enter at I, pass through the copper or brass gauze F, and leave again at O.

The thumb nuts enable the apparatus to be readily taken to pieces for cleaning and to be assembled again afterwards.

so that the final percentage COHb was about 70 per cent. The actual value of the percentage COHb was determined by means of the reversion spectroscope, and with a knowledge of the exact amount of CO dissolved in the water (obtained by titrating the CO water with a hæmoglobin

solution of known gas-combining capacity) it was easy to calculate the gas-combining capacity of the unknown hæmoglobin solution.

This method is about as accurate as the hæmoglobinometer method, but has the advantage of being applicable in artificial light as well as in daylight

- (iii) By shaking about 200 c c of the hæmoglobin solution in a gas sampling tube with a 10 c c gas phase containing an accurately known volume of CO. Analysis of the gas phase after equilibration gave the amount of residual CO in the gas phase, and the amount required to saturate the hæmoglobin could then be calculated in a manner to be described in another paper

This method could be made at least twice as accurate as (i) or (ii), and had the further advantage that it avoided any error which might have arisen through partial inactivation (and therefore loss of gas-combining capacity) of the hæmoglobin, which could not always be avoided in such dilute solutions

II —(i) THE ADEQUACY OF THE REACTION VELOCITY APPARATUS FOR COPING WITH SUCH RAPID REACTIONS

Preliminary tests showed that the reaction was a very rapid one, indeed, the time required for half-completion being in most cases between 1/100th and 1/1000th of a second. The adequacy of the apparatus for coping with such fast reactions had only previously been tested by us for the special case of monomolecular reactions (2), and it was pointed out that the same test (i.e., the

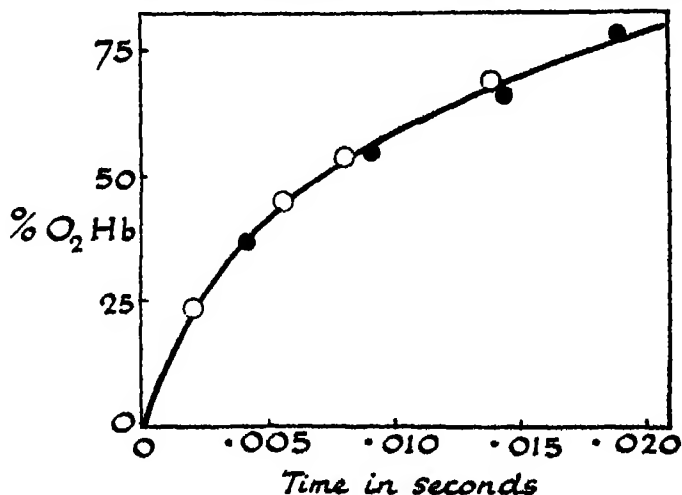


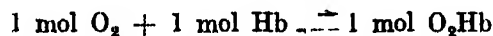
FIG. 3.

comparison of the results obtained with two widely different rates of flow) must always be repeated whenever a reaction of another type is being submitted to investigation. Fig 3 shows the results arrived at in such a test, the shaded circles representing readings obtained with a slow rate of linear flow (96 cms./sec) and the blank circles representing the readings obtained with a fast rate of linear flow (333 cms/sec). The two reacting solutions were in each of the experiments identical. The agreement between the two sets of values is extremely satisfactory, and left us no doubt that the apparatus was quite reliable, even when the time for half-completion of the reaction was only 0.002 seconds.

We also applied a much more stringent test for the velocity of mixing by means of a special thermal apparatus. Mixing was found to be complete in 0.0005 seconds. Details of this test have been given elsewhere (3).

II—(1) THE ORDER OF THE REACTION

In applying the Law of Mass Action to the interpretation of the results, we made, in the first place, the simplest possible assumption, namely, that of Hufner, viz., that the reaction could be expressed by the equation



On this assumption the rate of formation of O₂Hb should be given by the equation

$$\frac{d(\text{O}_2\text{Hb})}{dt} = k' (\text{O}_2) (\text{Hb}) - k (\text{O}_2\text{Hb}) \quad (\text{A})$$

or

$$\frac{dy}{dt} = k' (\alpha - y) (\beta - y) - ky, \quad (\text{B})$$

where α = Millimols* of O₂ per litre of solution both in physical solution and in reversible combination with Hb

β = Total gas-combining capacity of Hb per litre of solution expressed in millimols O₂

y = millimols of O₂ reversibly combined with Hb per litre of solution

In order to determine the value of k' by integration of this equation it is necessary also to know the value of k . This was always obtained by a separate reduction velocity experiment (1). The subsequent calculation of k' then depended upon whether the value of the second term of equation (B), i.e., $-ky$, could or could not be neglected over the range through which the calculation was made.

* 1 millimol = 1 mol \div 1000.

When the value of $-ky$ can be neglected, equation (B) simply integrates to

$$k'(t-t_0) = \frac{1}{\alpha - \beta} \left[\log_e \left[\frac{\alpha - y}{\beta - y} \right] \text{ at } t_0 - \log_e \left[\frac{\alpha - y}{\beta - y} \right] \text{ at } t \right],$$

and the value of k' can at once be calculated by substituting the experimental values of α , β , t and y in this equation

When, however, the value of $-ky$ is appreciable in comparison with dy/dt a more complicated procedure is necessary. We have

$$dy/dt + ky = k'(\alpha - y)(\beta - y),$$

$$e^{kt} \left(\frac{dy}{dt} + ky \right) = k' e^{kt} (\alpha - y)(\beta - y),$$

$$\text{i.e., } d/dt (e^{kt} y) = k' e^{kt} (\alpha - y)(\beta - y),$$

$$e^{kt} y = k' \int e^{kt} (\alpha - y)(\beta - y) + \text{constant}$$

From the experimental values of α , β , y , t and k (as determined by the separate reduction velocity experiment) the values of $e^{kt}(\alpha - y)(\beta - y)$ were calculated and plotted against t

Thus, if in such a graph, A be the area included between the curve, the t -axis and the ordinates to the curve at the points whose abscissæ are t_1 and t_2 , then

$$e^{kt_1} y_1 - e^{kt_2} y_2 = k' A,$$

$$k' = \frac{e^{kt_1} y_1 - e^{kt_2} y_2}{A}$$

It was found that the values of A could be determined with sufficient accuracy by means of the trapezoidal rule for evaluating areas

If, then, the assumption $1 \text{ mol O}_2 + 1 \text{ mol Hb} \rightleftharpoons 1 \text{ mol O}_2\text{Hb}$ were valid, the values of k' , as calculated by one of the above methods, should come out the same within the limits of experimental error both for all the points obtained in a given experiment and also for points obtained in other experiments with varying initial concentrations of O_2 and Hb , provided that the p_{H} , temperature and source of hæmoglobin were maintained constant. Tests of this kind were carried out both in the neighbourhood of $p_{\text{H}} 7.2$, and also in the neighbourhood of $p_{\text{H}} 10-11$. The reason for two sets of tests is that, in a brilliant series of experiments published recently, Van Slyke and his co-workers (4) have shown that the ionisation-constant of the "oxy-labile" hydrogen ion which dissociates from the hæmochromogen portion of the molecule has, in the case of reduced hæmoglobin, a value of 10^{-8} , so that at $p_{\text{H}} 7.2$ practically all the

reduced hæmoglobin molecules must retain their "oxy-labile" hydrogen ion, whereas at p_H 10-11 the opposite must be the case. The presence or absence of the "oxy-labile" hydrogen ion was found to have such a marked effect upon the rate of reduction of oxy-hæmoglobin that it seemed desirable to carry out all our tests on the rate of combination of oxygen with hæmoglobin, both at p_H 7.2 (where "oxy-labile-un-ionised" hæmoglobin predominates) and at p_H 10-11 (where "oxy-labile-ionised" hæmoglobin predominates)

Experimental Results at p_H 7.2, or near

The results of these experiments are summarised in Table II.

Table II.

No of Experiment	p_H	Temp	Concentration of O_2 in millimols/litre	Concentration of Hb in millimols/litre	k'	Mean value of k'
<i>Blood Sample I —</i>						
I(a)	7.7	17.5	0.165	0.151	2380, 3520	} 2975
I(b)	7.7	17.5	0.115	0.145	2690, 2910	
<i>Blood Sample II</i>						
II(a)	7.2	19.0	0.159	0.062	2910, 2760	} 2940
II(b)	7.2	19.0	0.301	0.078	2960	
II(c)	7.2	19.0	0.192	0.032	3180, 2990	

The hæmoglobin solutions for these five experiments were all prepared from two samples of different blood, the first of which furnished experiments IA and IB, whereas the second sample furnished experiments IIA, B and C. It will be observed that the calculated value of k' is not affected by doubling the O_2 concentration (Cp. IIA with IIB), nor by halving the Hb concentration (Cp. IIA with IIC). The constancy of k' is extremely satisfactory—better, indeed, than the accuracy of the experimental determinations would warrant us in expecting.

Experimental Results at p_H 10-11.

The reduced hæmoglobin solution required for these experiments was prepared by the very easy ammonium sulphide method mentioned in Section I. In order that the method should be efficacious it is necessary that the ammonium sulphide (α) should combine slowly but completely with all the oxygen present, both in physical solution and in reversible combination with the hæmoglobin, but (β) would not, when mixed suddenly with oxygenated water, combine with the dissolved oxygen at a rate appreciable in comparison with the rate at which the

latter combines with the reduced hæmoglobin, nor (γ) have any further chemical action upon the reduced hæmoglobin

That these requirements are met by ammonium sulphide is shown by the following evidence:—

(a) *Comparison of the Rate of Combination of O_2 and Hb with Rate of Reduction of O_2 Hb by Am_2S* —Reduced hæmoglobin solution was prepared by mixing about

3 parts whole blood

90 parts tap water

1 part ammonium sulphide (triple strength")

After standing at room-temperature for about half an hour the hæmoglobin was completely reduced

This solution was mixed with tap-water and the reaction velocity measured in

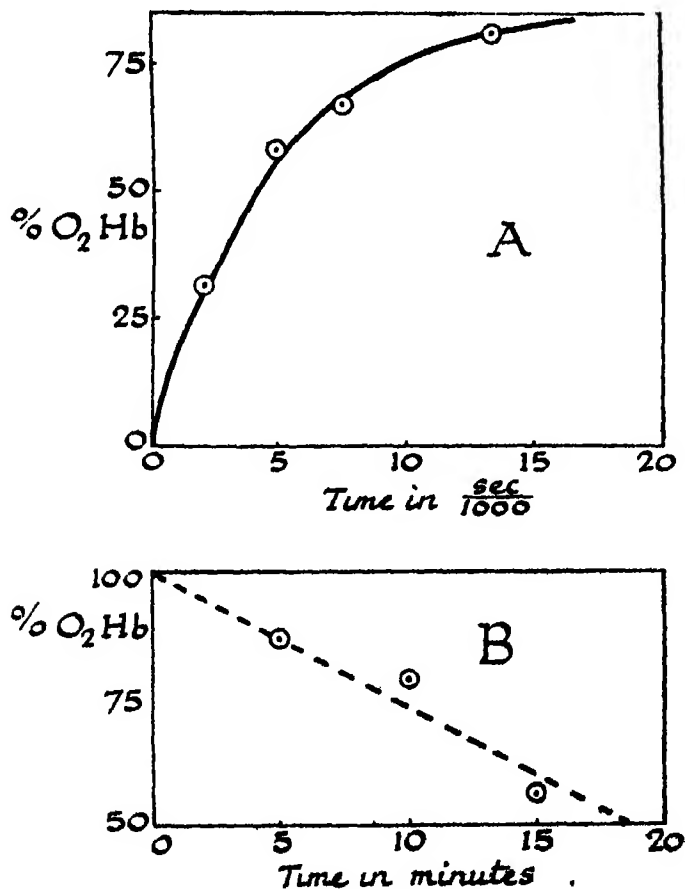


FIG. 4

the usual manner. The result is shown graphically in fig 4—A. The taps of the reagent bottles were then turned off suddenly and simultaneously, leaving in the observation tube a solution of oxyhæmoglobin and ammonium sulphide. The oxyhæmoglobin reduces so slowly that its rate can be easily followed by measuring the percentage O_2Hb with the spectroscope at intervals of five minutes. The rate of reduction is plotted in fig 4—B, and will be seen to be only about one hundred-thousandth of the rate at which oxyhæmoglobin is formed by combination of oxygen with reduced hæmoglobin.

(b) *The Effect of Different Concentrations of Ammonium Sulphide*—If the presence of ammonium sulphide had (α) any appreciable effect in retarding the combination of O_2 with Hb or (β) any chemical action on the hæmoglobin other than the removal of oxygen (e.g., the formation of "sulphhæmoglobin") then different results would be expected when varying amounts of ammonium sulphide were used in the preparation of the reduced hæmoglobin. Table III shows the results of experiments obtained with —

- (α) Solution I — reduced hæmoglobin containing $\frac{1}{2}$ per cent Am_2S Solution II = tap-water
 (β) „ I = „ „ „ 1 per cent Am_2S Solution II = tap-water
 (γ) „ I = „ „ „ 3 per cent Am_2S Solution II = tap-water

In each case solution I, after the addition of Am_2S , was allowed to stand half an hour before use.

The values obtained agree with one another within experimental error.

Table III —Percentage Oxyhæmoglobin

Time in Seconds	(α)	(β)	(γ)
0·00	0	0	0
0·0020	39	37	35·5
0·0048	59·5	59	64
0·0074	80	79	73

(c) *Comparison of Rate of Combination of O_2 with Physically Reduced Hb with Rate of Combination of O_2 with Chemically Reduced Hb*—Two samples of "physically reduced" Hb were prepared as above. The rate of combination of the first sample with oxygen was measured in the usual way. To the second sample Am_2S was added so as to make the concentration of Am_2S equal to

1 per cent After having been allowed to stand for half an hour, as in (b), the combination with O_2 was also determined The values obtained were within experimental error identical with those obtained on the first sample

(d) A determination of the gas-combining capacity of the dilute Hb solution was made both before the addition of Am_2S and after the latter had been allowed to act for several hours No difference at $p_H 10$ could be detected If, however, the solution were neutralised to $p_H 7.2$, then a speedy decline in the gas-combining capacity of the hæmoglobin ensued and a body with an absorption band in the red part of the spectrum made its appearance For this and other reasons the use of the ammonium-sulphide hæmoglobin was limited to the $p_H 10-11$ experiments The results of the experiments at $p_H 10-11$ are summarised in Table IV

Table IV

No of Experiment	p_H	Temp	Concentration O_2 in millimols/litre	Initial Concentration Hb in millimols/litre	k'	Average value of k'
Blood Sample I —		° C				
I(a)	10	13	0.330	0.145	2620, 1980	} 2090
I(b)	10	13	0.151	0.157	2150, 1610	
Blood Sample II —						
II(a)	10-11	15.1	0.100	0.112	6070, 6420	} 6150
II(b)	10-11	15.1	0.118	0.055	5970	
Blood Sample III —						
III(a)	10-11	15.0	0.394	0.112	3610	} 3145
III(b)	10-11	15.0	0.251	0.112	2680	

Again there is good agreement between the values obtained with different concentrations of the reacting substances, provided that the comparison is only made in cases in which the hæmoglobin solutions were prepared from the same sample of blood

III THE RELATION BETWEEN THE VELOCITY-CONSTANTS AND THE EQUILIBRIUM-CONSTANT OF THE REACTION $O_2 + Hb \rightleftharpoons O_2Hb$

A further and very crucial test both of the correctness of the equation $\frac{d(O_2Hb)}{dt} = k'(O_2)(Hb) - k(O_2Hb)$, and of the general validity of the experimental methods employed in this paper and preceding papers, was obtained by comparing the value of the equilibrium-constant of the reaction as calculated from the dissociation curve of the hæmoglobin solution in question

(which, if the above assumption is true, must be a rectangular hyperbola) with that obtained from the equation $K = \frac{\text{observed value of } k'}{\text{observed value of } k}$.

The Determination of the Dissociation Curve

General Method A few cubic centimetres of the hæmoglobin solution, whose dissociation curve was required, were introduced into a tonometer which had previously been filled with a gas mixture containing a suitable, and accurately measured, proportion of oxygen. The tonometer was rotated until equilibrium had been secured, and the ratio of $\frac{O_2Hb}{\text{Red } Hb}$ in the hæmoglobin was thereupon measured by means of the reversion spectroscope. The same procedure was then repeated with other proportions of oxygen in the gas phase. Thus the determination was carried out in accordance with the usual methods of blood-gas technique, but in order to obtain reliable results a considerable number of precautions were found to be essential. These will now be described in some detail.

(a) The Preparation of the Gas Mixtures

In most cases it is necessary to prepare gas mixtures containing very low partial pressures of O_2 (i.e., 0.1 to 0.5 per cent atmosphere), and to ascertain the numerical values of the latter with an accuracy of at least one part in a hundred. These requirements were satisfactorily met by replacing the air in the tonometer by O_2 -free nitrogen and by then forcing into the tonometer a small, but accurately-measured, quantity of ordinary air. From the volume of the latter, together with a knowledge of (i) the volume of the tonometer, (ii) the barometric pressure, and (iii) the O_2 per cent in the air used, i.e., 20.96, the final pO_2 in the tonometer was readily calculated.

(i) *The Preparation of the O_2 -free Nitrogen* The last traces of O_2 were removed from commercial N_2 by allowing the latter to stand for at least one day over a concentrated solution of alkaline sodium hydrosulphite ($Na_2S_2O_4$). The container and its connections, when not in use, were kept under water in order to guard against possible entry of atmospheric oxygen by leakage. Samples of the gas were at different times tested for traces of O_2 , but when once the technique had been mastered the results were always negative, so long as this was rigidly adhered to.

(ii) *The Filling of the Tonometer with O_2 -free Nitrogen*—The tonometer was first evacuated and filled with commercial N_2 , and evacuated again. It was then filled with the nitrogen whose purification has just been described,

evacuated a third time, and finally filled once more with the specially purified N_2 . The residual oxygen in the tonometer cannot have exceeded 0.001 per cent., a quantity which can be neglected in these experiments.

(iii) *The Introduction of the Known Volume of Ordinary Air*—The capacity of the tonometer which has been most used is 120 c.c., and the volumes of air to be introduced, therefore, range from 0.5 c.c. upwards. For this purpose a micro-burette and mercury reservoir of the same general design as that used by Barcroft (7) were found convenient. The volumes of air are measured off at atmospheric pressure (precautions having been taken to ensure that the air under measurement is saturated with water vapour at laboratory temperature) and then forced by mercury pressure into the tonometer. The burette which was used could be read without difficulty to 0.001 c.c. and was thus amply accurate enough.

(b) *The Introduction of the Hæmoglobin Solution into the Tonometer*

Having first had its gas-combining capacity measured in the usual way, the hæmoglobin was then shaken up with atmospheric air in order that the total amount of O_2 in each c.c. of the solution should be definitely known. A measured volume (usually 5 c.c.) of the hæmoglobin solution was then forced into the tonometer, and the quantity of O_2 which thereby enters, i.e., about $5 \times 0.008 = 0.04$ c.c., is allowed for in calculation of the final pO_2 in the tonometer, the accuracy of which is not appreciably affected by this correction.

(c) *The Rotation of the Tonometer*

The tonometer was fixed to a shaft which rotated in a water-bath at constant temperature. Up to the present the experiments have been done at laboratory temperature, but when other temperatures are used then thermostat arrangements will be necessary.

Control experiments showed that fifteen minutes' rotation was sufficient to secure equilibrium.

(d) *The Examination of the Solution after Equilibrium had been obtained*

In order to examine the hæmoglobin solution *in situ* (i.e., without removal from the tonometer, which is difficult to carry out anaerobically) a glass tube of diameter 1.2–1.3 cms. was either fused or attached by wide rubber tubing to the open end of a Barcroft tonometer. The tonometer, after having been rotated for a sufficient length of time (15 minutes), was unstrapped from the shaft and lowered, tap uppermost and tube downwards, through the hole in

the cork in the container W, until the bottom of the tonometer rested in the metal sheath M fixed to the base of the container (fig 5) The tonometer

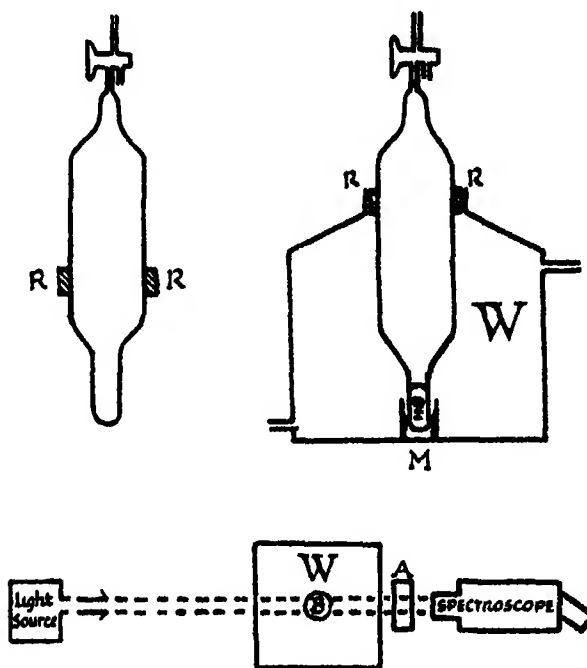


FIG 5

fitted closely in the hole in the cork, and thus together with the metal sheath M, ensured that the tonometer would take up an "identical" position each time it was inserted into W. The latter having been filled with water and an auxiliary trough containing COHb set in place, the spectroscopic examination was then carried out.

In view of the considerable effect of change of temperature upon the dissociation curve, it was necessary to maintain the Hb solution during the spectroscopic examination at the same temperature as the water-bath in which the tonometer had been rotated, otherwise (in these dilute solutions) considerable alterations in the percentage O_2Hb might occur.

(e) *The Number of Tonometers used and the Accuracy of the Observations*

The determination of the percentage O_2Hb of a given solution always required two spectroscopic readings.—(α) for the actual solution itself, and (β) for the same solution when saturated with O_2 . Each of these readings was subject to an experimental error of 1 A.U. Consideration showed that the use of a

single tonometer for all the points on the dissociation curve would yield more accurate results when the hyperbolic character of the dissociation curve was being tested, whereas a separate tonometer for each point was indicated when the absolute value of K was required. The reason for this statement is as follows :—

In the hyperbolic test, an error of 1 A.U. in the single spectroscopic reading for 100 per cent O_2Hb would cause a systematic error in all the values of the percentage O_2Hb as calculated for the several points obtained (i.e., they would all be either too high or too low), but if these points fell within experimental error on a rectangular hyperbola when they were calculated on the basis of the incorrect reading for 100 per cent O_2Hb then they would still fall (within experimental error) on another rectangular hyperbola when calculated on the correct basis. A single tonometer therefore gave the greater accuracy in determining the actual *shape* of the dissociation curve. Similar reasoning showed that for determining the true *position* of the dissociation curve (and therefore the absolute value of the equilibrium-constant) a series of tonometers, one for each point to be obtained, gave the more accurate result.

In the hyperbolic test, the volume of the first instalment of air forced into the tonometer was so adjusted that the percentage O_2Hb reached should be about 30 per cent. After equilibrium had been attained, and the spectroscopic measurement made, a further instalment of air was introduced, equilibration completed, and a second spectroscopic measurement made. This process was repeated once or twice more, the highest point not being allowed to exceed 75 per cent, on account of the limitations to the accuracy of the spectroscopic method mentioned previously (1). Finally, it was necessary to obtain the spectroscopic reading for the Hb solution when saturated with O_2 . This was readily obtained by replacing the gas mixture in the tonometer by ordinary air and shaking up the Hb solution therewith.

In determining the absolute value of K , suitable quantities of O_2 were introduced into the several tonometers so as to yield a series of values of percentage O_2Hb between 30 per cent and 70 per cent after equilibration, the spectroscopic readings were then made, the gas replaced by atmospheric air, and the readings for 100 per cent O_2Hb taken for each tonometer.

(f) *Decomposition of the Hæmoglobin Solution*

It has been pointed out by Douglas, Haldane and Haldane (8) that hæmoglobin in dilute solution is very prone to decompose into hæmatin-like products. The gas-combining capacity of the hæmoglobin solution at the end of the deter-

mination of the dissociation curve should therefore, in all cases, be compared with the gas-combining capacity at the outset of the experiment. No detectable change has been found at p_H 7.4 and temperatures below 18° C. At p_H s acid to 6.4 and temperatures above 25° C marked decomposition has, however, been noticed, and it is probable that the present method will not be applicable in such ranges.

Experimental Results

(a) *The Hyperbolic Character of the Dissociation Curve*—The results obtained on a haemoglobin solution at p_H 7.7, temp 17.5, are plotted in fig. 6. It will

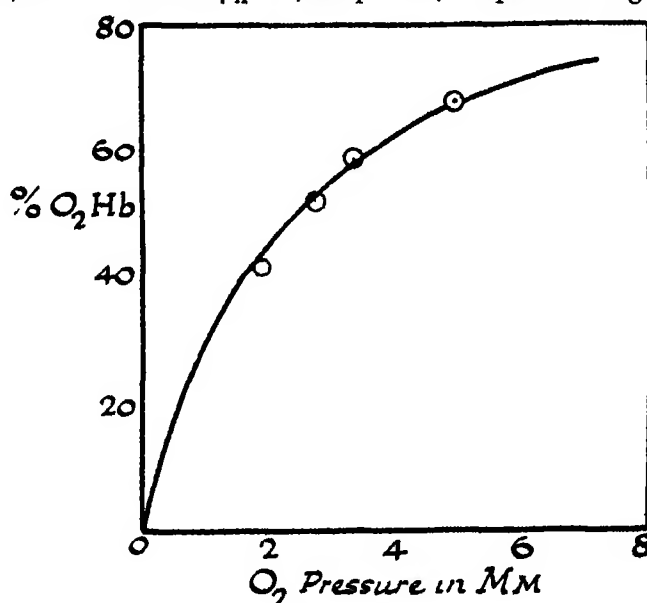


FIG. 6

be seen that the values fall very closely upon a rectangular hyperbola. The actual values of K , as calculated from the equation

$$K = \frac{\text{concn } O_2Hb}{\text{concn } Hb \times \text{concn dissolved } O_2 \text{ in millimols/litre'}}$$

are shown in Table V.

Table V

pO_2 in mm =	1.89	2.16	3.32	4.95
Percentage O_2Hb	42	52.5	59	68
K	201	218	228	226
Mean value of $K = 218$				

The agreement between the above values lies well within the experimental error

(β) *The Comparison of K with k'/k .*—The results of four such comparisons are summarised in Table VI

Table VI

No of Exp	p_H	Temp	Mean value of k'	Mean value of k	Value of k	
					Calculated from $k = k'/k$	Observed from dissociation curve
I	7.7	17.5	2875	17.5	164	218
II	7.2	18.9	2550	17.3	148	112
III	10.0	15.1	3145	4.5	700	730
IV	10.0	17.3	3540	8.1	438	130

In view of the fact that the values of k' , k and K were subject individually to possible experimental errors of ± 20 per cent., ± 10 per cent., and ± 15 per cent. respectively, the agreement is a good deal better than we had expected to obtain

IV—THE EFFECT OF P_H , TEMPERATURE, AND OTHER FACTORS

(1) *The Effect of P_H* —The results of a set of experiments at different P_H s are shown in Table VII. The Hb solutions were all prepared from the same sample of blood by means of the vacuum-spray method, and were found on examination to be completely reduced in every case. The different P_H s were obtained by adding suitable buffers to the aerated water with which the reduced Hb solution was subsequently mixed in the reaction velocity experiments.

In our previous paper on the rate of reduction of oxyhæmoglobin (1) we showed by control experiments that the inter-ionic changes of oxyhæmoglobin were too rapid to have any influence on the observed reduction velocities. A similar pair of control experiments, in which the constituents of the buffer were so distributed between the solutions that in one case the p_H of the hæmoglobin solution before mixture was the same as the p_H of the final mixture, whereas in the other case there was a large change, showed that the inter-ionic changes of reduced hæmoglobin were also too rapid to affect appreciably the observed oxygenation velocities.

The concentration of O_2 and of Hb in the mixed fluid were in all the experiments practically identical, so that the effect of p_H can be at once

Table VII

Time in seconds	$p_H = 5.8$	6.6	7.2	7.7	9	10
0*				25.5		
0.001	Percentage O ₂ Hb = 33	29	37.5	42	48	41.5
0.001		42	40	48	63	54.5
0.003		55	50.5			
0.004			56	(6)	75	64
0.005				69		
0.006						

* = Earliest reading obtainable

appreciated by mere inspection of the table. Unlike the effect on the reduction velocity-constant k , the effect of p_H on k' appears to be quite small, and the onus of accounting for the effect of p_H on the dissociation curve must fall mainly, if not entirely, upon the reduction velocity-constant. In one respect, the absence of any noteworthy effect of p_H is to be regretted. Had the difference between k' at p_H 7, and k' at p_H 10 been well outside the limits of experimental error, then it would have been possible, with the aid of the curve relating p_H and k' , to calculate the ionisation-constant for the dissociation of the oxylabile hydrogen ion from the haemochromogen portion of the reduced haemoglobin molecule, just as it was possible to calculate this ionisation constant for oxyhaemoglobin. Our value of the latter, *i.e.*, though necessarily much rougher, agrees very closely with the very accurate value obtained by an entirely independent method and subsequently published by Van Slyke and his co-workers. It would have been most interesting to see whether there would also have been the same agreement in the case of reduced haemoglobin, for which the value, according to Van Slyke, is $10^{-8.8}$ to $10^{-8.4}$. But the small effect of p_H on the velocity of oxidation of reduced haemoglobin makes such a comparison impossible.

(ii) *The Effect of Temperature and Light*—Different temperatures were obtained by cooling either or both of the solutions. In order that the effect of temperature should be at once discernible by inspection of the actual determinations, it was arranged that in all experiments on haemoglobin solutions prepared from the same sample of blood the total O₂ and total Hb in the mixed solutions should be constant. The results are summarised in Table VIII.

Table VIII

	p_H	Temp	At time = 0*		0 00185	0 00370 sec
Exp. No I	7.4	7° C	Percentage O ₂ Hb		59	75
	7.4	12° C			65	69
	7.4	17.5° C			60	72
Exp No II	P_H	Temp	$t = 0^*$	$t = 0.002$	0 00485	0 0077
	7.0	3.5	0	41.5	68	78
	7.0	14.5	0	42	63	83
Exp No III	P_H	Temp	$t = 0^*$	$t = 0.002$	0 00485	0 0077
	10	3.8	0	44	58	75
	10	14.5	0	36	63	81

* — Earliest reading obtainable

These figures point to the surprising conclusion that, both at neutral p_H s and alkaline p_H s, the temperature coefficient of k' per 10° C rise is little, if at all, greater than unity. Two explanations of this startling result occurred to us at once:—

- (α) That the mixing in our apparatus was not sufficiently rapid to enable the reaction to be properly followed. This possibility, however, was excluded by the fact that the time for half-completion in the case of all the reactions summarised in Table VIII was always greater than the figure for which the apparatus was shown to be reliable in Section II.
- (β) That the reaction might be a photo-chemical one, reactions of the latter type being often found to possess very low temperature coefficients (sometimes less than 1).

This possibility was tested by means of the arrangement shown in fig. 7. The first 2-cm. length of the observation tube could be illuminated either by the

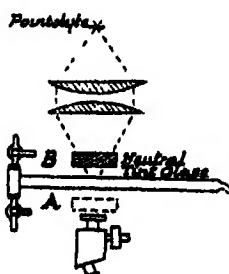


FIG 7

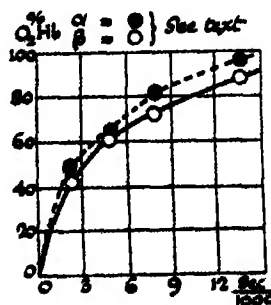


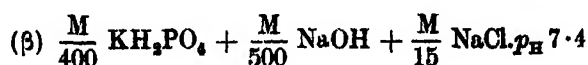
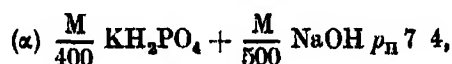
FIG 8

full beam of the 500 candle-power pointolyte lamp (with the neutral-tint glass in position A) or by a beam of only one-tenth intensity (neutral-tint glass

in position B) In both cases the spectroscope and the COHb auxiliary trough were placed between the eye of the observer and the neutral tint-glass, so that the COHb trough and spectroscope should be only illuminated by the one-tenth intensity beam Spectroscopic readings on the moving fluid were taken with neutral-tint glass in position A, the latter was then transferred to B and a fresh reading taken If light had any catalysing influence upon the reaction, then a different reading should have been obtained In actual fact, no difference could be found either at p_H 7 or at p_H 10, in spite of the fact that the procedure was repeated many times and that the observer did not know the position of the neutral-tint glass

A further experiment, in which a dilute Hb solution was equilibrated with N_2 gas phase containing about 0.4 per cent O_2 (α) in the dark and (β) in the pointolyte beam (with precautions to prevent rise of temperature due to the latter), showed that light also had no appreciable effect upon the equilibrium-constant of the reaction We have thus found no explanation for the very low temperature coefficient Its probable significance will be discussed again in Section V

(iii) *The Effect of Salts, i.e., of Ions other than H^+ or \bar{OH}* —Fig. 8 shows the results obtained with two widely differing concentrations of salt A solution of reduced hæmoglobin, prepared by the physical method, was mixed with aerated tap-water containing



The difference between the two sets of values which were obtained is very slight—barely, indeed, outside the limits of experimental error

(iv) *The Variability of Hæmoglobin in different Individuals of the same Species*.—Although the hæmoglobin solutions used in the experiments were all prepared from sheep's blood, the value of the velocity constant k' varied over a wide range, i.e., 6,200–1,000, thus confirming the remarks of previous writers who have commented upon the specificity of each individual's hæmoglobin

(v) *Physiological Application of the Results*—The main physiological interest of the results centres round the question "Can the combination of O_2 with the hæmoglobin in the red-blood corpuscles proceed so fast as not to retard, to an appreciable extent, the entry of oxygen into the blood as it passes through

the lung capillaries? Calculations, based on the values of the velocity-constants obtained in this paper (which have not, as yet, however, been proved by experiment to be valid for the highly concentrated Hb solutions in the red-blood corpuscles) indicate that under most circumstances the answer to this question is in the affirmative. The full details of the assumptions involved are to be given later in a paper by one of us.

V—FURTHER CONSIDERATIONS IN REGARD TO THE CHEMICAL KINETICS OF THE REACTION

(A) *The possible Existence of Aggregates in Solution*—The assumption that the reaction can be expressed by the equation $1 \text{ mol O}_2 + 1 \text{ mol Hb} \rightarrow 1 \text{ mol O}_2\text{Hb}$ was submitted to experimental verification and survived a considerable number of tests in Section II. In order, however, that such an assumption should be justifiable, it is *prima facie* essential that the molecule both of hæmoglobin and of oxyhæmoglobin should only contain one atom of iron, since, as Peters (9) has shown, the number of molecules of oxygen with which hæmoglobin can combine is equal to the number of atoms of iron which it contains. The molecular weight of hæmoglobin, in the event of there being only one atom of iron in the molecule, should amount to about 16,700, but recent measurements of osmotic pressure by G. S. Adair* go to show that the molecular weight, both of hæmoglobin and of oxyhæmoglobin, in dilute solution must be about 66,700. Adair therefore concludes that hæmoglobin and oxyhæmoglobin must both be present in the form of aggregates, which may be written Hb_4 and $(\text{O}_2\text{Hb})_4$ (where Hb and O_2Hb refer respectively to the equivalent weight, i.e., that weight which contains one atomic weight of iron) and that a partially saturated solution of hæmoglobin might not only contain $(\text{Hb})_4$ and $(\text{O}_2\text{Hb})_4$ but also contain aggregates of intermediate composition, i.e. $[\text{Hb}(\text{O}_2\text{Hb})_3]$, $[\text{Hb}_2(\text{O}_2\text{Hb})_2]$, $[\text{Hb}_3\text{O}_2\text{Hb}]$.

Even in this contingency we can, with the aid of a few additional and by no means improbable assumptions, arrive at the equation which was found satisfactory in Section II, namely,

$$\frac{d(\text{O}_2\text{Hb})}{dt} = k'(\text{O}_2)(\text{Hb}) - k(\text{O}_2\text{Hb})$$

(1) The test described in Section I showed that the α -absorption band of a single solution, which was ascertained by independent means to contain x equivalents of oxyhæmoglobin and $100-x$ equivalents of reduced hæmoglobin,

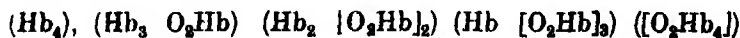
* Communicated privately to the Authors

was identical in position with the α -band of an optical mixture of two solutions containing x parts of fully saturated oxyhæmoglobin and $100-x$ parts of reduced hæmoglobin respectively, for several different values of x . We must therefore conclude that the reversion spectroscopy does give us the

$$\frac{\text{total number of "equivalents" of } (O_2Hb)}{\text{total number of "equivalents" of Hb}}$$

in any given solution whether these equivalents are combined together in aggregates or are separate from one another

Let us take a particular case for the sake of illustration. Suppose that all the hæmoglobin is present in aggregates containing four equivalents, *i.e.*, that we may have in solution



Then the total rate at which the number of equivalents of O_2Hb will increase will be given by an equation

$$\begin{aligned} \frac{d(O_2Hb)}{dt} = & (O_2) \{ k'_4(Hb)_4 + k'_3(Hb_3[O_2Hb]) + k'_2(Hb_2[O_2Hb]_2) + k'_1([O_2Hb]_4) \} \\ & + k_4([O_2Hb]_4) + k_3(Hb \cdot [O_2Hb]_3) + k_2(Hb_2 \cdot [O_2Hb]_2) \\ & + k_1(Hb_3[O_2Hb]) \} \end{aligned}$$

provided that the chances of two or more oxygen molecules combining or dissociating SIMULTANEOUSLY from an aggregate are so small as to be negligible. Now if

- (a) the portions of each Hb and O_2Hb grouping which combine together to form aggregates are sufficiently far removed from that part of the hæmochromogen grouping which combines with O_2 . And if, also,
- (b) the O_2 molecule must hit this sharply localised part of the hæmochromogen grouping in order that a combination should take place,

then it is not unreasonable to suppose that the chance of an O_2 molecule combining with an Hb_4 aggregate (which has four "free spaces") is four times greater than the chance of an O_2 molecule combining with an $Hb \cdot [O_2Hb]_3$ aggregate (since the latter has only one "free space") and, therefore, that

$$\frac{k'_4}{4} = \frac{k'_1}{1} = \text{on similar grounds } \frac{k'_2}{2} = \frac{k'_3}{3}$$

For the same reasons it may be plausibly assumed that

$$\frac{k_4}{4} = \frac{k_3}{3} = \frac{k_2}{2} = \frac{k_1}{1}.$$

$$\begin{aligned}
 &\text{On these suppositions, therefore, } d/dt \text{ (total number of equivalents of } O_2Hb) \\
 &= k'_1 (O_2) \{ 4 (Hb_4) + 3 (Hb_3[O_2Hb]) + 2 (Hb_2[O_2Hb])_2 + (Hb.[O_2Hb])_3 \} \\
 &\quad - k \{ 4 ([O_2Hb]_4) + 3 (Hb [O_2Hb]_3) + 2 (Hb_2 [O_2Hb]_2) + (Hb_3[O_2Hb]) \} \\
 &\text{or } d/dt \text{ (total number of equivalents of } O_2Hb) \\
 &= (O_2) k'_1 \text{ (total number of equivalents of Red Hb)} \\
 &\quad - k_1 \text{ (total number of equivalents of } O_2Hb)
 \end{aligned}$$

It is not difficult to see that similar assumptions as to the relations between the velocity constants lead to exactly the same equation, whatever the number of equivalents present in the aggregate. Nor is it necessary that all the aggregates should contain the same number of equivalents.

(B) *The Temperature Coefficient of the Reaction*—The experimental tests described in Sections II and IV have forced upon us the conclusion that the absence of any appreciable effect of temperature on the reaction is a genuine phenomenon, and not due to any instrumental defects. It becomes necessary, therefore, to seek for some physico-chemical explanation of this interesting result.

It is true that the velocities of many chemical reactions hitherto studied have a temperature coefficient for 10°C of from 2 to 3, and at one time a process with a temperature coefficient little, if at all, greater than unity would have been unhesitatingly classified a "physical" one. Recent work, in particular that of Langmuir (10), has, however, shown that the distinction between "physical" and "chemical" processes is an illogical one. The measurements by Langmuir (10) of the rate of combination of CO with O_2 in the presence of heated platinum filaments provide a close analogy with those described by us in the present papers. Langmuir found that at temperatures between 500°C and 800°C , and in presence of excess of O_2 , the rate of combination of CO with O_2 was proportional to the presence of CO and practically independent of temperature. His theory was that under these circumstances the platinum filament became almost completely covered with a monomolecular layer of O_2 molecules, and that every collision between a CO molecule and an oxygen atom of this monomolecular layer resulted in the formation of a molecule of CO_2 . By means of Herz's equation (derived from the kinetic theory of gases) Langmuir calculated the actual number of such collisions, and compared therewith the observed rate of formation of CO_2 molecules. The agreement was as good as could be expected.

We suggest that a similar theory may be applicable to the combination of O_2 with haemoglobin. It is probable that combinations between O_2 and

hæmoglobin can only be brought about by those collisions in which the O_2 molecule strikes a certain sharply localised portion of the hæmochromogen grouping in the neighbourhood of the iron atoms. But if we assume that ALL such collisions result in combinations, then it is clear that the only way in which a rise of temperature could accelerate the reaction would be by increasing the actual number of collisions per second. Since, according to the kinetic theory of gases, the number of collisions per second is proportional to the square root of the absolute temperature, it will readily be seen that the temperature coefficient per $10^\circ C$ would, on this theory, only amount to about 1.02, and would, therefore, be undetectable by our present methods.

Unfortunately we, at present, know nothing of the size or the nature of the "free space" which the oxygen molecule must hit, in order for combination with the hæmoglobin molecule to ensue. Nor do we know whether the O_2 molecule must possess any special internal orientation (e.g., must the line joining its two constituent atoms be perpendicular or parallel to the surface of the hæmoglobin molecule?) at the moment of collision. It is not, therefore, possible to compare observed velocities with those calculated on the basis of the theory, as was possible in the case of Langmuir's experiments. Nor has any other method of testing the theory yet presented itself. There is, however, one fact which is not inconsistent with the theory, though it has no evidential value. In a paper to be published shortly, we have made a similar set of measurements upon the velocity with which carbon monoxide combines with hæmoglobin. The velocity constant for this reaction (i.e., k'_{CO+Hb}) is only about one-fifteenth of k'_{O_2+Hb} at p_H 7.2 and $15^\circ C$. Assuming, as is generally held, that CO combines with hæmoglobin at exactly the same spot as O_2 , then, on the above theory, if $k'_{CO+Hb} = 1/15 k'_{O_2+Hb}$, only one-fifteenth of the collisions between CO and the sharply localized portion of the hæmoglobin molecule result in combinations at $15^\circ C$. If so, then there is scope for an increase in k'_{CO} with rise of temperature. This was found to be the case. Observations showed that k'_{CO+Hb} had a normal temperature coefficient of about 2.

Our thanks are due to the Medical Research Council for defraying in part the expenses involved in this research.

SUMMARY

SECTION I

In order to measure the velocity of combination of reduced hæmoglobin and oxygen it was necessary, in the first place, to devise methods of preparing

large quantities of reduced hæmoglobin solution and oxygenated water. Three methods were used in the preparation of the former: (1) The rolling method, (2) the vacuum spray method, (3) the chemical method, *e.g.*, by means of ammonium sulphide. In the preparation of the oxygenated water the first two methods were also used.

Experiment showed that the velocities obtained by causing these solutions to react were independent of the methods of preparation that had been employed.

The measurement, at different cross-sections of the observation tube of the velocity apparatus, of the percentage of O_2Hb in solution was effected by means of the reversion spectroscope.

The accuracy of the method was confirmed by comparing the values obtained spectroscopically for a number of mixtures of known concentration of reduced and oxyhæmoglobin.

SECTION II

The reaction between oxygen and reduced hæmoglobin was found to be very rapid, the time for half completion being 1/100 to 1/1000 of a second. Stringent tests of the velocity apparatus showed that it was adequate for dealing with such high velocities.

The velocity constants obtained with different concentrations of hæmoglobin and oxygen at P_H 7 (where un-ionised molecules predominate) and at P_H 10 to P_H 11 (where the ionised modification is in excess) agreed in showing that the reaction is a bimolecular one.

SECTION III

The investigation of the relationship between the two velocity constants and the equilibrium constant gives a very crucial test of our previous conclusions and methods. The filling of the tonometers with the correct gas mixtures required an elaborate technique which is described in detail. The experiments showed, firstly, that the dissociation curve (in dilute solution) is very closely of a hyperbolic character, and, secondly, that the quotient of the two velocity constants is equal (within the limits of experimental error) to the equilibrium constant.

SECTION IV

Neither change of salt concentration, hydrogen-ion concentration nor of temperature was found to have any marked effect on the velocity of the reaction. The low-temperature coefficient both at P_H 7 and P_H 10 suggested

that the reaction might be a photochemical one. Experiment showed, however, that such was not the case.

In view of the small effect of P_{H} on the oxidation velocity, the onus of accounting for the effect of P_{H} on the equilibrium constant must fall mainly, if not entirely, upon the reduction velocity constant.

SECTION V

The possible existence of aggregates in solution has been examined. The conclusion we have reached is, that the presence of such aggregates will not affect the velocity of oxygen uptake so long as the part of the hæmoglobin with which the oxygen combines is sharply localised and far removed from the part of the grouping which forms aggregates.

If in addition we assume that every collision of oxygen with this localised portion results in combination, we show how an explanation of the low-temperature coefficient of the reaction can be explained.

REFERENCES

- (1) Hartridge and Roughton, 'Roy Soc Proc,' A, vol 104, p 395 (1923)
 - (2) Hartridge and Roughton, 'Proc Camb Phil Soc,' vol 22, p 426 (1924)
 - (3) Hartridge and Roughton, 'Roy Soc Proc,' A, vol. 104, p 376 (1923)
 - (4) Hastings, Van Slyke, Neill, Heidelberger and Harrington, 'Journ of Biol Chem,' vol. 60, p 89 (1924)
 - (5) Hartridge, 'Journ of Physiol,' vol 44, p 1 (1912)
 - (6) Haldane, 'Respiration,' Yale and London, Appendix, p 424
 - (7) Barcroft, 'The Respiratory Function of the Blood,' p 307, London (1914)
 - (8) Douglas, Haldane and Haldane, 'Jour of Physiol,' vol 44, p 275 (1912).
 - (9) Peters, 'Journ of Physiol,' vol 44, p. 131 (1912).
 - (10) Langmuir, 'Trans. Far Soc,' vol 17, p 261 (1922).
-

The Structure of Molecules in Relation to their Optical Anisotropy.—Part I.

By K R RAMANATHAN, M A , D Sc , Assistant Lecturer in Physics,
University College, Rangoon

(Communicated by Prof C V Raman, M A , D Sc , F R S —Received June 23,
1924)

One of the most significant facts relating to the scattering of light in gases is the imperfection of polarisation of the light scattered in a direction perpendicular to the incident beam. The late Lord Rayleigh* and Born† explained this phenomenon as being due to the optical anisotropy of the molecule, that is, to the fact that the polarisation induced in a molecule depends on its orientation with respect to the electric vector in the incident light. Lord Rayleigh's theory does not go into the question as to how the anisotropy arises, but merely assumes that there are in each molecule three principal directions of vibration, along which the induced polarisations are different. If A, B, C are the moments induced in a molecule when its three principal directions are respectively along the direction of the electric vector in the incident light, then the ratio of the weak component to the strong in the transversely scattered light is given by

$$r = \frac{2(A^2 + B^2 + C^2) - 2(AB + BC + CA)}{4(A^2 + B^2 + C^2) + AB + BC + CA} \quad (1)$$

We now possess reliable measurements of the imperfection of polarisation in many gases and vapours, from the work of Lord Rayleigh‡ and of Raman and Rao§. Recently there has been carried out at Calcutta further measurement of the same quantity, in a series of organic vapours, by Mr A. S. Ganesan.|| Some of these results are collected together in Table I.

An examination of the table shows clearly the influence of the nature of the

* Rayleigh, 'Phil. Mag.', vol 35, p. 373 (1918).

† Born, 'Verh. Deutsch. Phys. Gesell.', vol 20, p. 16 (1918).

‡ 'Roy. Soc. Proc.', A, vol. 97, p. 435 (1920); vol. 98, p. 57 (1920), vol. 102, p. 190 (1923).

§ 'Phil. Mag.', vol 46, p. 427 (1923). Measurements have also been made by Gans ('Ann. der Physik,' vol 65, p. 97 (1921)), and J. Cabannes (Jour. de Physique,' vol 4, p. 429 (1923)).

|| Not yet published.

Table I.

	Weak component Strong component in per cent	Author
Argon	0.46	R
Mercury	Approximately complete	R
Helium	< 6.5	R
Hydrogen	3.83	R
	3.6	R and R
Oxygen	9.4	R
	8.4	R and R
Nitrogen	4.06	R
CO	3.4	Ramdas at Calcutta (not previously published)
CO ₂	11.7	R
	10.6	R and R
N ₂ O	15.4	R
	14.3	R and R
CS ₂	12.0	R (earlier work)
	16.7	G
Octane	2.7	G
Benzene	6.6	G
CCl ₄	1.0	G

R = Lord Rayleigh

R and R = Raman and Rao

G = Ganesan

molecule on the value of the imperfection Sir J. J. Thomson* has made suggestive attempts at connecting the variation of r with the departure of the shape of the molecule from spherical symmetry, but although among the mono-, di- and triatomic gases the value of the imperfection increases in general with the number of atoms in the molecule, this is by no means always the case. For example, octane, which is supposed to have a long molecule, shows even less imperfection than any of the diatomic gases in the table. It is, however, significant that in the case of the monatomic molecules, the imperfection is very nearly zero, and that among the polyatomic molecules, the smallest value of the imperfection is obtained for carbon tetrachloride, a molecule in which the chlorine atoms are presumably arranged at the corners of a regular tetrahedron.

The last-mentioned example suggests that a new way of approaching the problem is by considering the mutual influence of the different atoms composing a molecule. For example, in a diatomic molecule, when the electric vector is parallel to the line of centres of the atoms, the resultant polarisation would, owing to the mutual influence of the polarisations induced in each atom, be greater than if the atoms were far away from each other, while when the electric vector is perpendicular to the line of atomic centres, the polarisation

* 'Journal of the Franklin Institute,' vol. 195, p. 743 (1923).

would be smaller. On this view, a diatomic molecule must necessarily be anisotropic. With molecules containing more atoms, the anisotropy will depend on the nature and arrangement of the constituent atoms, and it may well be small even with long molecules. The recent success of Prof W. L. Bragg* in explaining the double refraction of calcite and aragonite on somewhat similar lines makes it worth while to examine how far we can explain the observed effects by considering the mutual influence of the atoms.

Diatomic Molecules

We shall assume that each atom by itself is isotropic, and that when placed in a periodic electric field behaves like a vibrating doublet placed at some point within the atom which we may call its "optical centre". Considering first the case of a diatomic gas like hydrogen in which both atoms are similar, let e be the charge on each equivalent doublet, m the mass of the vibrator and x the displacement. When the electric field E acts parallel to the axis of the molecule, the total electric intensity acting on one of the charges will be $E + 2ex_1/d^2$ where d is the distance between the optical centres of the atoms. Hence

$$mx_1 + fx_1 = e(E + 2ex_1/d^2)$$

where f is the restoring force on each charge per unit displacement.

When the periodicity of the electric intensity is introduced through the factor $\cos pt$

$$ex_1 = \frac{e^2/m}{n^2 - p^2 - 2e^2/md^2} E, \quad (2)$$

where $n^2 = f/m$.

The electric moment for the two atoms together is

$$AE = 2ex_1.$$

Similarly, when the electric field acts perpendicular to the axis of the molecule,

$$BE = 2ex_2 = \frac{2e^2/m}{n^2 - p^2 + e^2/md^2} E.$$

When the molecules are oriented at random, the average value of $2ex$ will be given by

$$2\overline{ex} = \left(\frac{A}{3} + \frac{2B}{3} \right) E$$

* W. L. Bragg, 'Roy Soc Proc,' A, vol 105, p. 370 (1924). Reference may also be made to a series of interesting papers by Dr Silberstein in 'Phil Mag.,' January, 1917, on "Molecular Refractivity and Atomic Refraction," etc.

and the refractivity

$$\begin{aligned}\mu^2 - 1 &= 4\pi v \left(\frac{A}{3} + \frac{2B}{3} \right) \\ &= \frac{4\pi v e^2}{3m} \left\{ \frac{2}{n^2 - p^2 - 2e^2/md^2} + \frac{4}{n^2 - p^2 + e^2/md^2} \right\},\end{aligned}$$

where v is the number of molecules per unit volume. Writing

$$\frac{4\pi v e^2}{m(n^2 - p^2)} = R_0$$

and

$$\frac{1}{2\pi v d^2} = k,$$

it is easy to put this into the convenient form

$$\mu^2 - 1 = \frac{2R_0}{3} \left\{ \frac{1}{1 - R_0 k} + \frac{2}{1 + \frac{1}{2}R_0 k} \right\}. \quad (3)$$

The optical anisotropy which may be defined as A/B is given by

$$\frac{A}{B} = \frac{1 + \frac{1}{2}R_0 k}{1 - R_0 k} \quad (4)$$

We shall now consider a few simple cases

1 *Hydrogen*—From our assumption of the isotropy of each atom, the molecule should have spheroidal symmetry. We can therefore write in equation (1) $B = C$, and we get

$$r = \frac{2(A^2 + B^2 - 2AB)}{4A^2 + 9B^2 + 2AB}$$

Taking r for hydrogen to be 3.7 per cent and solving, we get

$$A/B = 1.66 \text{ or } 0.543$$

Consistently with our physical assumptions we adopt the first value, and from (4) we calculate $R_0 k = 0.3047$. Using this value in (3) and taking R to be 0.0002812 (Cuthbertson's value for 0.486 μ), we get

$$\begin{aligned}R &= 1.328 \times 10^{-4} \\ \text{and } k &= 2.293 \times 10^9,\end{aligned}$$

leading to a value $d = 1.37 \times 10^{-8}$ cm*. This may be compared with the value of the molecular radius calculated from mean free path phenomena 1.34×10^{-8} cm†

* v has been assumed to be 2.708×10^{19} per c.c.

† Jeans, 'Dynamical Theory of Gases,' second edit., p. 341

2. *Nitrogen*— $r = 4.06$ per cent $A/B = 1.696$. $R_0 k = 0.3169$ from (4). Taking R to be 0.0006024 for 0.486μ and using (3), $R_0 = 2.832 \times 10^{-4}$,

$$k = 1.119 \times 10^8 \text{ and } d = 1.90 \times 10^{-8} \text{ cm.}$$

while the kinetic theory free path value of the "radius" of a nitrogen molecule is 1.90×10^{-8} cm.

3 *Oxygen*—For this gas, we shall take $r = 8.9$ per cent, the average of the values obtained by Rayleigh and by Raman and Rao

The corresponding value of $A/B = 2.211$ and $R_0 k = 0.4466$

$$\text{Taking } R = 0.000547 \text{ for } 0.486 \mu \text{ and } R_0 = 2.384 \times 10^{-4}, \\ k = 1.874 \times 10^8 \text{ and } d = 1.46 \times 10^{-8} \text{ cm.,}$$

while the mean free path value of the molecular radius is 1.81×10^{-8} cm. As will be noticed, while the kinetic theory diameter of an oxygen molecule is somewhat less than that of a nitrogen molecule, the distance between the optical centres seems to be much smaller in the former case

Triatomic Molecules.

Turning now to the case of a triatomic molecule like N_2O , CO_2 , or CS_2 , we can calculate its refractivity and optical anisotropy provided we know the structure of the molecule, the refractivities of the constituent atoms and the distance apart of the optical centres. For example, in the case of N_2O , let us suppose that the atomic centres are in a straight line, the oxygen being at the centre and let e_1 denote the charge on the equivalent doublet in the nitrogen atom, m_1 the mass of the vibrator and f_1 the restoring force per unit displacement. Let similar symbols with suffixes 2 denote the corresponding quantities in the oxygen atom. Then, when the electric field is parallel to the length of the molecule, the equations of motion of the charges in the nitrogen and oxygen atoms are respectively

$$m_1 \ddot{x}_1 + f_1 x_1 = e_1 \left\{ E + \frac{2e_2 x_2}{d^3} + \frac{2e_1 x_1}{8d^3} \right\} \\ m_2 \ddot{x}_2 + f_2 x_2 = e_2 \left\{ E + \frac{4e_1 x_1}{d^3} \right\}, \quad (5)$$

where d is the distance between the optical centres of the oxygen and nitrogen atoms.

Introducing the periodicity of the electric intensity through the factor $\cos pt$ and solving for $e_1 x_1$ and $e_2 x_2$, we get

$$e_1 x_1 = \frac{R_1}{4\pi\nu} \frac{1 + R_2 k}{1 - R_1 k/8 - 2R_1 R_2 k^2} F, \quad (6)$$

where

$$R_1 = \frac{4\pi v e_1^2}{m_1 (n_1^2 - p^2)} \quad R_2 = \frac{4\pi v e_2^2}{m_2 (n_2^2 - p^2)} \quad \text{and} \quad k = \frac{1}{2\pi v d^3},$$

and

$$e_2 x_2 = \frac{R_2}{4\pi v} \frac{1 + 15/8 R_1 k}{1 - R_1 k/8 - 2R_1 R_2 k^2} E.$$

The total moment along the length of the molecule is

$$2e_1 x_1 + e_2 x_2 = \frac{2R_1 + R_2 + 31/8 R_1 R_2 k}{1 - R_1 k/8 - 2R_1 R_2 k^2} \frac{E}{4\pi v} = AE, \text{ say}$$

Similarly, when the electric intensity is perpendicular to the line of atomic centres, the equations of motion are

$$m_1 x_1'' + f_1 x_1 = e_1 \left(E - \frac{e_2 x_2}{d^3} - \frac{e_1 x_1}{8d^3} \right),$$

$$m_2 x_2'' + f_2 x_2 = e_2 \left(E - \frac{2e_1 x_1}{d^3} \right).$$

Solving,

$$e_1 x_1 = \frac{R_1}{4\pi v} \frac{1 - R_2 k/2}{1 + R_1 k/16 - \frac{1}{2} R_1 R_2 k^2}$$

and

$$e_2 x_2 = \frac{R_2}{4\pi v} \frac{1 - 15/16 R_1 k}{1 + R_1 k/16 - \frac{1}{2} R_1 R_2 k^2}$$

and the corresponding moment is

$$2e_1 x_1 + e_2 x_2 = \frac{1}{4\pi v} \frac{2R_1 + R_2 - 31/16 R_1 R_2 k}{1 + R_1 k/16 - \frac{1}{2} R_1 R_2 k^2} E$$

$$= BE$$

As in the case of the diatomic molecules the refractivity is given by

$$\mu^2 - 1 = 4\pi v \left(\frac{A}{3} + \frac{2B}{3} \right) = R, \text{ say,}$$

$$= \frac{1}{3} \frac{2R_1 + R_2 + 31/8 R_1 R_2 k}{1 - R_1 k/8 - 2R_1 R_2 k^2} + \frac{2}{3} \frac{2R_1 + R_2 - 31/16 R_1 R_2 k}{1 + R_1 k/16 - \frac{1}{2} R_1 R_2 k^2}, \quad (7)$$

and the optical anisotropy as we have previously defined is

$$A/B = \frac{2R_1 + R_2 + 31/8 R_1 R_2 k}{1 - R_1 k/8 - 2R_1 R_2 k^2} \cdot \frac{1 + R_1 k/16 - \frac{1}{2} R_1 R_2 k^2}{2R_1 + R_2 - 31/16 R_1 R_2 k} \quad (8)$$

To calculate A/B, we require to know R_1 , R_2 and k . We have no direct means of determining any of these quantities, but let us tentatively assume that the refractivities R_1 and R_2 appropriate to the nitrogen and oxygen atoms are the same as in the respective molecules of N_2 and O_2 . The known

refractivity of N_2O will then enable us to calculate k from equation (7). The equation can be put in the form of a bi-quadratic :—

$$k^4 R\delta^2 - k^3 (R\gamma\delta + \beta\delta) - k^2 (5R\delta - 3\alpha\delta + 2R\gamma^2 + 2\beta\gamma) - k (2R\gamma - 2\alpha\gamma) + 4 (R - \alpha) = 0,$$

where

$$\alpha = 2R_1 + R_2 \quad \beta = 31/8 R_1 R_2$$

$$\gamma = R_1/8 \quad \text{and} \quad \delta = 2R_1 R_2$$

Taking

$$R = 10.28 \times 10^{-4} \text{ (for } \lambda = 0.480 \mu\text{)}$$

$$R_1 = 2.832 \times 10^{-4}$$

and

$$R_2 = 2.384 \times 10^{-4},$$

the equation becomes

$$1874k_1^4 - 402.4k_1^3 - 389k_1^2 - 1.58k_1 + 8.928 = 0,$$

where

$$k_1 = k \times 10^{-4}$$

The only root of this equation consistent with our physical assumptions is

$$k = 0.1460 \times 10^4, \text{ which leads to a value of } d = 1.59 \times 10^{-8} \text{ cm}$$

From (8),

$$A/B = 2.80,$$

and hence $r = 14.1$ per cent, while the value experimentally obtained by Lord Rayleigh was 15.7 per cent and that obtained by Raman and Rao was 14.3 per cent. Without laying too great stress on the numerical agreement, it seems to show that the general idea of the method is correct.

Carbon Dioxide.

We shall now take up the case of carbon dioxide. Since we have no direct means of determining the refractivity to be attributed to carbon in the molecule of carbon dioxide, we have to derive it from some other source. We may take the refractivity of carbon as derived from saturated organic compounds, but since it is likely that even there its value is likely to be influenced by the proximity of the neighbouring atoms, it is better to derive it from a source where the influence of the neighbouring atoms vanishes. In a crystal of diamond there is regular tetrahedral symmetry, and each carbon atom is bound by one electron each to its four nearest neighbours. We may adopt the value of the atomic refractivity of carbon in diamond for our present case, since here also all the four outer electrons of carbon are presumably bound up with the neighbouring oxygen atoms.

The refractive index of diamond for 0.480μ is 2.4370^* and taking its density to be 3.514,

$$\frac{\mu^2 - 1}{\mu^2 + 2} \cdot \frac{M}{\rho} = 2.124,$$

where M is the atomic weight of carbon and ρ is the density of diamond. The corresponding value of $\mu^2 - 1$ for free carbon atoms at 0°C and 76 cm. pressure is given by

$$2.124 = \frac{\mu^2 - 1}{3} \cdot \frac{2.016}{8.987 \times 10^{-5}},$$

where 2.016 is the molecular weight and 8.987×10^{-5} is the density of hydrogen

$$\text{Hence } R_2 = \mu^2 - 1 = 2.841 \times 10^{-4}$$

Using our previous value of R for the oxygen atom from its value in the oxygen molecule, and making use of equation (7), we obtain the appropriate biquadratic —

$$1663k_1^4 - 392k_1^3 - 322k_1^2 - 0.865k_1 + 5804 = 0, \quad \text{where } k_1 = k \times 10^{-4},$$

in which the refractive index of CO_2 at N.T.P. has been assumed to be 1.000453. The physically relevant root of the equation gives

$$k = 0.1284 \times 10^4 \quad d = 1.66 \times 10^{-8} \text{ cm},$$

and hence

$$A/B = 2.42$$

The imperfection of polarisation in a direction transverse to the incident light comes out as 10.8 per cent, which may be compared with Rayleigh's experimental value 11.7 per cent, and Raman and Rao's value 10.6 per cent.

The distance between the optical centres of the two nitrogen atoms in nitrous oxide is thus 3.18×10^{-8} cm, and the corresponding distance between the centres of the two oxygen atoms in CO_2 is 3.32×10^{-8} cm. Viscosity measurements indicate that the mean free-path size of the two molecules N_2O and CO_2 is practically the same. Since the size of the nitrogen molecule is larger than that of the oxygen molecule, the increased distance between the atomic centres in CO_2 is compensated by the smaller size of the oxygen atoms.

Carbon Disulphide.

We may expect that carbon disulphide has a constitution similar to carbon dioxide, and if we know the atomic refractivity of sulphur, we can calculate

* Landolt-Börnstein, 'Tabellen' (Martens), 1923 Edition, p. 918

the anisotropy of carbon disulphide, and hence the imperfection of polarisation of the transversely scattered light in its vapour. We may adopt the following empirical method of calculating the refractivity of sulphur. The refractivity of H_2S for 0.486μ is 13.12×10^{-4} , and since the refractivity of hydrogen is small compared with that of sulphur, we may to a first approximation obtain the value for sulphur by subtracting the refractivity of H_2 from that of H_2S . We thus get $R = 10.31 \times 10^{-4}$. Using the same value for the refractivity of carbon as in carbon dioxide,

$$R_2 = 2.841 \times 10^{-4}$$

We do not possess data for the refractivity of carbon disulphide vapour at wave-length 0.486μ , but from its refractivity for 0.589μ and its dispersion in the liquid state, we can easily calculate $\mu^2 - 1$, for 0.486μ . We thus get

$$R = 30.70 \times 10^{-4}$$

Making a similar calculation as in the two preceding cases,

$$k = 7.18 \times 10^3 \quad \text{and} \quad d = 2.02 \times 10^{-8} \text{ cm},$$

and

$$A/B = 2.61, \quad \text{and} \quad r = 12.5 \text{ per cent}$$

The imperfection of polarisation obtained photographically by Lord Rayleigh in his earlier work was 12 per cent, while that obtained visually by Ganesan at Calcutta was 16.7 per cent. The latter value is probably entitled to greater weight, as in this case the illumination of the vapour was limited to a time just sufficient for the observation to be taken, and thus the chance of formation of clouds was reduced to a minimum. The difference between the observed and calculated values is no doubt to be attributed to the uncertainty in the values of the atomic refractivity.

The general agreement, however, in the three cases investigated makes it fairly certain that a large part of the optical anisotropy of gaseous molecules arises from the mutual action of the atoms of the molecule. It is thus of great importance to extend the investigation to the case of other molecules, particularly in the organic region, where the influence of the structure of the molecule on the anisotropy stands out conspicuously.

Summary.

In the foregoing paper, the view is put forward that the optical anisotropy of gaseous molecules, as revealed by the polarisation of the light scattered from them, is due to the mutual action of the doublets induced by the incident light in the different atoms constituting the molecule. It is assumed that each atom by itself is isotropic.

From the known refractivity and polarisation of the scattered light in hydrogen, nitrogen and oxygen, the atomic refractivities and distances between the optical centres in the molecules are deduced. These distances are consistent with the size of atoms deduced from the kinetic theory.

The investigation is extended to the three triatomic gases, N_2O , CO_2 and CS_2 , and an expression is deduced for the imperfection of polarisation of the transversely scattered light in terms of the atomic refractivities of the different atoms and the distances apart of the optical centres. The calculated values of the imperfection are in satisfactory agreement with experiment.

I have great pleasure in acknowledging my indebtedness to Prof. C. V. Raman, at whose suggestion the above work was taken up, for his kind interest and helpful advice.

*On the Alternating Current Resistance of Solenoidal Coils **

By S. BUTTERWORTH, M.Sc.

(Communicated by F. E. Smith, F.R.S. —Received December 10, 1924.)

1. *Introduction*

In a paper published some time ago by the present writer† a formula was given for computing the alternating current resistance of single-layer coils in which the spacing of the wires is not too close. Recently Mr. C. N. Hickman‡ has made a comparison between the measured and computed values of the resistance of solenoidal coils and has used the above formula. Owing mainly to a misconception in regard to the scope of the formula, he came to the conclusion that the formula could be in error by as much as 300 per cent. It has been pointed out, however,§ that when the formula is legitimately applied the discrepancy is reduced to 30 per cent.

In order to account for the outstanding difference it is necessary to extend the theory so as to include closely wound coils. This extension has been made in the present paper, with the result that the difference between theory

* The author is indebted to the Admiralty for permission to publish this paper.

† 'Phil. Trans. Roy. Soc.,' A, vol. 222, p. 57, 1921.

‡ 'Scientific Paper Bureau of Standards,' No. 472.

§ 'Phys. Rev.,' June, 1924, p. 752.

and Hickman's observations is now reduced to an average value of 7 per cent. There are still outstanding differences, but these occur at much higher frequencies than those used by Hickman, and are probably due to want of uniformity of current distribution throughout the coil.

2 Preliminary Theory

The following equations, which were established in the author's previous paper, are required in the present investigation.

Let a long non-magnetic conducting cylinder of radius c be placed in a magnetic field alternating with frequency $\omega/2\pi$. The direction of the field is taken to be perpendicular to the axis of the cylinder, and it is assumed not to vary throughout the length of the cylinder. Let cylindrical co-ordinates r, θ, z be taken, having the axis of the cylinder as the axis of z , then if $P_0 e^{i\omega t}$, $Q_0 e^{i\omega t}$ be the rotors representing the components of the field in the directions of increase of r and θ when the cylinder is absent,

$$\left. \begin{aligned} P_0 &= \sum_{n=1}^{\infty} r^{n-1} (K_n \sin n\theta + L_n \cos n\theta) \\ Q_0 &= \sum_{n=1}^{\infty} r^{n-1} (K_n \cos n\theta - L_n \sin n\theta) \end{aligned} \right\} \quad (1)$$

in which K_n, L_n are in general complex coefficients independent of r and θ but depending on the form of the field. The eddy currents induced in the cylinder by the alternations of the field introduce a disturbing field whose components are represented by the rotors $P_1 e^{i\omega t}$, $Q_1 e^{i\omega t}$, such that

$$\left. \begin{aligned} P_1 &= \sum_{n=1}^{\infty} \frac{c^{2n}}{r^{n-1}} \chi_n (K_n \sin n\theta + L_n \cos n\theta) \\ Q_1 &= \sum_{n=1}^{\infty} \frac{c^{2n}}{r^{n+1}} \chi_n (K_n \cos n\theta - L_n \sin n\theta) \end{aligned} \right\} \quad (2)$$

in which

$$\chi_n \equiv -\{\phi_n(z) + i\psi_n(z)\} = J_{n+1}(\sqrt{-1}z)/J_{n-1}(\sqrt{-1}z), \quad (3)$$

$$z^2 = 4\pi k\omega c^2, \quad (4)$$

and $J_n(x)$ is Bessel's function of order n .

The energy dissipated in unit length of the cylinder in unit time is given by

$$W = \frac{1}{2}\omega \sum_{n=1}^{\infty} \{(K_n)^2 + (L_n)^2\} c^{2n} \psi_n/n, \quad (5)$$

where $(K_n), (L_n)$ represent the amplitudes of the coefficients K_n, L_n . The properties of the functions ϕ_n, ψ_n have been discussed in the author's

previous paper The sign of ϕ_n has been changed in equation (3) in order to make it always a positive quantity If the cylinder carries a current whose integral value is I we must add to Q_1 the term $2I/r$ and to the energy dissipation equation (5) the term

$$W_s = 2\omega I^2 \left(\frac{1}{z^2} + \frac{1}{2}\psi_2 \right) \equiv \frac{1}{2}R_0 I^2 (1 + F(z)) \quad (6)$$

in which R_0 is the direct current resistance of the cylinder per unit length and $F(z) = \frac{1}{2}z^2\psi_2$

These equations will be used to determine the losses in a single-layer plane system of equidistant parallel wires infinite in number—

(a) When the wires carry equal currents

(b) When the wires are placed in a uniform field parallel to the plane of the axes but normal to the directions of the axes

(c) When the wires are placed in a field normal to the plane of the system

It will then be shown how to combine the solutions of these three problems to determine the eddy current losses in a solenoidal coil having a large number of turns

3 Problem A

Let the cylinder of the previous section be one wire of an infinite single-layer system of coplanar parallel wires, each carrying a current I , the distance of successive wires being D Then, if the plane of the system be taken as the plane $\theta = 0$, we have from the nature of the symmetry

$$L_n = 0, \quad K_1 = K_3 = K_5 = \dots = 0$$

The vertical field at a point $r, 0$ in the neighbourhood of the wire under consideration, is made up of two portions,

$$Q_0 = K_2 r + K_4 r^3 + K_6 r^5 + \dots, \quad (7)$$

and

$$Q_1 = \frac{2I}{r} - \frac{c^4}{r^3} K_2 \chi_2 - \frac{c^6}{r^5} K_4 \chi_4 - \frac{c^{12}}{r^7} K_6 \chi_6, \quad (8)$$

the former portion being due to external causes (that is, to the currents in the remaining wires), and the latter is due to the current distribution in the wire in question.

Since the distribution is similar in each wire we may obtain an alternative expression for Q_0 by replacing r in (8) by $D + r, 2D + r, D - r, 2D - r, \dots$ and summing the results, noting that the fields due to wires on opposite sides of the wire under consideration are in opposition If the resulting sum is expanded in powers of r/D the expression for Q_0 is

identical in form with equation (7), so that the coefficient of r^n in the series must be equal to K_{n+1} . We are thus led to an infinite series of equations to determine the coefficients K_n . These equations are most simply expressed as follows —

$$\left. \begin{aligned} [1] [2] Y_2 &= 2(Y_0 S_2 + Y_2 S_4 + Y_4 S_6 + \dots) \chi_2 \\ [3] [4] Y_4 &= 2(Y_0 S_4 + Y_2 S_6 + Y_4 S_8 + \dots) \chi_4 \\ [5] [6] Y_6 &= 2(Y_0 S_6 + Y_2 S_8 + Y_4 S_{10} + \dots) \chi_6 \end{aligned} \right\} \quad (9)$$

in which

$$\left. \begin{aligned} Y_0 &= 2I, & Y_n &= -\chi_n K_n c^n / n \\ S_n &= [n-1] (c/D)^n \sigma_n & \sigma_n &= 1^{-n} + 2^{-n} + 3^{-n} + \dots \end{aligned} \right\} \quad (10)$$

In the same notation, if W_A represents the energy dissipated in unit length of one of the wires,

$$W_A = \frac{1}{4} \omega \left[8I^2 \left\{ \frac{1}{z^2} + \frac{1}{8} \psi_2(z) \right\} + \sum_1 \frac{(Y_n)^2 (|n|^2)}{(\chi_n)^2} \frac{\psi_n(z)}{n} \right] \quad (11)$$

The exact solution of equations (9) is probably impossible. We therefore proceed to attempt to obtain an approximate solution. Taking the case of "infinite" frequency, for which $\chi_n = -1$,

$$\psi_n = n\psi_1 = nF(z) R_0/\omega,$$

by (6) we have for the losses,

$$W_A = \frac{1}{4} R_0 \left[\{1 + F(z)\} I^2 + \frac{1}{4} F(z) \sum_1 (Y_n)^2 (|n|^2) \right], \quad (12)$$

while the values of Y_n are determined from (9), in which $\chi_n = \chi_2 = \dots = -1$. Equation (12) may be further simplified for this case, since $F(z)$ is very large. Then by (6)

$$\frac{W_A}{W_s} = 1 + \frac{1}{4} \sum_1 \left(\frac{Y_n}{I} \right)^2 (|n|^2) \quad (13)$$

The values of Y_n are found by successive approximations of (9), neglecting Y_4, Y_6 in the first approximation, Y_6, Y_8 in the second approximation, and so on. When the resulting values of Y_n are substituted in (13) the following results are obtained for the case of touching wires ($2c/D = 1$) —

No of approximation.	1	2	3	4	5	6
W_A/W_s	1.684	1.697	1.704	1.703	1.704	1.703.

A similar calculation for the case $2c/D = 0.9$ shows that the first approximation will give results within 1 per cent. of the true value. It may therefore

be inferred that when the frequency is not infinite and when the spacing does not exceed 0.9 it is sufficient if we neglect Y_4, Y_6 in equation (9). For "infinite" frequency and for any spacing the following table holds —

Table I

W_A = loss in one wire of infinite system

W_s = loss in solitary wire

d = diameter of wire = $2c$

D = distance of successive wires

d/D	0.1	0.2	0.3	0.4	0.5	0.6	0.7	0.8	0.9	1.0
W_A/W_s	1.000	1.002	1.011	1.034	1.080	1.158	1.270	1.409	1.555	1.703

For finite frequencies the first approximation yields the following formula —

$$W_A = \frac{1}{2} R_0 I^2 (1 + \lambda F) \quad (14)$$

in which

$$\lambda = 1 + \frac{1}{3} \sigma_2^2 \frac{d^4}{D^4} \left/ \left\{ \left(1 + \frac{2}{3} \sigma_4 \frac{d^4}{D^4} \phi_2 \right)^2 + \frac{1}{6} \sigma_4^2 \psi_2^2 \frac{d^8}{D^8} \right\} \right. \quad (15)$$

R_0 = direct current resistance of wire

F, ϕ_2, ψ_2 are functions of z tabulated in the appendix

$$\sigma_2 = 1^{-2} + 2^{-2} + 3^{-2} + \dots = \pi^2/6$$

$$\sigma_4 = 1^{-4} + 2^{-4} + 3^{-4} + \dots = \pi^4/90$$

d = diameter of wire.

D = distance of successive wires

It should be noted that this formula will not hold for a bounded system unless the wire is central. For non-central wires there is also a transverse field acting on the wires.

4. Problem B

If the wire system carries no nett current, but is acted upon by a uniform alternating field parallel to the plane of the system but normal to the axes of the wires, then considering the components P, Q in the neighbourhood of one wire, these components reverse in sign when θ increases by π , and, the plane of the system being the plane $\theta = 0$,

$$K_n = 0, \quad L_2 = L_4 = L_6 = \dots = 0$$

Following the same method as in Section 3, the radial field at the point $r, 0$ is made up of

$$P_0 = L_1 + L_3 r^2 + L_5 r^4 + \dots, \quad (16)$$

due to causes external to the wire of reference, and

$$P_1 = \frac{c^2}{r^2} L_1 \chi_1 + \frac{c^6}{r^4} L_3 \chi_3 + \frac{c^{10}}{r^6} L_5 \chi_5 + \dots \quad (17)$$

due to the eddy currents in this wire

Adding the fields due to all the remaining wires to the external field (represented by the rotor $H\epsilon^{i\omega t}$), expanding in ascending powers of r/D and equating coefficients of r^0, r^2, r^4 to L_1, L_3, L_5 , the equations to find L_1, L_3 , in terms of H are found to be

$$\left. \begin{aligned} Y_1 &= Hc\chi_1 + \frac{2}{[0][1]} \chi_1 (Y_1 S_2 + Y_3 S_4 + Y_5 S_6 + \dots) \\ Y_3 &= \frac{2}{[2][3]} \chi_3 (Y_1 S_4 + Y_3 S_6 + Y_5 S_8 + \dots) \\ Y_5 &= \frac{2}{[4][5]} \chi_5 (Y_1 S_6 + Y_3 S_8 + Y_5 S_{10} + \dots) \end{aligned} \right\}, \quad (18)$$

the notation being defined by equations (10), L_n replacing k_n . In the same notation the energy W_B dissipated in unit length of one wire in unit time is

$$W_B = \frac{1}{2} \omega \sum_{n=1}^{\infty} \frac{(Y_n)^2 (n)^2}{(X_n)^2} \frac{\psi_n(z)}{n} \quad (19)$$

By the same procedure as in Section 3, equation (19) becomes

$$W_B = \frac{1}{2} F(z) R_0 \sum_{n=1}^{\infty} (Y_n)^2 (n)^2 \quad (20)$$

when the frequency is very high, and in (18) χ_n becomes -1 . Under these conditions it is clear from (18) that Y_n/Hc depends only on c/D , and therefore (20) may be written

$$W_B = \frac{1}{2} F(z) R_0 H^2 c^2 f(c/D) \quad (21)$$

where

$$f\left(\frac{c}{D}\right) = \sum_n \left(\frac{Y_n}{Hc} \right)^2 (n)^2 \quad (22)$$

Solving (18) by successive approximations for Y_n/Hc and inserting these values in (22) we find for the case of touching wires ($2c/D = 1$),

$$f(c/D) = 0.301, 0.344, 0.346, 0.346,$$

for approximations 1, 2, 3, 4, respectively.

For other values of c/D the method of successive approximations yields the following results for $f(c/D)$

Table II

d/D	0.1	0.2	0.3	0.4	0.5	0.6	0.7	0.8	0.9	1.0
$f(c/D)$	0.984	0.937	0.867	0.781	0.689	0.598	0.515	0.445	0.389	0.346

Using only the first approximation for finite frequencies the following formula is obtained from (18) and (19) —

$$W_R = \frac{1}{8} \frac{R_0 G(z) H^2 d^2}{\left(1 + \frac{1}{2} \sigma_2 \phi_1 \frac{d^2}{D^2}\right)^2 + \frac{1}{4} \sigma_2^2 \psi_1^2 \frac{d^4}{D^4}} \quad (23)$$

in which $G(z) [\equiv \frac{1}{8} z^2 \psi_1]$, ϕ_1 , ψ_1 are tabulated in the Appendix, and the remaining symbols are defined under equation (15)

If equation (23) is applied to the case of "infinite" frequency we obtain for $f(c/D)$

$$f\left(\frac{c}{D}\right) = \left(1 + \frac{1}{2} \sigma_2 \frac{d^2}{D^2}\right)^{-2}. \quad (24)$$

This first approximation formula yields values of $f(c/D)$ which are too low by 8, 3, 6, 1, 4 per cent when $d/D = 0.9, 0.8, 0.7$

5 Problem C

When the field is normal to the plane of the system the conditions of symmetry make $L_n = 0$, $K_2 = K_4 = K_6 = 0$ in equations (1) and (2)

The procedure of Section (3) applied to the field Q at $r, 0$ yields a system of equations identical with (18) if the sign for χ_n is changed

The method of successive approximations for the case of touching wires fails, the value of W tending, presumably, to infinity. The method, however, is valid when $d/D = 0.9$. Denoting the dissipation by W_0 we have at high frequencies

$$W_0 = \frac{1}{4} F(z) R_0 H^2 c^2 g(c/D), \quad (25)$$

and when $d/D = 0.9$

$$g(c/D) = 8.95, 11.82, 12.35, 12.46$$

for the first, second, third and fourth approximation respectively. The nature of the convergency of these approximations indicates a value $g = 12.5$ for $d/D = 0.9$

For other values of d/D and for high frequency the following table holds:—

Table III

d/D	0.1	0.2	0.3	0.4	0.5	0.6	0.7	0.8	0.9	1.0
g	1.017	1.069	1.166	1.326	1.585	2.03	2.87	4.83	12.5	inf

For finite frequencies the first approximation formula is

$$W_0 = \frac{1}{8} \frac{R_0 G(z) H^2 d^2}{\left(1 - \frac{1}{2} \sigma_2 \phi_1 \frac{d^2}{D^2}\right)^2 + \frac{1}{4} \sigma_2^2 \psi_1^2 \frac{d^4}{D^4}}, \quad (26)$$

this formula yielding results 28, 8, 2 per cent low when $d/D = 0.9, 0.8, 0.7$ at very high frequencies

It will be noticed on comparison of (21) and (25) that for closely spaced wires the transverse field losses are very much in excess of the tangential field losses when the frequency is high. Also, if the spacing is so great that d^2/D^2 is negligible, formulæ (23) and (26) reduce to the known formula* for the losses in a solitary wire in a uniform field. The effect of neighbouring wires is to reduce the uniform field losses in the case of the tangential field and to increase them in the case of the transverse field. This is what would be inferred from a consideration of the physical effect of the induced eddy currents. These currents tend to thrust out the field from the substance of the wire, thus weakening the external field along the direction of the field and strengthening it in the equatorial plane. This means that in the case of the tangential field the effect of neighbouring wires is to weaken, and in the case of a transverse field to strengthen, the field acting on an individual wire.

6. Application to Solenoidal Coils

Let the parallel wire system now be acted upon by a uniform field, inclined to the plane of the system but normal to the axes of the wires, and let the system simultaneously carry a current I in each wire. From the consideration that the radial component P of the field changes sign when θ changes from 0 to π we have $L_2 = L_4 = L_6 = 0$. Further, if we write down the system of equations corresponding to (9) and (18) we find that these split up into the three sets discussed in the three preceding sections, so that the coefficients K_2, K_4, K_6 are determined solely by the current I , the coefficients K_1, K_3, K_5 by the transverse component of the field, and the coefficients L_1, L_3, L_5 by the tangential component of the field. Moreover, by (5) the losses corresponding to the separate coefficients are additive, so that the losses for this case are simply given by

$$W = W_A + W_B + W_C, \quad (27)$$

the values of H in the expressions for W_H and W_C being the tangential and transverse field components respectively. Now consider a single-layer solenoid of any length having an extremely large number of turns. An element of this solenoid lying between planes $x, x + \delta x$ normal to the axis may approximately be regarded as a system of straight parallel wires (since δx is infinitely small compared with the coil radius), infinite in number (since in the ideal coil the

* Butterworth, *loc. cit.*

number of turns are infinitely large) The losses in this slice are therefore given by (27), the appropriate values of the field components being calculated from the known formulæ for solenoids

For the whole solenoid the elementary losses are added This is equivalent to replacing the value of H^2 for any element by its mean-square value over the surface of the solenoid, and R_0 by the direct current resistance of the whole solenoid

Now for either component H^2 is proportional to I^2/D^2 where D is the distance of successive turns and the omitted factor depends only on the shape of the coil and position of the point considered Hence we may write for the mean square value of the transverse component $4u_1I^2/D^2$ for the mean square value of the tangential component $4u_2I^2/D^2$ Using these in (15), (23), (26), (27),

$$W = \frac{1}{2}RI^2 \left\{ (1 + \lambda F) + (1 + \frac{d^2}{D^2}) (\beta u_1 + \gamma u_2) \right\} \quad (28)$$

in which

$$\beta = 1 / \left\{ (1 + \frac{1}{2} \sigma_2 \phi_1 \frac{d^2}{D^2})^2 + \frac{1}{4} \sigma_2^2 \psi_1^2 \frac{d^4}{D^4} \right\} \\ \gamma = 1 / \left\{ (1 + \frac{1}{2} \sigma_2 \phi_1 \frac{d^2}{D^2})^2 + \frac{1}{4} \sigma_2^2 \psi_1^2 \frac{d^4}{D^4} \right\} \quad (29)$$

If further, we write

$$\alpha = (1 + \lambda F)/(1 + F),$$

we obtain from (28) the following formula for the alternating current resistance R' of the solenoid in terms of the direct current resistance R —

$$R'/R = \alpha (1 + F) + G (\beta u_1 + \gamma u_2) d^2/D^2. \quad (30)$$

α , β , γ are completely defined by the preceding equations and are functions of z and d/D , tending to unity when d/D is small A table of their values is given in the Appendix

The quantities u_1 , u_2 have still to be determined

7 Distribution of Magnetic Field over the Surface of a Solenoid.

The field at any point on the surface of a solenoid has a component H_T parallel to the axis and a component H_N acting radially outwards

These components may be calculated as follows —If the solenoid is very long, then, if a thin slice normal to the axis is supposed removed, the field in the gap, due to the remaining portions of the solenoid and at points near the surface of the solenoid, is wholly axial and has the value $2\pi nI$, where I is the current and n the number of turns in unit length This follows from the consideration that the field due to the removed portion has values $\pm 2\pi nI$

on either side, and that the value of the field when the slice is replaced is $4\pi nI$ inside and zero outside the solenoid. Hence $2\pi nI$ represents the field acting on the wires in the slice due to the remainder of the solenoid.

If the solenoid is finite this field is modified by the opposing magnetic action of its end poles. The modified field can be calculated from the known formulae for the field components due to a circular disc of poles. For points on the coaxial enveloping cylinder of a circular disc of radius a and at distance x therefrom these components are calculated by the elliptic integral formulae

$$H = \sigma \{ \pi - 2\sqrt{1 - k^2} K(k) \},$$

$$V = 2\sigma \{ (2 - k^2) K(k) - 2E(k) \} / k,$$

where K and E are elliptic integrals of the first and second kinds to modulus k , and

$$k^2 = 4a^2 / (4a^2 + x^2),$$

σ is the polar density, which in the case of the solenoid is nI , and H and V represent the axial and radial components respectively.

As regards the component V , this may be written $V = M\sigma/2\pi a$, where M is the mutual inductance between two coaxial circles, each of radius a and having separation x , so that use may be made of tables of mutual inductances in computing V .

The following values of $\sqrt{1 - k^2} K$ enable the value of H to be computed readily. It should be noted that these values represent one-quarter the field acting on the central wires when nI is unity and the length of the coil is $2x$.

Table IV —Values of $k'K$

$x/2a$	$k'K$	$x/2a$	$k'K$
0.1	0.368	2.0	1.485
0.2	0.595	3.0	1.529
0.3	0.767	4.0	1.547
0.4	0.902	5.0	1.555
0.5	1.009	6.0	1.561
0.6	1.098	7.0	1.563
0.7	1.167	8.0	1.565
0.8	1.224	9.0	1.566
0.9	1.272	10.0	1.567
1.0	1.311	inf	1.571

8 Mean-Square Values of Field over Solenoid.

The method for determining the mean-square value of the field is that of approximate integration, and has already been discussed in the author's

previous paper, in which the difficulty arising owing to the infinite value of the transverse field at the end of the solenoid is also dealt with. The resulting values of u_1 and u_2 are given in Table V below —

Table V—Values of u_1, u_2 in Formula (30)

a = radius of coil, b = length of coil

$b/2a$	0	0.2	0.4	0.6	0.8	1.0
u_1	3.29	3.13	2.83	2.51	2.22	1.94
u_2	0	0.50	1.23	1.99	2.71	3.35
$b/2a$	2	4	6	8	10	inf
u_1	1.11	0.51	0.31	0.21	0.17	0
u_2	5.47	7.23	8.07	8.52	8.73	9.87

Note — $b/2a = 0, u_1 = \pi^2/3, b/2a = \text{infinity}, u_2 = \pi^2$

9 Solenoid at very High Frequencies

When the frequency is infinitely large F and G both tend to infinity, but the ratio G/F tends to the value $1/2$, also $\alpha = \lambda, \beta = g, r = f$, so that if R_u represents the high frequency resistance of the uncoiled wire,

$$\frac{R'}{R_u} = \lambda + \frac{1}{2} \frac{d^2}{D^2} (gu_1 + fu_2) \quad (31)$$

Using Tables I, II, III the following values are obtained

Table VI—"Infinite" frequency resistance of solenoidal coil

a = coil radius d = wire diameter

b = coil length. D = distance of successive turns

Value of R'/R_u .

$b/2a =$	0	0.2	0.4	0.6	0.8	1.0	2	4	6	8	10	inf.
d/D												
1.0	inf	—	—	—	—	—	—	—	—	—	—	3.41
0.9	18.2	17.5	16.1	14.6	13.2	11.9	8.02	5.27	4.39	3.96	3.78	3.11
0.8	6.49	6.32	5.96	5.57	5.23	4.89	3.91	3.20	3.04	2.97	2.92	2.82
0.7	3.59	3.53	3.43	3.29	3.17	3.07	2.74	2.61	2.51	2.51	2.50	2.52
0.6	2.36	2.35	2.32	2.29	2.26	2.23	2.16	2.15	2.14	2.16	2.16	2.22
0.5	1.73	1.74	1.75	1.75	1.75	1.76	1.77	1.85	1.85	1.86	1.86	1.93
0.4	1.38	1.39	1.41	1.42	1.44	1.45	1.49	1.56	1.57	1.59	1.60	1.65
0.3	1.16	1.19	1.21	1.22	1.22	1.24	1.26	1.34	1.34	1.35	1.36	1.39
0.2	1.07	1.08	1.08	1.09	1.10	1.10	1.13	1.16	1.16	1.17	1.17	1.19
0.1	1.02	1.02	1.03	1.03	1.03	1.03	1.04	1.04	1.04	1.04	1.04	1.05

For this case the only result previously obtained has been that for a solenoid of infinite length and for which $d/D = 1$ Sommerfeld* gave for this case

$$R'/R_0 = 3.73$$

However, as Breit† has pointed out, there is an arithmetical error in Sommerfeld's calculation, and when this is corrected Sommerfeld's result becomes

$$R'/R_0 = 3.41,$$

which is identical with the tabulated value

10 Short Coils having a Finite Number of Turns

When the coil is very short $u_1 = \pi^2/3$ and $u_2 = 0$. If these are used in (30) and the formula is converted to a series formula in powers of d/D we find to the approximation d^4/D^4

$$\frac{R'}{R} = 1 + \left(1 + \frac{\pi^4}{72} \frac{d^4}{D^4}\right) F + \frac{\pi^2}{3} G \frac{d^2}{D^2} \left(1 + \frac{\pi^2}{6} \phi_1 \frac{d^2}{D^2}\right) \quad (32)$$

We proceed to find the formula corresponding to (32) when the number of turns is finite. Let there be $2n$ coplanar parallel wires, and let the wires be denoted $-n, -(n-1), \dots, -1, +1, +2, \dots, n$, p , n . For any one of these wires the equations of Section 2 apply, and if the plane of the system be the plane $0=0$, the coefficients L_n are zero. Further, the coefficients K_n will be different for each wire. Let the coefficient K_n , when the field is referred to axes having their origin in the wire p , be denoted by $K_n(p)$, and let the component Q of the field, when referred to the same axes and at a point distant r therefrom, be denoted by $Q(p, r)$. From the consideration that the field has odd symmetry about the centre of the whole system,

$$Q(\mu, r)_{0=0} = Q(-p, r)_{0=\pi} \quad (33)$$

If this be used in equations (1) and (2) we find

$$K_n(p) = (-)^n K_n(-p).$$

Now at a point $r, 0$ just outside the wire p , the field due to the currents in the remaining wires is by (1)

$$Q_0(p, r) = K_1(p) + rK_2(p) + r^2K_3(p) + \dots \quad (34)$$

* 'Ann. der Physik,' vol 28, p 609 (1907)

† 'Nature,' November 18, 1922.

and by (2) is also equal to

$$2I \left\{ \frac{1}{D+r} + \frac{1}{2D+r} + \frac{1}{(n+p-1)D+r} - \frac{1}{D-r} - \frac{1}{(n-s)(D-r)} \right\} \\ + [Q_1(p-1, D+r) + Q_1(p-2, 2D+r) + Q_1\{-n, (n+p-1)D+r\}]_{r=0} \\ - [Q_1(p+1, D-r) + Q_1(p+2, 2D-r) + Q_1\{n, (n-p)D-r\}]_{r=0} \quad (35)$$

If the expression (35) be expanded in ascending powers of r the coefficients of r^0, r, r^2, \dots must be identical with $K_1(p), K_2(p), \dots$ by (34). For the approximation sought we need only K_1, K_2 . The expansion then gives the equations

$$K_1(p) = \frac{2I}{D^2} \left\{ \frac{1}{n-p+1} + \frac{1}{n-p+2} + \frac{1}{n+p-1} \right. \\ \left. + \frac{c^2 I_1}{D^2} \left\{ k_1(p-1) + \frac{K_1(p-2)}{2^2} + \frac{K_1(1)}{(p-1)^2} + \frac{K_1(-1)}{p^2} \right. \right. \\ \left. \left. + \frac{K_1(-n)}{(n+p-1)^2} \right\} + K_1(p+1) + \frac{K_1(p+2)}{2^2} + \frac{K_1(n)}{(n-p)^2} \right\} + \quad (36)$$

$$K_2(p) = \frac{2I}{D^2} \left\{ 1 + \frac{1}{2^2} + \frac{1}{(n+p-1)^2} + 1 + \frac{1}{2^2} + \frac{1}{(n-p)^2} \right\} + \quad (37)$$

Regarding the term in c^2/D^2 in (36) as a correction, we can use the values of $K_1(p-1)$, etc., as given by the first term in (36) in this term.

We then have

$$K_1(p) = \frac{2I}{D} \left\{ \alpha_p - \frac{c^2 I_1}{D^2} \beta_p + \gamma_p \right\} \\ K_2(p) = \frac{2I}{D^2} (v_p + \dots) \quad (38)$$

in which

$$\alpha_p = \frac{1}{n-p+1} + \frac{1}{n-p+2} + \frac{1}{n+p-1} \\ \beta_p = \frac{\alpha_{p-1}}{1^2} + \frac{\alpha_{p-2}}{2^2} + \frac{\alpha_1}{(p-1)^2} + \frac{\alpha_{-1}}{p^2} + \frac{\alpha_{-n}}{(n+p-1)^2} \\ + \frac{\alpha_{p+1}}{1^2} + \frac{\alpha_{p+2}}{2^2} + \frac{\alpha_n}{(n-p)^2} \\ \gamma_p = 1 + \frac{1}{2^2} + \frac{1}{(n+p-1)^2} + 1 + \frac{1}{2^2} + \frac{1}{(n-p)^2} \quad (39)$$

Using (38) in equation (5) the dissipation in unit length of wire p is

$$W_p = \frac{\omega c^2 I^2}{D^4} \left[\left(\alpha_p^2 + 2\alpha_p \beta_p \phi_1 \frac{c^2}{D^2} \right) \psi_1 + \frac{1}{2} \frac{c^2}{D^2} \psi_2 \gamma_p^2 + \right], \quad (40)$$

to which must be added the ordinary skin effect

In the notation of preceding equations the whole dissipation in wire p is given by

$$\frac{1}{2} R_0 I^2 \left\{ 1 + F(z) \left(1 + \frac{1}{8} \gamma_p^2 \frac{d^4}{D^4} \right) + G(z) \frac{d^2}{D^2} \left(\alpha^2 p + \frac{1}{2} \alpha_p \beta_p \phi_1 \frac{d^2}{D^2} \right) + \right\}. \quad (41)$$

For the whole system α_p^2 , $\alpha_p \beta_p$, γ_p^2 must be replaced by their mean values. Let

$$\frac{1}{n} \sum_1^n \alpha_p^2 = u_n, \quad \frac{1}{n} \sum_1^n \alpha_p \beta_p = u_n v_n, \quad \frac{1}{n} \sum_1^n \gamma_p^2 = w_n \quad (42)$$

Also let R' be the alternating current resistance and R the direct current resistance of the whole system so that the dissipation is $\frac{1}{2} R' I^2$

Then from (41)

$$\frac{R'}{R} = 1 + F \left(1 + \frac{1}{8} w_n \frac{d^4}{D^4} \right) + u_n G \frac{d^2}{D^2} \left(1 + \frac{1}{2} v_n \phi_1 \frac{d^2}{D^2} \right) \quad (43)$$

The following table of values of u_n , v_n , w_n has been calculated from equations (39) and (42)

Table VII Values of u_n , v_n , w_n in equation (43)

n	u_n	v_n	u_n	v_n/u_n	w_n/u_n^2
2	1	-1	1	-1	1
3	1.500	-0.2500	2.375	-0.1667	1.056
4	1.806	+0.2081	3.458	+0.1153	1.061
5	2.014	0.5247	4.291	0.2605	1.058
6	2.166	0.7604	4.945	0.3511	1.054
10	2.514	1.3281	6.572	0.5283	1.040
20	2.833	+1.9088	8.215	+0.6738	1.024
inf	$\pi^2/3$	$\pi^2/3$	$\pi^4/9$	1	1

To interpolate for other values of n , u_n should be plotted against $1/n$, v_n/u_n against $1/\sqrt{n}$, w_n/u_n^2 against $1/n$. Approximately $w_n = u_n^2$.

11 Exact Solution for Two-Wire Coil at Infinite Frequency

In order to test the range of formula (43) it is important to obtain, if possible, an exact formula in certain cases. Formula (30) can be used when the number of wires is infinite, and it is possible to obtain an exact solution at very high frequencies in the case of two turns, assuming, of course, that these are suffi-

ciently represented by two parallel cylinders. At extreme frequencies the action of the eddy currents in a system of conducting cylinders is to annul the field within their substance, so that ultimately the surface of each cylinder becomes a stream-line in the magnetic field. Thus any problem on the high-frequency distribution of field due to currents in a system of parallel cylinders becomes analogous to an electrostatic problem, magnetic stream-lines replacing equipotential surfaces, integral currents replacing total charges, and the tangential field Q at any point on the surface of a cylinder corresponding to the electrical surface density σ multiplied by 4π .

Further, when Q is known, the energy dissipation per unit area of the cylindrical surface is identical with that for a uniform field tangential to the plane surface of an infinite conductor, since ultimately the radius of curvature of the cylinder is infinitely larger than the depth of penetration. Thus if k is the conductivity of the cylinder and f the frequency, the steady flow of energy into unit area of the surface of the cylinder is $Q^2(f/k)^{1/2}/16\pi$. The whole flow into unit length of a cylinder of radius c is thus $\frac{1}{2}Q_m^2 c^2 (\omega R_0/2)^{1/2}$, where $\omega = 2\pi f$, R_0 is the direct current resistance per unit length, and Q_m is the mean value of Q^2 over the surface.

Thus in the case of a single cylinder carrying current I , $Q = 2I/c$, and the dissipation of energy per unit length, is $\frac{1}{2}I^2 (R_0\omega/2)^{1/2}$, a result agreeing with that obtained by other methods.

Now the case of two parallel cylinders carrying equal charges has been treated by F. J. W. Whipple*. Let the cylinders each have radius c , and let their axes A, A' be at distance D . Let $D/2c = \cosh \alpha$. Then if B is the image of A' in A , B' the image of A in A' , B, B' lie on AA' , and $BB' = 2c \sinh \alpha$. Take a point P on one of the cylinders, and let $u = \widehat{BPB'}$. Whipple shows that the surface density σ at P is given by

$$\sigma = \frac{qKU}{\pi^2 c \sinh \alpha} (\cosh \alpha - \cosh u), \quad (44)$$

in which $U = \operatorname{dn} \frac{2uK}{\pi} + k \operatorname{cn} \frac{2uK}{\pi}$. Here q is the charge per unit length on

either cylinder, K is the real quarter period of the elliptic functions to a modulus k , which is of such value that

$$K'/K = 2\alpha/\pi \quad (45)$$

* 'Roy Soc. Proc.,' A, vol. 96, p. 465 (1920).

For the electromagnetic case q is replaced by the integral current I and σ by $Q/4\pi$, so that

$$Q = \frac{4IKU}{\pi\sigma \sinh \alpha} (\cosh \alpha - \cos u) \quad (46)$$

By integration the mean-square value of Q is found to be

$$Q_m^2 = \frac{4I^2}{\pi^2} \left[2 \coth \alpha \left(\frac{2K}{\pi} \right)^2 \left(\frac{E}{K} - \frac{k'^2}{2} \right) - 2 \operatorname{cosech}^2 \alpha \right], \quad (47)$$

so that the energy dissipated in unit length of the cylinder is

$$W = W_s \left[2 \coth \alpha \left(\frac{2K}{\pi} \right)^2 \left(\frac{E}{K} - \frac{k'^2}{2} \right) - 2 \operatorname{cosech}^2 \alpha \right] \quad (48)$$

where W_s is the dissipation in a solitary cylinder, viz -

$$W_s = \frac{1}{2} I^2 (R_0 \omega / 2)^{\frac{1}{2}} \quad (49)$$

For computation from (48) note that K and E are elliptic integrals of the first and second kinds to modulus k . Since k is only given indirectly by (45) it is preferable to treat k as known and calculate α by (45). The calculations lead to the following table -

Table VIII - High-frequency resistance of two parallel wires carrying similar currents

d = diameter of either wire - $2a$

D = distance of axes

$\sin^{-1} k$	d/D	W/W_s
0°		
10	0.087	1.004
20	0.175	1.010
30	0.264	1.034
40	0.352	1.061
50	0.440	1.091
60	0.540	1.134
70	0.640	1.180
80	0.754	1.234
89	0.905	1.301
90	1.000	1.333

12 Test of Range of Formula (43)

When the frequency is very high we obtain from (43)

$$\frac{W}{W_s} = 1 + \frac{1}{2} u_n \frac{d^2}{D^2} + \left(\frac{1}{8} w_n + \frac{1}{4} u_n v_n \right) \frac{d^4}{D^4} + \quad (50)$$

In the case of two wires

$$\frac{W}{W_s} = 1 + \frac{1}{2} \frac{d^2}{D^2} + \frac{1}{8} \frac{d^4}{D^4}, \quad (51)$$

and in the case of an infinite number of wires

$$\frac{W}{W_s} = 1 + \frac{\pi^2}{6} \frac{d^2}{D^2} + \frac{\pi^4}{24} \frac{d^4}{D^4} \quad (52)$$

The exact values for these cases are obtained from Tables VI and VIII. This yields the following comparison table --

d/D	Two wires		Infinite wires	
	Exact	by (51)	Exact	by (52)
1.0	1.333	1.375	inf	6.7
0.9	1.296	1.323	18.2	5.0
0.8	1.254	1.269	6.5	3.7
0.7	1.209	1.215	3.6	2.8
0.6	1.161	1.164	2.36	2.12
0.5	1.116	1.117	1.73	1.66

Formula (43) is therefore a good approximation throughout the whole range of d/D in the case of two wires, but in the case of an infinite number of wires breaks down when d/D exceeds, say 0.6 and the frequency is very high.

To include closer spacings a compromise must be made. It will be assumed that a formula of the type (30) will more nearly represent the truth and that the coefficients are such that formula (43) holds on expansion.

We have, then,

$$R'/R = 1 + F \left(1 + \frac{1}{8} w_n \frac{d^4}{D^4} \right) + \frac{u_n G \frac{d^2}{D^2}}{\left(1 - \frac{1}{4} v_n \phi_1 \frac{d^2}{D^2} \right)^2 + \frac{1}{18} v_n^2 \psi_1 \frac{d^4}{D^4}} \quad (53)$$

When this semi-empirical formula is compared with the exact results at infinite frequency we obtain the following comparison table

d/D	Two wires		Infinite wires	
	Exact	by (53)	Exact	by (53)
1.0	1.333	1.445	infinity	54.5
0.9	1.296	1.362	18.2	13.85
0.8	1.254	1.289	6.5	6.25
0.7	1.209	1.224	3.6	3.6
0.6	1.161	1.167	2.36	2.37
0.5	1.116	1.119	1.73	1.73

It appears from this table that if d/D is less than 0.8 the formula is always within 4 per cent of the exact result.

When $d/D = 0.9$ the formula is 5 per cent high in the case of two wires and 28 per cent low in the case of a very large number of wires. Since for finite frequencies the error is less, formula (53) should be reliable for very short coils for all frequencies, for any number of turns and for spacings up to $d/D = 0.8$.

Except at extremely high frequencies it should also be applicable even when $d/D = 0.9$.

13 Hickman's Formula

Hickman* has proposed a formula for calculating the alternating current resistance of a fairly long solenoid. His formula is as follows —

$$\frac{R'}{R} = U_{0/1} + \frac{G}{U_{0/2} + \frac{\lambda^2 F^2}{U_{0/2}}} + \frac{K}{U_{1/3} + \frac{\lambda^2 F^2}{U_{1/3}}}, \quad (54)$$

in which

$$\begin{aligned} G &= \frac{\lambda^2 d^2}{D^2} \left[\frac{D}{2a} + \tan^{-1} \frac{b}{2a} - \tan^{-1} \frac{D}{2a} \right]^2 \\ K &= \frac{\pi^2 \lambda^2 d^4}{144 D^4} \left[\frac{\pi^2}{6} + \frac{4bD}{b^2 + 4a^2} - \frac{4D^2}{D^2 + 4a^2} + \frac{D^2}{a^2} \right] \\ E - V_{0/2} &+ \frac{\pi^2 d^2}{24 D^2} - \frac{d^2}{4 D^2} \left[\frac{2bD}{b^2 + 4a^2} - \frac{2D^2}{D^2 + 4a^2} + \frac{D^2}{2a^2} \right] \\ F &= V_{1/3} + \frac{\pi^4}{1440} \frac{d^4}{D^4} \end{aligned}$$

$U_{0/n}$, $V_{0/n}$ are defined by the equation

$$Q_0/Q_n = U_{0/n} + i\lambda V_{0/n}, \quad (55)$$

in which

$$Q_n = \sum_{k=0}^{i-\infty} \frac{|n(i\lambda)^k|}{|k|k+n}, \quad (56)$$

while

$$\lambda = \pi d^2 k \omega / 4 \quad (57)$$

$\omega/2\pi$ is the frequency for which the formula holds, k is the conductivity of the wire, d its diameter, the wires in the coil are spaced at distance D , while the coil has length b and radius a . The formula strictly only holds for the effective resistance of the central wire in a system of parallel wires having the same number of wires as there are turns in the coil and the same spacing. The return of this system is a similar system at a distance equal to the radius of the coil.

* 'Scientific Paper, Bureau of Standards,' No. 472.

Hickman gives indirect reasons for supposing that this system will give similar results to that for a coil

He assumes that the loss in the central wire represents fairly the loss in the whole system, so that this will limit its application to fairly long solenoids

14 We now proceed to show the relation between Hickman's formula and the formula developed in the preceding sections. We first simplify the expressions for G, K, E, making use of the fact that the spacing is nearly always small compared with the radius and length of the coil

Neglecting D/a and its higher powers we have

$$\left. \begin{aligned} G &= \frac{\lambda^2 d^2}{12} \left(\tan^{-1} \frac{b}{2a} \right)^2, & K &= \frac{\pi^4 \lambda^2 d^4}{864 D^4} \\ E &= V_{0/2} + \frac{\pi^2 d^2}{24 D^2}, & F &= V_{1/3} + \frac{\pi^3 d^4}{1152 D^4} \end{aligned} \right\} \quad (58)$$

If in equation (56) we put $\lambda = -r^2/4$ it may be shown from the series for the Bessel functions that

$$Q_n = 2^n \left[n J_n(x) / x^n \right] \quad (59)$$

and then from (3), (4), (57), (59) we obtain the following equations connecting the functions $U_{s/n}$, $V_{s/n}$ with the functions ϕ_n , ψ_n defined in equation (3)

$$\left. \begin{aligned} U_{0/1} &= 1 + \frac{1}{8} z^2 \psi_2 & \lambda V_{0/1} &= \frac{z^2}{8} (1 - \phi_2) \\ U_{0/2} &= \frac{z^2 \psi_1}{8 (\phi_1^2 + \psi_1^2)} & \lambda V_{0/2} &= \frac{z^2 \phi_1}{8 (\phi_1^2 + \psi_1^2)} \\ U_{1/3} &= \frac{z^2 \psi^2}{24 (\phi_2^2 + \psi_2^2)} & \lambda V_{1/3} &= \frac{z^2 \phi_2}{24 (\phi_2^2 + \psi_2^2)} \end{aligned} \right\} \quad (60)$$

Since the values of ϕ , ψ can be computed for any value of z , these formulæ may be used to determine the functions U , V for values of λ beyond the range of Hickman's table (*loc cit*, p. 104)

By making use of equations (58) and (60) Hickman's formula (54) may now be written —

$$\begin{aligned} \frac{R'}{R} &= 1 + F(z) + \frac{\frac{\pi^4}{72} F(z) \frac{d^4}{D^4}}{\left(1 + \frac{\pi^4}{240} \phi_2 \frac{d^4}{D^4} \right)^2 + \left(\frac{\pi^4}{240} \psi_2 \frac{d^4}{D^4} \right)^2} \\ &\quad + \frac{uG(z) \frac{d^2}{D^2}}{\left(1 + \frac{\pi^2}{12} \phi_1 \frac{d^2}{D^2} \right)^2 + \left(\frac{\pi^2}{12} \psi_1 \frac{d^2}{D^2} \right)^2} \end{aligned} \quad (61)$$

where, as in equations (6) and (23),

$$F(z) \equiv \frac{1}{8} z^2 \psi_2, \quad G(z) = \frac{1}{8} z^2 \psi_1, \quad (62)$$

while

$$u = 4 (\tan^{-1} b/2a)^2$$

This formula is identical with that obtained in Section (6) (equation 10) if, in the formula there obtained, we suppose $u_1 = 0$ and u_2 to be defined by (62). Now u_1 is zero if the transverse field is negligible, as is the case for fairly long solenoids. The difference in the value of u is due to Hickman's assumption of two parallel wire systems as representing the solenoid. In fact, if the methods of the present paper were applied to solve Hickman's problem, equation (61) would be obtained.

To prove this we note that, so far as the losses in the central wire due to the wires in its own system are concerned, formula (14) holds good. As regards the losses due to the return system at distance a , these are given by formula (23) with $H = 2I/D \tan^{-1} b/2a$. Since the two losses are additive we obtain formula (61) for the high-frequency resistance of the central wire.

It may be noted here that formulæ (14) and (23) are approximate formulæ, and that the effect of non-uniformity of the field is represented by the third term in formula (61). Hickman has shown that this term contributes only a small amount to the total loss even when d/D is of the order 0.8. The error in applying the simple formula

$$R'/R = 1 + F(z) + uG(z) d^2/D^2$$

is therefore not mainly due to non-uniformity of the field over the section of an individual wire, but rather to the modification of the value of the uniform field due to the secondary eddy currents set up in the neighbouring wires (See Hickman's remarks, *loc. cit.*, p. 75).

15 Comparison with Experimental Results

Measurements of the alternating current resistance of fairly long solenoidal coils have been made by Howe* and by Hickman†. The conditions in regard to frequency and method were entirely different, Howe using radio frequencies and a thermal method, while Hickman used acoustic frequencies and a bridge method, the requisite skin effect being obtained by employing very thick wire and correspondingly large coils.

* 'Journ. I.E.E.', vol. 58, p. 152 (1920)

† Hickman, *loc. cit.*

Howe gives results for two coils in which ratio of length to diameter is 10, the coils differing in regard to spacing and diameter of wire.

The following tables show how formula (30) agrees with the observed values —

Howe's Observations

Coil 1.			Coil 2	
Wire diameter = 0.163 cm			Wire diameter = 0.264 cm	
Spacing = 0.33 cm			Spacing = 0.29 cm	
Turns = 62			Turns = 92	
$d\sqrt{f}$	Formula (30)	Observed	Formula (30)	Observed
25	1.8	1.7	2.9	2.7
50	3.6	3.5	6.1	5.5
100	7.1	7.0	13.1	10.9
150	10.6	10.5	20.1	16.4
200	14.1	14.0	27.3	21.8

It is seen that for the loosely spaced coil the agreement between theory and observation is very good, but in the closely wound coil the theoretical values are higher than the observed values.

In the latter case the loss due to the transverse field component is much more appreciable than in the former case. Now the losses due to the transverse field will be concentrated at the ends of the coil and will tend to make the temperature of the ends of the coil somewhat higher than that at the centre. Since Howe determined the resistance by measurement of temperature at the centre there will be a tendency for the observed results to be low.

Hickman's observations are compared with formula (30) in the following table.

It will be noticed that there is a slight tendency for the theoretical results again to be higher than the observed values, the mean discrepancy being about 7 per cent.

It may be noted here that Hickman's smallest coil is very similar in shape and spacing to Howe's coil No. 2, but while Hickman only works up to $d\sqrt{f} = 28$, Howe extends the observations to $d\sqrt{f} = 200$. Throughout the short range of overlapping the two methods check very well.

In view of the tendency for the theoretical formula to over-estimate the observed value, it may be well to emphasise that the theoretical formula assumes an infinite number of turns and a uniform current distribution, both

Hickman's Observations

Length = 96 cm. = b
 Wire diameter = 0.518 cm = d
 Spacing = 0.6 cm = D

Coil diameter, $2a$, cm	Frequency ν per second	Computed formula (50)	Observed, Hickman
8.24	1,000	1.72	1.69
	2,000	2.65	2.50
	3,000	3.19	3.04
15.8	1,000	1.68	1.59
	2,000	2.58	2.33
	3,000	3.13	2.88
22.6	1,000	1.64	1.55
	2,000	2.54	2.28
	3,000	3.12	2.84
30.4	1,000	1.59	1.54
	2,000	2.51	2.40
	3,000	3.16	2.75

of which conditions are violated in practice, non-uniformity of current distribution being due to capacity effects. As regards short coils for which formula (53) should hold, we may take a case given by Landemann and Hüter*. These experimenters found that, for short coils measured at a wave-length λ metres, their results could be expressed by the formula—

$$R' = \frac{A}{\sqrt{\lambda}} + \frac{B}{\lambda^2},$$

where A , B depend on the coil. In the case of a coil having a diameter of 31 cm, a length of 1.8 cm, and wound with seven turns of copper wire of 2.2 mm. diameter, they give—

$$A = 9.5, \quad B = 2.14 \times 10^4.$$

Using these values, we find when $\lambda = 7,300$ metres $R = 0.112$ ohm, while formula (53) gives $R' = 0.12$ ohm. When $\lambda = 455$ metres $R = 0.55$ ohm, by Landemann's formula, while formula (53) gives $R = 0.54$ ohm. For shorter wave-lengths the theoretical formula gives lower results than the experimental formula.

* 'Verh. Deutsch. Phys. Gesell.', vol. 15, p. 219 (1913).

APPENDIX TABLES

Table IX—Values of ϕ_1 , ψ_1 , ϕ_2 , ψ_2 , $F(z)$, $G(z)$ See formulæ (14), (23), (26), (30), (53) $z^2 = \pi k \omega d^2$. $\omega/2\pi$ = frequency k = conductivity of wire d = diameter of wire

z	ϕ_1	ϕ_2	ψ_1	ψ_2	$F(z)$	$G(z)$
0—0.5	$z^4/48$	$z^4/384$	$z^2/8$	$z^2/24$	$z^4/192$	$z^4/64$
0.5	0.0012	0.0002	0.0312	0.0104	0.000326	0.000975
1.0	0.0202	0.0026	0.1215	0.0415	0.00519	0.01519
1.5	0.0917	0.0129	0.246	0.0918	0.0258	0.0691
2.0	0.2262	0.389	0.345	0.156	0.0782	0.1724
2.5	0.377	0.0865	0.377	0.224	0.1756	0.295
3.0	0.500	0.1548	0.360	0.263	0.318	0.405
3.5	0.585	0.234	0.326	0.321	0.492	0.499
4.0	0.643	0.314	0.292	0.339	0.678	0.584
4.5	0.684	0.384	0.264	0.341	0.862	0.669
5.0	0.715	0.444	0.242	0.334	1.042	0.755
> 5	$1 - \frac{\sqrt{2}}{z}$	$1 - \frac{2\sqrt{2}}{z}$	$\frac{\sqrt{2}}{z} - \frac{1}{z^2}$	$\frac{2\sqrt{2}}{z} - \frac{6}{z^2}$	$\frac{\sqrt{2}z - 3}{4}$	$\frac{\sqrt{2}z - 1}{8}$

Table X—Values of α , β , γ in formula (30)

d/D	$z = 1$			$z = 2$			$z = 3$		
	α	β	γ	α	β	γ	α	β	γ
1.0	1.01	1.02	0.96	1.09	1.34	0.67	1.31	2.29	0.49
0.9	1.00	1.02	0.97	1.06	1.29	0.72	1.20	1.99	0.55
0.8		1.02	0.98	1.04	1.23	0.78	1.13	1.73	0.62
0.7		1.02	0.98	1.02	1.18	0.83	1.08	1.52	0.68
0.6		1.01	0.99	1.00	1.13	0.87	1.04	1.30	0.75
0.5		1.01	0.99		1.09	0.91	1.02	1.24	0.82
0.4		1.01	0.99		1.06	0.94	1.01	1.14	0.88
0.3		1.00	1.00		1.04	0.97	1.00	1.06	0.93
0.2					1.01	0.99		1.03	0.97
0.1					1.00	1.00		1.01	0.99

d/D	$z = 4$			$z = 5$			$z = \text{inf}$		
	α	β	γ	α	β	γ	α	β	γ
1.0	1.43	3.61	0.43	1.50	4.91	0.41	1.71	inf	0.35
0.9	1.30	2.75	0.49	1.37	3.39	0.46	1.55	12.45	0.39
0.8	1.21	2.12	0.55	1.25	2.48	0.53	1.41	4.83	0.44
0.7	1.12	1.71	0.62	1.15	1.94	0.60	1.27	2.87	0.52
0.6	1.07	1.51	0.70	1.09	1.60	0.68	1.16	2.03	0.60
0.5	1.03	1.32	0.78	1.04	1.37	0.76	1.08	1.59	0.69
0.4	1.02	1.19	0.85	1.02	1.22	0.84	1.03	1.33	0.78
0.3	1.00	1.10	0.91	1.00	1.11	0.90	1.01	1.17	0.87
0.2		1.04	0.96		1.05	0.98	1.00	1.07	0.94
0.1		1.01	0.99		1.01	0.99		1.02	0.98

On the Field of Force near the Neutral Point produced by Two Equal Coaxial Coils, with Special Reference to the Campbell Standard of Mutual Inductance.

By RAYMOND M WILMOTTE, B A , National Physical Laboratory.

(Communicated by Sir Joseph Petavel, F R S —Received December 16, 1924)

Introduction and Summary.

When a current is passed through two equal coaxial coils so that the component of the magnetic fields parallel to the common axis add, there is a circle, mid-way between the two coils, at which the magnetic field is zero. At all points in the plane of that circle lying outside it, the field of force is in one direction, and at all points within the circle it is in the opposite direction. It is evident, therefore, that if a coaxial turn of wire be placed in the plane of the circle, the mutual inductance between the two coils will be a maximum, when the wire coincides with the circle, and any small change in the radius of the turn will affect the value of the mutual inductance only to the second order of small quantities.

A Campbell (1) made use of this fact for the construction of a standard of mutual inductance. In this design two equal coaxial single layer coils formed the primary, and the secondary consisted of a large number of turns packed closely together, so that the mean circle of the secondary coincided with the neutral circle formed by the field of the two single layer coils. By this means it was not necessary to measure the diameter of the secondary coil with extreme accuracy.

The principle was also used by F. E. Smith (2) in the construction of an apparatus for measuring the absolute value of the ohm by the Lorenz method. A rotating disc formed the secondary of the mutual inductance with two single layer coaxial coils as the primary. Lord Rayleigh (3) had previously advocated the inverse system, in which the dimensions of the apparatus were adjusted so that a small change in the radius of the coils would have a very small effect on the value of the mutual inductance.

The accuracy of the apparatus designed on the principle first applied by A. Campbell depends largely on the terms of the second order in the evaluation of the mutual inductance. The conditions necessary to make the second order terms small do not seem to have been investigated, nor has the nature of the

small changes in the mutual inductance due to a displacement of the secondary in various directions been fully considered

These questions are investigated in this paper, and the variation of the value of the mutual inductance due to a radial displacement of the secondary is calculated and compared with the results obtained by A. Campbell for a particular case

The Variation of the Mutual Inductance due to a Small Displacement of the Secondary

1 *General Expression*—Throughout this paper the units used are absolute units unless otherwise stated. Coils P and Q (fig. 1) are equal and coaxial

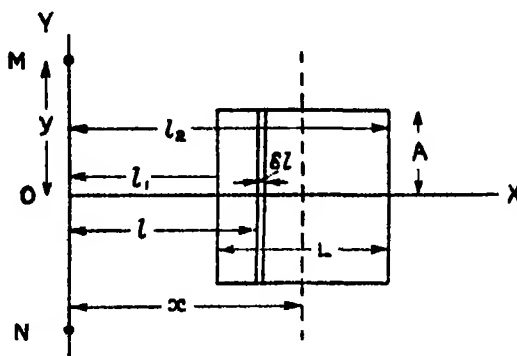


FIG. 1

These will be called the primary, and a single turn of radius y coaxial with the two equal coils will be called the secondary

Let M_1 and M_2 be the mutual inductance between the single turn, situated at a distance x from the centre of coil P, and coils P and Q respectively. Suppose the secondary be moved from the position MN to the position $M'N'$ where MM' is of length δr and makes an angle θ with the axis, then

$$\begin{aligned} \delta M_1 = & \left[\frac{\partial M_1}{\partial x} \delta x + \frac{\partial M_1}{\partial y} \delta y \right] + \frac{1}{2} \left[\frac{\partial^2 M_1}{\partial x^2} (\delta x)^2 + 2 \frac{\partial^2 M_1}{\partial x \partial y} \delta x \delta y + \frac{\partial^2 M_1}{\partial y^2} (\delta y)^2 \right] \\ & + \frac{1}{3} \left[\frac{\partial^3 M_1}{\partial x^3} (\delta x)^3 + 3 \frac{\partial^3 M_1}{\partial x^2 \partial y} (\delta x)^2 \delta y + 3 \frac{\partial^3 M_1}{\partial x \partial y^2} \delta x (\delta y)^2 + \frac{\partial^3 M_1}{\partial y^3} (\delta y)^3 \right] \\ & + \dots \end{aligned} \quad (1)$$

Now the co-ordinates of M' referred to OX , OY are $(x + \delta x, y + \delta y)$ and referred to $O'X$, $O'Y$ they become $(x + \delta x - 2b, y + \delta y)$. Hence, by putting M_2 for M_1 and $(x - 2b)$ for x in equation (1), the corresponding equation for

coil Q will be obtained. The total change in the mutual inductance to the terms of the first order of small quantities is, therefore, given by

$$\delta M_1 + \delta M_2 = \frac{\partial M_1}{\partial x} \delta x + \frac{\partial M_2}{\partial (x-2b)} \delta x + \frac{\partial M_1}{\partial y} \delta y + \frac{\partial M_2}{\partial y} \delta y$$

This will be zero for all values of the ratio $\delta x/\delta y$ where

$$\frac{\partial M_1}{\partial x} + \frac{\partial M_2}{\partial (x-2b)} = 0 \quad \text{and} \quad \frac{\partial M_1}{\partial y} + \frac{\partial M_2}{\partial y} = 0$$

Since M_1 and M_2 are similar, functions of these conditions will hold when

$$x = b \quad \text{and} \quad \frac{\partial M_1}{\partial y} = \frac{\partial M_2}{\partial y} = 0 \quad (2)$$

For these conditions, since $M = M_1 + M_2$, we have

$$\delta M = \left[\frac{\partial^2 M}{\partial x^2} (\delta x)^2 + \frac{\partial^2 M}{\partial y^2} (\delta y)^2 \right] + \left[\frac{\partial^2 M}{\partial x^2 \partial y} (\delta x)^2 \delta y + \frac{1}{2} \frac{\partial^2 M}{\partial y^2} (\delta y)^2 \right] + \quad (3)$$

If X and R are the axial and radial components respectively of the magnetic force at the secondary due to coil P alone, the following relations are easily deduced

$$2\pi y \quad X = \frac{\partial M}{\partial x} \quad \text{and} \quad 2\pi y \quad R = -\frac{\partial M}{\partial y}$$

Differentiating these relations and substituting equation (3) becomes

$$\begin{aligned} \delta M = 2\pi y \left[\frac{\partial x}{\partial y} (\delta y)^2 - \frac{\partial R}{\partial x} \cdot (\delta x)^2 \right] - \frac{2\pi}{3} \left[3y \frac{\partial^2 R}{\partial x \partial y} (\delta x)^2 \delta y \right. \\ \left. + 3 \frac{\partial R}{\partial x} \cdot (\delta x)^2 \cdot \delta y - y \cdot \frac{\partial^2 x}{\partial y^2} (\delta y)^2 - 2 \frac{\partial x}{\partial y} (\delta y)^2 \right] + \dots \end{aligned}$$

If Ω is the magnetic potential at the secondary

$$x = \frac{\partial \Omega}{\partial x} \quad \text{and} \quad R = \frac{\partial \Omega}{\partial y}$$

so that

$$\frac{\partial x}{\partial y} = \frac{\partial R}{\partial x} \quad \text{and} \quad \frac{\partial^2 x}{\partial y^2} = \frac{\partial^2 R}{\partial x \partial y}$$

The final result then is

$$\begin{aligned} \delta M = 2\pi y \left\{ \frac{\partial R}{\partial x} [(\delta x)^2 - (\delta y)^2] + \frac{1}{3} \left[\left(\frac{\partial^2 R}{\partial x \partial y} + \frac{2}{y} \frac{\partial R}{\partial x} \right) (\delta y)^2 \right. \right. \\ \left. \left. - 3 \left(\frac{\partial^2 R}{\partial x \partial y} + \frac{1}{y} \frac{\partial R}{\partial x} \right) (\delta x)^2 \cdot \delta y \right] + \dots \right\} \quad (4) \end{aligned}$$

If there are n_1 turns on the secondary, equation (5) becomes

$$\delta M = -2\pi y n_1 n_2 \left\{ \cos 2\theta \left(\frac{\partial R'}{\partial y} \right)_i (\delta r)^2 - \frac{\sin^2 \theta}{3} \left[\left(\frac{\partial R'}{\partial y} \right)_i^2 + \frac{2}{y} \left(\frac{R'}{\partial y} \right)_i + 3 \left(\frac{\partial R'}{\partial y} \right)_i \cot^2 \theta + \frac{3}{y} \left(\frac{R'}{\partial y} \right)_i \cot^2 \theta \right] (\delta r)^2 + \right\} \quad (6)$$

and the condition given by equation (2) becomes

$$\int_{l_1}^l X' dl = 0 \quad (7)$$

Alexander Russell (6) has shown that, for a coil of radius A

$$R' = \frac{2}{r_1} \left[\frac{2Al}{r_2^2} E - \frac{l}{y} (F - E) \right] \quad (8)$$

and

$$X' = \frac{2}{r_1} \left[\frac{2A(A-y)}{r_1^2} + (F - E) \right] \quad (9)$$

where $r_1^2 = (A + y)^2 + l^2$ and $r_2^2 = (A - y)^2 + l^2$, E and F being the complete elliptic integrals to the modulus $\sqrt{1 - r_2^2/r_1^2}$ of the first and second kinds

By means of these equations, the curves in figs 3 and 4 were calculated, taking the diameter of the primary as unity. These curves can be applied to any value of the diameter of the primary, since the magnetic force is inversely proportional to the linear dimensions of the coils.

The arithmetico-geometric means applied by L. V. King (7) for calculating the complete elliptic integrals can be used with convenience for obtaining these curves, if a calculating machine is available.

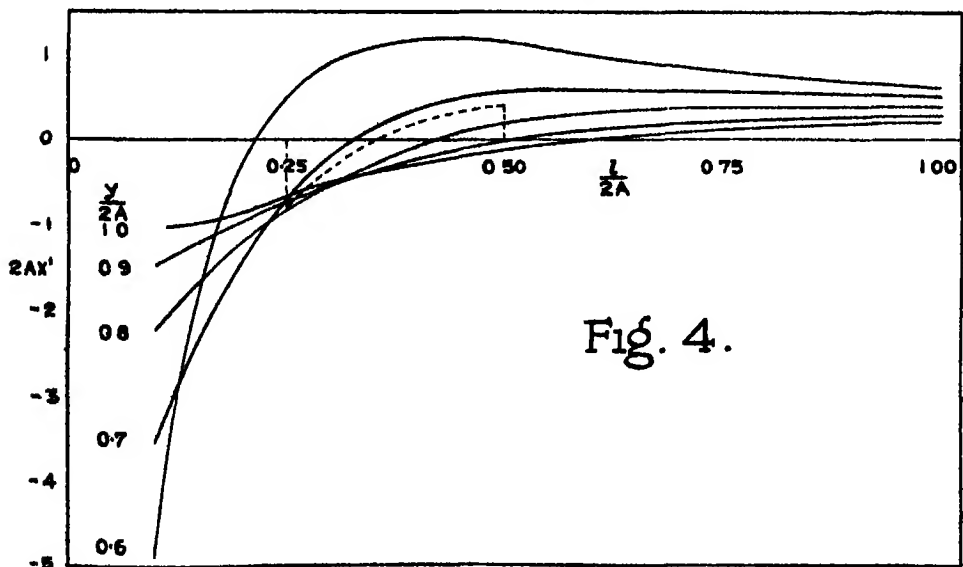
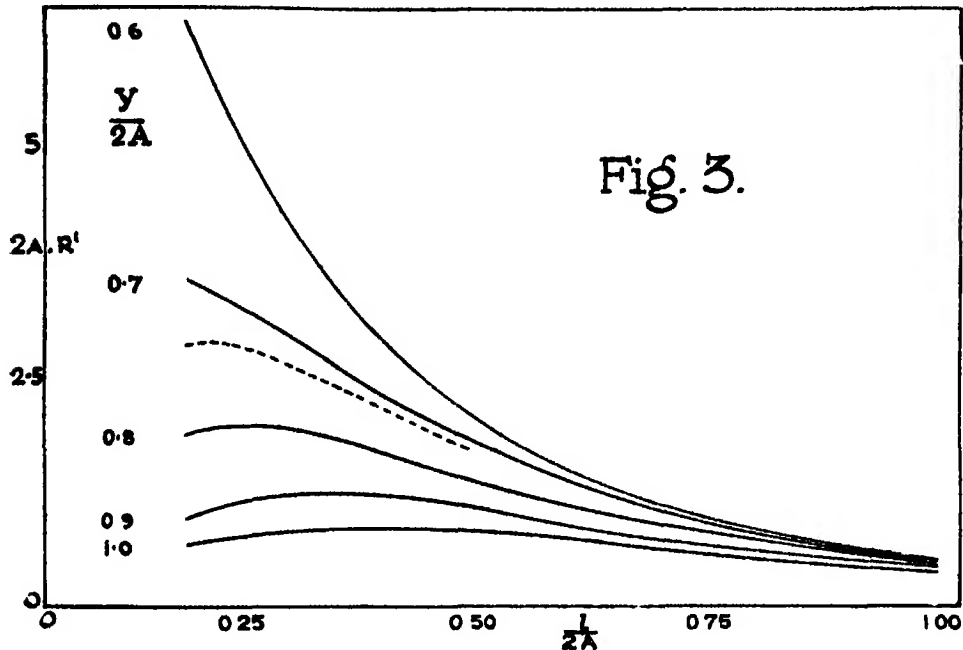
Since the terms of the third order are small, it is not necessary to evaluate $\partial R'/\partial y$ to any great accuracy. This can be obtained by estimating the gradient of the curves obtained by plotting R' against $y/2A$, from fig 3, at the required points. Should greater accuracy be required, it would be necessary to differentiate equation (7) with respect to y , remembering that, if k is the modulus,

$$\frac{\partial E}{\partial k} = \frac{1}{k} (E - F) \quad \text{and} \quad \frac{\partial F}{\partial k} = \frac{E}{k(1 - k^2)} - \frac{F}{k}$$

The relation obtained is rather cumbersome. Fortunately, the effect of the third-order terms is negligible in the calculation of the standard apparatus to which this paper mainly applies.

If the section of the secondary is finite, the variation of the value of the mutual inductance from the ideal case, when all the turns of the secondary are concentrated at the neutral circle, can be obtained by integrating equation

(4) over the whole section of the winding A Campbell (8) and D W Dye (9) evaluated the effect from a formula of G F C Searle deduced for a general



case of a coil having a rectangular cross-section in any field symmetrical about the axis of the coil To obtain a similar expression from equation (4) it is

necessary to expand the series to one other term, when a formula equivalent to that of G F C Searle will be obtained

3 *Comparison with the Campbell Standard of Mutual Inductance*—The dotted lines in figs 3 and 4 correspond to the design of the Campbell Standard of Mutual Inductance at present in the National Physical Laboratory A Campbell calculated the value of $\partial M/\partial y$, using the following formula obtained by differentiating the expression deduced by Vianam Jones (4) for the mutual inductance of a spiral and a circle

$$\frac{\partial M}{\partial y} = \frac{n_1 n_2 \sqrt{Ay}}{A(A+y)} \left[2AkF + \frac{(A+y)\sqrt{Ay}}{l} \psi \right]_{l_1}^{l_2} \quad (10)$$

where ψ is the complete elliptic integral of the third kind and n_2 is the number of turns per unit length of the spiral The values used were $A = 10$, $l_1 = 5$, $l_2 = 10$, $n_1 n_2 = 10,000$

From the curve obtained A Campbell deduced that

$$\frac{\partial M}{\partial y} = 0 \quad \text{when} \quad y = 14 \cdot 583$$

and

$$\frac{\partial M}{\partial y} = -0 \cdot 1077\xi + 0 \cdot 016\xi^2 +$$

where M is measured in millihenries and $\xi = y - 14 \cdot 583$

From fig 3 it will be seen that

$$\left[2AR' \right]_{0.25}^{0.5} = 1 \cdot 17 \quad \text{and} \quad \left[4A^2 \frac{\partial R'}{\partial y} \right]_{0.25}^{0.5} = 10 \cdot 2$$

Substituting the above values in equation (5) and putting $\theta = \pi/2$, we have

$$\delta M = -0 \cdot 054 (\delta r)^2 + 0 \cdot 0053 (\delta r)^3 +$$

in which M is measured in millihenries On differentiating this becomes

$$\frac{\partial M}{\partial r} = -0 \cdot 108\delta r + 0 \cdot 016 (\delta r)^2 +$$

This agrees with the result obtained by A Campbell It will be also seen that the area enclosed by the dotted line in fig 4 is zero, so that the condition required by equation (7) holds

If the terms of the third and higher orders are neglected, as was found admissible by A Campbell (8) and D W Dye (9) in the calculation of this standard of mutual inductance, δM varies as $\cos 2\theta$. This result is shown graphically in fig 5, in which polar co-ordinates are used, the radius being proportional to δM .

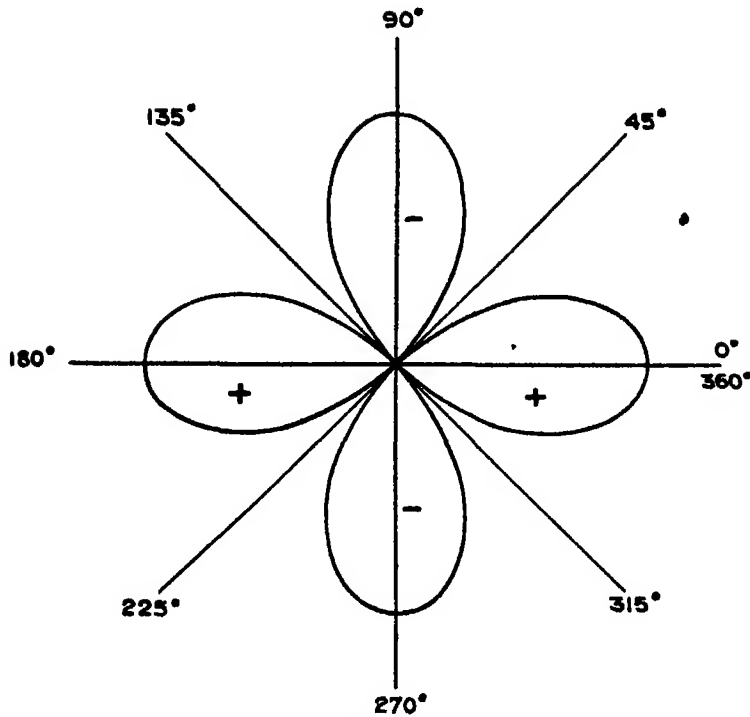


FIG 5

4. *Method of Finding Neutral Circle* -- Suppose the ratio of $y/2A$ is known, the approximate value of l_1 and l_2 which will make $\int_{l_1}^{l_2} X' dl = 0$ can be found from fig 4. The accurate value of this integral can then be calculated from equation (10), remembering that

$$\frac{\partial M}{\partial y} = 2\pi y \int_{l_1}^{l_2} X' dl$$

This can be made zero by adding $2\pi y X_2' \delta l_2$ where X_2' is the axial magnetic force due to a unit circular current at l_2 and can be read off from the curve in fig. 4. The value of δl_2 can then be found and added to l_2 , giving a second approximation to the dimensions of the primary coil. The process can be repeated until the necessary accuracy is attained.

Conclusion

It has been shown that, to keep the second-order terms small, it is necessary to make $[R']_{l_1}^{l_2}$ small, still retaining the condition given by equation (7). By

724 *Neutral Point produced by Two Equal Coaxial Coils.*

examining the curves of figs 3 and 4 it will be seen that this can be done by making the length of the single layer primary coils small, and the ratio of the diameters of the secondary to primary as large as possible

It is not advisable to reduce the diameter of the primary in order to increase the ratio of $y/2A$ for the accuracy in the measurement of the dimensions of the primary would thereby be decreased. On the other hand, it is not possible to increase the diameter of the secondary to any great extent, for the condition required by equation (7) shows that the distance between the primary and the secondary would have to be increased, rendering the apparatus very cumbersome and requiring a greater number of turns to give the same mutual inductance. This is a disadvantage, for the correction due to the self-capacity of the secondary becomes very important. The curves show, however, in which direction an improvement can be made, the best design depending on the kind of measurement to be made, and the ultimate size of the apparatus, which is considered convenient from a mechanical point of view.

The best shape for the secondary can be seen from fig 5. A displacement of the secondary at an angle of 45° with the axis produces a change in mutual inductance only to the third order of small quantities. This could have been deduced *a priori*, for the equipotential surface which cuts itself must do so in this case at an angle of 90° . It is not, however, usually practicable to use a complex shape for the section of the coil, for the new errors introduced would balance any advantage gained. A square section will, in general, be found most convenient.

In the case of the Lorenz apparatus a suggested refinement, as the outcome of the deductions of this paper, might be to bevel the rotating discs on which the brushes are applied, at an angle of 45° to the axis, so that any inaccuracy in the location of the brushes would only affect the result to the third order of small quantities.

In conclusion I wish to express my thanks to Dr G F C Searle for his kind criticism.

REFERENCES

- (1) 'Roy Soc Proc,' A, vol 79, p 428 (1907)
 - (2) 'Phil Trans,' A, vol 214, p 27 (1913)
 - (3) 'Phil Mag,' vol. 14 (1882)
 - (4) 'Roy Soc Proc,' A, vol 63, p. 192 (1898)
 - (5) 'B A Report,' p. 241 (1899).
 - (6) 'Phys Soc. Proc.,' vol 20, p 478 (1907).
 - (7) 'Roy. Soc. Proc.,' A, vol. 100, p. 60 (1921)
 - (8) 'Roy Soc Proc.,' A, vol. 87, p. 394 (1912).
 - (9) 'Roy. Soc. Proc,' A, vol. 101, p 315 (1922).
-

The Adiabatic Invariance of the Quantum Integrals.

By P A M DIRAC, St John's College, Cambridge

(Communicated by Prof Sir E Rutherford, F R S —Received December 19, 1924)

§ 1 *Introduction*

The postulate of the existence of stationary states in multiply periodic dynamical systems requires that if the condition of such a system, when quantised, is changed in any way by the application of an external field or by the alteration of one of the internal constraints, the new state of the system must also be correctly quantised. It follows that the laws of classical mechanics cannot in general be true, even approximately, during the transition. There is one kind of change, however, during which one may expect the classical laws to hold, namely, the so-called adiabatic change, which takes place infinitely slowly and regularly, so that the system practically remains multiply periodic all the time. In this case the quantum numbers cannot change, and it should be possible to deduce from the classical laws that the quantum integrals remain invariant. This was attempted by Burgers,* who showed that they are invariant provided there are no linear relations of the type

$$\sum_i m_i \omega_i = 0 \quad (1)$$

between the frequencies ω_i of the system, where the m_i are integers. In general, however, the frequencies will alter during the adiabatic change, and in so doing will pass through an infinity of values for which relations such as (1) hold. A closer investigation is therefore necessary, as was pointed out by Burgers himself.

In the following work, conditions which are rigorously sufficient to ensure the invariance of the quantum integrals, are obtained in such a form that it is possible for one to see whether they are satisfied or not without having to integrate the equations of adiabatic motion.

§ 2 *The Equations of Adiabatic Motion*

Let q_r, p_r ($r = 1, 2, \dots, n$) be a set of Hamiltonian co-ordinates of a multiply periodic dynamical system of n degrees of freedom. The quantum integrals J_r and their conjugate angle variables w_r form another set of Hamiltonian co-ordinates connected with the first by the contact transformation

$$\sum p_r dq_r = \sum J_r dw_r + dS. \quad (2)$$

* Burgers, 'Proc Amsterdam Roy. Acad. of Sciences,' vol 20, p 163.

Also the p_r and q_r , when expressed in terms of the J_r and w_r , are multiply periodic in the w_r with periods unity, and the Hamiltonian function H , when similarly expressed, is a function of the J_r only

Regarding S and the q_r as functions of the J_r and w_r , we have

$$\sum p_r \frac{\partial q_r}{\partial w_r} = J_r + \frac{\partial S}{\partial w_r}$$

and

$$\sum p_r \frac{\partial q_r}{\partial J_r} = \frac{\partial S}{\partial J_r}$$

The first of these equations shows that S is equal to a periodic function of the w_r , plus terms of the form $-\sum (J_r + \alpha_r) w_r$, where the α_r are independent of the w_r . The second now shows that the $(J_r + \alpha_r)$ are independent of the J_r . The $(J_r + \alpha_r)$ are therefore constants, and can be made zero by a suitable choice of the arbitrary constants that may be added to the J_r , as shown by Burgers. This makes S consist entirely of a periodic function of the w_r .

A change in the condition of the system is represented mathematically by the continuous variation (from a_1 to a_2 , say) of a parameter (a) occurring in the Hamiltonian function H , the Hamiltonian equations remaining valid, though H may involve a . An adiabatic change is the limiting case when a tends to zero in such a way that

$$a/a \rightarrow 0,^*$$

which makes

$$da/da \rightarrow 0$$

With (a) varying, equation (2) must be replaced by

$$\sum p_r \left(dq_r - \frac{\partial q_r}{\partial a} a dt \right) = \sum J_r dw_r + dS - \frac{\partial S}{\partial a} a dt.$$

This gives

$$\sum p_r dq_r - H dt = \sum J_r dw_r - \bar{H} dt + dS$$

where

$$\bar{H} = H - \sum p_r \frac{\partial q_r}{\partial a} a + \frac{\partial S}{\partial a} a.$$

Hence the transformation from p_r, q_r, H to J_r, w_r, \bar{H} is a contact transformation, so that

$$J_K = - \frac{\partial \bar{H}}{\partial w_K}, \quad w_K = \frac{\partial \bar{H}}{\partial J_K}. \quad (3)$$

For small values of a , H can be expanded in powers of a . Thus we can put

$$H = H_0 + aH_1.$$

* This relation cannot hold at the ends of the range of (a) from a_1 to a_2 , but we may make the intervals of (a) during which it does not hold as small as we please.

Here H_0 is the value of the Hamiltonian function when (a) is constant, so that

$$\frac{\partial H_0}{\partial w_K} = 0, \quad \frac{\partial H_0}{\partial J_K} = \omega_K,$$

where the ω_K may be considered as the instantaneous frequencies

Let

$$F = \sum p_r \frac{\partial q_r}{\partial a} - \frac{\partial S}{\partial a} - H_1$$

so that

$$\bar{H} = H_0 - aF$$

H_1 , being a function of the p_r and q_r , must be a periodic function of the w_r of period unity. Hence F is also a periodic function of the w_r of period unity, so we can write

$$\begin{aligned} 2\pi F &= \sum_{m_1, m_2, \dots, m_n} C_{m_1, m_2, \dots, m_n} \sin 2\pi (m_1 w_1 + m_2 w_2 + \dots + m_n w_n + \gamma_{m_1, m_2, \dots, m_n}) \\ &= \sum_m C_m \sin 2\pi (W_m + \gamma_m), \end{aligned} \quad (4)$$

say, W_m being equivalent to $\sum m_r w_r$, and the summation being taken over all integral values of m that make W_m positive. The coefficients C_m are functions of the J_K , a and α . We shall require the series $\sum m_K C_m$ to be absolutely and uniformly convergent, as is the case in general with continuous forces.

Equations (3) now become

$$\dot{J}_K = a \frac{\partial F}{\partial w_K}, \quad \dot{w}_K = \omega_K - a \frac{\partial F}{\partial J_K},$$

which may be written, when a does not vanish,

$$\frac{dJ_K}{da} = \frac{\partial F}{\partial w_K} \quad (5)$$

$$\frac{dw_K}{da} = \frac{\omega_K}{a} - \frac{\partial F}{\partial J_K} \quad (6)$$

These are the exact equations of adiabatic motion. Burgers derived them on the assumption that H does not contain a explicitly, but pointed out that it may be sufficient to assume that H involves a only through higher powers than the first*. The present method shows, however, that such assumptions are unnecessary, as $\partial H / \partial a$ can be absorbed in F .

§ 3 *The Conditions for Adiabatic Invariance.*

Suppose for definiteness that a is positive throughout the range of (a) from a_1 to a_2 , except at the ends, where it vanishes. Equations (4) and (5) show that

$$\left| \frac{dJ_K}{da} \right| \leq \sum_m |m_K C_m|,$$

* *Loc. cit.*, p. 169.

so that the dJ_K/da remain bounded as a tends to zero. Hence the J_K , and therefore also the C_m , dC_m/da , $d\gamma_m/da$, and $d\omega_K/da$, are also bounded.

Let a' to $a' + \delta a$ be a small interval of the range a_1 to a_2 , ultimately to be made to contract to zero about a certain point a_0 . Integrating equation (5) through this interval, we get

$$\begin{aligned}\delta J_K &= \int_{a'}^{a'+\delta a} \frac{\partial F}{\partial w_K} da = \sum_m \int_{a'}^{a'+\delta a} m_K C_m \cos 2\pi (W_m + \gamma_m) da \\ &= \sum_m m_K C_m \int_{a'}^{a'+\delta a} \cos 2\pi (W_m + \gamma_m) da + \delta a \epsilon(\delta a),\end{aligned}\quad (7)$$

where $\epsilon(x)$ is used to denote a quantity which tends to zero as x tends to zero. The C_m in (7) are the values of the coefficients for the point $a = a_0$, and the γ_m are also supposed to have their values for this point.

Let M be a large positive number, ultimately to be made to tend to infinity, and let m_0 denote the largest numerical value of the m 's in any specified set. We can divide the series on the right-hand side of (7) into two parts, one comprising only those sets of m 's whose m_0 is less than M , and the other comprising those sets of m 's whose m_0 is greater than or equal to M . This second part tends to zero as M tends to infinity, on account of the absolute convergence of the series $\sum m_K C_m$, and so it must be of the form $\delta a \epsilon(1/M)$. Thus

$$\delta J_K = \sum_m^M m_K C_m \int_{a'}^{a'+\delta a} \cos 2\pi (W_m + \gamma_m) da + \delta a \epsilon(\delta a) + \delta a \epsilon(1/M),$$

so that we are left with only a finite series with which to deal.

Consider now the contribution to δJ_K of a set of m 's for which

$$\left| \frac{dW_m}{da} \right| > \frac{m_0}{\eta} \quad (\alpha)$$

throughout the interval δa , where η is a small positive quantity which will ultimately be made to tend to zero in a certain way. We have

$$m_K C_m \int_{a'}^{a'+\delta a} \cos 2\pi (W_m + \gamma_m) da = m_K C_m \int_{a'}^{a'+\delta a} \left[\cos 2\pi (W_m + \gamma_m) \frac{dW_m}{da} \right] da$$

Now

$$\begin{aligned}\left| \frac{d}{da} \left(1 / \frac{dW_m}{da} \right) \right| &= \left| \frac{d^2 W_m}{da^2} / \left(\frac{dW_m}{da} \right)^2 \right| \\ &< \frac{\eta^2}{m_0} \left| \sum_K m_K \frac{d}{da} \left(\frac{\omega_K}{a} - \frac{\partial F}{\partial J_K} \right) \right| \quad \text{from (6) and } (\alpha) \\ &= \eta^2 \left| \sum_K \frac{m_K}{m_0} \left(\frac{1}{a} \frac{d\omega_K}{da} - \frac{\omega_K}{a^2} a - \frac{d}{da} \frac{\partial F}{\partial J_K} \right) \right|.\end{aligned}$$

This may be put equal to

$$\epsilon_m (\eta^2/a) + \epsilon_m (\eta^2 \ddot{a}/a^3)$$

$$\frac{d}{da} \frac{\partial F}{\partial J_K} = \frac{\partial^2 F}{\partial a \partial J_K} + \frac{\partial^2 F}{\partial a \partial J_K} \frac{da}{da} + \sum_i \left\{ \frac{\partial^2 F}{\partial J_i \partial J_K} \frac{dJ_i}{da} + \frac{\partial^2 F}{\partial w_i \partial J_K} \left(\frac{\omega_i}{a} - \frac{\partial F}{\partial J_i} \right) \right\}$$

Suppose (a) increases by Δa while W_m increases by $\frac{1}{2}$. During this time

$1 \left| \frac{dW_m}{da} \right|$ cannot change by more than $[\epsilon_m (\eta^2/a) + \epsilon_m (\eta^2 \ddot{a}/a^3)] \Delta a$, while

$\cos 2\pi (W_m + \gamma_m)$ changes sign. Hence the net contribution of two successive half-cycles to the integral we are evaluating must certainly be numerically less than

$$m_K C_m [\epsilon_m (\eta^2/a) + \epsilon_m (\eta^2 \ddot{a}/a^3)] \Delta a$$

Also, the fractions of complete cycles left over at the ends of the interval of

integration contribute terms that cannot numerically exceed $m_K C_m \left| \frac{dW_m}{da} \right|$,

which is of the form $m_K C_m \epsilon_m (\eta/\delta a) \delta a$, from (a). This gives

$$\left| m_K C_m \int_{a'}^{a'+\delta a} \cos 2\pi (W_m + \gamma_m) da \right| < m_K C_m \delta a$$

$$[\epsilon_m (\eta^2/a) + \epsilon_m (\eta^2 \ddot{a}/a^3) + \epsilon_m (\eta/\delta a)]$$

The sum of the right-hand side for all sets of m 's satisfying (a) and having $m_0 < M$ is of the form

$$\delta a [\epsilon (\eta^2/a) + \epsilon (\eta^2 \ddot{a}/a^3) + \epsilon (\eta/\delta a)],$$

owing to the absolute convergence of the series $\sum m_K C_m$, and to the fact that the ϵ_m 's tend to their zero values uniformly with respect to the m 's. Hence we have

$$\frac{\delta J_K}{\delta a} = \sum_m m_K C_m \frac{1}{\delta a} \int_{a'}^{a'+\delta a} \cos 2\pi (W_m + \gamma_m) da$$

$$+ \epsilon (\delta a) + \epsilon (1/M) + \epsilon (\eta^2/a) + \epsilon (\eta^2 \ddot{a}/a^3) + \epsilon (\eta/\delta a) \quad (8)$$

where the summation need include only those sets of m 's for which $m_0 < M$ and for which, at some point in the interval δa ,

$$\left| \frac{dW_m}{da} \right| = \left| \sum m_r \left(\frac{\omega_r}{a} - \frac{\partial F}{\partial J_r} \right) \right| \equiv \frac{m_0}{\eta}$$

or for which

$$|\sum m_r \omega_r| \equiv m_0^{\frac{1}{2}} a / \eta < M^{\frac{1}{2}} a / \eta, \quad (\beta)$$

the terms involving $\partial F / \partial J_r$ being negligible.

We can choose η to tend to zero with a in such a way that each of the quantities a/η , η^2/a and $\eta^2 \ddot{a}/a^3$ tends to zero, this being possible since a/a tends to zero. We can now make δa and $1/M$ tend to zero so slowly that $\eta/\delta a$, $a/\eta \delta a$ and

$M'a/\eta$ tend to zero. In this way all the ε terms in (8) (whose sum we shall denote simply by ε) tend to zero, and also $a/\eta\delta a$ and the right-hand side of (9) tend to zero.

We may assume that the J_K tend to certain limiting values J_{0K} at each point $a = a_0$ *. Throughout the interval δa the ω_K must lie within certain regions surrounding the values ω_{0K} that they take for $J_K = J_{0K}$, $a = a_0$, which regions ultimately contract to zero. There may be sets of m 's which make $\sum m_K \omega_{0K} = 0$ and these, if they exist, must be included in the summation in (8). Any other particular set of m 's originally satisfying (9), m_K 's say, must cease to do so sooner or later during the limiting process, since

$$|\sum_K m_K' \omega_K| > |\sum_K m_K \omega_{0K}|$$

at all points in the interval δa , and this will ultimately be greater than $M'a/\eta$. Hence we may choose M to be always sufficiently small to exclude all such sets of m 's from the summation in (8), while at the same time M tends to infinity during the limiting process. So the only sets of m 's that need be included are those which actually make $\sum m_r \omega_r = 0$ when $a = a_0$ and $J_K = J_{0K}$.

For any of these included sets m_r 's say, we have

$$\begin{aligned} \delta \sum_r m_r' \omega_r &= \sum_r m_r' \frac{\partial \omega_r}{\partial a} \delta a + \sum_{r,K} m_r' \frac{\partial \omega_r}{\partial J_K} \delta J_K + \delta a \varepsilon(\delta a) \\ &= \sum_r m_r' \frac{\partial \omega_r}{\partial a} \delta a + \sum_{r,K} m_r' \frac{\partial \omega_r}{\partial J_K} \sum_m m_K C_m \\ &\quad \int_a^{a'+\delta a} \cos 2\pi (W_m + \gamma_m) da + \varepsilon \cdot \delta a \end{aligned}$$

Now $\frac{1}{\delta a} \int_a^{a'+\delta a} \cos 2\pi (W_m + \gamma_m) da$ cannot numerically exceed unity, and may

therefore be put equal to $\cos \sigma_m$. Thus

$$\frac{\delta \sum_r m_r' \omega_r}{\delta a} = \sum_r m_r' \frac{\partial \omega_r}{\partial a} + \sum_{r,K} m_r' \frac{\partial \omega_r}{\partial J_K} \sum_m m_K C_m \cos \sigma_m + \varepsilon \quad (9)$$

$$\text{Suppose} \quad \left| \sum_r m_r' \frac{\partial \omega_r}{\partial a} \right| > \sum_m \left| C_m \sum_{r,K} m_K m_r' \frac{\partial \omega_r}{\partial J_K} \right| \quad (10)$$

* If they do not, then we could always choose a subsequence of the a 's which makes the J_K tend to certain limiting values J_K' (functions of a) at an infinite enumerable everywhere dense set of points, in which case it must also make $J_K \rightarrow J_K'$ for any intermediate point, on account of the continuity (uniform with respect to a) of J_K . The method of the text would now show that these J_K' are constants. In the same way we could choose another subsequence of a 's which makes $J_K \rightarrow J_K''$ not always equal to J_K' , and the J_K'' would also have to be constants. This is impossible since, initially, $J_K' = J_K''$.

when $a = a_0$ and $J_K = J_{0K}$. With this condition there is a lower bound b , to the value of $|\delta \Sigma_r m_r^* \omega_r / m_0^* \delta a|$ independent of the σ_m . This makes

$$|\delta \Sigma_r m_r^* \omega_r| > m_0^* b \delta a$$

where δa denotes any interval for which

$$\delta a \rightarrow 0 \quad \text{and} \quad \eta / \delta a \rightarrow 0$$

these being the only restrictions to which δa in equation (9) is subject. Thus $\Sigma_r m_r^* \omega_r$ satisfies the inequality (8) only during a small sub-interval whose extent cannot exceed any δa for which

$$m_0^* b \delta a > 2 (m_0^*)^2 a / \eta,$$

i.e., whose extent cannot exceed $2a / (m_0^*)^2 b \eta$, as this value for δa satisfies the above restrictions. It is only during this sub-interval that

$$|\cos 2\pi [W(m^*) + \gamma(m^*)] da$$

is of the same order of magnitude as the range of (a) through which it is taken. Hence,

$$m_K^* C(m^*) \int_{a'}^{a'+\delta a} \cos 2\pi [W(m^*) + \gamma(m^*)] da = \frac{m_K^* C(m^*)}{b} \epsilon_1 (a/\eta \delta a) \delta a$$

plus other ϵ terms like those already included in (8).

Summing this expression for all the sets of m 's left in (8) on the assumption that the inequality (10) holds for each of them, we get

$$\delta a \epsilon (a/\eta \delta a) \sum_{m=1}^M m_K C_m / b_m.$$

This series may be divergent, since the b_m may tend to zero as the m 's tend to infinity. We can avoid this difficulty by using the fact that there is no limitation on how slowly M tends to infinity. We may make the finite series $\sum_{m=1}^M m_K C_m / b_m$ tend to infinity more slowly than $\epsilon (a/\eta \delta a)$ tends to zero (however slowly that may be), so that their product tends to zero, and may be put equal to $\epsilon [af(M)/\eta \delta a]$.

Hence

$$\frac{\delta J_K}{\delta a} = \epsilon (\delta a) + \epsilon (1/M) + \epsilon (\eta^2/a) + \epsilon (\eta^2 \ddot{a}/a^3) + \epsilon (\eta/\delta a) + \epsilon [af(M)/\eta \delta a]$$

and this tends to zero if first a and then δa are made to tend to zero, the arbitrary quantities η and $1/M$ tending to zero in a suitable manner. So the J_K are constants in the limit provided, whenever a relation of the type

$$\Sigma_r m_r^* \omega_r = 0$$

holds for $a = a_0$ with integral m_r , and the corresponding coefficient $C(m')$ does not vanish, the inequality

$$\left| \frac{\partial}{\partial a} \sum_r m_r \omega_r \right| > \sum_{m_1, m_2} \left| C_{m_1, m_2} \sum_{r, k} m_k m_r \frac{\partial \omega_r}{\partial J_k} \right|$$

is satisfied, where the summation with respect to the m 's refers to all those sets of m 's for which

$$\sum m_r \omega_r = 0$$

when $a = a_0$

The maximum value of

$$\left| \sum_{r, k} m_r \frac{\partial \omega_r}{\partial J_k} \sum_m m_k C_m \cos 2\pi (W_m + \gamma_m) \right|$$

for all values of the w 's will in general be less than

$$\sum_m \left| C_m \sum_{r, k} m_k m_r \frac{\partial \omega_r}{\partial J_k} \right|$$

If this maximum is evaluated for any particular dynamical system (it cannot easily be done in the general case) and substituted for the right-hand side of (10), less stringent conditions for the adiabatic invariance will be obtained. If the improved conditions are not satisfied, the J_k can vary with suitable initial values of the phases of the motion, and will do so in such a way as to make $\sum m_r \omega_r$ remain equal to zero while (a) changes by a finite amount. As this contradicts the postulate of the existence of stationary states, one must conclude that in these cases the motion cannot be completely described by the use of classical mechanics.

If, however, there are relations of the type $\sum m_r \omega_r = 0$ holding identically for all values of the J 's, it is possible to reduce the number of J 's and w 's necessary to describe the system and to replace them by new conjugate variables α_r and β_r which do not enter into H . Equations (5) and (6) are still true, the only difference being that the C 's are now functions also of the α 's and β 's. It is easily verified that the $d\alpha/da$, $d\beta/da$ are bounded, and hence the same method applies to show that the reduced number of J 's are adiabatically invariant.

§ 4 *The Application of the Conditions.*

As there is an infinite number of inequalities to be satisfied for any variation in (a) , however small, the conditions would not be very useful unless it were possible to prove all of them except, perhaps, a finite number by general arguments. This does not seem to be possible for the general case of systems of more than two degrees of freedom.

For systems of two degrees of freedom, however, there is only a finite number of values of (a) for which

$$\omega_1 + x \omega_2 = 0 \quad \text{and} \quad \frac{\partial}{\partial a} (\omega_1 + x \omega_2) = 0$$

at the same time, x being a rational or irrational number, since there are two equations to determine the two unknowns (a) and x . In any closed interval of (a) which does not contain any of these values, there must be a lower limit to the value of

$$\left| \frac{\partial}{\partial a} (m_1 \omega_1 + m_2 \omega_2) / m_0 \right|,$$

where (a) and m_1/m_2 have values which make $m_1 \omega_1 + m_2 \omega_2 = 0$, otherwise there would be an infinite sequence of values of (a) and m_1/m_2 which make

$$m_1 \omega_1 + m_2 \omega_2 = 0 \quad \text{and} \quad \frac{\partial}{\partial a} (m_1 \omega_1 + m_2 \omega_2) / m_0 \rightarrow 0,$$

and the limiting values would give one of the points we have excluded. Hence, whenever

$$m_1' \omega_1 + m_2' \omega_2 = 0,$$

we have

$$\left| \frac{\partial}{\partial a} (m_1' \omega_1 + m_2' \omega_2) / m_0' \right| > \xi$$

say, so that the condition

$$\left| \frac{\partial}{\partial a} (m_1' \omega_1 + m_2' \omega_2) \right| > \sum_m \left| C_m \sum_{r,k} m_k m_r' \frac{\partial \omega_r}{\partial J_k} \right|$$

is satisfied if

$$\xi > \sum_m \left| C_m \sum_{r,k} m_k \frac{m_r'}{m_0'} \frac{\partial \omega_r}{\partial J_k} \right| \quad (11)$$

For any given ξ there can be only a finite number of values for m_1', m_2' which do not satisfy the inequality (11), since as $|m_1'|, |m_2'|$ tend to infinity the m 's included in the first summation in (11) also tend to infinity, so that the right-hand side of (11) tends to zero. Hence in any interval of (a) which does not contain any points at which

$$\omega_1/\omega_2 = \frac{\partial \omega_1}{\partial a} / \frac{\partial \omega_2}{\partial a},$$

there is only a finite number of points at which the J 's may not be constant.

The same result is true for a system of n degrees of freedom provided the coefficients $C_{m_1 \dots m_n}$ of the Fourier series vanish for all but a finite number of values of the suffixes m_1, m_2, \dots, m_n . The proof is the same as before, except that the factor $(m_1 \omega_1 + m_2 \omega_2)$ must be replaced by $\sum m_r \omega_r$, where m_1, \dots, m_n are restricted to have only values for which $C_{m_1 \dots m_n}$ does not vanish.

This case includes all the systems usually met with in the Quantum Theory, the vanishing of the C 's for certain values of the suffixes manifesting itself by selection principles which allow only a finite number of changes for each of the quantum numbers except at most two of them. The quantum integrals of such systems are invariant under any adiabatic change except at a finite set of points where

$$\omega_r/\omega_s = \frac{\partial \omega_r}{\partial a} \bigg/ \frac{\partial \omega_s}{\partial a},$$

ω and ω_s being the frequencies corresponding to the quantum numbers whose changes are unrestricted, and at another finite set (or possibly infinite enumerable set tending to points of the previous set) where relations of the type $\Sigma m_r \omega_r = 0$ hold

The writer is much obliged to Mr R. H. Fowler for suggesting this investigation, and for his help during its progress.

On the Theory of Elastic Stability

By W. R. DEAN, B.A., Fellow of Trinity College, Cambridge

(Communicated by Prof. G. I. Taylor, F.R.S.—Received December 20, 1924.)

The object of the present paper is to derive equations that are adequate to decide questions of the stability under stress of thin shells of isotropic elastic material. Equations for the same purpose have been given by R. V. Southwell,* who used a method that is closely followed in a part of this paper.

Such equations must contain terms that may be, and are, neglected in applications of the theory of elasticity to problems in which the stability of configurations is not considered. The truth of Kirchhoff's uniqueness theorem,† which has reference to the ordinary equations of elasticity, in which powers of the displacement co-ordinates above the first are neglected, is sufficient proof of this statement. In practice it is generally sufficient to retain only the first and second order terms,‡ and no terms of higher order are considered.

* "On the General Theory of Elastic Stability," 'Phil. Trans.,' A, vol. 213, p. 187.

† A. E. H. Love, 'Mathematical Theory of Elasticity' (3rd Edition), § 118.

‡ There are exceptions to this. Cf. a paper by J. Prescott, 'Phil. Mag.,' vol. 43, p. 97 (1922), which, though not immediately concerned with elastic stability, obtains equations which can be applied to this theory. See also § 9 below.

here To obtain such equations an extended form of Hooke's Law is necessary : the extension made by Southwell* is used in this paper There are then two methods available for the derivation of the equations Either we may obtain the three conditions for the equilibrium of an elementary volume of the substance by considering the forces acting upon it, or we may calculate the energy of strain correct to the *third* order of displacement co-ordinates and deduce the equations by variation of this function The first method has been used in one place here, as it would appear to be the simpler in the particular case of a plane plate, in which only one of the equations, and that the simplest, is required However, the stability equations for a cylindrical shell are also obtained, and then all three equations are necessary The derivation by the first method of each one of these is a laborious matter, while using the second method there is only one calculation, that of the strain energy function, to be made Consequently, for this purpose, as in general the second method seems to be preferable

The equations that are obtained by either of the methods outlined above refer in the first instance to the co-ordinates of displacement of any point of the shell Yet it is clearly desirable to have instead equations which connect the displacements of points only of the middle surface, for equations of this type will be simpler in so far as these displacements are functions of two variables only, while a knowledge of the behaviour of the middle surface is evidently sufficient to decide a question of stability What is wanted, in fact, is a method of reduction of equations involving the displacements of all points of the shell, to equations involving only the displacements of points of the middle surface,† precisely similar to that used in the Theory of Thin Shells ‡ The assumptions used in the reduction by this theory, however, are such that it is not clear how they can be used, or extended, to effect the reduction of second-order general equations that is required here

Consequently, no use of them has been made It is merely supposed that the displacement co-ordinates of any point of the shell can be expanded in power series of the normal distance of the point from the middle surface Second-order shell equations can then be deduced from the general equations by using the boundary conditions at the two faces of the shell The method will in the same way reduce general equations of the first order to the corre-

* *Loc cit*, p 192

† It will be convenient in what follows to call equations of these two types "general" equations and "shell" equations respectively

‡ Love, *op cit*, chap. 24

sponding shell equations. The assumption, therefore fundamental, as to the expansions of displacements may exclude some problems from the range of the method, but it does not appear likely that in elastic stability, where attention is of necessity confined to a consideration of the simplest types of stress, there will be any difficulty on this score. Moreover, the equations in their final form contain no explicit reference to the assumption, so that they may be, and certainly in first order problems often are, valid beyond the limits that might appear to be imposed. The equations thus obtained are not here applied to any new problem, but as it appeared desirable to check the results of a new method by a comparison with known formulae, the stability of a tubular strut has been briefly considered. The condition for instability in a symmetrical mode of distortion has been deduced by Southwell from general theory, and in other modes from the Theory of Thin Shells.* Equivalent results are obtained in each case by the methods of this paper.

The Strain Energy Function

2 We proceed to develop a method of finding in a suitable form the strain energy function of a thin cylindrical shell. The energy of strain is a quadratic function of the components of strain, which ordinarily need only be evaluated correctly to the second order of displacement co-ordinates. This accuracy is not sufficient if problems of stability are to be considered, and a more exact determination demands a complete revision of the usual processes of evaluation. In the first place an extended statement of Hooke's Law is necessary, as in its usual form it is not framed precisely enough if squares and products of displacements are to be included. We take that statement given by Southwell †

In a distortion of any magnitude of an elastic body there are associated with each point of the body three linear elements orthogonal both before and after strain, ‡ and these elements undergo stationary extension, as defined below. If a parallelepiped is constructed with these elements as coterminous edges, only normal stresses will act on its faces after strain, and if relations are assumed between these stresses and the corresponding strains, called respectively principal stresses and principal strains, they are sufficient to determine stress in terms of displacement completely. The extended form of Hooke's Law is that principal stresses and strains in a distortion of any magnitude are

* *Loc. cit.*, pp. 227-236.

† *Loc. cit.*, p. 193.

‡ Love, *op. cit.*, Appendix to chap. 1.

connected by the usual equations, that is to say, if the principal strains are extensions e_1, e_2, e_3 , and the corresponding principal stresses are S_1, S_2, S_3 , then

$$S_1 = 2\mu e_1 + \lambda(e_1 + e_2 + e_3), \text{ etc.} \quad (1)$$

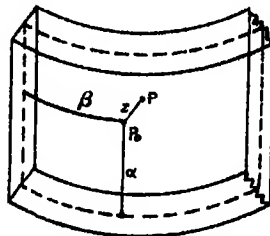
with Lamé's notation for the elastic constants

Extension is defined as the ratio of the increase in length of an element to its length *before* strain, and stress as the total action over an element of surface divided by the area of the element *before* strain. The energy of strain per unit volume of *unstrained* material, W , is then given by the equation

$$W = \frac{\lambda + \frac{2}{3}\mu}{2} (e_1 + e_2 + e_3)^2 - 2\mu (e_2 e_3 + e_3 e_1 + e_1 e_2) \quad (2)$$

With these assumptions and definitions the strain energy function of any elastic body can be calculated to any degree of accuracy that is required

We confine attention to a thin shell of uniform thickness of which the middle surface is generated by parallel straight lines. The position of any point P_0 of the middle surface is specified by α , the distance of P_0 , measured along a generator, from an arbitrary line of curvature and by β the distance of P_0 , measured along a line of curvature from an arbitrary generator. ρ , the radius of curvature of the normal section of this surface perpendicular to the generator at any point, is a function of β only*. The position of any point P of the shell is specified by drawing PP_0 normal to the middle surface, then if the length P_0P is z , the position of P is given by the orthogonal curvilinear co-ordinates α, β, z , as in the accompanying figure



3 We have first to find an expression for the extension of a linear element under strain. Let the displacements of $P, (\alpha, \beta, z)$, be u, v, w with regard to α, β, z axes at P , these axes being the normal to the middle surface through $P, (z)$, a line through P parallel to the generators, (α) , and a third perpendicular, (β) , u, v, w are then functions of α, β, z . Taking a neighbouring point $P', (\alpha + \delta\alpha, \beta + \delta\beta, z + \delta z)$, let the length PP' be r , and let its direction cosines with regard to α, β, z axes at P be l, m, n . The displacements of P' are

$$u + \frac{\partial u}{\partial \alpha} \delta\alpha + \frac{\partial u}{\partial \beta} \delta\beta + \frac{\partial u}{\partial z} \delta z, \text{ etc.,}$$

* Although the only application in this paper is to a problem wherein ρ is constant, other applications are meditated in which ρ is a function of β . The simplification in the work if ρ is supposed constant is very slight.

along α, β, z axes at P' , while to the first order of r

$$\delta\alpha = lr, \quad \delta\beta = \frac{m\rho r}{\rho - z},^* \quad \delta z = nr$$

The angle between the z axes of P and P' is to the same order $mr/(\rho - z)$. Thus the co-ordinates of P' after strain with regard to α, β, z axes at P are

$$\begin{aligned} u + r \left[l \left(1 + \frac{\partial u}{\partial \alpha} \right) + \frac{m\rho}{\rho - z} \frac{\partial u}{\partial \beta} + n \frac{\partial u}{\partial z} \right], \\ v + r \left[l \frac{\partial v}{\partial \alpha} + m \left(1 + \frac{\rho}{\rho - z} \frac{\partial v}{\partial \beta} - \frac{w}{\rho - z} \right) + n \frac{\partial v}{\partial z} \right], \\ \text{and} \\ w + r \left[l \frac{\partial w}{\partial \alpha} + m \left(\frac{\rho}{\rho - z} \frac{\partial w}{\partial \beta} + \frac{v}{\rho - z} \right) + n \left(1 + \frac{\partial w}{\partial z} \right) \right] \end{aligned}$$

The co-ordinates of P after strain are u, v, w , so that denoting by $r(1 + e)$ the length of PP' after strain, there results

$$\begin{aligned} (1 + e)^2 = & \left[l \left(1 + \frac{\partial u}{\partial \alpha} \right) + \frac{m\rho}{\rho - z} \frac{\partial u}{\partial \beta} + n \frac{\partial u}{\partial z} \right]^2 \\ & + \left[l \frac{\partial v}{\partial \alpha} + m \left(1 + \frac{\rho}{\rho - z} \frac{\partial v}{\partial \beta} - \frac{w}{\rho - z} \right) + n \frac{\partial v}{\partial z} \right]^2 \\ & + \left[l \frac{\partial w}{\partial \alpha} + m \left(\frac{\rho}{\rho - z} \frac{\partial w}{\partial \beta} + \frac{v}{\rho - z} \right) + n \left(1 + \frac{\partial w}{\partial z} \right) \right]^2 \end{aligned} \quad (3)$$

This expression gives e , the extension of a linear element, and shows that $(1 + e)$, the ratio of the length of the element after strain to that before, is inversely proportional to the central radius vector of a quadric in the direction of the element before strain. The equation to this quadric can be written

$$F(\xi, \eta, \zeta) = \text{const.} \quad (4)$$

if $F(l, m, n)$ denotes the right-hand side of (3), and the ξ, η, ζ axes coincide with the α, β, z axes at P . But if e_1, e_2, e_3 are the principal extensions at P we can also write the equation

$$(1 + e_1)^2 X^2 + (1 + e_2)^2 Y^2 + (1 + e_3)^2 Z^2 = \text{const.} \quad (5)$$

the X, Y, Z axes being through P and in the directions before strain of the linear elements that undergo principal extension. A comparison of equations (4) and (5) gives relations starting from which the expression (2) can be put in terms of u, v, w correctly to the third order of displacement co-ordinates. In the first place $\Sigma (1 + e_i)^2$ is equal to the sum of the coefficients of ξ^2, η^2

* With a proper choice of the sign of ρ

and ζ^2 in $F(\xi, \eta, \zeta)$. Subtracting 3 from each of these expressions and squaring,

$$\begin{aligned} 4(\Sigma e_1)^2 + 4(\Sigma e_1)(\Sigma e_1^2) \\ = 4 \left[\frac{\partial u}{\partial \alpha} + \frac{\rho}{\rho - z} \frac{\partial v}{\partial \beta} - \frac{w}{\rho - z} + \frac{\partial w}{\partial z} \right]^2 \\ + 4 \left[\frac{\partial u}{\partial \alpha} + \frac{\rho}{\rho - z} \frac{\partial v}{\partial \beta} - \frac{w}{\rho - z} + \frac{\partial w}{\partial z} \right] \left[\left(\frac{\partial u}{\partial \alpha} \right)^2 + \left(\frac{\rho}{\rho - z} \frac{\partial v}{\partial \beta} \right)^2 + \left(\frac{\partial u}{\partial z} \right)^2 + \left(\frac{\partial v}{\partial \alpha} \right)^2 \right. \\ \left. + \left(\frac{\rho}{\rho - z} \frac{\partial v}{\partial \beta} - \frac{w}{\rho - z} \right)^2 + \left(\frac{\partial v}{\partial z} \right)^2 + \left(\frac{\partial w}{\partial \alpha} \right)^2 \right. \\ \left. + \left(\frac{\rho}{\rho - z} \frac{\partial w}{\partial \beta} + \frac{v}{\rho - z} \right)^2 + \left(\frac{\partial w}{\partial z} \right)^2 \right], \end{aligned}$$

on each side terms of order higher than the third in e_1, e_2, e_3 , or in u, v, w have been ignored. The equation puts $(\Sigma e_1)^2$ in terms of u, v, w , but for some terms of the third order in e_1, e_2, e_3 . To evaluate the latter to our approximation it is clear that only relations of the first order in u, v, w are required. Thus we may use

$$\Sigma e_1 = \frac{\partial u}{\partial \alpha} + \frac{\rho}{\rho - z} \frac{\partial v}{\partial \beta} - \frac{w}{\rho - z} + \frac{\partial w}{\partial z}, \quad (6)$$

and

$$\begin{aligned} \Sigma e_2 e_3 = \left(\frac{\rho}{\rho - z} \frac{\partial v}{\partial \beta} - \frac{w}{\rho - z} \right) \frac{\partial w}{\partial z} + \frac{\partial w}{\partial z} \frac{\partial u}{\partial \alpha} + \frac{\partial u}{\partial \alpha} \left(\frac{\rho}{\rho - z} \frac{\partial v}{\partial \beta} - \frac{w}{\rho - z} \right) \\ - \frac{1}{2} \left[\left(\frac{\partial v}{\partial z} + \frac{\rho}{\rho - z} \frac{\partial w}{\partial \beta} + \frac{v}{\rho - z} \right)^2 + \left(\frac{\partial u}{\partial z} + \frac{\partial w}{\partial \alpha} \right)^2 + \left(\frac{\partial v}{\partial \alpha} + \frac{\rho}{\rho - z} \frac{\partial u}{\partial \beta} \right)^2 \right], \quad (7) \end{aligned}$$

two of the invariants of the ordinary theory of elasticity. Hence finally

$$\begin{aligned} (\Sigma e_1)^2 = \left[\frac{\partial u}{\partial \alpha} + \frac{\rho}{\rho - z} \frac{\partial v}{\partial \beta} - \frac{w}{\rho - z} + \frac{\partial w}{\partial z} \right]^2 \\ + \left[\frac{\partial u}{\partial \alpha} + \frac{\rho}{\rho - z} \frac{\partial v}{\partial \beta} - \frac{w}{\rho - z} + \frac{\partial w}{\partial z} \right] \left[\left(\frac{\rho}{\rho - z} \frac{\partial u}{\partial \beta} \right)^2 + \left(\frac{\partial u}{\partial z} \right)^2 + \left(\frac{\partial v}{\partial \alpha} \right)^2 + \left(\frac{\partial v}{\partial z} \right)^2 \right. \\ \left. + \left(\frac{\partial w}{\partial \alpha} \right)^2 + \left(\frac{\rho}{\rho - z} \frac{\partial w}{\partial \beta} + \frac{v}{\rho - z} \right)^2 \right. \\ \left. - \frac{1}{2} \left(\frac{\partial v}{\partial z} + \frac{\rho}{\rho - z} \frac{\partial w}{\partial \beta} + \frac{v}{\rho - z} \right)^2 \right. \\ \left. - \frac{1}{2} \left(\frac{\partial u}{\partial z} + \frac{\partial w}{\partial \alpha} \right)^2 - \frac{1}{2} \left(\frac{\partial v}{\partial \alpha} + \frac{\rho}{\rho - z} \frac{\partial u}{\partial \beta} \right)^2 \right] \quad (8) \end{aligned}$$

$\Sigma e_2 e_3$ is similarly expressed in terms of u, v, w . Evidently $\Sigma[(1 + e_2)^2 (1 + e_3)^2]$, the second invariant of quadrics (4) and (5), can be expressed in terms of u, v, w , while to our approximation

$$4\Sigma e_2 e_3 = 3 + \Sigma[(1 + e_2)^2 (1 + e_3)^2] - 2\Sigma(1 + e_1)^2 - 2(\Sigma e_1)(\Sigma e_2 e_3) + 6e_1 e_2 e_3$$

Thus we have $\Sigma e_2 e_3$ in terms of u, v, w , but for some terms of the third order in the principal extensions. As above these may be evaluated by (6) and (7) together with the third invariant of the ordinary theory,

$$\begin{aligned} e_1 e_2 e_3 = & \frac{\partial u}{\partial \alpha} \left(\frac{\rho}{\rho - z} \frac{\partial v}{\partial \beta} - \frac{w}{\rho - z} \right) \frac{\partial w}{\partial z} \\ & + \frac{1}{4} \left(\frac{\partial v}{\partial z} + \frac{\rho}{\rho - z} \frac{\partial w}{\partial \beta} + \frac{v}{\rho - z} \right) \left(\frac{\partial u}{\partial z} + \frac{\partial w}{\partial \alpha} \right) \left(\frac{\partial v}{\partial \alpha} + \frac{\rho}{\rho - z} \frac{\partial u}{\partial \beta} \right) \\ & - \frac{1}{4} \frac{\partial u}{\partial \alpha} \left(\frac{\partial v}{\partial z} + \frac{\rho}{\rho - z} \frac{\partial w}{\partial \beta} + \frac{v}{\rho - z} \right)^2 - \frac{1}{4} \left(\frac{\rho}{\rho - z} \frac{\partial v}{\partial \beta} - \frac{w}{\rho - z} \right) \left(\frac{\partial u}{\partial z} + \frac{\partial w}{\partial \alpha} \right)^2 \\ & - \frac{1}{4} \frac{\partial w}{\partial z} \left(\frac{\partial v}{\partial \alpha} + \frac{\rho}{\rho - z} \frac{\partial u}{\partial \beta} \right)^2 \end{aligned}$$

There results

$$\begin{aligned} 4\Sigma e_2 e_3 = & 4 \left[\left(\frac{\rho}{\rho - z} \frac{\partial v}{\partial \beta} - \frac{w}{\rho - z} \right) \frac{\partial w}{\partial z} + \frac{\partial w}{\partial z} \frac{\partial u}{\partial \alpha} + \frac{\partial u}{\partial \alpha} \left(\frac{\rho}{\rho - z} \frac{\partial v}{\partial \beta} - \frac{w}{\rho - z} \right) \right. \\ & \left. - \frac{1}{4} \left(\frac{\partial v}{\partial \alpha} + \frac{\rho}{\rho - z} \frac{\partial u}{\partial \beta} \right)^2 \right] \\ & + 2 \frac{\partial u}{\partial \alpha} \left[\left(\frac{\rho}{\rho - z} \frac{\partial u}{\partial \beta} \right)^2 + \left(\frac{\partial u}{\partial z} \right)^2 + \left(\frac{\partial v}{\partial z} \right)^2 + \left(\frac{\rho}{\rho - z} \frac{\partial w}{\partial \beta} + \frac{v}{\rho - z} \right)^2 \right] \\ & + 2 \left(\frac{\rho}{\rho - z} \frac{\partial v}{\partial \beta} - \frac{w}{\rho - z} \right) \left[\left(\frac{\partial u}{\partial z} \right)^2 + \left(\frac{\partial v}{\partial \alpha} \right)^2 + \left(\frac{\partial v}{\partial z} \right)^2 + \left(\frac{\partial w}{\partial \alpha} \right)^2 \right] \\ & + 2 \frac{\partial w}{\partial z} \left[\left(\frac{\rho}{\rho - z} \frac{\partial u}{\partial \beta} \right)^2 + \left(\frac{\partial v}{\partial \alpha} \right)^2 + \left(\frac{\partial w}{\partial \alpha} \right)^2 + \left(\frac{\rho}{\rho - z} \frac{\partial w}{\partial \beta} + \frac{v}{\rho - z} \right)^2 \right] \\ & - \left[\frac{\partial v}{\partial z} + \frac{\rho}{\rho - z} \frac{\partial w}{\partial \beta} + \frac{v}{\rho - z} + \frac{\rho}{\rho - z} \frac{\partial u}{\partial \beta} \frac{\partial u}{\partial z} + \left(\frac{\rho}{\rho - z} \frac{\partial v}{\partial \beta} - \frac{w}{\rho - z} \right) \frac{\partial v}{\partial z} \right. \\ & \left. + \left(\frac{\rho}{\rho - z} \frac{\partial w}{\partial \beta} + \frac{v}{\rho - z} \right) \frac{\partial w}{\partial z} \right]^2 \\ & - \left[\frac{\partial u}{\partial z} + \frac{\partial w}{\partial \alpha} + \frac{\partial u}{\partial \alpha} \frac{\partial u}{\partial z} + \frac{\partial v}{\partial \alpha} \frac{\partial v}{\partial z} + \frac{\partial w}{\partial \alpha} \frac{\partial w}{\partial z} \right]^2 \\ & - 2 \left[\frac{\partial v}{\partial \alpha} + \frac{\rho}{\rho - z} \frac{\partial u}{\partial \beta} \right] \left[\frac{\partial u}{\partial \alpha} \frac{\rho}{\rho - z} \frac{\partial u}{\partial \beta} + \frac{\partial v}{\partial \alpha} \left(\frac{\rho}{\rho - z} \frac{\partial v}{\partial \beta} - \frac{w}{\rho - z} \right) \right. \\ & \left. + \frac{\partial w}{\partial \alpha} \left(\frac{\rho}{\rho - z} \frac{\partial w}{\partial \beta} + \frac{v}{\rho - z} \right) \right] \end{aligned}$$

$$\begin{aligned}
 & + \frac{1}{2} \left[\frac{\partial u}{\partial \alpha} + \frac{\rho}{\rho - z} \frac{\partial v}{\partial \beta} - \frac{w}{\rho - z} + \frac{\partial w}{\partial z} \right] \left[\left(\frac{\partial v}{\partial z} + \frac{\rho}{\rho - z} \frac{\partial w}{\partial \beta} + \frac{v}{\rho - z} \right)^2 \right. \\
 & \qquad \qquad \qquad \left. + \left(\frac{\partial u}{\partial z} + \frac{\partial w}{\partial \alpha} \right)^2 + \left(\frac{\partial v}{\partial \alpha} + \frac{\rho}{\rho - z} \frac{\partial u}{\partial \beta} \right)^2 \right] \\
 & + \frac{1}{3} \left[\left(\frac{\partial v}{\partial z} + \frac{\rho}{\rho - z} \frac{\partial w}{\partial \beta} + \frac{v}{\rho - z} \right) \left(\frac{\partial u}{\partial z} + \frac{\partial w}{\partial \alpha} \right) \left(\frac{\partial v}{\partial \alpha} + \frac{\rho}{\rho - z} \frac{\partial u}{\partial \beta} \right) \right. \\
 & \qquad - \frac{\partial u}{\partial \alpha} \left(\frac{\partial v}{\partial z} + \frac{\rho}{\rho - z} \frac{\partial w}{\partial \beta} + \frac{v}{\rho - z} \right)^2 \\
 & \qquad \left. - \left(\frac{\rho}{\rho - z} \frac{\partial v}{\partial \beta} - \frac{w}{\rho - z} \right) \left(\frac{\partial u}{\partial z} + \frac{\partial w}{\partial \alpha} \right)^2 - \frac{\partial w}{\partial z} \left(\frac{\partial v}{\partial \alpha} + \frac{\rho}{\rho - z} \frac{\partial u}{\partial \beta} \right)^2 \right] \quad (9)
 \end{aligned}$$

Using equations (8) and (9) we have from (2) an expression for the strain energy function correct to the third order of u, v, w . By variation three conditions of equilibrium correct to the second-order of the co-ordinates of displacement can be derived. These are, of course, general equations, they are not needed in the deduction of shell equations, so that as they are complicated they are not set down here.

The Boundary Conditions

4 The reduction of general equations to shell equations is effected by means of the boundary conditions at the faces, $z = \pm h$, of the shell.

It happens that it is not necessary to calculate these conditions to the second-order in full. With the strain energy method first-order boundary conditions can be used, the extra terms of the more accurate conditions disappearing on substitution, while with the other method it is only necessary to know the form of the second-order conditions.

It is supposed in what follows that the faces are free from all external surface forces*. We write $\bar{\alpha}\bar{\alpha}, \bar{\beta}\bar{\beta}, \bar{z}\bar{z}, \bar{\beta}\bar{z}, \bar{z}\bar{\alpha}$, and $\bar{\alpha}\bar{\beta}$ for stresses referred to the actual (strained) elements of area upon which they act, and referred also to (α, β, z) axes at the point $(\bar{\alpha}, \bar{\beta}, \bar{z})$, to which point (α, β, z) is displaced by the strain. Thus $\bar{\alpha}\bar{\alpha}$, for instance, is the stress acting in the direction of the α axis of $(\bar{\alpha}, \bar{\beta}, \bar{z})$ upon an element of area normal to this direction, where by stress is meant action divided by strained element of area. Second order expressions for these stresses are not needed, to the first order they are of course known.

Suppose now that any point P of either face of the shell is displaced by the

* This is done as no problem is considered here, or is contemplated, in which the contrary is the case. It is pointed out below, § 6, that no loss of generality is involved.

strain to P_1 , which will be in the corresponding surface of the strained shell. The direction cosines of three orthogonal elements through P_1 , two of which are in the strained surface, are required to the first order. They must be referred to α, β, z axes at P_1 . The linear elements through P , whose direction cosines are $(1, 0, 0)$ and $(0, 1, 0)$ before strain, go through P_1 and lie in the surface after strain. A common perpendicular to these elements after strain gives the normal to the strained surface at P_1 . Hence we find that the direction cosines of an orthogonal set are given by the scheme

	$\bar{\alpha}$	$\bar{\beta}$	\bar{z}
1	1	$\frac{\partial v}{\partial \alpha}$	$\frac{\partial w}{\partial \alpha}$
2	$-\frac{\partial v}{\partial \alpha}$	1	$\frac{\rho}{\rho - z} \frac{\partial w}{\partial \beta}$
3	$-\frac{\partial w}{\partial \alpha}$	$-\frac{\rho}{\rho - z} \frac{\partial w}{\partial \beta}$	1

the element denoted by 3 being the normal to the strained surface at P_1 .

The conditions that there should be no action upon either face of the shell may now be written down at once. These are

$$\left. \begin{aligned} &\bar{z}z - \frac{2\rho}{\rho - z} \frac{\partial w}{\partial \beta} \bar{\beta}z - 2 \frac{\partial w}{\partial \alpha} \bar{z}\alpha = 0, \\ &\bar{\beta}z - \frac{\rho}{\rho - z} \frac{\partial w}{\partial \beta} (\bar{\beta}\beta - \bar{z}z) - \frac{\partial v}{\partial \alpha} \bar{z}\alpha - \frac{\partial w}{\partial \alpha} \bar{\alpha}\beta = 0, \\ &\bar{z}\alpha - \frac{\partial w}{\partial \alpha} (\bar{\alpha}\alpha - \bar{z}z) + \frac{\partial v}{\partial \alpha} \bar{\beta}z - \frac{\rho}{\rho - z} \frac{\partial w}{\partial \beta} \bar{\alpha}\beta = 0, \end{aligned} \right\} z = \pm h, \quad (10)$$

and

which are correct to the second order of u, v, w

The Stability of a Plane Plate.

5 Sufficient information has now been obtained to reduce the strain energy function to terms of the co-ordinates of displacement of points of the middle

surface of the shell, and hence to determine the shell equations. But it is also possible to write down the conditions for the equilibrium of an element of volume, and reduce them to shell equations. This is the first of the methods mentioned above as available. The work with the cylindrical shell considered hitherto is long, but in the case of a plane plate it is greatly simplified. The equation for a plane plate is, therefore, deduced in this way, in part as an example of the method, but more particularly because the process of approximation is exactly the same as that in the general case of the cylindrical shell. Consequently, the work in the latter instance can be set down more concisely after an easier problem has been handled by a similar procedure.

We take the middle surface of the plane plate in its unstressed configuration to be the x, y plane, and any normal as the z axis. All co-ordinates are referred to these fixed axes. Suppose that any point (x, y, z) of the shell is displaced by the strain to $(\bar{x}, \bar{y}, \bar{z})$. Then the condition that the force in the direction of the z axis on an element of volume should vanish* is

$$\frac{\partial \bar{\sigma}_z}{\partial \bar{x}} + \frac{\partial \bar{\sigma}_y}{\partial \bar{y}} + \frac{\partial \bar{\sigma}_z}{\partial \bar{z}} = 0 \quad (11)$$

The stresses that occur in this equation are defined exactly as are those above. It is easy to see that to the first order of u, v, w ,

$$\frac{\partial}{\partial \bar{x}} = \left(1 - \frac{\partial u}{\partial x}\right) \frac{\partial}{\partial x} - \frac{\partial v}{\partial x} \frac{\partial}{\partial y} - \frac{\partial w}{\partial x} \frac{\partial}{\partial z}, \text{ etc} \quad (12)$$

After calculation of the stresses to the second order, the general equation can be written down, but it need not be given here as the approximate shell equation can be derived directly.

Suppose that u, v, w can be expanded in power series of z , so that

$$u = u_0 + u_1 z + u_2 z^2 + \dots,$$

$$v = v_0 + v_1 z + v_2 z^2 + \dots,$$

and

$$w = w_0 + w_1 z + w_2 z^2 + \dots,$$

where u_0, v_0, w_0 , and the various coefficients of powers of z are all functions of x and y . u_0, v_0 and w_0 are evidently the co-ordinates of displacement of a point of the middle surface of the plate. With these values of u, v, w , we may reduce the left-hand side of (11) to a power series in z , the equation must be

* Cf. Southwell, *loc cit.*, p. 196, also for equation (12) below.

satisfied for all values of z , so that in particular the term independent of z in this expression must be zero. The resulting equation is

$$\begin{aligned} & \left(1 - \frac{\partial u_0}{\partial x}\right) \frac{\partial}{\partial x} (\bar{zx})_0 - \frac{\partial v_0}{\partial x} \frac{\partial}{\partial y} (\bar{zx})_0 - \frac{\partial w_0}{\partial x} (\bar{zx})_1 \\ & - \frac{\partial u_0}{\partial y} \frac{\partial}{\partial x} (\bar{yz})_0 + \left(1 - \frac{\partial v_0}{\partial y}\right) \frac{\partial}{\partial y} (\bar{yz})_0 - \frac{\partial w_0}{\partial y} (\bar{yz})_1 \\ & - u_1 \frac{\partial}{\partial x} (\bar{zz})_0 - v_1 \frac{\partial}{\partial y} (\bar{zz})_0 + (1 - w_1) (\bar{zz})_1 = 0 \end{aligned} \quad (13)$$

where, for instance, $(\bar{zx})_0$ stands for the term independent of z , and $(\bar{zx})_1$ for the coefficient of z , in the expansion of \bar{zx} . Equation (13) is not yet a shell equation, owing to the appearance of such terms as u_1, v_1, w_1 , to eliminate these the boundary conditions are used. For a plane plate equations (10) reduce to

$$\bar{zz} - 2 \frac{\partial w}{\partial y} \bar{yz} - 2 \frac{\partial w}{\partial x} \bar{zx} = 0, \quad (14)$$

$$\bar{yz} - \frac{\partial w}{\partial y} (\bar{yy} - \bar{zz}) - \frac{\partial v}{\partial x} \bar{zx} - \frac{\partial w}{\partial x} \bar{xy} = 0, \quad (15)$$

and

$$\bar{zx} - \frac{\partial w}{\partial x} (\bar{xx} - \bar{zz}) + \frac{\partial v}{\partial x} \bar{yz} - \frac{\partial w}{\partial y} \bar{xy} = 0, \quad (16)$$

each condition holding for $z = \pm h$

Therefore there are six conditions of which

$$\begin{aligned} & (\bar{yz})_0 - \frac{\partial w_0}{\partial y} (\bar{yy})_0 - \bar{zz}_0 - \frac{\partial v_0}{\partial x} (\bar{zx})_0 - \frac{\partial w_0}{\partial x} (\bar{xy})_0 \\ & + h^2 \left[(\bar{yz})_2 - \frac{\partial w_2}{\partial y} (\bar{yy} - \bar{zz})_0 - \frac{\partial w_1}{\partial y} (\bar{yy} - \bar{zz})_1 - \frac{\partial w_0}{\partial y} (\bar{yy} - \bar{zz})_2 \right. \\ & \quad - \frac{\partial v_2}{\partial x} (\bar{zx})_0 - \frac{\partial v_1}{\partial x} (\bar{zx})_1 - \frac{\partial v_0}{\partial x} (\bar{zx})_2 \\ & \quad \left. - \frac{\partial w_2}{\partial x} (\bar{xy})_0 - \frac{\partial w_1}{\partial x} (\bar{xy})_1 - \frac{\partial w_0}{\partial x} (\bar{xy})_2 \right] + \quad = 0, \quad (17) \end{aligned}$$

derived from the two equations from (15), is typical. These equations need only be used for the reduction of terms of the first order, for the others, simplified forms of these conditions, obtained by ignoring the second-order terms, are sufficiently accurate. Further, first of all we calculate a first

approximation to the equation (13) by ignoring h^2 . For the reduction of the second-order terms, then, we have the simple equations

$$(\lambda + 2\mu) w_1 + \lambda \left(\frac{\partial u_0}{\partial x} + \frac{\partial v_0}{\partial y} \right) = 0, \quad (18)$$

$$(\lambda + 2\mu) 2w_2 + \lambda \left(\frac{\partial u_1}{\partial x} + \frac{\partial v_1}{\partial y} \right) = 0, \quad (19)$$

$$v_1 + \frac{\partial w_0}{\partial y} = 0, \quad (20)$$

$$2v_2 + \frac{\partial w_1}{\partial y} = 0, \quad (21)$$

$$u_1 + \frac{\partial w_0}{\partial x} = 0, \quad (22)$$

and

$$2u_2 + \frac{\partial w_1}{\partial x} = 0 \quad (23)$$

These equations can also be used to simplify the more accurate boundary conditions (14), (15) and (16). For example, in (17) the terms $\frac{\partial w_0}{\partial y}(\bar{z}z)_0$ and $\frac{\partial v_0}{\partial x}(\bar{z}z)_0$ can both be ignored, by reason of equations (18) and (22), the other boundary conditions can be similarly dealt with.

In finding the first approximation, then, even for the reduction of terms of the first order, we have only to use the relatively simple equations

$$(\bar{z}z)_0 = (\bar{z}z)_1 = 0,$$

$$(\bar{y}z)_0 - \frac{\partial w_0}{\partial y}(\bar{y}y)_0 - \frac{\partial w_0}{\partial x}(\bar{x}y)_0 = 0,$$

and

$$(\bar{z}x)_0 - \frac{\partial w_0}{\partial x}(\bar{x}x)_0 - \frac{\partial w_0}{\partial y}(\bar{x}y)_0 = 0,$$

the other two conditions are not needed.

Again, what has been said as to the reduction of second-order terms shows that the first approximation to (13) is to be obtained from

$$\frac{\partial}{\partial x}(\bar{z}x)_0 + \frac{\partial}{\partial y}(\bar{y}z)_0 + (\bar{z}z)_1 = 0,$$

which by the conditions above is reduced to

$$\frac{\partial}{\partial x} \left[\frac{\partial w_0}{\partial x}(\bar{x}x)_0 + \frac{\partial w_0}{\partial y}(\bar{x}y)_0 \right] + \frac{\partial}{\partial y} \left[\frac{\partial w_0}{\partial y}(\bar{y}y)_0 + \frac{\partial w_0}{\partial x}(\bar{x}y)_0 \right] = 0.$$

All terms in this equation are of the second-order, so that the final reduction to terms of u_0 , v_0 , w_0 can be effected by equations (18) to (23). The resulting expression is

$$\begin{aligned} & \frac{\partial}{\partial x} \left[\frac{\partial w_0}{\partial x} \left\{ \frac{4\mu(\lambda + \mu)}{\lambda + 2\mu} \frac{\partial u_0}{\partial x} + \frac{2\mu\lambda}{\lambda + 2\mu} \frac{\partial v_0}{\partial y} \right\} + \mu \frac{\partial w_0}{\partial y} \left(\frac{\partial v_0}{\partial x} + \frac{\partial u_0}{\partial y} \right) \right] \\ & + \frac{\partial}{\partial y} \left[\frac{\partial w_0}{\partial y} \left\{ \frac{2\mu\lambda}{\lambda + 2\mu} \frac{\partial u_0}{\partial x} + \frac{4\mu(\lambda + \mu)}{\lambda + 2\mu} \frac{\partial v_0}{\partial x} \right\} + \mu \frac{\partial w_0}{\partial x} \left(\frac{\partial v_0}{\partial y} + \frac{\partial u_0}{\partial y} \right) \right] = 0 \quad (24) \end{aligned}$$

If a second approximation were required with complete accuracy it would present some difficulty, but it is possible to justify *a posteriori* in practical problems of elastic stability the neglect of terms of the second-order of displacements when multiplied by h^2 . Hence, what must be added to the left-hand side of (24) is merely the term in h^2 which appears in the Theory of Thin Shells,* that is to say.

$$-\frac{4\mu(\lambda + \mu)}{3(\lambda + 2\mu)} h^2 \nabla_1^4 w_0$$

The shell equation is finally

$$\begin{aligned} & \frac{2(\lambda + \mu)}{3} h^2 \nabla_1^4 w_0 - \frac{\partial}{\partial x} \left[\frac{\partial w_0}{\partial x} \left\{ 2(\lambda + \mu) \frac{\partial u_0}{\partial x} + \lambda \frac{\partial v_0}{\partial y} \right\} + \frac{\lambda + 2\mu}{2} \frac{\partial w_0}{\partial y} \left(\frac{\partial v_0}{\partial x} + \frac{\partial u_0}{\partial y} \right) \right] \\ & - \frac{\partial}{\partial y} \left[\frac{\partial w_0}{\partial y} \left\{ \lambda \frac{\partial u_0}{\partial x} + 2(\lambda + \mu) \frac{\partial v_0}{\partial y} \right\} \right. \\ & \quad \left. + \frac{\lambda + 2\mu}{2} \frac{\partial w_0}{\partial x} \left(\frac{\partial v_0}{\partial x} + \frac{\partial u_0}{\partial y} \right) \right] = 0, \end{aligned}$$

or

$$\begin{aligned} & \frac{h^2}{3} \nabla_1^4 w_0 - \frac{\partial}{\partial x} \left[\frac{\partial w_0}{\partial x} \left(\frac{\partial u_0}{\partial x} + \sigma \frac{\partial v_0}{\partial y} \right) + \frac{1 - \sigma}{2} \frac{\partial w_0}{\partial y} \left(\frac{\partial v_0}{\partial x} + \frac{\partial u_0}{\partial y} \right) \right] \\ & - \frac{\partial}{\partial y} \left[\frac{\partial w_0}{\partial y} \left(\sigma \frac{\partial u_0}{\partial x} + \frac{\partial v_0}{\partial y} \right) + \frac{1 - \sigma}{2} \frac{\partial w_0}{\partial x} \left(\frac{\partial v_0}{\partial x} + \frac{\partial u_0}{\partial y} \right) \right] = 0, \quad (25) \end{aligned}$$

σ denoting Poisson's ratio.

The equation of stability follows immediately from (25). Let the plate be stretched by external forces acting in its plane, so that the displacement of any point of the middle surface is $(u_0, v_0, 0)$. If the equilibrium of this configuration, called the "equilibrium configuration," is "neutral," there will be a neighbouring configuration of equilibrium, the "distorted configuration,"

* This expression can be obtained by the general method of this section without trouble, or it comes immediately from equation (32) below.

in which the displacement of a point of the middle surface is (u_0, v_0, w') . Then w' must satisfy the stability equation

$$\begin{aligned} \frac{h^2}{3} \nabla_1^4 w' - \frac{\partial}{\partial x} \left[\frac{\partial w'}{\partial x} \left(\frac{\partial u_0}{\partial x} + \sigma \frac{\partial v_0}{\partial y} \right) + \frac{1-\sigma}{2} \frac{\partial w'}{\partial y} \left(\frac{\partial v_0}{\partial x} + \frac{\partial u_0}{\partial y} \right) \right] \\ - \frac{\partial}{\partial y} \left[\frac{\partial w'}{\partial y} \left(\sigma \frac{\partial u_0}{\partial x} + \frac{\partial v_0}{\partial y} \right) + \frac{1-\sigma}{2} \frac{\partial w'}{\partial x} \left(\frac{\partial v_0}{\partial x} + \frac{\partial u_0}{\partial y} \right) \right] = 0, \end{aligned} \quad (26)$$

and certain boundary conditions which need not be considered here. The condition that there should be a non-zero solution w' with these properties determines the "critical" values of the external forces, if these are exceeded the plate will collapse

The equation (26) can be written*

$$D \nabla_1^4 w' - \frac{\partial}{\partial x} \left(T_1 \frac{\partial w'}{\partial x} + S \frac{\partial w'}{\partial y} \right) - \frac{\partial}{\partial y} \left(T_2 \frac{\partial w'}{\partial y} + S \frac{\partial w'}{\partial x} \right) = 0, \quad (27)$$

where T_1 , T_2 , and S are stress resultants† in the equilibrium configuration

In the general case the stability of an equilibrium configuration (u_0, v_0, w_0) is examined, and three shell equations must be considered. The equilibrium of this configuration is neutral if there is a neighbouring configuration $(u_0 + u', v_0 + v', w_0 + w')$ which will satisfy the equilibrium and boundary conditions

By subtracting the shell equations for the two configurations we have three equations containing terms of the types u' , $u_0 u'$, and u'^2 . The latter terms can be neglected, for, from the nature of the case, the absolute magnitudes of u' , v' , and w' can never be obtained, these quantities can therefore be supposed so small that their squares and products are negligible. Consequently, in general the stability equations are linear in u' , v' and w' , the coefficients being functions of u_0 , v_0 , and w_0 .

The simplification in the case of a plane plate comes from the fact that the question of stability arises only in connection with equilibrium configurations in which the middle surface is plane. It is then found that one stability equation contains only w' , if we take as the distorted configuration $(u_0 + u', v_0 + v', w')$, while the other two contain only u' and v' . There are therefore two distinct modes of collapse, and only one of these—that which is determined by the stability equation found here, and which is accompanied by the familiar buckling of the middle surface—is of physical interest‡

* Special cases of this equation have recently been considered by Southwell and Skan, 'Roy. Soc. Proc.', A, vol. 105, p. 582, and by the writer, 'Roy. Soc. Proc.', A, vol. 106, p. 268.

† The notation is that used in Love, *op. cit.*, chap. 22.

‡ See § 8.

The Reduction of the Strain Energy Function

6 Returning to the general case, we have now to express the strain energy, given by equations (2), (8) and (9), in terms of u_0 , v_0 and w_0 by means of the boundary conditions (10). Supposing, as in §5, that u , v and w are expanded in power series in z , an expression for W can be found of the form

$$W = W_0 + W_1 z + W_2 z^2 + \dots,$$

the energy of the whole plate is then

$$\iint d\alpha d\beta \int_{-h}^h \left(1 - \frac{z}{\rho}\right) (W_0 + W_1 z + W_2 z^2 + \dots) dz$$

It is proposed to evaluate this, neglecting terms in h^4 , terms of the fourth and higher orders of displacement co-ordinates, and terms of the third and higher orders when multiplied by h^2 . This accuracy is sufficient for most stability problems.

We have, then, to find W' given by

$$W' = W_0 + \frac{h^2}{3} (W_2 - W_1/\rho), \quad (28)$$

terms of the third order being neglected in W_1 and W_2 . The calculation is divided into two parts. First are obtained the terms not multiplied by h^2 , the deduction of the others is a problem in the ordinary theory of elasticity, and does not demand the special accuracy of the results given above. It may be remarked that there is no *a priori* reason to suppose that W_0 does not contain terms in h^2 as it will involve, for instance, terms in u_1 , v_1 and w_1 , and for the reduction of these to u_0 , v_0 and w_0 , conditions similar in form to (17) must be used. As pointed out below, however, W_0 does not in fact contain such terms, and this circumstance simplifies the reduction considerably.

W_0 is calculated exactly as in equation (24) above. For the reduction of the third-order terms we have the simple boundary conditions

$$(\bar{z}z)_0 = (\bar{z}z)_1 = 0,$$

$$(\bar{\beta}z)_0 = (\bar{\beta}z)_1 = 0,$$

and

$$(\bar{z}\alpha)_0 = (\bar{z}\alpha)_1 = 0,$$

the stresses being reckoned to the first order only, and these equations can be used to reduce the more accurate boundary conditions (10) to

$$(\bar{z}z)_0 = (\bar{z}z)_1 = 0,$$

$$(\bar{\beta}z)_0 - \frac{\partial w_0}{\partial \beta} (\bar{\beta}\beta)_0 - \frac{\partial w_0}{\partial \alpha} (\bar{\alpha}\beta)_0 = 0, \text{ etc.}$$

The only one actually required is the first, which can be written

$$(\lambda + 2\mu) w_1 + \lambda \left(\frac{\partial u_0}{\partial \alpha} + \frac{\partial v_0}{\partial \beta} - \frac{w_0}{\rho} \right) + F = 0, \quad (29)$$

where F is an unknown function of the second-order in u_0, u_1 , etc.

Simplifying the third-order terms of equations (8) and (9) by the simple boundary conditions, we have

$$\begin{aligned} [\Sigma e_1]_0^2 &= \left[\frac{\partial u_0}{\partial \alpha} + \frac{\partial v_0}{\partial \beta} - \frac{w_0}{\rho} + w_1 \right]^2 \\ &\quad + \left[\frac{\partial u_0}{\partial \alpha} + \frac{\partial v_0}{\partial \beta} - \frac{w_0}{\rho} + w_1 \right] \left[\left(\frac{\partial u_0}{\partial \beta} \right)^2 + u_1^2 + \left(\frac{\partial v_0}{\partial \alpha} \right)^2 + v_1^2 + \left(\frac{\partial w_0}{\partial \alpha} \right)^2 \right. \\ &\quad \left. + \left(\frac{\partial w_0}{\partial \beta} + \frac{v_0}{\rho} \right)^2 - \frac{1}{2} \left(\frac{\partial v_0}{\partial \alpha} + \frac{\partial u_0}{\partial \beta} \right)^2 \right], \end{aligned}$$

and

$$\begin{aligned} 4 [\Sigma e_1 e_3]_0 &= 4 \left[\left(\frac{\partial v_0}{\partial \beta} - \frac{w_0}{\rho} \right) w_1 + w_1 \frac{\partial u_0}{\partial \alpha} + \frac{\partial u_0}{\partial \alpha} \left(\frac{\partial v_0}{\partial \beta} - \frac{w_0}{\rho} \right) - \frac{1}{2} \left(\frac{\partial v_0}{\partial \alpha} + \frac{\partial u_0}{\partial \beta} \right)^2 \right] \\ &\quad + 2 \frac{\partial u_0}{\partial \alpha} \left[\left(\frac{\partial u_0}{\partial \beta} \right)^2 + u_1^2 + v_1^2 + \left(\frac{\partial w_0}{\partial \beta} + \frac{v_0}{\rho} \right)^2 \right] \\ &\quad + 2 \left(\frac{\partial v_0}{\partial \beta} - \frac{w_0}{\rho} \right) \left[u_1^2 + \left(\frac{\partial v_0}{\partial \alpha} \right)^2 + v_1^2 + \left(\frac{\partial w_0}{\partial \alpha} \right)^2 \right] \\ &\quad + 2 w_1 \left[\left(\frac{\partial u_0}{\partial \beta} \right)^2 + \left(\frac{\partial v_0}{\partial \alpha} \right)^2 + \left(\frac{\partial w_0}{\partial \alpha} \right)^2 + \left(\frac{\partial w_0}{\partial \beta} + \frac{v_0}{\rho} \right)^2 \right] \\ &\quad - 2 \left(\frac{\partial v_0}{\partial \alpha} + \frac{\partial u_0}{\partial \beta} \right) \left[\frac{\partial u_0}{\partial \alpha} \frac{\partial u_0}{\partial \beta} + \frac{\partial v_0}{\partial \alpha} \left(\frac{\partial v_0}{\partial \beta} - \frac{w_0}{\rho} \right) + \frac{\partial w_0}{\partial \alpha} \left(\frac{\partial w_0}{\partial \beta} + \frac{v_0}{\rho} \right) \right] \\ &\quad + \frac{1}{2} \left(\frac{\partial u_0}{\partial \alpha} + \frac{\partial v_0}{\partial \beta} - \frac{w_0}{\rho} - 2w_1 \right) \left(\frac{\partial v_0}{\partial \alpha} + \frac{\partial u_0}{\partial \beta} \right)^2 \end{aligned}$$

Using (29) to put w_1 in terms of u_0, v_0, w_0 in the expression for W_0 , it is found that the unknown function F disappears, there is therefore no need for the complete second-order boundary condition, a circumstance that reduces considerably the algebra that would otherwise be necessary

The final result is

$$\begin{aligned} W_0 &= \frac{2\mu(\lambda + \mu)}{\lambda + 2\mu} \left(\frac{\partial u_0}{\partial \alpha} + \frac{\partial v_0}{\partial \beta} - \frac{w_0}{\rho} \right)^2 - 2\mu \left[\frac{\partial u_0}{\partial \alpha} \left(\frac{\partial v_0}{\partial \beta} - \frac{w_0}{\rho} \right) - \frac{1}{2} \left(\frac{\partial v_0}{\partial \alpha} + \frac{\partial u_0}{\partial \beta} \right)^2 \right] \\ &\quad + \left(\frac{\partial w_0}{\partial \alpha} \right)^2 \left[\frac{2\mu(\lambda + \mu)}{\lambda + 2\mu} \frac{\partial u_0}{\partial \alpha} + \frac{\lambda\mu}{\lambda + 2\mu} \left(\frac{\partial v_0}{\partial \beta} - \frac{w_0}{\rho} \right) \right] \\ &\quad + \left(\frac{\partial w_0}{\partial \beta} + \frac{v_0}{\rho} \right)^2 \left[\frac{\lambda\mu}{\lambda + 2\mu} \frac{\partial u_0}{\partial \alpha} + \frac{2\mu(\lambda + \mu)}{\lambda + 2\mu} \left(\frac{\partial v_0}{\partial \beta} - \frac{w_0}{\rho} \right) \right] \\ &\quad + \mu \frac{\partial w_0}{\partial \alpha} \left(\frac{\partial w_0}{\partial \beta} + \frac{v_0}{\rho} \right) \left(\frac{\partial v_0}{\partial \alpha} + \frac{\partial u_0}{\partial \beta} \right) + \frac{\mu(3\lambda + 2\mu)}{4(\lambda + 2\mu)} \left(\frac{\partial u_0}{\partial \alpha} + \frac{\partial v_0}{\partial \beta} - \frac{w_0}{\rho} \right) \left(\frac{\partial v_0}{\partial \alpha} - \frac{\partial u_0}{\partial \beta} \right)^2. \end{aligned}$$

This represents in the first instance a first approximation to W_0 obtained by neglecting terms multiplied by h^2 . It remains to find the terms in h^2 . The result in this case is known, so that only an indication is given of the method of reaching it by the processes of this paper. The terms of the third-order can be ignored throughout, and we have merely to express in terms of u_0 , v_0 and w_0 the coefficient of h^2 in

$$W_0 + \frac{h^2}{3} (W_2 - W_1/\rho),$$

by means of six boundary conditions such as

$$(\lambda + 2\mu) w_1 + \lambda \left(\frac{\partial u_0}{\partial \alpha} + \frac{\partial v_0}{\partial \beta} - \frac{w_0}{\rho} \right) + h^2 \left[(\lambda + 2\mu) 3w_3 + \lambda \left(\frac{\partial u_2}{\partial \alpha} + \frac{\partial v_2}{\partial \beta} + \frac{1}{\rho} \frac{\partial v_1}{\partial \beta} + \frac{1}{\rho^2} \frac{\partial v_0}{\partial \beta} - \frac{w_2}{\rho} - \frac{w_1}{\rho^2} - \frac{w_0}{\rho^3} \right) \right] = 0$$

This can be done by successive approximation, the process being simple because it is found that upon combining the various terms none of the functions u , v , w appear with suffix greater than 2.

Were this not the case (as it is not if the alternative method of §5 is used for a second approximation), it would be necessary to use the relations that can be derived from general equations by equating to zero the coefficients of the various powers of z , to reduce the suffixes

The final expression* is

$$\begin{aligned} W'/\mu = & \frac{2(\lambda + \mu)}{\lambda + 2\mu} \left(\frac{\partial u}{\partial \alpha} + \frac{\partial v}{\partial \beta} - \frac{w}{\rho} \right)^2 - 2 \frac{\partial u}{\partial \alpha} \left(\frac{\partial v}{\partial \beta} - \frac{w}{\rho} \right) + \frac{1}{2} \left(\frac{\partial v}{\partial \alpha} + \frac{\partial u}{\partial \beta} \right)^2 \\ & + \left(\frac{\partial w}{\partial \alpha} \right)^2 \left[\frac{2(\lambda + \mu)}{\lambda + 2\mu} \frac{\partial u}{\partial \alpha} + \frac{\lambda}{\lambda + 2\mu} \left(\frac{\partial v}{\partial \beta} - \frac{w}{\rho} \right) \right] \\ & + \left(\frac{\partial w}{\partial \beta} + \frac{v}{\rho} \right)^2 \left[\frac{\lambda}{\lambda + 2\mu} \frac{\partial u}{\partial \alpha} + \frac{2(\lambda + \mu)}{\lambda + 2\mu} \left(\frac{\partial v}{\partial \beta} - \frac{w}{\rho} \right) \right] \\ & + \frac{\partial w}{\partial \alpha} \left(\frac{\partial w}{\partial \beta} + \frac{v}{\rho} \right) \left(\frac{\partial v}{\partial \alpha} + \frac{\partial u}{\partial \beta} \right) + \frac{3\lambda + 2\mu}{4(\lambda + 2\mu)} \left(\frac{\partial u}{\partial \alpha} + \frac{\partial v}{\partial \beta} - \frac{w}{\rho} \right) \left(\frac{\partial v}{\partial \alpha} - \frac{\partial u}{\partial \beta} \right)^2 \\ & + \frac{2h^2}{3} \left[\frac{\lambda + \mu}{\lambda + 2\mu} (\kappa_1 + \kappa_2)^2 + \tau^2 - \kappa_1 \kappa_2 \right. \\ & \quad + \frac{\lambda}{2(\lambda + 2\mu)} \left\{ \epsilon_1 + \frac{\lambda}{\lambda + 2\mu} (\epsilon_1 + \epsilon_2) \right\} \frac{\partial^2}{\partial \alpha^2} (\epsilon_1 + \epsilon_2) \\ & \quad + \frac{\lambda}{2(\lambda + 2\mu)} \left\{ \epsilon_2 + \frac{\lambda}{\lambda + 2\mu} (\epsilon_1 + \epsilon_2) \right\} \frac{\partial^2}{\partial \beta^2} (\epsilon_1 + \epsilon_2) \\ & \quad \left. + \frac{\lambda \omega}{2(\lambda + 2\mu)} \frac{\partial^2}{\partial \alpha \partial \beta} (\epsilon_1 + \epsilon_2) + \frac{\omega^2}{4\rho^2} \right] \end{aligned}$$

* From this point onwards the suffix 0 has been dropped ; all co-ordinates of displacement are of points of the middle surface.

$$+ \frac{3\lambda+2\mu}{2(\lambda+2\mu)\rho^2} \left\{ \epsilon_2 + \frac{\lambda}{\lambda+2\mu} (\epsilon_1 + \epsilon_2) \right\}^2 + \frac{3\lambda+2\mu}{\lambda+2\mu} \cdot \frac{\kappa_1 (\epsilon_1 + \epsilon_2)}{\rho} \\ - \frac{(5\lambda+4\mu)(\kappa_1 + \kappa_2)}{2(\lambda+2\mu)\rho} \left\{ \epsilon_2 + \frac{\lambda}{\lambda+2\mu} (\epsilon_1 + \epsilon_2) \right\} - \frac{\bar{\omega}\tau}{2\rho} \Big]$$

In the h^2 terms is used the notation of the Theory of Thin Shells,

$$\epsilon_1 = \frac{\partial u}{\partial \alpha}, \quad \epsilon_2 = \frac{\partial v}{\partial \beta} - \frac{w}{\rho}, \quad \bar{\omega} = \frac{\partial v}{\partial \alpha} + \frac{\partial u}{\partial \beta}, \\ \kappa_1 = \frac{\partial^2 w}{\partial \alpha^2}, \quad \kappa_2 = \frac{\partial}{\partial \beta} \left(\frac{\partial w}{\partial \beta} + \frac{v}{\rho} \right), \quad \tau = \frac{\partial}{\partial \alpha} \left(\frac{\partial w}{\partial \beta} + \frac{v}{\rho} \right)$$

The result (except for the third-order terms) is equivalent to one given by Basset *

The discussion has been limited for simplicity to the case in which there is no action on either face of the shell, but were such actions to exist no essential alteration in the procedure would be required. The expressions in equations (10) would then be equal to functions of the surface tractions, and therefore of α and β , and of the displacements of points of the surface †. The successive approximations could be made in exactly the same way, and the only difference would be that in the equations obtained by the method of §5, and in the strain energy of the present method, terms depending on the surface tractions would appear. It is true, as pointed out by the late Lord Rayleigh,‡ that if there are surface tractions no form for the strain energy entirely in terms of the displacements of the middle surface is possible, but for most purposes this does not constitute a difficulty, as the equilibrium or stability of configurations under given systems of external force is considered.

The Shell Equations.

7. In a position of equilibrium

$$\iint W' d\alpha d\beta$$

taken over the middle surface of the whole shell must be a minimum, so that

$$\iint \delta W' d\alpha d\beta = 0,$$

* 'Phil. Trans.,' A, vol. 181.

† Cf. Southwell, *loc. cit.*, p. 213.

‡ 'London Math. Soc. Proc.,' vol. 20, p. 372.

where δ denotes an arbitrary variation of u , v and w . This equation can be written in the form

$$\iint (A \delta u + B \delta v + C \delta w) d\alpha d\beta + \iint \left(\frac{\partial M}{\partial \alpha} + \frac{\partial N}{\partial \beta} \right) d\alpha d\beta = 0,$$

where A , B , C are functions of u , v , and w , by such relations as*

$$X \frac{\partial^2 \delta \phi}{\partial \alpha^2} = \frac{\partial^2 X}{\partial \alpha^2} \delta \phi + \frac{\partial}{\partial \alpha} \left(X \frac{\partial \delta \phi}{\partial \alpha} - \frac{\partial X}{\partial \alpha} \delta \phi \right),$$

$$2X \frac{\partial^2 \delta \phi}{\partial \alpha \partial \beta} = 2 \frac{\partial^2 X}{\partial \alpha \partial \beta} \delta \phi + \frac{\partial}{\partial \alpha} \left(X \frac{\partial \delta \phi}{\partial \beta} - \frac{\partial X}{\partial \beta} \delta \phi \right) + \frac{\partial}{\partial \beta} \left(X \frac{\partial \delta \phi}{\partial \alpha} - \frac{\partial X}{\partial \alpha} \delta \phi \right),$$

and

$$X \frac{\partial \delta \phi}{\partial \alpha} = - \frac{\partial X}{\partial \alpha} \delta \phi + \frac{\partial}{\partial \alpha} (X \delta \phi)$$

The second integral can be transformed into line integrals along the edge of the middle surface, from which the boundary conditions at the edges can be obtained. These are not usually of importance for a theory of elastic stability, and need not be considered here.†

The shell equations are given correctly to the second-order of u , v , w by

$$A = B = C = 0.$$

Written in full these equations are

$$\begin{aligned} & \frac{\partial}{\partial \alpha} \left[\frac{\partial u}{\partial \alpha} + \frac{1}{2} \left(\frac{\partial w}{\partial \alpha} \right)^2 \right] + \sigma \left\{ \frac{\partial v}{\partial \beta} - \frac{w}{\rho} + \frac{1}{2} \left(\frac{\partial w}{\partial \beta} + \frac{v}{\rho} \right)^2 \right\} + \frac{1+\sigma}{8} \left(\frac{\partial v}{\partial \alpha} - \frac{\partial u}{\partial \beta} \right)^2 \\ & + \frac{h^2}{3} \left\{ \frac{\sigma}{2(1-\sigma)} \frac{\partial^2}{\partial \alpha^2} (\epsilon_1 + \sigma \epsilon_2) + \frac{\sigma}{2(1-\sigma)} \frac{\partial^2}{\partial \beta^2} (\epsilon_2 + \sigma \epsilon_1) \right. \\ & + \frac{\sigma}{2(1-\sigma)} \frac{\partial^2}{\partial \alpha^2} (\epsilon_1 + \epsilon_2) + \frac{\sigma}{2} \frac{\partial^2 \omega}{\partial \alpha \partial \beta} + \frac{\sigma(1+\sigma)}{(1-\sigma)^2} \cdot \frac{\epsilon_2 + \sigma \epsilon_1}{\rho^2} \\ & \left. + (1+\sigma) \frac{\kappa_1}{\rho} - \frac{\sigma(2+\sigma)}{2(1-\sigma)} \frac{\kappa_1 + \kappa_2}{\rho} \right\} \\ & + \frac{\partial}{\partial \beta} \left[\frac{1-\sigma}{2} \left\{ \frac{\partial v}{\partial \alpha} + \frac{\partial u}{\partial \beta} + \frac{\partial w}{\partial \alpha} \left(\frac{\partial w}{\partial \beta} + \frac{v}{\rho} \right) \right\} \right. \\ & \left. - \frac{1+\sigma}{4} \left(\frac{\partial v}{\partial \alpha} - \frac{\partial u}{\partial \beta} \right) \left(\frac{\partial u}{\partial \alpha} + \frac{\partial v}{\partial \beta} - \frac{w}{\rho} \right) \right. \\ & \left. + \frac{h^2}{3} \left\{ \frac{\sigma}{2(1-\sigma)} \frac{\partial^2}{\partial \alpha \partial \beta} (\epsilon_1 + \epsilon_2) + \frac{1-\sigma}{2} \left(\frac{\partial \omega}{\partial \alpha} - \frac{\tau}{\rho} \right) \right\} \right] = 0, \quad (30) \end{aligned}$$

* See Love, 'Phil. Trans.,' A, vol. 179, p. 514.

† For instance, in the problem of the tubular strut examined below, it is impracticable to find the condition for the collapse of a strut of length l under given end conditions. What is done is to find the condition that a distortion of wave-length l may be maintained in an indefinitely long tube.

$$\begin{aligned}
& \frac{\partial}{\partial \alpha} \left[\frac{1-\sigma}{2} \left\{ \frac{\partial v}{\partial \alpha} + \frac{\partial u}{\partial \beta} + \frac{\partial w}{\partial \alpha} \left(\frac{\partial w}{\partial \beta} + \frac{v}{\rho} \right) \right\} + \frac{1+\sigma}{4} \left(\frac{\partial v}{\partial \alpha} - \frac{\partial u}{\partial \beta} \right) \left(\frac{\partial u}{\partial \alpha} + \frac{\partial v}{\partial \beta} - \frac{w}{\rho} \right) \right. \\
& \quad \left. + \frac{h^2}{3} \left\{ \frac{\sigma}{2(1-\sigma)} \frac{\partial^2}{\partial \alpha \partial \beta} (\epsilon_1 + \epsilon_2) + \frac{1-\sigma}{2} \left(\frac{\partial^2}{\partial \alpha^2} - \frac{\tau}{\rho^2} \right) \right\} \right] \\
& + \frac{\partial}{\partial \beta} \left[\frac{\partial v}{\partial \beta} - \frac{w}{\rho} + \frac{1}{2} \left(\frac{\partial w}{\partial \beta} + \frac{v}{\rho} \right)^2 + \sigma \left\{ \frac{\partial u}{\partial \alpha} + \frac{1}{2} \left(\frac{\partial w}{\partial \alpha} \right)^2 \right\} + \frac{1+\sigma}{8} \left(\frac{\partial v}{\partial \alpha} - \frac{\partial u}{\partial \beta} \right)^2 \right. \\
& \quad + \frac{h^2}{3} \left\{ \frac{\sigma}{2(1-\sigma)} \frac{\partial^2}{\partial \alpha^2} (\epsilon_1 + \sigma \epsilon_2) + \frac{\sigma}{2(1-\sigma)} \frac{\partial^2}{\partial \beta^2} (\epsilon_2 + \sigma \epsilon_1) \right. \\
& \quad + \frac{\sigma}{2(1-\sigma)} \frac{\partial^2}{\partial \beta^2} (\epsilon_1 + \epsilon_2) + \frac{\sigma}{2} \frac{\partial^2 w}{\partial \alpha \partial \beta} + \frac{1+\sigma}{(1-\sigma)^2} \cdot \frac{\epsilon_2 + \sigma \epsilon_1}{\rho^2} \\
& \quad \left. \left. + (1+\sigma) \frac{\kappa_1}{\rho} - \frac{2+\sigma}{2(1-\sigma)} \frac{\kappa_1 + \kappa_2}{\rho} \right\} \right] \\
& - \frac{1}{\rho} \left[\frac{1-\sigma}{2} \frac{\partial w}{\partial \alpha} \left(\frac{\partial v}{\partial \alpha} + \frac{\partial u}{\partial \beta} \right) + \left(\frac{\partial w}{\partial \beta} + \frac{v}{\rho} \right) \left(\frac{\partial v}{\partial \beta} - \frac{w}{\rho} + \sigma \frac{\partial u}{\partial \alpha} \right) \right. \\
& \quad - \frac{h^2}{3} \left\{ \frac{\partial}{\partial \beta} (\kappa_1 + \kappa_2) + (1-\sigma) \left(2 \frac{\partial \tau}{\partial \alpha} - \frac{\partial \epsilon_1}{\partial \beta} \right) \right. \\
& \quad \left. \left. - \frac{2+\sigma}{2(1-\sigma)} \frac{\partial}{\partial \beta} \left(\frac{\epsilon_2 + \sigma \epsilon_1}{\rho} \right) - \frac{(1-\sigma)}{2\rho} \cdot \frac{\partial w}{\partial \alpha} \right\} \right] = 0, \quad (31)
\end{aligned}$$

and

$$\begin{aligned}
& \frac{h^2}{3} \left[\left(\frac{\partial^2}{\partial \alpha^2} + \frac{\partial^2}{\partial \beta^2} \right) (\kappa_1 + \kappa_2) + (1-\sigma) \left(2 \frac{\partial^2 \tau}{\partial \alpha \partial \beta} - \frac{\partial^2 \kappa_2}{\partial \alpha^2} - \frac{\partial^2 \kappa_1}{\partial \beta^2} \right) \right. \\
& \quad + \frac{2-3\sigma^2}{2(1-\sigma)\rho} \frac{\partial^2}{\partial \alpha^2} (\epsilon_1 + \epsilon_2) - \frac{2+\sigma}{2(1-\sigma)\rho} \frac{\partial^2}{\partial \alpha^2} (\epsilon_2 + \sigma \epsilon_1) \\
& \quad \left. - \frac{2+\sigma}{2(1-\sigma)} \frac{\partial^2}{\partial \beta^2} \left(\frac{\epsilon_2 + \sigma \epsilon_1}{\rho} \right) - \frac{1-\sigma}{2} \frac{\partial^2}{\partial \sigma \partial \beta} \left(\frac{w}{\rho} \right) \right] \\
& - \frac{\partial}{\partial \alpha} \left[\frac{\partial w}{\partial \alpha} \left\{ \frac{\partial u}{\partial \alpha} + \sigma \left(\frac{\partial v}{\partial \beta} - \frac{w}{\rho} \right) \right\} + \frac{1-\sigma}{2} \left(\frac{\partial w}{\partial \beta} + \frac{v}{\rho} \right) \left(\frac{\partial v}{\partial \alpha} + \frac{\partial u}{\partial \beta} \right) \right] \\
& - \frac{\partial}{\partial \beta} \left[\left(\frac{\partial w}{\partial \beta} + \frac{v}{\rho} \right) \left(\frac{\partial v}{\partial \beta} - \frac{w}{\rho} + \sigma \frac{\partial u}{\partial \alpha} \right) + \frac{1-\sigma}{2} \frac{\partial w}{\partial \alpha} \left(\frac{\partial v}{\partial \alpha} + \frac{\partial u}{\partial \beta} \right) \right] \\
& - \frac{1}{\rho} \left[\frac{\partial v}{\partial \beta} - \frac{w}{\rho} + \frac{1}{2} \left(\frac{\partial w}{\partial \beta} + \frac{v}{\rho} \right)^2 + \sigma \left\{ \frac{\partial u}{\partial \alpha} + \frac{1}{2} \left(\frac{\partial w}{\partial \alpha} \right)^2 \right\} + \frac{1+\sigma}{8} \left(\frac{\partial v}{\partial \alpha} - \frac{\partial u}{\partial \beta} \right)^2 \right. \\
& \quad + \frac{h^2}{3} \left\{ \frac{\sigma}{2(1-\sigma)} \frac{\partial^2}{\partial \alpha^2} (\epsilon_1 + \sigma \epsilon_2) + \frac{\sigma}{2(1-\sigma)} \frac{\partial^2}{\partial \beta^2} (\epsilon_2 + \sigma \epsilon_1) \right. \\
& \quad + \frac{\sigma}{2(1-\sigma)} \frac{\partial^2}{\partial \beta^2} (\epsilon_1 + \epsilon_2) + \frac{\sigma}{2} \frac{\partial^2 w}{\partial \alpha \partial \beta} + \frac{1+\sigma}{(1-\sigma)^2} \frac{\epsilon_2 + \sigma \epsilon_1}{\rho^2} \\
& \quad \left. \left. + (1+\sigma) \frac{\kappa_1}{\rho} - \frac{2+\sigma}{2(1-\sigma)} \frac{\kappa_1 + \kappa_2}{\rho} \right\} \right] = 0 \quad (32)
\end{aligned}$$

σ as usual denotes Poisson's ratio, it has been found convenient to use the elastic constants λ , μ in the intermediate stages, though the equations themselves are simpler in terms of σ .

From these equations as in § 5 the equations of stability of any known configuration can be immediately set down

It will be seen that the complexity of the equations is not due to the second-order terms, which are comparatively few and in the main symmetrical, but to the terms in h^2 . The theory of thin shells simplifies the latter considerably by physical assumptions, but it does not appear possible to simplify the equations above on mathematical grounds in the general case. However, in a definite problem it is probable that it would be possible to see without difficulty which of these terms were important, and avoid unnecessary labour as is done in the problem considered below. It is not, therefore, thought worth while to abandon a process of approximation which, though unnecessarily accurate in some cases, is at least definite, in favour of one which it is legitimate to describe in the words of Rayleigh* as of "ill-defined significance"

Examples of General Theory

8 It has been remarked in § 5 that a plane plate in a configuration of equilibrium in which the middle surface is plane, can collapse in either of two independent modes, of which one only is of physical interest † The result of this is, as has been seen, considerably to reduce the work necessary in a problem of stability. It is of interest to show that this is the case from equations (30), (31), and (32). From them the corresponding equations for a plane plate can be deduced at once. They are

$$\begin{aligned} \frac{\partial}{\partial x} \left[\frac{\partial u}{\partial x} + \frac{1}{2} \left(\frac{\partial w}{\partial x} \right)^2 + \sigma \left\{ \frac{\partial v}{\partial y} + \frac{1}{2} \left(\frac{\partial w}{\partial y} \right)^2 \right\} + \frac{1+\sigma}{8} \left(\frac{\partial v}{\partial x} - \frac{\partial u}{\partial y} \right)^2 \right] \\ + \frac{\partial}{\partial y} \left[\frac{1-\sigma}{2} \left(\frac{\partial v}{\partial x} + \frac{\partial u}{\partial y} + \frac{\partial w}{\partial x} \frac{\partial w}{\partial y} \right) - \frac{1+\sigma}{4} \left(\frac{\partial v}{\partial x} - \frac{\partial u}{\partial y} \right) \left(\frac{\partial u}{\partial x} + \frac{\partial v}{\partial y} \right) \right] \\ + h^2 f_1(u, v) = 0, \quad (33) \end{aligned}$$

$$\begin{aligned} \frac{\partial}{\partial x} \left[\frac{1-\sigma}{2} \left(\frac{\partial v}{\partial x} + \frac{\partial u}{\partial y} + \frac{\partial w}{\partial x} \frac{\partial w}{\partial y} \right) + \frac{1+\sigma}{4} \left(\frac{\partial v}{\partial x} - \frac{\partial u}{\partial y} \right) \left(\frac{\partial u}{\partial x} + \frac{\partial v}{\partial y} \right) \right] \\ + \frac{\partial}{\partial y} \left[\frac{\partial v}{\partial y} + \frac{1}{2} \left(\frac{\partial w}{\partial y} \right)^2 + \sigma \left\{ \frac{\partial u}{\partial x} + \frac{1}{2} \left(\frac{\partial w}{\partial x} \right)^2 \right\} + \frac{1+\sigma}{8} \left(\frac{\partial v}{\partial x} - \frac{\partial u}{\partial y} \right)^2 \right] \\ + h^2 f_2(u, v) = 0, \quad (34) \end{aligned}$$

* *Loc. cit.*, p. 374.

† This was first pointed out by Southwell, *loc. cit.*, p. 202.

and

$$\frac{h^2}{3} \nabla_1^2 w - \frac{\partial}{\partial x} \left[\frac{\partial w}{\partial x} \left(\frac{\partial u}{\partial x} + \sigma \frac{\partial v}{\partial y} \right) + \frac{1-\sigma}{2} \frac{\partial w}{\partial y} \left(\frac{\partial v}{\partial x} + \frac{\partial u}{\partial y} \right) \right] - \frac{\partial}{\partial y} \left[\frac{\partial w}{\partial y} \left(\frac{\partial v}{\partial y} + \sigma \frac{\partial u}{\partial x} \right) + \frac{1-\sigma}{2} \frac{\partial w}{\partial x} \left(\frac{\partial v}{\partial x} + \frac{\partial u}{\partial y} \right) \right] = 0 \quad (35)$$

In equations (33) and (34), $f_1(u, v)$ and $f_2(u, v)$ are functions linear in u and v (35) is in agreement with equation (25) obtained by the alternative method. It is easy to see that if in these equations we substitute first $(u, v, 0)$ and then $(u + u', v + v', w')$, the displacements of the equilibrium and distorted configurations respectively, and then subtract the two sets of equations ignoring terms above the first-order in u' , v' and w' , the first two equations contain only u' and v' , and the third only w' . Consequently two independent modes of collapse are possible.

There is one point of importance. The condition that there should be a non-zero solution of the third equation will evidently require in general the strains such as $\partial u / \partial x$ in the equilibrium configuration to be of the order of h^2 . If instability in this mode is to appear before the breakdown of the material itself, if, that is to say, a theory of stability is to have practical value, the strains in the equilibrium configuration, and consequently h^2 , must be very small. But these are precisely the conditions that the approximations used in reaching (35) should be justifiable, for in this equation we have neglected terms similar to those that appear when multiplied either by a displacement or by h^2 . Consequently the condition that this instability should be possible in practice, is the condition that equation (35) should be competent to determine when it will take place.

The position in regard to instability of the other type is entirely different. From equations (33) and (34) it is clear that in general a non-zero solution in u' and v' cannot be obtained with small strains; the strains must be of the order of the coefficients of the terms in u' and v' alone. This result regarded as a first approximation shows, however, that there is no ground for neglecting any order of displacement co-ordinates, and there is no reason to suppose that further approximations would alter this conclusion as to the order of magnitude of the strains. This type of instability is then of no practical interest, and it is therefore a matter of indifference that sufficiently accurate equations would, in the general case, be impossible to obtain.* The theory of the stability of plane plates is, therefore, in the

* With the simplest types of stress there is, however, no difficulty.

fortunate position that it is only adequate to deal with problems that are of practical significance

The Stability of a Tubular Strut.

9 As a more interesting example the stability of a tubular strut is briefly considered. This problem has been solved by Southwell,* using in the case of distortions of axial symmetry his general theory of stability, but in the case of distortions of any type, the theory of thin shells. The general case, then, is here considered for the first time without the latter theory.

The equilibrium configuration of a long circular cylindrical shell in compression due to end thrust is given by

$$u = \theta\alpha, \quad v = 0, \quad w = \sigma\theta\rho.$$

θ is a constant and so, in this problem, is ρ . These displacements will evidently satisfy the shell equations. If the equilibrium of this configuration is neutral and a symmetrical distortion of the shell is liable to take place, the shell equations can also be satisfied by the displacements

$$u = \theta\alpha + u', \quad v = 0, \quad w = \sigma\theta\rho + w',$$

where u' and v' are independent of β . Subtracting the shell equations for the two configurations, and ignoring terms of order above the first in u' and w' , we have the two stability equations†

$$\begin{aligned} \frac{\partial}{\partial\alpha} \left[\frac{\partial u'}{\partial\alpha} - \frac{\sigma w'}{\rho} + \frac{h^2}{3} \left\{ \frac{\sigma}{2(1-\sigma)} \frac{\partial^2}{\partial\alpha^2} \left(\frac{\partial u'}{\partial\alpha} - \frac{\sigma w'}{\rho} \right) \right. \right. \\ \left. \left. + \frac{\sigma}{2(1-\sigma)} \frac{\partial^2}{\partial\alpha^2} \left(\frac{\partial u'}{\partial\alpha} - \frac{w'}{\rho} \right) + \frac{\sigma(1+\sigma)}{(1-\sigma)^2 \rho^2} \left(\sigma \frac{\partial u'}{\partial\alpha} - \frac{w'}{\rho} \right) \right. \right. \\ \left. \left. + \frac{2-2\sigma-3\sigma^2}{2(1-\sigma)\rho} \frac{\partial^2 w'}{\partial\alpha^2} \right\} \right] = 0, \quad (36) \end{aligned}$$

and

$$\begin{aligned} \frac{h^2}{3} \left[\frac{\partial^4 w'}{\partial\alpha^4} + \frac{2-3\sigma^2}{2(1-\sigma)\rho} \frac{\partial^2}{\partial\alpha^2} \left(\frac{\partial u'}{\partial\alpha} - \frac{w'}{\rho} \right) - \frac{2+\sigma}{2(1-\sigma)\rho} \frac{\partial^2}{\partial\alpha^2} \left(\sigma \frac{\partial u'}{\partial\alpha} - \frac{w'}{\rho} \right) \right] \\ - \theta(1-\sigma^2) \frac{\partial^2 w'}{\partial\alpha^2} \\ - \frac{1}{\rho} \left[\sigma \frac{\partial u'}{\partial\alpha} - \frac{w'}{\rho} + \frac{h^2}{3} \left\{ \frac{\sigma}{2(1-\sigma)} \frac{\partial^2}{\partial\alpha^2} \left(\frac{\partial u'}{\partial\alpha} - \frac{\sigma w'}{\rho} \right) \right. \right. \\ \left. \left. + \frac{1+\sigma}{(1-\sigma)^2 \rho^2} \left(\sigma \frac{\partial u'}{\partial\alpha} - \frac{w'}{\rho} \right) - \frac{\sigma(1+2\sigma)}{2(1-\sigma)\rho} \frac{\partial^2 w'}{\partial\alpha^2} \right\} \right] = 0. \quad (37) \end{aligned}$$

* *Loc. cit.*, pp. 227-236.

† Equation (31) is satisfied identically by both sets of displacements.

Writing

$$u' = U \sin \frac{q\alpha}{\rho},$$

and

$$w' = W \cos \frac{q\alpha}{\rho},$$

when U and W are constants, the condition for a non-zero solution of the equations can be written down at once in determinant form. As a first approximation ignore the terms in h^2 in (36) and (37), then

$$\begin{vmatrix} \frac{q}{\rho}, & -\frac{\sigma}{\rho} \\ -\frac{\sigma q}{\rho^2}, & \frac{1}{\rho^2} + \theta(1 - \sigma^2) \frac{q^2}{\rho^2} \end{vmatrix} = 0,$$

so that

$$\theta = -\frac{1}{q^2}$$

As a result, q must be large if the stress is to be one of practical interest. The next approximation, in which the terms in h^2 are included, is therefore written in the form

$$\begin{vmatrix} \frac{q}{\rho} + A \frac{h^2 q^3}{\rho^3} + B \frac{h^2 q}{\rho^3}, & -\frac{\sigma}{\rho} + C \frac{h^2 q^2}{\rho^3} + D \frac{h^2}{\rho^3} \\ -\frac{\sigma q}{\rho^2} + E \frac{h^2 q^3}{\rho^4} + F \frac{h^2 q}{\rho^4}, & \frac{1}{\rho^2} + \theta(1 - \sigma^2) \frac{q^2}{\rho^2} + H \frac{h^2 q^4}{\rho^4} + G \frac{h^2 q^2}{\rho^4} + I \frac{h^2}{\rho^4} \end{vmatrix} = 0,$$

where A, B, C, \dots are non-dimensional constants independent of q . Further, let

$$\theta = -\frac{1}{q^2} + \theta^1 \frac{h^2}{\rho^2},$$

and evaluate the determinant to order h^2

Then $\theta^1 q^2 = -(Lq^4 + Mq^2 + N)$,

where L, M, N are further constants independent of q .

The final form for θ is then

$$\theta = -\frac{1}{q^2} - \frac{h^2}{\rho^2} \left(Lq^2 + M + \frac{N}{q^2} \right),$$

and the minimum value of θ^1 for all values of q is given to a first approximation by

$$\theta = -\frac{2h}{\rho} \sqrt{L},$$

* This corresponds to the minimum thrust that will cause collapse in the mode considered; only this minimum value is of practical importance.

where

$$L = \frac{H}{1 - \sigma^2} = \frac{1}{3(1 - \sigma^2)}$$

With this value of θ we arrive at the known formula for the minimum total thrust, S , that in a strut of any radius will cause this type of collapse,

$$S = 8\pi E k^2 \sqrt{\frac{1}{3(1 - \sigma^2)}}.$$

To consider any type of distortion, the configuration adjacent to the equilibrium configuration must be taken to be

$$u = \theta\alpha + u', \quad v = v', \quad w = \sigma\theta\rho + w',$$

u' , v' , w' are now functions of α and β

Forming the stability equations in the usual way, the only terms in θ are found to be $\frac{(1 - \sigma^2)}{4} \theta \left(\frac{\partial^2 u'}{\partial \beta^2} - \frac{\partial^2 v'}{\partial \alpha \partial \beta} \right)$, $\frac{(1 - \sigma^2)}{4} \theta \left(\frac{\partial^2 v'}{\partial \alpha^2} - \frac{\partial^2 u'}{\partial \alpha \partial \beta} \right)$ and $-(1 - \sigma^2) \theta \frac{\partial^2 w'}{\partial \alpha^2}$, in the first, second and third equations respectively.

Setting in these equations

$$u = U \sin \frac{q\alpha}{\rho} \sin \frac{k\beta}{\rho},$$

$$v = V \cos \frac{q\alpha}{\rho} \cos \frac{k\beta}{\rho},$$

and

$$w = W \cos \frac{q\alpha}{\rho} \sin \frac{k\beta}{\rho},$$

a first approximation to θ (ignoring k^2) is found from the determinant

$$\begin{vmatrix} -\frac{1-\sigma}{2} k^2 - q^2 - \frac{1-\sigma^2}{4} \theta k^2, & \frac{1+\sigma}{2} kq - \frac{1-\sigma^2}{4} \theta kq & \sigma q \\ \frac{1+\sigma}{2} kq - \frac{1-\sigma^2}{4} \theta kq, & -k^2 - \frac{1-\sigma}{2} q^2 - \frac{1-\sigma^2}{4} \theta q^2, & -k \\ -\sigma q, & k, & 1 + (1 - \sigma^2) \theta q^2 \end{vmatrix} = 0.$$

Expanding and ignoring θ^2 , we have

$$\frac{(1 - \sigma)(1 - \sigma^2)}{2} \left[q^4 + q^2 \theta \left\{ k^2 (k^2 + 1) + 2k^2 q^2 + \frac{1 + \sigma}{2} q^2 + q^4 \right\} \right] = 0.$$

It is assumed that k is not zero,* as this case has been already discussed.

* The forms assumed for u' , v' , w' are not valid if $k = 0$.

Accordingly, q^2 must now be small if a stress of practical interest is to cause collapse. As a first result then

$$\theta = -\frac{q^2}{k^2(k^2 + 1)}$$

It is next necessary to find the various types of terms in the expansion of the determinant to order h^2 , the coefficients are not in the first instance required. It then appears that the minimum value of θ for given k (which must be integral) corresponds with a value of q which is such that θ , q^2 and h are small quantities of the same order. The determinant contains no terms independent of, or linear in, these three quantities. A first approximation to θ is therefore obtained from an evaluation of the determinant to the second order of these quantities. The terms in q^4 and θq^2 are known, none in θh or $q^2 h$ can appear, so that only terms in θ^2 and h^2 remain to be evaluated. There are physical grounds for ignoring the terms in θ^2 , and some mathematical grounds. Completely to determine them would of course require a revision of the preceding work, so that the shell equations should contain the relevant terms of the third-order. However, some of the terms in θ^2 already appear and are multiplied in every case by the square or higher power of q , this is also the case with those that arise in third-order shell equations which have been found in a special case for another purpose. It has therefore appeared impossible that these terms could affect the result, and they have not been calculated in full. The h^2 term is readily obtained. Writing the determinant

$$\begin{vmatrix} -\frac{1-\sigma}{2}k^2 - q^2 - \frac{1-\sigma^2}{4}\theta k^2 + A\frac{h^2}{\rho^2}, & \frac{1+\sigma}{2}kq - \frac{1-\sigma^2}{4}\theta kq + B\frac{h^2}{\rho^2}, & \sigma q + C\frac{h^2}{\rho^2}, \\ \frac{1+\sigma}{2}kq - \frac{1-\sigma^2}{4}\theta kq + D\frac{h^2}{\rho^2}, & -k^2 - \frac{1-\sigma}{2}q^2 - \frac{1-\sigma^2}{4}\theta q^2 + F\frac{h^2}{\rho^2}, & -k + G\frac{h^2}{\rho^2}, \\ -\sigma q + H\frac{h^2}{\rho^2}, & k + I\frac{h^2}{\rho^2}, & 1 + (1-\sigma^2)\theta q^2 + J\frac{h^2}{\rho^2} \end{vmatrix},$$

where A, B, C, \dots are constants, the term in h^2 is seen to be

$$-\frac{(1-\sigma)k^2 h^2}{2\rho^2}(F - kG + kI - k^2J).$$

In this expression only that part of F , for instance, independent of q is required, and this must come from the terms in v' not differentiated with regard to α in the second stability equation.

The final result is

$$\frac{1-\sigma}{2} \left[(1-\sigma^2)q^4 + (1-\sigma^2)\theta q^2 k^2 (k^2 + 1) + \frac{k^4(k^2 - 1)^2 h^2}{9\rho^2} \right] = 0.$$

The minimum value of θ is given by

$$q^2 = \frac{k^2 (k^2 - 1)}{\sqrt{3} (1 - \sigma^2)} \frac{h}{\rho},$$

the corresponding minimum total thrust, S , that will cause instability in the mode defined by k is

$$S = 8\pi E h^2 \frac{k^2 - 1}{k^2 + 1} \sqrt{\frac{1}{3(1 - \sigma^2)}},$$

verifying the result given by the 'Theory of Thin Shells.'*

*On the Fluorescence and Channelled Absorption of Bismuth
at High Temperatures.*

By K. RANGADHAMA RAO, M.A., Madras University Research
Scholar

(Communicated by Lord Rayleigh, F.R.S.—Received January 2, 1925)

[PLATE 12]

In a paper recently communicated to the Royal Society, experiments dealing with the absorption spectra of several metals were described, in which it was found that bismuth vapour shows both lines and bands in absorption. The banded spectrum consists of three groups of bands, each group consisting of a number of bands degraded towards the red, the group of bands in the visible region appearing at high temperatures

In the above experiments it was hoped that by raising the temperature of the absorption chamber sufficiently high, and raising the absorption in the lines of the several bands, it might be possible to detect a fine structure in some of these bands. Accordingly, the author modified the furnace previously used so as to blow through it a larger quantity of compressed air, and succeeded finally by using coke and this furnace to obtain a temperature of about 1500° C. to 1600° C. At this temperature the vapour emitted a fluorescent radiation orange yellow in colour.

In these experiments the spectra were photographed by a Hilger glass spectrometer of the constant deviation type. To obtain the fluorescence and absorption spectra in juxtaposition, the slit of the collimator is provided with

* Southwell, *loc. cit.*, p. 235.

a slotted diaphragm by which exposures were given of both the fluorescence and absorption spectra, without moving the photographic plate.

Fig 1 (Plate 12) represents the photograph of the fluorescence and channelled absorption of the vapour at this temperature, and the author succeeded in photographing about 20 of these fluorescence bands, the approximate wave-lengths of 16 of these are given in the table below, along with the wave numbers. It will be seen further from the photograph that the fluorescence spectrum is more or less the exact complement of the absorption spectrum in this region. When examined by a nicol, the fluorescent radiation did not exhibit any polarisation.

Fig 2 represents a section of the absorption spectrum at the high temperature. In contrast to the bands in the ultra-violet, some of these bands show a distinctly fine structure. According to Bohr's theory of band spectra, there seems to be little doubt that these bands correspond to triple quantification of the electronic, atomic and molecular motions of the bismuth molecule, and it may be that the large moment of inertia which we may suppose the bismuth molecule to have, leads to a small frequency interval between successive members of the line series in the bands. Further, the series consists of a large number of these members crowding together at the head.

Table 1 —(Fluorescence Spectrum)

λ	$\Delta\lambda$	ν	$\Delta\nu$
6533 0	—	15,307	—
6484 5	68 5	15,469	162
6389 0	75 5	15,652	183
6319 5	69 5	15,824	172
6248 5	71 0	16,004	180
6187 5	61 0	16,162	158
6117 5	70 0	16,347	185
6052 0	65 5	16,523	176
5991 5	60 5	16,699	167
5940 5	51 0	16,834	144
5886 5	60 0	17,005	171
5831 5	49 0	17,148	143
5776 5	55 0	17,312	168
5726 0	50 5	17,464	152
5680 0	46 0	17,606	142
5640 0	40 0	17,730	124

Electrical measurements of inelastic impact potentials and of ionisation of this element recently made by Ruark, Mohler and others* indicate that the

* 'Scientific Papers of the Bureau of Standards,' No. 490 (part of vol. 19), pp. 463-486 (June, 1924).

excitation potential is 1.9 volts. It is well known that the elements of the Fifth Group are polyatomic in the vapour state. The existence of the fluorescent banded spectrum in the above region indicates that banded spectra are a criterion for the presence of molecular radiation processes, and that the critical potentials of elements, which are polyatomic, are probably related to the molecule, and that the radiating systems here involved are molecules instead of atoms, so that, in addition to the energy associated with electrons, two other types of energy may be radiated due to the oscillations of the nuclei and the rotations of the molecule about its centre of gravity. It may, therefore, be assumed that the critical potentials of these elements correspond to the band spectra.

Further, these fluorescent bands are shaded towards the less refrangible side. Theoretically, these bands, therefore, correspond to a decrease in the moment of inertia of the molecule, as a result of the change in the molecular configuration involving a decrease in the internal energy.

I am deeply indebted to Prof. A. L. Narayan for his continued interest and help.

A Note on the Absorption of the Green Line of Thallium Vapour.

By K. RANGADHAMA RAO, M.A., Madras University Research Scholar

(Communicated by Lord Rayleigh, F.R.S.—Received January 2, 1925)

[PLATE 13]

Investigations on the structure of spectral lines indicate that lines of heavy metals like mercury and bismuth are generally complex in structure. The constitution of mercury and bismuth lines has been studied by several physicists, who have established the complexity of these lines.

Recently Metcalfe and Venkatesachar* described a series of interesting experiments on the absorption of $\lambda 5461$ by luminous mercury vapour, where it was found that all the satellites of the green line were strongly absorbed under suitable conditions and that the ratio of emission to absorption was fairly constant for all lines except — 0.237 A.U.

* 'Roy Soc. Proc.,' A, vol. 100, pp. 149–166 (1921), and vol. 105, pp. 520–531 (1924).

FIG. 1

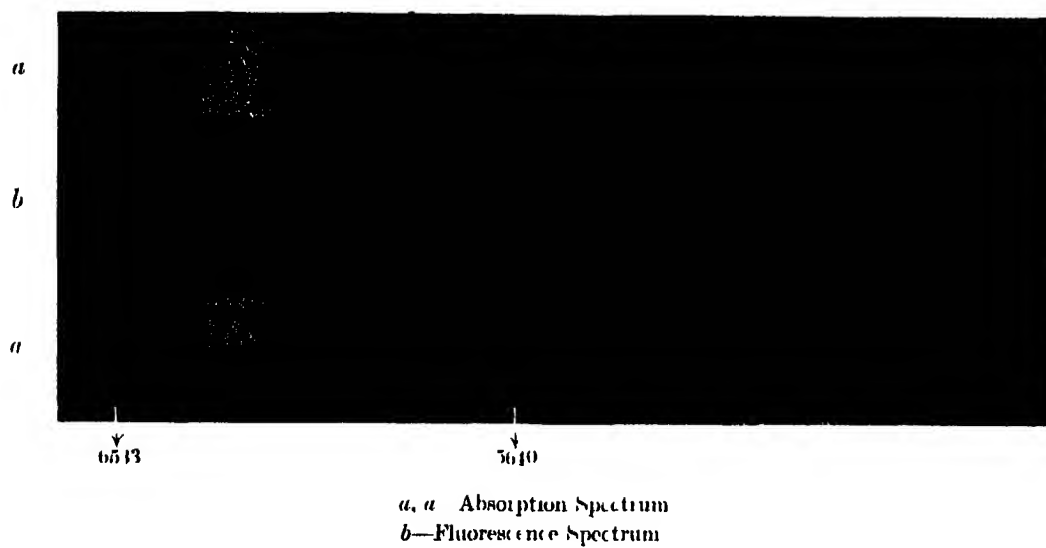


FIG. 2.



Absorption Spectrum

FIG. 1

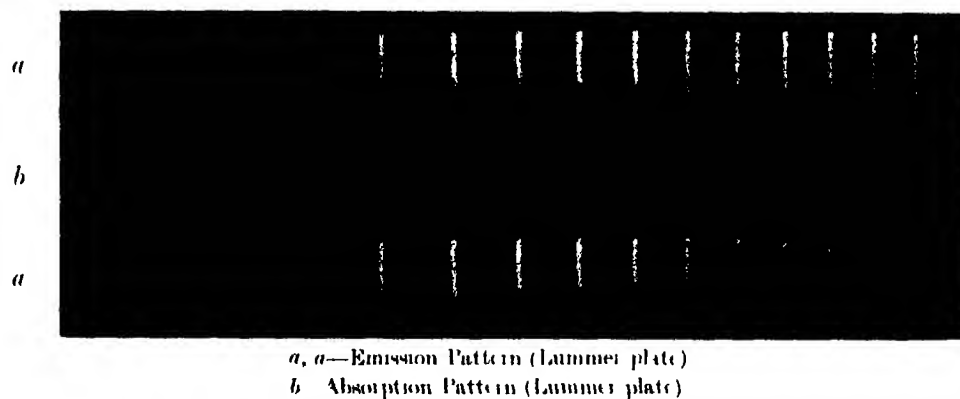
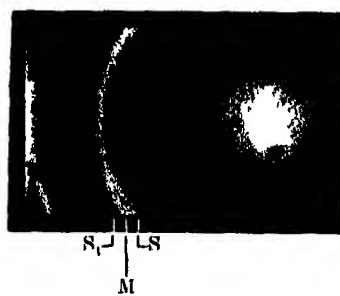


FIG. 2



FIG. 3



Numerous investigators studied the structure of the green line $\lambda 5350$ of thallium, notable among them being Michelson, Fabry and Perot, and Barnes, and found it to be complex in structure. In 1892 Michelson investigated the structure of this line by means of visibility curves, and found that the line consisted of two components, each of which was double. In 1899 Fabry and Perot investigated with their interferometer the structure of the same line and found that the line was triple, being composed of one bright and two weaker components, both of them being of the same intensity and lying on the red side, their separation being 0.02 \AA and 0.12 \AA respectively. In 1904 Barnes also studied the structure of this line and found that it consisted of the main line and two satellites, with a separation of 0.04 \AA and 0.1 \AA , the intensity of the first satellite being three times that of the latter.

In a previous paper* an account has been given of the experiments made by the author in collaboration with Prof. Narayan on "Absorption and Dispersion of Thallium Vapour," where it was found that $1\pi_2 - 1\pi_1$, corresponding to the first resonance potential, was not absorbed by the non-luminous vapour, and that the vapour exhibited anomalous dispersion more prominently at $\lambda 3775 (1\sigma - 1\pi_2)$ than at $\lambda 5350 (1\sigma - \pi_1)$, which is quite in keeping with the view that $1\pi_2$ is the ground orbit of the valence electron of the element.

From considerations based on the absorption of $\lambda 5461$ of mercury, it was thought that a more detailed study of the absorption of the green line of thallium would give interesting information. Further observations on the absorption of this line were therefore undertaken. As a preliminary to this, a cursory examination was made of the structure of this line.

In studying the constitution of this green line a glass Lummer-Gehrcke plate of resolving power about 300,000 for $\lambda 5350$ and a Fabry-Perot étalon (thickness of air layer 10.016 mm) were used. The source employed is the radiation from a vacuum tube through which a condensed discharge was passed from an induction coil between thallium electrodes. In order to avoid the necessity of knowing the order of the diffraction pattern in finding the separation of the satellites from the main line, and to make a more accurate determination of the intensities of these satellites relative to the main line, photographs containing the diffraction pattern on either side were obtained with the Lummer-Gehrcke plate. In these experiments the radiation constituting the green line was isolated by an auxiliary spectrometer.

Fig. 2 (Plate 13) is a reproduction of the diffraction pattern obtained with the Lummer plate. With the resolution attainable by the plate it is found

* 'Roy. Soc. Proc.,' A, vol. 106, pp. 596-601 (1924).

that the main line is a close doublet, and is accompanied by a satellite with separations 116 Å.

The resolving power of the plate is hardly sufficient to show the other satellite, but the photograph taken with the étalon (fig 3) clearly shows the existence of the other satellite also

The formula used in this experiment in measuring the fringe pattern obtained with the Lummer plate is the same as that used by McLennan,

$$\Delta\lambda = \frac{a_s^2 - a_m^2}{a_{m_2}^2 - a_{m_1}^2} d \lambda_{\max},$$

where the denominator is the difference between the squares of distances of two main-line fringes from the central line of the pattern

$a_m \rightarrow$ Distance of main-line fringe from the central line of the pattern

$a_s \rightarrow$ Distance from the central line of a satellite fringe of the same order

$d\lambda_{\max} \rightarrow$ Change in λ causing fringe of the m th order of the system of fringes due to $(\lambda + d\lambda)$ to coincide with fringe of the $(m + 1)$ th order of λ

In the absorption experiment, careful preliminary eye observations were made with the source of radiation the same as that used above, the resolving instrument being the Lummer plate. The column of absorbing vapour was contained at a low pressure in a seamless steel tube about 2 feet long with a plate-glass window at either end. As the temperature of the vapour was raised gradual absorption of the central doublet commenced at about 600° C, and it was completely extinguished at about 800° C while at this temperature the satellite was but very little absorbed. With further increase of temperature the absorption of the satellite took place till it was complete at about 950° C. Attempts to take a photograph when the main component alone was absorbed did not succeed, as it was found difficult to keep the vapour steadily at the temperature for the prolonged time of exposure necessitated by the presence of the very feeble satellite alone in the field, and, further, any slight alteration in the temperature would result in a reappearance of the central doublet or the absorption of the satellite also.

For photographing the spectrum in the stage of complete absorption of both the main line and satellite, the experiment was repeated with the source so modified as to give a sufficient continuous spectrum which would serve as a background on which the reversal could be obtained with clearness. A condensed discharge between thallium electrodes in hydrogen was found to

serve the purpose well. The photograph taken under these conditions is reproduced in fig. 1, where the absorption bands are found to exactly correspond with the emission pattern.

It is interesting to note that the absorption of the satellite commenced practically when the absorption of the main line was complete. This shows that although, according to the Quantum theory, the ratio of the number of atoms affecting the absorption of the main line and the satellite may be supposed to be constant under all conditions, it may be that the position of maximum absorption for the composite line would, on account of the exponential law of absorption, shift somewhat with the varying number of atoms taking part in the absorption at different temperatures.

As values of the intensities of the satellites relative to the main line are not generally in good agreement, attempts were also made to determine the intensities. For this purpose spectra taken with the Lummer plate and étalon were used, the method adopted being exactly the same as that previously used by Narayan for comparing the intensities of the satellites accompanying the lines of the principal Series of Potassium and described in detail elsewhere*. As a result of observations made on a number of plates it was found that the intensities of the satellites relative to the main line are 0.2 and 0.75 for 0.024 and 0.116 Å, respectively.

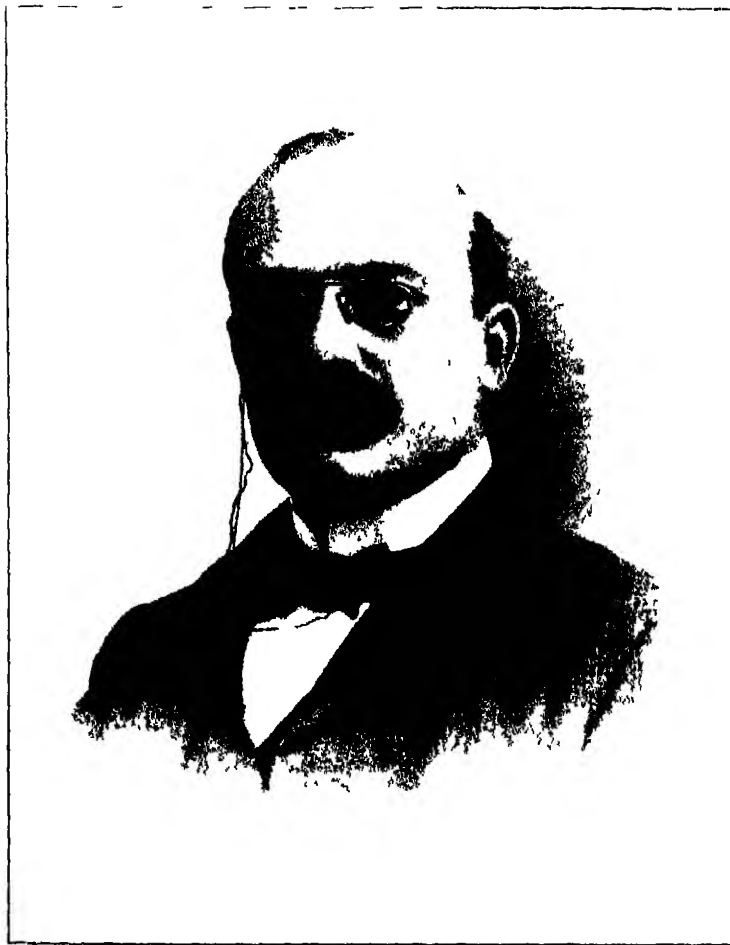
I am deeply indebted to Prof. A. L. Narayan for his continued interest and help.

* 'Proc. Phys. Soc. (London),' vol. 36, Part I, p. 35 (December 15, 1923)

OBITUARY NOTICES
OF
FELLOWS DECEASED.

CONTENTS.

	PAGE
S S. HOUGH (with portrait)	i
SIR JAMES JOHNSTONE DOBBIE (with portrait)	vi
JOHN EDWARD CAMPBELL (with portrait)	ix



S. J. Hough

S. S. HOUGH—1870-1923

SYDNEY SAMUEL HOUGH was born at Stoke Newington on June 11, 1870. He was educated at Christ's Hospital and at St John's College, Cambridge. After graduating as third wrangler in 1892, he was awarded a Smith's Prize in 1894 for his Essay on the oscillations of an ellipsoidal shell containing fluid, and in the following year he was elected to a fellowship at his college and to an Isaac Newton studentship.

He was a man of very quiet disposition, rather inaccessible, except in astronomical matters. Even in these he was reluctant to take part in public discussions, yet in private conversation he made it clear that he had very definite views, though it was not always an easy matter to elicit them. In private life he was extremely modest and unassuming, a very faithful friend, always cheerful and kindly, and inclined to regard unpleasant events and people from a humorous point of view.

His early papers were of outstanding merit. One of the first was "On the Rotation of an Elastic Spheroid," published in the 'Transactions' in 1896. It was a formal treatment of the calculation of the elastic deformation of a homogeneous sphere, and was elicited by the remarkable discovery of the variation of latitude made by Chandler, who about the year 1891 had completed a laborious and brilliant investigation which showed that there was a roughly periodic movement in the earth of the instantaneous axis of rotation, a complex movement which he proved to be made up of a superposition of two motions, one of period 427 days the other of period one year. Euler's period of nutation for a rigid earth was 306 days. Newcomb had, in 1892, at the instigation of Kelvin, shown from general considerations that the effect of elastic yielding would be to prolong the Eulerian period to about 440 days if the rigidity of the earth were equal to that of steel. Hough was the first to apply the mathematical theory of elasticity to the problem. His thorough examination of the question proved that Newcomb's treatment had been not quite complete, and his conclusion was that Chandler's period, 427 days, would be appropriate for an earth with a rigidity slightly greater than that of steel. The problem is one of enduring interest, on account of the light which it throws upon the internal constitution of the earth, and Hough's pioneering work upon it, supplemented by later investigations on similar lines, has shown how important a *datum* the length of the period of variation of latitude is for determining the manner and degree in which the earth yields to disturbing forces.

Hough's memoir "On the Oscillations of a Rotating Ellipsoidal Shell containing Fluid," based on his Smith's Prize Essay, and published in the 'Trans-

actions' in 1895, was also intended to deal with the problem of variation of latitude, by a formal proof that Fohe's suggestion, that a shell containing fluid would provide an explanation of Chandler's period of 427 days could not be accepted. Hough showed that, if the earth consisted of a rigid shell containing a homogeneous fluid, the Eulerian period of 305 days would be diminished by an amount which would increase with the size of the fluid nucleus, but that the result might be modified by elasticity of the crust.

Another paper of great geophysical interest was that on the "Influence of Viscosity on Waves and Currents"—'Proceedings of the London Mathematical Society,' vol. 28 (1897)—in some sense a preliminary, and in some sense a supplement, to the papers on tidal theory. By mathematical analysis, which was extremely simple if regard be had to the complexity of the subject, Hough showed that, with any reasonable assumptions as to the viscosity of sea-water and the nature of bottom friction, the rate of decay of current motions must be extremely slow, so that known physical causes would be sufficient to maintain such motions as actually exist. Proceeding to estimate the influence of friction on the tidal oscillations of the ocean, he arrived at results which fully confirmed Darwin's view as to the small influence of friction on the lunar fortnightly tide, or any other long-period tide, lunar or solar. These conclusions were opposed to the views of Laplace.

But the mathematical investigations for which Hough is likely to be best remembered are the two papers in which he revised the dynamical theory of the tides. These were published under the title "On the Application of Harmonic Analysis to the Dynamical Theory of the Tides" in the 'Philosophical Transactions' in 1897 and 1898. Laplace had formed the dynamical equations, and attempted to integrate them by means of series, the terms of the series being the functions which were, after him, named "Laplace's coefficients." Later, in the hands of Lord Kelvin, they came to be known as "spherical harmonics." In this attempt Laplace met with comparatively little success, so that Kelvin and Darwin had fallen back on a method of integration in terms of power-series. Hough was, however, convinced that Laplace's efforts at the integration, though unsuccessful, were well directed; for the method of expansion in spherical harmonics, if it could be applied effectively, would not only secure more rapid convergence, but would also render it possible to take account of the self-attraction of the water, thus introducing an important correction of the results that could be obtained by expansion in power-series. At the same time, he entertained some doubts as to the validity of the approximations which Laplace had permitted himself in forming the dynamical equations. He was thus led to investigate the whole problem from the beginning. By a brilliant application of some analysis, which had been developed by Poincaré, and already utilised by Bryan, for dealing with the oscillations of rotating fluid masses, he succeeded in placing the dynamical equations of the theory of the tides on a thoroughly sound foundation. Proceeding then to integrate

the equations in the case of symmetry about the axis of rotation, for which zonal harmonics only are required, he found that the coefficients of the terms in the series are connected by an "equation of three terms"—a linear difference equation of the second order—which is homogeneous in the case of free oscillations, but not in the case of forced. This equation could be solved by a method which had been used for the corresponding equation that arises in the theory of integration by power-series. Hough was thus able to determine the free oscillations, symmetrical about the axis of rotation, of an ocean supposed to cover the whole globe, for any law of depth which is also symmetrical. In the case of uniform depth he gave a complete numerical solution of the problem. He was also able to obtain by his method the results that had been found by others in regard to the forced oscillations of symmetrical type—the tides of long period. Further, he adapted the theory to give an account of the free steady motions of which the ocean, still with the same restriction as to symmetry, is capable. These free steady motions correspond to ocean currents in such an ocean. But, from a tidal point of view, they have an especial importance, first pointed out by the late Lord Rayleigh, because their effect is to diminish the calculated amplitudes of the long-period tides below their equilibrium values. The dynamical theory of the tides, as previously developed, had led to the result that, for an ocean covering the globe, these tides must be subject to such diminution, and this result had been felt to be disconcerting in view of attempts to base an estimate of the rigidity of the earth on observations of the actual height of the fortnightly tide.

All this theory—the dynamical equations, the symmetrical oscillations, and the theory of ocean currents—was contained in the first of the two papers. In the second Hough went on to apply the same methods to unsymmetrical oscillations, for which tesseral harmonics are required. The analysis is much more formidable, but again he found the key—the equation of three terms which had eluded previous attempts at a solution of the problem by expansion in series of spherical harmonics—and used it to determine both the free and the forced oscillations of unsymmetrical types, of an ocean covering the whole globe, still, however, with the restriction of symmetry as regards depth. The forced oscillations represent the actual tides, but the free oscillations are also of importance, from a tidal point of view, because of the possibility of resonance if there is a free period near to that of the disturbing forces. The possibility and the effects of resonance were examined minutely.

Darwin, in stating in the 'Encyclopædia Britannica' (1911) the dynamical theory of the tides, after alluding to Lamb's setting forth of Laplace's theory, refers to Hough as having undertaken an important revision of Laplace's theory. "He succeeded not only in introducing the effects of the mutual gravitation of the ocean, but also in determining the nature and periods of the free oscillations of the sea. A dynamical problem of this character cannot be regarded as fully solved unless we are able not only to discuss the 'forced'

oscillations of the system but also the 'free' Hence we regard Mr Hough's work as the most important contribution to the dynamical theory of the tides since the time of Laplace We shall accordingly present the theory briefly in the form due to Mr Hough " Darwin then proceeded to set forth the theory Apart from the original memoirs in the 'Transactions,' and in addition to this account in the 'Encyclopædia Britannica,' there is a brief *résumé* of the theory in Volume VI 1 B of the 'Encyclopédie der mathematischen Wissenschaften (Leipzig, 1908), in the article "Bewegung der Hydrosphäre," contributed by Darwin and Hough, and another brief account of the method, including some of the more important results, is given in Lamb's 'Hydrodynamics,' 3rd edition (Cambridge, 1906), and later editions

In September, 1898, Hough was appointed Chief Assistant at the Cape Observatory, on the recommendation of Sir David Gill, to whom he had been introduced by Sir George Darwin Under Gill's instigation he made a very complete discussion of the heliometer triangulation of the stars near the South Pole, and from a combination of this with the results of a photographic triangulation of the same region he deduced very accurate positions of the stars required in the southern observatories

Hough's work with the new transit circle obtained by Gill helped to make it the most perfect instrument for the purposes of fundamental astronomy and resulted in two fundamental catalogues, 1905-1911 and 1912-1916

In February, 1907, he was appointed H M Astronomer at the Cape on the retirement of Sir David Gill, and in this capacity he saw and contributed to an enormous output of work of high importance Dr Halm was appointed Chief Assistant in 1907, and in conjunction with him Hough carried out a discussion of radial velocities obtained with the Victoria telescope, and also a discussion of the systematic motions of the Bradley stars.

His work in regard to the 'Astrographic Catalogue' was very thorough, and a volume was completed giving the Right Ascensions and Declinations of 20,000 stars, including reference stars and all stars down to 9^m 0 in the Cape Photographic Durchmusterung of Kapteyn In conjunction with Backlund he compiled a series of fundamental reference stars for use in the 'Astrographic Catalogue'—the stars known as "Hough and Backlund fundamental stars."

The heliometer observations of the outer planets, instituted by Gill, were discussed, as well as the meridian observations of the inner planets

Hough was a mathematician who turned himself into a practical astronomer. Immediately before and after taking his B A degree his special subjects of study were Hydrodynamics and Elasticity, and he was thus well equipped to undertake those geophysical researches which afterwards made him famous. That he did not, in the engrossing pursuit of practical astronomy, lose interest in mathematics is evidenced by a remarkable paper, "On certain discontinuities connected with periodic orbits," published in the 'Acta Mathematica,' vol. 24 (1901), and reprinted in Sir G H. Darwin's 'Scientific Papers,' vol. IV. Darwin

had supposed that two of his orbits, one a closed oval and the other a figure-of-8, were members of the same family, a conclusion which was challenged by Poincaré. Hough, by the discovery of a whole new series of orbits, which he described as "retrograde," was able to trace backwards and forwards the history of both of Darwin's orbits, and to show that they belong to essentially distinct families

Altogether he leaves a splendid record of work accomplished in a life of only 52 years. He died in England on July 8, 1923, and was buried at Chingford Mount Cemetery

In 1906 Hough married Gertrude Annie, daughter of J. H. Lee, of Halstead, Essex. She had been a student at Newnham College. After twelve years of married life, Mrs. Hough died of pneumonia, after influenza, in 1918.

Hough became a Fellow of the Society in 1902. He was President of the South African Philosophical Society in 1907, and on the reconstruction of that Society as the Royal Society of South Africa he was its first President. He was also a Vice-President of the International Astronomical Union, and served as Chairman of the Committee on Fundamental Astronomy.

The accompanying portrait is reproduced from 'The Observatory' by the courtesy of the Editors.

A. E. H. L.
H. F. N.

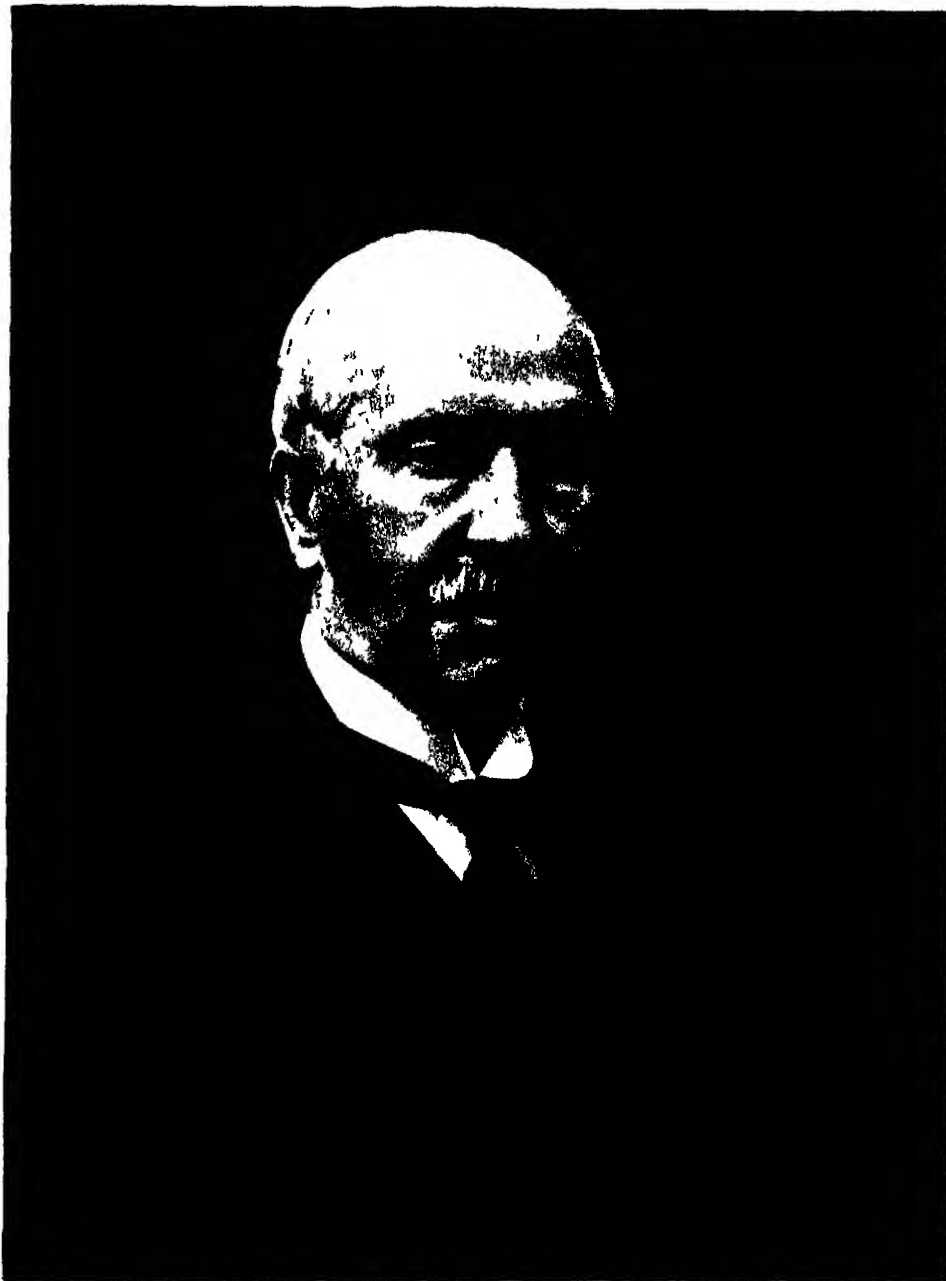
SIR JAMES JOHNSTONE DOBBIE—1852-1924

JAMES JOHNSTONE DOBBIE was born in Glasgow on August 1, 1852, a few months earlier than his fellow-townsmen future collaborator and friend, William Ramsay. He was educated at the High School of that city, and on leaving school took up architecture as a career, at the same time attending Humanity classes in the University. However, at the end of three years he abandoned his first choice of profession and became a regular student in the Faculty of Arts. Since he desired to graduate in science as well as in arts, and as there was then no science degree at Glasgow, he also attended classes in Edinburgh where degrees in science were offered. He graduated as M.A. of Glasgow in 1875, with honours in natural science. Ramsay, who had entered the University at the age of fourteen, was by that time tutorial assistant to Prof. Ferguson in the chemistry department. He and Dobbie first became acquainted in the summer of 1875, and the acquaintance soon ripened into collaboration and close friendship. During the next three years Dobbie worked partly at home and partly abroad, where he studied chemistry with Kolbe and mineralogy with Zirkel in Leipzig. Ramsay proposed to him in the summer of 1876 a joint investigation on the cinchona alkaloids, the method adopted being oxidation by permanganate. They conclusively showed a connection between these alkaloids and pyridine bases, having obtained pyridine carboxylic acids from quinine, cinchonine and quinidine. An account of the work was published in the 'Transactions of the Chemical Society' in 1878 and 1879. Dobbie graduated as B.Sc. of Edinburgh in the former year and as D.Sc. a year later, the work on quinine being made the subject of his thesis.

Dobbie's interest in mineralogy and geology, which he had studied with Archibald Geikie, led to his giving a course of lectures on mineralogy in the University of Glasgow during his tenure of the Clark Scholarship which had been awarded to him. In the long vacation of 1879 he and Ramsay went for a walking tour in Norway, in the course of which Dobbie made a collection of Norwegian minerals, afterwards presented to the College at Bangor, and gathered material for a number of papers which appeared in geological magazines.

On Ramsay's appointment to the Bristol chair in 1880, Dobbie succeeded him as assistant in the Chemistry Department, where he continued his work on alkaloids. He took part at this time in the establishment of the Scottish Section of the Society of Chemical Industry and became its first secretary.

In 1884 Dobbie was appointed to the chair of chemistry in the University College of North Wales at Bangor. The first years of his tenure were occupied in helping to place the new College on a firm footing, in creating a chemistry



James J. Dobbie

department out of hittle, and in organising instruction. When he was at length able to resume research work he attacked, in association with Dr. Alexander Lauder, the problem of the alkaloids of *Corydalis cava*, of which they isolated three. Their researches, which were published in a series of papers between 1893 and 1902, led to the determination of the constitution and relationships of the chief alkaloid, corydaline, and of many of its oxidation products and associated compounds.

In 1898 began a fruitful co-operation with W. N. Hartley, of Dublin, whose researches on absorption spectra had pointed a new way of attacking difficult problems of the constitution of organic compounds. The constitution of tautomeric organic substances first engaged the attention of the collaborators, and they were able to prove, for example, by comparison of the absorption spectra of isatin and its methyl derivatives, that the parent substance had the lactam, and not the alternative lactim, constitution. The method of investigation was afterwards applied to a large number of substances, including many alkaloids. Amongst the numerous papers of this period may be mentioned that on the constitution of cotarnine by Dobbie, Lauder and Tinkler as being of special interest and importance.

While at Bangor, Dobbie showed his marked capacity for organisation and his interest in problems of education outside his own immediate sphere. It was owing largely to his efforts that an agricultural department was instituted in the College, offering courses which led to a diploma, and later to a degree in agriculture. A chief part was also played by him in the negotiations which led to the foundation of the University of Wales.

He had married, in 1887, Violet daughter of Thomas Chilton, J.P., of Gresford, Wrexham, and the educational claims of a young family had their weight in prompting him to give up his teaching and research work at Bangor, and to accept in 1903 the post of Director of the Royal Scottish Museum in Edinburgh. This important position under the Scottish Education Department he held for six years with great success. His unfailing tact and wide interests enabled him nicely to balance the claims of competing sections of the Museum and to develop its usefulness in various directions. By keeping in touch with his former junior collaborators, he still contrived, despite heavy official work, to continue investigations on absorption spectra and the alkaloids. He retained his interest in agricultural education and became Convener of the College Committee of the Edinburgh and East of Scotland College of Agriculture.

In 1909, he succeeded Sir T. E. Thorpe as Principal of the Government Laboratory in London. The Laboratory was in process of reorganisation when he was appointed and became in 1911 a separate department, with himself at the head as Government Chemist. It will be readily understood that the war period imposed a great strain on this department and on its chief—a strain which, in the end, undoubtedly affected his health.

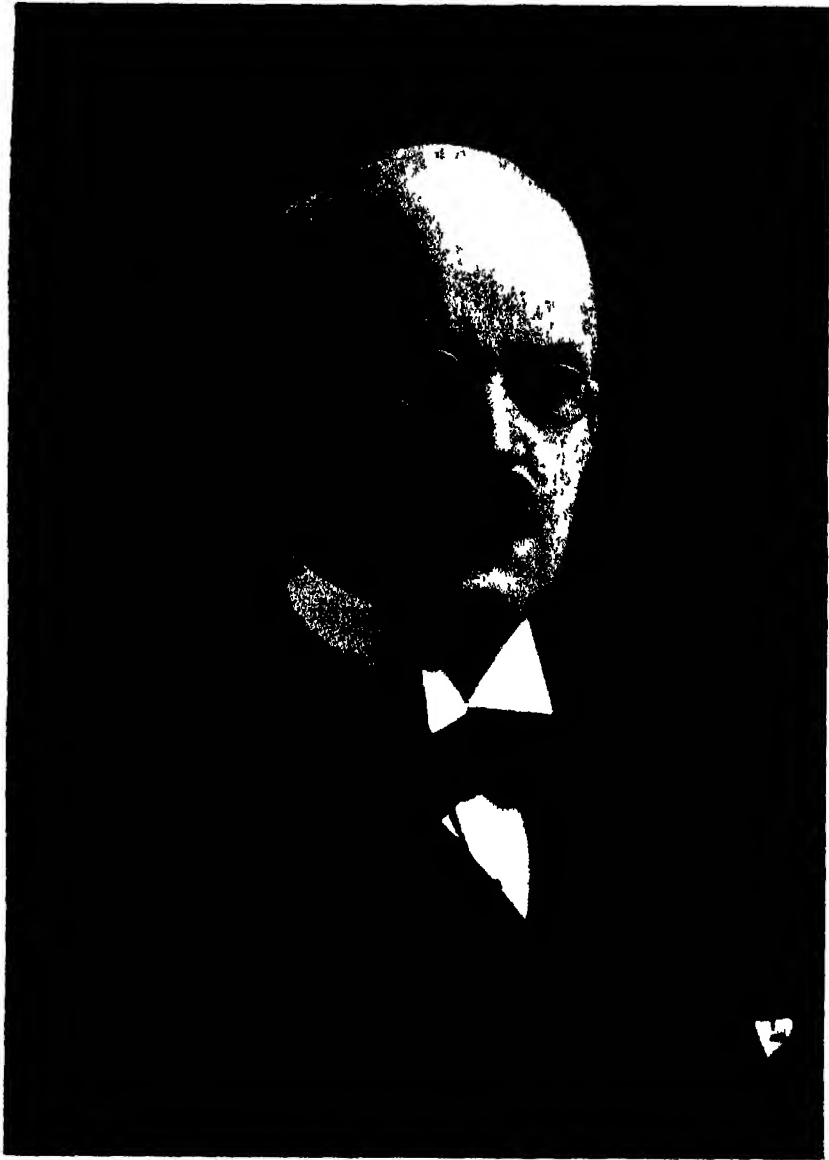
His investigations, now carried on chiefly with Dr. J J Fox as collaborator, still related mainly to the absorption spectra of the alkaloids, the general conclusion being that alkaloids which possess the same unreduced (benzenoid) nucleus have approximately the same absorption spectra, though they may otherwise differ considerably in composition and constitution. After the war, Dobbie found a new interest in applying measurements of absorption spectra to the constitution not of complex organic compounds, but to the simplest substances of all, the gaseous elements. He and Dr Fox published their results in three papers in the Proceedings of the Society in 1919-21. They found that the elements capable of being easily gasified in silica below a temperature of 1,350 deg may be divided into three classes in accordance with the behaviour of their spectra at gradually increasing temperatures – (1) Elements whose vapours exercise no absorption or show only a few well-defined bands, *e.g.*, mercury, zinc, cadmium, (2) elements in which the absorption gradually increases as the temperature is raised, *e.g.*, phosphorus, arsenic, antimony, (3) elements in which the absorption increases with increase of temperature and afterwards diminishes, *e.g.*, sulphur, selenium, tellurium, the halogens. The first group are monatomic, the second tetratomic, breaking down simply to diatomic molecules as the temperature increases. The behaviour of the third group is attributed to formation of a certain type of complex molecules as the temperature rises, and subsequent breaking down of the polymer at still higher temperatures.

Dobbie was elected to the Fellowship of the Society in 1904, and had conferred upon him the degree of LL.D. by the University of Glasgow in 1908, and of D.Sc. by the University of Wales in 1920. In 1915 he received the dignity of knighthood. He was President of the Institute of Chemistry from 1915 to 1917 and of the Chemical Society from 1919 to 1921.

He retired from his position as Government Chemist in 1920, but remained in London for a time to continue his valuable service on various public committees. Eventually he went to reside at Fairlie, a village on the Ayrshire coast with which his family had long been connected. Here he died after a short illness on 19th June 1924, being survived by his wife, one son and two married daughters. His elder son was killed in the war.

While his work was confined to science, teaching, and administration, his interests were many. Nature, literature, and art alike appealed to him. Methodical without rigidity, tactful yet firm, clear-sighted and judiciously minded, he was a valuable servant of the public at large, to an intimate circle he was a kindly, helpful friend.

J W.



J. E. Campbell,

—

JOHN EDWARD CAMPBELL—1862-1924

THE death of JOHN EDWARD CAMPBELL on October 1, 1924, was distressingly sudden. His powers were at their full, his health had seemed perfect, and for a wonder he was not at the time even working too hard. The loss is not only irreparable to his own family, but a grievous one to many admiring friends, to his College and to fellow-workers at mathematics in Oxford and out of it.

He was born on May 27, 1862, at Lisburn, Co. Antrim, where his father, John Campbell, M.D., the son of an earlier Dr. Campbell, was in practice. He once intended to enter the medical profession himself, as a brother did, and as his own eldest son has since done. In 1889 he married Sarah, eldest daughter of Mr. Joseph Hardman, cotton spinner, of Waterhead, Oldham. She survives him, as do two sons and a daughter. Another son, a scholar of his own College, fell near Ypres in October 1914, only a few days after landing as a hastily trained young officer.

After earlier education at home and at the Methodist College, Belfast, he entered Queen's College, Belfast, where he presently graduated in the Queen's University. He always remained a very loyal Ulsterman, in every sense, and expressed warm gratitude to those under whom he studied in his first University. Nor did Belfast forget him as he was earning distinction elsewhere. It conferred on him the Honorary Degree of D.Sc. in 1919.

In 1884 he came from Belfast to Oxford, with a scholarship, which could be held by one a little over the usual age, at the newly revived foundation, Hertford College. After getting in succession all the University distinctions open to a mathematical man, he became Fellow and Tutor of the same College. Later, for a good many years, he was also Lecturer of University College.

Of his devotion to duty in Oxford it is impossible to speak too highly, and the general affection felt for him can hardly be exaggerated. His success with pupils was marked, all the more marked because all saw that he was at home, mathematically, in regions above them and wondered that he could come down to their modest level. He possessed capacity for administration also, serving his College well as Vice-Principal, with Principal's authority, and as Bursar, at times of special need. He was a man of singular personal charm, cheery, unaffected, trust-inspiring. There was no selfishness in him. Differences of opinion, where principle was not at stake, did not worry him. He knew how to be sorry without complaining if misfortune or disappointment came his way.

His family are anxious that he should not be thought of only as a distinguished mathematician who was always at work. To them he was also the model of a sympathetic and truly Christian father, happy in sharing the interests of young people, and always ready to be straightforward with them, as intelligent friends, when they needed guidance. They felt that he instilled sincerity,

courage and fairness by daily example no less than by outspoken advice. His relaxations, other than domestic, were social among humble folk in a certain poor parish, but besides there was always a favourite book by Scott or Dickens or Jane Austen in his pocket, ready to hand for one more reading

He was elected F R S in 1905 For two years from November, 1918, he was President of the London Mathematical Society Quite recently he greatly appreciated the honour, a new one for an Oxford man, of being called upon to examine for the Cambridge Mathematical Tripos. He was understood to have things to tell us for our good from the sister University, but the opportunity will not come

As a researcher in, and writer of, mathematics, he disliked the petty, and was all for the general Finding himself, one may almost say by accident of environment, a student of geometry, but having all the same a decided bent towards differential analysis with a big object, he looked abroad for analysis bearing on geometry which needed making known at home, and began by saturating himself with knowledge obtained from Sophus Lie's "*Transformations-Gruppen*" A first period of great productiveness followed, as to the outcome of which Professor Burnside, the best qualified of judges, has kindly written the paragraph next following —

"Mr Campbell's interest in the theory of continuous groups was first shown in two papers on 'A Law of Combination of Operators,' in vols 28 and 29 of the '*Proc L M S*' In these papers he deals, from a point of view which is essentially his own, with the formal results which are at the base of Lie's theory In a paper published two years later, 'On the Theory of Simultaneous Partial Differential Equations,' he develops a system of formulæ by which it may be determined whether such a system is or is not integrable. His next contribution to the subject ('*Proc L M S*,' vol 33) was a 'Proof of the Third Fundamental Theorem in Lie's Theory' The proof given is essentially simpler than Lie's own, and, though it was subsequently criticised by Engel, it is recognised as being substantially complete. In 1903, not very long after the date of the last paper, Mr. Campbell's '*Introductory Treatise on Lie's Theory of Finite Continuous Transformation Groups*' was published. By writing this book he put English mathematicians under a lasting debt of gratitude It gives a wonderfully clear and complete account of a modern theory which, although it already had a literature of its own on the Continent, had, at the time when the book was published, attracted little or no attention in this country. Moreover, the book is not, in any sense whatever, a mere compilation from outside sources It is full of points of view and illustrations which are Mr Campbell's own. The chapters on contact transformations and on differential invariants may be specially referred to. The theory in which Mr Campbell was so specially interested underlies most of his more recent work on differential geometry in general, and on that particular branch of it connected with Einstein's gravitation-theory."

The last sentence in the above indicates how Campbell was led on to researches in the general differential geometry of surfaces and higher spaces, as associated by Gauss and his followers with the analysis of differential quadratic forms, and so to another study much pursued in other countries, but much neglected here. What may be looked upon as the second series of writings with which his name will be associated began in 1906 with a long and searching paper, "On Backlund's Transformation and the Partial Differential Equation $s = F(x, y, z)$ " ('Proc. L.M.S.', Ser. 2, vol. 5). Another paper in the next volume introduced an application of quaternion methods to the problem of the infinitesimal deformation of a surface, which in later work he followed up by considerable use of vectors and quaternions, and by the introduction of a notation of his own. His second period thus begun, was to last—with a break—for the rest of his life. It gave him great pleasure in 1909 to be invited by the delegates of the Common University Fund to give a special course of lectures in the University of Oxford on the subject of the differential geometry of surfaces which he had now made his own.

After the war period, during which Campbell lived as one unconscious of the existence of mathematics or of anything but his country and duties of service, he returned with fervour to his differential geometry (as well as his tutorial work). Now he began to attend, not only to the geometry of surfaces in Euclidean space, which had been his main concern beforehand, but to the geometry of quadratic differential forms in higher spaces, and in particular to the four-way space of the general theory of relativity. Though he never tired of confessing that he knew little about Physics, there is no doubt that the doctrine of gravitation according to Einstein appealed to him strongly. His valedictory address as President of the London Mathematical Society in November, 1920, is a memorable pronouncement, from a pure mathematician's standpoint, about the wonder that a hypothesis in the study of differential geometry, which he found natural, "should tell us about facts of the universe." The subject of the address was one that he returned to in at least one later paper.

A book on differential geometry was naturally expected from him—expected by some perhaps ever since his lectures of 1909—and he lived just long enough to write such a book. It is hoped that this will soon be published. It is complete, so far as he had intended it to go, except that a contemplated final chapter on the connexion of what had preceded with the theory of Einstein is only represented among writings that can be found by a fragment, if at all. In writing the book he is believed by his friends to have had in view, not so much the extension of knowledge, except in the chapters on higher spaces, as the enforcement of the usefulness and convenience of novel and neglected methods, those of the calculus of tensors and of vector geometry.

It must not be pretended that Campbell's work is easy reading. His analysis proceeds steadily, but is inevitably laborious because of his preference for

attacking problems in full generality, and of the small breathing space which he allows in the course of protracted investigations. Moreover, though when making a new start he carefully words an introduction descriptive of the aim of what is coming, there is sometimes not quite enough expression of the earlier stages of thought by which he has in the first place put the known, as derived from authorities or even from his own previous pages, in the form which is going to help him on. Yet there is a glowing enthusiasm about his confident advance which incites to determination in following him. He writes with the zeal of one who has a message to deliver, and the message will be carried on. His methods in differential geometry will receive the attention which they deserve. It may be expected that followers will improve on them, but his leadership will be recognised, and his actual production is not for the present day only.

E B E



INDEX TO VOL. CVII. (A)

- Address of the President, 1924, 1
- Aircrow, vibrations in blades and shaft of (Fage), 451
- Alpha-particles and ionisation in gases (Gurney), 332, stopping by gases (Gurney), 340.
- Allmand (A. J.) and Puri (V. S.) The Effect of Superposed Alternating Current on the Polarizable Primary Cell Zinc-Sulphuric Acid-Carbon. Part I. Low-frequency Current, 126
- Alternating current superposed on polarizable primary cell (Allmand and Puri), 126.
- Aluminium, distortion of single-crystal pieces of (Carpenter and Elam), 171
- Archimedean solids, development of (Thompson), 181
- Atomic fields of helium and neon (Jones), 157
- Barfield (R. H.) See Smith-Rose and Barfield.
- Bismuth, fluorescence and channelled absorption (Rao), 760
- Blackett (P. M. S.) The Ejection of Protons from Nitrogen Nuclei, photographed by the Wilson Method, 349
- Brinkworth (J. H.) On the Measurement of the Ratio of the Specific Heats, using Small Volumes of Gas—The Ratios of the Specific Heats of Air and of Hydrogen, 510
- Bucherer's experiments on ϵ/m (Lewis), 544
- Butterworth (S.) On the Alternating Current Resistance of Solenoidal Coils, 693.
- Campbell (A.) On the Determination of Resistance in Terms of Mutual Inductance, 310.
- Campbell (J. E.) Obituary notice of, ix.
- Carpenter (H. C. H.) and Elam (C. F.) Experiments on the Distortion of Single-crystal Test-pieces of Aluminium, 171
- Chapman (D. L.), Ramsbottom (J. E.) and Trotman (C. G.) The Union of Hydrogen and Oxygen in presence of Silver and Gold, 92
- Colours due to films on metals (Evans), 228.
- Constable (F. H.) The Catalytic Action of Copper Part VI.—An Explanation of the Reproducibility of the Catalyst and of the Periodic Change in its Activity, &c., 270.
- Constable (F. H.) See Palmer and Constable
- Copper, catalytic activity of (Palmer and Constable), 255, 270.
- Curtis (W. E.) The Fulcher Hydrogen Bands, 570.
- Dean (W. R.) On the Theory of Elastic Stability, 734.
- Dielectrics, law of electrical conduction in (Richardson), 101.
- Dirac (P. A. M.) The Adiabatic Invariance of the Quantum Integrals, 725.
- Dobbie (Sir J.) Obituary notice of, vi
- Dymond (E. G.) On the Precise Measurement of the Critical Potentials of Gases, 291.
- Elam (C. F.) See Carpenter and Elam.
- Evans (U. R.) The Colours due to Thin Films on Metals, 228.
- Fage (A.) An Experimental Study of the Vibrations in the Blades and Shaft of an Air-screw, 451.

- Farren (W S) and Taylor (G I) The Heat developed during Plastic Extension of Metals, 422
- Fowler (A.) The Structure of the Spectrum of Ionised Nitrogen, 31
- Fulcher hydrogen bands (Curtis), 570
- Gases, measurement of critical potentials of (Dymond), 291
- Gibbs (R E) The Variation with Temperature of the Intensity of Reflection of X-rays from Quartz, and its Bearing on the Crystal Structure, 561.
- Gurney (R. W) Ionisation by Alpha-particles in Monatomic and Diatomic Gases, 332 ; The Stopping Power of Gases for Alpha-particles of Different Velocities, 340
- Hæmoglobin, reduced, velocity of oxygen combining with (Hartridge and Roughton), 654.
- Hardy (G H) The Lattice Points of a Circle, 623
- Hartridge (H.) and Roughton (F J W) The Kinetics of Hæmoglobin III.—The Velocity with which Oxygen combines with Reduced Hæmoglobin, 654
- Heats, specific, measurement of ratio of (Brinkworth), 510
- Helium and neon, atomic fields (Jones), 157
- Hough (S S) Obituary notice of, 1
- Howard (J V) and Smith (S L) Recent Developments in Tensile Testing, 113
- Hydrogen and oxygen, union in presence of silver and gold (Chapman and others), 92.
- Hydrogen, regularities in secondary spectrum (Richardson and Tanaka), 602
- Ibbs (T. L) Thermal Diffusion Measurements, 470
- Indian and gallium spark spectra on ultra-violet region (Weinberg), 138
- Inductance, standard of mutual (Wilmotte), 716.
- Ingham (A. E) See Jones and Ingham
- Ionisation in gases by alpha-particles (Gurney), 332
- Iron crystals, magnetic properties of (Webster), 496
- Jeffreys (H) On the Formation of Water Waves by Wind, 189.
- Jones (J E) On the Atomic Fields of Helium and Neon, 157
- Jones (J E.), and Ingham (A E) On the Calculation of certain Crystal Potential Constants and on the Cubic Crystal of Least Potential Energy, 636
- Kingdon (K H) See Langmuir and Kingdon.
- Langmuir (J.) and Kingdon (K H) Thermionic Effects caused by Vapours of Alkali Metals, 61.
- Lattice points of a circle (Hardy), 623
- Lewis (T) The Interpretation of the Results of Bucherer's Experiments on e/m , 544.
- Light, total reflexion of (Schuster), 15
- Mann (F. G) and Pope (Sir W J) 1. 2 3—Triaminopropane and its Complex Metallic Compounds, 80.
- Martin (L. H) See Stoner and Martin.
- Merton (T R) and Pilley (J G.) On Experiments relating to the Spectrum of Nitrogen, 411
- Metals, colours due to films on (Evans), 228, heat developed during extension of (Farren and Taylor), 422, thermal and electrical conductivities (Schofield), 206.
- Molecules, structure of, in relation to optical anisotropy (Ramanathan), 684.
- Mosharafa (A. M) On the Quantum Dynamics of Degenerate Systems, 237.

Newbery (E) Overvoltage and Transfer Resistance, 486

Nicholson (J W) Spheroidal Wave functions, 43.

Nitrogen, spectrum of ionised (Fowler), 31

Obituary notices of Fellows deceased —

Hough, S S, 1

Dobbie, Sir J, vi

Campbell, J E, ix

Overvoltage and transfer resistance (Newbery), 486

Palmer (W G) and Constable (F H) The Catalytic Activity of Copper Part V —The Comparison of the Rates of Dehydration of Various Alcohols, 255

Pilley (J G) See Merton and Pilley

Pope (Sir W J) See Mann and Pope

Protons, ejection from nitrogen nuclei, photographed (Blackett), 349

Puri (V S) See Allmand and Puri.

Quantum dynamics of degenerate systems (Mosharafa), 237

Quantum integrals, adiabatic invariance of (Dirac), 725

Quartz, intensity of reflection of X-rays from, and bearing on crystal-structure (Gibbs), 544

Ramanathan (K R) The Structure of Molecules in relation to their Optical Anisotropy —Part I, 684

Ramsbottom (J E) See Chapman, Ramsbottom and Trotman

Rao (K R) On the Fluorescence and Channelled Absorption of Bismuth at High Temperatures, 760, A Note on the Absorption of the Green Line of Thallium Vapour, 762.

Refractory materials, electrically fused, making small pots of (Tritton), 287

Resistance in terms of mutual inductance (Campbell), 310

Richardson (O W) and Young (A F A.) The Thermionic Work functions and Photo-electric Thresholds of the Alkali Metals, 377

Richardson (O W) and Tanaka (T) Regularities in the Secondary Spectrum of Hydrogen, 602

Richardson (S W) The General Law of Electrical Conduction in Dielectrics, 101.

Roughton (F J W) See Hartridge and Roughton

Royal Society, life statistics of Fellows (Sohuster), 368

Royds (T) The Apparent Tripling of certain Lines in Arc Spectra, 360

Schofield (F H) The Thermal and Electrical Conductivities of some Pure Metals, 206.

Sohuster (Sir A) On the Total Reflexion of Light, 15, On the Life Statistics of Fellows of the Royal Society, 368.

Sélincourt (M. de) On the Effect of Temperature on the Anomalous Reflection of Silver, 247.

Sherrington (Sir C) Anniversary address, 1924, 1

Silver, anomalous reflection of (Sélincourt), 247.

Smith (S L) See Howard and Smith.

Smith-Rose (R. L.) and Barfield (R. H) On the Determination of the Directions of the Forces in Wireless Waves at the Earth's Surface, 587.

Solenoidal coils, alternating current resistance of (Butterworth), 693

Spectra, tripling of lines in arc (Royds), 360

- Spectrum of ionised nitrogen (Fowler), 31, of nitrogen, experiments relating to (Morton and Pilley), 411
- Stability, theory of elastic (Dean), 734
- Stoner (E C) and Martin (L H) The Absorption of X-rays, 312
- Tanaka (T) See Richardson and Tanaka
- Taylor (G. I) See Farren and Taylor
- Tensile testing, developments in (Howard and Smith), 113
- Thallium vapour, absorption of green line (Rao), 762
- Thermal diffusion measurements (Ibbs), 470
- Thermionic effects by vapours of alkali metals (Langmuir and Kingdon), 61.
- Thermionic work functions and photo-electric thresholds of alkali metals (Richardson and Young), 377
- Thompson (D'A W) On the 13 Semi regular Solids of Archimedes, and on their Development by Transformation of certain Plane Configurations, 181
- Triaminopropane and metallic compounds (Mann and Pope), 80
- Tritton (F S) A Centrifugal Method of Making Small Pots of Electrically Fused Refractory Materials, 287
- Trotman (C G) See Chapman, Ramsbottom and Trotman
- Wave-functions, spheroidal (Nicholson), 43
- Waves, water, formation by wind (Jeffreys), 189
- Webster (W L) The Magnetic Properties of Iron Crystals, 496
- Weinberg (M.) The Spark-spectra of Indian and Gallium in the Extreme Ultra-Violet Region, 138
- Wilmotte (R M.) On the Field of Force near the Neutral Point produced by Two Equal Coaxial Coils, with special reference to the Campbell Standard of Mutual Inductance, 716
- Wireless waves, directions of forces in, at earth's surface (Smith-Rose and Barfield), 587.
- X rays, absorption of (Stoner and Martin), 312, intensity of reflection of, from quartz (Gibbs), 544
- Young (A F A.) See Richardson and Young

I. A. R. I. 75

IMPERIAL AGRICULTURAL RESEARCH
INSTITUTE LIBRARY
NEW DELHI

Date of issue.	Date of issue.	Date of issue.
..		.
	..	
.	.	.
	..	
... .		
..		.

.	. .	
.
..
.		..
.
...